UNCLASSIFIED

AD 283 396

Reproduced
by the

ARMED SERVICES TECHNICAL INFORMATION AGENCY
ARLINGTON HALL STATION
ARLINGTON 12, VIRGINIA



UNCLASSIFIED

DISCLAIMER NOTICE

THIS DOCUMENT IS BEST QUALITY PRACTICABLE. THE COPY FURNISHED TO DTIC CONTAINED A SIGNIFICANT NUMBER OF PAGES WHICH DO NOT REPRODUCE LEGIBLY.

NOTICE: When government or other drawings, specifications or other data are used for any purpose other than in connection with a definitely related government procurement operation, the U. S. Government thereby incurs no responsibility, nor any obligation whatsoever; and the fact that the Government may have formulated, furnished, or in any way supplied the said drawings, specifications, or other data is not to be regarded by implication or otherwise as in any manner licensing the holder or any other person or corporation, or conveying any rights or permission to manufacture, use or sell any patented invention that may in any way be related thereto.

AD#2706:1

NOX

283 396

ECCANICA
EI SISTEMI
JOLO-VEICOLO

•

ECHANICS
F SOIL-VEHICLE
SYSTEMS

283396

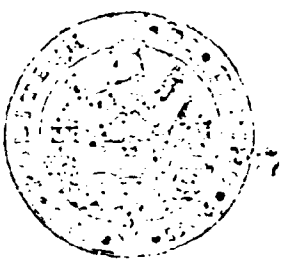
CATALOGED BY ASTIA
AS AD No. 1

MECCANICA DEI SISTEMI SUOLO-VEICOLO

MECHANICS OF SOIL-VEHICLE SYSTEMS

Atti del 1° Convegno Internazionale
del Movimento fuori strada

Proceedings of the 1st International Conference
on the Mechanics of Soil-Vehicle Systems



TORINO - SALIT VINCENZO 12 - 16 SETTEMBRE 1961

EDIZIONI
MINERVA
TECNICA

EDIZIONI MINERVA TECNICA

NO OTS

MECCANICA DEI SISTEMI SUOLO-VEICOLO

MECHANICS OF SOIL-VEHICLE SYSTEMS

MECCANICA DEI SISTEMI SUOLO-VEICOLO

MECHANICS OF SOIL-VEHICLE SYSTEMS

Atti del I Convegno Internazionale del Movimento Fuori Strada

Proceedings of the 1st International Conference on the Mechanics of Soil-Vehicle Systems

Torino - Saint Vincent, 12-16 Giugno 1961

EDIZIONI MINERVA TECNICA

TORINO (ITALY)

PUBBLICATO CON IL CONTRIBUTO
DEL
CONSIGLIO NAZIONALE DELLE RICERCHE

PROPRIETÀ LETTERARIA

INDICE

A. Capetti: *Prefazione* . . . . . pag. XIII

F. Garbari: *Introduzione* . . . . . » 1

MOBILITA' DEL VEICOLO E TEORIE SULLA PLASTICITA'
VEHICLE MOBILITY AND THEORIES OF PLASTICITY

1 — D. C. Drucker: On stress-strain relations for soils and load carrying capacity . . . . . pag. 15

Discussions: E. Leflaive; M. Juul Hvorslev . . . . . » 24

2 — R. M. Haythornthwaite: Methods of plasticity in land locomotion studies . . . . . » 28

Discussion: E. Leflaive . . . . . » 43

3 — R. L. Schiffman: Analysis of the displacements of the ground surface due to a moving vehicle . . . . . » 45

4 — L. J. Goodman, C. N. Lee: Effects of remolding on soil values related to vehicle mobility . . . . . » 63

Discussions: S. J. Knight, A. A. Rula; W. L. Harrison; R. Ariano; L. J. Goodman, C. N. Lee . . . . . » 76

5 — G. G. Meyerhof: The bearing capacity of soils under vehicle loads . . . . . » 81

6 — Trafficability Research Team: Forecasting of trafficability after traffic for sands possessing structures . . . . . » 87

Discussion: W. J. Turnbull . . . . . » 96

7 — E. T. Selig, K. E. Hofer, N. A. Weil: Elastic response of soil to tracked vehicles . . . . . pag. 97

Discussions: R. Ariano; N. A. Weil . . . . . » 107

CARATTERISTICHE TECNICHE DEI VEICOLI DESTINATI AL MOVIMENTO FUORI STRADA

ENGINEERING ASPECTS OF OFF-THE-ROAD VEHICLES

8 — F. L. Uffelmann: The performance of rigid cylindrical wheels on clay soil . . . . . pag. 111

Discussions: B. Mayfield, F. Sherratt; J. Phillips . . . » 126

9 — C. De Gregorio: Sul trasportatore tutta ruota . . . . . » 131

Discussions: N. W. Radforth; C. De Gregorio . . . . . » 135

10 — C. J. Nuttall, Jr.: The steering of tracked vehicle by articulation . . . . . » 136

11 — G. Bonmartini: Ruota strada; cingolo fuori strada . . . » 137

Discussions: J. Remus; L. Amici . . . . . » 157

12 — N. W. Radforth: Land factors and vehicle design in operations on organic terrain . . . . . » 158

Discussions: F. Bonmartini; N. W. Radforth . . . . » 169

13 — J. G. Thomson: Vehicle design from field test data . . . » 171

Discussion: N. W. Radforth . . . . . » 182

14 — S. Tsunematsu, K. Matsui: Relation of shape of track shoes to tractive force of the crawler-type tractor on peat soil . . » 183

Discussions: N. W. Radforth; D. Giacosa . . . . . » 190

ASPERITA' DEL TERRENO, VIBRAZIONI DEL VEICOLO E STABILITA' DIREZIONALE

TERRAIN ROUGHNESS, VEHICLE VIBRATION AND DIRECTIONAL STABILITY

15 — J. L. Bogdanoff, F. Kozin: On the statistical analysis of linear vehicle dynamics . . . . . pag. 195

16 — F. Kozin, J. L. Bogdanoff: On the statistical properties of the ground contour and its relation to the study of land locomotion . . . . . pag. 224

Discussions: E. Saibel; R. Ariano; F. Kozin; J. L. Bogdanoff; A. Castagna; V. E. Gough; L. Amici . . . . . » 240

17 — D. C. Clark, L. Segel: The steering and drawbar-pull performance of pneumatic-tired vehicles . . . . . » 244

Discussions: L. Amici; D. C. Clark . . . . . » 261

18 — Takashi Tanaka: The statical analysis and experiment on the force to the tractor wheel . . . . . » 262

Discussion: F. L. Uffelmann . . . . . » 271

MECCANICA DEL VEICOLO
VEHICLE MECHANICS

19 — W. Bergman, E. A. Fox, E. Saibel: Dynamics of an automobile in a cornering maneuver on and off the highway . . pag. 275

Discussions: J. L. Bogdanoff; E. Saibel; F. Kozin . . . » 303

20 — J. E. Shigley: The mechanics of walking vehicles . . . » 304

Discussions: S. Muratori; C. B. Lewis; J. E. Shigley . . » 321

21 — W. F. Buechele: Application of the soil parameters to vehicular mechanics . . . . . » 323

MISURA DEL SUOLO ED APPARECCHIATURE RELATIVE
SOIL MEASUREMENT AND INSTRUMENTATIONS

22 — F. Pavlics: Bevameter 100. A new type of field apparatus for measuring locomotive stress-strain relationships in soils . pag. 331

Discussions: F. L. Uffelmann; F. Pavlics . . . . . » 361

23 — I. J. Sattinger, S. Sternick: An instrumentation system for the measurement of terrain geometry . . . . . » 362

Discussions: L. Amici; I. J. Sattinger . . . . . » 370

24 — S. J. Knight, A. A. Rula: Measurement and estimation of the trafficability of fine-grained soils . . . . . » 371

Discussions: P. Brendeau; E. Lemke; N. W. Radforth . . » 384

25 — A. R. Reece, B. M. D. Wills: Forced-slip wheel-and-track tester . . . . . pag. 387

Discussion: W. Söhne . . . . . » 400

26 — G. E. Vanden Berg, I. F. Reed, A. W. Cooper: Evaluating and improving performance of traction devices . . . . . » 402

27 — D. E. Cobb, G. T. Colhon, J. D. Gentry: Scale model evaluation of earthmoving tools . . . . . » 412

Discussions: B. Mayfield; R. J. Sullivan; L. J. Goodman; E. Saibel . . . . . » 427

28 — W. F. Buechele: Instrumentation for land locomotion studies » 429

Discussion: J. Remus . . . . . » 437

29 — Trafficability Research Team: A proposed recording penetrometer . . . . . » 446

Discussion: W. J. Turnbull . . . . . » 453

30 — J. R. Phillips: Brief description of the six-component oblique-rolling-wheel machine recently constructed and tested at the University of Western Australia . . . . . » 454

RELAZIONE FRA SUOLO E VEICOLO
SOIL-VEHICLE RELATIONSHIP

31 — A. Finney: Special applications of high mobility tires . . . pag. 465

Discussions: L. Amici; L. Bogdanoff; A. Finney; S. G. J. Kelecom . . . . . » 484

32 — W. J. Turnbull, D. R. Freitag: The behavior of sand under pneumatic tires . . . . . »

33 — W. Söhne, F. J. Sonnen: Messungen von Rollwiderstand und Zugkraft von luftbereiften Ackerschleppern sowie mechanischen Bodenkenngrössen und Versuch einer Zuordnung . . . . » 506

Discussions: F. J. Sonnen; E. Lemke; W. Söhne; N. W. Radforth . . . . . » 536

34 — J. R. Phillips: The powered vehicular wheel plane-rolling in equilibrium: a consideration of slip and rolling resistance . » 541

Discussions: V. E. Gough; J. R. Phillips; A. R. Reece; W. F. Buechele . . . . . » 554

35 — G. W. Steinbrenner: The ideal tractive efficiency of soil . pag. 558

36 — S. J. Knight, M. P. Meyer: Soil trafficability classification scheme . . . . . » 567

37 — N. W. Mc Leod: Influence of multiple compartment tires on off-the-road vehicle mobility . . . . . » 575

38 — A. D. Seia: On the slip and the tractive effort . . . . . » 587

Discussion: M. G. Bekker . . . . . » 604

39 — A. Orlandi: Il fenomeno dell'aderenza di un cingolo fuori strada . . . . . » 605

40 — M. Weinblatm, S. Orlovski: Factors affecting wheeled tractor traction on sandy loess soils . . . . . » 618

Discussion: H. Meyer . . . . . » 639

SIMILITUDINE FRA VEICOLI IN GRANDEZZA NATURALE ED IN SCALA RIDOTTA

SIMILARITY BETWEEN FULL SIZE AND SMALL SCALE VEHICLES

J. Truelle: *Problèmes de similitude: déclaration d'ouverture* . . pag. 643

41 — H. H. Hicks, jr.: A similitude study of the drag and sinkage of wheels using a system of soil values related to locomotion » 645

42 — C. J. Nuttal Jr., R. P. McGowan: Scale models of vehicles in soils and snows . . . . . » 656

Discussion: Z. Janosi . . . . . » 676

43 — W. L. Harrison jr.: Analytical prediction of performance for full size and small scale model vehicles . . . . . » 678

Discussions: R. P. McGowan; W. L. Harrison; C. J. Powell, J. L. Smith . . . . . » 700

J. Truelle: *Problèmes de similitude: commentaire final* . . . . » 703

TEORIA E PREVISIONE DELLE PRESTAZIONI

THEORY AND PREDICTION

44 — Z. Janosi, B. Hanamoto: The analytical determination of drawbar pull as a function of slip for tracked vehicles in deformable soils . . . . . pag. 707

Discussions: A. R. Reece; Z. Janosi . . . . . » 727

45 — Z. JANOSI: An analysis of pneumatic tire performance on deformable soils . . . . . pag. 737

Discussions: R. D. WISMER, M. E. SMITH; Z. JANOSI; E. LEFLAIVE; W. L. HARRISON; F. L. UFFELMANN; F. FAUSTI . . » 762

46 — M. G. BEKKER: Evaluation and selection of optimum vehicle types under random terrain conditions . . . . . » 772

Discussions: F. L. UFFELMANN; M. G. BEKKER; S. J. KNIGHT, M. P. MEYER . . . . . » 786

DISCUSSIONE SUGLI ASPETTI DEL MOVIMENTO SULLA SUPERFICIE DELLA LUNA

PANEL DISCUSSIONS ON LUNAR SOILS

47 — J. A. RYAN: Some predictions as to the possible nature and behavior of the lunar soils . . . . . pag. 793

48 — N. A. WEIL: Probable soil conditions on the moon and terrestrial planets . . . . . » 803

Discussions: J. A. EVAN; N. A. WEIL; M. G. BEKKER; J. J. MURRAY; E. SAIBEL; W. J. TURNBULL; R. L. SCHIFFMAN . . . » 825

SUOLO E VEICOLI
SOIL AND VEHICLES

49 — TRAFFICABILITY RESEARCH TEAM: A suggested empirical combination between the Bekker and the Vicksburg methods in trafficability analyses of deep loose sands . . . . . pag. 837

Discussions: Z. JANOSI; D. R. FREITAG, E. S. RUSH . . . » 849

50 — E. T. VINCENT: Pressure distribution on and flow of sand past a rigid wheel . . . . . » 858

Discussion: Z. JANOSI . . . . . » 878

51 — J. REMUS: Etude de l'adhérence, en partant des moyen actuellement pratiqués pour tenter de l'améliorer . . . . . » 879

52 — H. VON SYBEL, F. GROSSE-SCHARMANN: Triebkraftsteigerung bei Geländefahrzeugen durch das Schub-Schritt-Verfahren . » 895

53 — A. ASSUR: Traffic over frozen or crusted surfaces . . . . » 913

ASPETTI DIDATTICI DEGLI STUDI DEL MOVIMENTO FUORI STRADA
EDUCATIONAL ASPECTS OF LAND LOCOMOTION STUDIES

54 — E. T. Vincent: Land locomotion in United States universities pag. 927

Discussions: L. Amici; A. R. Reece; J. R. Phillips; W. F. Buechele; E. Saibel . . . . . » 930

OSSERVAZIONI CONCLUSIVE GENERALI
SUMMATION AND CLOSING REMARKS

M. G. Bekker: *Where do we go from here?* . . . . . pag. 935

R. A. Weiss . . . . . » 944

Conclusione . . . . . » 947

PREFAZIONE

Questo volume contiene le memorie presentate al 1° Convegno Internazionale del Movimento fuori strada inaugurato a Torino il 12 giugno 1961, proseguito a Saint Vincent dal 13 al 15 e conclusosi nuovamente a Torino il 16. Sono pubblicati anche gli interventi nelle discussioni, alcuni dei quali assumono l'importanza di comunicazioni originali.

Il tema del congresso, più o meno chiaramente espresso nel conciso titolo italiano attribuitogli, riguardava principalmente il comportamento sui terreni più svariati che i veicoli possono incontrare nel movimento fuori dalle piste preparate per essi, e, viceversa, la proposta di mezzi più adatti per tale movimento.

L'importanza del tema riveste evidentemente vari settori, da quello militare, a quello agricolo ed a quello cantieristico per le opere costruzione di nuove strade o dighe, e per le ricerche di idrocarburi.

La materia trattata si è poi estesa naturalmente ad altri problemi della coppia veicolo-suolo.

Durante i lavori si sono pure avute proiezioni di film documentari e qualche dimostrazione pratica sul terreno.

Il convegno è stato organizzato dal Politecnico di Torino, che ne aveva ricevuto la proposta dal Servizio Tecnico dell'Ispettorato generale della motorizzazione militare italiana, e sotto il patrocinio dell'« U.S. Army Land Locomotion Research Laboratory (O.T.A.C.) ».

Il Politecnico ha una lunga tradizione negli insegnamenti relativi ai veicoli a motore, poichè da 30 anni funziona in esso un corso apposito post lauream, denominato dapprima « corso di perfezionamento nelle costruzioni automobilistiche » e poi « corso di specializzazione nella motorizzazione », s'intende, dei veicoli.

In questo corso, la cui fondazione è stata patrocinata dal compianto Gen. Angelo Pugnani e la direzione sempre tenuta dal Professor Giuseppe Pollone, hanno insegnato, oltre a docenti del Politecnico, i tecnici italiani più esperti nei diversi rami impegnati dal veicolo motorizzato: ricordo tra i civili gli ingegneri Gaudenzio Bono, ora amministratore delegato e direttore generale della FIAT; Antonio Fessia, ora direttore tecnico della Lancia; e Dante Giacosa, direttore

principale della Divisione Autoveicoli FIAT; tra i militari, il Gen. Amione, caduto in guerra, il Gen. Carrera e il Gen. Garbari, che del Comitato ordinatore di questo convegno ha accettato fattivamente la presidenza.

Il corso del Politecnico si è poi sviluppato secondo i crescenti bisogni dell'industria ed è attualmente articolato in tre sezioni rivolte rispettivamente agli automezzi militari, a quelli stradali ed a quelli dell'agricoltura. Da quest'anno poi, la specializzazione motoristica è offerta anche pre-laurea agli allievi ingegneri meccanici.

Un cenno agli organi che hanno preparato il convegno. Di promuovere la presentazione di memorie e vagliarne il merito, sono stati incaricati nei singoli Paesi, segretari nazionali che si meritano tutta la nostra riconoscenza. Un ringraziamento particolare spetta al Professor M. G. Bekker che ha messo a nostra disposizione l'alta sua competenza specifica sull'argomento del convegno.

Per l'organizzazione, dirò così, morale, è stato costituito un Comitato organizzatore nazionale, presieduto come già si è detto, dal Ten. Gen. S. T. e M. Ferruccio Garbari e composto dei Professori A. Castagna, E. Funaioli, D. Giacosa, G. Pollone, O. Sesini, L. Tocchetti e del Ten. Col. S. T. e M. Raffaele Tajani, quale Segretario generale.

Dell'organizzazione tecnica ed amministrativa in loco si è occupata una Giunta esecutiva composta del Rettore del Politecnico di Torino, Presidente, del Prof. G. Pollone, degli Ingegneri C. di San Germano e Franco Torazzi, e del Dott. F. Scalzotto, Segretario esecutivo.

A tutti i suoi collaboratori nella non lieve fatica, il Politecnico esprime vivi ringraziamenti. Essi si estendono agli Enti pubblici e privati che hanno contribuito alla riuscita dell'importante manifestazione tecnico-culturale, al Consiglio Nazionale delle Ricerche che ha contribuito al finanziamento per la pubblicazione degli « Atti » ed alla Casa Editrice Minerva Tecnica che se n'è assunta l'incarico, assolvendolo degnamente.

Torino, Luglio 1961.

ANTONIO CAPETTI
Rettore del Politecnico di Torino

PREFACE

This book contains all papers presented at the 1st International Conference on the Mechanics of Soil Vehicle Systems inaugurated in Turin on June 12th 1961 carried on at Saint Vincent from the 13th through the 15th and concluded in Turin again on June 16th. The discussions, some of which reach the importance of real papers, are also included.

The theme of the conference was mainly the behaviour on the most varied terrain that vehicles can meet, in off the road locomotion and viceversa the proposal of suitable devices for such locomotion.

The importance of this theme spread over different branches from the army, to agriculture, to road and dike building activities as well as to petroleum research.

The subjects dealt with spread over other soil and vehicle problems.

During the conference documentary films were shown as well as practical airplane and tracked vehicle demonstrations.

The conference has been organized by the « Politecnico » of Turin on proposal from the « Servizio Tecnico dell'Ispettorato generale della motorizzazione militare italiana », and under the sponsorship of « U.S. Army Land Locomotion Research Laboratory (O.T. A.C.) ».

The « Politecnico » has a long tradition in the teaching of motorization, through 30 years' experience in special « post-lauream » lectures called at first « course of specialization in motor cars construction » and later « course of specialization in motorization ».

This « Course » of the Politecnico has been developed according to the growing needs of industry and it now consists of three sections: military, road and agricultural vehicles. Since this year the specialization is offered also before the degree to students of mechanical engineering.

To this « Course », whose foundation was sponsored by Gen. Angelo Pugnani and whose direction was always held by Prof. Giuseppe Pollone, were appointed, besides the professors of the Politecnico, some of the Italian technicians more expert in the various

branches of vehicle motorization. Among the Civil engineers I remember Ing. Gaudenzio Bono, now Managing Director and General Manager of FIAT, Ing. Antonio Fessia, now technical manager of Lancia and Ing. Dante Giacosa chief manager of « Divisione Autoveicoli FIAT »; and among the Military engineers: Gen. Amione, Gen. Carrera, and Gen. Garbari that has accepted the chairmanship of the organizing Committee of this conference.

We would like to mention here all those who have contributed to the preparation of the conference. All our appreciation is deserved by the National Secretaries of the different Countries who have promoted the presentation of papers and selected them. Particular thanks are due to Prof. M. G. Bekker whose high special capacity concerning the subject has been at the disposal of the conference.

For the so to say moral organization a National Organizing Committee was formed, whose chairman as afore mentioned was Ten. Gen. S. T. e M. Ferruccio Garbari. Members were Prof. A. Castagna, Prof. E. Funaioli, Prof. D. Giacosa, Prof. G. Pollone, Prof. O. Sesini, Prof. L. Tocchetti and Ten. Col. S. T. e M. Raffaele Tajani, as General Secretary.

The technical and managing organization on the spot has been carried on by a General Arrangement Committee formed by the « Rettore » (President) of the Politecnico, chairman, by Prof. G. Pollone, Ing. C. di San Germano and Ing. Franco Torazzi, and Doct. F. Scalzotto, executive secretary.

The « Politecnico » wish to express their hearty thanks to all the collaborators in such not too easy organizing effort. Many thanks are due to the private and public companies that have contributed to the success of the important technical and cultural realization, to the « Consiglio Nazionale delle Ricerche » that have contributed to finance the publication of the Conference Proceedings and to the « Casa Editrice Minerva Tecnica » that worthily undertook it.

Turin, July 1961.

ANTONIO CAPETTI
Rettore del Politecnico di Torino

INTRODUZIONE

Eccellenze, gentili Signore, chiarissimi Professori, signori Congressisti,

La motorizzazione intesa quale sostituzione integrale del traino animale sulle strade si è ormai imposta da qualche decennio e incontrastata continua il suo sviluppo nel campo del trasporto delle persone e delle cose su qualsiasi striscia di terreno più o meno adattata o preparata che, per consistenza, livellamento della superficie e raggio di volta presenti le caratteristiche minime indispensabili per il passaggio sicuro di un veicolo.

Questa è la motorizzazione nel significato comune della parola e che si estrinseca negli innumerevoli tipi di autovetture e autocarri che oggi percorrono, sempre più numerosi e a velocità sempre crescenti, i vari tipi di strade. L'autoveicolo di oggi non è altro che il risultato del perfezionamento dei primitivi schemi architetturali che risalgono a una cinquantina di anni fa e le cui tappe sono segnate negli esemplari di veicoli che vedete raccolti in questo Museo dell'Automobile. Tali veicoli sono tutti caratterizzati, ancora oggi, dall'avere come organo propulsore la ruota motrice. Questo schema di veicolo, che potremmo definire a ruote portanti e motrici, rotolanti su una superficie praticamente piana ed indeformabile, ha oggi raggiunto un grado di rispondenza architetturale, costruttiva e tecnologica difficilmente suscettibile di ulteriore sensibile perfezionamento. Innumerevoli in questo settore sono le pubblicazioni tecniche che danno esaurienti e complete spiegazioni dei vari fenomeni, connessi al movimento del veicolo e al funzionamento dei vari organi che lo costituiscono e che nel contempo forniscono tutti gli elementi necessari per una rispondente progettazione del veicolo e dei suoi organi.

Non appena gli autoveicoli hanno cominciato ad imporsi quali mezzi per il trasporto di persone e di cose sulle strade — e siamo nel periodo susseguente la prima guerra mondiale — sono cominciati i primi tentativi, su scala abbastanza estesa, per sostituire sia nel campo agricolo che in quello militare la trazione animale con quella auto-

mobilistica. Nel ventennio tra la prima e la seconda guerra mondiale, assistiamo ad un fiorire di soluzioni e realizzazioni che riescono, dal 1930 in poi, a ridurre sensibilmente la presenza dell'animale da tiro nell'impiego agricolo e ad abolirlo totalmente in quello militare. Trattasi in genere di realizzazioni nelle quali l'organo propulsore rimane, come negli autoveicoli comuni, la ruota motrice, e che in sintesi sono caratterizzate da:

ruote tutte motrici di diametro relativamente grande, suscettibili di ricevere alla periferia organi di aderenza piuttosto pronunciati;

altezze minime da terra abbastanza elevate;

forti demoltiplicazioni nella trasmissione che realizzano elevati sforzi periferici alle ruote, tali da consentire il massimo sfruttamento dell'aderenza;

grande adattabilità alle asperità del terreno, ottenute in qualche caso mediante telaio snodato costituito da carrelli oscillanti attorno a un asse longitudinale e nella quasi totalità dei casi mediante opportuni tipi di sospensione;

trasmissione del moto alle ruote «differenziata», ma con possibilità di renderla rigida mediante bloccaggio dei differenziali;

raggi di volta alquanto ridotti, specie per i Paesi che, come l'Italia, sono caratterizzati da terreno impervio e da una viabilità come l'alpina e l'appenninica, molto tormentate altimetricamente e planimetricamente, con curve molto ristrette.

Il cingolo motore in sostituzione delle ruote motrici, fa la sua apparizione sui veicoli destinati al movimento fuori strada, prima ancora dei veicoli a ruote tutte motrici. Trattasi però di schemi architetturali di cingolatura che consentono velocità di traslazione dei veicoli molto basse, quali quelle raggiunte dalle primitive trattrici agricole industriali e dai primi carri armati apparsi sul teatro di guerra del lontano 1917. Il cingolo capace, per disegno e struttura, di rapidi spostamenti sia su strada che fuori strada fa la sua prima apparizione intorno al 1930; da allora è iniziata l'effettiva fase di sviluppo dei veicoli cingolati.

Nel ventennio tra la prima e la seconda guerra mondiale, si è sviluppata, come abbiamo accennato, quella branca della motorizzazione che potremmo definire motorizzazione per la marcia veloce su strada e fuori strada che alla fine dell'ultimo conflitto, è rappresentata in sintesi come segue:

veicoli a telaio rigido a quattro, a sei e a otto ruote, tutte motrici munite di pneumatici;

veicoli completamente cingolati;

veicoli semi-cingolati. Tali veicoli avevano tutti, in misura più o meno accentuata, la possibilità di movimento veloce su strada, unita ad una più o meno spiccata attitudine alla marcia veloce sulla quasi totalità dei tipi di terreno: da quello agricolo, sabbioso e fangoso, alle zone con forti pendenze e con rilevanti discontinuità superficiali.

A questa gamma di veicoli, costruiti in serie e per le esigenze più svariate, l'industria è giunta attraverso appropriati adattamenti e modifiche dei veicoli comuni adottando criteri suggeriti quasi esclusivamente dall'intuizione e perfezionati dall'esperienza. Possiamo anzi asserire che le soluzioni nuove e di avanguardia apparse in questo periodo, sono dovute in gran parte all'estro creativo dei singoli che hanno agito più per intuito che per raziocinio. E mi sia permesso a questo punto di aggiungere, per personale esperienza, che allo sviluppo della motorizzazione fuori strada hanno contribuito anche gli ardimentosi sperimentatori che hanno saputo portare il veicolo, divenuto per essi essere vivente come per altri il cavallo, al superamento degli ostacoli più impegnativi, facendo nascere fiducia nelle possibilità di impiego del mezzo fuori strada. Possiamo quindi asserire che, fino a una quindicina d'anni fa, le prime limitate conoscenze delle relazioni reciproche del complesso veicolo-suolo nel movimento fuori strada, erano prerogativa personale dei pochi sperimentatori e studiosi dello specifico problema.

A titolo puramente dimostrativo, desidero a questo punto accennare ad un episodio che risale all'ormai lontano 1941. Il Centro sperimentale della motorizzazione militare italiana aveva allora organizzato una dimostrazione pratica di movimento su un'ampia distesa di sabbia, in una zona litoranea vicino a Roma con 5 tipi di veicoli cingolati, aventi caratteristiche di peso, di potenza specifica e di architettura del cingolo completamente diverse. Alla dimostrazione prendevano parte, oltre alle Alte Autorità militari, i più competenti e sperimentati costruttori e progettisti d'Italia di veicoli fuori strada dell'epoca. Grande fu la sorpresa nel rilevare che il veicolo cingolato, dotato della maggior potenza specifica — circa 20 cavalli per tonnellata — si muoveva su quella particolare sabbia con una velocità intorno ai 15 km. all'ora, mentre un altro veicolo cingolato, avente

una potenza installata di poco più di 10 cavalli per tonnellata raggiungeva, su quella stessa sabbia, una velocità di circa 40 km. all'ora. Questa constatazione provocò, logicamente, l'inizio di una serie di indagini teoriche e sperimentali, aventi per obiettivo la ricerca degli elementi che influenzavano il movimento dei veicoli, sia a ruote, sia a cingolo sulla sabbia. Lo studio, condotto con criterio eminentemente pratico, consentì di dare una spiegazione, sia pure non del tutto rigorosa, del vasto e complesso problema delle reazioni tra organi propulsori e terreno, limitatamente a quello sabbioso. I risultati della indagine allora condotta, sono stati raccolti in due memorie pubblicate nel 1949 e 1950.

E' solo dopo il 1945 che tecnici e studiosi, di fronte alla multiforme varietà di veicoli fuori strada comparsi sui vari teatri della seconda guerra mondiale, incominciarono a dedicarsi all'esame sperimentale e scientifico di questo particolare problema, facilitati nel loro compito dal grande sviluppo quantitativo e qualitativo degli s[illegible] di misura in genere che consentono particolari applicazioni e p[illegible] rano rilievi molto esatti. Le prime rare memorie tecniche sull'a[illegible]mento incominciano ad apparire dopo il 1950 e si susseguono con una [illegible]erta frequenza, specie negli Stati Uniti d'America, dopo il 1955. [illegible] tal anno il Prof. Bekker dà alle stampe un testo sulla teoria del movimento fuori strada, nel quale, raccogliendo e sintetizzando con profondità di indagine quanto in precedenza è stato trattato sull'argomento, riunisce in un'opera di particolare valore i risultati ottenuti sulle indagini e le esperienze da lui stesso condotte, concretizzandole in una esauriente trattazione scientifica.

Il Prof. Bekker ha svolto la sua opera di direttore, di ricercatore e di studioso per molti anni nel Laboratorio di ricerche dell'esercito statunitense per il movimento fuori strada, Laboratorio molto interessante, razionalmente e bene attrezzato, al quale il Prof. Bekker accenna assieme ad altri laboratori del genere esistenti presso l'Università ed industrie degli Stati Uniti, nella sua recente pubblicazione «Il movimento fuori strada - ricerca e sviluppo nella meccanica del terreno».

La teoria della meccanica del movimento fuori strada degli autoveicoli convenzionali, quelli aventi cioè come organo propulsore la ruota motrice o il cingolo motore, è ancora nella sua prima fase di sviluppo, pur essendo già stata elevata a dignità universitaria, come materia di insegnamento, per vastità ed ampiezza di trattazione.

Questo I Convegno Internazionale del Movimento fuori Strada, al quale partecipano numerosi relatori provenienti da vari Paesi, americani, asiatici ed europei, assieme a molti tecnici, sta a dimostrare il particolare interesse che la motorizzazione fuori strada riveste per ogni Paese.

Potersi rendere infatti indipendenti dalle strade per raggiungere, rotolando sul terreno, qualsiasi località ed in qualsiasi condizione, rappresenta un'ulteriore ambita vittoria nel campo dei trasporti celeri terrestri. La conquista del fuori strada ha rappresentato in passato e rappresenta ancora oggi per i tecnici e per gli sperimentatori un ambito obiettivo che solo chi ne è stato attore può comprendere.

Le numerose memorie che saranno discusse nei quattro giorni di sedute tecniche del Convegno, porteranno certamente un reale contributo allo sviluppo della meccanica del movimento fuori strada, ma soprattutto ci auguriamo che da questa amichevole riunione di tecnici, studiosi ed appassionati di mezzi idonei alla marcia fuori strada, abbia inizio quello scambio fecondo e continuo di notizie e di idee che è condizione indispensabile per un rapido progresso, e che, nel contempo, sorga anche per questo particolare problema un entusiastico interesse, condizione essenziale per ben riuscire.

Tra gli argomenti che saranno discussi, non posso non rilevare con piacere che accanto a sistemi tradizionali, ruota motrice e cingolo motore, vi è qualche accenno a nuovi sistemi di locomozione. Il proiettarsi nel pratico con idee nuove è indice di progresso. La motorizzazione fuori strada di oggi si basa ancora sugli schemi architetturali tradizionali nei quali si stanno sempre più perfezionando gli organi propulsori — ruota gommata e cingolo motore — con l'obiettivo principe di diminuire la pressione specifica, favorire la galleggiabilità del veicolo su terreno cedevole ed aumentare l'aderenza.

Ed è appunto su questi elementi, ruota gommata, cingolo motore e loro aggruppamenti che si baseranno le discussioni di questi giorni che avranno per scopo di approfondire le relazioni fra questi organi di locomozione ed il terreno, per giungere a schemi architetturali di veicoli fuori strada che sfruttino la massima possibilità di movimento su qualsiasi terreno o che risultino più idonei ad operare in un determinato tipo di terreno. Questo non significa che in un domani più o meno lontano la tecnica non possa orientarsi in tutto o in parte verso altri sistemi di locomozione capaci di incrementare sensibil-

mente le prestazioni raggiungibili con gli schemi e con gli organi di locomozione attuali, che l'indagine e l'esperienza avranno perfezionato al massimo. Anzi la perfezione spinta al massimo degli organi propulsori attuali sarà certamente la base di partenza per eventuali future innovazioni.

Desidero ora, quale Presidente del Congresso, ringraziare l'On. Sotto-Segretario di Stato per la Difesa che rappresenta qui il Governo Italiano e le Alte Autorità che hanno voluto con la loro presenza rendere più solenne questa cerimonia; le Autorità dell'Esercito degli Stati Uniti d'America, che hanno, con il loro aiuto finanziario, consentito la realizzazione del Congresso; il Consiglio Nazionale delle Ricerche, che ci ha incoraggiato concedendoci il suo alto Patronato, e soprattutto il Politecnico di Torino, gloriosa fucina di tecnici italiani, che ha curato l'organizzazione del Convegno e quanti altri, con il loro contributo scientifico e con la loro presenza, hanno voluto rendere possibile questo I Convegno del Movimento fuori Strada, ed insisto nel dire Primo Convegno del Movimento fuori Strada, perchè sono certo che a questa iniziativa altre ne seguiranno, ora che per la prima volta i vari cultori di questa materia si trovano qui riuniti con i tecnici che realizzano veicoli idonei alla marcia fuori strada e con coloro che tali veicoli debbono impiegare. Non è senza significato che la seduta inaugurale di questo Convegno viene tenuta in un Museo che ci rammenta le glorie e le varie tappe del progresso della motorizzazione, in questa gloriosa città industriale dell'automobilismo italiano che, culla del Risorgimento, festeggia in questi giorni il Primo Centenario dell'Unità d'Italia.

Eccellenze, gentili signore, chiarissimi professori, signori congressisti; ho terminato la mia breve introduzione che ha solo voluto rammentare le tappe del progresso della motorizzazione fuori strada. Formulo di tutto cuore l'augurio che la piccola fiamma che oggi si accende possa essere il segnale di un rapido e continuo progresso in questo campo della tecnica.

FERRUCCIO GARBARI

Capo Servizio Tecnico della Motorizzazione
dell'Esercito Italiano

INTRODUCTION

Your Excellencies, Ladies and Gentlemen,

Motorization considered as entirely substituting animal traction on the road, has finally asserted itself in these last decades, and keeps on developing unhampered in the field of conveyance both of people and goods, on any strip of land more or less fit, or prepared, which for compactness, surface levelling, turning radius shows a minimum of indispensable features for the safe passage of a vehicle.

Such is motorization in its common meaning, which appears in the numberless types of motor cars, and lorries which crowd at an ever increasing speed the various types of roads. A motor vehicle nowadays is nothing but the result of the improvements on the early design practices, that reach back some fifty years ago, and whose stages are marked in the vehicle specimens shown in this Automobile Museum. Such vehicles are still characterized to this day, by their having as propelling organ, the driving wheel. This kind of vehicle which we may describe as carrying and driving wheel vehicles, rolling on a surface practically flat and undeformable, today has reached such a responsive architectural harmony, both constructive and technologic, that it is hardly apt to any remarkable further improvement. Numberless are in this domain the technical papers, giving thoroughly full explanations concerning the various phenomena, connected with the motion of the vehicle and the propelling of the various organs that make it up and meanwhile furnishing all the elements needed for a suitable design of the vehicle and of its organs.

No sooner did the motor vehicles prove satisfactory as means of conveyance for people and goods, on the road, after World War I, than the first attempts began on a rather extensive scale to substitute animal traction by motor traction both in the agricultural and military fields. In the twenty years between World War I and World War II the realizations multiply to such an extent that from the thirties on, animal traction has been remarkably reduced in the agricultural use and has disappeared altogether in the military field.

Generally in these realizations the propelling organ is the same as in the common motor vehicles, the driving wheel, and on the whole they are characterized by having:

— all driving wheels with a rather large diameter, apt to receive on their periphery quite conspicuous traction devices;

— rather high ground clearance;

— large reduction ratio in the power transmission in order to obtain high peripheral forces on the wheels such as to exploit at the utmost degree the available adherence;

— great adaptability to the roughness of the surface, obtained in some cases through the use of an articulated frame made up by subframes oscillating round a longitudinal axis and in almost every case through suitable types of suspension;

— power transmission to the driving wheels through differential gears with the possibility of the blockage of the differential itself.

The turning radius has been rather reduced, especially for such countries as Italy where the ground is impervious and the roads through the Alps and Apennines are altimetrically and planimetrically intricate with very narrow turns and bends.

The driving track system introduced to substitute the driving wheels first appears on the vehicles meant for off-the-road locomotion earlier than all-driving-wheels vehicles. However the design of these tracks is such as to allow very low speed and transport rates like those of the early agricultural and industrial tractors, and of the first armoured vehicles that appeared on World War I battle fields, far back in 1917. The tracked vehicle system capable of fast movements on account of its design and structure either on or off-the-road, first appeared about 1930.

Ever since an effective development of tracklaying vehicles has been carried on. In the twenty years' period between World War I and World War II, as above mentioned the branch of motorization, we may describe as fast locomotion on and off-the-road has been developed until at the end of the last war, it is represented on the whole as follows: four, six and eight wheel, rigid frame vehicles, furnished with tyres, and wholly tracked or half-tracked vehicles. Such vehicles had, more or less, the possibility of fast movement on the road, as well as a more or less pronounced aptness to speedy driving on almost every type of ground from agricultural soil sandy and muddy, to steepy areas and remarkable surface discontinuity.

Industry has reached such scale of standard vehicles for the most varied purposes, through the proper modification of common vehicles, adopting criteria suggested almost exclusively by intuition and improved through experience. We may even state that the new, pioneering solutions reached during this period are due mostly to the genial individual intuitions rather than to rational results. Let me add, through personal experience, that the development of off-the-road locomotion is not for the lesser part due to the daring experts who have brought the vehicle as a living being to them, like horses to others, to overcome the most engaging obstacles, rousing confidence in the possible use of off-the-road means of conveyance. Thus we may state that up to about fifteen years ago, the first limited notions as regards the mutual relations of the vehicle-soil system in the off-the-road traffic were the personal privilege of the few experts on that special problem.

As a mere demonstration I wish to point out an episode reaching far back in 1941. The experimental Centre of Italian miiitary motorization, had then organized a practical demonstration of locomotion on a wide stretch of sand, in a coast-line area near Rome, with 5 types of tracked vehicles, having altogether different features in weight, specific power and track design. The demonstration was attended by the High Military Authorities, and besides, by the most competent and expert Italian road vehicle builders and designers at the time. A great surprise was roused by the fact that the tracklayer, having the highest specific power — nearly 20 H.P. per ton — moved on that sand at a speed of about 15 km per hour, whereas another tracklayer having an installed power of hardly over 10 H.P. per ton, reached on the same sand a speed of nearly 40 km per hour. Logically this consideration brought about a series of theoretical and experimental investigation, with the purpose to find out the elements affecting the movement of the vehicles, either wheeled or tracked on the sand. The observation conducted on essentially practical criteria, allowed an explanation, though not strictly rigorous, of the far reaching complex problem of reaction between propelling organs and ground, limited to sandy soil. The results of the research were published in two papers in 1949 - 1950. It is only since 1945 that technicians and research experts confronted with the multiple variety of off-the-road vehicles that appeared everywhere during World War II, devoted themselves to the experimental and scientific study of this particular problem. They found greater facilities

in this task through the great development, both in quantity and quality, of the measuring instruments altogether, allowing particular applications and very exact findings. The earliest rare technical papers on the subject began to appear since 1950, rather frequently, especially in U.S.A. since 1955. In that year Prof. Bekker published a text on the off-the-road locomotion, in which gathering what had been said on the subject and digging deep into it, he collects in a specially valuable work, the results of his own researches and experiences and thoroughly deals with the matter scientifically.

Prof. Bekker has been Director, researcher, and a scientist for several years at Land Locomotion Laboratory, O.T.A.C. This Laboratory is very interesting, rationally equipped, and Prof. Bekker mentions it as well as others attached to Universities and Industries in U.S.A. in his recent publication: «Off-the-road locomotion - Research and development in soil mechanics».

The theory of off-the-road locomotion for conventional motor vehicle: those having as propelling organ the driving wheel and the driving track, is still in its early stage of development, though already raised to university dignity as a curriculum subject, for its wide and ample range. This first International Conference on the Mechanics of Soil-Vehicle Systems attended by quite a number of speakers from different countries, Americans, Asiatics, Europeans as well as technicians, proves the special interest roused in every country by the off-the-road motorization. In fact the possibility of reaching anywhere and everywhere indipendently from the road, represents further victory looked forward to in the field of fast land transport. Only who has been actively engaged in this conquest can fully appreciate it. The number of papers which are going to be discussed during the four days' technical meetings of the Conference will certainly contribute to the development of the mechanics of the off-the-road locomotion. But above all we trust that from such friendly meeting of technicians, scientists and keen supporters of devices fit for off-the-road locomotion, an exchange of mutual information may rise, as an indispensable condition to fast progress, as well as a keen interest essential to success.

Among the subject that are going to be dealt with I am pleased to remark that besides the traditional systems, there is a hint to new locomotion systems. New ideas in the way of traffic are a sign of progress. Off-the-road motorization, to day, is still based on traditional

architectural prospects, in which the propelling organs are ever improving, the tyred wheel and the driving track, with the main purpose of diminishing the specific pressure, facilitate the floating of the vehicle in soft ground and increase the adherence. In fact it is on such elements: tyred wheel, driving track and their grouping that will be the base of our discussions during the present meeting. Our purpose is to dig deep into the relations between the locomotion organs and the ground in order to reach design criteria for off-the-road vehicles affording to the utmost the conveyance on any kind of ground whatever and proving fitter to operate on specific kinds of soil. This does not exclude that in the near future technics may find a new trend of locomotion to enlarge the scope of activity.

However the starting point for further improvement will be the present prospects and locomotion organs, brought to a climax of perfection through research and experience.

In the quality of President of the Congress, I wish to thank the Honourable Secretary of State for the Defence, who represents the Italian Government and the Authorities that honour the present ceremony with their attendance, the Authorities of the United States Army that have financially supported the realization of this Congress; the National Council of Researches that has encouraged us by granting us its high Patronage, and above all the «Politecnico» of Turin a glorious maker of Italian technicians that has organized the Conference, and all those, as well those who have scientifically contributed or personally attend, this First Conference on the Mechanics of Soil Vehicle Systems and I insist on calling it the First Conference, as I feel sure that it will be followed by others after this meeting of all who are interested in the subject. There is a meaning in the fact that the opening Session of this Conference takes place in a Museum reminding us of the glories and the stages of motorization, in this City where Italian Motoring rose, this glorious cradle of Italian «Risorgimento» celebrating the first Centenary of the Unity of Italy.

Your Excellencies, Ladies and Gentlemen in closing this brief introduction to the Conference, I express the wish that the spark we light to day may lead the way to an ever increasing progress in this technical field.

FERRUCCIO GARBARI

Capo Servizio Tecnico della Motorizzazione
dell'Esercito Italiano

MOBILITA' DEL VEICOLO
E TEORIE SULLA PLASTICITA'

VEHICLE MOBILITY
AND THEORIES OF PLASTICITY

On stress-strain relations for soils and load carrying capacity *)

Relazione tra sollecitazioni e deformazioni del suolo e la capacità di carico

D. C. Drucker **)

ABSTRACT. -- *Although the art of soil engineering is old and in many respects well established, the science of soil mechanics is relatively recent. The word mechanics implies a mathematical formulation of the problem and of the basic equations to be used in its solution. In «soil» mechanics the essential set of equations clearly should be the relations between stress and strain in soils. Except for elastic and simple visco-elastic behavior, no such equations are now in actual use. It is the purpose of this paper to explore the stress-strain relations for plastic and frictional soil along with the associated means of determination of loads which will cause failure of a soil mass. Needed directions of study are indicated.*

Introduction

Soil mechanics, as the term implies, is a branch of mechanics of solids. A valid solution to a problem of the response of a soil mass to applied load must satisfy the boundary conditions on force and displacement, the equations of equilibrium or of motion, and the equations of compatibility. The key to obtaining valid solutions, therefore, is the establishment of the relation between force or stress quantities and compatible or geometric quantities. Without such basic knowledge of the stress-strain relations or their equivalent, a so-called solution is merely a guess.

Partly for simplicity in practice and partly because of the historical development of mechanics of solids, problems in soil mechanics are treated in several separate and unrelated ways. When no failure of the soil is involved, stresses at points in a soil mass under a footing, or behind a retaining wall, or under a moving vehicle [1,2 ***], are computed using linear elasticity. Problems of bearing capacity, stability of slopes, failure of retaining walls, land locomotion over weak terrain [3,4] now are considered in the realm of plasticity.

*) This paper reports work sponsored by the Land Locomotion Research Branch, Ordnance Tank-Automotive Command, Detroit Arsenal, under Contract DA-19-020-ORD-4566. Several of the topics discussed here were covered earlier in an unpublished Brown University Report DA-3763/1, March 1956.

**) Professor of Engineering, Brown University, Providence, Rhode Island.

***) Superscript numbers refer to the references at the end of the paper.

Settlement and consolidation problems, on the other hand, are treated as essentially visco-elastic.

The primary concern of this paper are those soil mechanics problems accepted in accordance with the usual terminology of the field as lying within the realm of plasticity. If texts and papers are consulted, a most surprising fact emerges. The description of stress-strain relations is restricted to the most elementary aspects of the simplest types of tests. No general relations have been written down and the need for them is almost never mentioned. This is in sharp distinction to the treatment of soil as an elastic or as a visco-elastic body where the basic equations not only are listed but actually are used. There is, of course, a reason for this omission of a detailed discussion of the relation between stress and strain. When soils with both cohesion and friction angle are studied, it is by no means clear what the fundamental relations are and much less how a solution could be obtained with them. Nevertheless it must be repeated here that without this fundamental knowledge or an appropriate idealization of soil behavior there can be no real solutions.

Henkel in his thesis [5] summarizing years of very careful triaxial experimentation on clay has established a most interesting set of results which will serve as reference for much of the discussion which follows. He finds that the maximum consolidation pressure is the controlling state variable for the behavior of over-consolidated clay. There is a remarkable degree of path independence. A common failure envelope is found for both drained and undrained tests. Henkel also demonstrates that for normally consolidated samples there is very closely a unique relation between the effective stresses and the water content. So well correlated a pattern of behavior indicates strongly that stress-strain relations of moderate complexity only must exist.

The mathematical theory of plasticity

The difficulties encountered in obtaining stress-strain relations for soils become clearer after a brief discussion, in pictorial and qualitative terms, of the basic features of the mathematical theory of plasticity. By definition, time and viscosity effects are absent. All significant features of the relation between stress and strain then are derived from the concept of a yield or loading surface and the postulate that in a cycle work cannot be extracted from the material and the system of forces acting upon it [4].

Two of the direct consequences of the postulate are: a) any yield or loading curve or surface must be convex and b) if axes of plastic strain are superposed on the axes of stress, the vector representing the increment of plastic strain is normal to the loading surface at the point representing the existing state of stress, or lies between adjacent normals at a corner, fig. 1. At a smooth point, therefore, the ratios of the components of the plastic strain increment are uniquely determined by the shape of the loading surface. At the stress point B or any point along the straight line AB of fig. 1, the ratio of the plastic extension rate to the plastic shear rate is constant at tan φ. If a zero

tension cut-off circle OD governs yielding, the ratio of plastic extension to plastic shear increases from D to O where it becomes infinite.

The assumption of perfect plasticity is the simplest and strongest idealization. Any « inside » path such as EB involves elastic or reversible behavior only, but at point B or any stress point on the single fixed yield surface

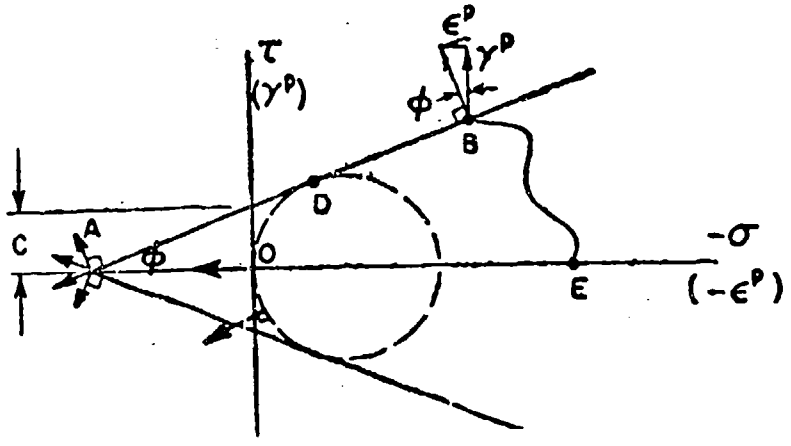


Fig. 1. — Plastic strain increment is normal to yield surface. If the material is unable to take tension, the upper half of the yield curve is ODB.

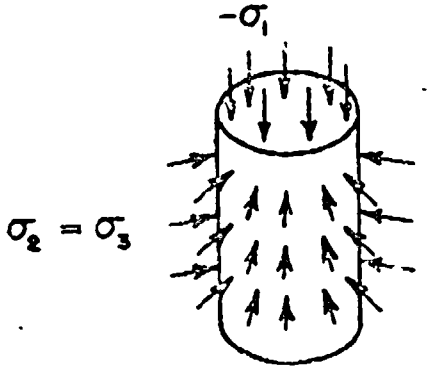


Fig. 2. — Triaxial test $\sigma_2 = \sigma_3$.

or curve there is no limit to the plastic deformation. A work-hardening material, on the other hand, is ready to deform plastically at a yield stress but requires an « increase » in stress to deform it. Consider, for example, the triaxial type of test with $\sigma_2 = \sigma_3$, fig. 2. Initial and subsequent surfaces which could be established by a path of loading are shown schematically in fig. 3. It is desirable and convenient to use σ_1 and $\sigma_2 \sqrt{2}$ as coordinates for plotting the yield and subsequent loading surfaces. In geometric terms this is a p re of the intersection of the surfaces in principal stress space by the plane $\sigma = \sigma_3$.

There is no reason to suppose that different loading paths will establish

the same loading surfaces although this assumption is made in the simplest of work-hardening theories of plasticity, the isotropic stress-hardening theories. In any case, the direction of the normal and, therefore, the ratio of the plastic strain increments generally will vary along the path of loading.

Soil as a plastic body

A perfectly plastic soil with constant friction angle φ may be postulated in an attempt to obtain a first approximation to the behavior of a real soil [7]. Some predictions of this enormous idealization are remarkably good. When, for instance, the inability of a soil to take appreciable tension is taken into

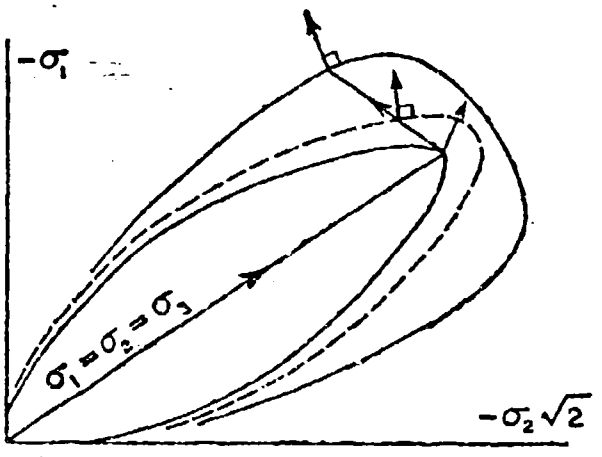


Fig. 3. — Loading surfaces are established by the path of loading.

account (cut-off circle of fig. 1), the computed critical height [8] of a free standing vertical bank is $H_c = \frac{2c}{\gamma} \tan\left(\frac{\pi}{4} + \frac{\varphi}{2}\right)$ in the usual notation. Also, in plane strain rigid body sliding, the lines of failure are either straight lines or logarithmic spirals [7]. Unfortunately, however, the dilatations which are predicted to accompany the shearing action are enormously in excess of those observed, a point emphasized by Brinch Hansen [4].

The concept of a soil as a work-hardening material was introduced [9] to obtain closer correlation between idealization and reality. This previously reported qualitative agreement of experimental data from fully drained triaxial tests on a silty clay with a predicted increase, decrease, or no change in volume was highly gratifying. Fig. 4 shows a plot of the plastic strain increment vectors of these tests in which the clay was pre-consolidated to B, then unloaded hydrostatically to C or D or E and finally subjected to increasing axial stress to failure at the line B″E″. Vectors normal to OB, the axis of symmetry in principal stress space, indicate zero plastic volume change, vectors inclined

to the right of this normal indicate volume decrease, those to the left indicate volume increase. The dashed line is the apparent yield surface established by the common pre-consolidation pressure. Except for point D', the normality condition is met very well. The volume change is seen to approach zero as the failure line is reached.

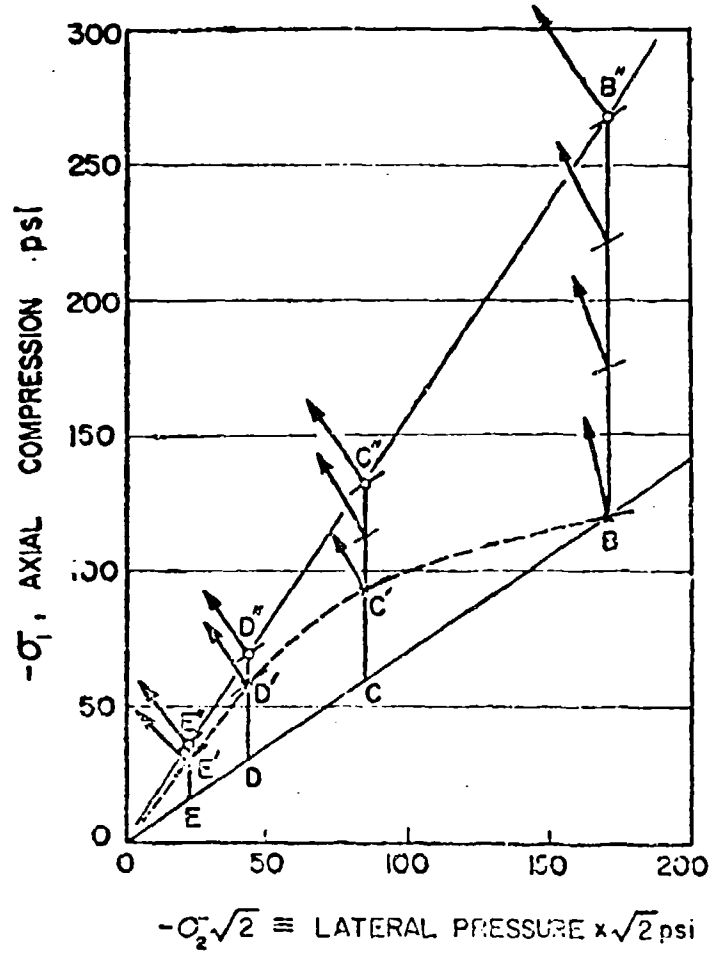


Fig. 4. — Drained triaxial compression test on a remolded silty clay[9]. Maximum or pre-consolidation pressure 120 psi. × indicates yield point; ○ maximum σ_1.

It is clear that no convex yield curve can be drawn which is normal to the plastic strain increment vectors beyond the initial yield curve. As mentioned previously, there is no reason to suppose that the yield surface established by loading from C' should be the same as that obtained from any other point such as D or E. Shield and Drucker[10] suggest the possibility of an intrinsic corner at failure and abrupt changes in the position of a pyramidal yield surface.

However, Henkel's data on both drained and undrained samples demonstrates quite conclusively that the preconsolidation pressure and the existing state of stress do determine the state of the soil. This contradiction with existing forms of plasticity theory cannot be passed off lightly.

Another indication that conventional plasticity theory does not apply fully to soils is that stress-strain curves for soil generally reach a maximum and then drop off. This is not in accord with the fundamental postulate and, if the discrepancy is very marked, the ordinary theory of plasticity cannot provide a suitable description of the behavior of soil.

Too much should not be expected of any idealization, no matter how elaborate, of a complicated heterogenous substance like soil. For many purposes the very rough agreement in general characteristics of a work-hardening

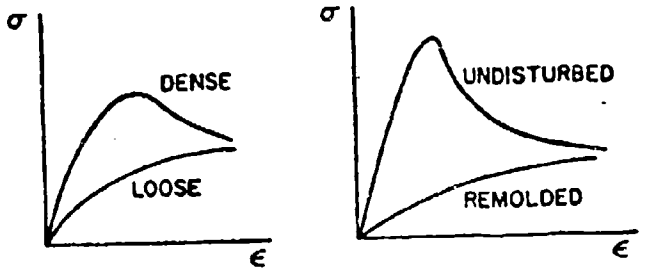


Fig. 5. — Curves with marked peaks do not fit within conventional plasticity.

material and actual soil will be adequate and for some the perfectly plastic assumption is sufficiently good. A distinction must be drawn between dense and loose sands and between overconsolidated clay in situ and remolded clay. The loose sand and the remolded clay behave more in accordance with conventional plastic stress-strain relations, the dense sand and the undisturbed clay peak very markedly, fig. 5.

There is, of course, no reason to restrict thinking to the type of plasticity theory which is suitable for metals. Points on the yield curve of fig. 4 represent states of stress with different water content. The curve of constant water content makes an appreciable angle with this yield curve. The water content of a clay is a highly significant variable and should somehow be included in the development of an appropriate theory. Stored and dissipated energy certainly are functions of water content. It would seem likely that a far more complicated normality condition would have to be found. No such theoretical development has yet been attempted but it would seem to offer real promise.

Soil as a body with friction

Soils are described as having both cohesion c and internal friction, φ, fig. 1. If they are truly frictional in behavior they are not plastic, or rather to the extent that they are frictional they are not plastic and viceversa.

This holds as well for assemblages of metals where the frictional action may in fact be plastic shearing on a microscopic scale. The converse situation may exist also. It is conceivable that frictional behavior on a very small scale may be equivalent in a very complicated material to plastic action on a gross scale. It is the macroscopic stress-strain relations which are of interest, not the microscopic.

The important difference between Coulomb friction and what might be termed *perfectly-plastic Coulomb action* is illustrated by a block sliding on or shearing a horizontal plane, fig. 6. In both cases the horizontal or tangential force is proportional to the vertical or normal force. However, frictional sliding is horizontal, while perfectly-plastic shearing involves large upward vertical (dilatational) motion as well. Work-hardening plastic action (as discussed previously, fig. 4) may lead to upward or downward vertical motion or neither.

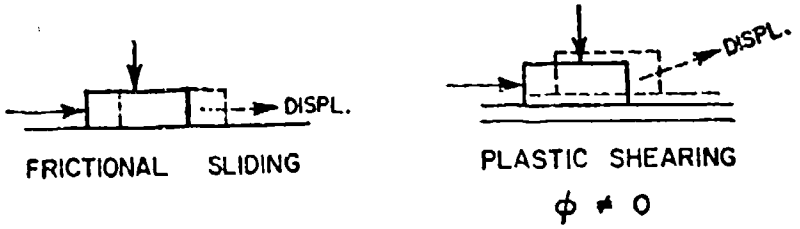


Fig. 6. — Dilatation accompanies *perfectly*-plastic shearing.

Failure of a soil mass under any type of loading

The details of the distribution of stress and strain in a mass of inelastic soil under arbitrary loading are obviously far beyond present understanding. A lesser goal but an even more useful one is the determination of loads which will cause failure of the mass. The weight of vehicle which can be supported, the maximum slope at which a given soil will stand, and the stability of a retaining wall are problems in this category.

If soil were perfectly plastic with a Coulomb or any other yield surface, there would be no difficulty, in principle, in computing load carrying capacities. With a moderate amount of work, the theorems of limit analysis [1] will give reasonably close bounds on the answer. The theorems are:

1) (lower bound) if an equilibrium distribution of stress can be found which balances the applied load and is everywhere below yield or at yield the soil mass will not fail or will be just at the point of failure;

2) (upper bound) the soil mass will fail if there is any compatible pattern of plastic deformation for which the rate at which the external forces do work exceeds the internal dissipation.

Theorem 1 states that a perfectly plastic soil will adjust itself to carry

the load if there is a possible way. Theorem 2 states that if a path of failure exists, the soil will fail.

If soil were work-hardening to an unlimited extent there would be no difficulty because there could be no failure. This ideal situation is irrelevant.

If soil were work-hardening with an open limiting stress surface, such as the Coulomb condition as found by Henkel [5] and illustrated in fig. 1 and 4, there would be grave difficulties in analysis. The plastic strain increment vector is normal to the loading surface but it is not normal to the limiting surface. Although this is a somewhat esoteric point it is by no means a trivial one. The proof of the limit theorems is intimately related to the fundamental postulate on which normality too is based. The upper bound theorem 2 is not even meaningful because the deformation pattern does not determine the dissipation uniquely. The sum of the principal stresses must be known.

If soil were frictional, precisely the same difficulty would arise. The normal stress on the plane of sliding governs the dissipation. Furthermore, it has been shown [12] that the lower bound theorem 1 does not hold for frictional systems. Frictional systems do not necessarily do the best they can to resist load.

There is a strong temptation to ignore all these considerations and to solve particular problems by special techniques. All too often, however, the technique will be found to have hidden in it the basic philosophy underlying one or both of the limit theorems. If so, and if the perfectly plastic idealization is not appropriate for the soil, the answer obtained will be without significance. Proper theorems which provide useful answers must be developed.

The following upper bound theorem would seem to provide a reasonable design or analysis procedure for a frictional soil. It does not have universal validity because it states that failure will occur if at all possible [13]. However, for a soil this concept may not be too conservative.

Failure should be assumed to occur if for a pattern of deformation the work done by the applied forces exceeds the allowable dissipation. The allowable dissipation is to be computed from any equilibrium distribution of normal stresses on the assumed surfaces of sliding.

The Swedish circle method then would be classed as giving an upper bound. That this is the general feeling is evidenced by a number of attempts to obtain a convenient lower answer.

The same theorem would seem reasonable for a work-hardening soil with the allowable dissipation computed from any equilibrium distribution of stress and the assumed deformation pattern. As for the frictional case, the word equilibrium includes both internal and surface traction conditions.

Concluding remarks

Intensive effort is required in both laboratory and field studies to determine the basic nature of the stress-strain relations for soil. A much clearer distinction can be made in the laboratory between plastic and frictional action if the path of loading is more completely under control. A true triaxial apparatus

is required, one in which all three principal stresses may be varied independently. Following earlier work of Hvorslev on the ring shear apparatus[13] and of Malishev[14] on the more general triaxial, a combined triaxial and ring shear apparatus was constructed by Haythornthwaite while at Brown University. Results obtained[15] seem to confirm the existence of a limiting stress surface but one which may well be quite anisotropic. Unfortunately, little light has yet been shed on the question of plastic vs. frictional behavior.

The main point to keep in mind is that satisfactory answers cannot be computed for the simplest problems of load carrying capacity until the stress-strain behavior of each of the various classes of soil is clarified and the appropriate extensions of the limit theorems have been developed. Until that happy day the engineer must continue to rely almost exclusively upon full scale and model experiments.

BIBLIOGRAPHY

1) Terzaghi K. Theoretical soil mechanics. John Wiley and Sons, New York, 1943.

2) Bekker M. G. Theory of land locomotion. University of Michigan Press, Ann Arbor, 1956.

3) Meyerhof G. G. The ultimate bearing capacity of foundations. Geotechnique, vol. 2, pag. 301-332, 1951.

4) Brinch Hansen J. Earth pressure calculations. Danish Technical Press, 1953.

5) Henkel D. J. The correlation between deformation, pore water pressure and strength characteristics of saturated clays. Ph. D. Thesis, University of London (Imperial College of Science and Technology), April 1958.

6) Drucker D. C. A more fundamental approach to stress-strain relations. Proceedings First U.S. National Congress for Applied Mechanics, A.S.M.E., pag. 487-491, 1951.

7) Drucker D. C. and Prager W. Soil mechanics and plastic analysis or limit design. Quarterly of Applied Mathematics, vol. 10, pag. 157-165, 1952.
Shield R. T. On Coulomb's law of failure in soils. Journal of the Mechanics and Physics of Solids, vol. 4, pag. 10-16, 1955.

8) Drucker D. C. Limit analysis of two and three dimensional soil mechanics problems. Journal of the Mechanics and Physics of Solids, vol. 1, pag. 217-226, 1953.

9) Drucker D. C., Gibson R. E. and Henkel D. J. Soil mechanics and work-hardening theories of plasticity. Proceedings A.S.C.E., vol. 81, 1955. Separate 798, Transactions A.S.C.E., vol. 122, pag. 338-346, 1957.

10) Jenike A. W. and Shield R. T. On the plastic flow of Coulomb solids beyond original failure. Journal of Applied Mechanics, vol. 26, pag. 599-602, 1959.

11) Drucker D. C., Prager W. and Greenberg H. J. Extended limit design theorems for continuous media. Quarterly of Applied Mathematics, vol. 9, pag. 381-389, January 1952.

12) Drucker D. C. Coulomb friction, plasticity and limit loads. Journal of Applied Mechanics, vol. 21, pag. 71-74, 1954.

13) Hvorslev M. J. and Kaufman R. I. Torsion shear apparatus and testing procedures. Bulletin 38, Waterways Experiment Station, U. S. Army, Vicksburg, Mississippi, 1952.

14) Malishev M. V. On the evaluation of the angle of internal friction and cohesion of a loose medium in the limit state of stress (in Russian). Izv. Akad. Nauk USSR Otd. Teckh. Nauk n. 7, pag. 122-132, July 1954.

15) Haythornthwaite R. M. Stress and strain in soils. Proceedings 2nd Naval Structural Mechanics (Brown University). Pergamon Press, pag. 185-193, 1960.

DISCUSSIONS

E. LEFLAIVE. — Je veux seulement signaler que, dans le cas du sol, une déformation irréversible engendre vraisemblablement une anisotropie et que l'introduction de ce facteur sera probablement nécessaire pour figurer aussi complètement que possible le comportement de ce type de matériaux. Des recherches sur ce point sont en cours à l'Université de Grenoble.

M. JUUL HVORSLEV. — Theoretical soil mechanics as applied to civil engineering and mobility problems involves many simplifying assumptions. The reliability of the practical methods of approximation is usually determined by comparison of the predicted and actual behavior of prototype structures. However, it should be realized that agreement between the predicted and actual behavior in many cases may be caused by compensating errors in the individual steps or operations, such as sampling, testing, and analysis. Therefore, great care should be exercised in generalization of the results obtained by the practical methods and in drawing conclusions with respect to the correctness of the individual operations. The reliability of the practical methods should be investigated whenever new problems or field conditions are encountered.

A more rigorous theoretical analysis of the problems is desirable as a guidance for research and for determination of the limits of reliability of the practical methods. As a first step it is logical to utilize the classical theories of elasticity, plasticity, and visco-elasticity as developed for idealized bodies. However, there are in many cases considerable differences between the properties of soils and those of the idealized bodies. The e differences may have only a minor influence on the solution of some problems but may cause misleading results in other cases. It is desirable that the influence of differences in properties of idealized bodies be estimated and discussed and that the classical theories be modified in such a manner that the special properties of soils are taken into consideration. When papers presenting solutions of soil mechanics problems by means of the classical theories are published in journals for applied mathematics, explanations of notations, special terminology, and underlying assumptions are usually omitted for the sake of brevity. However, the inclusion of such information in papers written for practical engineering journals and conferences would greatly increase the usefulness of and attention given to such papers.

Some of the voids mentioned in the foregoing paragraph are filled in the excellent paper by Professor Drucker, who clearly explains the assumptions and theorems which form the basis for the theory of plasticity and their relation to the actual properties of soils. He recognizes the need of modifications of the classical theories in conformity with the special properties of soils, and it is encouraging to learn that such theoretical developments do not present serious difficulties but seem to be a promising undertaking.

The writer would like to make some supplementary comments on current knowledge and needed research concerning deformation and strength properties of saturated fine-grained soils.

It has been known for many years that shearing stresses and strains tend to produce a volume decrease of normally consolidated and lightly overconsolidated clays (Casagrande, 1932) and a volume increase of strongly overconsolidated clays (Hvorslev,

1936 and 1937). These findings have not always been accepted because some of the early tests involved concurrent changes in both the mean normal stress and the deviatoric stresses. However, these findings have been confirmed in recent tests by Henkel (1958, 1960) and others during which the mean normal stress was held constant and only the deviatoric stresses were changed.

Current knowledge of the volume change characteristics of soils is limited to those occurring during direct and torsion shear tests, confined consolidation tests, and triaxial tests. Only the latter are suitable for fundamental research on the problem, since the value of the radial or lateral stresses in other tests cannot be determined or estimated with sufficient accuracy. Mathematical expressions have been developed for the relations between void ratio and all-round or hydrostatic pressure. Data on volume changes during other axially symmetrical stress conditions are available in form of the constant void ratio contours developed by Rendulic (1936, 1937) and extended by Henkel (1958, 1959). The first task would be to develop mathematical expressions for these contours. The ultimate object should be to obtain experimental data and develop mathematical expression for the volume change caused by an arbitrary change of any principal stress. Kjellman (1936) constructed triaxial equipment and performed a limited number of tests in which independent variation of any one of the three principal stresses was permitted. Further development of this type of equipment is needed but difficult, as stated by Professor Drucker.

Additional investigations of the influence of the rate of load application and of structural and thixotropic disturbances caused by distortional strains are needed also. A test specimen which has been consolidated under a given all-round pressure, then remolded and subjected to the same all-round pressure will undergo an additional volume change. Similarly, it is possible that distortional strains during a triaxial strength test may cause thixotropic changes which, in turn, enable additional volume changes to take place under a constant mean stress. The question then arises whether these volume changes, in energy equations, should be attributed to the mean stress and only indirectly to the deviatoric stresses. According to recent investigations by Mitchell (1960) and Bishop-Alpan-Blight-Donald (1960), thixotropic changes in deformation and strength characteristics of clays are manifested and explained by changes in pore water pressure and effective stresses.

Fairly rapid or transient load applications, such as those occurring in mobility and trafficability problems, cause only negligible volume changes of saturated clays. Under such conditions it is often convenient to operate with total stresses, but a full understanding of variations in strength and bearing capacity requires consideration of the influence of changes in pore water pressures and the Terzaghi concept that strength and deformation characteristics of soils primarily are governed by the effective stresses; that is, the difference between the total stresses and the pore water pressures.

As indicated by Professor Drucker, it has long been known that the strength of saturated and normally consolidated clays can be expressed as a simple exponential function of the void ratio or water content. However, more recent investigations by Taylor (1951, 1955), Henkel (1958, 1960), and others show that the strength is not defined by the void ratio alone but is also a function of the relative value of the intermediate principal stress at failure. For constant void ratio, the strength obtained in triaxial compression tests, $\sigma_1 > \sigma_2 = \sigma_3$, is considerably greater than that obtained by triaxial extension tests, $\sigma_1 = \sigma_2 > \sigma_3$. These differences in strength are partially explained by differences in pore water pressures and effective stresses under the various test conditions.

The constant-volume strength of overconsolidated clays may also be expressed as a function of the void ratio, but the function is more complicated than for normally consolidated clays, since the strength of overconsolidated clays also depends upon the stress history of the soil. As discussed later, these relations may be simpler for surface soils which have been subjected to many cycles of drying and swelling.

Stress-strain curves for undisturbed clays subjected to fairly rapid or transient loading generally exhibit a peak value followed by a gradual decrease in strength to that of a completely remolded clay. The latter strength is of great importance in trafficability and mobility problems. According to the concepts advanced by Roscoe-Schofield-Wroth (1958), the stress-void ratio relations of normally consolidated and overconsolidated clays approach at great strains a common «critical void ratio» line. Therefore, it is probable that the strength-void ratio relations for overconsolidated clays immediately after remolding approach the simple form of these relations for normally consolidated clays.

Stress-strain curves for clays, determined immediately after remolding, do not exhibit a peak value but approach in form the simple curves which form the basis for the classical theory of plasticity. However, most remolded clays undergo a thixotropic regain in strength with increasing time. This regain in strength is approximately proportional to the logarithm of the time elapsed after remolding. Stress-strain curves for a remolded clay, obtained after a thixotropic regain in strength, usually have a peak value, although this peak may not be as pronounced as that for the same clay in undisturbed condition.

The influence of a possible thixotropic regain in strength should be considered in the performance and evaluation of trafficability and mobility tests. It is probable that the possible number of passes of a vehicle over a given clay deposit may be increased by increasing the elapsed time between the individual passages of vehicles. However, the influence of a thixotropic regain in strength, obtained by stopping a single vehicle for an appreciable length of time, may be offset by an increase in sinkage and a corresponding increase in rolling resistance, as demonstrated in the paper by Schiffman (1961).

The mineral and organic constituents, water content, permeability, and capillarity of surface soils have been investigated in detail by soil physicists and agronomists. It is desirable that the deformation and strength characteristics of surface soils also be subjected to systematic research, since these soils are of primary interest in trafficability and mobility problems. The surface soils have been subjected to innumerable cycles of wetting and drying, which may cause the swelling and reconsolidation curves to approach each other and tend to establish simpler relations between void ratio and strength than those obtaining for overconsolidated soils from deeper strata. A higher content of organic matter in surface soils may also produce more pronounced thixotropic and visco-elastic properties.

It is apparent that considerable theoretical and experimental research is needed in order to gain a better understanding of the deformation and strength characteristics of soils and the application of this knowledge to practical problems. Close cooperation between theoreticians and experimentalists is needed in the planning and performance of this research. The former should recognize the need, as done by Professor Drucker, of taking the special properties of soils into consideration, and the latter should plan and perform their experiments in such a manner that the data needed by the theoreticians can be obtained directly rather than indirectly from the test results.

BIBLIOGRAPHY

Bishop A. W., Alpan I., Blight G. E. and Donald I. B. Factors controlling the strength of partially saturated cohesive soils. Proceedings ASCE Research Conference on Shear Strength of Cohesive Soils. University of Colorado, in press, June 1960.

Casagrande A. and Albert S. G. Research on shearing resistance of soils. Report, Massachusetts Institute of Technology, Cambridge, 1932.

Henkel D. J. The correlation between deformation, pore water pressure and strength characteristics of saturated clays. Thesis, University of London, 1958.

Henkel D. J. The relationship between the strength, pore water pressure and volume change characteristics of saturated clays. Geotechnique, vol. 9, pag. 119-135, 1959.

Henkel D. J. The relationship between the effective stresses and water content of saturated clays. Geotechnique, vol. 10, pag. 41-54, 1960.

Hvorslev M. J. Conditions of failure for remolded cohesive soils. Proc. First Int. Conf. Soil Mech. Found. Eng., Cambridge, vol. 3, pag. 51-53, 1936.

Hvorslev M. J. Ueber die Festigkeitseigenschaften gestorter bindiger Boden. Thesis, published by Danmarks Naturvidenskabelige Samfund, Ingeniorvidenskabelige Skrifter, Series A, No. 45, Copenhagen, 1937.

Kjellman W. Report on an apparatus for consummate investigation of the mechanical properties of soils. Proc. First Int. Conf. Soil Mech. Found. Eng., Cambridge, vol. 2, pag. 16-20, 1936.

Mitchell J. K. Fundamental aspects of thixotropy in soils. Proc. Am. Soc. Civ. Eng., Soil Mech. and Found. Div., vol. 86, No., SM3, pag. 19-52, 1960.

Rendulic L. Relation between void ratio and effective principal stresses for a remolded silty clay. Proc. First Int. Conf. Soil Mech. Found. Eng., Cambridge, vol. 3, pag. 48-51, 1936.

Rendulic L. Ein Grundgesetz der Tonmechanik und sein experimenteller Beweiss. Der Bauingenieur, vol. 18, pag. 459-467, 1937.

Roscoe K. H., Schofield A. N. and Wroth C. P. On yielding of soils. Geotechnique, vol. 8, pag. 22-53, 1958.

Schiffman R. L. Analysis of the displacements of the ground surface due to a moving vehicle. Paper No. 3 for the First Int. Conf. Mechanics of Soil-Vehicle Systems, Turin, 1961.

Taylor D. W. Review of research on shearing resistance of clay. Report to the USAE Waterways Experiment Station by Massachusetts Institute of Technology, 1955.

Taylor D. W. and Clough R. H. Research on shearing resistance of clay. Report to the USAE Waterways Experiment Station by Massachusetts Institute of Technology, 1951.

N. 2

Methods of plasticity in land locomotion studies *)

Studi del movimento fuori strada secondo la teoria della plasticità

R. M. Haythornthwaite **)

ABSTRACT. — *Successful application of plastic methods to problems of wheel and track sinkage is dependent on the availability of convenient methods of computation which are sufficiently flexible to allow for the extreme variability of ground conditions. In this paper, the basis of the plastic theory for soils is reviewed and it is shown how quick and convenient upper and lower bounds to carrying capacity can be obtained by the methods of limit analysis. As an example of interest in land-locomotion, the problem of the grouser plate (simulating a single lugged track element) is treated in detail for the case where ground weight is neglected. The paper closes with a brief review of the experimental basis of the theory.*

Introduction. — The theory of plasticity provides the means whereby practical engineering problems of ultimate strength can be solved through a knowledge of the basic mechanical properties of the material. Being parallel in development to elasticity theory, it rests upon a knowledge of stress-strain relations. In the case of soils, much fundamental work needs to be done to establish appropriate stress-strain relations and to explore the consequences. Nevertheless, the general ideas of plasticity have already been of great value conceptually in problems of soil mechanics, including those of land locomotion, and they hold great promise for the future.

Plasticity theory is founded on the concept of a stable material, one from which work cannot be extracted in any loading cycle. This requirement puts a severe restriction on the type of stress-strain relation which is admissible, causing it to be completely determined by the form of the yield condition for the material.

In the case of soils, the yield condition proposed by Coulomb [1] is now generally accepted. Thinking in terms of cohesion and frictional resistance across the possible slip planes in a mass of material, Coulomb, postulated that slip occurs when on any plane the shear stress reaches the value

$$\tau_0 = c - \sigma \tan \Phi \qquad (1)$$

*) This paper was originally prepared for Land Locomotion Laboratory, U. S. Army Ordnance Tank Automotive Command, Detroit, Michigan.

**) Professor of Engineering Science, The University of Michigan, Ann Arbor, Michigan, U.S.A.

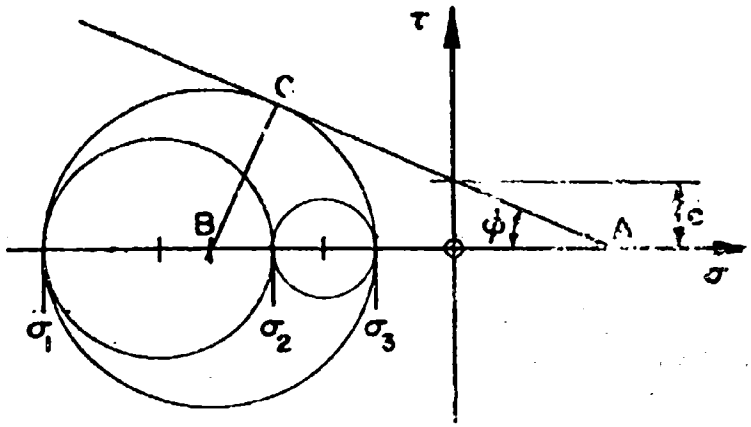


Fig. 1.

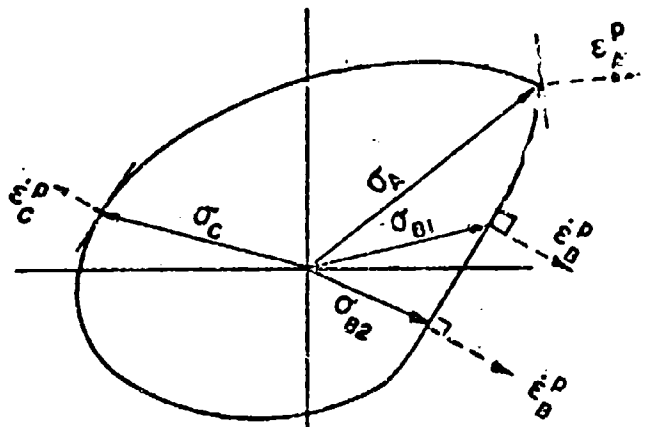


Fig. 2.

where **c** is the cohesion, σ the normal (tensile) stress on the plane and Φ a second empirical constant called the angle of internal friction. The corresponding principal stresses can be represented conveniently in the Mohr circle construction, fig. 1. Failure states are represented by circles touching the line (1). From the triangle ABC', $\sigma_3 - \sigma_1 = 2c\cos\Phi - (\sigma_1 + \sigma_3)\sin\Phi$, where σ_1, σ_3 are principal stresses; hence, after rearrangement,

$$\sigma_1 = \sigma_3 \tan^2\left(\frac{\pi}{4} + \frac{\Phi}{2}\right) - 2c\tan\left(\frac{\pi}{4} + \frac{\Phi}{2}\right) \qquad (2)$$

Here σ_1, σ_3 are the principal stresses with the greatest and smallest absolute values, respectively. Equation (2), with appropriate substitutions for σ_1 and

σ_3, defines the *yield surface* in the principal stress space with axes σ_a, σ_b, σ_c. If now a stress state, represented by a vector from the origin, is increased from zero, yield will be incipient when the vector reaches the surface, equation (2). For a non strain hardening material, the vector representing the stress state at any given point can never protrude beyond the surface, equation (2), otherwise it would represent a stress that the material could not sustain.

Turning now to the stress-strain relation, the stipulation that the material be stable requires that the strain rate vector is always normal to the yield surface when corresponding axes are superimposed [2] (see fig. 2). It can be shown [3] that the rate of energy dissipation per unit volume is

$$d = c \cot \Phi \, (\dot{e}_1 + \dot{e}_2 + \dot{e}_3) \tag{3}$$

where $\dot{e}_1$, $\dot{e}_2$, $\dot{e}_3$ are the principal strain rates, and that the principal strain rates are related by

$$\dot{e}_\alpha + \dot{e}_\beta + \dot{e}_\gamma \tan^2 \left(\frac{\pi}{4} + \frac{\Phi}{2}\right) = 0 \tag{4}$$

when $\dot{e}_\alpha$, $\dot{e}_\beta$ are positive and by

$$\dot{e}_\alpha \tan^2 \left(\frac{\pi}{4} - \frac{\Phi}{2}\right) + \dot{e}_\beta + \dot{e}_\gamma = 0 \tag{5}$$

when $\dot{e}_\beta$, $\dot{e}_\gamma$ are negative. The rates $\dot{e}_\alpha$, $\dot{e}_\beta$ and $\dot{e}_\gamma$ must be chosen so that the strain rate vector points towards the outside of the surface, equation (2).

Solutions. A problem is considered completely solved when:

a) a stress distribution has been found which satisfies the stress boundary conditions and the equations of equilibrium and also does not violate the yield condition (2) at any point; and

b) a velocity distribution has been found which satisfies the velocity boundary conditions and for which the corresponding strain rates are associated with the stresses in the manner indicated above.

Very few problems have been solved exactly in this sense and the techniques available will not be discussed here. One solution useful in the later discussion will be described to illustrate the features usually present, but the main effort will be devoted to a description of approximate solutions, one of which will be presented in detail as an example.

An exact solution holding a central place in land locomotion studies is that for the indentation of a flat surface by a long flat punch. Fig. 3 a indicates the directions of the surfaces of incipient slip associated with the stress distribution [i.e. surfaces on which (1) is satisfied] and fig. 3 b indicates the position of an initially square grid after a small downward displacement of the punch. The stress field was first obtained by Prandtl in 1920 [4]; the velocity field was added by Shield in 1953 [5]. Elsewhere [6], Shield has also extended the stress field throughout the rigid region, to confirm that the yield condition is nowhere

violated. The regions with straight slip lines (fig. 3 a) are regions of constant stress. Region ABC, in which the maximum principal stress is vertical, is referred to as an active Rankine zone, while ADE, in which σ_1 is horizontal, it an example of a passive Rankine zone.

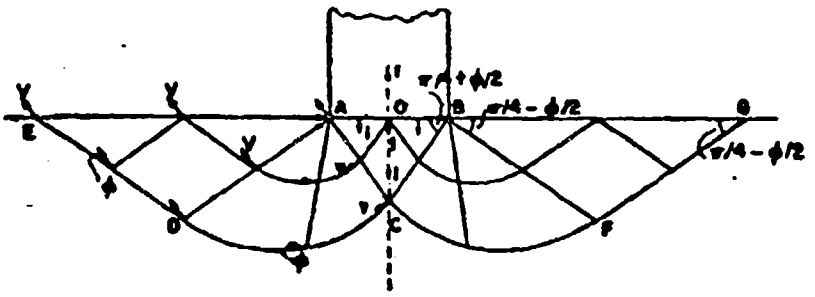


Fig. 3 a.

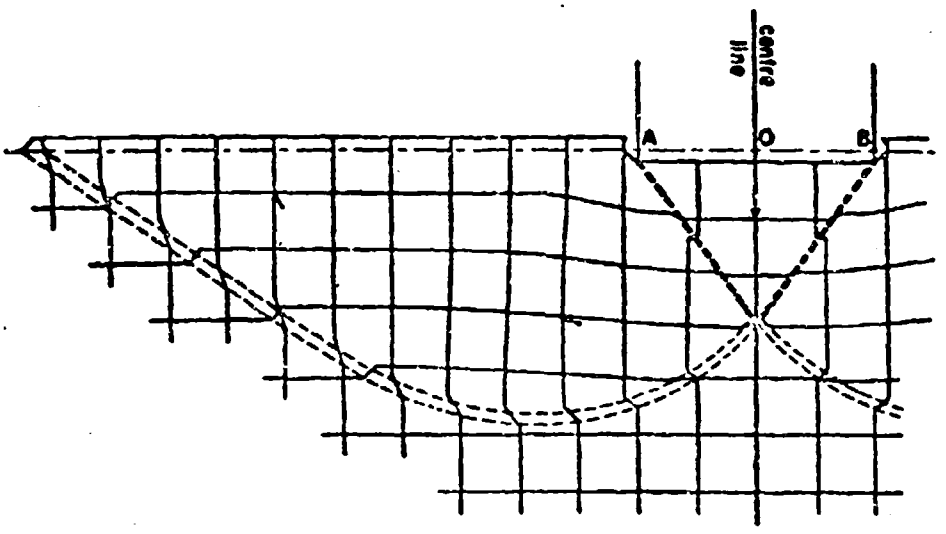


Fig. 3 b.

In fig. 3 a, both ABC and ADE move as rigid bodies, shearing motion occurring only along the boundaries. Region ACD is known as a region of radial shear and it will be discussed in detail later.

Few other complete solutions are known; however in the case of plane strain (of which the above is an example) there is a large number of stress solutions in the literature which satisfy condition (a) above, and the majority of these could probably be completed satisfactorily by associating velocity fields with them. Many partial solutions of this sort are given in Sokolovsky's book [1].

In the special case when $\Phi = 0$, the model reduces to that commonly used for metals and many solutions are available (see, for instance, [2-8]).

Approximate solutions. In view of the difficulty of obtaining exact solutions, approximate methods are frequently employed. The most satisfactory of these is the technique known as limit analysis, which was first introduced for soils in 1952 by Drucker and Prager [10]. The method rests on two propositions known as the *theorems of limit analysis* which can be stated as follows.

The lower bound theorem. Collapse will not occur if any state of stress can be found which satisfies the equations of equilibrium and the boundary conditions on stress and for which the yield condition is nowhere exceeded.

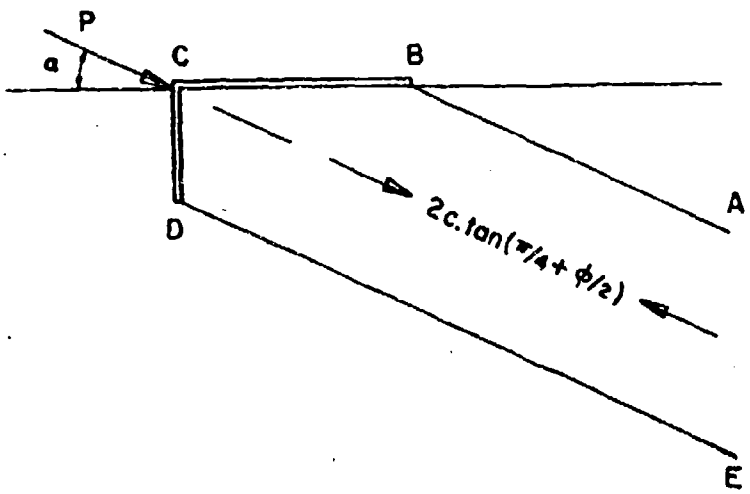


Fig. 4.

The upper bound theorem. Collapse must occur if, for any compatible flow pattern, the rate at which the external forces do work on the body equals or exceeds the rate of internal dissipation.

These theorems were established by Drucker, Greenberg and Prager [11] for the case of stress boundary conditions described by a single load parameter and by Hill [12] for cases like punch indentation where an imposed velocity is uniform in magnitude and direction along the boundary.

The actual techniques of limit analysis are best explained by means of a worked example. One is given in the next section.

An example of limit analysis

The example given below considers an idealisation of the familiar « grouser plate » or track tread element commonly met in land locomotion problems (see fig. 4). A vertical grouser plate of length H is rigidly attached to a horizontal plate of length L. The assembly is pressed into the soil by a force P inclined at an angle α to the horizontal. In this example it will be assumed that the line of action of the force P is such that the plate is displaced without rotation. Thus

the conditions conform to the usual practical problem, in which the plate element is attached to a vehicle.

Firstly crude upper and lower bounds will be found using very simple pictures of behavior, and then more elaborate pictures will be used in order to obtain closer bounds. In the process several important practical techniques are illustrated.

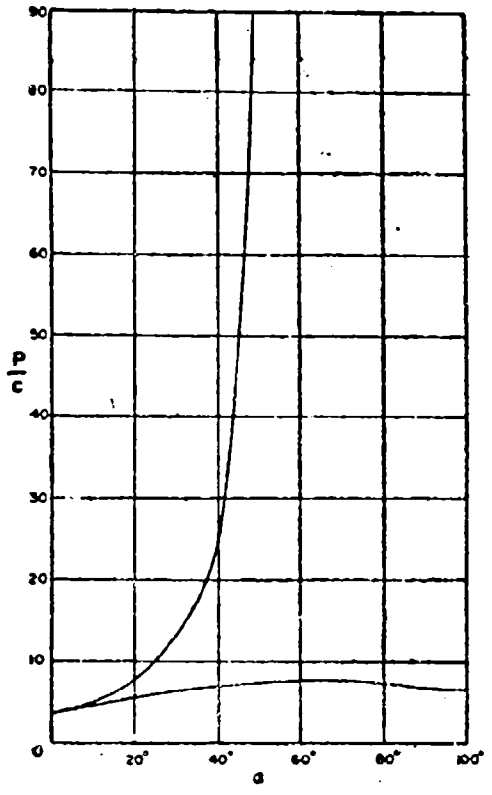


Fig. 5.

A first lower bound. — Consider the stress distribution shown in fig. 4. The soil carries a compressive stress in the zone ABCDE, which extends indefinitely into the soil, and zero stress elsewhere. Since the lateral stress is zero, the statically admissible stress is by (2), $-2c \cdot \tan(\pi/4 + \Phi/2)$ and for equilibrium

$$\frac{pL}{c} = 2(L \cdot \sin\alpha + H \cdot \cos\alpha) \tan\left(\frac{\pi}{4} + \frac{\Phi}{2}\right) \qquad (6)$$

when $\alpha < 90°$ and

$$\frac{pL}{c} = 2L \cdot \sin\alpha \tan\left(\frac{\pi}{4} + \frac{\Phi}{2}\right) \qquad (7)$$

when $\alpha > 90°$.

As a numerical example, consider the case where H = 1, L = 2 and $\Phi = 30°$. Equation (6) applies and the lower bound is as illustrated by the lower curve in fig. 5.

A first upper bound. — Consider the plane sliding mechanism shown in fig. 6. To compute the energy dissipation, we require the dilatation rate on the slip band AB. Consider first a slip band of width t, with points on the upper surface moving with velocity v relative to the lower surface, as shown. The non-zero rates of strain are

$$\dot{e}_y = \frac{v \cdot \sin \eta}{t} \qquad \dot{\gamma}_{xy} = \frac{v \cdot \cos \eta}{t}$$

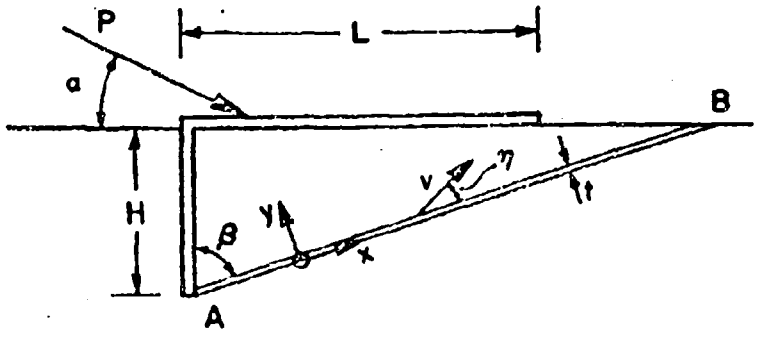


Fig. 6.

Substituting either (4) or (5), (nothing that $\dot{e}_x = \dot{e}_z = 0$), we obtain after some manipulation

$$\eta = \Phi$$

i.e. the direction of motion subtends an angle Φ to the slip plane. The rate of dilatation per unit area of slip surface is

$$(\dot{e}_x + \dot{e}_y + \dot{e}_z)\, t = v \cdot \sin \Phi$$

hence, at unit velocity on the slip surface, the rate of energy dissipation per unit area of the surface of sliding is, by (3),

$$c \cdot \cot \Phi \sin \Phi = c \cdot \cos \Phi \qquad (8)$$

The length of AB is $H \cdot \sec \beta$, so the total dissipation is

$$D = Hc \cdot \sec \beta \cos \Phi \qquad (9)$$

The rate at which work is done by the resultant force P is

$$W = P \cdot \cos \left(\alpha + \Phi + \frac{\pi}{2} - \beta \right) \qquad (10)$$

P is the resultant of the tractions over the length L and H which bear upon the soil. All points on these surfaces undergo the same displacement, so the upper bound theorem of limit analysis can be applied [12]. Thus $W > D$ or, substituting (9) and (10),

$$pU = \frac{He \cdot \cos\Phi}{\cos\beta \cos\left(\alpha + \Phi + \frac{\pi}{2} - \beta\right)} \qquad (11)$$

The angle β can be chosen to minimise pU and we obtain $\beta = \frac{\pi}{4} + \frac{\Phi}{2} + \frac{\alpha}{2}$, hence

$$pU = \frac{He \cdot \cos\Phi}{\cos^2\left(\frac{\pi}{4} + \frac{\Phi}{2} + \frac{\alpha}{2}\right)} \qquad (12)$$

The line of slip cannot intersect the horizontal plate, so when $\tan\beta < L/H$, (11) applies with $\beta = \tan^{-1}(L/H)$ substituted.

Considering the case where $H = 1$, $L = 2$ and $\Phi = 30°$, (11) applies when $\beta < \tan^{-1}(2) = 63.43°$, i.e. when $\alpha < 6.86°$, and (12) applies when $\alpha > 6.86°$: the resulting upper bound is illustrated by the upper curve in fig. 5.

The upper and lower bounds which have been obtained diverge sharply as α increases, but they almost coincide for $\alpha = 0$, and remain close enough to be of some practical use up to about $\alpha = 10°$. Thus, despite the simplicity of the pictures which have been employed, the problem has been solved for most practical purposes in the case of a relatively high tractive effort, as might occur on slopes or when the vehicle is towing *).

A second lower bound. — The lower bound can be improved by introducing a more complex statically admissible stress field. In making a choice, effective use can be made of intuition. This is one of the features that makes limit analysis particularly attractive to engineers. The next step might be to use the field shown in fig. 7 a. Instead of one there are now two zones of uniform stress which extend indefinitely into the soil, and also a zone formed by their intersection.

This stress field illustrates the use of discontinuity surfaces, which are well nigh essential if zones of uniform stress are to be matched. Discontinuities of stress can arise without violating equilibrium because the conditions of equilibrium across any surface specify only that the normal stress and the shear stress be continuous across the surface — the direct stresses parallel to the surface and on either side of it need not be related.

The application of this principle to the present problem is illustrated in the Mohr circle construction shown in fig. 7 b. The circle marked I refers to zone I in fig. 7 a — the pole is at P_I; similarly for circle II and circle III (zero radius), the poles are at P_{II} and P_{III} respectively. It should be noted that

*) It should be noted that the weight of the soil is being neglected.

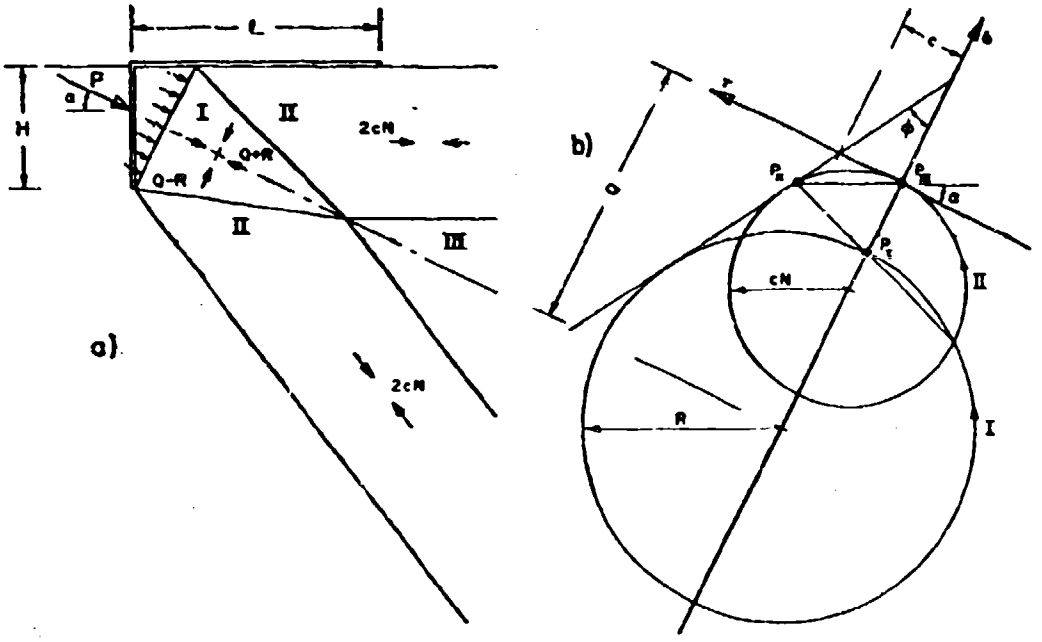


Fig. 7.

the stresses acting across a plane lying in a particular direction are given by the intersection with the circle of a parallel line drawn from the pole of that Mohr circle. The state of stress at the discontinuity between zones I and II must be represented by the intersections of the corresponding circles; also, by the above property of poles a line from either pole I or pole II which is parallel to the discontinuity must pass through the intersection; hence the three points are collinear. A similar argument applies to P_{II} and P_{III}. These facts serve to establish the relative sizes of the Mohr circles and also the angle α.

The angle α and the required pressure $Q + R$ (see fig. 7) are related analytically by

$$Q + R = 2cN \left[1 + \frac{1}{2} N^2 (1 - \cos 2\alpha + \sin 2\alpha \cot \eta)\right] \qquad (13)$$

where η is defined by the transcendental equation

$$(1 + 1/N^2) \cos 2 (\eta - \alpha) - 1/N^2 + \cos 2\alpha - \sin 2\alpha \cot \eta = 0 \qquad (14)$$

A numerical solution is necessary and it is much more convenient in practice to use a graphical construction based on the Mohr circles. Circle II remains constant for a given c and ϕ, and P_{II} can be located easily for circles I with various radii R. The angle α corresponding to each R can then be read off at once. The construction is valid when

$$\tan \alpha < L/H \qquad (15)$$

Above this value the vertical leg interferes with zone II and the bound is not clearly valid.

The lower curve in fig. 8 summarises the results from a graphical construction for the case $L = 2$, $H = 1$ and $\Psi = 30°$. Comparing figures 5 and 8, it

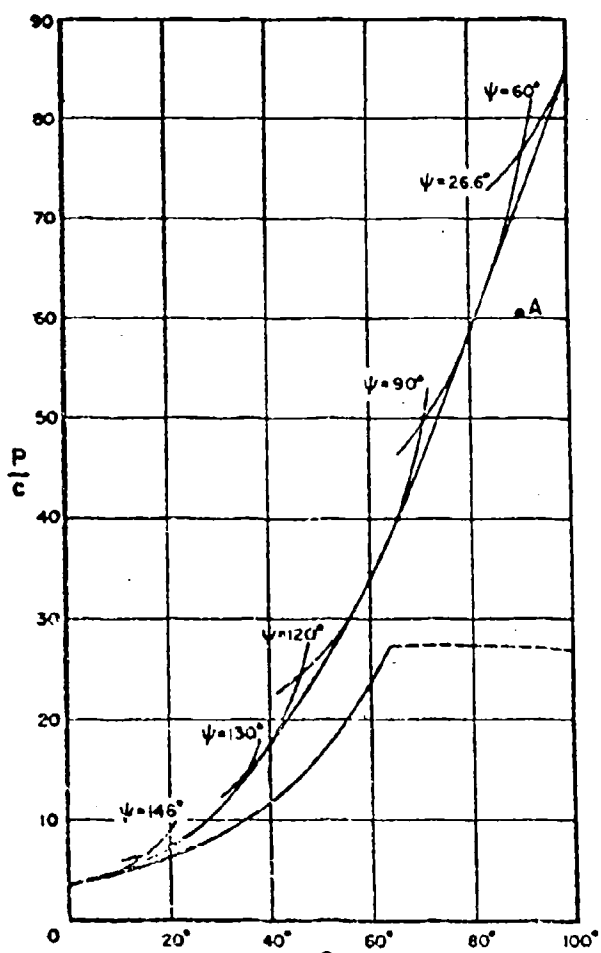


Fig. 8.

can be seen that a considerable improvement has been made for the larger values of α. The dotted part of the curve represents the results for the range where (15) is not satisfied.

A second upper bound. — The upper bound (11) is valid only when both terms in the denominator are positive and hence when $\alpha < \frac{\pi}{2} - \Phi$. At larger values of α, a more complicated velocity field becomes essential.

As in the case of the lower bound, intuition may be used with advantage to guide the choice of a new velocity field. In the problem under consideration the limiting cases $\alpha = 0$ and $\alpha = 90°$ are particularly valuable as a source of ideas for possible deformation patterns. The case $\alpha = 90°$ is quite close to the punch indentation solution (see fig. 3). The vertical grouser plate interferes with motion to one side of the center and may or may not increase the carrying capacity, depending on whether the soil tends to pull away from one side of the plate in the actual incipient motion. If it did the plate would act like a hole as far as soil to one side of it was concerned, so it is not obvious that the

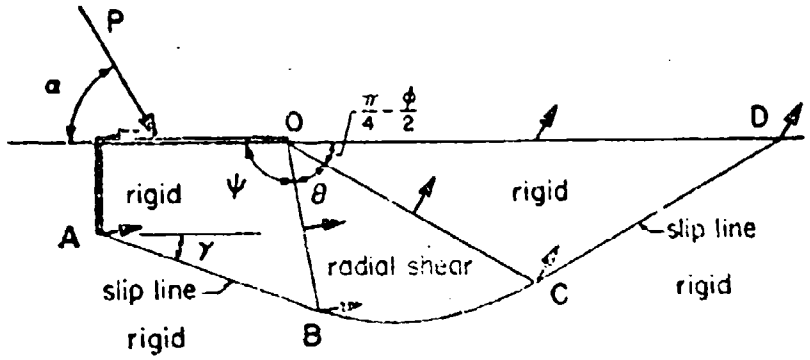


Fig. 9.

presence of the plate would always increase the load capacity. Nevertheless we might expect the deformation pattern to change to something like that shown in fig. 3 when α approaches 90°.

With the above consideration in mind the deformation pattern shown in fig. 9 was chosen as the basis for a second upper bound. It was intended that the angles be optimised to yield the lowest upper bounds possible with this pattern. The energy dissipation is concentrated on the slip line ABCD and in the zone OBC. Dissipation on a straight slip surface has been dealt with already in connection with the first upper bound; the zone of radial shear requires further special consideration before the total energy dissipation can be computed.

When one family of incipient slip directions is radial, the members of the other family will be inclined at an angle Φ to the circumferential direction (see fig. 10 a). An increment of length of one of the latter slip lines is $r \cdot d\Theta \sec \Phi = dr \cdot \operatorname{cosec} \Phi$ and after integration

$$r = r_0 \cdot e^{\Theta \cot \Phi} \tag{15}$$

where r_0 is the radius at $\Theta = 0$. Thus the second family consists of a set of logarithmic spirals.

In the particular case of the radial shear zone shown in fig. 9, the radial velocity is zero. The change in the circumferential velocity can be found by using the property that extensions along the slip lines must be zero[4]. Consider

a length AB along a slip line (fig. 10 b). At A the velocity v_1 in the direction of AB will be the orthogonal projection of v. If AB is not to extend the projection of $v + dv$ at B in the same direction must also be v_1; hence

$$v_1 = v_1 + dv_1 - v_1 \tan\Phi \, d\Theta$$

and after integration

$$v_1 = Ae^{\Theta \tan\Phi}$$

If $\Theta = 0$ at $v = v_0$,

$$v = v_1 \sec\Phi = v_0 e^{\Theta \tan\Phi} \tag{17}$$

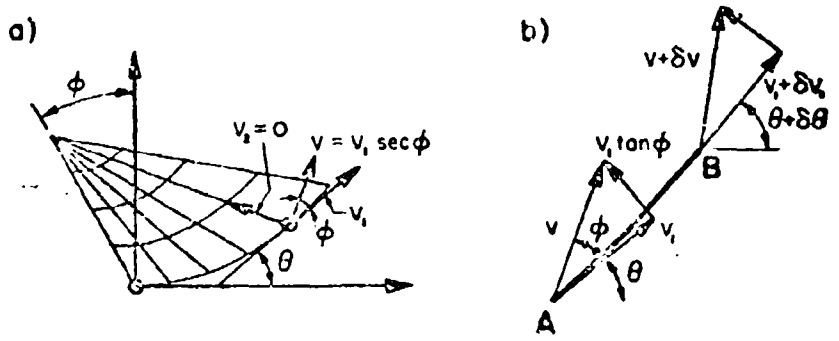


Fig. 10.

In polar coordinates the dilatation is

$$\Delta = \frac{1}{r}\frac{\delta}{\delta r}(ru_r) + \frac{1}{r}\frac{\delta u_\theta}{\delta\Theta} + \frac{\delta u_z}{\delta z} \tag{18}$$

where u_r, u_θ, u_z are the velocities in the radial, circumferential and axial directions, respectively (see, for instance [12], page 56). In our case, $u_r = 0$, $u_\theta = v$ and $u_z = 0$ and substituting (17)

$$\Delta = \frac{v_0}{r}\tan\Phi \cdot e^{\Theta \tan\Phi} \tag{19}$$

Substituting (19) in (3) and integrating over the zone OBC, the rate of energy dissipation in the zone is found to be

$$D_{OBC} = c \cdot \cot\Phi \int \Delta \, dv$$

$$= \int_0^\Theta \int_0^{r = r_0 e^{\Theta \tan\Phi}} c v_0 e^{\Theta \tan\Phi} \, d\Theta \, dr$$

$$= \frac{1}{2} c v_0 r_0 \cot\Phi \, (e^{2\Theta \tan\Phi} - 1) \tag{20}$$

when the velocity v_0 is the same at all radii, as in fig. 9. In the further analysis it is convenient to refer all other velocities to a unit velocity $v_0 = 1$ of the rigid zone OAB.

Considering next the slip surface AB, the velocity across the surface will be unity and its length $(r_0 \sin\psi - H)\operatorname{cosec}\gamma$, where

$$r_0 = \frac{L + H \cdot \cot\gamma}{\sin\psi \cot\gamma + \cos\psi} \tag{21}$$

is the length of OB. Using (8), the dissipation rate on AB is then

$$D_{AB} = c \cdot \cos\Phi \operatorname{cosec}\gamma \,(r_0 \sin\psi - H) \tag{22}$$

On BC the velocity (17) is $e^{\Theta \tan\Phi}$ and rate of dissipation is

$$D_{BC} = c \int_0^{\Theta} e^{\Theta \tan\Phi} r \cdot d\Theta$$

$$= \frac{1}{2} r_0 c \cdot \cot\Phi \,(e^{2\Theta\tan\Phi} - 1) \tag{23}$$

Finally, on CD, the length of which is equal to OC, the velocity is $e^{\Theta \tan\Phi}$ and the dissipation rate is

$$D_{CD} = c \cdot \cos\Phi \cdot r_0 e^{2\Theta\tan\Phi} \tag{23}$$

The total rate of energy dissipation found by adding (20), (22), (23) and (24) is equated to the rate at which work is done by P, given by $P \cdot \cos(\alpha - \gamma + \Phi)$ to produce the second upper bound

$$P^U = \frac{c\, r_0 \cot\Phi}{\cos(\alpha - \gamma + \Phi)} \left[(1 + \sin\Phi)\, e^{\pi\Theta\tan\Phi} - 1 + \frac{(\sin\psi - H/r_0 \sin\Phi)}{\sin\gamma}\right] \tag{25}$$

The result of numerical computations for the case $L = 2$, $H = 1$ and $\Phi = 30°$ is shown in the upper curves in fig. 8. The upper bound (25) was computed for several values of ψ and the envelope of the resulting curves gave a reasonable estimate of the optimum (lowest) values of P^U obtainable from (25). An alternative but less convenient procedure would have been to minimise (25) by computing the derivative with respect to ψ and equating to zero. (Note that r_0, γ, and Θ are all functions of ψ).

Exactly the same upper bound procedure can be applied to the punch indentation case illustrated in fig. 3, and as expected the correct expression

$$p = c \cdot \cot\Phi \left[e^{\pi\tan\Phi} \tan^2\left(\frac{\pi}{4} + \frac{\Phi}{2}\right) - 1\right] \tag{26}$$

is obtained for the punch indentation pressure. The corresponding value of P/c is shown as point A in fig. 8. As remarked earlier, this value is not necessarily either an upper or a lower bound for the grouser plate problem,

but we would not expect the two solutions to differ very much. Thus we wight expect the exact carrying capacity to lie quite close to the upper bound. This conjecture cannot of course be substantiated without further work.

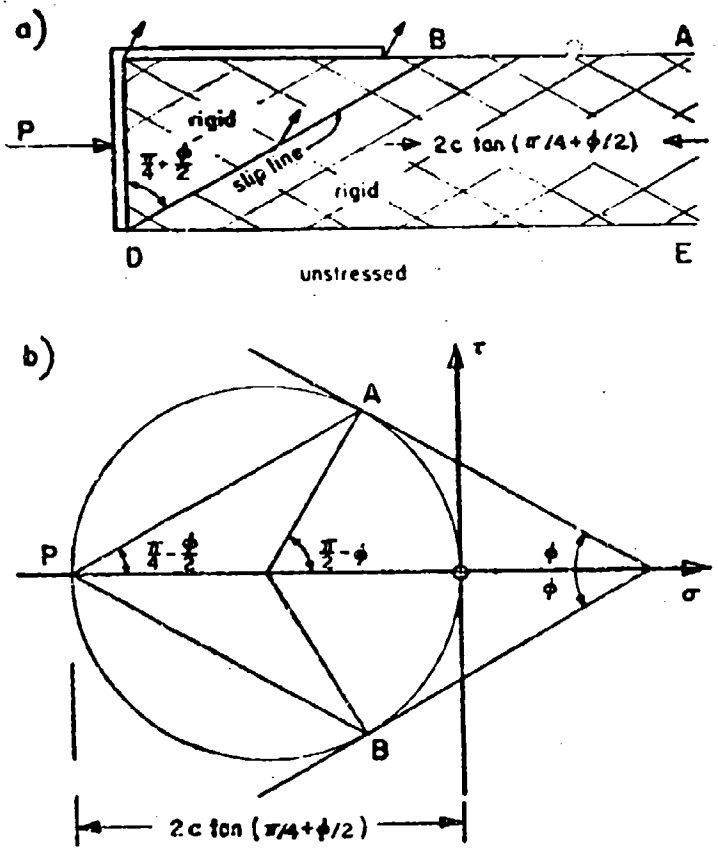


Fig. 11.

A complete solution. — For the particular case $\alpha = 0$, the upper and lower bounds nearly coincide (fig. 5), so they must be close to the true carrying capacity. If $\tan^{-1}(L/H) < \frac{\pi}{4} + \frac{\Phi}{2}$, so that (12) applies, this upper bound expression gives the same value as the lower bound (6) and the carrying capacity is

$$P = 2Hc \cdot \tan\left(\frac{\pi}{4} + \frac{\Phi}{2}\right) \qquad (27)$$

The solution can be shown to be complete. For completeness the velocity field must be shown to be associated correctly through the stress-strain law with the stress field and it must be shown that at no point in the soil, including all supposedly rigid zones, is the yield condition violated.

The case $\alpha = 0$ is hown in fig. 11. For the stress state in zone ABCDE, the Mohr circle is as shown in fig. 11 b. The pole is at P and slip will be incipient on the planes parallel to PA and PB. The assumed slip surface BD is one of these lines, so the deformation will be associated correctly with the stress field. All stresses are either zero or as represented in the Mohr circle, so the yield condition is not violated anywhere. Equilibrium is maintained across the stress discontinuity surface DE (the normal and shear stresses being zero on either side) and it is maintained in zone ABCDE providing the zone extends indefinitely to the right. Thus the solution is complete.

The extent of the deformable zone can be found quite simply by recalling that extension along a slip line is zero[5]. Since BC and CD are rigidly connected, the zone BCD moves as a rigid body; since the material below DE remains rigid, ABDE must also be rigid. Deformation is then restricted to the slip surface BD.

Plasticity in land locomotion studies

The theory of plasticity has played an important role in the development of land locomotion concepts. One need only mention as examples the notion of wheel and track spacing to prevent interaction between slip zones, an understanding of wheel sinkage by alternative sideways or back and front slip zones, and the development of the spaced link track[14].

Of special interest for the future is the possibility of using plasticity theory, particularly approximate limit analyses such as that presented in the previous section, to make quantitative estimates of vehicle performance. Here it should be noted that the methods of limit analysis are flexible and it is a relatively simple matter to make allowance for soil properties which vary with depth and for soil weight. Also the effects of design modifications can be explored quite easily.

In all such applications the methods of plasticity stand or fall on the appropriateness of the assumed yield condition and stress-strain law and it is in this area that experimental research is most urgently required. Even for sands the Coulomb law has not been confirmed beyond question for various levels of the intermediate principal stress[15], although tests under a punch in plane strain[16] seem fully consistent with the theory and may be accepted at least as circumstantial evidence in favour. In the case of silty soils[17], the evidence from triaxial tests would seem to support some type of strain hardening law, rather than ideal plasticity. Tests using a new triaxial-torsion machine which enables general complex stress states to be applied to a hollow cylindrical specimen have been completed recently at Brown University[18]. In these tests, failure was shown to be independent of loading path — a necessary condition for the establishment of a reasonably simple plastic theory. On the other hand, evidence obtained on the nature of the flow rule did not give full support to the theory of ideal plasticity, although the results may have been obscured by the apparent development of anisotropy. For clays,

behavior in the triaxial test is almost entirely cohesive, which suggests all the solutions developed originally for metals might be applicable, but again no information is available on the effects of the intermediate principal stress. It is clear that until these fundamental questions are resolved extreme caution must be exercised in applying plasticity theory and experimental confirmation is called for in each new application. Nevertheless the prospects are good that as our knowledge of the fundamental properties of soils improves, an important byproduct will be an extension in the range of application of plasticity theory.

ACKNOWLEDGMENT. — This study was made in the course of a research program in soil mechanics at Brown University which was supported by the Land Locomotion Laboratory, Ordnance Tank - Automotive Command, U.S. Army.

BIBLIOGRAPHY

1) Coulomb C. A. Essai sur une application des regles de maximis et minimis à quelques problems de statique relatif à l'architecture. Mem. Acad. Sci. (Savants Etrangers), 7, 343, 1773.
2) Drucker D. C. A more fundamental approach to plastic stress-strain relation. Proc. 1st. U. S. Nat. Cong. Applied Mechanics, 487-491, 1951.
3) Shield R. T. On Coulomb's law of failure in soils. J. Mech. Phys. Solids, 4, 10-16, 1955.
4) Prandtl L. Ueber die Harte plastischer Korper. Gottingen Nachr., math. Phys. Kl., 74, 1920.
5) Shield R. T. Mixed boundary value problems in soil mechanics. Q. Appl. Math., 11, 61-75, 1953.
6) Shield R. T. Plastic potential theory and Prandtl bearing capacity solution. J. Appl. Mech., 21, 193, 1954.
7) Sokolovsky V. V. Statika Cypuchey Credy. Statics of earthy mediums. Acad. Sci. U.S.S.R., 1st ed., 1942, 2nd ed., 1954.
8) Prager W. and Hodge P. G. Jr. Theory of perfectly plastic solids. John Wiley and Sons, Inc., New York, 1951.
9) Hill R. The mathematical theory of plasticity. Oxford Univ. Press, London, 1950.
10) Drucker D. C. and Prager W. Soil mechanics and plastic analysis or limit design. Q. Appl. Math., 10, 157-165, 1952.
11) Drucker D. C., Greenberg H. J. and Prager W. Extended limit design theorems for continuous media. Q. Appl. Math., 9, 381-389, 1952.
12) Hill R. On the state of stress in a plastic-rigid body at the yield point. Phil. Mag. Ser., 7, 42, 868, 1951.
13) Love A. E. H. Mathematical theory of elasticity. 4th Ed., Cambridge Univ. Press, London, 1927.
14) Bekker M. G. Theory of land locomotion. Univ. Michigan Press, Ann Arbor, 1956.
15) Haythornthwaite R. M. Mechanics of the triaxial test for soils. Proc. Am. Soc. Civil Engrs., 86 (SM5), 35-62, 1960.
16) Sylwestrowicz W. Experimental investigation of the behavior of soil under a punch or footing. J. Mech. Phys. Solids, 1, 258-264, 1953.
17) Drucker D. C., Gibson R. E. and Henkel D. J. Soil mechanics and work-hardening theories of plasticity. Proc. Am. Soc. Civil Engrs., 81, 798, 1-14, 1955.
18) Haythornthwaite R. M. Stress and strain in soils. Proc. 2nd Symposium Naval Structural Mechanics, Pergamon Press, 185-193, London, 1960.

D I S C U S S I O N

E. LEFLAIVE. — La théorie de la plasticité permet la détermination des contraintes à partir d'une hypothèse sur la forme de la rupture, qui se traduit par un schéma délimitant les zones de plasticité. Ce schéma n'est pas donné par la



Photo 1.

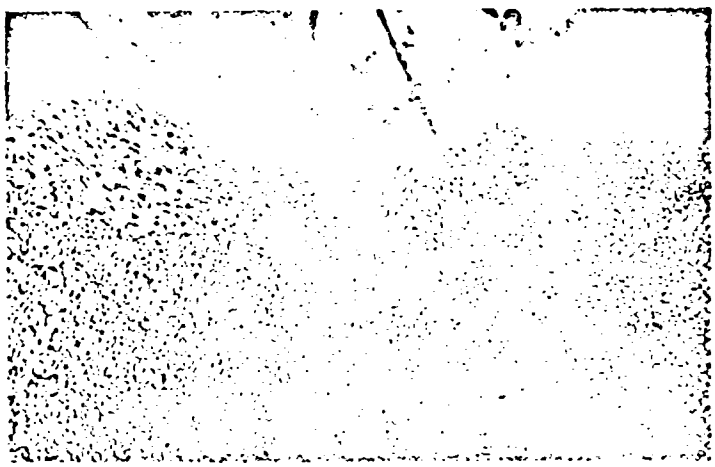


Photo 2.

théorie; des études expérimentales peuvent fournir des indications précieuses sur ce schéma; parmi ces méthodes, la réalisation d'un modèle expérimental à deux dimensions d'un matériau pulvérulent à l'aide de rouleaux, que nous avons utilisé, peut être d'un grand secours — et a d'ailleurs déjà rendu de grands services (cf. 1) — dans l'emploi des méthodes de calcul de plasticité appliquées aux sols. Quelques photographies prises sur ce modèle analogique fournissent notamment, pour l'étude à deux dimensions du problème du démarrage d'une roue, des indications sur l'évolution de la forme de la zone de cisaillement en fonction de la profondeur d'enfoncement de la roue.

---

1) J. Biarez, M. Burel: Contribution à l'étude de la force portante des fondations. Actes du Cinquième Congrès International de Mécanique des Sols et des Travaux de Fondations, Paris, 1961.

Analysis of the displacements of the ground surface due to a moving vehicle *)

Analisi degli spostamenti della superficie del terreno dovuti al movimento dei veicoli

ROBERT L. SCHIFFMAN **)

ABSTRACT. — *The problem of the displacement of the ground surface under the action of a moving vehicle is treated from an analytical point of view.*

The physical mechanisms of soil displacements are presented for the purpose of establishing various models of behavior of the soil system. Visco-elastic models of soil behavior are postulated on the basis of laboratory tests and field observations.

A theoretical study is made of the displacements of a loaded plate moving across the soil at relatively slow speeds. This study is based on theories of visco-elasticity.

The results of the study are presented in terms of analytical expressions and curves.

A physical interpretation of the results is presented, relating vehicular and soil parameters.

Introduction

The proper design of a vehicle requires knowledge and consideration of all the components affecting vehicle mobility.

Of all the components which play a part in vehicle mobility, the soil is the most variable and least understood. The soil also exhibits the most complex properties of all the mobility components.

For reason of soil behavior complexity, the mobility design of a vehicle must not only be related to the soil, but to the vehicle's use on a particular class of soils.

The use characteristic, as far as the soil is concerned, is the weight of the vehicle and the speed of its movement.

Soil can be grouped into three basic types, these being granular, clay, and mixtures of granular and clay-soils. Each of these soil groups has certain significant unifying characteristics. These characteristics can be used to predict soil-vehicle behavior for a given vehicle mobility consideration.

This paper develops certain soil deformation principles in terms of the vehicle characteristics of speed and weight.

---

*) This paper was originally prepared for Land Locomotion Laboratory, U.S. Army Ordnance Tank Automotive Command, Detroit, Michigan.

**) Associate Professor of soil mechanics, Rensselaer Polytechnic Institute, Troy, New York, U.S.A.

The soil considered is a clay. The vehicle characteristics are treated as a loaded plate subjected to repetitive loading.

In general, the behavior of the soil will be restricted to isotropic materials that follow linear laws with small strain. The stress-strain-time relations will be for a homogeneous continuum, although considerations of soil as a multi-phased system will be inherent in the analysis.

Behavior laws

Elastic behavior. — The stress-strain behavior for a homogeneous linear, isotropic, elastic material, exhibiting small strains is as follows:

$$\sigma_{ij} = \frac{3K - 2G}{3} \epsilon_{kk} \delta_{ij} + 2G\epsilon_{ij} \tag{1 a}$$

$$\delta = \begin{cases} 1 & i = j \\ 0 & i \neq j \end{cases} \tag{1 b}$$

Where:

K = Bulk modulus
G = Shear modulus

Equation (1) can be separated into volume change components (σ_{ij}) and (ϵ_{ij}), and deviator components (s_{ij}) and (e_{ij}).

$$\sigma_{ij} = 3K\epsilon_{ij} \tag{2 a}$$

$$s_{ij} = 2Ge_{ij} \tag{2 b}$$

The relations between the volumetric and deviator stress and strain components are:

$$s_{ij} = \sigma_{ij} - 1/3\, \sigma_{kk} \delta_{ij} \tag{3 a}$$

$$e_{ij} = \epsilon_{ij} - 1/3\, \epsilon_{kk} \delta_{ij} \tag{3 b}$$

The displacement of a loaded plate on the surface of an elastic half-space, as shown in fig. 1, can be expressed as follows:

$$w = \alpha \frac{3K + 4G}{4G\,(3K + G)} \frac{P}{\sqrt{A}} \tag{4}$$

Where:

w = Surface displacement of plate;
α = Geometric constant depending on shape of plate and position where displacement is measured;
P = Total load on plate;
A = Area of loaded plate.

Thus, the surface displacement of a plate can be expressed in terms of the elastic properties and the imposed load.

Visco-elastic behavior. — A visco-elastic stress-strain equation differs from the elastic relation only in the fact that the stresses and strains are related by time derivatives. The general linear visco-elastic stress-strain equation is:

$$\sum_{n=0}^{n} A_n \frac{\delta^n \sigma_{ij}}{\delta t^n} = \sum_{m=0}^{m} B_m \frac{\delta^m \varepsilon_{ij}}{\delta t^m} \tag{5}$$

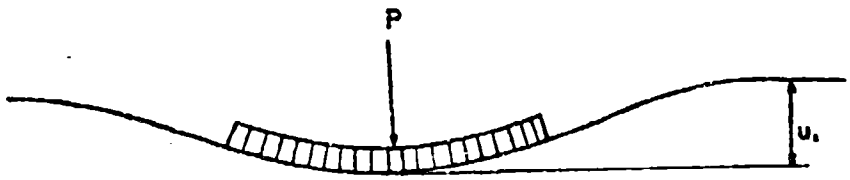


Fig. 1. — Loaded plate on half space.

Equation (5) can be written in operator form in terms of volume change and deviatoric components [1-2].

$$R(\sigma_{ij}) = S(\varepsilon_{ij}) \tag{6 a}$$

$$M(s_{ij}) = N(e_{ij}) \tag{6 b}$$

The operators, R, S, M, N, are time derivative operators multiplied by the material econstants associated with the equivalent stresses and strains. By this definition, the bulk and shear modulus are first order operators. As a result, the visco-elastic stress-strain law is:

$$\sigma_{ij} = \frac{MS - NR}{3RM} \varepsilon_{kk} \delta_{ij} + \frac{N}{M} \varepsilon_{ij} \tag{7}$$

Since the visco-elastic operators are linear, the elastic surface displacement equation is readily converted to a visco-elastic equation.

$$N(2MS + NR) w = M(MS + 2NR) P(t) \tag{8 a}$$

$$w = \frac{u_z \sqrt{A}}{\alpha} \tag{8 b}$$

Thus, given the visco-elastic properties of a soil system and the type of loading, the time-displacement relation can be developed.

Clay-soil behavior

The behavior of clays can be separated into three components.

1) Volume change behavior.
2) Deviator behavior.
3) Relation between volume change and deviator behavior.

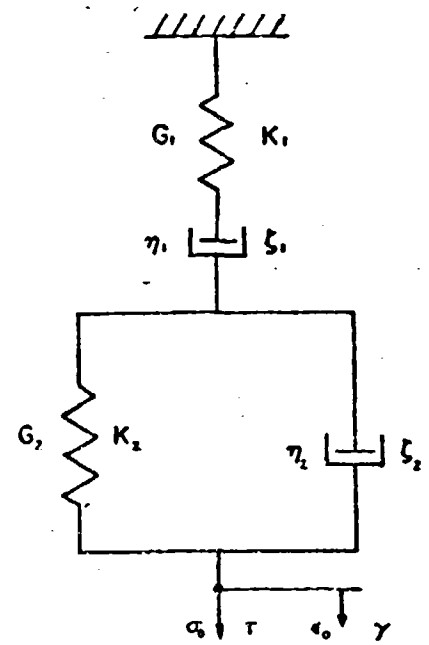


Fig. 2. — Burgers model.

The first two components listed above are known, at least for a series of general conditions. The third component is as yet quantitatively and qualitatively unknown. For the purposes of this paper, the coupling of volume change and deviator is relatively unimportant and will not be considered. It must be understood, however, that in a prototype design, the interdependence of volume change and deviator properties will substantially alter the magnitude of these properties, and must be considered.

Volume change. — The fundamental volume change theory of clay-soils is the Terzaghi theory of consolidation [3].

This theory considers the clay-soil mass to be a simplified saturated structure of incompressible particles and incompressible fluid.

From a rheologic point of view, the Terzaghi theory develops volume change as a Kelvin material [4].

The Terzaghi theory was developed for long term behavior under conditions of sustained loading. For a condition of short repetitive loads, the theory must be augmented [5]. The augmented theory of volume change behavior is rheologically a Burgers material [6], under stress (σ_o) and strain (ϵ_v).

The Burgers model, as shown in fig. 2 is in itself not sufficient.

The bulk modulus (K_2) cannot be a constant. If it were constant, the terminal volumetric deformation would be independent of the imposed stress. From tests and analyses by Bridgman [7], Seed [8], and Murnaghan [9], a tentative bulk modulus law is proposed.

$$K_2 = K_o + \lambda\sigma_o \tag{9}$$

Where:

K_o = Residual bulk modulus;
λ = Stress increment modulus.

Under sustained loading, the proposed volume change model must be compatible with the observations of terminal deformation. Thus, the volumetric viscosity (ζ_1) must increase with a decreasing volume, approaching infinity in the limit. As the fluid is squeezed out, the pores tend to close and the internal forces opposing fluid motion will increase. As a result, the viscosity (ζ_1) will increase both as a function of time and pressure. As a first approximation, the volumetric viscosity (ζ_1) can be considered to follow an exponential law.

$$\zeta_1 = \zeta_o \exp(a\sigma_o t) \tag{10}$$

Where:

ζ_o = Initial viscosity;
a = Constant.

The bulk modulus (K_1) expresses the effects of initial and final deformation and instantaneous reversibility. As such, it is dependent on the magnitude of the imposed stress and the time of loading to the point of unloading. Since the effects of imposed stress magnitude were considered in equation (9), the variation of (K_1) can be considered only in terms of deformation reversibility. Observations of repeated loading tests [10], have indicated that the instantaneous reversibility decreases with number of repetitions and the time of previous sustained loading. Since the problem considers only a limited number of repetitions, the modulus (K_1) will be considered to vary only in terms of the time of loading.

$$K_1 = \mu_o + \mu_1 (1 - e^{-bt}) \tag{11}$$

Where:

μ_o, μ_1 = Bulk moduli;
b = Constant.

The second volumetric viscosity (ζ_2) can be thought of as the initial permeability of the soil and as such, can be considered to remain constant.

The total volume change relation can be expressed as follows:

$$\varepsilon_v = \frac{\sigma_0}{K_1} + \int_0^t \frac{\sigma_0}{\zeta_1}\,dt + C\exp\left(-\int \frac{dt}{T_2}\right)$$

$$+ \exp\left(-\int \frac{dt}{T_2}\right)\int_0^t \frac{\sigma_0}{\zeta_2}\exp\left(\int \frac{dt}{T_2}\right)dt \qquad (12\,a)$$

$$T_2 = \frac{\zeta_2}{K_2} \qquad (12\,b)$$

Where:

ε_v = Volumetric strain.

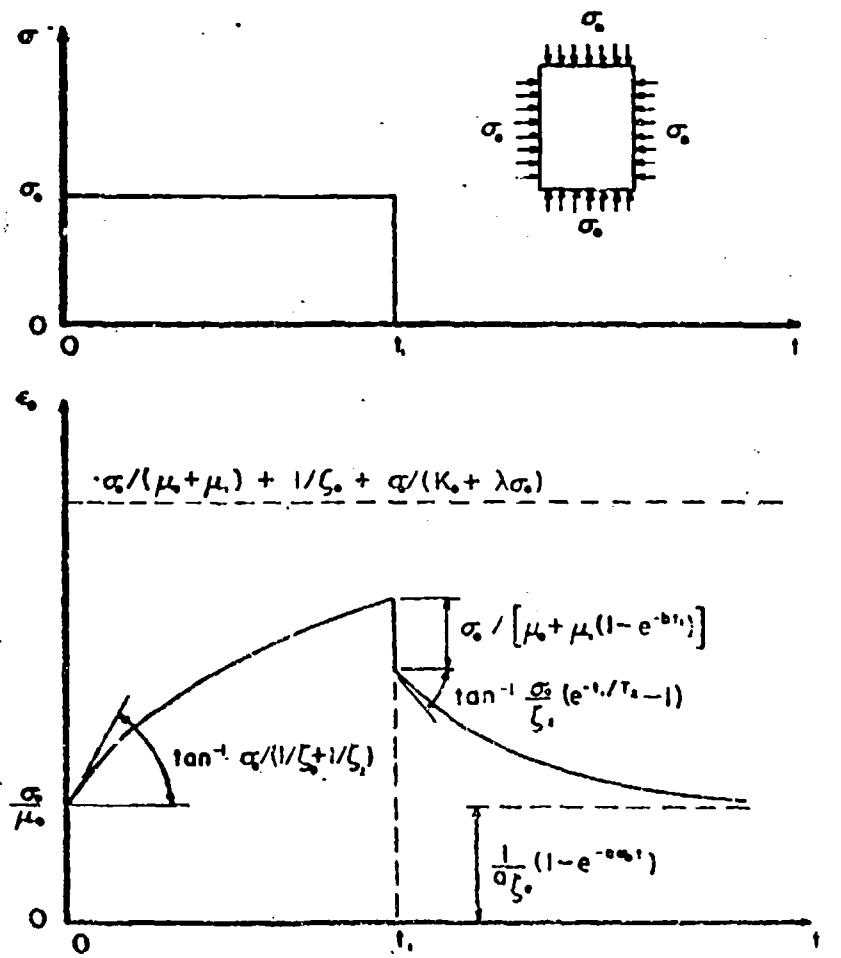


Fig. 3. — Volume change clay behavior.

The response (ϵ_0) due to a hydrostatic compression (σ_0) is:

$$\epsilon_0 = \frac{\sigma_0}{\mu_0 + \mu_1 (1 - e^{-b_1 t})} + \frac{1}{\eta \zeta_0} (1 - e^{-\eta \sigma_0 t}) + \frac{\sigma_0}{K_0 + \lambda \sigma_0} (1 - e^{-t/T_2}) \quad (13\,a)$$

$$T_2 = \frac{\zeta_0}{K_0 + \lambda \sigma_0} \quad (13\,b)$$

For a single load-unload cycle, the response is sketched in fig. 3.

As shown in fig. 3, the strain time behavior has all the observed phenomena for volume change of clay-soils. The effect of individual parameters in terms of such soil entities as moisture content, type of clay mineral, degree of saturation, temperature, etc., must as yet be determined. These however, will only change the magnitude of the properties.

Deviator behavior. — The deviator behavior of clay-soils in terms of rheologic properties has been described by Geuze [10-11-12-13], Tan [10-11-12-13-14], and Josselin de Jong [13], and Haefli [16].

The behavior reported generally follows the pattern shown in fig. 4.

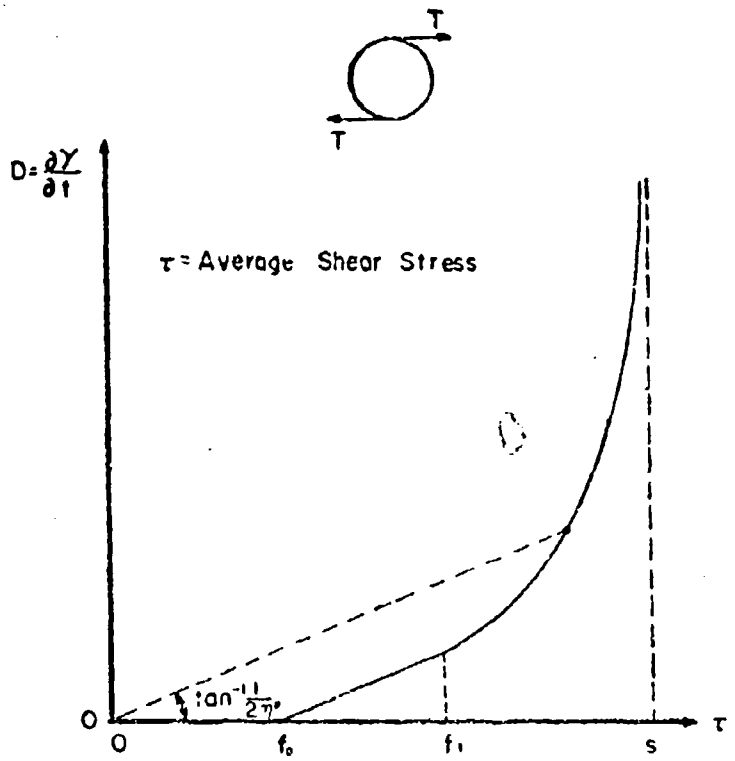


Fig. 4. — Deviator behavior of clay.

These results based on creep tests report the average shear stress (τ) as a function of the time rate of shear strain (D). The reported experiments show that for low stress levels below a yield value (f_0) the deviator behavior is elastic. Between (f_0) and (f_1) the behavior is viscous, and for stress levels above (f_1) the behavior exhibits shear thinning until the shear strength (s) is reached. The magnitudes of (f_0), (f_1), (s) and the slopes of the curve are dependent on the soil properties such as moisture content, previous load history, clay mineral, degree of saturation, temperature, etc. There is as yet insufficient experimental evidence to relate these magnitudes.

The discontinuity of the behavior can be treated analytically by considering the clay to be a thinning thixotropic Burgers material under stress (τ) and strain (γ). The deviator viscosity behaves as follows.

$$\frac{1}{\eta_1} = \Phi_0 e^{c\tau} + \Phi_2 e^{-dt} \tag{14}$$

The Burgers model is shown in fig. 2.

For the Burgers deviator model, the flow relation is:

$$D = \left(\frac{1}{\eta_1} + \frac{1}{\eta_2}\right)\tau + \frac{1}{G_1}\frac{\delta\tau}{\delta t} - \frac{1}{\eta_2 T_2} e^{-t/T_2}\int_0^t \tau e^{t/T_2}\,dt \tag{15 a}$$

$$J_2 = \eta_2/G_2 \tag{15 b}$$

Examining equations (15) with (η_1) as defined in equation (14), and considering time-strain equilibrium:

$$D = \Phi_1 \tau e^{c\tau} \tag{16}$$

The relation expressed in equation (16) can be used to approximate the shear thinning behavior for stresses greater than the yeld level (f_0), and is shown in fig. 5.

Clay-soil behavior. — The previous analysis outlines the establishment of soil properties in terms of rheologic behavior. It is thus possible to approximate the total stress-strain-time behavior of a clay in terms of its component behavior.

In volume change, the stress-strain behavior is expressed by the differential equation.

$$\frac{\delta^2\epsilon_{II}}{\delta t^2} + \frac{K_2}{\zeta_2}\frac{\delta\epsilon_{II}}{\delta t} = \frac{1}{3K_1}\frac{\delta\sigma_{II}}{\delta t^2} + \left[2\frac{\delta}{\delta t}\left(\frac{1}{3K_1}\right) + \frac{K_2}{3K_1\zeta_2} + \frac{1}{3\zeta_1} + \frac{1}{3\zeta_2}\right]\frac{\delta\sigma_{II}}{\delta t} + \left[\frac{\delta^2}{\delta t^2}\left(\frac{1}{3K_1}\right) + \frac{\delta}{\delta t}\left(\frac{K_2}{3K_1\zeta_2} + \frac{1}{3\zeta_1}\right) + \frac{K_2}{3K_1\zeta_1}\right]\sigma_{II} \tag{17}$$

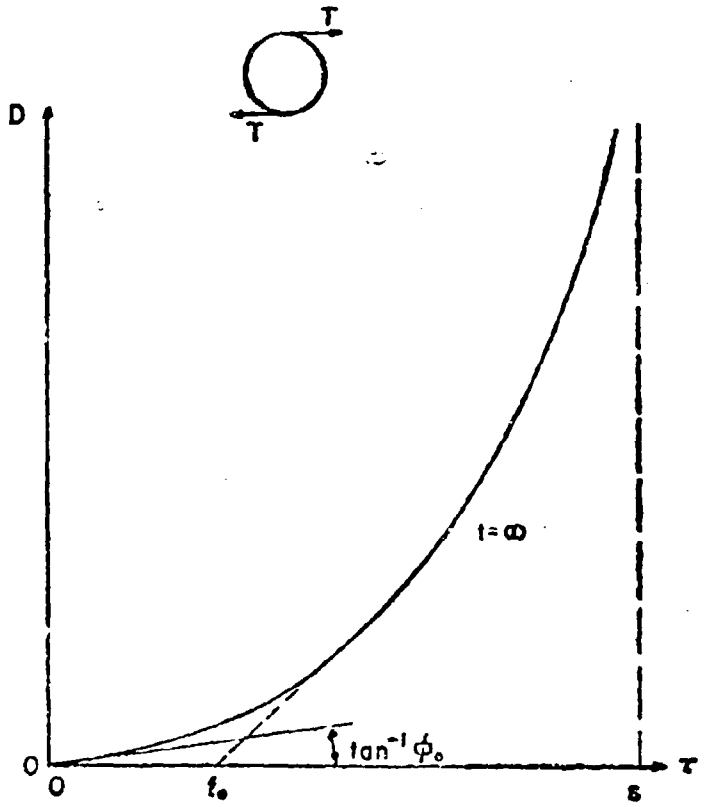


Fig. 5. — Shear behavior of clay ($\tau > f_o$).

The deviator stress-strain-time differential equation is:

$$s_{ij} = 2Ge_{ij} \qquad (s_{ij} < f_o) \tag{18 a}$$

$$\frac{\delta^2 e_{ij}}{\delta t^2} + \frac{G_2}{\eta_2}\frac{\delta e_{ij}}{\delta t} = \frac{1}{2G_1}\frac{\delta^2 s_{ij}}{\delta t^2} + \left[\frac{G_2}{2G_1\eta_2} + \frac{1}{2\eta_1} + \frac{1}{2\eta_2}\right]\frac{\delta s_{ij}}{\delta t}$$

$$+ \left[\frac{\delta}{\delta t}\left(\frac{1}{2\eta_1}\right) + \frac{G_2}{2G_1\eta_1}\right] s_{ij} \qquad (s_{ij} > f_o) \tag{18 b}$$

The initial conditions to equations (17) and (18) are dependent on the particular application and inherent soil initial stresses and strains.

Ground surface deformation

The deformation of the surface of the ground resulting from vehicular action is due to several factors. These are:

1) Speed of surface movement.
2) Imposed stresses as a function of vehicle weight.

Two problems of interest are those pertaining to a standing vehicle, and a moving vehicle.

In order to achieve indicative solutions, a linear theory will be used.

Standing vehicle. — In volume change, the most critical problem of a standing vehicle is the long time deformation. For this case, the theory of consolidation is applicable.

The deviator behavior is a function of the vehicle load. For light loads where the imposed deviator stresses are less than (f_o) the behavior is elastic. For imposed deviator stresses greater than (f_o) visco-elastic behavior is requisite.

As a first example, a light vehicle is considered. The volume change is considered to act as a Kelvin material while the deviator behavior is elastic.

$$\sigma_{ii} = 3K\varepsilon_{ii} + 3\zeta \frac{\delta \varepsilon_{ii}}{\delta t} \tag{19 a}$$

$$s_{ij} = 2G e_{ij} \qquad (s_{ij} < f_o) \tag{19 b}$$

The visco-elastic operators are:

$$R = 1 \tag{20 a}$$

$$S = 3K + 3\zeta \frac{\delta}{\delta t} \tag{20 b}$$

$$M = 1 \tag{20 c}$$

$$N = 2G \tag{20 d}$$

The displacement time relation from equations (8) becomes:

$$\frac{\delta w}{\delta t} + \frac{3K + G}{3\zeta} w = \frac{3K + 4G}{12G\zeta} P \tag{21 a}$$

$$w(o) = w_o \tag{21 b}$$

Equation (21) are the equations of a Kelvin model in which the soil is pre-deformed by a deformation (w_o)

$$w(t) = \frac{3K + 4G}{4G\,(3K + G)} P + \left[w_o - \frac{3K + 4G}{4G\,(3K + G)} \cdot P \right] e^{-t/T} \tag{22 a}$$

$$T = \frac{3\zeta}{3K + G} \tag{22 b}$$

The results presented in equations (22) indicate several features of the time-displacement relation. In the first place the time retardation of elastic displacement is greater than would be expected by pure consolidation. The additional delay is due to the shear deformation. Secondly, the previous load history plays an important factor in the total deformation. At a given vehicle

stand, if the elastic deformation is less than the previous deformation (w_o), the subsequent displacement will be a swell at the ground. If the previous deformation (w_o) can be matched to the elastic deformation, due the vehicle load, this vehicle can stand indefinitely without any sinkage what-so-ever. For a given residual settlement and vehicle load, the zero deformation condition can be established by adjusting the contact area and geometry of the track or standing platform.

For some soft soils, it is not possible to keep the deviator stress below (f_o). In these cases, the analysis must be based on a time-dependent deviator stress-strain relation. As on extreme example the deviator behavior will be considered as viscous.

$$\sigma_{ii} = 3K\epsilon_{ii} + 3\zeta \frac{\delta \epsilon_{ii}}{\delta t} \tag{23 a}$$

$$s_{ij} = 2\eta^* \frac{\delta e_{ij}}{\delta t} \qquad (s_{ij} > f_o) \tag{23 b}$$

The visco-elastic operators are:

$$R = 1 \tag{24 a}$$

$$S = 3K + 3\zeta \frac{\delta}{\delta t} \tag{24 b}$$

$$M = 1 \tag{24 c}$$

$$N = 2\eta^* \frac{\delta}{\delta t} \tag{24 d}$$

The displacement relation from equations (8) becomes:

$$\frac{\delta^2 w}{\delta t^2} + \frac{3K}{3\zeta + \eta^*} \frac{\delta w}{\delta t} = \frac{3K}{4\eta^* (3\zeta + \eta^*)} P \tag{25 a}$$

$$w(0) = 0 \tag{25 b}$$

The visco-elastic law is derived from a physical relationship in integral form. In order to convert to differential form, a second initial condition was built into the deformation relationship. Thus, equation (25 a) is a second order equation. One method of converting back to the integral relation consists of finding a visco-elastic model which is represented by equations (25). Since the volume change and deviator coupling is essentially a series coupling, the load-deformation model is as shown in fig. 6. The load-deformation relation is:

$$w(t) = \frac{1}{4\eta^*} \int_0^t P dt + \frac{3}{4(3\zeta + \eta)} e^{-t/T} \int_0^t P e^{t/T} dt \tag{26 a}$$

$$T = \frac{3\zeta + \eta^*}{3K} \tag{26 b}$$

For a given vehicle load (P) the deformation-time relation is:

$$w(t) = \frac{P}{4\eta^*} t + \frac{P}{4K}(1 - e^{-t/\tau}) \qquad (27)$$

As shown in fig. 7, the deformation increases with time, approaching a linear relationship.

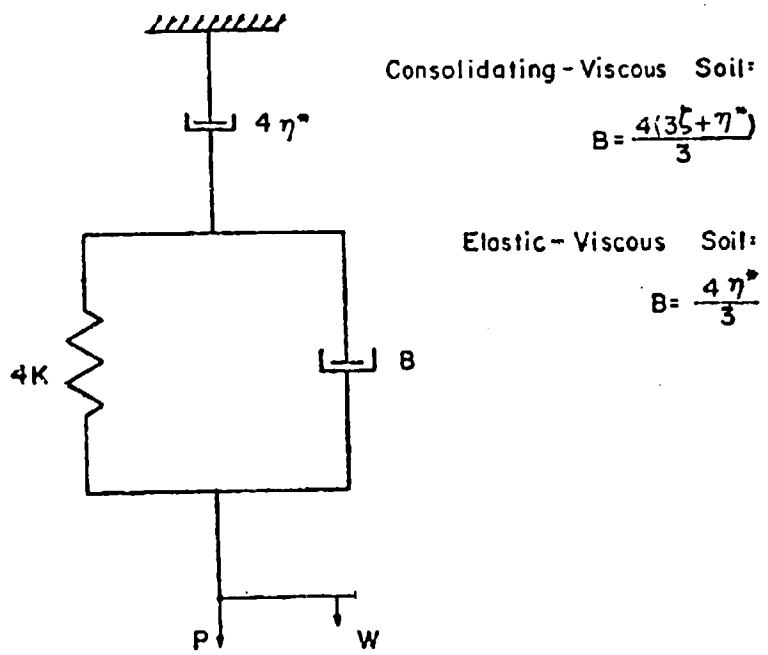


Fig. 6. — Load-deformation model.

From a design point of view, this relation indicates that for a given set of soil parameters, a given load and a given geometry of loaded area, the critical settlement with time can be established. Thus, the time of parking of a vehicle can be computed for field use.

The viscosity (η^*) is actually an apparent viscosity as indicated in fig. 4.

Moving vehicle. — The deformation-time analysis for a moving vehicle must include considerations of vehicle speed in addition to considerations of the soil properties and imposed stresses.

A high speed light vehicle will not develop any time-dependent volumetric stresses and will be in the range of elastic deviator stresses. The stress-strain relations for this type of activity are:

$$\sigma_{ii} = 3K\varepsilon_{ii} \qquad (28\,a)$$

$$s_{ij} = 2Ge_{ij} \qquad (28\,b)$$

The displacements will be instantaneous and elastic in direct proportion to the time of loading.

$$w(t) = \frac{3K_1 + 4G}{4G\,(3K_1 + G)}\,P(t) \tag{29}$$

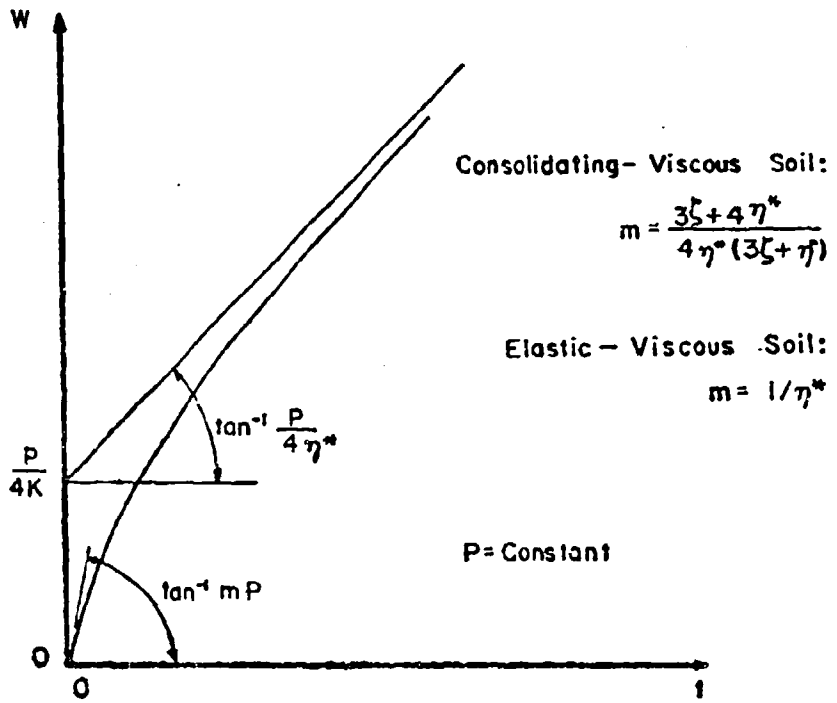


Fig. 7. — Deformation-time relation.

The same light vehicle for a relatively slow traverse of the ground will permit time dependent deformations in accordance with both the soil properties and the vehicle movement program.

$$\frac{\delta^2\sigma_{ij}}{\delta t^2} + \left(\frac{K_2}{\zeta_2} + \frac{K_1}{\zeta_1} + \frac{K_1}{\zeta_2}\right)\frac{\delta\sigma_{ij}}{\delta t} + \frac{K_2}{\zeta_1}\sigma_{ij}$$

$$= 3K_1\frac{\delta^2\epsilon_{ij}}{\delta t^2} + \frac{3K_1K_2}{\zeta_2}\frac{\delta\epsilon_{ij}}{\delta t} \tag{30 a}$$

$$s_{ij} = 2G\epsilon_{ij} \tag{30 b}$$

The visco-elastic operators are:

$$R = \frac{\delta^2}{\delta t^2} + \left(\frac{K_2}{\zeta_2} + \frac{K_1}{\zeta_1} + \frac{K_1}{\zeta_2}\right)\frac{\delta}{\delta t} + \frac{K_2}{\zeta_1} \tag{31 a}$$

$$S = 3K_1\frac{\delta^2}{\delta t^2} + \frac{3K_1K_2}{\zeta_2}\frac{\delta}{\delta t} \tag{31 b}$$

$$M = 1 \tag{31 c}$$

$$N = 2G \tag{31 d}$$

The basic load deformation equation is:

$$(3K_1 + G)\frac{\delta^2 w}{\delta t^2} + \left(\frac{3K_1K_2}{\zeta_2} + \frac{GK_2}{\zeta_2} + \frac{GK_1}{\zeta_1} + \frac{GK_1}{\zeta_2}\right)\frac{\delta w}{\delta t} + \frac{2GK_2}{\zeta_1}w$$

$$= \frac{3K_1 + 4G}{4G}\frac{\delta^2 P}{\delta t^2} + \left(\frac{3K_1K_2}{4G\zeta_2} + \frac{K_2}{\zeta_2} + \frac{K_1}{\zeta_1} + \frac{K_1}{\zeta_2}\right)\frac{\delta P}{\delta t} + \frac{K_2}{\zeta_1}P \tag{32 a}$$

$$w(0) = 0$$

The differential equation (32 a) can be represented by a five element visco-elastic model as shown in fig. 8. For this particular problem, the relation between the model parameters and the moduli and viscosities of the soil will not be developed, since they do not help the analysis.

The load-deformation-time relation for the five element model is:

$$w = \frac{P}{A_1} + \frac{1}{B_2}e^{-t/T_2}\int_0^t Pe^{t/T_2}\,dt + \frac{1}{B_3}e^{-t/T_3}\int_0^t Pe^{t/T_3}\,dt \tag{33 a}$$

$$T_2 = B_2/A_2 \tag{33 b}$$

$$T_3 = B_3/A_3 \tag{33 c}$$

A single passage of the load in time (t) results in a load-deformation relation as follows.

$$w = \frac{P}{A_1} + \frac{P}{A_2}(1 - e^{-t/T_2}) + \frac{P}{A_3}(1 - e^{-t/T_3}) \tag{34}$$

Thus, the vehicle passage will result in an instantaneous elastic deformation followed by additional viscous deformations. The longer the time of passage (the slower the vehicle) the greater the deformation. From the point of view of mobility, it can be seen, that a vehicle with a limiting deformation characteristic can be designed for a particular soil in terms of its time of passage.

The principles of design of a vehicle train can also be established by examining the five element model. The degree of relaxation of deformation is an exponential function of the speed and spacing between vehicles. For a given vehicle spacing and speed, the deformation will increase with length of train.

Using a limiting deformation as a design criteria, the number of vehicles can be increased by increasing their spacing.

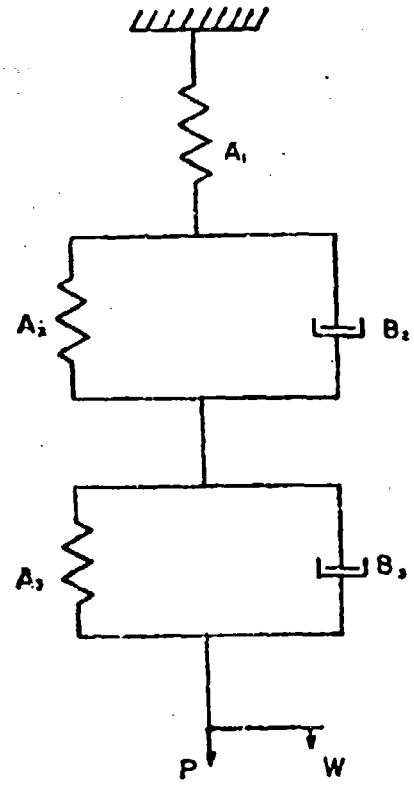


Fig. 8. — Five-element visco-elastic model.

Another consideration is the relatively high speed movement of a heavy vehicle over a soft soil. The volumetric stress-strain relation will be elastic while the deviator stress-strain relation can be considered to be viscous with an apparent viscosity (η^*).

$$\sigma_{ii} = 3K_1\varepsilon_{ii} \tag{35 c}$$

$$s_{ij} = 2\eta^* \frac{\delta \varepsilon_{ij}}{\delta t} \tag{35 b}$$

The operator relations are:

$$R = M = 1; \tag{36 a}$$

$$S = 3K_1; \tag{36 b}$$

$$N = 2\eta^* \frac{\delta}{\delta t} \tag{36 c}$$

The load-deformation differential equation then becomes:

$$\frac{\delta^2 w}{\delta t^2} + \frac{3K_1}{\eta^*}\frac{\delta w}{\delta t} = \frac{1}{\eta^*}\frac{\delta P}{\delta t} + \frac{3K}{4(\eta^*)^2}P \qquad (37\,a)$$

$$w(0) = 0 \qquad (37\,b)$$

The model which produces equation (37 a) is a three-element model similar to the one shown in fig. 6. The only difference is the value of the Kelvin dash-pot.

The deformation response of this model is:

$$w(t) = \frac{1}{4\eta^*}\int_0^t P\,dt + \frac{3}{4\eta^*}e^{-t/T}\int_0^t Pe^{t/T}\,dt \qquad (38\,a)$$

$$T = \eta^*/3K_1 \qquad (38\,b)$$

For a single traverse in time (t) the deformation becomes:

$$w(t) = \frac{P}{4\eta^*}t + \frac{P}{4K_1}(1 - e^{-t/T}) \qquad (39\,a)$$

$$\frac{\delta w}{\delta t}(0) = \frac{P}{\eta^*} \qquad (39\,b)$$

The relation in equations (39) is the same as shown in fig. 7 with a different magnitude of the initial slope.

As the load increases, the viscosity will decrease and the apparent viscosity (η^*) will drop very swiftly. As a result, the limiting design deformation will be approached exponentially with load and time of application. Thus, the mobility design must be balanced between load and speed. Higher loads will require greater speeds for a given deformation.

The effect of vehicle trains on the viscous portion of the deformation relation will be particularly pronounced. The first term of equation (39 a) indicates that the purely viscous portion of the deformation will never achieve recovery. Thus, successive vehicles in a train will impose linear increases on the deformation. The relaxation of the Kelvin unit will aid in the reduction of the total deformation, but it may not be enough to offset the large viscous deformations. As indicated previously, the proper train design will depend on the magnitude of the soil parameters and the balancing of the load and time of traverse.

By continuing the previous analysis, a vehicle load-deformation-time equation can be established for any combination of soil parameters. Furthermore, similar mobility design criteria can be established.

Conclusions

The foregoing analysis has attempted to develop rational relations for the soil parameters of importance in vehicle mobility, and to use the relations in terms of mobility design.

The mobility design was based on an assumed criteria, that the stresses imposed on the soil never reached the soil shear strength. This criteria was established since the achievement of shear strength by a single vehicle passage will remould the soil structure and thus make conditions of subsequent passage considerably less favorable.

The mobility design is a limiting deformation. Such a criteria can be established in terms of the type and desired speed of the vehicle.

The soil properties that have been established are:

1) The volume change behavior consists of an initial elastic deformation followed by a viscous delay, on loading. Unloading results in a partial elastic recovery followed by partial viscous recovery. Repeated load-unload cycles will increase the net deformation up to a deformation limit. Beyond the deformation limit, the soil will behave in a completely elastic manner.

2) The deviator behavior on loading consists of elastic behavior up to a yield stress (f_o). Beyond (f_o) the soil behaves as a shear thinning material with decreasing viscosity until shear failure is reached.

An analysis of load-deformation-time response for various conditions of loading, and soil conditions indicated the following:

1) The deformation of light vehicles when parked followed a Kelvin viseo-elastic relation. The deformation could be controlled to tolerable limits by altering the are and geometry of the loaded area. For soft soils this can be accomplished by using parking mats.

2) The deformation of heavy parked vehicles follows a Kelvin visco-elasticity augmented by a purely viscous deformation. In this case, deformation can only be controlled by restricting the time of parking. The maximum parking time is a function of the load and magnitude of the soil properties.

3) A light fast vehicle will impose only elastic deformations on the ground.

4) Heavy vehicles can be designed for a mobility criteria (maximum deformation), based on speed, load and magnitude of soil properties.

5) The design of vehicle trains depends on the balancing of the load and vehicle spacing to provide sufficient deformation recovery to satisfy the mobility criteria. Another design feature is the total deformation as a function of the number of vehicles in the train.

ACKNOWLEDGMENTS. — The work done in preparation for this paper has been supported by the Land Locomotion Laboratory, U. S. Army Ordnance Department under contract DA-30-069-ORD-2910 with Rensselaer Polytechnic Institute.

BIBLIOGRAPHY

1) Lee E. H. Stress analysis in visco-elastic bodies. Quarterly Applied Mathematics, 13, no. 2 July, pag. 183-190, 1955.

2) Radok J. L. M. Visco-elastic stress analysis. Quarterly Applied Mathematics, 15, no. 2 July, pag. 198-202, 1957.

3) Terzaghi K. Erdbaumechanik. F. Deuticke. Vienna, 1925.

4) Thomson W., (Lord Kelvin). Elasticity. Encyclopaedia Britannica, 9th Ed., 3, pag. 1-112.

5) Schiffman R. L. The use of visco-elastic stress-strain laws in soil testing. Soils-1959, Meetings, ASTM, STP, no. 254, pag. 131-155, 1959.

6) Burgers J. M. Model systems, phenomenological theories of relaxation and of viscosity, first report on viscosity and plasticity. Acad. of Sciences, Amsterdam. The Netherlands, pag. 30, 1935.

7) Bridgman P. W. Rough compressibilities of fourteen substances to 45,000 Fg/cm². Proc. Amer. Acad. Arts and Sciences, 72, pag. 207-255. 1938.

8) Seed H. B. and McNeill R. L. Soil deformations under repeated stress applications. Conference on soils for engineering purposes, Mexico City, ASTM, STP, no. 232, pag. 177-196, 1957.

9) Murnaghan F. D. Finite deformation of an elastic solid. John Wiley & Sons, Inc., N. Y., 1951.

10) Geuze E. C. W. A. and Tan T. K. The mechanical behavior of clays. Proc. Second International Conference on Rheology, Academic Press, N. Y., pag. 247-259, 1954.

11) Geuze E. C. W. A. and Tan T. K. The shearing properties of soils. Geotechnique, 2, no. 2, pag. 141-161, December 1950.

12) Geuze E. C. W. A Laboratory investigation including compaction tests. Improvement of soil properties, Proc. Third International Conference on soil mechanics and foundation engineering, 3. pag. 119-121, 1953.

13) Tan T. K. Investigations on the rheological properties of clays. PH. D. Thesis, Delft Technological University, the Netherlands, 1954.

14) Tan T. K. Structure mechanics of clays. Academic Sinica Inst. Civil Engineering and Architecture, Harbin, China, 1957.

15) Josselin De Jong G. and Geuze E. C. W. A. A capacitive cell apparatus. Proc. Fourth International Conference on Soil Mechanics and Foundation Engineering, 1, pag. 52-55, 1957.

16) Huefeli R. Creep problems in soils. Show and Ice Proc. Third International Conference on Soil Mechanics, and Foundation Engineering, 3, pag. 238-251, 1953.

Effects of remolding on soil values *) related to vehicle mobility

Effetti degli assestamenti sulle caratteristiche del suolo in relazione alla mobilità del veicolo

LOUIS J. GOODMAN **) - CHARLES N. LEE ***)

ABSTRACT. — *This paper summarizes the current results of a research study in progress to evaluate the effect of remolding of cohesive soils on stress-strain relationships embracing the two areas of wheel or track sinkage and slippage. Experimental equipment and procedures used to obtain load sinkage and horizontal shear soil values are described. Some thixotropic characteristics and an evaluation of vertical load and horizontal shear values proposed for use in soil-vehicle relationships are included.*

Experimental data to date show a marked reduction in the spread of cohesive and frictional moduli of soil deformation from remolding. Remolding also causes a decrease in these values, with subsequent increase noted with increased time after remolding. On the other hand, there seems to be no significant thixotropic regain of soil resistance to sinkage in the plastic flow range. Some discussion on preliminary horizontal shear observations and a comparison of sinkage from a rigid wheel in both undisturbed and remolded cohesive soil are presented.

Introduction

The need for more basic research on the ground properties which affect vehicle performance has been emphasized by experience with cross-country locomotion. Basically, the problem is to determine what types and conditions of natural surfaces can be used by various types of vehicles for a successful operation. An answer must also be provided for the number of these movements that can be successfully realized.

Among the difficulties encountered by land vehicles operating on various natural surfaces are the following:

1) Wheel or track slippage caused by combinations of insufficient shearing strength of the soil and vehicle characteristics.

2) Wheel or track sinkage due to the physical characteristics of both the soil and the vehicle.

---

*) This paper was originally prepared for Land Locomotion Laboratory, U. S. Army Ordnance Tank Automotive Command, Detroit, Michigan.

**) Associte Professor of Civil Engineering, Syracuse University Syracuse, New York.

***) Assistant Professor, New York State University, College of Forestry Syracuse, New York.

Much fundamental and applied research data are needed to determine and evaluated the various factors which influence the physical properties of soil affecting these vehicle actions. A possible outcome from these studies might be the use of soil mechanics criteria as a partial basis for vehicular design insofar as mobility in various « off-road » conditions is concerned.

M. G. Bekker emphasized that a solution to the mobility problem requires determination of stress-strain relationships of soil, with the vertical type of deformation relating to sinkage and the horizontal to slippage [1-2-3]. Based on this treatment of the problem, Bekker proposed that the following physical values be used to describe soil from the trafficability point of view:

1) *Vertical load values*

a) Frictional modulus of deformation . . . . . k_ϕ
b) Cohesive modulus of deformation . . . . . k_c
c) Exponent of sinkage . . . . . n

2) *Horizontal shear values*

a) Angle of internal friction . . . . . Φ
b) Cohesion c
c) Coefficients of slippage . . . . . k_1, k_2

Subsequent experimental work on artificial soils and snow by the Land Locomotion Research Branch of Detroit Arsenal [5-6] indicated that the proposed system as a whole was suitable for mobility studies and merited further study. A review of soil phenomena shows several factors that affect these characteristics, such as degree of remolding, water content, colloidal phenomena, rate of shear, etc. For example, remolding causes a pronounced reduction in strength and an increase in deformation tendencies for the majority of natural saturated clay deposits. If, however, a sample of remolded saturated clay is allowed to stand without further disturbance and without change in water content, it may regain part of its original strength and stiffness through a phenomenon known as « thixotropic regain » [7].

The purpose of this paper is to report on the findings of a beginning research effort to determine the effect of various degrees of remolding, such as might be realized from the actions of traversing vehicles, on Bekker's soil-vehicle parameters. The report is confined to preliminary results obtained from tests on both lacustrine and marine clay specimens, with special attention given to load sinkage at this time.

Sinkage and shear determinations have been made on these soils in both undisturbed and remolded states to ascertain and evaluate the full impact of remolding on the proposed vertical and horizontal soil values. Testing rates between dynamic and static have been used in an attempt to simulate field conditions. Thixotropic characteristics are also discussed.

Experimental program

Much of the work to date has been concerned with the load sinkage problem in soft to medium lacustrine clays. Some preliminary work has also been done with respect to horizontal shear considerations and determinations of different degrees of disturbance between undisturbed and completely remolded states.

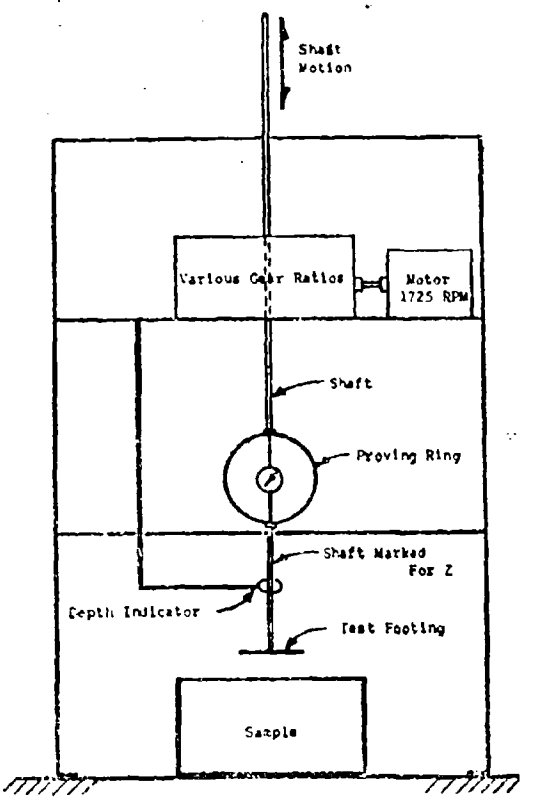


Fig. 1. — Load-sinkage test device.

Soil types. — The soil types used for the testing to date have been soft to medium lacustrine clays obtained from the general Syracuse area. Experimental work on a marine clay obtained from Boston, Mass. (Boston Blue Clay) is currently underway. The index properties of the clays used are shown in table 1.

Load sinkage. — A diagram of the test apparatus used in this part of the investigation is shown in fig. 1. Soil values k_c, k_ϕ and n have been obtained

from the following semi-empirical stress-strain relationship for vertical soil deformation proposed by Bekker [1,2]:

$$p = \left(\frac{k_c}{b} + k_\phi\right) z^n$$

where:

- p = the vertical unit load (psi)
- k_c = the « cohesive modulus » of soil deformation (lb/in^{n+1})
- k_ϕ = the « frictional modulus » of soil deformation (lb/in^{n+2})
- z = the vertical sinkage corresponding to p (in)
- b = the width of a rectangular footing or the radius of a circular footing (in)

TABLE I. — *Classification characteristics of soils investigated.*

Soil designation	Source	Mechanical analysis			Atterbergs		Natural water content	Unconfined comp. str.		Sensitivity	Description
		% Sand	% Silt	% Clay	L.L.	P.I.		Undisturbed	Remolded		
A	J. I. Case	0	42	58	55	31	45 ÷	0.88	0.18	4.9	Silty clay
B	J. I. Case	10	66	24	26	5	26 ÷	0.79	0.21	3.76	Clayey silt with trace sand
C	J. I. Case	6	55	39	32	13.9	29 ÷	—	—	—	Clayey silt with trace sand
D	Bongiovanni	0	72	28	21.3	2.7	25 ÷	0.75	0.2	3.8	Clayey silt
E	De Ruyter	0	67	33	30	12.4	27 ÷	2.5	0.3	8.3	Clayey silt
F	Boston	12	40	48	35.3	13.9	26 ÷	0.44	0.02	22.0	Silty clay with trace sand

Notes: L.L. = Liquid limit. P.I. = Plasticity index. Unconfined compressive strength - in tons per sq. ft. Soil C is a mixture of soils A and B.

Two successive load-sinkage tests are made with two different test footings and the values of pressure (p) and sinkage (z) are plotted on logarithmic paper, using p as the abscissa and z as the ordinate. The exponent (n) is obtained directly from the logarithmic plot, where n is the slope of the curves. The moduli of deformation are calculated from Bekker's equation as follows:

$$k_\phi = \frac{a_2 b_2 - a_1 b_1}{b_2 - b_1}$$

$$k_c = \frac{(a_1 - a_2)\, b_1 b_2}{b_2 - b_1}$$

where b_1 and b_2 are the widths of rectangular footings or radii of circular footings, and $a_1 = (k_c/b_1 + k_\phi)$ and $a_2 = (k_c\, b_2 + k_\phi)$. a_1 and a_2 are equal to

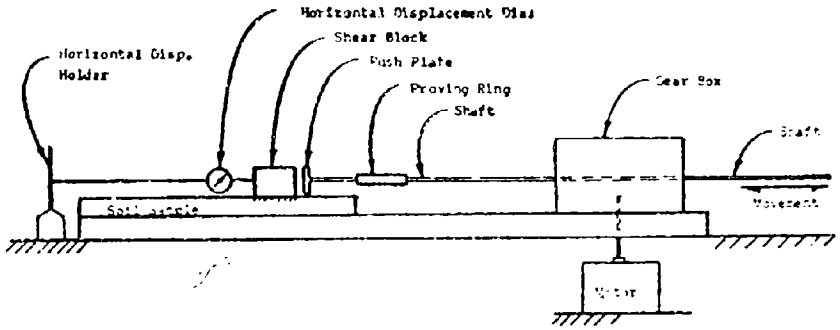


Fig. 2. — Horizontal shear test device.

the pressure for 1.0 inch sinkage of the smaller and larger size test footings, respectively.

Much of the work to date has been with test footing diameters of $\frac{3}{4}$ inch and 1 inch since preliminary experimental data indicated that a ratio of soil sample diameter to test footing diameter of 5 or 6 to 1 was necessary to eliminate side effects. It is possible to use a specimen size of 6 inches in diameter by 12 inches high with these footing sizes, thereby facilitating the field work in securing undisturbed samples. Test footings of $1\frac{1}{2}$ inches and 2 inches diameter have also been used with 1 cubic foot soil samples.

The penetration realized in the load sinkage tests is between 3 and 4 inches since bottom effects in the soil sample with a height of 12 inches seem to become apparent beyond this limit.

Experimental work has been carried out with constant rates of downward penetration which have been varied between 0.9 inches per minute and 2.25 inches per minute. The rate of vertical movement of the test footings used in the majority of the load sinkage runs has been 2.25 inches per minute.

Horizontal shear. — A diagram of the test apparatus used in this part of the investigation is shown in fig. 2.

A 3 inch × 3 inch shear plate has been used in this phase of the investigation which includes tests with both the horizontal shear device developed for this work and the standard laboratory direct shear machine. Much of the work with the horizontal shear device has been at a constant rate of shearing displacement of 2 inches per minute, with a fin spacing on the shear block of 9/16 inch and a fin depth and thickness of 0.125 inch and 0.025 inch respectively. Shear plates and fin designs of different shapes and sizes are currently being investigated using a forward motion varying between 1 and 4 inches per minute.

Different degrees of remolding. — Preliminary work on evaluating soil disturbance has been accomplished by means of passing a rigid wheel over the surface of a bed of clay. The present procedure is to make passes on both an

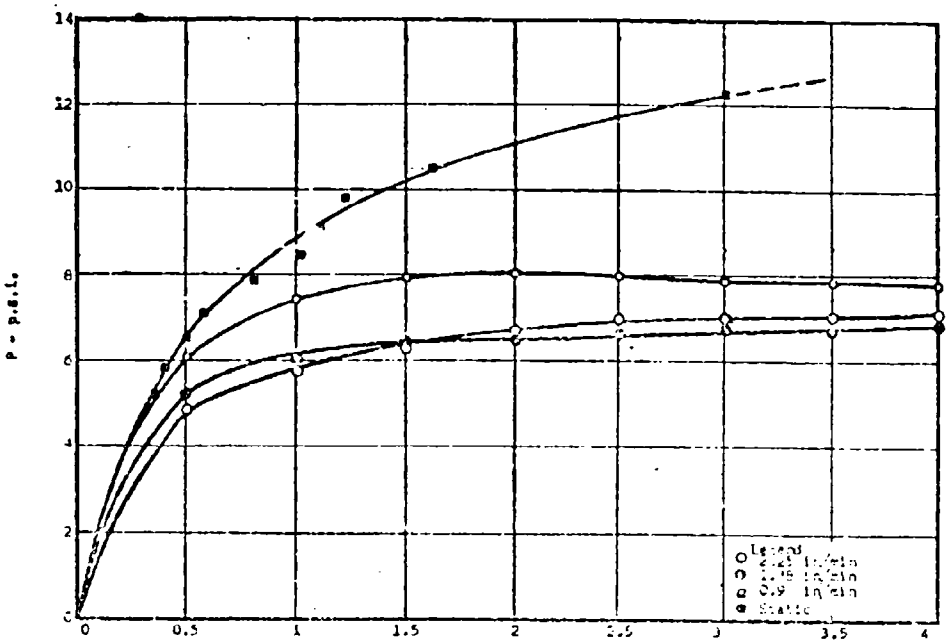


Fig. 3. — Sinkage-in. Load sinkage curves - Various rates of penetration. Clay A Remolded 0 time regain - 1" footing.

undisturbed and a remolded sample using a constant travel path and measuring the sinkage after each pass. These sinkage values are being evaluated for possible use as criteria for remolding by comparing the remolded and undisturbed sinkage patterns.

Discussion of results

Soil types. — Lacustrine clays are lake deposits and generally consist of alternate relatively thin strata of silt and clay. Deposition was such that these soils are often quite erratic with respect to homogeneity of composition in a vertical direction. This was found to be the case with Clays B and D in that the undisturbed specimens contain variable layers of silt, which would account for some of the erratic results obtained in the undisturbed state. Remolding has a homogenizing effect, which would tend to produce more uniform experimental data.

Clay deposits of marine origin are as a rule much more uniform in composition than lake deposits and are expected to give less variation in test results than those obtained on the lacustrine samples.

Effect of rate of sinkage. — In order to ascertain the effect of the rate of penetration on the soil values k_c, k_ϕ, and n, a series of sinkage tests was conducted on a soil sample (completely remolded Clay A), at different rates of

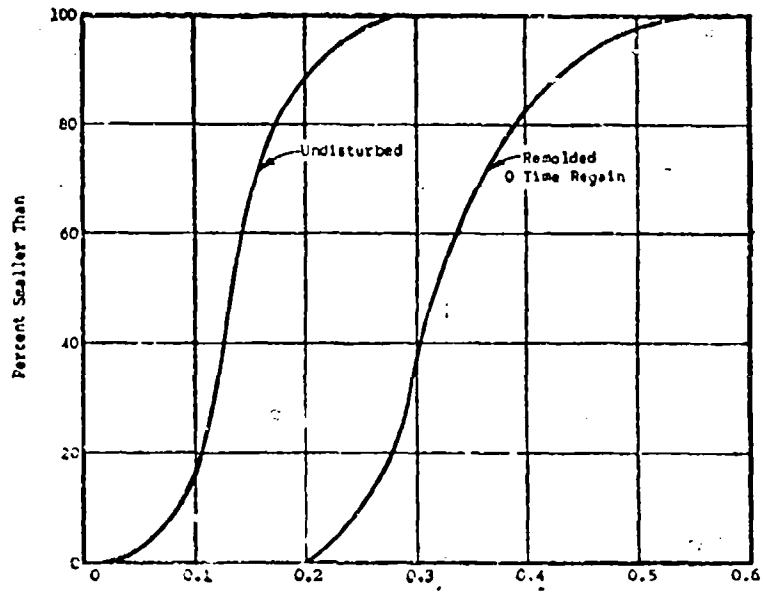


Fig. 4. — Cumulative Distribution Function of n - Clay B.

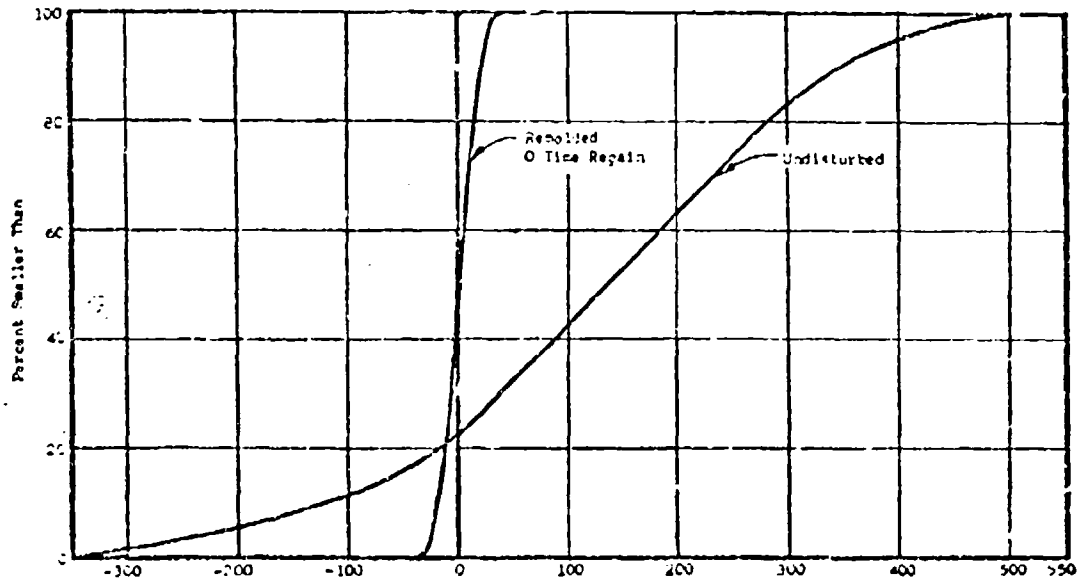


Fig. 5. — Cumulative Distribution Function of k_o - Clay B.

penetration. Test rates studied were static (with small load increments applied allowing for sinkage equilibrium between each increment), 0.9 in/min., 1.38 in/min., and 2.25 in/min. Typical pressure (p) vs. sinkage (z) curves are shown in fig. 3 where it can be seen that, except for the static case, the effect of the rate of penetration is not significant. It is therefore believed that for the study of mobility problems, soil values determined from an arbitrary rate of penetration other than static can be used.

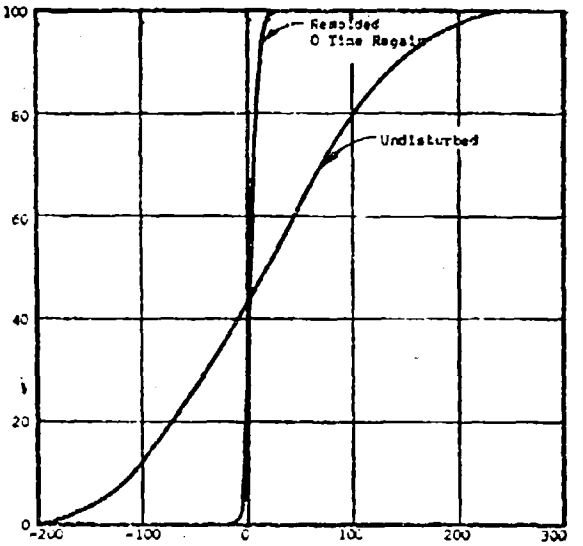


Fig. 6. — Cumulative Distribution Function of k_c - Clay B.

Effect of remolding on soil values in sinkage. — To determine the effect of remolding on the values of k_ϕ, k_c, and n, two general series of tests were conducted with lacustrine clay samples, one in the undisturbed state and the other in a completely remolded state. Values for both undisturbed and remolded states are shown for Clay B in figs. 4, 5 and 6 as cumulative distribution functions where it can be noted that the data follow fairly close to a normal distribution. These figures show the most significant effect of remolding to be a reduction in the dispersion of the values of k_ϕ and k_c which is felt to be a result of the homogenizing effect of the type of remolding used in the testing. Remolding also reduces the value of the mean for k_ϕ and k_c and increases the value for n, which is probably due to the removal of variable resistance to penetration from stratification or other non-homogeneous effects present in the undisturbed state. Recently obtained data on Boston Blue Clay specimens (Clay F) exhibit similar characteristics.

These observations suggest that, in predicting vehicle preformance in a given location, the soil values must be determined for the soil in the most critical condition expected from traffic types and amount.

Thixotropic regain of soil values in sinkage. — Results of tests on Clay A after complete remolding show that the value of n remains essentially constant with time while both k_c and k_ϕ increase with time, as shown in fig. 7. The increasing trend was more significant for the cohesive parameter k_c which is to be expected in this type of soil.

Thixotropic regain in plastic resistance in sinkage. — In the equation $p = (\frac{k_c}{b} + k_\phi) z^n$ suggested by Bekker, n is a positive number which

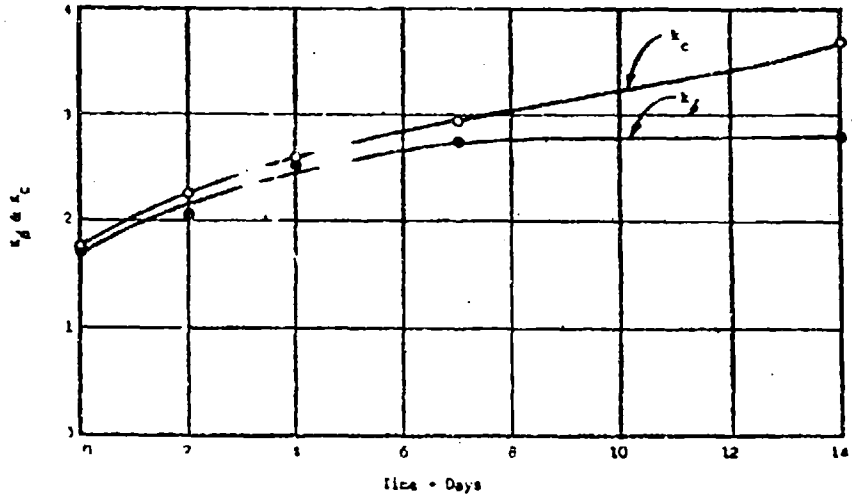


Fig. 7. — Thixotropic regain curves k_c and k_ϕ - Caly A.

implies that, for a given soil, p increases indefinitely with z. This relationship has been observed by other investigators in many cases whereas in the tests conducted with clays in this program, it was observed that p does increase with z at only low values of z. At larger values of z in the non-static rates of loading, penetration was observed to take place at a constant value of p Fig. 3 shows families of p vs. z curves, where it can be noted that p is practically constant for z larger than about 1 or 2 inches. Beyond this range, the soil is probably in plastic flow. It is believed that, in the study of large sinkage in clayey soils, the relationship between p and z for plastic flow will be of interest.

To study the thixotropic regain of the value of p for plastic flow, two initial series of tests were conducted, one with Clay A and the other with Clay C. The observed values of p for plastic flow are shown in figs. 8 a and 8 b. The dashed lines in these figures have been determined by the method of least squares and show a regain trend of the value of p in the plastic flow region. However, it is emphasized that no significance should be attached to this trend at this time in view of the wide scatter of points. A similar plot for Clay F is shown in fig. 8 c.

It is interesting to note that although there are increases of k_s and k_c with time and therefore changes in the shape of the p vs. z curves, the values of p at large z remain statistically unchanged:

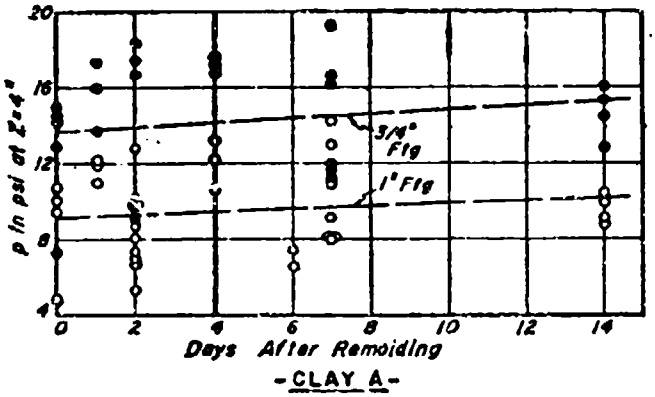


Fig. 8a. — Thixotropic regain of plastic resistance to sinkage.

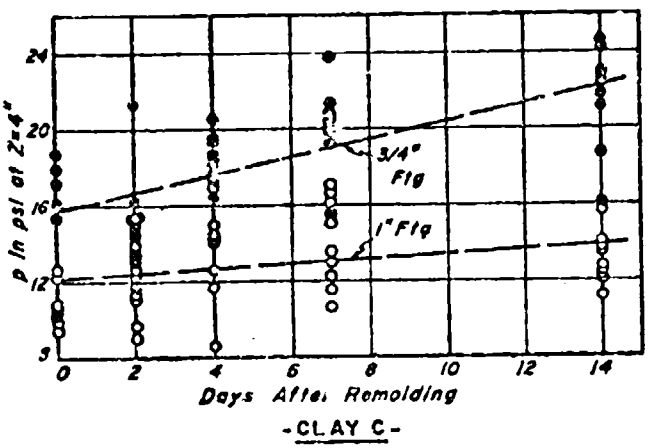


Fig. 8b. — Thixotropic regain of plastic resistance to sinkage.

Horizontal shear. — Preliminary tests show that unless the shear plate is properly seated in the clay specimen, considerable « bulldozing » action and also some tendency of the shear plate to submarine into the clay results. In order to reduce the heavy normal loads required for an adequate seating, experiments with various fin spacings and depths were undertaken. Results of these experiments show that a 3 inch square shear plate will properly seat itself in remolded clay specimens under low normal loads when the fin spacing is 9/16 in. and the fin depth and thickness is 0.125 in. and 0.025 in. respectively. Observations indicate that further refinements can be made that should give

test results in close accord with values related to actual track and tire prototypes.

Horizontal shear tests run with a 3" ×3" shear block on remolded samples indicate that disturbance takes place ahead of the block for a distance of approximately 1-½ inches when the peak condition for stress occurs. This means that an increase in shear area of about 50 % in excess of that from the block itself is necessary when evaluating values of c and Φ. Values computed using the 50 % additional shear area check out reasonably well with the c and Φ values obtained from direct shear tests on the same soil.

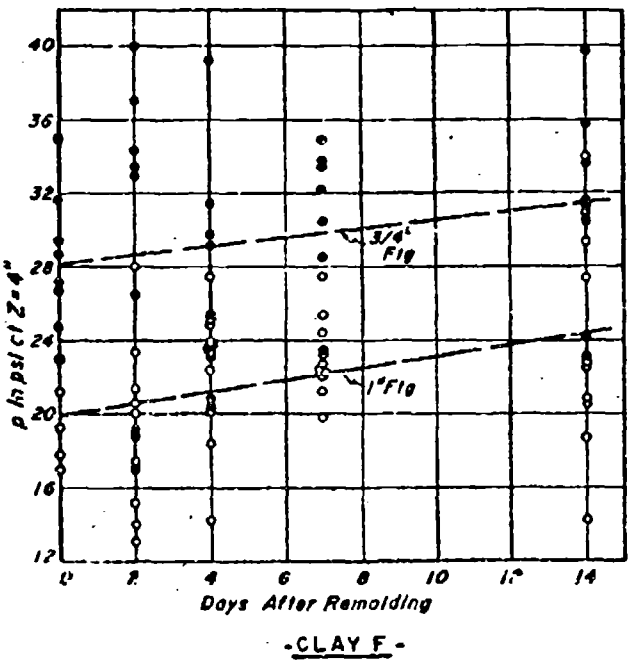


Fig. 8c. — Thixotropic regain of plastic resistance to sinkage.

Different degrees of remolding. -- The results of this phase of the investigation are inconclusive as yet. Fig. 9 shows the effect of the number of passes of a rigid test wheel on Clays B and F in both remolded and undisturbed states. Fig. 10 shows the relationship between the number of passes of the rigid wheel and resulting sinkage for thixotropic regain considerations for Clay F.

Much more experimental and theoretical work is needed in this area to determine not only a measure of the degree of disturbance, but also a mapping of the influence of various wheel and track shapes and traversing patterns under expected traffic loads and frequency.

test results in close accord with values related to actual track and tire prototypes.

Horizontal shear tests run with a 3" ×3" shear block on remolded samples indicate that disturbance takes place ahead of the block for a distance of approximately 1-½ inches when the peak condition for stress occurs. This means that an increase in shear area of about 50 % in excess of that from the block itself is necessary when evaluating values of c and Φ. Values computed using the 50 % additional shear area check out reasonably well with the c and Φ values obtained from direct shear tests on the same soil.

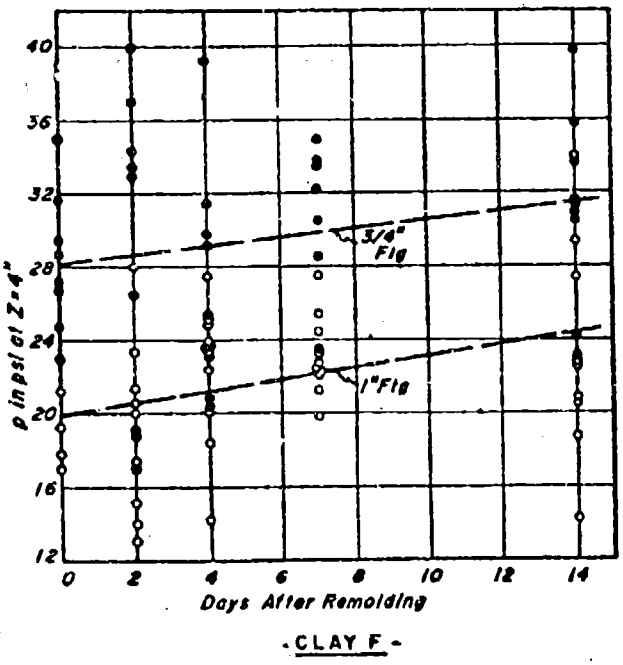


Fig. 8c. — Thixotropic regain of plastic resistance to sinkage.

Different degrees of remolding. — The results of this phase of the investigation are inconclusive as yet. Fig. 9 shows the effect of the number of passes of a rigid test wheel on Clays B and F in both remolded and undisturbed states. Fig. 10 shows the relationship between the number of passes of the rigid wheel and resulting sinkage for thixotropic regain considerations for Clay F.

Much more experimental and theoretical work is needed in this area to determine not only a measure of the degree of disturbance, but also a mapping of the influence of various wheel and track shapes and traversing patterns under expected traffic loads and frequency.

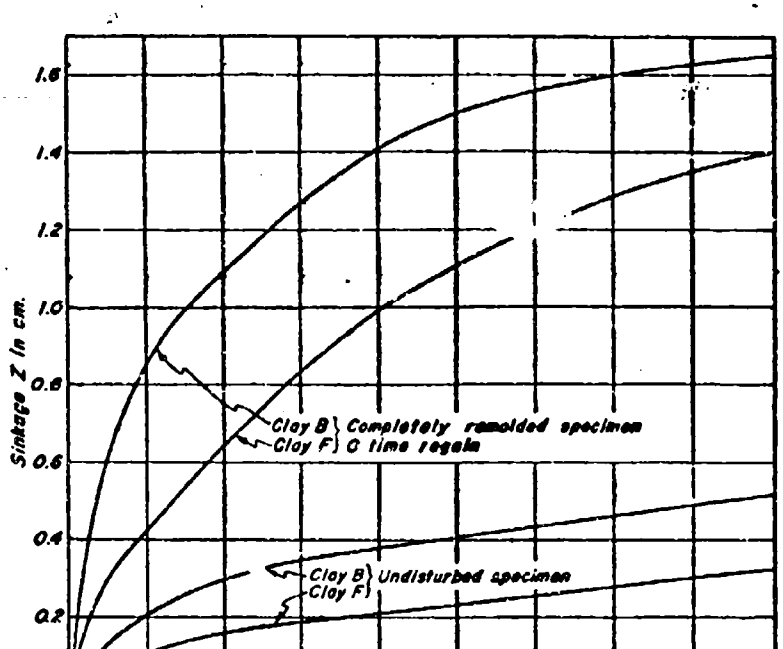


Fig. 9. — Effect of wheel travel on sinkage.

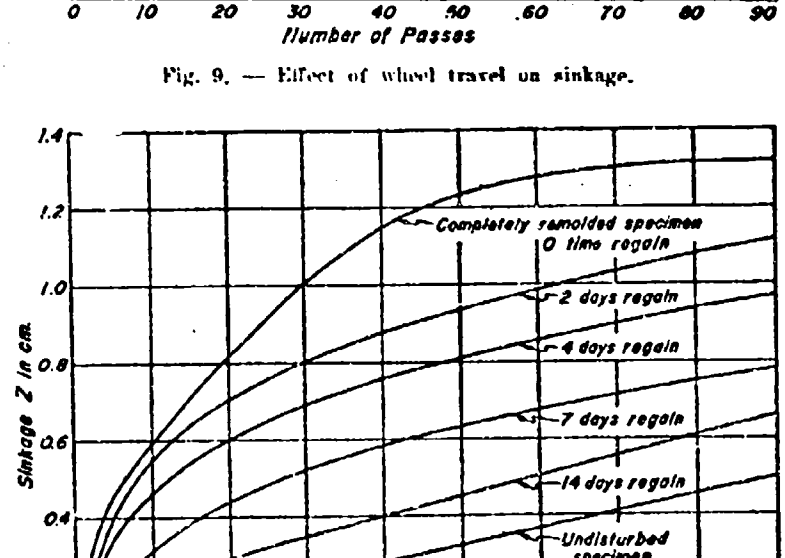


Fig. 10. — Effect of wheel travel on sinkage in Boston blue clay (clay F).

Closing remarks

The preceding discussion points out the fact that present results and analyses along the lines discussed in this paper are preliminary in nature and therefore inconclusive in many respects. As a result, additional investigations are needed to substantiate and refine the results of these preliminary studies and to establish and evaluate new relationships.

Some of the research plans for the immediate future include additional experimental and analytical work on both undisturbed and partially disturbed specimens of soft to medium clay. For example, a study of the progression of the degree of disturbance as caused by the shape, size, number of passes and tracking patterns of a disturbance wheel is needed. Also, thixotropic regain data for the various degrees of disturbance and with controlled time intervals in the range expected from various types of traffic is desirable.

The influence of the size of soil loading devices on soil value measurements must also be determined. This type of study should consist of the compilation of experimental data using various test footing and shear device sizes and shapes for both load sinkage and shear experimental work.

Finally, it should be stated that observations of experimental load sinkage relationships to date demonstrate that another area requiring immediate attention is an investigation on the plastic behavior of soils in mobility problems. The primary objective of such a study should be to develop a theory of plasticity for soils to be used in land locomotion mechanics.

ACKNOWLEDGMENTS. — This paper describes a research study in progress at Syracuse University which is sponsored by the Land Locomotion Laboratory of the Detroit Arsenal, Detroit, Michigan.

The authors express appreciation to Dr. Paul J. Brennan, Chairman, and Dr. Wen H. Li, Professor in the Department of Civil Engineering, and to personnel of the Land Locomotion Laboratory Detroit Arsenal, especially Col. M. G. Bekker and Capt. R. A. Liston for their interest and cooperation in this study.

Recognition is also given to Artinr Banazek and Sener Soyer, Graduate Students in the Department of Civil Engineering for their assistance on the project.

BIBLIOGRAPHY

1) Bekker M. G. A practical outline of the mechanics of automotive land locomotion. Detroit Arsenal, Land Locomotion Research Laboratory, June 1955.

2) Bekker M. G. A proposed system of physical and geometrical terrain values for the determination of vehicle performance and soil trafficability. Vehicle Mobility Symposium sponsored by the office of Ordnance Research and held at Stevens Institute of Technology, 18-20 April 1955. Repriated in Land Locomotion Research Report No. 4, 1956.

3) Bekker M. G. Theory of land locomotion. University of Michigan Press, Ann Arbor, 1956.

4) Taylor D. W. Fundamentals of soil mechanics. John Wiley and Sons, Inc., New York, 1948.

5) Hanamoto B. Artificial soils for laboratory studies in land locomotion. Ordnance Corps, Land Locomotion Research Branch, Research and Development Division, Ordnance Tank-Automotive Command, 15 November 1957.

6) Weiss S. J., Harrison W. L. Aborca Lt. L. C. and Bekker M. G. Preliminary study of snow values related to vehicle performance. Technical Memorandum M-02, Detroit Arsenal, Land Locomotion Research Laboratory, September 1956.

7) Mitchell, James K. Fundamental aspect of thixotropy in soils. Proceedings of the American Society of Civil Engineers, vol. 86, No. SM3, June 1960.

8) A soil value system for land locomotion mechanics. Department of the Army Ordnance Tank-Automotive Command, Research and Development Division, Land Locomotion Research Branch, Report No. 5, December 1958.

9) Harrison W. L., Janosi Z., Capt. Liston R. A., Capt. Lodewick L. S. Mobility studies. Ordnance Tank-Automotive Command, Detroit Arsenal, Centerline, Michigan, Report No. 59, December 1959.

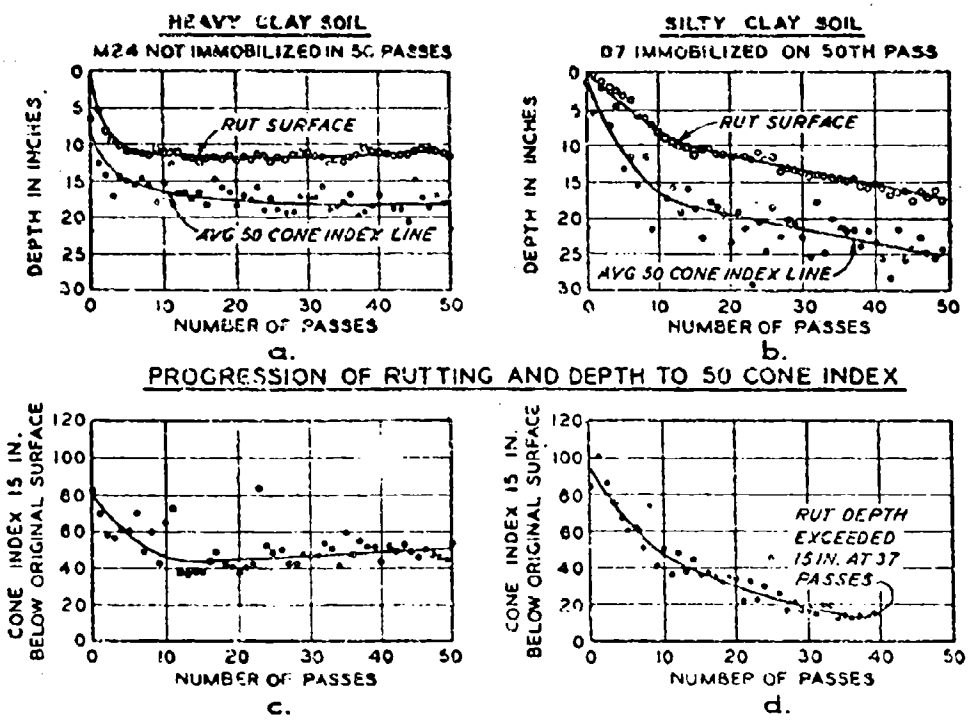
DISCUSSIONS

S. J. KNIGHT, A. A. RULA. — The Authors present the preliminary results of a study to determine the effect of various degrees of remolding, such as might be realized from the actions of traversing vehicles, on Bekker's soil-vehicle parameters. They demonstrate remolding to be extremely effective in altering the in-situ values of k_ϕ, k_c, and n, and suggest that « in predicting vehicle performance in a given location, the soil values must be determined for the soil in the most critical condition expected from traffic type and amount ». The Authors obviously have an appreciation of the importance of remolding in off-road locomotion, and it is hoped that they will pursue the experimental and theoretical research they recognize as being needed in this area.

In its early efforts to establish vehicle-soil relations by empirical means, the U. S. Army Engineer Waterways Experiment Station circumvented the remolding problem by testing vehicles on soils which had been substantially remolded by construction methods. However, in 1949, when the studies were extended to natural soils, the remolding problem had to be faced. Some insight into the process of soil remolding under actual vehicles may be gained from the following review of some of the results obtained from these early tests. Details may be found in WES Technical Memorandum No. 3-240, Tenth Supplement, « Trafficability of Soils, Tests on Natural Soils with Self-Propelled Vehicles, 1949 and 1950 ».

Typical curves that illustrate the effects of remolding under vehicle traffic on two natural fine-grained soils are shown in figure 1. Figure 1a illustrates the action of an M24 tank on a soft heavy clay (CH) *) soil which did not remold readily, while figure 1b shows the results of a D7 operating on a silty clay (ML) *) soil which was initially higher in strength than the heavy clay soil, but which did remold readily. In both cases the vehicle traveled forward, then backward, in the same path. In the test on the heavy clay, considerable rutting occurred early, as is generally the case in soft soils; but after 10 passes no further rutting occurred. This is evident in the curve labeled « rut surface », which, in fact, began to rise slightly at 25 passes. The isopleth for 50 cone index (see paper No. 24 for definition of cone index) is closely parallel. It indicates a softening of the soil early in the test but no further softening beyond about 15 passes. The two practically horizontal curves are indicative of a stable, balanced condition of vehicle and soil. The M24 tank completed 50 passes on the heavy clay and could have completed many more.

*) Classification according to the Unified Soil Classification System.



SOIL DATA FOR 6- TO 12-IN. DEPTH

	LL	PL	PI	USCS CLASS	WATER CONT- %	DENS LB/CU FT	CONE INDEX
HEAVY CLAY	61	23	38	CH	37.8	73.3	51
SILTY CLAY	37	25	12	ML	34.6	83.3	98

Fig. 1. — Effect of repetitive traffic on soil strength: a) progression of rutting and depth to 50 cone index, heavy clay soil; b) progression of rutting and depth to 50 cone index, silty clay soil; c) change in cone index at 15 in. below original surface, heavy clay soil; d) change in cone index at 15 in. below original surface, silty clay soil.

Figure 1 b shows that the D7 tractor began travel on a relatively high cone index (98 in the 6- to 12-in. layer), but traffic repetitions resulted in continued softening of the soil and progressively deeper ruts. As the rut surface descended, so also did the zone of remolding. The downward trend of the two curves might have been expected to indicate the immobilization which did occur on the 50th pass.

Figures 1 c and 1 d show plots of the variation in cone index at a depth 15 in. below the original ground surface for the same tests. For the heavy clay soil, figure 1 c, the curve descends for the first 13 passe, but then it continues with a slight rise as the number of passes increases. This indicate a rapid, but brief, strength loss to 13 passes and an actual slight increase in soil strength beyond 13 passes. Figure 1 d shows that cone index decreased progressively until 37 passes,

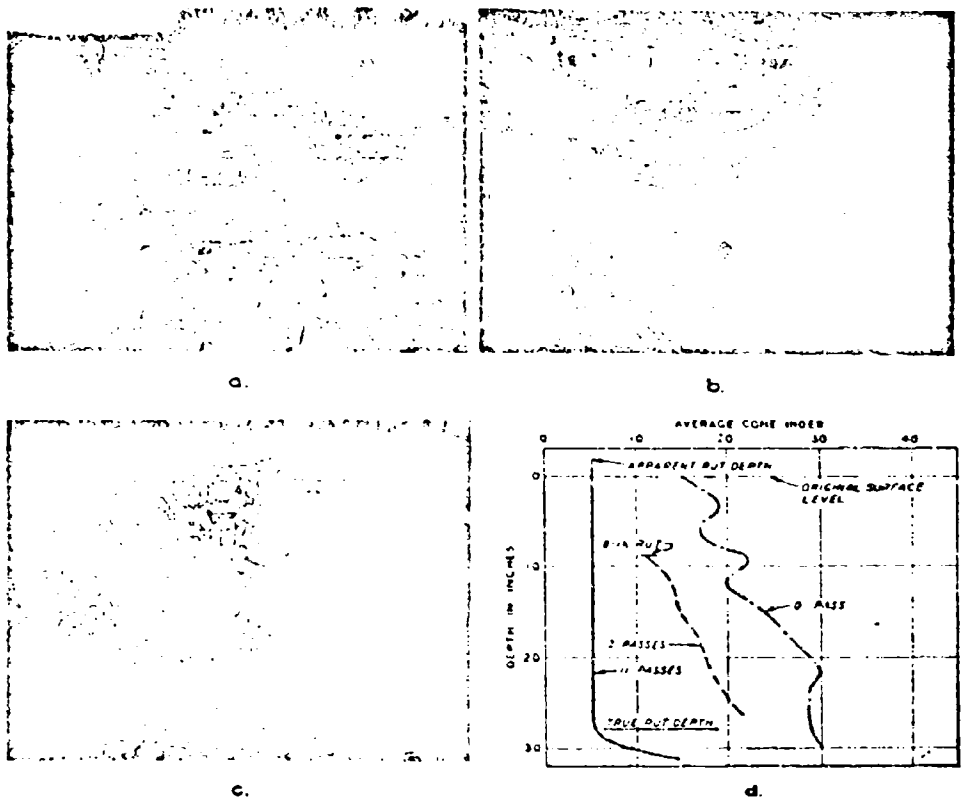


Fig. 2. — Remolding of wet sandy clay soil under the airoil: a) before traffic; b) after 3 passes; c) after 10 passes (airoil immobilized on 11th pass); d) cone index profiles.

at which time the ruts were 15 in. deep. The difference in behavior of these two soils is clearly evident in these contrasting curves.

The following general observations regarding remolding resulted from the 1949-1950 test programs. They have been verified by subsequent testing.

a) Practically any fine-grained soil, if sufficiently wet, will lose a portion of its strength when remolded under the action of vehicular traffic.

b) Wet, heavy (highly plastic) clay usually retains a high percentage of its strength, while wet, lean clay and silty clay may lose a high percentage of their original strengths. Many examples are available to show that silty soils can be weakened to only 30 % of their original strength. In such cases the remolding of the soil is accomplished so rapidly that a vehicle usually cannot negotiate even one pass across an area.

c) Even coarse-grained soils which contain as little as 10 % fine-grained material can be remolded or liquefied by the action of vehicles if the moisture content is high.

d) In order to predict vehicle performance successfully, the amount of remolding

to be encountered must be anticipated. (This is substantially the conclusion reached by Goodman and Lee).

Figure 2 is a pictorial illustration of remolding encountered in a recent Waterways Experiment Station test. The machine used was an Airoll, a test platform developed by the Borg-Warner Corporation for the U. S. Navy. Rubber bags (inflated to 8 psi in this test) are attached to chains which girdle the driving sprocket and idler similar to the track of a conventional vehicles. The machine weighs 19,000 lb and exerts an average ground pressure of only 1.9 psi on the projected track area. Figure 2 a shows the area before the test. Note the free water on the surface and that the personnel have no particular difficulty in walking over the area. Figure 2 b shows the test path after three passes of the Airoll. Note the saw-toothed pattern that has been formed on the surface. In figure 2 c repetition of traffic (10 passes) has remolded the soil in the path of the Airoll to near-liquid characteristics. On the next pass (the 11th) the Airoll became immobilized. Figure 2 d shows the cone index profiles corresponding to the three preceding figures.

W. L. HARRISON. — In answer to the previous comments, I wish to stress that Prof. Goodman's studies are directed towards the effect of remolding on the strength characteristics of soil. The primary interest is the change in soil strength caused by the leading wheels of multi-axle vehicles rather than changes caused by a great number of passes by a vehicle regardless of the number of wheels causing deformation on each pass.

The results of Prof. Goodman's studies will be used to provide more accurate predictions of vehicle performance. For purposes of vehicle design and evaluation, the factor of the number of passes a vehicle can make over a specific area of terrain is too irrational and much too qualitative to be of any value. In addition, I wish to say to Mr. Turnbull that we do not care to anticipate the effect of remolding for this is merely guessing, but we must be able to measure this effect and apply these measurements in the equations of land locomotion to determine its effect on vehicle performance.

Confusion has been injected into the discussions by entering the subject of trafficability which is concerned with vehicles passing one after another in the same rut as opposed to basic vehicle design which is concerned with the first pass.

R. ARIANO. — Nella comunicazione che è stata fatta precedentemente, ho sentito parlare e ho visto le figure relative all'assestamento dei terreni in rapporto al numero dei passaggi dei veicoli, ma non ho visto indicare quale era l'umidità dei terreni. Ora nella meccanica delle terre, è data fondamentale l'umidità all'atto del costipamento. Per noi stradini la determinazione del costipamento che può raggiungersi in un terreno è fatta sempre con riferimento a quella che è l'umidità ottima, risultante dalla prova Proctor. Evidentemente se noi andiamo ad umidità molto alte in modo che il materiale è molto fluido, in particolare se superassimo addirittura il limite liquido, il passaggio sui terreni non costiperebbe, ma sposterebbe semplicemente il materiale. Quindi sarebbe interessante verificare in rapporto alle varie umidità che cadono negli intervalli tra il limite liquido e il limite plastico, tra il limite plastico e il limite di ritiro e al di sotto del limite di ritiro, come influisce il numero di passaggi sul costipamento; non facendolo si rischia di attribuire il costipamento alla natura del terreno, all'essere una argilla, un'argilla limosa, un limo sabbioso, ecc., e le caratteristiche possono invece non essere un attributo specifico di quella terra, ma essere un attributo dalla umidità che c'è in quel particolare terreno.

W. L. HARRISON. — In answer to your question, if I have the correct understanding, when stress strain curves are measured to determine soil strength, and defined by the Bekker soil values, the soil moisture content is inherent as a function of soil strength. If your interest is in the effect of the change in moisture content throughout the various seasons on the strength of soil, then the change can be determined by the variation of soil strength parameters throughout the seasons. It is very difficult, if not impossible, to define soil strength by moisture content alone. Different soils such as sand, clay, and silt or the infinite combinations of these soils are influenced to a different degree by changes in moisture content.

R. ARIANO. — Vorrei solamente precisare che non è questione nei rapporti di umidità di vedere se siamo all'una o all'altra stagione e quindi di fare dei dati statistici. E' questione di vedere all'atto del passaggio dei veicoli, all'atto del costipamento naturale, quale è la quantità di acqua che c'è sulla terra e la quantità d'acqua può derivare da una pioggia che c'è stata poco prima, può derivare da ambiente umido, può derivare dall'essersi la terra asciugata per azione del sole, ecc. Noi nelle strade abbiamo sistematicamente messo in tutti i capitolati, — e stiamo preparando delle Norme in sede C.N.R. relative alle terre — in cui prescriviamo che quando si va a costipare un terreno, bisogna che vi sia quel determinato grado di umidità, perchè se no non si riesce a costiparlo bene. Non si riesce neanche se si insiste parecchio; c'è solo da notare che l'ottimo costipamento può variare col tipo di costipatore. Quanto poi all'influenza dell'acqua sul terreno costipato, è bene notare che se poi il terreno, per sua natura, per sua composizione è tale che in un certo senso è assimilabile a una terra stabilizzata granulometricamente, l'influenza dell'acqua che lo raggiunge a costipamento avvenuto può influire relativamente poco. D'altra parte, delle precauzioni si possono prendere; per esempio nella fondazione della strada di Caluses, provvedendo ad una impermeabilizzazione superficiale e alla protezione con cartone bitumato, ma questo è un aspetto diverso. Può bastare semplicemente un velo di bitume messo in superficie, per evitare una ulteriore filtrazione d'acqua a costipamento avvenuto. Ma è essenziale, prima costipare nel modo giusto, e ripeto, costipare nel modo giusto dipende enormemente dalla umidità del terreno all'atto del costipamento, umidità il cui tenore ottimo varia con il variare della natura e della composizione granulometrica del terreno.

L. J. GOODMAN and C. N. LEE. — We are taking advantage of the time interval between the Conference in Turin and the publication date of the proceedings to briefly mention current research activities in land locomotion mechanics at Syracuse University. The influence of the size of soil loading devices on the soil parameters used in the sinkage and shearing aspects of mobility studies is currently under investigation. Uniformity of soil conditions is being controlled by using completely remolded specimens of cohesive soil for both load-sinkage and horizontal shear experimental work. Investigations of different degrees of disturbance between undisturbed and completely remolded states of cohesive soils are also underway.

Finally, it may be of interest to note that a second research study on « Plastic Behavior of Soils in the Study of Land Locomotion Problems » has been recently initiated under the sponsorship of Land Locomotion Laboratory, U. S. Army Ordnance Tank Automotive Command, Detroit, Michigan. This study is under the direction of Dr. W. H. Li and Prof. L. J. Goodman at Syracuse University.

N. 5

The bearing capacity of soils under vehicle loads

La capacità portante del suolo sotto il carico del veicolo

Prof. Dr. G. G. Meyerhof *)

ABSTRACT. -- *Recent research on the bearing capacity of soils under inclined loads is applied to wheeled and tracked vehicles on soil or snow. It is found that the bearing capacity decreases rapidly with greater inclination of the load, while the corresponding maximum tractive effort increases to a maximum value and then decreases again.*

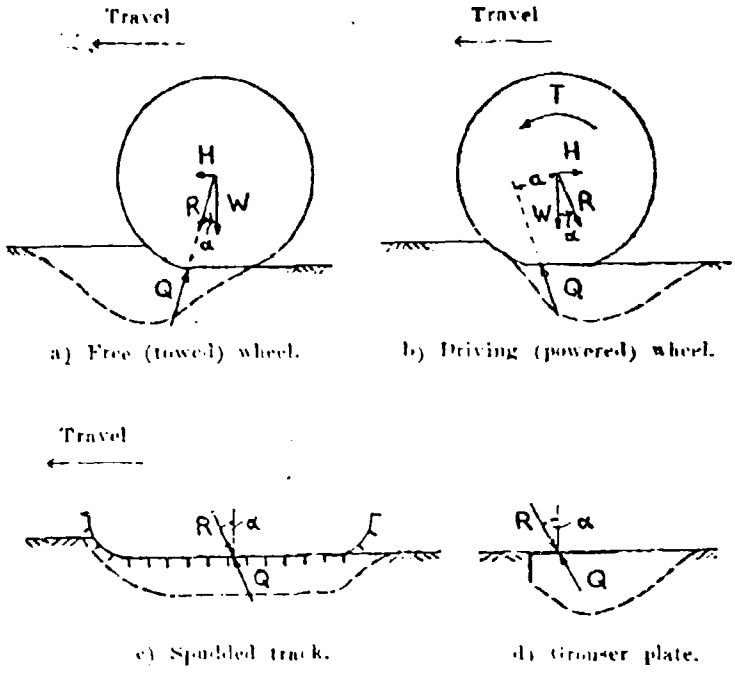
Introduction. -- One of the main problems in vehicle mobility off the road is the bearing capacity of soils, snow and ice under vehicle loads. Since this problem is related to the bearing capacity of foundations, some results of recent research in this field will be applied to wheeled and tracked vehicles. The bearing capacity of ice has been considered in a previous paper [1], and will not be discussed here.

Bearing capacity of wheels and tracks under inclined load. -- The load of vehicles is generally transmitted to soil or snow either by wheels or by tracks. The main forces acting at the centre of a free or towed wheel are the wheel load W and the horizontal pull H, which have a resultant R passing through the centre of the wheel and making an angle $\alpha = \tan^{-1}(H/W)$ with the vertical (fig. 1 a). This resultant force is balanced by the total reaction of the ground, which can reach a maximum value of the ultimate bearing capacity Q.

Similarly, for a driving or powered wheel the main forces on the wheel are the load W, the drawbar pull H and the torque T, which have a resultant R acting at a lever arm $a = T/R$ from the centre of the wheel and making an angle $\alpha = \tan^{-1}(H/W)$ with the vertical (fig. 1 b). The resultant R is balanced by the total ground reaction with a maximum possible value of Q, as before.

While the above relationships apply also approximately to wheels supporting a flexible track and to spudded wheels, the vehicle forces acting on a smooth or spudded track are more complex. However, for each track the resultant R acting at an angle α to the vertical must again be balanced by the

*) Head, Dept. of Civil Engineering, Nova Scotia Technical College, Halifax, N. S., Canada.



a) Free (towed) wheel. b) Driving (powered) wheel.

c) Spudded track. d) Grouser plate.

Fig. 1. — Forces on wheels and tracks.

total reaction of the ground with a maximum possible value of Q (fig. 1 c). A similar system of forces acts on an individual grouser plate (fig. 1 d).

For soil or snow the shearing strength can be expressed by

$$s = c + p \tan \Phi \tag{1}$$

where c is the apparent cohesion, Φ is the angle of internal friction or shearing resistance and p is the normal pressure on the shear plane. The vertical component of the average bearing capacity on such material can be represented by [2]

$$q_v = Q \cos \alpha / BL \tag{2}$$

$$q_v = (1 + 0.2\,B/L)\,cN_{cq} + (1 - 0.3\,B/L)\,\gamma BN_{\gamma q}/2 \tag{3}$$

where B is the width, D is the depth and L is the length of the ground contact area, γ is the unit weight of the material, and N_{cq} and $N_{\gamma q}$ are the resultant bearing capacity factors of a strip load and depend mainly on α, Φ and the depth ratio D/B of the contact area.

The horizontal component q_h of the bearing capacity cannot exceed the shearing resistance on the ground contact area plus the horizontal component

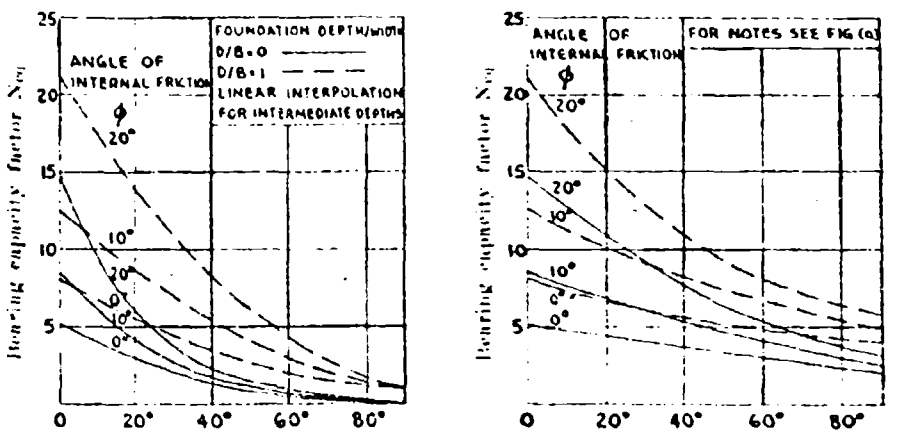
P_h of the passive earth or snow pressure on the front of the wheels or tracks. Thus,

$$q_h = Q \sin \alpha / BL = q_v \tan \alpha \tag{4}$$

$$q_h = c_a + q_v \tan \delta - P_h/BL \tag{5}$$

where c_a is the unit adhesion and δ is the angle of skin friction on the contact area. For greater inclinations α when q_h governs, eq. 3 must therefore be replaced by

$$q_v = \frac{c_a + P_h/BL}{\tan \alpha - \tan \delta} \tag{6}$$



a) Horizontal contact area. b) Inclined contact area.

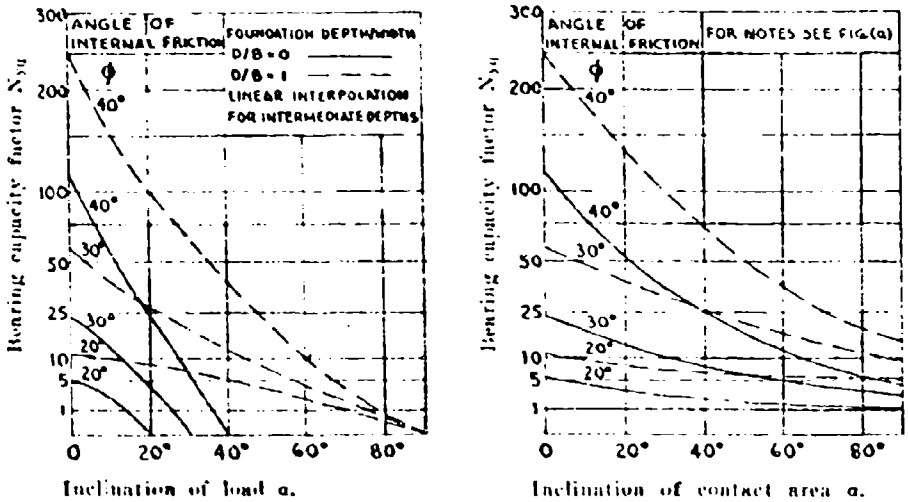
Fig. 2. — Bearing capacity factors for cohesive materials.

obtained from eq. 5. For spudded wheels and for tracks with grousers or spuds, the skin friction equals the shearing strength of the material (eq. 1) so that $c_a = c$ and $\delta = \Phi$ in eq. 6.

Two main basic cases of bearing capacity may be considered, namely, for horizontal contact areas and for contact areas normal to the load (i.e. area inclined at α to the horizontal). While the former case applies to tracks, the bearing capacity of wheels is between these limits and has to be interpolated. These limiting bearing capacity factors N_{cq} and $N_{\gamma q}$ for a rough base have been obtained previously [2] and are given in figs. 2 and 3, which show that for a given inclination α of the load an inclined contact area has a greater bearing capacity than a horizontal area; the factors for smooth areas are somewhat smaller in accordance with eq. 6.

The bearing capacity factors for horizontal contact areas decrease rapidly

with greater inclination α and become zero for a surface area if $\alpha = 90°$ on cohesive materials and if $\alpha = \Phi$ on cohesionless soils, when failure occurs by sliding on the ground. The bearing capacity factors for inclined contact areas also decrease rapidly with greater inclination α to the passive earth pressure coefficients for $\alpha = 90°$. The theoretical contact pressure distribution is similar to that of foundations with a vertical load. This pressure distribution is approximately uniform for the cohesive materials and roughly triangular for cohesionless soils.



a) Horizontal contact area. b) Inclined contact area.

Fig. 3. — Bearing capacity factors for cohesionless materials.

While the vertical component of the bearing capacity decreases for greater values of α (eqs. 2 and 3), the theoretical tractive effort or horizontal ground resistance, which is governed by the horizontal component of the bearing capacity, increases with inclination of the load to a maximum value and then decreases to a minimum for $\alpha = 90°$ (eqs. 4 and 5), as shown also in fig. 4. Within the practical range of the data given in figs. 2 and 3, the maximum tractive effort cannot exceed about one-quarter of the maximum value of the ultimate bearing capacity ($\alpha = 0$) in cohesionless soils or about one-half of the ultimate bearing capacity in cohesive materials.

Moreover, the maximum theoretical value of the tractive effort of an inclined contact area is greater than for a horizontal area, as would be expected. The results of loading tests on rough model footings with inclined loads on clay and sand [2] are found to be in good agreement with the theory (fig. 4). The tests with horizontal contact areas are representative of grouser plates

and show the importance of embedment depth on the horizontal ground resistance.

In order to apply the proposed method of analysis to vehicle loads in practice, the curved ground contact area has to be replaced by an equivalent plane rectangular area at an effective average depth. For wheels the average contact depth D is roughly one-half of the total sinkage, to which the depth

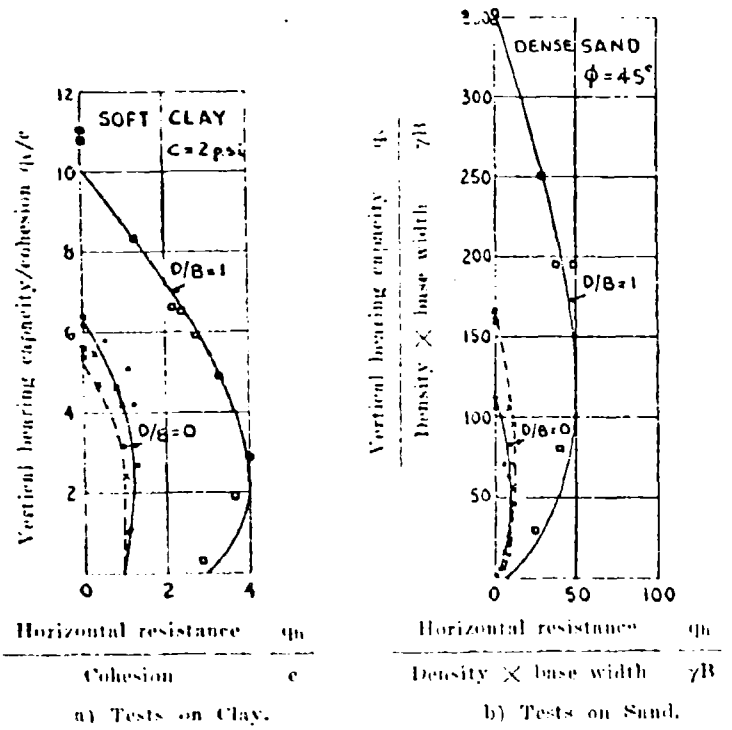


Fig. 4. — Results of loading tests on horizontal footings with inclined load. Legend: Test results: —; Theory: —; Strip D/B = 0 ×; Strip ——; Square D/B = 0 ○; Square ——; Duo. D/B = 1 □.

of the spuds has to be added in the case of spudded wheels. For smooth tracks the average depth D is approximately given by the total sinkage, while for grouser plates and spudded tracks the effective depth is equal to the sinkage plus the depth of the grousers or spuds. An estimate of the sinkage of vehicles is beyond the scope of this paper and can be based either on a semi-empirical approach[3] or a correlation of field observations with penetration or plate bearing tests for various loading and soil conditions.

Conclusions. — Recent research on the bearing capacity of soils under inclined loads can be applied to wheeled and tracked vehicles on soil or snow.

The theory indicates that the bearing capacity decreases rapidly with greater inclination of the load, which is supported by the results of loading tests with model footings. The maximum tractive effort is found to increase with inclination of the load to a maximum value and then decreases to a minimum for a horizontal load. The proposed analysis requires an estimate of the sinkage and further work on this problem is required.

BIBLIOGRAPHY

1) Meyerhof G. G. Bearing capacity of floating ice sheets. Proc. Am. Soc. Civ. Engrs., v. 86, No. EM 5, pag. 113, 1960.

2) Meyerhof G. G. The bearing capacity of foundations under eccentric and inclined loads. Proc. Third Int. Conf. Soil Mech., v. 1, pag. 440, 1953.

3) Bekker M. G. Theory of land locomotion. Univ. of Michigan Press, Ann Arbor, 1956.

Forecasting of trafficability after traffic for sands possessing structures

Previsione della possibilità di passaggi successivi su terreni sabbiosi

TRAFFICABILITY RESEARCH TEAM *)

ABSTRACT. -- *It has been found that in dry desert sands, apart from the leeward slope of dunes, the sand grains are cemented together, although the cementation may be destroyed by pressure of the fingers. Such sand is said to have a natural structure. Due to this structural characteristic, initial bearing strength of the ground prior to traffic is greater than after it.*

Sands possessing structure provide an example of a case where neither the Vicksburg method nor the Bekker method is adequate sufficiently to forecast trafficability.

Sands possessing structure require a field test in order to predict their trafficability after the sand is disturbed. The value obtained is a proper measure of the soil a military reconnaissance party.

After experimenting with several field methods, a crude but effective test was found satisfactory. A hole is dug in the sand and refilled by the same material. A soldier compacts the sand by tramping by foot until the original level of the natural surface is reestablished. Cone index values are taken from the location before and after the sand is disturbed. The value obtained is a proper measure of the soil strength after remolding. For practical purposes variations of ± 15% in cone index values, which are common, are not considered detrimental.

Introduction. — Soil trafficability prediction is based on a knowledge of combination of factors related to vehicles and those related to soil. Factors related to vehicles are fixed and are easily determined depending on the mechanical characteristics of those vehicles.

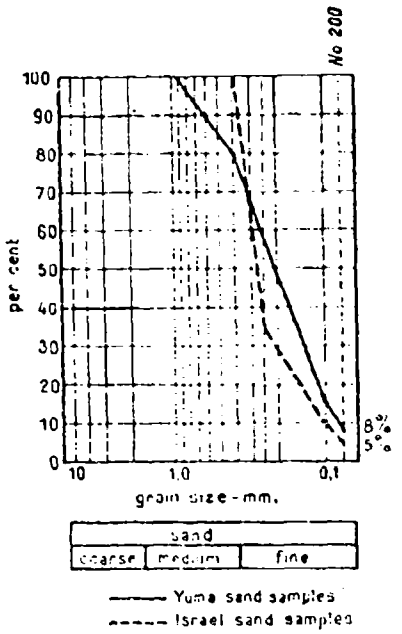
It has been found that in dry desert sands, except for the leeward slope of dunes, the sand grains are cemented together, although the cementation may be destroyed by the pressure of the fingers. Such sand is said to have a natural structure. Due to this structural characteristic, initial bearing strength of the ground prior to traffic is greater than after it.

The determination of properties of sands possessing structure poses a problem that does not have a complete solution by either of the two methods in use by the U. S. Army: the Vicksburg method used by the Corps of Engineers, and the Bekker method used by the Ordnance Corps.

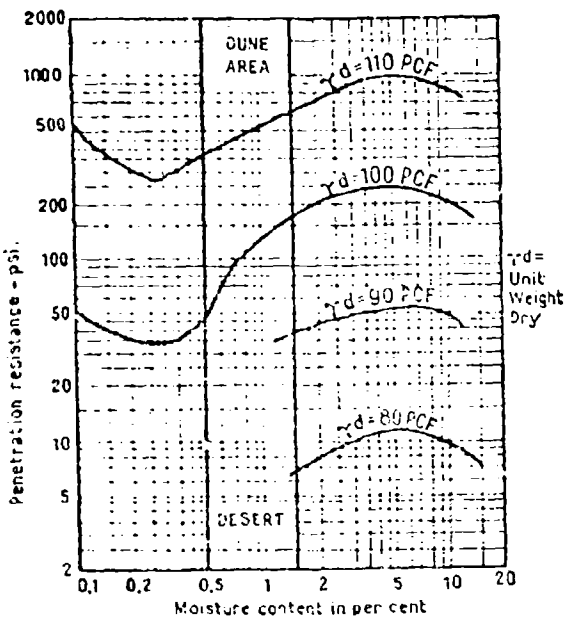
This paper reports the results of experiments made to find a quick practical method for establishing the usable Cone Index for sands having natural structure.

*) Corps of Engineers Israel Defence Army.

Strength characteristics of sands possessing structure. — A structural phenomenum in sands is a result of a cementation process by small grains. An appreciable cementation may be observed when the percentage of fines (passing No. 200 screen) ranges between 5% - 10%. Graph 1 depicts a comparison of mechanical analyses of sand from the dune region in Yuma U. S. [1] where the percent of soil passing a 200 screen is 8 % and sand from the dune regions in Israel where the per cent of soil passing a 200 screen is 5 %.



Graph 1.

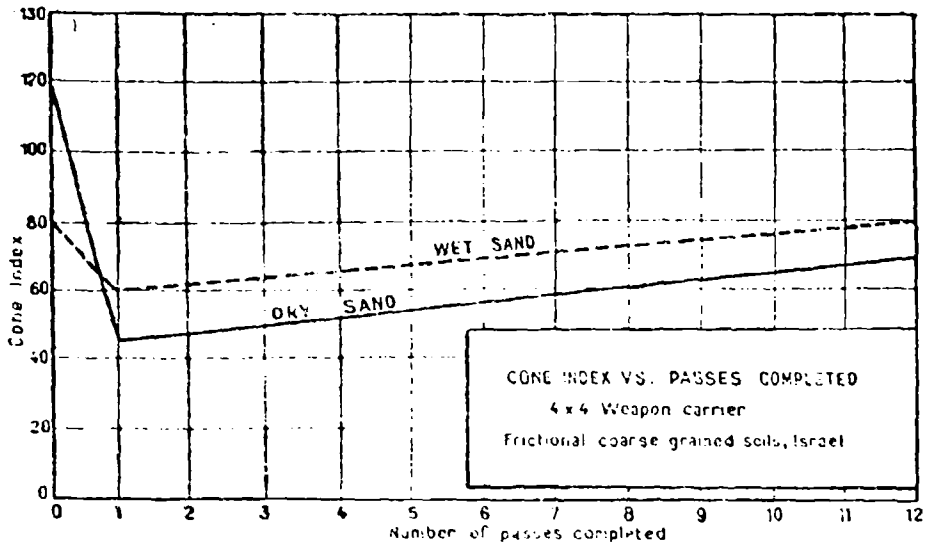


Graph 2.

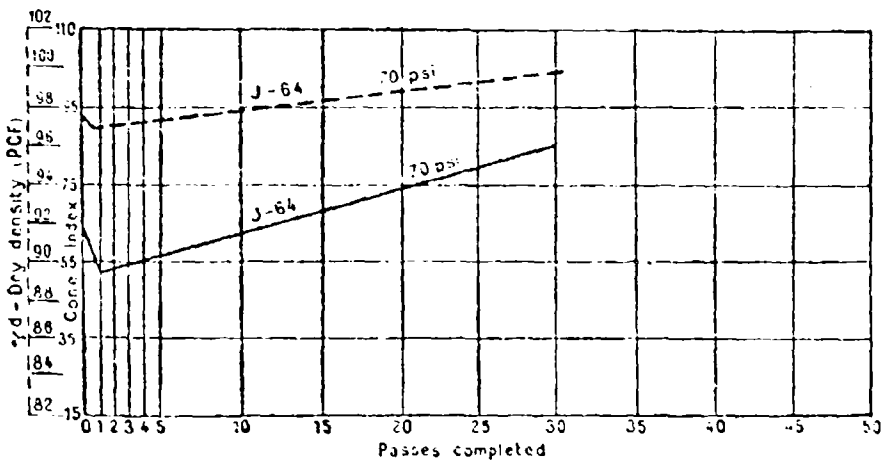
The structure found in sand in Israel was observed to be a temporary state, vanishing when the soil was soaked by rain, and reappearing when it had reached a moist to dry condition. Graph 2 [2] depicts ground strength (penetration resistance) versus moisture content relationships for sands of various densities. It is noticed that there exist great differences of strength within the limits of capillary moisture prevailing in deserts. A variation of 0,1 per cent of moisture within 0,5 - 1,5 % moisture range is highly influential in varying the sand strength, particularly at the high dry densities of the sand.

The relationship of Cone Index versus the number of completed vehicle passes for one site in Israel is shown in graph 3 for dry and for moist sands. The ordinate represents Cone Index reading of the 0 - 6" layer taken after a vehicle had completed its passes.

It is observed from this relationship that the initial sand bearing strength is reduced to almost one third of the original value after the first vehicle pass.



Graph 3.

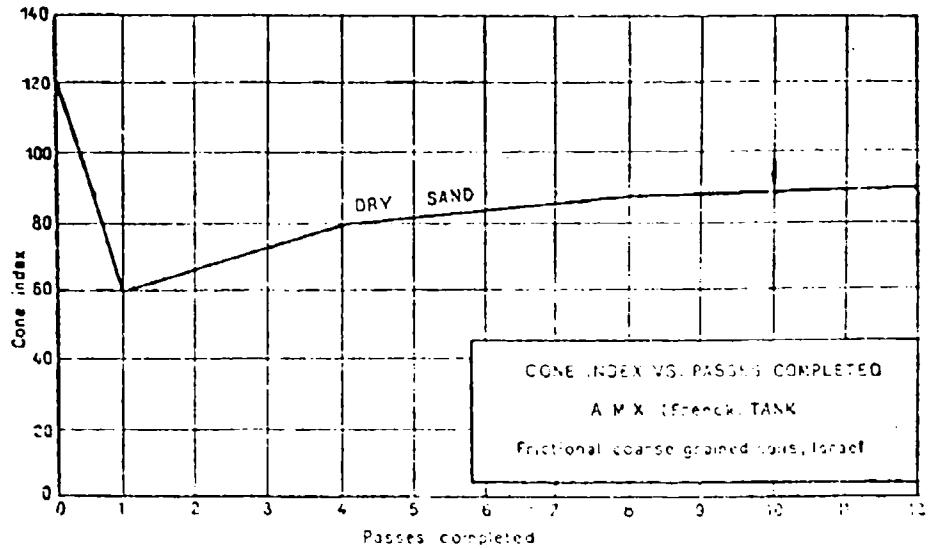


Graph 4. — Dry density vs. passes completed; cone index vs. passes completed. 2½ ton truck - 11.00 X 20 - 70 psi. Frictional coarse grained soils U.S.A.[3].

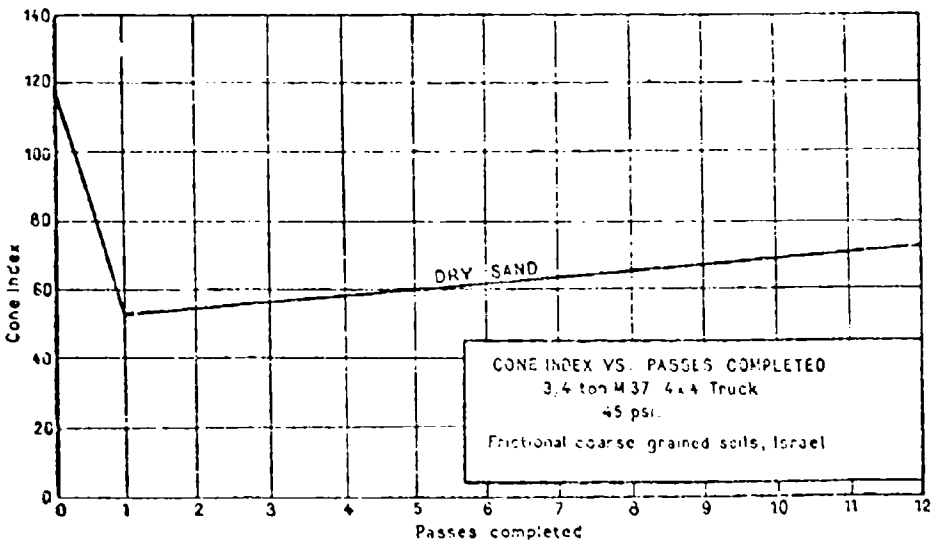
(From 120 to about 40 Cone Index in dry sand, and from 80 to 60 in moist sands).

Such a drop of strength determines the trafficability of the second vehicle.

It has become clear from experiments both in the U.S. and in Israel that variations in sand strength also arise from changes in dry density, as may be seen from graph 2 and graph 4[3]. The ordinate represents both Cone



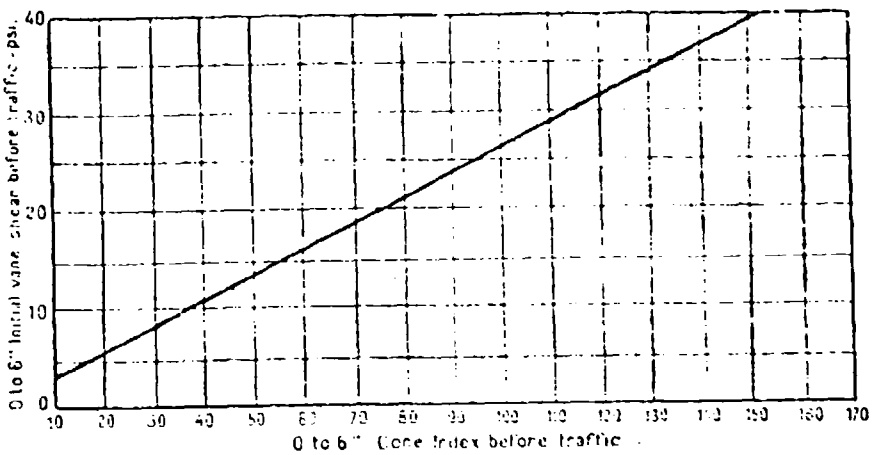
Graph 5.



Graph 6.

Index and dry densities while the abscissa represents the number of passes completed by a vehicle.

Graph 5 and 6 demonstrate experiments performed in Israel with a French AMX tank and with a 3/4 ton M 37 4 × 4 truck. It has been found that at a particular location the structure was destroyed to the same degree by two different vehicles. Pulverization of the sand by both the tank and the weapon carrier reduced the strength of the ground from a Cone Index of about 120 to 60.



Graph 7. — Comparison of initial vane shear with cone index in frictional course grained soils [3].

A suggested procedure for predicting strength after sand structure is destroyed. — Similar pulverization by two different vehicles, yielding identical ultimate Cone Index values justify the assumption that prediction of the strength after breakdown of sand structure by different types of vehicles could be done regardless of the characteristics of the vehicle.

It may also be assumed that when destruction of structure takes place there is only a change of bulk density not in moisture content.

The methods which have been employed in Israel for the purpose of predicting breakdown of structure included, using a shear vane and a penetrometer. Tests were also made as to the effectiveness of breaking down the structure by use of a bayonet and a shovel.

The purpose of the use of a shear vane was to establish the ratio of strength between initial strength for undisturbed conditions and the remolded value. There also exists a correlation between the shear vane values and the Cone Index graph 7 [3].

The vane used in the trials was a 6" by 2" vane. Satisfactorily consistent vane readings could not be determined for a number of reasons. Appreciable disturbance resulted from the penetration of the vane into the original ground, and the rate of rotation of the vanes.

The effectiveness of breaking down the structure was tried by the use of a bayonet and the use of a shovel. In the first instance the structure was broken with a bayonet within a 10 cm. diameter area and pressed back to the original ground level by foot pressure. Cone Index values were taken before and after this procedure. This procedure was not suitable. The resulting Cone Index values obtained were found to be too high, because of the passive resistance of the undisturbed sand surrounding the small volume of disturbed material tested.

The second instance, the use of a shovel in breaking down the structure led to the proposed procedure for determining the Cone Index after traffic.

A hole, about 40 cm. in diameter and 30 cm. deep, was dug with a shovel in a clean and flat place. The excavated sand was broken up and placed in a pile near the hole. Then the pulverized material was placed back in the hole and compacted by tramping by foot until the level matched that of the undisturbed ground. Cone Index readings were taken from the filled location before and after the hole was dug. With this procedure it was found that the ratio between the Cone Indexes before and after destruction of sand structure checked well with the actual field test results before and after the passing of a first vehicle. Although there were differences of about $\pm 15\%$ in the Cone Index for different sand locations, it was considered that such variations were not detrimental for practical purposes.

Conclusions. — Trafficability prediction in regions with sands possessing a natural structure presents a problem which is most satisfactorily solved by on the spot field trials.

The proposed method is a crude one, but it meets the requirements for the military man. It is simple, easy to perform and a rapid method.

ACKNOWLEDGMENT. — The Trafficability Research Team wishes to acknowledge its gratitude to Professor Joseph G. Zeitlen, Chairman, Department of Soil Engineering, Israel Institute of Technology, Haifa, for his guidance and assistance in the preparation of this paper.

BIBLIOGRAPHY

1) Corps of Engineers, U.S. Army. Tests on coarse grained soils with selfpropelled and towed vehicles. TM 3-240, Supplement 15, June 1950.

2) Air Force Surveys in Geophysics (U.S.). Remote determination of soil trafficability by the Aerial Penetrometer. No. 77, Oct. 1955.

3) Corps of Engineers, U.S. Army. Pilot tests on coarse grained soils. Supplement 13: Research and development report. TM 3-240, Nov. 1955.

APPENDIX

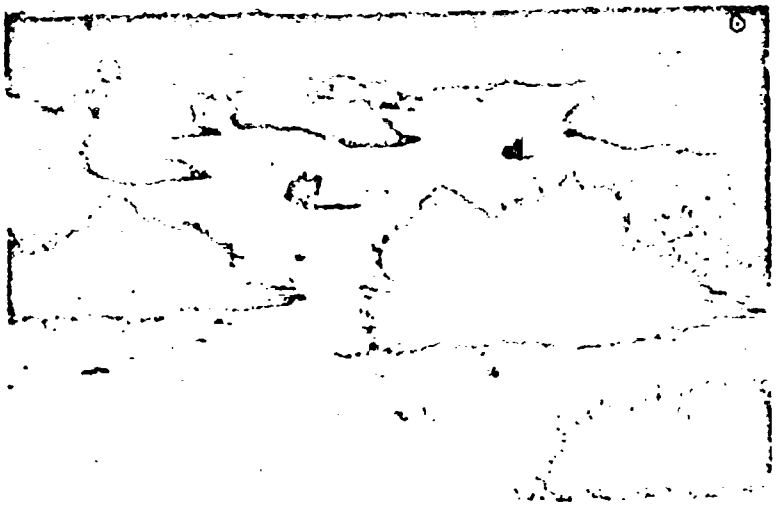


Fig. 1. — A general view. Region of sands possessing structure.



Fig. 2. — A) Destruction of sand in ruts. B) Undisturbed sand structure.



Fig. 3.

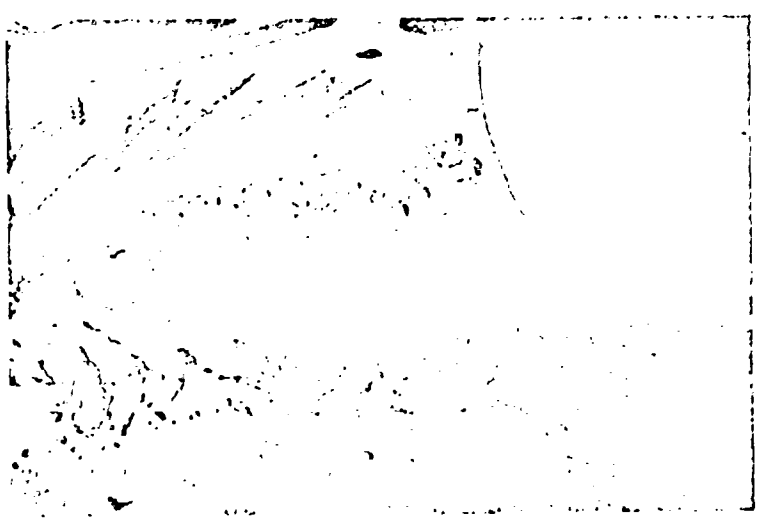


Fig. 4.

Fig. 3-4. — Destruction of sand structure by wheels.

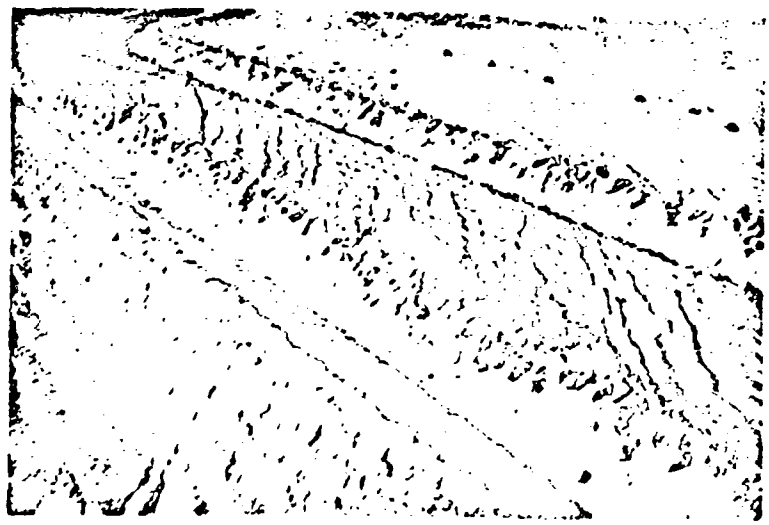


Fig. 5.

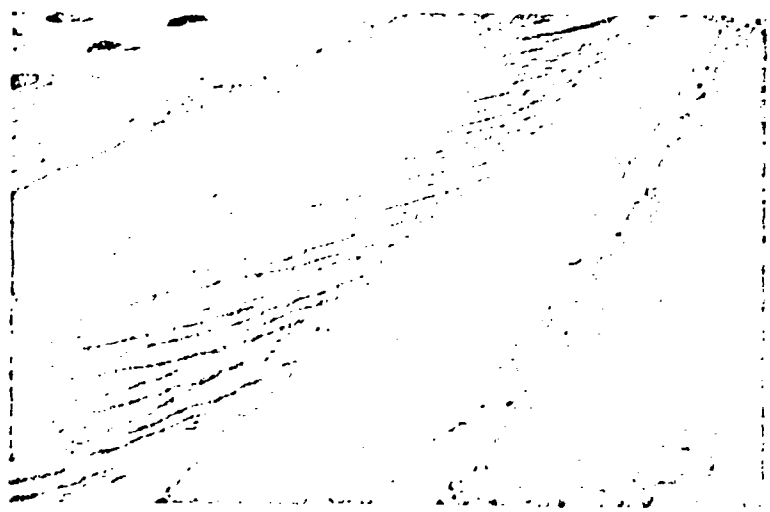


Fig. 6.

Fig. 5-6. — Types of ruts in sands possessing structure after traffic.

DISCUSSION

W. J. Turnbull. — In his presentation of the paper on trafficability forecasting Major Cohen gave an interesting discussion on sands possessing some structural strength. It is believed that structural strength in sands represents the exceptional rather than the normal case. It is further believed that structure in sands can usually be attributed to some form of chemical cementation occurring in nature. The problem here, as in fine-grained soils, involves a remolding process with a change in strength, usually downward, at least in the first few vehicular passes.

The U. S. Army Engineer Waterways Experiment Station has conducted relatively few tests in structured sands and consequently has not specifically developed a system for evaluating the strength loss upon disturbance. However, it is believed that this could be accomplished by forcing a thin-walled cylinder 6 inches to 8 inches in diameter into the soil and breaking the structure of the sand in the cylinder by ramming with a rod, care being used not to density the sand. The cone index would be measured in the cylinder in place.

The method proposed by the Israeli team has the merit of logic and simplicity, and if it can be shown to result in a good estimate of vehicle performance, it will undoubtedly receive wide acceptance. The Waterways Experiment Station will try out the method at the next opportunity. Meanwhile it would be interesting to study the results of any further testing that the Israeli Trafficability Research Team may have done on sands possessing structure.

Elastic response of soil to tracked vehicles

Reazione elastica del terreno al passaggio dei veicoli cingolati

E. T. Selig *) - K. E. Hofer **) - N. A. Weil ***)

ABSTRACT. — *This paper presents the results of an experimental study on the strain distribution in soils under loads simulating the complex loading pattern produced by tracked vehicles. The strain pattern produced by this loading was measured at twelve locations in two soils, a silty clay and a plastic clay.*

The experimental work was supported by analytical studies in which an exact solution was developed for the strain distribution in semi-infinite media, based upon Love's solution for an elastic, homogeneous and isotropic medium subjected to the prescribed surface tractions. Comparison of analytical and experimental results indicates that the theory can reasonably predict the actual response characteristics of the soil.

Introduction. — The purpose of the study reported in this paper was to determine the adequacy of the theory of elasticity to predict the stresses and strains in soils produced by vehicle loads on the surface. To accomplish this the theoretical differential displacements produced at various locations in a three dimensional soil medium by a tracked vehicle were first computed from the theory. The actual displacements at these locations were then measured in two soils in the field and the results compared with theoretical predictions.

Historically, the determination of stress and strain distributions in soil beneath a surface load has been the subject of many theoretical studies. However, few attempts have been made previously to evaluate these theoretical results experimentally. One of the few major efforts in this regard was a series of large-scale tests conducted at the Waterways Experiment Station ****). Primary consideration was given to measuring stresses at various locations in the soil beneath a footing on the surface. Although exact agreement with the

*) Associate Research Engineer, Soil Mechanics, Armour Research Foundation of Illinois Institute of Technology, Chicago, Illinois.

**) Assistant Research Engineer, Structural Mechanics, Armour Research Foundation of Illinois Institute of Technology, Chicago, Illinois.

***) Director, Mechanics Research Division, Armour Research Foundation of Illinois Institute of Technology, Chicago, Illinois.

****) U. S. Army Engineer Waterways Experiment Station, «Investigations of Pressures and Deflections for Flexible Pavements: Report No. 1, Homogeneous Clayey - Silt Test Section», Vicksburg, Miss., March 1951.

U. S. Army Engineer Waterways Experiment Station, «Investigations of Pressures and Deflections for Flexible Pavements: Report No. 4, Homogeneous Sand Test Section», Vicksburg, Miss., December 1951.

various theoretical solutions evaluated was not obtained, the general behavior observed conformed reasonably well with analytical predictions.

Inherently, it is difficult to obtain exact stress values in a three-dimensional soil mass. This is because of the unavoidable interaction between the gage and the soil which changes the stresses from those that would be obtained were the gage absent. Strains or, in effect, differential displacements on the other hand, potentially can be measured with less likelihood of influencing the soil response. This is because they can be determined with gages which have little resistance to deformation and, therefore, do not disturb « free field » effects. For these reasons the approach taken in the present study was to evaluate the theory



Fig. 1. — Representation of surface load applied by tracked vehicle.

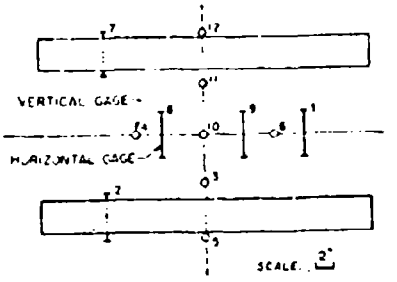


Fig. 2. — Location of gages for field test.

on the basis of displacements rather than stresses. In the following pages the assumptions involved in the theoretical formulation are listed, the experimental apparatus briefly described and the results of the field tests presented and compared with the theoretical predictions.

Theoretical solution. — In the theoretical solution, the soil is represented as a homogeneous, isotropic, linear elastic material. As such, the properties are completely described by two well known constants, the modulus of elasticity, E, and Poisson's ratio, r. The vehicle loading on the surface of the soil is represented for simplicity of theoretical analysis by a uniform pressure distribution over two parallel rectangular areas (fig. 1). Except for a small region directly beneath the load, this distribution was found to give results identical to that of a more realistic, but more involved, non-uniform distribution. The position coordinates x, y, z, are given in the dimensionless form x/a, y/a, z/a, where « a » is the half-width of the rectangle. We shall define transverse, longitudinal, and vertical to be the directions parallel to the x/a, y/a, and z/a axes, respectively. The length-to-width ratio of the rectangles is taken as 10, and the center-to-center spacing between them as 10 a.

The complete solution for the stresses and strains in a homogeneous isotropic, elastic half-space under uniform surface loading over a single rectangle has been derived by Love *). Due to their complexity, the equations

were programmed for the Univac 1105 electronic computer so that all of the components of strain could be determined at any point in the soil. The results for the assumed vehicle load representation were obtained by a suitable superposition of values given by these equations for two such rectangles spaced

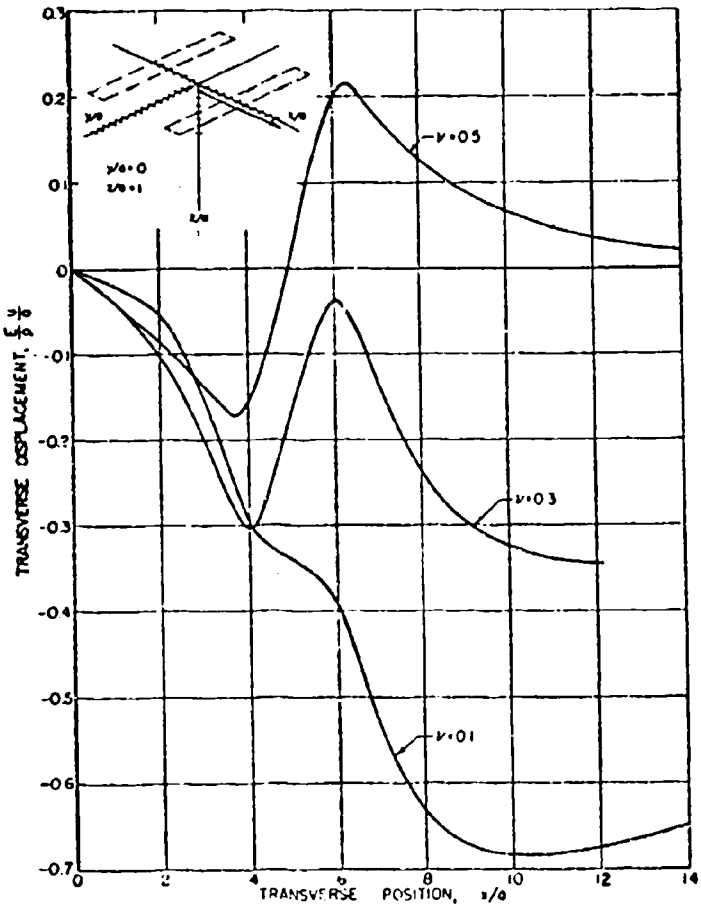


Fig. 3. — Theoretical transverse soil displacements.

according to fig. 1. The displacements were then computed by summing up the strains.

The resulting theoretical displacements of the soil along various paths, representative of those along which the gages for the test were located, are shown in figs. 3, 4, and 5. The arrows in the insert figures show the paths

*) Love A. E. H., «The Stress Produced in a Semi-Infinite Solid by Pressure on Part of the Boundary», Transactions, Royal Soc. London, England, Series A, vol. 228, pag. 377, 1929.

which correspond to each of the curves. The displacements u and w are given in the dimensionless form $\frac{E}{p}\frac{u}{a}$ and $\frac{E}{p}\frac{w}{a}$ corresponding to the transverse and vertical directions, respectively. These displacements are taken relative

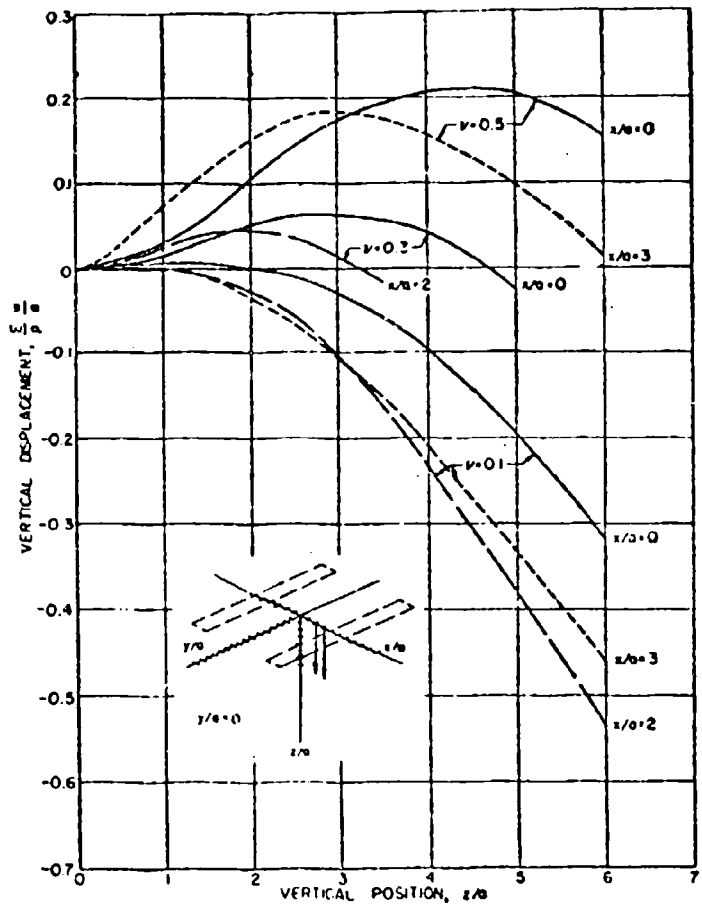


Fig. 4. — Theoretical vertical soil displacements outside of load.

to those of the coordinate planes. The latter are zero, due to symmetry, for the transverse case, but are equal to the movement of the ground surface for the vertical case. In other words, the displacements shown are absolute for the transverse direction, but for the vertical direction represent the difference in movement between the point in the soil and the point on the ground surface directly above. In either case, the correct differential displacement (magnitude and sign) between any two points along the paths shown are determined by subtracting the displacement at the point nearest the origin from that of the

point farthest from the origin. Negative values thus obtained indicate that the points moved together while positive values indicate that they moved apart. From figs. 3, 4, and 5, the significant influence of Poisson's ratio on the sign as well as magnitude of the displacements may also be readily seen.

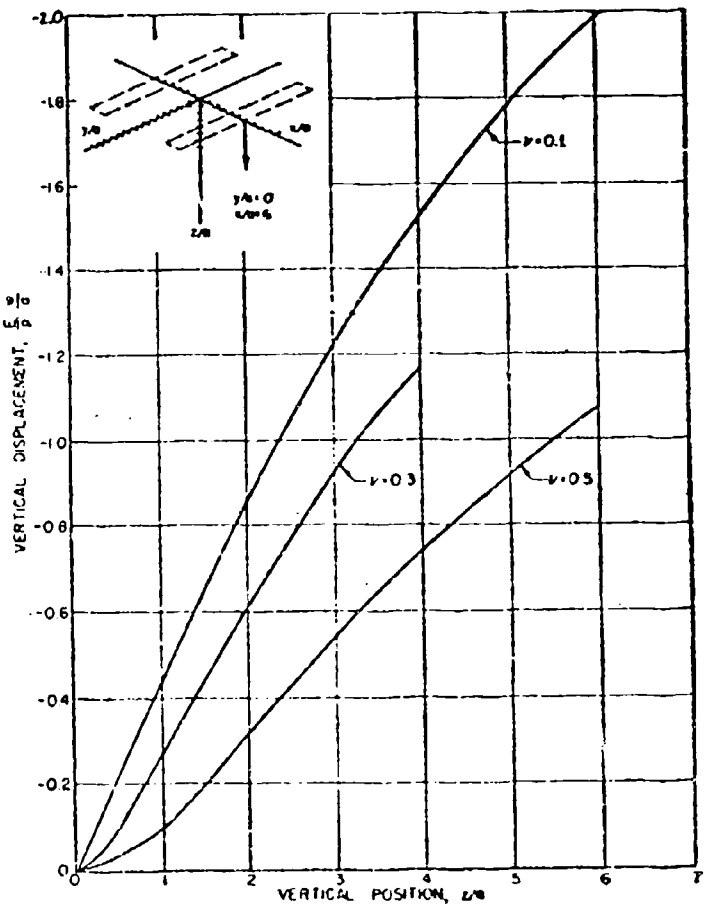


Fig. 5. — Theoretical vertical displacements beneath edge of load.

Experimental conditions. — Portable loading apparatus was constructed for duplicating the idealized loading assumed in the theoretical calculations. The fixture for distributing the load uniformly over two rectangular areas is shown in fig. 6. A large tank is placed on top of this fixture and filled with water to provide the desired load. The hydraulic jacks in fig. 6 are for keeping the tank level and the load uniform, even though the settlement may be uneven.

Twelve gages were buried in the soil, each to measure the differential displacement between two points 6 in. apart. The gages devised for this purpose are shown in fig. 7. Each end of the gage for vertical displacements

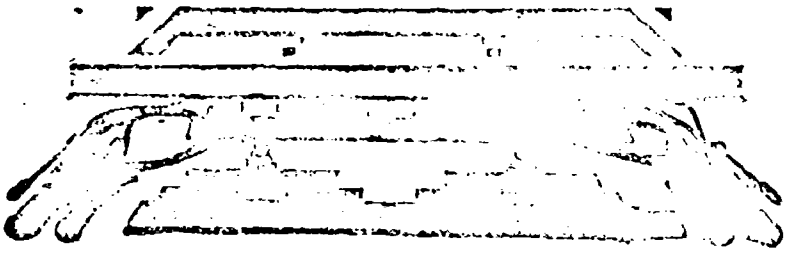


Fig. 6. — Fixture for distributing load to soil.

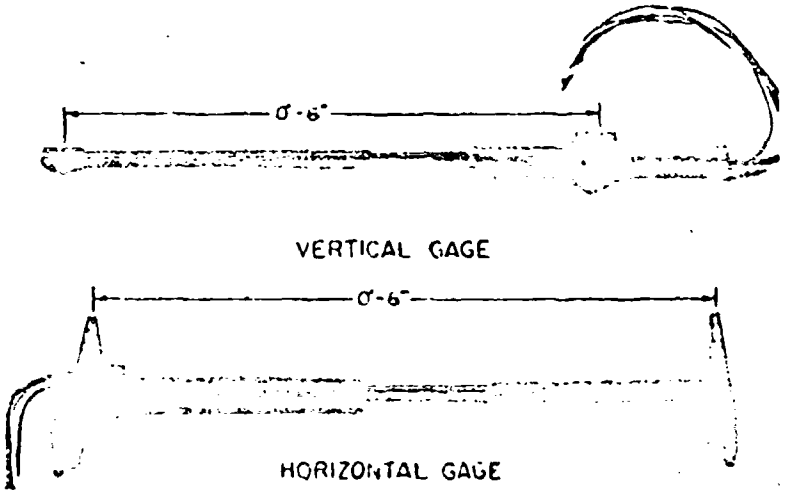


Fig. 7. — Differential displacement gages.

is coupled to the soil by an auger which is screwed into a pilot hole drilled into the soil. The ends of the horizontal gage are coupled to the soil by stakes which are pressed into the bottom of a narrow vertical slot cut into the soil. The gage locations are shown in fig. 2 and a photograph of the gages in place is shown in fig. 8. The horizontal gages were 2 ½ in below the surface and the reference points of vertical gages were 1 in. and 7 in. below the surface except for gages 5 and 12, which were ½ in. deeper.

The displacement sensing element of the gages was a linear differential transformer *). Relative movement of the two ends of the gages produced a

*) Linear Differential Transformer Lyn-SL-500, manufactured by Minatron Corporation, Belle Meade, New Jersey.

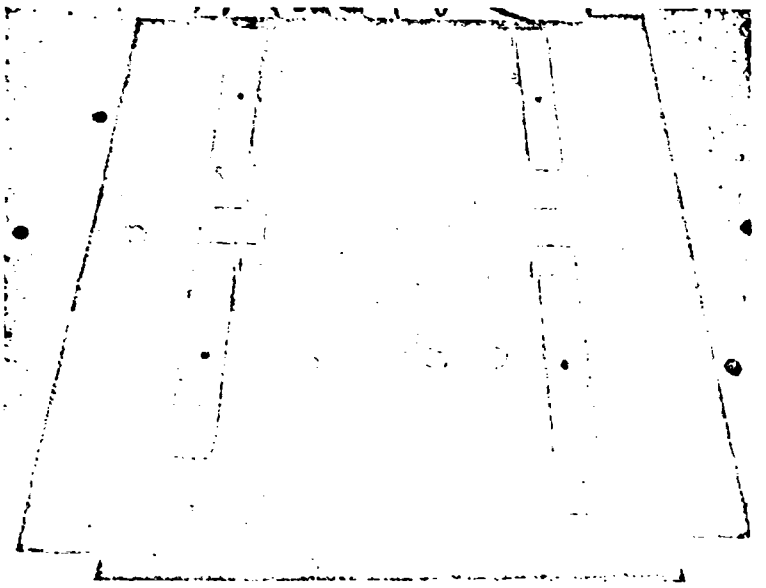


Fig. 8. — Gages in place for test.

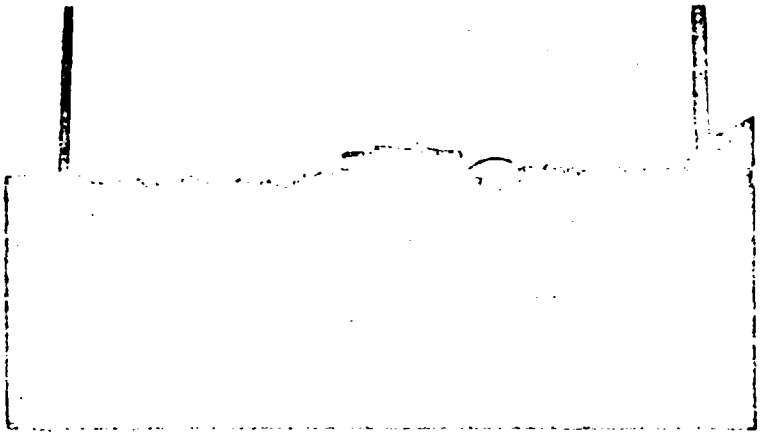


Fig. 9. — Test set-up.

voltage change directly proportional to this movement. With this equipment, differential displacements could be detected as small as 0.0001 in. over a range of ½ in.

The completed test setup is shown in fig. 9. At the beginning of the test, the water tank was raised off the temporary supports by the hydraulic jacks. Water was pumped into the tank from a nearby supply truck at a uniform rate to apply a slowly increasing load to the soil. After the full load had

been applied, it was then removed by pumping the water back out of the tank. Gage displacements were recorded during this entire loading cycle. The test was performed in two soils, one a silty clay and the other a plastic clay. The specifications of these soils are given in table 1.

TABLE 1. — *Specifications of soil.*

Type	Liquid limit, %	Plastic limit, %	Moisture content, %	Density, pcf	Void ratio	Percent saturation, %	Unconfined compressive strength, psi
Silty clay	31.5	25.1	27.9	117.2	0.79	79	7.5
Plastic clay	61.6	24.6	26.3	117.0	0.78	84	41.6



Fig. 10. — Representative gage displacement response in silty clay.

Results. — For each gage, the differential movement, δ, was plotted as a function of the applied ground pressure, p. Two examples showing both the loading and unloading response are given in fig. 10. There was considerable variation in the initial response of the gages probably as a result of placement conditions. For both soils tested the maximum ground pressure applied was much below the bearing capacity. Even so, upon unloading, the soil returned only partially to its original position. This non-recoverable response does not rule out the use of the elasticity theory; it merely requires that different constants be used in making predictions for the unloading portion as compared to the loading portion of the experiments.

For comparison with theory, the approximate slope (δ/p) of the loading portion of the curve for each gage was determined. The results are given in table 2. It may be seen that, in some cases, both the magnitude and sign of the differential displacements for a given location are different for each of the two soils. The vertical differential displacement, for example, may be either positive or negative in the zone between the loads.

From results such as given in figs. 3, 4, and 5, the theoretical values of δ/p, i.e., difference between appropriate u/p or w/p values, can be obtained

for each gage in terms of E, ν, and a. By inserting the values of « a » and δ/p from the field tests, a relationsl ip between E and ν is established for each gage that will make the theory exactly agree with the experimental results for that gage. This provides twelve independent equations with which to establish the two unknows E and ν. If the soil does respond according to the elasticity theory then a single pair of values will satisfy all 12 equations, assuming that the experimental method for obtaining the displacements provided a true measure of the soil response.

TABLE 2. — *Experimental gage response.*

Gage number	Gage response Δ/p, in/psi	
	Test in silty clay	Test in plastic clay
1	— 0,14 × 10^{-3}	
2	— 5,0 »	— 0,17 × 10^{-3}
3	— 0,72 »	— 0,093 »
4	+ 0,098 »	— 0,058 »
5	— 2,3 »	
6	+ 0,088 »	— 0,022 »
7	— 4,9 »	— 0,55 »
8	— 0,26 »	
9	— 0,28 »	
10	+ 0,091 »	— 0,020 »
11	— 0,86 »	— 0,11 »
12	— 1,89 »	— 0,38 »

The extent of agreement can best be observed by plotting the E-ν relationships for each gage on a coamon graph. These plots for the tests in plastic clay and silty clay are shown in fig. 11 a and 11 b respectively. In each case the region in which the intersections lie may be readily seen. Intersections at negative E must be excluded from consideration since they are physically untenable. The curves in fig. 11 a for gages 1, 5, 8, 9 were omitted since they appeared to malfunction either due to placement or instrumentation difficulties. The average values of E and ν for the positive intersections are indicated by a cross. For the silty clay these values are E = 600 psi and ν = 0.22; for the plastic clay E = 2200 psi and ν = 0.15.

From field observations it was known that neither of the soils was actually isotropic, the density and stiffness varying measurably in the vertical direction, particularly for the plastic clay. Also, some soil disturbance obviously did occur in placing the gages and by their presence during the test. For these reasons it could not be expected that the curves in fig. 11 relating E and ν would all intersect at a single point for each soil. Considering these difficulties, the regions within which the intersections lie are quite well delineated.

The relative values of ν actually obtained do explain such phenomena as the difference noted in the signs of the differential displacements for vertical gages 4, 6 and 10 when comparing the δ/p values for the two soils (table 2).

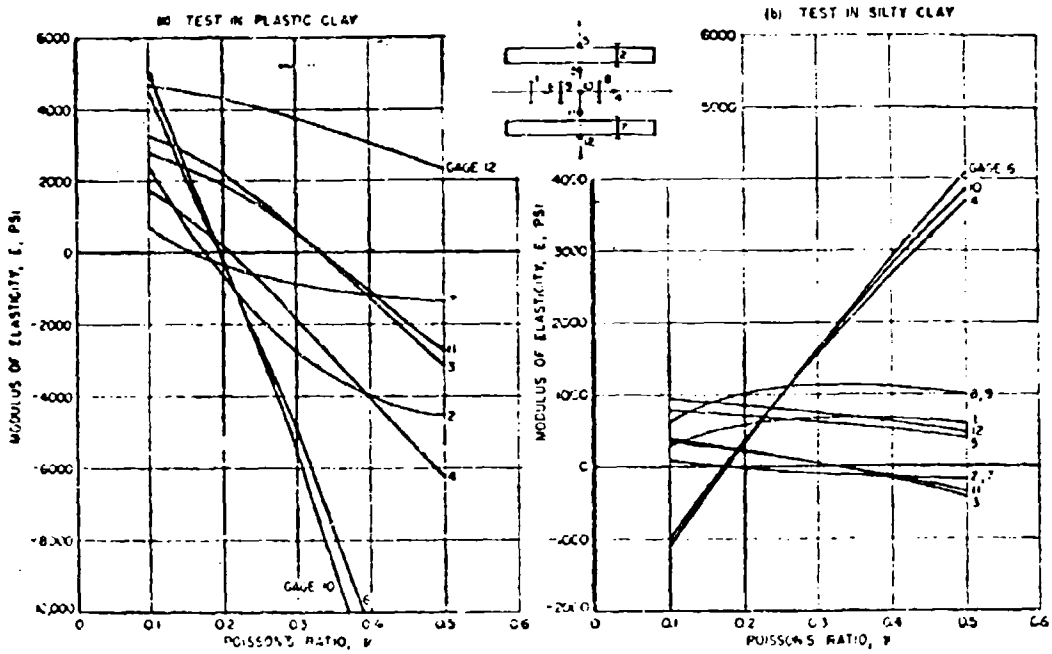


Fig. 11 a. Fig. 11 b.

Fig. 11. — Correlation of experimental results with theory.

Fig. 4 shows that these gages should extend for $\nu = 0.3$ and shorten for $\nu = 0.1$; the cross-over point is around $\nu = 0.2$. From table 2 it may be seen that these gages extended for the silty clay ($\nu = 0.22$) and shortened for the plastic clay ($\nu = 0.15$). Thus the change in sign of these vertical differential displacements can be explained by the theory based upon this small change in Poisson's ratio.

Conclusions. — The tests described in this paper were conducted to compare the differential displacements in soil beneath a tracked vehicle with those predicted by the theory of elasticity. The loads applied to the soil were considerably less than those which would cause failure of the soil. The principal objective was to evaluate the appropriateness of treating soils as homogeneous, isotropic, elastic media for the purpose of determining the stress and strain distributions created in soil under a complex loading pattern, such as imposed by a tracked vehicle. The comparison was made based upon differential displacements rather than stresses because of the inherent difficulty and uncertainty of accurately measuring the latter. The gages devised for measuring the displacements appeared to perform satisfactorily.

The results indicate that, while the soil does not exactly satisfy the theoretical assumptions, the theory can be used to predict reasonably well the

actual differential displacements of soil including reversal of sign with changes in Poisson's ratio. The correct values of E and ν must, of course, somehow be determined. The displacements are determined from strains which are in turn developed in response to the load applied to the soil surface. Hence to the extent the theory can be used to predict displacements, it can equally well be used to predict the stresses and strains in the soil.

DISCUSSIONS

R. ARIANO. — Io vorrei domandare all'illustre relatore semplicemente una spiegazione: quei moduli di elasticità e quei coefficienti di Poisson che egli ha indicati, sono stati determinati semplicemente per umidità, se non ho capito male, lievemente superiore al limite plastico. Non sono state fatte determinazioni anche per umidità diverse. Noi, per esempio, nel caso di strade prescriviamo che non si deve mai fare il manto se prima l'umidità non è stata portata al di sotto non solo del limite plastico, ma anche del limite di ritiro. Nel caso del terreno naturale, ci sarà quello che ci sarà. Quindi per svolgere la teoria mi pare che si dovrebbe dire: i moduli sono questi, se c'è tanto d'umidità; sono questi altri se l'umidità è minore; sono questi altri se l'umidità è ancora minore. La mia era semplicemente una domanda: è stata fatta qualche ricerca in quel senso o no?

N. A. WEIL. — If I understand the question correctly, I hope I can answer it. The actual moisture content of the soil was very near the plastic limit -- a little bit above it; however, in our approach to an attempt to find a suitable theory that would tend to predict the behavior of soils underneath loaded areas, we have set out first to investigate the adequacy of an elastic theory, isotopic homogeneous. If you assume that you are dealing with an elastic theory, the response of that semi-infinite medium will be entirely defined by two values only, notably the modulus of elasticity and Poisson's ratio. And our investigation at this time did not extend beyond the point of trying to find out this much. As I said, when we go into investigating the suitability of various plasticity theories, whether we assume ideally plastic behaviour, or a thixatropic, or some semblance of a *strain hardening* behaviour, which, by the way, is rather evident from the behaviour of the soil, then it would be valid to ask whether moisture content influenced the phenominological performance of the soil.

CARATTERISTICHE TECNICHE DEI VEICOLI DESTINATI AL MOVIMENTO FUORI STRADA

ENGINEERING ASPECTS OF OFF-THE-ROAD VEHICLES

N. 8

The performance of rigid cylindrical wheels on clay soil *)

Prestazione delle ruote rigide cilindriche su terreno argilloso

F. L. Uffelmann **)

ABSTRACT. — *A programme of measurement of the forces acting on full scale rigid cylindrical wheels when running on a purely cohesive soil of about 5 lbs. per square inch shear strength under various controlled load and slip conditions is described. The forces in question are those of rolling resistance, drawbar pull, tractive effort and both radial and tangential rim stresses; the added tractive soil reactions provided by ribbed side walls and radial rim spuds attached to the wheel are also evaluated.*

The experimental results are compared with a simple plastic theory of rut formation providing an estimate of rolling resistance, tractive soil reaction and the critical sinkage at which slip-stall occurs; the theory is extended to cover the effect of side wall traction. A static theory of spud reaction valid for low slip values is also given.

Finally suggestions are made for the design of a wheel to carry a load of 3 3/4 - 5 tons suitable for both on and off road use.

Introduction

Over the past few years a programme of experiment has been carried out at my Establishment on the performance of rigid cylindrical load carrying wheels on a soft clay soil, the object being to determine the forces acting and to provide a fuller understanding of the conditions under which such wheels may be used successfully. The experiments have been extended to the investigation of traction aids delaying slip stall failure.

The present account describes the methods used and the results obtained, a comparison being made with a simple plastic theory of deformation clarifying the problem of slip stall failure.

A special design of wheel is suggested which should give greatly improved soft ground performance over the simple cylindrical wheel without appreciable increase of overall dimensions, and yet be capable of reasonable performance on hard ground.

---

*) British Crown Copyright reserved. Published with permission of the Comptroller of Her Britannic Majesty's Stationery Office.

**) Fighting Vehicles Research and Development Establishment Chobham Lane, Chertsey, England.

1. Experimental procedure

1.1) **Scale of tests.** — Experiments were carried out at full scale to avoid errors of scaling, the series of wheels investigated being 54 ins. in diameter and with three widths, viz. 12 ins., 18 ins. and 24 ins.; this range being known to support the required loads of 3¾ to 5 tons at a sinkage not much exceeding six inches on a purely cohesive soil of shear strength about 5 lbs. per square inch.

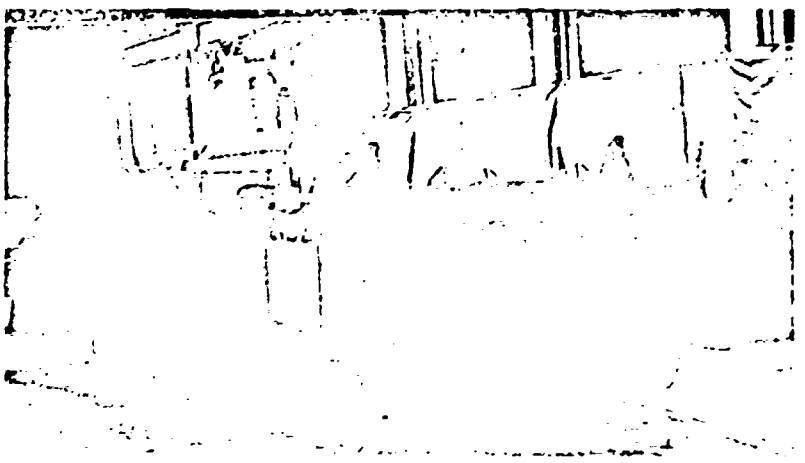


Fig. 1. — Wheel test rig.

1.2) **Test rig** (fig. 1). — The wheel under test is mounted is a steel framework rig linked to a David Brown 50 D tractor by a parallel linkage and pivot system, the linkage being adjustable for height so that it can maintain a horizontal working position for any particular test-wheel sinkage. The two axle bearings of the wheel are supported by ring springs of special design attached to the rig frame; the surface strain of these springs providing a measure of both horizontal and vertical forces acting on the axle via wire strain gauge transducers.

Two chain sprockets mounted on the wheel axle provide a drive for the test wheel at selected fixed slip rates ranging from zero to 40 % slip. This drive is achieved by chains linking to a second pair of sprockets mounted on an axle supporting three cable drums and running in bearings attached to the rig framework. Cable wound on a selected drum or pair of drums is unwound as the tractor proceeds forward thereby forcing the required degree of slip, the free cable end being anchored to the ground in the case of a single cable and drum or passed through an anchored pulley in the case of a looped cable and pair of drums. Three drums can thus provide six separate slip values and may include zero slip. Fixed negative slip rates would be obtainable if the cable were wound onto a drum from a point ahead of the tractor; provision for this is not made in the present design, but a natural negative slip value is obtainable when the wheel is undriven, i.e. when the cable is disconnected.

The rig frame together with the wheel weighs about 3,000 lbs., which load can be increased up to about 5 tons by the addition of steel slab weights to the panniers provided.

The pull in the cable is measured by a third ring spring attached to the cable anchor and is recorded together with the wheel axle thrusts and other relevant signals by an ultra violet galvanometer recorder. The system enables a determination of drawbar pull as the sum of horizontal forces acting on the wheel, together with its operating torque, for each condition of slip and axle loading.

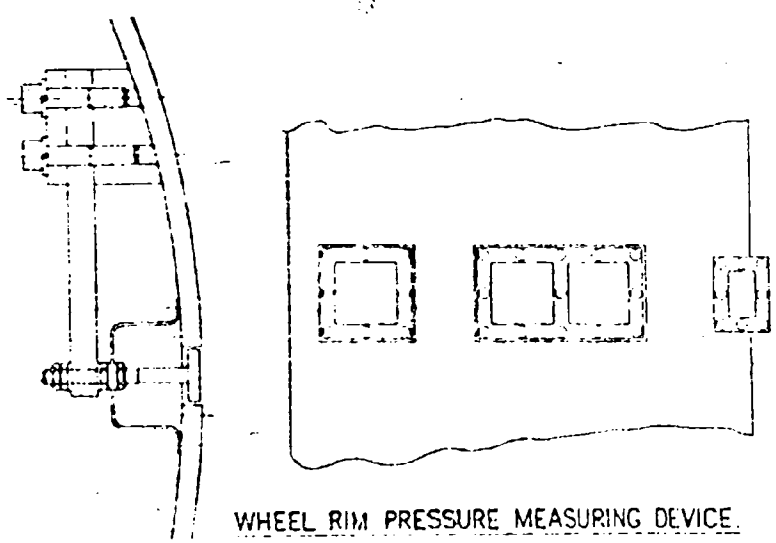


Fig. 2.

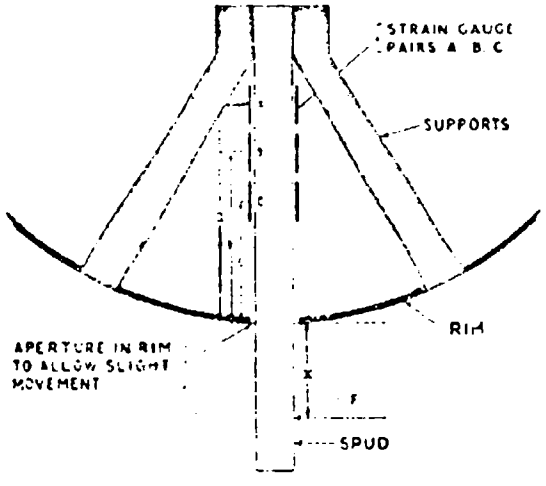
1.3) **Soil pit.** — The clay soil used for the experiments is contained in a pit dug in a concrete floor; it is 40 feet long, 4 feet 6 inches wide and some 7 feet deep. The top 4 ft. layer only is the test soil, the substrata consisting of sand and gravel. Provision is made for irrigation of the substrata while the surface moisture content of the clay test soil is maintained by spraying; surface losses, when the pit is not in use, are minimised by the use of a polythene cover. Shear strength is maintained at an approximately constant level by moisture control and by kneading with a dropping weight compactor. The kneading process also reforms the rut left by a wheel test, two or three passes being necessary for this purpose. A light roller is used to remove small surface irregularities left by the compactor.

The soil pit is sufficiently narrow to allow the tractor wheels to bridge across and run on firm concrete where they can develop the necessary tractive effort for the experiment.

1.4) **The measurement of radial and tangential forces acting on the wheel rim** (figs. 2 and 3). — Instrumentation has been provided for the measurement of radial pressure and tangential tractions acting on the wheel rim. For the case of a driven wheel the horizontal components of the tangential tractions integrated over the arc of contact of the rim with the soil give an independent measure



Fig. 3. — Tangential stress mensuring device.



Force « F » is equivalent resultant normal force on spud at distance « x » from rim.

Strain gauge pairs « A » « B » and « C » are attached to spud at distances « a » « b » and « c » from rim.

Signal from each pair is proportional to F (a ± x) or F (b ± x) or F (c ± x).

Signal from « B » is recorded.

Signals from « A » and « C » are differenced and recorded. The combined signal being proportional to « F » only and independent of « x ».

By calibration F can be found from this signal and thus « x » from the signal from gauges «B».

Forces axial to spud do not cause bending and are not recorded.

Fig. 4. — Instrumented spud.

of the tractive soil reaction; the horizontal component of the radial pressure integrated over the same are gives an independent measure of rolling resistance opposing the tractive soil reaction and forward movement. For the case of the unbraked towed wheel the sum of the two integrated horizontal components must represent the rolling resistance; here the total tangential traction would be expected to have a value zero to meet the zero torque condition of running, since the radial components can provide no torque. For the case of the braked wheel the total tangential traction would be negative, and the integrated horizontal components of the tangential tractions would add to the rolling resistance of deformation.

1. 5) Instrumented spud for tangential reation v. angle of rotation measurement (fig. 4). — An instrumented spud fixture is provided on the 18 ins. wide test wheel to give both a measure of the force developed by a spud in a direction tangential to the wheel rim, and its effective radius of application.

2. Theoretical considerations

2. 1) The simple plastic theory of rolling resistance *). — Here the wheel is assumed to have:

a) produced a rut equal to its instantaneous sinkage (plastic deformation without recovery), and

b) a uniform radial pressure q over the arc of contact with the soil.

For small angles of sinkage q may be identified with the surface strip load bearing capacity; by integration of the vertical component of q and equating to the vertical load W the sinkage δ can be shown to have the value

$$\delta = \frac{W^2}{q^2 a^2 D} \qquad (1)$$

where a is the width and D the diameter of the wheel rim.

Assuming that rolling resistance is due entirely to work done in compressing down the rut, we deduce

$$R = q \delta a = \frac{W^2}{q a D} \qquad (2)$$

Now in the case of the driven wheel let us assume a uniform tangential force to exist over the arc of contact with the soil **), which force increases with slip ***) and has a maximum value equal to the value of soil cohesion c. The integrated horizontal component of this force will be the tractive soil reaction T and at slip stall conditions will have its maximum value of

$$T_{max.} = c a l \qquad (3)$$

Where $l = r \sin \alpha$; α = angle of sinkage; r = wheel radius.

Under critical slip stall conditions

$$T_{max.} = R$$

$$\text{or:} \quad c a r \sin \alpha = q \delta a$$

$$= q a r \, [1 - \cos \alpha]$$

---

*) See Drucker I. L.R.L. Rep. 1 and 2, 1955.

**) This state of affairs has been found to be essentially correct at the high slip rates considered. See para. 3.4.

***) Defined as $\frac{V_w - V_a}{V_w}$ where V_a is the wheel rim velocity; V_g is the linear velocity of the axle relative to the ground.

Putting $q = 5.7c$ the surface bearing capacity value of an ideally « rough » strip footing we have

$$\sin \alpha = 5 \cdot 7 \, [1 - \cos \alpha]$$

from whence $$\alpha = 20° \quad \text{or} \quad \frac{\delta}{D} = 0 \cdot 03$$

Thus it would appear that a cylindrical wheel with no side walls would fail at the above sinkage on a purely cohesive soil irrespective of the actual value of soil cohesion or wheel width; it would stall before reaching this sinkage if the surface layers have a lower shear strength than the mean shear strength (slippery condition).

For a five foot diameter wheel this would mean a slip stall failure at a maximum of about 2 ins. sinkage, and the wheel cannot drive forward at greater sinkages without provision of additional tractive soil reaction.

2.2) **Side wall traction.** — An obvious source of additional tractive soil reaction for cohesive soils is that which can be obtained from suitably designed side wall plates. Using the same assumption on adhesion as for the wheel rim, the maximum horizontal component of slip resistance for side wall reaction is

$$T = c \, a \, r \sin \alpha + 2 \, c \, r^2 \, [\sin \alpha - \cos^2 \alpha \log_e (\sec \alpha + \tan \alpha)] \qquad (4a)$$

or approximately $$T = 1 \, c \, [a + 2\delta] \qquad (4b)$$

and the critical condition obtained by equating tractive soil reaction T to the rolling resistance R is now more dependent upon wheel rim width and occurs at a much increased sinkage.

Putting $R = q \, \delta \, a = N'_c \, c \, \delta \, a$ where N'_c is the appropriate bearing capacity constant for the footing shape and mean sinkage *), we find for a wheel of 5 ft. diameter and 1 ft. width that

$$\alpha = 45° \quad \text{and} \quad \frac{\delta}{D} = 0 \cdot 2$$

This means that a wheel of these dimensions fitted with effective side plates will not slip stall until a sinkage of about 1 ft. has been obtained.

2.3) **Tractive reaction available from spuds.** — Failing a sufficient tractive soil reaction from the wheel rim and side walls, recourse must be made to spuds projecting from the rim of the wheel. These may be a radial plate or an inclined plate type, but as the latter are unidirectional in performance, the radial type is usually preferable.

On static theory **) the peak tractive soil reaction provided by a single spud per unit width on purely cohesive soil is

$$P_p = \frac{W}{a \, l} \cdot h + 2 \, c \, h + \frac{1}{2} \gamma \, h^2 \qquad (5)$$

where: W is the total load; a is width of spud; l is the effective footing length; h = effective spud height; γ = soil density.

---

*) N'_c for a rough strip footing can be assumed to vary from 5.7 at the surface to 7.5 at deep sinkage $> 2.5 \, a$.

**) Retaining wall theory of Rankine.

End effects would slightly increase the value of P_p.

The third term represents the weight of the soil wedge above the line of shear and is negligible. The first term depending upon surcharge pressure can be most important, while the second term involving the soil cohesion is of increasing importance towards the end of the spud's passage through the soil when the surcharge is no longer acting above the shear surface and the first term vanishes.

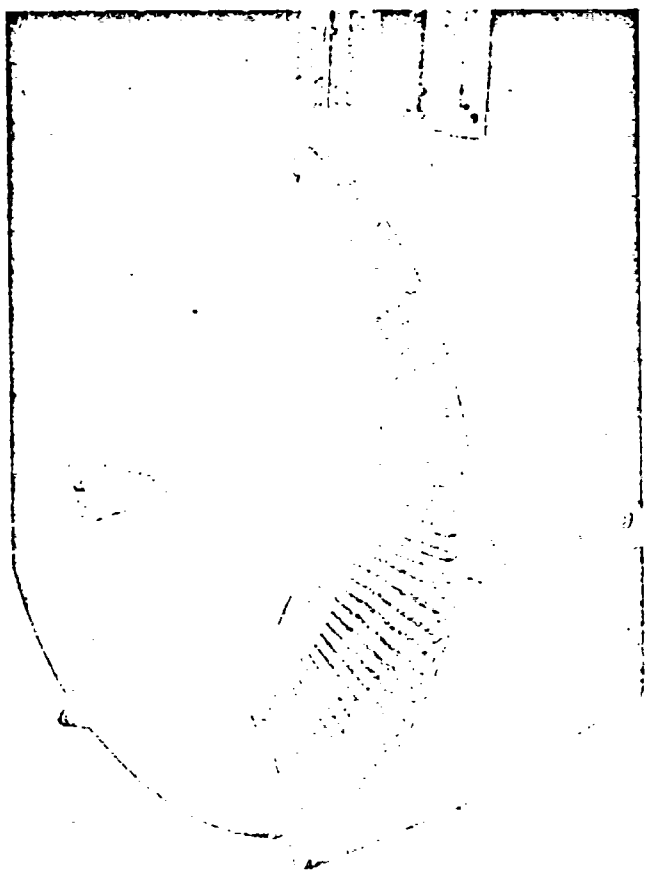


Fig. 5. — Side wall traction plates.

The first two terms have a common factor h and thus the tractive reaction would appear to be approximately proportional to the height of the spud.

The benefit of the surcharge pressure would not be obtained if the spuds were mounted, as is frequently done for convenience, to the side of the wheel rim carrying the axle load.

The variation of tractive reaction of a radial spud with slip rate is dependent upon the variation of soil shear strength with rate of shear and cannot therefore be calculated on static theory.

3. Experimental results

3.1) Rolling resistance (fig. 6). — Rolling resistance measurements made with the three test wheels were found to give a good correlation with the simple plastic theory and it would appear unnecessary to go to any greater sophistication in order to calculate rolling resistance of wide wheels at the shallow sinkage (0 - 2 ins. for the 24 in. wheel) and limited speed range (1 - 10 m.p.h.) of the tests.

The phenomenon of negative slip observed for the towed wheel increases rapidly with sinkage (12 ½ % at 2 ins. static sinkage; 25 % at 3"; 34 ½ % at 3.3" were observed for the 18 in. wheel); this must be due to upward soil flow components

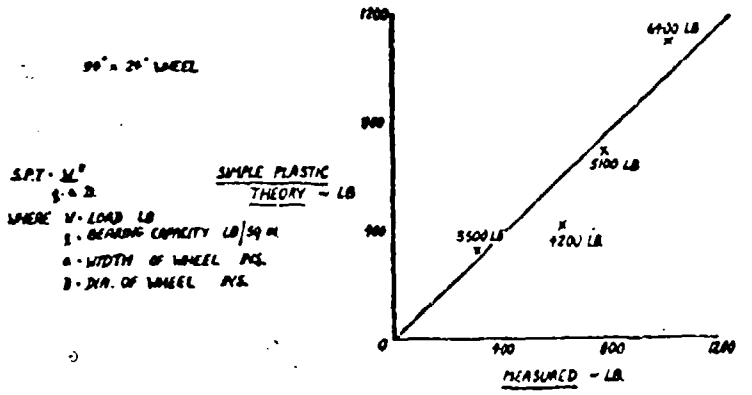


Fig. 6. — Rolling resistance correlation curve for 24 ins. wide wheel.

in front of the wheel and gives rise to added rolling resistance not estimated for in the theory. As a consequence the theory tends to underestimate at the deeper sinkages.

3.2) **Drawbar pull versus slip** (fig. 7). — The example given is the 12 in. wide wheel loaded to 6,000 lbs. on soil of cohesion 6.4 lbs. per square inch, this giving a dynamic sinkage of 6 ins. i.e. well beyond the theoretical slip stall condition at about 2 ins. It will be seen that the drawbar pull increases rapidly with slip covering the ranges — 1400 lbs. at zero slip to + 300 lbs. at 30 % slip. A single six inch radial spud mounted on the wheel rim provides + 300 lbs. (peak) at zero slip and + 3,500 lbs (peak) at 30 % slip. It is interesting to note the drawbar pull curve shews a positive rate of increase with slip and no signs of rounding off up to the 30 % slip value.

The drawbar pull provided by the spud when the soil surface is flooded remains unchanged; that due to the rim is considerably reduced.

An automatic device for sinkage measurement shows a recovery heave under these conditions of working of some 27 % (from 6 ins. to 4.4 ins.) during passage of the wheel, the total instantaneous sinkage measured from the raised lips of the rut being 7.5 ins. This plastic recovery increases the arc of contact of the wheel rim

with the soil and at high slip values can assist considerably to the total tractive soil reaction (See 3.4 below).

3.3) **Radial pressure measurement** (figs. 8 and 9). — The two examples given are again for the 12 in. wide wheel, fig. 8 being for the driven wheel at 30 % slip and 3.4 ins. static sinkage (6.7 ins. total rut depth), while fig. 9 is for the towed wheel at — 27 % slip and 4.8 ins. static sinkage (7.5 ins. total rut depth).

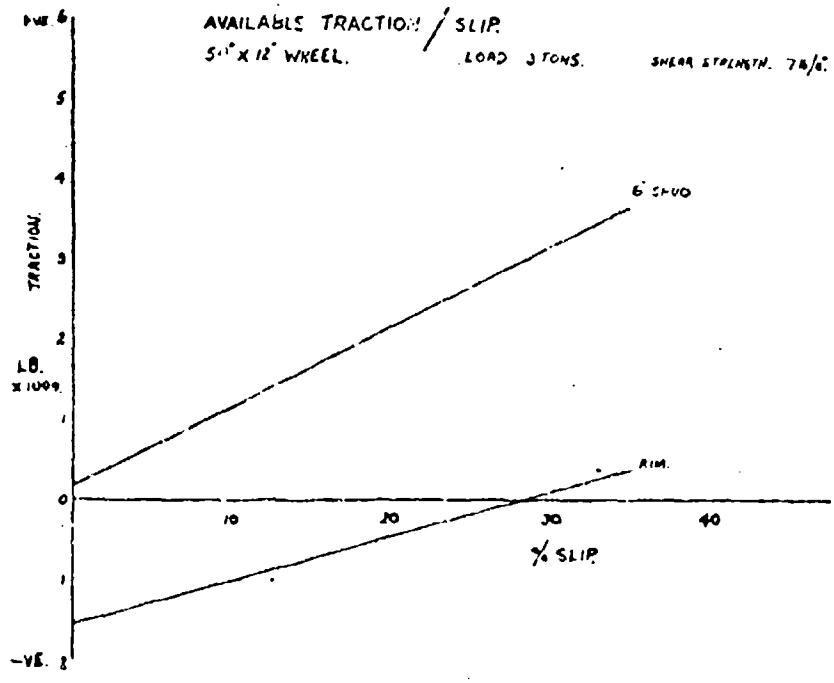


Fig. 7. — Available traction of 12 in. wide wheel versus slip.

The examples both show an approximately uniform radial pressure distribution from the first point of entry of the measuring pad into the soil until it is vertically beneath the axle (the towed wheel actually shows a 10 % increase in pressure over this range). The pressure drops rapidly beyond the vertical reaching zero at about 15° beyond, this corresponding to an inch soil heave recovery in the rut. Pressure distribution across the width of the rim (not shown) is sensibly uniform.

The assumption of uniform radial pressure made in the simple plastic theory is thus seen to be reasonably correct even for deep sinkages.

3.4) **Tangential stress measurement** (figs. 10-14). — The sensitive pad for this measurement is installed on the 18 in. wide wheel. The signatures obtained at a ground speed of 2.5 ft. per second, a total rut depth of 6 ins. and a total rim-soil contact are of 45-50° (15° of which is after the vertical) vary considerably with slip, as can be seen in the examples given. These cover a range of + 25 to — 15%.

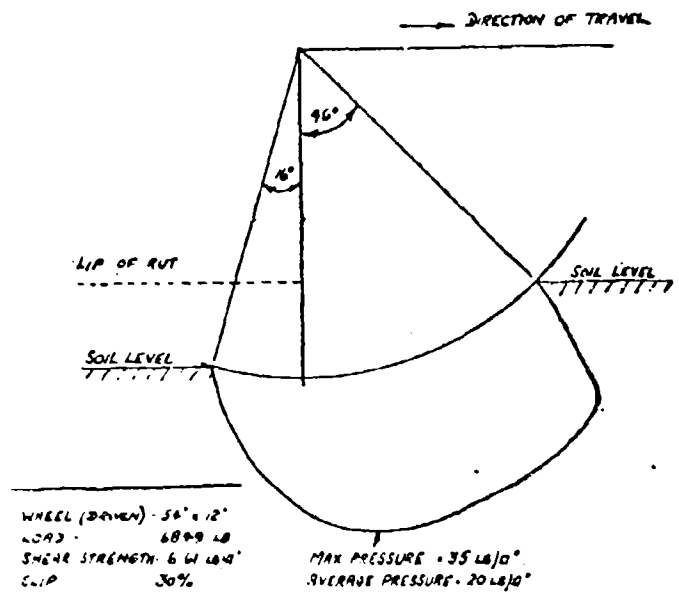


Fig. 8. — Radial pressure measurement driven wheel at 30 % slip. (12 in. wide wheel).

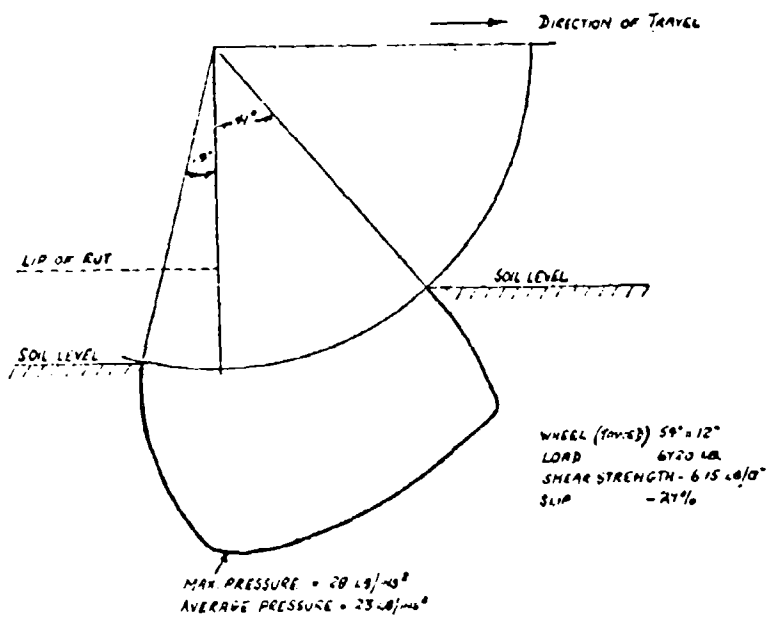


Fig. 9. — Radial pressure measurement towed wheel at — 27 % slip. (12 in. wide wheel).

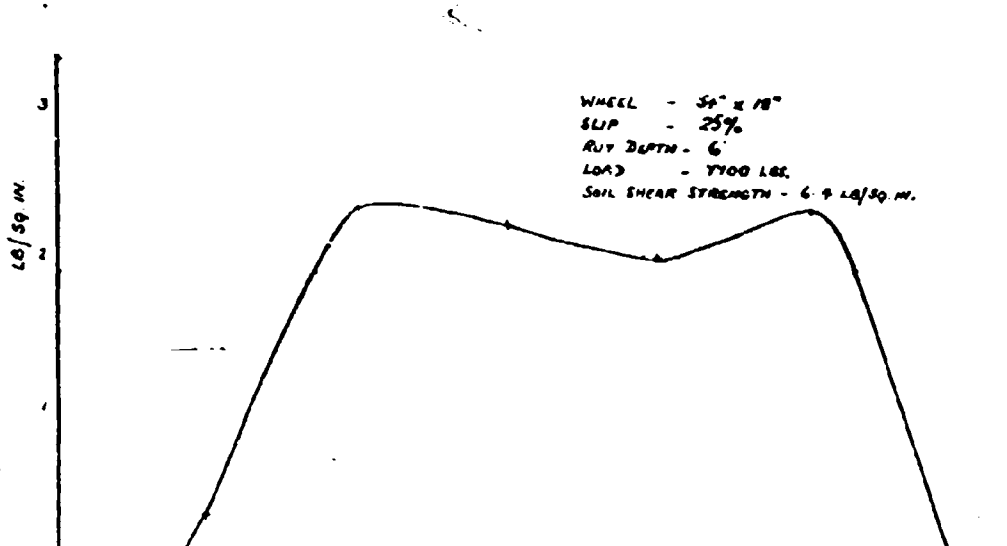


Fig. 10. — Tangential stress measurement 25% slip. (18" wide wheel).

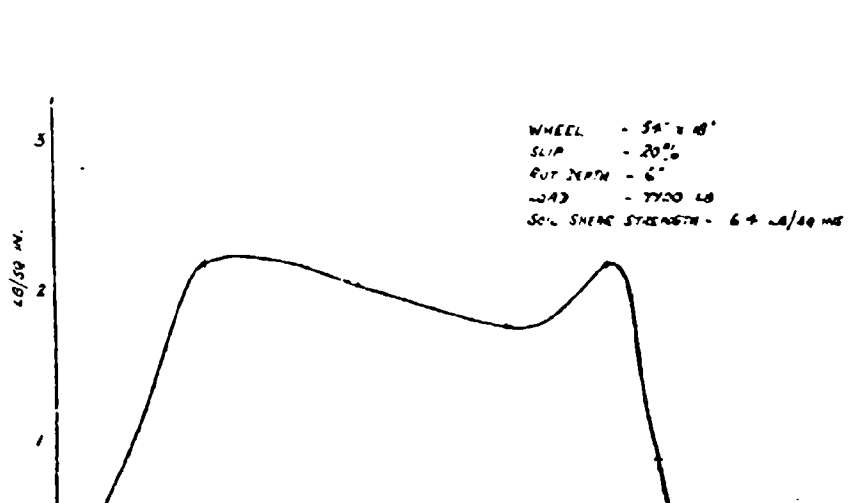


Fig. 11. — Tangential stress measurement 20% slip. (18" wide wheel).

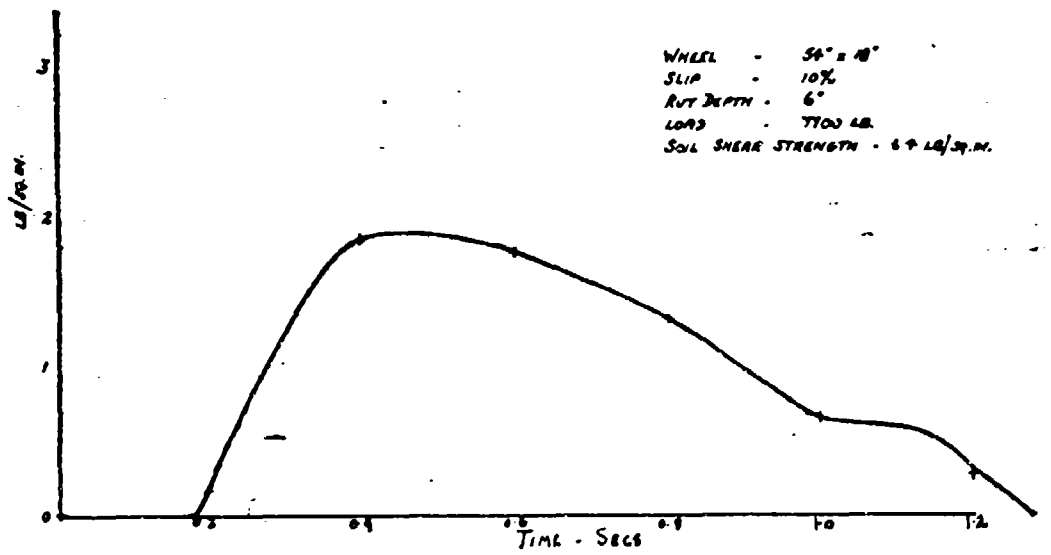


Fig. 12. — Tangential stress measurement 10 % slip. (18" wide wheel).

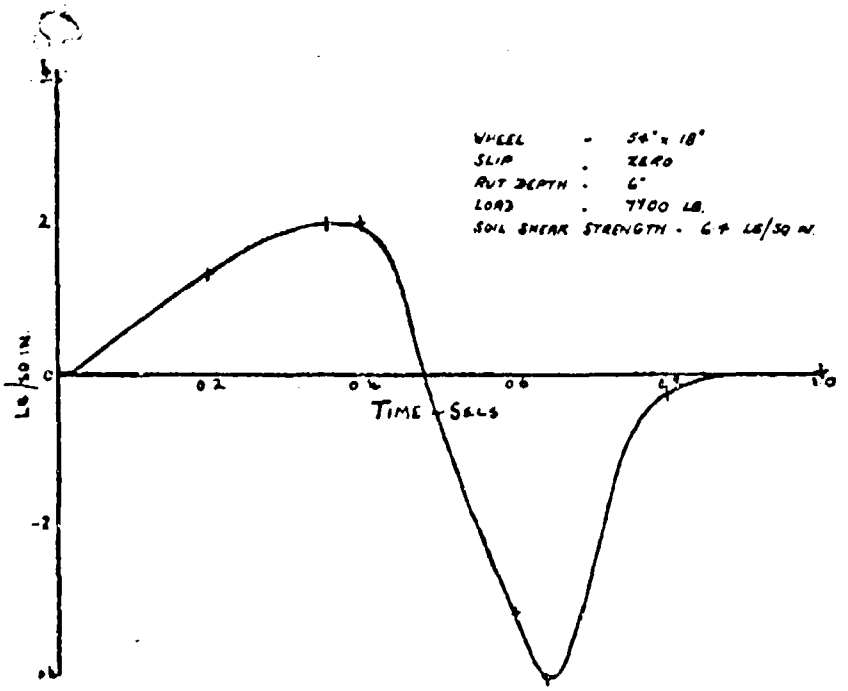


Fig. 13. — Tangential stress measurement 0 % slip. (18" wide wheel).

At all slip rates the stress rises rapidly on entry of the pad into the soil. For the higher slip rates (25 and 20 %) the stress drops gradually after entry and rises again just before exit where it drops rapidly to zero. At 10 % slip no recovery occurs before exit; at zero slip and for the negative slip of the unbraked towed wheel (— 15 % for the conditions of the experiment) the stress becomes negative before exit. For the towed wheel the average positive and negative stresses must be equal to produce the zero torque condition: the integrated horizontal components can be negative and add to the rolling resistance.

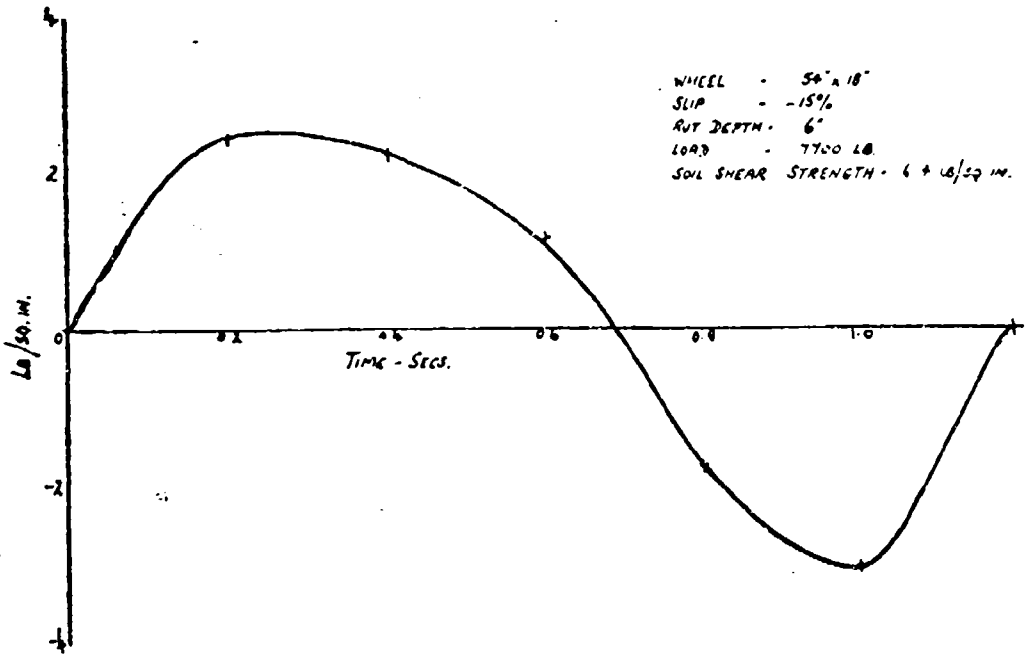


Fig. 14. Tangential stress measurement — 15 % slip. (18" wide wheel).

The maximum stress over the range 0 to 25 % slip appears to be linear with slip and for the tests made had a value of 0.4 c at 25 % and 0.2 c at zero slip.

The assumption of uniform tangential stress increasing with slip made in the simple plastic theory for the driven wheel for the estimation of tractive soil reaction is thus not greatly in error at the higher slip values, and under slip stall conditions (100 % slip) could easily have a value equal to or in excess of the value of soil cohesion. The theory does however underestimate the arc of contact at deep sinkage conditions due to plastic recovery of the rut and hence underestimates the total tractive soil reaction.

For the driven wheel the integrated horizontal component of this stress represents a measure of the actual tractive soil reaction of the rim under working conditions independent of rolling resistance.

3.5) **Side wall traction plates** (*e.g.* 5). — Two 120° plate sections with 1 in. deep close-spaced radial ribs were mounted on the 18 in. wide wheel. When operating at 5 ins. sinkage (3.7 tons loading) and 20 % slip, these plates increase the drawbar

pull by about 500 lbs. (recorded 750 lbs. rim only; 1,260 lbs. with side plates). This gain is still present when the soil surface is flooded (recorded — 700 lbs. rim only; — 200 lbs. with side plates).

It is clear therefore that the use of ribbed side plates on rigid cylindrical wheels delays wheel failures on clay soil.

It is interesting to note that flat unribbed side plates when fitted produced no measurable additional tractive soil reaction. This was found to be because soil contact was not made with the flat side plates; conical side plates might well produce an effect.

3.6) **Instrumented spud.** — The peak value of resistance recorded by the instrumented spud mounted on the 18 in. wide wheel is of the same order as that calculated by formula 5 in paragraph 2.3.

E.g. For the conditions of 7,000 lbs. load, $c = 6.4$ lbs. per square inch, slip = 20 %, sinkage = 4 ins.

the measured p max. = 3,600 lbs (at 20 % slip)

the calculated p max. = 3,330 lbs. (at zero slip).

For this estimate l was assumed equal to $r\ (\sin\alpha + \sin\alpha_1)$ where α is the angle of sinkage (31°30') and α_1 is the angle of soil rim contact to the rear of the axle (15°).

The centre of pressure on the spud at the position of maximum was found to be near the centre of the spud indicating a uniform pressure over the spud surface.

4. The development of a rigid rim wheel to carry 3-5 ton load and capable of good on and off road performance

The outside dimensions of such a wheel will be 5 ft diameter and 1 ½ ft. width. Such a wheel is being designed with a resiliently mounted rim using parallel layer rubber suspension pads spaced at 90° or 60° intervals around the axle, the degree of linear resilience being limited to 6 inches. The rim will be provided with radially ribbed side plates delaying slip stall failure and forming a rigid box structure.

The design provides adequate space for 4 or 6 automatic spuds which can be self injecting and retracting when operated from a cam mounted on the now eccentric axle, but can be retained within the rim when the cam is not in operation.

If the injection process is limited to 20° before and after the vertical through the wheel centre some advantages in soft ground running of the system over a rigid wheel with fixed spuds are apparent.

1) The mean vertical component of torque resistance is reduced while the useful horizontal component is maintained.

2) The excavation made by the spud is greatly reduced.

3) The rim will be self cleaning due to the soil shear surface reverting to the rim on withdrawal of the spud.

4) The wide spacing of the spuds in conjunction with the torsional resilience of the wheel will produce a variable slip velocity effect producing a higher average level soil reaction than would be obtained by a constant velocity rim (additional torsional resilience in the wheel drive may be necessary to produce this effect *and* to protect the drive from impulsive loading).

For hard ground running a cavity cushion tyre will be mounted in segments around the rim and will serve to increase the area of contact with the road and to attenuate high frequency vibration.

It is envisaged that the final wheel will have adequate traction due to rim and side wall effects to enable it to traverse all but the most difficult ground. Upon or before slip stall, the automatic spuds will be brought into operation so that the vehicle *can* proceed to firmer ground, when the spuds are retracted and the vehicle proceeds without their use. A safety device will be necessary to guard against the event of spuds being left extended on reaching a hard surface.

5. Conclusion

5. 1) The simple plastic theory as given is adequate for the calculation of rolling resistance of wheels of the dimensions used in the experiment when sinkage is limited to about 2 ins. At deeper sinkages increased upward flow components cause increased frontal resistance and high negative slip values; the latter result in negative tangential force components which can further add to the rolling resistance. Errors at deep sinkage are also present due to the approximate nature of the theory.

5. 2) At high positive slip values the assumption of a uniform tangential stress increasing with slip is approximately correct. The theory of tractive soil reaction underestimates unless allowance is made for the additional arc of contact due to soil recovery in the rut.

5. 3) The net result on the estimate of critical slip stall sinkage on a uniform medium is in some measure compensated for by the errors in the estimate of rolling resistance and tractive soil reaction.

5. 4) The separate measurement of radial and tangential rim stresses enables the rolling resistance and tractive soil reaction to be separated under working conditions.

5. 5) Ridged side plates have been shown to delay slip stall failure.

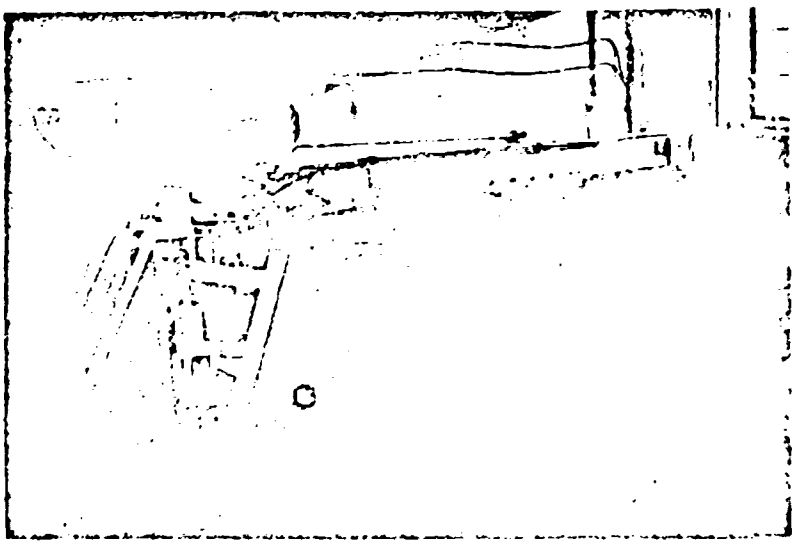
5. 6) Individual radial spuds give increasing benefit with slip up to (and apparently beyond) the limit of the experiments (30 % slip).

5. 7) It is thought that the described design of wheel with 4-6 self injecting spuds fitted to a 5 ft. diameter resiliently mounted rigid rim will carry axle loads of at least 3 tons over soil of 5 lbs. per square inch shear strength and yet give good performance on hard surfaces.

DISCUSSIONS

B. MAYFIELD, F. SHERRATT. — The Authors are working in the Civil Engineering Department of the University of Nottingham, England.

As a preliminary to the main on the problems of steering wheeled vehicles on soft ground investigation, a programme of basic research is being followed into the forces and couples acting on a rigid cylindrical wheel moving in various circular paths at various sinkage in an artificial clay. The wheel axle can also be



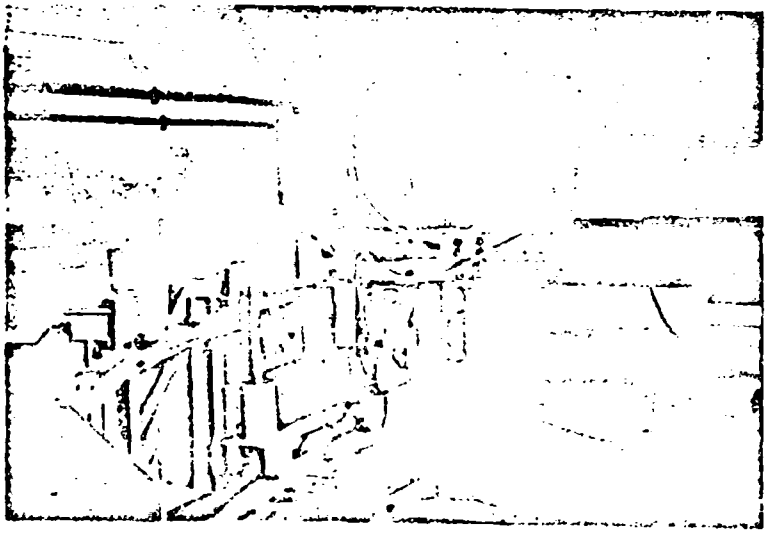
Slide 1. General view of apparatus.

set at varius angles to the path radius. The towed wheel at present under investigation is 9" dia. × $2\frac{11}{16}$" wide, being a scale model of the 5' drain × 18" wide wheels used by Mr. Uffelmann. It is intended to vary the wheel size in order to check the applied dimensional analysis, and to investigate wheels driven by hydraulic motors.

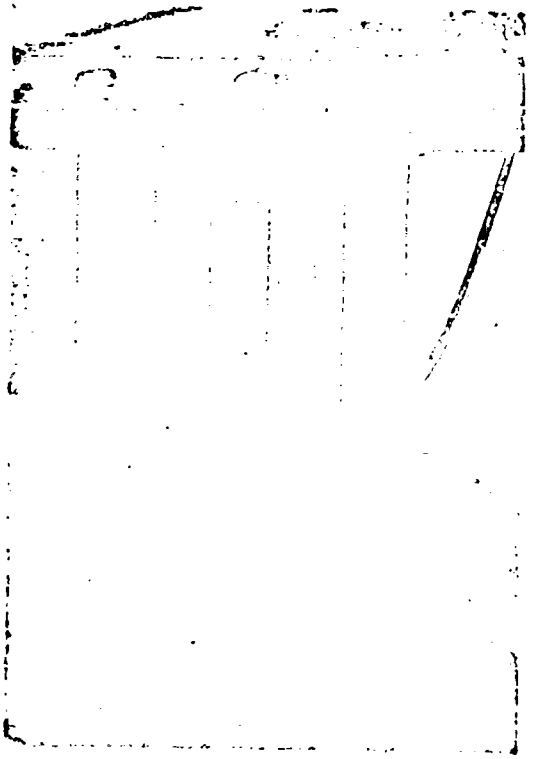
(Slide 1) The apparatus has a 12' long horizontal rotating arm to which the wheel can be attached in any of three positions, corresponding to the three soil troughs of differing radii. (Slide 2) It is driven by an electric motor at its outer extremity, acting through a pulley system and a magnetic clutch to a driving wheel on the upper track. The driving wheel is kept in contact with its track by two springs acting on the lower idling wheels.

(Slide 3) The test wheel is rigidly attached to the arm at a pre-set sinkage with its axle held in two load cells (slide 4) designed on the lines suggested by Close and Muzzey [*]). The load cells measure the vertical, horizontal and axial forces

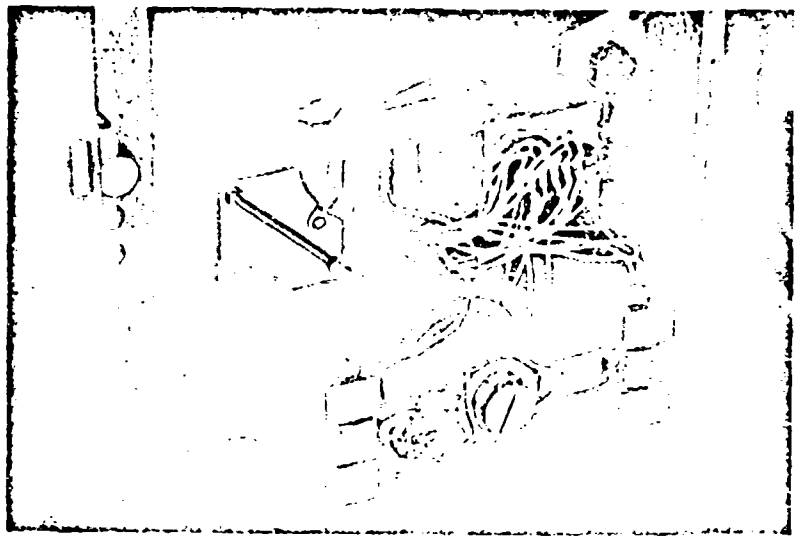
[*]) W. Close and C. L. Muzzey, «A device for measuring mechanical characteristics of tyres on the road», I. Mech. E. Proc. of the Automotive Division 1956-1957.



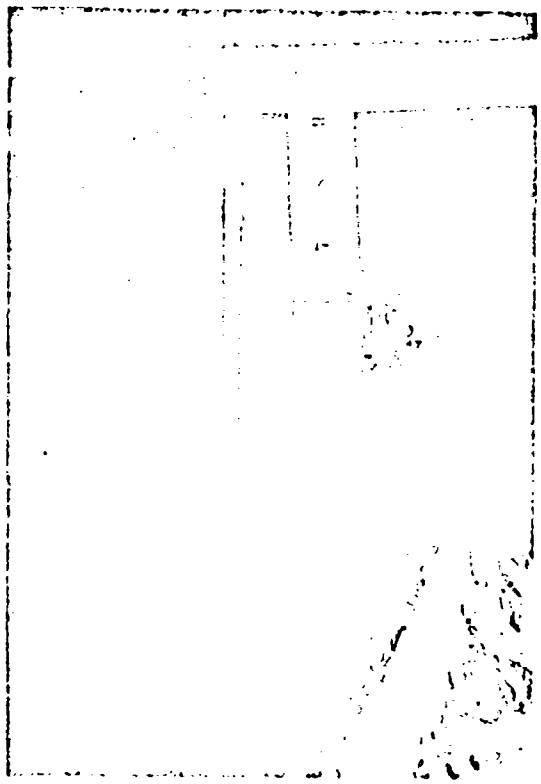
Slide 2. — Radial arm drive.



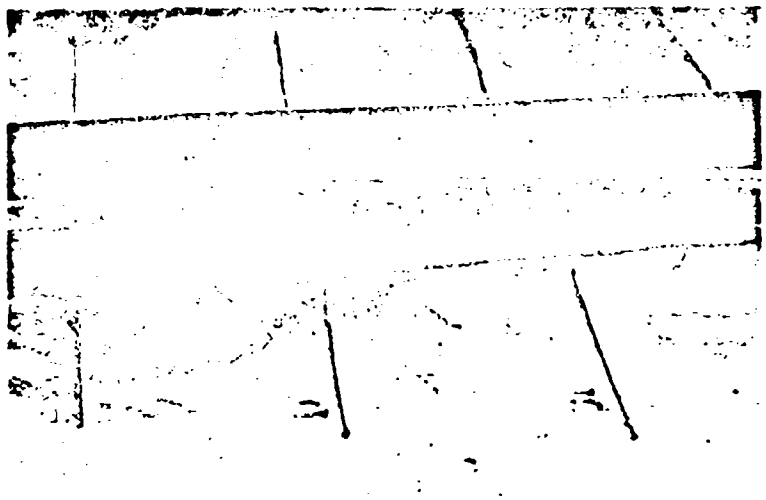
Slide 3. — Test wheel suspension.



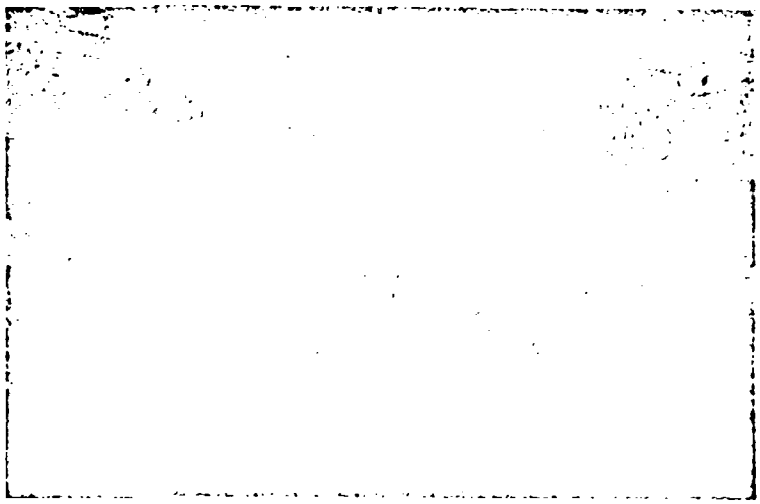
Slide 4. — Left-hand load cell.



Slide 5. — Example of side heave.



Slide 6. -- Forward movement of side heave



Slide 7. - Forward movement of track and lateral tension.

by means of electrical resistance strain gauged beams. The forces are recorded by means of a 12-channel recorder.

(Slide 5) Although working with clay entails track reforming difficulty, it simplifies observations on the rut. Considerable side heaves have been observed under certain condition, (slide 6) with large forward movements occurring within the « heave ».

(Slide 7) Radial lines drawn before a test run show forward movement of soil within this rut, increasing towards the outside of the path, together with considerable lateral tension.

J. PHILLIPS. — Gentlemen, Mr. Uffelmann, showed a number of slides giving the distribution of the radial and tangential stress on what many of us call the contact patch. It seems to me that three in particular, dealt with percentages of slip in the neighbourhood of zero, if I remember, slip 0, slip 5%, slip 10%, or some such figures. Now, you will notice that each of these diagrams, differed considerably from one another, and I had the impression any way that Mr. Uffelmann was asking us to draw important conclusions, about the distribution of the tangential stresses and the normal stresses in the neighbourhood of zero slip. I think Mr. Uffelmann will agree with me that in this work in particular, where the amount of sinkage of the wheel is considerable, that it is most important indeed to define very carefully what one means by slip. In a way this contribution, or this question of mine, of Mr. Uffelmann, is foreshadowing some remarks, which I think I will be making in connection with my paper if I remember on Wednesday.

N. 9

Sul trasportatore tutta ruota

All wheel carrier

Prof. Camillo De Gregorio *)

ABSTRACT. -- *A big «tyre», having the inside pneumatic filled with a liquid to transport, is, by itself, an off-the-road vehicle.*

Generally it should be drawn in one or more pieces, but could also be a self-moving.

The Author, explaining the principal characteristics, points out some solutions how to employ it.

Dal punto di vista della meccanica della locomozione, i pregi principali dei *trasportatori tutta ruota* possono riassumersi nei tre seguenti: minime pressioni specifiche trasmesse al suolo, facilità di deformazioni locali e quindi possibilità di «bere» gli ostacoli del terreno, grande inerzia al moto. La prima particolarità rende il mezzo idoneo alla marcia su terreni fangosi, sulla neve, sulla superficie gelata dei laghi; la seconda consente il movimento fuori strada su zone pietrose, o a forte rugosità, su terreno di campagna, con asperità vegetali, o con buche, ecc.

In linea di massima si può pensare di scendere sino a 0,2 ÷ 0,3 kg/cm² come pressione media specifica, riferita a tutta l'*area di impronta*. Si tratta di valori talmente piccoli da permettere il moto sui fondi terrestri, che presentino le più basse *capacità portanti*.

Le dimensioni massime delle deformazioni sul corpo del trasportatore sono legate alla pressione interna, alla flessibilità del ricoprimento esterno, al peso totale.

In genere, penso che la grandezza dell'ostacolo sul terreno completamente ammortizzabile, sia da porsi in relazione diretta e con la larghezza e con il diametro del contenitore rotolante.

Nel caso di forma «a ruota», è da ritenersi che le dimensioni dell'asperità, perfettamente superabile, siano di poco inferiori al diametro dell'anello, se la pressione interna non supera la mezza atmosfera e se il raggio totale esterno della ruota è almeno doppio del diametro dell'anello.

Questo sistema di trasportatori per liquidi, costituito da copertoni giganti, nel cui interno, al posto della camera d'aria a pressione, si trova un serbatoio in gomma, è nato in seguito al perfezionarsi dei procedimenti tecnologici per la costruzione dei pneumatici.

---

*) Direttore dell'Istituto dei Trasporti, Facoltà di Ingegneria, Università di Palermo.

Il caricamento (e lo svuotamento) avviene attraverso tubazione, che passa in corrispondenza dell'asse di rotazione della « ruota ». E' la pressione del liquido da trasportare a mantenere gonfio il grosso pneumatico.

Se non sono previste particolari aggressività chimiche da parte dei prodotti immagazzinati, è lo stesso *copertone* a fare da serbatoio. Il trasporto avviene per semplice rotolamento della « ruota » e non vi è quindi bisogno di carro o di *chassis*. La « ruota » fa cioè da recipiente e, nello stesso tempo, da veicolo. Naturalmente occorre provvedere ad un mezzo di trazione che potrebbe essere, ad esempio, un trattore cingolato, o un veicolo automobilistico di opportuna potenza.

E' ancora da pensare alla possibilità del contenitore rotolante automotore.

Se i trasportatori sono trainati, essi vengono opportunamente accoppiati, sì da costituire un « treno » di due o più pezzi.

Il trasportatore rotolante, a parte esigenze di trazione, non ha quindi bisogno, per il moto, di una vera e propria via a manto apparecchiato. Esso pertanto, non solo è adoperabile su strade in pessimo stato di manutenzione ed in condizioni meteorologiche avverse, ma su terreni agricoli accidentati, su cattive piste sabbiose, in zone artiche.

Gli impieghi fin'oggi adottati riguardano trasporti militari.

A completamento di quanto detto deve aggiungersi che, non avendosi a temere fenomeni di usura nel *battistrada*, così accentuati come nei pneumatici degli autoveicoli, il materiale con cui è fabbricato il *copertone* può presentare una maggiore flessibilità ed un minor peso per unità di superficie.

Tenuto conto di questo fattore e della mancanza di un vero e proprio veicolo (per cui la *tara* risulta parecchie volte inferiore al carico trasportato), si osserva che la resistenza alla trazione del trasportatore rotolante, riferita al peso del liquido, è inferiore a quella che si riscontra nelle normali autobotti, in marcia su strade ordinarie.

• • •

Il miglior impiego del trasportatore rotolante può attuarsi con il suo completo riempimento. Il moto è altrimenti possibile solo a velocità minime e su tratte pianeggianti.

Quando il trasportatore è pieno e la sua velocità di rotazione è sufficiente, non si ha scorrimento relativo tra pareti e liquido. La massa fluida rotola anch'essa, incrementando l'inerzia giratoria del complesso. E' quindi possibile il superamento di ostacoli di un balzo, senza sensibili variazioni di velocità e senza strappi sull'organo trainante.

Più precisamente, potremmo dire che il *peso d'inerzia* del trasportatore, durante la fase iniziale del moto, cresce sino a stabilizzarsi, in corrispondenza di una data velocità, ad un valore massimo costante. La velocità di rotazione alla quale il peso d'inerzia raggiunge il suo massimo è tanto più bassa quanto minore è il rapporto tra larghezza dell'anello e diametro esterno della ruota. Un grande diametro, d'altra parte, porta con sè un minor numero di giri a pari velocità di avanzamento, e agisce quindi sfavorevolmente, in tal senso.

L'alettatura interna, o meglio ancora, la scompartimentazione, fa sì che tutta la massa del liquido trasportato roti sincronicamente all'involucro esterno.

La scompartimentazione consente, in particolare, il trasporto di sostanze solide pulverulente o granulari. Naturalmente occorre prevedere, in tal caso, un sistema diverso di caricamento, per esempio, munendo il trasportatore rotolante di bocche laterali, a chiusura ermetica.

L'uso prevalente dei trasportatori è per i prodotti petroliferi e per i rifornimenti d'acqua. Solo in tali applicazioni sono stati finora utilizzati.

Questo mezzo di trasporto trova il suo normale settore d'impiego nell'approvvigionamento di basi polari, di località site in zone forestali o impervie, in prossimità di lande acquitrinose ed in genere in zone prive di strade. Le sue prestazioni sono particolarmente apprezzate dal punto di vista militare e tattico (campi aerei *avanzati*, *teste di ponte*, ecc.), durante grandi lavori di bonifica e di costruzioni (piste aeroportuali, cantieri stradali, dighe, ecc.).

Si potrebbe ancora pensare che il trasportatore rotolante sia particolarmente impiegabile su terreni di corsa extraterrestri assai scabrosi, duri, in cui l'accelerazione di gravità sia particolarmente bassa.

I trasportatori rotolanti si prestano ad essere tra loro collegati, in modo da formare dei veri e propri « treni », e poichè la loro capacità di trasporto è notevole, non è da escludersi che possano sostituire, in parecchi casi, le autobotti e le autocisterne. A notarsi che il loro impiego non desta alcuna preoccupazione di sicurezza e che il loro costo può risultare inferiore a quello degli automezzi convenzionali, tenuto anche conto della necessità di uno speciale trattore.

Il sistema si presenta pure idoneo, oltre che per i trasporti congiunturali (mancanza iniziale di strade, casi di impraticabilità), a veri e propri trasporti regolari di grandi quantitativi di prodotti petroliferi, o altri liquidi in genere. A quest'ultimo proposito bisogna tener conto della possibilità che le pareti interne dei serbatoi flessibili vengano attaccate dalle sostanze trasportate.

La « The Four Wheel Dive Auto Co. », a cui si debbono alcune realizzazioni, ha messo in uso dei serbatoi in gomma, che resistono bene al trasporto dei combustibili, aventi un contenuto aromatico sino al 40 % e che possono lavorare sino a temperature di — 20° e di + 50° C.

I contenitori a pneumatico possono venire agevolmente caricati su carri ferroviari e su aeroplani. Da questi ultimi possono essere anche lanciati con paracadute.

Oltre che da veicolo, i contenitori servono da serbatoi statici, con grande economia di impianto, facilità di trasloco, eliminazione di travasi intermedi.

Si tenga infine presente la possibilità di impiego dei contenitori su buone strade di pianura: data la bassissima resistenza specifica di rotolamento essi consentono ad un autocarro di potenzialità medie (che non rinunzia al suo normale carico), di poter trainare sino a velocità dell'ordine di 30 km/h, una ventina di tonnellate di prodotti.

* * *

Il rimorchio di più trasportatori rotolanti può agevolmente attuarsi, purchè essi siano uniti tra loro da tiranti rigidi. Se la lunghezza di questi tiranti è regolabile, può scegliersi, per ogni tipo di terreno, un adatto distanziamento. Ciò, sia per evitare orme troppo profonde (suoli di bassa *capacità portante*), sia per poter meglio sfruttare la notevole inerzia del veicolo (suoli molto accidentati).

In questo secondo caso la distanza tra le ruote va commensurata, oltre che al suo diametro, alla dimensione media degli ostacoli sulla superficie di corsa, per modo che la resistenza istantanea al moto dell'intero « treno » rimanga costante.

I tiranti debbono essere collegati da una timoniera, attraversante l'asse di rotazione e quindi munita di boccole.

Su ogni ruota vanno applicati, da ambedue i lati, i tamburi dei freni, per esempio del tipo automobilistico ad espansione, con ganasce rivestite di ferodo. L'azione non può che essere pneumatica: è quindi necessario un adatto impianto a bordo del trattore.

Il cilindro a freno può porsi sulla timoniera, da un lato.

Il comando al tamburo opposto deve avvenire attraverso l'asse, che pertanto va previsto cavo.

L'arresto e la direzionalità di un veicolo tutta ruota automotore potrebbero attuarsi a mezzo di aria compressa. Da una bombola ad alta pressione l'aria verrebbe inviata sui bordi gonfiabili, posti trasversalmente sulla superficie esterna. Una prestabilita dissimetria su tali bordi creerebbe dei risalti, per provocare il cambiamento di direzione.

Ma, evidentemente, è meglio ricorrere alle ruote binate quando si desidera un veicolo automotore.

Per quanto mi risulta, nessuna prova è stata fin'oggi effettuata su trasportatori automotori. La difficoltà principale consiste nell'equilibrare la spinta esercitata dal motore.

Motore e guidatore verrebbero collocati a sbalzo, a ciascun lato della ruota.

Servendosi di un trasmettitore pneumatico o idraulico e ricorrendo al sistema di sacche gonfiabili, questa difficoltà rimane superata.

L'aria compressa viene immessa, ciclicamente, a mezzo di un distributore rotante, su ciascuna sacca periferica, in modo da produrre azione di moto. Oppure può adoperarsi il sistema inverso: tenere rigonfi tutti i serbatoi esterni e scacciare ciclicamente l'aria da ciascuno di essi, in modo che sia raggiunto l'effetto voluto. In questo secondo caso la ruota si presenterebbe come avente una dentatura esterna a grande risalto. E' possibile ancora pensare a sporgenze rigonfiabili « a spina », oppure « a chevron ».

Il sistema permette, indifferentemente, la marcia nei due sensi e quindi anche l'azione di arresto. Tutto sta nella adatta regolazione sincrona del distributore dell'aria alla rotazione del trasportatore.

Lo schema proposto non permette, evidentemente, elevate velocità di marcia,

ma evita allo speciale veicolo la necessità di venire trainato da un mezzo estraneo.

Il dispositivo autonomo descritto è misto ad aderenza e ad impuntamento.

Come dati per una calcolazione preventiva darei i seguenti valori (veicoli trainati):

— rapporto tra tara e carico	1/3 ÷ 1/4
— resistenza alla trazione su ottima strada	20 kg/tonn
— idem su terreno fangoso di campagna	30 kg/tonn
— idem su terreno sabbioso	40 kg/tonn
— idem su terreno roccioso o pietroso	40 ÷ 100 kg/tonn
— velocità massima su strada	30 km/h
— idem su pista	25 km/h
— idem su terreno accidentato	20 km/h
— carico massimo trasportabile per unità	da 500 a 1000 kg ed oltre
— coefficiente d'inerzia per la determinazione del peso fittizio	$k_a = 2 \div 2{,}5$
— rapporto tra sforzo di trazione allo spunto e sforzo di trazione a regime	2,5 ÷ 3,5

Il trasportatore tutta ruota è un veicolo al cui impiego conviene indirizzarsi per talune speciali applicazioni.

La presente relazione ha appunto lo scopo di invito e introduzione agli studi relativi.

DISCUSSIONS

N. W. RADFORTH. — It is important to establish a concept of what is meant by «Marsh». What are the reference features accepted by Prof. De Gregorio for this troublesome type of terrain? It is my experience that a wheeled vehicle has virtually no chance of exhibiting effective tractive effort on marshy terrain.

C. DE GREGORIO. — Ringrazio l'interlocutore principalmente perchè egli mi permette di correggere una parola della traduzione in inglese della mia breve esposizione.

Io non ho parlato di marcia su «palude». Il contenitore non è difatti adatto al movimento su fondi acquitrinosi, aventi un certo battente d'acqua. Esso può solo marciare su terreno consistente fangoso, di bassa capacità portante.

Il contenitore rotolante ha anche un'altra posibilità d'impiego, che sta in un campo perfettamente opposto: marcia su terreno sabbioso, rugoso o pietroso.

Evidentemente la traduttrice è incorsa in una involontaria imprecisione riportando in inglese la parola italiana «palude».

Il contenitore ha tuttavia delle qualità «anfibie» nel senso che, con opportuni accorgimenti, se ne può studiare il moto nell'acqua profonda sfruttando doti di galleggiabilità.

N. 10

The steering of tracked vehicle by articulation

La sterzatura dei veicoli cingolati mediante articolazione

– C. J. Nuttall, Jr. *)

The Author not having been able to attend the meeting and to present his paper has expressed the wish not to have it published.

L'Autore, non avendo potuto presentare personalmente al Convegno la sua relazione, ha espresso il desiderio che essa non venisse inclusa negli Atti.

---

*) Wilson Nuttall Raimond, Engineers inc., Chestertown, Maryland, U.S.A.

Ruota strada: cingolo fuori strada

Wheels for the road tracks for cross-country

G. Bonmartini (Roma)



LEONARDO DA VINCI

in una lettera del 1484 diretta a Ludovico Sforza

« Item farò carri coperti e sicuri inoffensibili, i quali entrando intra li inimici con sue artiglierie non è sì grande moltitudine di gente d'arme che non rompessino. E dietro a questi potranno seguire fanterie assai illese e senza alcuno impedimento ».

in a letter, dated 1484, addressed to Ludovico Sforza

« Also, I shall make covered vehicles, invulnerable and safe, equipped with guns, to penetrate into the enemy's ranks; these will crush the resistance of any number of armed soldiers. Such vehicles will be followed by infantry, which will proceed safely and without any impediments whatsoever ».

Ricordo qui, in ordine alfabetico, i miei valenti Collaboratori: Dott. Ing. Ferdinando Bordoni (calcoli matematici), Comandante Gian Giacomo Chiesi (prove ed esperienze), Dott. Ing. Carlo Gianini (progettazione meccanica), e ringrazio la Fiat S.p.A. per il disinteressato e prezioso aiuto prestatomi.

ABSTRACT. — *In the present Report the Author wishes to express his opinion, based on many years of diligent and thorough research, as follows:*

1) the track is the only means permitting reliable off-the-road circulation;

2) in order to yield the best possible performance, the track has to be pneumatic.

This Report gives a condensed description of the studies and research carried out in order to obtain a high speed pneumatic track consisting of one continuous band.

Furthermore, as a result of intensive studies on frictions in the track and on the ground, it describes a track where the sliding friction is converted into rolling friction together with a new joint for connection of the links of the chain.

Il problema dei mezzi atti ad operare fuori strada, mi si presentò in maniera precisa, nel 1928 e, più precisamente, sotto il profilo aeronautico.

Avevo, allora, messo allo studio un piccolo bimotore da turismo a 5 posti, non senza prima avere indagato sulle facoltà di assorbimento del mercato internazionale, per un aereo del genere.

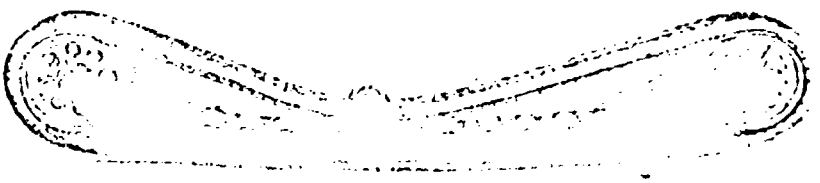


Fig. 1.

Mi sembrò, come ancora mi sembra, che il vero turismo aereo non fosse rappresentato dalla facoltà di trasferimento da un regolare campo di aviazione ad un altro, bensì dalla possibilità di trasferimento molto più vasto, e cioè da un punto qualsiasi ad un altro.

Mi misi, allora, a studiare il problema e mi convinsi che l'unica strada da seguire era quella di realizzare un cingolo adatto allo scopo (fig. 1, 2, 3).

Nelle illustrazioni annesse alla presente Relazione, è possibile trovare traccia delle diverse vie seguite nei vari tentativi di realizzazioni pratiche e, in qualche caso, anche delle esperienze compiute.

A parte le leggi che limitavano (e, purtroppo, limitano ancora) l'impiego dei mezzi aerei privati, un piccolo bimotore, originale anche come sistemazione della potenza motrice — fig. 4 — atto ad operare presso a poco dovunque e anfibio, avrebbe potuto avere una certa fortuna commerciale.

Nel 1941, per esigenze belliche, fui costretto ad un lungo soggiorno in un Paese dove il problema dei trasporti dimostrò la sua importanza vitale e mi convinsi allora, sempre più, che l'impiego del cingolo integrale era il solo mezzo atto a risolvere il problema.

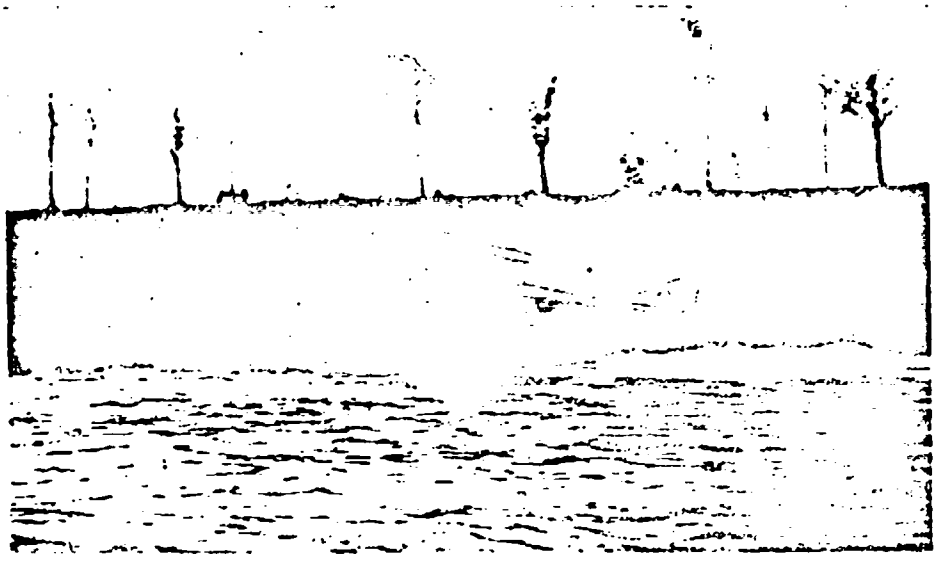


Fig. 2.

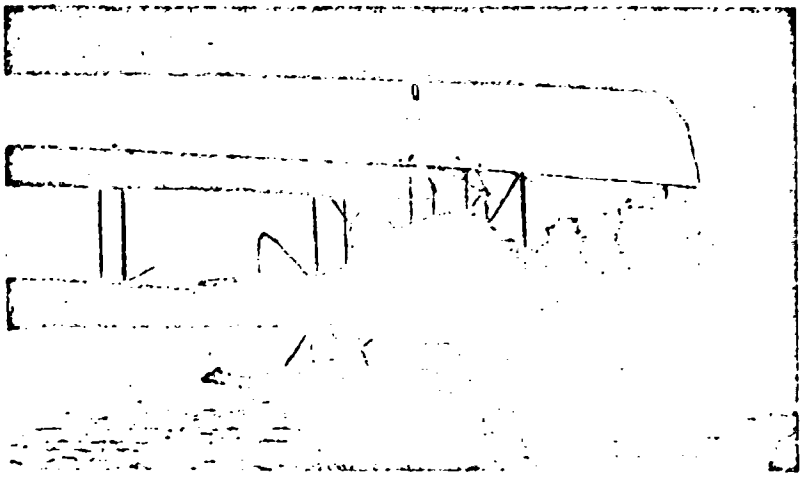


Fig. 3.

Un articolo del Generale Guderian, pubblicato sulla « Wehr-Wissenschaftliche Rundschau » del maggio 1952, commentò chiaramente questo asserto.

Venuta la pace, proseguii i miei studi e nel 1949 con l'aiuto della Superga S.p.A. (Gruppo Pirelli), realizzai, a mie totali spese, il primo tubolare pneumatico che fu esperimentato, praticamente, sotto un vecchio Piper 65 HP e che dette, già dalle prime prove, risultati che non esito a definire, per quell'epoca, strabilianti (fig. 5, 6, 7).

Ma il tubolare in sè e per sè aveva numerosi difetti.

La Pirelli S.p.A. avocò, allora, a sè il problema della messa a punto del tubolare e, sempre a mie totali spese e grazie al valore dei Collaboratori della Pirelli stessa, si arrivò alla produzione di tubolari perfetti, non solo, ma dei quali la Pirelli riuscì a metterne a punto anche il sistema di produzione industriale.

Con grande meraviglia io constato ancora oggi, che non solo si discute sulle facoltà del cingolo, nei confronti della ruota, per tutti i mezzi di trasporto,

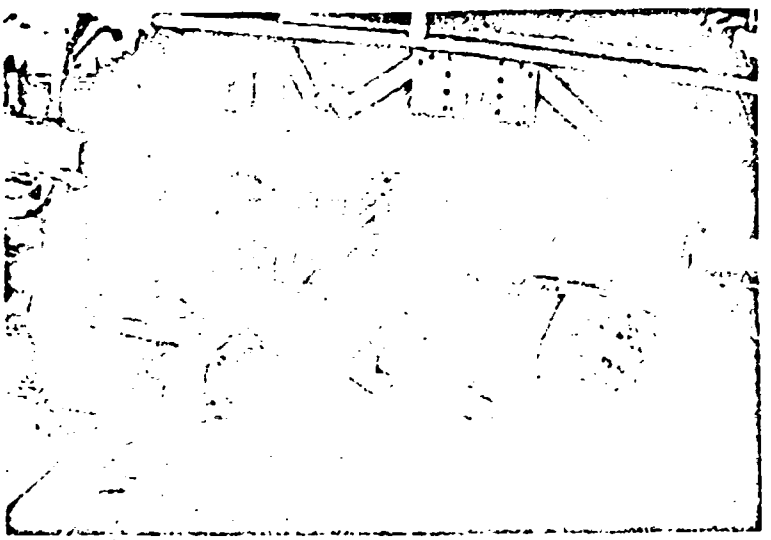


Fig. 4.

siano essi aerei che terrestri, atti ad operare fuori strada, ma che studiosi e Ditte, anche di primo ordine, seguitano a profondere patrimoni di intelligenza, di mezzi e di denaro, su strade scientifiche e tecniche, a mio avviso, senza uscita.

Vale la pena, penso, di fare insieme un poco di storia ed un poco di critica costruttiva e fare il punto della situazione.

Il mezzo di trasporto, nelle prime origini, era o umano, o a dorso di quadrupedi, o con una specie di treggia.

Venne, poi, verso il quarto millennio a.C. la grande invenzione della ruota che sostituì all'attrito radente della treggia sul terreno, quello volvente della ruota sul suo asse. E la ruota portò alla creazione della strada, perchè la ruota, per la sua limitata area di appoggio, aveva grande tendenza ad affondare sui terreni molto spesso poco consistenti.

Ne consegue, quindi, come prima constatazione storica, che la ruota, per questo fattore, non è adatta a far galleggiare l'automezzo fuori strada.

La prima prova di questo asserto si ebbe durante la prima guerra mondiale 1914-1918. L'intuizione di Leonardo da Vinci era diventata realizzabile, inquan-

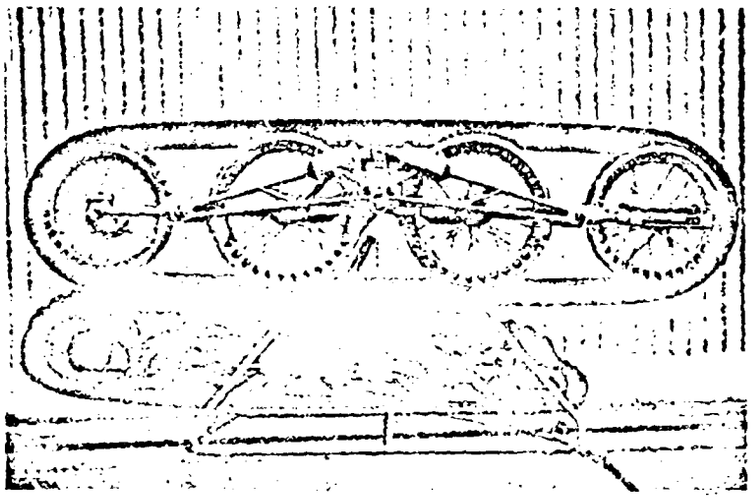


Fig. 5.

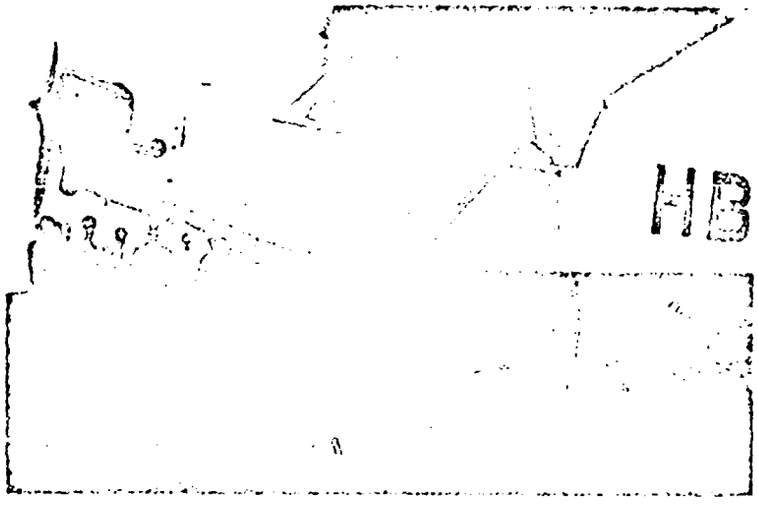


Fig. 6.

tochè il motore a combustione interna, questo nuovo, grande schiavo dell'uomo, era diventato una realtà.

I campi di battaglia del Nord della Francia erano il centro tattico e strategico della guerra. Dal lato germanico lo sfondamento della linea difensiva nemica significava tagliare i rifornimenti dal mare agli eserciti alleati; da quello alleato, arrivare al Ruhr significava, per lo meno, privare l'esercito germanico della principale base industriale e del maggior centro di produzione di energia.

Nessun mezzo, allora conosciuto, riusciva nell'intento di sfondare le rispettive croste corazzate; sorse allora negli Stati Maggiori francese ed inglese, indipendentemente l'uno dall'altro, l'idea di creare un fortino semovente, corazzato per la difesa dell'uomo avanzante, e munito di armi per l'offesa.

Ma data la poca consistenza del terreno della zona, la ruota si dimostrò inadatta allo scopo, in quanto affondava. Inoltre le buche provocate dagli infiniti bombardamenti ed i fossati rappresentati dalle numerose file di trincee, nelle quali le ruote cadevano, rendevano impensabile l'impiego della ruota stessa.



Fig. 7.

Ebbe così inizio la prima, grande realizzazione del cingolo, atto a consentire l'impiego del carro armato e che risolveva il problema numero uno dei mezzi fuori strada: *cioè quello della galleggiabilità e, quindi, della transitabilità su tutti i terreni.*

Nacque il cingolo, ma con difetti fondamentali che tuttora permangono e sui quali i tecnici di tutto il mondo, sino ad oggi, non sono riusciti a dire una parola definitiva.

Praticamente il cingolo era costituito da una serie di piastre metalliche rettangolari, munite di pinne di aggrappamento sul terreno collegate da cerniere metalliche, simili ai cardini intorno ai quali ruotano, da secoli, le porte.

Questa soluzione, che è quella ancora impiegata ai giorni nostri, ha soprattutto, i seguenti difetti di base:

a) Un cospicuo attrito radente sul suolo, che limita l'ampiezza del cingolo: attrito esaltato dalle pinne di aggrappamento che affondano nel terreno, rendono difficile la manovra del veicolo, assorbono gran parte della potenza disponibile

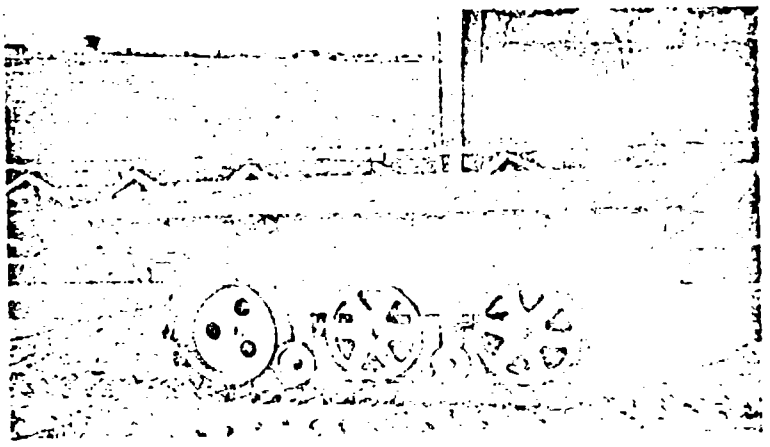


Fig. 8.



Fig. 9.

e costringono ad effettuare detta manovra, per mezzo di frizioni di sterzo pesanti, costose e delicate.

Questi sono, per inciso, i motivi veri per i quali non esistono, praticamente, in commercio, rimorchi cingolati.

Questo problema è stato risolto applicando al rimorchio cingolato le stesse suole a rulli in gomma da me studiate per i trattori, che per la loro conformazione eliminano l'attrito radente sul terreno (fig. 8, 9).

b) Il secondo grave difetto è rappresentato dalle cerniere che uniscono le suole fra loro e consentono al cingolo l'avvolgimento attorno alle ruote terminali del telaio.

Esse sono costituite da perni metallici dalle superfici indurite, sui quali ruotano gli occhi terminali delle piastre di catenaria e le relative boccole.

Queste cerniere sono soggette a rapida usura ed assorbono, a loro volta, una quantità ingentissima dell'energia disponibile.

Vi sono dei cingoli che al posto dei perni metallici impiegano dei tipi speciali di silentblok in gomma con scarso rendimento.

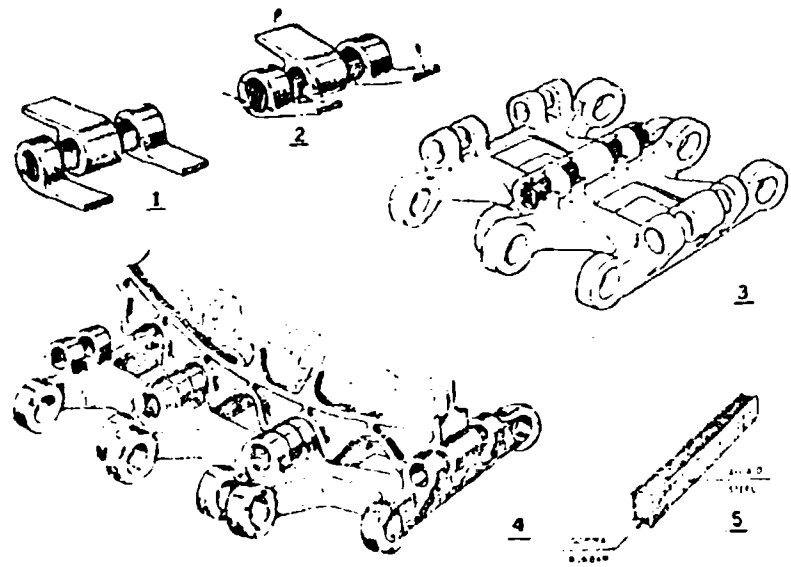


Fig. 10.

Anche questo problema è stato da me praticamente risolto attraverso un dispositivo di collegamento che consente la rotazione relativa attorno ad un asse fisso, sostituendosi al normale perno metallico ed eliminando, in tal modo, ogni attrito fra perno e boccole della catenaria (fig. 10, 11).

c) A causa dei materiali impiegati nella costruzione dei cingoli, e per gli accessori aggiunti all'automezzo per renderlo atto ai molteplici sforzi ed alle necessità che scaturiscono dall'impiego di questi tipi di cingoli, il peso totale del mezzo cingolato, rispetto a quello del tradizionale mezzo a ruote, è sempre di gran lunga superiore.

A parte l'inevitabile, conseguente aumento di costo, questo rappresenta un ulteriore grossissimo ostacolo al raggiungimento di un basso carico unitario sul terreno, limitandone le facoltà di impiego.

d) Infine il peso del veicolo e soprattutto dei cingoli, lo snodarsi a scatti di questi ultimi, i martellamenti delle piastre metalliche contro il terreno e le sue irregolarità, rendono difficile il raggiungimento di quelle velocità elevate che, specie per i veicoli militari, sono, oggi, una imperativa necessità.

SAGA LABORATORIO	Perno elastico per cingolo (brev Bonmartini) Prova dinamica Fr. 1/84231	N.° 1842/L Firma [illegible] Data VISTO 24.2.61

Prova di torsione

Deformazione angolare 0°÷28°

frequenza: 150 cicli al min.

provino conf. in sala prove C.11

Mescola Mesa 55

Vulcanizzazione 30' 151°

ved. l'esito della prova, su diagr. 1843/L

ved. il disegno del provino 9603 SAGA

Diagramma Statico

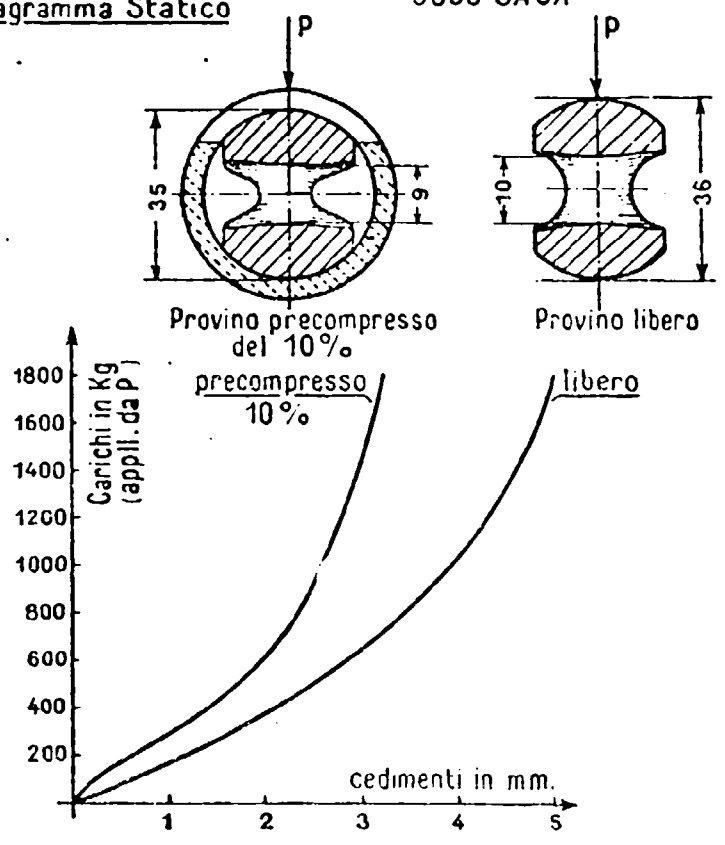


Fig. 11.

Malgrado tutti i difetti suaccennati, il cingolo come all'inizio ho detto, permise, durante la guerra 1914-1918, la realizzazione di veicoli corazzati e armati, capaci di muoversi, fuori delle strade, su terreni sconvolti, irregolari e molli.

Come sempre avviene, le guerre risolvono anche problemi che interessano in tempo di pace e creano delle macchine che diventano, poi, di uso comune; così avvenne anche nel caso del cingolo.

Infatti, finita la guerra, nacquero, derivate dai mezzi militari, le trattrici agricole e tutta una serie di automezzi atti a muoversi su terreni non predisposti alla viabilità.

Oggi esistono, pertanto, due impieghi fondamentali dei veicoli fuori strada: impiego civile ed impiego militare.

Ma *solo ed unico* il cingolo, malgrado la sua rudimentalità, sormonta le irregolarità del terreno, supera le buche ed i fossati e « galleggia » sopra terreni anche poco consistenti.

Quest'ultima prerogativa è dovuta alla grande superficie di appoggio che è possibile ottenere con i cingoli e che consente di ridurre grandemente il carico unitario sul terreno.

Uno dei grandi vantaggi dei cingoli, nei confronti delle ruote, consiste, infatti, nella loro notevole proprietà di appoggiare a terra una frazione importante (un terzo circa) dello sviluppo della loro superficie esterna totale; l'area di appoggio di una ruota, invece, è una quota assai modesta (di solito circa un dodicesimo) dello sviluppo della superficie totale del battistrada.

Pertanto, a parità di carico e di pressione sul terreno, e quindi di area di contatto, la superficie totale di un cingolo è necessariamente minore rispetto a quella necessaria in una ruota dato il rapporto stabilito da 1 a 4.

Vediamo la cosa un po' più da vicino.

Dal punto di vista che qui interessa, un cingolo è costituito da una zona di appoggio sul terreno, la cui area indichiamo con s, da un tratto di ritorno, pressapoco parallelo e di superficie identica al tratto a terra, e di 2 raccordi, anteriore e posteriore che, di solito, hanno una superficie complessiva vicina al valore s anzidetto, ammesso che la ruota anteriore e quella posteriore abbiano lo stesso diametro.

Si può, pertanto, dire che l'area totale di un cingolo è, all'incirca uguale ad $s + s + s = 3s$; cioè l'area di appoggio a terra è presso a poco un terzo dell'area totale, come avevo già asserito.

Naturalmente, se il cingolo affonda sensibilmente nel terreno, la zona di appoggio aumenta ancora, per il concorso di ulteriori tratti dei raccordi anteriore e posteriore, giungendo ad un valore limite vicino alla metà della superficie totale, se il cingolo affonda fino ai mozzi delle ruote.

Tale condizione è, naturalmente, eccezionale, ma l'area a terra è vicina ad un siffatto valore limite anche per affondamenti moderati; talchè si può affermare che la superficie utile di un cingolo è compresa fra la metà ed un terzo di quella totale.

I cingoli attuali non consentono di arrivare ad un carico sul terreno così

basso da eliminare ogni preoccupazione riguardante la consistenza ed il tipo del terreno di impiego del veicolo.

In una ruota, invece, la corda della zona di contatto è, di solito, una frazione di raggio r' di battistrada della ruota; se, ad esempio, supponiamo che la suddetta corda sia la metà di r', l'area della superficie di contatto sarà: $\frac{1}{2} r' c'$, essendo c' la larghezza del battistrada; e poichè l'area della superficie totale di quest'ultimo è, ovviamente, pari a $2 \pi r' c'$, il rapporto fra le aree suddette sarà dato da

$$\varphi' = \frac{\frac{1}{2} r' c'}{2 \pi r' c'} = \frac{1}{4 \pi} \cong \frac{1}{12},$$

cioè l'area a terra sarà circa un dodicesimo dell'area totale del battistrada, come avevo prima asserito.

Tale rapporto è ¼ di quello trovato precedentemente per i cingoli.

Naturalmente, se il terreno è cedevole e la ruota affonda, la zona di contatto cresce, ed il rapporto, impronta a terra - area totale, migliora fino al valore limite di circa ⅓. Tale valore limite si raggiunge quando la ruota affonda fino al mozzo; ma contrariamente a quanto avviene per i cingoli, i valori normali del suddetto rapporto sono, di solito, assai lontani da tale valore limite, poichè, in queste condizioni, si verifica il ribaltamento della macchina, mentre la potenza motrice a disposizione è incapace di spostare il veicolo.

D'altro canto tutte queste mie considerazioni sono superflue perchè ritengo che le opere del Prof. Bekker, per la loro scientifica, fondamentale importanza, siano a conoscenza di tutti coloro i quali si interessano al problema della locomozione fuori strada e che, quindi, sia facile per tutti convincersi che il cingolo è il mezzo tipico per operare in tal senso.

Se si vuol tentare di realizzare un veicolo a ruote che abbia gli stessi carichi unitari sul terreno, e sia in grado di superare ostacoli, buche e fossi, anche modesti, occorre, evidentemente, ricorrere a ruote enormi, di ingombro, peso e costo elevatissimi.

Va altresì detto che tali grandi ruote sarebbero facilmente vulnerabili e danneggiabili (e non si potrebbe certamente pensare di portare con sè delle ruote di scorta, anche per l'impossibilità pratica della rapida sostituzione di quella avariata); inoltre, con ruote di tali dimensioni e di così estesa area a terra, risorgerebbero, in pieno, i problemi di strisciamento e di conseguente attrito radente nei percorsi in curva, di cui avevo precedentemente fatto cenno.

Con i cingoli, invece, anche se di dimensioni raccolte e normali, è facile raggiungere pressioni sul terreno bassissime; è altrettanto facile valicare fossi, buche e superare ostacoli (specialmente se i cingoli sono del tipo a ruota anteriore rialzata, come è generalmente praticato); la vulnerabilità è ridotta e le riparazioni sono abbastanza facili, giacchè i mezzi cingolati possono portare a bordo elementi di cingolo o, addirittura, un cingolo intero di ricambio.

Naturalmente, accanto a tanti pregi, il cingolo ha ancora i numerosi difetti che ho messo già in evidenza nelle prime pagine di questo scritto e che occorrerà eliminare od attenuare.

Si può dire, a tale riguardo, che il cingolo è ancora nella sua infanzia, come lo erano le ruote di legno o di metallo, di secoli fa.

E' indubbio che senza l'adozione dei pneumatici, gli automezzi odierni non esisterebbero. E nessuno degli infiniti tentativi tesi a sostituire i pneumatici con soluzioni meccaniche, ha mai superato le soglie dei sogni dorati.

Ma ad oggi la lezione non è servita nei riguardi dei cingoli che perseguono, più o meno, la strada delle soluzioni meccaniche. Molti tentativi sono stati fatti, sostituendo con ruote pneumatiche le ruote metalliche sulle quali corre il cingolo, e molti sono stati gli studi e le realizzazioni in argomento.

Ma il cingolo vero e proprio è rimasto, fondamentalmente, sempre metallico, complesso e pesante e di impiego non semplice.

Se poi a questo si aggiunge quell'ibridio dei mezzi semi-cingolati che ai difetti di impiego dei cingoli, aggiungono quelli delle ruote (fossati, buche, carico concentrato sul terreno, inefficienza direzionale, ecc.), c'è da disperare che il problema, almeno dal punto di vista militare veramente angoscioso, arrivi ad una soluzione corretta.

Lo stesso avviene per il decollo ed atterragio degli aerei che, se per degli aerei da caccia può essere risolto con la partenza verticale, non risolve sensatamente quello non meno importante e non meno grave degli aerei da trasporto.

In una guerra futura fra i primi obiettivi da colpire ci saranno le piste di involo, danteggiate le quali sarà inutile possedere gli aerei da trasporto.

E non saranno certamente gli elicotteri, stupende realizzazioni del genio umano, ma militarmente senza difesa, a risolvere il problema dei trasporti in tempo di guerra.

E così per i veicoli terrestri è ecvità assoluta pensare di utilizzare gli automezzi odierni su ruote, atti solo per impiego stradale. Fra le distruzioni dei ponti, bombardamenti aerei, missilistici, mitragliamenti e la guerra partigiana, le strade diverranno inservibili.

E allora! Io penso che il cingolo stia subendo, storicamente, le stesse vicende della ruota: nata rigida, cerchiata con materiale non elastico, ha subìto la prima, fondamentale trasformazione, verso il 1870, quando, valendosi della scoperta delle qualità della gomma, si cominciò a ricoprire il cerchione metallico con gomma piena.

Nel 1888 J. B. Dunlop tentò, per primo con successo, la sostituzione della gomma piena con un tubo di gomma chiuso ad anello e gonfiato con l'aria e lo applicò alle ruote del triciclo del figlio, il quale potè, giovandosi di questa applicazione, vincere tutte le corse, per tricicli, alle quali prese parte in quegli anni.

Questa fu una rivelazione che finì per sconvolgere la complessa architettura degli autoveicoli.

Questa breve storia della ruota, alla quale la pneumaticità ha spalancato la porta al più formidabile sviluppo e perfezionamento dei mezzi di locomozione,

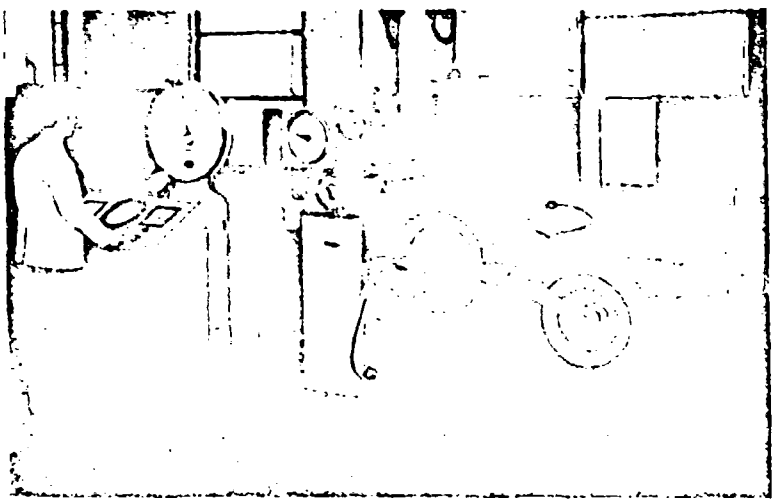


Fig. 12.

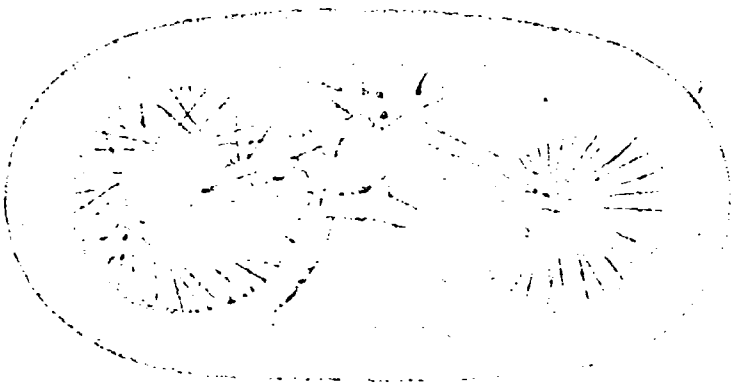


Fig. 13.

avrebbe pur dovuto essere una lezione valida e preziosa nel dare, almeno, un indirizzo agli studi dei cingoli.

Invece questo non è avvenuto.

Il cingolo è nato meccanico, con piastre metalliche incernierate fra loro.

In un secondo tempo, soprattutto per consentire ai mezzi cingolati di circolare sulle strade, che dalle piastre metalliche venivano gravemente deteriorate, queste furono ricoperte da una superficie di gomma piena.

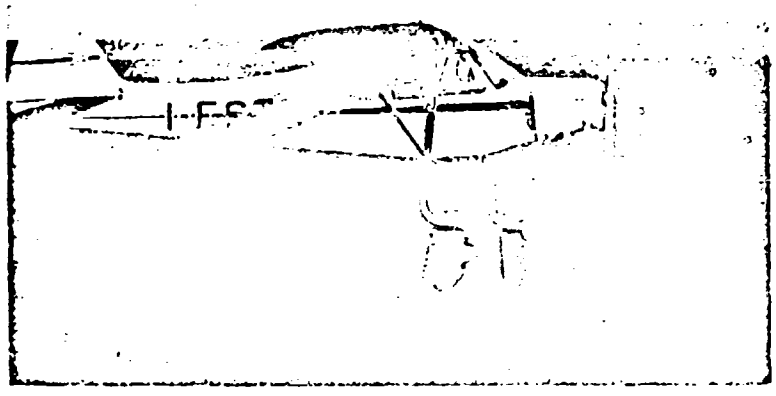


Fig. 14.

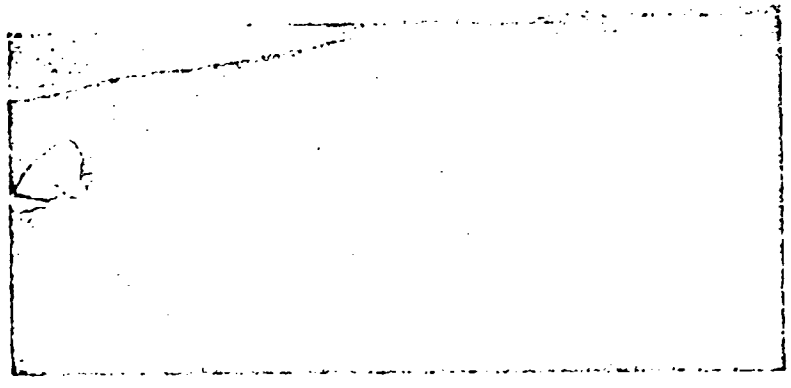


Fig. 15.

La mia netta e precisa convinzione, suffragata dalle molteplici esperienze compiute, è che nessuna soluzione potrà, veramente, migliorare il funzionamento del cingolo, se questo rimane fondamentalmente e strutturalmente ancora quello di 50 anni fa: metallico, meccanico, a catena, a piastre, ecc.

Affermo che l'unica soluzione possibile e alla quale, fatalmente, si finirà per giungere, è quella di passare dalle attuali strutture metalliche, discontinue, a strutture pneumatiche continue, ed è in questa direzione che debbono essere

indirizzati gli studi per risolvere il grave problema della cingolatura degli automezzi fuori strada, terrestri ed aerei.

Un cingolo pneumatico, per usi aeronautici, già esiste ed è stato da me realizzato col concorso tecnico della « Pirelli ». Ha superato, con pieno successo, la fase sperimentale e le prove pratiche ed è stato *regolarmente omologato dal competente Registro Aeronautico Italiano* (fig. 12, 13, 14, 15, 16).

Tale cingolo, denominato « cingolo pneumatico liscio Bonmartini », è costituito da un tubo chiuso di materiale flessibile (gomma telata), munito di battistrada sulla superficie dorsale esterna, ed armato con due sottili trecce metalliche chiuse, flessibili ma non estendibili annegate nei fianchi del tubo.

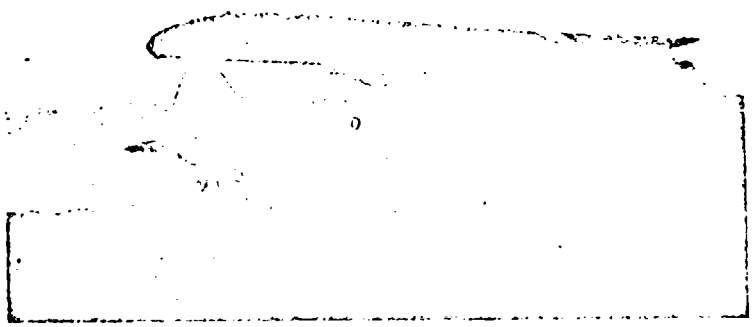


Fig. 16.

Numerosi aerei leggeri hanno volato con carrelli muniti di siffatti « cingoli pneumatici lisci » e dato il carico unitario sul terreno di soli 500 gr. cmq. hanno avuto la possibilità di partire ed atterrare normalmente, senza alcun inconveniente, su campi arati e solcati da fossi o su spiagge marine sabbiose, a velocità normale di decollo ed arrivo (fig. 17, 18, 19, 20, 21).

Per la sua estrema scorrevolezza, inoltre, il « cingolo pneumatico liscio », non allunga il percorso normale di rullaggio dell'aereo e all'atterraggio vince il suo momento di inerzia senza dover ricorrere ad un preavviamento del cingolo stesso.

Per gli aerei di peso rilevante il problema è diverso: più facile e più difficile.

Occorre inquadrarlo, studiarlo, esperimentarlo a gradi senza stancarsi. L'obiettivo ne vale la pena.

Gli stessi tubolari lisci (fig. 22) possono essere impiegati su veicoli terrestri in sostituzione delle normali catenarie. E' ovvio che in questo caso sia la parte

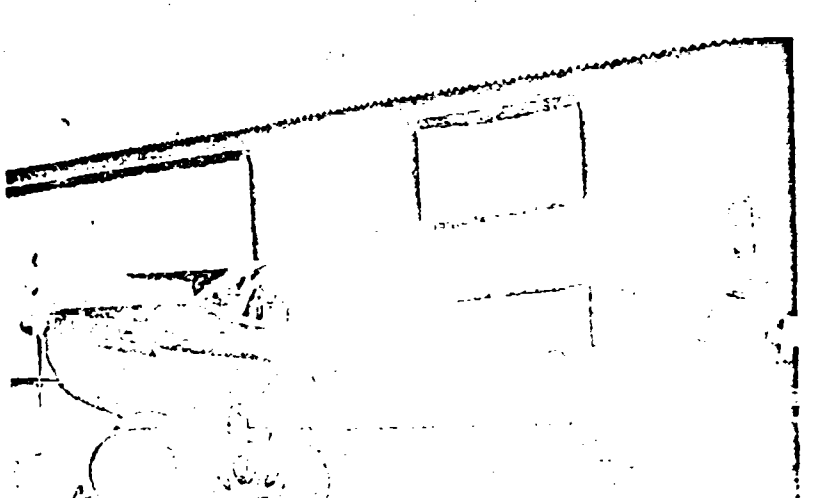


Fig. 17.



Fig. 18.

ventrale che la parte dorsale (battistrada) dovranno essere opportunamente rinforzate e configurate in funzione del loro diverso impiego.

Gli stessi tubolari sempre impiegati su veicoli terrestri e modificati in particolare sulle fiancate, impegnati entro opportune ruote motrici a gola (formate da due flangie distanziate fra loro e libere nell'interno per lo sfogo del fango o della neve), possono lavorare correttamente a trazione, comportandosi come normali cinghie di trasmissione (rettangolari o trapezoidali).

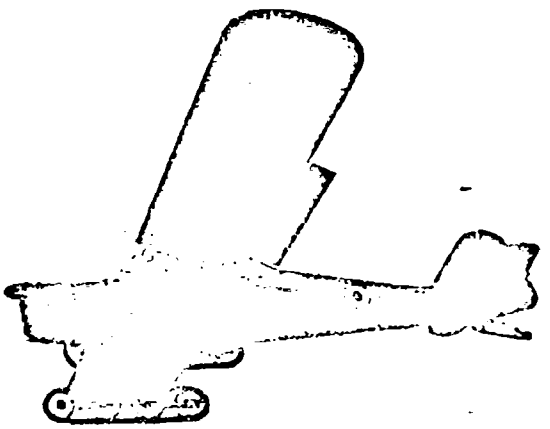


Fig. 19.

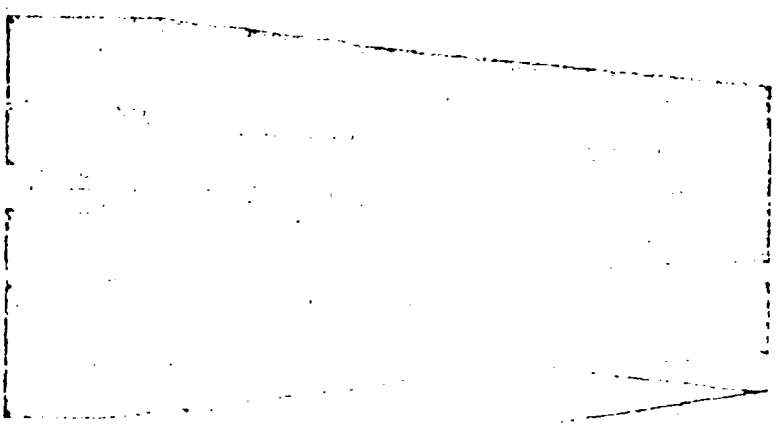


Fig. 20.

E' presumibile che ancor meglio si comporteranno i tubolari a superficie ondulata, giacchè le loro ondulazioni ventrali sono molto adatte ad « impegnarsi » con i denti di opportune ruote dentate motrici. Questi cingoli pneumatici ondulati, sono molto simili a quelli precedentemente descritti e l'unica differenza sostanziale consiste nel fatto che il tubo chiuso di materiale flessibile, che ne costituisce l'elemento fondamentale, non è a superficie liscia, bensì ondulata.

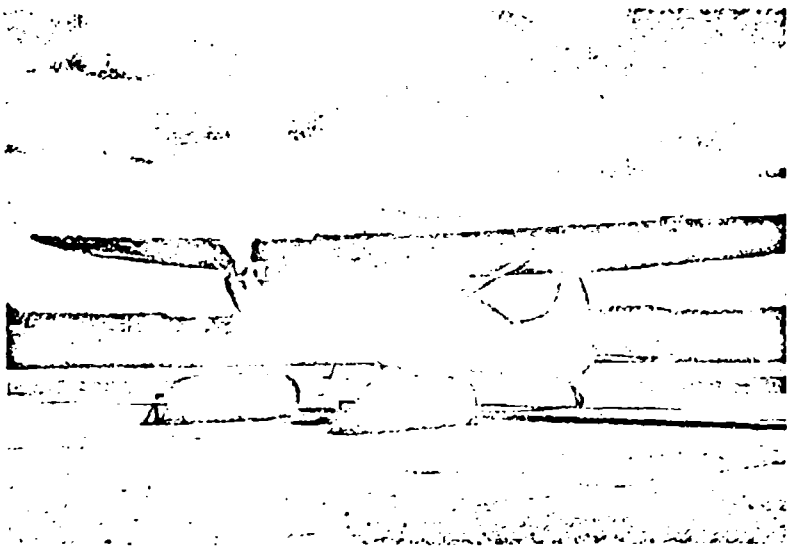


Fig. 21.

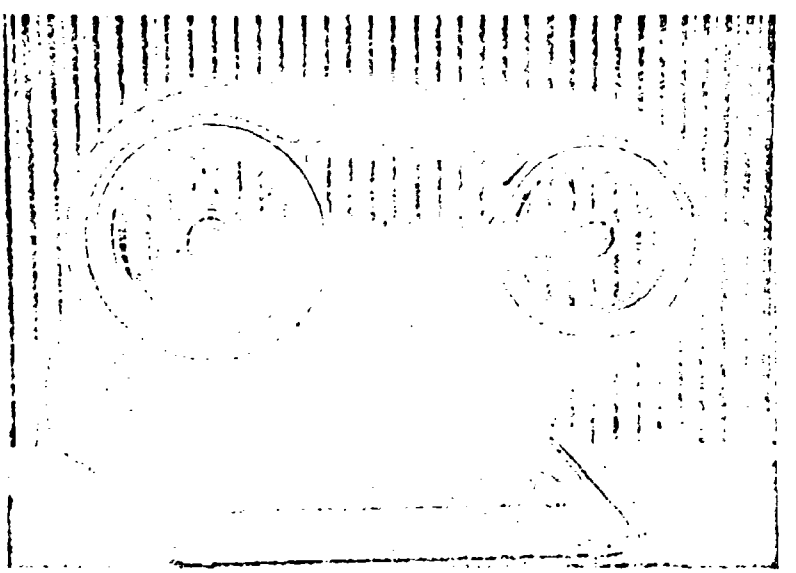


Fig. 22.

Come è facile comprendere la sua particolare struttura permette la massima flessibilità ed « avvolgibilità » attorno alle ruote guida e motrici, anche se di diametro ridotto e *indipendentemente dalla pressione interna di gonfiaggio.*

E' questo il primo suo vantaggio rispetto al « tubolare liscio ».

E' chiaro, inoltre, che per effetto della sua forma ondulata, l'importanza

dell'isteresi della gomma viene fortemente ridotta e questo a tutto vantaggio delle alte velocità.

Nell'impiego terrestre, poi, particolare vantaggio del cingolo ondulato su quello liscio, consiste nel fatto che esso si presta assai bene a sostenere rilevanti sforzi di trazione.

Infatti, per la sua particolare conformazione, sulla parte dorsale (esterna) le ondulazioni fornite di resistenti battistrada, servono anche da pinne di aggrappamento, in quanto mordono il terreno, mentre nella parte ventrale (interna) i solchi fra una ondulazione e l'altra, servono, come per una catenaria tradizionale, di aggrappamento alla ruota dentata motrice.

I vantaggi offerti dall'impiego del cingolo pneumatico saranno veramente notevoli e tali da compensare, largamente, le fatiche della loro messa a punto.

Anzitutto le cerniere che costituiscono l'elemento più delicato ed importante dei cingoli attuali, spariscono completamente e, con loro, i relativi difetti di rapida usura, di assorbimento di energia, per attrito, di funzionamento a scatti e martellante, a tutto vantaggio del maggior rendimento della macchina e, quindi, maggior potenza a disposizione per l'impiego, minore consumo e minori soste per riparazioni.

Inoltre, il materiale costitutivo di un cingolo pneumatico è di gran lunga più leggero di quello degli ordinari cingoli; pertanto i veicoli cingolati pneumatici saranno assai più leggeri dei cingoli attuali.

Non solo, ma secondo il rapporto prima accennato, tra sviluppo ruota e cingolo, il cingolo pneumatico sarà di gran lunga più leggero di una ruota enorme o di più ruote adatte ad identica prestazione del cingolo.

Il peso minore, oltre a permettere un più basso carico unitario, significa anche un minor costo di produzione. Questo porterà, quindi, ad un minor costo di acquisto e di esercizio, perchè è chiaro che i tubolari prodotti su larga serie verranno a costare meno del cingolo metallico tradizionale, composto di innumerevoli parti.

Inoltre, come esercizio, il costo dovrebbe essere, se non minore, almeno uguale a quello delle ruote in funzione del minor carico unitario da sopportare.

In conseguenza, poi, di questo minor carico unitario, i tubolari saranno di una maggiore durata e di difficile perforazione.

Qui va sottolineato il fatto che il ricambio del cingolo tubolare è facilissimo e che è possibile portare sulla macchina, per il suo basso peso e il poco ingombro, l'eventuale ricambio.

Il problema delle alte velocità, difficilmente solubile con gli attuali cingoli a catena, viene automaticamente risolto dai cingoli tubolari pneumatici.

Altro vantaggio presentato dal tubolare corrugato, impiegato su carrelli di atterraggio per aerei, è quello di addolcire l'impatto col terreno in funzione della sua forma. Inoltre le sue ondulazioni anulari si presentano al contatto sul terreno, in progressione numerica flettendosi all'indietro rispetto al senso di moto, rendendo meno violento l'avviamento del cingolo stesso.

Va, altresì detto che siffatti cingoli, grazie alla forma arrotondata del loro battistrada, si apriranno automaticamente la strada nel fango e nella

neve, con maggiore facilità dei cingoli a piastre rettangolari e che l'attuale forte rumore dei mezzi cingolati sarà, ovviamente, del tutto eliminato.

A questo proposito gli studi del Generale Garbari sulla resistenza al movimento dei veicoli a ruote su terreno cedevole, sono fondamentali.

Io penso che l'impiego di due tubolari affiancati opportunamente distanziati fra di loro, migliorerebbe ulteriormente il galleggiamento del veicolo.

Inoltre le pinne di aggrappamento in gomma nel tubolare pneumatico, ridurrebbero l'accumulo del terreno sullo stesso.

Oltre a ciò un cingolo tubolare corrugato pneumatico, potendo avvolgersi con facilità sulle ruote portanti, queste potranno essere ridotte di diametro con conseguente riduzione di ingombro, di peso e di costo.

Per completare questo rapido panorama del funzionamento del cingolo pneumatico, ci resta soltanto da dire due parole sul loro comportamento in curva e nelle evoluzioni.

Dobbiamo anzitutto notare, a tale riguardo, che le continue piccole variazioni di direzione che, inevitabilmente, si verificano anche nella marcia rettilinea, verranno assorbite dalla pneumaticità e flessibilità del tubolare pneumatico.

Nelle forti variazioni di direzione, invece, saranno inevitabili gli strisciamenti dei cingoli sul terreno, con conseguente attrito radente; il problema sarà, però, meno drammatico che non nel caso dei cingoli metallici, grazie al minor peso dei cingoli e, quindi, del carico unitario sul terreno e grazie alla forma arrotondata dei fianchi dei cingoli stessi, che, ovviamente, facilita il loro spostamento trasversale.

Infine, durante le evoluzioni, il cingolo tende a torcersi su se stesso, ma come l'impiego aeronautico ha già ampiamente dimostrato, tali fenomeni torsionali vengono frenati dalle funi laterali di irrigidimento, mantenute distanziate dalla pressione interna del pneumatico che svolge, pertanto, anche questo ulteriore, importante compito, indispensabile al buon comportamento del cingolo durante le evoluzioni.

Ho così terminato la mia esposizione; essa è stata forzatamente breve, ma spero che abbia sufficientemente lumeggiato i miei convincimenti.

Io affermo che le più belle pagine della storia dei cingoli attendono ancora di essere scritte.

Come la ruota è il mezzo idoneo per muoversi sulla strada, così il cingolo è lo strumento più adatto per circolare fuori strada; e come la ruota stradale ha assunto la sua veste definitiva sotto forma di ruota gommata pneumatica, così le strutture cingolate si trasformeranno in forme pneumatiche e, allora, mentre la ruota resterà ancorata al solo impiego stradale, il cingolo pneumatico sarà l'unico, vero mezzo atto a consentire la viabilità degli automezzi su strada e fuori strada.

Ho ritenuto utile riassumere, il più brevemente possibile, le conclusioni alle quali sono arrivato dopo trentacinque anni di studi ed esperienze difficili, costose e, spesso, anche pericolose, con l'augurio che la mia immane fatica intellettuale, materiale e finanziaria, possa servire a quanti credono, sinceramente e fattivamente nel progresso, ed il cui intelletto, energia e coraggio,

sono tesi all'obiettivo grandioso di piegare il nuovo, grande schiavo dell'uomo: « il motore a combustione interna », all'impiego dei mezzi motorizzati, non solo sulle strade ed alle sempre più imponenti piste di decollo e di atterraggio degli aerei, ma alle più ampie vie del mondo.

DISCUSSIONS

J. REMUS. — Je voudrais simplement poser une question qui m'a été inspirée par la lecture des différentes communications et de pubblications antérieures du Comte Bonmartini, dont j'ai eu l'occasion de suivre les travaux déjà depuis plusieur années. C'est à propos de la chenille tubulaire utilisée aussi bien sur des véhicules agricoles que sur des trains d'atterrissage d'avion. M. Bonmartini condamne l'emploi du pneumatique en dehors des routes, ce qui m'inquiète un peu pour mon avenir personnel mais ceci est une autre question. Je voudrais simplement qu'il puisse nous préciser, et peut être je crois que beaucoup d'autres auront la même préoccupation, comment à partir d'une certaine vitesse sur le pneumatique tubulaire lisse ou même ondulé, on peut éviter la formation d'une onde de refoulement lorsqu'on dépasse une certaine vitesse. Ce problème existe déjà sur le pneumatique, on le constate en particulier grâce à l'analyse ultraphotographique, mais je pense que dans le cas de la chenille tubulaire ce problème doit être encore beaucoup plus grave.

L. AMICI. — Riguardo ai fenomeni di onda dinamica che si constatano sul pneumatico bisognerebbe dire che si è un po' esagerato. Anzitutto si sono viste spessissimo in pubblicazioni tecniche, fotografie di onde dinamiche però su ruota-strada e non su strada. Sino ad ora nessuno ha misurato le onde dinamiche su strada. Su ruota-strada data la curvatura di quest'ultima è più facile che si verifichino. Probabilmente sono sensibili in realtà solo in pneumatici da corsa per velocità oltre i 200 km all'ora.

Nel caso dei cingoli Bonmartini per applicazioni stradali, credo che l'unica risposta possibile sia questa: prima aspettiamo di fare i cingoli che vanno a 200 km/ora e poi si vedrà. Per ora gli obiettivi sono un po' più modesti: ci accontentiamo di andare a 80 km/ora. Credo che il Conte Bonmartini sia d'accordo. (Mi segnala che è d'accordo all'80 %, e questo vuol dire che vuole andare a 100 km/ora).

Ci sono indubbiamente i pericoli di un'onda di « refoulement » come diceva M. Remus. Però ci sono anche molti modi per combatterli su cui è inutile adesso dilungarsi. Alludo ad esempio a elementi rinforzati di tipo longitudinale. Entrando un po' nella meccanica del pneumatico, tutti sanno che esistono i pneumatici di tipo radiale, cioè pneumatici muniti al di sotto del battistrada di fili longitudinali, con carcassa radiale. Ora i cingoli Bonmartini, e non credo svelare nessun mistero, sono fatti con fili esclusivamente radiali, senza alcun rinforzo longitudinale, che per ora hanno dato ottimi risultati a tutti gli effetti, cioè anche agli effetti di decollo ed atterraggio dove le sollecitazioni longitudinali sono abbastanza gravi. Per ora ce l'abbiamo fatta esclusivamente con fili radiali. Siamo pronti evidentemente a introdurre rinforzi ed anche angolazioni dei fili e chi sa quali altre diavolerie. Ce ne sono molte a disposizione dei tecnici. In conclusione non siamo per niente intimoriti dal problema del « refoulement ».

N. 12

Land factors and vehicle design in operations on organic terrain

Caratteristiche del terreno e struttura del veicolo operante su terreno organico

NORMAN W. RADFORTH, F. R. S. C. *)

ABSTRACT. — *It is illustrated and explained that structural features of peaty terrain are cosmic as to arrangement. This phenomenon accounts for the presence of terrain conditions that are characteristic and predictable on inspection from the ground or the air.*

The majority of these conditions (land factors) have primary significance in relation to basic design of vehicles intended for operations on organic terrain, but compensation for them is usually lacking. The conditions are described and it is indicated how they limit the performance of vehicles of modern design.

By application of aerial survey methods the frequency, sequence and arrangement of land factors in a given traverse are conveyed and related to vehicle response.

It is well established that successful vehicular mobility on soils can be expected only if design parameters are pertinent to soil relations as well as to mechanical principle inherent in vehicle construction. There is a third factor that is basic, the nature of the operations for which the vehicle is required. The writer holds the view that the most important factor of the three is soil. It has priority in that it is already « designed » and the other factors are in this sense secondary and must conform.

It could well be claimed that a fourth factor, climatic, should have equal prominence as to fundamental significance especially when water in either the frozen or liquid phase does so much to modify the mechanical response of soils.

In the last analysis the human factor, e.g. the operator of the vehicle may be a controlling, even limiting factor in the operation. But even the human factor is secondary in the relative scale. His judgment and action will be revealed as influenced by the soil factor if he is trained.

The primary position of soil may be accepted, when everything is considered, with but one qualification. This is, that to prescribe for successful operation soil must be assessed not only in terms of mechanical indices but also in relation to the concept of soil being a component of terrain. This means that terrain, with soil as an important element, is the factor to be analysed in the procurement of vehicular design.

*) Professor of Botany, McMaster University, Hamilton College, Hamilton, Ontario, Canada.

The objection to this proposal may arise through suggestion exemplified by Bekker (1958) who is justifiably hopeful that we shall be « less dependent on qualitative "indices" and "factors" of unspecified dimensions » in seeking to establish formulae for mobility. If qualitative indices are adequate particularly in locating the critical areas in which quantitative assessment is essential, they are useful. Variation in terrain character, often conducive to statistical expression (Radforth, 1958 a) could conceivably be so important as to overshadow physico-geometric data derived *from an assumed soil type*. This is particularly applicable for organic terrain, with which the Author is concerned, because the terrain and its soil are products of biological processes, the effects of which may now be judged.

The cosmotic state of organic terrain

On every continent there exists a kind of terrain in which the soil is constituted of fossilized plant remains that accumulate in depth to form an organic mantle over the mineral subsoil. Most of it forms at the onset of certain persistent climatic conditions typified by those that accompany glacial retreat. The prominent agent essential for the origin of organic terrain is water which is prevalent in the environment and consistently saturates the soil.

The first plants to colonize the saturated land did not totally degenerate following death. Structurally whole parts remained in the ground or fell to the ground and they, like the mineral soil particles, became saturated with water which sharply curtailed degeneration and effected structural preservation indefinitely (fossilization).

These plants were succeeded by others and the process repeated itself. Eventually, there resulted a fossilized organic layer covered by a living layer of vegetation (fig. 1). This extended laterally and gradually covered the mineral sublayer.

Colonization was not uniformly incident Therefore, the organic mantle was at first markedly disrupted.

The process of accumulation persisted. As the organic layer increased in depth, lateral spread also increased until patches of the organic mantle became contiguous. In several areas of the earth's surface e.g., in Northern Canada, the organic cover is continuous for several hundred miles in several directions and often in depths exceeding 30 feet (fig. 2). Where interruptions occur they are secondary as far as characterization of the main land surface is concerned.

It has been suggested that colonization takes place in a consistently and persistently wet environment. This condition is typified in fig. 3. If the water factor prevails, accumulation generates on all types of mineral soil. Indeed it may occur over water or over bare rock where no soil exists. Where sublayer constitution changes there are accompanying changes in rate of accumulation and consequently depth. If there is a distributional effect in sublayer types, depth variability in the organic overburden will conform.



Fig. 1.

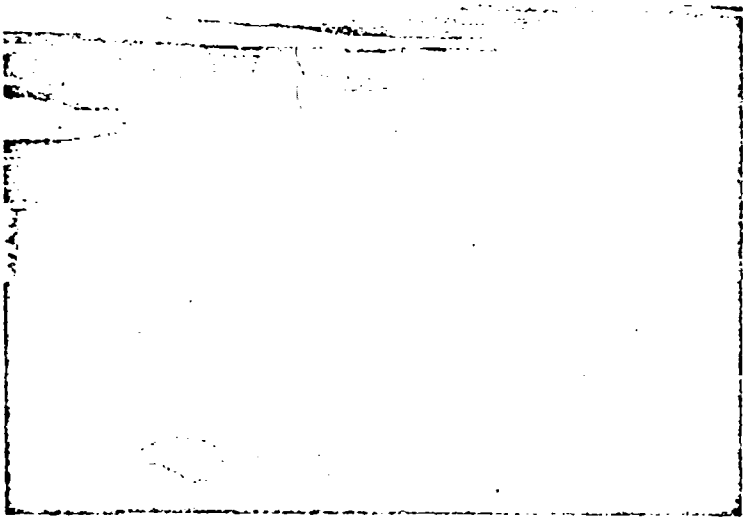


Fig. 2.

Variability in accumulation also occurs in response to a geomorphic factor. The affect of this factor has been recorded at length elsewhere (Radforth, *In press*). It is through this factor that topographic variability arises in the organic mantle. In this respect variability may occur as a result of irregularity in the mineral sublayer (fig. 4). On the other hand, it may be caused by difference and irregularity in ice pattern. It may also arise for hydrological

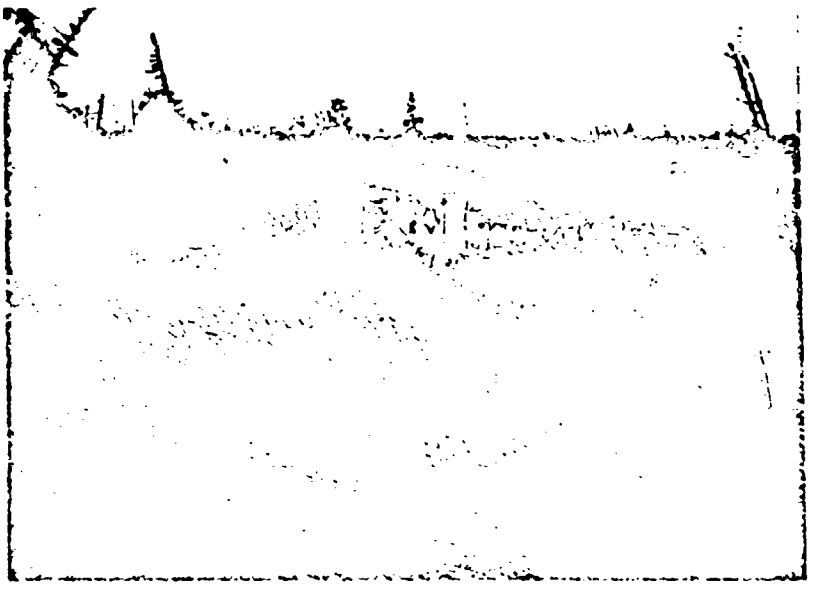


Fig. 3.

reasons. Finally, difference in accumulative rate and constitutional properties of the organic matter itself may induce topographic difference (cf. figs. 5, 6, 7, 8).

Variability in organic terrain is appreciated at once by the observer who inspects the terrain first hand for even the first time. The reason that someone untrained can detect difference is largely not because of topographic variation but because of variation reflected in vegetal cover, — the living component of the organic mantle. When the observer is asked to express what he sees, he usually answers in terms of structural values. In other words, vegetal cover in one area of organic terrain is characterized by a set of structural values (stature, form, texture and spatial relationships among components) that differ from those characterizing cover in another area.

If cover varies structurally, the fossilized component will, likewise, vary because the living cover is the structural forerunner of the fossil increment. Thus, it arises that structurally, there are « kinds » of organic terrain and « kinds » of fossil organic matter within the terrain. This principle can be

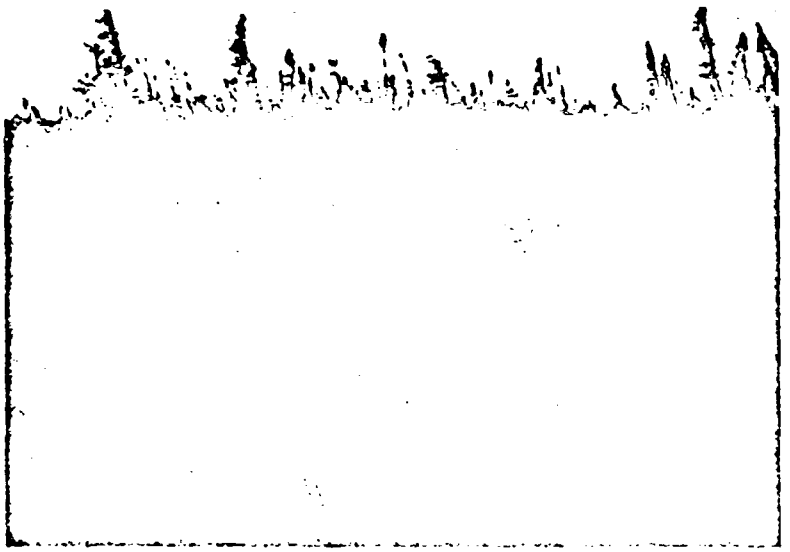


Fig. 4.

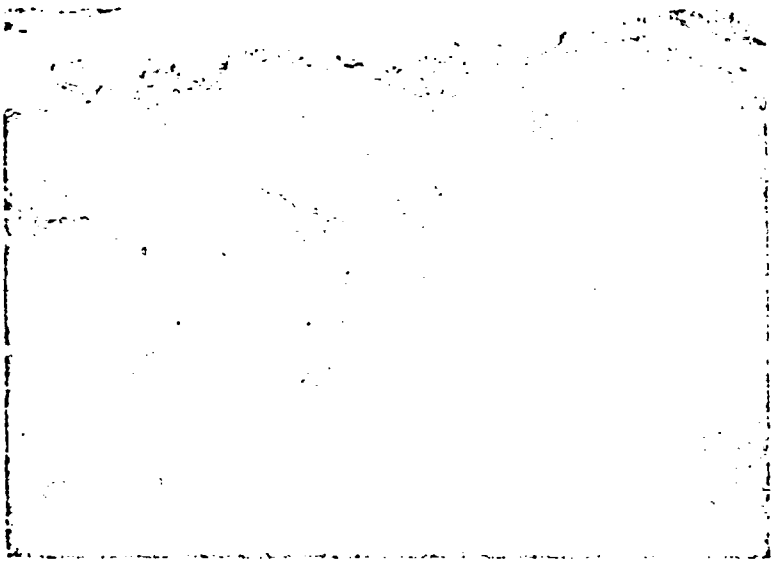


Fig. 5.

demonstrated readily by inspection of gross samples of the organic matter (peat, as it is known in English-speaking countries).

The reader will begin to appreciate that organic terrain differs fundamentally from mineral terrain apart from the contrast conveyed by the expressions « organic » and « mineral ». Contrast is also established on a generic basis. Mineral implies geological origin, whereas, organic biological (botanical) origin.

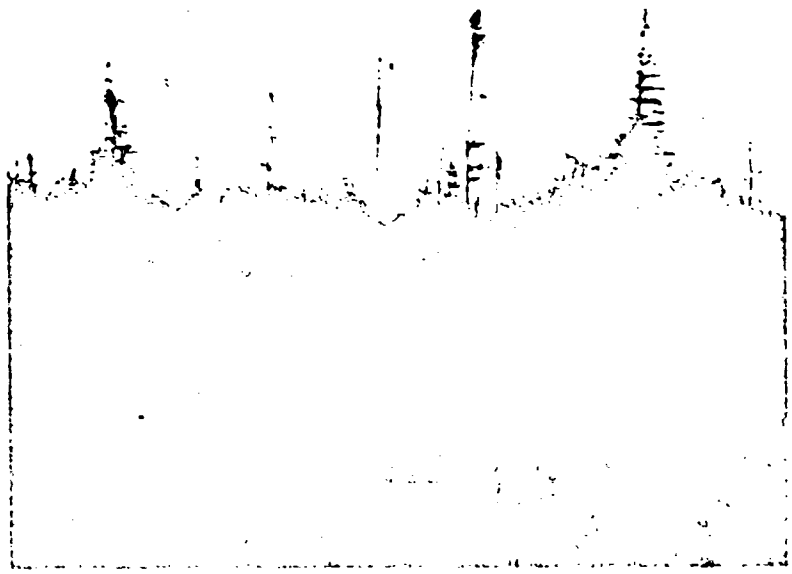


Fig. 6.

On the generic basis a sample of organic terrain is rarely derived from materials and effects of erosion that have been incident at a location other than that at which the sample occurs. Peat deposits are essentially primary geographically, and accumulation has occurred *in situ*. Also the controls governing accumulation are basically biotic for organic terrain. Thus, sedimentary or glacial agents play no significant part in the accumulation of peat. Finally, the composition of peat constituted as it is of plant remains cannot be assessed by the same values (size, shape, kind and arrangement of constituent particles) that are used for identifying and differentiating mineral soils. This contrast prompts enquiry into how field and laboratory reference can best be made for organic terrain. The biotic factor has proved important in this connection for, by applying palaeobotanical principles, it has been shown that peat, as it accumulates, reflects organization.

To reveal this organization is difficult if gross structure of the peat is used as the reference basis. There are sometimes local aberrations in structure

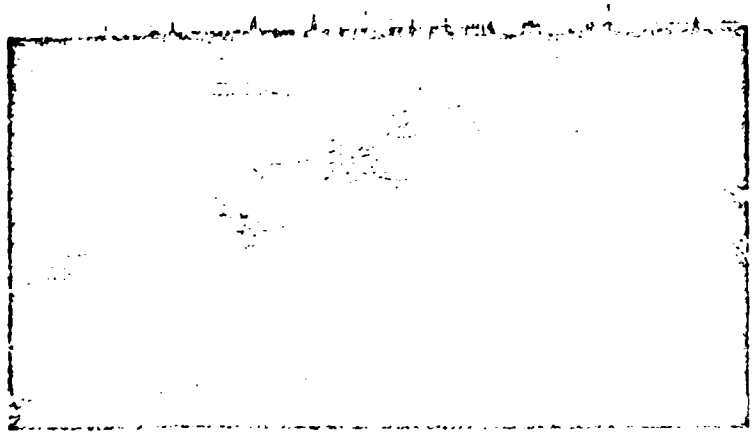


Fig. 7.

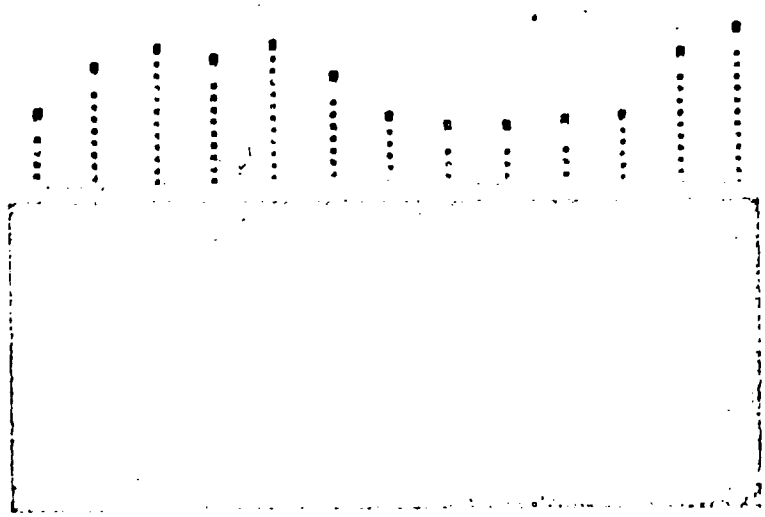


Fig. 8.

caused by transient local circumstances, an unusually large fossilized log may displace normal accumulative structural pattern and relative abundance of constituents generally characteristic for the area. Also, when research disclosing the principles of organization was begun it was difficult to establish how gross structure in depth (often inconvenient or impractical to expose) signified a valid historical biological trend. When the components were large, as was often the case, it was difficult to tell where the delineation of type structural pattern lay.

It was not until microfossils were used to reveal successional trends in peat history that a means of demonstrating organization became clear (Radforth, 1952). The microfossils (pollen and spores) chiefly of *in situ* plants comprising the peat, showed change in relative frequency in a given core depth of peat. If microfossil peat cores were compared, characteristic frequency patterns revealed themselves. Then when a characteristic pattern was related to gross structure of the peat sample from which the core was removed, the natural and characteristic parameters of gross structure could be confidently expressed.

The microfossil history also exposed the vegetal trends which culminated in contemporary vegetal cover. In other words, it helped to disclose delineation of structural type in the living cover as it did for gross macrofossil composition (Radforth, 1955).

The critical principle through which organization is expressed can now be reasoned. If a given microfossil pattern is equivalent to both surface and subsurface structural pattern, then that surface pattern is indicative for the subsurface structural condition. This is most helpful because it can be demonstrated that characteristic vegetal cover patterns recur. They are not fortuitous, and therefore subsurface structural difference can now be designated over wide areas simply from surface inspection. Moreover, this can be applied on an inter-continental basis.

Predictability as applied to organic terrain

With organization present in the entire organic overburden, classification of the phenomena of variation becomes a possibility. Classification as developed by the writer (Radforth, 1952) emphasizes the following principles:

a) natural (biological) events and circumstances are basic;

b) classification is a system on a manifold basis;

c) the system is universally applicable, e.g. for purposes of environmental analyses, engineering planning, and biological, geographical and certain geological studies.

The classification system (loc. cit. Radforth, 1952) is already in wide use in Canada and to some extent in the U.S.A. for engineering programmes of terrain interpretation. Surface cover is usually elected for the main approach to analysis and the use of the cover formula method of reference is the practice.

Classification affords prediction. Accordingly, prediction has been attempted in the present work and off-the-road access has been emphasized. The kinds

of access hazards are listed in Table 1, column 1. The predominating cover formulae pertinent to them are shown in column 2. The first step towards prediction of vehicle performance in so far as the terrain factor is concerned is to locate the formulae on a proposed access route.

TABLE I. — *The relationship of critical access hazards and corresponding vehicular response to identification aids for organic terrain.*

Access hazard	Predominating cover formulae	Predominating 30,000 ft. airform pattern	Vehicular performance
1	2	3	4
Low density organic	FI, EI, DFI	Dermatoid	Partial to total subsidence, loss of tractive effort
Low tensility organic	FI, HE	Dermatoid, marbloid	Total subsidence
Heterogeneous organic	DFI, EI, FEI	Stipploid, terrazzoid	Differential subsidence
Coarse peat components	AEH, AEI	Stipploid	Track damage, pitching
Unconsolidated sublayer	EI, FI	Reticuloid	Subsidence, loss of tractive effort
Perforated ice inclusion	FI, FEI	Reticuloid	Total or differential subsidence
Polygonal ice inclusion	HE, EHI	Marbloid, terrazzoid	Differential subsidence, pitching
Knolled ice inclusion	AEI, AEH, BEI, BEH	Stipploid	Track damage, inadequate steerability, pitching
Miscellaneous ice condition	FI, FEI, DEI	Reticuloid, terrazzoid	Partial subsidence
Elevated irregularity	EH, HE, EI	Marbloid, terrazzoid	Axial pitch, differential subsidence, localized load intensification
Depressed irregularity	DFI	Dermatoid, stipploid	Lateral and axial pitch, partial and differential subsidence
Rock inclusions	FEI, FI, BFI	Terrazzoid	Track damage
Mounding	DEI, EI, EH, BDE	Terrazzoid, marbloid	Inadequate steerability
Ridging	FI, EHI, BEI, BFI	Terrazzoid, reticuloid	Differential subsidence, lateral pitch
Rough microtopography	BDE, ADE, DFI	Stipploid	Severe pitch, track damage, partial subsidence
Vertical peat face	HE, EI	Marbloid	Localized load intensification, loss of tractive effort
Interrupted organic terrain	(Mineral terrain adjacent)	All patterns	Variable response
Tree cover	AEI, AH, AEH, BEI, BEH	Stipploid	Excessive deviation, inadequate steerability
Tree fall	ADE, AEI	Stipploid	High frequency pitching, track damage
Ponded terrain	FI, FEI, HE	Dermatoid, reticuloid, marbloid	Total subsidence, high deviation rate
Inclined terrain	FI, EI	Dermatoid	Loss of tractive effort

The interpreter must then survey the route to determine the frequency and extent of each kind of cover. This may be done by surface traverse through conventional methods. The most convenient way to survey is by direct observation from the air preferably by helicopter from 500 feet. Direct observation from 1,000 feet in conventional low speed aeroplane flight is next best. If high altitude flight is essential (30,000 feet), prediction is still possible (Radforth, 1956). Indi. erial inspection using air photographs is often the only means available. In this case, interpretive procedure is necessary (cf. Radforth, 1955 - 1958).



Fig. 9.

Fig. 9 shows a recommended traverse over 5 miles of organic terrain in northern Canada. It has been chosen as the straight line route offering best performance and thus, has the lowest frequency of critical access hazards. Frequency of given hazards is determined as a function of the extent of that cover formula containing the characteristic hazards. To arrive at the number of hazards of a given kind per mile of known cover, the average distance between successive similar hazards is used as the factor. Thus, for approximately half the route (Muskeg, Tr5, E1) elevated irregularities will occur every 100 feet on the average or 52 per mile or approximately 130 from the beginning of the route to the next major change in the terrain.

It will be noted in Table II that there are three other access hazards occurring in the first half of the route. Their frequencies are lower by far than that for the first (elevated irregularities). When total frequencies for all access hazards are compared for the two types of terrain, it works out that the second half of the route has nearly four times as many hazards as the first half.

Optimum speed on the type of terrain shown in the first half of the route is determined as 5 m.p.h. per mile of terrain. Thus, the terrain all being similar for about 2½ miles, the distance would be covered in half an hour. If all access hazards consume the same time (a not unreasonable assumption) the second half of the traverse would take about 4 times as long to cover, about 2 hours.

TABLE II. — *Comparison of frequencies for occurrence of access hazards in the two halves of the access route, fig. 9.*

Predominating cover formulae	Access hazard	Frequency (per 2½ miles)	
1	2	3	
HE, EI	Elevated irregularity	130	First half of access route
	Ponded terrain	45	
	Low tensility organic	30	
	Polygonal ice inclusion	23	
	Total	228	
FI, FEI	Low density organic	265	Second half of access route
	Low tensility organic	265	
	Ponded terrain	130	
	Perforated ice inclusion	130	
	Unconsolidated sublayer	28	
	Miscellaneous ice hazard	15	
	Ridging	15	
	Rock inclusions	0	
	Inclined terrain	0	
	Total	848	

To achieve this result, the vehicle would have to be designed with the following features: Buoyancy in open fresh water, coordinated winch-track speed, adequate approach angle on tracks, appropriate flexibility in the lower run of track and in the grousers, design for optimum thrust relative to the structural constitution of the terrain, centre of gravity and load distribution appropriate to the amplitude of irregularity that the terrain in fig. 9, characterizes, and lowest possible ground pressure.

If it is judged that mobility as outlined in this work does not meet requirements, the only recourse is modification through route selection. This would be approached by eliminating as much as possible of the type of terrain shown in the second half of the traverse (fig. 9). It is not feasible to circumvent all of this kind of terrain and perhaps it would be more realistic to devise other systems of access such as that proposed by the Slipe-Haul system (Cuthbertson and Radforth, 1958).

ACKNOWLEDGMENT. — The writer is a recipient of grants from the National Research Council of Canada and the Defence Research Board (Canada) for the support of the work fundamental to the considerations in this paper. This is gratefully acknowledged.

BIBLIOGRAPHY

Cuthbertson J. and Radforth N. W. Muskeg access, the « Slipe-Haul » method. Canadian Oil and Gas Industries, pag. 50-51, October 1958.

Bekker M. G. Operational definitions of mechanical mobility of motor vehicles. Ordnance Corps, Land Locomotion Research Branch R and D Division OTAC, Report No. 40, June 1958.

Radforth N. W. Suggested classification of muskeg for the engineer. Engineering Journal, 35, 1-12, 1952.

Radforth N. W. Organic terrain organization from the air. Handbook No. 1 (altitudes less than 1,000 feet). Defence Research Board, DR No. 95, 1955.

Radforth N. W. Range of structural variation in organic terrain. Trans. Roy. Soc. Canada, series III, vol. 49, sec. V, pag. 51-67, 1955.

Radforth N. W. The application of aerial survey over organic terrain. Roads and Engineering Construction, August 1956.

Radforth N. W. The theory of measurement in relation to drainage and bearing strength of muskeg. Proceedings of the Fourth Muskeg Conference, Tech. Memo. No. 54, National Research Council, Canada, pag. 59-73, 1958.

Radforth N. W. Organic terrain organization from the air. Handbook No. 2 (altitudes 1,000 to 5,000 feet). Defence Research Board, DR No. 122, 1958.

Radforth N. W. Organic terrain. (In press).

DISCUSSIONS

F. BONMARTINI. — I am here as one of my father's aids but am an employee of Standard Oil of New Jersey. However, I have spent several years in Canada working with one Standard Oil's affiliates, Imperial Oil, a company extremely interested in solving the problems of muskeg trafficability because of the area's oil resources.

I remember the problems faced by the oil searching parties in traversing the muskeg, and I myself saw caterpiller tractors sink and disappear from view like sinking ships. Dr. Radforth has just said, I believe that he can determine the trafficability of the muskeg through aerial photographs and thus avoid these mishaps.

However, I continue to think that one of the major problems of travelling over muskeg is preventing the track from cutting the surface. The muskeg is like a floating carpet, the moment the wheel or traction system cuts through it, the machine sinks unless, a Dr. Radforth says, it is buoyed up. However, I would like to ask how, even if the machine si buoyed, will it be able to get out of a rut should it go into one?

N. W. RADFORTH. — Mr. Chairman, the first question referred to the possibility of prediction of trafficability of this muskeg or organic terrain. And the answer is favourable: yes, we can predict, we can not only indicate where the route shall be, but we can also indicate what the experience is going to be if that route is travelled and what the experience would be if another route, still on organic terrain were travelled. The interesting thing about this is that whatever can be done in Canada, we feel reasonably certain that we can do it in other countries, shall we say in other continents, in the circumpolar aspect indeed. I think the question n. 2 was: do we have to cut the mat, that is to say this living layer or the roots supplied by this

living layer of contemporary plants. The answer is that if you do cut the mat, then of course the number of passes that you can achieve will be depleted; depending upon the kind of organic terrain, the number of passes will be depleted much faster in one case than in another. But we can also predict, with regard to this feature, that in connection with the building of roads on this organic terrain, we recognize, or we shall say that the local engineers recognize three types of failure with regard to roads. I think it is pertinent because failure on roads built over organic terrain really relates to the business of cutting this mat. These three types of failures are as follows: sinkers in which the road disappears like the vehicle that my colleague was making reference to, here 400 feet or more of road embankment can disappear. The second kind of failure is known colloquially as a *folder*, and in this case the road folds along its centre line, forms in cross-section a V and disappears out of sight. The third kind of failure is known as a slider, in which the road embankment tips and then slides nicely out of sight. These three things arise when for instance, or one of these three things may arise, when ditching is brought too close to the centre line of the road. We can therefore predict, depending upon the kind of organic terrain, where ditching should be done. We can predict, with respect to a given kind of vehicle where and when the organic mat will be severed and where embarrassment and zero mobility shall obtain. Thank you.

N. 13

Vehicle design from field test data

Progettazione di veicoli in base ai dati sperimentali del terreno

J. G. Thomson *)

ABSTRACT. — *Difficult terrain, including five hundred thousand square miles of muskeg have almost prohibited development of the Canadian Northland. Severe economic penalties have had to be absorbed by the few developments which have been undertaken.*

In particular, the exploration efforts of the Canadian oil industry have been adversely affected by the low trafficability soils of the Western Sedimentary Basin. Until recently winter trails, water routes and airlifts were the only means of access to huge areas. Now, through the application of standard engineering practice, all-season land travel over muskeg and other difficult soils and snow is possible with mass transportation vehicles.

To solve the problem of muskeg mobility it was first necessary to know precisely what muskeg is and to determine a certain number of its properties. A very excellent qualitative description and classification of muskeg was published nine years ago by N. W. Radforth. His orderly classification in turn provided a basis from which determination of some of the mechanical properties of muskeg was possible. In fact, his simple nine-part classification has been used as quasi-quantitative in conjunction with some vehicle mobility studies.

The requirement for vehicles became so urgent that design and construction of the first few vehicles were carried out before any data on the mechanical properties of the environment were available. Some of these vehicles were successful within limits but in no case was a really satisfactory vehicle produced. Some of the mechanical properties of muskeg have now been determined and are being used to optimize vehicle design.

To speed vehicle development the critical experiment method is being used with some frequency. Based on previous experience with vehicles in other media an assumption is made as to the effect of an arbitrary design change. The modified vehicle is then tested in comparison with the standard vehicle. If the assumed effect is found to occur substantially as predicted the modification is then accepted as a design principle.

To avoid the pitfalls which can be caused by continuous application of the method, a somewhat more basic approach is also used. One such approach was the application of a standard shear vane to the media. Apparent shear strength of a muskeg mat was determined by shear vane and the results compared with vehicle performance determined by the «pull-slip» method. A tentative correlation was obtained.

Based on the results of the critical experiments and the shear vane-vehicle correlation a vehicle design program was undertaken. To date this design program has produced vehicles of 4, 10 and 20 tons payload capacity. All of these have displayed excellent mobility characteristics in the design media. There is no apparent reason why the information so gathered cannot be applied to vehicles in any weight class.

Introduction

The transportation systems involved in oil exploration must be capable of operating over a wide variety of terrains and be amenable to extremes of climate. Canada's active oil exploration area, about 780,000 square miles in extent, runs through Temperate, Sub-Arctic and Arctic regions.

*) Imperial Oil Limited, Canada.

To meet the terrain, climatic and other operational limits it has been necessary to design and develop special vehicles. The methods applied to this development program have been those promising an economy of time, money and material while still holding good promise of success. The « critical experiment » has been the technique commonly applied to the development of one family of vehicles for this area.

Much of the design information gathered in this program is in the form of definition of the limiting terrain types. This data can be used to set limits on the suitable operational areas for conventional wheeled and tracked vehicles in all of northern Canada. Optionally, the data can be applied to the design of any class of vehicles with sufficient mobility to operate throughout the area.

The problem

a) **Topography and Soils of the Western Sedimentary Basin.** — The Western Sedimentary Basin is Canada's active oil exploration area. The large variety of topographic features and soil types found throughout this basin include soft remoldable clays, boulder fields, organic terrain, forested and grassland plains and slopes, sharp river margins, sand dunes, gravel eskers and mountains. Each poses its own set of mobility and trafficability problems in addition to those common to all. Permafrost in association with any of these soil types will cause variations of vehicle response to the terrain. In addition, several of the soil types have completely different characteristics on a seasonal basis.

An outstanding example of seasonal change of characteristics is exhibited by the organic terrain or muskeg which covers an estimated 500,000 square miles of northern Canada. Organic terrain requires that vehicles have low ground contact pressure and high tolerance to sinkage but little suspension for summer travel. In winter, sinkage is non-existent in the frozen material but surface roughness is extreme. Deep, soft suspensions are the main requirement for successful winter operation of vehicles over muskeg.

The development program to be described was applied to providing high mobility transportation vehicles for muskeg. However, since muskeg is not a continuous operating media, the solutions have been influenced by other soil types and topography.

b) **Climatology of the Western Sedimentary Basin.** — The climate of the Western Sedimentary Basin varies widely in the range of temperatures and in precipitation. It also varies widely from one area to another so that a general statement of characteristics cannot suffice. However, the range of temperatures is from a daily minimum of — 70° F to a daily maximum of + 100° F. In northwestern Canada, that is, from Hudson's Bay to the Rocky mountains, there is normally less than 30 inches of snow on the ground at any time. Naturally the winter climate of the southerly portion of the basin is

much warmer than the minimum noted above. In the south, there is normally only a few inches of snow on the ground during the winter season.

c) **Vehicle Operation in the Western Sedimentary Basin.** — Obviously, this large area with its great variety of soil types, topography and climate poses many problems for vehicle movements.

With some exceptions the civilian transportation requirements are for exploration purposes at this time. This statement carries with it the implication that very little money can be spent on building roads or even trails. True off-road mobility must be provided for mass transportation. Both the mining and oil industries are actively engaged in exploration over terrain which until recently had never been traversed. Exploration of these areas has in part been made feasible through recent vehicle developments.

Muskeg, the major limiting soil type to vehicle travel in northern Canada, « has become the term designating organic terrain, the physical condition of which is governed by the structure of the peat it contains and its related mineral soil sub-layer considered in relation to topographic features and the surface vegetation with which the peat co-exists » [1]. Muskegs can be classified into combinations on nine major components suggested by Radforth [2]. In addition, Radforth has classified the ground forms and topography associated with organic terrain [3].

Each muskeg type calls for variations in the vehicle characteristics to achieve optimum mobility. For example, type « FI » muskeg is composed only of mosses and grasses and is characterised by low bearing strength which results in deep vehicle sinkages and moderate motion resistance. Transportation can be conducted over this material by special high mobility vehicles. Type « AFI » is composed of mosses, grasses and trees to about 40 ft. height. The roots of the « A » element (trees) increase the bearing and shear strengths of the muskeg and thereby reduce the motion resistance acting on the vehicle. But the tree trunks are a physical obstacle to vehicle traffic. Either the vehicle must have the ability to push over and trample the trees or a trail must be cleared if type AFI muskeg is to be traversed. The first solution must be used for exploration transportation only if a trail has not been winter-cut in anticipation of a summer operation.

d) **Transportation requirements for oil exploration.** — In attempting to devise an off-road transportation system certain practical conditions are imposed. First and most important, the solution must be both functionally and economically effective. The solution must also be arrived at with a minimum research and development expenditure. To protect the individual company's competitive position it must be achieved in a minimum of time. A limited solution, namely a piece of hardware, is required and therefore a continuing program or facilities for such a program cannot be accepted. Thus the possibility of applying the methods of a terradynamic laboratory cannot be considered. However, it would be foolhardy to attempt a field development program without

a thorough awareness of the general design trends indicated by the work of the terradynamics laboratories.

With the above limiting conditions in mind the solution to the transportation problems of one specific company engaged in oil exploration in the northern portions of the Western Sedimentary Basin were undertaken by a field evaluation method. The first phase of the program was to delineate a group of vehicles which would facilitate exploration.

Several phases in the oil exploration scheme are dependent on transportation vehicles. The first of these is the transportation required for surface geology reconnaissance. This may be done with small surface vehicles but is more conveniently done with helicopters or light aircraft. The second stage of exploration is the geophysical survey, and requires surface vehicles. Vehicles in sizes suitable for geophysical work are supplied by commercial manufacturers. Tracked vehicles for this service are conventional in design but provide adequate mobility over much of the terrain at the low gross vehicle weights involved. The third stage of exploration involves drilling wildcat wells. In this case, approximately 600 tons of drilling equipment and supplies must be moved to the drilling location which frequently is remote from any road or trail network. Suitable off-road vehicles were not commercially available for this mass transportation role over organic terrain.

Generally, if mineral soils are prevalent in the area a summer trail will be prepared and conventional wheeled transportation vehicles applied to drilling rig moves. Where organic soils (muskeg) form a substantial part of the terrain to be traversed tracked vehicles must be used except for a few months each winter. Trail preparation is carried out in the winter with conventional bulldozers and, if logistically possible, the drilling rig is transported on the frozen trail by wheeled vehicles. In some cases the drilling equipment is not available until after the spring thaw and tracked carriers must be used in summer.

Experience in exploration transportation has shown that a vehicle cannot be designed for one specific set of circumstances. An analysis of a large number of exploration well locations has shown that the common case is that of a route composed of mineral and organic soils which will traverse both flat and hilly areas. In addition several stream crossings will be encountered in the usual 50- to 100-mile route length. Therefore the requirement for an all-purpose vehicle arises.

The all-purpose vehicle is unrealistic. The vehicle's performance must be compromised in some terrains in order to achieve the level of performance needed for others. Generally, the vehicle must have sufficient mobility to traverse the softest soil to be encountered, in this case muskeg, the ruggedness to withstand the roughest terrain, mountain trails, and the power to propel it through the terrain which generates the highest motion resistance, fat, remoldable clays. The resulting vehicle is a hybrid rather than an all-purpose vehicle. In terms of performance this means that a practical muskeg vehicle will normally be both overpowered and overweight for service in its primary design environment.

The general outline of a vehicle is often preconceived by an analysis of its role. Standard oil well drilling rigs have maximum single component weights up to 31 tons but more commonly only up to 23 to 25 tons. Since only two components on any rig exceed 20 tons, about 550 of the total 600 tons to be transported can be moved by a 20-ton carrier. The remaining overweight pieces can be moved by the same carrier if the operating speed is reduced. A 20-ton payload capacity seems to be a reasonable maximum nominal size for oil exploration transportation vehicles.

The load compositions set the deck dimensions. A drilling rig requires a clear deck of not less than 8 ft. × 24 ft. for the largest pieces of machinery. If the deck is only 24 ft. long, end clearances must allow for the overhang of up to 40 ft. long tubular goods.

At this point it can be estimated that the vehicle cannot be shorter than 45 ft. nor have a gross weight of less than 50 tons. At least 300 hp. will be required to propel it through the most commonly encountered soil conditions at 10 mph. If differential track steering were to be employed the overall vehicle width would have to be 30 to 35 feet. This width is unacceptable on the basis of the cost of clearing a wide trail and the cost of building a structure four times the width of the loads it will carry. Also, the vehicle would have a very wide belly on which it could easily « hang-up » in soft clay and muskeg.

Similar practical design limitations have been experienced in the evaluation and design of oversnow vehicles. In that media substantial progress toward good mobility had already been made using various forms of articulated vehicles [2,3]. Two or more « bellyless » units « en train » steered by joint forces appear to best exploit the general principle of articulation. This form of articulation also appears to be the only one suitable for use on large vehicles. There is no known or even suspected size limit to this principle.

From the foregoing it is seen that at least the morphology of the vehicle has been established without specific reference to the soil-imposed limitations. However, the selection of features is not purely objective. They are subjective on the basis of successful experience with very similar principles in other soft media.

Designing for mobility

a) **Available methods.** — If the mechanics of the transmittal of forces between the track or wheel and the soil can be determined, then an optimum vehicle can be designed for any specific soil. This is the approach used in laboratory investigations and the result frequently has the disadvantage of being specific. A vehicle designed by this method should produce optimum performance when operating in the design conditions but may be an especially poor performer if it is divorced from them. In addition, a vehicle designed for optimum mobility performance may not be morphologically suited to the remainder of its role. That is, it may be unable to carry the requisite payload or, if it can carry the payload, it may not be able to accomodate the load size or composition.

The critical experiment at or near full scale can produce satisfactory design solutions to mobility problems. In this case the test work is carried out in one or several real environments and substantial weight is placed on the morphological conformance of the machine with its envisioned role. At any time during the program the range of conditions can be extended merely by extending the number of practical soils in which the tests are made.

The method is quite simple to apply. From various sources and considerations a possible design solution to a specific mobility problem is deduced. A specific modification is then designed and applied to a vehicle of known performance and the resulting change of performance determined in a brief field test program. If the expected result is in fact achieved it is accepted that the deduced solution was correct.

This method has another advantage. Either the modified vehicle is a prototype or only a minor design step is required between the test and prototype vehicle. It is not necessary to design, construct and evaluate a prototype based on small-scale, model data.

Critical experiments may also be used to demonstrate in general terms the soil-imposed limits to the vehicle design which has been outlined morphologically in the manner noted in the preceding section.

b) **Personnel.** — Neither of the two mobility design methods outlined above are purely objective. The results produced by a terradynamics laboratory are influenced by the question put to the apparatus and the limits imposed on the apparatus. However, over a period of time and after the construction of several prototypes, it should be possible to set practical test limits which will compensate for lack of objectivity. The critical field experiment is by nature subjective.

It follows then that by either method the resulting vehicle will only be as good as the personnel engaged in the pre-design evaluations. Relatively inexperienced technicians and scientists can produce good data from a laboratory under a skilled project director. However, the field test method must be under the close direction of the head of the design team. The test director must know specifically what he is seeking and how the result will be applied to the design of the vehicle. Obviously long experience and a thorough understanding of the general problem to be solved are required of the personnel using the field test method.

The critical experiment applied

During the summer seasons of 1957 and 1958 critical experiments were applied to the problem of providing mobility in muskeg for oil exploration vehicles. The first series of field tests was designed to evaluate and improve the muskeg mobility performance of two existing vehicles. The guiding assumption was that muskeg responds to vehicles substantially as a classic soil. Muskeg trafficability data which could be applied to the design of a family of vehicles which would have much higher mobility than those used for the tests

were also sought. Basic to the test program was the already existing knowledge of how to improve vehicle mobility in snow and that snow responds to a vehicle substantially as a soil [4,5]. It was then assumed that vehicle characteristics which improve mobility in snow would do the same in muskeg if adequate shear strength to provide propulsion could be made available from the surface mat of the muskeg by controlling sinkage. The test program partially outlined below verified these assumptions.

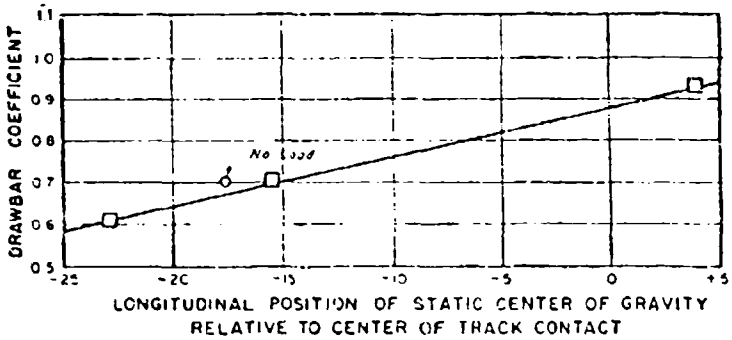


Fig. 1. — Scout car weight distribution tests. - Test specifications: date: 18 oct. 1957; gross vehicle weight: 7108 lbs.; payload: 1630 lbs.; test media: type - Fl - muskeg; nominal unit ground pressure: 1.65 p.s.i. - Note: results not corrected for shift of centre of gravity due to drawbar pull above line of action of tracks or vehicle trim angle.

The aims of the 1957 test program were quite modest. The two most important of these were to attempt to determine the maximum allowable nominal contact pressure between the track and the ground and to determine the effect of variations in the position of the centre of gravity of the vehicle with respect to the centre of track contact.

The test vehicle was known to be tail-heavy and it was therefore obvious that although it had a nominal contact pressure of 1.65 psi at least a portion of the track must be operating at a considerably higher ground pressure. It was therefore fundamental to the determination of the allowable nominal contact pressure to adjust the load distribution so that the nominal and actual contact pressures would be as nearly as possible the same. By placing the payload at various points on the load deck and on a special platform built in front of the vehicle it was possible to vary the position of the centre of gravity of the loaded vehicle from 25" behind the centre of the track contact to 4" ahead of that centre. The vehicle's excess traction (or drawbar pull) was measured in each of the load conditions and was found to increase in a straight line as the centre of gravity was moved forward. This result is shown in fig. 1. Over the test range an improvement of 50 % in net traction was achieved.

Observation of the vehicle during that portion of the test program strengthened the assumption that the nominal unit ground pressure limit could be

increased from the then accepted maximum of 2 psi. Some trafficability tests were therefore undertaken at nominal unit ground pressures of 3 psi and 5 psi. Because of the large volume of the payload required to achieve these ground pressures it was not possible to operate the vehicle at the most favourable position for the centre of gravity.

Even at non optimum load distribution, 50 passes were made through the same path at the nominal 3 psi ground contact pressure. At the conclusion of the 50th traverse the muskeg surface mat was depressed but substantially intact. Drawbar pull tests could not be completed since engine power was not sufficient to permit maximum traction from the tracks to be exceeded at this contact pressure.

The gross vehicle weight was then increased to produce a nominal contact pressure of 5 psi. Since the vehicle, a half-ton carrier, was grossly overloaded only a few passes were attempted in one track. Observation of the test gave the impression that the muskeg could sustain at least 25 and probably 50 or more traverses.

Details of the test techniques and results of the 1957 program were the subject of an earlier publication*.

From this test program it was concluded that muskeg had much better trafficability characteristics than many vehicles had made it appear. In setting up the 1958 program a number of steps which had at first been thought necessary were eliminated on the basis that the problems no longer appeared to be terrain-generated.

After the initial assumptions regarding muskeg response to vehicular traffic were verified by the test program they were generalized. It was tentatively concluded that information now existed on the relationships among sinkage, weight and weight distribution, motion resistance, allowable ground pressure, etc. The second field program, carried out in the summer of 1958, was aimed at confirming and extending the first year's work using a larger vehicle. In addition to the vehicle traction tests a shear vane was applied to the measurement of shear strengths in the muskeg. Generally, it was shown that areas of high shear strength as measured with the shear vane produced high net vehicle traction and vice versa.

An elementary analysis related the instantaneous strain caused by the shear vane to the instantaneous strain under various segments of the vehicle track. A theoretical vehicle performance curve of similar shape to the measured vehicle performance curve was obtained. Theoretical performance was substantially higher than actual. Although it is not suggested that a rigorous correlation was established it is pointed out that gross theoretical traction was calculated whereas net vehicle traction was measured. A comparison of theoretical and actual performance is shown in fig. 2.

Towed motion resistance tests, the results of which are loosely associated with powered motion resistance, were carried out. The sum of towed motion resistance and net traction was shown to approach the theoretical traction.

To permit a more effective sprocket design than employed on the test

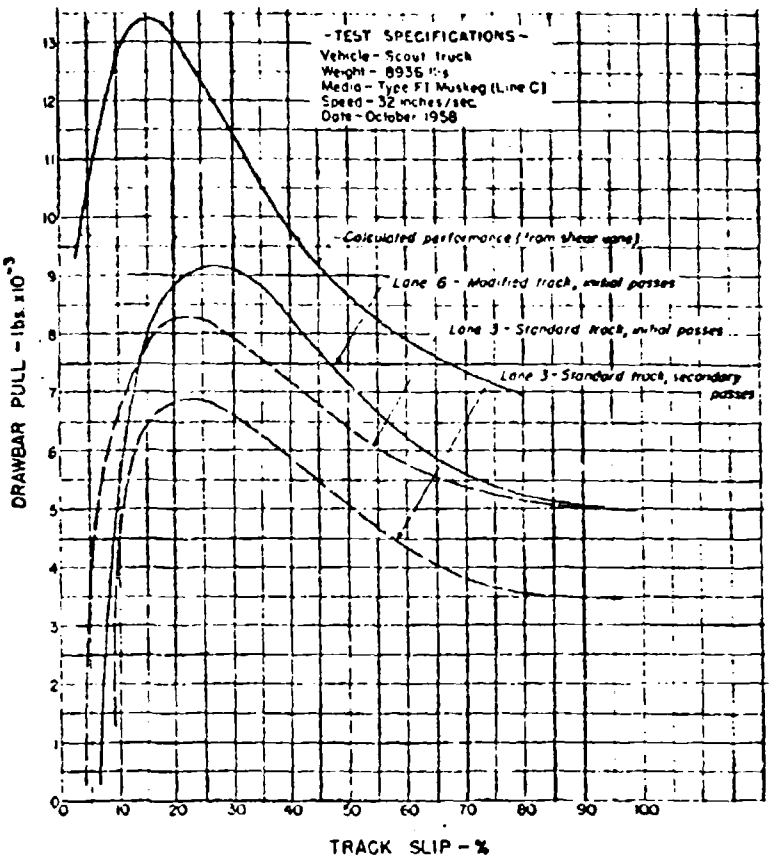


Fig. 2. — Effect on drawbar pull of doubling track pitch comparison of theoretical and test results.

vehicle it was desiderable to increase the grouser spacing. Observation of the interaction of the track and muskeg indicated that and optimum grip was not achieved between the grousers and the muskeg at the standard grouser pitch. In the late stages of the test program, therefore, every second grouser was removed from the band track and the net traction again determined. The substantial improvement attributable to the longer track pitch is indicated in figure 2.

The results of the 1958 field test program have been published in detail [7].

On the basis of the conclusions which had been drawn from the first field program a test rig, which was later accepted as a rough prototype of an articulated 10 ton trasporter, was constructed. The reasoning behind the selection of the joint force steered, articulated vehicle has been detailed in earlier publications [5,6]. It was impossible to determine the net traction of this vehicle during the second test period since there was no other vehicle in exis-

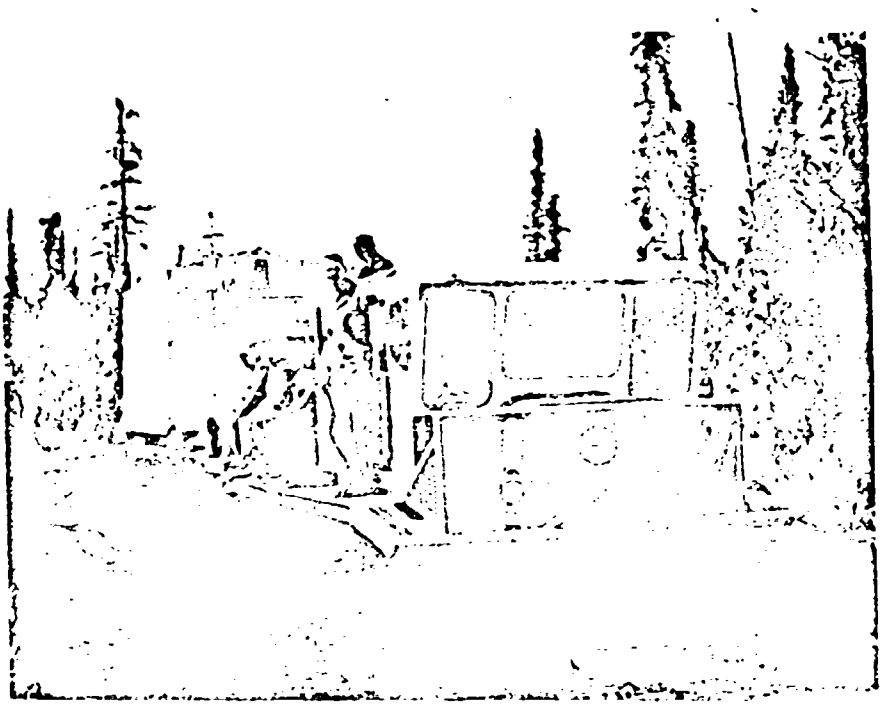


Fig. 2. — « Musk Ox » operating on muskeg trail.

tence of sufficient size and mobility to act as dynamometer vehicle. The only tests that could be carried out were trafficability evaluations at the then rated 8 ton pay-load. It was found that the vehicle had excellent mobility and manoeuvrability.

Since the test muskeg failed to challenge the test rig's (the term vehicle is purposely avoided) ability it was released from the test program and assigned a field role as a transportation vehicle. No mobility failures or even difficulties were encountered in this service. Mechanical failures were frequent since the rig was originally intended to have a life of only a few weeks under test field conditions.

This test rig (or 10 ton prototype) was expanded later in 1958 into the 20 ton payload articulated vehicle named « Musk-Ox ». Immediately after construction this vehicle was put into full field service without testing or evaluation. The payload capacity at which the field test results were applied is a good indication of the level of confidence placed on the design data obtained by the methods outlined. Specific conditions and assumptions applied to the design as well as a description of the principles and components employed in the vehicle are given in an earlier paper [2].

The « Musk-Ox », shown in figure 3, has now been in service during two summer-seasons. Its mobility performance and mechanical reliability have been outstanding in all organic and mineral terrains encountered.

Summary of method

The design method outlined in this report is as simple as it is successful. Basically, it is composed of the following steps.

1) Identify the role of the vehicle accurately in terms of mobility and function.

2) Establish the range of conditions through which the vehicle will be required to operate and then determine:

a) the allowable nominal ground contact pressure for the softest terrain;

b) the power requirement for the highest motion resistance terrain; and,

c) the structural ruggedness required in the machine for the roughest terrain.

3) Conduct sufficient field work with existing vehicles to establish the feasibility of the solution outlined from the results of 1) and 2) above.

4) Design and construct a prototype vehicle and apply it to the field service. Proving ground evaluation does not duplicate field conditions and is therefore not a useful development step.

It is most important to note that primary consideration is placed on the fact that every vehicle is terrain-limited and morphological characteristics must be reconciled with both terrain limitations and the vehicle's operational role through that terrain. In view of this predominance of terrain over mechanical limitations the vehicle solution may be considered general. For example, the « Musk-Ox » is a vehicle of 54 tons gross weight which is mobile in a very large variety of muskegs. It is quite incidental that this is a transportation vehicle. It could just as easily be a fighting vehicle on which 20 tons of armor and armament would replace the payload.

In determining the ability of muskeg to support vehicular traffic the work was done in such a way as to be capable of very wide generalization. This was accomplished by minimising the use of tests which give specific information. Therefore although the test work was done in only a few of the muskeg types found in the Western Sedimentary Basin of Canada the findings will be applicable to all muskegs which occur in areas of similar climatology. The muskegs within this climatological regime will occur in northeastern Canada, northern Europe and Asia and southern South America. This does not say that the vehicle's muskeg performance will be identical in every muskeg found throughout the world. It says merely that a vehicle with a substantial muskeg capability in northwestern Canada will have a similar muskeg capability in any other geographical area with approximately equivalent climatology.

BIBLIOGRAPHY

1) **Radforth N. W.** Organic terrain organisation from the air. Handbook No. 1, Defence Research Board, Canada. DR No. 95, Ottawa, October 1955.

2) **Radforth N. W.** A suggested classification of muskeg for the engineer. National Research Council of Canada, Technical Memorandum No. 24, Ottawa, May 1952.

3) **Radforth N. W.** Organic terrain organisation from the air. Handbook No. 2, Defence Research Board, Canada. DR No. 124, Ottawa, February 1958.

4) **Thomson J. G.** A study of some factors influencing vehicle mobility in snow. Defence Research Board, Canada. D Eng R Report No. 1, Ottawa, December 1957.

5) **Thomson J. G., Wilson C. W.** A study of some phases of the snow-vehicle interaction, vol. III, Defence Research Board, Canada, Report No. D.R. 128, Ottawa, April 1958.

6) **Thomson J. G.** Vehicle mobility performance in muskeg. (A preliminary report). Proceedings of the Fourth Muskeg Research Conference, National Research Council of Canada, Technical Memorandum No. 54, Ottawa, August 1958.

7) **Thomson J. G.** Vehicle mobility in muskeg. (A second report). Proceedings of the Fifth Muskeg Research Conference, National Research Council of Canada, Technical Memorandum No. 61, Ottawa, June 1959.

8) **Nuttall C. J., Thomson J. G.** Design and muskeg operation of the 20 ton payload carrier: the « Musk-Ox ». Society of Automotive Engineers, Preprint No. 213 B, New York, September 1st, 1960.

9) **Thomson J. G.** Vehicles in muskeg. The Engineering Journal. The Engineering Institute of Canada, Montreal, May 1960.

DISCUSSION

N. W. RADFORTH. -- Mr. Chairman, I apologize for appearing again, but because of the nature of your comments, Sir, which suggested that analyses of these two papers should be in some degree considered together, I feel that the following remarks are appropriate. With regard to Mr. Thomson's presentation, I can say, as a result of the data that he has presented from time to time, and as a result of his tests, we have a vehicle which can effectively traverse a large percentage of organic terrain. I must emphasize that I mean organic terrain wherever it exists over the surface of the earth — not just in Canada.

It is possible to predict, and Mr. Thomson has effectively done this, the response of the vehicle to the terrain in terms of budgeting — not only in terms of whether an operation will succeed, or as to whether it shall succeed in this way or that way. I think that this is a very advanced step indeed, and I must congratulate Mr. Thomson in this respect. He has shown that by considering the vehicle and terrain together, the cost of certain operations can be predicted once the nature of the operation has been designated.

This can be done before any vehicle is sent out, and often before any on-the-ground reconnaissance, by examination, initially, of air photographs.

Relation of shape of track shoes to tractive force of the crawler-type tractor on peat soil

Relazione tra la forma dei pattini del cingolo e lo sforzo di trazione dei trattori cingolati su terreno cedevole

S. Tsunematsu *) - K. Matsui **)

ABSTRACT. — *The crawler-type tractors equiped with wide tracks have been adapted to swampy soils such as the peat ground in Hokkaido. The tracks are effective for reducing the rate of sinking on such loose-type soils. The flat track shoes having the conventional lugs tend to cut and strip the surface of the ground, causing the deceases of traction force. Thus, it has become very important to design the most effective shape of track shoes.*

From this view point, this investigations were carried out to determine the relation of the shape of track shoes to the traction force of tractor. This paper summarizes several experiments on the traction force of two tractors, trailing a ditcher plow, ordinary moldboad plow, harrow and trailer on the peat soil in Hokkaido.

Three types of shoes were tested for the experiments. The first type of shoes had triangular cross sections. The cross sections of the second type of shoes were a little different from that of first type of shoes, because they were welded with surplus metal along one edge of each shoes. The third shoes had semi round cross sections.

These three shoes were respectively, named a-shoes, b-shoes and c-shoes in this paper.

The conclusions obtained from these studies were as follows:

1) The maximun traction force were 85 % of the tractor weight for the a- and b-shoes. The trend of cutting and stripping the soil surface for the b-shoes was larger than that for the a-shoes. This trend for c-shoes was smaller than that for a- and b-shoes, while the maximum traction force of c-shoes was 75 % of the tractor weight and it was smaller than that of a-shoes.

2) The traction force on the stripped surface was largely decreased, comparing with that on the unstripped surface. The decreasing rate of traction force was proportional to the stripping depth of the soil surface.

The influences of the shape of track shoes on the traction force were small for the stripped ground. Namely, for all the shape of shoes, the maximum traction force were, respectively, 40 and 65 % of the traction weight on the 15 cm and 10 cm stripped ground.

Introduction

The bulldozer is one of the effective machines for public works and is widely used on peat soil in Hokkaido, Japan. However there are several problems in increasing its tractive force, because of the special physical properties of peat soil. Such factors as weakness of pressure resistance, high

*) Head, Dept. of Agricultural Machinery, Faculty of Agriculture Hokkaido University, Sapporo, Japan.

**) Faculty of Agriculture, Hokkaido University, Sapporo, Japan.

water content, residual dead plants, etc. are not favourable to the use of the regular track shoes of a bulldozer. Usually, wide track shoes have been used to reduce the tendency of bulldozers to sink into soil such as loose peat soil. There are several effective special-type track shoes designed so as to prevent a side slip of tracks, and shearing and stripping of soil surface on this type of soil.

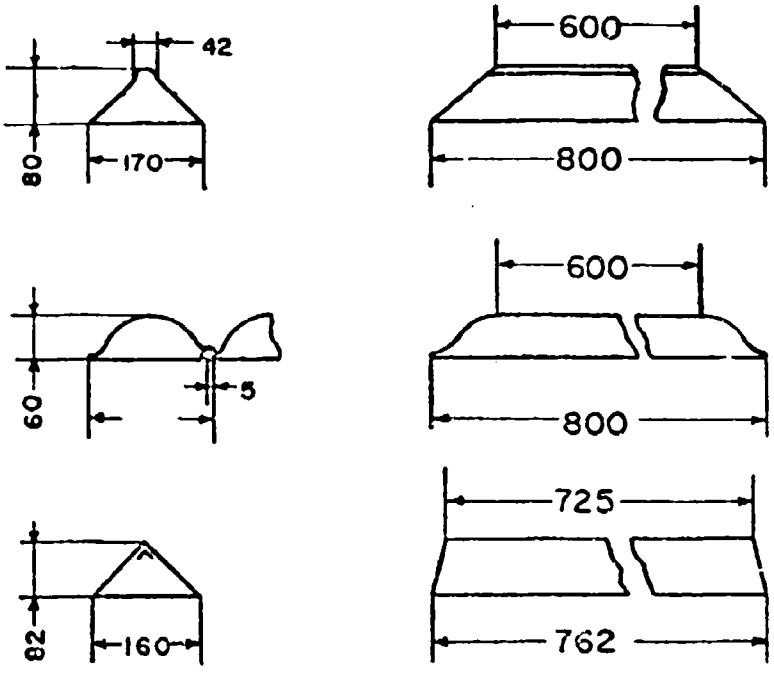


Fig. 1. — Test track shoes.

The present paper reports the results of tests on the tractive force of three types of the track shoes in connection with conditions of soil surface and the position of the center of gravity of the tractor.

Method of the tests

1) *Tractors and track shoes.* — Two tractors, N and K were used for these tests, and they were equipped with the special wide track shoes designed by the manufacturer for the purpose of decreasing the pressure of ground contact, instead of the regular type shoes. The width of the regular and special track shoes were 40 cm. and 80 cm., respectively, for K-tractor, and 33 cm. and 76 cm. for the N-tractor. The pressure of ground contact of both tractor equipped with the regular track shoes was 0.41 Kg./cm^2; however that of the K- and N-tractors decreased, respectively, to 0.25 Kg./cm^2 and 0.21 Kg./cm^2 with the special track shoes. The three types of track shoes are shown in fig. 1,

a- and b-shoes belong to the N-tractor and c-shoes belong to the K-tractor. Though the a-shoes form a triangle section, there is a special figure at the point of the shoes as shown in fig. 1. The shape of this point was formed by welded steel. The outline of the b-shoes is almost round, and their shape was designed taking into consideration the fact that peat fiber would not be cut by the point of the shoes. Another special feature of the b-shoes was that they over-lapped about 5 cm. with next shoe. This lapping was effective in preventing soil from coming out between the shoes, and in decreasing the pressure of ground contact. The c-shoes of the K-tractor were in the form of a right angle isosceles triangle.

TABLE 1. — *Specification of test bulldozers.*

	K-tractor Shoes			N-tractor Shoes	
		Winch			
Length (mm)			4540		3760
Width (mm)			3150		2502
Height (mm)			2200		2094
Weight (kg)	a-shoes	with	10600	c-shoes	7020
	b-shoes	with	10200		
	b-shoes	without	9800		
Width of track shoes (mm)			800		760
Length of the ground contact (mm)			2580		2140
Tread (mm)			2200		1650
Pressure of the ground contact (kg/cm)	a-shoes	with	0.26	c-shoes	0.21
	b-shoes	with	0.25		
	b-shoes	without	0.24		
Blade, width × height (mm)			3150×790		2502×800
Rated H.P.			55		46

The K-tractor was equipped with a winch drum at the rear end of the body, and the center of gravity was located 11 cm. behind the center of the whole track length in contact with the earth, i.e. between the front wheel shaft and the rear driving wheel shaft. When the winch was taken away, the center of gravity moved forward about 8 cm., and was at about the center of the tractor. Table 1 shows the main specifications of both tractors. The reason that there was some difference in the weight of the N-tractor in this table was due to the difference of the track shoes.

2) *Soil conditions.* — The tests were carried out on lower peat soil at Shinotsu village near Sapporo in Hokkaido. The section of ground is shown in fig. 2. The soil was very moist, and was covered with marsh-reed and horse tail. The top layer consisted of the root or rhizome of those plants.

The soil conditions could be divided into the following four types. The A- and B- conditions were just of the surface of the soil, however there was difference in level of underground water in each case. The height of underground water was about 24 cm. in the A-condition, and 38 cm. in the B-condition. The water content of the B-condition was lower than that of the A-condition as shown in table 2. The C-condition was about 10 cm. under the B-condition, and it was prepared by stripping the surface layer of the B-condition by a bull-dozer. The D-condition, was about 15 cm. under the C-condition, and it was softest of the four conditions. Some physical characteristics of these test places are shown in table 2.

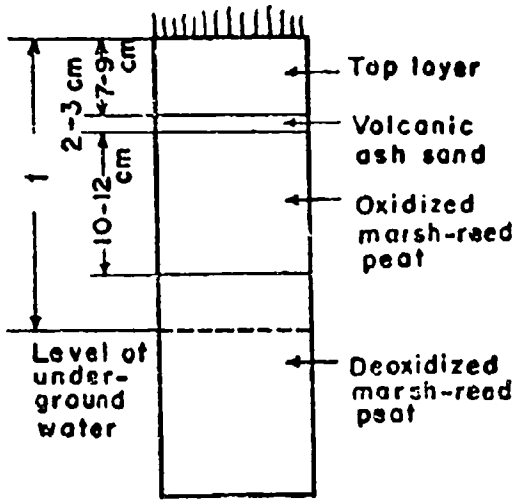


Fig. 2. — Section of ground.

TABLE 2. — *Physical properties and hardness of the soil.*

Sym. of soil condition	Depth cm	Rate of water content %	Capacity of water content %	Apparent specific gravity	Hardness of soil	
					Depth from suface cm	Hardness mm
A	0-10	131	165	0.44	0	57.3
	10-20	766	796	0.11	10	51.0
	20-30	364	371	0.22	20	62.5
B	0-10	93	129	0.51	0	72.5
	10-20	452	526	0.15	10	66.7
	20-30	686	755	0.11	20	80.0
C					0	77.5
D					0	96.5

*) Diameter of hollow made by the scale of conical soil hardness (pressure is 50 kg).

3) *Methodology of the tests.* — By measuring of the tractive force and slippage at the same time, the influence of the soil condition and the shape of the track shoes on the tractive force were tested with the K-tractor equipped with the winch. For this test, a- and b-shoes were used, and the soil conditions, A, B, C, and D-condition were given for a-shoes, and then B- and D-condition were selected for b-shoes. To determine the influence of the position of the

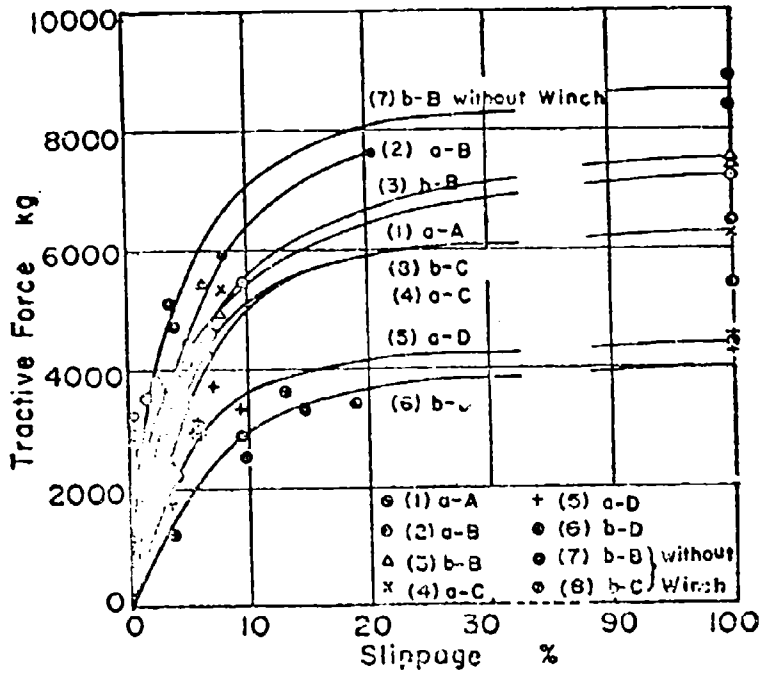


Fig. 3. — Tractive force-slippage.

center of gravity on the tractive force, the K-tractor, equipped with b-shoes, and without the winch drum was used on B- and C-conditions. The value of the tractive force under both conditions, equipped with and without the winch would be compared in discussing the influence of the center of gravity.

For the N-tractor, the maximum tractive force was measured on the C-condition.

Another bulldozer was used as a load tractor for the test tractors. The various load were provided by adjusting the engine and foot brake, and the blade of the load tractor. The pulling of the tractor was done carefully so as not to add the vertical load on the track shoes. The tractor was in first gear and the throttle lever was set at full speed.

Results and discussion

The results of the tests are summerized in fig. 2 and table 3. The maximum tractive force, and the tractive force and the coefficient of traction at 16 % slippage given by fig. 2 are shown in table 3.

TABLE 3. — *Results of the tests.*

No.	1	2	3	4	5	6	7	8	9
Shape of track shoes	a	a	b	a	a	b	b	b	c
Soil condition	A	B	B	C	D	D	B	C	C
Sym. of tractors	K	K	K	K	K	K	K	K	N
Winch	with	with	with	with	with	with	without	without	
Max tractive force (kg)	7200	7000*	7400	6300	4300	3900	8000	6300	4600
Tractive force at 16 % slippage (kg)	6200	7000	6400	5750	4150	3600	7800	5750	
Coefficient of traction at 100 % slippage	67.8		72.5	59.4	40.6	38.2	87.7	64.2	65.5
Coefficient of traction at 16 % slippage	58.5	66.0	62.7	54.2	39.2	35.3	79.6	58.7	

*) Stoppage of the engine.

1) *The influence of the soil conditions on the tractive force.* — In case of the natural surface (A- and B-condition), the amount of underground water content influenced on the tractive force as shown by the comparison between No. 1 and No. 2 of table 3. Stoppage of the tractor engine noted in No. 2 was a special case, due to some trable with the fuel nozzle. The maximum coefficient of traction on the surface of this peat soil was a little smaller than that of 70 - 80 % [1] on a common soil surface. However, the fact that these relatively good values were obtained was due to the effect of the special track shoes.

On the other hand, a decrease in the tractive force on the stripped ground face (C- and D-condition) was evident as shown by No. 4, 5, and 6 in table 3. And also, it was a very interesting point that the deeper the tractive force became. This result can be justified by comparison with the report of Manai [2] that the strength of peat soil decreases more and more according to increasing depth from the surface of ground. This is one of the important characteristics of peat soil. The above mentioned fact shows that tractors or bulldozers traveling on peat soil must be equipped with special track shoes designed so as not to destroy or strip the natural top surface of the soil. Likewise the travel of a tractor should not be repeated on the same place, if possible.

2) *The influence of the shape of the track shoes on the tractive force.* — The results of the tests on a- and b-shoes showed that the coeficient of traction of a-shoes was 2-4% (actual value of the coefficient of traction) higher than that of b-shoes on B- and D-conditions. This result could be explained on the basis that the shearing area of the soil of a-shoes which existed between the projections of shoes adjoining each other, was wider than that of b-shoes. It was assumed for b-shoes that the curved surfaces near the projections of the shoes just translated the friction force between the face of the shoes and the peat soil to the tractive force. The traveling resistances of these two shoes on peat soil were rather smaller than that on common soil, as shown in table 4. Also, a difference of traveling resistance between these shoes was not evident. Therefore it is not necessary to discuss the traveling resistance of these shoes. For the above mentioned reason, it is concluded that in general track shoes having a wider shearing area are better on peat soil. One of the weak points of the a-shoes was that the welded steel at the point had tendency to strip the top face of peat soil. This shape should be improved.

TABLE 4. — *Relationship between shape of track shoes and traveling resistance.* (0.8 *m/sec. speed*).

Shape of track shoes	Soil-coudition	Traveling resistance kg	Coeficient of travelling resistance %
a	B	1150	10.9
b	B	910	8.8
a	C	1340	12.9
b	C	1150	11.3

3) *The influence of the position of the center of gravity on the tractive force.* — The influence of the position of the center of gravity on the tractive force on fresh soil conditions (B-condition) can be illustrated by a comparison of No. 3 and No. 7 in table 3. The tractive force of the tractor equipped with the winch was lower than that of the tractor without the winch. By analogy the same relationship on the stripped soil conditions can by demonstrated by the values in No. 4-8, and No. 5-6 of table 3. The reason that these results were obtained was due to the fact that the tractor with the winch tilted backward. The tractor traveled in the position of climbing up a slop. However, the tractor without the winch maintained a level position, and all faces of the track shoes pressed uniformly against the soil. The fact that there was a difference of 8-10% in the coeficient of traction due to the slight difference in the position of the center of gravity. Thus, the position of the center of gravity is more important than the shape of the shoes. The tractive force of the N-tractor was high as shown in No. 9 of table 3. This value was given by the design to position the center of gravity at the center of the tra[illegible] as near as possible, in addition to a consideration of the shape of the s[illegible]

and the pressure of ground contact. In regard to the influence of the position of the center of gravity, Kühner has stated that it had much influence on the tractive force on sandy soil. The position of the center of gravity is especially important on soft soil such as peat soil. When the center of gravity is located too far forward, the front of tractor sink deeper than the rear end. Therefore, the traveling resistance increases. On the other hand, if the center of gravity is put too far to the rear, the tractor tends to travel in a position as if climbing a slop. Thus the maintenance of a level position of tractors is very important.

Conclusion

From the results of the tests on the tractive force of tractors on peat soil, the tractive force was found to be influenced by the water content of peat soil which had a close relationship with the height of underground water. The depth of stripped soil also influenced in the tractive force. As to the type of the shoes, it was found that a-shoes were superior to b-shoes under any soil condition. The track shoes should have a shape that does not strip the natural soil surface. Also, they should have a soil shearing area as wide as possible. The position of the center of gravity should also be considered, because it had a close relationship with the tractive force. When a tractor or bulldozer was equipped with efficient shoes and the position of the center of gravity was correct, it was possible to increase the maximum coefficient of traction as high as 85 % on the B-condition and 65-70 % on the C-condition.

These factors of the center of gravity and the shape of the track shoes are important to increase the coefficient of traction for field works, such as plowing and disking, etc.

BIBLIOGRAPHY

1) Tsunematsu S., Yoshida T. and Matsui K. Study on the maximum tractive force of tractor on the different soil conditions. Journal of the Society of Agricultural Machinery, Japan, vol. 17, No. 2, pag. 37, November 1955.
2) Manai K. On the stability of a peat-bed at ishikari district. Bulletin of the Faculty of Engineer, Hokkaido University, Japan, vol. 17, No. 2, pag. 1, March 1952.
3) Kühner K. Gelände fahrzeug und Gelände. V.D.I., Bd. 81, Nr. 7, pag. 161, 1937.
4) Report on an investigation on the performance of the tractors for soil improvement. Section of Agricultural Administration, Department of Agriculture, Hokkaido, Japan, pag. 161, 1937.
5) Bekker M. G. Soil-vehicle concepts found impending design. S.A.E. Journal, May 1950.

DISCUSSIONS

N. W. RADFORTH. — It is encouraging to learn of attempts to relate mechanical aspects of track units to gradient of difference in peat (the fossilized element in organic terrain). There is urgence in connection with procuring illustrative result for peat-deapth

gradients and water content difference. The quantitative information available in this account serves as a useful foundation for future analysis. The approach to the problem by dealing with: 1) influence of soil conditions; 2) influence of shape of track shoes; 3) influence of position of center of gravity on tractive force is fundamental and useful to us.

In trafficability problems of peat I have found it is important to know whether the original peat surface has been rehabilitated thus changing the structural relations that would have typified the peat under natural circumstances. Is the reed, horse-tail cover primary or secondary?.

Also under soil conditions, softness of the order shown for « D » soil type is not always experienced as being low as compared with the top layer. My own experience is that peat structure differs as to strength or harness moreso in the horizontal dimension than in the vertical. Are the Authors able to concur with this? Are they concerned only with so-called agricultural peats?

In achieving mobility to 70-80 % effectiveness of the result on a common soil can this in fact be attributed to favourable effect of special track shoes or to a good peat type fortuitously chosen? It is anticipated by the commentator that the « a-shoes » would in fact not strip the top face of peat soil if the latter is very woody as is often the case. Has this shoe been examined for all coarse peats? It might be markedly useful and not inappropriate as claimed.

The center of gravity with few exceptions changes when winch action is applied, as the Author indicates. Synchronization of winch and track speed obviates this difficulty.

As a comment on the conclusion of this paper the Author may be interested to know that in some of our categories of Canadian peat sheer strength increases with depth, contrary to common understanding.

D. GIACOSA. — E' ultimata la serie di relazioni prevista per il primo giorno del Convegno. Poichè non sono stati richiesti altri interventi e non vedo alcuno farsi avanti, la riunione ha termine.

Purtroppo è mancata la presentazione di due relazioni molto interessanti. La relazione di Mr. Thomson e quella di Mr. Tsumenatsu che avrebbero completato il quadro comprendente i numerosi e complessi problemi del movimento fuori strada nel caso particolare del terreno organico.

Tutte le relazioni presentate oggi sono state interessanti e meriterebbero un ampio commento. Come costruttore di veicoli penso che date le enormi differenze tra le configurazioni del terreno e le caratteristiche del suolo sia estremamente difficile e forse addirittura impossibile realizzare un veicolo che possa andare su tutti i terreni. E' necessario per ogni terreno preparare il veicolo che meglio si adatti al genere di operazioni che su quel particolare terreno deve compiere. E' vero che alcune condizioni sono comuni a tutti i veicoli che devono agire fuori strada; queste condizioni, ben note, sono la più bassa possibile pressione specifica sul terreno e una giusta posizione del centro di gravità nei confronti della superficie di contatto col suolo; ma per tutti gli organi di trazione che sono a contatto diretto col suolo è necessario che il disegno si adegui alle particolari caratteristiche del suolo stesso.

Gli studi vasti ed approfonditi e le ricerche fatte specialmente dai Laboratori delle Università Americane contribuiranno in forma decisiva a raggiungere dei risultati positivi e a progredire in questo particolare settore della locomozione.

ASPERITA' DEL TERRENO, VIBRAZIONI DEL VEICOLO E STABILITA' DIREZIONALE

TERRAIN ROUGHNESS, VEHICLE VIBRATION AND DIRECTIONAL STABILITY

On the statistical analysis of linear vehicle dynamics *)

Analisi statistica della dinamica del veicolo lineare

J. L. Bogdanoff - F. Kozin **)

ABSTRACT. — *Statistical analyses of the dynamics of some two-dimensional linear vehicles traveling on a rough track are performed to determine the influence on two aspects of vehicle ride of a set of parameters which include wheel base length, idealized tire imprint length, speed, and damping constant. It is assumed that the vehicles move with constant horizontal velocity on a second order, weakly stationary and mean square continuous random track with contact maintained at all times between the idealized tires and the track. The two aspects of vehicle ride used as measures of the ride roughness are peak value of power spectral density and variance of frame acceleration, the frame acceleration being either vertical at the c. g. of frame, vertical at the point over idealized wheel, or angular (pitching).*

For the same speed, damping, and power spectral density for the track, for two particular vehicles, the idealized tire imprint length was a relatively unimportant parameter over a fairly large range of values. On the other hand, one parameter which included the wheel base length was found to be important under the same conditions.

Four sets of parameter values were found which at the same speed produced best or optimal rides for vertical acceleration at the frame c. g. and over the wheel, depending upon which measure of ride roughness was employed. The influence of speed was then examined on vehicles having these sets of parameter values. In all cases, increasing speeds produced sharp increases in ride roughness.

1. - Introduction

The motivation for the investigation reported in this paper and the need for a statistical description of the ground in the investigation are described in the Introduction to the preceding paper. Hence, the remarks of this section only need be directed to those aspects of vehicle dynamics and « optimal ride » not previously commented upon.

A wide variety of one, two and three dimensional models have been suggested for a study of the dynamics of real vehicles. Some of these models are linear while others are non-linear. The one we shall employ in this paper [1-2] is sufficiently simple so that the mathematics is reasonably tractable and yet sufficiently complicated so as to make parameter studies interesting. A sketch of this linear two-dimensional vehicle is given in figure 1.

This vehicle consists of a rigid frame connected at each end via a parallel arranged spring and damper suspension element to an idealized wheel-tire. In

*) This paper was originally prepared for Land Locomotion Laboratory, U.S. Army Ordnance Tank Automotive Command, Detroit, Michigan.

**) Midwest Applied Science Corp. and Purdue University.

the initial stages of the investigation, a number of wheel-tire models were considered. However, on simplifying each of them to a case which could be described in a reasonable mathematical form, the wheel-tire model shown was obtained. It has mass but no moment of inertia, and it is connected to the ground of track through a spring-damper arrangement distributed along a massless rigid bar. Contact with the track over the entire foot-print length is assumed. Thus, the idealized tire acts much like a deformable slipper gliding over the track. Bouncing is not permitted in the sense that contact over the entire foot-print length is maintained at all times, but the wheel mass may oscillate vertically on the suspension element and the idealized tire.

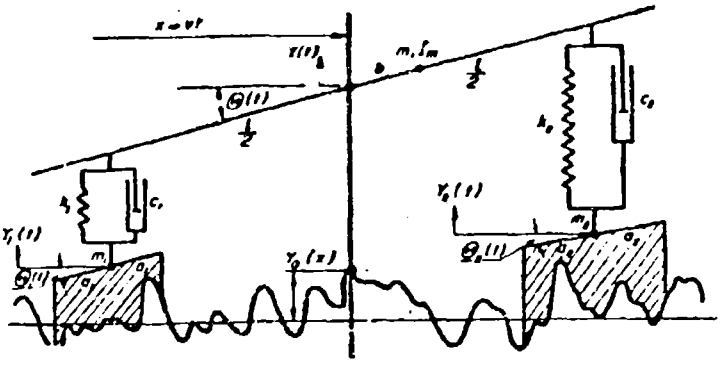


Fig. 1.

We also assume that the elements shown vertical always remain in that position. The vehicle of figure 1 thus possesses the frame translation and pitch and some of the simpler aspects of wheel-tire dynamics common to a real vehicle. However, it is clear that frame roll, tire bounding off the track, etc., are excluded.

To estimate whether one vehicle design can be driven faster than another design, or whether a given vehicle design can be driven at a definite speed over a terrain of specified roughness requires that there be some quantitative ride criterion against which projected vehicle capability can be measured. At the present time, a universally accepted ride criterion is not available.

It is a commonly held view among individuals associated with the military wheeled-vehicle field that such vehicles have the reserve power and sufficient mechanical strength to go to much greater speeds than presently being attained under off-road conditions. Moreover, if speeds are reached that begin to break parts, or if more power is needed to increase speed, these individuals believe that the needed strength and power can easily be supplied. The driver, occupants, or cargo of vehicles thus appear to provide a basic limitation on vehicle speed.

The frame motion of the vehicle model is limited to vertical translation and pitch. The acceleration of each appears to influence certain aspects of

ride. For example, bouncing of the driver, say, upon his seat is associated with large vertical frame acceleration. When such bouncing becomes sufficiently severe, it results in physical injury. Severe oscillatory acceleration in pitch results in loss of visual perception (this also occurs with severe oscillatory vertical acceleration) and loss of equilibrium. In most cases, the driver reduces vehicle speed before either the oscillating vertical or pitching acceleration reaches such extreme values, or the occupants insist that he do so. Damage tests with humans to determine when vertical acceleration causes injury, pitch acceleration causes loss of visual perception, etc., have been conducted using simple harmonic motions. Results [2,3] of such tests cannot be directly converted to the case in which the oscillations are random in character. Hence, bounds on vertical acceleration (also transverse, etc.) and pitching acceleration set by these two tests are not useful to us. Tests in progress and also projected will be with randomly oscillating acceleration, and, when these results are available, they should establish quantitative bounds on human tolerance to acceleration in random oscillation. In any event, it is reasonable at this time to base ride criteria on random oscillatory acceleration in vertical acceleration and pitch.

A number of drivers of military vehicles also pointed out that when large gun tubes are carried in a turret, limiting vehicle speed was frequently set by violent oscillations occuring in these tubes as a result of severe vehicle pitch.

We shall select two quantities as measures of the severity of a random oscillation. One is the magnitude of the largest peak in the power spectral density. The smaller the maximum peak, the lower the ordinate bounding the entire spectral density curve. While the work of Goldman [4] is not applicable, it does suggest that low values of this bounding ordinate may be associated with a comfortable ride from the human standpoint in random oscillatory acceleration.

The variance is a measure of the spread of a probability distribution about its mean. A large variance implies that the probability of a significant deviation from the mean is large. For a reasonably smooth random oscillation, the variance may thus be used as a measure at any time of the probability of the oscillation deviating from its mean by some specified amount. Hence, by reducing variance, the probability of large excursion in such an oscillation is in general reduced.

It is well to point out that other aspects of vehicle acceleration may provide useful ride criteria. In particular, the work of Von Gierke [4] and others [5] suggests that minimum acceleration power spectral density (vertical translation or pitch) in a band from 3 c p s to 10 c p s might produce the best ride from the human standpoint. Thus, the peak in this band could be a measure of the severity of a random acceleration.

In this paper, we shall study the influence of several vehicle parameters upon an optimal ride criterion based either on minimizing the largest peak in power spectral density or on minimizing the variance in vertical translation

or pitch acceleration. All numerical results presented pertain to these optimal ride criteria.

We shall begin the main portions of the paper by presenting some elementary remarks on such statistical quantities as mean, variance, covariance, power spectral density, m.s. continuity, etc., as they apply to the track on which the model moves. The physical aspects of the model considered in the equations of motion are then discussed. Section IV presents the equations of motion and shows how the power spectral density of vertical translation of the frame, etc. are obtained. Numerical results on parameter studies for two special cases of the vehicle of figure 1 and some general observations are given in the final section.

II. - Track model

A detailed discussion of a stochastic model of ground roughness is being presented elsewhere [2]. It suffices for the purposes of this paper to simply assume that the track elevation vs horizontal distance is a random function possessing statistical properties that ground roughness along a line of reasonable length is likely to possess. In particular, we shall confine our assumptions to second order properties [3], i.e. to properties which can be deduced from covariances. Thus, explicit probability distributions of ground roughness or elevation are not employed.

The mean response of a linear vehicle to a non-zero mean track elevation may be treated by deterministic and well known methods. The fluctuations of the response about the mean motion, on the other hand, must be treated by probabilistic methods. Since we are primarily interested in the latter, we shall assume that the mean track elevation has the constant value zero. As we wish to employ second order properties, it is required that the track of elevation be a second order [4] random function (r. f.). Member functions of ground elevations are, of course, oscillatory in nature, but they should not contain discontinuities involving more than finite jumps. The assumption of mean square (m. s.) continuity [5] is usually sufficient to eliminate unreasonable member functions and we shall employ it. Finally, in order to be able to employ the concept of power spectral density and the techniques associated with it [6], we shall assume that ground elevation vs horizontal distance is at least weakly stationary [7]. This means that at least the first two probability distributions do not depend upon the location of the origin of the horizontal distance.

As an additional comment upon the fact that results given in this paper only depend upon second order properties and not upon particular types of distributions, let us note that whether a particular representation of ground elevation as a r. f. is Gaussian or not is of no consequence.

There are essentially two ways in which it is convenient to represent ground or track elevation $y_0(x)$ as a r. f. of the horizontal coordinate x.

In one way, an explicit formula for $y_0(x)$ in terms of a family or set of random variables (r. v's.) is adopted, and, in the other, certain statistical requirements are postulated (zero mean, second order, m. s. continuity, and at least weak stationarity) and a certain integral representation meeting these requirements employed. Each procedure has certain advantages; hence we shall discuss them.

A formula adopted in previous papers [1-2] is

$$y_0(x) = 2\sum_{j=1}^{n} a_j \cos(\lambda_j x + \Phi_j) \tag{2.1}$$

where a_j and λ_j are ordinary constants and the Φ_j are independent r. v's. uniformly distributed over an interval of length 2π. Thus, $y_0(x)$ is a sum of cosine functions having randomly distributed phases. The λ_j have the dimensions of length to the minus one power; and, when divided by 2π give cycles per unit length. Hence, they may be regarded as angular «length» frequencies. The a_j are, of course, the amplitudes of the simple harmonic elements. The statistical properties of (2. 1) are well known [3]; we easily find that

$$E = [y_0(x)] = 0$$

$$\Gamma_{y_0}(x_1, x_2) = E\left\{ y_0(x_1)\, y_0(x_2) \right\} = \sum_{j=1}^{n} a_j^2 \cos\lambda_j (x_2 - x_1) \tag{2.2}$$

$$\sigma^2_{y_0}(x) = \Gamma_{y_0}(x, x) = 2\sum_{j=1}^{n} a_j^2$$

It is perhaps appropriate to review briefly the meanings of these equations. The first states that the mean of $y_0(x)$ is zero. The third states that $\sigma^2_{y_0}(x)$ is independent of x and since for finite a_j and finite n it is finite, $y_0(x)$ is of second order. $\Gamma_{y_0}(x_1, x_2)$ is differentiable any number of times with respect to x_1 and x_2; thus, $y_0(x)$ is m. s. differentiable any number of times. (Indeed, the member functions are differentiable to any order). Finally, since $\Gamma_{y_0}(x_1, x_2)$ depends only upon $x_2 - x_1$ and the mean is constant, we know that $y_0(x)$ is at least weakly stationary. Hence, the requirements enumerated above for the random function which is to represent ground elevation vs horizontal are met.

If n is replaced by infinity, there are conditions — which we need not state here — on the a_j and λ_j if $y_0(x)$ is to be second order and m. s. continuous.

The power spectral density of $y_0(x)$ is given by the formula [3]:

$$P_{y_0}(\lambda) = 2\sum_{j=1}^{n} a_j^2\, \delta(\lambda - \lambda_j) \tag{2.3}$$

where $\delta(\lambda - \lambda_j)$ is the delta function centered at λ_j with the properties

$$\int_{-\infty}^{\infty} \delta(\lambda - \lambda_j)\, d\lambda = 1\,, \quad \delta(\lambda - \lambda_j) = 0\,, \quad \text{if } \lambda \neq \lambda_j$$

We shall call $2\,a_j^2$ the weight of the power spectral density at λ_j. If $y_0(x)$ is interpreted as a voltage applied to a resistance of one ohm and x is interpreted as the time, then the integral of $P_{y_0}(\lambda)\,d\lambda$ between λ_a and λ_b $(> \lambda_a)$ is the average power in $y_0(x)$ between those values of λ. On setting $x_2 - x_1 = x_0$ we may write down the well known[3] formulas

$$\begin{aligned} \Gamma_{y_0}(x_0) &= \int_0^{\infty} P_{y_0}(\lambda) \cos \lambda x_0\, d\lambda \\ P_{y_0}(\lambda) &= \frac{2}{\pi} \int_0^{\infty} \Gamma_{y_0}(x_0) \cos \lambda x_0\, dx_0 \\ \sigma_{y_0}^2 &= \int_0^{\infty} P_{y_0}(\lambda)\, d\lambda \end{aligned} \tag{2.4}$$

That is, the covariance $\Gamma_{y_0}(x_0)$ and the power spectral density $P_{y_0}(\lambda)$ are Fourier transforms of one another.

If a set $\Phi_1, \ldots, \Phi_n$ of the Φ_j are selected with the aid of a table of random numbers, say, then one member function

$$y_0(x) = 2 \sum_{j=1}^{n} a_j \cos(\lambda_j x + \Phi_j) \tag{2.5}$$

of $y_0(x)$ is obtained. Different selections of the Φ_j lead to different member functions. We have shown elsewhere[1] how it is possible to select the a_j and λ_j so that the integrated power spectral density

$$\int_0^{\lambda} P_{y_0}(\lambda')\, d\lambda'$$

of (2.3) approximates as closely as is required to the integral

$$\int_0^{\lambda} P(\lambda')\, d\lambda'$$

of some prescribed or given power spectral density $P(\lambda)$. Since such a procedure determines the a_j and λ_j, it is thus possible with (2.5) to obtain a deterministic member function $y_0(x)$ of the random function (2.1), and the integrated power spectral density of this $y_0(x)$ approximates to the integral of the prescribed power spectral density $P(\lambda)$. A graph, or for that matter, an actual track*) of a section of the member function (2.5) belonging to this $y_0(x)$ can therefore be constructed.

*) A track calculated on this basis has been constructed at the Detroit Arsenal.

The advantages in employing or considering (2.1) are that a simple and readily interpretable formula for $y_a(x)$ is available, member functions are easy to obtain and present in graphical form, if desired, and the power spectral density (2.3) possesses an interpretation in terms of well known electrical engineering concepts. These advantages of (2.1) prompted us to introduce it for the benefit of those readers whose background in random function theory needs refreshing. The disadvantage in using (2.1) in analytical work stems from the fact it often leads to a good deal of unnecessary algebra.

Let us now examine the formula

$$y_a(x) = \int_{-\infty}^{\infty} e^{i\lambda x}\, dZ(\lambda) \tag{2.6}$$

where the integral is to be interpreted in the m.s. sense[3] and the random set function $Z(\lambda)$ is an orthogonal process[1] with the properties

$$\begin{gathered} E\{Z\} = 0 \\ \frac{d}{d\lambda} E\{|Z(\lambda)|^2\} = \frac{1}{2} P_{y_a}(\lambda) \\ P_{y_a}(\lambda) = P_{y_a}(-\lambda) \\ \frac{1}{2}\int_{-\infty}^{\infty} P_{y_a}(\lambda)\, d\lambda < \infty, \quad \frac{1}{2}\int_{-\infty}^{\infty} \lambda^2 P_{y_a}(\lambda)\, d\lambda < \infty \end{gathered} \tag{2.7}$$

From these equations, we find that

$$\begin{gathered} E\{y_a(x)\} = 0 \\ \Gamma_{y_a}(x_1, x_2) = \frac{1}{2}\int_{-\infty}^{\infty} e^{i\lambda(x_2 - x_1)} P_{y_a}(\lambda)\, d\lambda = \int_0^{\infty} P_{y_a}(\lambda) \cos\lambda x_0\, d\lambda \\ \sigma^2_{y_a}(x) = \frac{1}{2}\int_{-\infty}^{\infty} P_{y_a}(\lambda)\, d\lambda < \infty \end{gathered} \tag{2.8}$$

Thus, $y_a(x)$ has a zero mean, is of second order, and, since the covariance depends only upon $x_2 - x_1$ and the mean is constant, it is at least weakly stationary. The last of (2.7) and second of (2.8) enable us to demonstrate the m.s. continuity of (2.6). Hence, all the requirements which we wish to impose on the r.f. representing ground or track elevation vs horizontal distance are met.

In what follows, we shall employ (2.6) rather than (2.1), because the former lends itself to certain computations we wish to make.

III. - Vehicle model

Figure 1 shows the idealized linear two-dimensional vehicle that is to be discussed. The rigid frame has wheel base length l; its mass is M; and its moment of inertia about its c. g. is I_m. The c. g. is at distance b from the wheel base center O. $y(t)$ is the vertical displacement of O, and $\Phi(t)$ is the angular displacement of the frame. We shall assume that O has a constant horizontal speed v so that its x-coordinate is vt, t being the time.

The ends of the frame are supported on linear springs and viscous dampers arranged in parallel. k_j and c_j ($j = 1,7$) are the rear ($j = 1$) and front ($j = 2$) spring and viscous damper constants respectively. These elements are taken as massless, the upper and lower pivots are assumed frictionless, and they remain vertical throughout the motion.

Idealized tires are assumed. Each has a rigid massless frame of length $2a_j$ and a mass m_j concentrated at the frame center. These frames are connected by frictionless pivots to the bottoms of the parallel arranged spring and damper elements, as shown. $K_j(\xi_j)$ and $\gamma_j(\xi_j)$ are, respectively, the linear spring constant per unit length and the viscous damping constant per unit length which are distributed in a parallel arrangement over the bottoms of the frames; we assume these elements are massless. We shall make the initial assumption that $K_j(\xi_j)$ and $\gamma_j(\xi_j)$ are even functions of ξ_j; at a latter stage, we shall simply assume they are independent of ξ_j. Contact of the tire spring and damper elements with the track or road is assumed to be maintained at all times. $\Phi_1(t)$ is the angular displacement of the rear tire frame and $\Phi_2(t)$ is the angular displacement of the front frame. The vertical displacements of the masses m_1 and m_2 are $y_1(t)$ and $y_2(t)$, respectively.

Gravity will be neglected. Further, all angles are assumed to be sufficiently small so that cosines may be replaced by unity and the sines by the angles in radians.

IV. - Analysis of vehicle dynamics

For the vehicle model just described, we find the equations of motion to be

$$\begin{aligned} M(\ddot{y} + b\ddot{\Phi}) &= -F_1(t) - F_2(t) \\ I_m\ddot{\Phi} &= \left(\frac{l}{2} + b\right)F_1(t) - \left(\frac{l}{2} - b\right)F_2(t) \\ m_1\ddot{y}_1 &= F_1(t) - F_3(t) \\ m_2\ddot{y}_2 &= F_2(t) - F_4(t) \end{aligned} \tag{4.1}$$

where

$$F_1(t) = k_1\left(y - \frac{l}{2}\Theta - y_1\right) + c_1\left(\dot{y} - \frac{l}{2}\dot{\Theta} - \dot{y}_1\right)$$

$$F_2(t) = k_2\left(y + \frac{l}{2}\Theta - y_2\right) + c_2\left(\dot{y} + \frac{l}{2}\dot{\Theta} - \dot{y}_2\right)$$

$$F_3(t) = \int_{-a_1}^{a_1}\left\{k_1(\xi_1)\left[y_1 + \xi_1\Theta_1 - y_0\left(x - \frac{l}{2} + \xi_1\right)\right]\right.$$

$$\left. + \gamma_1(\xi_1)\left[\dot{y}_1 + \xi_1\dot{\Theta}_1 - \dot{y}_0\left(x - \frac{l}{2} + \xi_1\right)\right]\right\} d\xi_1 \qquad (4.2)$$

$$F_4(t) = \int_{-a_2}^{a_2}\left\{k_2(\xi_2)\left[y_2 + \xi_2\Theta_2 - y_0\left(x + \frac{l}{2} + \xi_2\right)\right]\right.$$

$$\left. + \gamma_2(\xi_2)\left[\dot{y}_2 + \xi_2\dot{\Theta}_2 - \dot{y}_0\left(x + \frac{l}{2} + \xi_2\right)\right]\right\} d\xi_2$$

and where derivatives and integrals are to be interpreted in the m.s. sense[7].

To simplify the analysis from this point on, it is convenient to assume that the vehicle is symmetrical, i.e.

$$\begin{aligned} k_1 &= k_2 = k & c_1 &= c_2 = c \\ a_1 &= a_2 = a & K_1(\xi) &= K_2(\xi) = K(\xi) \\ \gamma_1(\xi) &= \gamma_2(\xi) = \gamma(\xi) & m_1 &= m_2 = m \\ & & b &= 0 \end{aligned} \qquad (4.3)$$

The equations of motion may now be written in the form

$$\ddot{y} + 2\zeta_\gamma\omega_\gamma\dot{y} + \omega_\gamma^2 y - \frac{1}{2}\left(2\zeta_\gamma\omega_\gamma\dot{y}_1 + \omega_\gamma^2 y_1\right) - \frac{1}{2}\left(2\zeta_\gamma\omega_\gamma\dot{y}_2 + \omega_\gamma^2 y_2\right) = 0$$

$$\ddot{\Theta} + 2\zeta_\theta\omega_\theta\dot{\Theta} + \omega_\theta^2\Theta + \frac{1}{l}\left(2\zeta_\theta\omega_\theta\dot{y}_1 + \omega_\theta^2 y_1\right) - \frac{1}{l}\left(2\zeta_\theta\omega_\theta\dot{y}_2 + \omega_\theta^2 y_2\right) = 0$$

$$- a_1\left(\frac{2\zeta_\gamma\omega_0^2}{\omega_\gamma}\dot{y} + \omega_0^2 y\right) + \frac{a_1 l}{2}\left(\frac{2\zeta_\theta\omega_0^2}{\omega_\theta}\dot{\Theta} + \omega_0^2\Theta\right) \qquad (4.4)$$

$$+ \ddot{y}_1 + \left(2\zeta\omega_0 + a_1\frac{2\zeta_\gamma\omega_0^2}{\omega_\gamma}\right)\dot{y}_1 + \omega_0^2(1 + a_1)\,y_1$$

$$= \omega_0^2 \int_{-a}^{a} \left[\frac{k(\xi)}{k} y_0\left(x - \frac{l}{2} + \xi\right) + \frac{2\zeta_0}{\omega_0} \frac{\gamma(\xi)}{c} \dot{y}_0\left(x - \frac{l}{2} + \xi\right) \right] d\xi$$

$$- \alpha_1 \left(\frac{2\zeta_\gamma \omega_\gamma^2}{\omega_\gamma} \dot{y} + \omega_\gamma^2 y \right) - \frac{\alpha_1 l}{2} \left(\frac{2\zeta_\theta \omega_\theta^2}{\omega_\theta} \dot{\theta} + \omega_\theta^2 \theta \right)$$

$$+ \ddot{y} + \left(2\zeta_0 \omega_0 + \alpha_1 \frac{2\zeta_\gamma \omega_\gamma^2}{\omega_\gamma} \right) \dot{y}_2 + \omega_0^2 (1 - \alpha_1) y_2$$

$$= \omega_0^2 \int_{-a}^{a} \left[\frac{k(\xi)}{k} y_0\left(x + \frac{l}{2} + \xi\right) + \frac{2\zeta_0}{\omega_0} \frac{\gamma(\xi)}{c} \dot{y}_0\left(x + \frac{l}{2} + \xi\right) \right] d\xi$$

where now

$$\omega_\gamma^2 = \frac{2k}{M} \qquad 2\zeta_\gamma \omega_\gamma = \frac{2c}{M} \qquad \omega_\theta^2 = \frac{kl^2}{2I_m}$$

$$2\zeta_\theta \omega_\theta = \frac{cl^2}{2I_m} \qquad \omega_0^2 = \frac{k}{m} \qquad 2\zeta_0 \omega_0 = \frac{c}{m} \tag{4.5}$$

$$\alpha_1 = \frac{k}{K} \qquad k = \int_{-a}^{a} K(\xi)\, d\xi \qquad c = \int_{-a}^{a} \gamma(\xi)\, d\xi$$

These symbols have the usual interpretations given in small vibration theory. The angles $\Phi_1(t)$ and $\Phi_2(t)$ drop out of the third and fourth of (4.4) since we have taken $K(\xi)$ and $\gamma(\xi)$ to be even functions of ξ.

We must now employ a representation for $y_0(x)$. As mentioned above, it is convenient to use (2.6). It is also convenient at this time to assume the forms of $K(\xi)$ and $\gamma(\xi)$ are the same. Thus,

$$\frac{K(\xi)}{k} = \frac{\gamma(\xi)}{c} = \frac{g(\xi)}{2a}$$

where $g(\xi)$ is even in ξ and the two non zero terms on the right hand sides of (4.4) become

$$\omega_0^2 e^{\pm \frac{i\omega l}{2v}} \int_{-\infty}^{\infty} G\left(\frac{\omega a}{v}\right) \left(1 + i \frac{2\zeta_0 \omega}{\omega_0}\right) e^{i\omega t}\, dZ\left(\frac{\omega}{v}\right) \tag{4.6}$$

respectively, where

$$\omega = \lambda v$$

$$G\left(\frac{\omega a}{v}\right) = \frac{1}{2a}\int_{-a}^{a} g(\xi)\, e^{-\frac{i\omega\xi}{v}}\, d\xi \tag{4.7}$$

With v a constant, $y_a(vt)$ and $\dot{y}_a(vt)$ are still at least weakly stationary. It follows[9] that $y(t)$, $\mathfrak{F}(t)$, $y_1(t)$, $y_2(t)$ are also at least weakly stationary, since they are related to $y_a(vt)$ and its m.s. derivative $\dot{y}_a(vt)$ through a system of constant coefficient linear differential equations. Thus, we may write

$$\begin{aligned} y(t) &= \int_{-\infty}^{\infty} e^{i\omega t}\, dU(\omega) \\ \mathfrak{F}(t) &= \int_{-\infty}^{\infty} e^{i\omega t}\, dV(\omega) \\ y_1(t) &= \int_{-\infty}^{\infty} e^{i\omega t}\, dW_1(\omega) \\ y_2(t) &= \int_{-\infty}^{\infty} e^{i\omega t}\, dW_2(\omega) \end{aligned} \tag{4.8}$$

the random set functions $U(\omega)$, $V(\omega)$, $W_1(\omega)$, $W_2(\omega)$ being orthogonal processes. The substitution of (4.6) and (4.8) into (4.4) provides us with the following equations for the determination of $dU(\omega)$, $dV(\omega)$, $dW_1(\omega)$ and $dW_2(\omega)$:

$$\begin{aligned} &(\omega_\gamma^2 - \omega^2 + i2\zeta_\gamma\omega_\gamma\omega)\, dU(\omega) - \frac{1}{2}(\omega_\gamma^2 + i2\zeta_\gamma\omega_\gamma\omega)\, dW_1(\omega) \\ &\quad - \frac{1}{2}(\omega_\gamma^2 + i2\zeta_\gamma\omega_\gamma\omega)\, dW_2(\omega) = 0 \\ &(\omega_\theta^2 - \omega^2 + i2\zeta_\theta\omega_\theta\omega)\, dV(\omega) + \frac{1}{l}(\omega_\theta^2 + i2\zeta_\theta\omega_\theta\omega)\, dW_1(\omega) \\ &\quad - \frac{1}{l}(\omega_\theta^2 + i2\zeta_\theta\omega_\theta\omega)\, dW_2(\omega) = 0 \\ &-\alpha_1\left(\omega_v^2 + i\frac{2\zeta_\gamma\omega_n^2\omega}{\omega_\gamma}\right) dU(\omega) + \frac{\alpha_1 l}{2}\left(\omega_v^2 + i\frac{2\zeta_\theta\omega_v^2\omega}{\omega_\theta}\right) dV(\omega) \\ &\quad + \left[\omega_v^2(1+\alpha_1) - \omega^2 + i\left(2\zeta_v\omega_n\omega + \alpha_1\frac{2\zeta_\gamma\omega_v\omega}{\omega_\gamma}\right)\right] dW_1(\omega) \end{aligned} \tag{4.9}$$

$$= \omega_0^2 e^{-\frac{i\omega l}{2v}} G\left(\frac{\omega R}{v}\right)\left(1 + i\frac{2\zeta_0\omega}{\omega_0}\right) dZ\left(\frac{\omega}{v}\right)$$

$$- \alpha_1\left(\omega_0^2 + i\frac{2\zeta_\gamma\omega_0^2\omega}{\omega_\gamma}\right) dU(\omega) - \frac{\alpha_1 l}{R}\left(\omega_0^2 + i\frac{2\zeta_\theta\omega_0^2\omega}{\omega_\theta}\right) dV(\omega)$$

$$+ \left[\omega_0^2(1-\alpha_1) - \omega^2 + i\left(2\zeta_0\omega_0\omega + \alpha_1\frac{2\zeta_\theta\omega_0^2\omega}{\omega_\gamma}\right)\right] dW_2(\omega)$$

$$= \omega_0^2 e^{\frac{i\omega l}{2v}} G\left(\frac{\omega R}{v}\right)\left(1 + i\frac{2\zeta_0\omega}{\omega_0}\right) dZ\left(\frac{\omega}{v}\right)$$

The solution of the first two of (4.9) for $dW_1(\omega)$ and $dW_2(\omega)$ gives

$$dW_1(\omega) = \frac{-w_1 dU(\omega) + w_2 dV(\omega)}{w} \qquad (4.10)$$

$$dW_2(\omega) = \frac{w_1 dU(\omega) + w_2 dV(\omega)}{w}$$

with

$$w = (\omega_\gamma^2 + i2\zeta_\gamma\omega_\gamma\omega)(\omega_\theta^2 + i2\zeta_\theta\omega_\theta\omega)$$

$$w_1 = 2(\omega_0^2 + i2\zeta_\theta\omega_\theta\omega)(\omega_\gamma^2 - \omega^2 + i2\zeta_\gamma\omega_\gamma\omega) \qquad (4.11)$$

$$w_2 = 1(\omega_\gamma^2 + i2\zeta_\gamma\omega_\gamma\omega)(\omega_\theta^2 - \omega^2 + i2\zeta_\theta\omega_\theta\omega)$$

The last two of (4.9) with (4.10) determine $dU(\omega)$ and $dV(\omega)$:

$$dU(\omega) = \frac{-z}{n_1 + \frac{nw_1}{w}} \cos\frac{\omega l}{2v} dZ\left(\frac{\omega}{v}\right) \qquad (4.12)$$

$$dV(\omega) = \frac{-iz}{n_2 + \frac{nw_2}{w}} \sin\frac{\omega l}{2v} dZ\left(\frac{\omega}{v}\right)$$

where

$$n_1 = \alpha_1\left(\omega_0^2 + i\frac{2\zeta_\gamma\omega_0^2\omega}{\omega_\gamma}\right)$$

$$v_1 = \frac{a_1 l}{2}\left(\omega_\theta^2 + i\frac{2\zeta\omega_0^2\omega}{\omega_\theta}\right)$$

$$u = \omega_0^2(1+a_1) - \omega^2 + i\left(2\zeta_0\omega_0\omega + a_1\frac{2\zeta_T\omega_\theta^2\omega}{\omega_T}\right) \qquad (4.13)$$

$$z = \omega_0^2 G\left(\frac{\omega a}{v}\right)\left(1 + i\frac{2\zeta_0\omega}{\omega_0}\right)$$

The power spectral density of $y(t)$, for example, is given by a formula similar to the second of (2.7); it is

$$\frac{1}{2}P_y(\omega) = \frac{d}{d\omega}E\left\{\left[U(\omega)\right]^2\right\}$$

Hence, with the first of (4.12) and the second of (2.7), we find that

$$P_y(\omega) = \frac{1}{2v}\left[1 + \left(\frac{2\zeta_0\omega}{\omega_0}\right)^2\right]\left[1 + \left(\frac{2\zeta_T\omega}{\omega_T}\right)^2\right]\left|\left[a_1\left(1 + i\frac{2\zeta_T\omega}{\omega_T}\right)^2\right.\right.$$
$$+ 2\left\{1 + a_1 - \frac{\omega^2}{\omega_\theta^2} + i2\left(\zeta_0 + a_1\frac{\zeta_T\omega_0}{\omega_T}\right)\frac{\omega}{\omega_\theta}\right\}\left(1 - \frac{\omega^2}{\omega_\theta^2}\right.$$
$$\left.\left. + i\frac{2\zeta_T\omega}{\omega_T}\right)\right]^2\Bigg|^{-1}\left(1 + \cos\frac{\omega l}{v}\right)\left[G\left(\frac{\omega a}{v}\right)\right]^2 P_z\left(\frac{\omega}{v}\right) \qquad (4.15)$$

and similarly,

$$P_{\circledR}(\omega) = \frac{1}{2vl^2}\left[1 + \left(\frac{2\zeta_0\omega}{\omega_0}\right)^2\right]\left[1 + \left(\frac{2\zeta_\theta\omega}{\omega_\theta}\right)^2\right]\left|\left[\frac{a_1}{2}1 + i\frac{2\zeta_\theta\omega}{\omega_\theta}\right.\right.$$
$$+ \left\{1 + a_1 - \frac{\omega^2}{\omega_\theta^2} + i2\left(\zeta_0 + a_1\frac{\zeta_T\omega}{\omega_T}\right)\frac{\omega}{\omega_\theta}\right\}\left(1 - \frac{\omega^2}{\omega_\theta^2}\right.$$
$$\left.\left. + i\frac{2\zeta_\theta\omega}{\omega_\theta}\right)\right]^2\Bigg|^{-1}\left(1 - \cos\frac{\omega l}{v}\right)\left[G\left(\frac{\omega a}{v}\right)\right]^2 P_z\left(\frac{\omega}{v}\right) \qquad (4.16)$$

Two special cases of the system shown in figure 1 are of particular interest in this paper. The first is obtained by replacing the idealized tires by massless point follower. The power spectral densities of the vertical displacement $y(t) + z\circledR(t)$ at a point on the frame at a distance z along the frame from the c. g. and of $\circledR(t)$ are

$$P_y(z,\omega)_1 = \frac{1}{2l^2}\left[\left(1-\frac{\omega^2}{\omega_\gamma^2}\right)^2 + \left(2\zeta_\gamma\frac{\omega}{\omega_\gamma}\right)^2\right]^{-1}\left[\left(1-\frac{\omega^2}{\omega_\theta^2}\right)^2 + \left(2\zeta_\theta\frac{\omega}{\omega_\theta}\right)^2\right]^{-1}$$

$$\times\left\{l^2\left(1+\cos\frac{\omega l}{v}\right)\left[1+\left(2\zeta_\gamma\frac{\omega}{\omega_\gamma}\right)^2\right]\left[\left(1-\frac{\omega^2}{\omega_\theta^2}\right)^2+\left(2\zeta_\theta\frac{\omega}{\omega_\theta}\right)^2\right]\right.$$

$$+ 8lz\sin\frac{\omega l}{v}\left[\zeta_\gamma\frac{\omega^3}{\omega_\gamma^3}\left\{\frac{\omega^2}{\omega_\theta^2}-1-\left(2\zeta_\theta\frac{\omega}{\omega_\theta}\right)^2\right\}\right.$$

$$\left.\left.-\zeta_\theta\frac{\omega^3}{\omega_\theta^3}\left\{\frac{\omega^2}{\omega_\gamma^2}-1-\left(2\zeta_\gamma\frac{\omega}{\omega_\gamma}\right)^2\right\}\right] + 4z^2\left(1-\cos\frac{\omega l}{v}\right)\right.$$

$$\left[1+2\zeta_\theta\frac{\omega}{\omega_\theta}\right)^2\left]\left[\left(1-\frac{\omega^2}{\omega_\gamma^2}\right)^2+\left(2\zeta_\gamma\frac{\omega}{\omega_\gamma}\right)^2\right]\frac{P_{y_0}\left(\frac{\omega}{v}\right)}{v}\right.$$

$$P_{\mathfrak{B}}(\omega_1)_1 = \frac{2\left(1-\cos\frac{\omega l}{v}\right)\left[1+\left(\frac{2\zeta_\theta\omega}{\omega}\right)^2\right]}{\left[\left(1-\frac{\omega^2}{\omega_\theta^2}\right)^2+\left(\frac{2\zeta_\theta\omega}{\omega_\theta}\right)^2\right]^2 l^2 v}\,P_{y_0}\left(\frac{\omega}{v}\right) \tag{4.17}$$

The power spectral densities of $y_1(t)$, $y_2(t)$ and of the vertical motion at points on the vehicle frame other than its c.g. may be found in the same manner, respectively, where the frequency range is from $-\infty$ to ∞. The second case is obtained from the system shown in figure by making the two elements connecting the frame and the tire masses rigid and lumping the tire masses in with the mass of the frame; we find that the spectral densities of $y(t) + z\mathfrak{F}(t)$ and $\mathfrak{G}(t)$ are

$$P_y(z,\omega)_2 = \left[G\left(\frac{\omega l}{v}\right)\right]^2 P_y(z,\omega)_1$$

$$P_{\mathfrak{G}}(z,\omega)_2 = \left[G\left(\frac{\omega l}{v}\right)\right]^2 P_{\mathfrak{G}}(z,\omega)_1 \tag{4.18}$$

We have omitted derivations of (4.17) and (4.18) since they follow almost the same sequence of steps that we employed in obtaining (4.15) and (4.16) from (4.1).

V. - Discussion and results

It is possible to draw a few general conclusions from the results given in the previous section.

Examination of (4.15) and (4.16), say, reveals that the half-tire frame

or half foot print length a only enters these equations through the term $G\left(\frac{\omega a}{V}\right)$ where [see (4.7)],

$$G\left(\frac{\omega a}{V}\right) = \frac{1}{2a}\int_{-a}^{a} g(\xi)\, e^{\frac{i\omega\xi}{V}}\, d\xi$$

and $g(\xi)$ is the distribution along the frame of the parallel arranged linear spring and viscous damper tire elements. Since $G\left(\frac{\omega a}{V}\right)$ is an integral of

$$g(\xi)\, e^{\frac{i\omega\xi}{V}}/2a$$

over the foot print length, $G\left(\frac{\omega a}{V}\right)$ represents the smoothing of the roughness in the track due to the idealized tires. Thus,

$$\left[G\left(\frac{\omega a}{V}\right)\right]^2 P_{y_0}\left(\frac{\omega}{V}\right) \tag{5.1}$$

may be regarded as the power spectral density of the input to the vehicle obtained from the power spectral density of $y_0(x)$ after smoothing by the idealized tires. This suggests that in the analysis we could have ignored the tire-foot print length provided the track $y_0(x)$ with power spectral density $P_{y_0}\left(\frac{\omega}{V}\right)$ were replaced by a smoothed track with power spectral density (5.1). Advantage of this point may therefore be taken in future investigations. The conclusion that a tire is a smoothing device in some sense is in agreement with results obtained on large low pressure tires.

In the numerical results presented below, we shall assume that

$$g(\xi) = 1 \tag{5.2}$$

and, thus,

$$\left[G\left(\frac{\omega a}{V}\right)\right]^2 = \left(\frac{\sin\frac{\omega a}{V}}{\frac{\omega a}{V}}\right)^2 \tag{5.3}$$

It is clear from this equation that the larger a, the narrower the peak in the term on the right. Hence, the larger a, the smaller the high frequency portion of (5.1) and the greater the smoothing influence of the tires. Conversely, the smaller a, the broader the peak in the right of (5.3), and the less the smoothing effect of the tires. Actually, the selection (5.2) is not particularly realistic,

since $g(\xi)$ should approach zero as $\xi \to \pm a$. However, (5.3) is easy to compute with, provides an estimate of the influence of the tire on spectral density of various quantities, and so is adequate for present purposes.

The power spectral density $P_y(\omega)$ contains the wheel base length l in just one term, namely in $(1 + \cos \omega l/v)$. Since this term multiplies $P_{y_0}(\omega/v)$, just as does $[G(\omega a/v)]^2$, it may also be regarded as a filter acting on $P_{y_0}(\omega/v)$. Clearly, the term filters periodically, depending upon the value of l/v. Thus, wheel base length and speed v may be expected to have a substantial influence on certain aspects of vehicle ride. The term $(1 - \cos \omega l/v)$ in $P_{\ddot{y}}(\omega)$ may be interpreted in the same sense.

From the first of (4.8), we deduce that

$$\Gamma_y(t_1, t_2) = \frac{1}{2} \int_{-\infty}^{\infty} e^{i\omega(t_2 - t_1)} P_y(\omega)\, d\omega$$

The r.f. $y(t)$ has two m.s. derivates $\dot{y}(t)$ and $\ddot{y}(t)$; it follows[5] that the covariances of these r.f. are

$$\begin{aligned} \Gamma_{\dot{y}}(t_1, t_2) &= \frac{\delta^2}{\delta t_1\, \delta t_2} \Gamma_y(t_1, t_2) \\ \Gamma_{\ddot{y}}(t_1, t_2) &= \frac{\delta^4}{\delta t_1\, \delta t_2} \Gamma_y(t_1, t_2) \end{aligned} \tag{5.5}$$

Hence, on combining (5.4) and (5.5) and making use of the definition of the covariances of $\dot{y}(t)$ and $\ddot{y}(t)$ in terms of integrals of their power spectral densities, we find that

$$\begin{aligned} P_{\dot{y}}(\omega) &= \omega^2 P_y(\omega) \\ P_{\ddot{y}}(\omega) &= \omega^4 P_y(\omega) \end{aligned} \tag{5.6}$$

thus, the power spectral density of the first or second m.s. derivative of a suitable r.f. may be found by multipying its power spectral density by ω^2 or by ω^4, respectively. This rule is quite general[5] and we shall use it without further comment in what follows to obtain the power spectral densities of $\ddot{\mathfrak{F}}(t)$, and $\ddot{y}(t) + z\ddot{\mathfrak{F}}(t)$.

The constants which define the vehicle and track enter the spectral densities of interest in a fairly complex manner. Further, the measures of ride roughness that are being employed involve these power spectral densities either through an integral (variance) or a derivative (peak value). Hence, we shall not employ analytical methods to perform quantitative parameter studies on ride roughness but instead use numerical methods.

A definite formula for $P_{y_0}(\lambda)$ is now required

$$P_{y_0}(\lambda) = \frac{\sigma^2_{\lambda_0}}{\lambda_0 \sqrt{2\pi}} e^{-\frac{\lambda^2}{2\lambda_0^2}} \tag{5.7}$$

The quantity $\sigma^2_{y_0}$ is the variance of $y_0(x)$; λ_0 is a constant which may be used to adjust the spread of the single peak possessed by $P_{y_0}(\lambda)$. This formula appears to give a reasonable fit to a power spectral density which we obtained from ground measurements. Further measurements may well suggest different expressions for the right hand side of (5.7) *). However, for the present, it is a reasonable selection.

A set of dimensionless parameters we have found convenient to employ in numerical calculations is the following:

$$\alpha = \frac{l\omega\gamma}{v_0} \qquad \beta = \frac{\lambda_0 v_0}{\omega_\gamma} \qquad \nu = \frac{v_0}{v}$$
$$\frac{a}{l} \qquad \zeta_\gamma \qquad \bar{K} = \frac{l}{2\rho} \tag{5.8}$$

where v_0 is a reference speed and ρ is the radius of gyration about the c.g. of the frame. In terms of these parameters, the first of (4.17) can be rewritten as

$$\frac{P_\gamma(z,\omega)_1}{\sigma^2_{y_0}/\omega_\gamma} = \frac{1}{2}\left[(1-r^2)^2 + (2\zeta_\gamma r)^2\right]^{-1}\left[\left(1-\frac{r^2}{\bar{K}^2}\right)^2\right]^{-1}$$
$$\left\{(1+\cos\alpha\nu r)\left[1+(2\zeta_\gamma r)^2\right]\left[\left(1-\frac{r^2}{\bar{K}^2}\right)^2+(2\zeta_\gamma r)^2\right]\right.$$
$$+ 8\zeta_\gamma r^3\frac{z}{l}\sin\alpha\nu r\left[\left(\frac{r^2}{\bar{K}^2}-1-4\zeta_\gamma^2 r^2\right)-\frac{1}{\bar{K}^2}\left(r^2-1-4\zeta_\gamma^2 r^2\right)\right]$$
$$\left.+4\frac{r^2}{l^2}(1-\cos\alpha\nu r)\left[1+(2\zeta_\gamma r)^2\right]\left[(1-r^2)^2+(2\zeta_\gamma r)^2\right]\right\}\frac{\nu}{\beta\sqrt{2\pi}}e^{-\frac{r^2\nu^2}{2\beta^2}} \tag{5.9}$$

for example. The other spectral densities can be put in a similar form.

As mentioned in the introduction, the two ride criteria which we shall employ are either the magnitude of the largest peak in the power spectral density or the value of the variance for acceleration. The accelerations of the

*) The covariance corresponding to (5.7) is analytic; thus, the r.f. having this covariance is m.s. analytic [6]. While m.s. analyticity has certain predictibility implications, we shall ignore them.

frame we shall consider are $\ddot{y}(t)$, $\ddot{y}(t) + \frac{1}{2}\ddot{\Phi}(t)$ and $\ddot{\Phi}(t)$; the first is vertical acceleration at the c.g., the second is vertical acceleration over idealized wheel-tire, and the third is pitching acceleration.

Only the two special cases of the vehicle shown in fig. 1 will be considered at this time. The formulas needed for the power spectral densities are obtained from either (4. 17) or (4. 18). Ordinate values for vertical acceleration results are divided by $\sigma_{y_0}^2 \omega_y^4$ and those for angular acceleration results by $\sigma_{y_0}^2 \omega_\theta^4/l^2$; these factors will be omitted on the graphs. We shall also omit the subscripts 1 or 2 on the ordinate designation, since the subscripts 1 and 2 refer to the cases $a/l = 0$ and $a/l \neq 0$, respectively, and these are indicated explicitly upon the graphs.

Figures 2 - 4 present numerical results on the maximum value of the power spectral densities and on the variances of $\ddot{y}(t)$, $\ddot{y}(t) + z\ddot{\Phi}(t)$ and $\ddot{\Phi}(t)$ as functions of the parameters α and a/l.

It is immediately clear that results on variance with $a/l = 0$ and $a/l = 0.0625$ and also on magnitude of the maximum value of the power spectral density do not differ appreciably until α becomes larger than 4 or 5. We note that $a/l = 0.0625$ corresponds to a total foot print length — rear plus front — of 25 % of the wheel base length l; most wheeled vehicles have a value of approximately 10 %. Thus, a/l does not appear to be a significant parameter with the ride criteria we are employing unless α exceeds 4 or 5. In what follows, therefore, it is convenient to set $a/l = 0$.

On the other hand, changes in the parameter α have a pronounced influence on the magnitude of the largest peak in the power spectral density and the variance of the various accelerations. This strong influence is due to the fact that the location of the bands on the ω-axis which the trigonometric terms containing α filter change with α, sometimes reducing peaks sharply and sometimes reinforcing them.

For the vertical acceleration, there is a unique value of α which makes the peak magnitude and variance a minimum. Thus, if the best ride under the conditions assumed is determined either by the minimum peak magnitude in the spectral density or by the minimum value of variance, we see that for each point on the frame there is a unique value of α which provides such a best ride; the range of α values being from .4088 to 2.[illegible]0. We also note, however, that slight changes from these α values produced large changes in minimum peak magnitude and variance, i.e. the best ride is a sharply tuned function of α. For too large a value of α with $z = \frac{1}{2}$ the variance is larger than with a very small α; but with $z = 0$, the variance is always reduced below its value at $\alpha = 0$ by increasing α.

The peak value in the spectral density and the [illegible]ance for the pitching acceleration exhibit a different dependence upon α t[illegible]n encountered with the vertical acceleration, as may be seen from figure 4. Each is zero when α equals

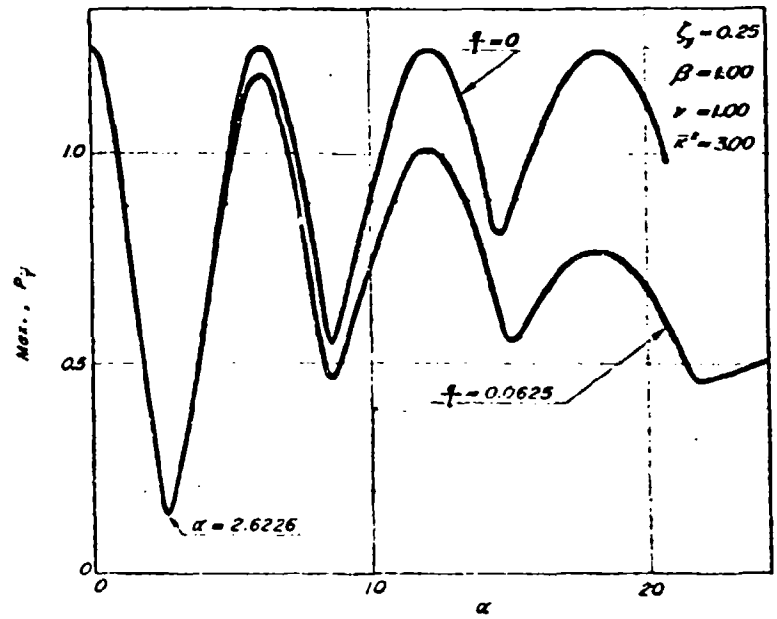

$\zeta_y = 0.25$
$\beta = 1.00$
$\nu = 1.00$
$\bar{\kappa}^2 = 3.00$
$\frac{q}{f} = 0$
$\frac{q}{f} = 0.0625$
$\alpha = 2.6226$
Max., P_y
1.0
0.5
0
0
10
20
α

Fig. 2a.

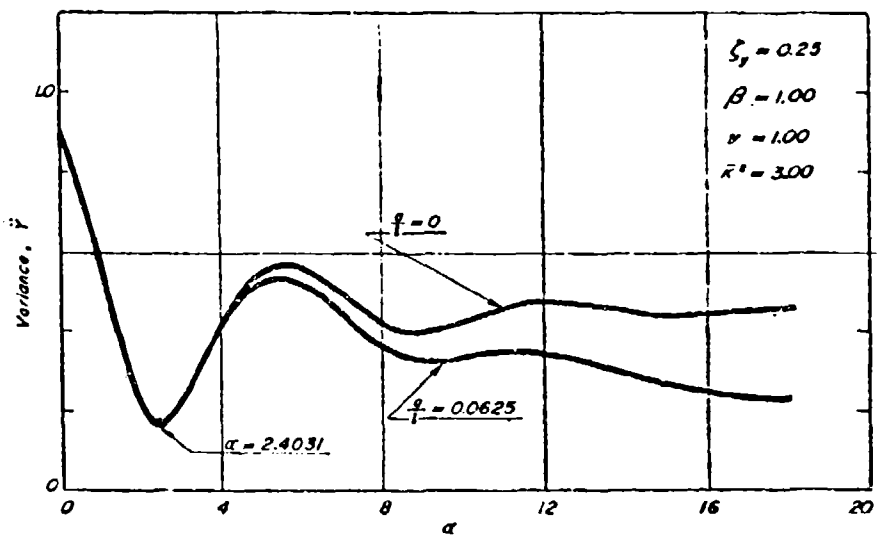

$\zeta_y = 0.25$
$\beta = 1.00$
$\nu = 1.00$
$\bar{\kappa}^2 = 3.00$
$\frac{q}{f} = 0$
$\frac{q}{f} = 0.0625$
$\alpha = 2.4031$
Variance, $\bar{y}^2$
1.0
0
0
4
8
12
16
20
α

Fig. 2b.

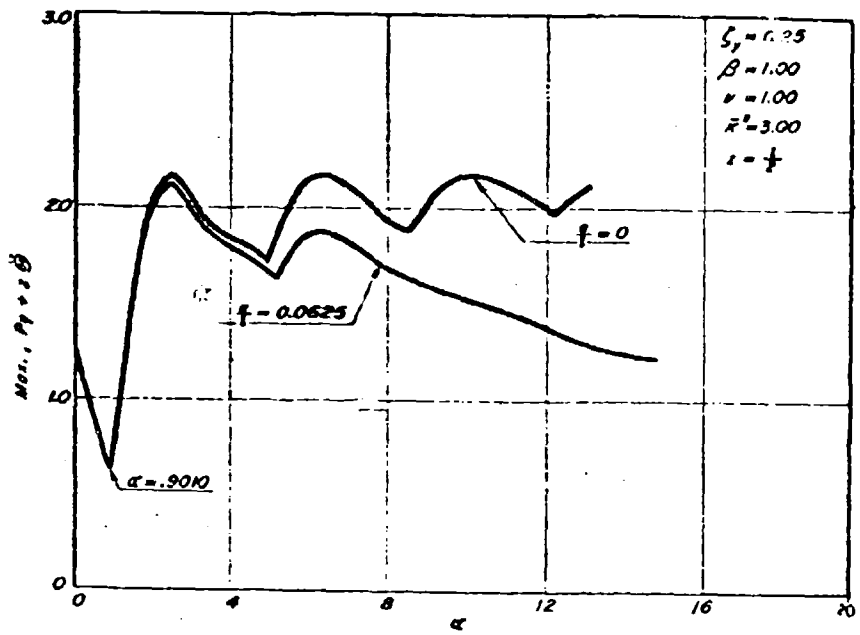

3.0
2.0
1.0
0
0
4
8
12
16
20
α
Max., $P_y + \bar{z}\bar{\theta}$
ζ_y = 0.25
β = 1.00
ν = 1.00
$\bar{R}^2$ = 3.00
$\frac{z}{l}$ = $\frac{1}{2}$
$\frac{f}{l}$ = 0
$\frac{f}{l}$ = 0.0625
α = .9010

Fig. 3 a.

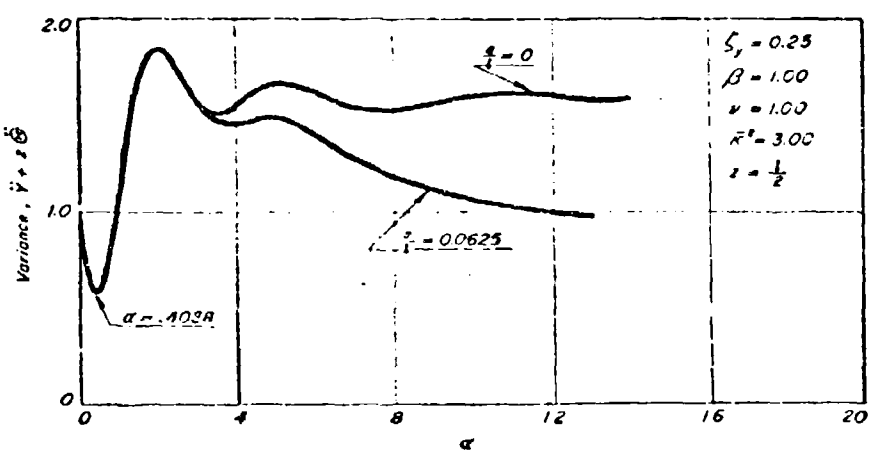

2.0
1.0
0
0
4
8
12
16
20
α
Variance, $\ddot{Y} + \bar{z}\ddot{\theta}$
ζ_y = 0.25
β = 1.00
ν = 1.00
$\bar{R}^2$ = 3.00
$\frac{z}{l}$ = $\frac{1}{2}$
$\frac{f}{l}$ = 0
$\frac{f}{l}$ = 0.0625
α = .1038

Fig. 3 b.

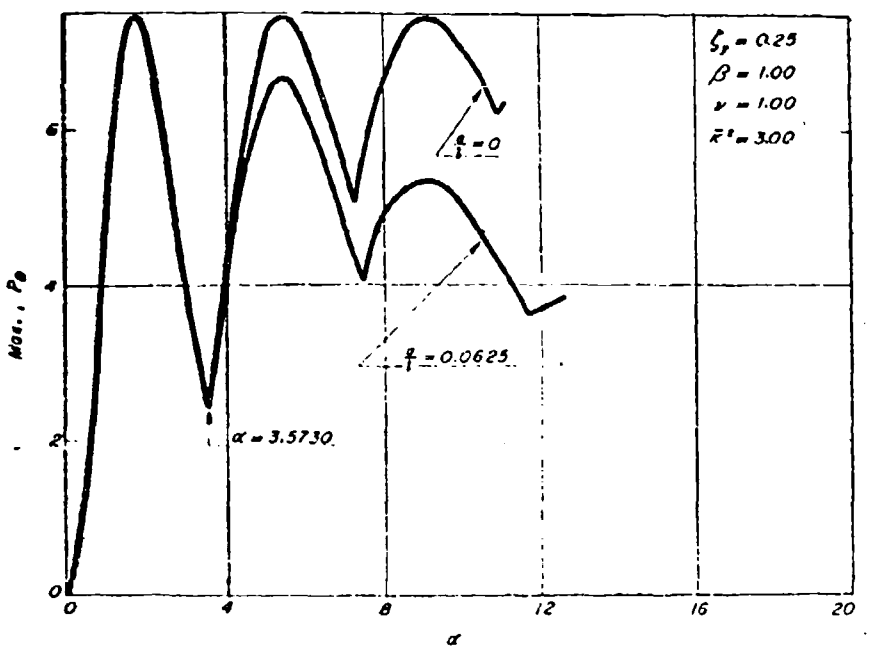

$\zeta_y = 0.25$
$\beta = 1.00$
$\nu = 1.00$
$\bar{\kappa}^2 = 3.00$
$\frac{\rho}{l} = 0$
$\frac{\rho}{l} = 0.0625$
$\alpha = 3.5730$
Max., P_θ
0
2
4
6
0
4
8
12
16
20
α

Fig. 4 a.

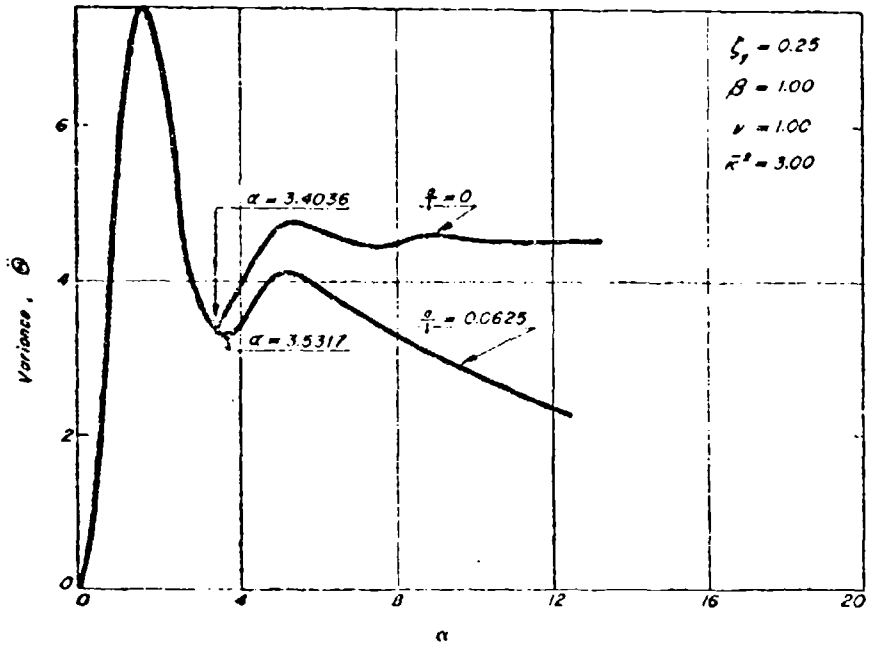

$\zeta_y = 0.25$
$\beta = 1.00$
$\nu = 1.00$
$\bar{\kappa}^2 = 3.00$
$\alpha = 3.4036$
$\frac{\rho}{l} = 0$
$\alpha = 3.5317$
$\frac{\rho}{l} = 0.0625$
Variance, Φ
0
2
4
6
0
4
8
12
16
20
α

Fig. 4 b.

zero; as α increases each reaches a maximum value, falls to a minimum and then oscillates. The value of α which gives the best ride in vertical acceleration does not give a best ride in pitch. However, it must be remembered that the parameter $\overline{K}$ is adjustable. Hence, it may be possible to select α and $\overline{K}$ to give a best ride from the point of view of vertical acceleration and pitch, or, at least, a good compromise to a best ride in both cases; this point is now under investigation.

The ride criterion used in figure 5 is the magnitude of the largest peak in the power spectral density of $\ddot{y}(t)$. With $\frac{a}{l} = 0$; $\beta = 1.00$; $\nu = 1.00$; the value of α which makes the peak a minimum is plotted as a function of ζ_y (see figure 5 a). In addition, the minimum peak value is plotted. Although the range of the minimum peak is not large for the ζ_y considered, there is a unique ζ_y (= .6953) and α (= 1.9170) which makes this minimum peak a minimum. Thus, one pair of ζ_y and α give the best ride in the peak of power spectral density sense. Figure 5 b is a graph of the peak in the power spectral density of $\ddot{y}(t)$ as a function of ν with $\frac{a}{l} = 0$; $\beta = 1.00$; $\zeta_y = .6953$; $\alpha = 1.9170$. Λ $\nu > 1$ corresponds to $v < v_0$ and $\nu < 1$ corresponds to $v > v_0$. Thus, as speeds decrease below v_0, which may be looked upon as design speed, the peak value falls gradually; however, as ν increases above ν_0 the peak value rises sharply, i. e. the ride rapidly gets worse.

The results presented in figure 6 correspond to results given in figure 5 except that the ride criterion is now the value of the variance of $\ddot{y}(t)$. Figures 7 and 8 correspond to figures 5 and 6 but for $\ddot{y}(t) + \frac{1}{2}\ddot{\Theta}(t)$. The conclusions drawn from figure 5 are reflected in these three figures.

Figures 8 and 9 present results on $\ddot{\Theta}(t)$ that are the same as given in figures 5 and 6, respectively, for $\ddot{y}(t)$. However, with $\ddot{\Theta}(t)$ neither the minimum variance nor minimum peak value has a minimum value as a function of ζ_y. This result agrees with the observation that the oscillations of $\ddot{\Theta}(t)$ may be reduced to zero by making l infinite and using a rigid suspension system. For arbitrarily selected ζ_y, these two figures again show the great sensitivity of variance and maximum peak value of power spectral density to changes in ν in the neighborhood of $\nu = 1$.

The parameter β was not changed in the studies reported in this paper. We recall that β contains λ_0 which is a measure of the spread of $P_{r_0}(\lambda)$. At this time, we have no numerical value for λ_0 moreover, we are not certain that (5.7) is the most reasonable choice for $P_{r_0}(\lambda)$. Hence, it does not seem appropriate to obtain results with other than one value of β. It is worthy of note, however, that since

$$\alpha\beta = \lambda_0 l \tag{5.10}$$

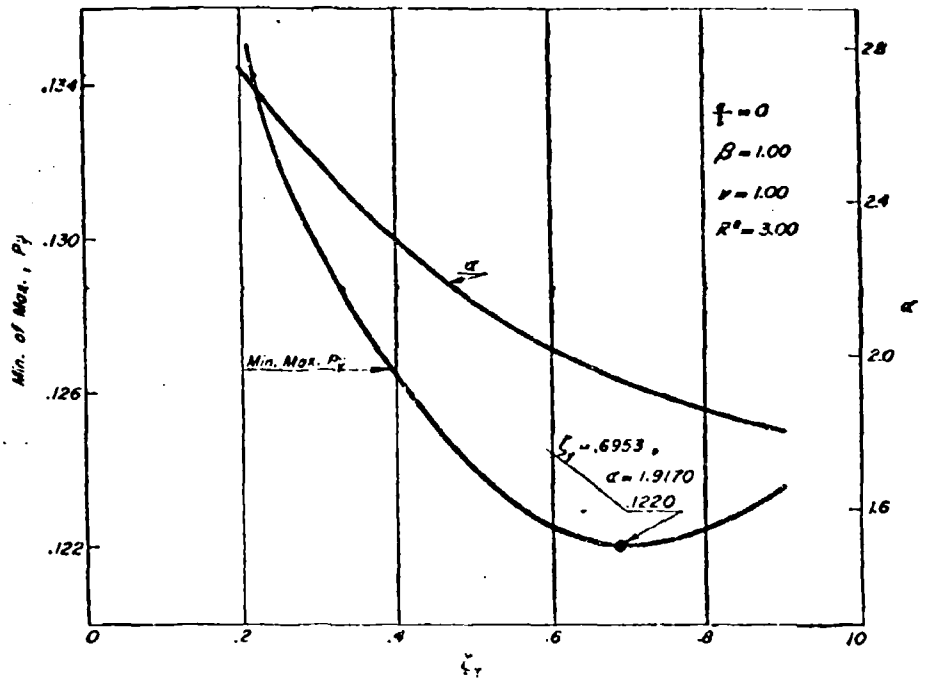

.134
.130
.126
.122
Min. of Max., P_y
0
.2
.4
.6
.8
1.0
ζ_r
2.8
2.4
2.0
1.6
α
$\frac{e}{t} = 0$
$\beta = 1.00$
$\nu = 1.00$
$R^0 = 3.00$
α
Min. Max. P_y
$\zeta_r = .6953$,
$\alpha = 1.9170$
.1220

Fig. 5 a.

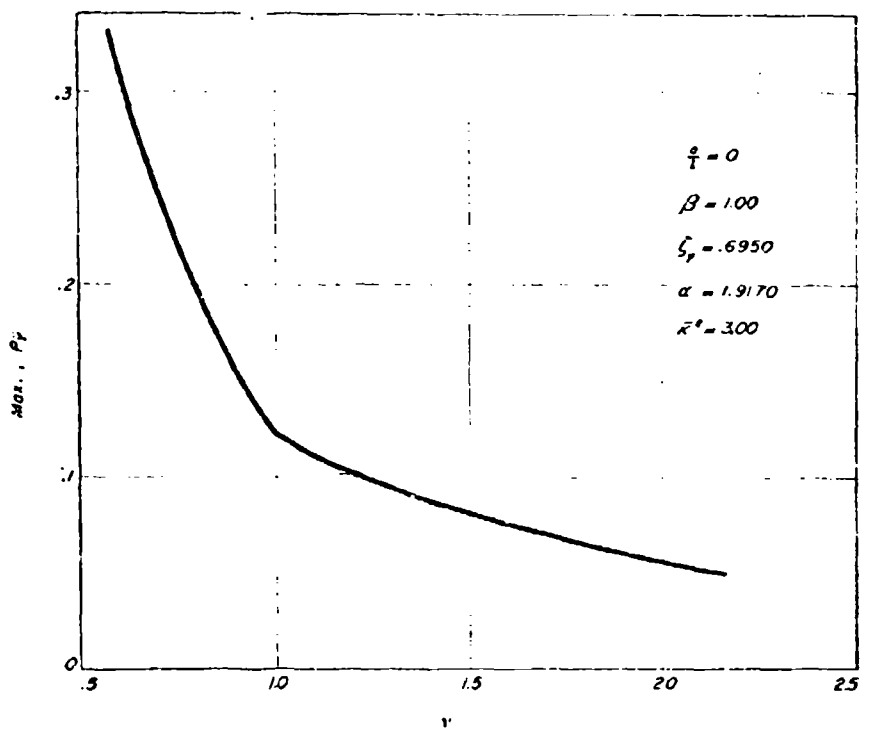

.3
.2
.1
0
Max., P_y
.5
1.0
1.5
2.0
2.5
ν
$\frac{e}{t} = 0$
$\beta = 1.00$
$\zeta_r = .6950$
$\alpha = 1.9170$
$R^0 = 3.00$

Fig. 5 b.

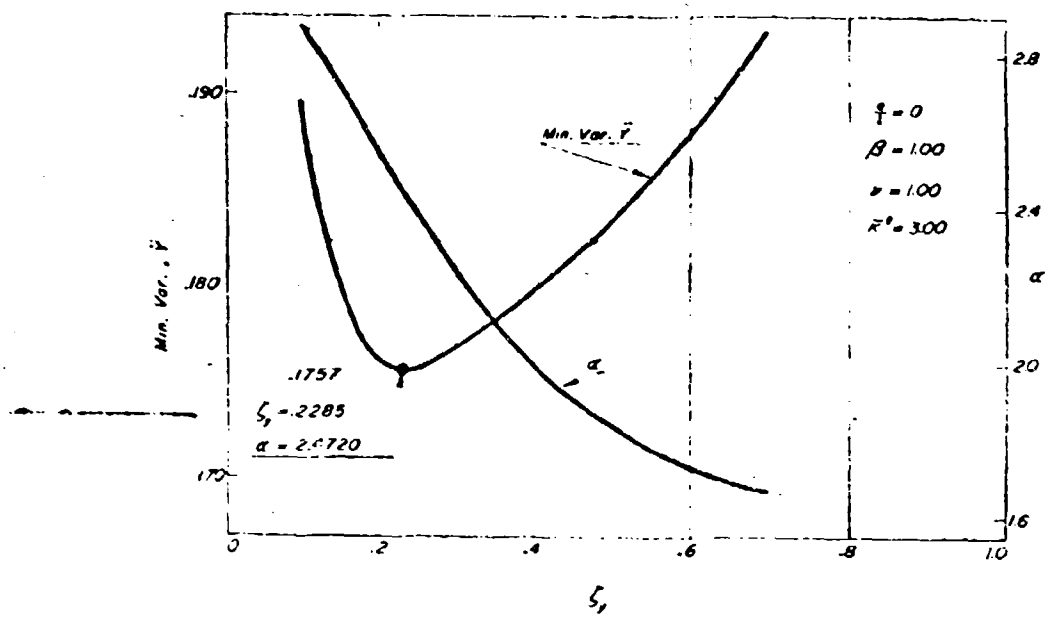

Min. Var., $\bar{V}$
.190
.180
.170
Min. Var. $\bar{V}$
α_c
.1757
ζ_y = .2285
α = 2.4720
$\frac{q}{t}$ = 0
β = 1.00
ν = 1.00
$\bar{K}^0$ = 3.00
2.8
2.4
2.0
1.6
α
0
.2
.4
.6
.8
1.0
ζ_y

Fig. 6a.

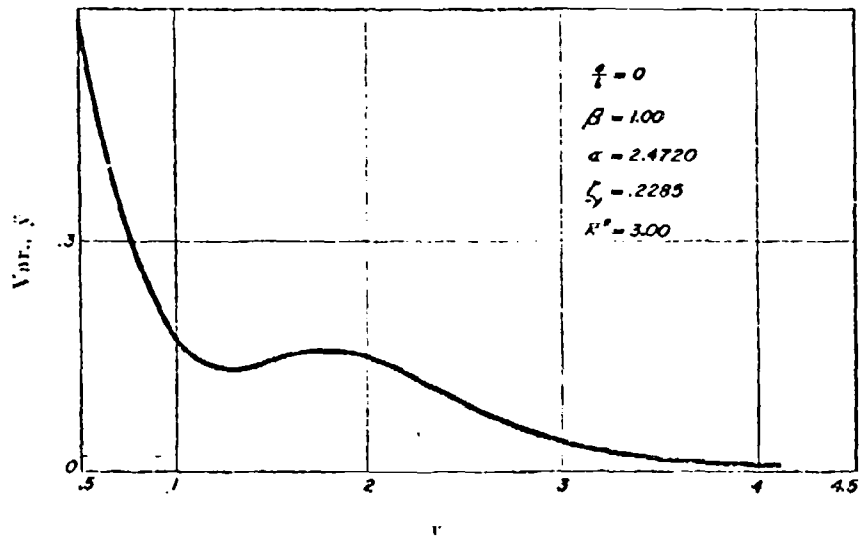

Var., $\bar{V}$
.3
0
$\frac{q}{t}$ = 0
β = 1.00
α = 2.4720
ζ_y = .2285
$\bar{K}^0$ = 3.00
.5
1
2
3
4
4.5
r

Fig. 6b.

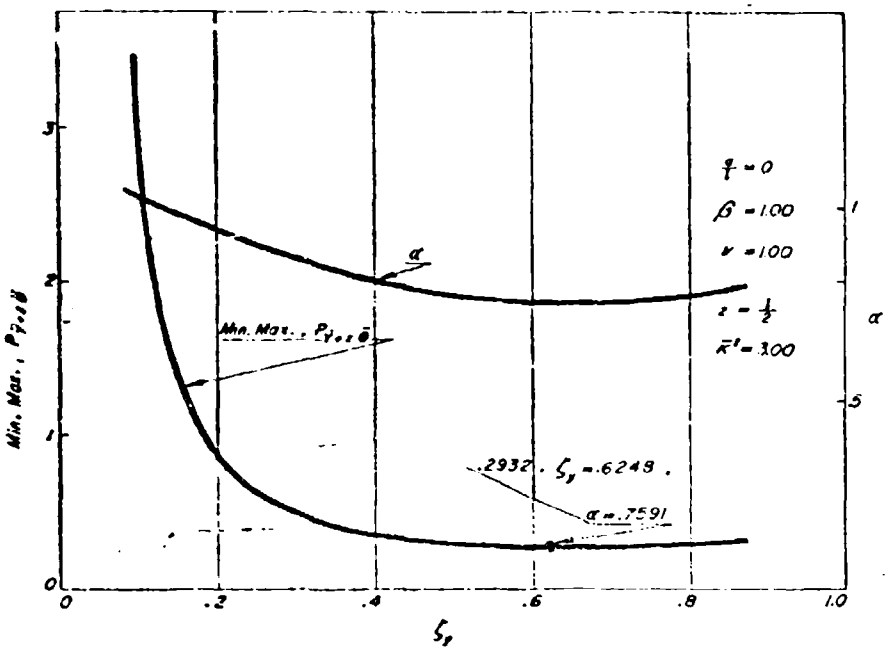

Min. Max., $P_{y=0}$
α
Min. Max., $P_{y=0}$
$\frac{a}{l} = 0$
$\beta = 1.00$
$\nu = 1.00$
$z = \frac{1}{2}$
$\bar{\kappa}' = 3.00$
α
.2932 . ζ_y = .6248 .
α = .7591
ζ_y

Fig. 7 a.

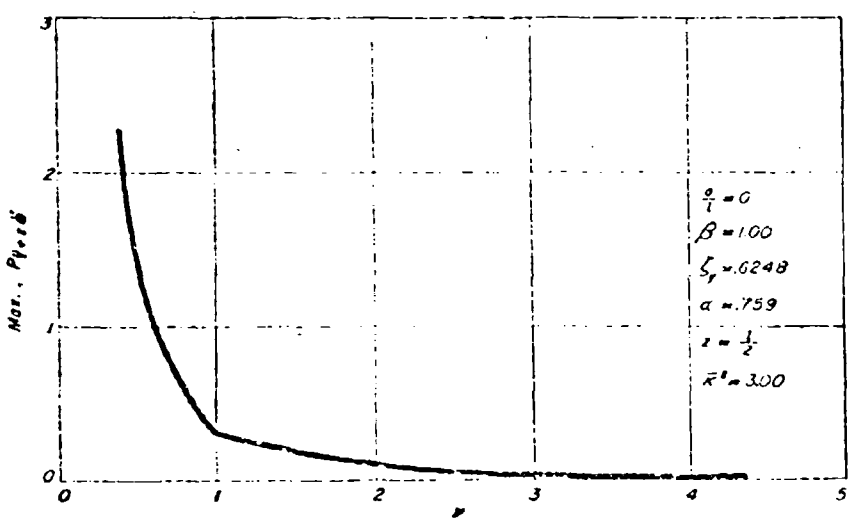

Max., $P_{y=0}$
$\frac{a}{l} = 0$
$\beta = 1.00$
ζ_y = .6248
α = .759
$z = \frac{1}{2}$
$\bar{\kappa}' = 3.00$
ν

Fig. 7 b.

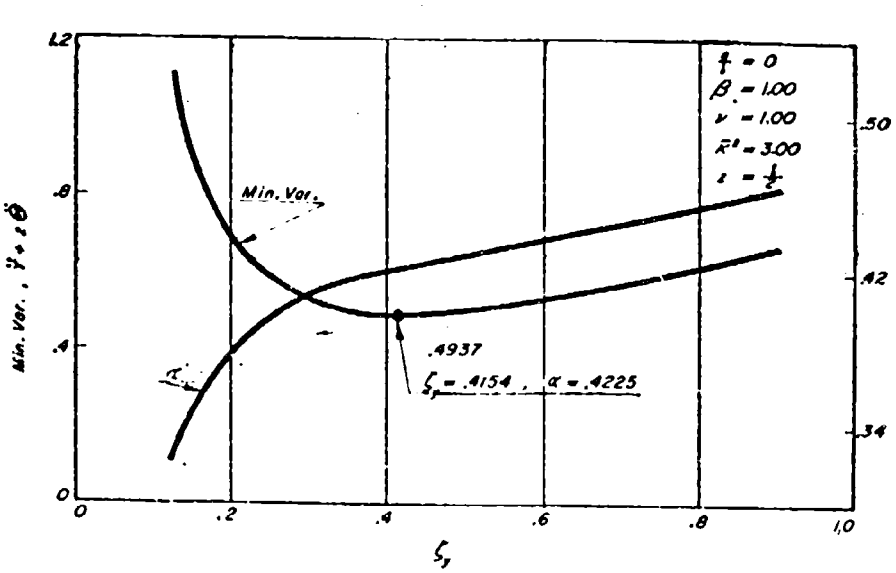

1.2
.8
.4
0
Min. Var., $\bar{V} + \bar{\theta}$
Min. Var.
$\bar{\alpha}$
.4937
ζ_y = .4154 , α = .4225
$\bar{q}$ = 0
β = 1.00
ν = 1.00
$\bar{R}^a$ = 3.00
τ = 1/2
.50
.42
.34
0
.2
.4
.6
.8
1.0
ζ_y

Fig. 8a.

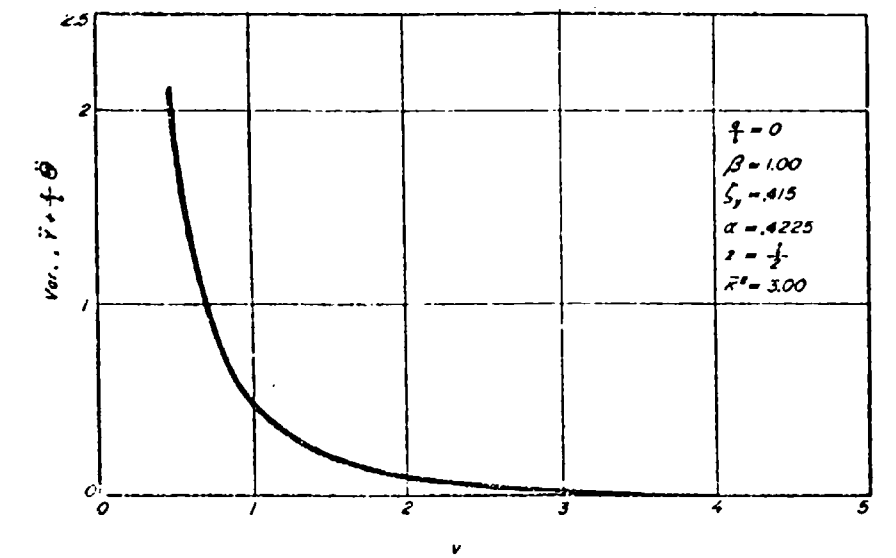

2.5
2
1
0
Var., $\bar{V} + \bar{\theta}$
$\bar{q}$ = 0
β = 1.00
ζ_y = .415
α = .4225
τ = 1/2
$\bar{R}^a$ = 3.00
0
1
2
3
4
5
ν

Fig. 8b.

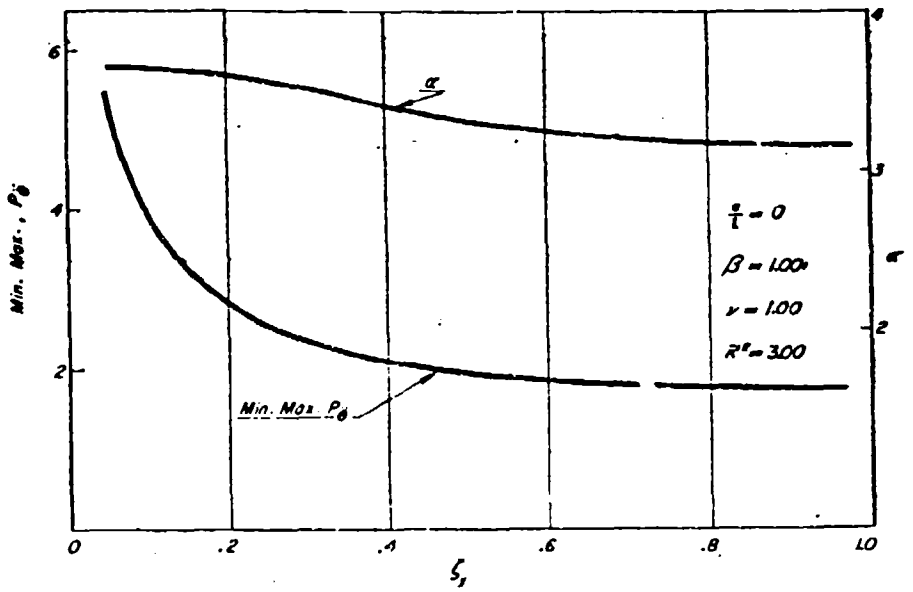

Min. Max., P_θ
α
Min. Max P_θ
$\frac{a}{t} = 0$
$\beta = 1.00$
$\nu = 1.00$
$R^* = 3.00$
ζ_1

Fig. 9 a.

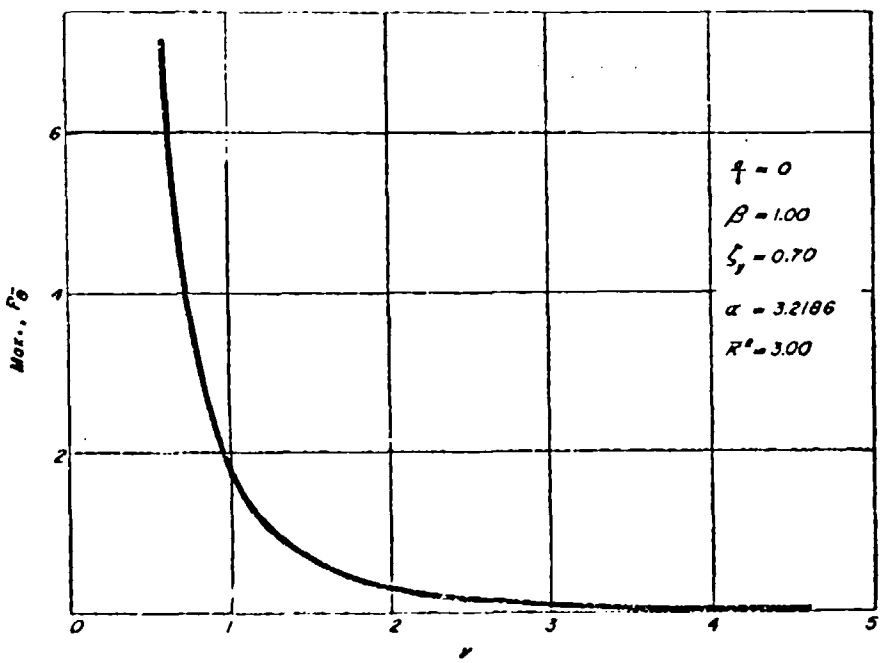

Max., P_θ
$\frac{a}{t} = 0$
$\beta = 1.00$
$\zeta_1 = 0.70$
$\alpha = 3.2186$
$R^* = 3.00$
ν

Fig. 9 b.

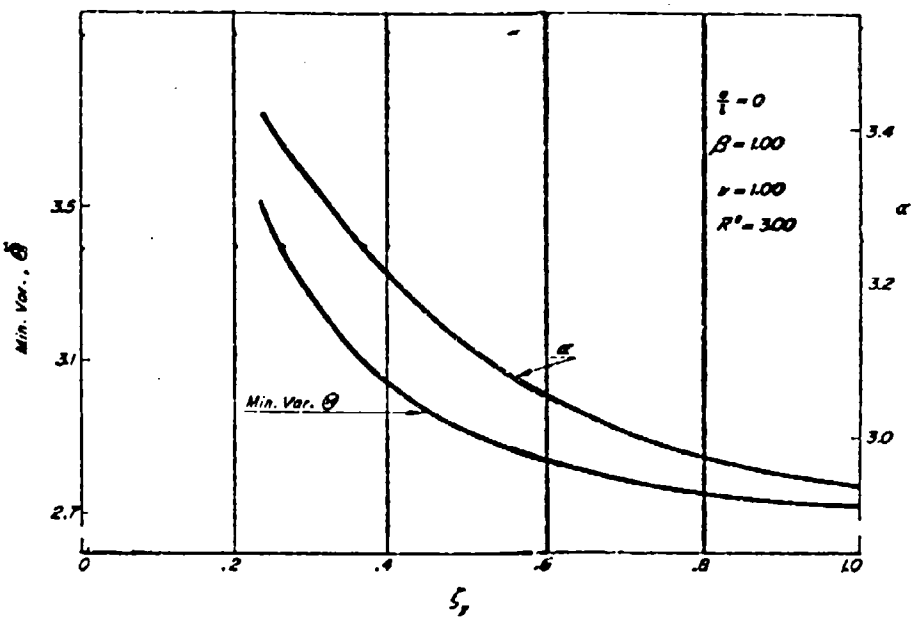


Fig. 10 a.

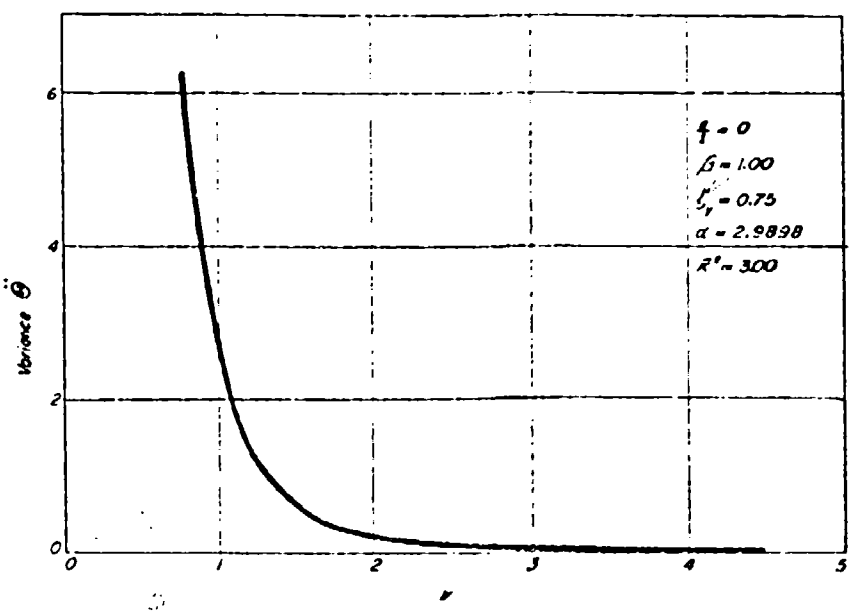


Fig. 10 b.

if we had a numerical value for λ_c and the α associated with a best ride in same sense for a given ζ_y, β, etc., then a numerical value for the corresponding wheel base length could be obtained.

The results presented in this paper represent the beginnings of an attack on the interesting problem of how to design a vehicle to achieve higher speeds than obtained at present under off-road conditions. A large effort will surely have to be devoted to obtaining a statistical characterization of ground contour geometry and quantitative ride criteria before either the method of attack proposed can be justified here and definitive design results can be obtained.

ACKNOWLEDGMENT. — The Authors wish to express their thanks to M. G. Bekker, and Capt. Liston and Capt. Tyler of the Land Locomotion Laboratory, Detroit Arsenal, for helpful discussion given during the course of the investigation.

REFERENCES

1) Bogdanoff J. L. and Kozin F. Behavior of a linear one-degree of freedom vehicle moving with constant velocity on a stationary gaussian random track. Report No. 48, Land Locomotion Laboratory, Detroit, February 1959.

2) Kozin F. and Bogdanoff J. L. On the statistical analysis of the motion of some simple two-dimensional linear vehicles moving on a random track. International Journal of Mechanical Sciences, Vol. 2, No. 3, p. 168, 1960.

3) Goldman D. E. Effects of vibration on man. Handbook of Noise Control, McGraw-Hill, New York, 1957.

4) Von Gierke H. E. Transmission of vibratory energy through human body tissue. Proc. of First Nat. Biophysics Conf., 1957, Yale University Press, 1959.

5) Coermann R. R. The mechanical impedance of the human body in the sitting and standing position, etc. Third Annual Meeting of the Biophysical Society, Pittsburgh, Penn., February 1959.

6) Kozin F. and Bogdanoff J. L. On the statistical properties of the ground contour and its relation to the study of land locomotion. (See preceeding paper).

7) Moyal J. E. Stochastic processes and statistical physics. Journal of Royal Statistical Society, Sec. B., Vol. 11, p. 150, 1950.

8) Bartlett M. S. An introduction to stochastic processes. Cambridge University Press, Cambridge, 1955.

9) Rice S. O. Mathematical analysis of random noise. Bell System Tech. Journal, Vol. 23, p. 282, 1944; and Vol. 24, p. 46, 1945.

N. 16

On the statistical properties of the ground contour and its relation to the study of land locomotion *)

Proprietà statistiche della superficie del terreno e loro influenza sullo studio del movimento dei veicoli fuori strada

F. Kozin - J. L. Bogdanoff **)

ABSTRACT. — *The ground plays a fundamental role in the study of the ground-vehicle-driver complex which comprises the subject of Land Locomotion. Through the pioneering efforts of people such as Col. M. G. Bekker, formerly of the Land Locomotion Laboratory of the U. S. Army Ordnance Corp. Detroit Arsenal, great progress has been made concerning the role of ground soil properties and mechanics in determining the tractive ability of a vehicle traveling on the surface. However, until quite recently, very little has been studied concerning the role of the ground surface contour in determining the speeds of vehicles especially on off-road conditions.*

The Authors [3] have found that for a simplified vehicle traveling on a random ground contour there is a quantitative relation between the ground described by its spectral density function and the optimal wheel-base relative to the criterion of maximizing driver's comfort. This was only an initial study but points the way to the fact that the geometry of the ground surface must be clearly studied to try to characterize it in such a way that quantitative results concerning significant vehicle parameters may be derived.

In this paper statistical models of the ground surface contour are considered along with possible forms for the two dimensional power spectral density. The advantages and disadvantages of the models are pointed out. Perturbations in the power spectral density of the surface are studied to determine the magnitude of their effect on an optimum criterion chosen for vehicle parameter studies. Finally, the power spectral densities from an actual ground surface survey are presented and discussed.

I. - Introduction

The remarkable speed range of modern passenger and commercial motor vehicles on a modern highway is due partly to the power available in contemporary power packages, partly to the suspension system, partly to the straightness of the highway, but it is mainly due to the *smoothness* of the surface upon which they operate. One immediately realizes the importance of the smoothness

*) This paper was originally prepared for Land Locomotion Laboratory, U.S. Army Ordnance Tank Automotive Command, Detroit, Michigan.

**) Midwest Applied Science Corp. and Purdue University.

of the surface when these vehicles are required to operate off the road. Certain wheeled military vehicles have nearly equivalent speed ranges when operating on the same types of smooth pavements. It must be remembered, however, that of necessity, a military vehicle may be required to operate off paved roads. Under off-road conditions, these military vehicles like modern passenger and commercial vehicles have a very limited speed range. This fact is, of course, not strange, since the same considerations are used in the design of the three types of vehicles.

The basic design criteria for all wheeled vehicles in most categories is much the same-good speed and control on the highway together with, in some cases, load carrying capacity. A vehicle designed using such criteria does not operate and cannot be expected to operate at even moderate speeds when the assumption that it will operate on a modern smooth highway is changed to the assumption of operation under off-road conditions.

To secure reasonable off-road speeds of wheeled or other types of vehicles, it is obvious that fundamental studies must be made of the factors which limit speed under these conditions.

The Land Locomotion Laboratory, Detroit Arsenal, has advocated that such studies be made. The material presented in this paper and the one that follows is the result of such studies conducted by the Midwest Applied Science Corporation, of Lafayette, Indiana, U.S.A.

These studies pertain to the over-all problem of land locomotion as governed by the geometrical properties of the ground surface when that surface is viewed from the statistical point of view.

The work divides itself rather naturally into three parts: a statistical description of the ground surface, vehicle dynamics, and possible criteria for ride performance. The first is discussed in the present pa

II. - The ground. Introductory remarks

It is a remarkable fact that although the very earliest form of transportation was land locomotion, the way in which the ground characteristics should enter into the design of vehicles has been the least understood of the three major environments of travel, that is, of land, sea, and air travel.

We shall be primarily concerned here with the ground part of the ground-vehicle driver complex. Any study of the Theory of Land Locomotion must start with the ground for it is the primary and continual input into any vehicle that moves by way of its contact with the ground, whether the contact is through tires, tracks, skis, or any other mode.

The characteristics of the ground can be broken up into two major areas, the physical properties of the ground as a material and the geometrical properties of the ground as a two dimensional surface.

The material properties of the ground are those associated with its elas-

ticity, plasticity and trafficability. Bekker [1], and his associated have made many interesting and important studies of these ground properties and their relation to the Theory of Land Locomotion.

It is the ground as a geometrical surface that has been the least studied relative to the Theory of Land Locomotion. Furthermore, the surface apparently has not been analytically characterized in any realistic fashion. This can be thought to be mainly due to its irregular nature and the lack, until relatively recently, of methods of analyzing and characterizing surfaces with such peculiarities or — if you will — randomness in elevation. The methods we refer to are those found within the scope of the theory of probability and random functions.

Only recently have statistical analyses of road surfaces been considered, in particular the work of Hoboult et al. [2] in determining the spectral properties of airport runways. Even here ground vehicles were not the primary consideration!

In the studies over the past two years by Bogdanoff and Kozin of the Midwest Applied Science Corporation [3,4] under contract with the Land Locomotion Laboratory of the Detroit Arsenal OTAC, U.S.A., ground elevation surveys have been performed along lines on typical plowed ground in central Indiana. Spectral analyses were then performed from these surveys. Within their studies the statistical analysis was performed of simple vehicles traveling on a track whose contour is one membre function of a random process having spectral properties approximating those found from the surveys. Full details of these studies are given in the next paper. At the time of the writing of this paper the results of these surveys concerning the field as random surface have not been fully appraised. Therefore, even though the statistical properties are known along particular straight lines on this field, its general two-dimensional statistical character remains unknown. It is probably safe to say that the question of the statistical character of arbitrary ground surfaces is quite new and yet to be answered.

In this paper we shall consider two aspects of the theory of random ground surfaces, the theoretical and the experimental. Under the theoretical considerations we shall discuss a possible analytical model of the random ground surfaces along with the associated two dimensions spectral density functions. The advantages and short-comings of using these model will also be discussed. It is certain that approximations to ground surfaces through spectral densities will have to be employed in studying the motion of vehicles traveling over random surfaces. Hence, the magnitude and nature of the errors introduced into the analysis by using such approximations will also be studied.

Under the experimental considerations we shall present and discuss the results of a ground surface survey that was designed specifically to try to characterize the spectral properties along straight lines in any direction for that particular field. This survey will be compared with the theoretical results discussed in this paper in order to determine the feasibility of a spectral characterization of the type we propose.

III. - The ground. Random models

The model of a random surface that has gained great favor among oceanographers and meteorologists studying the surface of the sea [4] is simply the two dimensional analogue of the Rice random functions [2] that are used as models for the random tracks in the paper to follow. To this end, consider the expression

$$z(x,y) = \sum_{k=-n}^{n} c_k \exp i(u_k x + v_k y + \Phi_k) \tag{1}$$

where c_k, u_k, v_k are real numbers satisfying

$$\begin{aligned} &c_k = c_{-k}, \quad c_0 = 0 \\ &u_{-k} = -u_k \\ &v_{-k} = -v_k, \quad u_k, v_k \text{ have the dimension } L^{-1} \end{aligned} \tag{2}$$

The Φ_k's are independent random phases, each uniformly distributed on the interval $(0, 2\pi)$ satisfying $\Phi_{-k} = -\Phi_k$. Hence, we see that $z(x,y)$ is real and, indeed, is no more than a linear combination of cosine terms with random phases. Conceptually this fits the picture that one has of a ground surface full of miniature mounds and valleys.

One immediate objection to the form (1) is that as $n \to \infty$, $z(x,y)$ must become a Gaussian Process [3]. However, it is strongly suspected that the ground surface in general is not Gaussian. It is known that except for a very small error due to non-linearities in the hydrodynamic equations [5] the sea surface is Gaussian in character and hence (1) modified to include time variation fits the phenomenon quite well.

But this objection can be dispensed with since our studies of vehicle dynamics have been directed toward analysing the so-called second-order properties. These are properties that are determined by the covariance function. It can easily be shown [4] that when studying second order properties of an arbitrary second order random process, that is, a process whose mean square exists, the process may be replaced by a Gaussian process with the same covariance function. Thus no contradiction is created by using (1). We realize fully that (1) may not suffice if we must study subtle properties of the vehicle motion that are based upon considerations of the probability densities themselves and not second moments.

Upon taking the first two moments of $z(x,y)$ as given by (1) we find

$$E[z(x,y)] = 0$$

$$E[z(x,y)\, z(x+x', y+y')] = \sum_{k=-n}^{n} c_k^2 \exp i(u_k x' + v_k y') = \Gamma(x', y') \tag{3}$$

where E [ ] denotes the expectation or ensemble average of the quantity within the brackets.

In words (3) states that the mean is zero and the covariance function exists, being dependent only upon the differences of the abcissas and ordinates. Therefore, by definition, z (x, y) is second order and at least weakly stationary random process.

Because of the weak stationarity expressed by (3), one may define its Fourier inverse as

$$\Gamma(x, y) = \int du \int dv\, E(u, v) \exp i(ux + vy) \tag{4}$$

[Note: Unless explicitly stated otherwise, all integrals will be over the range $(-\infty, \infty)$].

Hence,

$$E(uv) = \frac{1}{4\pi^2} \int dx \int dy\ \Gamma(x, y) \exp i(xu + yv) \tag{5}$$

The function E (u, v) is the two-dimensional power spectral density function. That is E (u, v) $\Delta u\, \Delta v$ yields approximately the average amount of power of the random process that is found in the frequency rectangle $(u, u + \Delta u) \times (v, v + \Delta v)$.

We may write explicitly,

$$E(u, v)\, \Delta u\, \Delta v = \sum_{k'} \sigma^2_{k'} \tag{6}$$

where the index k' runs over those frequency pairs (u'_k, v'_k) that are in the rectangle $(u, u + \Delta u) \times (v, v + \Delta v)$.

This is merely the extension to two dimensions of the power spectral density function that one encounters when studying one-dimensional records.

A major question may now be asked. The question is, « How does one determine a useful approximation, economically, in both time and expense, of E (u, v) for an actual ground surface? ».

Furthermore, what can be said about E (u, v) restricted to a given path on the surface?

The reason we feel that these are major questions is due to the fact the power spectrum of the surface appears to be the most readily available way of characterizing the surface statistically. Whether or not one may be able to determine simpler characteristics of a random surface that can be used significantly for vehicle design purposes seems to be unknown at present. Much research remains to be performed in this area.

The remainder of this paper will be devoted to trying to answer the questions posed above.

IV. - Spectral properties along paths

We shall first consider straight line paths through arbitrary points (x_0, y_0) having directions determined by the angles formed with the positive x -axis, as shown in fig. 1.

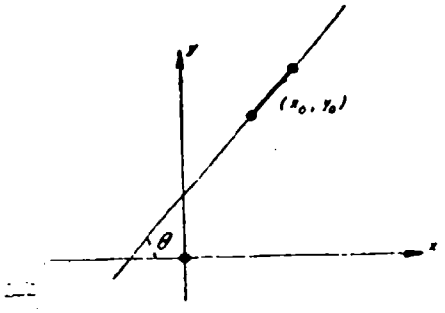


Fig. 1.

Following the procedure in (6) consider the transformation

$$T; \quad \begin{aligned} \xi &= (x - x_0)\cos\Theta + (y - y_0)\sin\Theta \\ \eta &= -(x - x_0)\sin\Theta + (y - y_0)\cos\Theta, \end{aligned} \tag{7}$$

and its inverse

$$T^{-1}; \quad \begin{aligned} x &= x_0 + \xi\cos\Theta - \eta\sin\Theta \\ y &= y_0 + \xi\sin\Theta + \eta\cos\Theta \end{aligned}$$

The line in question is given by η identically equal to zero.

Let us first notice that for a weakly stationary process along a line, l, we have

$$\Gamma(\vec{v}') = E\left[z(\vec{v})\, z(\vec{v} + \vec{v}')\right] \tag{8}$$

where

$$\vec{v} = \vec{v}_0 + k\vec{u} \qquad \text{and} \qquad \vec{u} = 1, \vec{v}_0 \cdot \vec{u} = 0$$

This is given schematically in fig. 2.

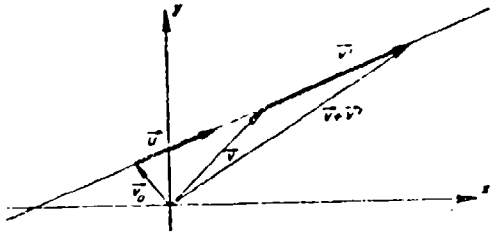


Fig. 2.

Also

$$\bar{v}' = k' \bar{u} \tag{9}$$

Thus we see that the covariance along any line depends only upon the angle Θ, or the direction of the line. Therefore all classes of parallel lines have the same covariance function, and it follows that they shall have the same spectral density function.

Now, using (4) and (7) with $(x_o, y_o) = (0, 0)$, we find

$$\left.\begin{aligned} \Gamma'(\xi, \eta) &= \int du \int dv \left\{ E(u, v) \exp i \left[(\xi \cos\Theta - \eta \sin\Theta)\, u + (\xi \sin\Theta + \eta \cos\Theta)\, v \right] \right\} \\ &= \int du \int dv \left\{ E(u, v) \exp i \left[\xi (u \cos\Theta + v \sin\Theta) + \eta (-u \sin\Theta + v \cos\Theta) \right] \right\} \\ &= \int du' \int dv' E'(u', v') \exp i (\xi u' + \eta v') \end{aligned}\right| \tag{10}$$

where

$$\left.\begin{aligned} u' &= u \cos\Theta + v \sin\Theta \\ v' &= -u \sin\Theta + v \cos\Theta \\ E'(u', v') &= E\left[u(u', v'),\ v(u', v') \right] \end{aligned}\right|$$

and the Jacobian of the transformation is unity.

Placing $\eta = 0$ for the line in question yields

$$\Gamma_\Theta(\xi) = \Gamma'(\xi, 0) = \int du' \int dv' E'(u', v') \exp i (\xi u') \tag{11}$$

But the covariance and spectral density functions are Fourier transform pairs, so that,

$$E_\Theta(u') = \int dv' E'(u', v') = \int dv\, E(u, v) \tag{12}$$

which is the spectral density function along the line in the given direction.

At this point we wish to strongly stress the fact that all of the results so far obtained in this section are based only upon the weak stationarity of the random surface process and not upon explicit forms or processes.

From (11), we obtain an interesting result concerning weakly stationary random surfaces.

$$\sigma^2_\Theta = \Gamma_\Theta(0) = \int du' \int dv' E'(u', v') = \int du \int dv\, E(u, v) \tag{13}$$

But the last double integral is independent of Θ. Therefore, the variance must be the same along any direction! Apparently this has been found to be the case for sea surfaces, but it is not clear that one shall find this to be true for the ground surface. The consideration of weakly stationary random processes to describe the ground surface could break down seriously at this point.

Let us now study paths that are not necessarily straight lines. What can be said about their power spectral density functions? We shall approach the question by first considering the covariance function along a path.

We shall parametrize the path using arc length, s, along the path as the parameter. The elevation for the path [x (s), y (s)] on the surface (1) is

$$z\,[x\,(s), y\,(s)] = \sum_{k=-n}^{n} c_k \exp i\,\left[u_k\,x\,(s) + v_k\,y\,(s) + \Phi_k\right] \tag{14}$$

The mean is still zero.

For the covariance, one finds,

$$\left.\begin{aligned} &E\,[z\,[x\,(s), y\,(s)]\,z\,[x\,(s+s'), y\,(s+s')]] \\ &= E\,\Big[\sum_{k=-n}^{n}\sum_{j=-n}^{n} c_k\,c_j \exp i\,[u_k\,x\,(s) + v_k\,y\,(s) \\ &\quad + u_j\,x\,(s+s') + v_j\,y\,(s+s') + \Phi_j + \Phi_k]\Big] \\ &= \sum_{j=-n}^{n} c_j \exp i\{u_j\,[x\,(s+s') - x\,(s)] + v_j\,[y\,(s+s') - y\,(s)]\} \end{aligned}\right\} \tag{15}$$

since there can only be a contribution to the average if $k = -j$. But in order for this to be a function of s' alone so that a spectral density function exists along the path, it follows that

$$\left.\begin{aligned} x\,(s+s') - x\,(s) &= g\,(s') \\ y\,(s+s') - y\,(s) &= k\,(s') \end{aligned}\right\} \tag{16}$$

for any s, s' along the path.

The obvious example of (16) is the straight line path that we have already considered. Are there any other cases? The answer is easily seen to be no by simply differentiating the relations (16) with respect to s and setting s equal to zero, yielding

$$\frac{dx}{ds} \quad \frac{dy}{ds} = \text{constant.} \tag{17}$$

Therefore, a spectral density function cannot be expected to characterize paths other than straight lines on a weakly stationary random surface.

V. - Spectral models for real ground surfaces

From the preceding considerations, we know that spectral densities exist along straight lines on weakly stationary random surfaces. We may assume that fields free from streams, shell holes, or other man-made singularities such as irrigation channels, etc. have the required stationary properties, so that

spectral densities of the ground elevations along straight line paths can be obtained. Our problem in this section is inverse to that considered in the previous section, namely, how can we determine E (u, v) from spectral properties of straight line paths?

From several samples of surveys taken along actual rough ground, it appears that the power spectral density function has the general form for straight lines as given by the exponential function

$$\frac{\sigma^2}{u_0\sqrt{2\pi}} \exp\left(-\frac{u^2}{2u_0^2}\right) \tag{18}$$

where u_0 is a measure of the spread of frequencies about zero and σ^2 is a measure of the area under the curve, that is, the variance. We hasten to add that (18) is by no means definitive, since the statistical characterization of ground surfaces is still in its infancy. Qualitative results may be based upon the form (18), but quantitative results based upon (18), must contain inaccuracies. The magnitude and effect of errors based upon inaccuracies in the estimate of the power spectral density function will be considered in the following section.

Upon initial considerations, there are two possible ways of extending the function (18) into a two dimensional spectral density function. Each of the extensions represent distinct modes of attack on the problem of obtaining the E (u, v) function in the easiest possible fashion. The functions extensions are

$$\left.\begin{aligned} E(u,v) &= \frac{\sigma^2\sqrt{ac-b^2}}{\pi} \exp -\left[au^2 + 2buv + cv^2\right] \\ E_{\Theta}(u) &= \frac{\sigma^2}{u_0(\Theta)\sqrt{2\pi}} \exp -\frac{u^2}{2u_0^2(\Theta)} \end{aligned}\right\} \tag{19}$$

The first expression is simply an extension of the one dimensional exponential function to a two dimensional one. The second expression represents the variation in (18) along linear paths defined by Θ the angle between the line and the positive x-axis.

To explicitly determine the functions (19) one would need a, b, c in the first case. In the second case the variation of u_0 with Θ would be needed. The factor σ^2 is an amplification factor that represents the variance. It must be constant along any line as derived above. Notice that E (u, v) = constant in the first expression of (19) correspond to ellipses in the (u, v) — plane.

To help substantiate the form chosen for the first of (19), we notice that one may define moments for E (u, v) as (6)

$$m_{pq} = \int du \int dv\, E(u,v)\, u^p v^q \tag{20}$$

This allows us to define moments along straight lines in various directions by making use of the transformation given in (10).

$$\begin{aligned} m_n(\Theta) &= \int du' E_\Theta(u') u'^n \\ &= \int du' \int dv' E'(u', v') u'^n \\ &= \int du \int dv E(u, v) (u \cos\Theta + v \sin\Theta)^n \end{aligned} \tag{21}$$

Notice, in particular, that the second moment is

$$m_2(\Theta) = m_{20} \cos^2\Theta + 8 m_{11} \cos\Theta \sin\Theta + m_{02} \sin^2\Theta \tag{22}$$

This function of Θ is continuous in its domain of definition and must attain its extreme values. However, determining these values is equivalent to finding the stationary values of the quadratic form

$$m_{20} x^2 + 2 m_{11} x y + m_{02} y^2 \tag{23}$$

subject to the conditions $x^2 + y^2 = 1$

The solution to this classical eigenvalue problem is given by

$$\begin{vmatrix} m_{20} - \lambda & m_{11} \\ m_{11} & m_{02} - \lambda \end{vmatrix} = 0 \tag{24}$$

We have, then, two distinct directions for which $m_2(\Theta)$ is stationary. These directions can be considered to correspond to the directions of the major and minor axes of the elliptical power spectral density distribution.

To determine the elliptical power spectral density function for a given field one would have to determine a, b, c. This can be accomplished by surveying three linear paths along three distinct directions. We shall discuss a survey devoted to this task later.

The second of the forms in (19) can be useful if there is a definitely preferred direction of the variations in contour of a particular ground surface. This corresponds to the so-called long crested property in a wave pattern. Such a state would presumably exist shortly after a field had been plowed, or if there happens to be a prevailing weather and wind direction creating a distinct grain to the surface. Fig. 3 represents schematically this effect.

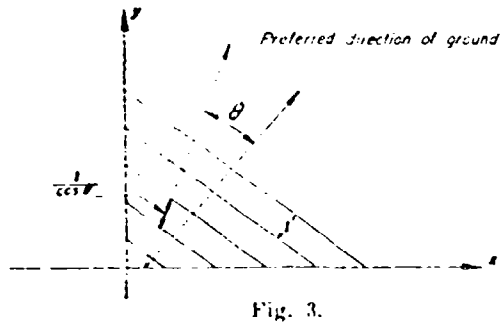


Fig. 3.

Therefore for a wave length of l in the preferred direction, we find that the length becomes $\frac{l}{\cos\Theta}$ along the direction defined by $\Theta, -\frac{\pi}{2} < \Theta < \frac{\pi}{2}$.

The original frequency u becomes $u\cos\Theta$ along the new direction. If the power spectral density function along the preferred direction E (u) then

$$E_{\Theta}(u) = \frac{1}{\cos\Theta} E\left(\frac{1}{\cos\Theta}\right) \tag{25}$$

Hence, using (25) the second of (19) must become

$$E_{\Theta}(u) = \frac{\sigma^2}{u_0 \cos\Theta \sqrt{2\pi}} \exp - \frac{u^2}{2u_0^2 \cos^2\Theta} \tag{26}$$

Therefore $u_0(\Theta)$ becomes $u_0 \cos\Theta$. We now have the spectral properties along any linear path on the surface merely from the results found along the preferred direction. For fields that can be recognized to have the properties mentioned above only one survey will suffice for the determination of its spectral properties.

VI. - The effect of errors in the estimate of the power spectral density function

The nature of the errors in vehicle parameter studies based upon inaccurate power spectral density forms and measurements is of prime importance in our studies. As one must expect, we may only obtain the spectral density function from surveys within some confidence band.

In the following paper two criteria are used upon which to make optimum judgements concerning the parameters that characterize the simple vehicles considered. The criteria concern the variance of the vertical acceleration and the stationary values of the power spectral density of the vertical acceleration.

One can easily show that the power spectral density of the output of a linear system which is subjected to a stationary random input is simply, assuming one dimensional spectra

$$P(\lambda) = |H(i\lambda)|^2 P(\lambda) = h(\lambda) P(\lambda) \tag{26 bis}$$

where $H(i\lambda)$ is the frequency response of the linear system.

We must recognize that $h(\lambda)$ is really $h(\lambda, \vec{p})$ where $\vec{p}$ is the parameter vector whose values we wish to optimize relative to the criteria mentioned above. We shall consider first order effects on the second of the criteria mentioned above. from errors in the power spectral density function.

Consider the power spectral density $P(\lambda) + P^*(\lambda)$, where $P^*(\lambda)$ is the perturbation or error term. The maximum values of $h(\lambda)\,[P(\lambda) + P^*(\lambda)]$ are determined as usual from the equation

$$\frac{dh(\lambda, p)}{d\lambda}\left[P(\lambda) + P^*(\lambda)\right] = h(\lambda, p)\frac{d\left[P(\lambda) + P^*(\lambda)\right]}{d\lambda} = 0 \tag{27}$$

We have specialized the parametric study to only one parameter p. We write the solution to (27) as $\lambda(p) + \lambda^*(p)$ where $\lambda(p)$ is the root if there is no error in the power spectral density estimate. The curve of the maxima as a function of p has the form

$$h[\lambda(p) + \lambda^*(p), p]\ \left[P[\lambda(p) + \lambda^*(p)] + P^*[\lambda(p) + \lambda^*(p)]\right] \qquad (28)$$

From (27) we may find the first order estimate of $\lambda^*(p)$ by substituting $\lambda(p) + \lambda^*(p)$ into (27), then expanding this expression about $\lambda(p)$. Upon using the fact that

$$\frac{dh\ [\lambda(p), p]}{d\lambda}\ P[\lambda(p)] + h[\lambda(p), p]\ \frac{dP\ [\lambda(p)]}{d\lambda} = 0 \qquad (29)$$

we find

$$\lambda^*(p) = -\ \frac{\frac{d}{d\lambda}\left[h[\lambda(p), p]\ P^*[\lambda(p)]\right]}{\frac{d^2}{d\lambda^2}\left[h[\lambda(p), p]\ P[\lambda(p)]\right]} \qquad (30)$$

Proceeding in the same fashion with equation (28), we can determine the first order difference in the curve of the maxima as being

$$h[\lambda(p), p]\ P^*[\lambda(p)] \qquad (31)$$

By use of the relation (30) and (31) we can therefore estimate the magnitude of the errors involved by approximating the power spectral density function as exponential.

VII. - Ground surveys and conclusions

The Midwest Applied Science Corporation has under contract with the Land Locomotion Laboratories undertaken the task of analyzing actual ground survey data to determine the nature of real ground spectra, and make decisions regarding characterizations of the surface. To the best of our knowledge this has not been undertaken in the U.S.A. before. The oceanographers are certainly well ahead in this approach.

Since there is no readily available data for our purpose of studying the ground as a surface, we have performed a survey on a field that has been, in its history, plowed, cultivated and grazed. This field is located in North-central Indiana, adjacent to Purdue University, and is part of the Purdue dairy farms.

The survey on this field was taken along five concentric lines that divide a circle into equal sections, as shown in fig. 4.

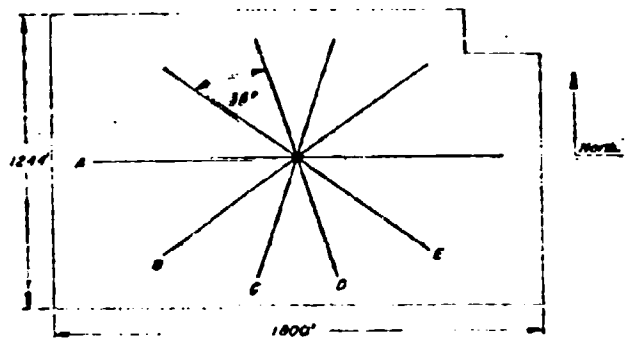


Fig. 4.

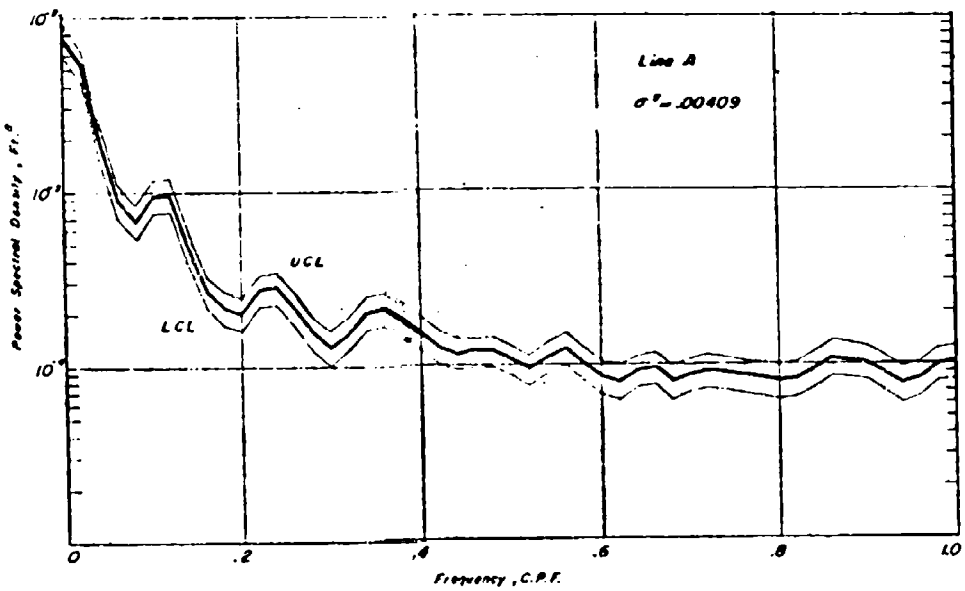


Fig. 5.

The lengths of the lines vary from fifteen hundred feet for line A to twelve hundred feet for line D. The elevations were taken at six inch intervals along each line, thereby yielding a spectral resolution of one cycle per foot.

It was decided to use the lines in the configuration shown rather than a rectangular grid on the surface due to the fact that we are primarily interested, for the land locomotion problem, in the spectral properties as a function of direction. Hence a polar survey appeared more suitable than a rectangular survey.

The use of five lines was dictated by the fact that if we are to try to fit ellipses to the constant power contours, then this elliptical distribution of

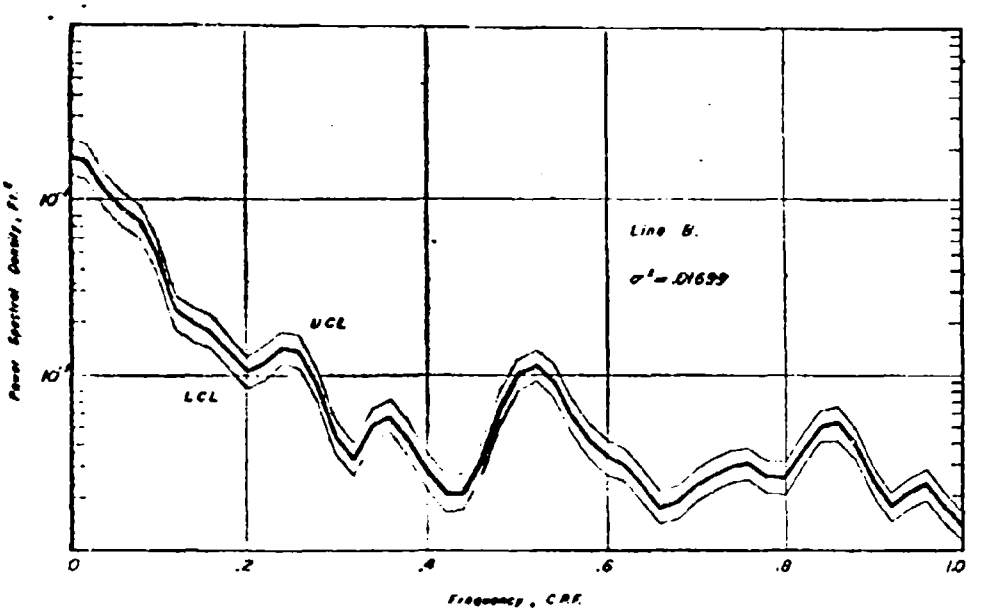

Line B.
$\sigma^2 = .01699$
UCL
LCL
10^1
10^0
0
.2
.4
.6
.8
1.0

Fig. 6.

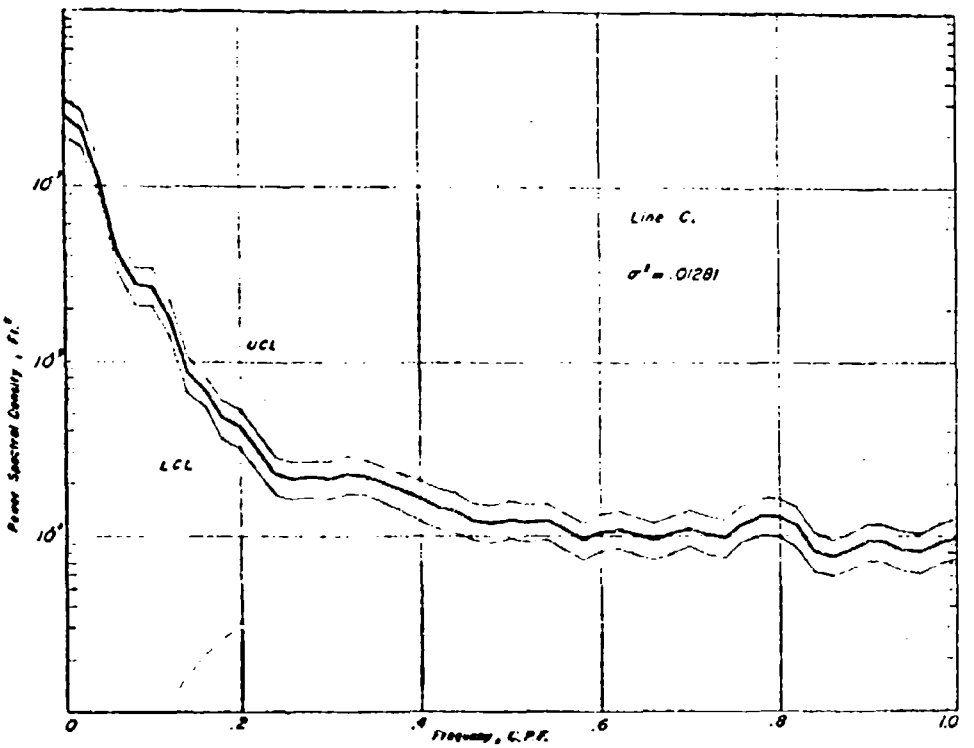

Line C.
$\sigma^2 = .01281$
UCL
LCL
10^1
10^0
0
.2
.4
.6
.8
1.0

Fig. 7.

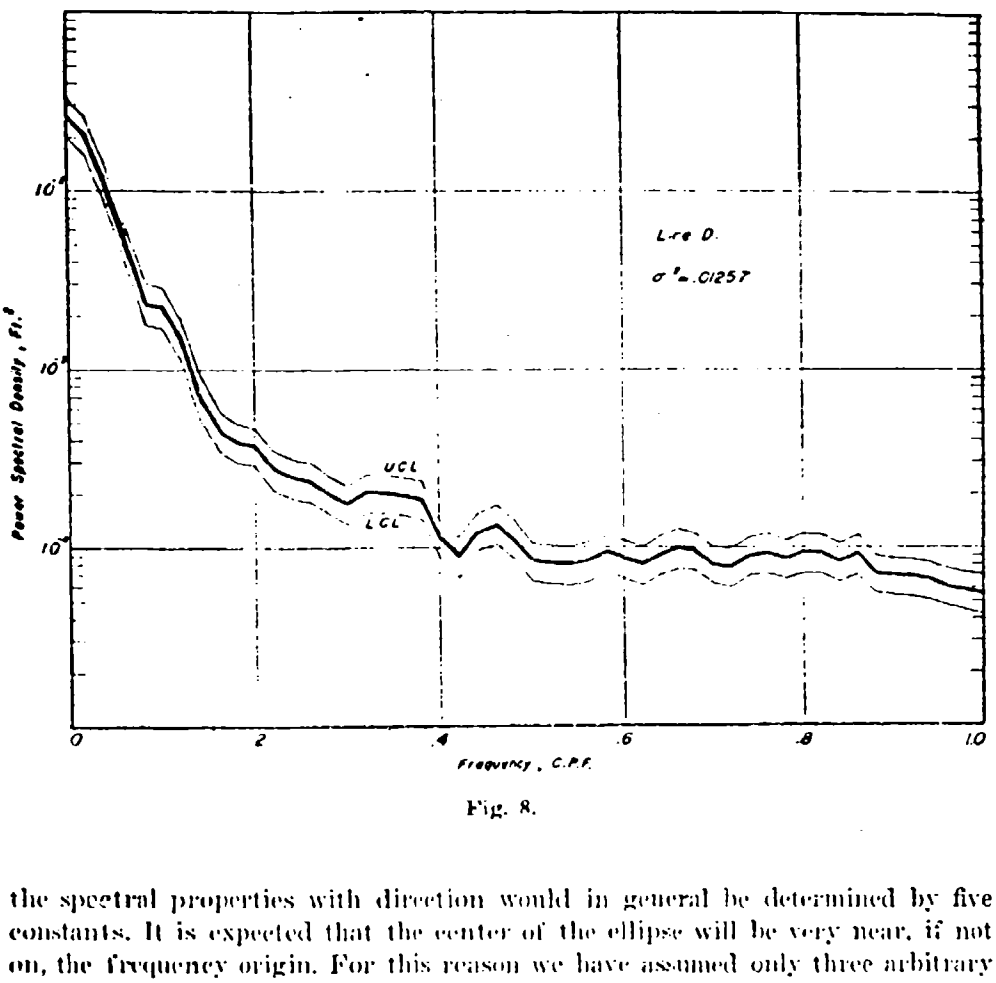


Fig. 8.

the spectral properties with direction would in general be determined by five constants. It is expected that the center of the ellipse will be very near, if not on, the frequency origin. For this reason we have assumed only three arbitrary constants in the previous analysis. However, we shall continue to use five lines for the first few surface surveys.

To obtain the power spectral densities a numerical analysis was performed on the raw data, and programmed for computation on a digital computer. These are presented along with their ninety per cent confidence limits and their variances in figures 5-8. The numerical procedure used on the raw data was first to subtract out least squares parabolic base lines along each contour in order to delete the extremely low frequencies, for these frequencies do not effect the trafficability of vehicles. The resulting data were then analyzed according to the methods of Blackman and Tukey [8].

The method of deleting the very low frequencies is still open to investigation due to the possibility of introducing high frequency components from the points at which the parabolic base lines are connected. This may account for the large power concentrated around 5 cycles/ft. on line B, and on the large

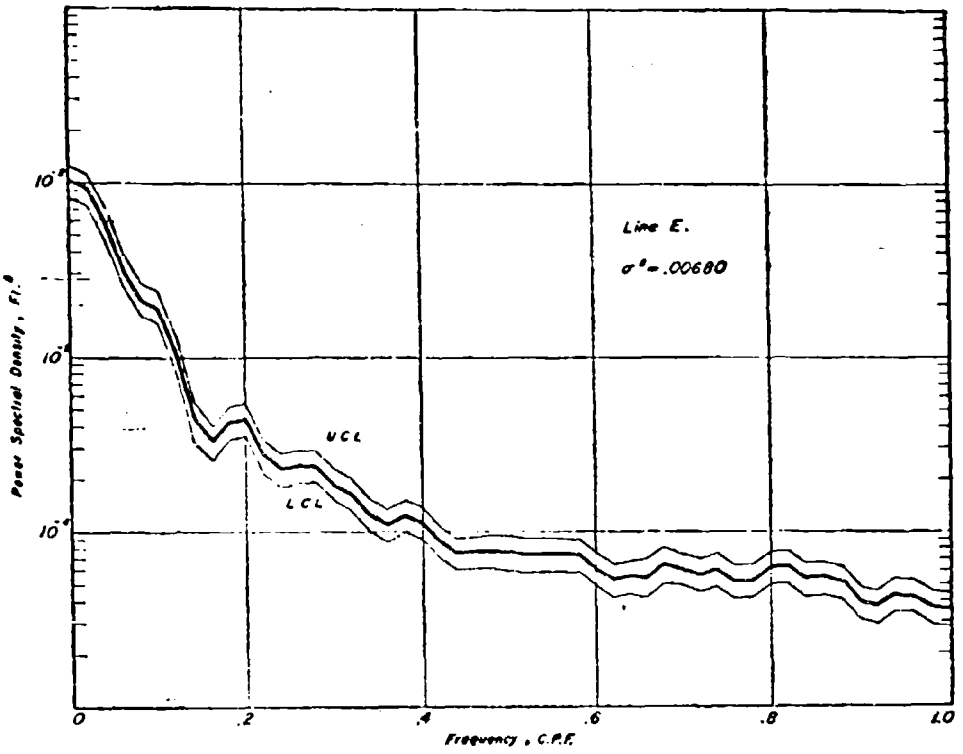


Fig. 9.

variations of the computed variances. Clearly, the base lines must effect these variances.

The complete analysis of these power spectral is presently in progress, therefore it is too early to say whether this data fits the models described previously. Preliminary studies have indicated a change in the functional form to fit the curve at the lower frequencies more faithfully. But since this is intimately connected with the initial data reduction procedures, we cannot make a decision on this point until further studies are performed.

It is our feeling that the future will see the off-road vehicle that will be adaptively controlled to adjust itself to the terrain that it must operate on. The signal that the control mechanism must operate on is derived from those aspects of the ground surface that will be continuously measured, or sampled, and the optimizing criterion that is built into the system. But what aspects of the ground surface contour should be measured remembering that it is a random surface? We feel that this can be answered by studies along the lines presented in this paper. We hasten to add that this is just an initial study of the general problem from the off-road mobility point of view. Therefore while particulars may change, the general philosophy presented will remain fixed.

BIBLIOGRAPHY

1) Bekker M. G. Theory of land locomotion. University of Michigan Press, Ann Arbor, Michigan, 1956.

2) Holoult J. C. et al. On spectral analysis of runway roughness and loads developed during taxiing. NACA Tech., note no. 3484, July, 1955.

3) Bogdanoff J. L. and Kozin F. On the statistical analysis of the motion of some simple vehicles moving on a random track. Report no. RR 20-LL 65, Land Locomotion Laboratory Research Division, Detroit Arsenal, Detroit, Michigan, November 1959.

4) Bogdanoff J. L. and Kozin F. On the statistical analysis of the motion of some simple two-dimensional linear vehicles moving on a random track. Report no. RR 19-LL 65. Land Locomotion Laboratory Research Division, Detroit Arsenal, Detroit, Michigan, April 1960.

5) Pierson W. T. Jr. Wind generated gravity waves, advances in geophysics, vol. 2, Academic Press, New York, 1956.

6) Longuet-Higgins M. S. The statistical analysis of a random moving surface, Phil. Trans. of the Royal Soc. of London, series A, Math. and Phys. Sci., pag. 321, vol. 249, no. 966, February 1957.

7) Rice S. O. Mathematical analysis of random noise. Selected Papers on Noise and Stachastic Processes, Edited by N. Wax, Dover Publications, New York, 1954.

8) Loeve M. Probability theory. Ch. 8, Von Nostrand, New York, 1955.

9) Blackmann R. B. and Tukey J. W. The measurement of power spectra from the point of view of communications engineering. Dover Publications, New York.

DISCUSSIONS

E. SAIBEL. — I too would like to congratulate Prof. Bogdanoff and Kozin for an extremely interesting and important contribution. And I should just like to suggest one direction in which their statistical analysis might be of great help to people who are particularly intersted in off-the-road locomotion, and to some extent, those who are interested in on-the-road-locomotion. That is, the use of the statistics of extreme values. The authors take samples, and from these samples predict statistical distribution of waviness of the surface, local imperfections and so on. But then, I think a statistics of extreme values would supplement this work, in that it could predict major changes from this picture. In other words, the frequency with which one might find crevasses or pits; or, on the road, the frequency with which one might find, holes in the concrete for example. I think between the two one could get an admirable estimation of the terrain, and could predict what could happen as a vehicle moved over it.

R. ARIANO. — Volevo rivolgere semplicemente una domanda ai nostri precedenti oratori, ed è questa: per giudicare del grado di confortevolezza del movimento, dal quale, desumere se la strada è più o meno rugosa — e tra parentesi per misurare la rugosità vi sono appositi apparecchi; io ne ho fatto costruire uno dal mio Istituto —, e me sembra che il metodo più adatto debba essere quello di determinare le variazioni dell'accelerazione in funzione del tempo, che vengono impresse all'individuo. Una accelerazione costante non è disturbante. In nessun altro momento più che in questo in cui abbiamo i voli dei Gagarin e compagni, si può riconoscere che effettivamente

non è l'accelerazione e non è la frequenza quelle che influiscono sul disturbo; lo *fanno* la variazione di tali variabili nel tempo, e la velocità di loro variazione. I nostri studi nel passato su strade ordinarie hanno dimostrato che effettivamente la detta variazione dà un'idea della confortevolezza. Volevo domandare agli illustri relatori se hanno impostato il problema in questo senso, se hanno fatto qualche esperienza, se possono darci degli ordini di grandezza che illuminino qual'è il disturbo veramente disturbante, veramente non tollerabile.

F. KOZIN. — Of course, we ourselves have not been directly concerned with the actual measurements of human discomfort, but I do know of course that for example von Gierke at Wright Field, in Dayton Ohio, has made extensive studies on the discomfort of a man to various frequencies, and this was not necessarily a tonic factor. But as a matter of fact he found two, I think two, significant frequency bands in which there were definite discomforts, and these were associated with the natural frequencies of certain organ levels within the body. Now, that is one thing: you had so many things, questions, Sir, that I cannot remember exactly all of them that were asked. Now, of course, the time-wise accelerations — I think you put forth this particular question. Of course, these accelerations are also random in this case; you see, when we speak about a problem cast in a random, or probabilistic way, we are looking at the average properties. We cannot look at a distinct property because the ground is continually changing. We look at the average properties, so that we can always discuss, and when we are talking of the power spectral densities we are mentioning, or discussing, the average power over these various grounds, within a certain class of random processes. Now I don't know if I have answered any or all of your questions, but.

J. L. BOGDANOFF. — Before answering the question that was just asked, I'd like to comment a moment upon remarks made by Prof. Saibel. The question of the useful extreme value statistics was considered by us at a certain stage in our investigation. However, an amount of information is available as to how extreme value statistics is related to human response; human estimates of the roughness of a ride has not, to my knowledge, been investigated at all. We did not see, at the time we looked at the extreme value problem how we could obtain, or how we could even adopt a posture which would be plausible, and for that reason we dropped the extreme value statistics work. It is possible, when tests are completed on shaking a human under random conditions, that the line of investigation suggested by Professor Saibel will be a useful one; but until then we have nothing further to say on it. And now with regard to the chairman's comment: as I understand it, the question has to do with the rate of change of acceleration. I believe this quantity is referred to as jerk under certain circumstances, or it is referred to colloquially that way in the United States. The methods which we have adopted would apply quite well either to acceleration, third derivative, fourth derivative, any derivatives for which you wish to consider spectral densities, following immediately from spectral densities of input and the transfer functions of the systems involved. But again, there is nothing of a quantitative nature that would enable us to say that a certain third derivative, for example, would be a useful measure of ride roughness. It may be, but there is not sufficient experimental tests on human beings at this time to go along this line of investigation at all.

Does that answer your question, Mr. Chairman?

A. CASTAGNA. — Se mi è consentito vorrei dire che, a mio sommesso avviso, il lavoro dei professori Bogdanoff e Kozin è ammirevole per il criterio informatore del procedimento.

Appare irrilevante che l'ipotesi sulle asperità del terreno posta dagli Autori sia, o meno, proprio la più gravosa agli effetti dell'eccitazione di perturbazioni nel moto del veicolo con riferimento ai riflessi fisiologici sui passeggeri. Ugual cosa può dirsi nei riguardi della schematizzazione del veicolo.

Mi sembra essenziale la caratterizzazione delle asperità del terreno mediante gruppi di famiglie di irregolarità, confuse e cooperanti « a caso » con la soggezione a solo poche o ben fondate limitazioni, espresse mediante il campo dei valori del parametro densità dello spettro di potenza (power spectral density) ma del resto rappresentative di condizioni di terreno estremamente variate; e, naturalmente, stabilite sulla scorta di estese rilevazioni valutate statisticamente; nonchè la considerazione di un pneumatico in contatto col terreno per una certa lunghezza, così da risentire la simultanea azione di tratti più o meno ampi di più irregolarità, similmente ad una condizione media di effettivo esercizio.

Ad una materia così sfuggente gli Autori hanno saputo dare una forma matematica precisa tanto che al problema delicato e difficile della dinamica dell'accoppiamento del veicolo col terreno attraverso il pneumatico hanno saputo dare una chiara soluzione matematica fondata su ipotesi significative.

Qui sta il valore della memoria; e, ritenendo di interpretare anche l'opinione dell'Uditorio, ne porgo agli Autori i più vivi rallegramenti.

V. E. GOUGH. — These papers are very important and, as the Chairman has said, the authors are to be congratulated.

In order to help those whose knowledge is not developped in this necessary from of analysis but who have some knowledge of conventional analysis assuming simple harmonic road surfaces, could the speakers, at some time in the future, make available the conventional analyses of the simplified vehicle they have studied together with the new form of analyses expressed in the statistical terms P.S.D and variance. This may help the assimilation of the new and necessary concepts.

F. KOZIN. — Just two points: first, that we have not limited this strictly to just a mathematical analysis but, indeed, we do have a test facility that is nearly completed at the Land Locomotion Laboratories of the Detroit Arsenal. I believe only instrumentation is the last step to be taken before the test facility is operated. The facility consists of a model vehicle, a wheel base, a four wheel vehicle wheel base, approximately one meter running on a track which is a member function of a process, of a random process, which meets, or is very close to the types of processes that we have found from our surveys of the ground surface. That is one point.

The other point is this: that concerning the last remark, we have indeed considered a simple harmonic road. However, one finds in this case that you do not have a best ride. You find... of course, perhaps we have had to go through these things rather quickly this morning... in the dynamic analysis, using the input power spectral densities, we found that there was a unique set of parameters, wheel bases in this particular case, that gave us a best ride. For the case of the random... that is, of the simple deterministic harmonic case, we have, I do not know if it is... I think it is in this particular report. One find that there is not best ride, but that are many, many at the same level. Thank you.

L. AMICI. — E' al microfono l'Ing. Amici della Società Pirelli di Milano. Noi da circa cinque anni studiamo il pneumatico anche dal punto di vista della trasduzione delle vibrazioni; e per fare questo ci siamo attrezzati con apparecchiature adeguate. Abbiamo poi cercato di riprodurre il comportamento del pneumatico mediante modelli meccanici caratterizzati da alcuni parametri e ci siamo sforzati di riprodurre mediante una macchina calcolatrice analogica il comportamento vibrazionale del pneumatico in marcia. Negli ultimi tempi ci siamo accorti che questi studi sono ben lungi dall'arrivare ad una soluzione e si può dire anzi che ogni giorno si complicano di più invece di semplificarsi. Quindi mi pare che l'ipotesi fatta dall'oratore di un pneumatico molto semplice — ridotto direi ai minimi termini — sia forse un po' troppo lontana dal vero. In sostanza il pneumatico è risuonatore che ha moltissime frequenze proprie ed ha un comportamento diversissimo a seconda del tipo, cioè a seconda della disposizione e della natura delle sue strutture interne.

Quindi io desidererei da parte degli autori che hanno fatto un lavoro evidentemente complesso e ben sviluppato, che ci si limiti a descrivere la strada; poi dopo, al resto, per così dire, ci penseremo noi « pneumaticari ». Cioè a dire: dateci il disotto, — che per noi è molto difficile da avere — e per cui occorrono effettivamente studi molto particolari e grandi energie; poi, dopo per quanto riguarda il di sopra cercheremo di farlo insieme.

A. CASTAGNA. — Se mi è lecito esprimere il mio avviso su quanto ha detto l'Ing. Amici, e con licenza dei Prof. Kozin e Bogdanoff, mi permetterei di soggiungere che, mentre è comprensibile che lo studioso del pneumatico chieda la definizione matematica del terreno con le sue irregolarità, non sembra lecito separare le due parti.

Chi provvede la forma matematica del terreno deve tenere presente che essa è destinata allo studio della dinamica dell'accoppiamento col pneumatico. Il solo esame statistico delle asperità in se stesse, astraendo da tale considerazione, non è sufficiente.

Si tratta pertanto di dare l'espressione matematica della geometria di un terreno accettabile e realistico, e ciò naturalmente con riferimento al fatto che un pneumatico deve percorrerlo.

Bisogna d'altra parte ricordare che la sostanza delle memorie di Bogdanoff e Kozin non è limitata dalla scelta di un tipo particolare di pneumatico e di una elementare forma di terreno. Le asperità previste sono di forma ampiamente generalizzata; ed è pure notevole l'ipotesi dell'appoggio esteso del pneumatico. Da rilevare infine il non semplice sviluppo matematico della trattazione.

N. 17

The steering and drawbar-pull performance of pneumatic-tired vehicles *)

Sterzatura e caratteristiche di trazione alla barra dei veicoli su pneumatici

D. C. CLARK **) - L. SEGEL ***)

ABSTRACT. — *An analysis is made of the steering and drawbar-pull performance of a tractor-trailer combination consisting of a two-axle, pneumatic-tired tractor towing a single-axle, pneumatic-tired trailer. The analysis is valid only for a restricted range of lateral accelerations, since it is based on closed-form solutions obtained from an approximate theory. Calculations have been made to determine:*

1) the influence of towed load, steer configuration, and stability margin on the location of the turn center of the vehicle as a function of thrust;

2) the influence of towed load, steer configuration, and stability margin on the thrust-speed relationship in a steady turn.

3) the influence of stability margin on the thrust-speed relationship for a tractor, without a towed load, negotiating curved paths of constant turn radius; and

4) the incremental horsepower required in a turn versus velocity, as a function of steering geometry, stability margin, and drawbar pull.

The calculations show that, for a given level of available horsepower, the speed will decrease markedly in a turn or, conversely, a large horsepower increment is required to maintain speed in a turn due to an «induced drag» created by the longitudinal component of the centrifugal acceleration vector.

Introduction. — Heretofore, the attention of the researcher in land locomotion has been focussed upon the task of maximizing the drawbar-pull or load-carrying capacity of cross-country vehicles. Existing theoretical analyses and experimental measurements have been concerned almost entirely with straight-line vehicle motions and have, in large part, neglected the tractive performance of vehicles moving in a curved path. At the present time, a vehicle designer has no means of predicting vehicle performance in a turn as a function of a particular steer geometry, towed-load geometry, suspension-roll properties, or propulsion configuration (viz.: front, rear, or four-wheel drive). It is postulated that the ability to make such a prediction should be a valuable tool in the vehicle evaluation and design process.

Consider the tractor and trailer element pictured in fig. 1. It can be noted that the drawbar pull created in the towing linkage by a given level of tractive

---

*) This paper was originally prepared for Land Locomotion Laboratory, U.S. Army Ordnance Tank Automotive Command, Detroit, Michigan.

**) Associate Research Engineer Vehicle Dynamics Department Cornell Aeronautical Laboratory, Inc.

***) Assistant Department Head Vehicle Dynamics Department Cornell Aeronautical Laboratory, Inc.

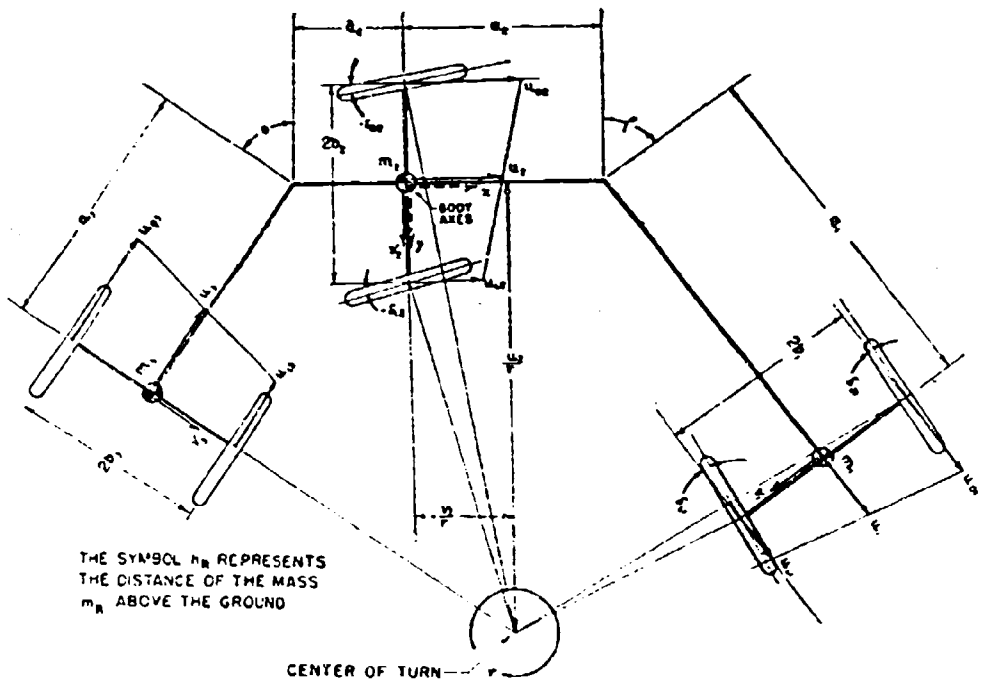


Fig. 1. — Plan view of tractor-trailer showing geometry and velocities for combined Ackermann and articulated steering.

effort applied at two or more wheels is affected not only by path curvature but also by geometrical factors that control the angle at which the towed load trails the tractor. If it is assumed that the towing hinge is a free pivot that supports no moment, then the towed load must align itself in such manner that the moment about the hinge will always be zero. It is thus seen that the centrifugal acceleration produced in the turn will have a bearing on the resultant trailer angle, since it will be necessary for the tires supporting the trailer mass to produce side forces in order to maintain the specified equilibrium condition.

In essence, the above statements emphasize the fact that drawbar pull has *directional* properties when a tractor vehicle is negotiating a turn. Evaluation of the drawbar-pull and speed performance of a towing vehicle, therefore, cannot proceed without knowledge of the geometric configuration of the towed load. By the same token, it is necessary to define the geometry of the towing vehicle, as well as the existing steer configuration and the wheel locations at which driving thrust is applied in order to produce forward locomotion.

It is apparent that tractive performance during the turning process is a function of the form of the locomotion element (i.e., wheel or track) and the characteristics of the supporting soil. In view of the lack of data on the mechanics of wheels and tracks yawing and sideslipping in deformable soils,

the analysis presented herein deals only with pneumatic-tired vehicles turning on a flat, nondeformable surface. Efforts are currently under way to describe the turning behavior of an articulated track-laying tractor towing a wheel-supported towed load.

The detailed derivation of the equations of equilibrium defining the force and moment balance that must exist in a steady turn is straightforward, but the equations themselves are numerous and rather involved. Since the conclusions to be presented in this paper are based on solutions yielded by a simplified theory, the derivation of the exact equations will only be indicated, together with a listing of pertinent assumptions and restrictions. The solutions obtained from an approximate theory (relying primarily on the validity of treating tires as a linear force producing element for a restricted range of slip angles) are compared with results obtained in earlier studies[1,2] of automotive steering behavior. The accuracy of these approximate solutions is evaluated by comparing both approximate and exact predictions of tractor-trailer turning performance. Use is made of the approximate solutions to perform a brief parametric study indicating the manner in which tractive performance is influenced by basic vehicle parameters such as steer configuration and stability margin.

Equations of equilibrium. — The equations of equilibrium express the force and moment balance that must exist in a steady-state turn. Forces must be generated both in the ground plane and perpendicular to the ground plane in order to balance the centrifugal forces and moments arising from the presence of path curvature. The forces in the ground plane derive from the tire-ground interface and consist of:

1) the tractive efforts produced by driving torques generated by the vehicle power plant, and

2) the side forces that act perpendicular to the center plane of the tire when the tire has a lateral component of velocity relative to the ground.

Since previous investigators have shown that the lateral (or side) force produced by a tire is a function of the angle which the velocity vector of the tire makes with the tire center plane, it is necessary that kinematic relations be written to yield the slip angle of each tire as a function of the motion variables of the vehicle and the angular displacements that are used for purposes of steering. The tire side forces are also a function of the vertical load on the tire and the tractive effort being generated in the plane of the tire. Note also that the vertical load on the tire will change from its zero speed value because of load transfer produced by (1) the finite height of the center of gravity above the ground plane, (2) finite vehicle width, and (3) the centrifugal acceleration vector. In summary, the equations of equilibrium of the four-degree-of-freedom system can be expressed symbolically as:

$$\text{Tractor:}\quad \Sigma X = \Sigma Y = \Sigma M = 0 \qquad (1)$$

$$\text{Trailer:}\quad \Sigma M_{\text{hinge}} = 0 \qquad (2)$$

where Y, X, and M are forces and moments in the ground plane acting on the tractor, expressed in terms of the body axes shown in fig. 1;
and ΣM_{hinge} is the moment about the towing hinge.

The pneumatic tire slip angles are given by:

$$\alpha_{jk} = \arctan\left(-\frac{v_k}{u_{jk}}\right) - \delta_{jk} \; ; \qquad \begin{matrix} j = 0, i \text{ *} \\ k = 1, 2, 3 \end{matrix} \tag{3}$$

where α_{jk} is the slip angle of each tire.

$$u_{jk}, v_k = f(u_2, v_2, r, \Theta, \rho) \tag{4}$$

$$Z_{jk} = f(m_k, b_k, h_k, a_k, r) \tag{5}$$

where Z_{jk} is the vertical load on each tire.

$$\overline{Y}_{jk} = f(C_{jk}, \alpha_{jk}, \overline{X}_{jk}, Z_{jk}, \mu) \tag{6}$$

where

$\overline{Y}_{jk}$ is the force on each tire perpendicular to its center plane,

$$C_{jk} = -\lim_{\alpha_{jk} \to 0} -\left(\frac{\delta \overline{Y}_{jk}}{\delta \alpha_{jk}}\right)$$

$\overline{X}_{jk}$ is the tractive effort in the tire plane, μ is the coefficient of friction between tire and ground, and the remainder of the symbols used in equations (1) through (6) are defined in fig. 1.

It should be noted that equation (6) of the above set of equations is the key relationship that ultimately determines the turning behavior of the tractor-trailer vehicle under consideration. This equation represents the *tire mechanics* of the complete vehicle system and, as such, defines the manner in which forces are created to hold the vehicle in the turn. In the above nonlinear equations, the functional relationship indicated in equation (6) can be represented by a mathematical function derived by Fiala [5], as later modified [4], to account for the effects of longitudinal thrust by application of the « friction circle » concept **).

Figure 1 is a plan view of a generalized tractor-trailer vehicle of unspecified geometry, steering configuration and thrust-input location to which equation (1) through (6) apply. Note that the total mass of the tractor is divided into two portions, each portion assumed to have its center of gravity (cg) above its respective axle location. If the front and rear masses are sized according to the location of the cg of the total mass, then the centrifugal force vectors associated with each separate mass will sum vectorially to equal the centrifugal

*) The subscripts 0 and i relate to outer (left hand) and inner (right hand) for a right turn. The subscripts k are 1, 2 and 3 representing the front and rear sections of the tractor, and the trailer, respectively.

**) The friction circle concept assumes that the maximum tire reaction force in the horizontal ground plane is limited to the friction coefficient-vertical load product.

force vector produced by the total mass at the cg of the total mass. This technique of separating the total mass into two equivalent masses proves to be particularly convenient in deriving the centrifugal force terms in the equations.

To summarize, the following assumptions are made in writing equations (1) through (6):

1) The tractor-trailer vehicle turns on a nondeformable level surface possessing isotropic Coulomb-friction properties.

2) A total of four degrees of freedom are considered, namely:
   a) two translational degrees of freedom of the tractor,
   b) one rotational degree of freedom of the tractor, and
   c) one rotational degree of freedom of the trailer relative to the tractor.

3) The tractor and trailer are rigid bodies with fixed center of gravity locations.

4) Motion resistance created at the tire-ground interface is independent of vehicle velocity.

5) Vertical tire loads are independent of the longitudinal component of centrifugal acceleration.

6) The drawbar hitage is frictionless; i.e., it does not resist motions of the trailer relative to the tractor.

7) The combined vehicle moves in a constant-speed, constans-radius right-hand turn with the turning center always to the right of the inner (right) tires.

8) The independent variables are steering input, δ_{jk} or ρ, and thrust, $\overline{X}_{jk}$, in the plane of the tire.

Solution of simplified approximate equations. — It is possible to obtain a solution of equations (1) through (6) to yield u_z, v_z, r, and Θ as a function of the independent variables, δ_{jk}, ρ, and $\overline{X}_{jk}$, by means of an iterative solution technique. An extensive parameter study to determine speed-thrust relationships as a function of tire properties, vehicle geometry, steer configuration, and drive configuration is quite feasible if machine computing methods are used. Programming of these equations for solution on a Datatron 204 computer has been accomplished but, since the objective of this paper is to implement a physical understanding of the vehicle turning process, attention will be directed primarily to the closed-form solutions that can be derived when equations (1) through (6) are appropriately simplified.

In addition to the usual simplification achieved by assuming all angles sufficiently small such that $\cos\gamma = 1$, $\sin\gamma = \gamma$, and $\tan\gamma = \gamma$, two additional assumptions are made to assist in simplifying the problem. The first assumption is that the width of the vehicle is small in relation to its radius of turn. This assumption permits collapsing the vehicle to a zero width such that the subscript, j, to denote inner or outer wheels, disappears. The second, and major, assumption is that equation (6) can be replaced by

$$\overline{Y}_k = -C_k \alpha_k \qquad (7)$$

where C_k is the tire constant that is commonly referred to as « tire-cornering stiffness » or tire « cornering power ». Note that C_k represents the combined cornering stiffness of the right and left tires on each axle. The above three steps lead to a set of simplified equations from which it is possible to derive the below tabulated solutions for the yawing velocity, r, and the location of the turn center from the vehicle x axis and ahead of the rear axle, a_2/r and v_2/r, respectively, as a function of the thrust, $\bar{X}_k$, and the steer angle δ_k, or the articulation angle, ρ. It is convenient to write these solutions separately for the Ackermann and articulated steering cases. Thus:

Ackermann steering

$$r = \sqrt{\frac{(\bar{X}_1 + \bar{X}_2 + \bar{X}_3)\ (\delta_1 - \delta_2)^2}{(m_1 + m_2 + m_3)\ \left(\frac{m_2}{C_2}\ \delta_1 - \frac{m_1}{C_1}\ \delta_2\right)\ \lambda^2}} \tag{8}$$

$$\frac{a_2}{r} = \frac{\lambda}{\delta_1 - \delta_2}\left[1 + \frac{\lambda}{(\delta_1 - \delta_2)^2}\left(\frac{m_1}{C_1} - \frac{m_2}{C_2}\right) r^2\right] \tag{9}$$

$$\frac{v_2}{r} = \delta_2\left(\frac{a_2}{r}\right) - \frac{m_2}{C_2}\left(\frac{a_2}{r}\right)^2 r^2 \tag{10}$$

Articulation steering

$$r = \sqrt{\frac{(\bar{X}_1 + \bar{X}_2 + \bar{X}_3)}{\left(\frac{m_1^2}{C_1} + \frac{m_2^2}{C_2} + \frac{m_3^2}{C_3}\right)\left(\frac{\lambda}{\rho}\right)^2}} \tag{11}$$

$$\frac{a_2}{r} = \frac{\lambda}{\rho}\left[1 + \frac{\lambda}{\rho^2}\left(\frac{m_1}{C_1} - \frac{m_2}{C_2}\right) r^2\right] \tag{12}$$

$$\frac{v_2}{r} = -\frac{m_2}{C_2}\left(\frac{a_2}{r}\right)^2 r^2 \tag{13}$$

Note that equations (8) through (10) hold for either front- or rear-wheel Ackermann steering, as well as for steering the front and rear wheels simultaneously. For right turns, δ_1 and ρ are always positive angles and δ_2 is always a negative angle. If rear-wheel steering is assumed to be zero (i.e., $\delta_2 = 0$), it is seen that equations (9), (10), (12), and (13) are identical in form, which result states that, for small angles, articulation steer is equivalent to front-wheel Ackermann steer. The above equations yield the yawing velocity in the turn,

the distance of the turn center from the X axis (longitudinal axis) of the vehicle, and the distance of the turn center from the y axis (lateral axis) in that order. Figure 1 shows these distances clearly. In addition to the input variables, $\overline{X}_k$, δ_k, and ρ, three vehicle parameters appear; namely, vehicle mass, tire cornering stiffness, and vehicle wheel base.

The most significant result obtained from solution of the simplified, linearized equations of equilibrium is the relationship between yawing velocity and input thrust, expressed by equations (8) and (11). In essence, these equations yield the incremental thrusts that must be provided, over and above the thrust values needed to maintain constant velocity in straight-line motion, when the vehicle is put into a turn by means of a steering input, δ_k or ρ. For a fixed value of steer angle, the yawing velocity in a turn increases as the one-fourth power of the tractive effort. The physical explanation of this theoretical result derives from the manner in which pneumatic tires produce the side forces required to hold the vehicle in the turn against the action of centrifugal force. Since the tires must operate at a slip angle, the entire vehicle must assume an attitude angle with respect to its velocity vector and accordingly, in a turn, there exists a component of centrifugal force along the x axis of the vehicle, in the negative or rearward direction. This centrifugal force component constitutes, in effect, an « induced drag » that does not exist for straight-line motion. The question naturally arises as to whether there are vehicle design features that have a significant bearing on the level of the drag that is induced in a turn. This question is particularly pertinent when a tractor is used to tow a trailer that has a sizeable mass as well as a given level of rolling resistance or drag in straight-line motion.

Equations (9), (10), (12), and (13) shed additional light on the phenomenon of turn-induced drag, since they yield the locus of the turn center as a function of the yawing velocity of the vehicle. Equations (10) and (13) demonstrate that the turn center must move forward, relative to the y axis location in the tractor, as speed is increased in the turn. With increasing forward movement of the turn center, the component of centrifugal acceleration along the longitudinal (i.e., x) axis of the tractor becomes a retarding force of significant magnitude.

Equations (9) and (12) yield the y location of the turn center; i.e., the perpendicular distance from the x axis of the tractor to the center of the turn. In effect, u_2/r is approximately equivalent to the radius of turn, and equation (9) constitutes a restatement of the relationship between turning radius and various vehicle parameters that has been derived previously in investigations of the stability and control of automotive vehicles[2]. It should be noted that the quantity $m_1/e_1 - m_2/e_2$ is positive when the vehicle has a positive stability margin as defined in reference 2. If the terminology of « understeer » and « oversteer » is used to designate vehicles with positive and negative stability margins, respectively, equations (9) and (12) show that the distance from the turn center to the x axis of the tractor increases with increasing speed for an understeer vehicle and vice versa for an oversteer vehicle.

The turning performance of a hypothetical tractor-trailer vehicle. — Before proceeding to examine the turning behavior of an assumed tractor-trailer combination with the aid of equations (8) and (13), some consideration should be given to indicating the degree to which the solutions of the approximate theory agree with the results yielded by equations (1) through (6). Fig. 2 shows a comparison between « exact » and linearized theory, where the calculations have been based on the tractor-trailer vehicle specified in table 1. Shown

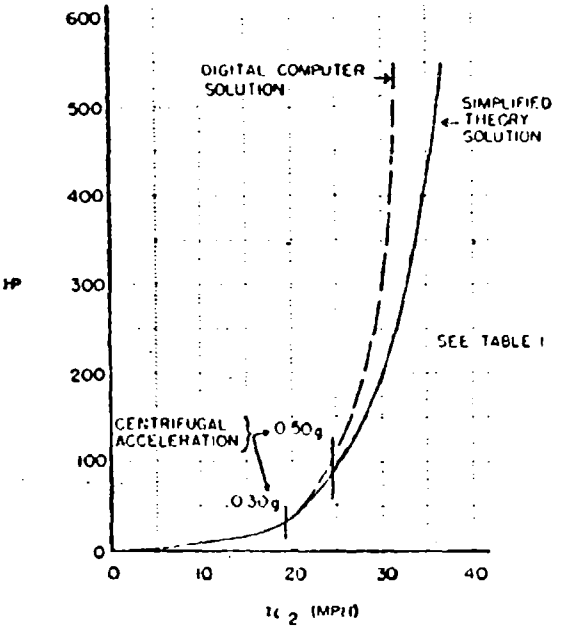


Fig. 2. — Incremental horsepower required in a turn produced by a fixed-steering displacement vs. Forward velocity.

plotted are the incremental horsepower required in a turn produced by a steer angle, $\delta_1 = 10.37$ degrees *), as a function of the velocity, u_2, along the longitudinal axis of the tractor. It can be observed that the difference in the two solutions is practically nonexistent at centrifugal accelerations below 0.3 g and that the difference is still not appreciable at 0.5 g. For the assumed vehicle, approximately thirty additional horsepower are required to turn at 0.3 g lateral acceleration and approximately one-hundred additional horsepower at 0.5 g.

Figures 3 through 11 have accordingly been plotted on the basis of calculations using equations (8) through (13). It should be realized that the trends shown become qualitative in nature for centrifugal accelerations above 0.5 g.

---

*) $\delta_1 \triangleq \frac{1}{2}(\delta_{w1} + \delta_{w1})$.

Note that the incremental thrust, T, shown plotted on these figures, is defined as:

$$T = \bar{X}_1 + \bar{X}_2 + \bar{X}_3 \tag{14}$$

The term « incremental » is used to designate that the thrust, T, is the additional thrust required to maintain a given velocity and path curvature over and above any straight-ahead motion resistance.

TABLE 1. — *Ackermann steering solution for curves of figure 2.*

Digital computer parameters		Equivalent narrow vehicle simplified equation parameters	
δ_{01}	10 deg.	δ_1	10.37 deg.
δ_{11}	10.74		
C_{01}	24,700 lb/rad	C_1	49,400 lb/rad
C_{11}	24,700 lb/rad		
C_{02}	24,700 lb/rad	C_2	49,400 lb/rad
C_{12}	24,700 lb/rad		
C_{03}	26,700 lb/rad	C_3	53,400 lb/rad
C_{13}	26,700 lb/rad		
$\bar{X}_{01}$	Input independent	$\bar{X}_1$	Input independent
$\bar{X}_{11}$	variable		variable = $\bar{X}_{01} + \bar{X}_{11}$
$\bar{X}_{02}$	Input independent	$\bar{X}_2$	Input independent
$\bar{X}_{12}$	variable		variable = $\bar{X}_{02} + \bar{X}_{12}$
$\bar{X}_{03}$	— 100 lb	$\bar{X}_3$	— 200 lb
$\bar{X}_{13}$	— 100 lb		

In addition, the following quantities were assumed:

$m_1 = m_2 = 248$ slugs
$m_3 = 310$ slugs
$h_1 = h_2 = h_3 = 0.5$ ft
$a_1 = a_2 = 7.5$ ft
$\bar{a}_2 = 2.0$ ft
$a_3 = 10$ ft
$b_1 = b_2 = b_3 = 3.0$ ft
$\mu = 1.0$
$g = 32.2$ ft/sec^2

It is believed that considerable insight into vehicle-turning behavior can be obtained by referring to figures 3 through 11. The effects on vehicle behavior of the stability margin and the presence or lack of a towed load, as well as the method of steering, are highly significant quantities to be evaluated. Accordingly, it was decided to select a set of parameters for a reasonable vehicle configuration and evaluate the steering, stability, and drawbar-pull effects upon the location of the turning center, the thrust-speed relationship, and the incremental horsepower-speed relationship. Table 2 indicates the eighteen cases that were considered (three steering methods, three stability margins, and two drawbar-pull configurations) and defines « case » numbers that appear on the figures. The actual parameter values for each case can be determined from tables 3 and 4.

Figures 3 and 4 describe the influence of centrifugal acceleration on the location of the turning center. The figures are plotted to scale with the vehicle shown at the top and the turn center locus shown at the bottom with net thrust as a parameter. Note that the location of the turning center always moves

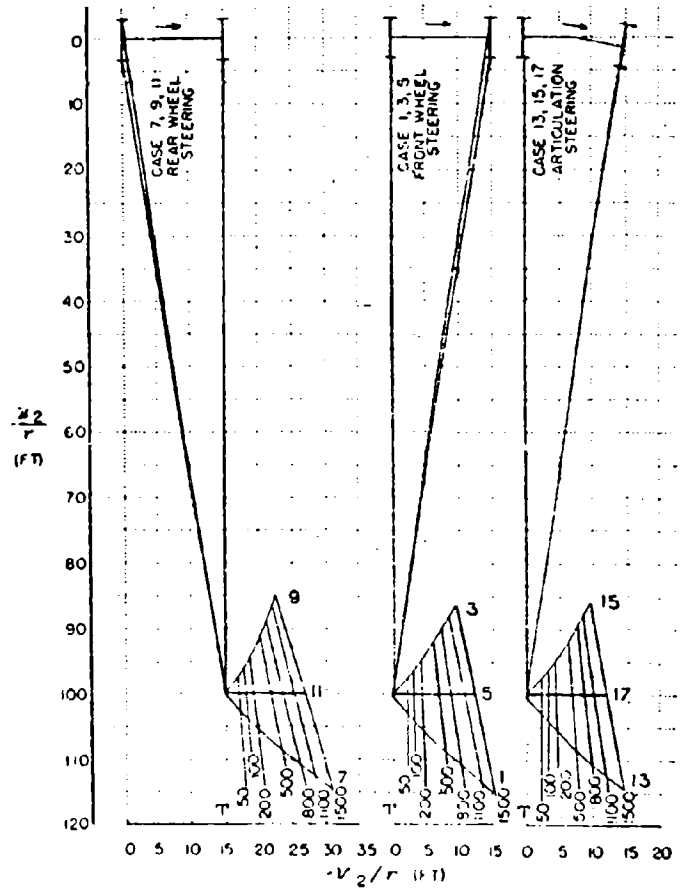


Fig. 3. — Turn center location for three steering geometries as a function of input thrust-no drawbar load.

forward with thrust (or speed). This is because of the previously discussed necessity of generating negative slip angles to create positive side forces to hold the vehicle in the turn. This result obtains for all cases. When the stability margin is positive (or understeer), the location of the net side force vector is aft of the location of the tractor cg, resulting in a yawing moment that tends to steer the vehicle out of the turn, thus increasing the turn radius. A zero value of stability margin requires the net side force vector to be coincident with

TABLE 2. — *Key to vehicle configurations (see figures 2-6, 8-10).*

Case	Steering geometry	Stability margin	Drawbar load
1	Front wheel	+	without
2	Front wheel	+	with
3	Front wheel	—	without
4	Front wheel	—	with
5	Front wheel	0	without
6	Front wheel	0	with
7	Rear wheel	+	without
8	Rear wheel	+	with
9	Rear wheel	—	without
10	Rear wheel	—	with
11	Rear wheel	0	without
12	Rear wheel	0	with
13	Articulated	+	without
14	Articulated	+	with
15	Articulated	—	without
16	Articulated	—	with
17	Articulated	0	without
18	Articulated	0	with

TABLE 3. — *Assumed vehicle parameter values (width effects neglected).*

Cases		Neutral steer tractor 5, 6, 11, 12, 17, 18	Oversteer tractor 3, 4, 9, 10, 15, 16	Understeer tractor 1, 2, 7, 8, 13, 14
a_1	ft	7.5	8.5	6.5
a_2		7.5	6.5	8.5
a_3		2.0	2.0	2.0
a_4		10.0	10.0	10.0
m_1		248	214	282
m_2	slugs	248	282	214
m_3		310	310	310
C_1		49,400	46,600	51,400
C_2	lb/rad	49,400	51,400	46,600
C_3		53,400	53,400	53,400

TABLE 4. — *Steering inputs-degrees.*

Steering geometry	δ_1	δ_2	ρ
Front wheel	8.6	0	0
Rear wheel	0	8.6	0
Articulated	0	0	8.6

the cg such that no yawing moment is generated in a turn, thus causing the turn center to remain a constant distance from the center line of the vehicle. The oversteer, or negative stability margin, cases create a positive yawing moment in the turn due to the net side force vector lying ahead of the cg. The

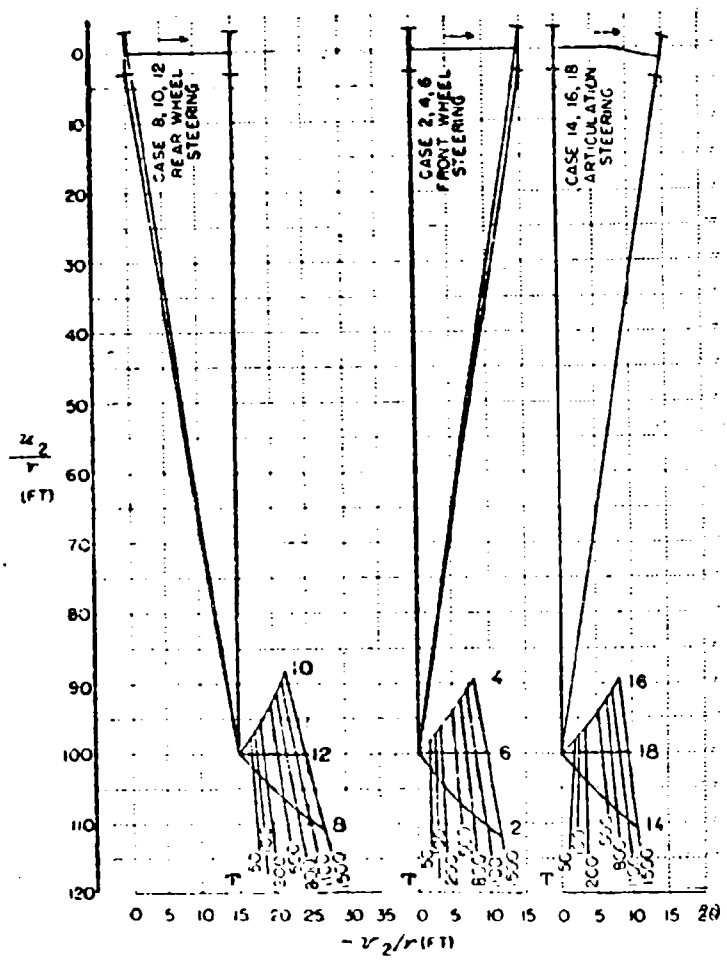


Fig. 4. — Turn center location for three steering geometries as function of input thrust-with drawbar load.

positive yawing moment tends to tighten the turn, or reduce the turn radius. The curves shown as figures 3 and 4 are the same on each figure for the same steering configuration. Note that a given amount of thrust modifies the turn center location of the tractor-trailer combination less than the tractor alone. This is because the centrifugal acceleration generated at a given thrust is less with a drawbar-load because of the reduced speed resulting from the thrust increment required to tow the load. No significant advantage of one steering method over another is evident from the figures.

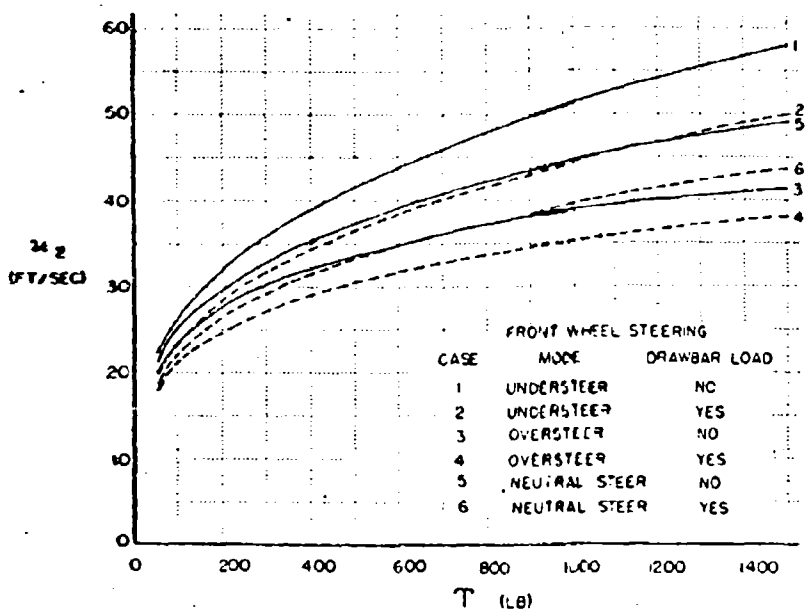


Fig. 5. — Forward velocity vs. Total driving thrust for three stability margins; with and without drawbar load-front wheel Ackermann steering.

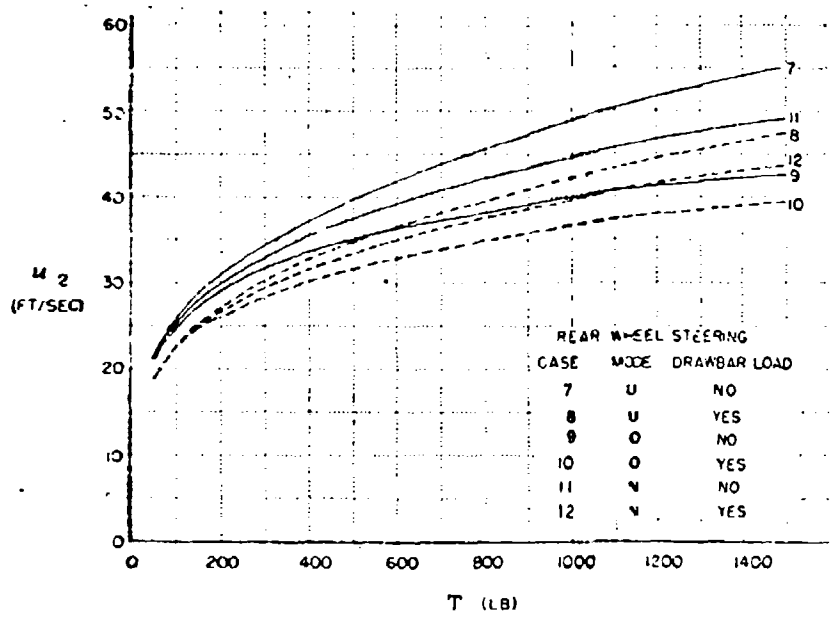


Fig. 6. — Forward velocity vs. Total driving thrust for three stability margins; with and without drawbar load-rear wheel Ackermann steering.

Figures 5, 6 and 7 show the manner in which forward velocity, u_2, varies with incremental thrust, T, required in a turn (steering displacement held fixed) as a function of stability margin and presence of a towed load for front-wheel steering, rear-wheel steering and articulation steering, respectively. On examination of a typical plot, e.g., fig. 5, it is seen that, to maintain a speed of 30 ft/sec at a steer angle, $\delta_1 = 8.6$ deg., incremental thrusts will be required ranging from 160 lbs (approximately), for the understeer tractor,

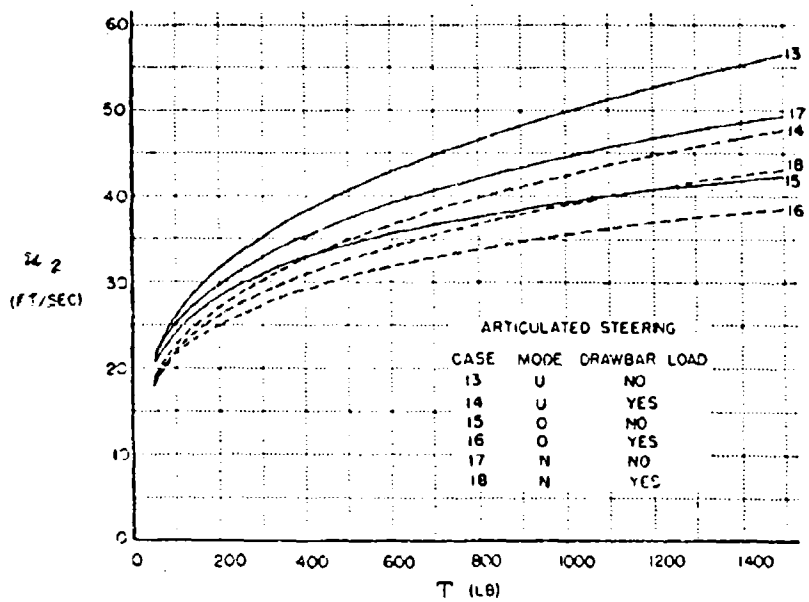


Fig. 7. — Forward velocity vs. Total driving thrust for three stability margins; with and without drawbar load-articulated steering.

without a trailer, to 460 lbs (approximately) for the oversteer tractor pulling the specified trailer. For the rear-wheel steering configuration, the incremental thrust required (for $u_2 = 30$ ft/sec and $\delta_2 = -8.6$ deg.) ranges from approximately 180 lbs to 400 lbs with the minimum thrust requirement again existing for an understeer vehicle without trailer and the maximum thrust requirement for the oversteer tractor with trailer. The results plotted in fig. 7 for the articulated steer configuration are very similar to the results shown in fig. 5 for the front-wheel steer configuration.

The computations discussed above have the disadvantage that they apply to a fixed value of steering input with the result that the path curvature or radius of turn is changing continually with speed as a function of the stability margin. By crossplotting a suitable set of calculations, it is possible to derive curves similar to those shown in figures 5 through 7, except that path curvature or turn radius is held fixed instead of steer angle. This procedure permits

drawing conclusions about the influence of stability margin on thrust requirements in a turn for locomotion operations as they would occur in practice. Fig. 8 shows that a front-wheel steering tractor without a towed load turning at 30 ft/sec on a 100 ft radius has an incremental thrust requirement ranging

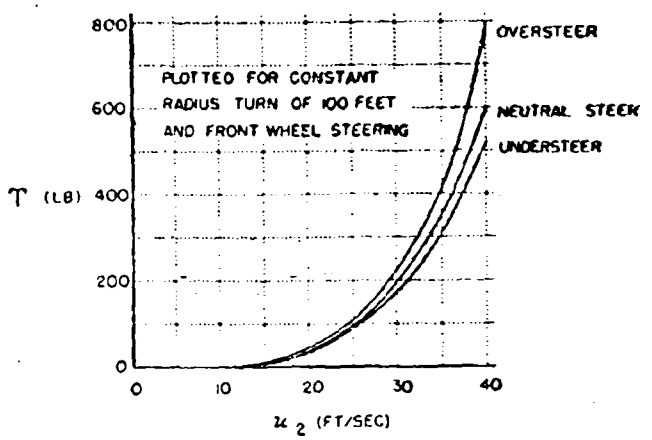


Fig. 8. — Thrust required to maintain a one-hundred foot, constant-radius turn as a function of forward velocity for three stability margins.

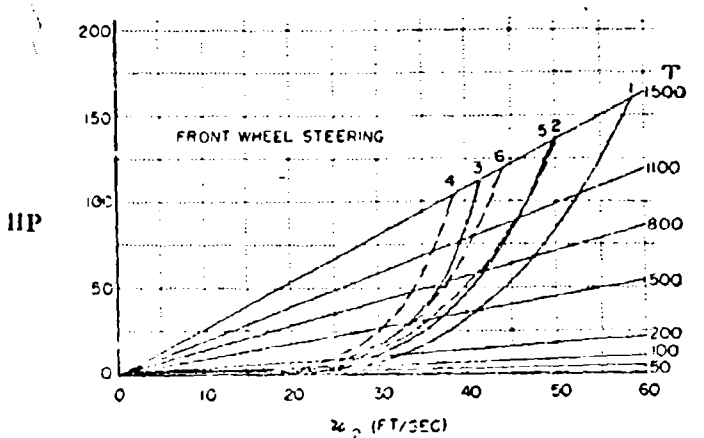


Fig. 9. — Power required to maintain a constant velocity in a turn for three stability margins; with and without a towed load-front wheel Ackermann steering.

from 175 lbs to 220 lbs for the levels of stability margin assumed in these calculations. It should be observed that an oversteer vehicle requires more driving thrust than the understeer vehicle.

The incremental horsepower required to maintain a constant-speed, constant-steer angle turn is shown for the eighteen combinations of stability margin, steering geometry, and drawbar-pull in figures 9 through 11. The most significant

feature to be noted in these figures is the rapid increase in power requirements with *speed* for all eighteen cases. As previously noted, this is caused by the forward motion of the turning center and the consequent, rearward component

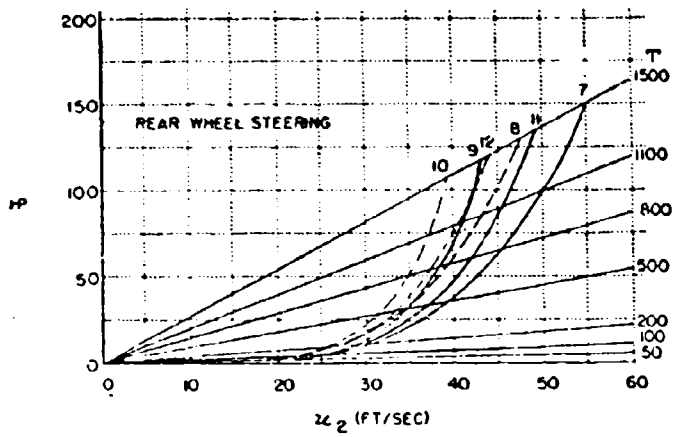


Fig. 10. — Power required to maintain a constant velocity in a turn for three stability margins; with and without a towed load-rear wheel Aekermann steering.

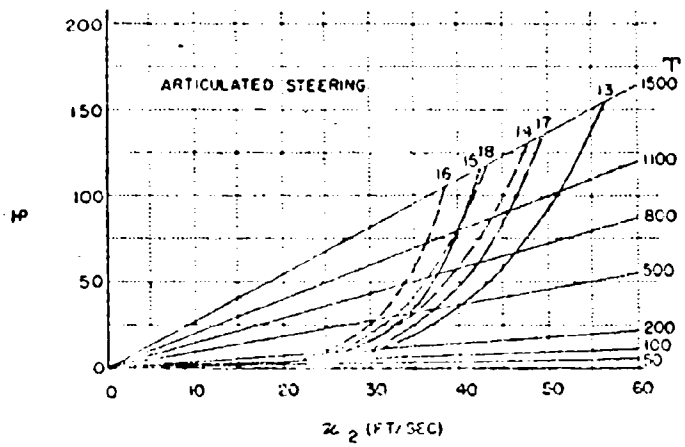


Fig. 11. — Power required to maintain a constant velocity in a turn for three stability margins; with and without a towed load-articulated steering.

of centrifugal force, or induced drag. It is apparent that, for the assumed vehicle, speeds up to thirty feet per second can be realized at horsepower increments of twenty-five or less. Further increases in speed cause drastic increments in power for all cases.

It is significant that the simplified theory does not indicate that any one steering method has any advantage over any other, with respect to power

requirements. On the other hand, the « exact » theory, which retains the significant nonlinearities due to tire behavior, shows that it is necessary to consider the distribution of power, steering, and load transfer to all four wheels of the vehicle at high centrifugal accelerations. Consequently, it cannot be stated categorically that the method of steering has no influence whatsoever on the steady-state turn performance of a pneumatic-tired vehicle, even though the simplified theory says that speed-horsepower relationships in a turn are not influenced by steering geometry.

Concluding remarks

1) For centrifugal accelerations below 0.5 g, the thrust required to overcome the induced drag in a turn increases as the fourth power of the velocity of the vehicle.

2) The turn center of a pneumatic-tired vehicle always moves forward with increasing velocity and moves out (or away) from and in towards the vehicle depending on whether the stability margin is positive or negative.

3) A towed load or drawbar-pull requirement will necessitate additional thrust to be provided by a tractor in a turn, which thrusts will be primarily a function of the mass of the towed load rather than a function of its straight-motion resistance.

4) For a turn of constant radius, an oversteer vehicle will require more incremental thrust versus velocity than will be required by an understeer vehicle, over the range of velocities or centrifugal acceleration for which the derived, simplified theory is valid.

5) For a restricted range of centrifugal acceleration, steering geometry has no influence on speed-thrust relationship in a turn.

ACKNOWLEDGMENT. — The Authors acknowledge, with many thanks, the support of both the Land Locomotion Research and Dynamic Simulations Laboratories, U. S. Army Ordnance Tank-Automotive Command, in the performance of the research leading to results described herein. In particular, acknowledgment is made to Mr. F. Pradko for permission to publish this information.

BIBLIOGRAPHY

1) Segel L. Research in the fundamentals of automobile control and stability. Transactions of the Society of Automotive Engineers, vol. 65, pag. 527-540, 1957.

2) Segel L. Theoretical prediction and experimental substantiation of the response of the automobile to steering control. Proceedings of the Automobile Division, the Institution of Mechanical Engineers, no. 7, 1956-1957.

3) Fiala E. Lateral forces on rolling pneumatic tires. Zeitschrift, V.D.I., vol, 96, no. 29, pag. 973-979, 1954.

4) Pacejka H. B. Study of the lateral behavior of an automobile moving upon a flat, level road and of an analog method of solving the problem. Report of the Laboratorium voor Voertuigtechniek, Technische Hogeschool, Delft, 1958.

DISCUSSION

L. AMICI. — Volevo chiedere all'Oratore se, come ha esaminato l'influenza dovuta alle variazioni di velocità nello spostamento del centro di rotazione del veicolo, ha pure esaminato l'influenza delle variazioni delle caratteristiche di deriva; cioè di quelle caratteristiche laterali del pneumatico di cui si è parlato. E in particolare occorrerebbe esaminare le variazioni in funzione della pressione di gonfiamento dei pneumatici. Sarebbe molto interessante da esaminare, in conclusione, quali influenze hanno le variazioni di pressioni di gonfiamento sulla sovrasterzatura ed entro quali limiti si può correggerla mediante correzioni delle pressioni di gonfiamento.

D. C. CLARK. — The analysis presented in this paper has assumed the cornering stiffness of the individual tires to be arbitrarily specified quantities. Values of cornering stiffness were selected that are representative of the sizes of tires required to support the assumed weights. The static margin of the towing vehicle was varied in this study by adjusting the relative lateral stiffnesses of the front and rear tires. For a given tire installation a change in lateral stiffness could be produced by changes in tire inflation pressure. However, to calculate the exact change in static margin produced by variations in tire pressure, it is necessary to obtain experimental data from appropriate tire tests.

N. 18

The statical analysis and experiment on the force to the tractor wheel

Analisi statistica ed esperimenti sulla forza alle ruote del trattore

TAKASHI TANAKA *)

ABSTRACT. — *Application of the statical analysis which has been used to the vehicles on the road, automobile and other cars, to the farm wheel of tractor gives us the false results sometimes by the differences of soil conditions. Then the new idea must be given to force analysis of the farm wheel. In this paper, the idea of wheel efficiency «the ratio of power which was used for forward against power on axle» was conducted, and this efficiency η_w was* $\eta_w = \frac{Z\,V}{T\,V_0/r}$; *where Z is the horizontal force for forward, T is torque force on axle, V is the forward velocity of wheel, V_0 is the circunferential velocity of the any point on the wheel surface and r is the radius of the wheel.*

It was proved that there were differences between rolling resistences of drawn wheel Qr and that of driving wheel Qd theoretically.

$Qr = G \cdot \sin(\delta + \alpha) \cdot \cos\delta$. $Qd = G \cdot \sin\delta \cdot \cos(\delta + \alpha)$. *where α is the gradient of the soil surface, and G is the axle loads. From these theories, the necessary torque forces of wheel axle T were calculated from soil reaction.* $T = [P \cdot \cos\delta + G \cdot \sin(\delta + \alpha)] \cdot r$. *These theory were all confirmed by experiment.*

Application of the statical analysis which has been used to the vehicle on the road, automobile or the other cars, to the farm wheel of tractor gives us the false results sometimes. For, there are many differences between the road and the farm soil surface. Soil under the tractor wheel are travelled greatly by the action of wheel and the are more severe on the humid soil or mud surfaces. Then the new analysis must be considered to the old treatments. In this paper, the wheel efficieney and the rolling resistences which were considered from the new standpoints were reported, and the torque force, that is, moment of the driven axle of the tractor were calculated from reaction force of soil to the wheel. All results were confirmed by the experiments reported in the last section of this paper.

Wheel efficiency. — Power of engine which is transmitted to the driving wheel axle is changed to power for forward by the wheel. The tractive efficieney have been used to show the rate of effective power to the axle horse power, but there were nothing to determine the performances of the wheel which

*) Assistant Professor, Shiga Prefectural College, Kusatsu Shiga, Japan.

the purpose was the support of the body only as that of the power tiller, then the wheel efficiency were conducted and were given a definition as «the ratio of power which was used for forward against power of axle trasmitted from engine», and wheel efficiency η_w may be written

$$\eta_w = Z V / \frac{T}{r} V_0 \tag{1}$$

where Z is the horizontal force for forward, T is torque force on axle, V is the velocity of wheel, V_w is the circumferential velocity of any point on the wheel surface and r is the radius of the wheel. In the wheel on the road, Z has been treated approximately to equal to T/r and V/V_0 has been called efficiency of forward. On the farm wheel, however, there may be arised the false results.

As the case shown in fig. 1, Z is

$$Z = \frac{T}{r} \cos \delta \tag{2}$$

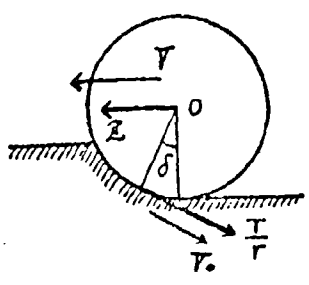


Fig. 1.

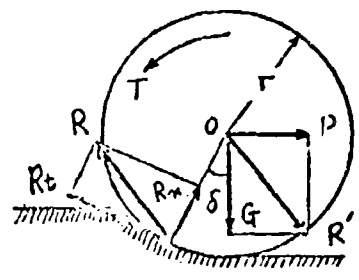


Fig. 2.

On the humid soil, δ which is called angle of repose becomes considerably large. The equation (1) may be changed by using equation (2) as follows

$$\eta_w = \cos \delta \cdot \alpha = \cos \delta \ (1 - \mu) \tag{3}$$

where $\alpha = V/V_0$ and μ is slip ratio of wheel. This equation shows the performance of tractor wheel will be decided by δ and μ, and may be improved by decrease of them.

Rolling resistances. — Rolling resistances are reaction forces of soil to the wheels which are rolling and they have an opposite direction to the forward. Statistical equilibrium of the forces in fig. 2 are given as follows

$$Rt \cos \delta - Rn \sin \delta = G \sin \alpha + P \tag{4}$$

$$Rt \sin \delta + Rn \cos \delta = G \cos \alpha \tag{5}$$

$$Rt \cdot r = T \tag{6}$$

In order to go ahead, the horizontal forces or torque force must be worked to the wheel axle and even if there are no drawbar loads, they must be worked and these working forces are balanced with the rolling resistances. Magnitudes of them are given by $Rn \cdot \sin \delta$ in equation (4) which is $P = 0$, and have opposite direction to the forward.

The measurement of rolling resistances are usually conducted by methods of traction or inertia under the condition which the wheel axle are free from the torque force, but they are measured only the resistances of wheel which is drawn, moreover the friction of bearings and the gears are calculated as the rolling resistances. Then, the rolling resistances of the drawn wheel and that of driving wheel must be considered separately.

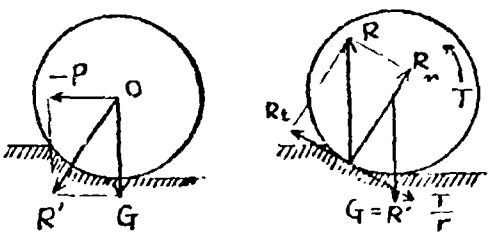


Fig. 3.

Fig. 3 shows the worked fore of the wheel to soil, and (a) is the drawn wheel and (b) is the driving wheel. In the case (a), the pulling force $-P$ and the axle load G are worked to the axle, and the resultant force of them R' is balanced with soil reaction $R = Rn$, and $Rn \cdot \sin \delta$ which is the horizontal component of R is the rolling resistance of drawn wheel Qr. If the torque force $T = 0$, and climb gradient $\alpha = 0$ in the equation (4) and (6)

$$Qr = Rn \cdot \sin \delta = -P \tag{7}$$

and equation (7) may be written as shown in fig. 3 (a)

$$-P = Rn \cdot \sin \delta = G \cdot \tan \delta \tag{8}$$

In the driving wheel as fig. 3 (b), the worked force to the soil are quite different from (a), then it may be considered that the soil movement under the wheel will be different, too. And it is supposed that this differences becomes larger on the humid soil. T/r in fig. 3 (b) is the tangential force at the contact surface to the soil. The horizontal component of soil reaction Rt is balanced with the rolling resistance of driving wheel Qd. That is

$$Qd = Rn \cdot \sin \delta - Rt \cdot \cos \delta = G \sin \delta \cdot \cos \delta \tag{9}$$

Each rolling resistances are different as shown in equation (8) and (9), but they are both function of the load to the axle G and angle of depose δ.

From the equation (4) and (5), unknown quantities Rn and Rt may be calculated as

$$Rt = -P \cos \delta + G \sin (\delta + \alpha) \tag{10}$$

$$Rn = -P \sin \delta + G \cos (\delta + \alpha) \tag{11}$$

As rolling resistance of driving wheel is $Rn \cdot \sin \delta$ at the time when $P = 0$,

$$Rn \cdot \sin \delta = G \cdot \sin \delta \cdot \cos (\delta + \alpha) = Qd \quad (12)$$

Axle torque force which must be transmitted for ascending the slope which has the gradient angle α, is given as

$$T = Rt \cdot r = [P \cdot \cos \delta + G \cdot \sin (\delta + \alpha)] \cdot r \quad (13)$$

In the case of drawn wheel, $Rt = 0$, then equation (4) and (5) are

$$-Rn \cdot \sin \delta + P - G \cdot \sin \alpha = 0 \quad (14)$$

$$Rn \cdot \cos \delta - G \cdot \cos \alpha = 0 \quad (15)$$

From these equations, the rolling resistance of drawn wheel is

$$Qr = P = G \cdot \sin (\delta + \alpha)/\cos \delta \quad (16)$$

At the horizontal surface, $\alpha = 0$, then the equation (12) and (16) are able to be written as same as equation (9) and (7) respectively. It is noted that these equations are all conducted by neglecting the inertia force because of slow velocity of the wheels.

From the axle torque force T (Kg./cm.) in the equation (13) the diameter of the wheel axle to persevere to that torque force may be given. Dianeter of wheel d (cm.) are

$$d = \sqrt[3]{\frac{16 \cdot T}{\pi f d}} \quad (17)$$

where fd is allowable torsion stress of the axle materials. Fig. 4 is the calculation chart of the T and d. K in fig. 4 is

$$K = \zeta \cos \delta + \sin (\delta + \alpha) \quad (18)$$

where ζ is the tractive coefficient, P/G. The numbers affixed to the broken line on the chart show the procedure to require. The adequate cross point of the net formed by the lines of gradient of soil surface α and lines of angle of repose δ is connected with the point which shows the tractive coefficient of tractor wheel at first, and the point of K line is got. The necessary torque T is got by connecting with point of K and the point of product number of axle load G and radius of wheel r. At last the axle diameter d is shown on the cross point of line 3 which is connected T and allowable torsion stress fd of axle materials. The magnitudes of angle of repose has been reported in many past papers.

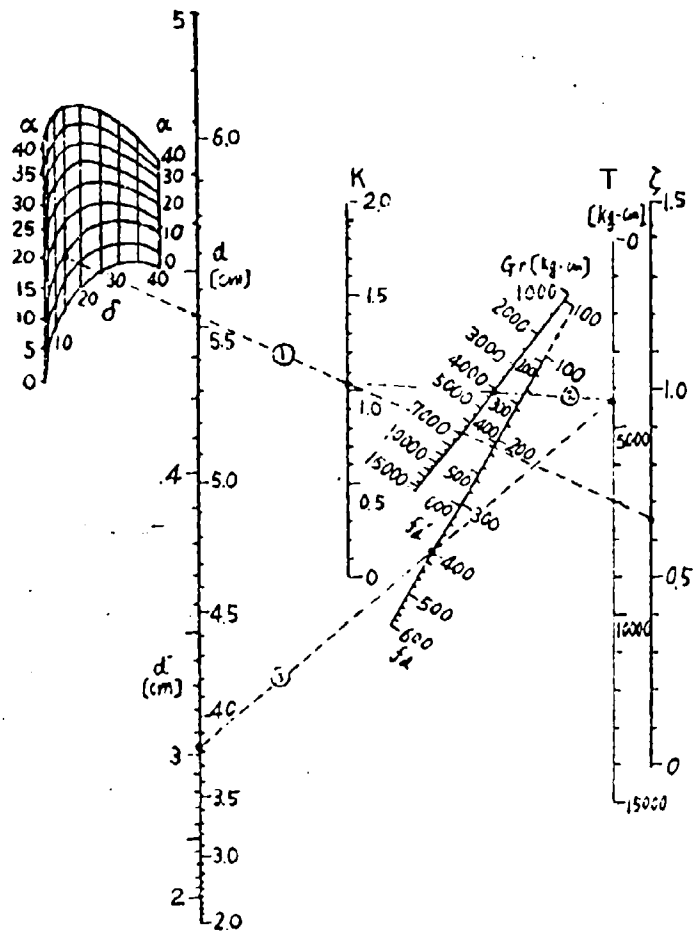


Fig. 4. — Calculating chart.

Experiment. — The test to confirm the above equation were performed. Tractor used in this test was a hand tractor made in Japan, and the table I shows the each terms of the tire used in this test.

TABLE I.

Tire	Kind	Diameter	Width	Inflation press.	Weight
Pneumatic Tire	4.00 - 8,2 ply	440 mm.	124 mm.	1.75 Kg./cm²	6.8 Kg.
Steel Tire	Steel plate welded	710 mm.	130 mm.	—	13.4 Kg.

Several soil conditions were selected. Tchy were the hard soil road which is pressed and contained clay and gravel, loamy field which was used as the seed bed of the colza and soil moisture contents was 16 per cent, sandy loam paddy field which has been harvested, moisture content was 19.3 per cent, the same field and moisture content was 38 per cent, the same field which is covered water about 1 centimeter and the same field which was plowing and harrowing and moisture content was 20.2 per cent.

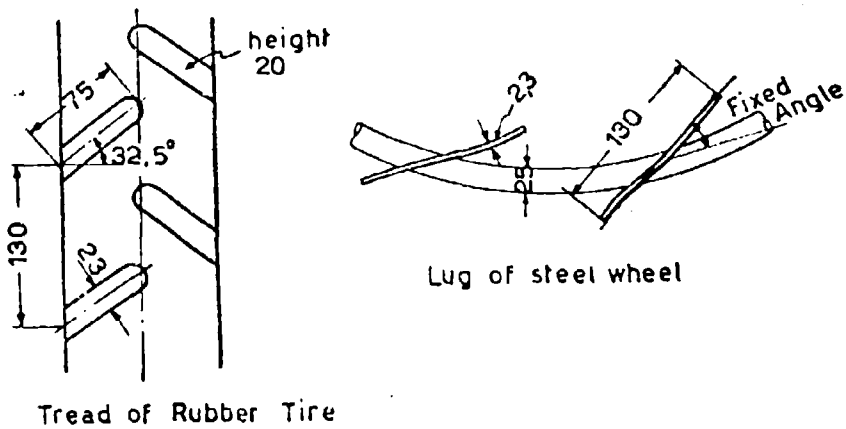


Fig. 5.

The electric three phase induction motor 3 Hp. was taken in instead of water cooled petroleum engine of hand tractor. The mechanical effieiency of motor and tractor were calculated previously and the driving horse power of wheel axle was calculated by that effieiency and in put of the motor measured by electric power meter. Drawbar resistances were given by pulling the sled loading concrete block. The rolling resistances of drawn wheel were measured by taetive method which the test wheel were drawn by the other tractor and the drawing velocity were 0.6 - 0.7 meter per second.

Performance curves of tractor driving wheel. — Fig. 6 is the one example of the test results. The relations of the drawing force which is tangential to the wheel surface T/r, forward force $Z = \frac{T}{r} \cdot \cos \delta$, coefficient of forward force Z/G, drawbar pull P, coefficient of drawbar pull P/G, and torque force worked on the axle T to the wheel axle horse power were straight line, for the circumferential velocity of tractor wheel surface has been constant, and the relation between each forces were same, too. Forward force Z at the time when P = 0 is the rolling resistance of driving wheel Qd and the horse power necessary for this forward are given at the left end of abscissa. Maximum drawbar pull and the horse power at that time are shown in the right end.

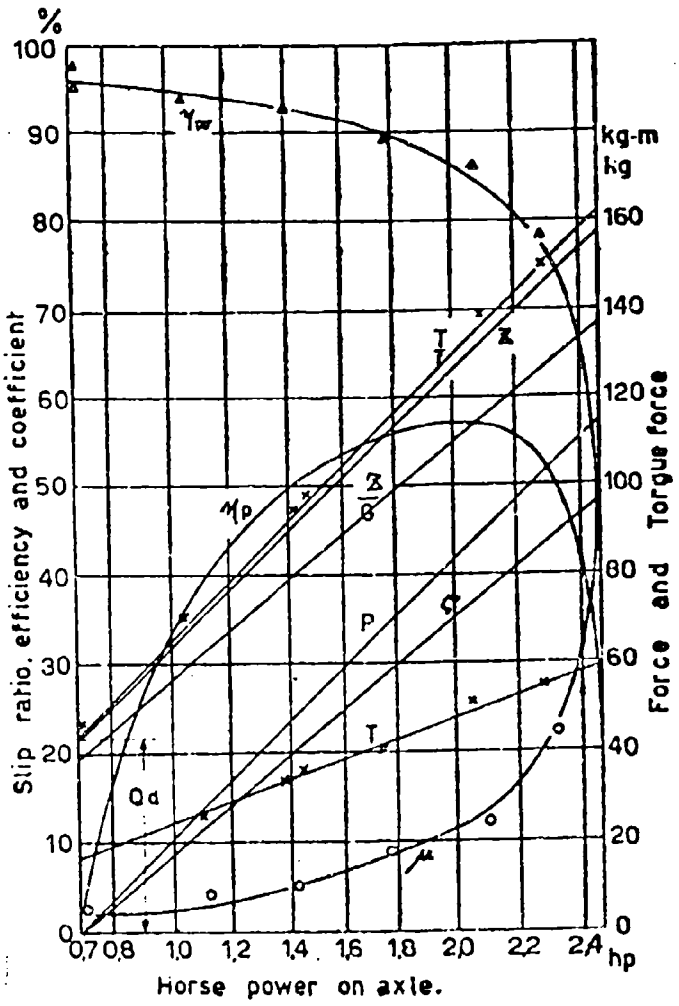


Fig. 6. -- Performance curve.

Torque forces of the axle measured from the motor in put were quite agreed with the values calculated by the equation (13) and forward force Z was evidently shown as the sum of rolling resistance Qd and drawbar pull P.

The curves of tractive efficiency and wheel efficiency separate the area to three parts and upper part of them shows the rate of lost horse power due to the slippage and sinking of wheel, the middle part shows the rate of horse power spended by the rolling resistances and lower part shows the rate of drawbar horse power in axle horse power. This chart which shows the all performances of wheel may be called the performance curve of tractor wheel.

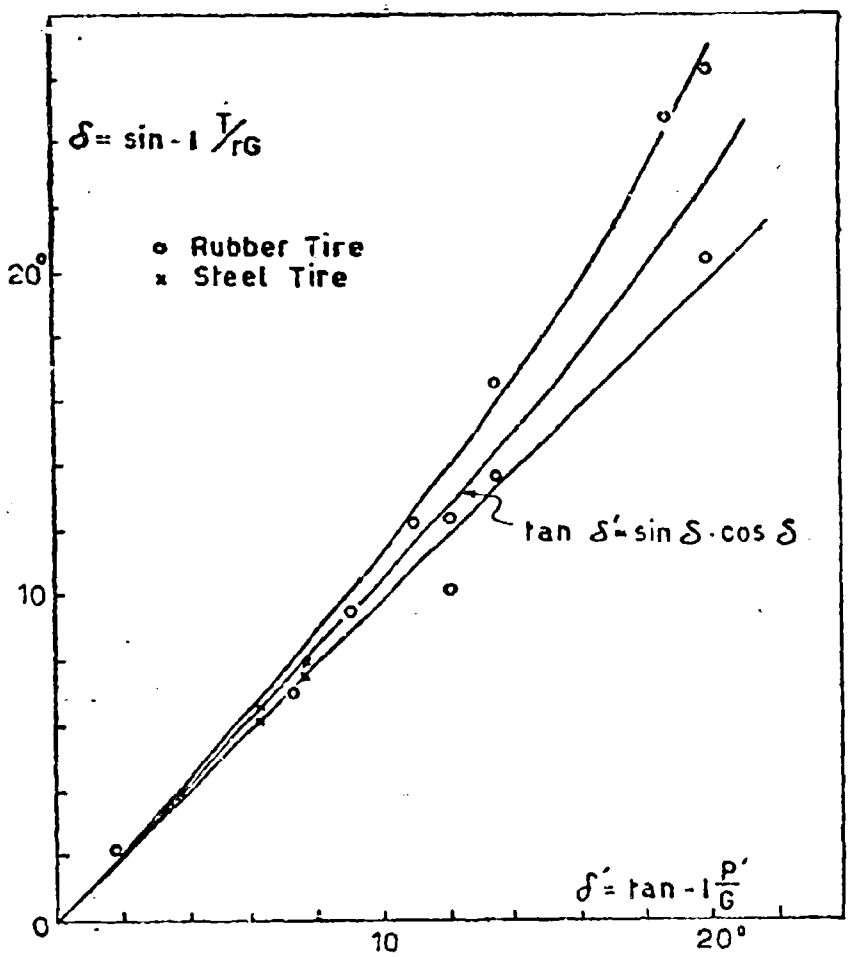


Fig. 7. — Relation of δ and δ'.

Rolling resistance and angle of repose. — It has been mentioned that there were deferences between the rolling resistances of driving wheel and that of drawn wheel, but there were not differences particularly. It is suppose that there were not such soil deformations to cause the differences.

Then, from the relation $Qr = G \cdot \tan \delta'$ and $Qd = G \cdot \sin \delta \cdot \cos \delta$, it is resulted that $\tan \delta' = \sin \delta \cdot \cos \delta$. The results obtained from the tests are well contented this relation as fig. 7.

Torque force of wheel axle were well agreed with the calculation value by the equation (13), too, as fig. 8.

The other many results were obtained by this tests, but they did not

give the direct suggestion to this paper's object. Then, they were simply showed on the table 2. The suffixed numbers on the steel tire on table 2 shows the fixed angle of the plate lug to the wheel rim as fig. 5.

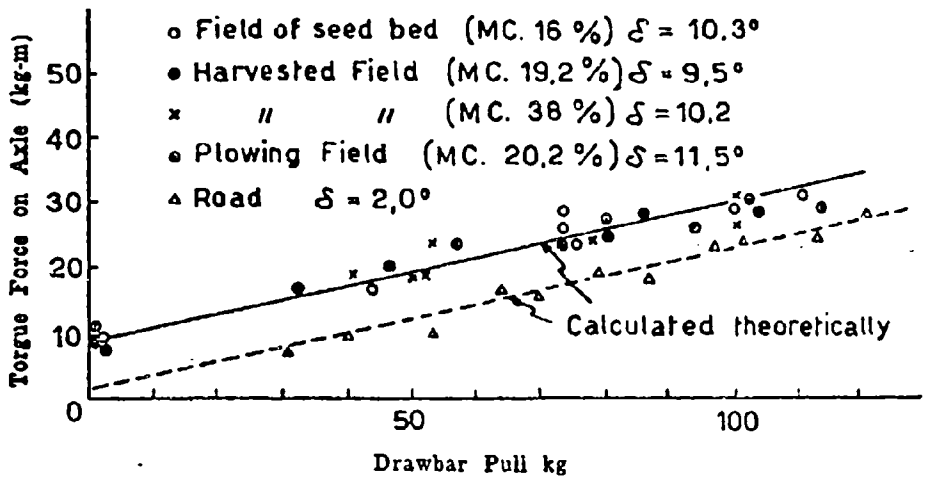


Fig. 8. — Torque Force on Axle.

TABLE 2.

Tire	Soil Cond.	Mois. Cont. %	δ degree	Qd Kg.	Z-max. Kg.	Z-max./G %	P-max. Kg.	P-max./G %	η_p-max. %
Rubber	Road	—	2.0	7	136	61.0	127	57.0	80.0
	FSD	16.0	10.3	39	152	68.2	113	50.7	49.5
	PLF	20.2	11.7	46	159	71.3	111	49.8	47.0
	Ha.F	19.3	9.5	36	148	66.4	109	48.9	50.0
	Ha.F	38.0	10.2	40	148	66.4	104	46.7	41.0
Steel 53	PLF	20.2	11.5	46	167	70.7	120	50.7	55.5
	Ha.F	19.3	11.2	46	162	68.6	115	48.7	58.0
	WC.F	—	9.5	40	187	79.1	149	63.0	66.5
Steel 48	WC.F	—	5.0	20	170	71.8	150	63.5	77.0
Steel 43	FSD	16.0	8.3	34	174	73.7	144	61.0	61.0
	PLF	20.2	8.0	36	150	63.5	116	49.1	60.5
	Ha.F	19.3	11.2	46	167	70.7	116	49.1	54.5
	Ha.F	38.0	8.7	36	185	78.3	149	63.0	63.5

FSD: Field of seed bed; PLF: Plowing and harrowing field; Ha.F: Harvested field; WC.F: Water covered field. η_p: Tractive efficiency.

DISCUSSION

F. L. UFFELMANN. — Prof. Tanaka has obtained formulae of rolling resistance of towed and driven wheels on soft ground without any reference to soil constant but in terms of axle load (G) and an angle (δ) describing the direction of the resultant radial and tangential forces.

The assumption of a common angle δ for both these forces tacitly assumes a balanced (or uniform) distribution of radial and tangential stresses on the are of contact of the wheel rim with the soil. Under these conditions 2 δ would be the angle of sinkage and the theory would be approximately correct for a non frictional soil and high slip values (see paper 7). For an unbalanced distribution of stresses two separate angles (say δ_R and δ_T) would be required to describe the direction of the radial and tangential resultants and Prof. Tanaka's conclusions would no longer be valid. The self driving wheel on a non frictional soil would be such an instance when running at low slip values (see paper 7). Non uniform distribution also occurs on sand (see paper 46).

It is interesting to note that for the tacit assumptions made the rolling resistance of the self driven wheel is ($\cos^2 \delta$) (the towed rolling resistance). For all practical purposes this difference is not large amounting to only 3 % for $\delta = 10°$.

MECCANICA DEL VEICOLO

VEHICLE MECHANICS

N. 19

Dynamics of an automobile in a cornering maneuver on and off the highway

La dinamica del veicolo in curva su strada e fuori strada

W. Bergman *) - E. A. Fox - E. Sabel **)

ABSTRACT. - *The handling characteristics of a four wheeled vehicle equipped with pneumatic tires is discussed quantitatively. The vehicle is treated as a dynamic system with 6 degrees of freedom. The mathematical model of the vehicle consists of a sprung mass connected with the wheels by means of springs and dash pots. This mathematical model includes propulsion of the vehicle by means of an engine, various types of suspensions and drives (front, rear and four wheel drive).*

Particular emphasis is placed on the non-linear characteristics of the pneumatic tire. A precise definition of steering stability is given, as is a definition of «break away», and the method of applying these definitions is indicated. The methods are applicable to either on-the-road or off-the-road vehicles, the difference being solely in the nature of the tire-ground relationships.

Introduction

Vehicle handling is one of the most complex phenomena in the field of vehicle dynamics. In modern automobiles, for instance, low pressure tires, soft suspension springing and horizontal suspension and steering compliance have added to the problems of the engineer responsible for vehicle handling. To develop satisfactory handling qualities, considerable experimentation is necessary in obtaining the optimum compromise between handling and other suspension requirements.

The suspension engineer, through his experience, has become familiar with the qualitative effect of the many parameters which influence handling, and is able to apply his knowledge qualitatively in order to achieve a desirable response in the vehicle. However, because of the complex interrelationship between the parameters involved, it is logical to seek a more efficient method of accomplishing this results. A quantitative analysis of the parameters would permit a more direct approach toward the achievement of an optimum relationship between these factors and would thereby reduce the manpower, material and time required to obtain satisfactory handling.

Such a method of quantitative analysis of the relationship between handling parameters and the variables of motion has been desired by vehicle

*) Ford Motor Company, Dearborn, Michigan, U.S.A.
**) Rensselaer Polytechnic Institute, Troy, New York, U.S.A.

engineers for many years. In the automobile field, for instance, many theories have been developed relating these factors. Until recent years, their practical application has been handicapped by the lack of electronic computers to solve the complex simultaneous equations which are usually involved and it has been necessary to make use of many simplifying assumptions which limit the practical utility of the analysis. To our knowledge, these theories are all related to a four-wheeled vehicle with pneumatic tires, operating on a hard surface; none of them discussed the behavior of a vehicle cornering on a deformable surface or considers the non-linear characteristics of the tire.

The theory presented in this paper constitutes a more rigorous analysis of a vehicle than has hitherto been treated considering all important design parameters with particular emphasis on the non-linear characteristic of the pneumatic tire. The theory previously developed by one of the authors[1] is utilized to deserive the forces when the pneumatic tire is rolling on a hard surface.

Although the equations describing the relationship between the tire and the ground surface are directly applicable only to a hard surface, the lateral characteristics of a tire operating on deformable soil are also discussed in a general way. This paper indicates that handling characteristics are adversely affected to a major extent by the deformability of the soil, in off the road locomotion. Therefore, it is important that further studies of the handling characteristics of a vehicle in *off* the road operation be conducted.

The equations of motion are applicable to vehicles with front or rear wheel drive or four wheel drive and having various suspension configurations.

The mathematical model of the vehicle used in this theory consists of a sprung mass connected with the wheels by means of springs and dash pots. The vehicle is treated as a dynamic system with six degrees of freedom. The non-linear effects of change of wheel loads, traction, camber and slip angles on lateral tire forces are discussed. Vehicle design parameters affecting these factors are incorporated in the equations of motion.

From these equations can be derived the understeer or oversteer characteristics of the vehicle, as well as other types of stability.

A new theory of vehicle motion

In order to establish a criterion of stability of control of the steering of a vehicle, it is necessary to set up a mathematical model which will embody the important dynamical characteristics of the car itself and which will have acting on it all of the important externally impressed forces that actually exist.

The model we have chosen is that of a sprung mass mounted to the wheels by means of springs and dash pots. The motion of the sprung mass relative to wheels will be completely specified by the deflections of the springs. These will be found from the Z_i, $i = 1, 2, 3, 4$ and will be considered small quantities.

The Z_i are the vertical distances from the centers of the wheels to the points of attachment of the sprung mass respectively.

The wheels, which may be steered, have camber, toe-in, etc. will be thought of as being attached to a real or imagined rigid frame.

The center of the right rear wheel will be taken as a point of reference and a coordinate system moving with the rigid frame will be set up through the center of the wheel, see fig. 1.

In the first analysis, the wheels will be considered weightless. Thus their momenta and moments of momentum will be neglected. This has the effect of making the center of mass of the entire vehicle coincide with that of the sprung

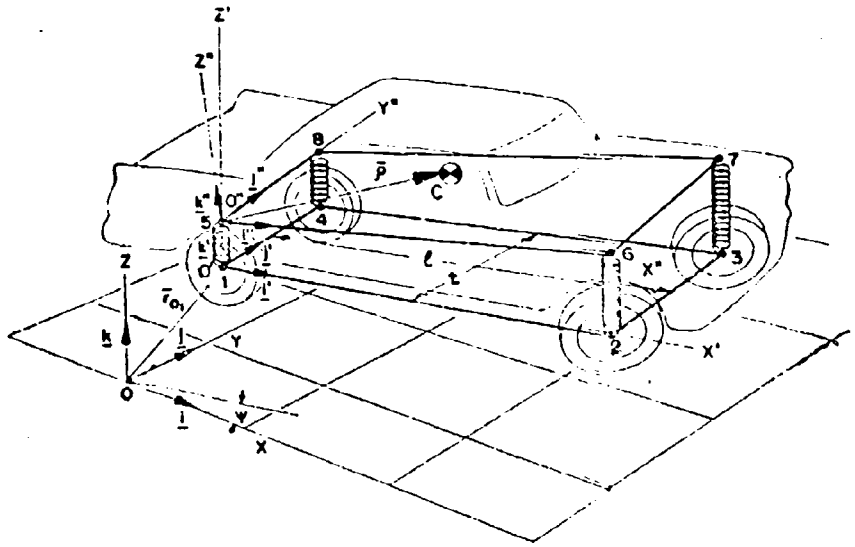


Fig. 1. — Inertial frame.

mass. As will be shown below this is not a bad approximation and if at a later stage it is desired to consider the mass of the wheels and their gyroscopic effects on the steering, the results obtained from the first approximation can be used as a basis for solving the more general problem.

In addition to the coordinate system fixed in the frame (real or imaginary) to which the wheels are attached and designated by X', Y', Z'; two other coordinate systems are useful. One of these will be fixed in the sprung mass and will be designated by X'', Y'', Z''. In the normal rest position of the vehicle the origin of the double-prime system will be directly under that of the single-prime system and the axes will be respectively parallel, the Z' and Z'' axes coinciding.

The third system is a set of fixed axes on the earth constituting our *inertial frame*. We shall write our equations of motion with respect to these last axes and then transform them over to the more convenient system, the primed coordinates, for calculational purposes. By choosing to describe the motion of the sprung mass relative to the frame by means of the spring deflections, related to Z_i, we have eliminated all of the ambiguities attendent upon

[redacted] use of such concepts as roll-axis, [redacted] found useful to couch results in these terms, they can easily be found from the "i"s.

In each system of axes, the unit vectors will be designated by i, j, and k respectively, the unprimed vectors belonging to the inertial frame and the others as specified above.

Review of existing theories

Huber [2] was the first to recognize that non-linearity between lateral tire force and wheel load is one of the most important factors in determining vehicle stability.

Rieckert and Schunk [3] developed a classic theory of vehicle motion, in which they employed Huber's findings regarding tire characteristics. In their analysis, they considered not only tire forces and inertia forces, but also aerodynamic forces. Stability conditions were established from their analysis.

Mitschke [4] expanded an analysis of vehicle motion previously developed by Rieckert and Schunk to describe a four wheeled automobile with front, rear or four wheel steering.

W. Kamm [5] in his thesis on directional stability provided an analysis of static and dynamic stability with particular emphasis on the effect of side winds on vehicle stability.

Kamm's theory was extended by Gebelein and Schlick [6], who confirmed the stability requirements previously formulated by Kamm; namely, apply more load at the front axle and locate the center of pressure behind the C. G. by using fins.

Schilling [7] made a classic analysis of an automobile by treating the vehicle as a linear dynamic system with three degrees of freedom. He also considered roll of the car body. Schilling's theory was further extended by Segel [8], who incorporated more design parameters in the equations of motion and introduced the concept of static stability margin as a criterion of vehicle stability.

H. Kohr [9] employed Segel's equations of motion for an extensive study of vehicle motion which was simulated on analog and digital computers.

Goland and Jindra [10] in their treatment of the motion of an automobile introduced the effect of dynamic wheel loads on lateral tire forces, employing empirical equations developed by Smiley and Horne [11].

Paslay and Slibar [12] made a significant contribution to the theoretical analysis of vehicle dynamics by describing the motion of a four wheeled automobile as a dynamic system with six degrees of freedom. In their analysis, the authors considered inertia forces and all tire forces including traction on each individual wheel.

Enke [13] employed in his analysis a more realistic model of an automobile than did his predecessors. He considered various types of suspensions and the effect of suspension guidance on wheel rate. Unlike other authors, he used the

iteration technique in his calculations and utilized tire curves instead of equations.

Mitterlehner [14] showed how stability of the vehicle improves with an increase in the natural frequency of the steering system. He advocated the use of positive easter to improve vehicle stability.

Fiala [15] emphasized the importance of flexibility of the steering system and body roll on vehicle stability. In determining deflections of the wheels due to flexibility of the system he considered not only easter but also aligning torque and precession torque.

W. Zuk [16] studied the motion of an automobile with all four wheels blocked on a road having non-uniform friction properties, on a transverse slope and in a flat curve.

Radt and Milliken [17] considered the effect of traction and braking forces on lateral tire forces in their equation of motion. This allowed them to study the motion of the vehicle up to the condition of skidding.

In contrast with previous authors, who confined their studies to the behavior of a vehicle on a paved surface, Bekker [18] in his monumental work, presented a comprehensive theory of land locomotion, which particularly emphasized off-the-road locomotion. In his book, this author discusses and analyzes the mechanics of various types of vehicles; the mechanics of a wheel; soil and snow mechanics and many other related phenomena.

Kinematical analysis

Let $\bar{r}_{01}$ designate the vector from the origin of the inertial frame to the center of the right rear wheel, point 1, which is the reference point for the primed system of axes.

The velocity of point 1, $\bar{v}_1$ is given by

$$\bar{v}_1 = \dot{\bar{r}}_{01} \tag{1}$$

the dot indicating differentiation with respect to time.

The angular velocity of the sprung mass $\bar{\omega}_s$, is given by

$$\bar{\omega}_s = \frac{d}{dt}\left[\frac{z_4 - z_1}{t}\right]\bar{i}'' + \frac{d}{dt}\left[\frac{z_2 - z_1}{l}\right]\bar{j}'' + \frac{d\psi}{dt}\bar{k} \tag{2}$$

the quantities Z_1, Z_2, Z_3 and Z_4 being considered small. Thus,

$$\Theta = \frac{z_4 - z_1}{t} = \frac{z_2 - z_3}{t} \tag{3}$$

is the roll angle, and

$$\varphi = \frac{z_1 - z_2}{l} = \frac{z_4 - z_3}{l} \tag{4}$$

is the pitch angle.

Equations 3 and 4, which are consistent, imply that

$$z_4 = z_1 + z_3 - z_2 \tag{5}$$

a relationship which exists by virtue of the fact that the sprung mass is rigid and its lower side may be considered to constitute a plane.

It should be noted that by assuming the motion of the four points of suspension of the unsprung mass to be vertical, we have assumed yaw relative to the motion of the wheel frame to be unimportant. The rotation of the car about the Z axis is ψ.

Equation (2) can be written

$$\bar{\omega}_s = \dot{\phi}\bar{i}'' + \dot{\varphi}\bar{j} + \dot{\psi}\bar{k} \tag{6}$$

Let us designate the center of gravity of the sprung mass by c. Then the distance from the origin of the inertial frame to point c expressed vectorially is

$$\bar{r}_{oc} = \bar{r}_{o1} + z_1\bar{k} + \bar{\rho} \tag{7}$$

Note that $\bar{k} = \bar{k}'$ since point 1 moves only in a vertical direction. The vector $\bar{\rho}$ is the vector from point, 5, the origin of the coordinate system fixed in the sprung mass to the centroid of the sprung mass. It may be expressed as follows

$$\bar{\rho} = a\bar{i}'' + b\bar{j}'' + c\bar{k}'' \tag{8}$$

where a, b and c are the coordinates of the centroid measured from point 5 in the double prime coordinate directions.

We can now differentiate equation (7) with respect to time to obtain

$$\dot{\bar{r}}_{oc} = \dot{\bar{r}}_{o1} + \dot{z}_1\bar{k} + \bar{\omega}_s\bar{\rho} + \dot{\bar{\rho}}_r \tag{9}$$

where $\bar{\rho}_r$ is the vector from the centroid of the sprung mass to the centroid of the total mass and

$$\ddot{\bar{r}}_{oc} = \ddot{\bar{r}}_{o1} + \ddot{z}_1\bar{k} + \bar{\omega}_s \times (\bar{\omega}_s \times \bar{\rho}) + \dot{\bar{\omega}}_s \times \bar{\rho} + \ddot{\bar{\rho}}_r + 2\bar{\omega}_s \times \dot{\bar{\rho}}_r \tag{10}$$

The last term is called the Coriolis acceleration. If we assume that the centroid of the entire system and the centroid of the sprung mass coincide, we may drop the last two terms in equation (10) and the last two in equation (9) since ρ is fixed in magnitude, $\dot{\bar{\rho}}_r$ and $\ddot{\bar{\rho}}_r$ will both be zero. Equations (9) and (10) then become

$$\dot{\bar{r}}_{oc} = \dot{\bar{r}}_{o1} + \dot{z}_1\bar{k} + \bar{\omega}_s \times \bar{\rho} \tag{11}$$

$$\ddot{\bar{r}}_{oc} = \ddot{\bar{r}}_{o1} + \ddot{z}_1\bar{k} + \bar{\omega}_s \times (\bar{\omega}_s \times \bar{\rho}) + \dot{\bar{\omega}}_s \times \bar{\rho} \tag{12}$$

If x_1 and y_1 are the coordinates of the center of the right rear wheel in the inertial frame of reference, it may easily be shown that

$$\ddot{\bar{r}}_{o1} = \underline{i}'(\ddot{\bar{x}}_1 \cos\psi + \ddot{\bar{y}}_1 \sin\psi) + \underline{j}(-\ddot{\bar{x}}_1 \sin\psi + \ddot{\bar{y}}_1 \cos\psi) \tag{13}$$

$$\bar{\omega}_s \times (\bar{\omega}_s \times \bar{\rho}) = -\underline{i}' a\dot{\psi}^2 - \underline{j}' b\dot{\psi}^2 \tag{14}$$

and

$$\dot{\bar{\omega}}_s \times \bar{\rho} = \underline{i}'(c\ddot{\varphi} - b\ddot{\psi}) + \underline{j}'(a\ddot{\psi} - c\ddot{\theta}) + \underline{k}'(b\ddot{\theta} - a\ddot{\varphi}) \tag{15}$$

In obtaining the above, small quantities of the second order and higher have been neglected. These relationships are useful since the equations of motion are written with respect to the inertial frame of reference but the primed frame is the most convenient to work with.

Dynamical analysis

Let us calculate the inertia tensor for the sprung mass with respect to axes passing through its centroid parallel to the double-prime system. Since there is a plane of symmetry, two of the products of inertia vanish and the tensor reduces to

$$I = \begin{bmatrix} I_x & 0 & -I_{xz} \\ 0 & I_y & 0 \\ -I_{xz} & 0 & I_z \end{bmatrix} \tag{16}$$

where

I_x is the moment of inertia about the X_c'',
I_y is the moment of inertia about the Y_c'',
I_z is the moment of inertia about the Z_c'',
I_{xz} is the product of inertia about X_c'' Z_c''.

The components of angular momentum about these same axes are given by

$$H_{x_c''} = I_x \omega_{x''} - I_{xz}\omega_{z''}; \quad H_{y_c''} = I_y \omega_{y''}; \quad H_{z_c''} = -I_{xz}\omega_{x''} + I_z \omega_{z''} \tag{17}$$

which reduce to

$$H_{x_c''} = I_x(\dot{\theta} - q\dot{\psi}) - I_{xz}\dot{\psi}$$

$$H_{y_c''} = I_y(\dot{q} - \dot{\psi}\theta) \tag{18}$$

$$H_{z_c''} = -I_{xz}(\dot{\theta} - q\dot{\psi}) + I_z\dot{\psi}$$

The components of time rate of change are

$$\dot{H}_{x''_c} = I_x(\ddot{\Theta} - \varphi\ddot{\psi} - \dot{\varphi}\dot{\psi}) - I_{xz}\ddot{\psi}$$

$$\dot{H}_{y''_c} = I_y(\ddot{\varphi} - \Theta\ddot{\psi} - \dot{\Theta}\dot{\psi}) \tag{19}$$

$$\dot{H}_{z''_c} = -I_{xz}(\ddot{\Theta} - \varphi\ddot{\psi} - \dot{\varphi}\dot{\psi}) + I_z\ddot{\psi}$$

The general equations for the motion of a rigid body tell us that for axes fixed in the center of mass of a body sum of the moments of the forces about the point c becomes:

$$\overline{L_c} = (\dot{H}_x - \omega_z H_y + \omega_y H_z)\,\underline{i}'' + (\dot{H}_y - \omega_x H_z + \omega_z H_x)\,\underline{j}''$$

$$+ (\dot{H}_z - \omega_y H_x + \omega_x H_y)\,\underline{k}'' \tag{20}$$

where the subscripts on the H's and ω's indicate the fixed axes through the centroid of the sprung mass. These equations become, when transformed to the primed axes

$$\overline{L_c} = (I_x\ddot{\Theta} - I_{xz}\ddot{\psi})\,\underline{i}' + I_y\ddot{\varphi}\,\underline{j}' + (I_z\ddot{\psi} - I_{xz}\ddot{\Theta})\,\underline{k}' \tag{21}$$

if terms of a higher order of magnitude in smallness are dropped.

Equations (21) constitute three of the dynamical equations of motion.

$$\overline{F} = M\ddot{\bar{r}}_c \tag{22}$$

The quantity $\ddot{\bar{r}}_c$ has already been calculated in equation (11) and the components of acceleration of the center of mass may be put into the following useful form in the prime-coordinate system.

$$\ddot{\bar{r}}_c = \underline{i}'(\ddot{x}_1\cos\psi + \ddot{y}_1\sin\psi - a\dot{\psi}^2 + c\ddot{\varphi} - b\ddot{\psi})$$

$$+ \underline{j}'(-\ddot{x}_1\sin\psi + \ddot{y}_1\cos\psi - b\dot{\psi}^2 + a\ddot{\psi} - c\ddot{\Theta}) \tag{23}$$

$$+ \underline{k}'(\ddot{z}_1 + b\ddot{\Theta} - a\ddot{\varphi})$$

Our system of equations thus consists of three from equation (21) and three form equations (23) in the six unknowns z_1, z_2, z_3, x_1, y_1, and ψ since Θ and φ may be expressed in terms of z_1, z_2, and z_3.

For purposes of determining the signs of forces and moments, we have dealt exclusively with right-handed systems of coordinates.

If we designate by $\overline{P}_i$ the system of forces acting on the i — th wheel (i = 1, 2, 3, 4), and by $\bar{r}_{Gi}$ the vector running from the center of gravity to the i — th point of application of $\overline{P}_i$ we have (G and e are presumed to coincide).

$$\overline{L}_G = \sum_{i=1}^{4} \bar{r}_{Gi} \overline{P}_i + \bar{r}_{GE} \overline{E} + \sum_{i=1}^{4} \overline{M}_i \tag{24}$$

where $\overline{E}$ will be considered the aerodynamic forces and $\bar{r}_{GE}$ a similar position vector for the aerodynamic forces $\overline{M}_i$ are the tire aligning torques at i-th wheel.

The indicated vector products are to be carried out automatically in accordance with the rule illustrated by the following

$$\bar{r}_{Gi} \times \overline{F}_i = \begin{bmatrix} \underline{i}' & \underline{j}' & \underline{k}' \\ x'_i & y'_i & (z'_i + r_w) \\ F_{ix'} & F_{iy'} & F_{iz'} \end{bmatrix} \tag{25}$$

where

r_w is the loaded radius of the wheel.

It is somewhat simpler to obtain the moments of the externally applied forces in the following manner

$$\bar{r}_{c1} = -\bar{\rho} - (z_1 + r_w)\,\underline{k} \tag{26}$$

$$\bar{\rho} = a\,\underline{i}'' + b\,\underline{j}'' + c\,\underline{k}''$$

where

$$\bar{\rho} = \bar{r}_{3c} = -\bar{r}_{c3} \tag{27}$$

The other distances are found in a similar manner

$$\begin{aligned} \bar{r}_{c2} &= \bar{r}_{c6} - (z_2 + r_w)\,\underline{k} \\ \bar{r}_{c3} &= \bar{r}_{c7} - (z_3 + r_w)\,\underline{k} \\ \bar{r}_{c4} &= \bar{r}_{c8} - (z_4 + r_w)\,\underline{k} \end{aligned} \tag{28}$$

Also

$$\begin{aligned} \bar{r}_{c6} &= \bar{r}_{c5} + l\,\underline{i}'' = -\bar{\rho} + l\,\underline{i}'' \\ \bar{r}_{c7} &= \bar{r}_{c6} + t\,\underline{j}'' = -\bar{\rho} + l\,\underline{i}'' + t\,\underline{j}'' \\ \bar{r}_{c8} &= -\bar{\rho} + t\,\underline{j}'' \end{aligned} \tag{29}$$

It can be shown that

$$\bar{\rho} = (a + e\varphi)\,\underline{i}'' + (b + e\Theta)\,\underline{j}'' + (e - a\varphi - b\Theta)\,\underline{k}'' \qquad (30)$$

and that the double-prime unit vectors are related to the single prime ones through

$$\begin{aligned} \underline{i}'' &= \underline{i}' - \varphi\,\underline{k}' \\ \underline{j}'' &= \underline{j}' - \Theta\,\underline{k}' \\ \underline{k}'' &= \varphi\,\underline{i}' + \Theta\,\underline{j}' + \underline{k}' \end{aligned} \qquad (31)$$

so that all the moments may easily be worked out.

List of symbols

Parameters

W = Vehicle total weight (lb.)
W_s = Vehicle sprung weight (lb.)
a, b, e = Coordinates of C.G. in double prime coordinate system (ft.)
l = Wheelbase (ft.)
h_r = Rear roll center height (ft.)
t = Tread (ft.)
h_s = C.G. height
I_x = Moment of inertia of the vehicle about X-axis (in roll) (lb. ft. sec.^{2})
I_y = Moment of inertia of the vehicle about Y-axis (in pitch) (lb. ft. sec.^{2})
I_z = Moment of inertia of the vehicle about Z-axis (in yaw) (lb. ft. sec^2.)
I_{xz} = Product of inertia of the vehicle about X and Z axis
k_φ = Body roll coefficient, due to engine torque (non-dimensional)
k_φ = 1.0 for symmetrical rigid driven axle suspensions
k_φ = 0 for suspended carrier suspensions
k_{ind} = Independent rear suspension coefficient (non-dimensional)
k_{ind} = 1.0 for independent rear and swing axle
k_{ind} = 0 for solid axle suspensions
k_{fd} = Front wheel drive coefficient (non-dimensional)
k_{fd} = 1.0 for front or four wheel drive vehicle
k_{fd} = 0 for rear wheel drive vehicle
k_{rd} = Rear wheel drive coefficient (non-dimensional)
k_{rd} = 1.0 for rear or four wheel drive vehicle
k_{rd} = 0 for front wheel drive vehicle
t_s = Rear spring base (ft.)
Subscripts: fl, fr, rl, rr = front left, front right, rear left, rear right wheel
Subscripts: f, r = front, rear
W_{fl}°, W_{fr}°, W_{rl}°, W_{rr}° = Static wheel loads (lbs.)

k_f = Front ride rate (lb./ft.)
k_r = Rear ride rate (lb./ft.)
k_f' = Front stabilizer bar rate at the wheel (lb./ft.)
k_r' = Rear stabilizer bar rate (lb./ft.)
k_{sf} = Front shock absorber rate $\left(\frac{\text{lb. sec.}}{\text{ft.}}\right)$
k_{sr} = Rear shock absorber rate $\left(\frac{\text{lb. sec.}}{\text{ft.}}\right)$
k_m = Effective mass factor (non-dimensional)
i = Axle ratio (non-dimensional)
η_a = Axle efficiency (non-dimensional)
η_t = Transmission efficiency (non-dimensional)
r_w = Tire rolling radius under load (ft.)
ζ = Rear ride rate increase coefficient due to twisting of the spring in roll (non-dimensional)
μ_o = Static coefficient of friction between tire and road surface (non-dimensional)
A_f = Frontal area of the vehicle ($ft.^2$)
φ = Air density $\left(\frac{\text{lb. sec.}^2}{\text{ft.}}\right)$
c_x = Aerodynamic drag coefficient (non-dimensional)
c_y = Aerodynamic lateral force coefficient (non-dimensional)
c_z = Aerodynamic lift coefficient (non-dimensional)
c_{xx} = Aerodynamic roll coefficient (non-dimensional)
c_{yy} = Aerodynamic pitch coefficient (non-dimensional)
c_{zz} = Aerodynamic yaw coefficient (non-dimensional)

Incremental input values

$\frac{dt_{fl}}{df_{fl}}, \frac{dt_{fr}}{df_{fr}}, \frac{dt_{rl}}{df_{rl}}, \frac{dt_{rr}}{df_{rr}}$ = Rate of tread change at the tire-road contact point, with respect to vertical wheel displacement (anti-roll angle) (non-dimensional)

$\frac{dl_{fl}}{df_{fl}}, \frac{dl_{fr}}{df_{fr}}, \frac{dl_{rl}}{df_{rl}}, \frac{dl_{rr}}{df_{rr}}$ = Rate of wheel base change with respect to vertical wheel displacement (anti-pitch angle) (non-dimensional)

$\frac{dt'_{fl}}{df_{fl}}, \frac{dt'_{fr}}{df_{fr}}, \frac{dt'_{rl}}{df_{rl}}, \frac{dt'_{rr}}{df_{rr}}$ = Rate of tread change at the wheel center, with respect to vertical wheel displacement (non-dimensional)

Independent and dependent variables (2 dependent, 6 independent)

δ_s = Steering wheel angle (radians)
T_a = Axle torque (lb. ft.)
x, y = Coordinates of the geometrical center of the right rear wheel
ψ = Angle through which car has rotated about the z-axis (radians)
f_{fl}, f_{fr}, f_{rr} = Vertical wheel deflections (ft.)

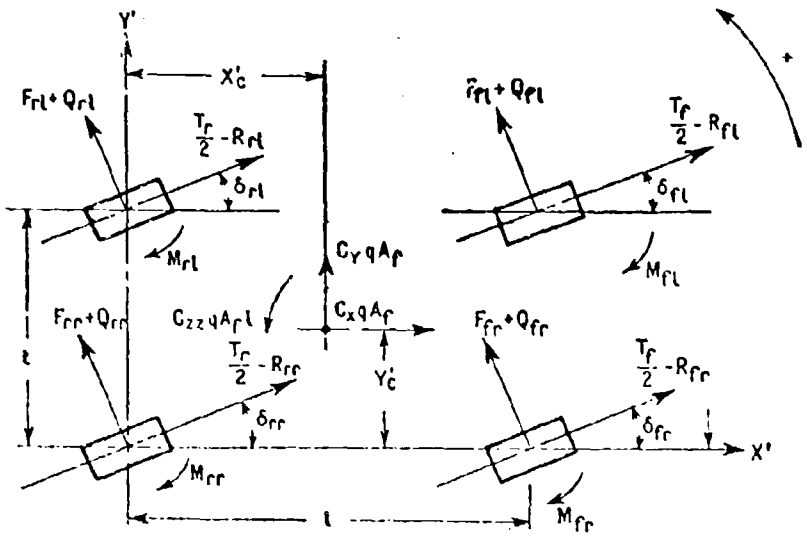


Fig. 2. — Forces and moments acting on the vehicle in the plan view.

Auxiliary variables

Θ = Roll angle (radians)
φ = Pitch angle (radians)
δ_{fl}, δ_{fr}, δ_{rl}, δ_{rr} = Dynamic steer angle (radians)
β_{fl}, β_{fr}, β_{rl}, β_{rr} = Angle between velocity vector and x^1 axis (radians)
α_{fl}, α_{fr}, α_{rl}, α_{rr} = Slip angle (radians)
x'_c y'_c z'_c = Coordinates of C.G. in $x^1y^1z^1$ system (ft.)
v_{rr} = Vehicle velocity or velocity at the center of the right rear wheel (ft./sec.)
q = Aerodynamic pressure (lbs. /ft.^{2})
W_{fl}, W_{fr}, W_{rl}, W_{rr} = Vertical wheel reactions (lb.)
R_{fl}, R_{fr}, R_{rl}, R_{rr} = Rolling resistance (lb.)
T_f, T_r = Traction force (lb.)
Q_{fl}, Q_{fr}, Q_{rl}, Q_{rr} = Camber thrust (lb.)
M_{fl}, M_{fr}, M_{rl}, M_{rr} = Tire aligning torque (lb. ft.)
W^b_{fl}, W^b_{fr}, W^b_{rl}, W^b_{rr} = Components of the vertical wheel reactions due to compression of the rubber bumpers
F_{fl}, F_{fr}, F_{rl}, F_{rr} = Lateral tire force (lb.)

Discussion

In order to solve the system of equations embodied in equations (22) and (24) it is necessary to have explicit relationships for the external forces. These forces consist of tire forces and aerodynamic forces.

When inserted into the equations of motion, we arrive at the following system of equations, see figures 2, 3, 4.

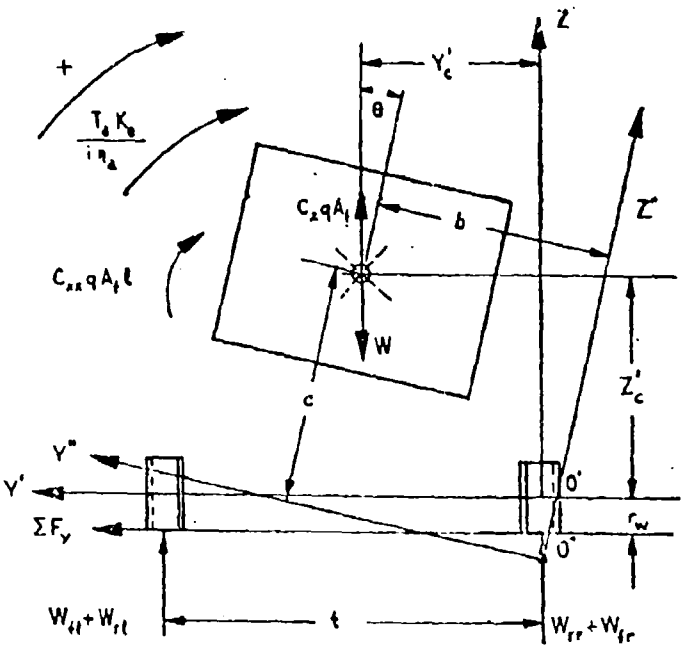


Fig. 3. — Forces and moments acting on the vehicle in the front view.

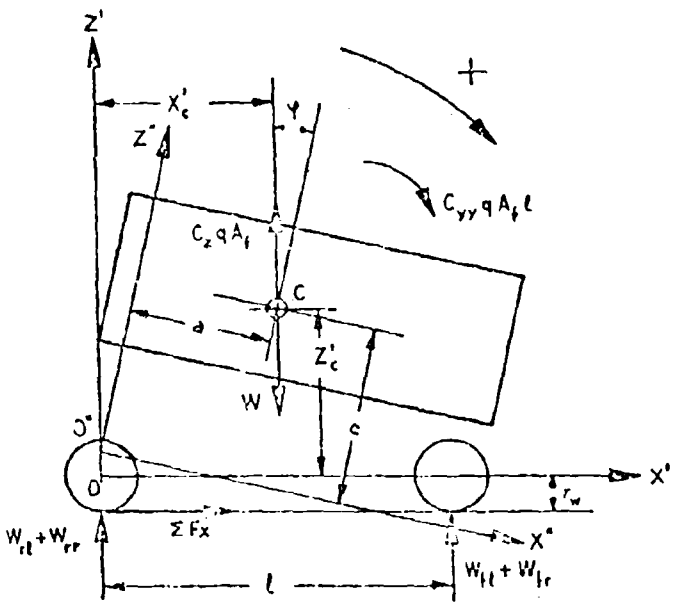


Fig. 4. — Forces and moments acting on the vehicle in the side view.

$$\Sigma F_x = -(F_{fl} + Q_{fl}) \sin\delta_{fl} + \left(\frac{T_f}{2} - R_{fl}\right) \cos\delta_{fl} - (F_{fr} + Q_{fr}) \sin\delta_{fr} + \left(\frac{T_f}{2} - R_{fr}\right) \cos\delta_{fr} - (F_{rl} + Q_{rl}) \sin\delta_{rl} + \left(\frac{T_r}{2} - R_{rl}\right) \cos\delta_{rl} - (F_{rr} + Q_{rr}) \sin\delta_{rr} + \left(\frac{T_r}{2} - R_{rr}\right) \cos\delta_{rr} + c_x q A_f = \frac{k_m W}{g} \left(\ddot{x}_{rr} \cos\psi + \ddot{y}_{rr} \sin\psi - a\dot{\psi}^2 + \frac{W_a}{W} c\ddot{\varphi} - b\ddot{\psi}\right) \quad (32)$$

$$\Sigma F_y = (F_{fl} + Q_{fl}) \cos\delta_{fl} + \left(\frac{T_f}{2} - R_{fl}\right) \sin\delta_{fl} + (F_{fr} + Q_{fr}) \cos\delta_{fr} + \left(\frac{T_f}{2} - R_{fr}\right) \sin\delta_{fr} + (F_{rl} + Q_{rl}) \cos\delta_{rl} + \left(\frac{T_r}{2} - R_{rl}\right) \sin\delta_{rl} + (F_{rr} + Q_{rr}) \cos\delta_{rr} + \left(\frac{T_r}{2} - R_{rr}\right) \sin\delta_{rr} + c_y q A_f = \frac{W}{g} \left(-\ddot{x}_{rr} \sin\psi + \ddot{y}_{rr} \cos\psi - b\dot{\psi}^2 + a\ddot{\psi} - \frac{W_a}{W} c\ddot{\Theta}\right) \quad (33)$$

$$\Sigma F_z = W_{fl} + W_{fr} + W_{rl} + W_{rr} - W + c_z q A_f = \frac{W_a}{g} \left(-\ddot{f}_{rr} + b\ddot{\Theta} - a\ddot{\varphi}\right) \quad (34)$$

$$\Sigma M_x = \left[(F_{fl} + Q_{fl}) \cos\delta_{fl} + \left(\frac{T_f}{2} - R_{fl}\right) \sin\delta_{fl} + (F_{fr} + Q_{fr}) \cos\delta_{fr} + \left(\frac{T_f}{2} - R_{fr}\right) \sin\delta_{fr} + (F_{rl} + Q_{rl}) \cos\delta_{rl} + \left(\frac{T_r}{2} - R_{rl}\right) \sin\delta_{rl} + (F_{rr} + Q_{rr}) \cos\delta_{rr} + \left(\frac{T_r}{2} - R_{rr}\right) \sin\delta_{rr}\right] (z_c' + r_w) - (W_{fr} + W_{rr}) y_c' + (W_{fl} + W_{rl}) (t - y_c') + c_{xx} q A_f l + c_y q A_f (z_c' + r_w) + \frac{T_a k_a}{i \eta_a} = I_x \ddot{\Theta} - I_{xz} \ddot{\psi} \quad (35)$$

$$\Sigma M_y = (W_{rl} + W_{rr}) x_c' - (W_{fl} + W_{fr}) (l - x_c') - \left[-(F_{fl} + Q_{fl}) \sin\delta_{fl} + \left(\frac{T_f}{2} - R_{fl}\right) \cos\delta_{fl} - (F_{fr} + Q_{fr}) \sin\delta_{fr} + \left(\frac{T_f}{2} - R_{fr}\right) \cos\delta_{fr} - (F_{rl} + Q_{rl}) \sin\delta_{rl} + \left(\frac{T_r}{2} - R_{rl}\right) \cos\delta_{rl} - (F_{rr} + Q_{rr}) \sin\delta_{rr} + \left(\frac{T_r}{2} - R_{rr}\right) \cos\delta_{rr}\right] (z_c' + r_w) + c_{yz} q A_f l - C_x q A_f (z_c' + r_w) = I_y \ddot{\varphi} \quad (36)$$

$$\Sigma M_z = \left[(F_{fl} + Q_{fl}) \cos\delta_{fl} + \left(\frac{T_f}{2} - R_{fl}\right) \sin\delta_{fl} + (F_{fr} + Q_{fr}) \cos\delta_{fr}\right.$$

$$\left. + \left(\frac{T_f}{2} - R_{fr}\right) \sin\delta_{fr}\right] (l - x_c') - \left[(F_{rl} + Q_{rl}) \cos\delta_{rl} + \left(\frac{T_r}{2} - R_{rl}\right) \sin\delta_{rl}\right.$$

$$\left. + (F_{rr} + Q_{rr}) \cos\delta_{rr} + \left(\frac{T_r}{2} - R_{rr}\right) \sin\delta_{rr}\right] x_c' - \left[\left(\frac{T_f}{2} - R_{fl}\right) \cos\delta_{fl}\right.$$

$$\left. - (F_{fl} + Q_{fl}) \sin\delta_{fl} + \left(\frac{T_r}{2} - R_{rl}\right) \cos\delta_{rl} - (F_{rl} + Q_{rl}) \sin\delta_{rl}\right] (t - y_c')$$

$$+ \left[\left(\frac{T_f}{2} - R_{fr}\right) \cos\delta_{fr} - (F_{fr} + Q_{fr}) \sin\delta_{fr} + \left(\frac{T_r}{2} - R_{rr}\right) \cos\delta_{rr}\right.$$

$$\left. - (F_{rr} + Q_{rr}) \sin\delta_{rr}\right] y_c' - M_{fl} - M_{fr} - M_{rl} - M_{rr} + c_{xz}\, q\, A_f\, l$$

$$= I_z \ddot{\psi} - I_{xz} \ddot{\Theta} \tag{37}$$

where:

$$T_f = k_{f\delta} \frac{T_s}{r_w} \qquad T_r = k_{r\delta} \frac{T_s}{r_w} \qquad q = \frac{\rho v_{rr}}{2}$$

It is pointed out that the equations of motion (32-37) employ subscripts rr, fr, fl, and rl for identification of the individual wheels instead of the previously used 1, 2, 3, 4 indices. Tire forces designated by $\overline{P}_i$ in equation (24) are broken down into individual components F, Q, T, R and W. Since the vertical distance between the origins of the prime and double prime systems (points O′ and O″) affects the value of the coordinate C of the centroid of the sprung mass, this distance cannot be selected arbitrarily. For instance, in the case of a vehicle equipped with independent front suspension, and solid rear axle (see fig. 5) this distance becomes:

$$z_0 = -r_w + \frac{h_r (l - a)}{l} \tag{38}$$

and the value C may be expressed as follows:

$$c = h_s - \frac{h_r (l - a)}{l} \tag{39}$$

The coordinates of the centroid of the total mass of the vehicle x_c' y_c' and z_c' may be obtained from simple geometrical relationships:

$$x_c' = a + \frac{W_s}{W} c\varphi \tag{40}$$

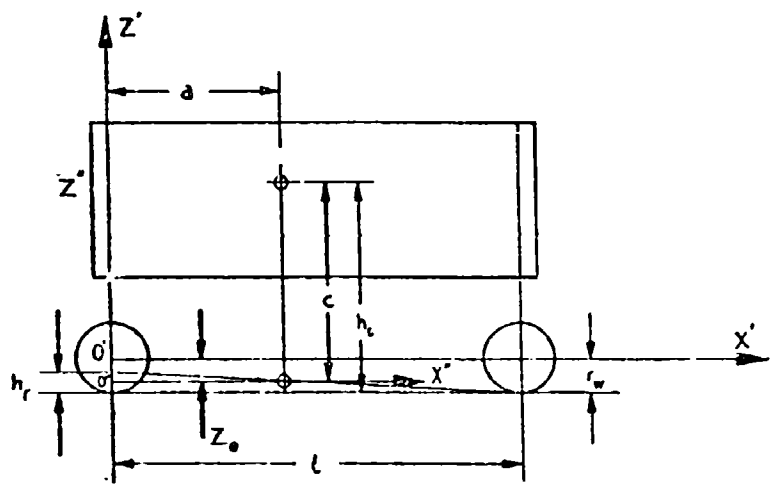


Fig. 5. — Determination of the coordinate z_c' of the centroid of a vehicle equipped with solid rear axle.

$$y_c' = h - \frac{W_s}{W} e\theta \tag{41}$$

$$z_c' = \frac{W_s}{W} e - a\varphi + b\theta + z_1 \tag{42}$$

Tire forces. — Lateral tire forces and their distribution between front and rear are recognized as the major factor in determining the vehicle's behavior in cornering. Non-linearity of lateral tire forces must be emphasized, since this is a primary cause of the understeering or oversteering response of the vehicle. The tire theory previously developed by one of the present authors [4] is utilized to describe lateral tire force and aligning torque as non-linear functions of slip angle, wheel load, traction force, camber and friction coefficients. Therefore, this paper does not cover the explicit relationships describing tire characteristics. Lateral tire forces are greatly influenced by numerous design parameters, including dynamic wheel load, wheel camber, power application and geometrical steer.

In off-the-load locomotion, an additional factor not associated with design must be considered: the character of the terrain traversed, particularly the deformability of the soil. This important subject is discussed in a general way in a later section of this paper.

Dynamic wheel load: dynamic wheel load is defined as the instantaneous value of the vertical reaction between the tire and the road surface. It is governed by the six factors listed and discussed below.

1) Static weight distribution between front and rear: It is quite obvious that the static load is a major component of the dynamic load.

2) Lateral weight transfer through the springs: This results from the total rolling moment acting on the car body, which is composed of a) the moment produced by the lateral component of inertia force, applied at the C. G. of the sprung mass; b) the moment resulting from lateral displacement of the C. G. of the sprung mass due to roll; c) the aerodynamic rolling moment and d) the rolling moment due to driveshaft torque, in the case of a solid rear axle only. The driveshaft torque produces not only a moment resulting in body roll, but also a moment transmitted directly through the rear axle and not associated with roll. Therefore, we will discuss the effect of driveshaft torque on lateral weight transfer separately.

The rolling moment of the sprung mass, which is produced by the factors a) b) and c) as listed above, is determined by roll center heights, roll angle and height of the center of pressure. The rolling moment transmitted through the suspension springs to the wheels is distributed between front and rear in proportion to the respective roll rates.

3) Lateral weight transfer bypassing the springs: This is produced by that moment of lateral tire forces which equals the sum of the products of front and rear lateral tire forces and their respective roll center heights.

In the case of independent suspensions, roll center height is not a constant but rather a variable which is determined by tread change. In the equations of car motion, the concept of anti-roll forces is used instead of roll center height. Anti-roll force is defined as the vertical component of lateral tire force. This force equals lateral tire force multiplied by the angle between the tangent to the wheel path curve and a line vertical with respect to the road surface.

4) Lateral weight transfer due to engine torque: on a vehicle equipped with a solid rear axle, a torque reaction, caused by driveshaft torque, develops at the rear axle; this results in roll of the car body to the right. The rolling moment produced by driveshaft torque adds to the moments produced by the lateral components of the inertia forces applied at the C. G. of the sprung mass and by aerodynamic forces. The resultant moment acting on the rear axle is composed of that part of the moment due to driveshaft torque which is transmitted from the body to the axle through the springs and the reaction moment at the rear axle.

5) Fore and aft weight transfer: This is produced by the sum of all moments acting about a horizontal lateral axis through the C. G. of the vehicle. These moments in turn are determined by the longitudinal components of inertia forces, by the fore and aft displacement of the C. G. of the sprung mass resulting from pitch and by the aerodynamic pitching moment.

6) Lift caused by aerodynamic and inertia forces: Both aerodynamic and inertia forces have components which act upward and result in lift of the car body and reduction of vertical wheel reactions. This effect increases with

speed; at high speeds it can have a very pronounced influence on vehicle stability because of the interrelation between vertical and lateral tire forces.

Determination of dynamic wheel loads, taking into consideration all the factors discussed above, is expressed in equations 43-46.

$$W_{fl} = W_{fl}^{0} + k_f f_{fl} - \frac{k_f'}{2}(f_{fr} - f_{fl}) + k_{ar}\dot{f}_{fl} - \left[(F_{fl} + Q_{fl})\cos\delta_{fl} + \left(\frac{T_f}{2} - R_{fl}\right)\sin\delta_{fl}\right]\frac{d\,t_{fl}}{d\,f_{fl}} - \left[-(F_{fl} + Q_{fl})\sin\delta_{fl} + \left(\frac{T_f}{2} - R_{fl}\right)\cos\delta_{fl}\right]\frac{d\,l_{fl}}{d\,f_{fl}} + W_{fl}^{b} \quad (43)$$

$$W_{fr} = W_{fr}^{0} + k_f f_{fr} + \frac{k_f'}{2}(f_{fr} - f_{fl}) + k_{ar}\dot{f}_{fr} + \left[(F_{fr} + Q_{fr})\cos\delta_{fr} + \left(\frac{T_f}{2} - R_{fr}\right)\sin\delta_{fr}\right]\frac{d\,t_{fr}}{d\,f_{fr}} - \left[-(F_{fr} + Q_{fr})\sin\delta_{fr} + \left(\frac{T_f}{2} - R_{fr}\right)\cos\delta_{fr}\right]\frac{d\,l_{fr}}{d\,f_{fr}} + W_{fr}^{b} \quad (44)$$

$$W_{rl} = W_{rl}^{0} - \left[\zeta k_r \frac{t_a^2}{t^2}\frac{(f_{rr} - f_{rl})}{2} - \frac{k_r}{2}(f_{rr} + f_{rl})\right](1 - k_{bd}) + \left[-(F_{rl} + Q_{rl})\sin\delta_{rl} + \left(\frac{T_r}{2} - R_{rl}\right)\cos\delta_{rl}\right]\frac{d\,l_{rl}}{d\,f_{rl}} + k_{ar}\dot{f}_{rl} + \left[k_r f_{rl} - \frac{k_r'}{2}(f_{rr} - f_{rl})\right]k_{bd} - \left[(F_{rl} + Q_{rl})\cos\delta_{rl} + \left(\frac{T_r}{2} - R_{rl}\right)\sin\delta_{rl}\right]\frac{d\,t_{rl}}{d\,f_{rl}}k_{bd} - \left[(F_{rl} + Q_{rl})\cos\delta_{rl} + \left(\frac{T_r}{2} - R_{rl}\right)\sin\delta_{rl} + (F_{rr} + Q_{rr})\cos\delta_{rr} + \left(\frac{T_r}{2} - R_{rr}\right)\sin\delta_{rr}\right]\frac{h_r(1 - k_{bd})}{t} + \frac{T_a k_\varphi}{t\,i\,\eta_a} + W_{rl}^{b} \quad (45)$$

$$W_{rr} = W_{rr}^{0} + \left[\zeta k_r \frac{t_a^2}{t^2}\frac{(f_{rl} - f_{rr})}{2} + \frac{k_r}{2}(f_{rr} + f_{rl})\right](1 - k_{bd}) + \left[-(F_{rr} + Q_{rr})\sin\delta_{rr} + \left(\frac{T_r}{2} - R_{rr}\right)\cos\delta_{rr}\right]\frac{d\,l_{rr}}{d\,f_{rr}} + k_{ar}\dot{f}_{rr}$$

$$+ \left[k_r f_{rr} + \frac{k_r'}{2}(f_{rr} - f_{rl})\right] k_{bd}$$

$$+ \left[(F_{rr} + Q_{rr}) \cos \delta_{rr} + \left(\frac{T_r}{2} - R_{rr}\right) \sin \delta_{rr}\right] \frac{d\, t_{rr}}{d\, f_{rr}} k_{bd}$$

$$+ \left[(F_{rl} + Q_{rl}) \cos \delta_{rl} + \left(\frac{T_r}{2} - R_{rl}\right) \sin \delta_{rl} + (F_{rr} + Q_{rr}) \cos \delta_{rr}\right.$$

$$\left. + \left(\frac{T_r}{2} - R_{rr}\right) \sin \delta_{rr}\right] \frac{h_r (1 - k_{bd})}{t} - \frac{T_a k_e}{t\, i\, \eta_a} + W_{rr}^{b} \qquad (46)$$

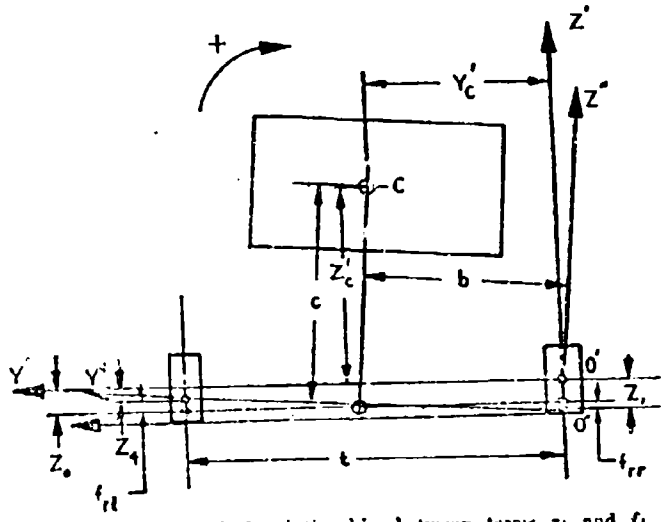


Fig. 6. — Geometrical relationship between terms z_i and f_i.

The most significant terms in these equations are expressed as functions of vertical wheel displacement f_{rr}, f_{rr}, f_{rl}, f_{rl}.

The term « vertical wheel displacement » is more commonly found in automotive design practice than the previously employed values z_i. The relationship between f_i and z_i is shown in fig. 6.

Wheel camber: Wheel camber produces a lateral tire force which is additive to those produced due to slip angle. The front wheels of a vehicle equipped with independent front suspension usually lean toward the outside of the turn; therefore, camber thrust reduces the resultant lateral tire force at the front. Camber thrust is proportional to the dynamic camber angle, which comprises static design camber, camber change in roll and roll angle. Camber thrust is a non-linear function of wheel load (see equation 46 in ref. 1).

Power application: The application of power to the driving wheels influences lateral tire forces on the driving tires, fore and aft weight transfer

and lateral weight transfer. Its effect on lateral tire force is explained by the « interaction effect » and by reduction of the effective lateral coefficient of friction, as described in detail in reference [1].

Power application also produces forward acceleration of the vehicle, which brings about another longitudinal component of the inertia force and therefore produces additional fore and aft weight transfer and pitch. Since power application requires an increase of the drive shaft torque, additional lateral weight transfer and roll of the car body also result.

Effect of geometrical steer. — Geometrical steer is defined as steer of the front or rear wheels which results from causes other than driver action. It may result from any of the following factors: steering geometry, toe change, initial toe-in setting, rear axle roll steer and suspension and steering flexibility. Geometrical steer causes changes in slip angles and consequently changes in lateral tire forces.

Steering geometry: Steering geometry determines the distribution of slip angle values between outer and inner wheels. True Ackerman geometry produces larger slip angles at the front inner wheel than at the outer wheel. Parallel steering results in approximately equal slip angles on outer and inner wheels, provided the radius of the turn is sufficiently large. Since the lateral tire force reduces with a decrease of wheel load, the slip angle at the inner wheel is comparatively ineffective. Therefore, the vehicle with Ackerman steering develops smaller resultant lateral forces at the front tires than the same vehicle with parallel steering. Consequently, in a given cornering maneuver, the vehicle with Ackerman steering requires larger steering corrections than an equivalent vehicle with parallel steering. Therefore, if parallel steering is considered as a base line then we can say that Ackerman steering geometry produces an understeering effect on the vehicle.

Toe change: Typical toe change geometry on the front, namely, toe-out in jounce and toe-in in rebound, results in reduction of the slip angles at the front tires, which in turn causes a reduction of lateral tire force at the front. The resulting understeering effect increases with an increase of toe change as described above.

Initial toe-in setting: This is another factor governing the distribution of slip angles between inner and outer wheels in a cornering maneuver. Under actual driving conditions it reduces or may even reverse to become toe-out, because of free play and flexibility in the steering system. Therefore, in studying vehicle dynamics, we deal with so called « dynamic » toe-in or toe-out. It is not difficult to see that dynamic toe-in will increase the slip angle at the outer wheel and decrease the slip angle at the inner wheel. This results in an increase of the resultant lateral force on the front tires; in other words, it has an oversteering effect. Therefore, dynamic toe-in opposes the understeering effect produced by Ackerman steering geometry. Dynamic toe-out brings about the opposite trend, resulting in a decrease of the resultant lateral force at the front tires and thus has an understeering effect.

Rear axle roll steer: The most commonly used kind of rear axle steer, forward displacement of the jounce wheel relative to the displacement of the rebound wheel, results in an increase of slip angles at the rear tires. This produces an increase of lateral tire forces at the rear and therefore results in an understeering effect.

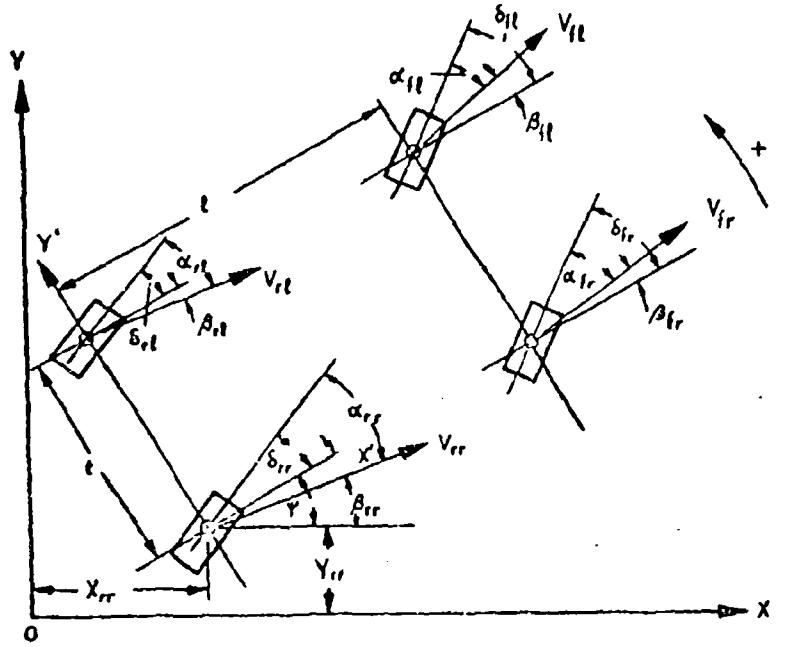


Fig. 7. — Position of the vehicle in the plane of the road surface.

Flexibility in the steering system: Flexibility in the steering system influences the angular displacement of the front wheels produced by torque transmitted through the steering system. For a given initial static toe-in setting, dynamic toe-in decreases with an increase in the flexibility of the steering system. In cornering, this flexibility tends to cause toe-out displacement of the outer wheel and « toe-in » displacement of the inner wheel. Therefore, flexibility of the steering system has an understeering effect. This can be illustrated by the fact that a vehicle equipped with a rack pinion steering, which is comparatively rigid, has less understeer than the same vehicle equipped with a conventional steering system having identical static steering geometry.

The effect of geometrical steer is described in the equations of motion by empirical relationships, most of which are presented in terms of vertical wheel displacements.

Lateral tire force is a function of the variables discussed above and also of slip angle. The slip angle may be expressed in terms of other variables of motion as shown in equations 47-54 below (see fig. 7).

$$\psi + \beta_{rr} = \tan^{-1} \frac{\dot{y}_{rr}}{\dot{x}_{rr}} \tag{47}$$

$$\beta_{rr} = -\alpha_{rr} + \delta_{rr} \tag{48}$$

$$\beta_{fr} = \delta_{fr} - \alpha_{fr} \tag{49}$$

$$\beta_{fr} = \tan^{-1} \frac{l\dot{\psi} + v_{rr} \sin \beta_{rr} - \frac{d\, t'_{fr}}{d\, f_{fr}} \dot{f}_{fr} + k_{hd} \frac{d\, t'_{rr}}{d\, f_{rr}} \dot{f}_{rr}}{v_{rr} \cos \beta_{rr}} \tag{50}$$

$$\beta_{fl} = \delta_{fl} - \alpha_{fl} \tag{51}$$

$$\beta_{fl} = \tan^{-1} \frac{l\dot{\psi} + v_{rr} \sin \beta_{rr} + \frac{d\, t'_{fl}}{d\, f_{fl}} \dot{f}_{fl} + k_{hd} \frac{d\, t'_{rr}}{d\, f_{rr}} \dot{f}_{rr}}{v_{rr} \cos \beta_{rr} - t\dot{\psi}} \tag{52}$$

$$\beta_{rl} = -\alpha_{rl} + \delta_{rl} \tag{53}$$

$$\beta_{rl} = \tan^{-1} \frac{v_{rr} \sin \beta_{rr} + k_{hd} \frac{d\, t'_{rl}}{d\, f_{rl}} \dot{f}_{rl} + k_{hd} \frac{d\, t'_{rr}}{d\, f_{rr}} \dot{f}_{rr}}{v_{rr} \cos \beta_{rr} - t\dot{\psi}} \tag{54}$$

The dynamical problem thus resolves itself to a system of six differential equations in the eight variables, all of which may be functions of time.

The basic independent variables are x_1, y_1, ψ, f_{rr}, f_{fr}, f_{fl}, T_a, and δ_s. Six of these may be solved for when two of them are specified. In our problem T_a and δ_s will be specified together with the initial conditions on the other six, thus

$$x_1\ (0) \qquad \dot{x}_1\ (0)$$

$$y_1\ (0) \qquad \dot{y}_1\ (0)$$

$$\psi_1\ (0) \qquad \dot{\psi}_1\ (0)$$

will be assumed given.

Since we can solve for any of the variables of motion, quantitative evaluation of a vehicle's understeering or oversteering response is also possible. Understeer or oversteer describes a change in motion produced by a given input of drive shaft torque, of steer angle or of a lateral force such as a wind gust. In the case of a step input, understeering and oversteering characteristics of the

vehicle can be described quantitatively by the time history of the response: input ratio. Response of the vehicle may be expressed in terms of variables of motion such as yawing acceleration, yawing velocity or radius of curvature of the vehicle path. To obtain the absolute value of the understeer-oversteer response of an actual vehicle, it has to be evaluated against a so called « neutral » response. The difference between these two responses provides the actual value of understeer or oversteer. To illustrate this, let us assume that for a given steer it is known what radius of curvature a car will move in when traveling exceedingly slowly under steady conditions. We shall refer to this as a quasi-static radius of curvature. Let us now suppose that a car moving with constant speed in a circle of radius ρ_o is powered by a certain constant torque T_o. Let a unit change be applied to T_o and solve the dynamical equations of motion for the new radius of curvature; the method for doing this will be described below. On comparing the new radius of curvature ρ_d with ρ_o, we shall say that oversteering has occurred if $\rho_d < \rho_o$.

Another test that may be applied is to give the steer angle a unit change. Again, solving the dynamical equations for the radius of curvature of the path taken by the car and comparing this with the radius of curvature under-steady, slow conditions for the new steer angle, we again use the criterion of

and

$$\rho_d < \rho_o \qquad \text{oversteer}$$

$$\rho_d > \rho_o \qquad \text{understeer.}$$

When the car is moving with constant speed in a straight line and is acted on by a lateral unit force e.g. the wind, the dynamical equations are solved and the radius of curvature is determined as a function of time. In the case of understeer, the car turns in the direction of the wind, in the case of oversteer it will eventually turn toward the wind.

It is important to note that a vehicle may not perform the same way under the three different conditions described above. It is also important to note that because of the non-linearity of the problem the solution must be carried out over a finite duration of time in order that the essential characteristics of the motion be determined; furthermore, these effects cannot be linearly superimposed and will depend upon the initial velocity.

Thus, the quantity we shall solve for is

$$\rho = \frac{(\dot{x}_1^2 + \dot{y}_1)^{3/2}}{\dot{x}_1 \ddot{y}_1 - \dot{y}_1 \ddot{x}_1}$$

Furthermore, the computed ψ (t) when compared to the tangent of the trajectory $\dot{y}/\dot{x}$ will indicate such phenomena as break-away. In addition, the values of the z's will indicate whether or not undesirable oscillations of the sprung mass will occur.

It is evident that the complexity of the problem precludes obtaining a solution other than a numerical one. However, with the use of a high speed digital computer, it is feasible to solve the problem as outlined above. In fact, the authors are at present carrying out such a program for a vehicle on a hard pavement. For that case values of the physical parameters entering into the equations have been found and results are being obtained which can be and are being compared with experiment.

In the case of vehicles on soil, the relationships of load and displacement must be found before numerical work can be carried out.

There is one area, however, which can be treated with present knowledge; we should like to point out that the problem of a vehicle traveling on a hard, frozen terrain is amenable to solution.

Lateral characteristics of a tire rolling on soft soil

Vehicle handling characteristics are determined mainly by forces between the tire and the ground and by deformations of these two media. Lateral forces and lateral deformations are of particular importance in cornering maneuvers of an automobile. Other forces such as vertical loads and longitudinal forces (traction, rolling resistance) and corresponding deformations are also important since they have a secondary effect on lateral forces and deformations. Lateral deformations of the tire and of the ground are particularly important since they produce a slip angle at the rolling tire and therefore determine the behavior of the vehicle in cornering. To the best of our knowledge tire theories [19-20-21-22] developed in the past were concerned exclusively with tires operating on hard, friction type surfaces. The coefficient of friction between the tire and the ground was the only factor describing ground properties which these theories considered.

Solving the equation of motion for a vehicle operated on a hard surface with high and low coefficients of friction would show that a vehicle moving on a low friction surface has a considerably larger understeering or oversteering response than the same vehicle on a high friction surface. Therefore, the handling characteristics of vehicles moving across frozen cross-country terrain could become critical even at moderate speeds.

Although the tire equations (1) used in the solution of the equations of motion are limited to friction type hard surfaces, they can also be adapted to cohesive type surfaces by replacing the coefficient of friction by a cohesive coefficient and by using the size of the tire contact area instead of wheel load.

In order to establish the effect of lateral deformability of the soil on the relationship between lateral tire force and slip angle, let us determine the slip angle produced by a given lateral force applied to the rolling wheel for the cases of a wheel rolling on a hard surface and a wheel rolling on deformable soil. Fig. 8 shows an elastic wheel rolling with a constant forward velocity v_x in the direction parallel to the X-axis of an arbitrarily selected X Y Z coordinate

system. The plane of the wheel is parallel to the X Z plane and the centerline of the wheel is located at an arbitrarily selected distance y_o from the Y axis. No lateral forces act on the wheel, therefore, the velocity vector is parallel to the plane of the wheel and the slip angle is equal to zero.

Fig. 9 shows the same wheel with a lateral force F acting on it. As a result of this force application, the wheel moves laterally during a time increment Δt at a distance $\Delta y_1 = y_o - y_1$ where y_1 is a new coordinate of the centerline of the wheel. Therefore, the lateral velocity component of this wheel

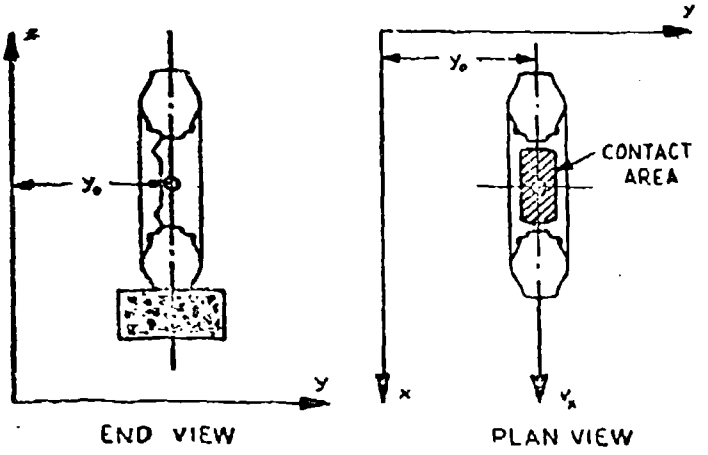


Fig. 8. — Elastic tire rolling on a hard surface at a slip angle equal to zero.

becomes $v'_y = \frac{\Delta y_1}{\Delta t}$. This lateral velocity component produces an angle α_1 between the resultant velocity vector $\bar{v} = \bar{v}'_y + \bar{v}_x$ and the plane of the wheel. Since the forward velocity v_x is constant, the magnitude of this slip angle will be proportional to the lateral velocity component v'_y or the lateral displacement Δy_1. We assume that the lateral force F does not exceed the friction or cohesive limits between the tire contact area and the ground surface. Therefore, the tire contact area is not displaced laterally and the lateral displacement of the wheel results in a lateral deformation of the tire which is equal to the lateral displacement of the wheel from its initial position.

Figure 10 shows a wheel rolling under the conditions described above and subjected to the same lateral force F acting upon it, except that in this case we assume the wheel to be rigid and the soil to be deformable in the lateral direction. In order to simplify this problem, we first omit the effect of sinkage of the wheel on its lateral flexibility. Since the wheel is rigid and no sliding takes place between the tire contact area and the soil surface, the lateral displacement of the wheel will be determined by the lateral displacement of a soil segment underneath the contact area. The amount of lateral displacement of the

soil produced by a given lateral force F will be determined exclusively by the soil's deformation properties. Let us assume that as a result of lateral soil deformation, the wheel displaces laterally during a time increment Δt at a

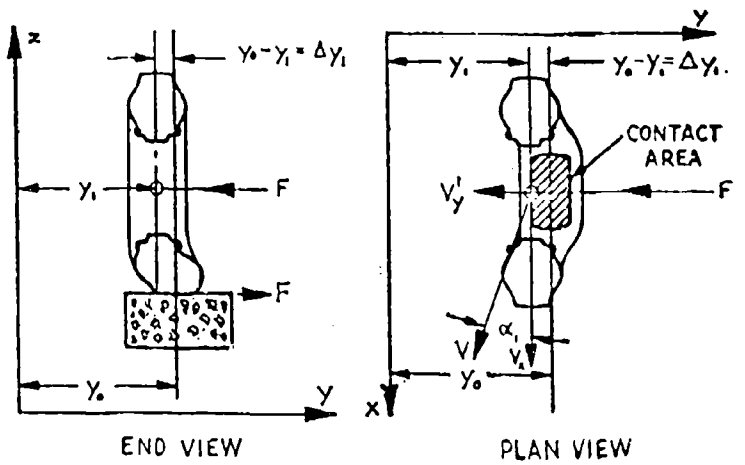


Fig. 9. — Elastic tire rolling on a hard surface at a finite slip angle.

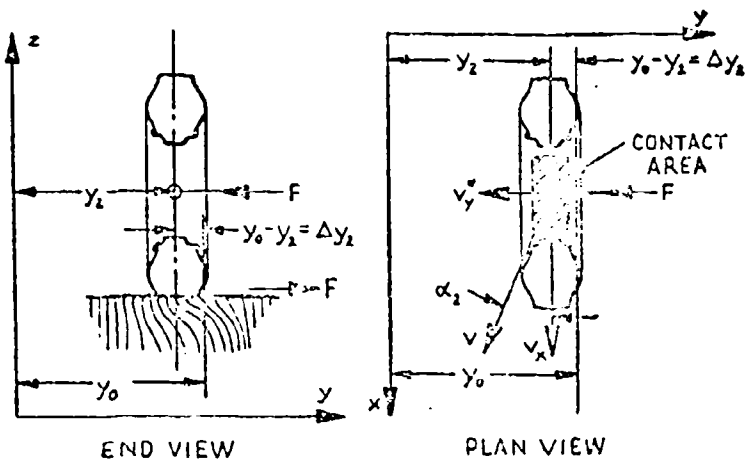


Fig. 10. — Rigid tire rolling on a deformable soil at a finite slip angle.

distance $\Delta y_2 = y_0 - y_2$ where y_2 is a new coordinate of the centerline of the wheel. Therefore, the wheel will operate at a slip angle which will be proportional to deformation of the soil. This illustrates that a slip angle can result either from lateral deformation of a tire or from lateral deformation of the soil.

Figure 11 shows an elastic wheel rolling over soil deformable in the lateral direction. Total lateral displacement of the wheel is composed of individual

lateral displacements caused by deformation of the tire and the soil respectively

$$\Delta y_3 = \Delta y_1 + \Delta y_2$$

Naturally, the resultant slip angles will be larger than those in the case of a hard surface. Therefore, deformability of the soil contributes to an increase of understeering-oversteering response of the vehicle.

In the discussion above, we were concerned only with lateral deformability of the soil and ignored its deformability in the vertical direction, which causes sinkage of the wheel. Sinkage of the wheel results in a restrained lateral defor-

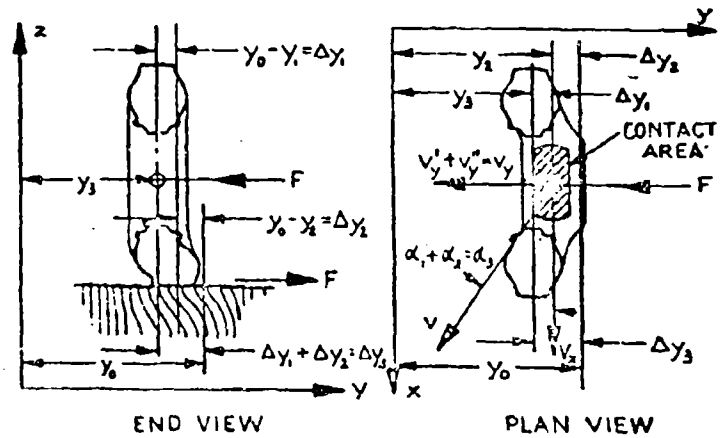


Fig. 11. — Elastic tire rolling on a deformable soil at a finite slip angle.

mation of that part of the tire which is submerged in the soil; it also results in an increased rolling resistance. Restrained lateral deformation of the submerged part of the tire will cause an increase of overall lateral tire stiffness and therefore a decrease in the slip angle corresponding to a given value of lateral tire force. According to the concept of the « interaction effect » increased rolling resistance results in decreased overall lateral tire stiffness. Therefore, sinkage of a tire produces two opposite effects, one of which reduces and the other increases lateral tire stiffness. It is not possible to determine the effect of wheel sinkage on the resultant lateral tire properties quantitatively without knowledge of the mechanics of the interrelation between soil and tire.

The above discussion is merely an attempt to outline some of the basic problems which would be encountered by anyone interested in studying lateral tire-ground forces and deformations on cross-country vehicles. Since, to the best of our knowledge, neither experimental nor theoretical work has ever been conducted in this field, we would recommend that this study be initiated by measurements of lateral tire forces and slip angles in cross-country terrain. Some of the existing trailer type test rigs could be utilized for this purpose. It is also essential to measure vertical wheel loads, rolling resistance, speeds and

tire pressures prevailing during the test. The measurement of coefficient of friction or cohesion between tire and the soil surface is also necessary in order to evaluate the test results. Of course, tests to determine load-deflection characteristics of the soil in all three dimensions are also required. Particular emphasis should be placed on determining the effect of a load acting in one plane on the load-deflection characteristics of the soil in the other planes perpendicular to the force's plane of action. Studies along these lines have already been conducted by Bekker [23]. He measured the relationship between vertical wheel load and maximum shearing force in the soil. Bekker found that shearing force increases nonlinearly with an increase of wheel load, reaches a certain maximum and then experiences no further change incident to a further load increase.

BIBLIOGRAPHY

1) Bergman W. Theoretical prediction of the effect of traction on cornering force. Paper presented at the SAE Summer Meeting, Chicago, Illinois, June 1960.

2) Huber L. Die Fahrtrichtungsstabilität des Schnellfahrenden Kraftwagens. Deutsche Kraftfahrtforschung Heft. 44, 1940.

3) Rickert P. and Schunck T. Zur Fahrmechanik des gummibereiften Kraftfahrzeuges. Ingenieur Archiv, 12, pag. 240-224, 1940.

4) Mitschke M. Fahrtrichtungshaltung und Fahrstabilität von vierrädrigen Kraftfahrzeugen. Deutsche Kraftfahrtforschung und Strassenverkehrstechnik Heft, 135, 1960.

5) Kamm W. Directional stability of motor vehicles. Technical memorandum, no. 103, Stevens Institute of Technology, Hoboken, New Jersey, 1953.

6) Gebelein H. and Schlick G. Untersuchungen zur Erhöhung der Sicherheit der Kraftfahrzeuge durch Verbesserung der Stabilität und der Fahrtrichtungshaltung. Deutsche Kraftfahrforschung und Strassenverkehrstechnik Heft, 122, 1959.

7) Schilling R. Directional control of automobiles. Journal of the Industrial Mathematics Society, vol. 4, pag. 64-77, 1953.

8) Segel L. Theoretical prediction and experimental substantiation of the response of the automobile to steering control. Automobile Division, the Institution of Mechanical Engineering Proceedings, 1956.

9) Kohr R. H. The application of mathematics to a basic study of automobile control and stability problems. General Motors Engineering Journal, April-May-June, pages 14-19, 1959.

10) Goland M. and Jindra F. Directional stability and control of a four wheeled vehicle in a flat turn. Paper presented at the SAE National West Coast Meeting, San Francisco, California, August, 1960.

11) Smiley R. and Horne W. Mechanical properties of pneumatic tires. NACA Technical Note, 4110, 1958.

12) Paslay P. R. and Slibar A. The motion of automobiles in unbanked curves. Ingenieur Archiv, vol. 24, pag. 412-424, 1956.

13) Euke K. Ein Verfahren zur Berechnung der Kurvenlage des Kraftwagens. Dissertation, Technische Hochschule Karlsruhe, 1957.

14) Mitterlehner G. Die Lenkstabilität des luftbereiften Kraftwagens. Ingenieur Archiv, vol. 27, pag. 88-103, 1959.

15) Fiala E. Zur Fahrdynamik des Strassenfahrzeuges unter Berücksichtigung der Lenkstabilität. ATZ, pag. 71-79, March 1960.

16) Zuk W. The dynamics of vehicle skid deviation as caused by road conditions. Paper presented at the First International Skid Prevention Conference, Charlottesville, Virginia, August 1959.

17) Radt H. S. and Milliken W. F. Motions of skidding automobiles. Paper presented at the SAE Summer Meeting, Chicago, Illinois, June 1960.

18) Bekker M. G. Theory of land locomotion. University of Michigan Press, Ann Arbor, 1956.

19) Von Schlippe B. and Dietrich R. Shimmying of a pneumatic wheel. NACA, T.M. 1365, pag. 125-147, translation from. Das flattern eines bepneuten Rades, Bericht 140 der Lilienthal Gesellschaft, pag. 35-45, 1941.

20) Temple G. The dynamics of the pneumatic tyre.

21) Fiala E. Seitenkräfte am rollenden Luftreifen. V.D.I., pag. 973-979, October 1954.

22) Fromm H. Sideslip and guiding characteristics of the rolling wheel. NACA, T.M. 1365, pag. 191-203. Translation from «Seitenschlupf und Führungswert des rollenden Rades», Bericht 140 der Lilienthal Gesellschaft, pag. 56-63.

23) Bekker M. G. Relationship between soil and a vehicle. SAE Quarterly Transactions, vol. 4, pag. 331-397, July, 1950.

DISCUSSIONS

J. L. BOGDANOFF. — I would like to first congratulate the speaker on a very fine piece of work. The calculation of breakaway is indeed unusual, and while I am not an expert in this field, I am aware of its significance. One question that I would like to put: when you spoke of being able to compute breakawey, over and understeering off the road, what procedure did you have in mind for dealing with the ground, if you take it as a hard but rough surface?

E. SAIBEL. — It is in answer to that question that I was interested in the work of Bogdanoff and Kozin, because the characteristics between tire and ground have to be found experimentally. Now, when those characteristics are variables, then obviously the only thing we can do is to get average values and treat the problem from statistical point of view. This is quite possible to do because we have methods as were shown this morning, for averaging these quantities in a rational way, and these values can fit directely into our equations.

F. KOZIN. — I'd just like to ask Prof. Saibel to perhaps state in a little bit more detail the stability of a limit cycle in which you perform. Could you comment on that?

E. SAIBEL. — The simplifications that we made in the problem were on the dynamical side. In many haste I did not mention the fact that we are expressing the motion of the vehicle in terms of the deflections of the springs, and we are assuming these deflections to be small. That is our first simplification. This means that since we take the deflections in this paper to be small, we are limiting ourselves to pitch and roll, no yaw. Second assumption: in the kinematical and dynamical analysis, certain quantities came up which were small quantities of the second order; these were dropped. So that, the dynamical side of the equations are linear. The non-linearities occur on the force side of the equation. Consequently, we have a well defined system which we known will have a unique solution, with the initial conditions that we impose.

N. 20

The mechanics of walking vehicles *)

La meccanica dei veicoli che camminano

JOSEPH E. SHIGLEY **)

ABSTRACT. — *A criteria for qualitatively judging the merits of proposed walking mechanisms is first established. It is found that the shape of the locus of the foot relative to the vehicle is of prime importance in obtaining a balance of inertia forces, and that this locus is useful in the creation of a nomenclature for walking machines. Walking mechanisms driven by a rotating source of power are investigated and found to be useful only for slow speeds because of the difficulty of control and of obtaining balanced inertia forces. It is found that hydraulically operated walking mechanisms satisfy most of the quality requirements. Another conclusion of the paper is that walking machines should be capable of traversing rough terrain at slightly greater speeds than wheeled or tracked vehicles.*

Introduction

The number of references on the mechanics of animal locomotion are indeed sparse. Bekker [1,2] cites Rashevsky [3,4] and states that all jumping or running quadrupeds utilize a system of extremities consisting of levers. Both Bekker and Rashevsky reach the conclusion that running is most efficient when the vertical movement of the center of gravity is a minimum. Bekker uses the polygon analogy to develop relationships which give the power required for walking as a function of the velocity.

In 1948 Levens, Inman, and Blosser [5,6] reported an interesting means of investigating the mechanics of human locomotion. Vertical and horizontal displacements of various points on the leg and body in a single plane were determined photographically by an interrupted-light technique. For a normal subject in level walking, the results show a smooth and continuous curve for the motion of the center of gravity with only a slight vertical motion. On the other hand the path generated by the heel is quite discontinuous with large velocity changes.

Note: The superior numbers refer to the bibliography at the end of the paper.

*) This paper was originally prepared for Land Locomotion Laboratory, U.S. Army Ordnance Tank Automotive Command, Detroit, Michigan.

**) University of Michigan, Ann Arbor, Michigan, U.S.A.

Current research in prosthetics at the University of Michigan, Case Institute of Technology, the University of California, and others, may yield valuable techniques for the investigation of animal locomotion.

Bernhard [7] recently made a preliminary study of mechanical means of running and jumping and suggested that additional investigation is desirable.

With this meager background an investigation into the problems of mechanical walking appeared particularly interesting.

The elements of a walking vehicle may be illustrated by the block diagram of fig. 1. The *power source* is used to overcome friction between the feet of

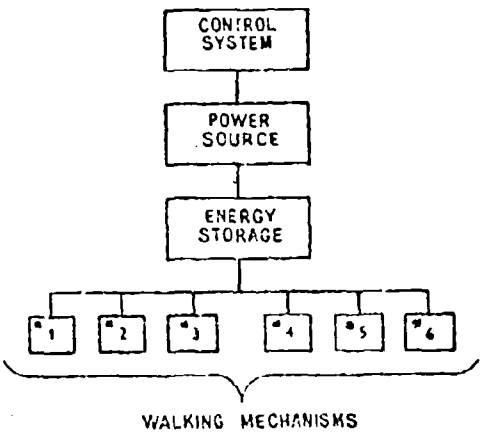


Fig. 1. — Block diagram of a walking vehicle.

the vehicle and the terrain, to make up for frictional losses which occur in the moving parts, and to lift the vehicle over obstructions and up grades. The *control system* provides a means of controlling the *speed, direction, length of stride, height of step,* and *elevation of vehicle* above the mean terrain level. The legs or unit means of locomotion are defined as *walking mechanisms* and are identified by the numbered blocks. The *energy-storage device* serves to level the power requirements by providing energy for acceleration of some of the walking mechanisms and absorbing or storing the energy released by the deceleration of other mechanisms.

An ideal walking mechanism is one which fulfills the following requirements:

1) It must have a uniform velocity while the feet are in contact with the ground.

2) The stride must be long in relation to the physical dimensions of the walking mechanism.

3) The length of stride must be controllable by the vehicle operator.

4) The height of the step (return stroke of foot) should be large compared to the dimensions of the walking mechanism.

5) The height of the step should be controllable by the vehicle operator.

6) It should have a high stride-time to return-time ratio. This means that the foot should be in contact with the terrain during a major portion of a cycle of operation.

7) The speed of a walking mechanism should be capable of variation independently of other walking mechanisms on the same vehicle. This requirement provides the means for direction control.

8) The walking mechanism should be such that it can move the vehicle in either the forward or the backward direction.

9) The inertia forces and inertia torques acting on the vehicle should be balanced.

10) The energy required to lift the foot at the end of stride and return the foot to the beginning of stride should be recoverable.

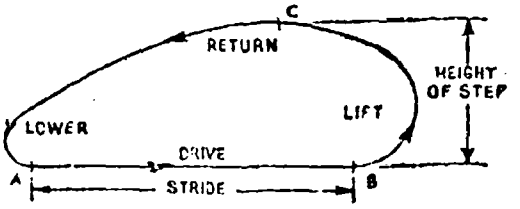


Fig. 2. — Locus of the foot.

11) The height of the body of the vehicle above a mean terrain level should be capable of control by the operator.

A useful means of obtaining a preliminary estimate of the value of a proposed walking mechanism is to graphically generate the closed curve or locus containing all points of the foot as it moves relative to the vehicle (fig. 2). In fig. 2 the foot drives the vehicle during stride, and a point traversing this portion of the locus should do so at a constant velocity. The remaining portion of the locus are the *lift*, *return*, and *lower* phases of the action. A complete traverse of the locus by the foot constitutes a *cycle*. The shape of the lift and lower phases of the locus are useful in determining the action of the foot in initial and final contact with the ground. The shape of the return portion is immaterial except as it affects the acceleration.

Figure 3 illustrates a group of loci. The limiting or degenerate case in (a) is the same as a wheel. The rectangular locus of (b) is interesting because, during return, the foot is always the same distance from the terrain. It is a poor locus because of the infinite acceleration at the corners, and because a descending foot encountering higher terrain would either slide across the terrain or cause the vehicle to stop for a period of time. The loci of (c) and (d) represent extreme cases which can be obtained using the crank and rocker linkage in which the foot is attached to the coupler. The locus of (c) offers the most attractive possibilities because of its symmetry. It has a long straight stride. The return portion of the locus is direct and promises to give minimum

accelerations. The lift and lower phases of the action resemble that of a wheel and so their acceleration characteristics should not be too different. Furthermore, a symmetrical locus offers the attractive possibility of getting balanced inertia forces and torques by properly phasing a number of walking mechanisms on like paths. And finally, the shape of the lift and lower phases seems to be the best compromise between the circular locus of (a) and the rectangular one of (b).

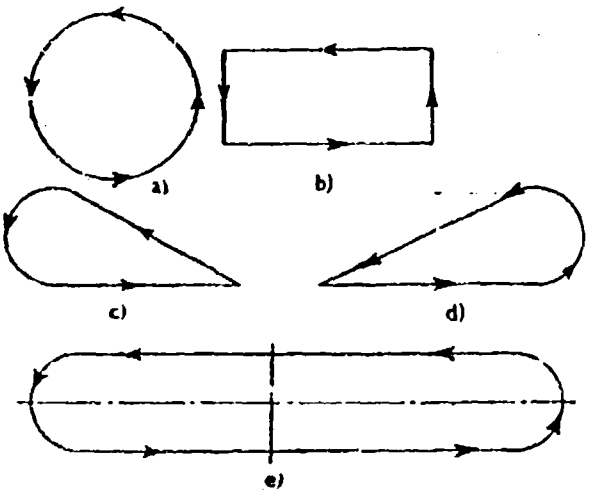


Fig. 3. — Foot loci.

It is interesting to contrast the operation of a wheel when meeting an obstruction to that of the foot of a walking machine when meeting the same obstruction. Both cases are shown in fig. 4. In (a) a wheeled vehicle moving with a velocity V meets with an obstruction. Point A is the point of contact and the periphery of the wheel has the same velocity (tangential) V as the vehicle, but its horizontal component V^h is less than V and consequently the vehicle (except for the effect of the elasticity of the tire) tries to change its velocity to V^h causing shock to the vehicle. In (b) the walking machine meets the same obstruction. The velocity of the foot V^h also differs from the vehicle velocity V. But it is not unlikely that a walking mechanism can be developed in which the tangential component of the velocity of the foot on the lower phase of the locus can be substantially increased above the vehicle velocity so as to increase the horizontal component when meeting an obstruction and thus decrease the shock. Furthermore, a foot does not contact every particle in its path of travel so that, by simple probability, we know that a walking machine will not encounter as many obstructions as a wheeled vehicle. This leads to the conclusion that a walking machine ought to have an advantage over a wheeled or tracked vehicle over rough terrain if speed is the governing

consideration. It is also clear from this discussion that walking mechanisms should be designed to permit some relative motion or sliding between the shoe and the foot of the mechanism or between the shoe and the terrain.

When a pair of legs, on a walking machine, are separated by a reasonable distance and synchronized, then their lower extremities may be joined by runners or skis in order to provide a very long narrow shoe. Such an arrangement should be especially useful for walking over soft terrain such as snow, swampy ground, or loose sand. The possibility is noted, however, that the use of two legs in synchronism by its very nature prevents the phasing of one leg relative to another in order to balance inertial effects.

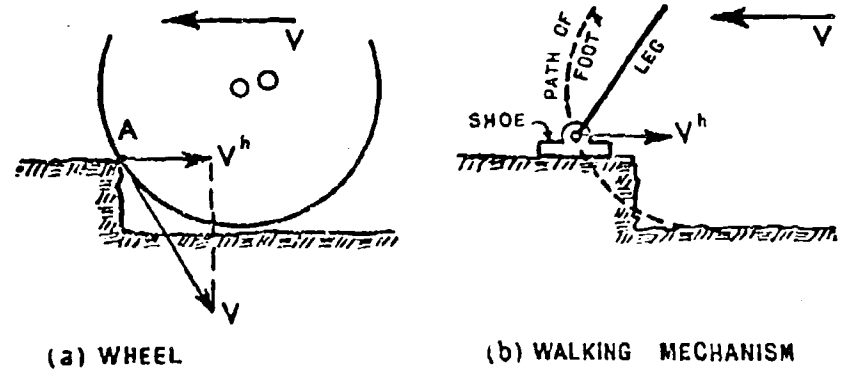


Fig. 4. — Comparison of a wheel and a foot.

Figure 5 illustrates an *equivalent walking mechanism* with a foot A generating the ideal locus. It is called an equivalent mechanism for convenience and because we wish it to represent the general class of all mechanisms capable of generating the ideal locus. Point O is attached to the frame of the vehicle and provides a pivot for the rocking block 3. Link 3 is the leg and it can slide through the rocking block. The driving force must be supplied at point B but it is not necessary for this discussion that we specify the details.

We might visualize point A as traversing the path at a uniform velocity always tangent to the path. Then, because the distance OA is always changing, the leg will always have an angular acceleration. A vertical component of acceleration also exists during the lift and lower phases of the action.

For the problem as described, the vertical acceleration during lift has a sense which is exactly opposite to the vertical acceleration during the lower phase of the action. This means that, if two legs on a vehicle are out of phase by one half a cycle, then, during lift and lower, the vertical inertia forces will be exactly opposite in direction. If the masses of the two legs are the same, and if the lines of action of the two inertia forces are coincident, then the resulting inertia force on the vehicle is zero. This explains the meaning of balancing and how the vertical components of the inertia forces can be balanced.

Next we consider the horizontal components of the inertia forces. If the leg is statically balanced these result in an inertia torque on the vehicle and it is in this torque that our interest lies. It is clear from fig. 5 that the inertia forces during stride will be opposite in direction to those which occur during return. It is not so clear that their magnitudes will be different. During lift of the leg the mass center changes its position too. Furthermore the angular acceleration of the leg is different in magnitude during return than it is during stride because the foot A is closer to the center of rotation O.

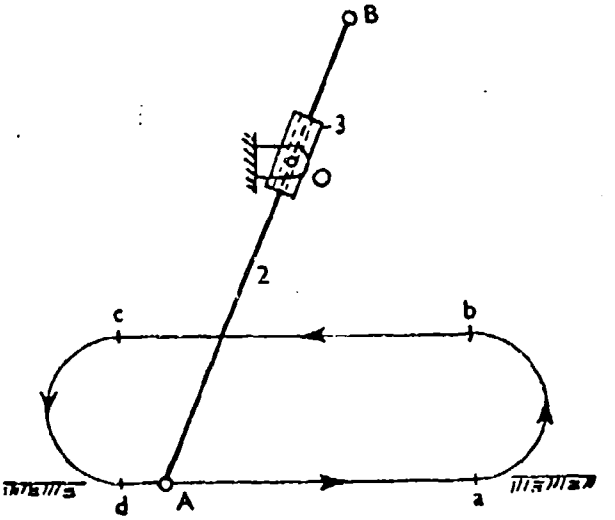


Fig. 5. — Equivalent mechanism.

Thus a pair of legs separated by a phase of one half cycle will only have their inertia torques partly balanced during the stride and return events. It can be demonstrated, however, that, because a torque vector is a free vector, by using sixteen or more legs, the inertia torque reaction on the entire vehicle can be made very small.

The preceding discussion shows that the four corners of a vehicle should be supported by a minimum of sixteen legs, four per corner.

Mechanically operated walking mechanisms

By mechanically operated walking mechanisms we refer specifically to any walking mechanism consisting of mechanical links driven by a rotating source of power.

Figure 6 is not a solution to the problem but it represents the general configuration of the class of linkages which were investigated, and is presented as an illustration of some of the problems involved.

The linkage of fig. 6 is called the crank and rocker linkage. The *crank* or driver is link 2; it rotates about a center O_2 fixed to the vehicle frame.

Link 4 is the *rocker* and it oscillates about center O_4 also fixed to the vehicle frame. Link 3 is called the *coupler*, and it is connected to the foot at point B. Link 1, the frame of the vehicle, is not shown.

The linkage and the locus are *not* compatible since the one will not generate the other. The problem is this: What are the dimensions of the four links which will generate the required locus?

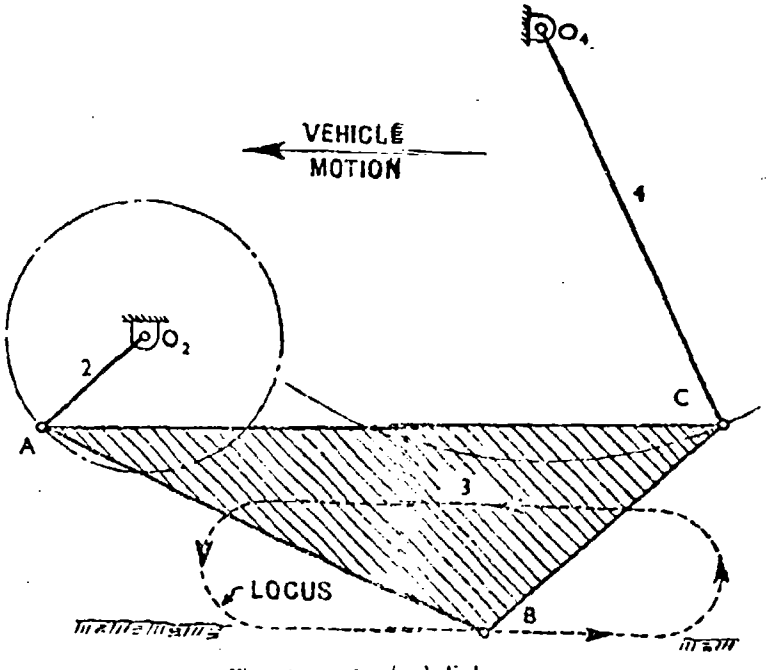


Fig. 6. — Desired linkage.

Three methods of synthesizing such a linkage are available. The Hrones-Nelson [5] synthesis consists in inspecting a very large number of paths generated by linkages of different dimensions until a suitable one is found. The second method is due to Kurt Hain [3] and is called *point-position-reduction*. It consists of choosing five points on the path to be generated. Then a proper choice of points O_2 and O_4 together with the crank length O_2A enables one to locate points B and C by an inversion process so that point B will pass through the five preselected points. Freudenstein [6] has programmed Hain's method on the IBM 650 computer so as to obtain a linkage which will generate the locus with the least error. Since, theoretically at least, there are an infinite number of solutions to the problem, an infinite number still remain after these methods have been used. Furthermore, in point-position-reduction there is no assurance in advance that the resulting linkage will permit the crank to rotate in a complete circle.

A linkage, representing a group of similar solutions obtained by the Hrones-Nelson method, is shown in fig. 7. The locus is shown by dashed lines. The distance between the numbered station points on the locus gives a good idea of the velocities involved since these correspond with equally spaced points on the crank circle. The stride is fairly straight and has good velocity characteristics, but the height of step is much too small.

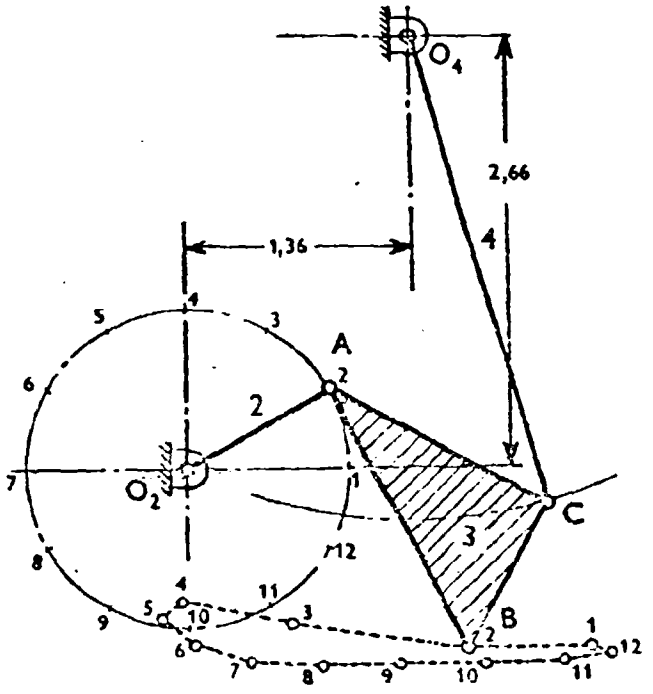


Fig. 7. — A four-bar walking linkage.

A thorough search of Hrones and Nelson reveals only a few linkages which will generate the required locus and none of these seem to be any better than the one of fig. 7. On the other hand if link 4 is permitted to oscillate about a point which is near or below the roadway surface then a great many configurations become available for study. Since the pivot for link 4 cannot physically be located beneath the roadway surface it is necessary to replace link 4 with a slider operating in a cam groove having a center of curvature below the roadway surface.

The best of the cam-groove mechanisms is the one of fig. 8. The locus shows a good stride, a fairly good return-stroke clearance, and a lower phase of the action which is not too poor. The lift is not good, and the locus is not symmetrical about either the vertical or the horizontal center lines. The fact that the foot velocity during stride is not uniform requires that the crank

be driven at a non-uniform velocity. This is a correction means and it can be accomplished by driving the crank with a pair of non-circular gears.

Since the cam groove need not be constant curvature slight changes can be made in it in order to refine the locus. Figure 9 shows an improved locus obtained by such a correction.

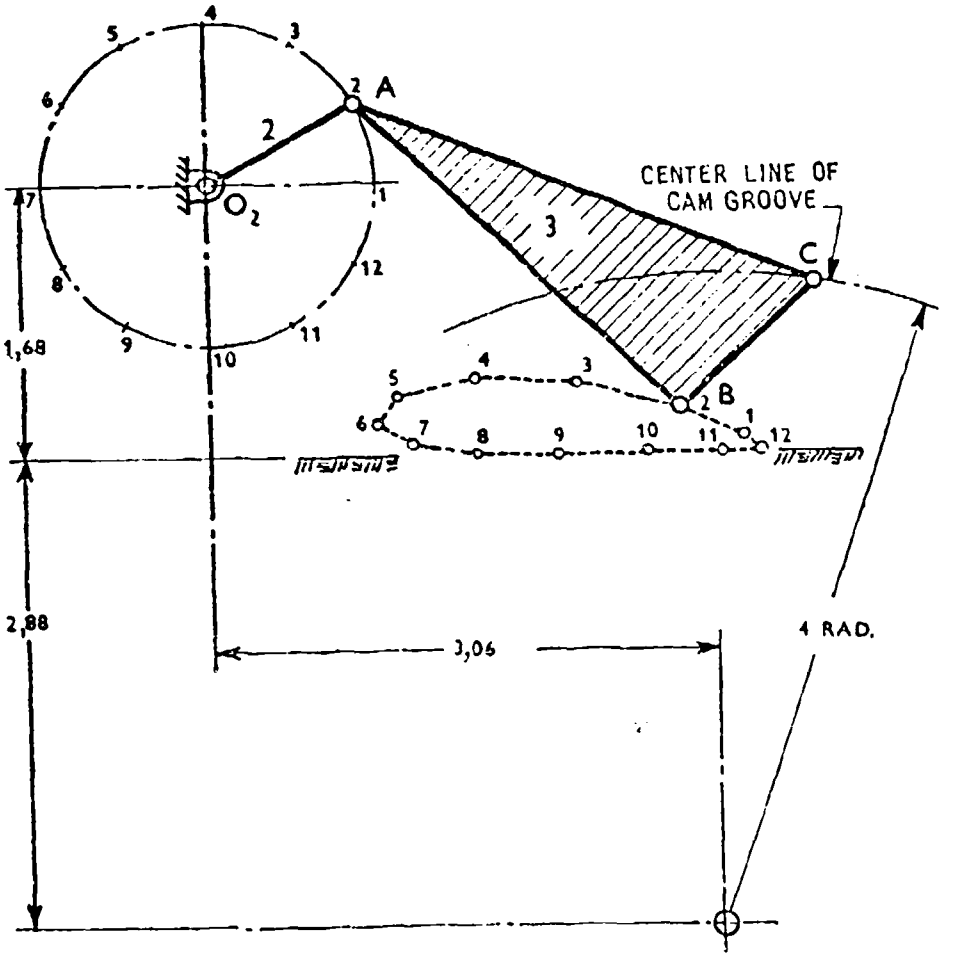


Fig. 8. — The cam-groove linkage.

The existence of the cam groove is quite a disadvantage. In an effort to overcome this, and still take advantage of the large group of linkages like that of fig. 8, the one of fig. 10 was developed. This amounts to taking the linkage of Fig. 8, turning it upside down, and connecting another link to point B having the foot on the other end. In fig. 10 we wish to connect the leg at point C. But a leg connected only at C would not have constrained

motion. Consequently we add links 5, 7, and 8 to the system and get a linkage consisting of two feet M and N, or a single ski or runner.

A small-scale working model of a walking machine was constructed by the Land Locomotion Laboratory at the Detroit Arsenal based upon the linkage of fig. 10. A photograph of this model is shown in fig. 11.

The performance of the class of walking mechanisms capable of being driven by a rotating crank cannot be described as being very satisfactory.

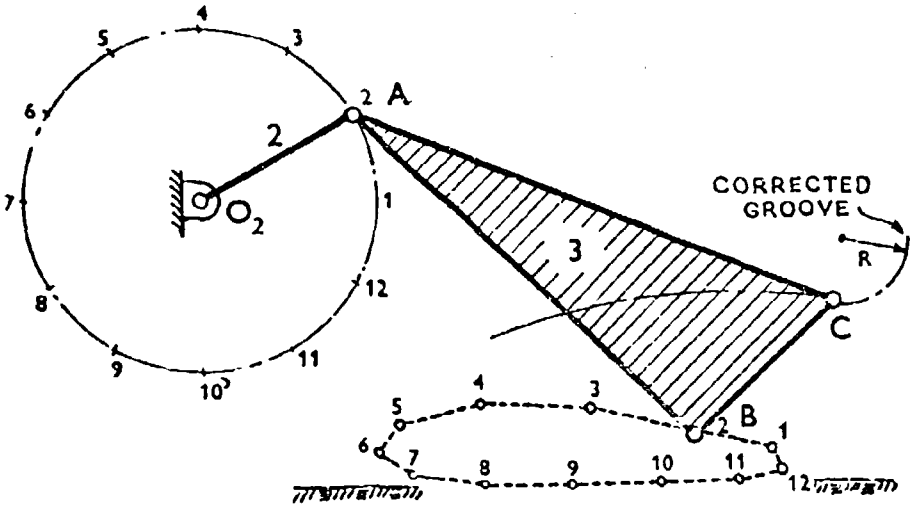


Fig. 9. — A corrected cam-groove mechanism.

None of them fulfill the uniform velocity requirement although they can be made to do so utilizing pairs of non-circular gears as drivers. Also, none of the strides are very long when compared to the overall space required by the entire mechanism. In all of the mechanisms the length of stride is fixed by the dimensions of the linkage and cannot be controlled by the vehicle operator. The height of step is not controllable by the operator either and it can be made larger only by increasing the dimensions of the linkages; this is equivalent to using a large vehicle to obtain high steps.

All of these mechanisms can be operated forward and backward, but direction control would have to be obtained using controlled differentials. Note too that, with a rotating power source, the addition of a flywheel will satisfy the requirement for energy storage during a cycle of operation. Finally, analysis reveals that the inertia torques for a number of these mechanisms connected to a vehicle can be balanced, but the inertia forces cannot. The existence of these unbalanced inertia forces means that a walking vehicle driven by a rotating power source can only be operated at a very slow speed.

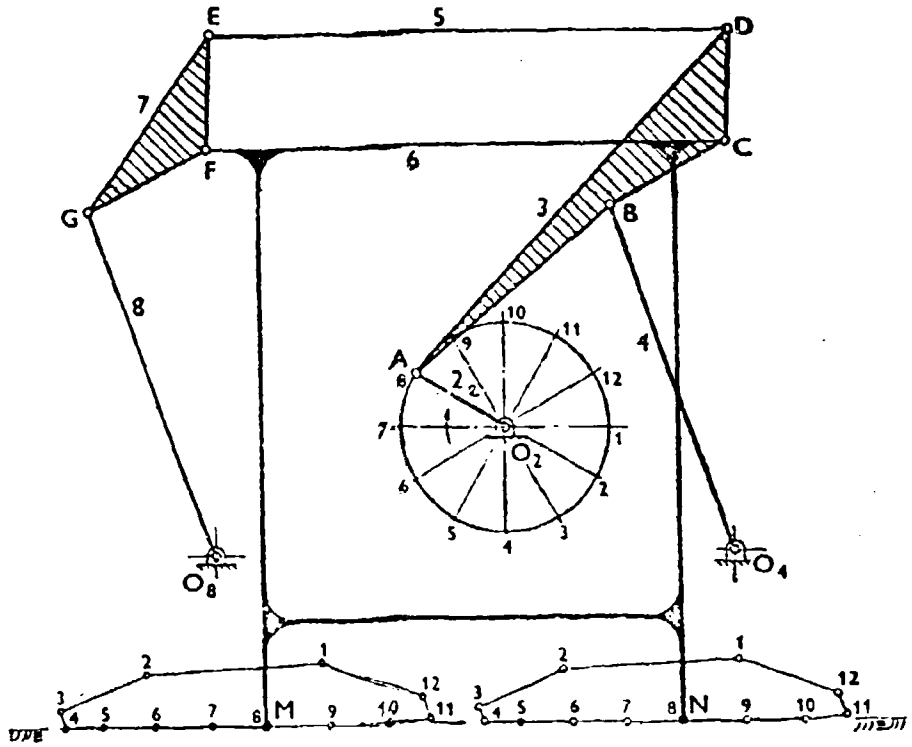


Fig. 10. — The double rocker mechanism.



Fig. 11.

It is noted, however, that the existence of an infinite number of solutions to the walking mechanism means that the possibility of finding a mechanism capable of being balanced still exists.

Vehicle geometry

Let us now interest ourselves in the arrangement of the walking mechanisms on the vehicle itself in order that the shaking and rocking of the vehicle due to inertia forces and torques can be reduced or eliminated. Figure 12 is a side view of a vehicle having legs (not shown) mounted at points A and B. If the legs are properly phased, then, at some instant in time, the inertia torque T_A will be counterclockwise and the torque T_B will be clockwise. Since a torque vector is a free vector, these torques will cancel one another, if their magnitudes are equal, regardless of the location of points A and B.

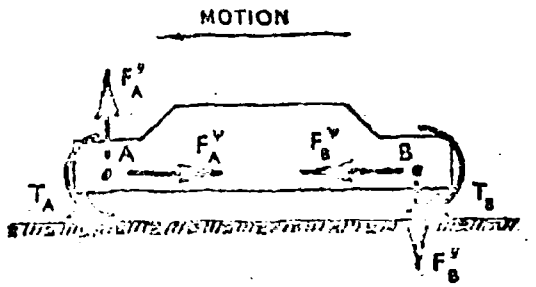


Fig. 12. — Forces on the vehicle.

The horizontal components of the inertia forces F_A^x and F_B^x will cancel each other if their magnitudes are equal and if their elevation on the vehicle are the same. Thus, except for elevation, the location of A and B on the vehicle is not important.

Finally, examining the vertical components F_A^y and $-F_B^y$, we see that these forces form a couple which will tend to rock or oscillate the vehicle about a horizontal axis through the side. In order to achieve cancellation of the vertical components it is necessary for points A and B to be coincident.

Thus it is necessary to mount enough properly phased legs *at one point* to balance the inertia forces in the vertical direction; and enough properly phased legs *on one side* to balance the inertia torques and the horizontal components of the inertia forces. Aside from considerations of support and traction these are the guiding principles which must be used in selecting and arranging the legs. A machine employing perfect walking mechanisms would have a minimum of eight legs on each side, four at A and four at B, properly phased, in order that the resultant inertia forces and torques be zero at all times.

Hydraulically operated walking mechanisms

The mechanism of fig. 13 uses a hydraulic cylinder to position the foot for all phases of the action, but the drive is with a rotating power source. Although the addition of the hydraulic cylinder gives control over the height of step, the locus is quite poor and shows high values of acceleration. The mechanism must still be driven by a source of power at a non-uniform velocity and so we have not gained anything.

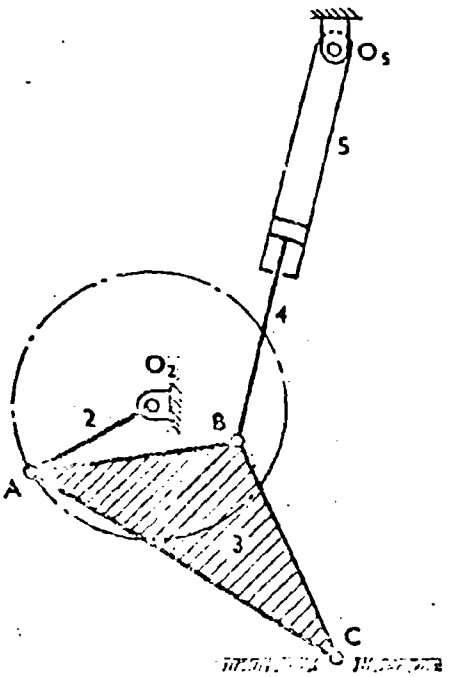


Fig. 13. — A hydraulic walking linkage.

Figure 14 shows a two-cylinder walking linkage in which one cylinder is used for driving and another cylinder for lifting. By programming the flow to these two cylinders properly, the foot B can be made to generate the required locus. Unfortunately, the driving cylinder and piston rod are placed in bending by the weight of the vehicle, and so this is not a good solution.

The mechanism of fig. 15 was developed in an attempt to eliminate the bending on the piston rods. This is one of the best in a large class of mechanisms in which rigid links are used in combination with two cylinders. In this figure, cylinder 2 is intended to accomplish the driving function, and cylinder 5 the lifting function. The mechanism is quite versatile. For example,

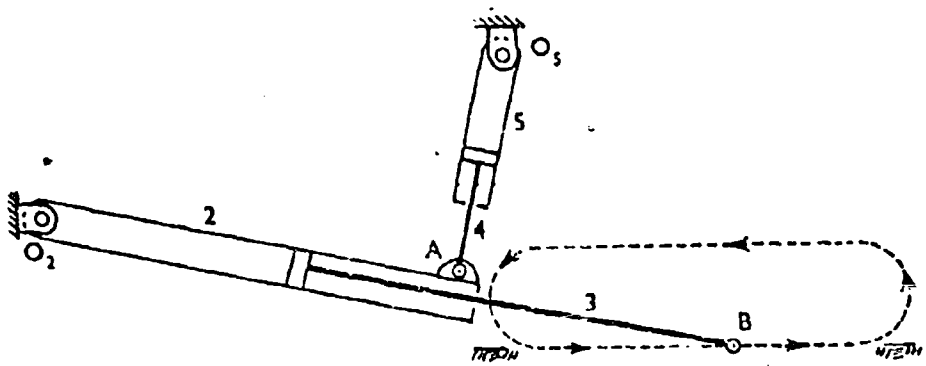


Fig. 14. — A two-cylinder walking linkage.

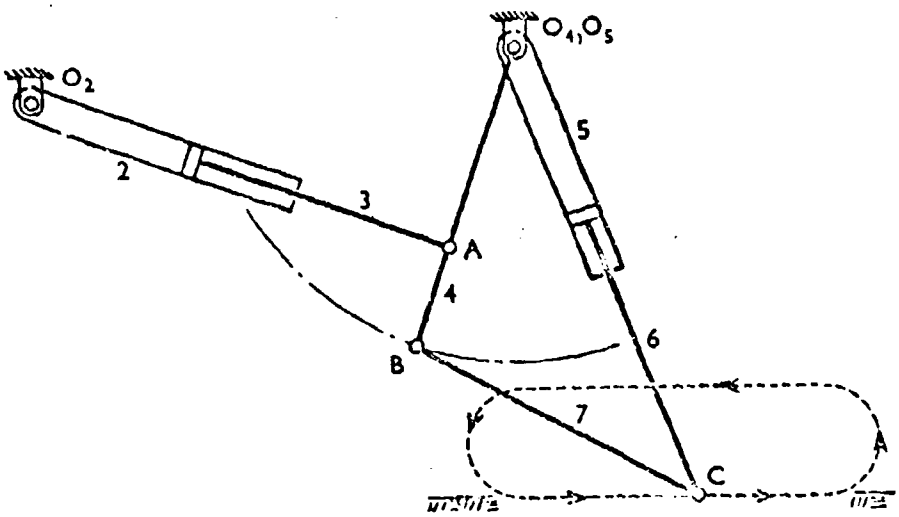


Fig. 15. — Improved model.

the one of fig. 15 has the piston rod of the driving cylinder connected to rocker 4 between point B and the pivot point O_4. Thus, the piston motion is less than the length of stride. But, if the piston rod is connected to the rocker outside of point B, then we get the reverse, and the piston motion is now more than the stride. Also, the piston rod of the lifting cylinder need not be connected at point C. It can be connected anywhere between B and C on link 7 in order to multiply the action of the lifting cylinder. Finally, O_4 and O_5 need not be coincident. If O_5 is located on the vertical center line of the locus, then the rocking motion of the lift cylinder will be symmetrical about this center line.

One of the difficulties of these two-cylinder mechanisms is that the piston

motion for lifting and driving are not independent of each other. Thus, if the height of step is varied without changing the length of stride then another set of flow programs must be used for the two cylinders. Consequently we look for a hydraulic mechanism in which the lift and drive functions are completely independent of each other.

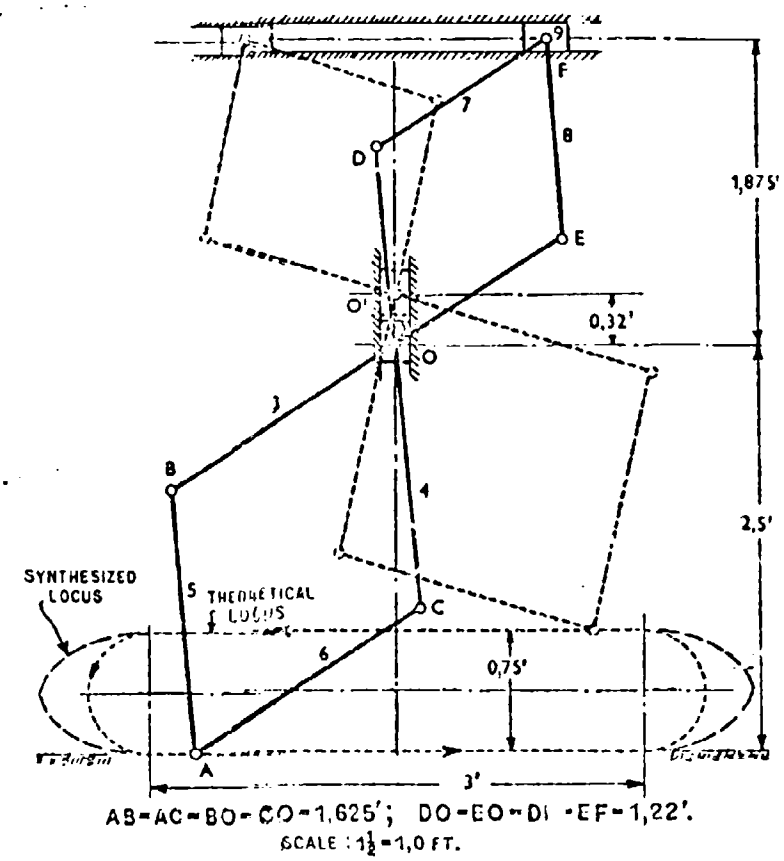


Fig. 16. — The pantograph mechanism.

One method of getting this independence is to use the pantograph mechanism and use one cylinder (fig. 16) to obtain the horizontal motion and another cylinder to obtain the vertical motion. Thus the pantograph center at O is driven up and down by the lift cylinder, while a separate cylinder drives slider 9 in a horizontal direction. With this arrangement one flow-control program is sufficient for each cylinder regardless of the values set for the stride or the lift. Thus the generated locus will always be symmetrical about both the horizontal and vertical center lines.

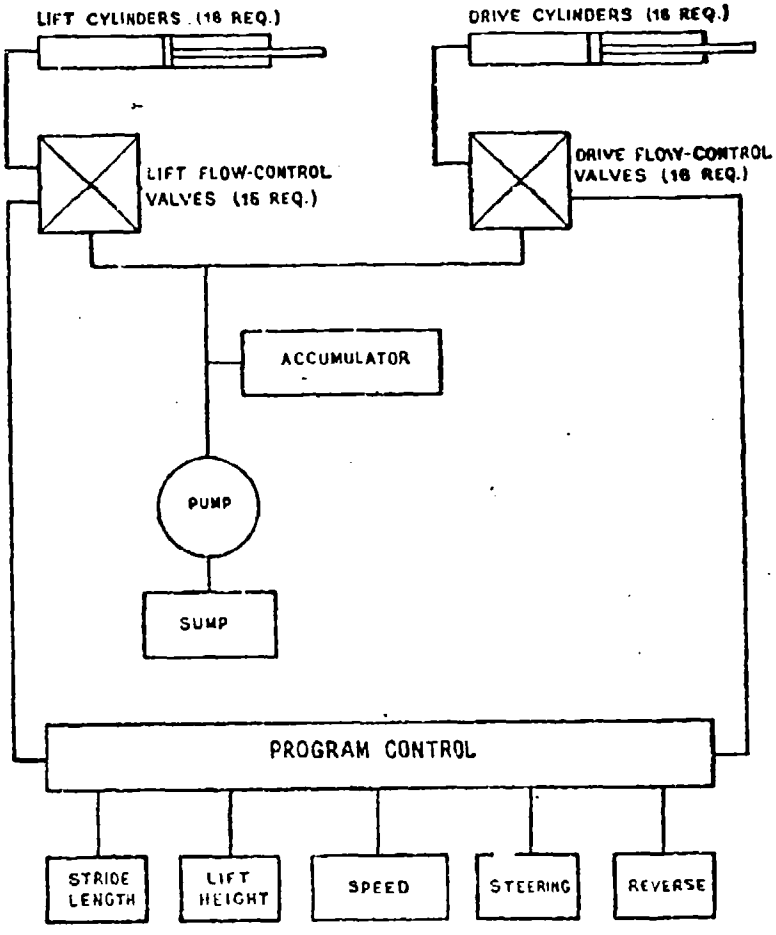


Fig. 17. — Block diagram of control system.

A dynamic analysis of the pantograph linkage shows that the inertia forces and torques can be reduced to very small values using a minimum of 16 legs on the vehicle. Thus, for all practical purposes, balancing of all inertia forces and torques on the pantograph mechanism is possible. The use of an accumulator in the hydraulic system serves the same purpose as a flywheel in a rotating system. Thus the requirement for energy storage during acceleration and deceleration is satisfied.

A block diagram of a proposed control system for a sixteen-legged vehicle is shown in fig. 17. We visualize four legs at each corner and all sixteen legs phased so as to obtain the best balance of inertia forces. In particular we desire the following:

1) Ability to control the length of stride of each gang of four legs.

2) Ability to control the height of step of each gang.

3) Ability to change the vehicle speed and to reverse its motion.

4) Ability to steer the vehicle by changing the speed of the legs on one side relative to the other side.

The stride and lift for each gang of four legs would be controlled by ganged three-dimensional cams, four cams for stride and four for lift. The axial dimensions of these cams would control the length of stride and the height of lift, respectively. The radial shapes would initiate and control the four events of the cycle. The phase relationship of the four legs is dictated by the relative angular position in which the cams are fastened to the cam shaft. The cams representing two gangs of legs on one side of the vehicle could be on the same cam shaft. Then the speed of the cam shaft dictates the speed of the legs on that side.

Steering would be accomplished by speeding up the legs on one side of the vehicle. Since the legs on a single side are quite well balanced this would have a negligible effect on the inertia forces and torques transmitted to the vehicle. It would, however, increase the peaks to be supplied by the accumulator. Taking shorter steps on one side of the vehicle could be used for steering because this does not change the speed.

The pantograph mechanism satisfies all the requirements outlined at the beginning except number 6. It may well be that a high stride-time to return-time ratio is impossible to obtain and still get balanced inertia forces, no matter how the walking means is accomplished.

BIBLIOGRAPHY

1) Bekker M. G. Theory of land locomotion. The University of Michigan Press, Ann Arbor, 1956.

2) Bekker M. G. Off the road locomotion. The University of Michigan Press, Ann Arbor, 1960.

3) Rashevsky N. Mathematical Biophysics. Chicago, 1948.

4) Rashevsky N. On the locomotion of mammals. Bull. of Math. Biophysics, vol. 10, 1948.

5) Levens A. S., Inman V. T. and Blosser J. A. Transverse rotation of the segments of the lower extremity in locomotion. Jour. of Bone and Joint Surgery, vol. 30-a, no. 4, 1948.

6) Levens A. S. Graphics. John Wiley and Sons, New York, pag. 513-522, 1954.

7) Bernhard R. K. Preliminary study on jumping and running types of locomotion. Research Report No. 43, Land Locomotion Research Laboratory, Detroit Arsenal, 1958.

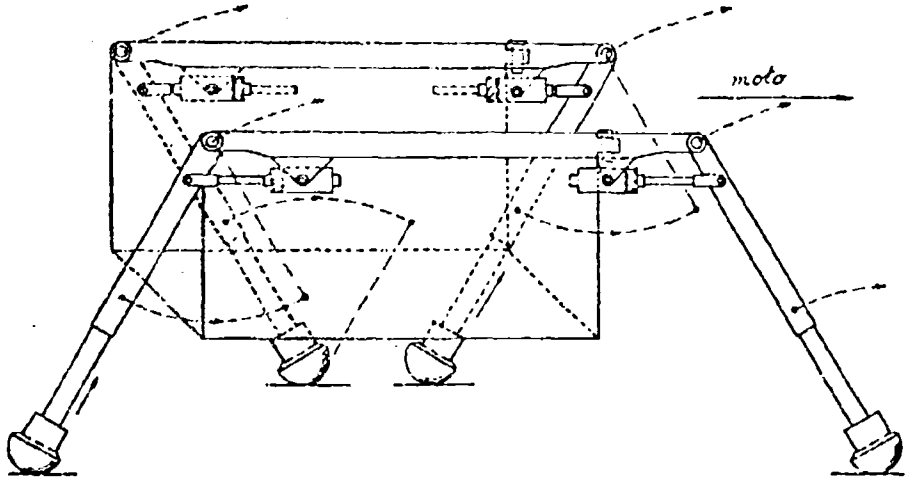
8) Hrones John A. and Nelson George L. Analysis of the four-bar linkage. Published jointly by Technology Press, M. I. T., Cambridge, Mass, and John Wiley and Sons, Inc., New York, 1951.

9) Kurt Hain. Angewandte Getriebelehre. Hannover-Darmstadt: Shrodel, 1952.

10) Freudenstein F. Approximate synthesis of four-bar linkages. Trans. ASME, 77, 853, 1955.

DISCUSSIONS

S. MURATORI. — Ho ascoltato con grande particolare interesse la dotta relazione del Prof. Joseph E. Shigley sul veicolo camminante essendomi dedicato io pure, in questi ultimi anni, allo studio di un veicolo a motore muoventesi su appoggi discontinui allo scopo di cercar di rendere più facile ed economico lo sviluppo delle comunicazioni nei vasti territori impervi o desertici che esistono più o meno in tutte le parti del mondo e la valorizzazione di essi.



Nel progetto Cin Ma presi le spunto dal movimento dei quadrupedi in genere e del cavallo in particolare che, come tutti sanno, ha quattro andature fondamentali: il passo, il galoppo, l'ambio e il trotto. Nel passo i piedi si muovono uno per volta mentre nelle altre tre andature si muovono accoppiati e le andature stesse rappresentano tutte le combinazioni possibili.

La lunghezza del passo che è semplicemente misurata dallo spazio coperto dai piedi nel loro ritmico movimento varia nell'andatura passo e si riduce ai $\frac{2}{3}$ di quella che sarebbe ottenuta alle altre andature per una stessa apertura angolare delle gambe.

Ad ogni coppia di muscoli agenti sugli arti si può immaginare di sostituire, per analogia di funzionamento, un cilindro a doppio effetto o un dispositivo analogo.

La figura rappresenta lo schema di un veicolo nella posizione di trotto quando cioè si muovono contemporaneamente i piedi diagonalmente opposti. La figura di base ottenuta collegando perimetralmente i piedi è in tal caso un trapezio mentre è un rettangolo nel caso del galoppo ed un rombo per l'ambio e cambia ad ogni semipasso. Nel caso del passo è alternativamente un trapezio e un rombo e cambia ad ogni quarto di passo.

Osservando la figura si vede che se si scambiano i piedi che si sollevano dal suolo con quelli che su di esso posano, il veicolo inverte la direzione del suo spostamento.

La velocità di un veicolo di questo tipo è data dal prodotto della lunghezza

del passo per il numero dei passi eseguiti nell'unità di tempo ed essendo questi fattori variabili ne deriva un'ampia gamma di velocità.

I problemi tecnici per realizzare le varie andature di un veicolo a 4 gambe non presentano difficoltà particolari ma soltanto una certa complessità che scompare completamente se si raddoppia il numero delle gambe portandolo a 8 e sistemandole, a coppie ed in fase opposta, sull'asse del medesimo perno di rotazione. In questo semplice modo le tre andature di galoppo ambio e trotto si unificano in una sola identica andatura ed il veicolo si troverà sempre in condizioni di stabilità paragonabili a quelle di un'automobile e mentre quattro piedi poseranno al suolo durante un intero semipasso, gli altri quattro, in fase opposta ai primi, saranno in movimento per assumere una nuova posizione alla fine del semipasso stesso.

Qualora si utilizzasse un sistema oleodinamico per ottenere i movimenti [illegible] la distribuzione ed i comandi relativi sarebbero molto semplici e facilmente [illegible] caso per caso, alla vastissima gamma dei possibili veicoli di questo tipo.

Le speciali caratteristiche del movimento di tali veicoli in cui gli appoggi, capaci di sollevarsi dal suolo e superare ostacoli e che si posano solamente, sembrano rendere tali veicoli preferibili ad ogni altro per affrontare, sia pure a velocità moderata, condizioni di suolo incognite e difficili quali possono presentarsi in esplorazioni terrestri od extraterrestri.

C. B. LEWIS. — Mr. Chairman, Gentlemen I have been interested in ambulatory vehicles for quite a long time. If you are interested in designing a walking vehicle which will operate on extremely soft terrain, there seems to be a fundamental limitation in that the maximum amount of footprint area you can use is related to the plan area of the vehicle: it is difficult to get more than roughly half of this plan area fully utilized in footprints in contact with the ground at any moment. Thus, compared with a more conventional bellyless tracked vehicle (such as the Canadian RAT) of the same weight and plan area, the walking vehicle must have roughly double the nominal ground pressure.

The other thing I found very interesting in Prof. Shigley's paper is his departure from the rigid four bar chain type of mechanism in using programmed hydraulic jacks. It occurs to me that if a walking vehicle is to move over very irregular ground, this vehicle should be able to sense the profile of the ground ahead of it, by either some device such as sonic sensors or even small feeler wheels out ahead of the vehicle, and use this information automatically in programming the jack movements to compensate for the irregular profile. I should like to ask Prof. Shigley whether he had that sort of thing in mind in programming his hydraulic jacks. The other thing that I am interested in is whether it is possible, in a high speed ambulatory vehicle, to utilize the effect of the plasticity of the soil during the very momentary contact of the footprint with the ground; perhaps the full sinkage hasn't got time to develop if the footprint is only in contact with the ground for a very short time. Thank you.

J. E. SHIGLEY. — With regard to the first question, I recognize the desirability of sensing the type of terrain. In my research I did nothing toward looking into that, or how it could be accomplished; but I realize that if one could sense the terrain, then it might give one a great deal more control over the vehicle, and we could use the information from the senser to automatically control, perhaps, the height of lift, or something of that nature, in order to produce a smoother ride. With regard to the second question, I'm afraid I can't comment.

Application of the soil parameters to vehicular mechanics

La meccanica del veicolo in base ai parametri del suolo

WESLEY F. BUCHELE *)

ABSTRACT. — *Vehicular mechanics equations, which govern the dynamic weight transfer of a two-wheel drive tractor, were derived. Soil value equations, derived by Bekker, were applied to the above equations to show the effect of soil parameters upon the dynamic weight transfer of the tractor.*

The resulting equations showed that the dynamic weight transfer of a two-wheel drive vehicle increases as drawbar pull (P), cohesion (C), angle of internal friction (Ø), modulus of cohesion (k_c), modulus of deformation ($k\phi$), width of tire (b) and length of tire contact (L) increases, and decreases as the terrain coefficient (n) increases.

Introduction. — Two-wheel drive tractors are used by farmers and military men alike as prime movers for off-the-road operations.

While the two-wheel drive tractor is cheaper to purchase than a four-wheel drive tractor, it tends to be less stable under certain operating conditions. Tip-over-backward accidents killed approximately 390 farmers in the United States during 1958 [1].

The purpose of this paper is to apply soil value parameters to vehicular mechanics equations in order to predict the dynamic weight transfer of a two-wheel drive tractor.

The dynamic weight transfer is critical because under a heavy pull, the vehicle must not only be stable, but enough weight must remain on the front-wheels to provide good steering. Thrust and motion resistance of a vehicle depends on the dynamic weight placed by the wheels of the vehicle on the soil.

The classical vehicular equations used by engineers were derived by superimposing forces on a static vehicle and calculating the resulting moments about the soil-tire contact point [2]. While these derivations provide simplified equations, they failed to (a) accurately predict the dynamic weight transfer of the vehicle or (b) utilize soil value information in predicting the vehicular performance under various soil conditions.

---

*) Paper authorized for publication as Journal Article No. 2853 of the Michigan Agricultural Experiment Station, East Lansing, Michigan. The Author, Wesley F. Buchele, is Associate Professor of Agricultural Engineering at Michigan State University.

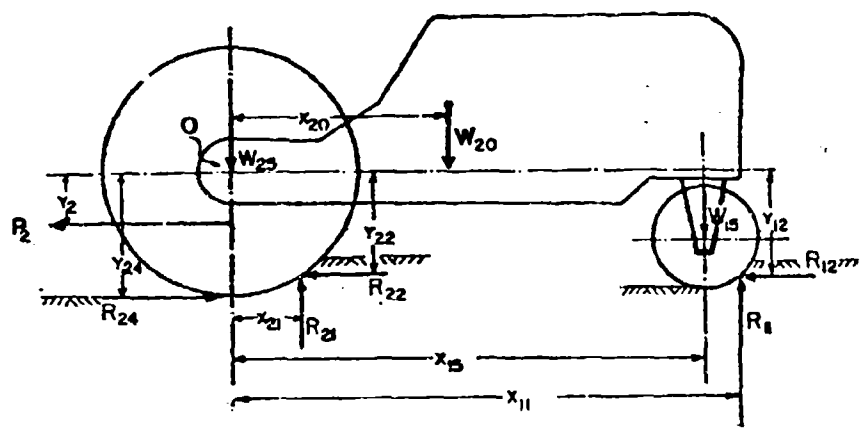


Fig. 1. — The direction and place of application of various forces on two-wheel drive vehicles.

Derivation of vehicular mechanics equations. — Dynamic equations using soil value information will be developed in this paper for the two-wheel drive vehicles shown in figure 1. The following assumptions were made in the derivation of the equations:

1) The rear wheels rotate or tend to rotate clockwise (tend to move the vehicle forward).

2) The towed load P_2 is constant and is applied to the tractor drawbar.

3) Rear axle torque is positive at all times.

4) Acceleration is equal to zero.

5) Wind resistance is equal to zero.

6) Tractor is moving or tending to move in a strainght line.

The subscript of each number has been selected so that the first number of the notation indicates the place of action of the force and the second number designates the force under consideration. Thus, R_{21} is force 1 (resultant of all vertical upward forces on the tire) operating at No. 2 (rear) wheel of the vehicle.

$$\Sigma \vec{F_H} + = 0 = -R_{22} + R_{24} - R_{12} - P_2 \qquad (1\,a)$$

$$P_2 = R_{24} - R_{22} - R_{12} \qquad (1\,b)$$

$$F_V\,\uparrow + = 0 = R_{21} + R_{11} - W_{25} - W_{20} - W_{15} \qquad (2)$$

The moments operating on a vehicle may be summed about any point. The point of intersection of R_{21} and R_{22} (the intersection may or may not be on the periphery of the tire) has often been used because the moments created by the soil reaction forces equal zero. Because this point continually changes and because it is desired to calculate the value of the soil reaction, the moment

summation will be made about point « 0 », the center of the rear axle. Soil value information can then be applied to the derived equations.

$$\Sigma \; M_C \curvearrowleft + = 0 = P_2Y_2 - R_{21}X_{21} + R_{22}Y_{22} + R_{24}Y_{24} + W_{20}X_{20} - R_{11}X_{11} + R_{12}Y_{12} + W_{13}X_{13} \tag{3}$$

Dynamic weight transfer when soil conditions limit the drawbar pull of the vehicle. — The dynamic weight transfer W_D of a vehicle is defined in equation 4.

$$W_D = R_{11}\,\text{static} - R_{11}\,\text{Dynamic} \tag{4}$$

Where:

$$R_{11}\,\text{static} = \frac{W_{13}X_{13} + W_{20}X_{20}}{X_{13}} \tag{5}$$

and

$$R_{11}\,\text{Dynamic} = \frac{P_2Y_2 - R_{21}X_{21} + R_{22}Y_{22} - R_{24}Y_{24} + W_{20}X_{20} + R_{12}Y_{12} + W_{13}X_{13}}{X_{13}} \tag{6}$$

Note: X_{11} is assumed as equal to X_{13}. This assumption introduces an error of the order of 2 percent. This error decreases, however, as the weight transfer increases, because as R_{11} dynamic approaches zero, X_{11} approaches X_{13}.

$$W_D = \frac{R_{21}X_{21} + R_{24}Y_{24} - P_2Y_2 - R_{22}Y_{22} - R_{12}Y_{12}}{X_{13}} \tag{7}$$

The land locomotion equations derived by Bekker which govern the forward thrust and motion resistance of the vehicle[3] are substituted in equation 7.

$$W_D = \frac{(W_{20} + W_D)X_{21} + [bLC + (W_{20} + W_D)\tan\Phi]Y_{24} - P_2Y_2}{X_{13}} - \frac{Y_{22}}{n+1\,(k_c + bk_\phi)^{\frac{1}{n}}}\left[\frac{(W_{20} + W_D)}{L}^{\frac{n+1}{n}} + \frac{(W_{13} - W_D)}{L}^{\frac{n+1}{n}}\right] \Big/ X_{13} \tag{8}$$

Where:

Y_{12} is assumed $= Y_{22}$

$R_{24} = bLC + R_{21}\tan\Phi$

$$R_{22} = \frac{1}{n+1\,(k_c + bk_\phi)^{\frac{1}{n}}}\left(\frac{R_{21}}{L}\right)^{\frac{n+1}{n}}$$

$$R_{12} = \frac{I}{n+1\,(k_c + bk_\phi)^{\frac{1}{n}}} \left(\frac{R_{11}}{L}\right)^{\frac{n+1}{n}}$$

$R_{21} = W_{2s} + W_D$
$R_{11} = W_{1s} - W_D$
bL = ground contact area of rear wheels

$$W_{2s} \text{ (static weight on rear wheels)} = W_{2s} + \frac{(X_{1s} - X_{2s})_{W_{2s}}}{X_{1s}}$$

$$W_{1s} \text{ (static weight on front wheels)} = W_{1s} + \frac{X_{2s}W_{2s}}{X_{1s}}$$

C = cohesion
k_c = modulus of cohesion
k_ϕ = modulus of deformation
n = terrain coefficient
Φ = angle of internal friction.

The above equation cannot be solved explicitly for W_D as the weight transfer of the vehicle at all times depends upon the weight which the rear-axle drive wheels place on the ground. It must be solved by a series of approximation in which W_D is set equal to a percent of the static weight on the rear wheel (W_{2s}).

Equation 8 shows that the weight transfer increases as drawbar pull (P), cohesion (C), angle of internal friction (Φ), modulus of cohesion (k_c), modulus of deformation (k_ϕ), width of tire (b), and length of tire-soil contact (L) increases, and decreases as the terrain coefficient (n) increases.

The thrust of the vehicle depends upon the dynamic weight (R_{21}) of the drive wheels, thus the thrust of the vehicle increases as W_D increases. In like manner, the motion resistance of the rear wheels increases as W_D increases while, simultaneously, the motion resistance for the front wheels decreases as W_D increases. When the W_D is shifted from small front wheels to large rear wheels of a vehicle, as in the case of a farm tractor, the motion resistance decreases as the dynamic weight transfer increases.

Weight transfer when engine torque limits the drawbar pull of the vehicle. — A summation of the moments operating on a free body diagram (fig. 2) of the rear tractor tire (a powered wheel) is shown in equation 9 a.

$$\Sigma M_a \left(+\right) = 0 = -R_{21}X_{21} + R_{22}Y_{22} - R_{24}Y_{24} + TRE_2 \qquad (9\,a)$$

$$-TRE_2 = -R_{21}X_{21} + R_{22}Y_{22} - R_{24}Y_{24} \qquad (9\,b)$$

The dynamic weight transfer equation involving rear axle torque (TRE) is gained by substituting equation 9 b in equation 7.

$$W_D = \frac{TRE_2 - P_2Y_2 - R_{12}Y_{12}}{X_{1s}} \qquad (10)$$

The motion resistance equation is substituted for R_{12}.

$$W_D = \frac{TRE_2 - P_2 Y_2 - \frac{Y_{12}}{n+1(k_c + bk_\phi)^{\frac{1}{n}}} \left(\frac{W_{12} - W_D}{L}\right)^{\frac{n+1}{n}}}{X_{12}} \qquad (11)$$

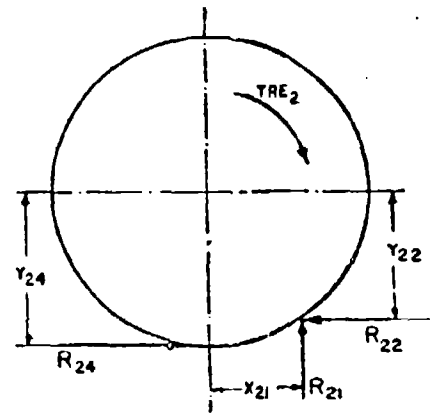


Fig. 2. — Free body diagram of a powered wheel.

Equation 11 provides weight transfer information when rear axle torque is limiting the performance of the vehicle. It is also used under test conditions where the rear axle torque is actually being measured in order to calculate the magnitude of soil reactions operating against the tractor tire.

AKNOWLEDGMENT. — The Author aknowledges the support of the Land Locomotion Laboratory, Detroit Arsenal, Centerline, Michigan.

BIBLIOGRAPHY

1) Fiske K. V. Cost and extent of tractor accidents. Seminar on Environmental Health and Safety of the Tractor Operator. Michigan State University, 1959.

2) McKibben E. G. Kinematics and dynamics of the wheel type farm tractor. Part V, Stability. Agricultural Engineering, 8, 119-122, 1927.

3) Bekker M. G. A practical outline of the mechanics of automotive land locomotion. Land Locomotion Laboratory, Detroit Arsenal, 1955.

MISURA DEL SUOLO
ED APPARECCHIATURE RELATIVE

SOIL MEASUREMENT
AND INSTRUMENTATIONS

Bevameter 100. A new type of field apparatus for measuring locomotive stress-strain relationships in soils *)

Il « Bevameter 100 » un nuovo tipo di apparecchio da campo per misurare le relazioni tra sollecitazioni e deformazioni del suolo dovute al movimento dei veicoli

FERENC PAVLICS **)

ABSTRACT. — *The objective of this paper was to develop a test method utilizing rigid wheels for measuring physical soil parameters used in land locomotion mechanics. This new approach was proposed to provide a quick and continuous method for soil testing on field.*

Theoretical analysis was made on the load-sinkage and traction-slip relations for a rigid wheel. Tests were performed in two different kinds of soil. Finally a comparison was made between the soil values obtained from wheel tests and conventional bevameter tests.

The conclusion was drawn, that the wheel type soil measuring instrument is feasible, practical for field tests. The results show that the soil parameters obtained from wheel tests are in good agreement with the ones obtained from conventional bevameter tests. By this instrument a large number of test data can be obtained quickly for statistical evaluation of soil values.

Symbols

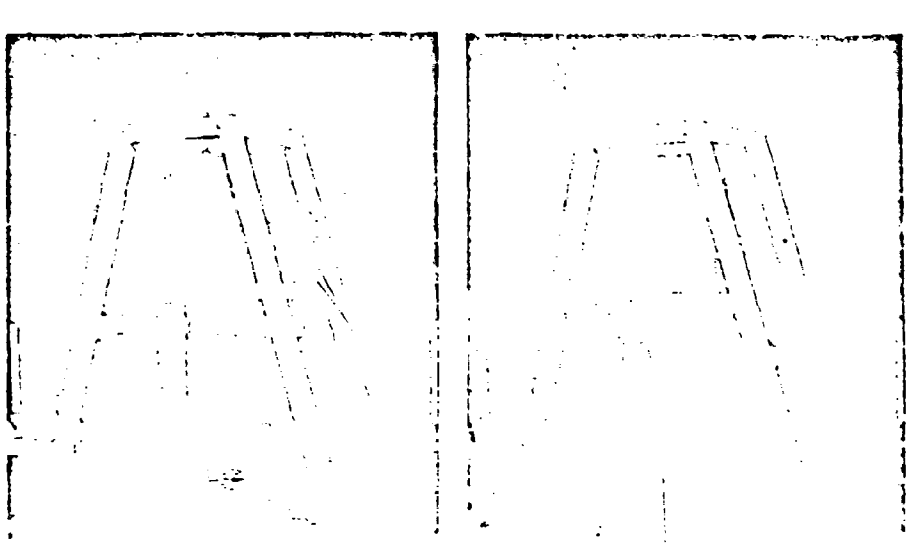
n	=	Exponent of sinkage	p	=	Normal pressure
k_c	=	Cohesive modulus of sinkage	S	=	Shear stress in the soil
k_ϕ	=	Frictional modulus of sinkage	W	=	Normal load
c	=	Cohesion	A	=	Ground contact area
Φ	=	Angle of internal friction	l	=	Length of the ground contact area
K	=	Deformation modulus	D	=	Diameter of the wheel
H	=	Traction, tractive effort	b	=	Width of the wheel
i	=	Slip	Z	=	Sinkage of the wheel

1. - Introduction

A) **Problem.** — The objective of this paper was to develop a test method utilizing rigid wheels for determination of physical soil values used in land locomotion mechanics to describe stress-strain relations of the soil.

*) This paper was originally prepared for Land Locomotion Laboratory U.S. Army Ordnance Tank Automotive Command, Detroit, Michigan.

**) General Motors Corporation Land Mobility Laboratory Warren, Michigan.



a b

Fig. 1. — Conventional bevameter. a) Sinkage plate side; b) Shear ring side.

B) **Background.** — The measurement of physical soil values proposed by Bekker, which utilized sinkage plates and shear annulus as described elsewhere [1-2-3], has been quite successful. However, the measuring procedure is lengthy; it requires two different size plates each of which has to be forced into the soil and a shear annulus which has to be rotated at three or more normal pressures (fig. 1). For each test run the equipment has to be moved and set up which prolongs the process of measurement. Even with the most advanced type of this instrument, called the bevameter (mounted on a vehicle and operated hydraulically), the time of a test cycle cannot be reduced to less than 10 minutes. This has a serious handicap in view of the necessity for a large number of data required for statistical evaluation of soil values.

To provide a quick and continuous method of operation a new approach has been proposed by Bekker for the recording of soil parameters. In this approach two rolling rigid wheels having the same diameter but different widths were substituted for flat plates previously used in load-sinkage tests, and the circumference of such wheels equipped with grousers were substituted for the shear annulus. In this manner, the load-sinkage curves and the shear-slip curves may be recorded continuously without stopping the measuring device. From such curves the sinkage and shear parameters as defined by Bekker [2-3], can be subsequently computed.

The practicability of this new idea for the determination of sinkage para-

meters was first described in reference 4. In this paper the problem will be discussed further, and the results of shear tests performed by means of slipping wheel circumferences will be reported.

II. - Theoretical analysis

A) Determination of load-sinkage parameters. — When towing a rigid wheel at varying loads and measuring the corresponding sinkage we can plot the load-sinkage function.

The sinkage of a rigid wheel of diameter D and width b can be expressed by the following equation [5]:

$$Z = \left[\frac{3W}{(3-n)(k_c + b k_\phi)\sqrt{D}}\right]^{\frac{2}{2n+1}} \tag{1}$$

where W is the normal load on the wheel, k_c, k_ϕ and n are the sinkage soil parameters. Expressing the normal load and taking the logarithm of both sides, we have:

$$\log W = \frac{2n+1}{2}\log Z + \log\frac{(3-n)(k_c + b k_\phi)\sqrt{D}}{3} \tag{2}$$

For two wheels of the same diameter and normal load, but different width b_1 and b_2 we can write:

$$\log W = \frac{2n+1}{2}\log Z_1 + \log\frac{(3-n)(k_c + b_2 k_\phi)\sqrt{D}}{3}$$

and (3)

$$\log W = \frac{2n+1}{2}\log Z_2 + \log\frac{(3-n)(k_c + b_1 k_\phi)\sqrt{D}}{3}$$

By varying the load W and plotting log W vs log Z we get two straight lines for the two wheels (fig. 2).

The slope of these lines is equal to $\frac{2n+1}{2}$, and the exponent of sinkage can be expressed as

$$n = \tan\alpha - \frac{1}{2} \tag{4}$$

The ordinates at Z = 1 are equal to

$$a_1 = \frac{(3-n)(k_c + b_1 k_\phi)\sqrt{D}}{3}$$

and (5)

$$a_2 = \frac{(3-n)(k_c + b_2 k_\phi)\sqrt{D}}{3}$$

Hence the values of k_c and k_ϕ may be determined in accordance with standard procedure (2) (7):

$$k_c = \frac{3}{(3-n)\sqrt{D}} \frac{a_1}{b_1} - \frac{a_2}{b_2} \frac{b_1 b_2}{b_2 - b_1} \tag{6}$$

$$k_\phi = \frac{3}{(3-n)\sqrt{D}} \frac{a_2 - a_1}{b_2 - b_1} \tag{7}$$

A sample computation of the sinkage soil values (n, k_c, k_ϕ) form actual test data in two different soils is given in figures 12 and 13.

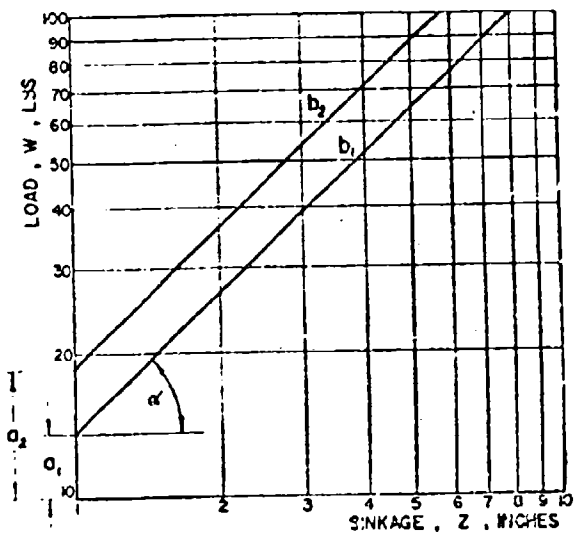


Fig. 2. — Load vs. sinkage curves.

B) **Determination of shear-slip parameters.** — When towing a rigid wheel equipped with grousers along its circumference and then producing a relative displacement between the wheel and the soil by means of driving or braking the wheel, we can measure the tractive effort (H) and the corresponding slip (i). From these test data we can plot the traction-slip curve.

Considering large diameter wheels and relatively small sinkages we can substitute the arc of the wheel in contact with the soil with a straight line (fig. 3).

For such case the traction can be expressed by the following equation (6):

$$H = A\,(c + p\tan\phi)\left[1 - \frac{K}{i\,l}\left(1 - e^{-\frac{i\,l}{K}}\right)\right] \tag{8}$$

where:

A = bl contact area

$p = \frac{W}{A}$ normal pressure

l = length of the contact area

$i = \frac{v_t - v_a}{v_t}$ slip

c, Φ and K = shear-slip soil values

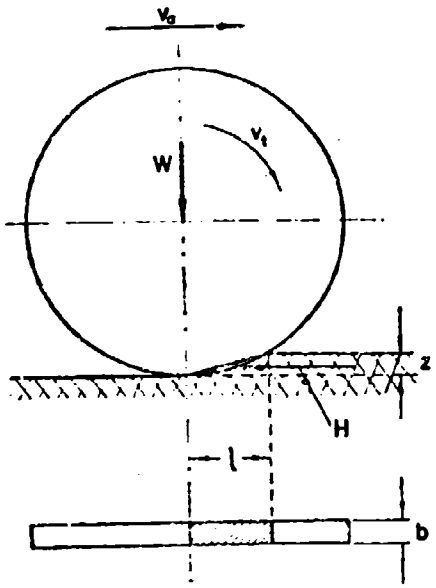


Fig. 3. — Contact area of a wheel.

The typical form of a tractive effort-slip curve is shown in figure 4. Taking the first derivative of H as a function of i we get from (8)

$$\frac{dH}{di} = A\,(c + p\tan\Phi)\left[\frac{-l\,e^{-\frac{H}{K}} - K\,(e^{-\frac{H}{K}} - 1)}{i^2\,l}\right] \qquad (9)$$

To find the value of $\frac{dH}{di}$ at $i = 0$, we use l'Hospital's rule:

$$\left[\frac{dH}{di}\right]_{i=0} = \lim_{i \to 0} A\,(c + p\tan\Phi)\left[\frac{\frac{l}{K}\,e^{-\frac{H}{K}}}{2}\right] \qquad (10)$$

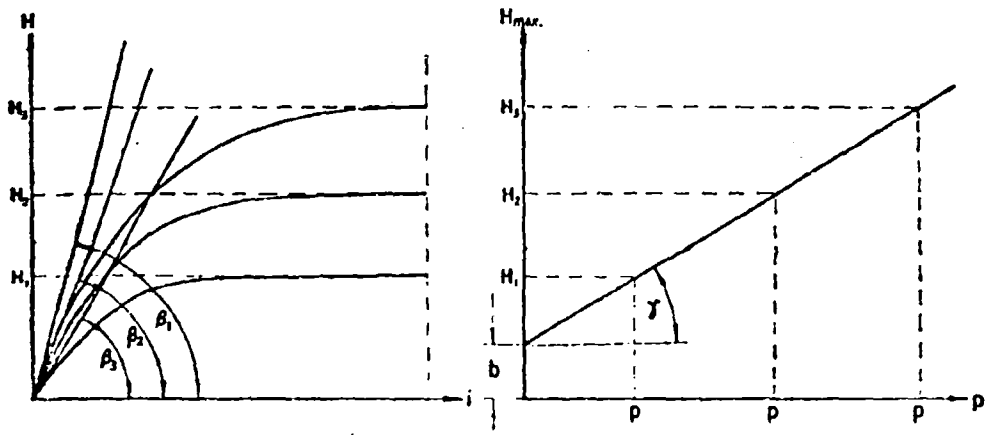


Fig. 4. — Tractive effort-slip curves.

and,

$$\left[\frac{dH}{di}\right]_{i=0} = A\,(e + p\tan\Phi)\,\frac{1}{2K} \tag{11}$$

Since $\left[\frac{dH}{di}\right] i = 0$ is the slope of the tangent to the H — i curve at the origin, we can write:

$$K = \frac{1\,A\,(e + p\tan\Phi)}{2\tan\beta} \tag{12}$$

and rearranging:

$$e + p\tan\Phi = \frac{2K\tan\beta}{A\,l} \tag{13}$$

Assuming that the maximum tractive effort occurs at i = 1 (100 % slip), we can write from equation (8):

$$H_{max} = A\,(e + p\tan\Phi)\left[1 - \frac{K}{l}\,(1 - e^{-\frac{l}{K}})\right] \tag{14}$$

Since $\frac{H_{max}}{A}$ is the maximum shear strength, S_{max}:

$$S_{max} = (e + p\tan\Phi)\left[1 - \frac{K}{l}\,(1 - e^{-\frac{l}{K}})\right] \tag{15}$$

Substituting equation (13) into (15):

$$S_{max} = \frac{2K\tan\beta}{A\,l}\left[1 - \frac{K}{l}\,(1 - e^{-\frac{l}{K}})\right] \tag{16}$$

or,

$$\frac{A\,l^2\,S_{max}}{2\tan\beta} = Kl - K^2 + K^2\,e^{-\frac{l}{K}}$$

Since the ratio $\frac{l}{K}$ is always larger than five, as practical experience indicates, which means that $e^{-\frac{l}{K}}$ is smaller than 0.006, the last term in equation (16) can be neglected, and from (16)

$$K^2 - K l + \frac{A l^2 S_{max}}{2 \tan \beta} = 0 \qquad (17)$$

The solution for K gives:

$$K = \frac{l}{2} \left[l \pm \sqrt{l - \frac{2 A S_{max}}{\tan \beta}} \right] \qquad (18)$$

which has two roots:

1) For

$$K = \frac{l}{2} \left[l + \sqrt{l - \frac{2 A S_{max}}{\tan \beta}} \right]$$

it can be seen that $K > \frac{l}{2}$

It follows then from equation (12) that $A (c + p \tan \Phi) > \tan \beta$ (19)

2) Similarly for

$$K = \frac{l}{2} \left[l - \sqrt{l - \frac{2 A S_{max}}{\tan \beta}} \right]$$

and, in this case: $K < \frac{l}{2}$. Accordingly: $A (c + p \tan \Phi) < \tan \beta)$ (20)

The meaning of equation (19) and (20) can be seen in figure 5. Since the H — i curves are always of the type shown in figure 5 b, solution (1) has to be rejected, and:

$$K = \frac{l}{2} \left[l - \sqrt{l - \frac{2 A S_{max}}{\tan \beta}} \right] \qquad (21)$$

Since l, A, S_{max} are recorded test data, and $\tan \beta$ can be determined from the H — i curve, the value of K can be computed from equation (21).

Repeating the traction-slip tests for various loads W_1, $W_2 \ldots W_n$, a number of H — i curves will be obtained, all showing certain peak values H_1, $H_2 \ldots H_n$ (fig. 4). The H and W values may be divided by the contact area, A, and the maximum shearing strength, S_{max}, under corresponding pressure, p, may be determined as follows:

$$S_{max} = \frac{H_{max}}{A}$$

$$p = \frac{W}{A} \qquad (22)$$

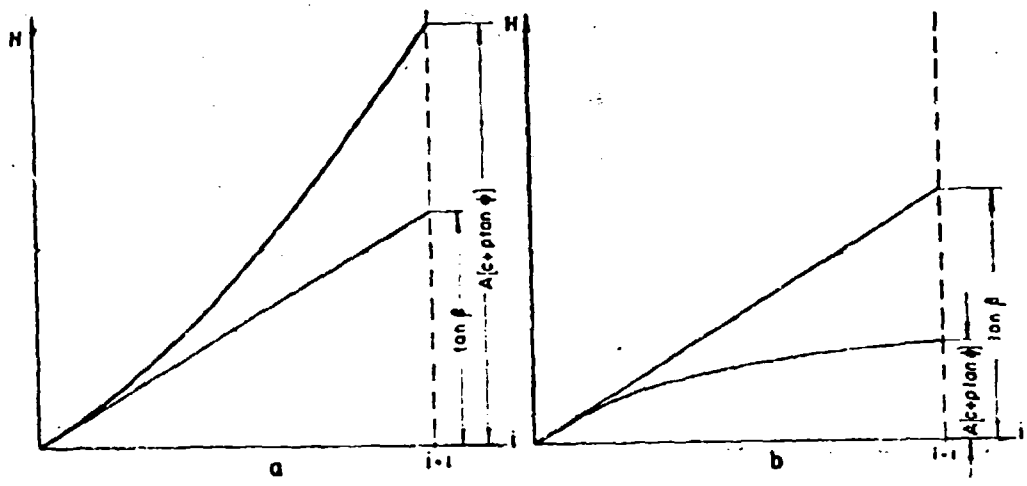


Fig. 5. — Determination of deformation modulus.

Plotting the values of S_{max} as a function of p, one may obtain a straight line as shown in figure 4. The equation of this line is:

$$S_{max} = (c + p \tan \Phi) \left[1 - \frac{K}{l} \left(1 - e^{-\frac{l}{K}}\right)\right]$$

Let b be the ordinate at $p = 0$, and tan γ the slope of the straight line. Then the soil values c and Φ can be expressed as follows:

$$c = \frac{b}{1 - \frac{K}{l} \left(1 - e^{-\frac{l}{K}}\right)} \tag{23}$$

$$\tan \Phi = \frac{\tan \gamma}{1 - \frac{K}{l} \left(1 - e^{-\frac{l}{K}}\right)} \tag{24}$$

A sample computation of the shear-slip soil values (K, c, Φ) from actual test data in two different soils is shown in figures 14, 15, 16 and 17.

III. - Test procedure

A) **Test apparatus.** — A schematic drawing of a wheel type test device for determining sinkage soil parameters is shown in figure 6. The functioning of the apparatus is as follows:

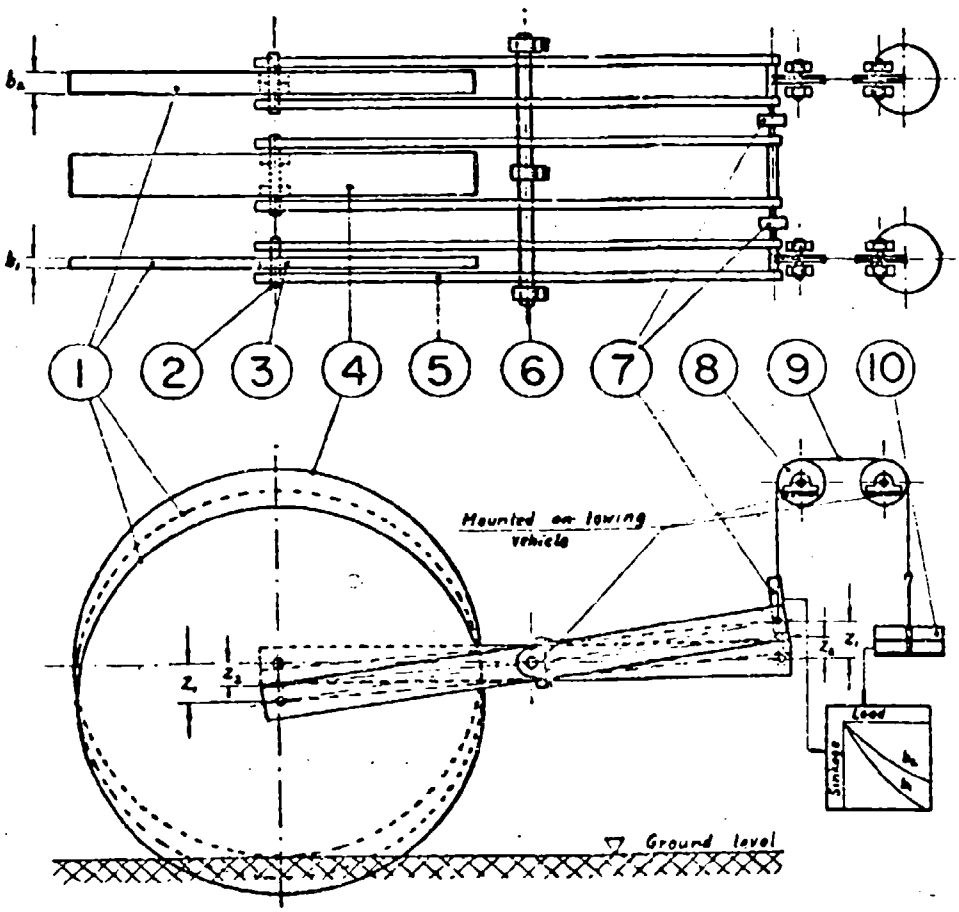


Fig. 6. — Schematic drawing of a wheel type test device for determining load-sinkage relations in the soil.

Test wheels (1) are free to turn about axle (2) on ball bearings. Wheel arms (5) are free to rotate about shaft (6) which is mounted on the towing carriage. The loading of the wheels is provided by weight (10) through a cable (9) and pulley (8) system. The pulleys are mounted on the towing carriage. The measurement of the sinkage is obtained by linear potentiometers (7) using wheel (4) as reference wheel (rolling on the surface of the soil).

A schematic drawing of a wheel type test device for determining shear-slip soil parameters is shown in figure 7. The functioning of this device is as follows: test wheel (1) equipped with grousers along its circumference is free to turn around axle (3) on ball bearings. Wheel arms (4) can rotate about shaft (6) which is mounted on the towing carriage. Chain drive system (5) provides connection between the test wheel (1) and an adjustable electromagnetic friction brake (8). The gradually applied braking torque is measured by torquemeter (7).

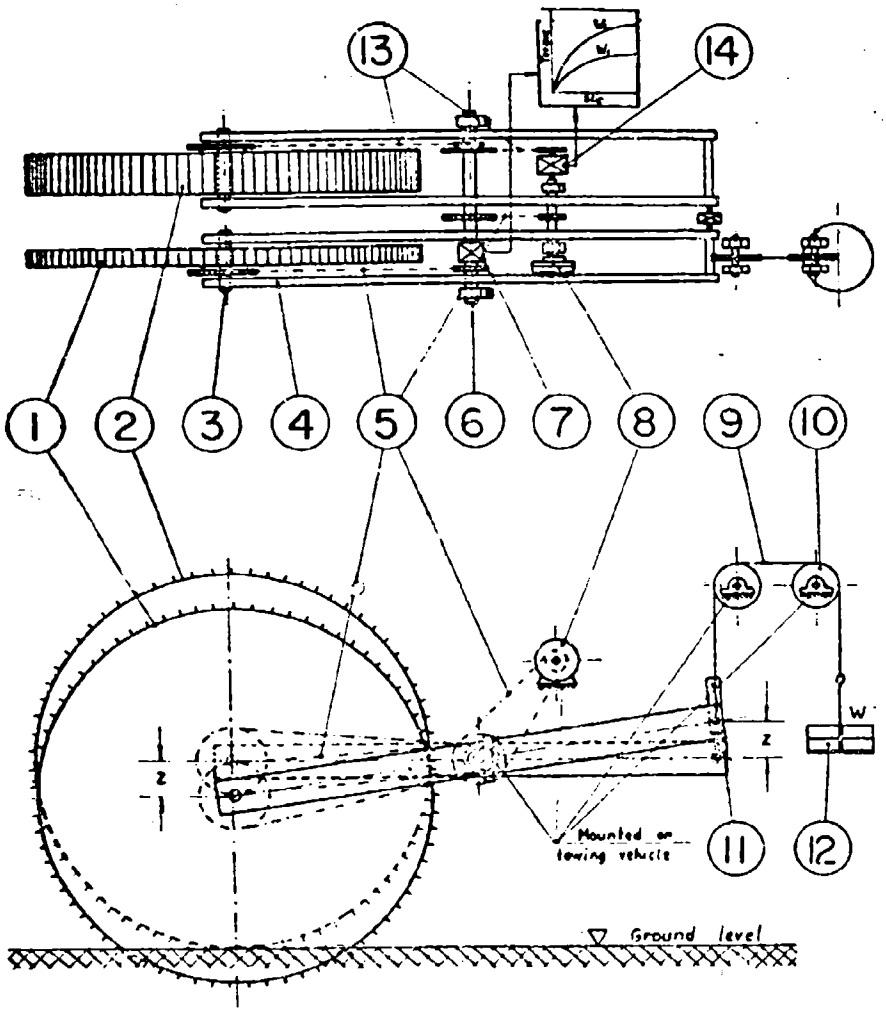


Fig. 7. — Schematic drawing of a wheel type test device for determining shear-slip relations in the soil.

The loading of the test wheel is provided by weight (12) through a cable (9) and pulley (10) arrangement. A differential type slip measuring device (14) records the speed difference between the test wheel (1) and reference wheel (2) which is rolling without slip. The measurement of sinkage is performed by linear potentiometer (11) using wheel (2) as a reference.

The above described test equipment was mounted on a soil bin dynamometer carriage. The soil bin was 40 ft long, 5 ft wide and 2 ft deep. The towing carriage was equipped with soil processing and leveling device.

A general view of the test set-up is shown in figure 8.

Figure 9 shows the test wheels with the towing carriage during a test run.

Figure 10 shows a rear view of the towing carriage, where the loading of the test wheels, the sinkage measuring potentiometers and the soil processing and leveling device can be seen.

Figure 11 shows the wheel type test device with the presently used soil value measuring instrument (bevameter).



Fig. 8. — General view of the test equipment.

B) **Instrumentation.** — *Sinkage measurements.* - The sinkage of the test wheels was measured by linear potentiometers with a range of 0-8 inches using the reference wheel as base. The reference wheel counterbalanced to almost zero load was rolling between the test wheels far enough from them so that any bulding of the soil surface due to flow under wheel loads did not influence its action in establishing the zero point.

Tractive effort measurement. — The traction force was measured by electric resistance strain gauge type torquemeters which were mounted on the shaft transmitting the torque from the test wheels to the brake. The torquemeters were calibrated directly to traction force.

Slip measurement. — A differential gear arrangement was used for measuring slip directly.

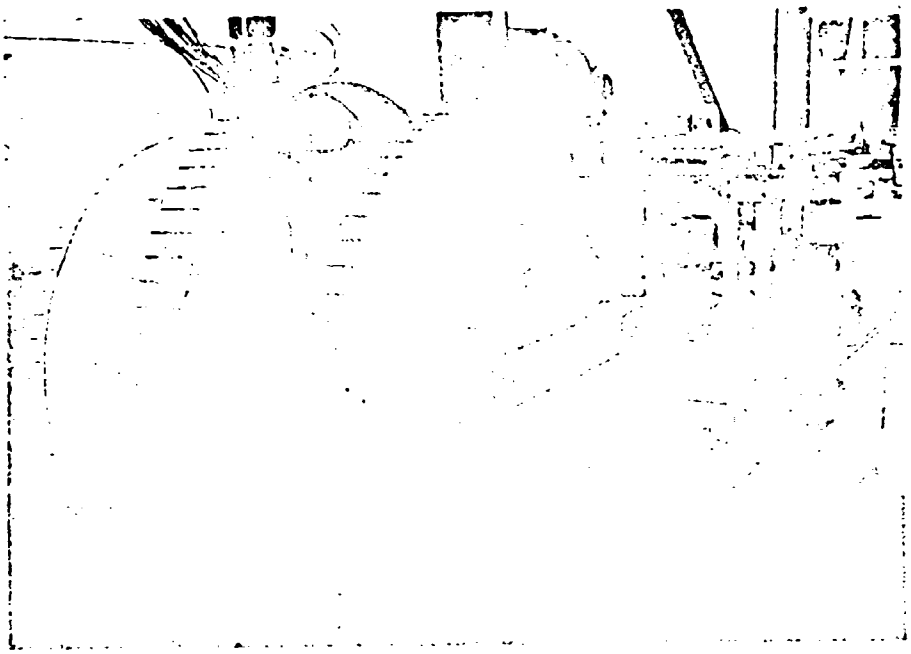


Fig. 9. — Front view of the test equipment.

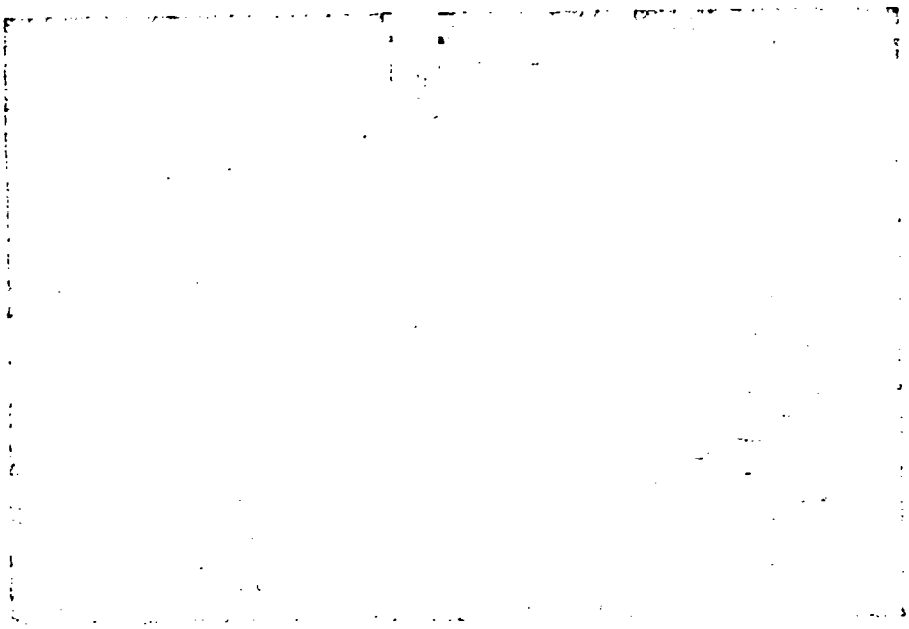


Fig. 10. — Rear view of the towing carriage.

Recording instrument. — A six channel Sanborn type electronic amplifier and recording oscillograph was used for recording test data.

(') **Conduct of tests.** — The load on each test wheel was varied from 50 to 800 lbs. The towing velocity was kept constant, approximately 1 fps. The length of each test run was approximately 30 ft. Test data were recordered

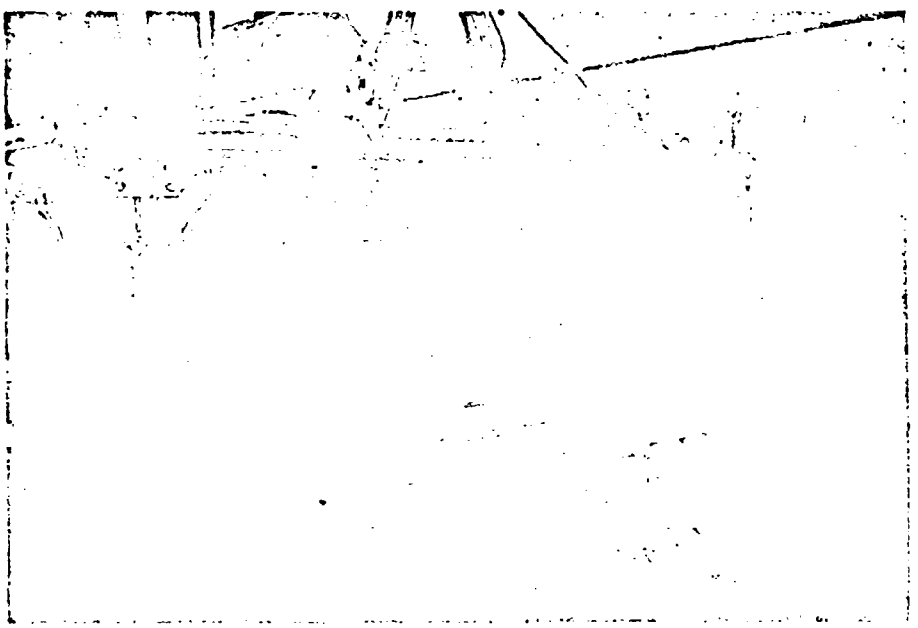


Fig. 11. — Wheel type test apparatus with the bevameter.

continuously during tests. The slip was varied gradually from 0 to 100 % for the shear-slip tests, so each test run produced a complete traction-slip curve. 20-25 tests were performed for statistical evaluation of the results. Soil values were measured before each run by conventional bevameter. Moisture content also was checked frequently. The soil was processed and leveled before each test.

Tests were performed in two basic types of soil: dry sand and loam. The detailed description of these soils is presented in appendix 4.

Due to the arrangement of the test equipment various effects on the test results had to be considered:

1) Weight transfer due to the tractive effort.

2) Weight transfer due to the positioning of the towing arms.

3) Towing speed.

4) Driven or braked wheel.

The effect of these factors on test results is discussed in detail in appendix 1.

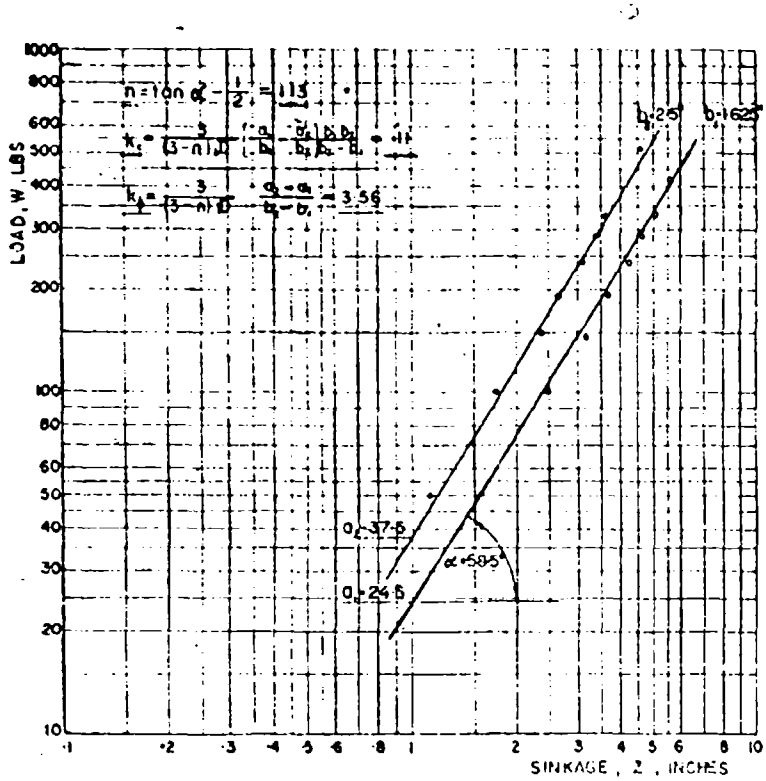


Fig. 12. — Sample computation of the sinkage soil values from test data; wheel sinkage test; soil: dry mason sand.

IV. - Test results

A) **Test result data.** — Because of the extensive test data (tests were repeated 20-25 times for statistical evaluation) we present only one sample test sheet for sinkage test and shear test for each soil (see figs. 12 to 17).

The determination of frequency distribution, mean values, and standard deviations of the test results obtained from wheel tests is presented in appendix 2.

The soil parameters measured by conventional bevameter were also evaluated statistically. The results are presented in appendix 3.

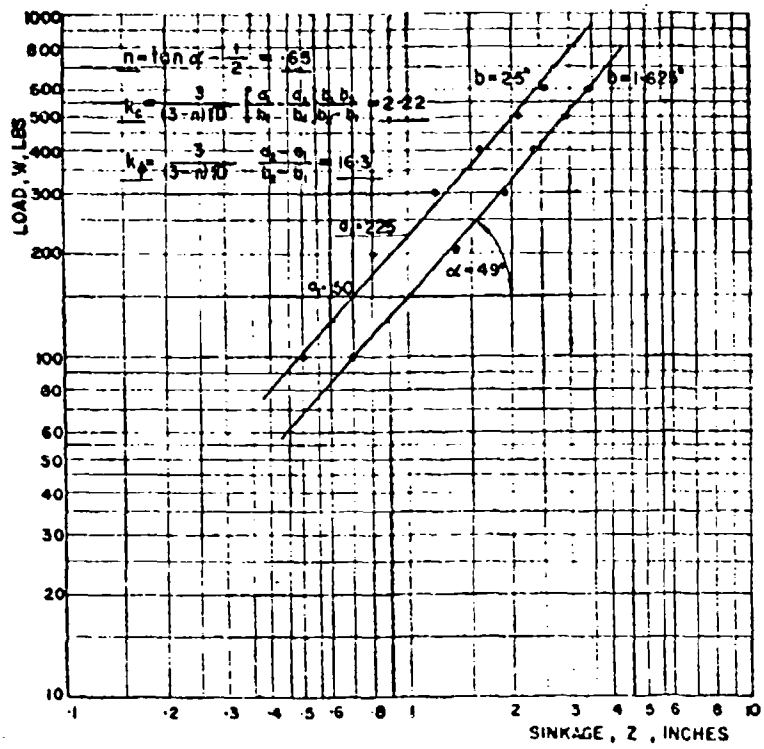
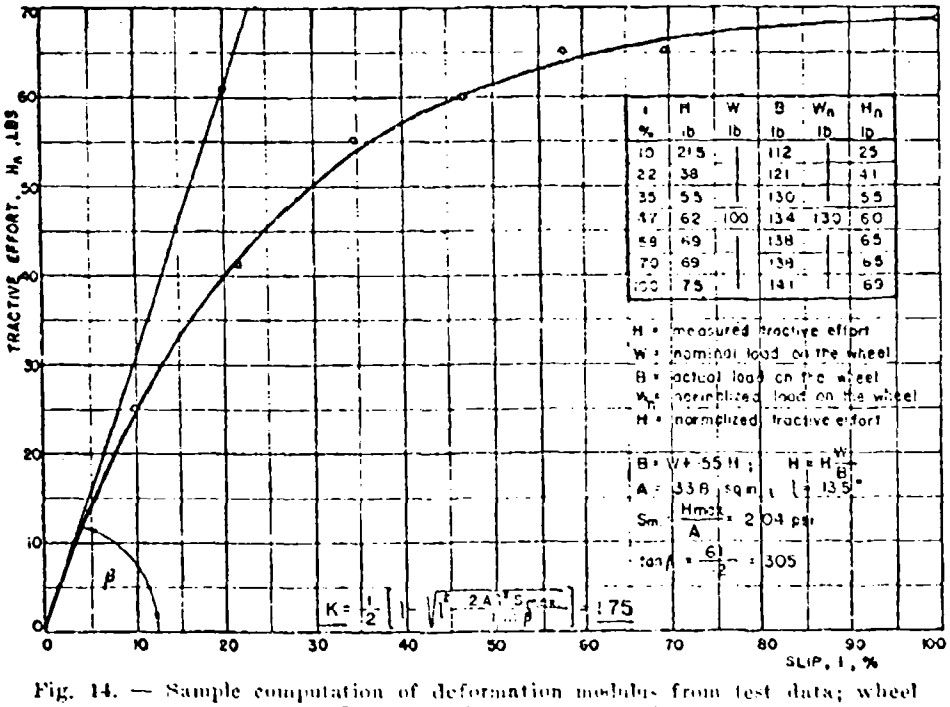


Fig. 13. — Sample computation of the sinkage soil values from test data; wheel sinkage test; soil: loam.



i %	H lb	W lb	B lb	W_n lb	H_n lb
10	21.5		112		25
22	38		121		41
35	55		130		55
47	62	100	134	130	60
59	69		138		65
70	69		139		65
100	75		141		69

Fig. 14. — Sample computation of deformation modulus from test data; wheel test: D: 46"; soil: dry mason sand.

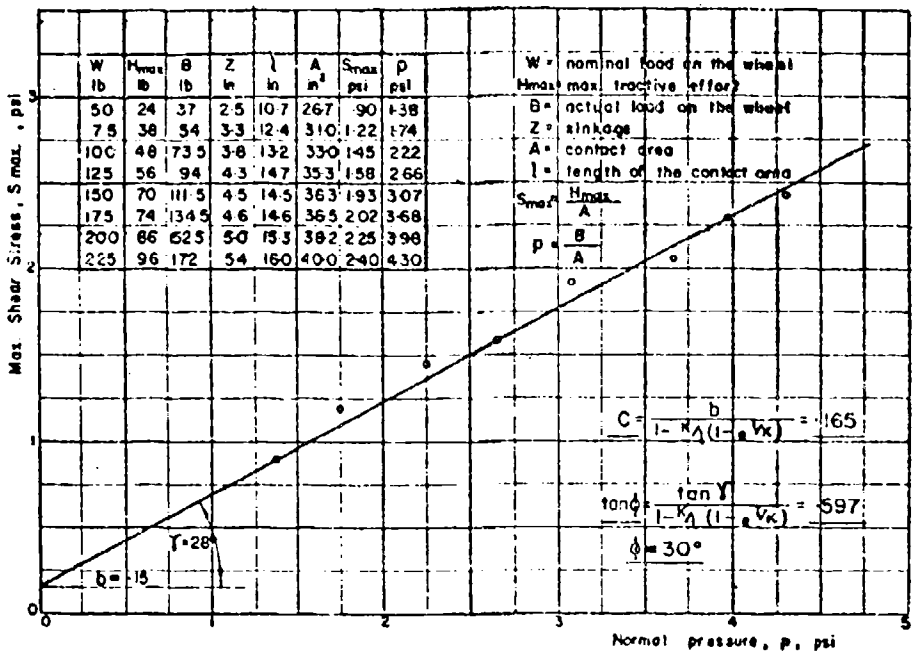


Fig. 15. — Sample computation of shear soil values from test data; wheel test; dia: 46"; soil: dry mason sand.

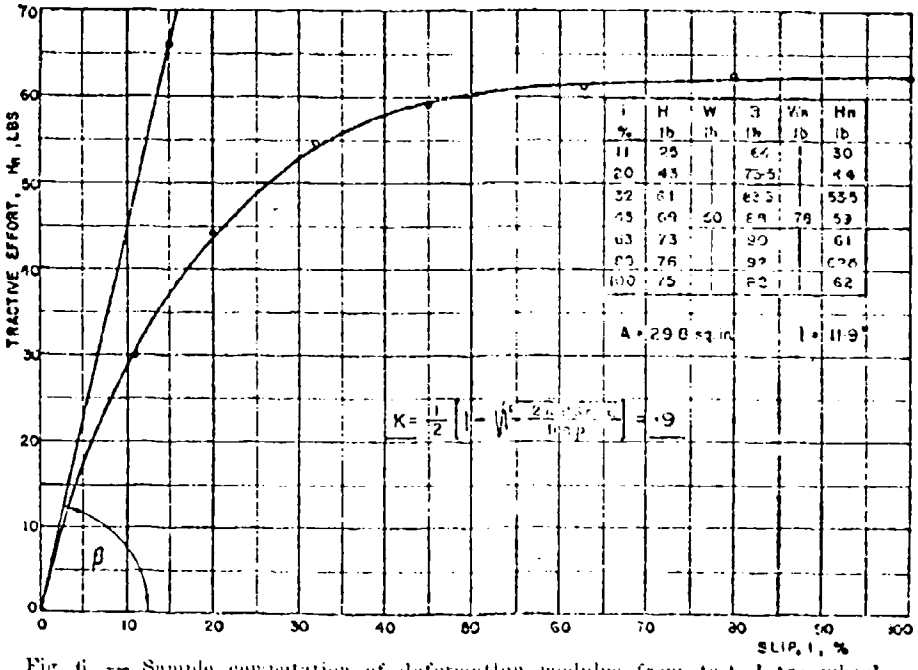


Fig. 6. — Sample computation of deformation modulus from test data; wheel test; d: 46"; soil: loam.

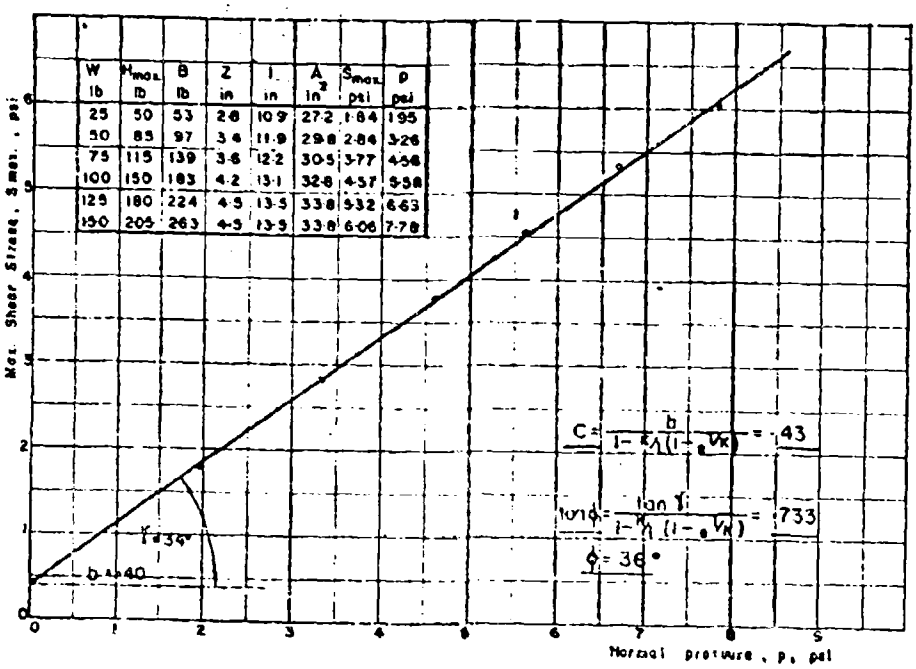


Fig. 17. — Sample computation of shear soil values from test data; wheel test; dia: 46"; soil: loam.

B) Comparison of test results obtained from wheel tests with the conventional Bevameter test data.

1) Soil: Dry muson sand

Soil values	Wheel type test device		Conventional bevameter	
	Mean value	Standard deviation	Mean value	Standard deviation
n	1.1825	.0554	1.110	.046
k_c	.04	.325	.112	.257
k_ϕ	3.58	.410	3.925	.504
c	.2375	.086	.150	.093
Φ	29.5	2.09	28	1.85
K	1.50		.70	

2) Soil: Loam (farm soil)

Soil values	Wheel type test device		Conventional bevameter	
	Mean value	Standard deviation	Mean value	Standard deviation
n	.680	.143	.690	.079
k_c	2.40	1.24	2.31	1.72
k_ϕ	15.78	1.32	16.85	2.30
c	.44	.104	.25	.061
Φ	33.66	1.07	29.7	1.09
K	1.10		.50	

V. - Discussion of test results and conclusions

As a comparison of test results obtained from wheel tests, with those obtained with the conventional bevameter shows, the sinkage soil parameters (n, k_c, k_ϕ) are in a very close agreement, irrespective of the instrument used.

When comparing shear soil parameters (c and Φ) we find however the values obtained from wheel tests to be slightly higher than those obtained from bevameter tests. This is due to the fact, that in the case of a braked wheel the previously mentioned bulldozing resistance was measured as a part of the traction. When driving, however, the test wheel instead of braking it, this error can be minimized, should it be considered undesirable

There also is a significant difference between the values of the deformation modulus, K, obtained from wheel tests and the bevameter tests. However, we have never been satisfied with original bevameter data as they always tended to produce too low a slip for the maximum of traction. After developing the wheeled soil testing device we found a much better agreement between predictions and actual vehicle test data, which indicates that the new instrument reproduces soil shear conditions imparted by vehicle action with greater fidelity than the bevameter.

BIBLIOGRAPHY

1) Bekker M. G. Practical outline of the mechanics of automotive land locomotion. Detroit Arsenal, Land Locomotion Research Branch, June, 1955.
2) Bekker M. G. A proposed system of physical and geometrical terrain values for the determination of vehicle performance and soil trafficability. Interservice Vehicle Mobility Symposium, Office of Ordnance Research, Duke University and Stevens Institute of Technology. Published by Land Locomotion Research Branch, OTAC, Detroit, 1955.
3) A soil value system for land locomotion mechanics. Research Report no. 5. Detroit Arsenal, Land Locomotion Research Branch, December 1958.
4) Czuko T. and Bekker M. G. Determination of vehicle sinkage parameters by means of rigid wheels. Detroit Arsenal, Land Locomotion Research Branch, May 1958.
5) Bekker M. G. Theory of land locomotion. University of Michigan Press. Ann Arbor, Michigan, 1956.
6) Janosi Z. and Hanamoto B. An analysis of the drawbar-pull slip relationship for tracks. Land Locomotion Laboratory, OTAC, December 1960.
7) Bekker M. G. Off-the-road locomotion, research and development in terramechanics. University of Michigan Press, Ann Arbor, Michigan, 1959.

APPENDIX 1

The effect of various factors on the test results

1) Effect of weight transfer due to the tractive effort (fig. 18):

The moment equilibrium for point « A »:

$$B + HR - WI - FR_1 = 0$$

Since $F = \frac{R}{r_2}$ from the equilibrium about « 0 » we have

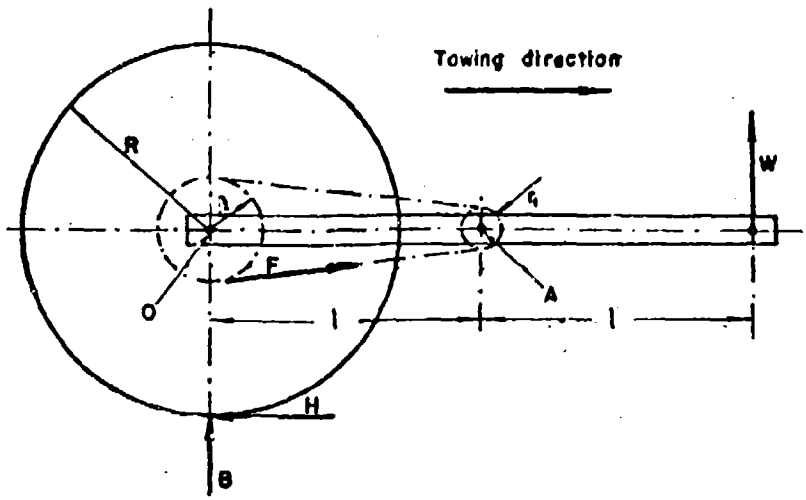


Fig. 18. — Effect of weight transfer due to the tractive effort.

$$B\,l + H\,R - W\,l - H\,\frac{R}{r_2}\,r_1 = 0$$

Solving for B, we have

$$B = \frac{W\,l - H\,R\,\left(1 - \frac{r_1}{r_2}\right)}{l}$$

In our case $\frac{r_1}{r_2} = \frac{1}{3}$, and $\frac{R}{l} = .82$

Then the value of B for pulled wheel

$$B = W - .55\,H$$

In the case of a pushed wheel (towing direction opposite to that indicated in figure 18)

$$B = W + .55\,H$$

The weight transfer due to the tractive effort was considered when computing the normal pressure, p.

2) Effect of weight transfer due to the positioning of the towing arms (figure 19):

The towing force, T, has a vertical component which results in a weight transfer when the towing arm is not horizontal. We have from figure 19,

$$T_V = T \sin \alpha = T\,\frac{Z/2}{l}$$

Then T can be expressed as follows:

$$T = \frac{T_H}{\cos \alpha} = \frac{H}{\cos \alpha}$$

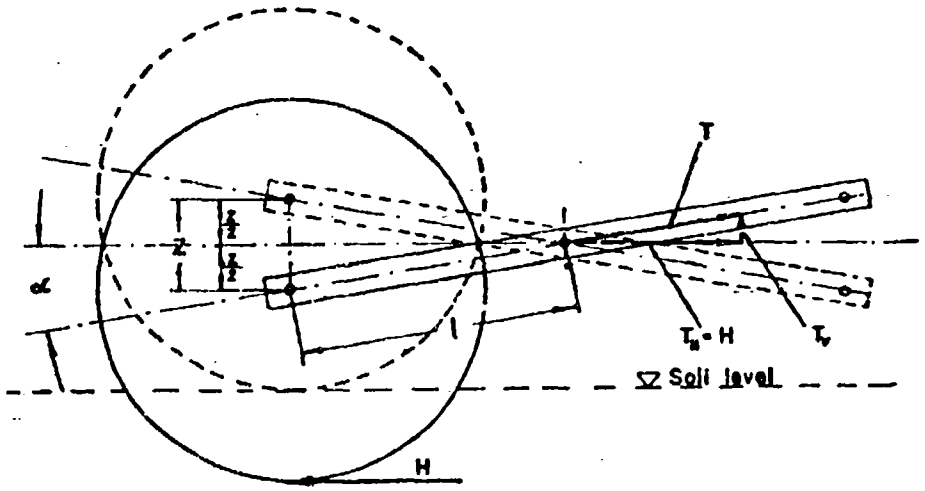


Fig. 19. — Effect of weight transfer due to the towing arm position.

In our case at the maximum sinkage (8 in),

$$Z = 8 \text{ in} \qquad l = 28''$$

$$\text{So } T_v = \frac{4}{28} T = (.14)\ (1.05)\ H = .147\, H$$

Since H is approximately one third of W, the weight transfer is less than 5 % of the normal load at the worst condition, thus can be neglected.

3) Effect of the towing speed.

The effect of the towing speed on both sinkage and shear test results was investigated and it was found that the towing speed in the range of ½ to 6 fps has no effect at all on the test results.

4) Effect of driving or braking the wheel.

When driving the wheel, the slip was defined as follows:

$$i = \frac{V_t - V_a}{V_t}$$

In the case of braked wheel the slip

$$i = \frac{V_a - V_t}{V_a}$$

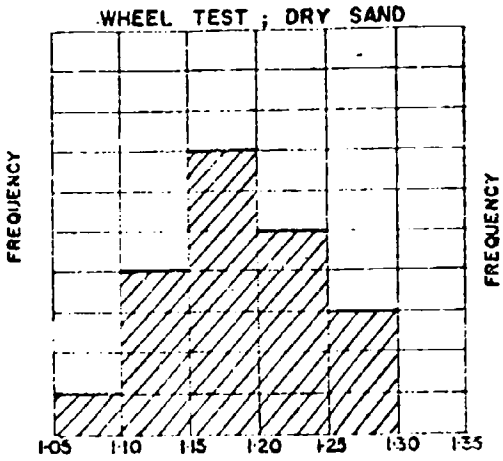
where: V_a = the towing speed;
V_t = the wheel circumferential speed.

In the case of the braked wheel there was an additional bulldozing resistance in front of the wheel, which was included in traction measurement. However, comparison tests with driven and braked wheels showd no practical significant difference between the two cases.

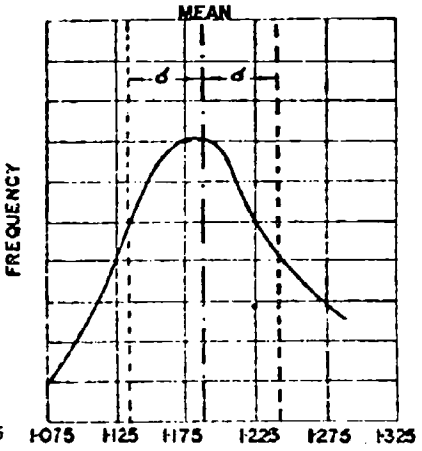
APPENDIX 2

Statistical evaluation of soil values obtained from wheel tests

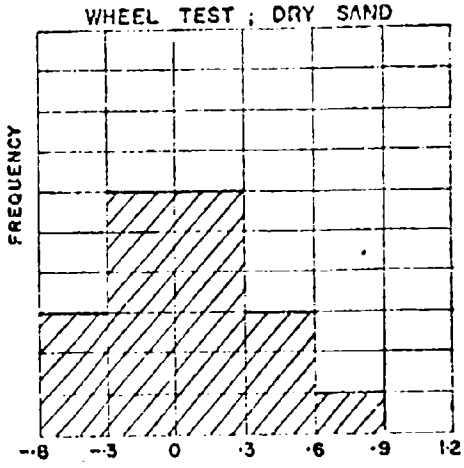
HISTOGRAM FOR « n »



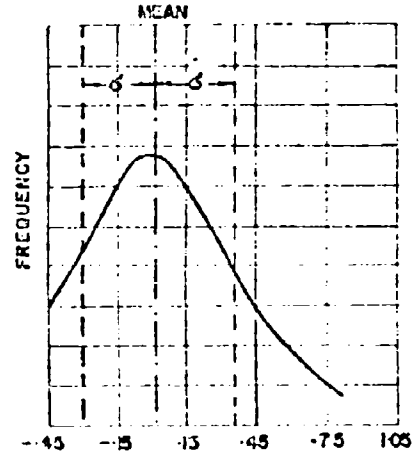
FREQUENCY DISTRIBUTION CURVE



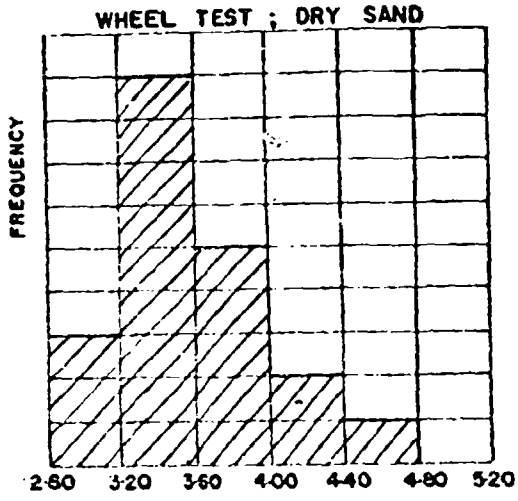
HISTOGRAM FOR « k »



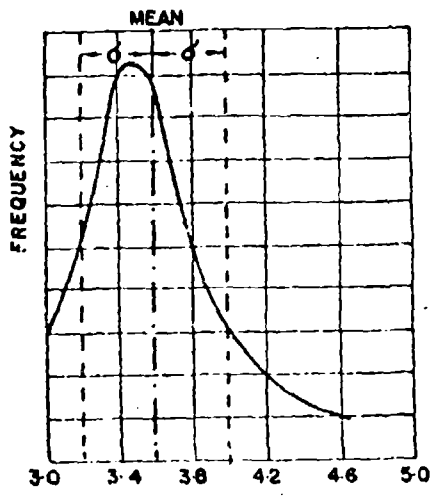
FREQUENCY DISTRIBUTION CURVE



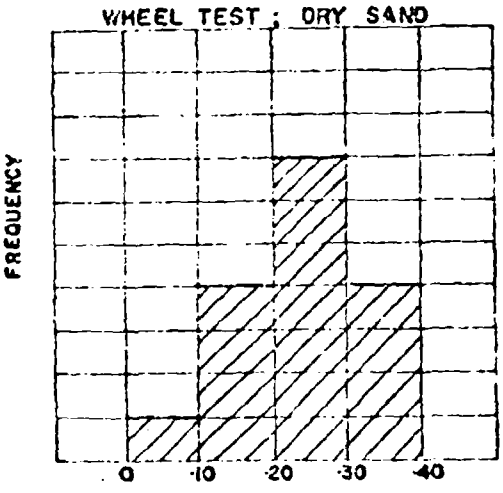
HISTOGRAM FOR « k »



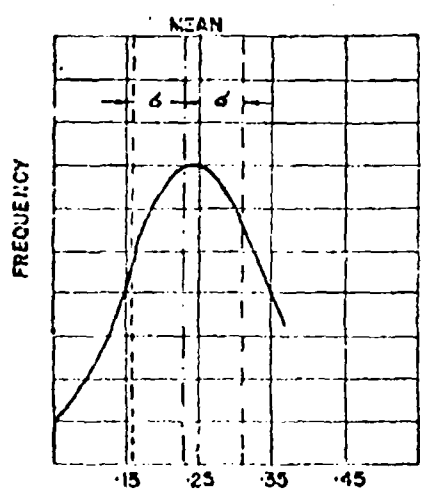
FREQUENCY DISTRIBUTION CURVE



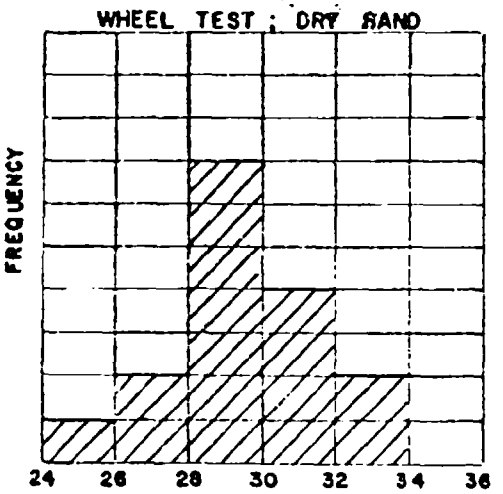
HISTOGRAM FOR « c »



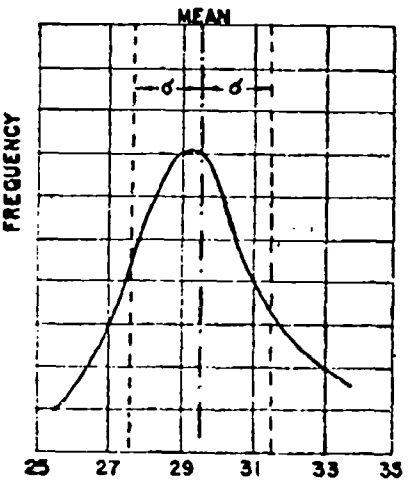
FREQUENCY DISTRIBUTION CURVE



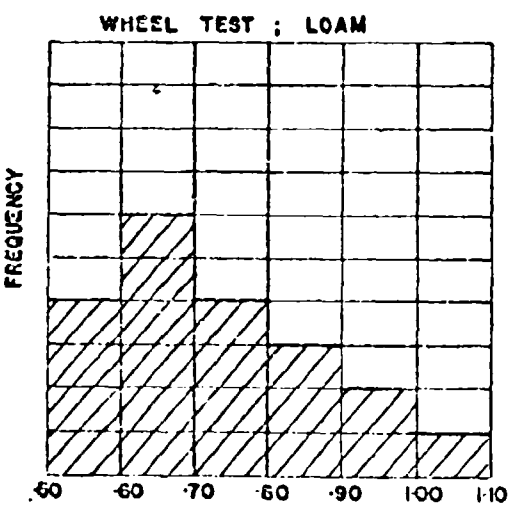
HISTOGRAM FOR « Φ »



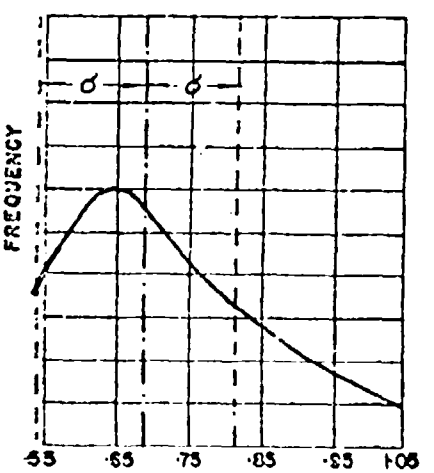
FREQUENCY DISTRIBUTION CURVE



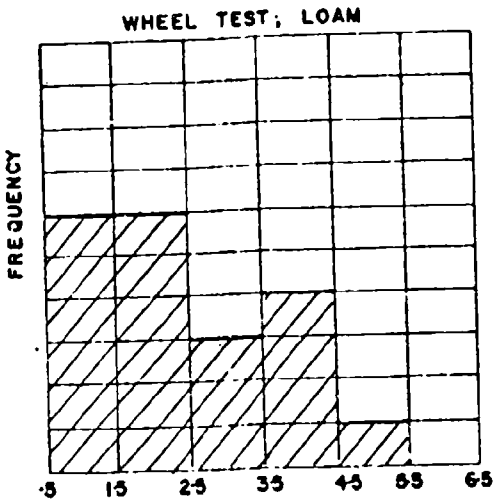
HISTOGRAM FOR « n »



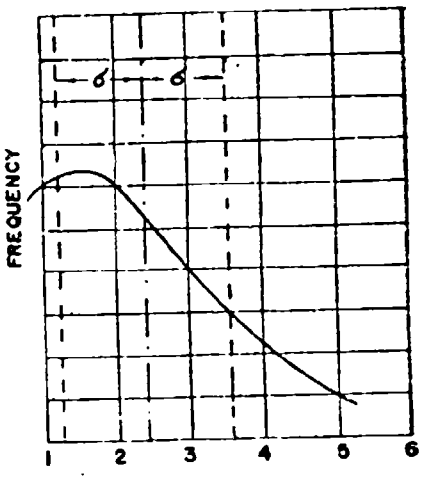
FREQUENCY DISTRIBUTION CURVE



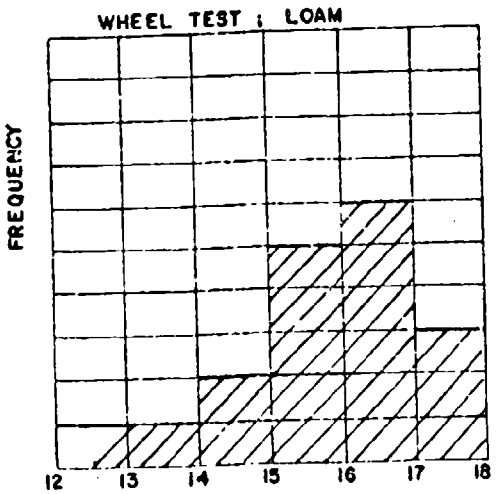
HISTOGRAM FOR « k₁ »



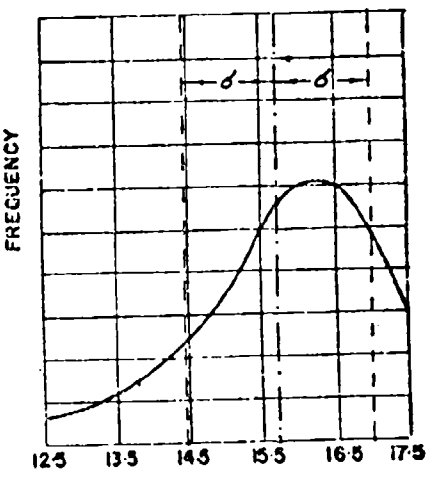
FREQUENCY DISTRIBUTION CURVE



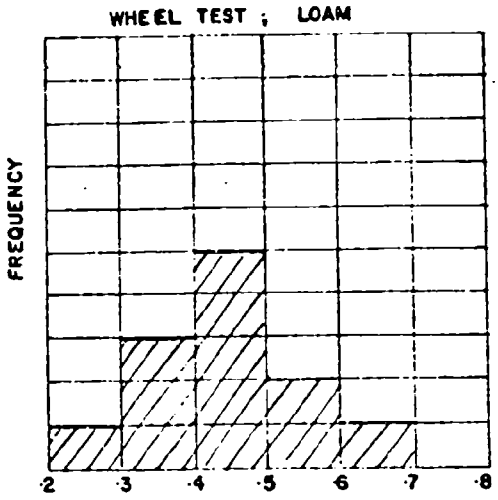
HISTOGRAM FOR « k₂ »



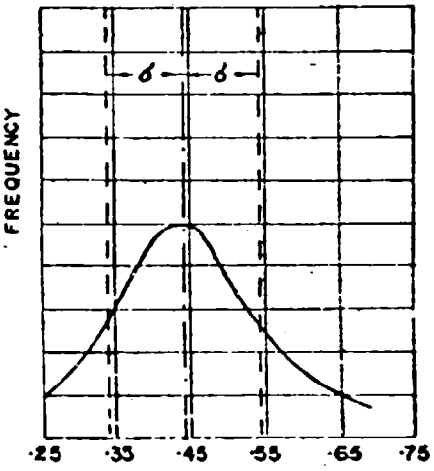
FREQUENCY DISTRIBUTION CURVE



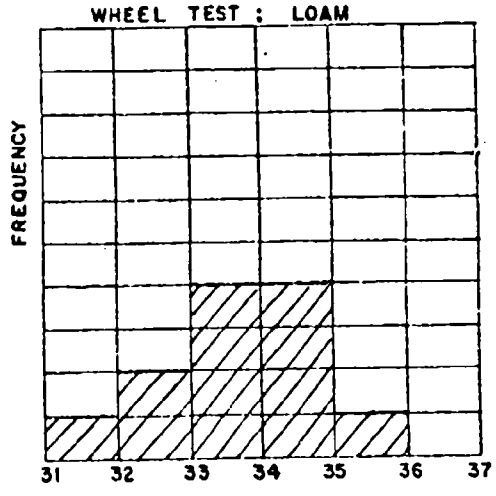
HISTOGRAM FOR « c »



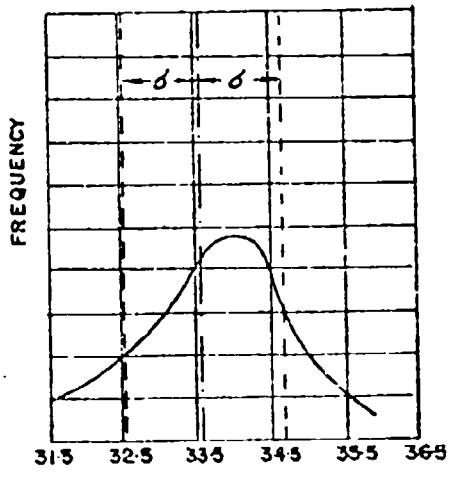
FREQUENCY DISTRIBUTION CURVE



HISTOGRAM FOR « Φ »



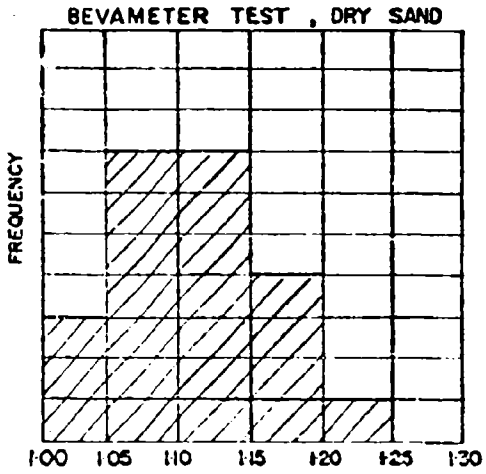
FREQUENCY DISTRIBUTION CURVE



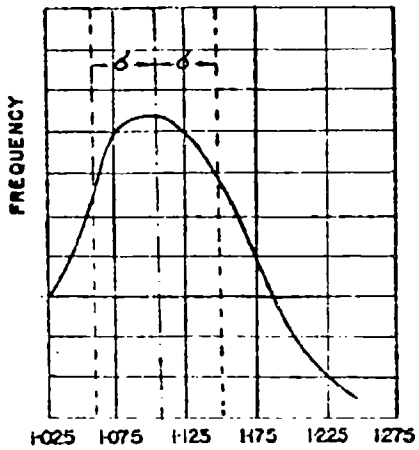
APPENDIX 3

Statistical evaluation of soil values obtained from bevameter tests

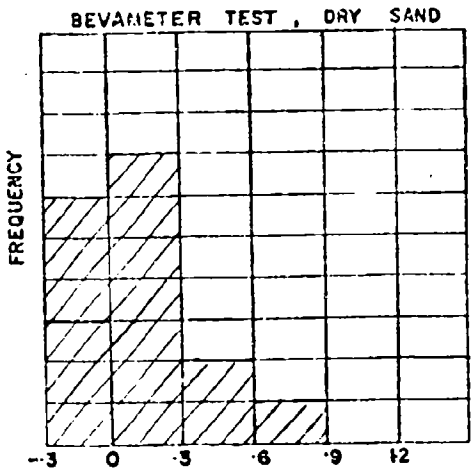
HISTOGRAM FOR « n »



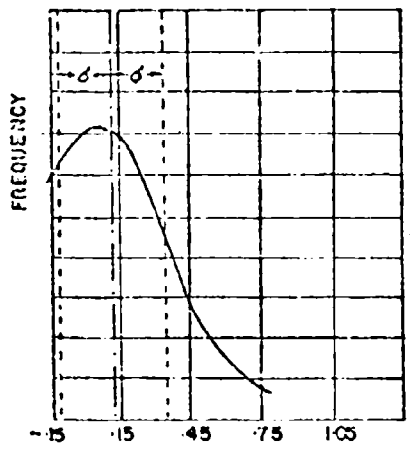
FREQUENCY DISTRIBUTION CURVE



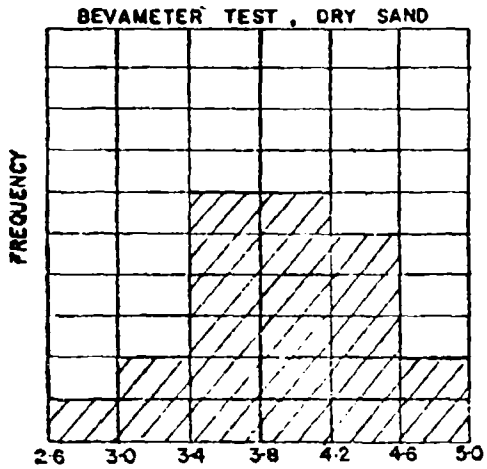
HISTOGRAM FOR « k »



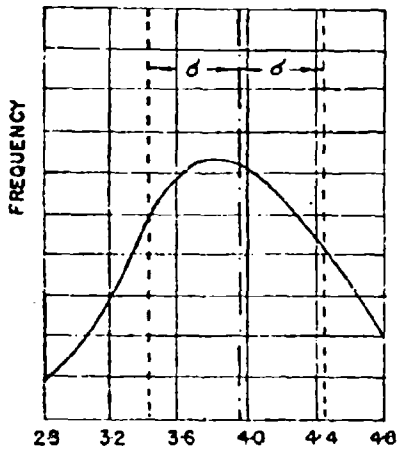
FREQUENCY DISTRIBUTION CURVE



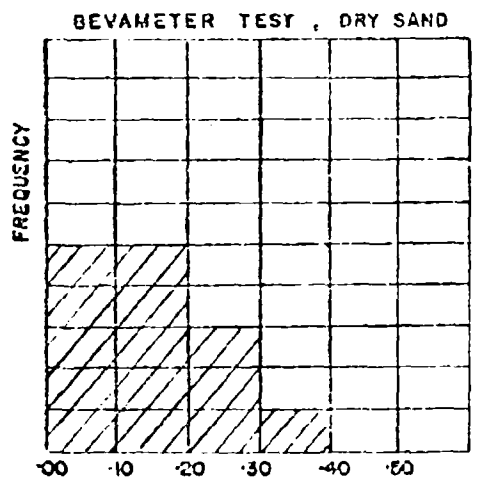
HISTOGRAM FOR « Φ »



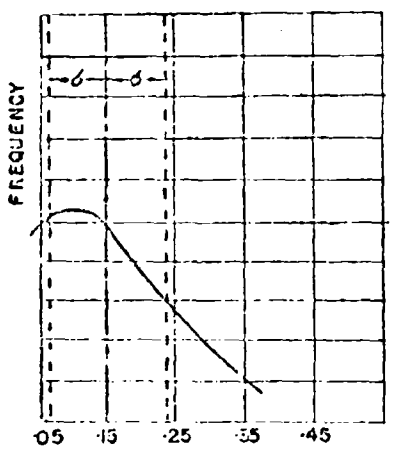
FREQUENCY DISTRIBUTION CURVE



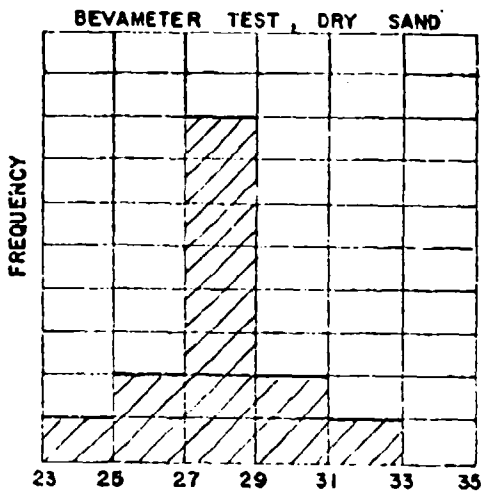
HISTOGRAM FOR « c »



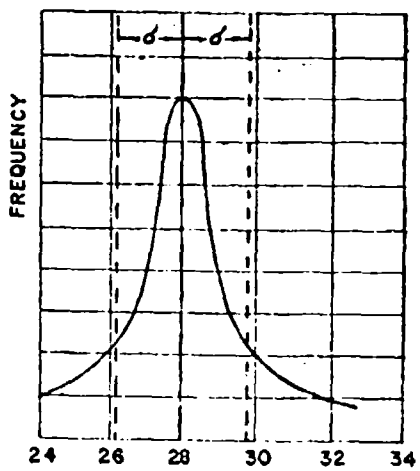
FREQUENCY DISTRIBUTION CURVE



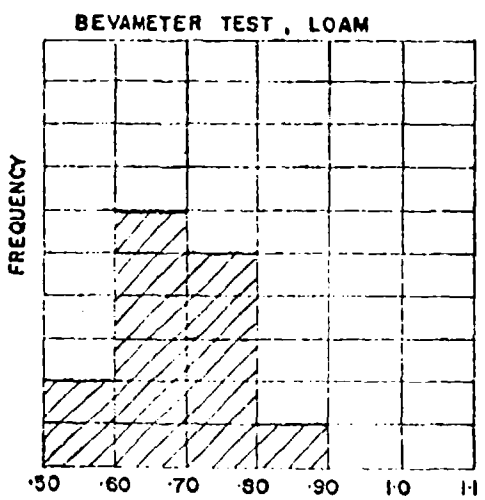
HISTOGRAM FOR « Φ »



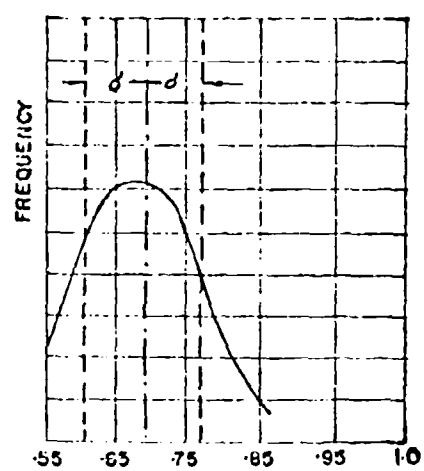
FREQUENCY DISTRIBUTION CURVE



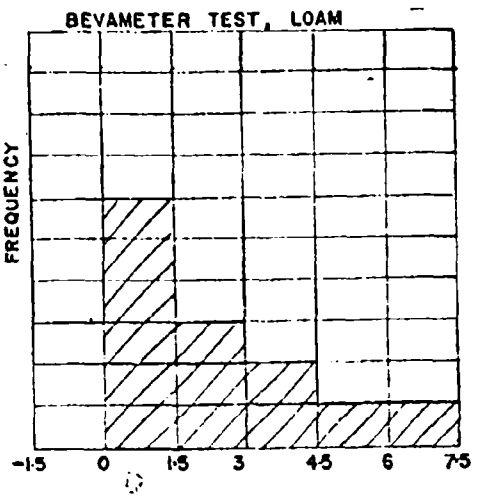
HISTOGRAM FOR « n »



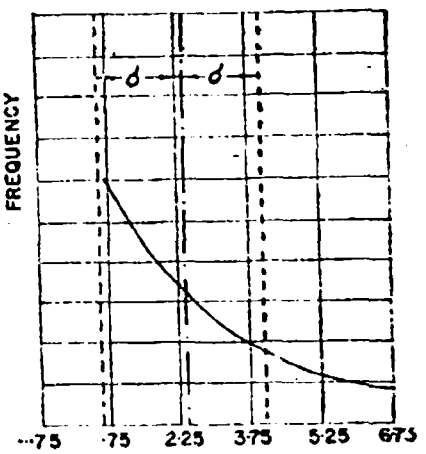
FREQUENCY DISTRIBUTION CURVE



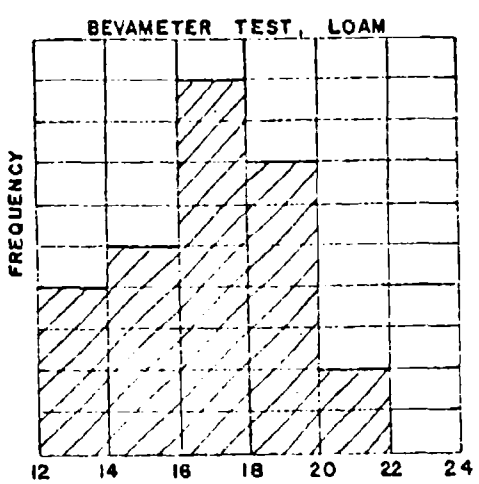
HISTOGRAM FOR « k »



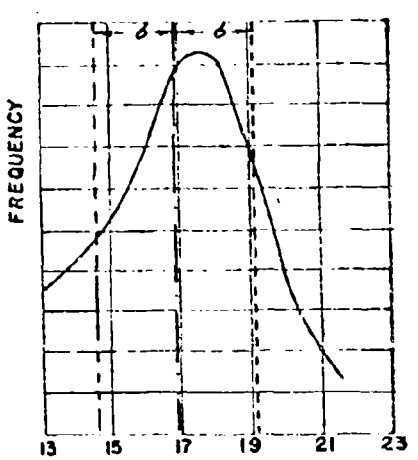
FREQUENCY DISTRIBUTION CURVE



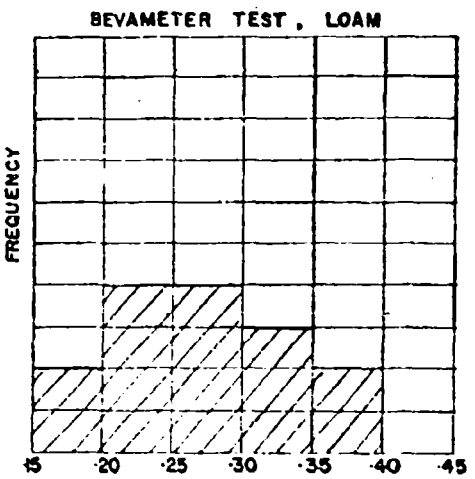
HISTOGRAM FOR « k₀ »



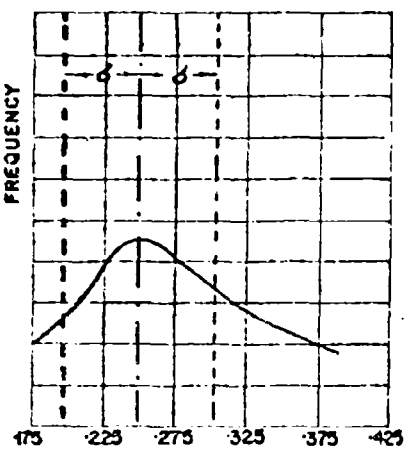
FREQUENCY DISTRIBUTION CURVE



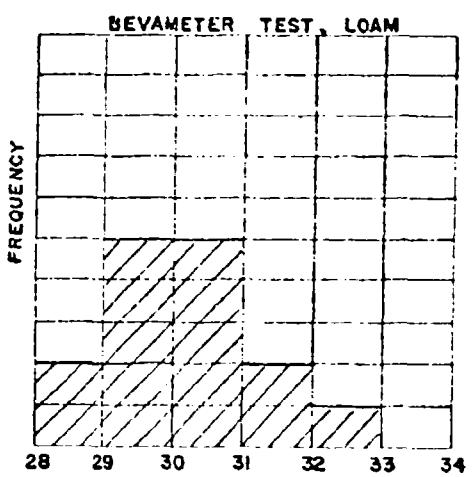
HISTOGRAM FOR « c »



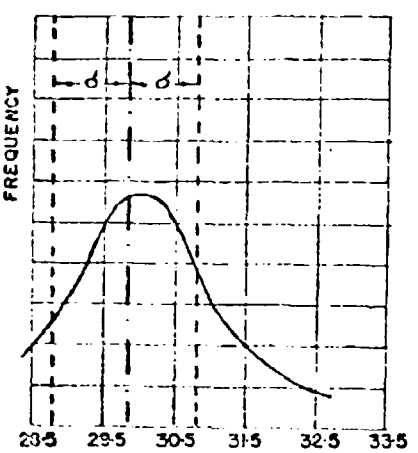
FREQUENCY DISTRIBUTION CURVE



HISTOGRAM FOR « d »



FREQUENCY DISTRIBUTION CURVE



APPENDIX 4

Description of soils used for tests

Description of soils.

1) *Dry mason sand*
Density: 103 lb/ft³
Moisture content: 2 %
Direct shear test data
Friction angle: 31°
Cohesion: 0.1 lb/in²

2) *Loam* (Michigan farm soil)
Density: 78 lb/ft³
Moisture content (average) 14 %
Direct shear test data
Friction angle: 34°
Cohesion: 0.50 lb/in²

The grain size distribution diagram is shown in figure 20.

DISCUSSIONS

F. L. UFFELMANN. — Mr. Pavlics is to be congratulated on the design of this equipment which will enable a speedier evaluation of Mr. Bekker's 6-7 constants than was possible with previous static equipment. It would appear to require further development to provide a truly continuous evaluation with distance as it is noted the increments of loading are not automatic.

The slip constant K recorded by the wheel system is about twice that recorded by the static type bevameter. I should like to suggest the reason for this must be attributed to the approximate nature of the calculation where the wheel footing is considered equivalent to a uniformly loaded rigid plane footing with a linear distribution of slip displacement (see paper 41) while actually the wheel can have a non-uniform radial pressure distribution (see paper 46) and has a non linear horizontal component of slip displacement distribution.

There is no indication as to how the length of the equivalent footing is estimated; the area of plastic recovery after passage of the wheel should not be forgotten in this estimate as this can add considerably to the traction of the wheel.

It is suggested that a direct measurement of the horizontal force on the axle would be preferable to the torque measurement divided by the wheel radius, as the latter method gives the true horizontal force at zero sinkage only.

F. PAVLICS. — The test device shown in my paper is an experimental test device, not an operation field test equipment yet. So there are many things to be corrected and to be modified, as for instance a more practical way of loading the wheels, which can be solved by hydraulic loading mechanism; and also for measuring properties like force, slip, and sinkage, also can be arranged in some more practical way. As far as the loading area is concerned, the equation I have shown for the relationship between the load and sinkage of the wheel is considering that the loading area is not a flat plate, but a part of a circle. In case of the shear test, when we are breaking or driving the wheel we substituted the curve with a straight line. This of course is an assumption which is permissible only when the sinkage is quite small. But in case of a large diameter wheel, and that is the reason why we suggest to use a large enough diameter wheel, this error is quite small, and we do not think that it would be advisable to go into a more complicated mathematical formulation of the problem. I do not know if I answered all of your questions or not

N. 23

An instrumentation system for the measurement of terrain geometry *)

Apparecchiature per la misurazione della geometria del terreno

I. J. Sattinger - S. Sternick **)

ABSTRACT. — *An instrumentation system for the measurement of terrain geometry has been developed and tested. The purpose of this device is to provide a means for the rapid and accurate collection of terrain profile data, which will be useful in the analysis of the rough-ground performance of cross-country vehicles. The field equipment consists of a two-wheeled measuring assembly which is towed across the ground. Electrical instruments mounted on the assembly continuously measure the slope of the ground and the distance travelled along the surface of the ground. These quantities are continuously recorded on magnetic tape. The magnetic tape is then returned to a laboratory data-processing system which obtains the profile data by a mathematical process of integrating the slope of the ground with respect to surface travel. Preliminary tests indicate that the system is capable of obtaining terrain profile with an error which does not accumulate to more than 4 inches in 100 feet.*

1. - Introduction

An important characteristic of an off-the-road vehicle is its rough-ground performance, as indicated, for example, by the speed which it can safely achieve across rough terrain. Allowable speeds tend to be limited by the effects of vehicle motion on human passengers and on equipment carried aboard the vehicle. In order to design vehicles with improved rough-ground performance, methods must be developed and implemented for analyzing and predicting such performance. Although a first systematic, analytical approach in this direction was made by Leiber prior to 1944 [1], the whole question was not sufficiently recognized until the early 1950's when Bekker reformulated the problem in his lectures delivered at the Graduate School, Stevens Institute of Technology [2], and stressed it again during his studies at the Operations Research Office, John Hopkins University [3].

The development of a suitable methodology for dealing with this aspect of off-the-road locomotion requires research in two main directions. First,

*) This paper was originally prepared for Land Locomotion Laboratory, U.S. Army Ordnance Tank Automotive Command, Detroit, Michigan.

**) Institute of Science and Technology, University of Michigan, Ann Arbor, Michigan, U.S.A.

accurate comprehensive information on the geometric characteristics of the terrain over which cross-country vehicles must operate is needed to replace the present sketchy and incomplete information. This requires a research program for the collection of such data on representative samples of the earth's surface and the analysis and organization of these data.

Second, techniques must be developed for using known vehicle characteristics to predict vehicle performance over given terrain. In addition to experimental field testing, a considerable amount of work has been done on theoretical analysis of vehicle dynamics. The early methods of analysis were based primarily on the assumption that the suspension system is linear [1-4]. These methods are presently being extended to permit the analysis of vehicle performance by the representation of terrain profile and vehicle motion in terms of power spectral density distributions [5]. Analog computer simulation methods have also been developed recently which take into account the important non-linearities of the suspension system as well as the irregular character of the ground surface [6-7].

The instrumentation system described in this paper is intended to provide the means for carrying out research of the first type described above, namely, the collection and organization of necessary information on terrain geometry. This instrumentation system was developed for the purpose by the Institute of Science and Technology of the University of Michigan under the sponsorship of the Land Locomotion Laboratory, Ordnance Tank-Automotive Command of the United States Army.

2. - Required characteristics of instrumentation system

2.1) **Types of information required.** — The profile data of a particular section of ground form a record of the elevation of each point along a selected route as a function of the horizontal distance along the route. Methods of analysis of the ground wave performance of cross-country vehicles make use either of a ground profile record or of some other form of data derived from it. Profile data are thus the basic information required in a terrain measuring program.

If the data are to be used to determine the dynamic response of the vehicle in pitch and bounce only, it is sufficient that the profile along a single line be obtained. To make more comprehensive studies which include the roll response, data can be collected along two parallel lines separated by the track width of a vehicle.

Since studies of vehicle mobility may be expected to cover entire areas [8], it is desirable to supplement the profile data collected along specific paths with information covering the general area in which the data were taken. A plan view of the area should be provided to show the natural and man-made features. Such topographical data may already be available either in the form of topographic maps similar to those prepared by the U.S. Geological Survey or in the form of aerial photographs available from civilian or military agencies.

2. 2) **Performance and operating characteristics.** — The required characteristics of a profile measuring system include accuracy, economy, reliability, mobility and usability of the form of the output data. The accuracy required of the data depends on the effect which errors in profile measurement have on the calculation of the pitch, bounce, and roll of a number of types of wheeled and tracklaying vehicles as they travel over terrain at various speeds. In terms of response to a sinusoidal road function of a given amplitude, only small motions of the vehicle body occur for ground wavelengths less than about one-half or greater than 5 times the wheel-base or ground contact length of the vehicle being studied. Wheel-bases of interest range from 4 to 22 ft; therefore, reasonably accurate measurements of sinusoidal components with wavelengths greater than 2 ft and less than 100 ft should be sufficient. To obtain such accuracy, a horizontal resolution (i.e., horizontal spacing of individual measurements) equal to about 1 ft is adequate. However, a greater degree of horizontal resolution is useful, since it permits detailed measurement of individual non-sinusoidal irregularities. With respect to vertical accuracy required, errors of 1 in. over horizontal distances of the order of a wheelbase length and errors of 4 in. over distance of 100 ft result in errors in calculation of body motions small enough to be ignored. In determining the accuracy of a system, systematic errors, accumulating in one direction only, appear as a difference in average slope and are therefore of no significance in vehicle studies.

A data collection system which depends on highly trained technical personnel is expensive and might be difficult to operative if they are not readily available. For this reason, simplicity of operation and ease of maintenance are important characteristics of a suitable system.

The ground over which measurements are to be made will contain obstacles of various sizes and shapes, will vary widely in composition or consistency, and may be covered with snow or vegetation. In many cases it will be difficult to reach the location where measurements are to be made. The instrumentation vehicle chosen should have the mobility to function properly under these conditions.

Since extensive amounts of data on terrain geometry are required as an adequate basis for vehicle performance analysis, it is advisable to develop measurement methods which are suitable for the rapid and accurate collection of terrain data on a large scale. The measuring system should produce data in a form convenient for subsequent use. Two specific uses for terrain geometry data are anticipated. They can be used to provide road-function inputs to an analog simulation of a vehicle suspension system or they can be subjected to harmonic analysis techniques to characterize each road sample in terms of its spectral density (i.e., the amplitude of each sinusoidal component as a function of ground wavelength). In either case, a record of elevation, y, as a function of the horizontal component of distance, x, provides the necessary data in a form adaptable to the intended use.

3. - Description of instrumentation system

3. 1) Theory of operation. — The measurement technique adopted in the system described in this paper was selected as a result of an initial study of various possible methods of measuring terrain geometry [4]. Vehicular surveying systems have been developed by several inventors since 1865. Several of these operate on what may be called the slope integration method, a recent development of this type being the Johnson Elevation Meter [9-10]. This meter is intended chiefly for use in measuring total elevational differences between widely separated points, perhaps several miles apart, rather than for obtaining continuous profiles. However, the integration of ground slope, which is the basic principle of operation, is adaptable to a profiling instrument.

To perform its function, a device based on the slope integration method is designed so that it mechanizes the equations:

$$y - y_o = \int_o^s \sin \Theta \, ds, \tag{1}$$

$$x = \int_o^s \cos \Theta \, ds, \tag{2}$$

in which

s is the total distance traveled along the surface of the ground;
y is the elevation of the ground for total travel, s;
y_o is the elevation of the ground at the beginning of the run;
x is the horizontal component of distance along the ground for total travel, s;
Θ is the slope angle of the ground under the vehicle at the distance s from the origin.

For these equations, the two quantities which must be measured continuously are the distance traveled by the vehicle and the slope of the ground over which the vehicle is traveling. To determine these two quantities, a trailing arm towed by a powered vehicle supports a measuring assembly consisting of two wheels mounted in tandem so as to follow a common track (see fig. 1). An angular reference device carried by the trailer provides a continuous indication of the pitch angle of the wheel frame, assumed to be the same as the slope of the ground over which the wheels are traveling. The forward travel of the vehicle is measured by an odometric device connected to one of the measuring wheels. The electrical outputs of the angular reference and the distance indicator are fed through a data recording and conversion system to a digital computer which uses these outputs to perform the mathematical computation corresponding to equations (1) and (2).

3. 2) Detailed description of system. — The measuring assembly of the terrain geometry measurement system is attached to the rear unit of the towing vehicle by means of a pivoted support, which allows the trailing arm

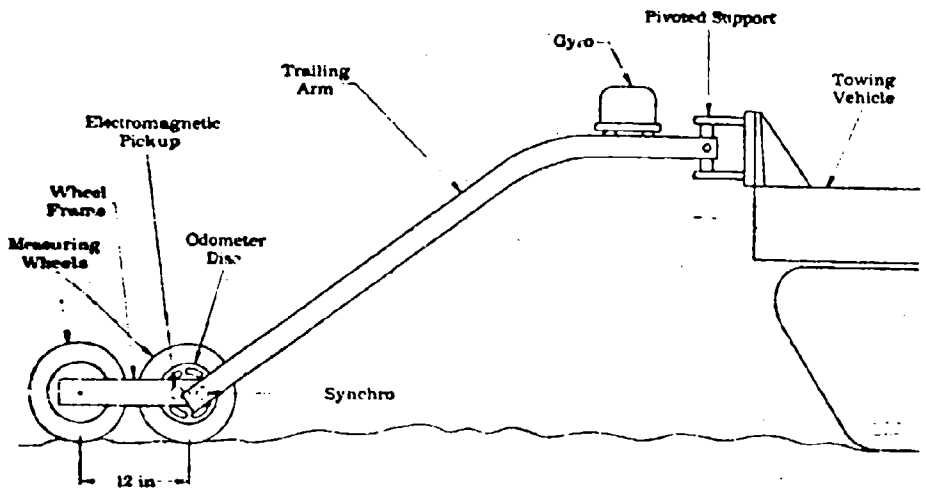


Fig. 1. — Terrain measuring assembly.

to rotate in both yaw and pitch. The slope of the ground is sensed by a pair of 11-inch-diameter wheels, mounted in tandem on a frame of 12-inch wheelbase at the rear of the assembly.

An odometer system produces a voltage pulse at constant increments of s, the travel of the wheel along the surface of the ground. The odometer system operates in the following manner. A metal disc mounted on the axle of the front measuring wheel contains a number of evenly-spaced slots. As the wheel rotates, these slots pass in front of an electromagnetic pick-up whose magnetic reluctance varies with its proximity to a metal surface. The voltage output of this pick-up is amplified, and used to control the closure of a relay contact during the period when a slot is in front of the pick-up; hence, each closure indicates an increment of travel of the front measuring wheel. A voltage transmitted through the relay contact is recorded on one channel of an Ampex AR 200 magnetic tape recorder.

A synchro system is used to indicate continuously the pitch angle which the wheel frame makes with the vertical, total allowable range being from $-90°$ to $+90°$. One synchro is attached to the front measuring wheel in such a manner as to indicate the angle between the wheel frame and the trailing arm. A second synchro is attached to the pitch gimbal of a vertical gyroscope mounted on the trailing arm, so that it measures the angle between the trailing arm and the vertical spin axis of the gyro. The stator windings of the two synchros are electrically connected in such a manner that the voltage of the output rotor winding is proportional to the sine of the angle between the longitudinal axis of the wheel frame and the vertical. This output signal consists of a 400 cps carrier voltage whose amplitude and phase correspond to the sine of the angle. A demodulator converts this carrier voltage to a

varying d-c voltage, having a magnitude and sign also corresponding to the sine of the angle. This varying d-c voltage is recorded on a second channel of the Ampex AR-200 tape recorder, in parallel with the odometer voltage.

In addition to the measuring assembly and magnetic tape recorder described above, the terrain measurement system includes power supplies for generating the necessary electrical power used in the system. The primary source of this power is a gasoline-driven engine which operates a 60 cps electrical generator. Auxiliary power supplies use the 60 cps power to produce 400 cps required by the synchros and the gyro motor.

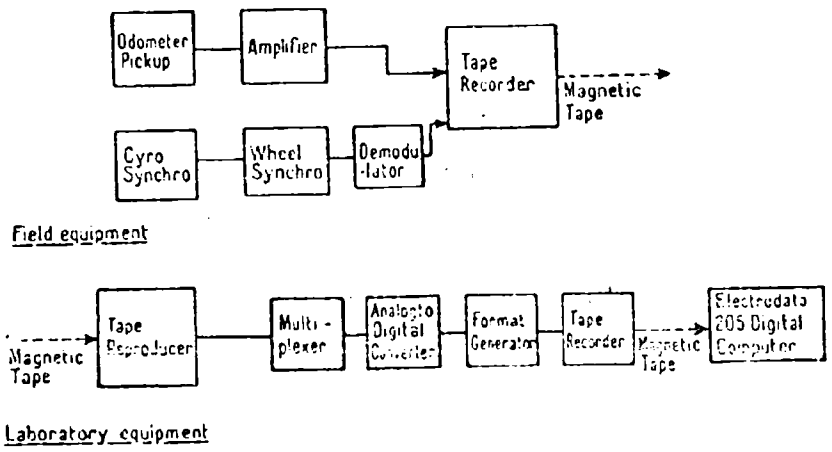


Fig. 2. — Data-processing facility.

In order to obtain terrain geometry data in its final form, the raw data, as originally recorded on magnetic tape, must be processed in a digital computer. This is accomplished by means of a general-purpose data-processing facility located at the Ordnance Tank-Automotive Command (see fig. 2). This facility contains a magnetic tape reproducer by means of which the original electrical outputs of the measuring instruments are reproduced in analog form. A multiplexer sequentially samples the individual channels of the tape reproducer. The sampled data are routed to an analog-to-digital converter, which converts the analog samples into digital form. The numerical data are then organized by means of the format generator into a format which is compatible for use with an Electro Data 205 digital computer. This further processing is accomplished by the use of a set of computer instructions inserted along with the data. Since the computer instructions can be modified by preparing and inserting a new program, maximum flexibility can be obtained in the data processing operation.

In this paper, one particular method of obtaining profile data from the raw data recorded by the field system will be described. Variations of this

data-processing operation are possible; however, additional study is required to determine the optimum method of mathematical analysis of the raw data.

In the data processing operation the increments of distance, Δy and Δx of the ground profile are computed for constant increments, Δs, along the ground surface. For each increment, Δs, amounting to 4 inches, the following computations occur:

$$(\sin \Theta)_i \, \Delta s = \Delta y_i \tag{3}$$

$$(\cos \Theta)_i \, \Delta s = \Delta x_i \tag{4}$$

$$\sum_0^i \Delta x_i = x_i \tag{5}$$

$$\sum_0^i \Delta y_i = y_i \tag{6}$$

The computed values of x_i and y_i can be plotted by a digital plotter or the values can be stored on magnetic tape for subsequent analysis.

4. - Performance characteristics

The system described in this paper has been constructed and is presently undergoing tests (see fig. 3). Some of the preliminary test results are reported here as an indication of the performance of the system.

The performance characteristic which is of primary importance is the accuracy of the system. Several sources of error are possible. Mechanical and electrical errors affect the measurement of slope angle and surface distance and their conversion to profile data. In addition, limitations in the horizontal resolution of the slope measurement device can result in a distortion of the short wavelength components of the profile.

The system has been designed so that the combination of mechanical and electrical errors will fall within the accuracy requirements discussed in Section 2.2. These requirements can be expressed in terms of the standard deviation of the slope angle. If the errors of individual increments of elevation change are assumed to have a normal distribution, a standard deviation of the slope angle amounting to 2 degrees could be permitted, without exceeding an error of 4 in. in a distance of 100 ft. Preliminary tests indicate that errors due to the electrical system can be kept within 1 degree.

Mechanical errors are primarily those due to bouncing of the measurement wheels. These can be kept within acceptable limits by restricting the speed of the measuring vehicle. A speed of 5 fps has been achieved over several samples of terrain without appearing to cause undue wheel bounce.

Errors are inherent in any measuring system which has a finite horizontal resolution. The system described here may be thought of as having a horizontal resolution of 1 ft., since this is the wheelbase of the measuring frame. However, the slope integration process approaches a continuous operation, since data

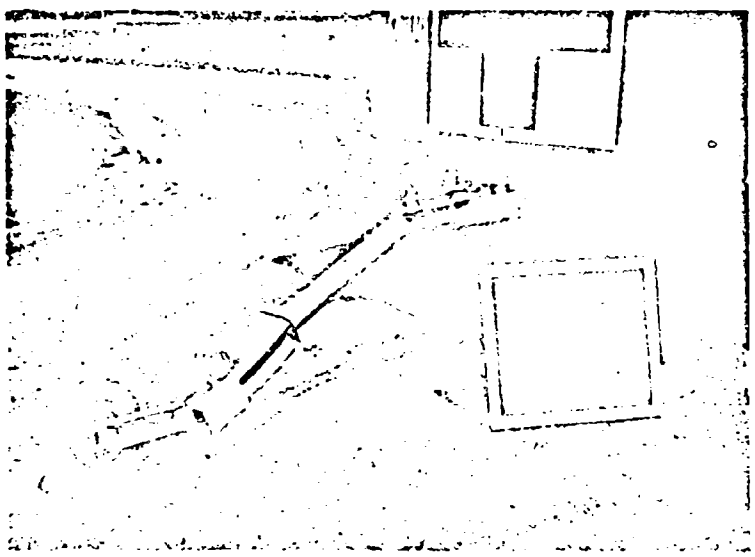


Fig. 3. — Field equipment for terrain measurement.

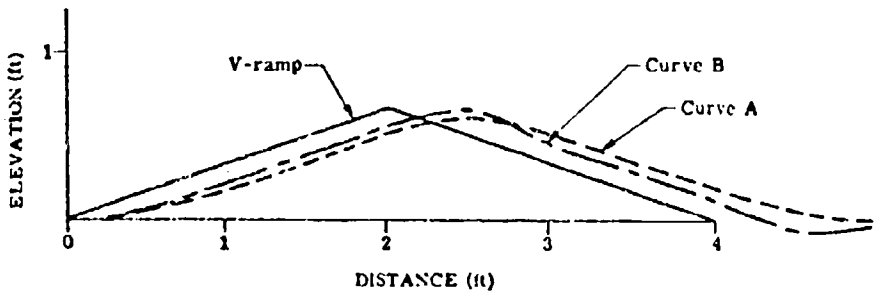


Fig. 4. — Representation of terrain sample.

samples are taken every 4 in. Hence, improved resolution may be obtained by proper processing of the resultant data.

The method of data reduction described in Section 3.2 produces profile data which meet the accuracy requirements specified in Section 2.2. Figure 4 is an example of the data obtained by the measurement system using this method. The terrain irregularity used for this example is a V-ramp 4 ft. long and 8 in. high. Curve A represents the profile obtained by the computation process previously described. Note that the amplitude and general shape of the curve are similar to the original irregularity, but that the location of the peak has been retarded about 8 in. Curve B has been obtained by modifying Curve A. In this modification, the short wavelength components of Curve A

(especially those less than about 2 feet) have been emphasized by being passed through a frequency-selective filter. The characteristics of this filter are such that the magnitude of all wavelength components of the original irregularity down to about 1.1 ft. are measured with less than 10 % error. In the case shown, the primary effect of the transformation is to reduce the shift in position of the peak to about 5 in.

Although the results obtained with the present system produce data of satisfactory accuracy, it is believed that system accuracy can be still further increased by further improvement of the electrical and mechanical design and refinement of the data processing operation.

BIBLIOGRAPHY

1) Lehr E. Springing and damping of the suspension of armored vehicles. Translation by the School of Tank Technology, British Ministry of Supply, 1945.
2) Bekker M. G. Theory of land locomotion. The University of Michigan Press, Ann Arbor, Michigan, 1956.
3) Bekker M. G. Methods of evaluation of off-the-road locomotion. ORO-T-247, Operation Research Office, Johns University, pag. 38-41, 17 August 1953.
4) Bertschinger U. Dissertation of the vibrational characteristics of tracked vehicles. Translation by Fighting Vehicle Design, Dept., Chertsey, England.
5) Bogdanoff J. L. and Kozin F. On the statistical analysis of the motion of some simple vehicles moving on random track. Land Locomotion Report No. 65, OTAC, Detroit, Michigan, 1959.
6) Sattinger I. J. and Smith D. F. Computer simulation of vehicle motion in three dimensions. Report No. 2901-10-T, The University of Michigan, Willow Run Laboratories, May 1960.
7) Sattinger I. J. Methods of evaluating the effects of terrain geometry on vehicle mobility. Proceedings of Interservice Vehicle Mobility Symposium, conducted by Office of Ordnance Research, U. S. Army, 18-20 April 1955.
8) Sattinger I. J. Final engineering report on terrain geometry measurements. Report No. 2384-13-F, The University of Michigan, Engineering Research Institute, April 1956.
9) U. S. Patent No. 2,647,323, Elevation Meter, F. L. Johnson, et al., 4 August 1953.
10) Kostrop J. E. Sun oil co's. mobile elevation meter. World Oil, vol. 128, No. 13, pag. 76-78 and pag. 80, April 1949.

DISCUSSIONS

L. AMICI. — E' stata osservata una differenza nei risultati variando la velocità nell'apparecchiatura e la velocità di avanzamento?

I. J. SATTINGER. — The question has been asked as to whether the accuracy of the system is affected by the speed with which the measuring vehicle travels over the ground. The answer is that if it does not travel above approximately 5 to 10 ft/sec., then the profile which is recorded will not be affected by the speed. If the vehicle travels too rapidly, the wheels of the measuring system begin to bounce and this introduces errors into the measurement. If we travel at a slow enough speed, say 5 to 10 ft/sec. at the most, then our measurement should be reasonably accurate.

Measurement and estimation of the trafficability of fine-grained soils

Misure e valutazione delle possibilità di traffico su terreni a grana fine

S. J. Knight *) - A. A. Rula **)

ABSTRACT. — *Instruments and techniques developed by the U.S. Army Corps of Engineers for the direct measurement and remote estimation of the trafficability of fine-grained soils and prediction of performance of military vehicles are summarized in this paper. A simple, empirical measure of soil strength, called rating cone index, adequately describes the trafficability of a fine-grained soil and serves as the basis for confident prediction of military vehicle performance in terms of single or multiple passage across a level area, drawbar pull available for towing loads or climbing slopes, and forces required to tow nonself-propelled vehicles.*

Introduction. — In the context of this paper the trafficability of a soil is defined as its ability to support the passage of a military vehicle; a fine-grained soil is defined as one in which more than half (by weight) of its constituent materials are finer than 0.074 mm. In a final sense, the trafficability of a soil can be assessed fully and comprehensively only by a consideration of the forces brought to bear by the vehicle concerned and the behavior of the soil under those forces. But theories and laws of mechanics of soil-vehicle systems, now being vigorously sought, may require several more years of intensive research for their complete fruition. Military commanders cannot afford to wait. Their responsibilities demand that they be able to differentiate passable and impassable areas for the vehicles under their command. They must do this rapidly and in simple terms of reference. Recognizing these requirements and realizing the tremendous difficulties involved in a truly theoretical approach to the problem, the U.S. Army several years ago decided that satisfactory solutions could best be achieved quickly by a rational experimental or empirical course of investigation. Accordingly, the Waterways Experiment Station (WES) of the U.S. Army Corps of Engineers, at Vicksburg, Mississippi, was asked to undertake a program aimed at quickly developing instruments and techniques whereby military commanders could ascertain whether or not the vehicles under their command could travel over the soil surfaces they would encounter. This program is now largely complete. This paper presents a summary

*) Engineer, Chief, Army Mobility Research Center, Soils Division, U.S. Army Engineer Waterways Experiment Station, Vicksburg, Miss.

**) Engineer, Chief, Trafficability Section, Army Mobility Research Center, Soils Division, U.S. Army Engineer Waterways Experiment Station, Vicksburg, Miss.

description of instruments and techniques developed by the Corps of Engineers, U. S. Army, for directly measuring and remotely estimating the trafficability of fine-grained soils. Details may be found in the WES reports on this subject listed in Appendix A.

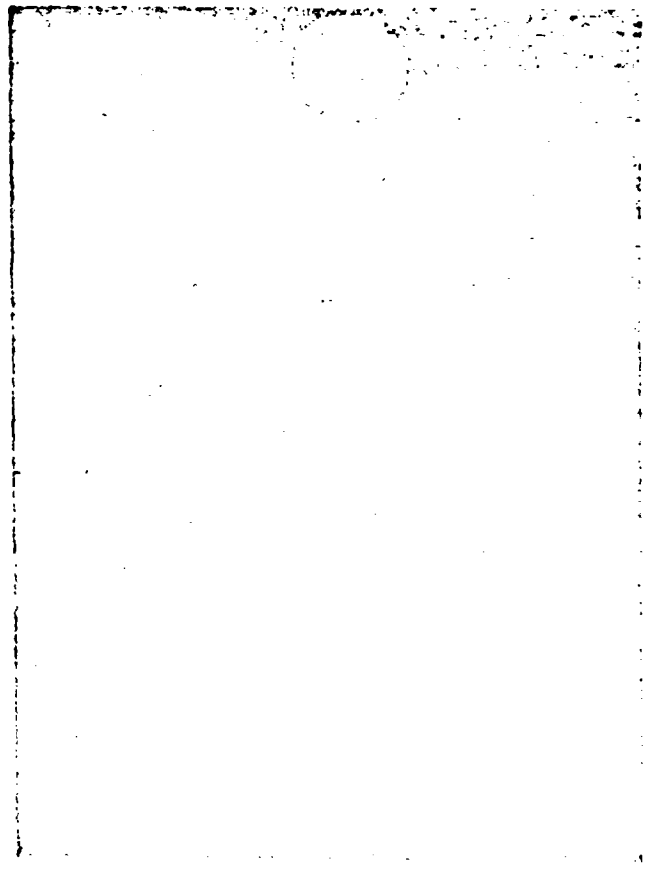


Fig. 1. — Cone penetrometer in use.

General soil-vehicle consideration. — To be adequate for passage of a vehicle, a soil must have sufficient bearing capacity to prevent the vehicle from sinking too deeply and sufficient traction capacity to provide the necessary forward thrust of the vehicle's wheels or tracks. Bearing capacity and traction capacity are both functions of the shear strength of a soil. Usually an immobilization of a vehicle is caused by a concurrent failure in bearing and traction and it is not easy to separate the two effects. Traction failure can occur on a soil with adequate bearing strength, as when a rubber-tired vehicle merely spins its wheels on the surface of a slippery clay soil but does not sink

appreciably; however, sinkage failure does not occur without being accompanied by traction failure.

Instruments. — Bearing-traction capacity is measured empirically in terms of the cone index, which is the pounds of force that must be applied to the handle of the cone penetrometer (shown in fig. 1) per square inch of its cone base area in order to force it into the ground. The right circular, 30-degree cone, not visible in the photo, has a cone base area of ½ sq in. The cone is pushed slowly downward and readings of the dial gage are made at desired vertical increments.

Many soils whose strengths are low in situ will become even weaker under the action, or remolding effect, of a vehicle. To estimate the cone index that will prevail under the moving vehicle, a remolding test is necessary. This tests consists of measurement of the cone index of a sample of soil confined in a small cylinder before and after pounding it with 100 blows of a 2-½-lb hammer falling 12 in. A « remolding index » is obtained by dividing the cone index of the soil, after it has been pounded, by its cone index before the blows were applied. Figure 2 illustrates the various stages of this test. A « rating cone index », the final measure of a soil's trafficability, is obtained by multiplying the in-situ cone index by the remolding index.

Vehicle performance. Cone index correlations. — From data collected in hundreds of tests with several types of military vehicles on fine-grained soils (loams, silts, clays, etc.) it has become feasible to predict the performance of these vehicles on the basis of the rating cone index. If the rating cone index of a given area is known, it can be confidently predicted whether a given vehicle will be able to cross it once, whether 50 vehicles can cross in the same path, how heavy a load the vehicle can tow through it, or how steep a slope the vehicle can climb.

Table 1 shows the rating cone index in the critical soil layer (usually 6 to 12 in.) necessary for completion of one pass and 50 passes by a few typical military vehicles. Cone indexes required for 50 passes of a vehicle up a given slope or for 50 passes towing a given load on level terrain may be determined be estimated using the curves in fig. 4.

TABLE 1.

Vehicle	Description	Rating cone index for 1 pass	Rating cone index for 50 passes
M 29 C weasel	5,500-lb, tracked, amphibious cargo carrier	20	25
D 7 engineer tractor	35,000-lb Caterpillar type construction tractor	30	40
M 48 tank	90,000-lb medium tank	40	50
3/4-ton weapon carrier	7,400-lb (with load of 1,500 lb) 4 × 4 truck	50	65
2-1/2-ton cargo truck	16,200-lb (with load of 5,000 lb) 6 × 6 truck	45	60

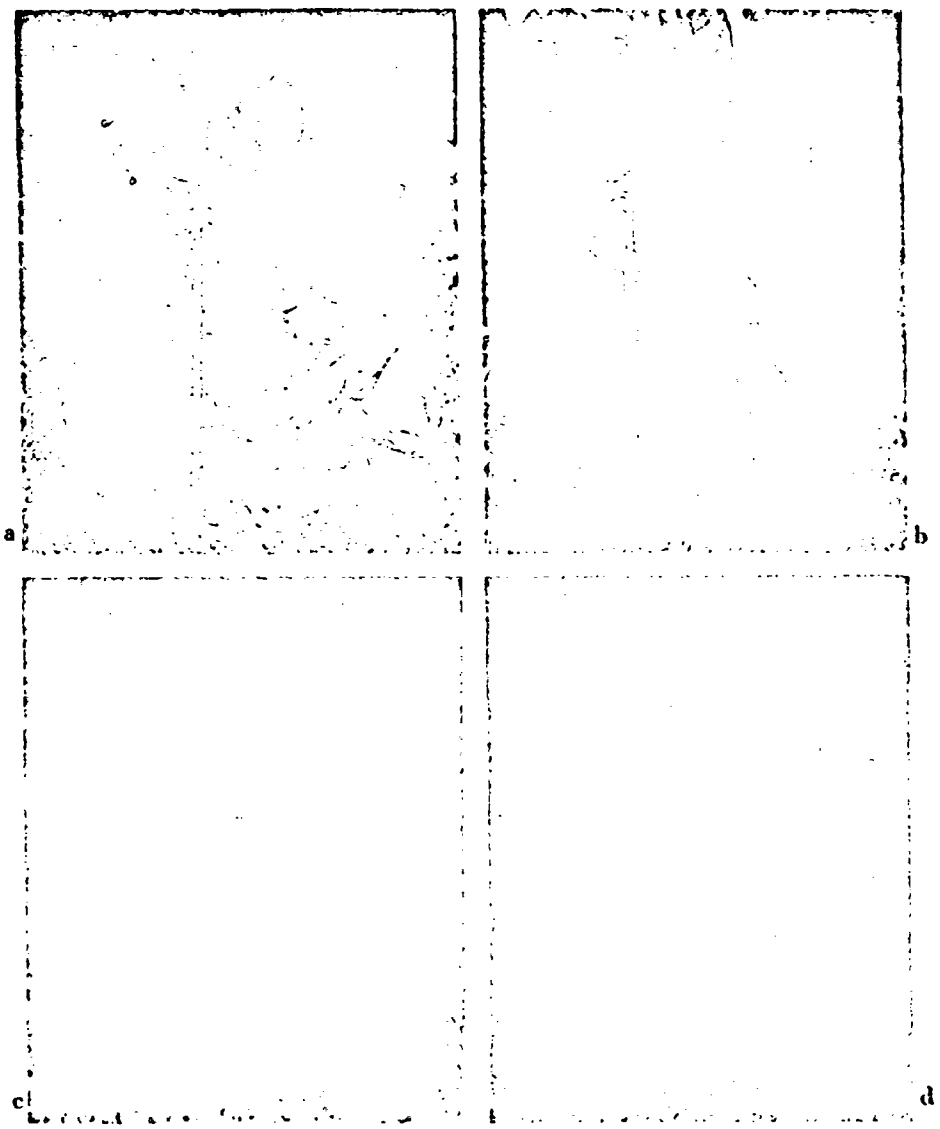


Fig. 2. — Remolding test. a) Taking sample; b) loading remolding cylinder; c) measuring cone index in remolding cylinder; d) appiying hammer blows.

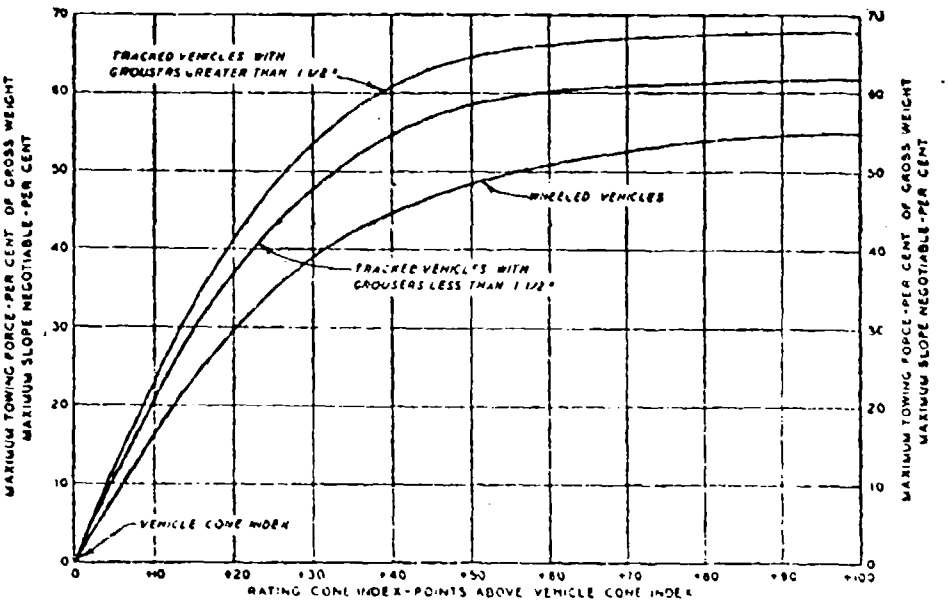
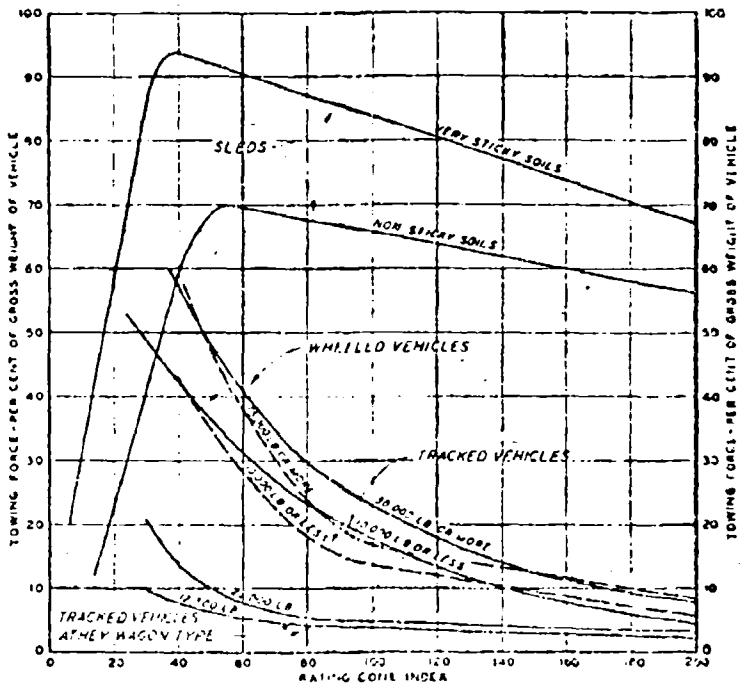


Fig. 3. — Maximum continuous tractive effort on level ground, maximum slopes and maximum towing force VS rating cone index expressed as point above vehicle cone index.

Using the data collected in actual vehicle tests, a system was developed for evaluating the effects of a vehicle's characteristics (weight, contact, pressure, etc.) in terms of the cone index required for the vehicle. The system comprises four formulas — one formula for self-propelled tracked vehicles, another for self-propelled wheeled vehicles, and one each for towed tracked and wheeled vehicles. These formulas are shown in Appendix B. The formula for self-propelled tracked vehicles has been verified by several tests on vehicles not used in its development and found to be entirely satisfactory. The formula for self-propelled wheeled vehicles has only been checked by a few tests, and while these tests bear out the formula, additional tests are needed before it can be fully accepted. No opportunity has as yet presented itself for checking the two formulas for towed vehicles.

Soil classification. — The principal influence on the rating cone index of a fine-grained soil is the amount of water it contains. Almost any soil in a comparatively dry state is trafficable to all military vehicles, but if its moisture content is increased, its trafficability may be reduced to the point where only certain vehicles can traverse it. A further increase in moisture may render the soil untrafficable to all vehicles. It is apparent that moisture conditions must be recognized in any evaluation of the trafficability of a soil, and further that soils must be at similar or equivalent conditions of moisture in order that they may be rated fairly in comparison with each other.



Note: The towing force required in an area whose cone index is 20 points or more below the minimum for the vehicle may equal or exceed the weight of the vehicle.

Fig. 4. — Towing force required on level ground.

The WES studies have shown that in a humid climate the top 12 in. or so of a given fine-grained soil attains a certain maximum soil moisture early in the wet season and maintains this moisture with very little deviation throughout this season. This field maximum offers a practical moisture datum for evaluation of the trafficability of soils, at least in humid U.S. locations. Although actual moisture content varies widely from soil type to soil type, a soil whose moisture content is at field maximum is at its poorest condition from a trafficability standpoint.

A scheme of classifying soils from the standpoint of their trafficability in the west season is shown in table 2.

Remote estimation of trafficability. — In military situations it is not always possible to enter an area and make cone penetrometer measurements. Therefore, a substantial amount of study has been devoted to estimating trafficability when physical contact with the soil is denied.

Soil types can be identified from aerial photos or deduced from soils, topographic, or geologic maps, and, once they are identified, their strengths can be estimated on the basis of their moisture contents. Use of table 2 will provide a rough estimate of soil strengths in the wet season, but greater accuracy

TABLE 2. — *Trafficability characteristics of soils in wet season.*

Group	SOILS	Unified soil classification system *)	Probable cone index range	Probable remolding index range	Probable rating cone index range	Slipperiness effects	Stickiness effects	COMMENTS
A	Coarse-grained, cohesionless sands and gravels	GW, GP, SW, SP	80 to 300	> 1	80 to 300	Slight to none	None	Will support continuous traffic of military vehicles with tracks or with high-flotation tires. Moist sands are good, dry sands only fair. Wheeled vehicles with standard tires may be immobilized in dry sands.
B	Inorganic clays of high plasticity, fat clays	CH	53 to 165	0.75 to 1.35	65 to 140	Severe to slight	Severe to slight	Usually will support more than 50 passes of military vehicles. Going will be difficult at times.
C	Clayey gravels, gravel-sand-clay mixtures	GC	85 to 175	0.45 to 0.75	45 to 125	Severe to slight	Moderate to slight	Often will not support 40 to 50 passes of military vehicles, but usually will support limited traffic. Going will be difficult in most cases.
	Clayey sands, sand-clay mixtures	SC						
	Gravelly clays, sandy clays, inorganic clays of low to medium plasticity, lean clays, silty clays	CL						
D	Silty gravels, gravel-sand-silt mixtures	GM	85 to 180	0.25 to 0.85	25 to 120	Moderate to slight	Slight	Usually will not support 40 to 50 passes of military vehicles. Often will not permit even a single pass. Going will be difficult in most cases.
	Silty sands, sand-silt mixtures	SM						
	Inorganic silts and very fine sands, rock flour, silty or clayey fine sands or clayey silts with slight plasticity	ML and CL-ML						
	Inorganic silts, micaceous or diatomaceous fine sandy or silty soils, elastic silts	MH						
	Organic silts and organic silty clays of low plasticity	OL						
	Organic clays of medium to high plasticity, organic silts	OH						

*) Developed by Bureau of Reclamation and Corps of Engineers.

is desired by the Military. Accordingly, studies are in progress to permit the prediction of the amount of water a given soil will contain at any time and, from the water content, the strength the soil will have. With the cooperation of the U. S. Forest Service, methods have been developed that permit the prediction of moisture content from actual rainfall data with very good accuracy. Mainly, these methods consider two phenomena, accretion and depletion. The amount of moisture that a soil will accrete from rainfall depends mainly upon the moisture content of the soil before the rain and the amount of rain. Graphs and charts have been constructed that permit fairly accurate prediction of accretion quantities for all soil types located in the humid areas of the United States. Soil moisture is depleted by evaporation, transpiration, and drainage. Depletion rates vary mainly according to season, soil type, and topography. Hundreds of soils in widely scattered locations of the U. S. have been used in developing accretion and depletion data, and these data are now being analyzed to develop criteria that will permit extrapolation to other soils and climates of the world.

Reflectance and emissivity by soils of energy in the electromagnetic spectrum may lend themselves to correlation with soil type and moisture content, and hence serve as another tool in deducing the trafficability of soils by remote means. Laboratory studies have recently been started at the WES to determine the degree of correlation between controlled changes in soil type, moisture content, and density and the reflectance and emissivity of the laboratory samples. Preliminary analysis indicates promising results and the studies are therefore being continued. If a thorough program of laboratory research confirms the feasibility of electromagnetic means of estimating soil trafficability, studies will then be extended to field conditions.

Conclusions. — Pursuing a rational, empirical philosophy of research, simple instruments and techniques for the direct measurement and remote estimation of the trafficability of fine-grained soils were developed by the WES. When soil strength has been measured or estimated in terms of an empirical index, called rating cone index, the performance of any conventional vehicle can be predicted with confidence.

APPENDIX A

Reports published by Army Mobility Research Center under projet t 8870-05-001, trafficability and mobility research

Reporting agency	Report number	TITLE	Date of report
WES		Trafficability of soils	Sep. 1945
WES	TM 3-240	Pilot tests - Self-propelled vehicles	Nov. 1947
WES	TM 3-240 1st supplement	Laboratory tests to determine effects of moisture content and density	Mar. 1948
WES	TM 3-240 2nd supplement	Trafficability studies - Fort Churchill, Summer 1947	Aug. 1948
WES	TM 3-240 3rd supplement	Development of testing instruments	Oct. 1948

Reporting agency	Report number	TITLE	Date of report
WES	TM 3-240 4th supplement	Tests of self-propelled vehicles - Yuma, Arizona, 1947	Apr. 1949
WES	TM 3-240 5th supplement	Analysis of existing data	May 1949
WES	TM 3-240 6th supplement	Tests on self-propelled vehicles - Vicksburg, Mississippi, 1947	Sep. 1949
WES	TM 3-240 7th supplement	Tests on towed vehicles, 1947-1948	Jun. 1950
WES	TM 3-240 8th supplement	Slope studies	May 1951
WES	TM 3-240 9th supplement	Vehicle classification	May 1951
WES	TM 3-240 10th supplement	Tests on natural soils with self-propelled vehicles, 1949-1950	Jan. 1954
WES	TM 3-240 11th supplement	Soil classification	Aug. 1954
WES	TM 3-240 12th supplement	Tests on natural soils with self-propelled vehicles, 1951-1953	Nov. 1954
WES	TM 3-240 13th supplement	Pilot study, tests on coarse-grained soils	Nov. 1955
WES	TM 3-240 14th supplement	A summary of trafficability studies through 1955	Dec. 1956
WES	TM 3-240 15th supplement	Tests on coarse-grained soils with self-propelled and towed vehicles, 1956 and 1957	Jun. 1959
WES-TES	TR ENG 37	Soils trafficability	Jul. 1959
WES	TM 3-331 No. 1	Forecasting trafficability of soils	Oct. 1951
WES	TM 3-331 No. 2	Forecasting trafficability of soils	Jun. 1952
WES	TM 3-331 No. 3	Forecasting trafficability of soils	Oct. 1954
WES	TM 3-331 No. 4	Forecasting trafficability of soils	Feb. 1957
WES	TM 3-331 No. 5	Forecasting trafficability of soils	Jun. 1959
WES	TM 3-414 No. 1	Vehicles in snow: A critical review of the state of the art	Aug. 1955
WES	TM 3-414 No. 2	Greenland studies 1954	Aug. 1955
WES	TM 3-414 No. 3	Greenland studies 1955 and 1957	May 1960
WES	TM 3-414 No. 4	Test on subarctic snow	Dec. 1960
WES	TR 3-462 No. 1	Studies on aerial cone penetrometer, Laboratory study of mechanical principles	Jul. 1957
WES	TR 3-462 No. 2	Studies of aerial cone penetrometer, field tests	Apr. 1958
WES-ACFEL	TR 3-505	Approach roads, Greenland 1955, program	Jun. 1959
WES	TR 3-516 No. 1	Deflection of moving tires	Jul. 1959
WES	TR 3-545 No. 2	Stresses under moving vehicles (wheeled)	May 1960
WES	TR 3-545 No. 3	Stresses under moving vehicles (tracked)	Jul. 1960
WES	MP 4-101	Trafficability survey of selected areas, Camp Stewart, Georgia	Nov. 1954
WES	MP 3-117	Field tests of nuclear instruments for the measurement of soil moisture and density	Mar. 1955
WES	MP 4-135	The development of methods for predicting soil moisture content, report on the Fairbanks, Alaska, Extension	Jul. 1955
WES	MP 4-230 No. 1	Stresses under moving vehicles, a pilot study of WES earth pressure cell action in comparatively soft soil	Jul. 1957
WES	MP 4-241	Vehicle mobility	Oct. 1957
WES	MP 4-238	Statistical occurrence of soil strength	Dec. 1957
WES	MP 4-282	Comparison of performance characteristics in snow of the polecat and weasel	Aug. 1958
WES	MP 4-284	A limited study of factors that affect soil strength	Aug. 1958

Reporting agency	Report number	TITLE	Date of report
WES	MP 4-298	Meteorological and trafficability data, U.S. Canadian Arctic Weather Stations	Jan. 1959
WES	MP 4-300	Aerial penetrometer demonstration at Fort Rucker, Alabama	Jan. 1959
WES	MP 4-322	A limited study of snap-tracs	Feb. 1959
WES	MP 4-327	Effect of mold size and other factors on laboratory cone index measurements	Mar. 1959
WES	MP 4-350	Pilot study to evaluate the squeeze test for use in vehicle-mobility research	Jul. 1959
WES	MP 4-355 No. 1	Trafficability predictions in tropical soils (Panama)	Sep. 1959
WES	MP 4-355 No. 2	Trafficability predictions in tropical soils (Puerto Rico)	Feb. 1960
WES	MP 4-362	Preliminary stresses under off-road vehicles	Oct. 1959
WES	MP 4-371	Laboratory tests of liquid nitrogen soil-moisture samplers	Jan. 1960
WES	MP 4-404	The Army Mobility Research Center testing facility	Jul. 1960
WES	MP 4-412	A limited study of the performance of the 2-ton meili flex-trac	Nov. 1960
Purdue U.		Application of airphoto pattern analysis to soil trafficability studies	Jun. 1951
Purdue U.		Application of airphoto pattern analysis to soil trafficability studies, glacial deposited materials	Jun. 1951
Purdue U.		Application of airphoto pattern analysis to soil trafficability studies, miscellaneous materials	Jun. 1951
Purdue U.		Application of airphoto pattern analysis to soil trafficability studies, water deposited materials (revised)	Dec. 1952
Purdue U.		Application of airphoto pattern analysis to soil trafficability studies, wind deposited soils	Feb. 1954
Purdue U.		Application of airphoto pattern analysis to soil trafficability studies, aeolian materials	Mar. 1954
Purdue U.		Application of airphoto pattern analysis to soil trafficability studies, residual materials	Jun. 1954
Purdue U.		Techniques for predicting soil trafficability information from aerial photographs	Sep. 1956
Purdue U.		Application of airphoto pattern analysis to soil trafficability studies, supplement No. 1	Sep. 1956
Purdue U.		Application of airphoto pattern analysis to soil trafficability studies, supplement No. 2	Dec. 1957
WES		Landig strip evaluation (office report)	Jul. 1952
Purdue-WES		Trafficability conditions in camp atterbury area, Indiana (office report)	Jul. 1952
Purdue-WES		Trafficability conditions in an area in Norfolk County, East Anglia, England	Sep. 1952
Purdue-WES		Statistical analyses of trafficability data (office report)	Nov. 1953
Purdue U.		Effect of soil moisture and other natural variables on aerial photo gray tones (office report)	Oct. 1954

Note: All Purdue U. reports are on work under contract with WES.

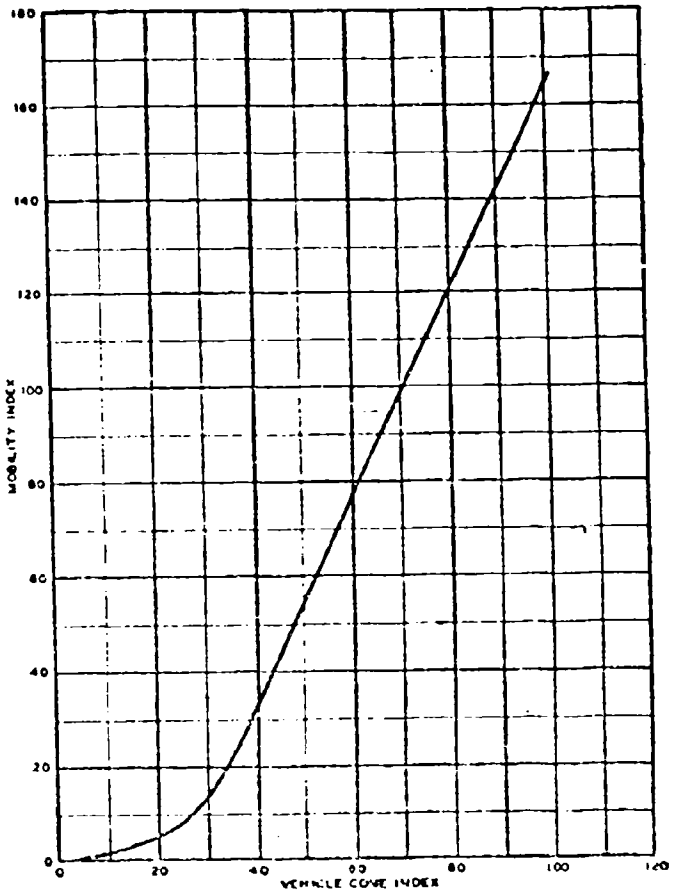


Fig. 5. — Mobility index VS vehicle cone index.

APPENDIX B

Mobility index

The mobility index is a dimensionless number obtained by applying certain characteristics of a vehicle to the formulas given subsequently. The mobility index can then be applied to the curve shown in fig. 5 to determine the vehicle cone index.

Self-propelled tracked vehicles

$$\text{Mobility index} = \left(\frac{\text{contact pressure} \times \text{weight factor}}{\text{track factor} \times \text{grouser factor}} + \text{bogie factor} - \text{clearance factor} \right) \times$$

$$\times \text{engine factor} \times \text{transmission factor}$$

wherein,

$$\text{contact pressure} = \frac{\text{gross weight in lb}}{\text{area of tracks in contact with ground in sq in.}}$$

weight factor: less than 50,000 lb = 1.0
50,000 to 69,999 lb = 1.2
70,000 to 99,999 lb = 1.4
100,000 lb or greater = 1.8

$$\text{track factor} = \frac{\text{track width in in.}}{100}$$

grouser factor: grousers less than 1.5 in. high = 1.0
grousers more than 1.5 in. high = 1.1

$$\text{bogie factor} = \frac{\text{gross weight in lb divided by 10}}{\text{(total number of bogies on tracks in contact with ground)} \times \text{(area of 1 track shoe in sq in.)}}$$

$$\text{clearance factor} = \frac{\text{clearance in in.}}{10}$$

engine factor: 10 or greater hp per ton of vehicle wt = 1.0
less than 10 hp per ton of vehicle wt = 1.05

transmission factor: hydraulic = 1.0; mechanical = 1.05

Self-propelled wheeled vehicles

$$\text{Mobility index} =$$

$$= 0.6\left[\left(\frac{\text{contact pressure factor} \times \text{weigth factor}}{\text{tire factor} \times \text{grouser factor}} + \text{wheel load} - \text{clearance factor}\right) \times \right.$$

$$\left. \times \text{engine factor} \times \text{transmission factor}\right] + 20$$

wherein,

$$\text{contact pressure factor} = \frac{\text{gross weight in lb}}{\text{tire width} \times \text{rim diam} \times \text{number of tires}}$$

weight factor: greater than 35,000 lb = 1.1
15,000 to 35,000 lb = 1.0
less than 15,000 lb = 0.9

$$\text{tire factor} = 1.25 \times \text{tire width in in. divided by 1.00}$$

grouser factor: with chains = 1.05
without chains = 1.00

$$\text{wheel load} = \frac{\text{gross weight in kips}}{\text{number of wheels}} \text{ (wheels may be single or dual)}$$

$$\text{clearance factor} = \frac{\text{clearance in in.}}{10}$$

engine factor: greater than 10 hp per ton = 1.0
less than 10 hp per ton = 1.05

transmission factor: hydraulic = 1.0; mechanical = 1.05

Towed tracked vehicles

$$\text{Mobility index} = \left(\frac{\text{contact pressure} \times \text{weight factor}}{\text{track factor}} + \text{bogie factor} - \text{clearance} \right) + 30$$

wherein,

$$\text{contact pressure} = \frac{\text{gross weight in lb}}{\text{area of tracks in contact with ground in sq in.}}$$

weight factor: 15,000 lb or greater = 1.0
below 15,000 lb = 0.8

$$\text{track factor} = \frac{\text{track width in in.}}{100}$$

$$\text{bogie factor} = \frac{\text{gross weight in lb divided by 10}}{(\text{total number of bogies on track in contact with ground}) \times (\text{area of 1 track shoe in sq in.})}$$

clearance = clearance in in.

Towed wheeled vehicles

$$\text{Mobility index} = 0.64 \left(\frac{\text{contact pressure factor} \times \text{weight factor}}{\text{tire factor}} + \text{axle load} - \text{clearance} \right) + 10$$

wherein,

$$\text{contact pressure factor} = \frac{\text{normal tire pressure in lb per sq in.}}{2}$$

weight factor: 15,000 lb per axle or greater = 1.0
12,500 to 14,999 lb = 0.9
10,000 to 12,499 lb = 0.8
7,500 to 9,999 lb = 0.7
less than 7,500 lb = 0.6

$$\text{tire factor:} \qquad \text{single tire} = \frac{\text{width in in.}}{100}$$

$$\text{dual tire} = \frac{1.5 \times \text{width in in.}}{100}$$

$$\text{axle load} = \frac{\text{axle load in lb}}{1000}$$

$$\text{clearance} = \text{clearance in in.}$$

DISCUSSIONS

P. BRINDEAU.

Monsieur le Président, Messieurs,

Je félicite Monsieur Jackson pour l'excellent rapport qu'il a présenté. Je tiens à signaler que parmi les études d'ordre pratique que nous avons faites en France, nous nous sommes posés un problème analogue à celui que s'est posé l'Ecole de Vicksburg, mais dans un domaine un peu particulier.

Il s'agissait pour nous de définir dans quelles conditions un avion pouvait se poser sur un terrain naturel. Lorsque je parle d'avion, il s'agit du « Nord 2506 » dont la charge du train d'atterrissage est de 20 tonnes sur deux roues. Pour ce faire nous avons utilisé un pénétromètre à cône — de même angle que celui utilisé à Vicksburg — mais basé sur un principe un peu différent. L'enfoncement du cône s'obtient à l'aide d'une masse frappante, exactement comme pour un pilot, on évalue l'indice de cône par la quantité de kilogrammètres qu'il faut pour enfoncer la pointe du cône de 10 cm. Nous avons donc en France un indice de cône qui est peu différent de celui utilisé par Vicksburg et qui par ailleurs a pu être rattaché à l'indice C.B.R. utilisé dans la technique routière. Nous avons fait en quelques années de très nombreux essais et maintenant il est possible avec toute chance de réussite, d'atterrir et de décoller sur le terrain reconnu à priori; en effet, il ne s'agit pas seulement d'atterrir, il faut encore que le terrain offre une résistance à l'avancement suffisamment faible pour permettre le décollage de l'avion sur sol naturel. Plus récemment nous avons utilisé la même technique, avec les mêmes appareils pour étudier les possibilités d'évolution des véhicules militaires sur des terrains variés, à faible portance, c'est à dire avec indice C.B.R. inférieur à 1.

Je tenais simplement à signaler ces études et la tendance que nous avons à rattacher les données fournies par des appareils tels que le pénétromètres aux données obtenues avec des matériels plus importants l'indice C.B.R. par exemple.

E. LEMKE — Zunächst einmal bitte ich den Herrn vortragenden zu sagen wie, in dem Fall der Beobachtungen in USA, die Länge dieser nassen Jahreszeit tatsächlich liegt, und wie im einzelnen die Plätze beobachtet und ausgewählt wurden. Es wäre möglich, auf Grund von Bodenkarten, typische Stellen für bestimmte Streubereiche auszusuchen; es wäre auf der anderen Seite auch möglich wahllos die Stellen zu

nehmen, ohne Rücksicht darauf ob sie an der Grenze oder im inneren Bereich irgend eines Bodentyps liegen.

Und dann, die andere Frage: ob bereits in grösserer Zahl fortlaufende Beobachtungen ganz bestimmter typischer Stellen von Bodenarten vorgenommen worden sind.

Zu dem Schema, das im Vortrag N. 24 auf Tafel 2 gegeben wurde, sind also eine Reihe von Gruppen aufgestellt worden — a, b, c, d — und diese sind für unsere Arbeit ausserordentlich wichtig, und sehr interessant. Es würde aber für die praktische Arbeit im Gelände sehr nützlich sein, wenn wir diese Abgrenzungen zwischen diesen Bodengruppen genauer wüssten, etwa in einem Messungsdreieck mit den Ecken: Ton, Schluff und Sand. Ich würde es begrüssen, wenn hier eine Zusammenarbeit, in Unterstützung unserer Arbeit durch das Forschungsinstitut in Vicksburg, zustande käme.

Denn man sieht klar, dass eine Gruppe auf der Sandecke steht, die Gruppe a) der reinen Sande, die Frage ist nur: wie weit reicht dies Sandgruppe gegen die Ton- und Schluffecke hin? Im übrigen ist klar, dass die Grenze dieser Sandgruppe nicht für die verschiedenen Korngrenzen des Sandes gleich ist, sondern mit Abnehmen der Korngrenze des Sande in die Sandecke hineinschrumpft, weil ja der Sand, mit abnehmender Korngrenze, selbst sich dem Schluff nähert; also zum Beispiel bei Kleinsand sehr viel kleiner sein sollte als bei Grobsand. Es ist nur die Frage: wieviele Gruppen muss man da unterscheiden? Etwa nur eine Gruppe, die den feinen bis mittelfeinen Sand noch einschliesst, bis zum Grobsand? Oder noch mehr? Es ist nämlich in dieser Gruppierung nur von Grobsand und Kies, auf der einen Seite, und dann eben von Feinsand und Feinsandgemischen gesprochen; es fehlt dabei der Uebergang Mittel- bis Grobsand, Mittel-sand, Fein- bis Mittelfein, die sehr häufig vorkommen und da eben noch nicht beurteilt sind.

Dann ein weiterer Hinweis. In dem zuletzt gezeigten Schema steht zu unterst der Torf, und darüber sind die « rating cone indexes » gegeben worden; ich schliesse daraus, dass der Torf, also das Moor, mit dem Kegelpenetrometer getestet worden ist. Ich sprache schon vorher, dass wir in trockensten Zeiten, bei Ausbildung starker tragender Decken auf Torf, zu nicht allgemein verwertbaren Zahlen, mit Hilfe des Kegelpenetrometer, gekommen sind; Zahlen die besonders nicht übereinstimmen mit dem Fahrverhalten schwerer, mehrerer zehner Tonner wiegender, Fahrzeuge. Also, die Frage: ist der Torf mit dem Kegelpenetrometer getestet worden, und sind da Schwierigkeiten aufgetreten? An sich, in der nassen Jahreszeit, für die diese Gliederung gilt, erwarte ich diese Schwierigkeit nur von der lebenden Vegetationsdecke und ihren Wurzeln, weniger von der Schicht die zu wenig, oder weniger als normal Wasser enthält. Das Bild wird viel extremer wenn der Torf im trockenen Zustand betrachtet wird, wobei sich also die Moore ähnlich einem Fächer auseinanderfalten wie es die Mineralböden im nassen Zustand machen; die also im trockenen Zustand im Grunde genommen alle sich gleich verhalten, und im nassen Zustand aufblättern, das selbe tut das Moor im trockenen Zustand, oder auch noch im trockeren Zustand. Dann, zu diesem Schema, das im Aufsatz N. 24 gegeben wurde, ist es in mancher Hinsicht im Gelände wichtig das Profil des Bodens zu betrachten, das sich bis an diese geringen Tiefen von 30 cm auswirkt; wobei ja der Herr vortragende von der kritischer Schicht von 15-30 cm — oder 6-12 Zoll — gesprochen hat. In dieser Tiefe liegen massgebende Grenzen bei den Böden die von oben her Humusgehalte oder Humusauflagen haben; besonders im flachliegenden Gelände Mitteleuropas reichen, bis in 20 cm Tiefe, auf sehr grossen tiefgelegenen ebenen Flächen, hohe Humusgehalte bis 15 % — wir nennen sie « humus » und stark « humus » bei unseren Bodenaufnahmen —, aber darüber hinaus auch noch an Moor, teilweise bei nicht grösserer Tiefe, 15-30 % organischer Gehalt, und es gibt auch Torfe die nicht mächtiger sind, die flächer liegen als 30 cm. Die üblichen Boden-

karten haben vielfach diese Torfgrenzen nicht gezeigt, und man hat dann vielleicht vermutet der Torf wäre sehr mächtig, aber unsere Aufnahmen zeigten dass grosse Flächen existieren von Mooren, an den Rändern besonders, die keine 30 cm Mächtigkeit erreichen. Ich würde also für notwendig halten, dass in den Klassifizierungen, neben der Ausscheidung der Grenzen in einem Dreieck, auch diese Profilbildungen berücksichtigt werden.

N. W. RADFORTH. — In response to Mr. Lemke's questions I should like to suggest that there is no limit to the list of attributes (subjectively or objectively arising) that obtains for a classification system pertaining to terrain. Sufficient to say therefore, that if a classification system (artificial or natural) works, then it is useful and does not lead to half-truth or inadequacy. We surely need many classification systems all of which if valid can be coordinated. Coordination therefore, is the mechanism which avoids over-complication in classification. In this general light the system of Knight and Meyer is valid, useful and much in need.

I am able to confirm from field analysis that the penetrometer approach is applicable for peats and indeed helps to differentiate them. It is important first to classify the peats and for this, surface cover is useful as a reference index whether cover is primary (natural) or secondary (induced by fire, harvesting or agriculture).

N. 25

Forced-slip wheel-and-track tester

Misuratore di scorrimento forzato di ruote e cingoli

A. R. Reece - B. M. D. Wills *)

ABSTRACT. — *A special purpose machine is described which can measure the tractive effort, rolling resistance, and slip of a wide range of rigid and resilient wheels and tracks. It works on the forced slip principle, in which the test wheel or track is obliged to rotate at a controlled slip by the unwinding of a wire rope from a drum which is geared to the wheel or track under test.*

The input torque and output thrust are simply measured as they are a function of the forces exerted by the towing tractor and the cable. Instrumentation is accordingly simplified. The machine has the virtues of versatility and simplicity at low cost.

1. - Introduction

Research into tractive performance and rolling resistance requires the testing of a wide range of rigid and resilient wheels and tracks, and is facilitated by using a special purpose testing machine rather than normal vehicles.

To evaluate the performance of the driven rear wheels on an ordinary vehicle, one must measure the input torque to the wheels, allowing for the rolling resistance of the front wheels and evaluate the load transfer effect due to the draught force applied by the loading car. Methods and apparatus have been evolved to measure these variables but the apparatus has always been complicated and unwieldy and the results obtainable only after lengthy computation. To do this for a number of wheel and track sizes would require instrumentation for several types of tractors, making a research programme of this type quite impracticable.

Full-scale and long-term research into wheel and track performance in the field, therefore, requires a special machine. A single wheel tester for this purpose was designed and built at the National Institute of Agricultural Engineering in 1950 [1]. This machine applies a controlled torque to the test wheel by means of an electrical transmission and measures the resulting slip and thrust. The machine works well but is limited to the testing of wheels, as it is not easily adaptable for use with tracks. It is also of complicated design and expensive to make. The farm tractor on which it is based cannot be used for other work.

*) King's College, University of Durham, Newcastle upon Tyne, U.K.

A full-scale laboratory test rig in use by Mr. F. L. Uffelmann at the Fighting Vehicles Research and Development Establishment, operates on the forced-slip principle, where slip is controlled and tractive effort and torque input are the measured variables. The machine described here is a versatile version of this rig, intended to take a wide range of wheel and rigid and resilient tracks, and capable of testing them in a wide variety of field conditions.

2. - The principle of the forced-slip tester

2.1) **Slip.** — The test wheel, of rolling radius « r », has a concentric slip drum, of radius « a », rigidly attached to the wheel axle as in fig. 1. Wire rope,

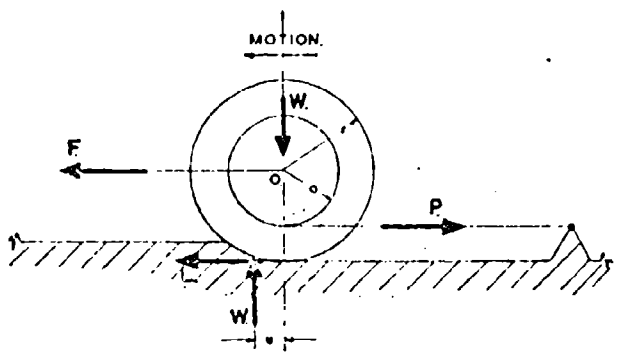


Fig. 1. — Positive slip.

wound around the slip drum, is led off and anchored behind the wheel, which is then pulled forward by a winch or tractor. The distance moved forward by the wheel in one revolution, equals the length of cable unwound from the circumference of the slip drum, because the drum is obliged to rotate without slip on the wire rope.

$$\therefore \quad \text{Slip } i = \frac{2\pi r - 2\pi a}{2\pi r}$$

$$\text{i.e.} \quad i = 1 - \frac{a}{r} \tag{1}$$

As « a » decreases the slip tends assymtotically to 100 %, and as « a » increases towards « r », zero slip is approached.

2.2) **Skid, or negative slip.** — If « a » becomes larger than « r », as in fig. 2, and the rope is anchored in front of the wheel, the cable will be wound on to the drum as the wheel is pulled forward; resulting in negative slip or skid.

In this case the actual distance moved forward per revolution of the axle is greater than the no-slip distance $2\pi r$, and the slip is negative.

$$\therefore \quad \text{Slip} = i = -\left(\frac{a}{r} - 1\right)$$

2.3) **The geared forced-slip system.** — It will be apparent that the arrangement in fig. 2 is diagrammatic only and would not be possible in the field. A practical version of this arrangement is obtained by separating the

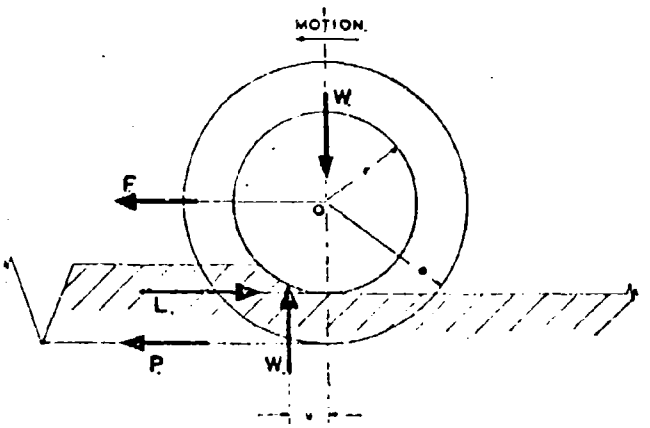


Fig. 2. — Negative slip or skid.

drum and the wheel and connecting them by a chain drive. The effective radius of the drum then depends upon the ratio of the chain drive. If « n » is the ratio of the number of teeth on the drum to the number of teeth on the wheel sprocket then:

$$i = 1 - \frac{n}{nr}$$

$$\text{or} \quad i = 1 - \frac{A}{r}$$

here $A = \frac{r}{n}$ and is the effective drum radius.

2.4) **The equilibrium of the forced-slip system.** — Considering the equilibrium of the wheel and drum assembly we have:

$$\text{From} \quad \Sigma F_x = 0$$

$$L = P - F \tag{2}$$

$$\text{From} \quad \Sigma M_o = 0$$

$$Wu = Pa - Lr \tag{3}$$

« Wu » is the rolling resistance torque and some workers may care to convert this to a notional horizontal retarding force acting at the rolling radius by writing Rr = Wu. Combining this with 1 and 2 gives.

$$R = P\left(\frac{a}{r} - 1\right) + F$$

$$\text{or} \quad R = F - Pi \tag{4}$$

The power input to the tester is through the towing tractor via the force F, and it is entirely devoted to overcoming the rolling and slip losses of the test wheel or track, since no useful work is done.

$$\therefore \quad \text{Power input} = \frac{Fv}{550}$$

$$= \frac{v}{550}(Pi + R) \tag{5}$$

2.5) **Theoretical force relationships for the forced slip system.** — The use of the tester at high slip values is limited by the maximum pull which the towing tractor can develop. It is therefore important to determine the relation between F and L (and P and L) in order to obtain the limiting slip.

From equations 1, 2 and 3 we obtain.

$$F = \frac{Li}{1-i} + \frac{R}{1-i} \tag{6}$$

From equations 1 and 3 we obtain.

$$P = \frac{L}{1-i} + \frac{R}{1-i} \tag{7}$$

Assuming rolling resistance to be zero equation 6 and 7 reduce to $\frac{F}{L} = \frac{i}{1-i}$ and $\frac{P}{L} = \frac{1}{1-i}$. These have been plotted in figure 8 and are a fair approximation to the operating conditions when testing a track in field or a tyre on concrete or tarmac.

The track presents the worst possible operating conditions for the tester as the track under test will develop large tractive forces compared to the wheels of the towing tractor and if say 50 % slip is to be reached the drawbar pull developed by the tractor must be greater than the tractive effort developed by the track. $\left(\frac{F}{L} > 1\right)$

Tracklayers under normal industrial and agricultural conditions work at very low slip values, usually not exceeding 20 %. Working on loose sand in the field, with the Bristol track, slip values up to 27 % have been reached

with the ordinary wheeled tractor, but using dual rear wheels. This slip range would be quite adequate for normal track testing. However, for research work it is useful to explore higher slip ranges and this can easily be attained by using two towing tractors or by fitting half tracks or four wheel drive the existing tractor.

The tester has been designed to operate with a range of wheels up to an 11"-36" tyre. Tyres of this size are used on the rear wheels of the towing tractor. The weight on the test wheel is approximately equal to that on each rear tractor wheel so that ideally, for no rolling resistance the tester should operate up to slip values determined by $\frac{F}{L} = 2$. (approx. 65 % slip), this it does on a hard ground (tarmac or concrete) test.

The effect of rolling resistance is to increase the pull required from the towing tractor. It has been observed from published reports of tests on agricultural tractor wheels that the highest rolling resistance is encountered with steel lugged wheels in soft ground and here the resistance may be as much as a third as great as the maximum drawbar pull. The dotted lines in figure 8 have been calculated for such a condition and it will be observed that the maximum slip obtainable is reduced from 65 % to 50 %.

3 - The design of the tester

The machine as shown in figure 4, has been designed to be pulled by any 40 to 50 h.p. farm tractor. It is connected to the tractor by the standard 3 point linkage and provided some counterbalance weights are added to the front of the tractor the machine can be lifted on the linkage, and the whole outfit is then very manoeuvrable. The tractor is not permanently fixed to the tester. It is used for cultivating the test plots between experiments and is available for other work when testing is not in progress.

The machine consists of a large welded rectangular tubular frame. The main lower tube is very long and because it is one sided and provided with a continuous row of bolt holes, it is easy to bolt on wheels of different sizes, and trains of wheels or various types of tracks. The tube will take the place of the track frame of a rigid type track or the vehicle hull in the case of a resilient track. The front of the frame widens out to form the triangle needed for the 3 point linkage attaching points.

The drive drum is mounted at the top of an « A » frame which is welded to the main tube. The rope comes off the drum down to a tail pulley near the ground and away to the anchor. This position for the drive drum has been chosen to keep the centre of gravity of the machine forward for ease of lifting, and to give a uniform pressure distribution on a track. It is high up so that it can clear the largest wheel that it is anticipated using on the tester.

Two different drums have been provided, each drum being approximately conical in shape, with the outside diameter increasing in 5 separate steps.

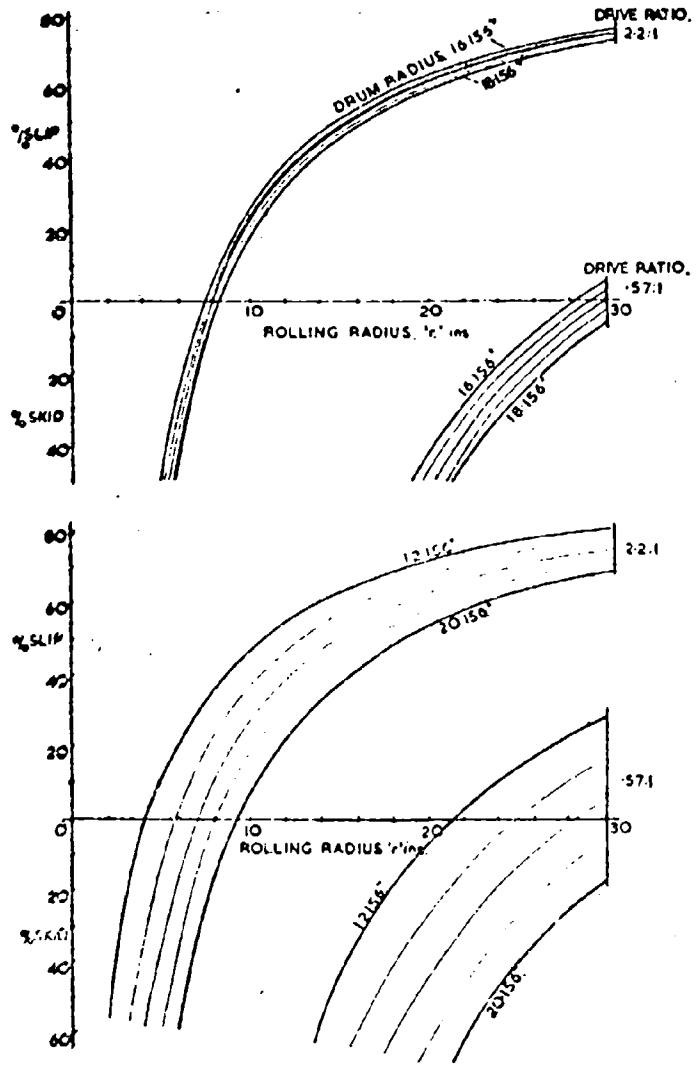


Fig. 3. — *Slip range against rolling radius for maximum and minimum drive ratio.*

In use the cable is wound round the drum stepping up from one diameter to the next. Each run with the machine, therefore, gives five different slip values. This arrangement has been chosen in preference to a conical drum so that conditions are stabilized for at least three revolutions of the largest wheel or track. This enables five sets of three readings at each slip value, to be obtained from force and pressure-measuring equipment in the periphery of the wheels or tracks.

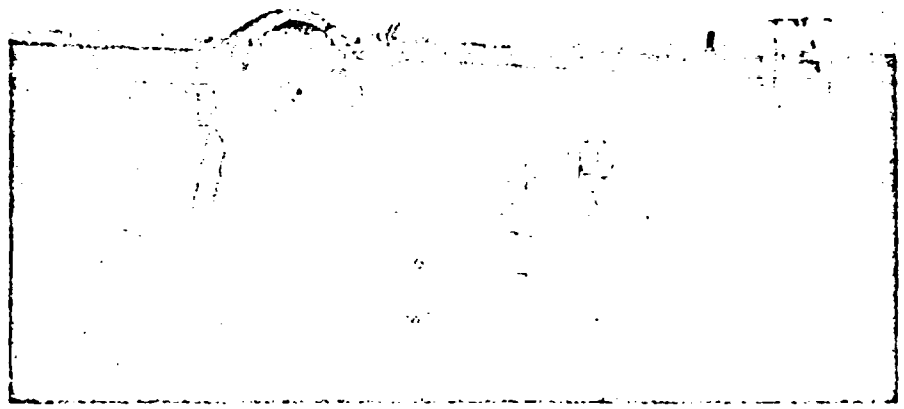


Fig. 4.

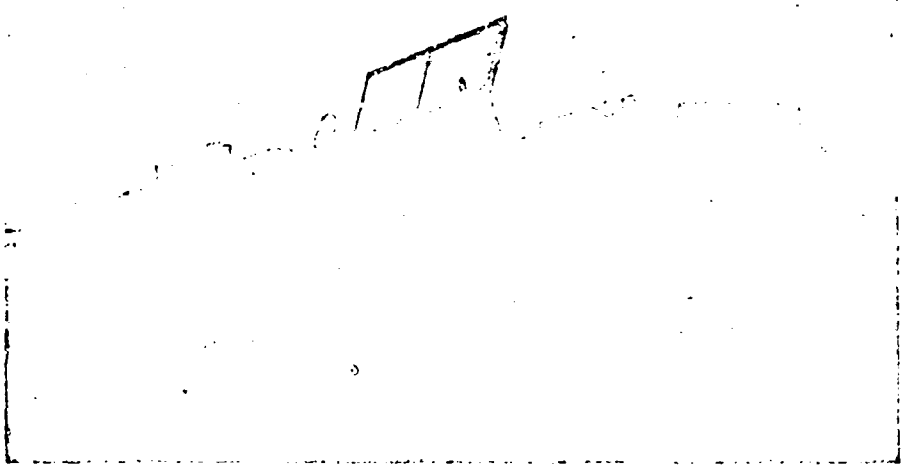


Fig. 5.

The drum is connected to the wheel or track sprocket by a 1" pitch chain drive. Six sprockets are available for this drive and by different arrangements of pairs, twelve different drive ratios are available. Figure 3 shows the slip range which is available using the two different drums for maximum and minimum gear ratio. The other ten ratios completely fill the intervening space between the curves shown in the two graphs of figure 3. The close ratio drum has been provided for use with long tracks. On such a track there is a very great increase in tractive effort for quite small increments in slip.

The drums are free to rotate on their shaft but can be coupled to a driving plate on the shaft by a simple spring loaded pin to enable them to drive the sprocket. When the coupling is disconnected the drum can be turned by hand and the cable wound on.

When a wheel is being tested, the three links of the 3 point linkage are in use and provision has been made for adjusting the link points on both the tractor and the tester. The links are kept parallel and horizontal so that no load transfer takes place. When the track is in use only the lower links are used so that the track is free to pitch. In this case the lower links are kept as low as possible, and the height of the tail pulley from which the cable is taken, is adjusted so that the load transfer effects at front and rear, approximately cancel each other. The actual weight distribution during the test can be easily calculated from the values of the forces and the height of the links and cable.

For a skidding test, a low gear ratio is chosen and the wire rope is brought off the top of the drum, round the tail pulley and along beneath the towing tractor via the guide pulleys. A reeving device is provided so that the cable is wound neatly on to the drums without any overlapping.

The very best wire rope that it was possible to buy has been chosen in order to minimize the weight involved and to facilitate the handling of the considerable lengths required. It is a 5/16" diameter galvanized aircraft control cord with a minimum breaking load of 8,800 lb. A shear pin set to fail at 6,000 lb, is provided at the anchor end of the rope to prevent it breaking.

The anchor for the fixed end of the wire rope is required to withstand pulls of up to 6,000 lb and must be readily movable. A suitable device has been provided by fitting a Land Rover with two large, hydraulically actuated sprags. These sprags are forced into the ground and the Land Rover lifted up on to them. In this way the whole of the weight of the Land Rover is applied to the anchors so that the maximum use is made of the frictional component of the strength of the soil beneath the anchors. The recording instruments are housed in the Land Rover and connected to the tester by long trailing cables. It also carries a large and powerful Bevameter, which is used with the vehicle jacked up to form a stable base. The Land Rover also pulls a trailer which carries the tester and the whole outfit is, therefore, able to transport itself along the road. The Land Rover with sprags and recording instruments is shown in figure 5.

To determine the efficiency of the chain and rope drive a steel rimmed

wheel is mounted on the tester frame as for a normal wheel test, and the tester is allowed to rest on its stands behind the towing tractor with the steel wheel several inches clear of the ground, as in figure 9.

A steel cable is wound on to one of the slip drums in the normal manner and led off under the tail pulley wheel. The other end of the cable is attached, through a recording dynamometer, to what can be called the input tractor.

Another steel cable is anchored by one end to the periphery of the steel loading wheel and is led off under the wheel, forward under the towing tractor and is attached through a recording dynamometer to the output tractor which is used as a loading car.

As the input tractor is driven away from the tester it rotates the slip drum, and the output tractor, exerting a specified load is pulled toward the tester as the loading wheel winds on cable. A calibration of all sprocket ratios over a wide range of loads may be obtained in this way.

A representative figure for the efficiency of all the sprocket ratios under varying loads in 98 %.

4. - Specification

The tester has been designed to operate with a wide range of wheel sizes from an 8"-24" tyre (rolling radius 18.3") to an 11"-36" tyre (rolling radius 27") and also a corresponding range of rigid wheels. It is also possible to operate with double or tandem wheels. Various types of track may be fitted and an experimental rigid track is in use in which the width may be varied from 7" to 10" and the contact length varied from 50" to 25". Tractive efforts of up to 2,400 lb are possible.

The minimum weight of the tester, less test wheel or track, is about 1,500 lb and this constitutes one of the main limitations of the machine's use. The weight can of course be increased, but not reduced. The position of the centre of gravity of the machine can be easily adjusted by sliding a 100 lb weight along the gantry projecting from the front of the machine.

5. - Instrumentation

It is only necessary to measure the cable pull, and the force between the tractor and tester, to carry out a normal wheel test. It was originally intended that these two forces should be measured by means of hydraulic dynamometers. One such dynamometer was inserted between the fixed end of the cable and the anchor, and the dial read by the driver of the Land Rover. The front of the machine was originally connected to the tractor 3 point linkage via a large parallel linkage, and the force between tractor and tester was measured by a

single hydraulic dynamometer with the dial on top of the linkage. This version of the machine is shown with an 11"-36" tyre in figure 6.

It later became apparent that serious research would require further force and stress measuring instruments in the periphery of the test wheels and tracks and, therefore, multi-channel recording was essential. It was decided to standardize on strain gauge transducers recording on to a 6 channel direct writing mirror galvanometer recorder manufactured by New Electronic Products Ltd.

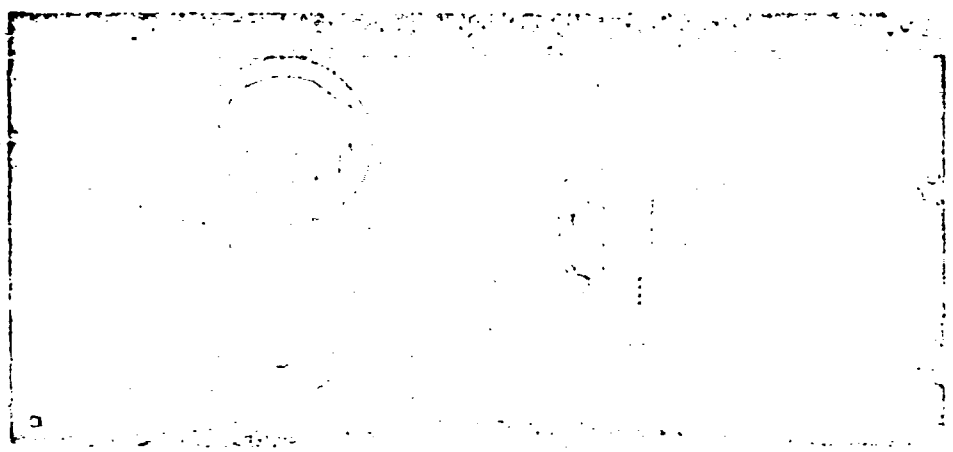


Fig. 6.

The use of strain gauge dynamometers enabled the parallel linkage at the front of the tester to be removed. The force exerted by the 3 point linkage on the tester is measured by means of three special cantilever pins which support the tractor ends of the linkage. These pins record only the horizontal components of the pull; the three components are electrically added and the resultant force is recorded. This arrangement has been described in full by one of the writers [3]. The removal of the parallel linkage made a very great reduction in the total weight of the tester and it was only then that it was possible to lift the machine on the tractor linkage.

The rope force is measured by a steel ring-type strain gauge dynamometer at the anchor end. All the dynamometers can be calibrated in the field by means of a dial gauge proving ring or dead weights and a special loading frame mounted on the front of the tractor. This is shown in fig. 7.

The slip of the test wheel during a given test can be calculated from the radius of the drum in use, but in practice it is preferred to measure this from the distance moved forward in each revolution of the wheel. This distance is obtained very simply by providing the wheel with a marker which makes a

mark in the soil for each revolution. The procedure takes care of any small variation in slip due to kinking of the wire rope or loose winding on to a drum, or stretch of the rope under load.

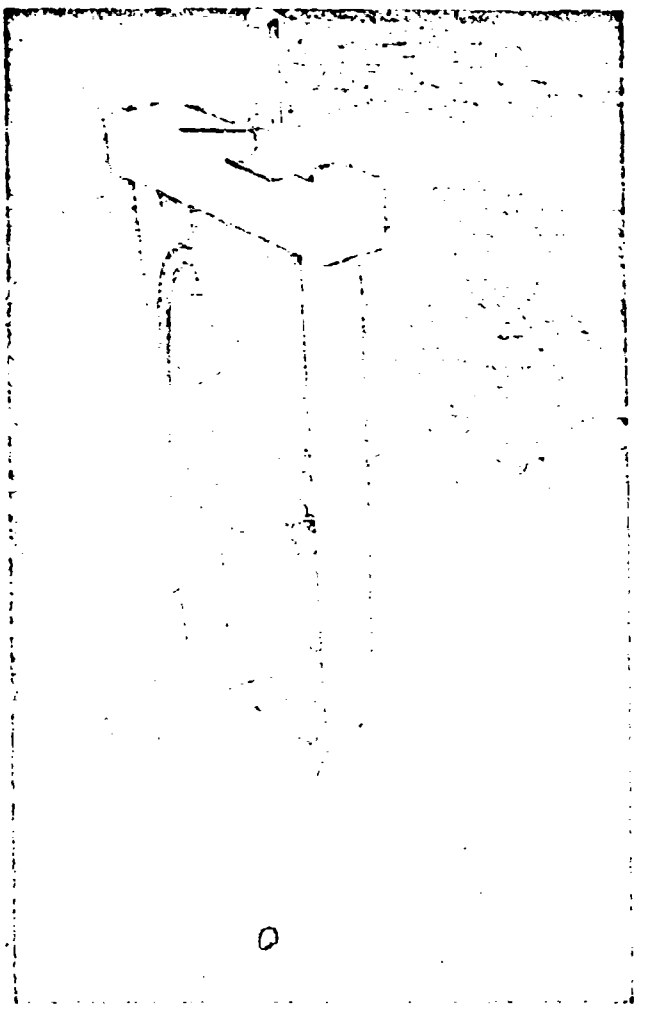


Fig. 7.

6. - Operating procedure

It is necessary that the test site should be flat over the length of a test run. A normal run covering five slip values requires about 250 ft. If only shorter lengths are available then the number of slips per run is reduced by winding a shorter rope on to a smaller number of the different drum radii. After each

run the tester is lifted and backed slowly up to the Land Rover while the instrument operator winds in the rope. Just before reaching the anchor the tractor is swung sideways and placed in position for its next run. The Land Rover jacks are retracted and it is also moved across. Test can be conducted by two men only.

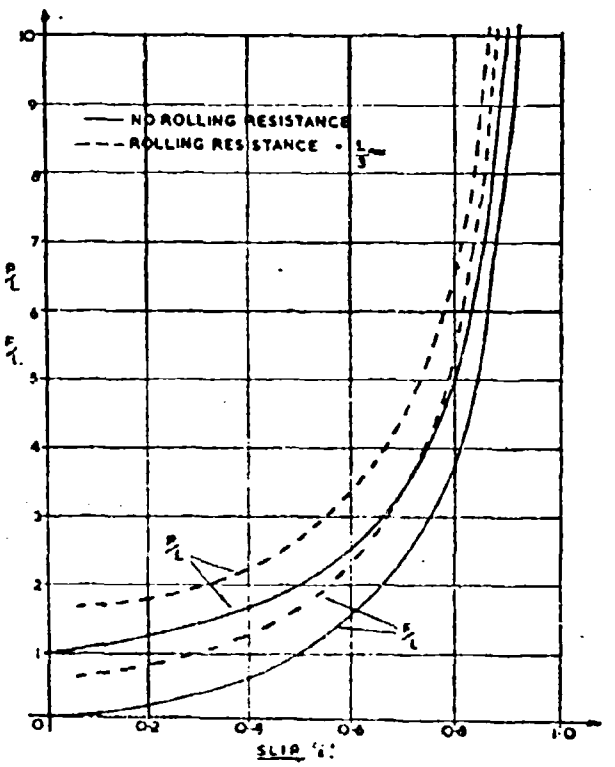


Fig. 8. — Force relationship as a function of slip.

Before each run all the dynamometers are zeroed at no load. This requires the separation of the tester and tractor to ensure that there is no load in the connecting 3 point linkage. For positive slip values the wire is wound on to the drum so that the test begins at low slip values and as it progresses the cable automatically runs off the larger drums on to the smaller ones. This ensures that as the length of cable off the drums increases so does the tension avoiding sagging and resulting contact with the soil surface.

The tester is operated at a speed controlled by the engine governor of the towing tractor. As the slip of the test wheel increases, the required pull from the tractor rises, and due to the slip of its wheels the speed of the test is reduced.

7. - Conclusions

The machine described here has taken the writers 2.½ years to develop, and during this time the form and method of operation have changed considerably. In its final form it is a simple machine that is cheap to make with the outstanding virtue of accommoduting a very wide range of ground drive equipment. The major limitation lies in the rate of working which is lower than that of an electrically or hydraulically powered machine.

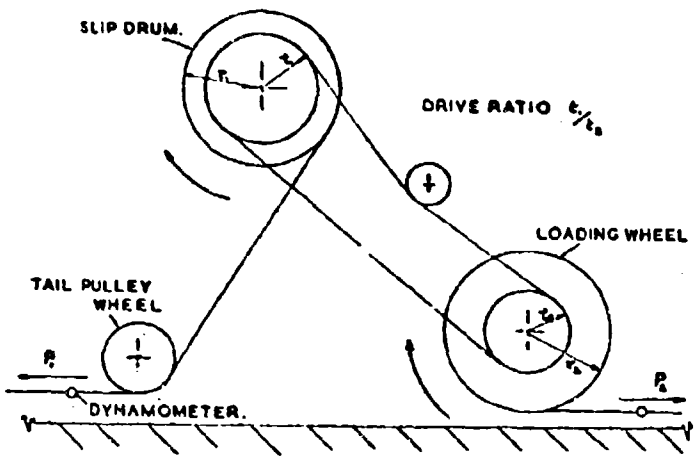


Fig. 9. — Transmission efficiency calibration.

8. - Notation

r: rolling radius; a: drum radius; u: horizontal displacement of vertical soil component; n: chain drive ratio; v: tractor speed; i: slip; A: effective drum radius; W: weight of test wheel; F: tractor force; P: rope tension; L: nett tractive effort; R: rolling resistance.

BIBLIOGRAPHY

1) Bailey P. H. The N.I.A.E. Single Wheel Tester. An apparatus for research on the performance of tractor wheels. Report No. 40. Nat. Inst. Agric. Engng., Silsoe, 1954.

2) Payne P. C. J. Winch sprag design to utilize soil friction. J. Agric. Engng. Research, vol. 1, No. 1, 1956.

3) Reece A. R. A three point linkage dynamometer. J. Agric. Engng. Research, vol. 6, No. 1, 1961.

DISCUSSION

W. SOEHNE. — **Im Institut für landtechnische Grundlagenforschung wurde ein von einem Traktor gezogenes Einzelrad-Prüfgerät mit Zwangsschlupf (Forced-slip single-wheel tester) entwickelt. Bei diesem Gerät befinden sich auf der Achse des Test-rades zwei spiral-kegelförmige Trommeln, von denen zwei Seile ablaufen, die**

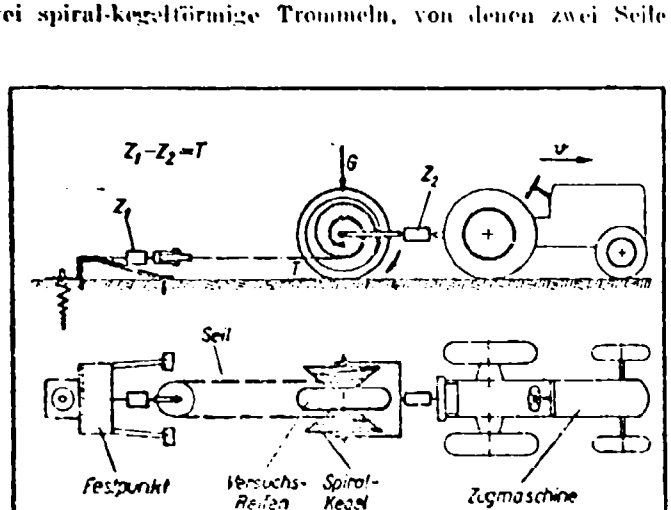


Bild 1. — Zeigt eine schematische Darstellung der Einzelprüfgerätes; als Festpunkt wurde ein zweiter schwerer Schlepper verwendet, der im Boden verankert ist.

an einem Fest-Punkt im Boden verankert sind. Dadurch wird dem Testrad beim Abrollen der Seile ein Schlupf erteilt, der von 8 bis 60 % zunimmt, so dass auf einem Wege von etwa 25 m eine vollständige Zugkraftschlupfkurve aufgenommen werden kann. Durch zwei hydraulisch gemessene Zugkräfte Z_1 und Z_2 ist es möglich, das Zugkraft-Schlupfverhalten und den Rollwiderstand in Abhängigkeit von dem zwangsweise erteilten Schlupf zu ermitteln. Das Gerät ergab befriedigende Werte bei relativ feuchtem und lockerem Boden. Bei trockenem, harten Boden traten am Prüfrad Vertikal- und Drehschwingungen auf, die das Ergebnis fälschten. Diese Schwingungen scheinen jedoch keine typische Eigenschaft dieses Testers, sondern ganz allgemein eine Eig nart on stark beanspruchten Gummireifen zu sein.



Bild 2. — Zeigt das Versuchsrad mit den spiral-kegelförmigen Trommeln.

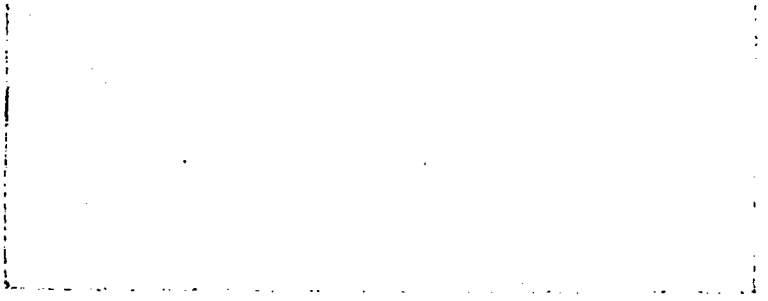


Bild 3. — Zeigt die gesamte Versuchseinrichtung.

N. 26

Evaluating and improving performance of traction devices

Valutazione e miglioramento delle prestazioni dei dispositivi di trazione

G. E. Vanden Berg - I. F. Reed - A. W. Cooper *)

ABSTRACT. — *The forces acting on any traction device using the principle of converting rotary motion into useful pull are discussed and defined. Equilibrium conditions are applied to show the relationships that must exist between these forces. The concepts of thrust and rolling resistance are discussed and the assumptions now used to calculate their magnitudes are shown to be incorrect in general.*

The relative motion between a traction device and soil is discussed and two different phenomena, designated slip and travel ratio, are shown to be important. They are respectively, (1) the relative movement of the contact surface of the traction device with respect to the soil and (2) the actual forward travel of the traction device with respect to a theoretical forward travel.

Methods and facilities at the National Tillage Machinery Laboratory for testing traction devices are presented. Simultaneous measurement of necessary variables together with an analog computer and multi-channel recorder are shown to permit calculating and recording instantaneously the coefficient of traction and mechanical efficiency.

Determining how traction is developed by measuring the forces in the mutual contact surface of the traction device and soil is suggested as a method of improving traction. That these measurements may lead to the optimum force distribution for maximum traction is also suggested.

Introduction

To evaluate the performance of a traction device, certain specific objectives must first be set forth. The primary purpose of any traction device is to develop pull; consequently, one of the objectives of evaluating performance is to determine the pull capabilities of the device. In particular, the maximum pull of a given soil condition needs to be known. Situations often exist where the maximum pull that a device is capable of developing is of primary concern as in loose sand or any other condition of low traction. In other cases where the traction device has the capacity to develop the necessary pull and where it will be used a large number of hours, efficiency becomes important. The efficiency at which a traction device operates can perhaps become the most

*) Agricultural Engineer, Agricultural Engineer, and Director, National Tillage Machinery Laboratory, Crop Production Engineering Research Branch, Agricultural Engineering Research Division, Agricultural Research Service, U.S. Department of Agriculture, Auburn, Alabama.

important characteristic of the device since a small superiority in efficiency may make a large economical difference in operation. The major objectives of a program to evaluate the performance of traction devices, therefore, should be to determine, first, the maximum pull the traction device is capable of developing for a given soil condition and second, the efficiency at which the pull is developed. The pull and efficiency should be determined over a range of soil conditions and a range of operating conditions for the traction device. There are other objectives in evaluating performance of traction devices, such as good riding qualities, depe labilit , low initial cost, and low maintenance requirements but these will .et be considered in this paper.

In this paper, the measured quantities necessary to evaluate a traction device will be defined. The method of testing used at the National Tillage Machinery Laboratory, Auburn, Alabama, USA, will be discussed and the advantages and disadvantages of that method pointed out. Finally, different approaches for improving the performance of traction devices will be discussed.

Objectives and definitions

The forces acting on a rigid wheel operating under various conditions are depicted in fig. 1. In defining the measures of the performance of a traction device, these forces must be considered and they apply to all traction devices employing the principle of converting rotary motion into useful pull. In devices other than a wheel, the distribution of forces may be different from those shown but the principles to be discussed will be the same as for the wheel. Note that the forces shown are those that act on the wheel only and to obtain overall performance of a vehicle, the interaction between vehicle and wheel must be considered.

The forces shown in fig. 1a represent a wheel acting as a transport device rather than a traction device. The forces acting at the contact surface are shown normal to the surface of the wheel where the length of vectors represent a possible reasonable distribution of forces. Neglecting friction, the moment at the axle must be zero; therefore all forces in the contact area must pass through the axle so no tangential forces can exist. From equilibrium conditions, the pull P required to move the wheel must be equal in magnitude but opposite in direction to the sum of the horizontal components of all forces in the contact area (rolling resistance). Similarly, the sum of the vertical components of all forces must be equal in magnitude but opposite in direction to the weight carried, W. The resultant, R, of all forces acting in the contact area must pass through the axle of the wheel, since the moment at the axle is zero.

Fig. 1b depicts the wheel acting as a traction device using rotary energy $T\omega$ applied to the axle and developing a useful output energy Pv where T represents torque, ω (omega) rate of angular rotation, and v forward speed. The forces in the contact area are shown in a possible reasonable distribution normal and tangent to the surface of the wheel. Applying equilibrium conditions since accelerations are assumed to be zero, the components of the

resultant R are again precisely P and W; but, since the moment at the axle is not zero, R must be located so that the relation T = Rl is satisfied.

Researchers have discussed the concepts of thrust and rolling resistance for various traction devices and values have been reported for tractor tires operating in various soil conditions[1-3]. Fig. 1c shows that all horizontal

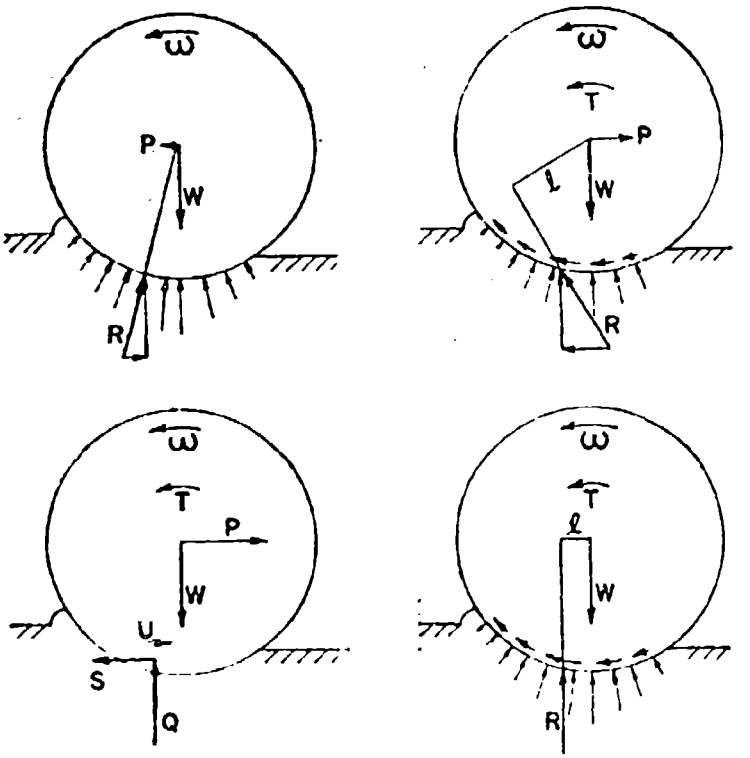


Fig. 1. — Forces acting on a rigid wheel operating (a) as a transport device, (b) as a traction device, (c) as a traction device showing hypothetical thrust and rolling resistance forces, (d) as a traction device where pull is zero.

components of forces in fig. 1b acting in the direction of travel can be summed and their sum defined as thrust, S. Similarly, the sum of the horizontal components of forces acting opposite to the direction of travel might be defined as rolling resistance, U. Thrust is equal to rolling resistance plus pull from equilibrium conditions. That such physical quantities do exist in the contact area seems logical when defined as above.

Determining the magnitude of thrust and rolling resistance is a problem. In the past workers have used the rolling radius (the radius of a theoretical circle that will roll the same distance as the wheel when the wheel develops zero pull) and said that thrust acted on a lever arm equal in magnitude to the

rolling radius. Neglecting contributions of vertical forces to the moment about the axle, thrust could then be calculated by dividing torque by the rolling radius. The fallacy of such reasoning can be seen by examining fig. 1c where S is thrust and U is rolling resistance as defined above and Q is the resultant of all vertical components in the contact area. Each is located at a possible reasonable centroid for the distribution shown in fig. 1b. If the wheel is assumed rigid, its rolling radius will theoretically be equal to the actual radius so that thrust will be assumed to act at the very bottom of the wheel. The centroid of thrust forces must lie closer to the axle as shown in fig. 1c since the vertical distance below the axle of nearly all of the thrust forces is less than the actual radius of the wheel. The rolling radius thus gives a lever arm that is too long.

In a rubber tire, the error is even greater. Experience has shown that the rolling radius of a rubber tire is closely related to the circumference of the tire and not the actual distance between the axle and the soil's surface. The deflections of the tire would bring the axle closer still to the location of thrust but the rolling radius would still be approximately the same as if the tire acted as a rigid wheel. Therefore, the difference between the actual lever arm and the one given by the rolling radius would be even greater than for a rigid wheel. Unless the actual lever arm of the thrust forces can be determined, as for example, during a condition when no rutting occurs, neither thrust nor rolling resistance can be accurately determined. Furthermore, since both occur in the same physical area and are thus difficult to separate, perhaps their hypothetical existence is a confused model of the actual forces occurring in the contact area

Besides the forces acting on a traction device, the relative motion between the device and soil must be defined. Considerable confusion and argument have prevailed concerning the definition of such motion. In the case of a rubber tire where flexing of rubber, deforming of soil, and twisting or bending of lugs all occur simultaneously, the motion is particularly confusing. Conceivably, relative motions of part of a tire in the contact area could appear to be aiding while other parts of the tire are hindering forward travel. Such a phenomenon has in reality been observed by the authors. From an efficiency standpoint and from the intended purpose of a traction device (developing useful pull), the actual distance traveled is of primary concern regardless of the amount of relative movement occurring between the mutual contact surface of the traction device and soil. Two distinct phenomena are thus of interest, the relative movement at the contact surfaces and the actual distance traveled forward. This paper suggests recognizing the two phenomena and attempting to separate them by definition. Slip may be defined as the actual relative movement that occurs between the surface of the traction device and the surface of the soil. Travel ratio may be defined as the ratio of the distance traveled with a finite pull developed to the distance traveled when pull is zero for a given angular rotation. Travel at zero pull and at a finite pull both will change with each soil condition and operating condition of the traction

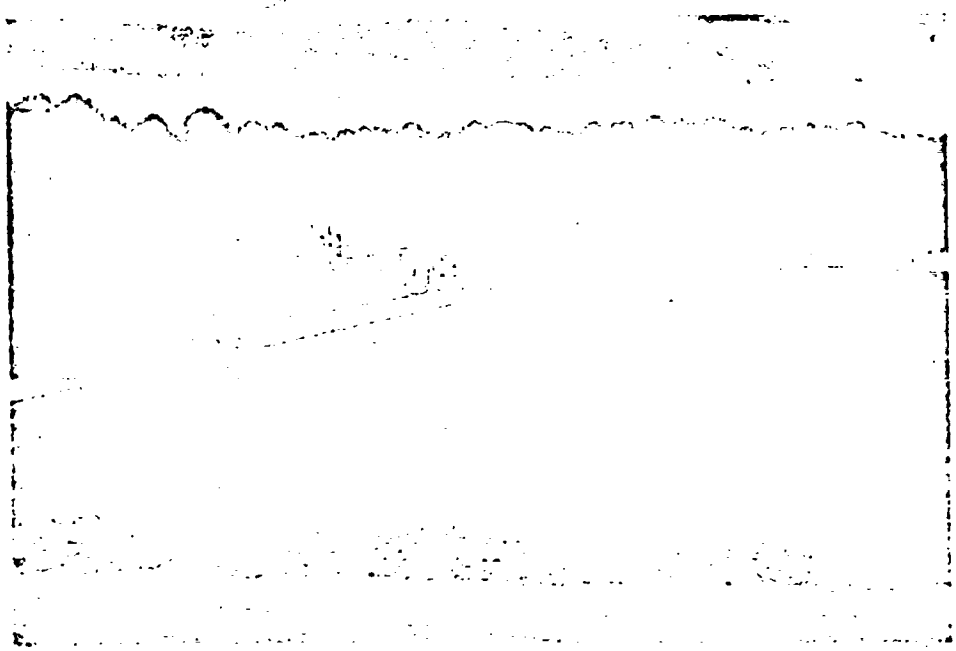


Fig. 2. — Overall view of National Tillage Machinery Laboratory showing soil bins with left to right, tillage test unit, special traction test equipment and soil fitting car.

device. These definitions recognize that slip and travel ratio can be exactly the same or can be widely different for a given traction device in a given soil condition.

The distance traveled at zero pull is the special operating condition of the traction device occurring when the sum of horizontal forces equals zero (fig. 1d). At this condition input torque is just sufficient to overcome rolling resistance. Where travel reduction is defined as one minus travel ratio, a negative travel reduction would mean the device requires a towing force and acts as a transport device. A positive travel reduction indicates the device develops pull and acts as a traction device. Zero travel reduction would thus represent the transition point between acting as a transport device and a traction device. Soehne and Bock [5] have used the same definition except the term slip was used where this paper has suggested travel reduction. Travel reduction and slip defined as above are separate and distinct quantities and both must be recognized in evaluating traction devices.

Evaluating the pull and efficiency performance of a traction device thus involves measuring the pull, torque input, load carried, forward speed, and angular rotation of the torque input at various degrees of travel reduction. The magnitude of pull and the efficiency at which the pull is developed characterize the performance of the device. Efficiency, as has been implied,

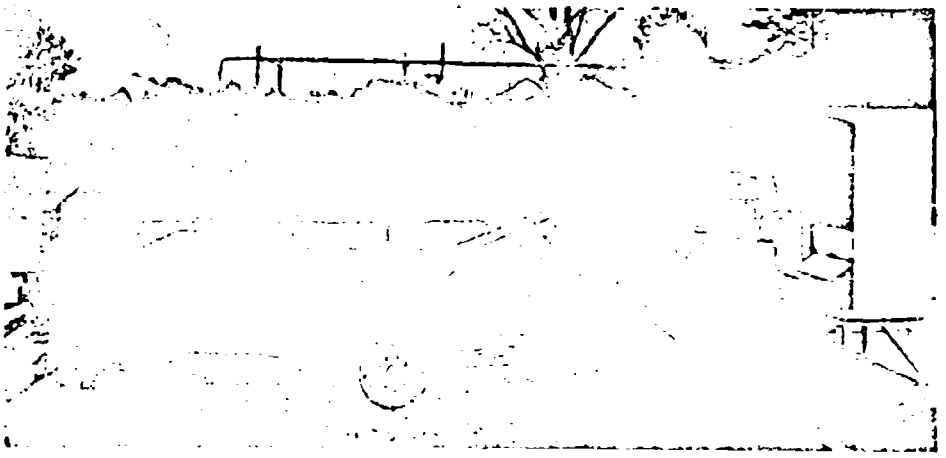


Fig. 3. — Special traction test equipment showing detailed construction.

is the ratio of output energy Pv divided by input energy T_w. Since the pull a traction device develops is directly related to load carried and, since in most present testing devices the phenomenon of weight transfer occurs, the coefficient of traction is often used to characterize the traction device. Comparing the pull of one device against another where both were tested in an apparatus where weight transfer occurs leads to a slight bias since increased pull causes increased weight transfer which in turn causes more pull. Pull divided by total load carried is defined as the coefficient of traction and removes any bias due to weight transfer in the testing apparatus.

Testing facilities and methods

Unique facilities at the National Tillage Machinery Laboratory (fig. 2) were especially designed for testing traction devices. Soil bins 20 feet wide and 250 feet long are available. The special equipment shown in fig. 3 permits only the traction device to come in contact with the soil since the testing apparatus is carried on steel rails on the walls of the bins. Because of the control over soil preparation, a uniform soil condition can be obtained in a given soil bin. However, in spite of nearly 25 years of experience, a soil condition which is exactly equivalent to a previous soil condition cannot be obtained. Obtaining as much information per soil fitting as possible is therefore essential. In any type of testing where space is limited, in this case soil available, the maximum utilization of test area can be made by continuously and slowly changing one variable during a test. Such testing, of course, requires that all the measured variables be continuously and simultaneously recorded. The only other type of testing is to measure the desired variables at a series of conditions repre-

senting dynamic equilibrium. The average values during the period of dynamic equilibrium are determined and calculations performed on these data to evaluate the test results.

Prior to the fall of 1959, traction tests at the National Tillage Machinery Laboratory were conducted by the latter method. In tests at that time, the travel reduction of the traction device was controlled and the other variables measured and recorded. During a test a specific travel reduction would be adjusted and the apparatus allowed to equilibrate and records made for a short period of time. All of the recording charts were then coded and the next level of travel reduction was adjusted and the apparatus again allowed to equilibrate and the recording made and charts coded. In this manner, proceeding as rapidly as the operators could, data were recorded for five to six different travel reductions in one pass down the length of the soil bin. In the fall of 1959, instrumentation was modified so that all the variables could be measured continuously and simultaneously. Since the modification, travel reduction is varied gradually and continuously from 0 % to 100 % or the maximum percent desired and, instead of only five or six travel reductions, all of the values over the range tested are obtained. Furthermore, three such tests can be run in one length of the soil bin. Consequently, besides getting more data per test, three times the number of tests can be run in a given soil condition.

To continuously and simultaneously record the measured variables, a multi-channel, direct-recording oscillograph is employed. The basic oscillograph assembly is composed of the necessary amplifiers, balancing mechanisms, and power supplies so that the sensing transducers can be connected directly to the oscillograph assembly. Pull is measured using an electrical resistance strain gage tension dynamometer. Torque is measured using a specially constructed hub which employs reluctance gage transducers that sense the deflection of spokes of the hub. The static load carried by the traction device is weighed on a platform scale. The load added to the traction device due to weight transfer of the tractor is measured by supporting the front end of the tractor on cantilever beams instrumented with electrical resistance strain gages and recording the weight lifted off during a test. The forward speed of the traction device is measured using a DC generator driven from the rail as the test car moves forward. Travel reduction is measured by recording the difference between the DC voltage generated due to the forward speed of the test car and a DC voltage generated on the tractor which is proportional to the angular rotation of the driving hub. Through simple calibrations at the 0 and 100 % points, travel reduction is measured directly as a percentage. Fig. 4 shows a schematic diagram of the travel reduction meter circuitry. The zero percentage point is determined when the traction device and the test car are traveling forward at the same speed and the pull of the traction device is zero. The potentiometer associated with the rail generator (fig. 4) is adjusted so the meter reads zero under the above conditions. The 100 % point is determined when the forward travel of the test car is zero while the traction device is operating at its rated

rpm. By calibrating the potentiometer associated with the rail generator, the rolling radius can be read directly from the dial. Five simultaneous signals are thus measured and recorded on the multi-channel oscillograph: pull, torque, travel reduction, weight transfer, and forward speed. The theoretical rolling radius and static weight on the traction device are obtained prior to a test. The engine rpm of the tractor is maintained constant and thus the angular rotation of the driving hub is constant during a test.

By recording continuously and simultaneously all of the measured variables during a traction device test, other electronic equipment can be employed to speed data analysis and reduction. For example, the travel reduction and the

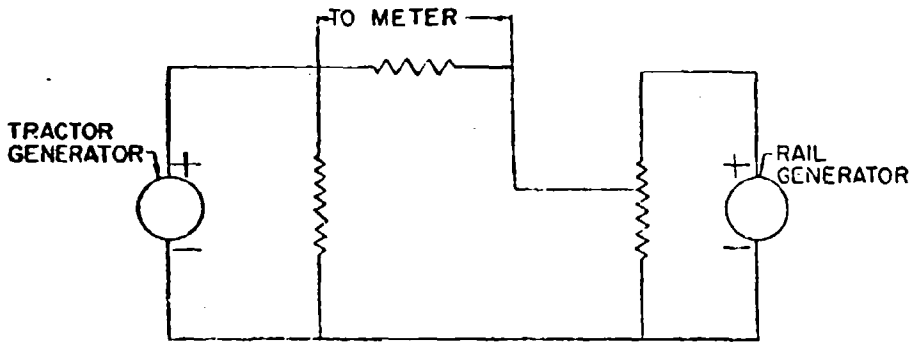


Fig. 4. — Schematic diagram of travel reduction meter.

pull signals can be fed directly into an XY plotter and a travel reduction-pull curve constructed employing all of the data that were measured. Without using an XY plotter, travel reduction and pull must be read at simultaneous times from the oscillograph chart, necessitating that a finite number of discreet points be selected so the curve can be plotted. Since an XY plotter will plot all of the measured points rather than a finite number and, since it eliminates the need to critically read the multi-channel oscillograph, a more accurate curve can be obtained more easily and quickly using this equipment.

Even further data reduction is possible. To compute the efficiency of the traction device, the pull, forward speed, and torque must be read from the chart at simultaneous times. By employing an analog computer properly programmed to use the signals representing the pull, torque, speed, and angular rotation of the driving hub, power efficiency will be computed directly. As with the XY plotter, all of the measured data rather than a limited number of selected points will be used. The output of the analog computer can be recorded on the multi-channel oscillograph chart so that the original data and the computed data will be recorded simultaneously and continuously. Such a procedure not only speeds up the data reduction but enables a more accurate determination of maximums and minimums and where they occur. For example, maximum efficiency occurs when the pull is large, the speed is high, and the

torque is low. To visually inspect the data and determine such a point is nearly impossible. Furthermore, to accurately locate maximum efficiency by calculation requires a large number of points and considerable time and effort. Thus the analog computer used in conjunction with the multi-channel oscillograph can greatly speed and improve data analysis procedures. The coefficient of traction, of course, could also be computed employing an analog computer. Signals representing the pull and the weight transfer can be fed into the computer and manipulated to give coefficient of traction which again can be recorded continuously and simultaneously on the multi-channel oscillograph.

Improving performance

Two basic approaches seem logical in attempting to improve the performance of traction devices. The first approach involves the direct comparison of similar traction devices having some variable changed. The magnitude of the variable that results in superior performance can then be concluded to be better but not necessarily best in designing a traction device. Such an approach is the one that has most often been followed in developing farm tractor tires. Studies of this type were used in determining the effect of such factors as lug spacing, lug height, lug angle, and effect of rim width[1,2,3]. Such an approach can and does lead to rather quick results. However, the method does not answer the questions of how and why each variable affects the performance of the traction device. Furthermore, there is no assurance that the ultimate performance has been obtained.

The second logical approach is to determine how traction is developed through the forces which act between the traction device and the soil in the mutual contact area as depicted in fig. 1. Examples exist where two similar tires carry precisely the same dynamic load, operate in the same soil condition and yet one tire outpulls the other. The difference in the pulls must appear in the different distributions of the forces within the contact area. An approach for determining the differences of performance of traction devices is thus to measure the distribution of forces in the contact area and determine how basic factors affect traction. Such factors as lug height, or spacing, or angle, would appear as differences in the stress distributions in the contact surface. The relationship between such distributions and the characteristics of the traction device would answer some of the hows and whys of traction.

The approach can be carried one step further. The distribution of stresses « desired » by the soil to give maximum traction can be determined experimentally. Knowing the « desired » or optimum distribution permits attempting to design a traction device that will produce that distribution. Such procedures will result in the ultimate performance of which a soil is capable in terms of traction.

Determining stress distributions will be time-consuming. With modern advances in instrumentation, however, the task will not be as formidable as it once appeared. Measurements of contact pressures or stresses normal to the

contact surface have already been made. The work of Kraft, which was reported by Soehne [5], was perhaps the first attempt. More recently, work by Vanden Berg and Gill [7] and Trabbic, Lask, and Buchele [6] reported measurements made in smooth tires and lugged tires, respectively. While these measurements have admittedly been rather crude, they never the less point out that such measurements can be successfully made and with the proper refinement will result in good, valid data. At the present time, there appears to have been little success in measuring tangential stresses in the contact area in connection with rubber tires. A track shoe dynamometer was designed and used by Reed [4] and is a first approach at measuring the normal and tangential stresses occurring in a track. Perhaps the device can be miniaturized and installed in the lug of a rubber tire so that normal and tangential stresses can be simultaneously measured. Certainly there are other solutions which, when properly applied, will permit the necessary measurements.

Several possibilities present themselves as means of determining the stress distributions « desired » by the soil. Laboratory models representing the different configurations of traction devices can be tested in a model box. Contact pressures and tangential stresses within the contact area can be simultaneously measured. The pull or draft of the model can be measured as well as soil-material friction. By varying the loading or normal pressures of the model, by simulating lug height and thickness and flexibility, it should be possible to determine the maximum pull a soil is capable of developing while in a given physical condition. Only after such information is available and traction devices are capable of applying stresses similar to the distribution « desired » by the soil will maximum traction be possible.

BIBLIOGRAPHY

1) McKibben E. G., Reed I. F. and Reaves C. A. Some effects of rim width on tractor tire performance. Agr. Engr., 33, 487-490, 496, 1952.

2) Reed I. F. and Shields J. W. The effects of lug height and rim width on the performance of farm tractor tires. SAE Journal, pag. 40-41, December 1950.

3) Reed I. F., Reaves C. A. and Shields J. W. Comparative performance of farm tractor tires weighted with liquid and wheel weights. Agr. Engr., 34, 6, 391-395, 1953.

4) Reed I. F. Measurement of forces on track-type tractor shoes. Transactions of ASAE, 1, 1, 15-18, 1958.

5) Soehne W. Kraftuebertragung zwischen schlepperreifen und ackerboden (stress transmission between tractor tires and soils). Grundl Landtech. 3, 75-78, 1952.

6) Trabbic G. W., Lask K. V. and Buchele W. F. Measurement of soil-tire interface pressures. Agr. Engr., 40, 11, 678-681, 1959.

7) Vanden Berg G. E. and Gill W. R. Pressure distribution between a smooth tire and soil. Paper presented at annual meeting of ASAE, Ithaca, N. Y., June, 1959.

N. 27

Scale model evaluation of earthmoving tools

Valutazione degli attrezzi per i movimenti di terra su modelli in scala

D. E. Cobb - G. T. Cohron - J. D. Gentry *)

ABSTRACT. — *A test facility is described which is used for scale-model studies of earthmoving tools, and test procedures are discussed. Models, inexpensively constructed of sheet metal, are of very small scale. A variety of realistic field operating conditions can be simulated, through the use of strain-gaged load-sensing devices and electrical controls. A standard soil preparation routine has been developed. Artificial soils are employed, using oil as the moistening agent, which are more stable than natural soils. Model analysis for the soil cutting process is incomplete, in that the only soil properties to be controlled are shear strength and density. Distortion is therefore possible, and the need is cited for further work to identify and evaluate other soil factors of importance. Results to date indicate that earthmoving processes are well suited to scale-model investigation. Models offer many advantages, including low cost, rapid testing, and reduction in variability of test conditions and results.*

Introduction

For many years, models of footings and retaining walls have been used to aid in the formulation of theories relating to problems in soil mechanics. More recently, scale models of both tracked and wheeled vehicles have been employed to determine vehicular mobility. Models have also been used to study tillage tools. At Caterpillar Tractor Co. small-scale models are being used to study performance of the soil-engaging parts of our machines.

Since a large percentage of our model analysis has been directed toward specific machines within our product line, it would be well for the reader to become acquainted with the types of earthmoving equipment produced by our company.

Figure 1 shows a track-type tractor operating with a bulldozer. It is one of the most versatile machines in our line, particularly on jobs involving the moving of large quantities of materials for short distances, clearing land of trees and brush, and pushing other machines. The wheel-type tractor-scraper unit shown in figure 2 is used for moving overburden and construction soils at high speeds over longer distances. A track-type loader appears in figure 3. Its functions, like those of the track-type tractor and bulldozer, are varied, but it is widely used wherever materials must be excavated and stockpiled or loaded into hauling units.

*) Caterpillar Tractor Co., Peoria, Illinois.



Fig. 1. — Bulldozer on track-type tractor.

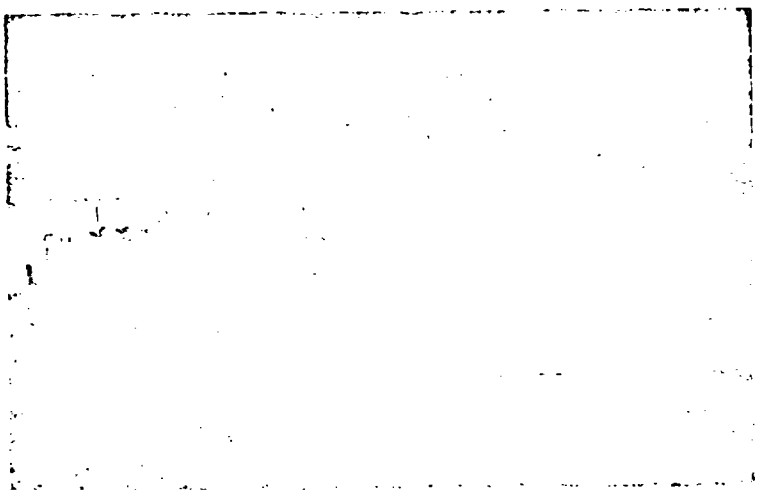


Fig. 2. — Wheel type tractor-scraper.

In the movement of all types of earth ranging from weak soil to rock, other important earthmoving functions must be performed besides moving material from one location to another. A ripper on a track-type tractor such as in figure 4, is a tool for breaking up many types of rock formations. Another important earthmoving tool is the motor grader shown in figure 5. It has many uses, but is generally used for road maintenance and leveling operations.

The problem of accurately evaluating the performance of each of the above earthmoving tools has been — for many years — severely handicapped by the variability of field soils. The machine operator also contributes to the

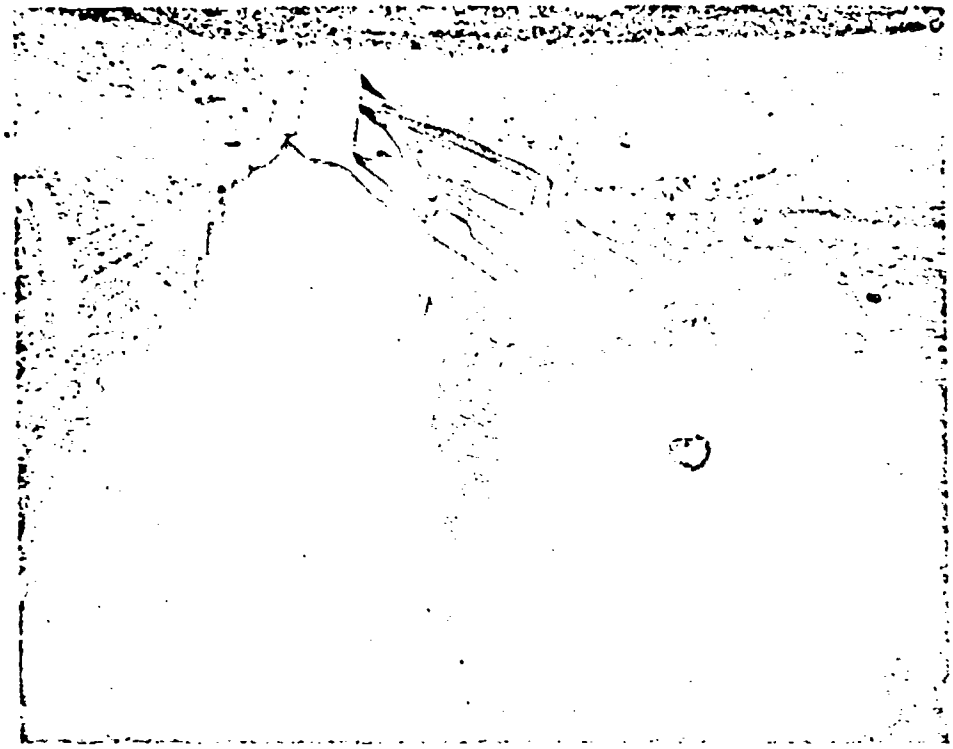


Fig. 3. Track-type loader.



Fig. 4. — Ripper on track-type tractor.

variability of field test data, since he cannot accurately reproduce adjustments of the cutting element on successive tests. Minimizing these two factors has been of prime consideration in the establishment of an indoor scale-model testing facility.

In this paper, a facility used by the soil mechanics engineers at Caterpillar Tractor Co. will be discussed. Model testing techniques are presented in some detail. While being aware of many of the shortcomings, we are optimistic about the ability of scaled models to provide accurate and useful information in the evaluation of earthmoving tools.

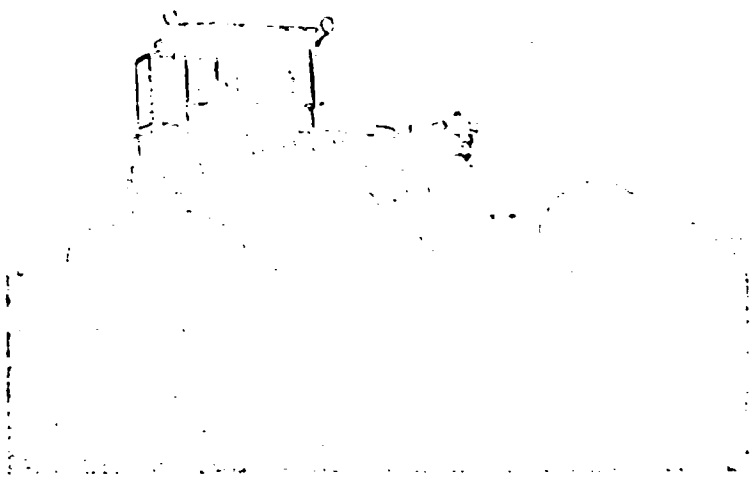


Fig. 5. — Motor grader.

Model testing facility

The model testing facility used to evaluate earthmoving tools is a soil bin (figure 6). Over all dimensions are 18 feet long by 3 feet wide by 5.5 feet high (5.49 × 0.91 × 1.68 meters). A monorail on which the dynamometer carriage travels is positioned 2.5 feet (76 cm) above the top of the trough. The bin is mounted on rollers and can be moved easily or tipped to produce a sloped soil surface. It was designed to contain soil 1.5 feet (46 cm) deep. However, as mostly small-scale models of earth-cutting tools are tested in this facility, a shallow wooden-box insert was found to be sufficient. The wooden trough is 16 feet long by 2 feet wide by 4 inches deep (4.88 m × 61 cm × 10 cm) and expedites testing because the small volume of soil is easily prepared. The amount of soil used for testing is only 8 cubic feet (0.226 cubic m); therefore, it can be quickly replaced with a different soil.

Soil preparation consists of « rototilling », leveling, and rolling. The

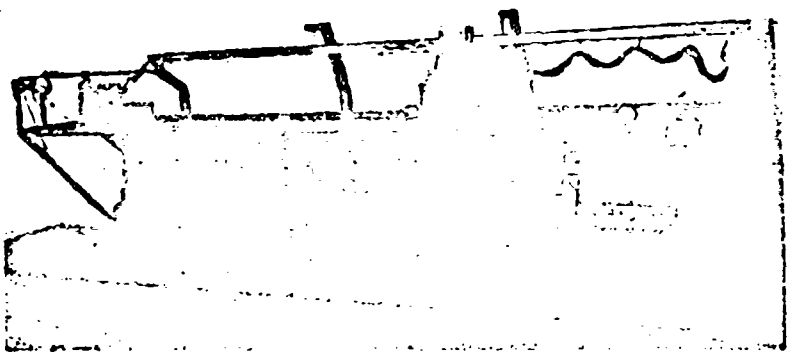


Fig. 6. — General view of soil bin.

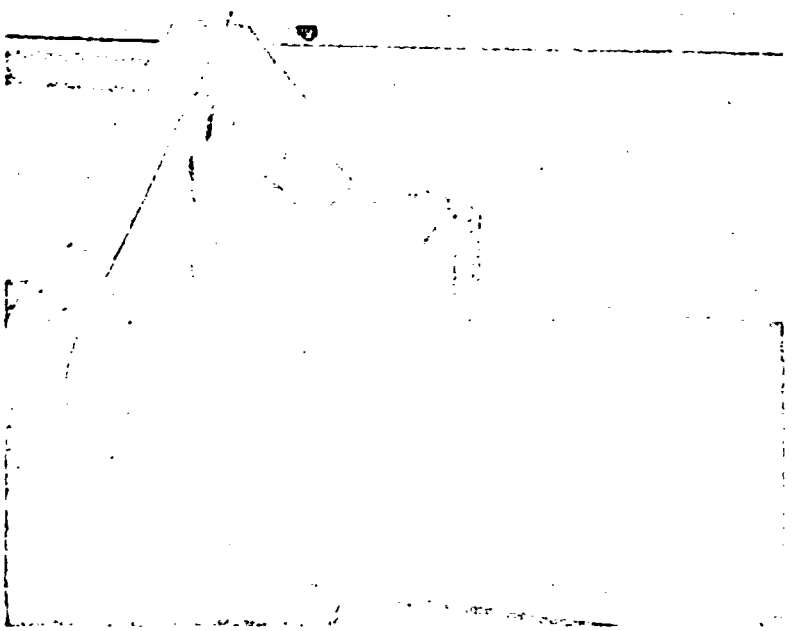


Fig. 7. — Rototiller.

rototiller (figure 7) is a small electrically-powered commercial unit, mounted on guide rails and towed by the dynamometer carriage. One pass of the rototiller thoroughly loosens the soil. A leveling blade precedes the rototiller to fill the previous test excavation. Another leveling blade is used in front of the roller.

The compacting roller (figure 8) is 1 foot (30.5 cm) in diameter, 1.5 feet (45.7 cm) wide, and weighs 150 pounds (68 kg). Any number of roller passes can be made, depending on the type of soil being used and the soil shearing strength desired. The final roller pass leaves a relatively smooth, level surface.

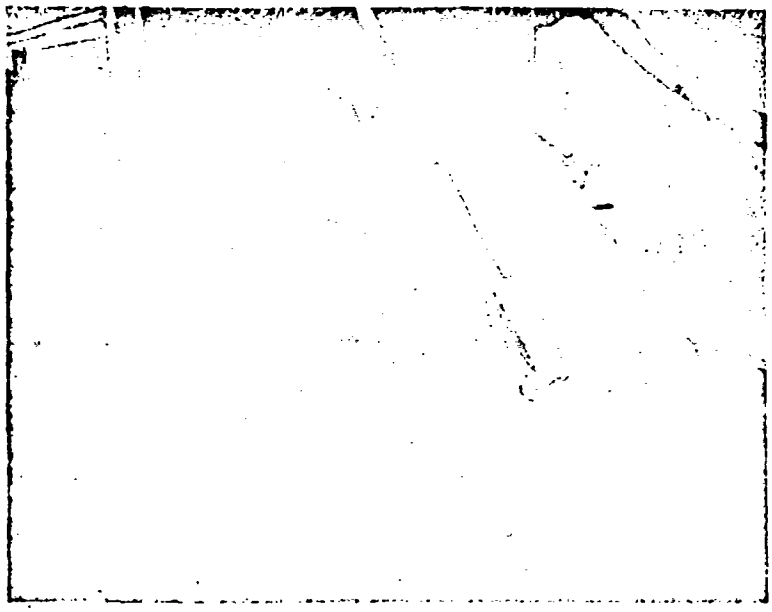


Fig. 8. — Compacting roller.

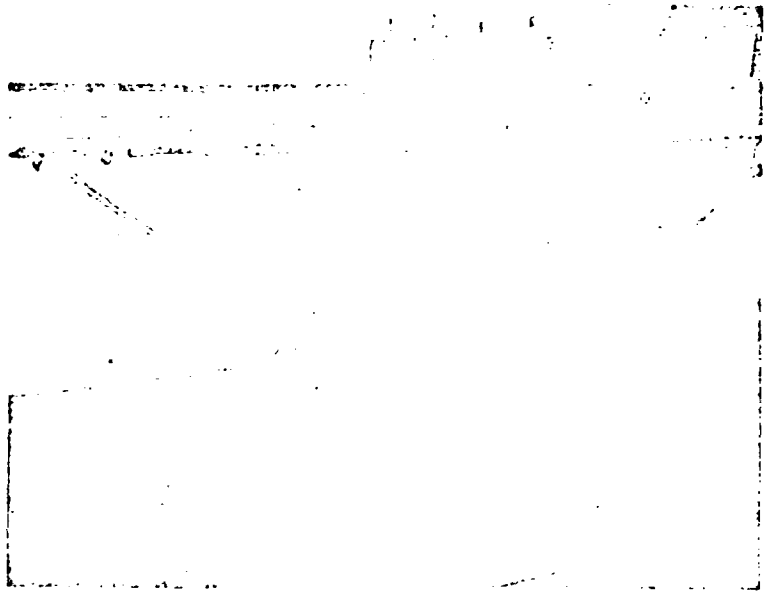


Fig. 9. — Dynamometer carriage.

A cable drum, rotated by a hydraulic motor, tows the dynamometer carriage (figure 9) in either direction through a cable-pulley system. Carriage speed is controlled with a hydraulic flow-control valve. A flow-direction valve reverses the direction of travel of the dynamometer carriage.

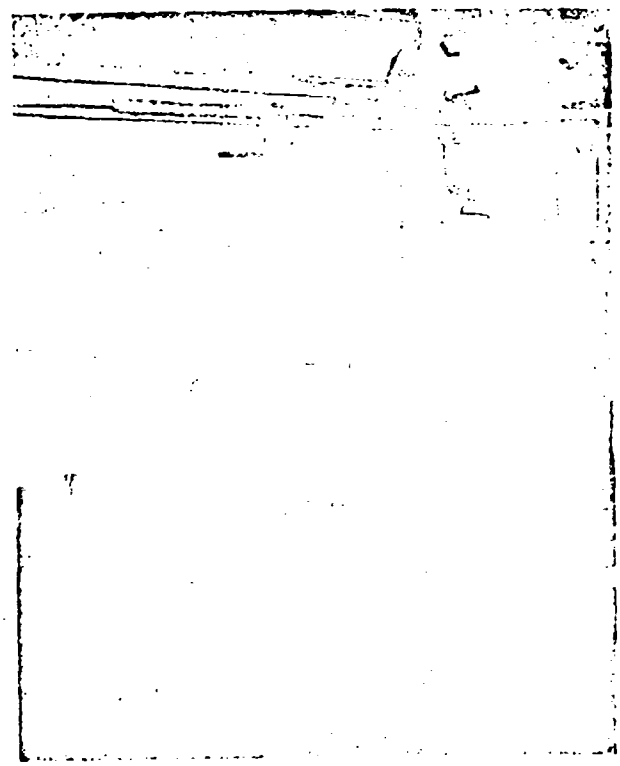


Fig. 10. — Model mounting and load-cell arrangement.

The facility is capable of producing model testing speeds from 0.15 to 2.20 feet per second (4.6 to 67.1 cm/sec.). The maximum testing distance is 14 feet (4.27 m). The power available to propel the model is approximately 1 horsepower (1.01 metric hp).

Various force-measuring load cells are used on the dynamometer carriage. The cells are of the strain-gaged type, and mount between the carriage and the model (figure 10). Forces in any direction can be measured and located as required by the test procedure. These forces range from 0 to 100 pounds (45 kg). Strain-gage signals from the load cell are fed through appropriate amplifiers to a recording oscillograph to provide a continuous record of the measured forces. The weight of the soil moved by the model can be determined from the vertical force record, for scrapers and loader buckets, when the model

is raised from the soil. For bulldozers, the load is pushed into a pan and weighed on a platform scale.

The models being tested in this facility range from 1/15 to 1/8 scale. Loader buckets can be tested at 1/8 size, while most bulldozers are evaluated at 1/10 or 1/12 scale. Model scrapers are 1/12 to 1/15 in size depending upon the size of the full-scale machine.

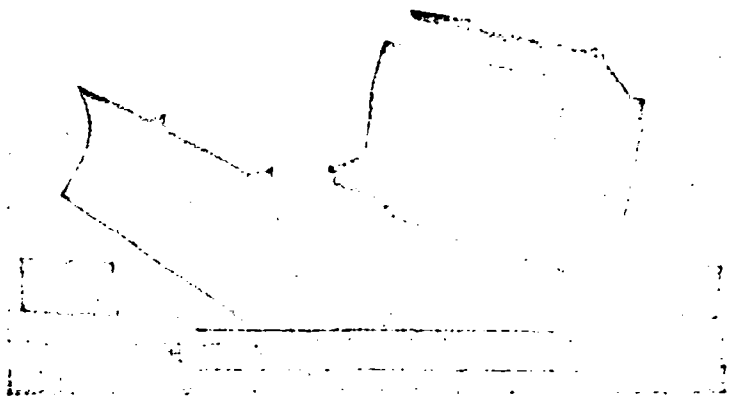


Fig. 11. — Model bulldozer and scraper.

Small-scale models may be constructed from sketches of a new machine. These models are fabricated from .050 inch (1.27 mm) thick galvanized sheet metal (figure 11). The sheet metal is easy to form, and joints are made by soft soldering. Thus, major design changes may be made quickly and inexpensively in the models.

Soils used for model tests

Artificial soils are used for most of our model tests since they are more stable than natural soils. The engineering properties of the soil at the time it is being cut and loaded are of primary interest. Changes that occur in natural soils over long periods of time are not important to the model test. Therefore, we want a soil that can be disturbed and quickly returned to its original condition repeatedly, without any change in engineering properties. This can be done more easily with an artificial soil than with a field soil.

Fire clay, sand, and a low viscosity oil are the three ingredients used to make the artificial soils. Different proportions of these materials produce

a wide range of soils. Figure 12 shows the engineering properties of some of the soils that have been used. These properties are for specific compactions. Oil Soils No. 1A through 1D, for example, are the same mixture with different compactions. Thus, by simply varying the number of passes with the roller, the properties of the soil were changed. This was a quick way to produce a variety of soils.

The internal shear strength of the soil has been given in terms of apparent cohesion and internal angle of friction. Both peak and ultimate shear strengths of the soil were recorded in this manner. The ultimate external shear strength of soil on steel was recorded in a similar manner, in terms of apparent adhesion and external angle of friction.

The shear strengths of the soils shown in figure 12 were obtained with a small shear plate 3 inches wide by 6 inches long (7.62 × 15.24 cm). The shear plate had cleats extending across the 3 inch dimension, at right angles to the direction of travel, which were 0.010 inches thick, 0.25 inches high, and spaced 1.12 inches apart (0.25 × 6.35 × 28.45 mm). Dead weights were used to produce different normal loads on the shear plate. The shearing forces were measured with a spring scale. These forces were gradually applied manually during a time of approximately 4 seconds. A flat steel plate of the same size was used to measure the shearing force of steel on soil. This method of measuring shear stress has several limitations, but for the purpose of many of our tests, it was satisfactory.

OIL SOIL PROPERTIES

		SHEAR STRENGTH—QUICK SHEAR					
		INTERNAL (SOIL ON SOIL)				EXTERNAL (SOIL ON SOIL)	
		Peak		Ultimate		Ultimate	
Oil Soil No.	Bulk density lb/yd³	Cohesion psi	Angle of friction deg	Cohesion psi	Angle of friction deg	Adhesion psi	Angle of friction deg
1 A	1920	0	30	0	30	0	24
1 B	2830	.18	40	0	35	0	27
1 C	2870	.60	40	0	35	0	27
1 D	2890	.76	41	0	35	0	27
3	2950	.18	20	.18	29	.02	10
4	3550	.35	27	.04	37	.(illegible)	18
5	3250	.38	47	0	40	0	25

Fig. 12. — Table of engineering properties of Oil Soils.

Artificial soils of this type appear to be stable over long periods of time. The same soil can be used for several months without any noticeable change in engineering properties. It should be mentioned, however, that even though we have been able to obtain much worthwhile information by using these soils, more work needs to be done in developing a wider range of artificial soils.

Requirements and limitations of model tests

Theoretically, it is possible to predict the behavior of a full-scale earthmoving machine by testing small-scale models. If all the important variables are recognized and properly scaled, accurate full-scale results can be predicted. This is done by using model theory as explained in many publications on dimensional analysis.

The factors that are important in earthmoving involve the tool and the soil. The variables of the tool include its geometry, motion, and applied forces. The variables of the soil which are controlled include its bulk density and shear strength.

Our small-scale models are made geometrically similar to the full-scale machine. However, only the surfaces that touch the soil have to be reproduced in detail, and even they are often simplified when the performance of the tool is not affected.

The physical properties of the soil can be scaled in more than one way for the model tests. However, using materials that are readily available, it is convenient to keep the bulk density of the model soil the same as that of the field soil being simulated. If this is done, the shear strength of the model soil must be made equal to the shear strength of the field soil multiplied by the scale factor. (The scale factor is the ratio of a characteristic length on the model to a similar full-scale length). This means that cohesion must be multiplied by the scale factor, while the angle of friction remains the same. The same is true for adhesion and external angle of friction of the soil on steel, respectively.

When the forces required to accelerate the soil are important, the velocity of the model must be equal to the velocity of the full-scale machine multiplied by the square root of the scale factor.

If the variables mentioned were the only ones of importance, and they were scaled according to model theory as noted, then the amount of soil loaded by the full-scale machine would be equal to the model load divided by the scale factor cubed. However, if some important variable were not properly scaled, the results would be distorted.

As an example, assume the performance of a bulldozer in a particular field soil is to be predicted from tests of a 1/10 size model. For the purpose of this example, assume that the variables discussed above are the only ones of importance, and that the model soil can be scaled as needed. All important linear dimensions on the model should be made 1/10 size. Angles must be the same on the model as on the full-scale machine. A model soil should be selected which has the same bulk density as the field soil. If the strength of the soil is expressed in terms of apparent cohesion and internal angle of friction, then the cohesion of the model soil should be made 1/10 the cohesion of the field soil, while keeping the angle of internal friction the same. The adhesion and external angle of friction of the soil on the metal moldboard must be scaled in a corresponding manner. The shear strength of the soil on the moldboard of

the bulldozer can be adjusted by changing the roughness of the metal surface rather than by altering the soil. The model should be run at a speed equal to the full-scale speed multiplied by the square root of 1/10. In addition, if the model were to be run at a constant value of force, the horizontal thrust should be regulated at 1/1000 the full-scale force. Each pound of soil bulldozed by the model will then represent 1000 pounds full-scale.

Since earthmoving tools are used in a wide range of materials, we are interested in evaluating models in many different soils. This simplifies the testing to the extent that in many cases it is not necessary to scale any one particular field soil. By testing the model in a range of model soils, design features can be evaluated.

We realize there are other soil variables that affect soil cutting and loading. These variables, such as soil compressibility or compressive strength, may also be important. In the past we have made few attempts to control other properties. As a result, our model data are no doubt distorted in many cases. In the future, more soil properties will be evaluated in order to determine their influence on the performance of different earthmoving tools.

Presently our experience in predicting full-scale performance from model tests is somewhat limited. We have not run enough controlled full-scale tests to be able to determine the accuracy of our model tests under a wide range of conditions. However, results have been encouraging from both a qualitative and quantitative standpoint.

We are especially interested in developing a more complete understanding of basic soil cutting and loading processes. More information of this type is needed for the design of efficient soil engaging tools.

Test conditions and techniques

A great deal of effort has been expended to duplicate field operations, to make our model tests realistic and meaningful. Earthmoving equipment works under a wide range of conditions. The machine operator can vary the thrust, speed, and power being used by changing the cutting depth of the tool. The way these variables are controlled on the model test, therefore, becomes somewhat arbitrary. The method that is used depends upon the information desired. In most cases it is sufficient to hold the speed and thrust constant. Thrust is controlled by adjusting the depth of cut.

For example, let us assume that a certain track-type tractor has a constant drawbar pull and speed, and operates at its maximum horsepower. If it is further assumed that this condition is best for cutting and moving soil with a bulldozer on this machine, these conditions are sufficient to establish the operational techniques for the model test.

Figure 13 shows a schematic diagram of the constant-force control system used for testing a bulldozer blade. The strain-gaged load cell is sensitive only to the horizontal component of cutting and loading resistance (F_H). Thus, the voltage change in the strain gage bridge circuit gives a direct indication

of F_H. The amount of horizontal force which is available to the blade is adjusted by changing a reference voltage with a potentiometer in the electronic controls. As the test begins with the blade resting on the soil surface, the horizontal

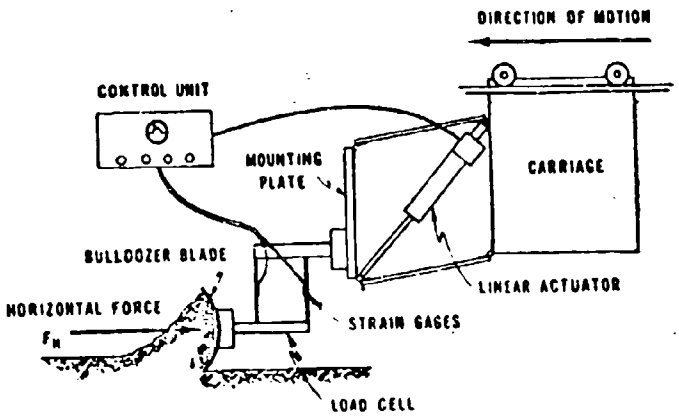


Fig. 13. — Schematic diagram of constant-force control system.

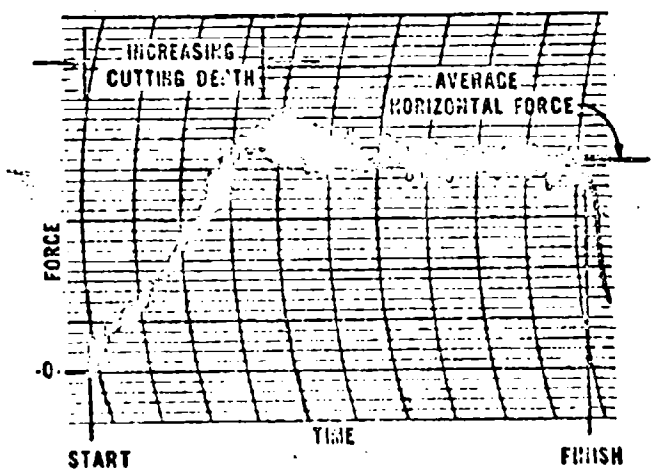


Fig. 14. — Typical force-time record.

force will be less than the value selected to be held constant. In this condition, a set of relays closes, causing the electrical linear actuator to force the bulldozer blade deeper into the soil. When the horizontal force on the model equals the desired level, the relay contacts open, causing the linear actuator to stop. Any increase in horizontal force will then cause the actuator to reduce the cutting depth until the selected and actual horizontal forces (reference and load-cell voltages) again are in equilibrium. This process is repeated rapidly

and continually throughout the test, and maintains the average horizontal force on the model at the desired level. The force-time trace in figure 14 is a typical record of the force exerted on a model bulldozer during loading in the soil bin. Deviations from the average force result form control corrections and the intermittent nature of the soil shear failures.

In some field operating conditions, the speed is higher at the start of a bulldozing pass than at the end. This is natural since the small cutting and loading resistances at the start of the pass allow the machine to utilize its horsepower in higher speed when the drawbar pull requirements are low. If it is desirable to simulate a particular drawbar pull-speed relationship, an auxiliary control system is used. Figure 15 shows a schematic diagram of this system which can regulate force and speed in any preselected manner.

The speed of the model dynamometer carriage is determined by the angular position of a hydraulic flow control valve which regulates the amount of oil passing through the hydraulic motor. The position of the valve, in turn, is controlled by an electric motor. Therefore, when the motor turns at a constant speed, the model will be decelerated at a constant rate. The rheostat in figure 15 is preset manually to control the rate of deceleration.

Since a tractor has a specified maximum drawbar pull at any given speed, it is therefore necessary to adjust the available thrust on the model when the speed is changed. To accomplish this, a cam is connected directly to the sprocket of the flow-regulating valve, so that its angular position would be proportional to the speed of the model. The instantaneous radius of the cam controls an electrical resistance potentiometer through a rack and pinion arrangement. The position of the potentiometer determines the reference voltage (available drawbar pull) for the force-control system. The shape of the cam is taken from the pull-speed curve of the tractor under consideration. The terminal speed, with its characteristic drawbar pull, will be reached when the limit switch at the end of the rack is contacted, interrupting the power to the motor. Thus, the cam puts into the control system the specified relationship between drawbar pull and speed. The characteristics of a tractor are therefore duplicated by the manipulation of a few controls.

The two systems just described are easily adaptable to a wide variety of testing conditions. Figure 16 shows the control stand as it actually appears in the soil bin setup.

Figures 17 and 18 show two typical curves obtained from scraper loading studies in the field and in the soil bin. Points for the curves were obtained by loading the scraper for different lengths of time and weighing each load. A series of such points gives a curve which shows the average load in the unit at any specific time during the loading cycle. These figures indicate that the data obtained from model tests are sufficiently reproducible to determine small differences in the performance of earthmoving tools. Because of the amount of scatter in field test data, much more testing would be required to detect small differences in full-scale machines.

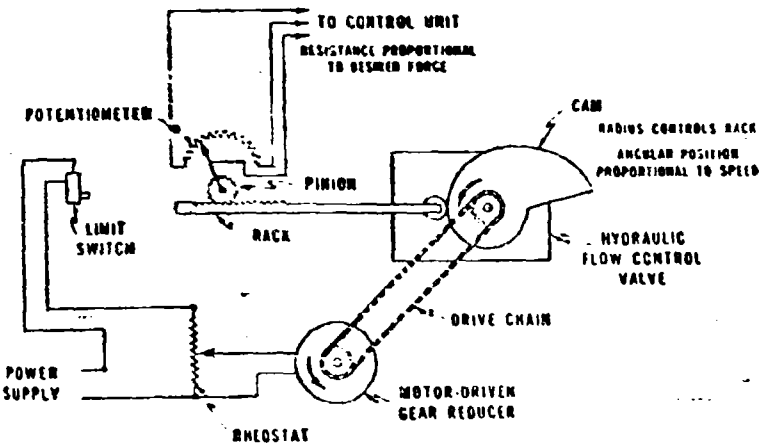


Fig. 15. — Schematic diagram of variable-force control system.

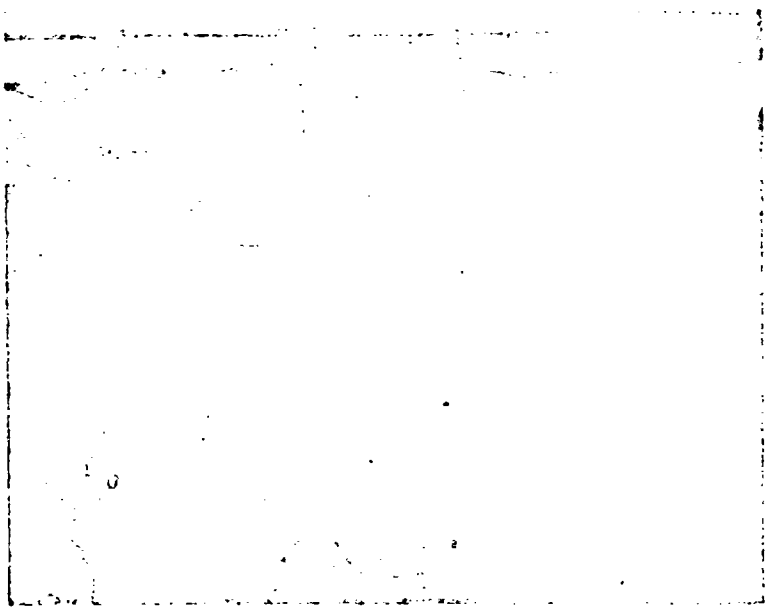


Fig. 16. — Operation and control stand.

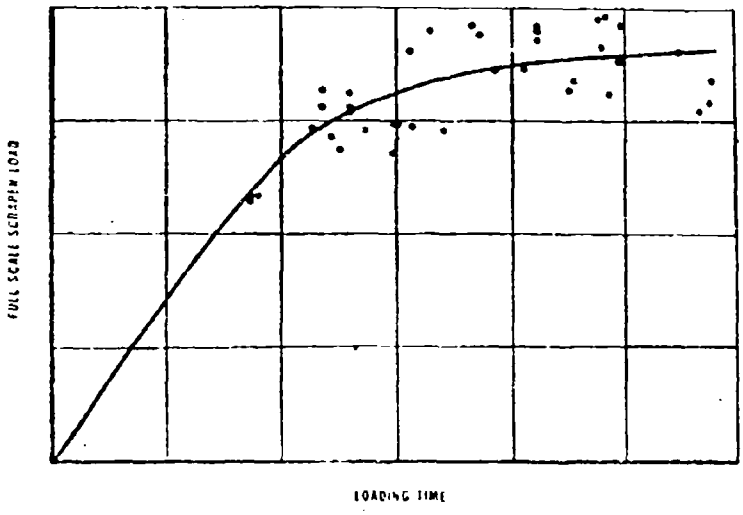


Fig. 17. — Field scraper loading curve.

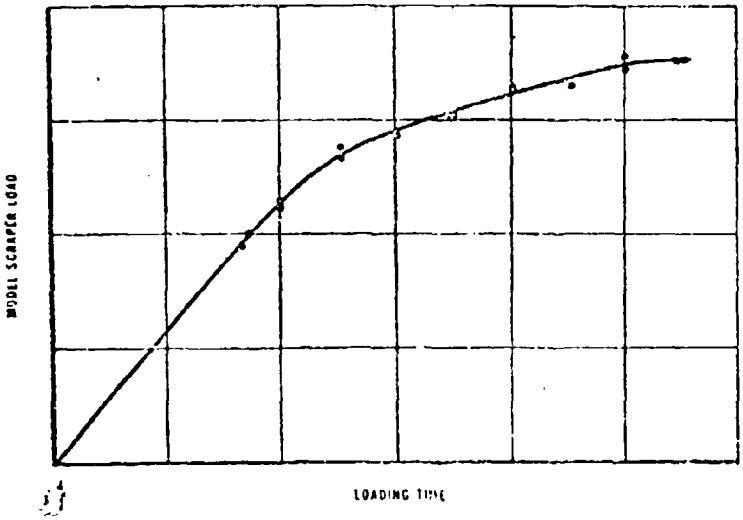


Fig. 18. — Soil bin scraper loading curve.

DISCUSSIONS

B. MAYFIELD. — I should like to question one or two of the authors' assertions in the section in the paper headed «Requirements and limitations of model tests», in connection with the scaling of various test quantities. Prof. Goodman mentioned yesterday, and Mr. Nuttall has mentioned in previous papers, that velocity considerations are not the same as stated in this paper. I should like to ask the author if possible, please, whether the velocity requirements, in other words that the velocity of the model must be equal to the velocity of the full-scale machine multiplied by the square root of the scale factor, is based purely on theory, that is Froude's number, or based on practical tests.

R. J. SULLIVAN. — In answer to the question: the basis is theoretical in other words a dimensional analysis, with various resulting dimensionless groups. I do not recall whether the Froude number as such appears as one of the groups, but at least with the variables we consider, the velocity did come out scaled as indicated. Test results indicate the scaling to be of the right order of magnitude.

L. J. GOODMAN. — I would like to ask Mr. Sullivan a question as to whether or not determinations of the shearing strength of soil were made by using the models, and if so: what is used for the shear area?

R. J. SULLIVAN. — For determination of shear strength we have used mostly a simple flat grouser plate, pressing down with various amounts of normal force, and determining the force required to shear the soil horizontally. The area we took is the geometrical area of the plate.

L. J. GOODMAN. — I would like to ask one further question. We have observed in some of our work, at Syracuse University, on the shearing strength of a soil by using a similar technique, that in a clay soil the area is somewhat larger then the geometric area of the plate itself. And I would like to ask if the people at the tractor company had made any observations on this.

R. J. SULLIVAN. — No. I had read that statement in your paper and was interested in it, but we are not able to compare this with our experience. We simply took the area that was available, and so I cannot say whether that applies to our situation.

E. SAIBEL. — I would like to ask Mr. Sullivan if he would give us a little more information about the parameter groupings by which he gets results for the prototype from the models. Just what these variables are, how they are grouped, and if he can give us some information about how good the results are from the model; how they project the prototype behaviour.

R. J. SULLIVAN. — I will rely on memory. I think I have already stated, Prof. Saibel, that the actual quantitative prediction of performance from a model to a full-scale, particularly with a very small scale model as we are using, is not a precise thing at this time. We are relying on visual appearance, on being able actually to observe the full-scale vehicle also; at the present time we would not want to take a model, run it in the towing tank and say: it did this, therefore a full-scale machine will do so many times this. We are not able to take that for granted. I would have to write out the dimensionless terms, but I can say that the variables we considered were the depth of cut, the linear dimension of the machine, the acceleration of gravity, the density, the velocity, the force, the weight of soil being moved, the cohesion and the friction angle of the soil — if that is nine it is all of them; I would have to sit down and work out the terms.

Instrumentation for land locomotion studies

Apparecchiature per lo studio del movimento fuori strada dei veicoli

WESLEY F. BUCHELE *)

ABSTRACT. — *The use of a number of instruments designed, constructed and developed for various research projects at Michigan State University were discussed. Three diaphragm transducers containing strain gauges were used to measure the normal stresses in the soil and soil-tire interface pressures. A three-inch diameter brass ball, containing twelve flush-mounted three-quarter-inch diameter transducers, was used to measure the stresses at a point in the soil. An undisturbed core sampler capable of pulling a sixty-inch long core was developed. A mean stress transducer and a recording volumeter were used to record dynamic test data. The combining of soil renovating equipment and soil test bins provided a means of securing replicated tests with the same soil under standard conditions.*

Introduction. — In order to gain data for the study of the behavior of soils under the influence of wheel traffic and tillage implements, a number of instruments have been designed, constructed and developed at Michigan State University. The purpose of this paper is to present the soil measuring instruments developed and to indicate the uses of each instrument.

Diaphragm strain transducers. — Cooper et al.[1,2] developed a Type A diaphragm transducer, shown in figure 1 and 3, to measure stresses normal to the surface of the diaphragm. The biscuit-shaped transducer was two inches in diameter and three-fourths of an inch in height. Two active Type A A-18 SR-4 strain gauges were glued to the inside wall of the cylindrical box. The range of the transducer, with 0.025 inch diaphragm, was linear between 0 and 40 psi. The transducers were used to measure the stress distribution in the soil as wheels and tillage implements traveled over a line of gauges placed at various depths across the path of the vehicle. Numerous isopiestic graphs were drawn to show the normal stress distribution in the soil under tires and implements.

Measurement of tire-soil interface pressure. — Because the Type A diaphragm transducers were too large to be placed in the lugs of rubber

*) Paper authorized for publication as Journal Article No. 2854 of the Michigan Agricultural Experiment Station, East Lansing, Michigan. The author, Wesley F. Buchele, is Associate Professor of Agricultural Engineering at Michigan State University.

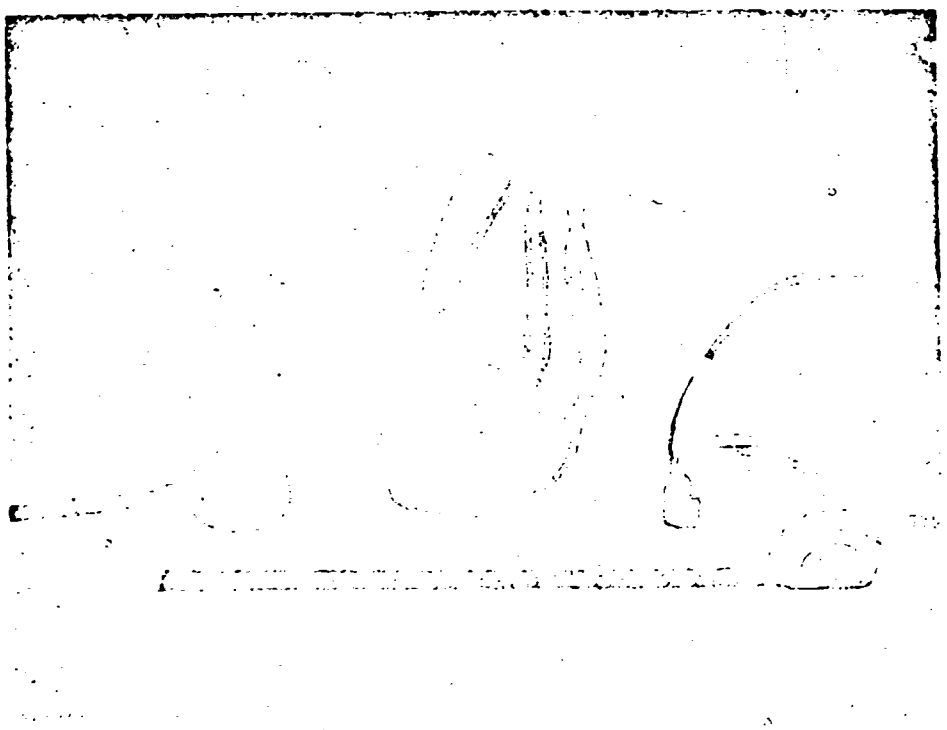


Fig. 1. — Diaphragm transducers. Type A transducer on the left, Type D transducer in the middle. The sensing transducer of the mean stress transducer is shown on the right. Type C transducers are shown located in the Type D transducer and mean stress transducer.

agricultural tractor tires, a Type B diaphragm transducer one-half inch in height was developed by Trabbic, Lask and Buchele[4]. One Type A-18 SR-4 strain gauge was glued to the diaphragm. Three dummy gauges were located on a block placed near the tractor. Several layers of cotton cloth covered with masking tape were used to insulate the nontemperature-compensated transducers from the soil as the tire rolled on the soil. Five Type B transducers were placed on the leading and trailing sides and on the top of a lug of an agricultural tractor tire. Since each lug ends on the parting line of the tire, a total of ten transducers were used in the two adjacent lugs. Ten other diaphragms were placed in the undertread between the two lugs.

The ten transducers spaced across the tire presented a graphical picture of the magnitude of the pressure developed at the soil-tire interface as the tire rolled on the soil. The transducers provided information concerning the rolling resistance of the wheel, the tractive force developed by the wheel, and the dynamic weight of the tractor. Since the tire rotated, the instantaneous tire-soil interface pressure was recorded on a time-base graph through the entire angle of contact. The location against the tire of the resultant of all the soil reactions

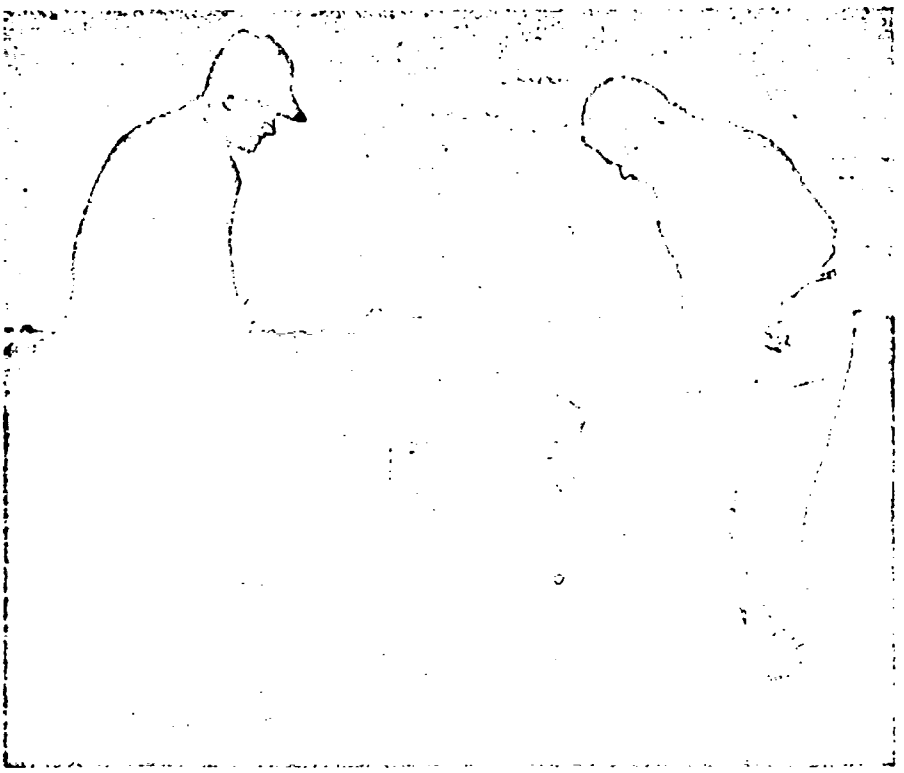


Fig. 2. — The undisturbed core sampler is operated by two men and can pull cores up to 60 inches in length. Approximately 1 to 2 minutes is required to take a soil sample.

was calculated from the data. The relationships between rear axle torque, drawbar pull, tire pressure, and slip were studied.

Powered undisturbed soil sampler. — The effect of wheel traffic, weathering, plant root growth, etc., upon the bulk density of the soil has interested many research workers.

A powered undisturbed soil core sampler, shown in figure 2, was developed by Buchele [4]. This sampler was capable of pulling (depending on the ability of the soil to support its own weight) a 60-inch long core.

An open-centered auger (containing a concentrically located soil tube) cut an annulus in the soil larger in diameter than the soil tube and below the trimming edge of the soil tube. The soil tube (containing the tube liners three inches in height) followed the auger bits and trimmed the emerging soil column to an exact dimension. When the desired depth had been reached, the soil tube, complete with liners and tube, was pulled from the sampler. The soil column and the tube liners were pushed from the soil tube and sectioned with

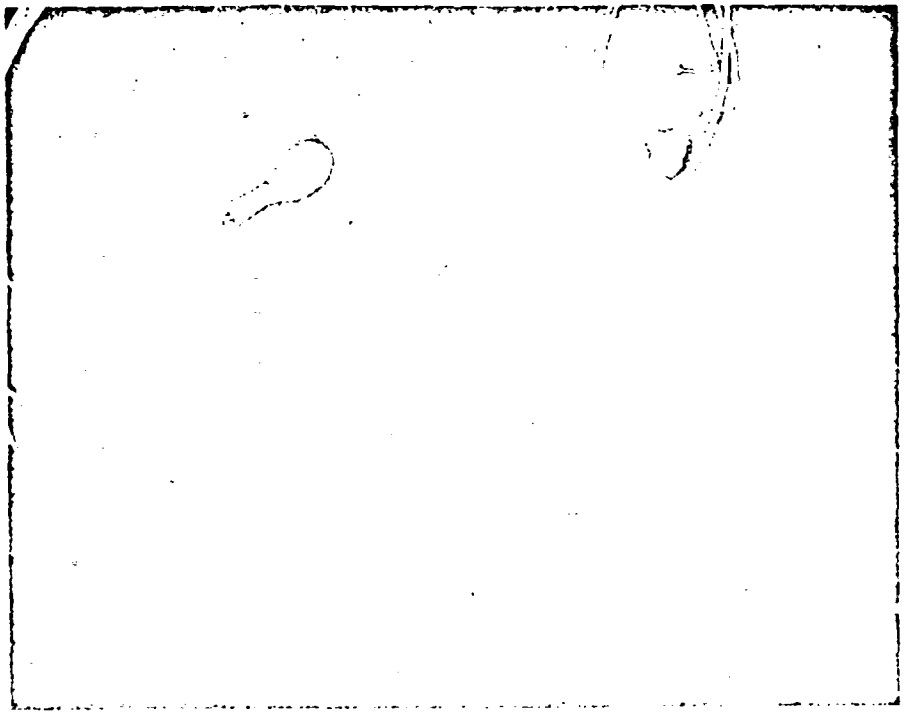


Fig. 3. — The location of the Type A and Type D transducers and the recording volumeter balloon on a circle concentric with the soil tank. Notice the positions of the Type A transducers.

a knife by cutting between the tube liners. The diameter of the core was equal to that of the trimming edge of the soil tube while the height was equal to that of the tube liner.

Stress-strain relationship in soil. — The hypothesis, that changes in mean stress are related to changes in bulk density, was studied by Vanden Berg, Buchele and Malven[5]. An attempt to establish a stress-strain law was made by using continuum mechanics concepts and appealing to rotational symmetry. Type A diaphragm transducers and the balloons of an indicating volumeter (fig. 3) were located on the periphery of a circle at various depths and a loading plate was concentrically placed on the surface of the soil.

While the hypothesis was not proved at the 95 % confidence level, neither was it disproved. Changes in bulk density were found, however, to be best related to changes in mean stress.

The above hypothesis proposed by Vanden Berg[5] was dynamically studied by Harris[6]. A Type D diaphragm six-directional stress transducer was constructed by locating twelve Type C diaphragm transducers in a three-inch diameter brass ball, as shown in figure 1. The Type C transducer was similar

to the Type B except that it contained a one-half inch Bradshaw foil gauge consisting of two independent circuits.

A pair of Type C transducers was located flush with the surface of the ball diametrically opposite each other on each of the three mutually perpendicular planes of the Type D transducers. The other six transducers were oriented in the planes that bisect any two of the three mutually perpendicular planes.

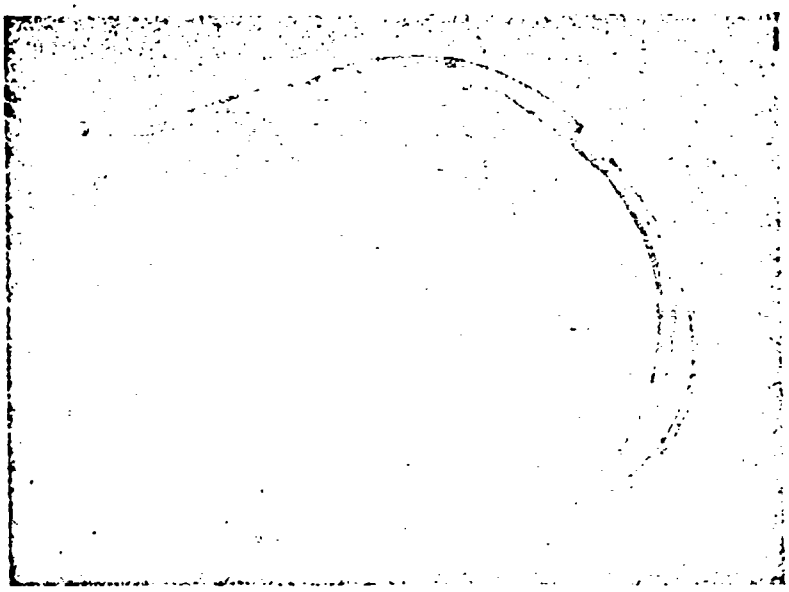


Fig. 4. — The mean stress transducer consists of a toy balloon filled with water, rigid plastic tubing and a Type C transducer held in an adapter.

The two arms of the two diametrically opposite Type C transducers were hooked together into a wheatstone bridge circuit. The bridge arrangement gave an average of the two separate readings.

A mean stress transducer shown in figure 1 and figure 4 was assembled by attaching a water-filled balloon to one end of a length of rigid plastic tubing. The other end of the tubing was attached by an adaptor to the diaphragm side of the Type C transducer. The Type D transducer and the mean stress transducer were placed in the soil at various depths and in concentric circles with the Type A transducer and the recording volumeter.

The effect of rates of loading and moisture content upon changes in density under various stress states was studied dynamically.

Of the various dynamic relationships studied, the changes in bulk density were found best related to changes in maximum shear stress.

In situ measurements of bulk density. — The undisturbed soil sampler (fig. 2) indicated the initial and final bulk density but did not show how or

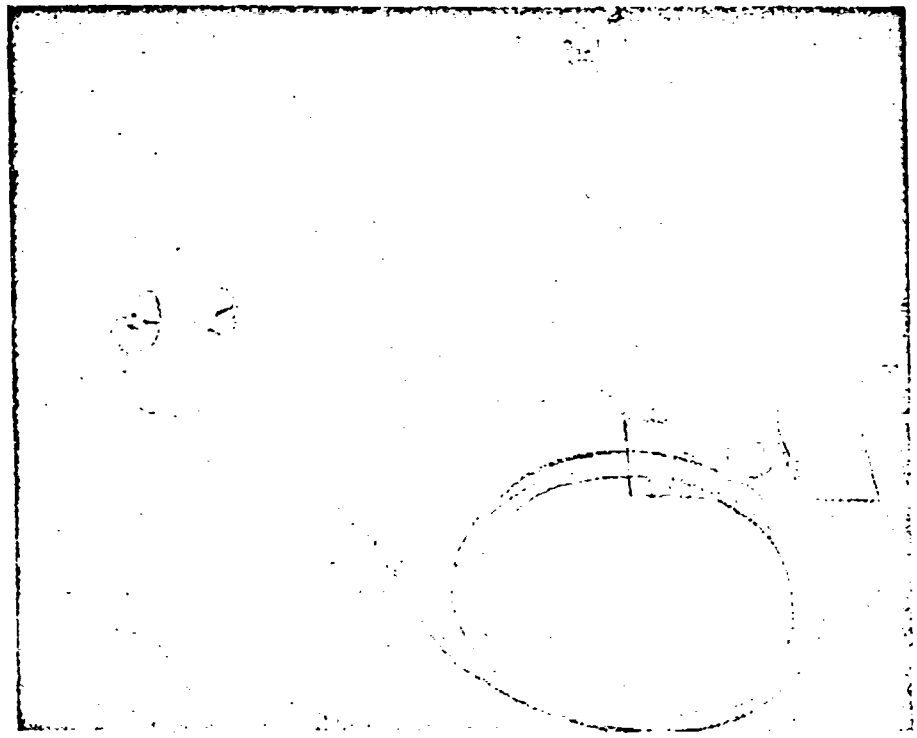


Fig. 5. — The recording volumeter consists of a toy balloon filled with soil, rigid plastic tubing and a diaphragm housing. The initial and final bulk density is determined by weighing the balloon in and out of water.

when these changes occurred. The static changes in bulk density were measured with an indicating volumeter developed by Hovanesian, Vanden Berg and McColly.

The dynamic changes in bulk density were measured with a recording volumeter shown in figure 5 developed by Hovanesian and Buchele [7]. This work was conducted concurrently with Vanden Berg [8].

The recording volumeter consisted of a volumetric transducer, rigid plastic tubing, and a toy balloon. The transducer contained a 0.007-inch thick stainless steel diaphragm housed between two air chambers. Four Type A-18 SR-4 strain gauges were glued to the diaphragm, two in the center, and two diametrically opposite each other on the periphery. One air chamber was sealed and the other was attached to a length of rigid plastic tubing. The other end of this tubing was attached to the toy balloon. Disturbed soil from the experimental site was placed in the balloon before the balloon was attached to the plastic tubing.

The recording volumeter was used to study the dynamic relation between changes in mean stress created in a hydraulic pressure chamber and changes

in bulk density. The bulk density γ was found related to mean stress σ_m by the equation

$$\gamma = \gamma_0 + B \ln \frac{\sigma}{\sigma_0}$$

Where:

σ_0 = the initial mean stress state;
γ_0 = the initial bulk density (before loading);
B = a parametric constant depending on soil parameters.

Hydraulic operated bevameter. -- The bevameter developed at the Land Locomotion Laboratory was further developed by Stong [5] by welding three-point-hitch attaching points to the frame. A three-point-hitch tractor was used to raise, transport and lower the bevameter and supply hydraulic power to operate the shear head and penetrometer. They studied the effect of tillage operations, wheel traffic, weathering and freezing and thawing upon the Bekker values, soil moisture and bulk density.

On the soil tested, between the moisture range of 11 and 22 percent, changes in bulk density from 1.05 to 1.28 affected the soil values more than moisture content.

Freezing and thawing increased cohesion and decreased the angle of internal shear (Φ) but did not affect k_ϕ, k_c, and n.

Plowing decreased C and Φ. Disking increased Φ and k_c and decreased the other parameter.

Soil renovating equipment. — Harris [6] and Stong [5] constructed a soil renovator for the mechanical processing, handling and containing the soil for test purposes. The renovator shown in figure 6 consisted of two removable bottomed tanks, two soil conveyor belts, central elevator, screens, and spray equipment.

Two tanks (5 feet diameter X 4 feet deep) were located over the soil conveyor belts. Only one tank of soil was used at a time and renovation of the soil was accomplished by moving the soil from one tank to the other tank and back to the first tank. Water was added at the discarge points of the conveyor belts.

Each conveyor belt discarged into a central hopper where the soil was immediately elevated and dumped into the opposite tank.

Since the soil measuring instruments were located above one of the tanks, the other tank was used only for storage during a particular set of experiments. The size of the clods and the height of fall of the soil was controlled by placing a screen over the instrumented tank and letting the soil fall through it into the tank.

Vibrators were placed below one of the tanks and were used to consolidate the soil into various bulk densities. Air tampers were used to produce layers of soil of high bulk density. The hydraulic bevameter was located above one tank and a 20-inch diameter pressure plate operated by a hydraulic ram was placed above the other tank.

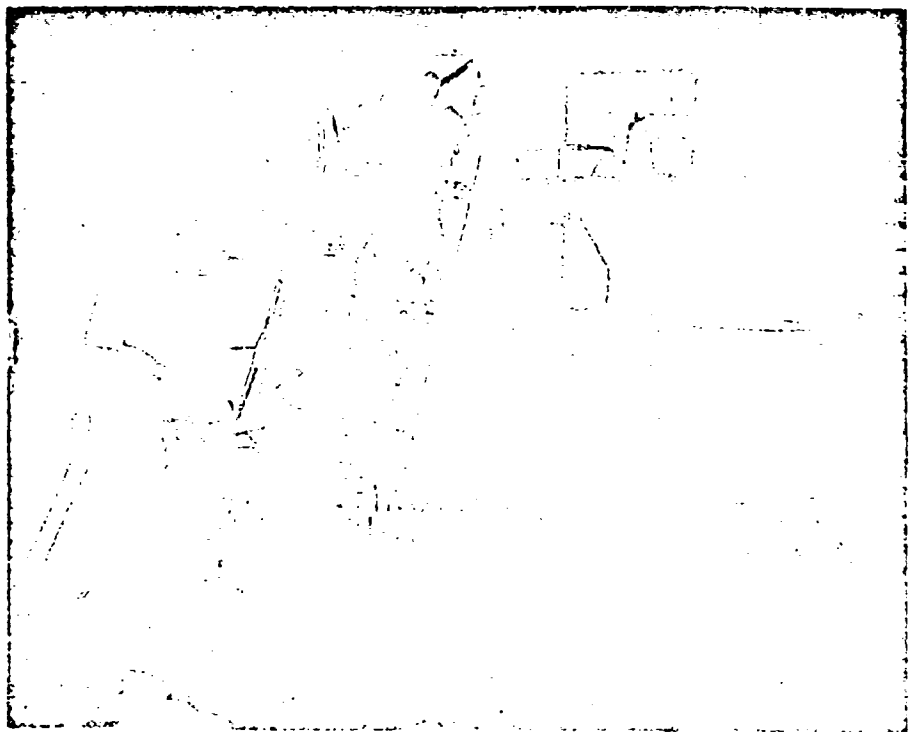


Fig. 6. — The soil renovator reconditioned the soil after each test to provide a means of securing replications of a treatment on a standard soil condition using the same soil. The pressure plate used by Harris [6] and hydraulic pump is also shown.

Discussion. — The research work in soil mechanics has lead to the development of a number of soil instruments, has provided theoretical and empirical information concerning soil behavior under the influence of load and weather, and has motivated the teaching of a graduate course in this area.

The development of dynamic recording instruments has increased the understanding of the soils under the influence of moving vehicles.

Conclusions. — 1) Stress-strain laws can be tested under dynamic conditions.

2) Bulk density has a definite effect upon soil parameters.

3) A soil renovator for reconditioning and handling laboratory soils has been constructed.

4) Design, construction and development of instruments is an important part of soil mechanics research.

ACKNOWLEDGMENT. — The Author acknowledges the support of the Land Locomotion Laboratory, Detroit Arsenal, Centerline, Michigan.

BIBLIOGRAPHY

1) Cooper A. W., Vanden Berg G. E., McColly H. F. and Erickson A. E. Strain gauge cell measures soil pressure. Agricultural Engineering, 32, 232-235, 246, 1957.

2) Vanden Berg G. E., Cooper A. W., Erickson A. E. and Carleton W. M. Soil pressure distribution under tractor and implement traffic. Agricultural Engineering, 38, 854-859, 1957.

3) Trabbic G. W., Lask K. V. and Buchele W. F. Measurement of soil tire interface pressures. Agricultural Engineering, 40, 678-681, 1959.

4) Buchele W. F. The design of an undisturbed core sampler. Transactions of ASAE, In press, 1961.

5) Vanden Berg G. E., Buchele W. F. and Malvern L. E. Application of continuum mechanics to soil compaction. Transaction of ASAE, 1, 24-27, 1958.

6) Harris, Wesley Lamar. Dynamic stress transducers and the use of continuum mechanics in the study of various soil stress-strain relationships. Unpublished PhD thesis, Michigan State University Library, 1960.

7) Hovanesian J. E. and Buchele W. F. Development of a recording volumetric transducer for studying effects of soil parameters on compaction. Transaction of ASAE, 2, 78-80, 1959.

8) Stong Jack V. Basic factors affecting the strength and sinkage of tillable soils. Unpublished MS thesis, Michigan State University Library, 1960.

DISCUSSION

J. REMUS. — Je voudrais simplement revenir sur l'un des points de l'exposé tellement interessant qui vient de nous être fait. Il révèle un ensemble d'équipement qui a la particularité d'être extrêmement mobile, et par conséquent de permettre des recherches aussi bien sur des sols en place que sur des sols homogénéisés et amené en laboratoire. Je voudrais signaler que sur un point particulier nous avons poursuivi en France des recherches depuis environ une dizaine d'années sur le problème du tassement du sol par le passage des véhicules agricoles. Le compactage du sol, qui est un avantage dans le cas des travaux publics, par exemple, est au contraire un inconvénient en agriculture puisqu'il est nécessaire de préserver les espaces lacunaires dans le sol et d'éviter la compaction. D'ailleurs, mes collègues allemands qui sont ici se sont eux-mêmes depuis longtemps penchés sur cette question. Nous avons utilisé en France une méthode analogue, c'est-à-dire nous avons eu recours aux jauges de contrainte, mais nous nous sommes systématiquement désintéressés des essais dans des sols homogénéisés en laboratoire. Si l'on examine une coupe de sol arable, on rencontre trois zones parallèles:

— *Les cinq premiers centimètres* sont au contact direct de l'air extérieur, de la pluie et du vent. Le passage des véhicules et des animaux s'y fait sentir dans tous les cas, et plus particulièrement le patinage des roues. Ce dernier phénomène, conséquence d'une adhérence inévitablement imparfaite, a pour effet un brassage des terres de structures fines et la lacération des petites racines.

— *La zone régulièrement labourée.* - Si ce labour est convenablement effectué, il doit, au moins une fois par an (sauf dans les luzernières), détruire toutes les conséquences vraies ou supposées d'un éventuel tassement. Il n'y a pas de risque d'effet durable. Néanmoins, on peut considérer le cas de la culture en cours de végétation

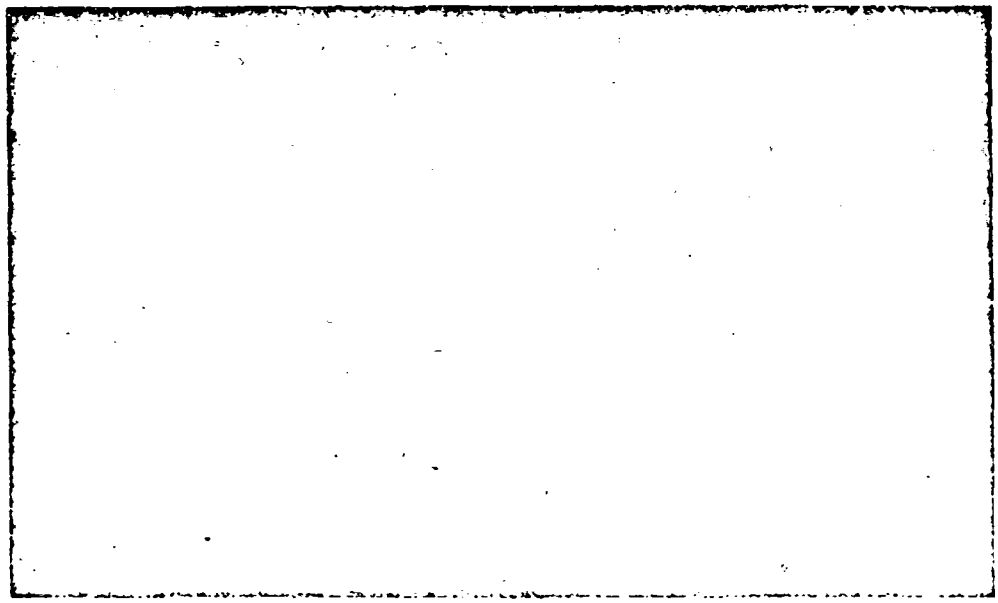


Fig. A.

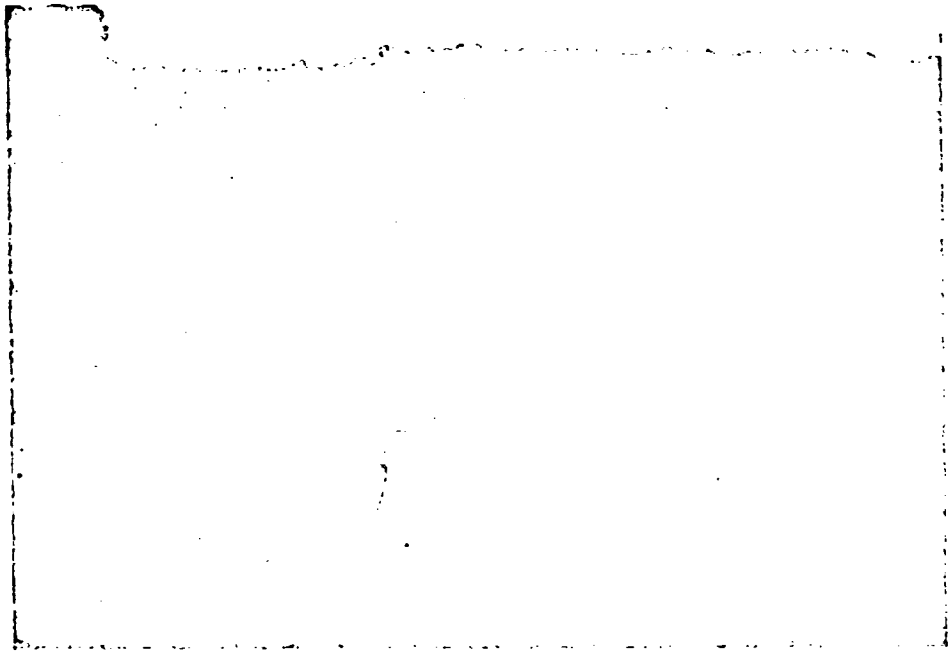


Fig. B.

dont le développement pourrait théoriquement être retardé ou compromis par des passages de tracteurs et de machines après les semis. Dans le cas des traitements antiparasitaires par exemple.

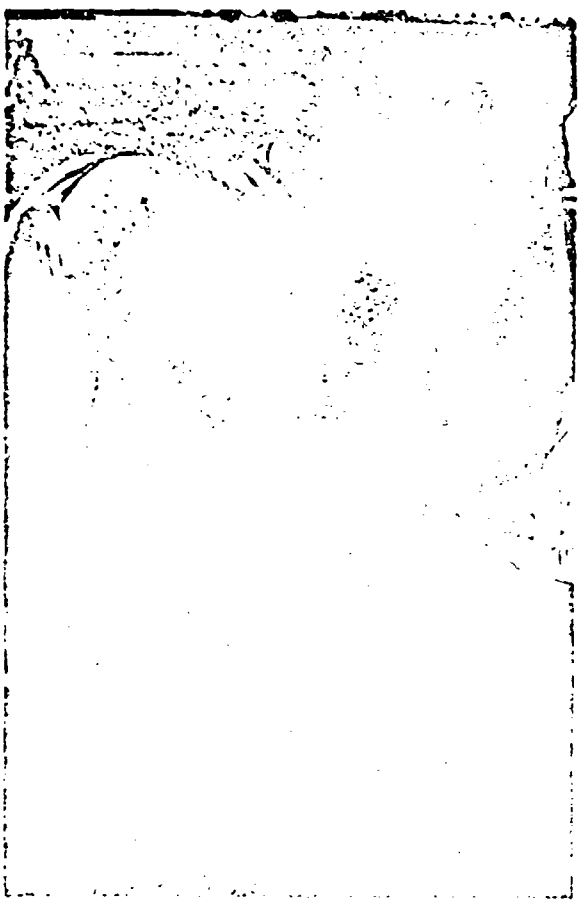


Fig. C.

— *Enfin, la zone sous-jacente.* - Celle-ci n'est pratiquement jamais disloquée, aérée, regonflée. Or, il a été constaté une brusque diminution de la porosité au-dessous de la couche labourée. Il y a par conséquent, à ce niveau, une asphyxie du sol dont il faut trouver les causes et les remèdes.

Il y a longtemps, en fait, qu'on essaie d'étudier la circulation des liquides et de l'air dans le sol, et le développement des racines en fonction des espaces lacunaires.

Lorsque le sol a subi une compression, il faut examiner les causes, la durée et les conséquences pour la porosité du sol, et, ce qui est la seule chose qui, en définitive, nous intéresse, le comportement de la plante dans le sol comprimé.

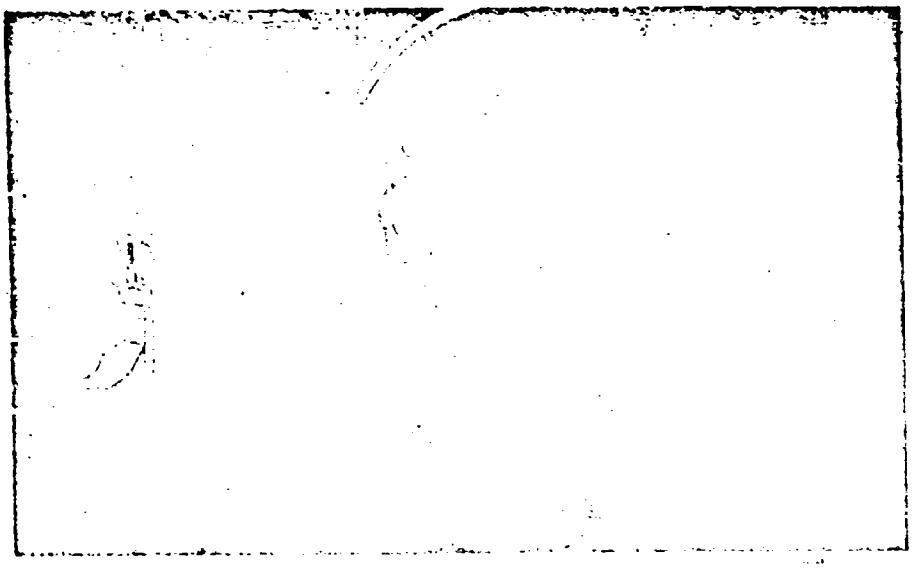


Fig. D.

Faute d'un moyen direct d'étudier jusqu'à présent cette compression dans le sol en place, on en a souvent examiné les conséquences, soit :

— la variation du poids spécifique du sol comprimé (Fontaine et Payne);

— soit la variation de la vitesse de l'écoulement de l'eau (Sékéra);

— le temps de passage d'un volume d'air (Buesse avec l'appareil de Von Janert);

— soit, enfin, le développement des systèmes radiculaires dans des sols tassés ou non (Johannès Görbing).

Ces différentes méthodes, qui nécessitent des prélèvements d'échantillons mal délimités et inévitablement non identiques, ont donné cependant des résultats intéressants, mais ne nous ont rien appris sur les compressions dont elle examinent les conséquences plus ou moins lointaines.

Par ailleurs, on a également essayé des mesures avec des manomètres à huile, à quartz et à self, mais ces appareils se sont montrés encombrants, fragiles et inefficaces.

La méthode que nous allons examiner maintenant permet d'opérer des mesures sur le sol en place, sans prélèvement, ni perturbation préalable.

Elle tente, par ailleurs, d'analyser le phénomène lui-même et non plus ses conséquences.

Elle est pratiquée depuis 1953 et utilise la technique des mesures par « strain-gage » qui était à l'époque peu répandue, mais est maintenant couramment appliquée aux mesures de contraintes dans le sol, ainsi que le montre la communication de M. Buchele.

Mais elle reste originale en ce sens que, comme nous venons de le dire, elle permet de faire des mesures dans de sols en place.

En quoi consiste la méthode?

On creuse dans le champ une fosse de m. 1,50 de long et de la profondeur voulue. Les extrémités de la fosse doivent être horizontalement à m. 1,50 de la zone où l'on veut effectuer la mesure.

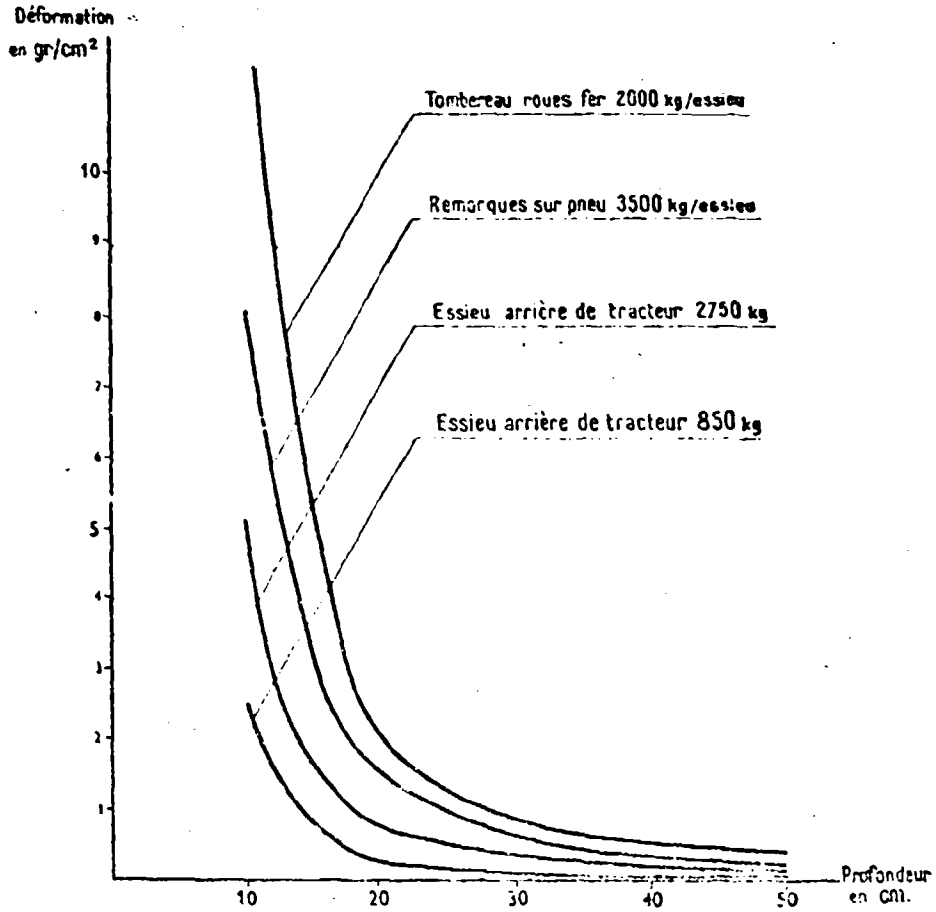


Fig. 1. — Déformation d'un même sol (argilo-siliceux, humidité 18 %) sous différentes charges. C'est la déformation maximum à la fin du stationnement du véhicule à la verticale du capteur.

On effectue horizontalement, à la profondeur désirée pour la mesure, un carottage dans la paroi de la fosse à l'aide d'une mince canne d'acier creuse à l'extrémité tranchante. L'opération est menée de façon à éviter toute compression de cette canne sur les parois du tunnel qu'elle creuse.

On introduit à sa place ensuite une seconde canne de section légèrement inférieure et qui porte à son extrémité une capsule d'acier portant des jauges de contraintes.

On peut introduire simultanément plusieurs cannes à des profondeurs différentes et orienter les capsules dans le sens désiré pour la mesure, par rapport au plan horizontal.

Les jauges sont reliées à un système d'amplification et d'enregistrement, avec des montages classiques en pont de Wheatstone.

L'appareillage a été réalisé en 52/53 par le Laboratoire de Technique Electronique sur les directives de M. de Wreden de la S. A. Dunlop et du Professeur S. Henin, Directeur du Laboratoire du Sol.

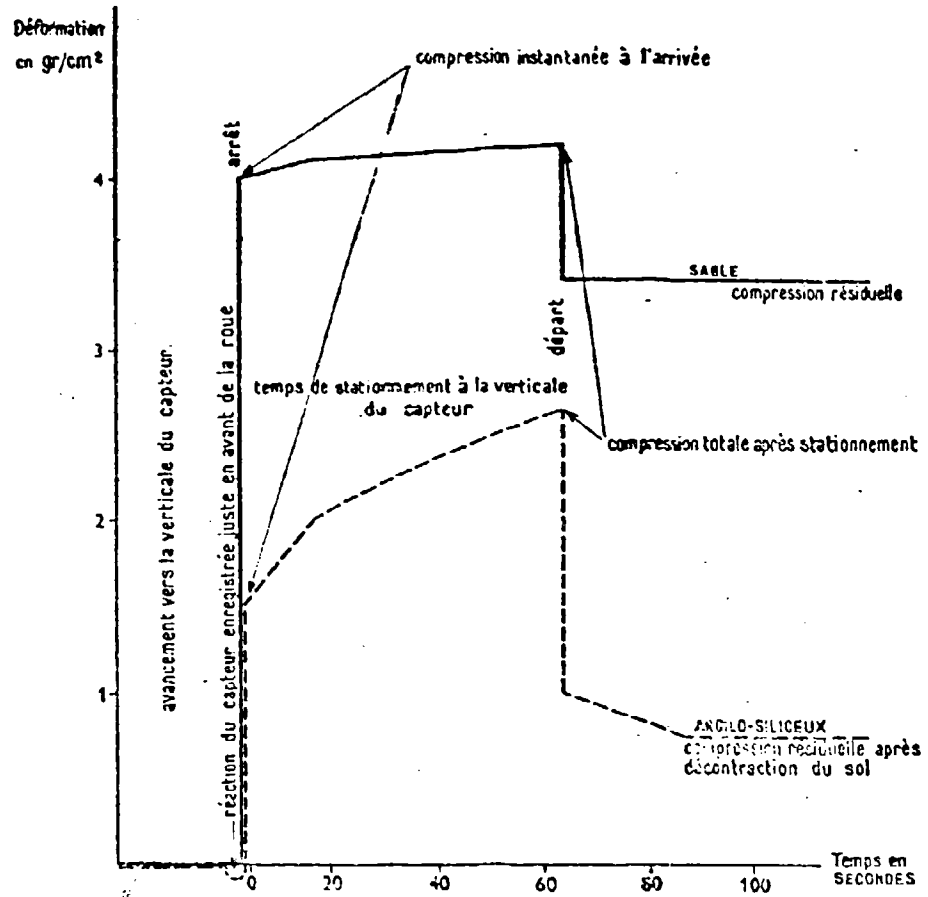


Fig. 2. — Comparaison de la compression instantanée, de l'effet du stationnement de la roue immobile, et de la compression résiduelle, pour un pneu de tracteur de 850 kg. de charge sur l'essieu, sur friche de betteraves à 10 cm. de profondeur: 1) argilo-siliceux, humidité 14 %; 2) sol totalement sableux, humidité 8 %.

Que mesure-t-on?

Le sol n'est pas un corps homogène, on ne mesure donc pas des pressions, mais des compressions. Les unités, arbitraires, sont exprimées en gr/cm² par analogie avec les mesures d'étalonnage des sondes sous pression d'huile. Les valeurs sont donc comparables entre elles.

Quelle est l'intensité de la déformation?

Elle est liée aux différents éléments: la nature du terrain, son degré d'humidité, la nature, le poids et la vitesse du véhicule, le gonflement des pneus.

Rappelons que la pression des pneus au travail sur le champ est normalement comprise entre 800 et 1.200 grammes pour les pneus simples et 500 à 600 grammes pour les pneus jumelés. Ce qui se traduit par une pression sur le sol égale à la pression

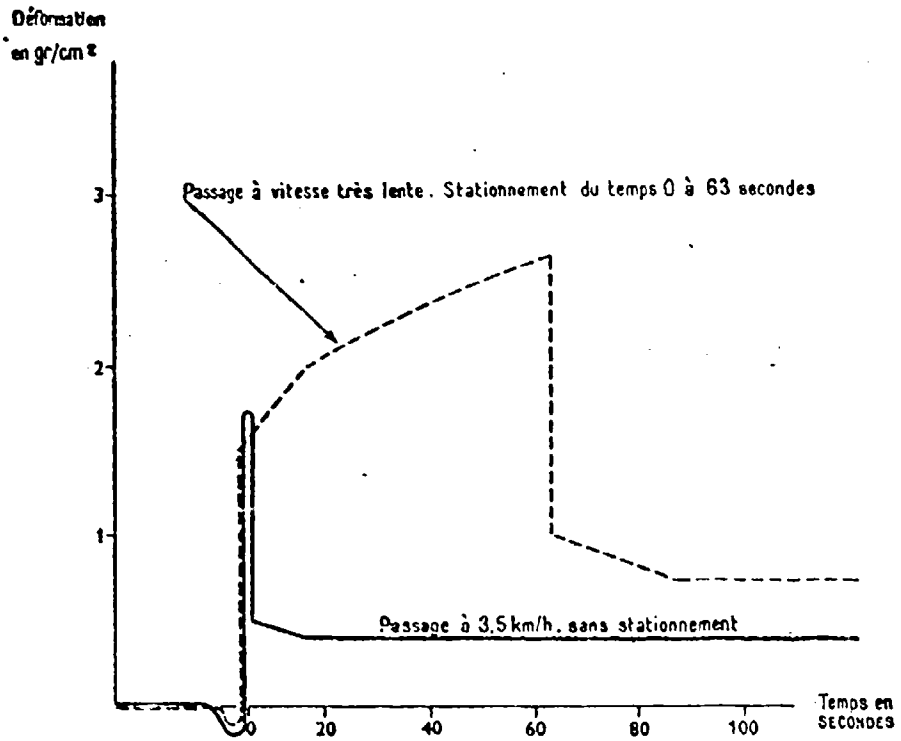


Fig. 3. — Comparaison entre les effets de compression sur sol argilo-siliceux, humidité 14 % à 10 cm. de profondeur du même tracteur: 1) arrivée à vitesse lente, arrêt et départ; 2) passage sans arrêt à 3,6 km/h.

de gonflement (condition essentielle de l'équilibre du pneu) majorée d'une certaine quantité, environ 10 %, due à ce que l'enveloppe du pneu n'est pas idéalement élastique. A 10 centimètres de profondeur, la compression est d'environ 5 à 10 gr/cm² pour un sol argileux compact, et va jusqu'à quelques dizaines de grammes dans un sol sablonneux sans cohésion.

Comment se déroule le phénomène?

Laissons la parole au Professeur Henin:

« Grâce à cet appareil on peut alors suivre en détail les modifications subies par le sol à une profondeur donnée soit par le passage d'un instrument, soit par l'application d'une charge fixe. En particulier quand un véhicule vient se mettre en station on observe à son approche une légère décompression du sol. Celle-ci correspond à l'effet foisonnement qui compense partiellement l'enfoncement du terrain consécutif à l'application de la charge. Puis lorsque l'engin arrive à la verticale de la sonde, on constate un effondrement plus ou moins marqué, mais qui n'atteint sa valeur maxima qu'après un temps qui s'élève parfois à plusieurs secondes. Au moment du départ de l'engin, on observe une décompression d'importance extrêmement variable, mais cette détente n'est également complète qu'après un temps qui peut atteindre lui-même plusieurs

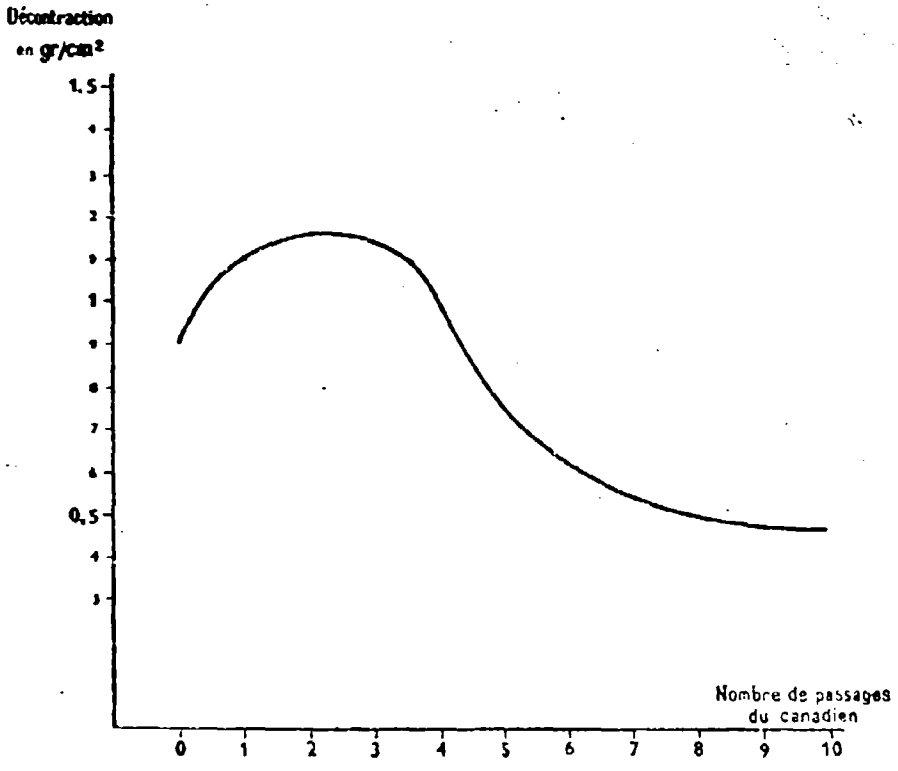


Fig. 4. — Variations de la décontraction (écart entre la compression initiale et la compression résiduelle) sous l'effet du travail d'un sol (passages multiples du canadien). Mesure à 10 cm. sol argilo-siliceux à 18 % d'humidité; friche de betteraves. Passage d'un tracteur de 1200 kg. par essieu, après travail du sol au canadien. (Les mesures sont faites chaque fois en un point différent de la même bande de terrain après un passage, deux passages, etc., du canadien).

secondes. Si le véhicule passe sans s'arrêter, on constate une compressione brutale suivie d'un effet élastique qui paraît d'autant plus marqué que le déplacement du véhicule est plus rapide, du moins pour les terrains présentant une élasticité notable. Nous pensons que ces effets élastiques sont dus à l'atmosphère du sol qui en se détendant provoque un regonflement du terrain. Si la charge est appliquée pendant un temps assez long, l'air a le temps de s'échapper et les effets élastiques sont moins prononcés. Quant aux réactions lentes, elles nous paraissent attribuable à l'expulsion ou à la réabsorption de l'eau imbibant la masse colloïdale, comme dans le cas des mesures oedomètriques » *).

Résultat

Influence de la nature du sol. — Elle est évidente et les mesures confirment celles qui ont pu être faites par ailleurs en laboratoire sur échantillons.

La « décontraction » d'un sol argilo-sablonneux est plus importante que celle

*) Comptes rendus hebdomadaires des séances de l'Académie d'Agriculture de France, séance du 30 Juin 1954.

d'une sable qui peut même être nulle. Mais répètons-le, ce n'est pas dans le domaine de la nature même des sols que cet appareil a fourni des éléments nouveaux.

Influence de l'état du sol. — Là, les mesures sont intéressantes, car elles révèlent qu'un sol riche en humus se regonfle mieux qu'un sol de même densité et de même granulométrie, mais inerte.

On peut également mesurer l'influence du travail mécanique du sol. On constate qu'après plusieurs passages consécutifs d'un canadien par exemple, l'élasticité d'un sol argilo-silicieux augmente jusqu'à une certaine limite. Au-delà de celle-ci, l'accumulation des passages ne fait que comprimer davantage le sol. Donc un sol régulièrement cultivé et biologiquement sain, a une plus grande élasticité.

L'*humidité* du sol a bien entendu une influence certaine. La décontraction d'un sol d'humidité moyenne est de 9/10e, mais si l'humidité dépasse 40 % des espaces lacunaires, la décontraction tombe endessous de 3/10e.

Ceci est important dans les termins à forte rétention. Les travaux de printemps y sont souvent retardés et le cultivateur est souvent tenté de travailler des terres humides, de peur d'être distancé par la saison.

Il semble donc qu'il risque de détériorer sa terre qui ne « revient » pas après le passage du véhicule.

Influence du temps de passage. — Il a été signalé ci-dessus par le Professeur Henin.

C'est un phénomène qu'il faut probablement relier à la constatation suivante:

Si l'on compare un tracteur à roues et un tracteur à chenilles de même poids, le second provoque une compression plus faible que le premier, dans le 30 premiers centimètres. Mais cette compression, audelà des 30 centimètres, devient comparativement plus importante pour le tracteur à chenilles, quoique faible pour les deux tracteurs.

On peut supposer que, le temps d'appui de la chenille en un point du sol étant plus grand que celui d'un pneu pour deux vitesses d'avancement identiques, c'est effect de temps qui l'emporte sur celui de poids.

Signalon pour finir un inconvénient pour ce système de mesure qui est d'ailleurs commun à tous les moyens de mesures de compressions de sols que nous connaissons: il ne permet pas d'analyser correctement ce qui se passe dans les cinq premiers centimètres de profondeur.

Comparaisons mesurées à des profondeurs constantes, sur sol argileux, à 18 % *d'humidité, entre tracteur à chenille de* 4 *tonnes au total et un tracteur à roues de* 1750 *kgs/essieu moteur.*

Profondeur	Chenille	Roues
10 cm.	1,2	3,0
20 cm.	0,16	1,9
30 cm.	0,12	0,13
40 cm.	0,09	0,04

N. 29

A proposed recording penetrometer

Proposta di un penetrometro registratore

TRAFFICABILITY RESEARCH TEAM *)

ABSTRACT. — *Soil trafficability has become a subject of great importance to the military man, the tactical planner. For a long time it has just been in a category of research.*

Soil trafficability prediction, whether it be by a theoretical or an experimental method, requires the evaluation of certain factors related to soil physical properties beforehand. Such evaluation of factors requires instrumentation.

In the development stage, the cone penetrometer was designed to fulfill the requirements of research work in soil trafficability, as well as to be simple in operation. It works best when handled by trained people under quiet conditions and yields precise individual readings. For practical use, when these instruments serve as equipment for reconnaissance parties, it is important that they be operative by the smallest possible crew, not necessarily highly trained, by day and by night, and yield recorded readings for later interpretations.

In this light a discussion is being made on several instruments usable for the evaluation of soil trafficability, such as a cone index measuring instrument (the penetrometer) a soil shear measuring device (the shear vane), and slope measuring instruments. Special description is given of a cone penetrometer developed in Israel which records graphically the penetration resistance versus depth.

Introduction. — Soil trafficability has become a subject of great importance to the military man, the tactical planner. For a long time it has just been in a category of research.

Soil trafficability prediction whether it be by a theoretical or an experimental method, required the evaluation of some other factors related to soil physical properties beforehand. Such evaluations of factors require instrumentation.

In the development stage the cone penetrometer was designed to fulfill the requirements of research work in soil trafficability. It worked best by trained people under quiet conditions and yielded precise individual readings. For practical use, when this instrument should serve as equipment for reconnaissance parties, it is important that it be operative by the smallest possible crew, not necessarily highly trained, by day and by night and yield recorded readings for later interpretations.

In this light, a special description is given of a cone penetrometer developed in Israel which records graphically the penetration resistance versus depth.

*) Corps of Engineers Israel Defence Army.

Factors to be measured. — A close observation of factors which govern the trafficability properties of an area indicates the importance of

ground strength,
ground slope.

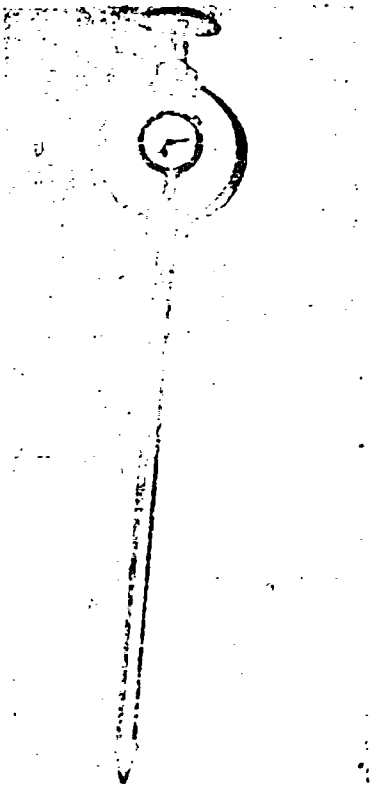


Fig. 1. — Dial penetrometer.

On the other hand, these factors are dependent on other variables such as soil physical properties and soil moisture. Evaluation of those other variables are not needed if there were means to determine the main factors precisely. Ground strength and slope constitute the key to trafficability forecasts from on-the-spot quick field tests.

Present day instruments. — Existing instruments in military use fall in two groups corresponding to the two factors they have been designed to measure:

Strength measuring instruments:
- cone penetrometer [2] (fig. 1),
- aerial penetrometer [1],
- shear vane [3],
- remolding instruments [4].

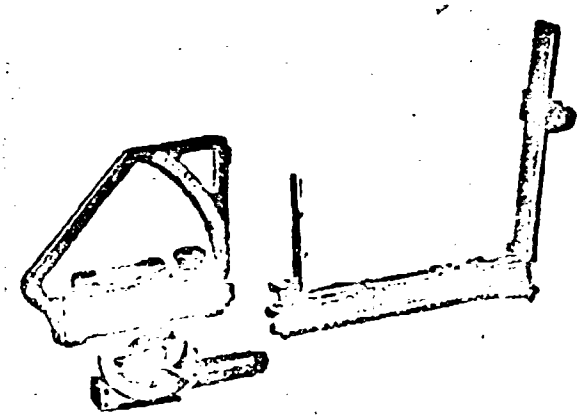


Fig. 2. — Inclinometers.

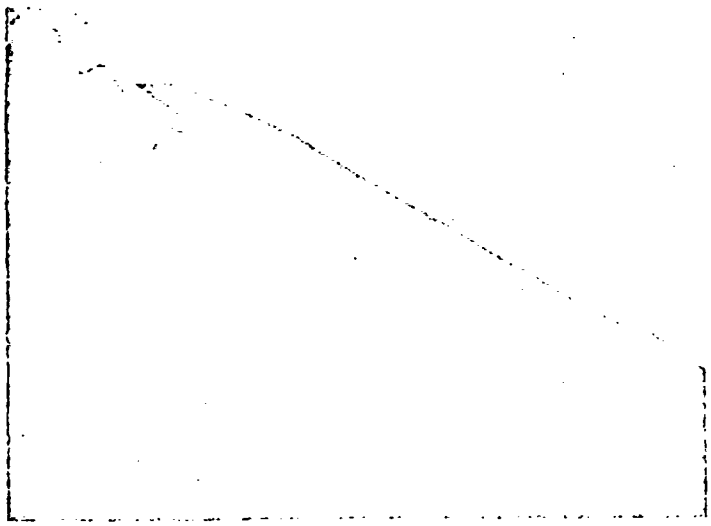


Fig. 3. — Proposed recording penetrometer.

Slope measuring instruments (fig. 2):
hand level,
inclinometer.

Not listed are the usual instruments found in the soil mechanics laboratories.

Drawbacks of present day instruments. — Most of the present day trafficability instruments in practical military use were originally developed for trafficability research work. Few were designed specifically for military use. Most of these instruments possess a number of drawbacks in application for

practical work. It is worthwhile to examine these disadvantages in order to better develop improved instruments.

Listed below are a number of important drawbacks to instruments presently in use which may be partially or completely characteristic of them:

1) Require an operating crew of two or more.

2) Not designed for speedy operations, where and when a great number of readings have to be taken.

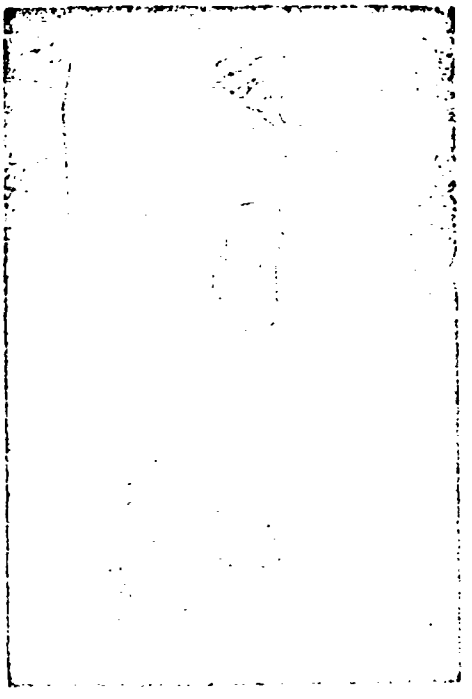


Fig. 4. — Recording penetrometer in operation.

3) Require observation and recording of separate readings.

4) Require instantaneous readings of small instruments. Human error under such an arrangement may be large, particularly with not very experienced operators, or under strained working conditions.

5) Not designed for night work.

6) Constructed of precise and fine parts, such as a deflectometer on a penetrometer.

Suggested improvements for the newly developed instruments. — 1) Must be rugged, shockproof and should not consist of delicate springwork or other parts.

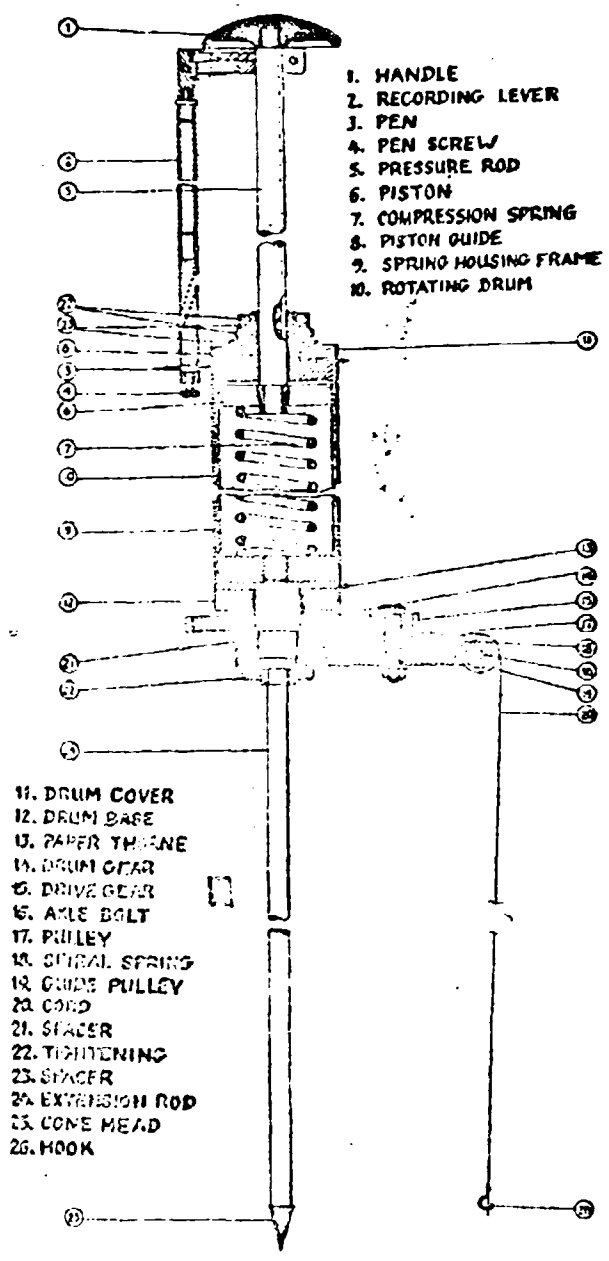


Fig. 5. — Recording penetrometer detail.

2) It should, where possible, be a self recording device. In this way much of the error caused in night reading or under strained conditions could be avoided.

3) Designed for a great number of readings, to be taken in the shortest possible time.

4) If it is not to be a recording instrument, it should still be suitable for night operation.

5) Should be light and transportable.

6) Be suitable for operation by one man.

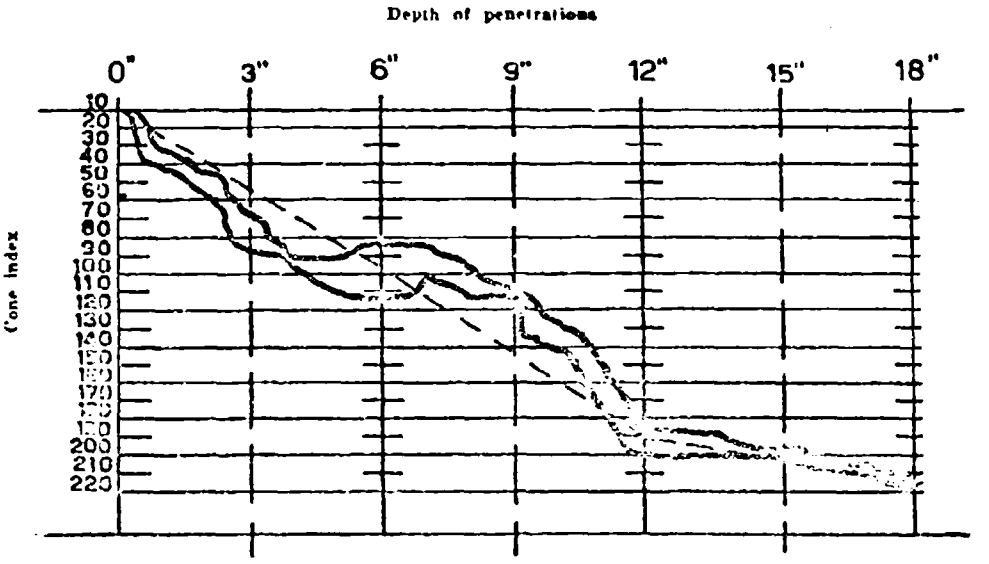


Fig. 6. — Example of recorded penetrations.

A proposed recording penetrometer. — The cone penetrometer measures soil strength through the resistance to penetration by a standard cone of various depths. The penetrometer developed by the U. S. Corps of Engineers measures the force applied in forcing the cone through the soil by the deflection of a proving ring as shown by a strain dial (fig. 1).

In spite of a number of advantages over other types of instruments, the present day penetrometer has most of the drawbacks listed above.

With the list of suggested improvements in mind a new penetrometer was developed on the principle of a recording instrument (fig. 3, 4, 5).

A description and discussion of the newly developed recording penetrometer is given below. It is expected that similar modifications may be made to other instruments used for the trafficability evaluation of a soil.

Principle : The recording penetrometer measures simultaneously the force required to push a standard cone (0,5" cross sectional area), into the ground

and its depth of penetration. The readings are recorded on a paper attached on to a rotating drum. The rotation of the drum is activated by loosening of a cord allowing a spiral spring to unwind.

Method of operation: The starting position of the penetrometer is as follows: the penetrometer is set on its two extension rods with the point of the cone just touching the ground surface. The cord is pulled out and tied to the operator's foot. At this position the cord length is about that of the extension rods. In pulling out the cord an internal spiral spring is wound up, thereby causing the drum to rotate and reach a starting position. As soon as force is applied from above to push the cone into the ground a vertical spring is compressed so that a recording pen is lowered. At this time the cord hooked to the operator's foot loosens, allowing the spiral spring to unwind and rotate the drum back. A line drawn on the paper is hence a resultant of a vertical component (that of the force of penetration) and a horizontal component (that of the depth of penetration).

About six penetrations are needed at one spot in order to provide a usable average.

Interpretation of ground strength of a desired layer is being achieved as follows. A line (dotted line) is drawn to combine the means of cone index values of whatever penetrations there were, at the 6", 12" and 18" marks. The 3", 9", 15" marks are midmarks for the 0-6", 6"-12" and 12"-18" layers respectively. The intersections of the dotted line with the 3", 9" and 15" marks are taken as the mean cone index values for the respective layers (fig. 6).

Calibration: a pressure of 100 psi. results in a 3 cm contraction of the contraction spring. A penetration of 24" results in a peripheral rotation of about 15 cm movement of a point on the circumference of the rotating drum.

Conclusions. — This paper introduces a proposed recording penetrometer. The suggestion has arisen as a result of a long period of observation of present day instruments. The recording penetrometer is believed to be superior to the dial penetrometer. It provides a picture of what happens throughout a particular layer, not just at specified boundaries.

Whereas the recording penetrometer has answered to most of the requirements, there is another penetrometer in production already with further modifications.

Future work will be aimed at the modification of other classes of instruments used in trafficability analyses.

ACKNOWLEDGMENT. — The Trafficability Research Team wishes to acknowledge its gratitude to Professor Joseph G. Zeitlen, Chairman, Department of Soil Engineering, Israel Institute of Technology, Haifa, for his guidance and assistance in the preparation of this paper.

BIBLIOGRAPHY

1) Air Force Surveys in Geophysics (U.S.). Remote determination of soil trafficability by the Aerial Penetrometer No. 77, October 1955.

2) Corps of Engineers U.S. Development of testing instruments TM 3-240. Supplement 3, October 1948.

3) Corps of Engineers, U.S. Army. Research and development report TM-3-240. Supplements 13, 14, 15.

DISCUSSION

W. J. TURNBULL. — In his presentation of the paper Major Cohen listed some features of the U.S. Army Engineer Waterways Experiment Station cone penetrometer that he feels are detrimental to the efficient gathering of cone index data in the field. In his opinion, many of these deficiencies can be eliminated by a device to record automatically the cone index-depth relation. The Israeli Trafficability Research Team is to be complimented on its ingenuity in developing such a device for field use.

Some of the shortcomings of the cone penetrometer described by Major Cohen have been noted by others who have used it, including the Waterways Experiment Station itself. However, it has been concluded that the advantages of the present model of the penetrometer outweigh the disadvantages and that, for the most part, the instrument is quite practical for military use. The penetrometer and detailed procedures for its use in fine-grained soils are described in U.S. Department of the Army Technical Bulletin ENG 37, « Soils Trafficability ».

This is not to say, however, that the self-recording feature would not be a desirable improvement if it could be achieved without sacrificing other favorable characteristics. The self-recording penetrometer devised by the Israelis utilizes a helical spring in compression to measure the applied loads. It has been the experience of the Waterways Experiment Station that this type of load-measuring device is not entirely satisfactory. Such a spring with a large travel has a nonlinear load-compression relation. Because of the relatively great movement of the spring the instrument is very difficult to control in soils of irregularly varying strength and, for similar reasons, the results are sometimes greatly influenced by the skill of the operator.

It is suggested that a proving ring or beam, or perhaps a helical spring in tension, should replace the compression spring and that a relatively stiff spring be employed with a device to amplify deflections at the recorder.

N. 30

Brief description of the six-component oblique-rolling-wheel machine recently constructed and tested at the University of Western Australia

Breve descrizione di una macchina a ruota inclinata a sei componenti recentemente realizzata e sperimentata dall'University of Western Australia

J. R. Phillips *)

ABSTRACT. — *The machine being described is a «six-component» machine in that it will measure all three components both of the oblique reaction-force and of the oblique reaction-couple which act from the ground on a rolling wheel. A single wheel, stationary in the machine, may ben set to any chosen combination of drift and camber angles, it may be driven or braked with any chosen hub-torque, it may be caused to carry whatever vertical load is chosen, and it will roll on a continuous, deformable, sandy «road», which is caused to travel rearwards relative to the wheel. Some remarks are made about the advantages and disadvantages of this machine as a laboratory device, and the general purposes for which it was designed and built are briefly mentioned.*

Introduction. — The behaviour of the flexible vehicular wheel when powered and oblique-rolling on deformable ground is not well understood. Indeed the much simpler behaviour of what might be called the powered, plane-rolling wheel is even mysterious enough to warrant further study. A sound, fundamental mechanics of powered, plane, and oblique rolling is slowly developing; but special laboratory machines are still required for studying the phenomena and for isolating the numerous variables which are involved.

Such a laboratory machine has been designed, built and tested at the University of Western Australia. It will permit the forces and couples acting upon a driven-or-braked, oblique-rolling wheel to be measured while the wheel itself may be set to run within a wide range of different conditions of rolling. Camber angle, drift angle, torque at the hub, vertical load, angular and linear velocities of the wheel, nature of the wheel-rim, and nature of the ground on which the wheel in caused to roll, are all either separately alterable or freely adjustable. Measurements may be made under each condition of rolling which will, when suitably processed, give all the information required for quoting the total, force-plus-couple reaction from the ground upon the wheel. Also

*) University of Western Australia, Nedlands, Australia.

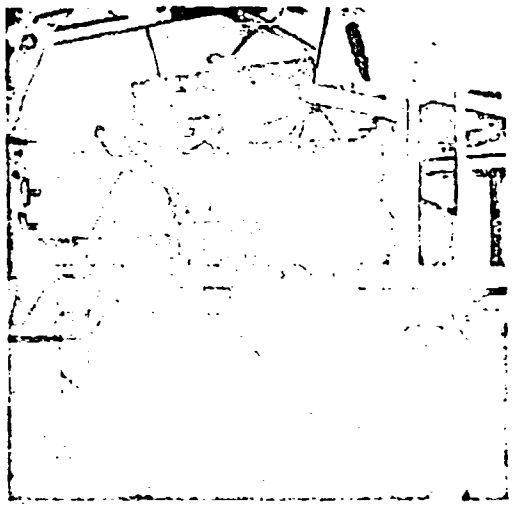


Fig. 1.

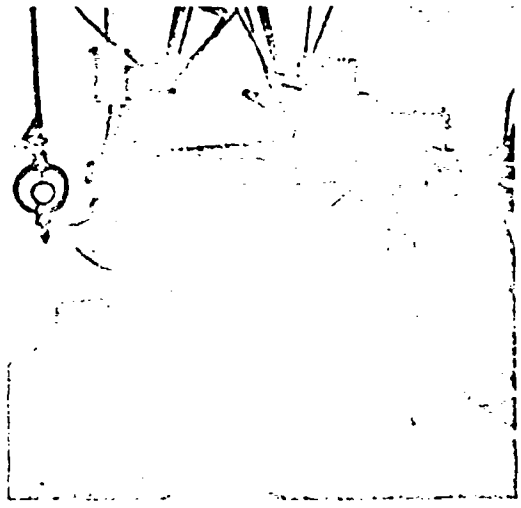


Fig. 2.

« slip », « rolling resistance », and other such arbitrarily defined phenomena, may be studied by using the machine.

What follows is a description, without diagrams, of the machine. Numbers in parentheses at the ends of paragraphs, however, refer to the appended photographs, 1 to 10. These should be consulted as required for clarification of the text.

General working principles. — The wheel — there is only one wheel — helps to support the rear end of a special chassis. The chassis, to be described in further detail later, does not « travel » but remains at rest; it is prevented from « toppling-over » by being also supported at its front end by two freely-swinging, flexible cables which extend from adjustable fixings on the roof of the laboratory down to adjustable fixings disposed on either side of the centre-line of the chassis itself. The wheel rolls on a treadmill-like conveyor belt, suitably surfaced. The conveyor belt is supported, below the wheel, by a platen of special rollers; this platen helps to provide a firmly based, yet moving, « ground » on which the wheel may roll. The ground travels rearwards relative to the wheel (fig. 3-4).

When the machine is working the chassis is at rest in equilibrium; the external forces and couples acting on the chassis sum to zero. These external forces and couples are: a) the weight of the whole chassis-and-wheel assembly acting downwards through its centre-of-mass; b) the tension in one of the supporting cables acting obliquely upwards along that cable; c) the corresponding tension acting obliquely upwards along the other cable; d) the force-plus-couple reaction from the ground upon the wheel.

Briefly speaking the three pure forces a), b) and c) are measured and located; their equilibrant, the total force-plus-couple reaction on the wheel, is

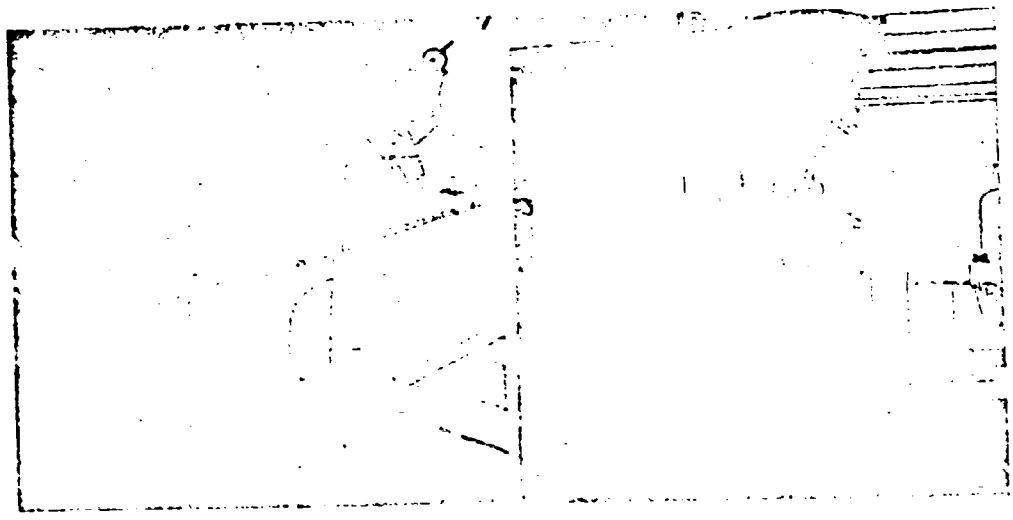


Fig. 3.

Fig. 4.



Fig. 5.

Fig. 6.

calculated by a method of direct vector-addition. In general the three pure forces mentioned are not concurrent; nor are they coplanar, so that performed vector-additions (one for each setting of the machine) are necessarily three-dimensional.

Reference (1959) describes some previous work on oblique-rolling wheels of a similar, but much cruder, kind, while reference (1955) describes a graphical method which has been used, in conjunction with numerical methods, for the vector-additions of the forces.

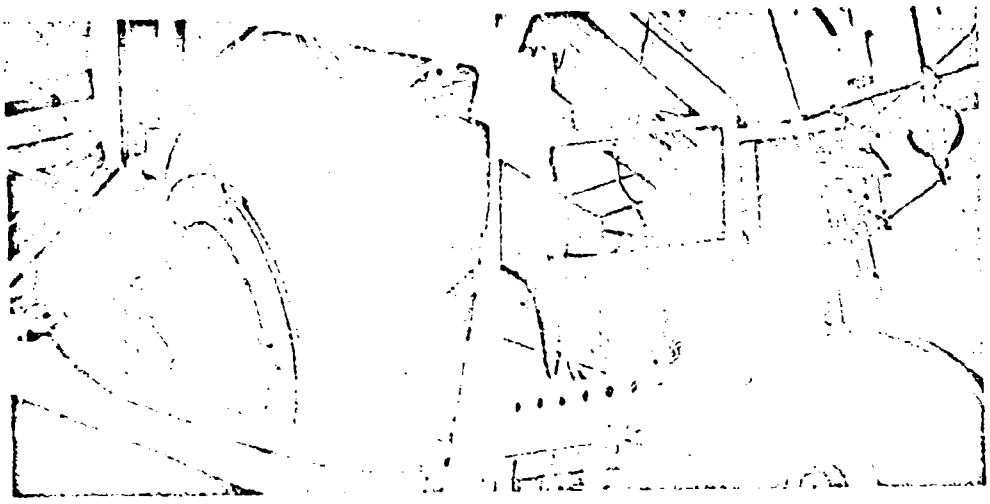


Fig. 7.

Fig. 8.

Wheel-drive assembly. — The wheel, its axle, its driving motor and power-transmission are all mounted on a compact, rigid frame. This frame may be tilted adjustably about a horizontal hinge which is mounted at right angles to the axle, so that a chosen camber angle β for the wheel may be set. The horizontal hinge is supported within a second, circular frame which may be swung adjustably about a vertical axis so that a chosen angle ϵ, in plan, may be set between the line-of-intersection of the peripheral plane of the wheel and some horizontal plane, and the centre-line of the chassis. Thus the whole wheel-drive assembly, which is carried within a circular, horizontal housing in the chassis, permits the wheel to be set at any oblique angle (fig. 1, 7, 8).

Whereas the camber angle β may be set to any chosen value by means of the adjustment provided — the chassis is arranged always to run in a « level » position — the drift angle α at which the wheel will actually run on the road cannot be so set. If κ is the angle in plan which happens to occur between the centre-line of the chassis and the direction-of-travel of the ground, then the drift angle $\alpha = \epsilon \pm \kappa$.

The driving motor mentioned is a 1.0 HP, 250 volt, DC motor designed to run at 1500 RPM and to carry a maximum current of 3.5 amperes. Its field winding is separately excited with a constant 250 volt DC supply, while the voltage applied across its armature is adjustable from + 250 volts DC through zero to — 250 volts DC. Whenever, therefore, the wheel is not in contact with the road — the whole chassis may be hoisted up — the wheel may be caused to rotate with any chosen angular velocity, positive or negative, within a range. The power-transmission system from the motor to the wheel includes a 15:1 speed-reduction ratio, so the maximum and minimum angular velocities of the wheel under the mentioned circumstances are roughly + 100 RPM and — 100 RPM (fig. 2, 7).

The particular wheel mounted in the machine at present has a pneumatic tyre of nominal size 3.50 × 10, that is it has a peripheral diameter of roughly 17 inches. Camber angles β of up to 45° are obtainable, and the angle α may be set at intervals of 5° throughout the range 360°. As an indication of the overall size of the wheel-drive assembly, the diameter of the circular housing in the chassis, which is the « equatorial » diameter of an imaginary sphere enclosing the whole assembly, is roughly 22 inches (fig. 8).

Within the wheel-drive assembly there is also accommodated, concentric with, and near to the « hub » of the wheel, a mechanical torquemeter; the torquemeter indicates on the face of an ordinary dial gauge the torque M applied at the hub of the wheel; the torque M is not the torque applied at the axle, but the algebraic sum of the torque applied at the axle, say M_p, and the « friction » torque, say M_q, which is « lost » at the supporting bearing. It is accordingly possible while the wheel is rolling, by means of the mentioned electrical control, to adjust the torque M directly, to whatever chosen value might be required. M may be made zero (and thus the wheel neither driven nor braked), or decreased in the direction of braking to roughly — 125 lb.ft., or increased in the direction of driving to roughly + 75 lb.ft. Except to say that the torquemeter works on the principle of measuring an axial twist due to the bending of two equally loaded, ball-ended cantilevers, no detailed description of its working is given here (fig. 7).

Provision is made around the hub of the wheel for attaching various sizes of split-rim for accommodating various sizes and kinds of pneumatic tyre. Tyres may accordingly be changed or « turned over » without disturbing any part of the wheel-drive assembly or the torquemeter already described (fig. 7, 8).

The travelling ground. — A rubberised, 3-ply conveyor belt 33 inches wide is carried on two, 21 inches diameter pulleys set with their centres 140 inches horizontally apart. In the neighbourhood of the wheel (which rolls on the top side of the upper-run of the conveyor belt) a platen of six steel rollers (2.25 inches diameter and at 2.50 inches centres) supports the weight of the wheel, the platen bearing upwards against the underside of the upper-run. The six rollers are each deeply indented with three V-grooves which accommodate three endless V-belts firmly rivetted to the inside of the mentioned conveyor belt. The function of these V-belts and grooves is to accept and to resist the heavy sideways loads on the belt occasioned by the oblique-rolling action of the wheel (fig. 8, 1).

Because the six rollers of the platen are deeply indented with the V-grooves they are unable to support themselves in strength as beams. They accordingly run, with ball-thrust bearings (not axially located) at their ends, supported platen-wise on another parallel set of seven, unindented rollers; these latter rollers are mounted, with ball-journal bearings at their ends, in a fixed frame immediately below. The whole 13-roller assembly extends all the way across the underside of the upper-run of the conveyor belt (fig. 8).

At the present time a « hard road » surface is made on the belt with

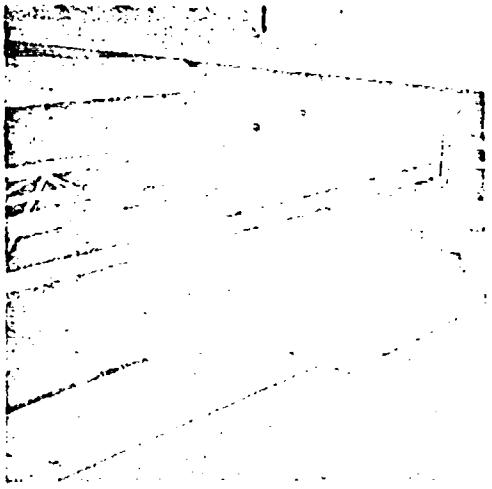


Fig. 9.

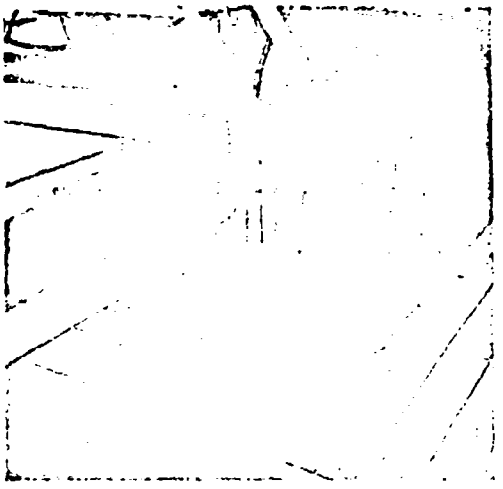


Fig. 10.

a heavy sprinkling of Leighton Buzzard sand embedded in a thin layer of « Neoprene » liquid-rubber cement. This surface has, so far, shown itself to be resistive to abrasion, and sufficiently elastic to negotiate the fairly steep curvature of the conveyor pulleys without cracking (fig. 1, 2).

The belt is driven by a 440 volt AC, 3-phase, 5.0 HP motor provided with a built-in, mechanical, « Brottby » variator, delivering its power through a motor-car gear box and a roller-chain speed-reduction system in such a way that a range of linear speeds for the belt, from 2 to 20 feet/second are obtainable (fig. 3, 4).

It is proposed ultimately to feed loose, dry sand onto the road from a hopper, to be smoothed under an adjustable « grader » for consistency of depth, before it is carried along and under the wheel, the sand to be then returned to the hopper for continuous recirculation. Presently, however, the machine is being used to advantage in its « hard road » condition, that is with no loose sand being used at all.

Chassis and supporting cables. — Looking in the direction-of-travel of the road, the chassis is seen to extend from left to right across the road; at its left and right extremities it extends downwards in the form of two « legs » which straddle the conveyor belt; underneath the lower-run of the conveyor belt the chassis extends acrosswise, joining together the two extremities of the legs. The chassis, in other words, is a rigid « box » surrounding the road yet making contact with it only via the single wheel; nowhere else but at the wheel does the chassis-and-wheel assembly touch the conveyor-belt assembly (fig. 3, 10, 9).

At the top of the chassis, at the « front » end (opposite to that of the wheel), two adjustable devices are mounted which permit the gimbal-jointed,

lower ends of the supporting cables to be set, polar-wise and horizontally, within a range of different positions (fig. 6, 5, 4).

Correspondingly, and attached to the concrete roof of the laboratory, there is a system of rails, adjustable gantries, and travelling trolleys which permit the gimbal-jointed, upper ends of the supporting cables to be set, Cartesian-wise and horizontally, within a range of different positions (fig. 5, 4).

The supporting cables themselves are of flexible steel rope, 0.125 inches diameter. For each cable provision is made, by means of a somewhat complicated hoisting and locking arrangement, for adjusting the actual length of cable extending between the upper and lower gimbal-joints (fig. 5, 4).

As an integral part of the lower part of the chassis (the part below the lower-run of the conveyor belt), a mechanical arrangement is provided for moving a basket of lead blocks from place to place Cartesian-wise. Blocks may be inserted or removed from the basket, and the basket may be locked in any desired position. It is by this means that both the mass and the position of the centre-of-mass of the chassis-and-wheel assembly may be altered as desired. The mass may be altered from roughly 650 pounds to roughly 850 pounds, and the position-in-plan of the centre-of-mass may be adjusted within a roughly circular area of roughly 30 inches diameter (fig. 9, 3).

It is important to notice here that, although the total mass of the chassis-and-wheel assembly cannot be reduced below the mentioned 650 pounds or thereabouts, the vertical load sustained by the wheel may quite easily be reduced to values approaching zero. The operator needs simply to watch an imaginary line, which extends between the gimbal-joints at the lower ends of the cables, and to adjust this line closer and closer to the position-in-plan of the centre-of-mass (fig. 3, 4).

Position measurement. — On the roof, or, rather, within the roof-assembly, five adjustable reference-buttons are permanently and accurately set in a widely dispersed, cruciform arrangement; these act as a horizontal reference grid from which all measurements are made Cartesian-wise, with plumb-bobs, rule, dumpy level, etc., in the three orthogonal directions (fig. 5, 4).

Within the chassis, which is rigid, heights between important levels and horizontal distances between important plan-positions are accurately known, so that a) a vertical, graduated scale on the chassis which is viewed with a telescope and cross-hair fixed in space, and b) other, horizontally arranged, angular and linear scales on the chassis, permit us to fix a) the overall « height » at which the chassis is running, and b) the positions-in-plan, relative to the chassis, of the lower gimbal-joints of the supporting cables (fig. 2, 6).

It should be mentioned here that three glass manometer tubes, connected by flexible tubing to a central reservoir of colored fluid, are mounted vertically at three widely dispersed points on the chassis frame. These manometers are used for judging by eye when the chassis (the horizontal circular housing mentioned) is running level. If the chassis is « rocking » a little, as it sometimes does, the flexible tubes may be throttled slightly to steady the manometer levels (fig. 1, 3).

The angle « was mentioned earlier, namely, the angle which happens to occur in plan between the centre-line of the chassis and the direction-of-travel of the ground. To measure this angle, and to locate, in plan, the whole chassis-and-wheel assembly relative to the reference grid, a special apparatus is used. Two « pencils » (ball-point pens affixed in the ends of hard brass tubes 0.5 inches diameter and 20 inches long) are separately free to slide upwards and downwards in a frame fixed to the roof; the pencils, whose axes are accurately vertical, known in position, and accurately 72 inches apart, laterally straddle the chassis; as the chassis gently « rocks », the pencils write on two « record-papers » which are clipped to two, specially constructed, horizontal « drawing boards » which are fixed to the chassis and accordingly rock with it; as the gentle rocking proceeds the pencils describe irregular, though clearly « centred » marks on the record-papers. At known points in each board, two fixed, upward-pointing pins pierce the record-papers so that, after both papers have been removed and measurements have been made, the « average plan-position » of the chassis may be located in relation to the reference grid (fig. 2, 4).

This latter job is done graphically. Also graphically, with the aid of special templates and other devices to hasten the work, the two upper and the two lower gimbal-joints are located in both plan and elevation views of the machine drawn to scale. Thus the positions and directions of the two supporting forces (acting obliquely upwards along the cables) are established. How the magnitudes of these two forces are measured and how the position and magnitude of the force of gravity on the chassis are measured, however, have yet to be explained.

On the question of accuracy it might be mentioned here that all dimensions within the machine are set or measured so as to be well within the accuracy obtainable in graphical computation. The location in space of the geometric centres of the upper gimbal-joints, for example, are held within spherical tolerances not exceeding 0.1 inches diameter.

Force measurement. — Near the lower gimbal-joint in each cable a proving ring (of range 600 pounds) is inserted for measuring the cable-tension. These proving rings are designed and calibrated in such a way that the cable-tensions may be accurately measured to within 5 pounds — even when the tensions are fluctuating about mean values due to slight rocking of the chassis. Arrangements are being made to counterweight the proving rings in such a way that the centres-of-mass of the proving rings will coincide with the geometric centres of the lower gimbal-joints; until this counterweighting is done, the present masses (about 6 pounds for each ring) will continue slightly to interfere with the accurate assessment of the directions of the tensile forces (fig. 4, 5, 6).

The only remaining force to be measured now is the force of gravity which acts through the centre-of-mass of the chassis-and-wheel assembly. In order to measure this, three « hooks » fixed on the chassis are disposed in a triangular manner so as to straddle, in plan, the position of the centre-of-mass. There are two of these hooks at the front, and one at the rear of the chassis; and their positions-in-plan on the chassis are accurately known. Three proving rings,

similar to those already mentioned, are supported on three other hooks suitably fixed in space so as to match the three hooks fixed on the chassis. A simple arrangement of hand-powered, ratchet winches permits the whole chassis-and-wheel assembly to be hoisted and hung on the three suspended proving rings, this being usually done after each running of the wheel has been otherwise recorded. From this it will be clear how the total mass, and the position-in-plan of the centre-of-mass of the chassis-and-wheel assembly may be determined (fig. 10, 8, 2).

When « hung on the hooks », incidentally, the chassis is level, so that general maintenance work, checkings of dimensions, calibrations of the torquemeter, settings of the manometer zeros, etc., may all be done conveniently with the chassis in this position (fig. 2, 3, 8).

Some final remarks. — In this descriptive explanation of the machine the author sees no proper place for arguing what it believes to be the merits or demerits of the machine. He would however like to argue here that, because the wheel is free to « find its own level » in this machine, the machine is able to « accommodate itself » to local irregularities in the wheel itself, and in the ground, without causing the troublesome, transient disturbances in the force-indicating apparatus which would be a feature of other, more « rigid » machines. The dial gauges of the proving rings remain remarkably steady; this, associated with the obviously stable « centreing » tendency of the pencil marks made on the record-papers, leads one to argue that the machine « absorbs its own transient disturbances », by virtue both its freedom to « accommodate » and its inertia.

Another relevant comment here is that, because the machine is « universal », it may be used to study the mechanics of the plane-rolling wheel as well. The plane-rolling condition, of course, is extant whenever $\alpha = 0$ and $\beta = 0$.

It must be admitted that the required graphical and/or numerical computations hinted at in the above explanation are fairly laborious; for while working the machine it will be necessary to explore gradually, test by test, a series of chosen « regions of enquiry », and thus to construct, stage by stage, a series of performance curves for the various phenomena: without some quicker methods of computation or a computing machine, the speed of this work will be relatively slow. The author, however, is particularly interested in the couple associated with the reaction force which acts from the ground on powered oblique-rolling wheels and its mechanics, and in the question of « rolling resistance » as applied to powered wheels rolling in deformable media; so at least for the present he has available an accurate, universal, laboratory machine with which to study, albeit slowly, these phenomena.

BIBLIOGRAPHY

Phillips J. R. A graphical method for skew forces and couples. Australian Journal of Applied Science, vol. 6, n. 2, pag. 131-148, 1955.

Phillips J. R. Experimental determination of the forces on some towed drifting wheels. Journal of Agricultural Engineering Research, vol. 4, n. 4, pag. 294-306, 1959.

RELAZIONE FRA SUOLO E VEICOLO

SOIL-VEHICLE RELATIONSHIP

Special applications of high mobility tires

Speciali applicazioni di pneumatici ad alta mobilità

ADDIS FINNEY *)

ABSTRACT. — *Present-day operating conditions and service requirements for off-highway vehicles have become more difficult. The evolution of tire sizes and types used in off-highway operations, particularly those demanding a high degree of mobility and flotation, is reviewed and photographs of vehicles in actual use are shown to illustrate typical as well as unusual service requirements. Many new tire sizes have been introduced to carry larger, heavier vehicles and to meet the more severe service conditions. Trend has been toward larger tires and low section-height shape of tire cross-section as being most efficient in providing the desired tire performance characteristics.*

Introduction. — This paper, which will not be highly technical in character, is intended to accomplish two purposes:

1) Review the evolution of tire sizes and types used primarily for off-highway operations, particularly those which demand a high degree of mobility and flotation.

2) Show typical service requirements, including several which are unusual and for which new and different tire sizes, tread designs and constructions have been developed.

Review of requirements. — The service field under consideration has been divided into four categories, each of which is comparatively unique:

1) *Construction field* as typified by dam, waterway and highway projects which require movement of large quantities of earth and rock. In this service, changes have occurred in:

Speeds, which were originally 6-8 miles per hour but now go up as high as 25-50 miles per hour,

Length of hauls, which are now as long as 10 miles whereas one mile was once considered a long haul, and

Size of loads and equipment. Present equipment includes trucks of 4-5 cu.yd. capacity, self-loading scrapers of 25 cu.yd. capacity and specialised vehicles such as coal haulers going up to 75 cu.yd. capacity.

2) *Logging, mining and petroleum.* Heavier units, such as mobile

*) European Technical Coordinator, The Firestone Tire & Rubber Co. Paris, France.

cranes and self-contained pumps and power plants, are being used in this service for increased efficiency and are being taken into areas previously considered inaccessible. This demands tires with flotation characteristics and load-carrying capacities which once would have been considered impractical.

3) *Military operations.* Here also, heavier equipment is being developed which must operate over a great variety of surfaces in cross-country transport. For this service, reliability of particular importance.

4) *General transportation* into newly-developing areas without adequate highways or railways. Land trains are now operating into territory where surface transportation was previously very primitive. Such units must have flotation and mobility under heavy loads, without need for extensive preparation and maintenance of roads or tracks.

Mobility problems. — Mobility is perhaps the most important requirement for off-highway service with heavy equipment and entails ability to operate over a wide variety of surface conditions, such as:

Sand, met mainly on beach and desert operations and of special importance in many petroleum-producing areas.

Soft soil and mud, of primary concern in construction and earth-moving projects and quite often encountered in cross-country operations.

Snow and bogs, found in arctic transport and in many mining and logging areas.

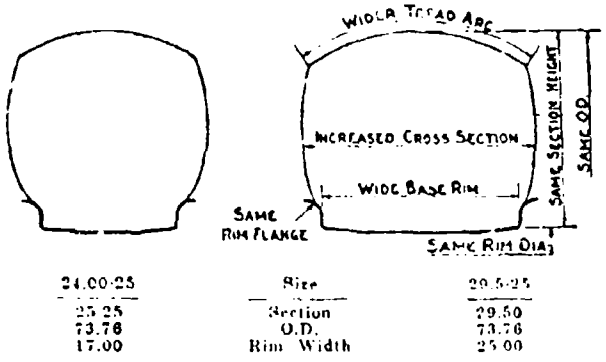
1934	1961	
	Conventional	Wide-base
13.50-20	14.00-20	
	-24	
	16.00-21	
	-25	20.5-25
17.25-24	18.00-25	23.5-25
	-33	
	-49	
	21.00-25	26.5-25
	-29	-29
	-35	
	24.00-25	29.5-25
	-29	-29
	-33	-33
		-35
	27.00-33	33.5-33
		-39
	30.00-33	37.5-33
	36.00-41	
		48 × 68

Fig. 1. — Off-highway tire sizes.

Hills. This includes not only hilly or mountainous terrain but also slopes of any size, such as fill gradients and desert sand dunes.

Tires sizes and types. — The growth of off-highway operations has brought about a great diversification in tires to meet all service requirements. A study of this phase of the subject brings out several interesting developments.

1) *Number of sizes*: In fig. 1, tire sizes are shown as they existed in 1934 and as they exist today. In addition to noting the increase from 2 to 28 regularly manufactured sizes, we see that tires have become larger both in cross-section and in rim diameter. This change to larger tires permits higher loads per tire without sacrificing flotation and mobility characteristics.



24.00-25	Size	29.5-25
25.25	Section	29.50
73.76	O.D.	73.76
17.00	Rim Width	25.00

Fig. 2. — Conventional 24.00-25 vs 29.5-25 Traction Rock.

2) *Conventional vs. wide-base*: Two types of tires now exist, namely conventional and wide-base. Fig. 2 illustrates the differences between these two types of tire by comparing the 24.00-25 conventional and 29.5-25 wide-base sizes. Without changing rim diameter or tire overall diameter, the cross-section width on the 29.5-25 tire has been increased by using a wider rim.

With the same tire loadings, inflation pressures on the wide-base tire can be reduced 10 lbs./sq.in. The wider cross-section gives improved traction and flotation and the lower unit ground pressure improves resistance to damage from stones and other objects.

3) *Low section-height tires*: The wide-base principle is carried still further in low section-height tires. Fig. 3 compares the 36.00-41 conventional and 48 × 68 low section-height sizes, both of which are used in off-highway transportation where flotation is important. The low section-height shape of the 48 × 68 tire permits a 27″ increase in bead diameter and 9″ increase in cross-section width with only a minor increase of 6″ in overall diameter. This makes possible a wider cross-section for improved flotation without increasing overall diameter or tire weight, as would have been necessary if conventional tire shape had been maintained.

4) *Single vs. duals*: Another application of the low section-height principle is in the use of larger single tires to replace dual tires. Fig. 4 compares a special 24-20.5 low section-height tire with the 14.00-20 dual sand tires which it replaces in desert exploration and transportation services. The 24-20.5

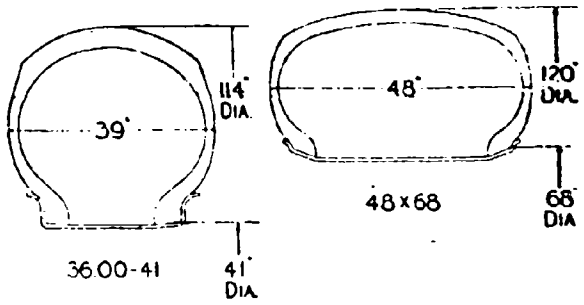


Fig. 3. — Example of low section-height off highway tire.

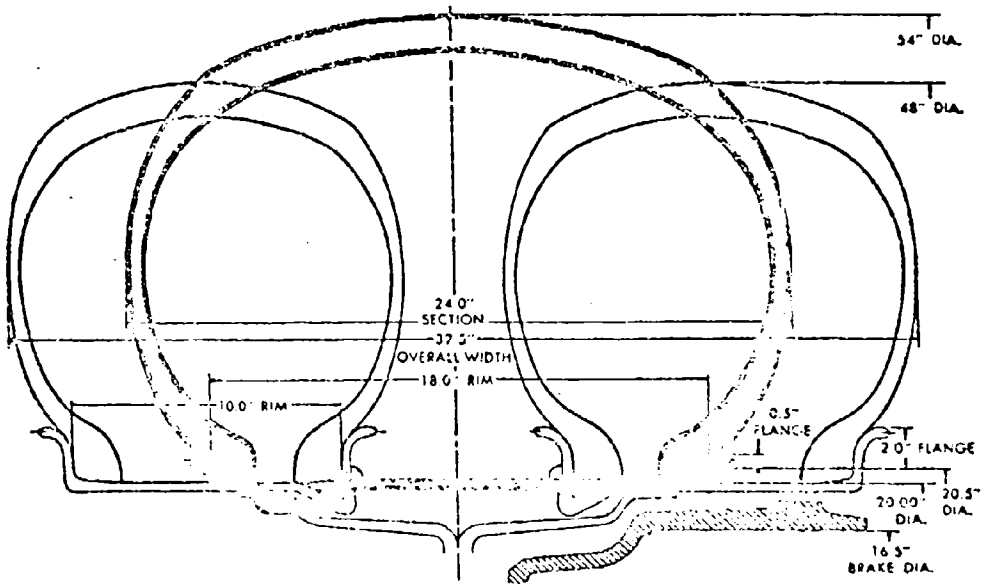


Fig. 4. — Sand tires. - 24-20.5 single to replace 14.00-20 duals.

tire has the overall diameter of a 16.00-20 tire because clearances permitted this and because conversion from 14.00-20 duals to 16.00-20 duals has been gaining headway. Although the change from dual tires to one large single tire reduces total ground contact area, experience is showing that flotation and mobility are improved without reduction in total load-carrying capacity.

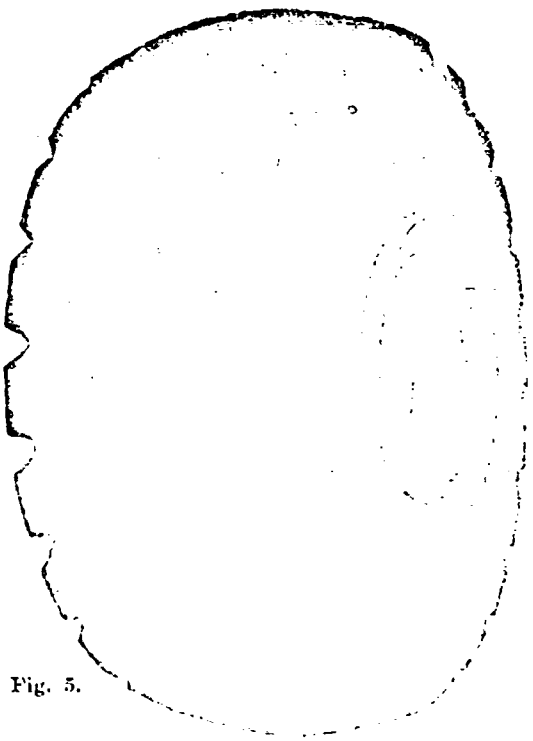


Fig. 5.

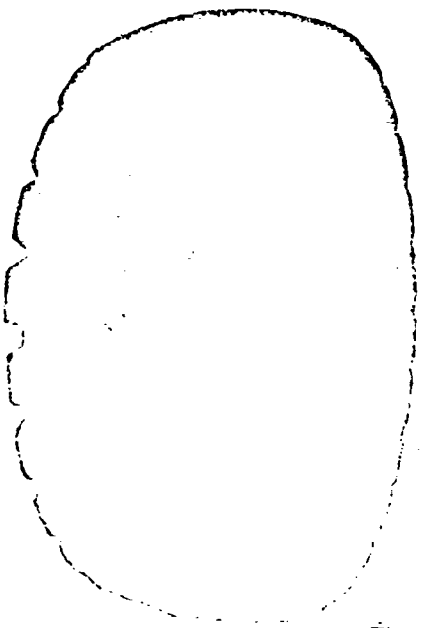


Fig. 6.



Fig. 7.



Fig. 8.

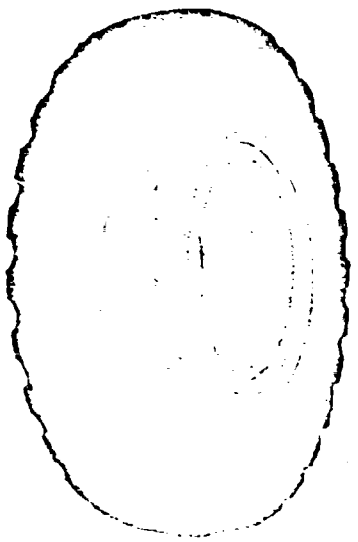


Fig. 9.

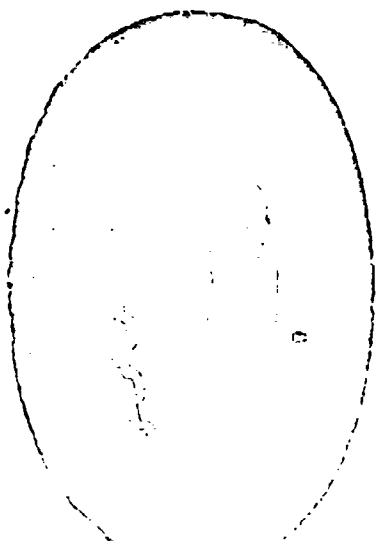


Fig. 10.

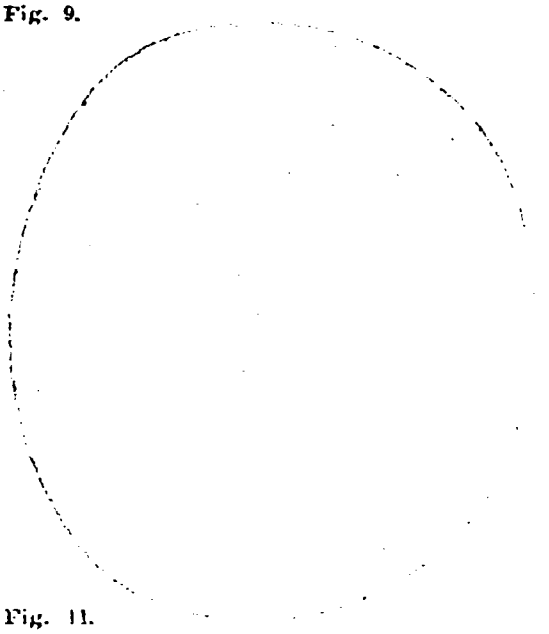


Fig. 11.

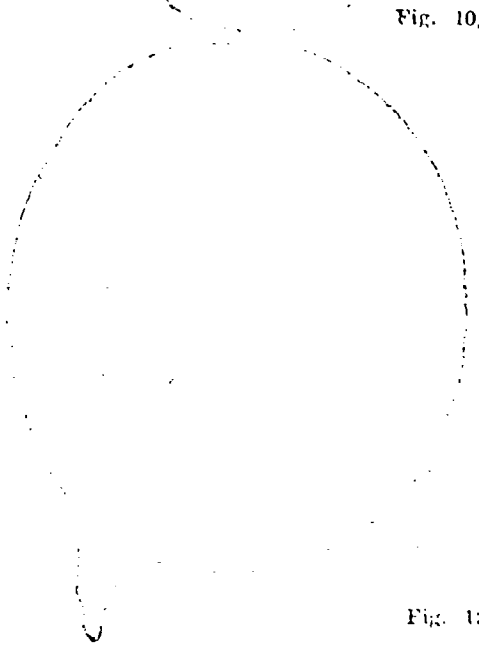


Fig. 12.

5) *Tread patterns.* All off-highway operations do not need the same degree of traction. As a result, separate tread designs are used for different degrees of tractive effort. A few current designs have been chosen to illustrate this.

Maximum traction. Fig. 5 shows a representative tread pattern designed for maximum traction requirements, as in earthmoving or excavating operations.

Fig. 6 shows a variation of this pattern in which deep grooves have been added to the traction elements to reduce rubber mass and provide lower tire operating temperatures in high-speed service.

Medium traction. Fig. 7 illustrates a medium traction design used mainly in military operations and fig. 8 a design which gives extra traction in off-highway service and still performs satisfactorily if used part of the time on the highway.

Free-rolling. Fig. 9 shows a ribbed tread pattern and fig. 10 a shallow-depth button-type tread pattern, both of which types are widely used on free-rolling wheels. Choice of design would depend upon the exact service requirements involved.

Special requirements: Unusual service conditions sometimes demand a special choice of tread pattern. In desert operations, for example, maximum traction on drive wheels is necessary but use of an aggressive design is not always advisable because it may tend to dig in and become stuck when a « no-go » situation is encountered in soft sand. In this case, a ribbed design, such as in fig. 11, may be used, the lack of traction elements being offset by large ground contact area. Operations in snow present similar problems and fig. 12 illustrates a shallow-depth design which has been successful on powered as well as free-rolling wheels in this type of service.

Tire construction. — Consideration of tire construction is a subject in itself and no attempt is being made to explore it at this time. It need only be understood that the tire must possess the characteristics of durability, load carrying ability, speed capability and low operating temperature to the degree which service requirements demand.

High tensile cord materials must be used to provide sufficient strength in a thin body construction to give flexibility to the tire, and rubber compounds must be as cool-running as possible, consistent with toughness and abrasion resistance, to keep tire operating temperatures down to a safe level.

Examples of service operations. — To illustrate points which have been discussed and to indicate the extent to which off-highway operations have grown in scope and complexity, a few examples of vehicles in actual service have been selected.

Fig. 13. — A typical earthmoving operation, the vehicles being self-loading scrapers with a track-type tractor to assist in the loading operation.

Fig. 14. — A stripping operation involving rocky terrain and flotation requirements. Material is being carried by track, with mechanical shovel loading.

Fig. 15. — A bull-dozer operating in conditions which require maximum traction plus mobility.

Fig. 16. — The same type of bull-dozer as shown in Fig. 15 is here being used in a filling operation on a small body of water where greater emphasis is placed on flotation.

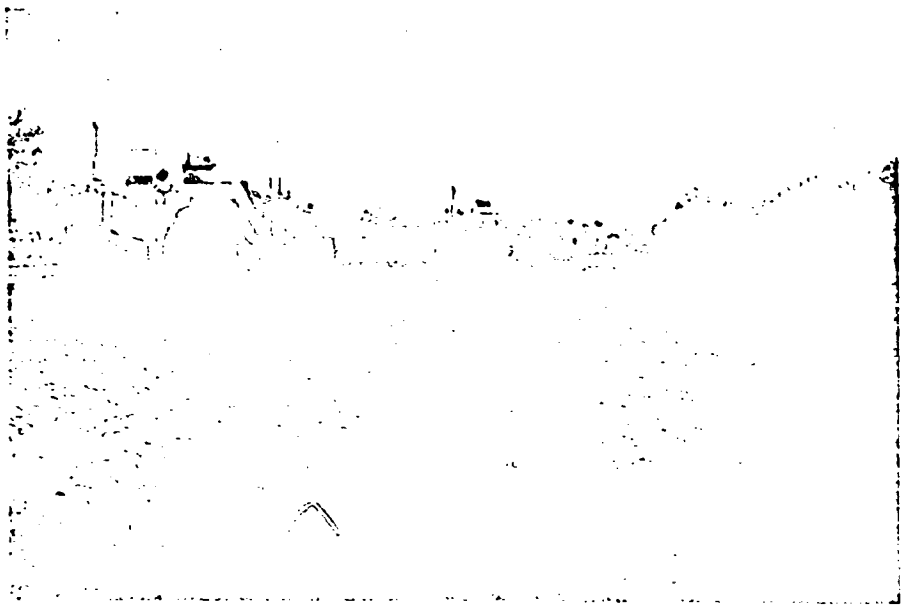


Fig. 13.

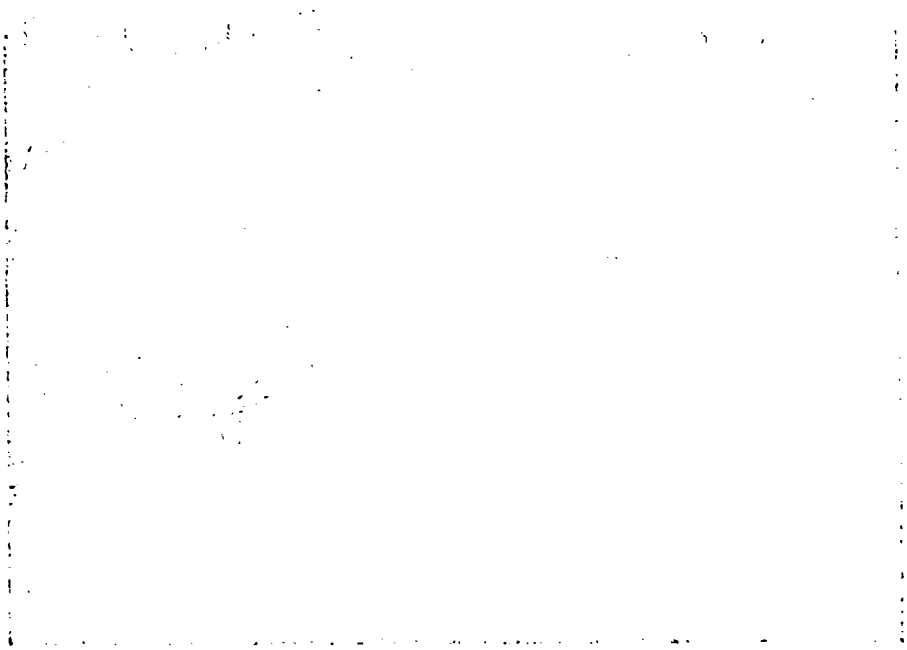


Fig. 14.

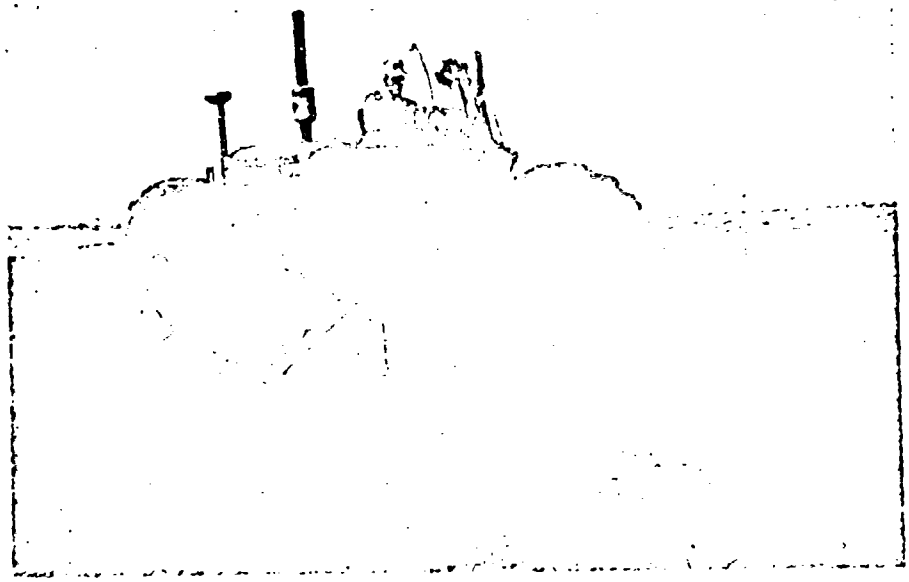


Fig. 15.

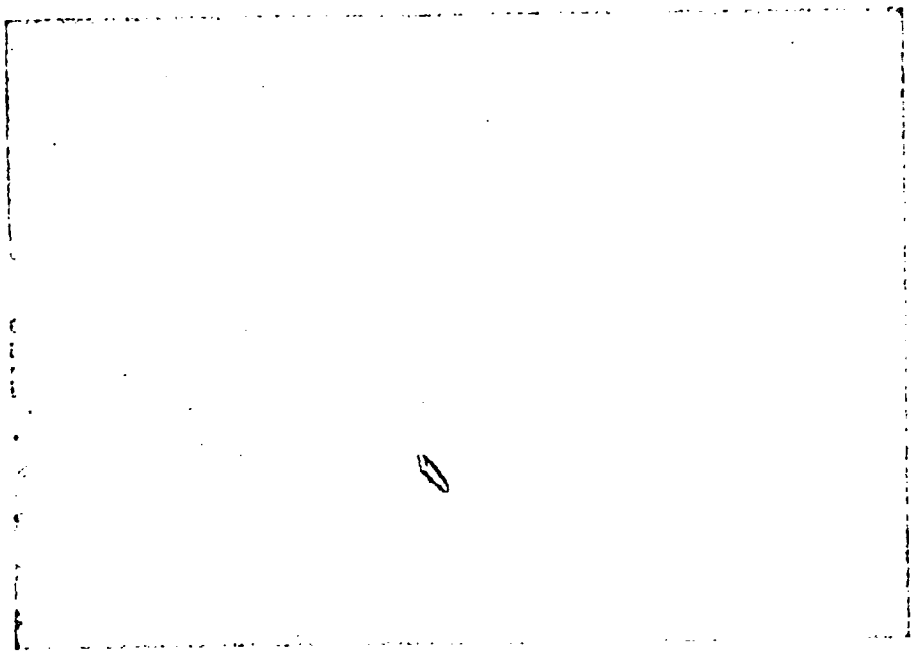


Fig. 16.

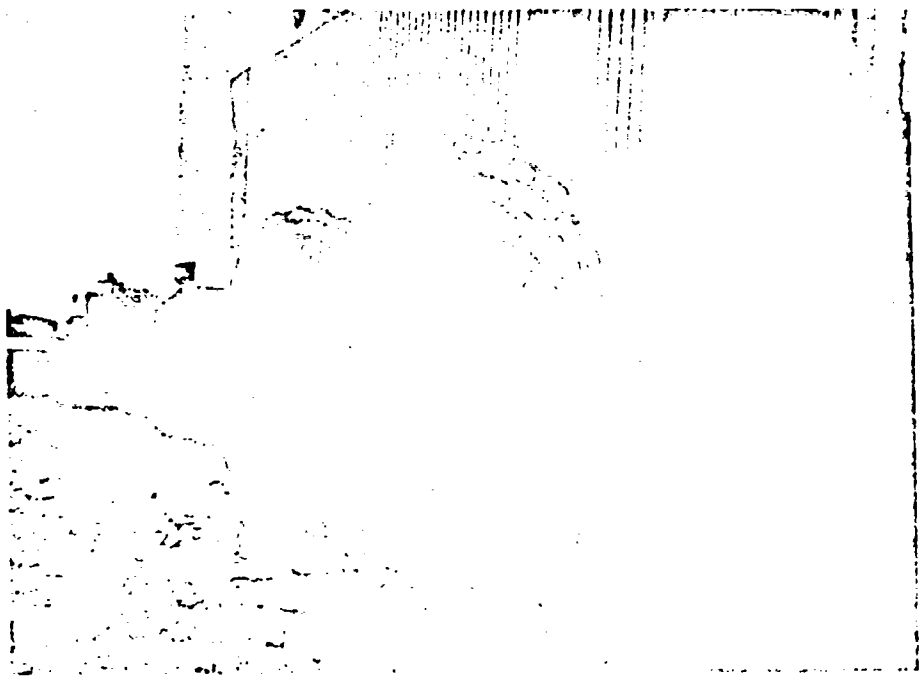


Fig. 17.

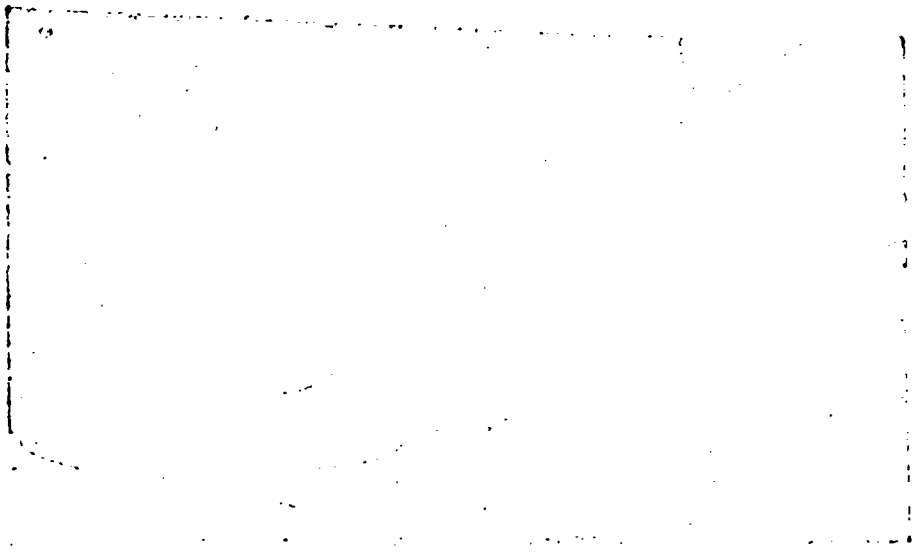


Fig. 18.

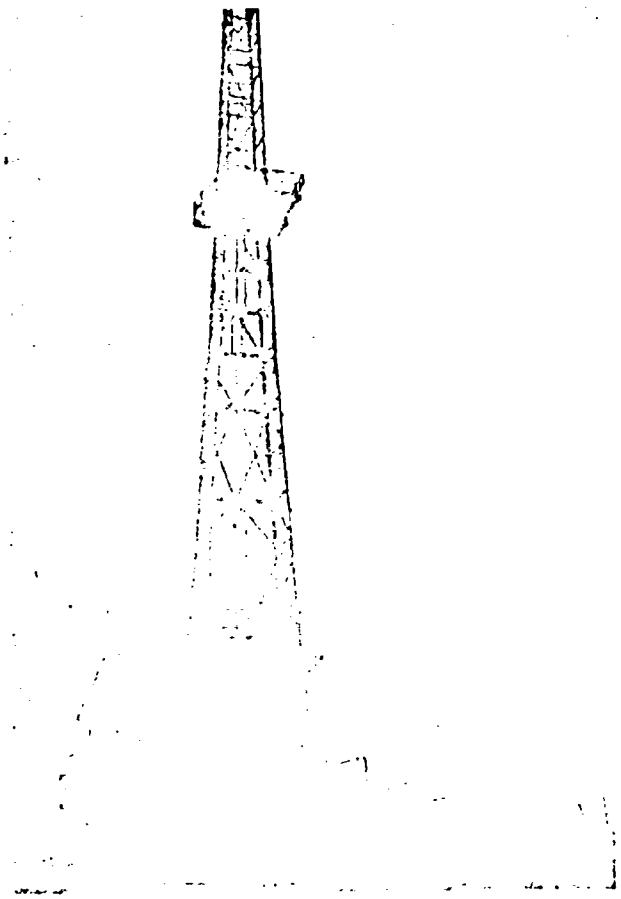


Fig. 19.

Fig. 17. — Typical rough, rocky terrain which is met in oil-company operations in the Middle East. Tire size is 36.00-41 being used in transport of a large indivisible load.

Fig. 18. — The same 36.00-41 size in transport of material for pipeline maintenance. Loadings in this service go as high as 70,000 lbs per tire.

Fig. 19. — 36.00-41 tires being used in the transport of a drilling rig in one unit, without up-ending it.

Fig. 20. — A truck stuck in soft sand in a typical desert operation. Drive wheels are equipped with 14.00-20 dual sand tires.

Fig. 21. — Special 24-20.5 low section-height sand tires which are used as singles to replace 14.00-20 or 16.00-20 dual tires.

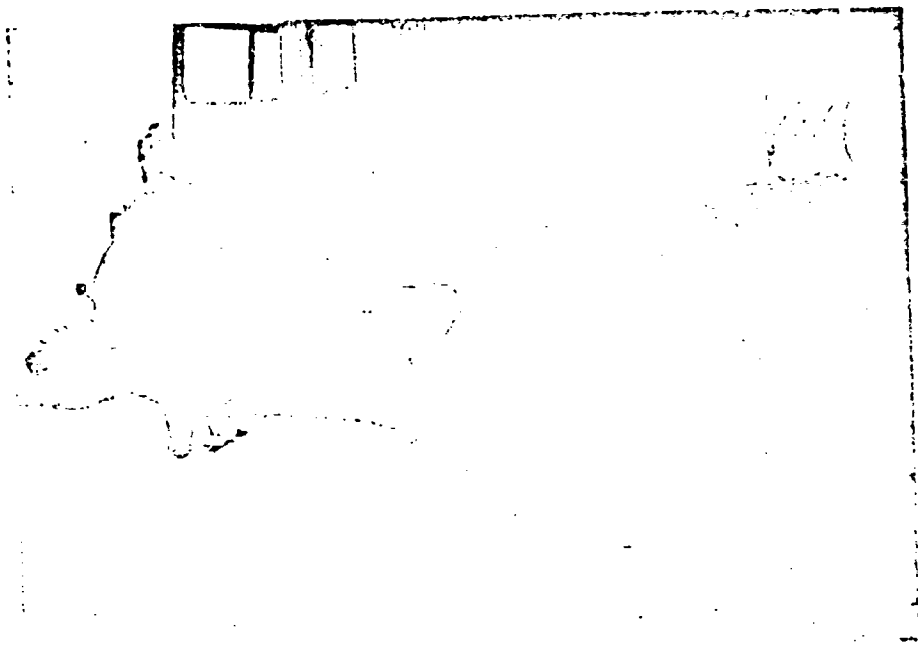


Fig. 20.

Fig. 21.



Fig. 22.

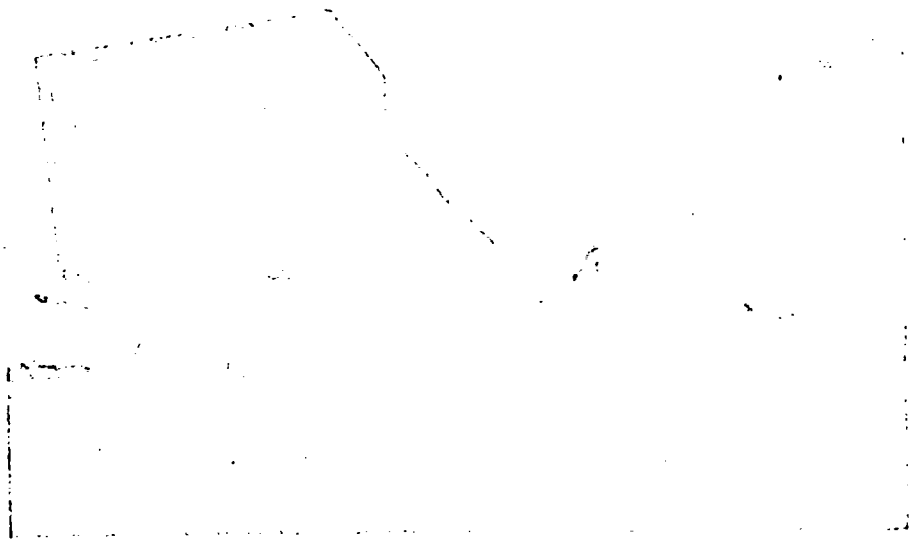


Fig. 23.



Fig. 24.



Fig. 25.

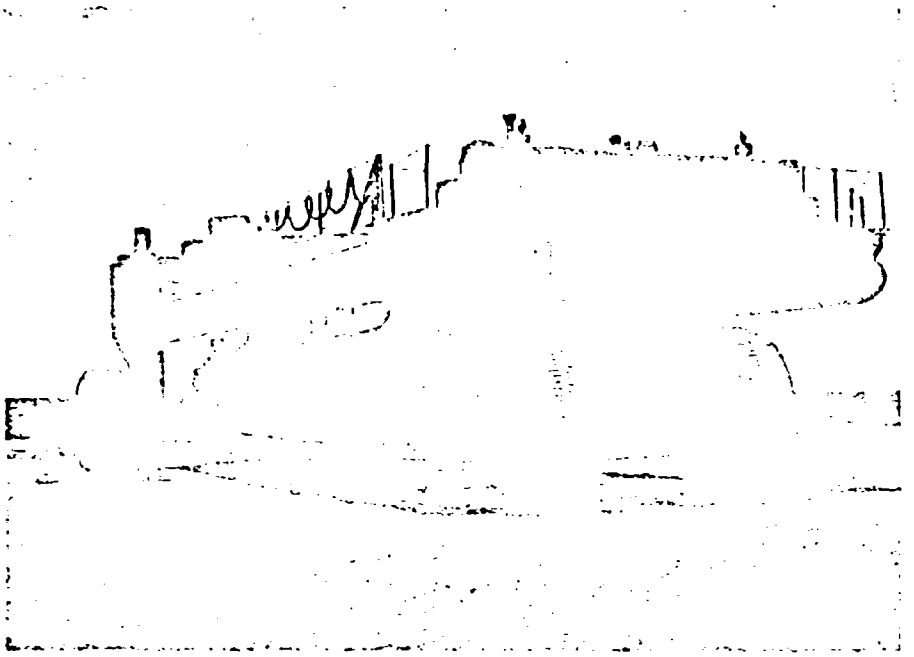


Fig. 26.



Fig. 27.

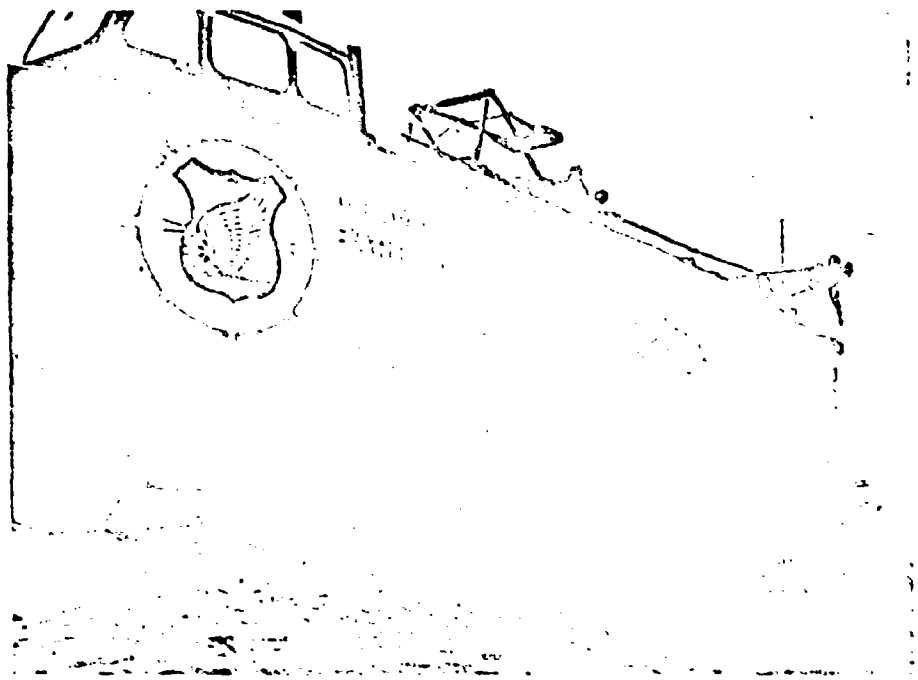


Fig. 28.

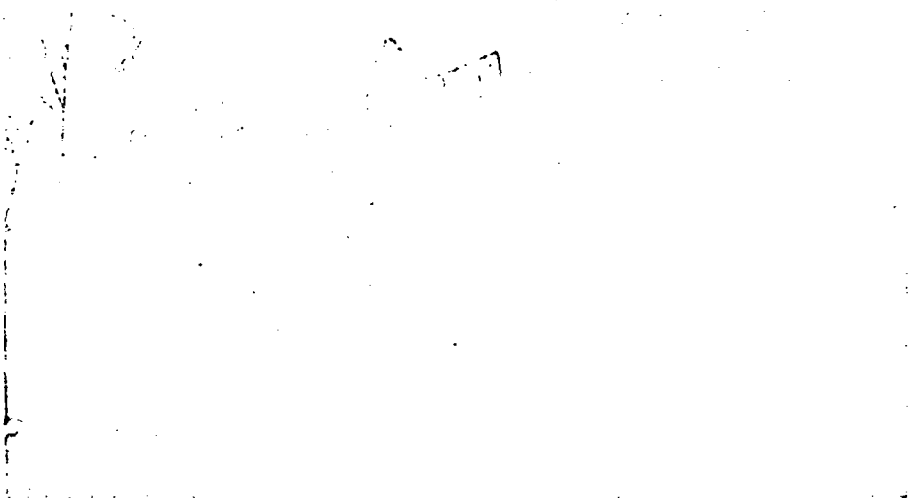


Fig. 29.

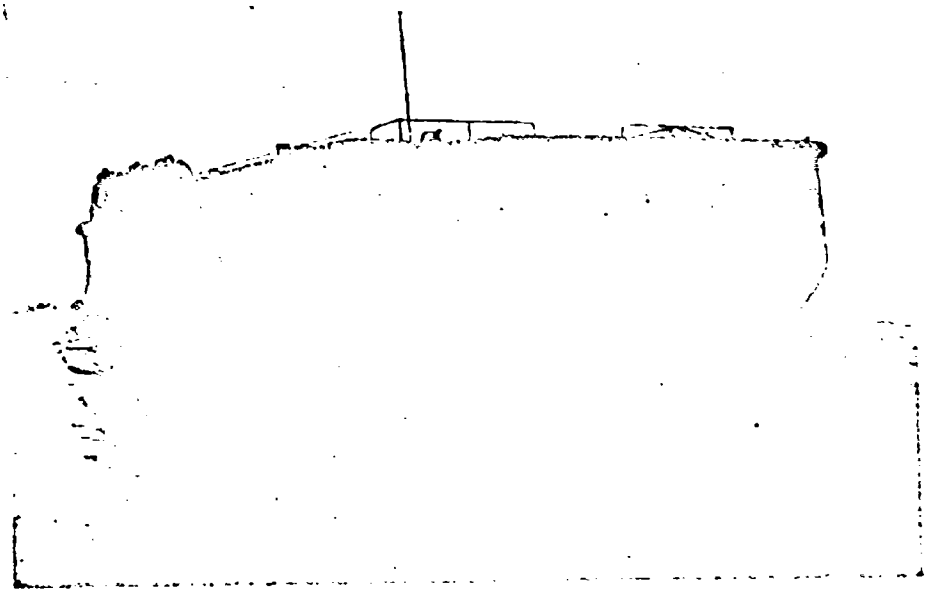


Fig. 30.



Fig. 31.

Fig. 22. — Typical tractor-trailer unit for use in desert transport and oil exploration service, equipped with 24-20.5 sand tires on drive and trailer positions.

Fig. 23. — Snow train, equipped with special 89" low section-height tires, for use in transportation to newly-developing areas.

Fig. 24. — 48 × 68 low section-height tires on a larger power unit for snow train service.

Fig. 25. — 48 × 68 tires on a giant bull-dozer. Large ground contact area supplants aggressive trend pattern for traction, at the same time providing improved flotation characteristics.

Fig. 26. — Military application of 48 × 68 tires on a landing craft retriever.

Fig. 27. — GOER high mobility military vehicle which is capable of fast cross-country operation. Special 29.5-25 wide-base tires with light construction are used.

Fig. 28. — BARC amphibious vehicle with 36.00-41 tires, for taking cargo directly from ship and transporting it inland. Note the low inflation pressure used in the beaching manoeuvre.

Fig. 29. — BARC in cross-country operation. Tire inflation pressure is increased while vehicle is in motion, once the beaching manoeuvre is completed.

Fig. 30. — BARC re-entering the water for another trip to the ship.

Fig. 31. — This photograph, which was a taken in 1943, shows a low-pressure tire which has a large ground contact area, very low unit ground pressure and excellent mobility. It was a fore-runner to the Rolligon and Terratire.

Duplex highway tire. — It is interesting to see how off-highway experience can be applied in highway service. Fig. 32 shows technical data for an experimental 18 - 19.5 Duplex tire which has been developed for use as singles to replace 11 - 22.5 or 10.00 - 20 dual tires. Tires inflation pressure is the same and load-carrying capacity is virtually unchanged. However, spring rate is greatly reduced on the 18 - 19.5 tire, as might be expected from a comparison of loaded and unloaded radii, and this is helpful in reducing vehicle maintenance and damage to fragile merchandise.

	Conventional 11-22.5	Duplex 18-19.5
Ply rating	12	16
Inflation	75 psi	75 psi
Load/tire	4,580 lbs	9,000 lbs
Loaded radius	19.6"	19.3"
Spring rate	10,700 lbs/inch as Duals	6,600 lbs/inch

Fig. 32. — « Duplex » tire data.

Fig. 33 shows the cross-sectional relationship of the 18 - 19.5 Duplex and 11 - 22.5 dual tires. Flotation characteristics of the Duplex tire are very good and interest is being shown in its use on highway vehicles which occasionally go into off-highway service.

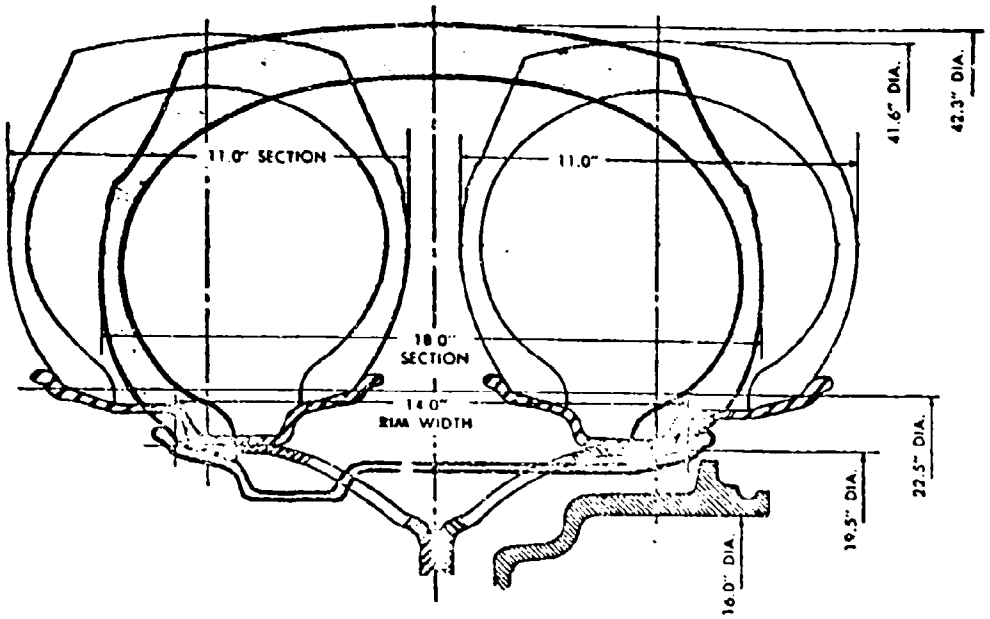


Fig. 33. — Duplex tire, 18-19.5 single to replace 11-22.5 duals.

Fig. 34.

Fig. 34 illustrates the appearance of the two types of tires when mounted on the rear of a vehicle. The 18-19.5 tire is the fore-runner of a line of tires which will be used as singles to replace duals up through 12.00-24 size.

ACKNOWLEDGMENTS. — Photographs used in connection with this paper are through the courtesy of:

R. G. Le Tourneau, Inc.
Arabian American Oil Co.
U. S. Army Transportation and Ordnance Depts.
Firestone Tire & Rubber Co.

DISCUSSIONS

L. AMICI. — Per desiderio di completezza credo sia opportuno, da parte di uno studioso di pneumatici, di ricordare che accanto ai tipi di pneumatici visti ora e che rappresentano in un certo senso la massima punta dei pneumatici tradizionali, esistono pneumatici di tipo nuovo — o relativamente nuovo, perchè esistono già da un certo numero di anni, e cioè i pneumatici radiali, ovvero pneumatici di cui la struttura interna è fatta con fili radiali cioè giacenti in piani passanti per l'asse di rotazione in cui sotto al battistrada vi è un rinforzo longitudinale che può essere di vario tipo.

Questo rinforzo racchiude la carcassa e la costringe ad avere un certo diametro. Ora, su questo semplicissimo principio è basata tutta una teoria nuova, un'ondata nuova, diciamo, una parola nuova nel campo dei pneumatici. Si riesce ad avere con questo tipo una maggiore capacità di carico, cioè a pari dimensioni i pneumatici di tipo radiale portano più carico oppure portano lo stesso carico con pressione inferiori. Ciò è dovuto al fatto che il fianco del pneumatico radiale può schiacciarsi di più mentre il pneumatico con struttura incrociata non può schiacciarsi senza danno oltre un certo limite, che è abbastanza ristretto. Si noti anche che, essendo nel radiale i fili disposti secondo direzioni geodetiche si ha il massimo sfruttamento del materiale. Quindi la struttura può resistere a una certa pressione, avendo il minimo peso. Di conseguenza i radiali pneumatici sono leggeri. Essendo leggeri, l'assorbimento della potenza peristeresi dei materiali è minore, cioè il pneumatico radiale assorbe minore potenza. Ciò è di estremo interesse per i pneumatici fuori strada.

I vantaggi del pneumatico radiale sono poi ancora molti e non si finirebbe quasi più di elencarli minuziosamente. Limitiamoci a dire ancora che la durata dei battistrada in rettilineo, ma soprattutto in curva, è molto maggiore. La ragione di questo è un po' complicata e non la posso indicare qui; comunque rimando a una nostra conferenza al congresso di Parigi, sui pneumatici radiali di tipo agricolo che è stata pubblicata per intero sulla Revue Générale du Caoutchouc (numero dell'ottobre 1959).

Dal punto di vista delle applicazioni del fuori strada il radiale si presta particolarmente bene, direi, nel senso che appunto la mobilità e la gallegiabilità sono qualità caratteristiche del radiale. E' abbastanza intuitiva la ragione: questo grande tegolone che il pneumatico ha sotto al battistrada, lo mette in condizioni di eccellenza, nel senso che l'appoggio sulla strada viene straordinariamente ben ripartito su una lunga superficie. Si può accennare a qualche difetto dei radiali,

oppure a qualche difficoltà di adattamento, diciamo (perchè altrimenti uno si potrebbe chiedere come mai tutti i pneumatici di questi mondo non sono radiali?). Essi hanno talvolta condizioni di adattamento un po' più difficili dei pneumatici normali, e cioè occorre studiare molto bene l'adattamento al singolo veicolo. In particolare danno mobilità trasversale al veicolo, maggiore della normale, e quindi il guidatore del veicolo deve adattarsi a un tipo di guida leggermente diverso. Questo, per qualunque veicolo. Nel caso dei fuori strada tuttavia, questa particolarità che talvolta è dannosa date le basse velocità in gioco, non ha molta importanza; quindi direi che quello del fuori strada è un campo ideale per i pneumatici radiali.

L. BOGDANOFF. — In regard to the equipment which Mr. Finney has shown on the slides I have noticed a great deal of violent bouncing occassionally a... equipment goes across the rough ground, and I am curious to know, Mr. Finney has looked at this problem of vehicle bounce which seems to me to be related quite closely to tractive ability, especially on rough ground. Again the question is: what about the dynamics of the tire-vehicle-soil combination? You have spoken of traction only. What have you done on this?

A. FINNEY. — As I mentioned at the start of my paper, I did not prepare it to be technical in any way. It merely shows the practical application of some tire developments as they are now being used in the field. So I am not prepared to go into deeply technical discussion as we are hearing with some of the other papers. For that reason, I prefer not to take any of your time just to give my own impressions on this question.

S. G. J. KELECOM. — Je voudrais simplement ajouter à cette liste de pneus déjà présentés un nouveau type en essai depui quelques années à la F.N.: le pneu Lypsoid dont la caractéristique principale est la faible pression spécifique et l'absence de flancs latéraux.

Par suppression de ceux-ci on peut augmenter fortement la déformation de la bande de roulement sans craindre une dérive latérale excessive; c'est l'objet de cette nouveauté inventée par le Suisse Straussler.

Les caractéristiques propres de ce pneu nous ont incité à mettre au point un petit véhicule léeger qui, comme vous le voyez sur la photo, est équipé de 3 roues Lypsoid dont une directrice.

Ce véhicule conçu plus spécialement pour servir d'intermédiaire entre le fantassin et la jeep, spécialement pour les troupes aéroportées, est extraordinairement maniable malgré le faible poids sur la roue AV et peut passer sur des sols réputés infranchissables par des véhicules normaux. Il est spécialement adapté aux sables et boues molles.

La photo montrée ici donne une idée de cet engin à grande vitesse où le vol plané n'est pas exclu.

N. 32

The behavior of sand under pneumatic tires

Il comportamento della sabbia sotto il pneumatico

W. J. Turnbull *) - D. R. Freitag **)

ABSTRACT. — *Tests to determine the behavior of sand under pneumatic tires are being conducted in a special facility of the Army Mobility Research Center, U. S. Army Engineer Waterways Experiment Station, Vicksburg, Mississippi. The operation of a dynamometer carriage-soil bin system provides a continuous record of the performance of a tire or track for slip values ranging from slightly negative to 100 per cent. Tests with three pneumatic tires of the same over-all diameter but of different cross-section widths have been conducted on an air-dry sand. Results show that the performance of these tires on the first pass in dependent only upon wheel load and sinkage. If other factors exert an influence on performance, their effects are reflected in sinkage. The test data show that the total traction force developed by the test tires is approximately 0.39 times the tire load. These results are supported by an analysis of the forces acting on the wheel. Problems yet to be solved are outlined briefly.*

A laboratory for the conduct of research on vehicle mobility has been established at the Waterways Experiment Station (WES), Vicksburg, Mississippi, by the U. S. Army Corps of Engineers. This laboratory, a major facility of the Army Mobility Research Center (AMRC) [1], was planned and equipped to provide a broad capability for studying the interaction of a vehicle's running gear with soft soil surfaces. Work now in progress at the AMRC includes the measurement of pressures at the contact interface of a pneumatic tire and soft yielding soils, a study of the magnitude and distribution of stresses induced within a soft soil mass by tracked and wheeled vehicles, the determination of the shape assumed by a loaded pneumatic tire rolling on various types of surfaces, and a study of the influence of tire geometry on the performance of soils subjected to the action of pneumatic tires. This latter study as it applies to sand is the subject of this paper.

The behavior of soils, normally measured or indicated in classic soil mechanics studies by stress-strain relations, failure occurrence, changes in moisture content, density, strength, etc., is also measured in these terms in vehicle mobility research whenever feasible. However, because present instrumentation and techniques are not adequate for the rapid measurement of

*) Engineer, chief, soils division, U. S. Army Engineer Waterways Experiment Station, Vicksburg, Miss.

**) Engineer, chief, Mobility Section, Army Mobility Research Center, Soils Division, U. S. Army Waterways Experiment Station, Vicksburg, Miss.

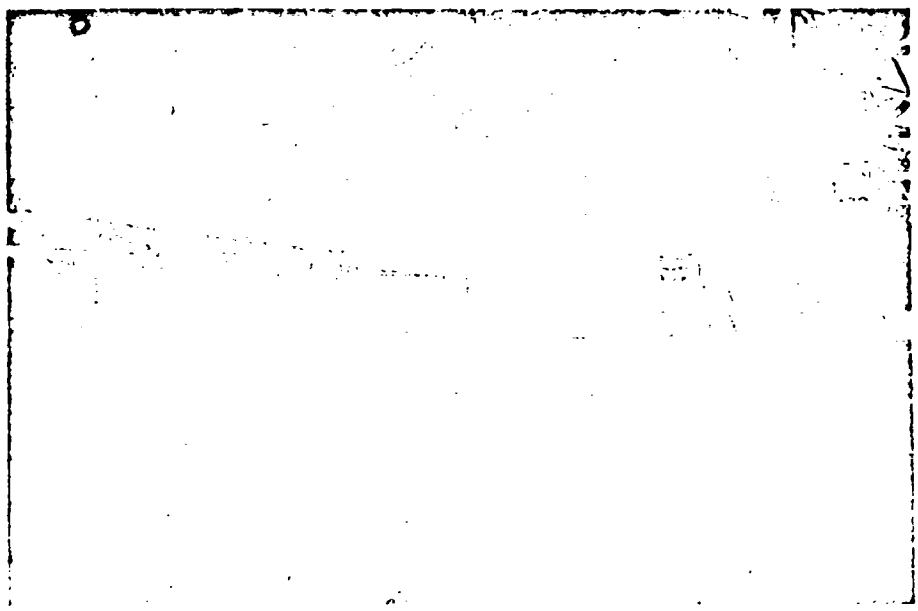


Fig. 1. — Interior of AMRC test facility.

soil behavior, compromises must be effected. Measurements of moisture, density, and strength are made before and after the soil has been loaded but seldom during the actual loading. Stress-strain relations are expressed mainly in terms of loads imposed, contact areas, tire deflection, and sinkage. These are difficult factors to measure with accuracy and even more difficult (at the present time) to employ in formula or equation form. As a result, it has been necessary to measure soil behavior in terms of its effects on vehicle performance. These effects, in turn, are expressed mainly by sinkage, slippage, drawbar pull, etc.

The principal tool employed in the research on the behavior of soils under pneumatic tires is a dynamometer carriage-soil bin system. With this system, model or full-scale vehicle components are studied in controlled soil conditions in much the same manner that aircraft parts are studied in a wind tunnel by the aerodynamicist. The AMRC soil bin is composed of a series of large soil cars or containers-on-wheels that can be joined to form a continuous bin 165 ft long. (See fig. 1).

Cantilevered over the joined soil cars is a pair of carefully aligned rails upon which the dynamometer test carriage assembly is carried. Fig. 2 is a close-up of the details of the carriage, the rail system, etc. A basic supporting frame rides on the rails and is towed by a continuous cable on an electrically powered winch. The wheel to be tested is attached to the supporting frame. The attachment is made in such a manner that the wheel can be loaded and powered and yet be free to move up or down as the soil conditions dictate. The mechanical linkages permit the separation and measurement of horizontal and



Fig. 2. — View of test carriage.

vertical forces. Measurements are also made of driving torque, wheel speed, speed of carriage advance, slip, vertical movement of the wheel, and, by means of special gages inside the tire, the deflection of the tire while moving through the soft soil.

The dimensions of the test apparatus permit the testing of wheels up to 32 in. in outside diameter and 16 in. in width on filled soil cars. Vertical loads up to 3000 lb may be applied either by lead weights or by air pressure. With light vertical loads, tests may be conducted at speeds reaching about 25 mph in the central portion of the soil car line.

Since the determination of the behavior of soils under pneumatic tires is a primary objective of the test program, considerable effort is made to provide uniform, homogeneous soil conditions for each test and to study a broad range of soil conditions. Tests are being conducted on sand, clay, and silt soils. The strength of soil desired for a particular test can be obtained by proper control of the density and the water content of the soil.

The sand normally is tested in the air-dry state, and satisfactory control of its properties can be achieved by varying its density. Since the strength of a cohesive soil is primarily related to its water content, this factor is the principal variant in controlling the properties of the clay and the silt. To prepare the clay and silt soils for testing, a system composed chiefly of standard brick-making equipment is used to mix carefully metered portions of soil and water. This equipment can be seen to the right in fig. 1. After being blended, the soil-water mixture is placed in the soil cars and compacted with a heavy roller.

Several kinds of tests to evaluate the state of the soil are made before a test is run. Cone index is determined with a mechanized version of the WES cone penetrometer [2], plate bearing tests are made with three different sizes of circular plates, and torsion shear and vane shear tests are made. Soil samples are taken for determination of the water content and dry density of the soil and for use in conventional laboratory shear tests. Thus, a complete set of test

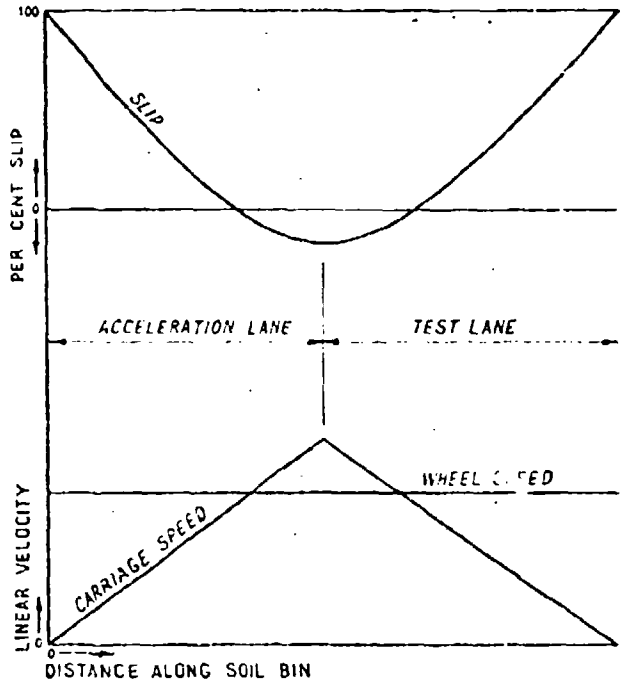


Fig. 3. — Schematic of operating technique.

data includes not only the usual soil data such as water content, density, cohesion, and angle of friction, but also the WES cone index, the seven soil values proposed by Bekker [3], and the relative plate bearing resistance, C_r, employed in the U. S. Army Transportation Corps model-vehicle research programs [4]. Some of these data are also obtained at intervals during the course of the test to determine the changes caused by the applied traffic.

The tires used in the test program are intended to represent as broad a range of geometrical characteristics as possible within the limitations of the test apparatus. One basic set of test tires is composed of tires with the same over-all diameter (about 28 in.) but of different cross-section widths. Another set is composed of tires that have the same cross-section width (about 4-½ in.) but are of different over-all diameters. Also, tires of the same size but of different ply ratings, low-profile tires, radial-ply tires, bag-type tires, etc.,

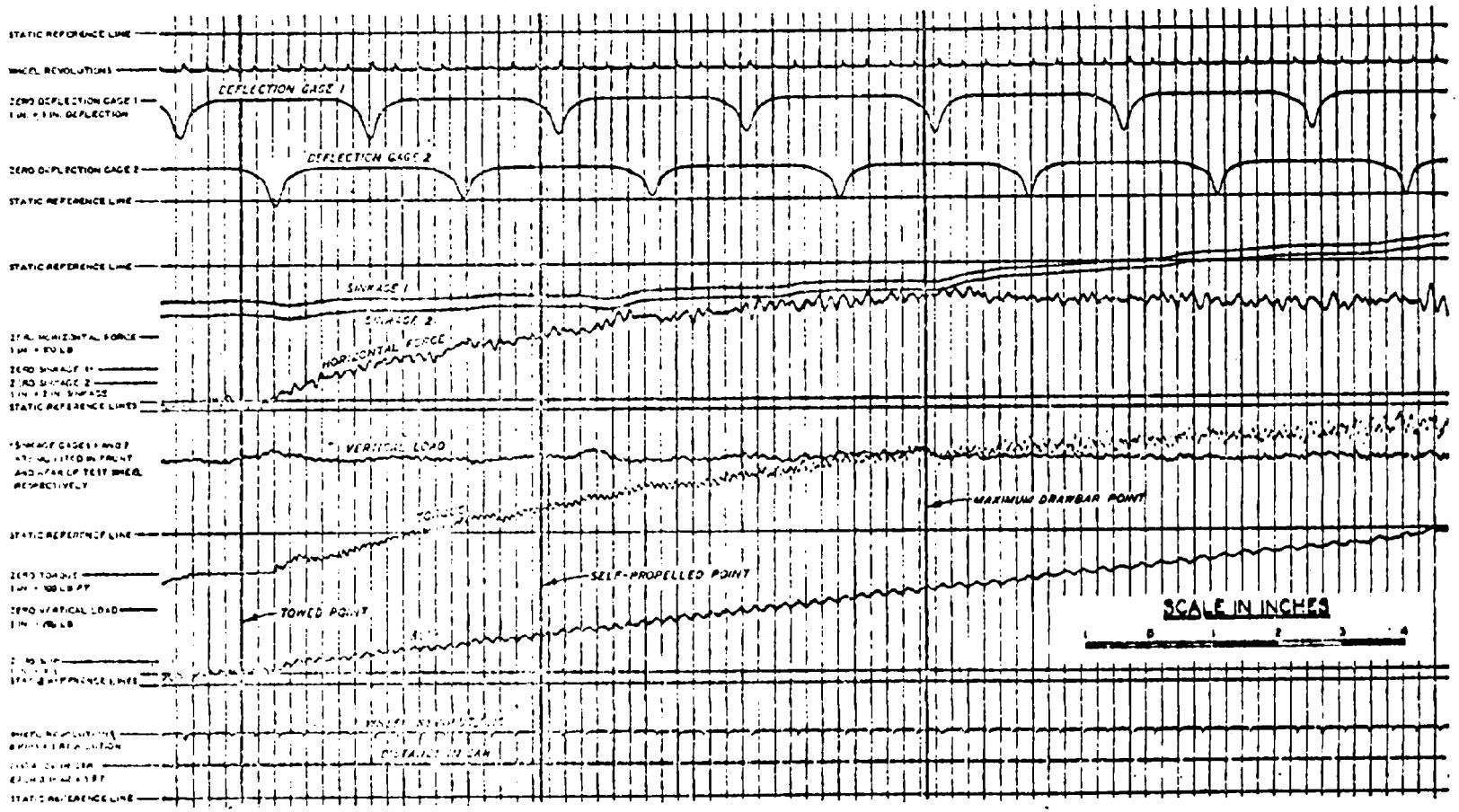


Fig. 4. — Typical oscillograph trace.

are to be used. Several loads, inflation pressures, and deflections are used for each tire in the test program. Normally, for each load, inflation pressures are selected that will result in tire deflections of 15, 25, and 35 per cent of the unflected height of the tire cross-section (as measured from the rim flange). In the research to date, the effect of tread pattern has been eliminated by using treadless tires. This feature will be included in later tests.

A multiple-pass run is made with each tire in each test condition. A complete drawbar pull-slip curve is developed on each pass. The operating technique employed to accomplish this is shown diagrammatically in fig. 3. The speed of rotation of the wheel is held constant while the forward speed of the carriage is varied. When the carriage speed is equal to the theoretical forward speed of the wheel (i.e., the rotational velocity times the circumference of the wheel), the wheel is at zero slip. When the carriage speed exceeds the theoretical wheel speed, slip is negative. When the carriage speed is zero, the wheel is at 100 % slip. The actual data run is made by increasing the slip from negative values through zero to 100 %. Since some time is required to accelerate the carriage to the required speed, the first two cars in the line are used for this purpose. The data are collected during the time the wheel is running in the third and fourth cars in the line-up.

A section of a test oscillograph, obtained in an actual test run, fig. 4, illustrates the nature of the raw data records obtained. In fig. 5, the horizontal force and torque data from the oscillograph have been plotted against slip, also from the oscillograph, to show a typical drawbar-slip and torque-slip curve. Points on the drawbar-slip curve that are of major interest in this study are the zero torque (towed) point, the zero drawbar pull (self-propelled) point, and the maximum drawbar pull point. These points are indicated in figs. 4 and 5. Performance at certain constant slip values (e.g., 20 % slip) also has been considered worthy of study. Performance data collected at each of these reference points for each pass include the vertical load, horizontal force (i.e., the drawbar pull, either positive or negative), torque input, wheel sinkage, wheel slip, and deflection of the tire.

At the time this paper was written, the majority of investigations had been conducted on sand using only three different sizes of tires. The scope of this paper is therefore limited by these considerations. In the interest of brevity, this paper is further limited to typical results obtained with one tire on its first run through the sand, selected comparisons to show the effects of variations in cross-section width of tires, and examples of certain trends such as the influence of repetitive traffic on the behavior of the sand. Most of the data shown will be those obtained with the 4.50-18 tire, since it was used to explore test program techniques, determine capabilities of various components of the test apparatus, check data reproducibility, etc. Normally, fewer investigations will be conducted with each tire than are suggested by the data available for the 4.50-18 tire.

The horizontal forces in pounds measured on the first pass at the towed point and at the maximum drawbar pull point have been selected to represent

the effects of soil behavior on tire performance. The horizontal force at the towed point (hereafter referred to as the towed force) acts in a direction opposite to the direction of the horizontal force at the maximum drawbar pull point. Therefore, for clarity, the towed force has been considered a negative

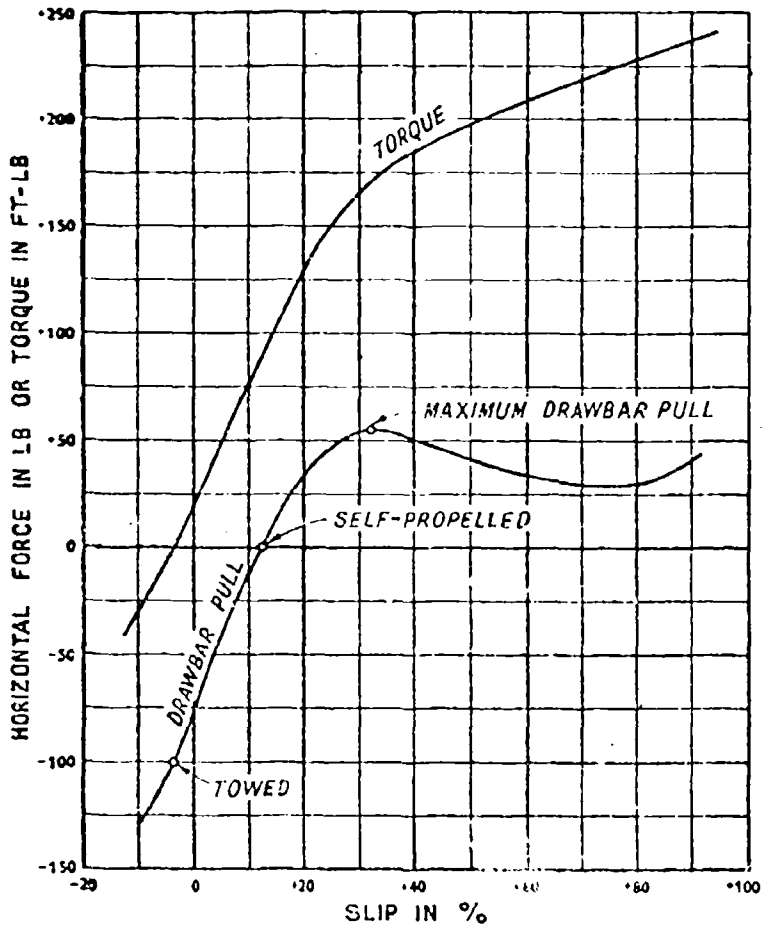


Fig. 5. — Typical drawbar pull-slip and torque-slip curve.

pull and is so plotted on the accompanying figures. The sinkage of the wheel measured at the points under consideration has been selected to indicate the relative severity of the test conditions.

In fig. 6, first-pass towed force has been plotted against sinkage for all runs with the 4.50-18 tire loaded to 900 lb. It will be noted that test data for 15, 25, and 35 % deflection (70-, 31.7-, and 19.9-psi inflation pressures, respectively) and for various sand densities are included on the plot. Although the data for 35 % deflection are somewhat scattered, a single curve suffices to

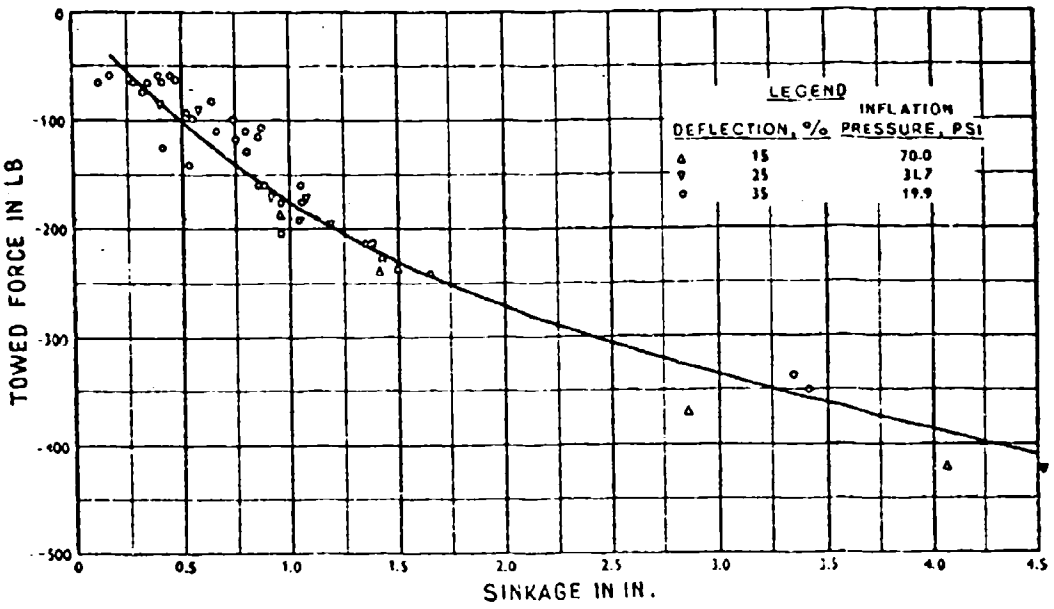


Fig. 6. — Towed force vs sinkage, first pass, 4.50-18 smooth tire, 900-lb load.

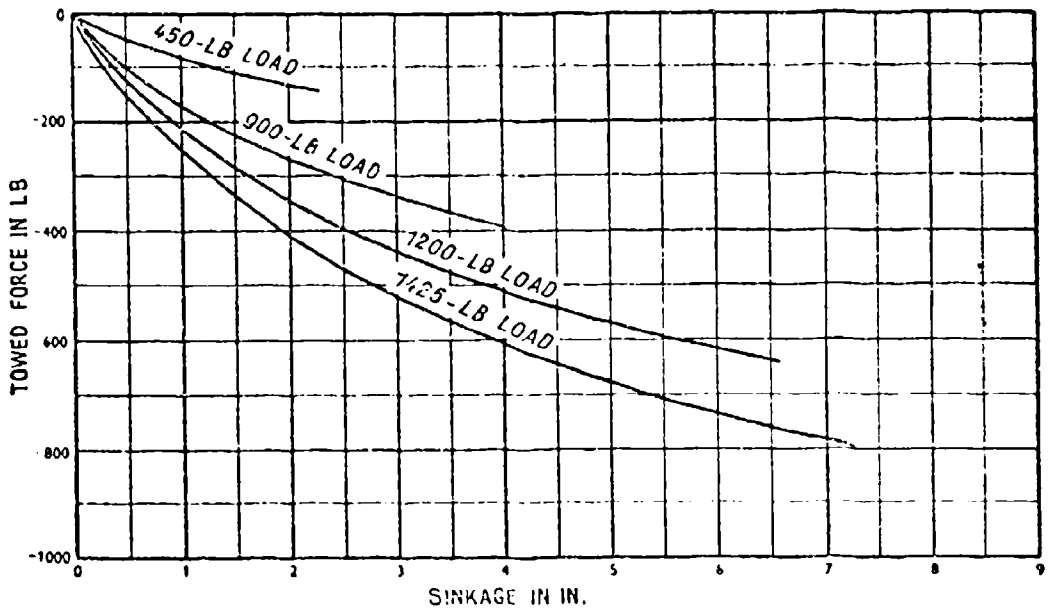


Fig. 7. — Towed force vs sinkage, first pass, 4.50-18 smooth tire, various loads.

characterize all the data. This suggests that the influence of inflation pressure and tire deflection on performance at the towed point is reflected in the sinkage measurement.

A distinct relationship between towed force and sinkage can be developed for each of the test loads used with this tire. As is the case of the 900-lb load, the curves for the 450-lb, 1200-lb, and 1425-lb loads were better defined at high sinkages than at low sinkages. A family of curves representing test results for a wide range of loads is shown in fig. 7. Similar curves were obtained from data from tests of the other two tires.

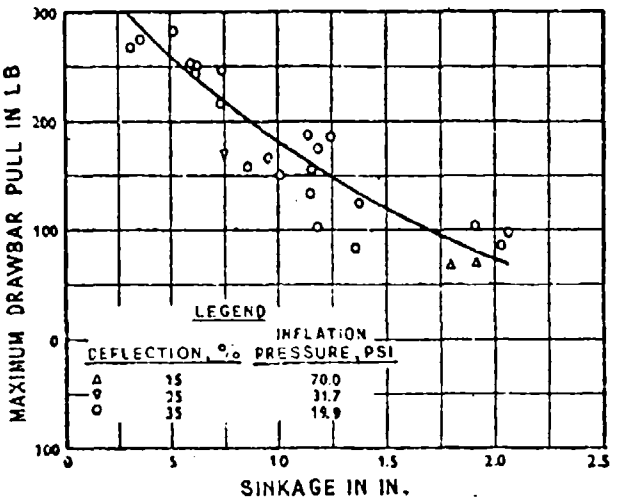


Fig. 8. — Maximum drawbar pull vs sinkage, first pass, 4.50-18 smooth tire, 900-lb load.

Maximum drawbar pull obtained on the first pass with the 4.50-18 tire loaded to 900 lb is plotted against sinkage in fig. 8. The sinkage plotted is that measured at the maximum drawbar pull point. It should be noted that the sinkage at the maximum drawbar pull point in a test run is greater than at the towed point in the same run. This effect, which can be noted in fig. 4, is apparently a function of slip. Again, results obtained with the specified load at all inflation pressures and on all sand conditions have been included and a single smooth curve has been drawn to represent all the data. As with the towed force, it appears that if factors other than load influence the performance of the tire, they are reflected in sinkage.

A family of curves representing the maximum drawbar pull versus sinkage relation for the 4.50-18 tire for three loads is shown in fig. 9. It will be noted that the curve for the 1425-lb load indicates that the maximum drawbar pull becomes negative when the sinkage exceeds about 3 in. A negative maximum drawbar pull means that the resistance to the motion of the wheel through

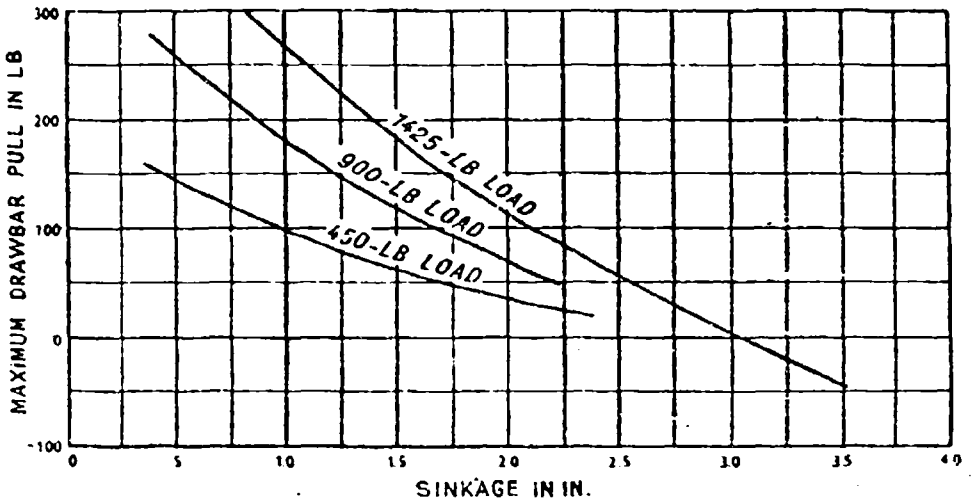


Fig. 9. — Maximum drawbar pull vs sinkage, first pass, 4.50-18 smooth tire, various loads.

the sand was so great that the powered wheel could not derive enough tractive force from the sand to propel itself and it was effectively immobilized. This state was not reached in tests at lesser loads, but the shapes of the curves suggest that the maximum drawbar pull would become zero also at about 3 in. of sinkage.

It does not require a careful scrutiny of the two families of tire-performance curves to recognize the regular pattern established by varying the load on the tire. In fig. 10a the ratio of maximum drawbar pull to load (maximum drawbar pull coefficient) has been plotted against sinkage; and in fig. 10b, a similar plot of ratio of towed force to load (towed force coefficient) has been made. In both plots all the available data with the 4.50-18 tire have been used without regard to load, inflation pressure, soil strength, soil density, or any other factor.

In fig. 11a and 11b, the data obtained from tests on the 9.00-14 tire also are plotted in terms of maximum drawbar pull and towed force coefficients. As with the 4.50-18 tire, the data appear to be less precise at small sinkages than at the greater sinkages. Further study is needed in this region to determine if the scatter is caused by inadequate measuring techniques or if an inherently unstable condition exists as a result of purely physical factors.

The curves drawn to represent the 9.00-14 tire test results are exactly the same as for the 4.50-18 tire. The fit is remarkably good. Since the 9.00-14 tire is almost twice as wide as the 4.50-18 tire, this indicates that tire section width, like inflation pressure, has an effect on performance only insofar as it influences the amount of sinkage. The two tires have very nearly the same overall diameter, so no inference can be drawn concerning the effect of this dimension.

The similarity in the shapes of the towed force-sinkage and maximum drawbar pull-sinkage curves is remarkable. In fig. 12, the towed force coefficient and maximum drawbar pull coefficient for the same sinkage have been added without regard to sign and plotted against the sinkage. To do this logically, it has been necessary to assume that the resisting force experienced by the

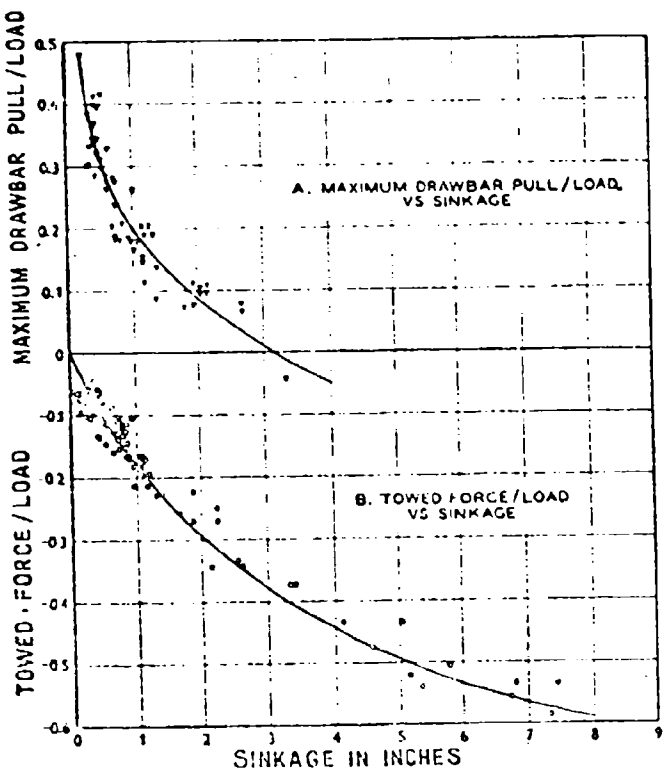


Fig. 10. -- Performance vs sinkage, first pass, 4.50-18 smooth tire.

powered wheel at the maximum drawbar pull point is the same as that measured for the towed wheel, when the sinkage is the same. As a result of this combination, a traction coefficient has been derived that, except at low sinkages, is a constant. If the towed force plus the maximum drawbar pull represents the total horizontal thrust developed by the wheel, then the constant can be considered a coefficient of friction for the interaction between tire and sand.

Another measure of the thrust developed by the tire rotating on the soil is the torque input. In fig. 13a, the torque measured at the maximum drawbar pull point has been plotted against load for the tests with the 4.50-18 tire and in fig. 13 b, the same plot is shown for the 9.00-14 tire data. Straight lines

have been drawn through the origin to represent both sets of data. While there is a satisfactory fit for the 9.00-14 tire, it appears less satisfactory for the 4.50-18 tire, particularly at the largest loads.

Some of the scatter evident in these data plots is believed to result from different degrees of slip that are associated with the maximum drawbar pull

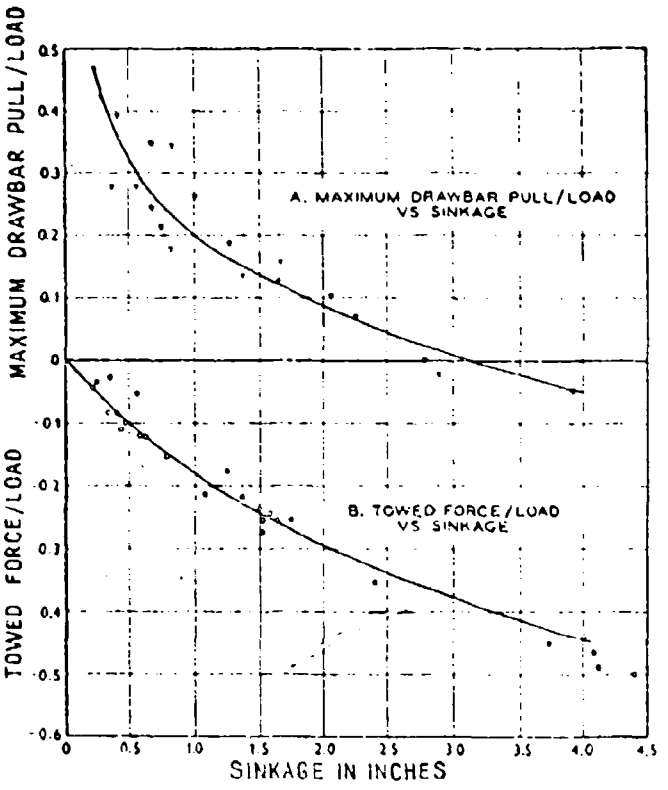


Fig. 11. — Performance vs sinkage, first pass, 9.00-14 smooth tire.

point under the various test conditions. This factor may account for about half the dispersion of the test results. The reason for the remainder cannot be identified at this time.

The straight-line relation of torque to load provides a basis for checking the results of the towed force plus maximum drawbar pull analysis. In fig. 14, the forces acting upon a wheel are diagrammed both for the towed-wheel condition and for the powered-wheel condition. In the case of the towed wheel in a steady state, the wheel load W is balanced by the vertical soil reaction RV, and the towed force TF is equal and opposite to the horizontal soil reaction RH. Since in the steady towed condition there is no torque on the wheel, the algebraic sum of moments about the axle must equal zero. Therefore, the

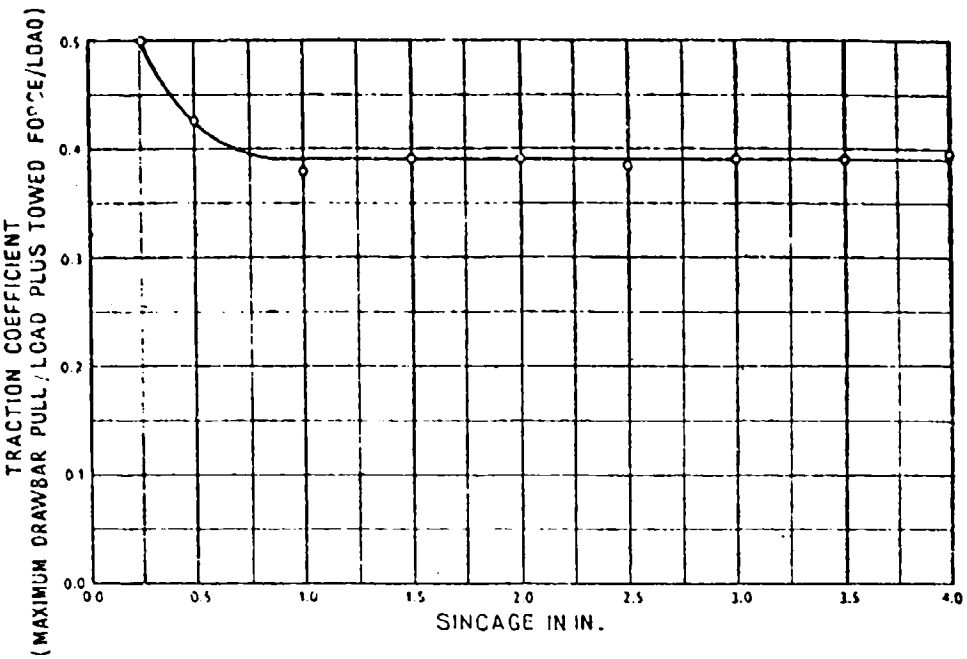


Fig. 12. — Traction coefficient vs sinkage, first pass, 4.50-18 and 9.00-14 smooth tires.

resultant of the vertical soil reaction must be shifted forward a distance mv so that:

$$\overline{RV}\ (mv) = \overline{RH}\ (mh) \qquad \text{(Eq 1)}$$

In the case of the powered wheel, the horizontal force at the axle normally changes direction and becomes the drawbar pull. A torque input, TO, is added, as is the horizontal traction force TE. The equations of equilibrium require that:

$$W = \overline{RV} \qquad \text{(Eq 2)}$$

$$\overline{TE} = \overline{DB} + \overline{RH} \qquad \text{(Eq 3)}$$

$$\overline{TO} + \overline{RH}\ (mh) = \overline{RV}\ (mv) + \overline{TE}\ (rd) \qquad \text{(Eq 4)}$$

Only the forces W and DB and the torque TO are measured directly. The moment arm rd can be calculated from the undeflected tire radius and the deflections measured by the gages inside the tire. The remaining values can be supplied only if certain assumptions are made. If it is assumed that the force RH is a function only of sinkage, then from the experimental data discussed previously (fig. 12), it can be stated that for the tires tested, the traction force $\overline{TE} = 0.39W$. If it is further assumed that $\overline{RV}$ (mv) = RH (mh) as in the case of the towed wheel, then $\overline{TO} = \overline{TE}$ (rd).

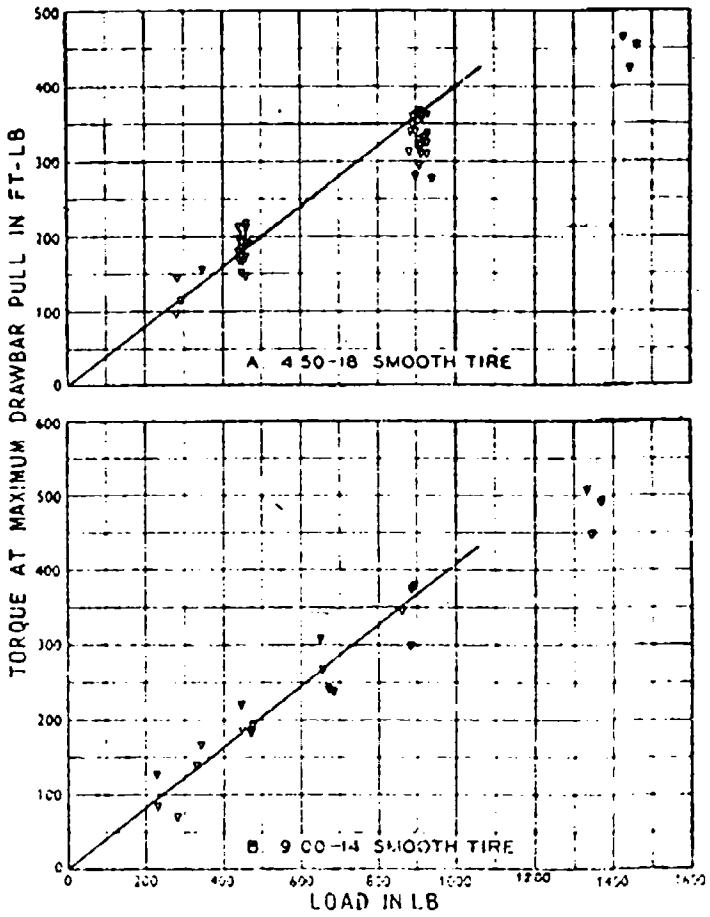


Fig. 13. — Torque at maximum drawbar pull vs load, first pass.

The average deflected radius, rd, measured in the tests on the 4.50-18 tire is 12.3 in. and for the 9.00-14 tire about 12.6 in. Therefore, for the 4.50-18 tire:

$$\overline{TO} = \frac{12.3}{12}(0.39)W = 0.40W \text{ ft-lb}$$

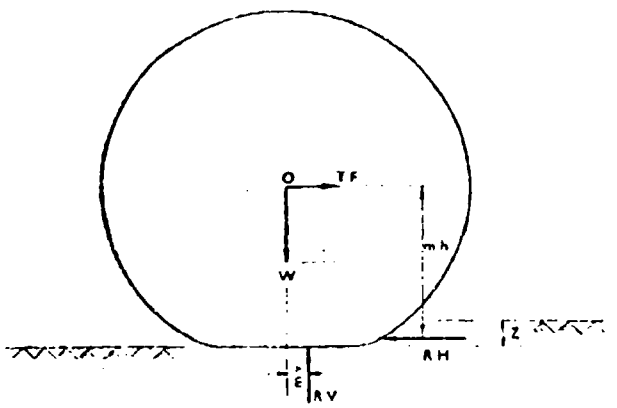
and for the 9.00-14 tire:

$$\overline{TO} = \frac{12.6}{12}(0.39)W = 0.41W \text{ ft-lb}$$

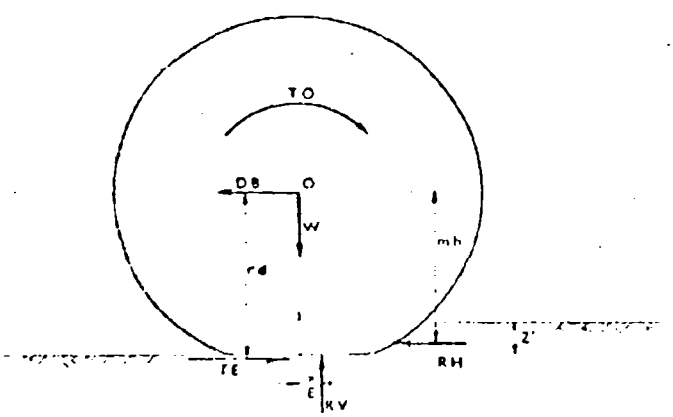
The straight lines delineated by these equations are those that have been

drawn through the data points in fig. 13a and 13b. The fit is quite reasonable except, as noted previously, for the higher loads.

From the data and discussions presented thus far, it can be concluded that the effect of sand condition on the performance of a tire on its first pass



A. TOWED WHEEL



B. POWERED WHEEL

Fig. 14. — Diagram of forces on wheel in sand.

can be predicted if the sinkage that will occur can be predicted. Unfortunately, at the time of this writing the sinkage cannot yet be predicted satisfactorily. Existing analytical approaches such as classical bearing capacity equations and Bekker's sinkage equations were found to be inapplicable. The experimental data form regular patterns, however, and it should not be too difficult to derive a general equation for sinkage in terms of tire size, load, soil strength, etc.

A typical load-sinkage curve is shown in fig. 15. The data are for the 4.50-18 tire at 35 per cent deflection on a medium-strength sand. The sinkages are those measured at the towed point. Although there is some scatter of the data, no difficulty is experienced in drawing an average curve. The effect of sand

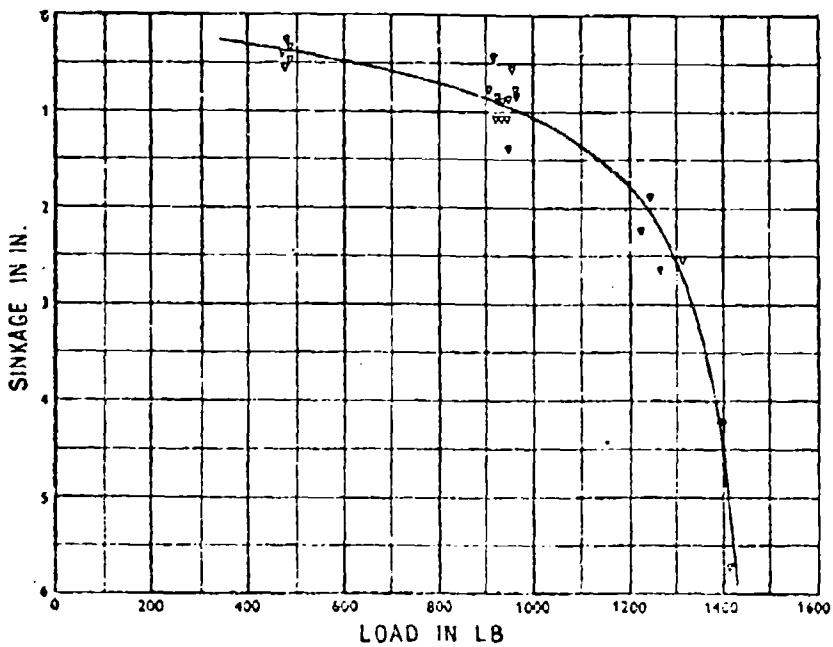


Fig. 15. — Sinkage vs load, first pass, towed 4.50-18 smooth tire, 35 % deflection, medium strength sand.

strength is illustrated in fig. 16 where load-sinkage curves for soft, medium, and firm sand are drawn. Approximate numerical evaluations of the sand condition described by the terms soft, medium, and firm can be obtained from the table below:

Descriptive term	Soft	Medium	Firm
Dry density, lb/cu ft	97.5	99.5	101.5
Friction angle, degrees	34	34 ½	35
Cone index [2], psi	25	40	55
K_ϕ [3], lb/in.$^{n+2}$	10.0	13.5	19.3
K_c [3], lb/in.$^{n+1}$	0	0	0
n [3], dimensionless	0.8	0.8	0.8
C_r (14-in.-diameter plant) [4], dimensionless	0.44	0.61	0.78

The curves in fig. 16 show, as would be expected, that the strongest sand can carry the greatest load without excessive sinkage. Also, the general shapes of the load-sinkage curves are not unlike those obtained in the plate bearing tests. The influence of tire deflection on the load-sinkage curves is shown in fig. 17a. Tire prints made on an unyielding surface show that the area of the

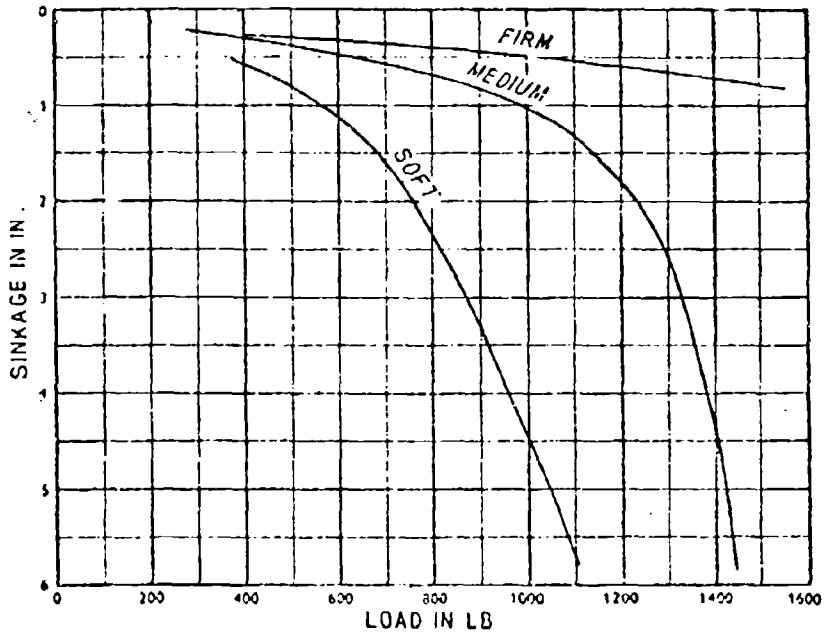


Fig. 16. — Sinkage vs load, first pass, towed 4.50-18 smooth tire, 35 % deflection.

tire in contact with the surface is about the same for all loads if the deflections are the same. For the 4.50-18 tire, the hard surface contact areas approximately double with each 10 % increase in deflection. The actual areas are about 12.5 sq in. at 15 % deflection, 23 sq in. at 25 % deflection, and 36 sq in. at 35 % deflection. A load-sinkage curve for a constant deflection, then, can also be considered a contact pressure-sinkage curve. At any given load the three deflections also represent different contact pressures. However, if the data of fig. 17a are replotted on the basis of contact pressure instead of load, fig. 17b, the curves do not collapse except for small sinkages.

In fig. 18, load-sinkage curves for two tires are compared. All test conditions were closely similar in these tests, except that the 9.00-14 tire has a section width approximately twice that of the 4.50-18 tire. The data are too few to be conclusive, but the trend suggests at least that the load per unit width may be a useful factor in comparing the performance of different sizes of tires.

All of the results described thus far have been only for the first pass of the wheel through the sand. Since almost all military vehicles have two or three driving wheels following one behind the other, it is of considerable

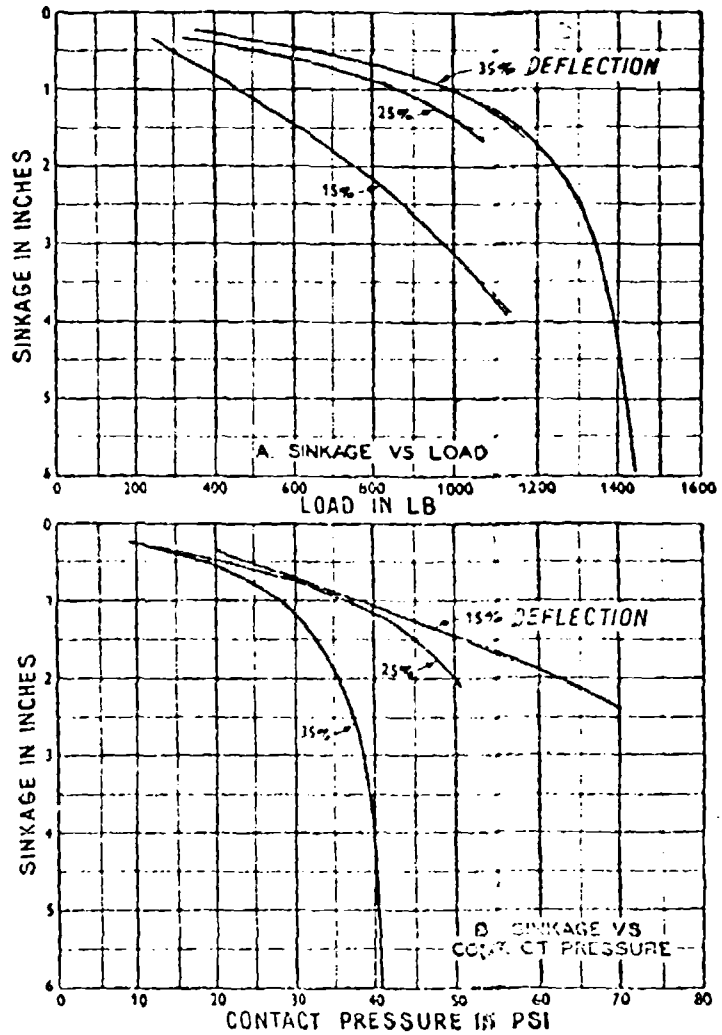


Fig. 17. — Sinkage vs load and contact pressure, first pass, towed 4.50-18 smooth tire, medium strength sand.

importance to study the effects of repetitive traffic. Data of this nature are being collected on all tests conducted by the AMRC, but as yet they have not been given detailed study. Discussion of this aspect of the work will be sufficient only to outline the nature of the problems involved.

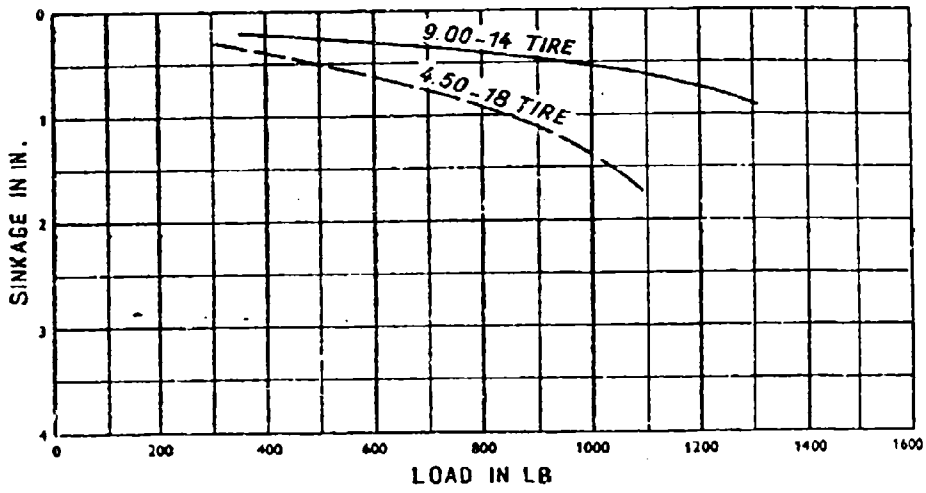


Fig. 18. — Sinkage vs load, first pass, towed smooth tires, 25 % deflection, medium strength sand.

Analysis of multiple-pass data is complicated by the fact that practically all the conditions except the tire itself and its load are constantly changing. One of the more perplexing problems is that the percentage of slip at which the maximum drawbar pull occurs varies with the conditions created on the previous pass. This presents difficulties not only in analysis but also in establishing the manner in which the test should be run. For illustrative purposes, two test conditions have been selected. Various data items measured during the test have been plotted against the number of passes in fig. 19 to show in graphic form the changes that occur during the test.

In general, as the plotted data suggest, it is found that there is a definite trend for many of the test parameters to approach an equilibrium value. This value may be either greater than or less than the first-pass magnitude of the parameter, depending upon the initial condition of the sand. This is of considerable interest in the operation of long, train-like vehicles or in multiple-vehicle operations, for the effect is to lessen the importance of the first wheel over a given point. In poor going, the data suggest that trains should be advantageous but that on firm sands, dispersed, single-unit operation may be more efficient.

It is readily evident that there is much yet to be learned concerning the effects of sand behavior on the operation and performance of pneumatic tires. It is hoped that the experiments being conducted at the AMRC will provide the data that will eventually fill the gaps in the knowledge in this area. In the future, the study will be extended to include pneumatic tires on soft clay and tracks on both sand and clay where even more challenging problems are believed to lie.

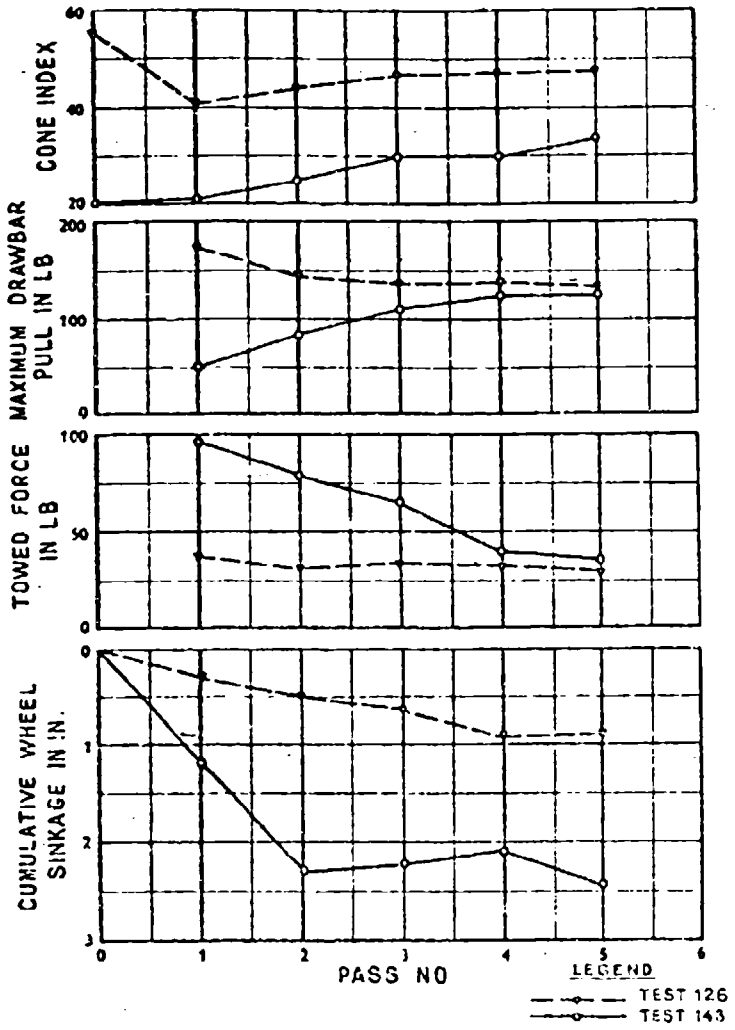


Fig. 19. — Effects of repetitive traffic, 4.50-18 smooth tire, 150-lb load.

BIBLIOGRAPHY

1) Knight S. J. The Army Mobility Research Center. The Military Engineer (Society of American Military Engineers, Mills Bldg., Pennsylvania Ave., at 17th St., N. W., Washington 6, D. C.), vol. 52, No. 347, pag. 208-212, May-June 1960.

2) Knight S. J. A summary of trafficability studies through 1955. Technical Memorandum no. 3-240, 14th Supplement, U. S. Army Engineer Waterways Experiment Station, Vicksburg, Mississippi, December 1956.

3) Bekker M. G. A proposed system of physical and geometrical terrain values for the determination of vehicle performance and soil trafficability. Interservice Vehicle Mobility Symposium, Office of Ordnance Research, Published by Land Locomotion Research Branch, OTAC, Detroit, 1955.

4) Nuttall C. J. Jr. and Wilson C. W. Scale-model vehicles in snow. Report No. 29-3 prepared under contract with TRECOM, Chestertown, Md., 1959.

N. 33

Messungen von Rollwiderstand und Zugkraft von luftbereiften Ackerschleppern sowie mechanischen Bodenkenngrössen und Versuch einer Zuordnung

Comparison between relationships of agricultural tractors and mechanical soil values

Misure di resistenza al rotolamento di trattori agricoli con pneumatici in relazione alle caratteristiche del terreno

W. Söhne *) - F. J. Sonnen **)

ABSTRACT. — *After World War II the Departments of Tractor Research and of Basic Research in Agricultural Engineering in the Agricultural Research Center Braunschweig-Völkenrode began some investigations on the relationships between vehicle and agricultural soils, basing on previous studies in this field. Besides other work measuring devices and methods were set up which enabled investigations on the traction performance of entire vehicles in relation to slip and the rolling resistance as well as determination of shearing resistance of soils and vertical soil deformation under loaded plates.*

These devices were used for measurements on different kinds of mineral soils and on peat soil. The tests on mineral soils were to show the differences in rolling resistance, traction and soil coefficients on tough and settled stubble fields and on ploughed soils.

As to be expected, each cultivation of the soil decreased the traction performance and increased the rolling resistance. The pressure tests indicated that pressure increase complies with the Gorjatschkin formula practically only on settled and uniformly moist mineral soils. Loose mineral soils with tillage boat or, in the whole, soils with structure and humidity variations, differ widely.

It proved that the Gorjatschkin formula does not apply to peat soils. Contrary to mineral soils, which show always an increasing pressure with growing depth, peat soils indicate a maximum with decreasing or only remaining pressures. Moreover the characteristics of pressure are considerably influenced by rooted sods or by firmer or drier surface layer.

As shearing tests have proven, structure variations of mineral soils due to soil cultivation and plants growth have an influence on the course of the shear stresses in relation to the shearing and gliding way. Likewise even very intense cultivation does not alter the angel of internal friction to a mayor extent, provided humidity and

---

*) Privatdozent Dr. Ing. Walter Söhne ist wissenschaftlicher Mitarbeiter am Institut für Landtechnische Grundlagenforschung (Direktor: Prof. Dr. Ing. W. Bätel) der Forschungsanstalt für Landwirtschaft, Braunschweig-Völkenrode.

**) Dipl. Ing. Franz-Joseph Sonnen ist wissenschaftlicher Mitarbeiter am Institut für Schlepperforschung (Direktor: Prof. Dipl. Ing. H. Meyer) der Forschungsanstalt für Landwirtschaft, Braunschweig-Völkenrode.

pressure remain constant. Cohesion varies considerably in relation to the texture, but can be put to zero for some time by agricultural cultivation. According to the results hitherto, testing methods and devices should be improved so far, that better correlations between physical soil characteristics and coefficients of rolling resistance and traction can be obtained.

In der Landwirtschaft müssen vorwiegend ausserhalb fester Fahrbahnen Lasten transportiert und Geräte zur Bodenbearbeitung, Pflanzenpflege und Ernte gezogen werden. Dazu wurden in der Vergangenheit Tiere verwendet, die sich schwierigen Bodenverhältnissen relativ gut anpassen können, die jedoch durch den landwirtschaftlichen Traktor zunehmend verdrängt werden.

Die Ausbildung der Fahrwerke dieser Ackerschlepper, der Arbeitsmaschinen und -geräte und der Transportfahrzeuge erfolgte im wesentlichen empirisch. Dabei stützte man sich auf Fehlversuche, deren Ergebnisse jedoch keinen Einblick in die Zusammenhänge der Vorgänge zwischen Reifen und Boden gestatten. Allerdings setzten bereits vor dem ersten Weltkrieg Bemühungen um ihre Erforschung ein [1].

Nach dem zweiten Weltkrieg wurde anknüpfend an diese Arbeiten die Erforschung der Zusammenhänge wieder aufgenommen. Ihr Ziel ist, die Bewegung der Fahrzeuge ausserhalb fester Fahrbahnen so sicher wie möglich zu machen. Dazu müssen die Rollwiderstände der Laufwerke gesenkt und die Vortriebskräfte gesteigert werden. Als Voraussetzung hierfür müssen zunächst die vom Boden aufnehmbaren Drücke, die Schubspannungen und die Verformungen in der Berührungsfläche zwischen Laufwerk und Boden bestimmt werden. Neuerdings werden in der Forschungsanstalt für Landwirtschaft, Braunschweig-Völkenrode, Untersuchungen durchgeführt, die eine Korrelation zwischen den physikalischen Bodenkenngrössen und den Rollwiderständen und Vortriebskräften gestatten sollen.

1. - Messmethoden und -einrichtungen

1.1) Messmethoden und -einrichtungen zur Ermittlung von Zugkraft, Schlupf und Fahrwiderstand von Laufwerken.

Das Institut für Schlepperforschung führt seine Versuche auf Acker oder Wiese durch, es nimmt die damit verbundene Ungleichförmigkeit von Textur und Struktur des Bodens in Kauf, um sich den praktischen Verhältnissen anzunähern. Innerhalb der einzelnen Versuchsreihen muss jedoch die Ungleichförmigkeit möglichst gering sein. Die zu untersuchenden Fahrwerke werden an geeigneten Fahrzeugen entsprechenden Gewichts und passender Motorleistung angebracht. Diese werden von einem Messwagen gezogen bzw. abgebremst. Die zwischen Versuchsfahrzeug und Messwagen ausgeübte Kraft wird über einen Zugkraftmesser registriert. Rollwiderstände einzelner Achsen eines Fahrzeuges werden getrennt aufgenommen.

Als Messwagen (Bild 1.01) wird ein geländegängiges Fahrzeug mit Allradantrieb und Allradbremse benutzt. Für die Registrierung der Zugkraft

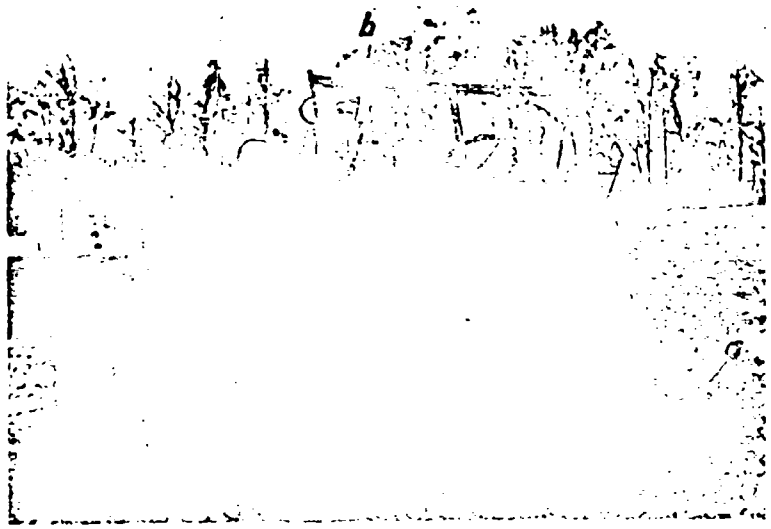


Bild 1.01. — Zugkraft-Messwagen mit Zugkraftschreiber. a) Höhenverstellbarer Geber. b) Registriergerät für Zugkraft und Schlupf.

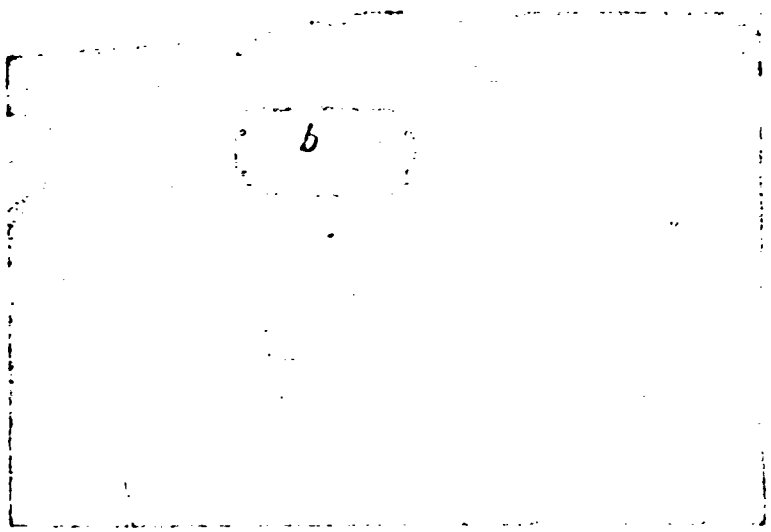


Bild 1.02. — Registriergerät für Zugkraft und Schlupf. a) Schreibeinrichtung. b) Rechengetriebe f. Schlupf. c) Geber für Weg. d) Geber für Triebradumdrehungen.

genügt eine Einrichtung mit hydraulischer Kraftübertragung auf das Schreibgerät, da hohe Frequenzen nicht erfasst werden müssen. Zugleich mit der Zugkraft wird der Schlupf bei treibenden Fahrwerken aufgezeichnet (Bild 1.02). Ein zusätzlicher Funktionsschreiber (XY-Recorder) hierfür ist noch nicht erprobt.

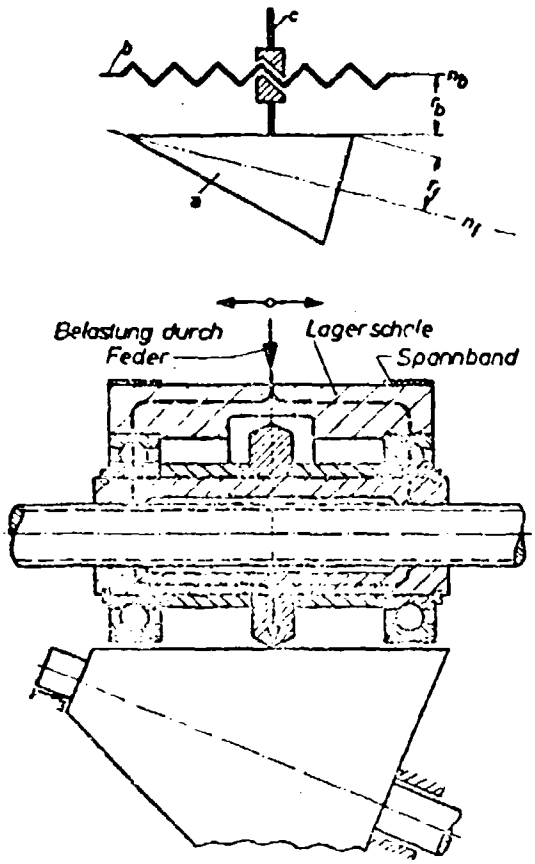


Bild 1.03. — Rechengetriebe des Schlupfmessers.

Der Schlupf lässt sich nach Freise [3] dadurch messen, dass man die Differenz zweier Drehzahlen bestimmt und sie zu einer von beiden ins Verhältnis setzt. Bezeichnet man die für eine bestimmte Strecke erforderliche Anzahl der Umdrehungen der Triebräder unter Schlupf mit z, die Anzahl der Umdrehungen bei schlupflosem Abrollen der Triebräder auf der gleichen Strecke mit z_0, dann gilt für den Schlupf

$$\sigma = \frac{z - z_0}{z} \cdot 100 = \left(1 - \frac{z_0}{z}\right) \cdot 100\ \%$$

Bei dem Entwurf des Messgerätes wurde von einer von Freise angegebenen grundsätzlichen Anordnung ausgegangen (Bild 1.03), mit der diese Beziehung ausgewertet werden kann. Es handelt sich dabei um ein stufenlos einstellbares Getriebe aus einem Reibkegel und aus einem Reibrad, das auf einer mit Gewinde versehenen Welle (Spindel) gelagert ist. Das Reibrad wird an den Kegel ohne Belastung der Welle angepresst. Reibrad und Kegel haben infolge der zwischen ihnen bestehenden Reibung gleiche Umfangsgeschwindigkeiten. Aendert sich die Drehzahl von Kegel oder Welle, so verschiebt sich

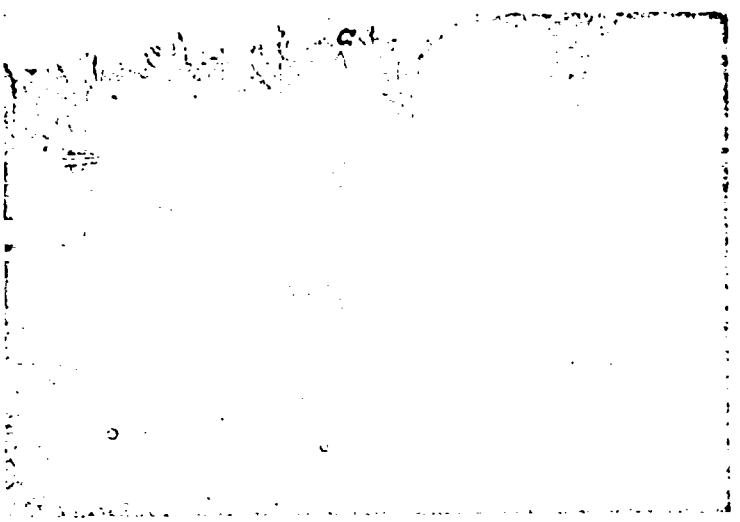


Bild 1.04. — Zugkraftmesswagen. a) Geber für Weg (Ablaufeinrichtung f. Drahtseil mit Variatorgetriebe). b) Messeinrichtung f. Zugwiderstände.

das Reibrad auf der mit Gewinde versehenen Welle axial so lange, bis die Drehzahldifferenz ausgeglichen ist. Die axiale Lage des Reibrades ist ein direktes Mass für den Schlupf, sie wird auf dem gleichen Messstreifen wie die Zugkraft aufgezeichnet. Die Anzeigegenauigkeit des Schlupfmess- und Schreibgerätes beträgt $\pm$ 1 % Schlupf. Die Einstellzeit ist kleiner als 0,5 sec. bei Aenderung des Schlupfes von 20 %. Der Reibkegel wird von der Zapfwelle des Versuchsschleppers angetrieben, deren Umdrehungen in einem festen Verhältnis zu denjenigen der Triebräder stehen. Die Spindel wird entweder von einem Mitlaufrad oder bei schwierigen Ackerverhältnissen von einer Seilrolle aus gedreht, über die ein im Boden verankertes Seil abläuft (Bild 1.04). Um die Uebersetzung den wechselnden Reifendurchmessern und Fahrbahnbedingungen anpassen zu können, ist ein weiteres stufenloses Getriebe zwischen Spindel und Seilrolle geschaltet. Die Uebersetzung wird dann jeweils so gewählt, dass dass Messgerät bei schlupflosem Abrollen der Reifen auf dem Boden die Nullanzeige gibt. Das Gerät wird seit 1953 auch unter schwierigsten Ackerverhältnissen benutzt und

hat sich sehr gut bewährt. Ein Schlupfschreibgerät in ähnlichem Aufbau wird nach Zschange seit 1957 auch im Institut für Landtechnik, Potsdam-Bornim, verwendet [3].

1.2) Messeinrichtung zur Bestimmung mechanischer Bodenkenngrössen.

Der Rollwiderstand von Laufwerken wird ausserhalb fester Fahrbahnen überwiegend von der vertikalen Verformung des Bodens unter dem Laufwerk

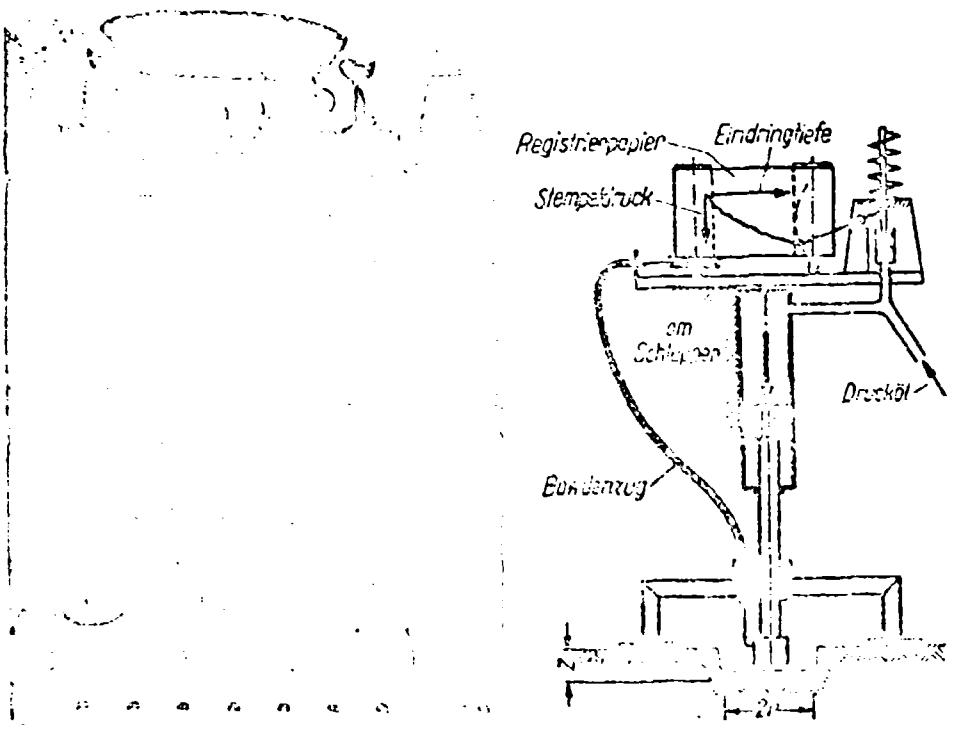


Bild 1.05 u. 1.06. — Hydraulisch betriebener Bodendruckstempel am Schlepperheck.

beeinflusst; die Zugkräfte hängen vom Schubspannungsverlauf in Abhängigkeit von der horizontalen Verformung des Bodens ab. Zur Bestimmung beider bodenmechanischer Kenngrössen wurden vom Institut für Landtechnische Grundlagenforschung die unten beschriebenen Geräte entwickelt. Sie sind Schlepperanbaugeräte und benutzen die Schlepperhydraulik als Kraftquelle.

1.21) Bodendruckstempel. — Zum Bestimmen der vertikalen Verformung des Ackerbodens in Abhängigkeit von einer Last wurde ein hydraulisch betriebener Bodendruckstempel (Bild 1.05, 1.06) entwickelt. Dieses Gerät ist starr am Schlepperheck angebaut. Es besteht im wesentlichen aus einem hydraulischen

Arbeitszylinder, dessen Kolbenstange mit Druckplatten verschiedenen Durchmessers von 70 bis 400 mm bzw. mit Rechteckplatten entsprechender Flächengrösse mit einem Seitenverhältnis 4:1 versehen werden kann. Das Eindringen der Platten in den Boden wird über einen Bowdenzug auf einen Indikator übertragen und dient als Abszisse für den Druck im Arbeitszylinder, der als Mass der Eindrückkraft vom Indikator gemessen und aufgeschrieben wird.

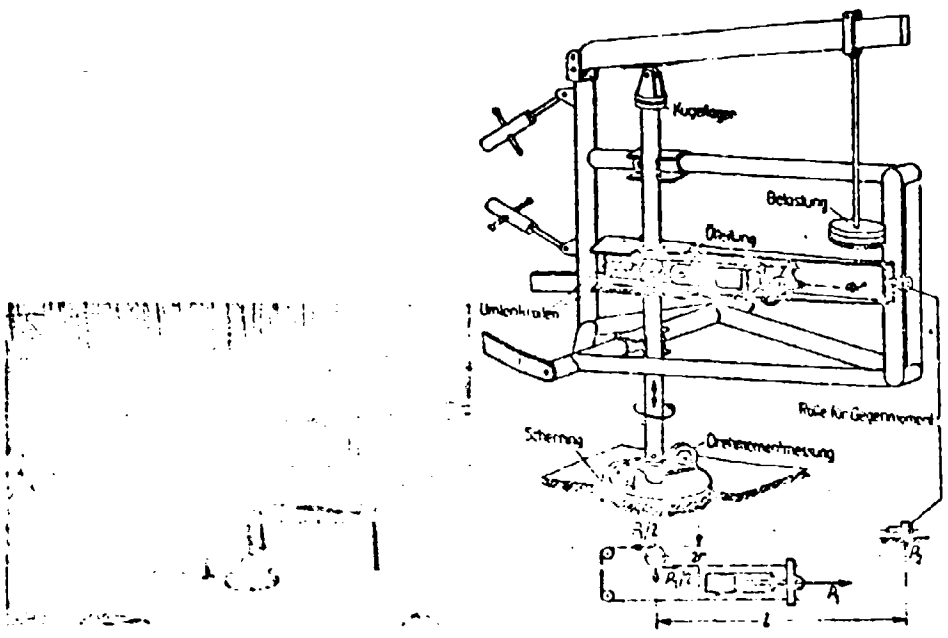


Bild 1.07 u. 1.08. — Hydraulisch betriebenes Ringschergerät am Dreipunktgestänge des Schleppers.

1.22) **Ringschergerät.** — In Anlehnung an ein älteres, handbetätigtes Ringschergerät [4], das vornehmlich im Laboratorium verwendet wird, wurde ein grösseres Ringschergerät für Feldversuche gebaut (Bild 1.07, 1.08), das mit einer vertikalen Last bis 400 kg arbeiten kann. Es wird am Dreipunktanbau des Schleppers befestigt und durch einen zusätzlichen Diagonallenker in seiner Stellung festgehalten. An dem verwindungssteifen Rohrrahmen des Gerätes ist die Welle des Scherringes gelagert, die über einen Hebel mit Gewichten belastet wird. Der Scherring wird von einem hydraulischen Arbeitszylinder gedreht. Das Drehmoment der Welle wird über zwei hydraulische Messdosen (Bild 1.09) auf den Scherring (Bild 1.10) übertragen und mit Hilfe eines Indikators gemessen und aufgezeichnet.

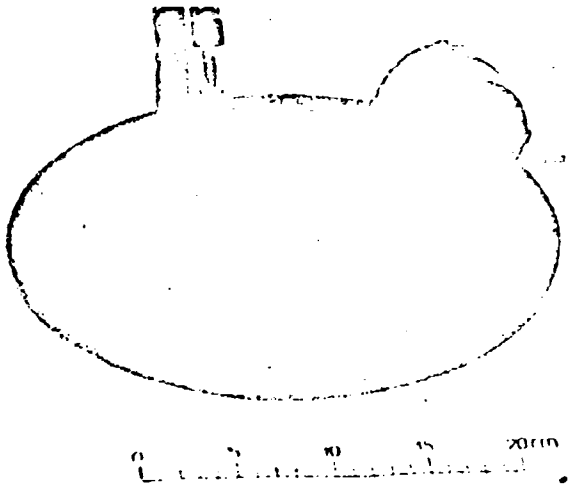


Bild 1.09 — Drehmomentenmesseinrichtung am Ringschergerät.

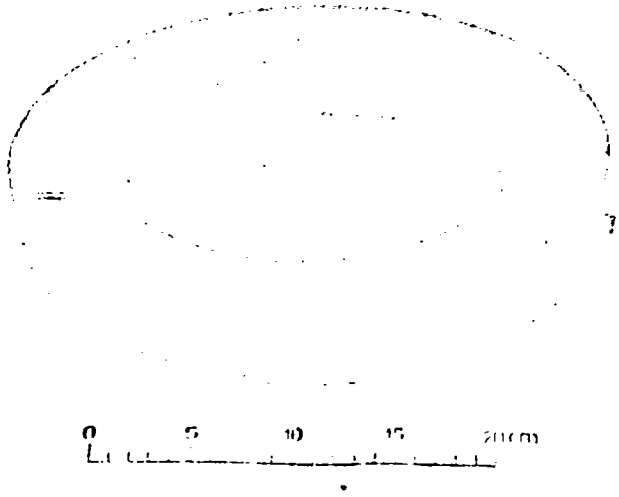


Bild 1.10. — Scherring zum Ringschergerät.

2. - Messergebnisse

Die Messungen wurden auf drei Mineralböden bei jeweils zwei verschiedenen Bodenzuständen und auf Moorboden durchgeführt. Die Korngrössenverteilung und die Bodenfeuchtigkeit der Mineralböden bei den einzelnen Versuchen sind in Tabelle 1 wiedergegeben. Nähere Angaben über Moorböden finden sich bei den Ergebnissen dieser Böden.

Tabelle 1.

Boden	Bodenzustand	Feuchtigkeit Gewichts-%		Korngrössenverteilung in %			
				Grobsand %	Feinsand %	Schluff %	Ton %
Sandboden A	a) Stoppelfeld	8,3	Zugkraftmessungen	63,1	34,1	1,3	1,5
	b) Gepflügt, geeggt und 8 Tg. abgesetzt	8,0	u. Druck- u. Scherversuche				
Sandiger Lehm B	a) Stoppelfeld	20 22	Zugkraftmessungen Druck- u. Scherversuche	45,5	35,5	12,0	7
	b) Gepflügt, geeggt, 5 Wochen abgesetzt	17 14	Zugkraftmessungen Druck- u. Scherversuche				
Sandig-toniger Lehm C	a) Stoppelfeld	20 25	Zugkraftmessungen Druck- u. Scherversuche	36,1	20,0	11,2	32,7
	b) 8-10 cm geschält, ca. 6 Wochen abgesetzt	32 24	Zugkraftmessungen *) Druck und Scherversuche				

*) Infolge Witterungsumschlages konnte das gesamte Versuchsprogramm nicht an einem Tag durchgeführt werden. Daher musste ein Teil der Messungen unter geänderten Bedingungen gemacht werden.

2. 1) Fahrwiderstand und Zugkraftverhalten auf verschiedenen Böden.

Der Versuchsschlepper war an der Triebachse bei einer statischen Hinterachslast von 1400 kp mit Reifen der Grösse 10-28 AS mit einem Reifeninnendruck von 0,8 atü ausgerüstet; die Vorderachse war bei einer statischen Achslast von 544 kp mit Reifen 5,50-16 mit einem Innendruck von 1,5 atü versehen. Bei den Moorversuchen, die weiter zurückliegen, war ein anderer Schlepper mit Sonderausrüstung eingesetzt worden, die später angegeben wird.

2. 11) Sandboden A. — Bei den Messungen auf dem *Stoppel feld* wurden Rollwiderstandsbeiwerte an der Vorderachse von 0,081 und an der Hinterachse von 0,064 gefunden. Auf *gepflügtem*, geeggten und etwa 8 Tage abgelagerten Boden betrugen sie an der Vorderachse 0,093, an der Hinterachse 0,097.

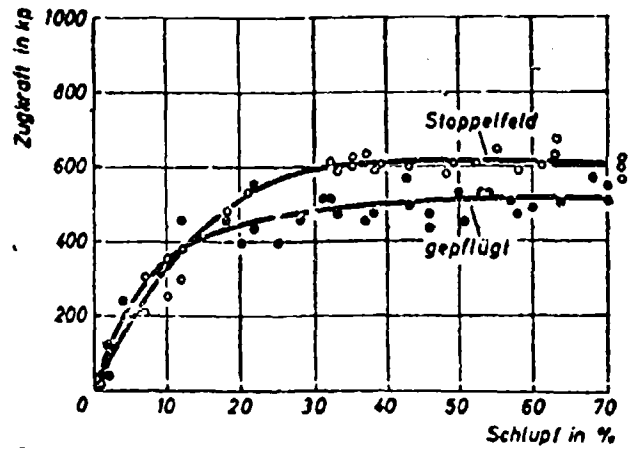


Bild 2.01. — Zugkraft in Abhängigkeit vom Schlupf auf Sandboden A, (Stoppelfeld und gepflügter Zustand).

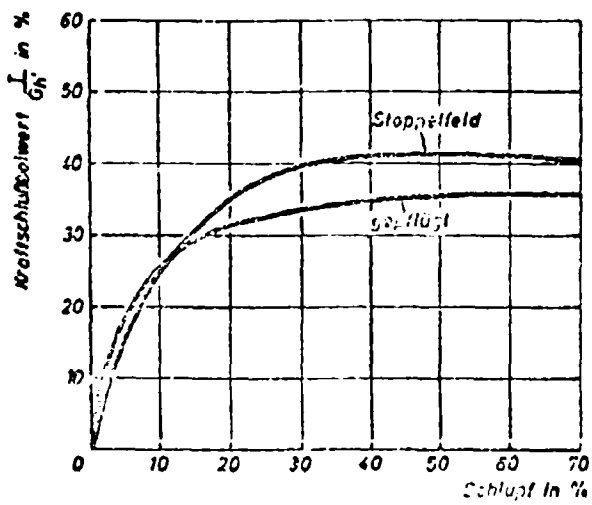


Bild 2.02. — Triebkraftbeiwert (Kraftschlussbeiwert) in Abhängigkeit vom Schlupf auf Sandboden A, (Stoppelfeld und gepflügter Zustand).

In Bild 2.01 sind die Zugkräfte in Abhängigkeit vom Schlupf dargestellt. Die Kurve der Messungen auf dem Stoppelfeld hat auch im Bereich geringen Schlupfes nur einen verhältnismässig flachen Anstieg und biegt bei etwa 30 % Schlupf zur Horizontalen ab. Auf dem gepflügten Boden steigt die Kurve auch bei höheren Schlupfwerten noch an. Die Messwerte beider Versuche streuen nur wenig.

In Bild 2.02 sind die aus den Zugkraftschlupfmessungen errechneten Triebkraft-Beiwertkurven aufgezeichnet. Im unteren Schlupfbereich bis etwa 10 % sind die Triebkraft-Beiwerte etwa gleichwertig; oberhalb dieses Grenz-

wertes sind die des gepflügten Sandes geringer. Auf dem Stoppelfeld wie auf dem gepflügten Boden wurden nur verhältnismässig kleine Triebkraft-Beiwerte erzielt.

2.12) **Sandiger Lehmboden B.** — Die Rollwiderstandsbeiwerte betrugen auf dem *Stoppelfeld* an der Vorderachse 0,048, an der Hinterachse 0,044. Auf *gepflügtem* und 5 Wochen abgelagerten Boden waren sie an der Vorderachse 0,13 und an der Hinterachse 0,118.

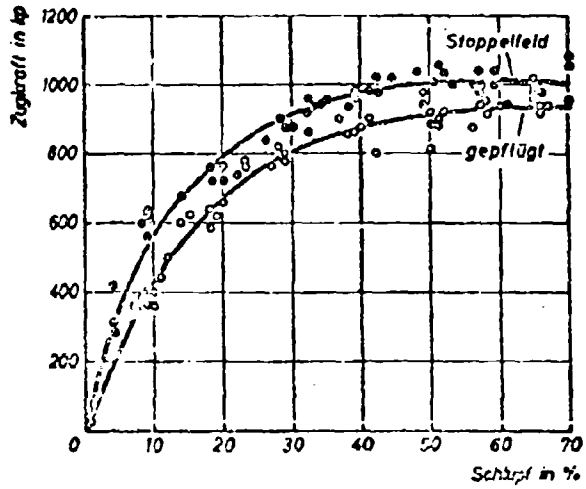


Bild 2.03. — Zugkraft in Abhängigkeit vom Schlupf auf sandigem Lehm B, (Stoppelfeld und gepflügter Zustand).

Die Ergebnisse der Zugkraftschlupfmessung sind in Bild 2.03 eingezeichnet. Der zunächst verhältnismässig steile Anstieg der Kurve auf *Stoppelfeld* nimmt mit grösser werdendem Schlupf ab und nähert sich oberhalb von etwa 40 % Schlupf der Horizontalen; im Bereich von 60 70 % Schlupf deutet sich ein leichter Abfall an. Auf *gepflügtem* Boden verläuft der Anstieg der Kurve flacher und nimmt mit steigendem Schlupf ab. Die Lage der Messwerte lässt auch im Bereich sehr hohen Schlupfes kein Abbiegen des Kurvenverlaufs erkennen. Ihre Streuung ist verhältnismässig gering.

In Bild 2.04 sind die Kurvenzüge der Triebkraft-Beiwerte eingetragen. Sie erreichen auf Stoppelfeld verhältnismässig günstige Werte und sind auch auf dem gepflügten Boden nicht viel kleiner.

2.13) **Sandig-toniger Lehm C.** — Als Rollwiderstandsbeiwerte wurden auf dem *Stoppelfeld* an der Vorderachse 0,068 und an der Hinterachse 0,063 ermittelt. Auf *geschältem* Boden betrugen die Rollwiderstandsbeiwerte auch infolge der höheren Feuchtigkeit an der Vorderachse 0,228 und an der Hinterachse 0,138.

Die in Abhängigkeit vom Schlupf gemessenen Zugkräfte streuen nur wenig (Bild 2.05). Die Kurve des Stoppelfeldes steigt über den ganzen Schlupfbereich

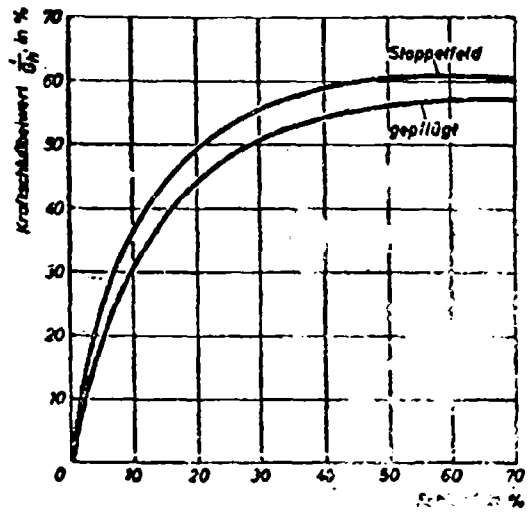


Bild 2.04. — Triebkraftbeiwert (Kraft-Ausnutzwert) in Abhängigkeit vom Schlupf auf sandigem Lehm B, (Stoppelfeld und gepflügter Zustand).

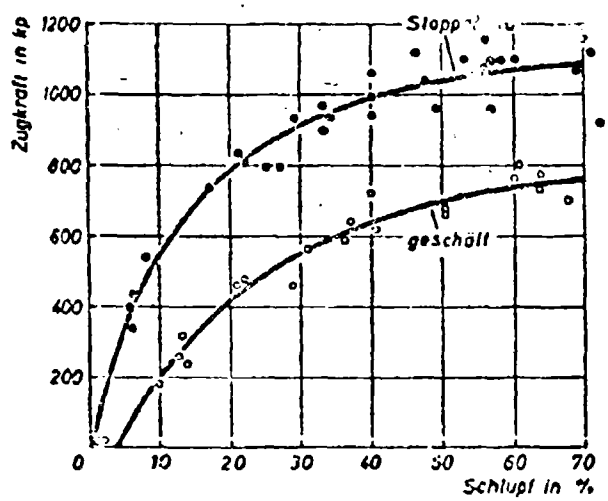


Bild 2.05. — Zugkraft in Abhängigkeit vom Schlupf auf sandig-tonigem Lehm C, (Stoppelfeld und geschälter Zustand).

an, am stärksten im Bereich bis etwa 15 % Schlupf. Die Messungen auf geschältem Boden mussten an einer anderen Stelle des gleichen Feldstücks gemacht werden. Infolge des höheren Rollwiderstandes beginnt die Zugkraft-schlupfkurve erst bei etwa 4 % Schlupf.

Die Darstellung der Triebkraftbeiwerte (Bild 2.06) lässt die günstigen Werte auf Stoppelfeld und den beträchtlichen Unterschied der beiden Kurvenverläufe erkennen.

Neben diesen hier aufgeführten Versuchen wurden Vergleichs- bzw. Ergänzungsversuche mit Reifen gleicher und anderer Grösse sowie mit unterschiedlichen Radlasten gemacht. Auf Böden ohne Strukturschwellen ist auf Grund zahlreicher Versuche zu erwarten, dass der Verlauf des Triebkraftbeiwertes in Abhängigkeit vom Schlupf mit befriedigender Genauigkeit mit einer Exponentialfunktion der Form

$$K = K_{max} - A e^{-kx}$$

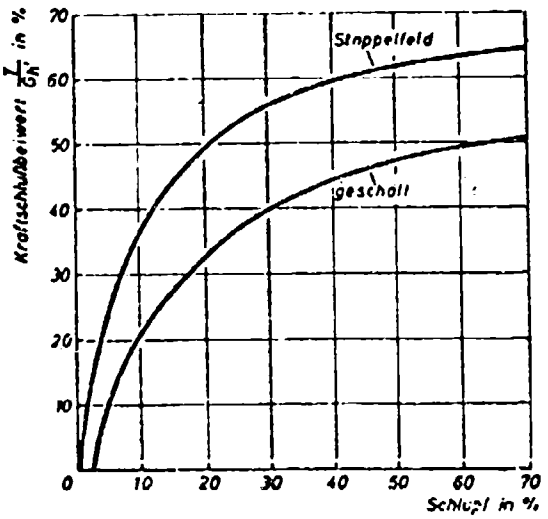


Bild 2.06. — Triebkraftbeiwert (Kraftschlussbeiwert) in Abhängigkeit vom Schlupf auf sandigtonigem Lehm C, (Stoppelfeld und geschälter Zustand).

wiedergegeben werden kann. Alle Versuche zeigten, dass die Rollwiderstände mit lockerer werdendem Boden ansteigen, die Vortriebskräfte aber geringer werden, wobei aber für das Ausmass dieser Veränderungen bisher keine Gesetzmässigkeit angegeben werden kann. Ausnahmen sind nur dann zu erwarten, wenn die gelockerte Schicht nicht tief ist und die Reifenstollen in die darunter liegende feste Bodenschicht eingreifen.

2.14) **Moorböden.** — Als Beispiel für Böden mit sehr geringer Tragfähigkeit wurden schon früher Versuche auf kultivierten Moorböden durchgeführt. Hierbei ist die richtige Reifenauswahl und Belastung besonders wichtig. Reifenausrüstung und Achslasten waren bei diesen Versuchen:

Reifen	Innendruck	Achslast	
		Hinten	Vorn
7·36	0,8 atü	840 kp	550 kp
7·36 Zwilling	0,8 atü	969 kp	550 kp
10·28	0,4 atü	1570 kp	550 kp

In allen Fällen waren die Vorderräder mit Moorverbreiterung ausgerüstet.

Abweichend von der Darstellung der anderen Ergebnisse ist in Bild 2.07 der Zugkraftbeiwert Z/G in Abhängigkeit vom Schlupf dargestellt. Die Bereifung 7-36 ergibt nur geringe Zugkraftbeiwerte. Die Kurve steigt bis zu etwa 50 % Schlupf an und fällt dann wieder leicht ab. Der Anstieg der Kurve ist flach. Bei der Verwendung des breiteren Reifens 10-28 mit einem auf 0,4 atü abgesenkten Innendruck wird die Zugfähigkeit im ganzen gemessenen Bereich erheblich verbessert. Durch die Verwendung von Zwillingsreifen wird die

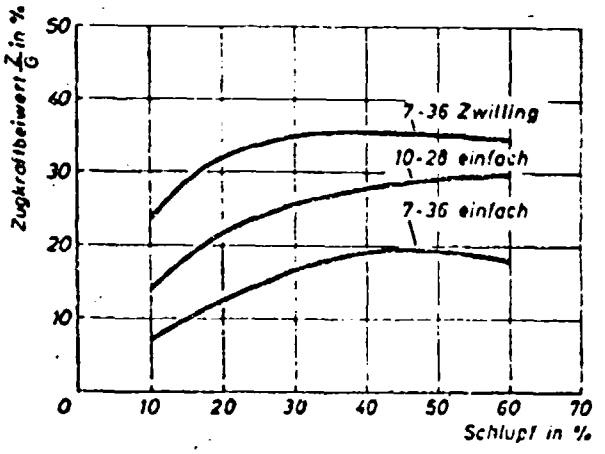


Bild 2.07. — Zugkraftbeiwert Z/G in Abhängigkeit vom Schlupf auf Hochmoor, geschälte Stoppel, bei Radschleppern mit verschiedener Hinterachsbereifung.

Zugfähigkeit weiter beträchtlich erhöht. Im Bereich bis etwa 20 % Schlupf ist der Anstieg der Kurve verhältnismässig steil; er wird nach Ueberschreiten dieses Wertes flacher und weist ein Maximum bei etwa 45 % Schlupf auf. Gegenüber der Bereifung 7-36 verbesserten sich durch den Reifen 10-28 und die Zwillingsreifen die maximalen Zugkraftbeiwerte um 30 und 85 %. Weitere Möglichkeiten zur Verbesserung der Zugkräfte sind von Bock[5] beschrieben und untersucht worden.

2.2) Stempeldruck- und Scherversuche.

2.21) **Stempeldruckversuche.** — Mit dem Stempeldruckgerät wurden auf den gleichen Böden, auf denen die Fahrversuche gemacht waren, die Kräfte unter Stempeln in Abhängigkeit von der Eindringtiefe gemessen.

2.211) *Sandboden A.* - In Bild 2.08 a-e sind die Ergebnisse von Stempeldruckversuchen auf *Stoppelfeld* und in *gepflügtem* Zustand mit verschiedenen Stempeldurchmessern aufgetragen. Die Druckverläufe ergeben im doppellogarithmischen Netz angenähert Geraden und entsprechen somit der Formel von

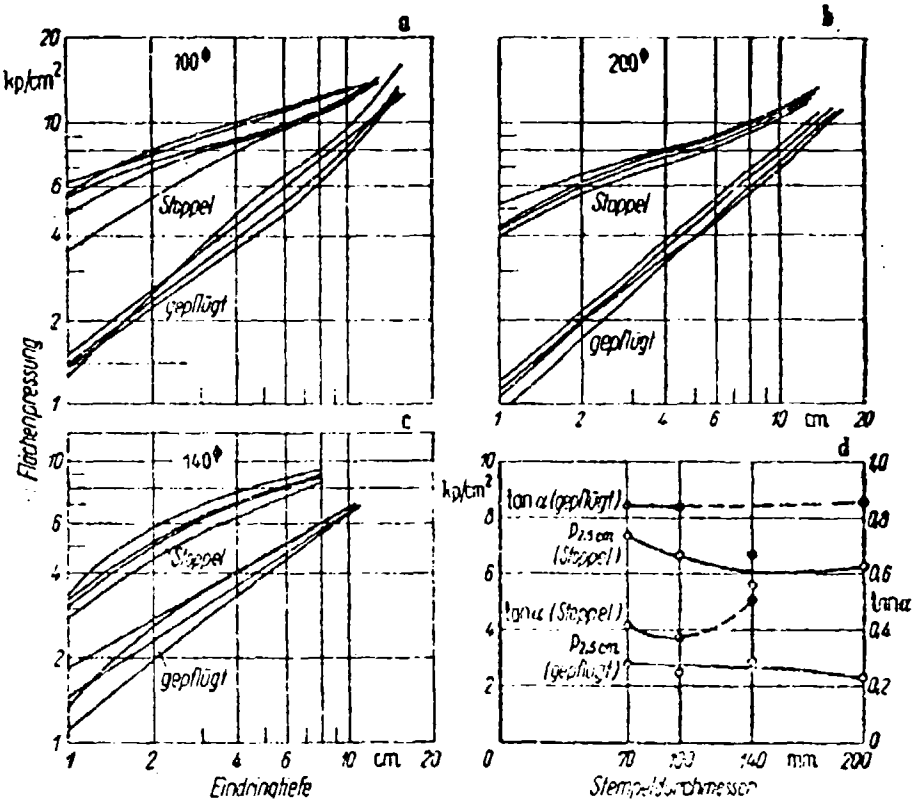


Bild 2.08. — a-c) Flächenpressung unter Stempeln verschiedenen Durchmessers in Abhängigkeit von der Eindringtiefe auf dem Sandboden A, Stoppelfeld und gepflügter Zustand. d) Flächenpressungen bei einer Eindringtiefe von 2,5 cm und Neigung der Eindringkurven tan α in Abhängigkeit vom Stempeldurchmesser.

Gorjatschkin $p = k\ z^n$. Es treten beträchtliche Streuungen auf, die auf dem Stoppelfeld von Vorverdichtungen wie z.B. Schlepperspuren herrühren können. Die erforderlichen Flächenpressungen sind auf dem Stoppelfeld in geringen Eindringtiefen erheblich höher als auf dem gepflügten Boden; doch nähern sich die beiden Kurvenstreufelder einander im Bereich von etwa 18 cm Tiefe, d.h. bei Annäherung an die Bearbeitungsgrenze.

In Bild 2.08 d sind in Abhängigkeit vom Stempeldurchmesser die Flächenpressungen aufgetragen, die erforderlich sind, um die verschiedenen Stempel bis zu einer Tiefe von 2,5 cm in den Boden hineinzudrücken. Diese Flächenpressungen nehmen mit zunehmendem Stempeldurchmesser auf dem Stoppelfeld geringfügig ab. Gleichzeitig ist der Exponent $n = \tan\alpha$ der Gleichungen der Eindrückkurven, d.h. die Neigung der Kurven in doppeltlogarithmischem Netz aufgetragen. Dieser Wert ist auf dem Stoppelfeld erheblich kleiner als auf dem gepflügten Boden.

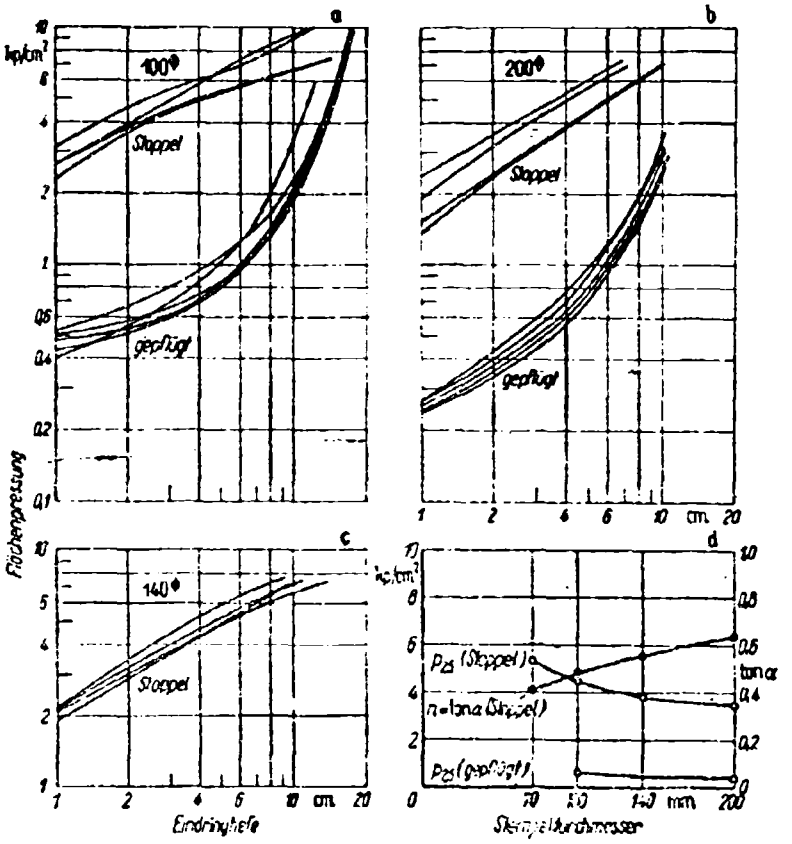


Bild 2.09. — a-c) Flächenpressung unter Stempeln verschiedenen Durchmessers in Abhängigkeit von der Eindringtiefe auf dem sandigen Lehmboden B, Stoppelfeld und gepflügter Zustand. d) Flächenpressungen bei einer Eindringtiefe von 2,5 cm und Neigung der Eindringkurven tan α in Abhängigkeit vom Stempeldurchmesser.

2.212) *Sandiger Lehmboden B.* - In Bild 2.09 a-c sind die Ergebnisse von Stempeldruckversuchen auf Stoppelfeld und auf gepflügtem, etwa 5 Wochen abgesetzten Boden wiedergegeben. Auf dem *Stoppelfeld* lassen sich die Eindrückungskurven wieder recht gut durch die Formel von Gorjatschkin darstellen. Auf *gepflügtem* Boden dagegen ergab sich ein völlig abweichendes Verhalten. Die Pflugtiefe betrug etwa 18 cm. Das Pflügen bedeutet eine erhebliche Auflockerung und damit eine Störung der natürlichen Lagerungsdichte. Infolgedessen dringen die Stempel zunächst schon bei relativ niedrigen Drücken in den Boden ein. Je tiefer sie kommen, umso mehr wirkt sich der Einfluss der Bearbeitungsgrenze, d.h. des nicht mehr aufgelockerten Untergrundes aus, und die Flächenpressungen steigen steil an. In Bild 2.09 d sind die erforderlichen

Flächenpressungen für eine Eindrücktiefe von 2,5 cm sowie die Neigung der Kurven auf Stoppelfeld angegeben.

Auf dem gepflügten Boden wurden neben den Druckversuchen mit Stempeln von 100 und 200 mm Ø solche mit Rechteckstempeln gleicher Flächengrösse durchgeführt, Bild 2.10. Die erforderlichen Flächenpressungen sind bis zu Eindrücktiefen von 6 cm unter den kleinen Stempeln grösser als unter den grossen und unter den Rechteckstempeln grösser als unter den runden.

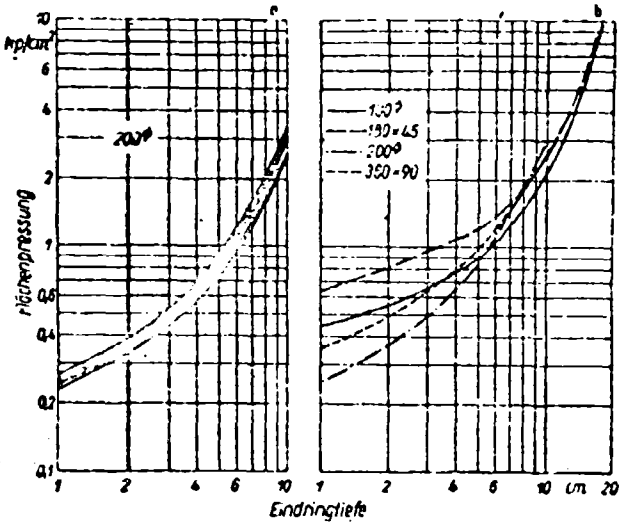


Bild 2.10. — Flächenpressung unter runden und rechteckigen Stempeln verschiedener Grösse in Abhängigkeit von der Eindringtiefe auf sandigem Lehmboden B, gepflügter Zustand.

2.213) *Sandig-toniger Lehmboden C.* - In Bild 2.11 sind die Stempeldruckkurven verschiedenen runder und rechteckiger Stempel auf *Stoppelfeld* in Abhängigkeit von der Eindringtiefe dargestellt. Dabei zeigen die Bilder 2.11 a-c die Streubreiten der einzelnen Versuche, Bild 2.11 d den Verlauf der Mittelwertkurven der verschiedenen Stempel. Auch hier weichen die Kurvenverläufe erheblich von dem nach der Gorjatschkin'schen Formel zu erwartenden Verlauf ab. Zunächst nimmt die Neigung der Kurve bis zu einer Tiefe von rund 10 cm mehr und mehr ab und nähert sich fast einer Horizontalen. Dann beginnt sie aber wieder anzusteigen und wird verhältnismässig gross.

Als Grund für dieses Verhalten kann folgendes angenommen werden: das steile Ansteigen der Flächenpressung in grösseren Tiefen als 10 cm ist auf die Annäherung des Stempels an die Bearbeitungsgrenze mit einem relativ härteren Untergrund zurückzuführen. Das Flacherwerden zwischen 3 und 8 cm Tiefe ist vermutlich dadurch zu erklären, dass unter einer dünnen abgetrockneten Schicht an der Oberfläche eine leichter verformbare Schicht höheren Wassergehaltes lag. In Bild 2.11 d sind die Mittelwerte bei verschiedenen Stempelab-

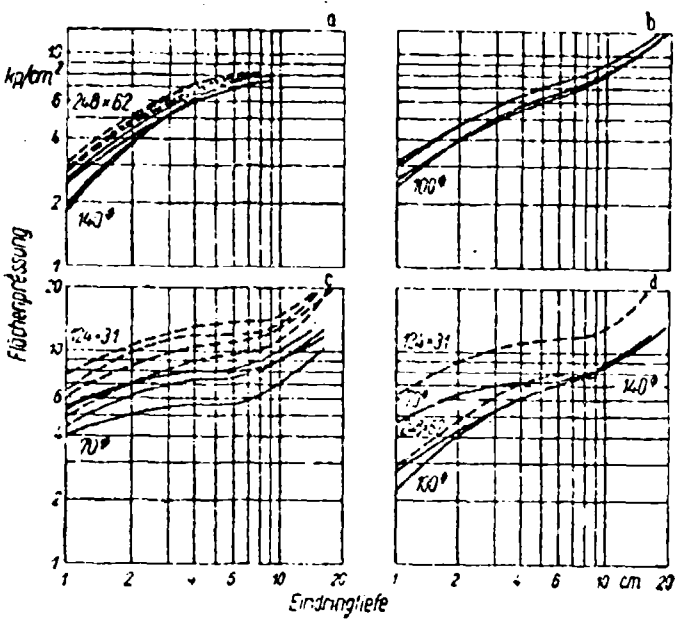


Bild 2.11. — a-c) Flächenpressung unter Stempeln verschiedenen Durchmessers in Abhängigkeit von der Eindringtiefe auf einem sandig-tonigen Lehmboden C, Weizenstoppel. d) Mittelwertkurven der einzelnen Stempel.

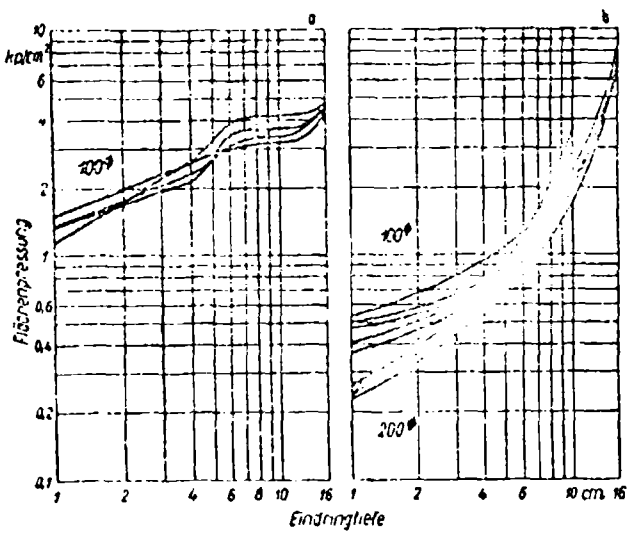


Bild 2.12. — Flächenpressung unter Stempeln in Abhängigkeit von der Eindringtiefe. a) Auf dem sandig-tonigen Lehmboden C, geschälter Zustand. b) Auf dem sandigen Lehm B, gepflügter Zustand.

messungen einander gegenübergestellt. Die Stempel mit kleinerem Durchmesser können wiederum höhere Flächenpressungen aufnehmen als die grösseren, die rechteckigen Stempel höhere als die runden. Auf Grund des Einflusses der Kohäsion ist das auf diesem Boden auch zu erwarten.

Auf etwa 8-10 cm tief geschältem Boden zeigt der Kurvenverlauf deutlich ein Ansteigen der Flächenpressungen bei Annäherung an die Schältiefe

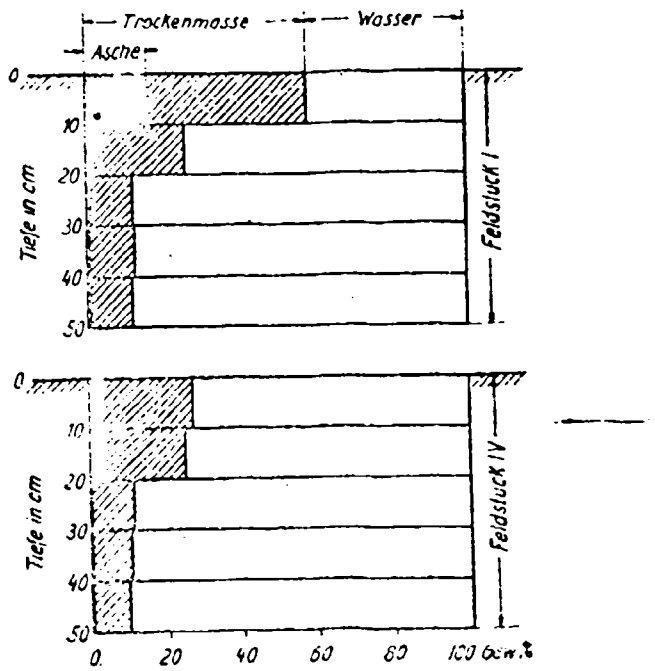


Bild 2.13. — Wasser- und Aschengehalt von zwei Moorböden in verschiedenen Tiefen.

(Bild 2.12 a). Anschliessend bleiben die Werte mit grösser werdender Tiefe annähernd konstant und steigen erst bei Annäherung an die ursprüngliche Bearbeitungsgrenze wieder an.

2.214) *Moorböden.* - Auf den untersuchten Moorböden befindet sich eine gut entwickelte Grasnarbe mit 8-10 cm tief reichendem Wurzelwerk, das die Mooroberfläche erheblich verfestigt. Der Wassergehalt des Torfes nimmt mit zunehmender Tiefe zu; entsprechend nimmt die Fliessfestigkeit des Bodens ab (Bild 2.13). In 20-50 cm Tiefe erreicht der Wassergehalt einen Wert von 87-90 %. Der Grundwasserspiegel lag infolge künstlicher Vorentwässerung durch Gräben in einer Tiefe von etwa 75 cm. Auf Grund der Abnahme der Fliessfestigkeit mit der Tiefe war bei den Druckstempelversuchen ein von Mineralböden völlig verschiedenes Verhalten zu erwarten. Wegen der geringen

Tragfähigkeit des Bodens konnten auch Stempel mit Durchmessern von 300 und 400 mm verwendet werden.

Die Bilder 2.14 und 2.15 oben zeigen Diagramme, die mit dem Stempeldruckgerät auf den Moorböden D und E an der Oberfläche aufgenommen wurden. Die einzelnen Messungen streuen infolge des Einflusses der verwurzelten Grasnarbe beträchtlich. Beim Eindrücken des Stempels in den Boden

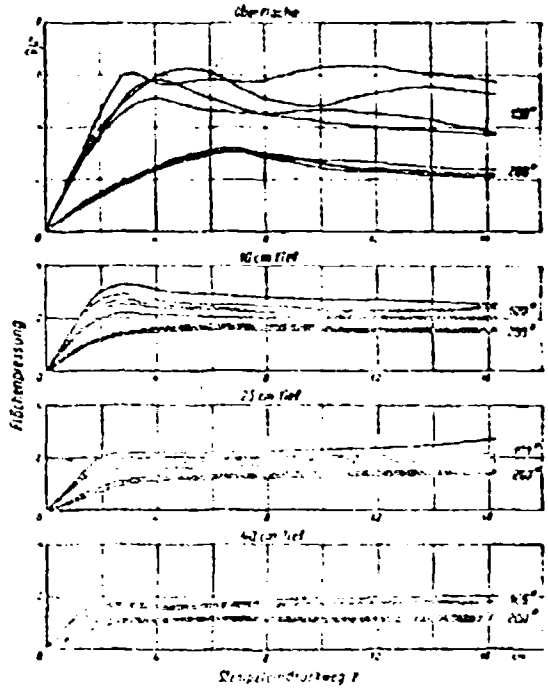


Bild 2.14. — Flächenpressung unter Stempeln verschiedenen Durchmessers auf dem Moorboden D in Abhängigkeit von der Eindringtiefe an der Oberfläche auf der Grasnarbe und in verschiedenen Tiefen Ausgangstiefen.

steigt die Flächenpressung zunächst im Bereich der überwiegend elastischen Verformung der Grasnarbe und des Moores fast linear an. Mit zunehmender plastischer Verformung wird ihr Anstieg flacher. Der Druck erreicht ein Maximum, bei dem die verwurzelte Grasnarbe durchgeschert wird. Anschliessend fällt er merklich ab und bleibt dann nahezu konstant. Beim Stempel von 200 mm Ø ist das Maximum nicht so stark ausgeprägt.

Nach dem Ausheben entsprechend tiefer und so ausgedehnter Gruben, dass Randeinflüsse nicht zu erwarten waren, wurden die Versuche in 10, 25 und 40 cm Ausgangstiefe wiederholt (Bild 2.14, 2.15). Dabei sind bei Bild 2.15 nur noch die Mittelwerte auf jeweils vier Messungen wiedergegeben. Auch bei diesen Versuchen steigt zunächst der Druck im überwiegend elastischen Bereich an, der Verlauf wird dann allmählich flacher und der Druck bleibt anschliessend

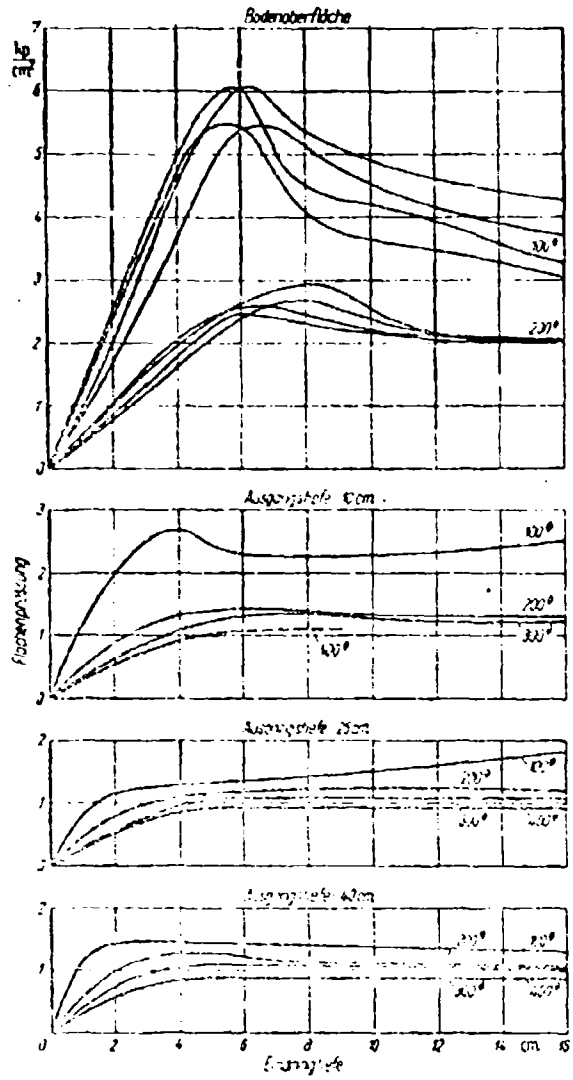


Bild 2.15. — Flächenpressung unter Stempeln verschiedenen Durchmessers auf dem Moorboden E in Abhängigkeit von der Eindringtiefe an der Oberfläche auf der Grasnarbe und in verschiedenen Ausgangstiefen.

nahezu konstant bzw. nimmt mit zunehmender Eindringtiefe geringfügig wieder ab. Mit zunehmender Ausgangstiefe wurden bei allen Stempelgrössen geringere Flächenpressungen gemessen. Dabei war der Unterschied zwischen den Ergebnissen an der Oberfläche und in 10 cm Ausgangstiefe besonders gross. Ferner wurde mit zunehmender Ausgangstiefe der Eindrückweg bis zum Maximum bzw. bis zum Abbiegen der Kurven in die Horizontale kleiner. Er war in allen Ausgangstiefen umso grösser, je grösser der Stempeldurchmesser war.

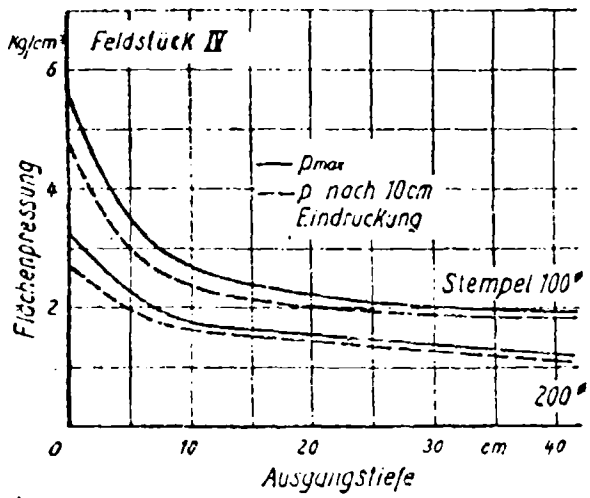


Bild 2.16. — Maximale Flächenpressungen und Flächenpressungen nach 10 cm Eindrücktiefe auf Moorboden D in Abhängigkeit von der Ausgangstiefe bei verschiedenen Stempeldurchmessern.

In Bild 2.16 sind die maximalen Flächenpressungen sowie die Flächenpressungen in einer Eindrücktiefe von 10 cm in Abhängigkeit von der Ausgangstiefe auf dem Moorboden D eingetragen. Dabei zeigt sich der grosse Einfluss der Grasnarben besonders unter dem 100 mm Ø - Stempel und das Absinken der erreichten Flächenpressungen mit zunehmender Ausgangstiefe. Man kann die jeweilige Flächenpressung p_{f1}, bei der die Tragfähigkeit des Bodens erschöpft ist, aufteilen in einen kohäsiven Anteil $p_o : r$, wobei r der Radius der Stempelplatte ist, und einen von den Abmessungen der Stempelplatte unabhängigen Anteil p_k.

$$p_{f1} = \frac{p_o}{r} + p_k$$

Damit lässt sich auch die voraussichtliche Flächenpressung, bei der die Tragfähigkeit unter grösseren Flächen erschöpft ist, berechnen.

In Bild 2.17 a und b sind für die Moorböden D und E die gemessenen und ebenso die aus obiger Formel errechneten Flächenpressungen über dem

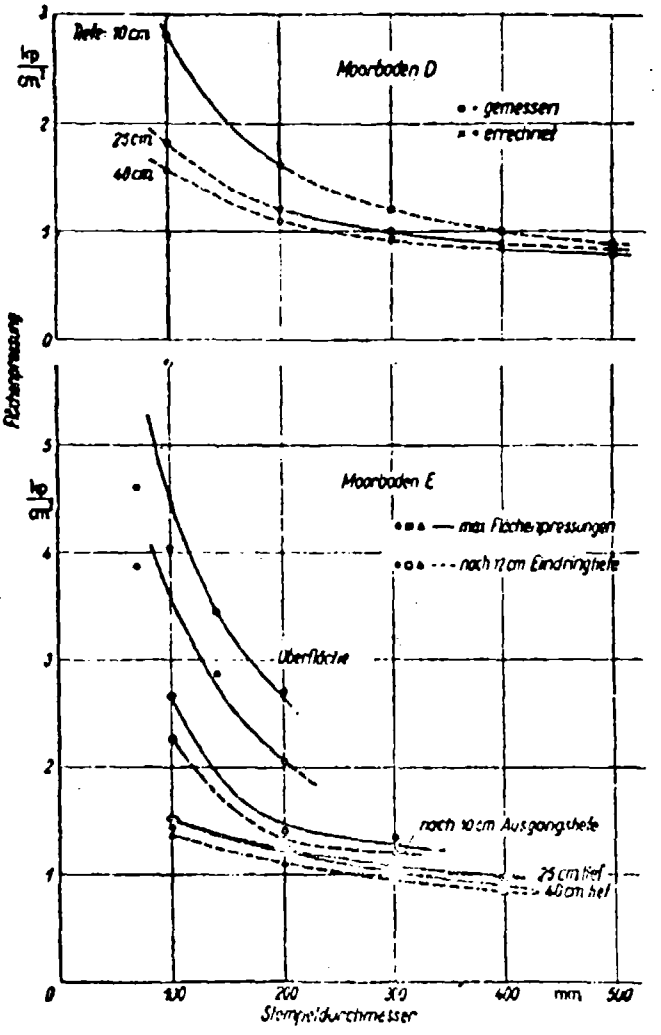


Bild 2.17. — Maximale Flächenpressungen auf Moorboden D und E in Abhängigkeit vom Stempeldurchmesser bei verschiedenen Ausgangstiefen.

Stempeldurchmesser aufgetragen. Unter einem Druckstempel oder unter einer Lastfläche findet das grösste plastische Fliessen keineswegs unmittelbar unter der Stempelfläche statt. Unter ihr befindet sich durch die Reibung in dieser Fläche eine unter allseitigem Druck stehende Zone, in der im wesentlichen nur eine Verdichtung, aber kein Fliessen erfolgt. Diese Zone ist von dem eigentlichen Fliessbereich umgeben, in dem Fliessen wie Verdichtung stattfindet. In diesem Bereich sind die Schubspannungen und die Scherverformung am grössten.

Zur Erläuterung dieses Vorganges kann vielleicht ein anderer Versuch

herangezogen werden. Bild 2.18 zeigt die plastische Verformung eines Mineralbodens unter einem Druckstempel. Dabei ist die Verdichtung und das Fliessen durch ein vorher eingebrachtes Gitternetz aus vertikalen Gipssträngen und horizontalen Kalkschichten sichtbar gemacht. Aus diesen sowie zahlreichen Parallelversuchen geht hervor, dass die Zone grössten plastischen Fliessens in einer Tiefe von 0,5 bis 0,8 des Stempeldurchmessers bzw. bei Rechteckflächen von 0,6 bis 0,9 der Breite der Belastungsfläche unter ihr liegt. Unter der Voraussetzung, dass die Verhältnisse bei organischen Böden ähnlich sind, liegt

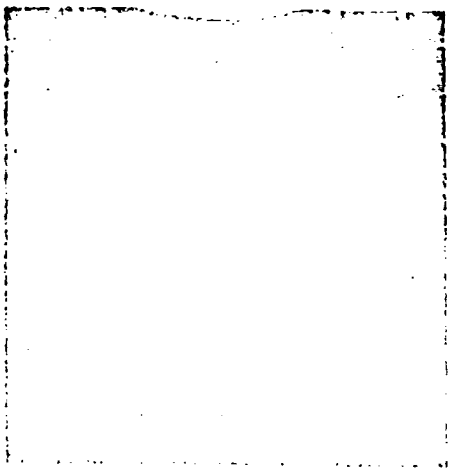


Bild 2.18. — Plastische Verformung eines Mineralbodens unter einem Druckstempel.

die Zone grössten plastischen Fliessens also unter einem Druckstempel von 100 mm Ø noch im Bereich der Grasnarbe mit höherer Festigkeit und bei einem Druckstempel von 262 mm Ø unmittelbar unter der Grasnarbe. Bei einem Durchmesser von 40 cm liegt die Zone des grössten plastischen Fliessens bereits in einer Tiefe von 20–30 cm.

Die Stempeldruckversuche zeigen, dass die Tragfähigkeit des Moorbodens nach Ueberschreiten des Maximalwertes bei einer bestimmten Eindringtiefe wieder absinkt. Im Gegensatz zu den Mineralböden, bei denen mit zunehmender Eindrücktiefe die Flächenpressungen immer anwachsen, ergibt sich also bei Moorböden durch das Abscheren der Grasnarbe eine Herabsetzung der Tragfähigkeit, die sich gefährlich auswirken kann. Für die Dimensionierung von Reifen oder Gleisketten zum Befahren von Moorböden darf man daher nicht von den an der Bodenoberfläche gemessenen Werten ausgehen, da besonders bei Uebertragung von Schubkräften durch Gleisketten oder Reifen immer mit einer Zerstörung der Grasnarbe gerechnet werden muss. Man muss vielmehr von den Werten ausgehen, die das Moor unterhalb der Grasnarbe tragen kann.

2.22) **Scherversuche.** — **Parallel zu den Stempeldruckversuchen wurden zu gleicher Zeit Scherversuche auf den verschiedenen Böden durchgeführt.**

2.221) *Sandboden A.* - **Die Ergebnisse der Scherversuche auf *Stoppelfeld* sind in Bild 2.19 a und b und auf demselben Boden im *gepflügten* Zustand in Bild 2.19 c und d wiedergegeben. Dabei sind in Bild 2.19 a und c der Schubspannungsverlauf in Abhängigkeit vom Scher- und Gleitweg und in Bild**

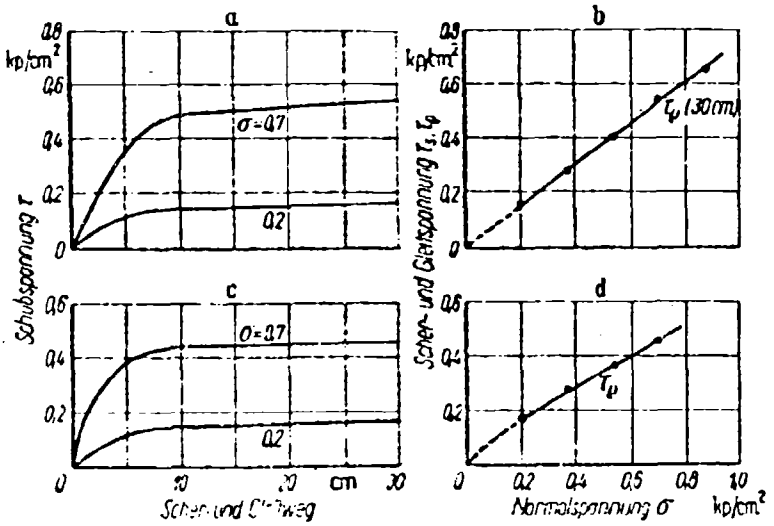


Bild 2.19. — a, c) Schubspannungsverlauf in Abhängigkeit vom Scher- und Gleitweg. b, d) Scher- bzw. Gleitspannungen in Abhängigkeit von der Normalspannung auf dem Sandboden A, Stoppelfeld und gepflügter Zustand.

2.19 b und d die Scher- bzw. Gleitspannungen in Abhängigkeit von der Normalspannung aufgetragen.

Der Sandboden A zeigt sowohl als Stoppelfeld wie als gepflügter Boden keine Kohäsion und auch keine wesentlichen Unterschiede im Schubverlauf über dem Scher- und Gleitweg.

2.222) *Sandiger Lehmboden B.* - Die Messergebnisse auf *Stoppelfeld* sind in Bild 2.20 a und b und im *gepflügten* Zustand in Bild 2.20 c und d dargestellt. Dabei sind wieder in a und c der Schubspannungsverlauf in Abhängigkeit vom Scher- und Gleitweg und in b und d die Scher- bzw. Gleitspannungen in Abhängigkeit von der Normalspannung aufgetragen.

Als Stoppelfeld hat der Boden eine Kohäsion in der Grössenordnung von etwa 0.1 kp/cm². Die Reibungsbeiwerte bei Stoppel und gepflügtem Boden unterscheiden sich nicht viel. Der wesentliche Unterschied ist vielmehr, dass im dichtgelagerten Zustand die maximale Spannung schon bei sehr kleinem Scherweg von 2,5-3 cm erreicht ist, auf dem locker gepflügten Boden dagegen

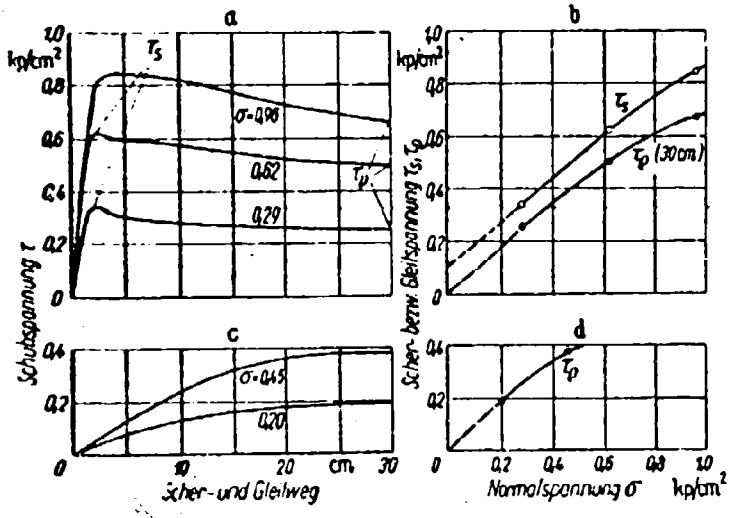


Bild 2.20. — a, c) Schubspannungsverlauf in Abhängigkeit vom Scher- und Gleitweg. b, d) Scher- bzw. Gleitspannungen in Abhängigkeit von der Normalspannung auf dem sandigen Lehmboden B, Stoppelfeld und gepflügter Zustand.

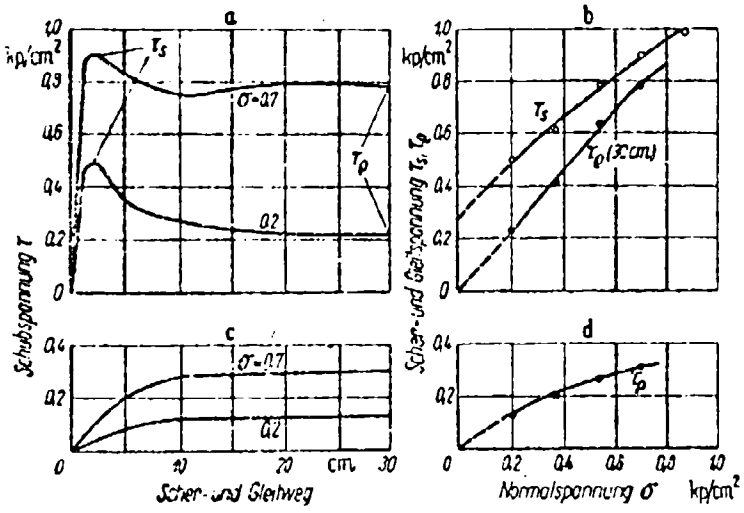


Bild 2.21. — a, c) Schubspannungsverlauf in Abhängigkeit vom Scher- und Gleitweg. b, d) Scher- bzw. Gleitspannungen in Abhängigkeit von der Normalspannung auf dem sandig-tonigen Lehmboden C, Stoppelfeld und geschälter Zustand.

die maximale Reibungsspannung erst nach einem relativ grossen Verformungsweg erreicht wird.

2.223) *Sandig-toniger Lehmboden C.* - Dieser Boden hat als *Stoppelfeld* erhebliche Kohäsionswerte (Bild 2.21 a und b), die nach dem *Schälen* verschwunden sind (Bild 2.21 c und d). Entscheidend ist aber wieder, dass auf dem

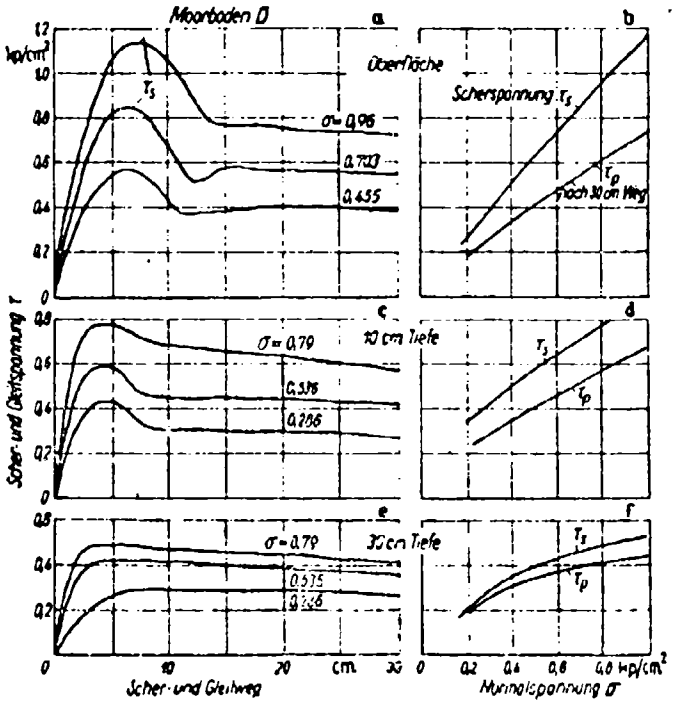


Bild 2.22. — Schubspannungsverlauf in Abhängigkeit vom Scher- und Gleitweg auf Moorboden D. Scher- und Gleitspannungen in Abhängigkeit von der Normalspannung.

abgesetzten festen Stoppelfeld die maximale Scherspannung relativ schnell erreicht ist, während bei dem geschälten Boden ein grosser Verformungsweg benötigt wird, ehe der maximale Reibungsbeiwert $\mu = \text{tg } \rho$ erreicht wird.

2.224) *Moorboden D.* - Die Scherfestigkeit an der Oberfläche wird in starkem Masse durch das Wurzelwerk der Grasnarbe (Bild 2.22 a-d) beeinflusst. Die maximale Scherspannung wird nach einem grösseren Scher- und Gleitweg erreicht als bei Mineralböden in fester Lagerung. Während an der Oberfläche und in 10 cm Ausgangstiefe die Scher- und Gleitspannungen etwa proportional dem Normaldruck ansteigen, ist dies bei 30 cm Ausgangstiefe nicht mehr der Fall.

3. - Vergleich der Messergebnisse

Auf den drei Mineralböden A, B, C werden die Ergebnisse der Rollwiderstands- und Zugkraftmessungen mit denen der Stempeldruck- und Scherversuche verglichen. Ein entsprechender Vergleich auf den Moorböden ist nur in der Tendenz möglich, da die früheren Zugkraftmessungen auf einem mit Scheibenegge geschälten Stoppelfeld, die Stempeldruck- und Scherversuche dagegen auf Grasland stattfanden.

3. 1) Rollwiderstandsmessungen und Stempeldruckversuche.

Auf dem gepflügten Sand A war der Rollwiderstandsbeiwert der Vorderachse um 20 % und der der Hinterachse um 50 % grösser als auf dem Stoppelfeld. Dieser Unterschied lässt sich aus der Differenz der Flächenpressungen tendenzmässig aber noch nicht quantitativ erklären (Tabelle 2).

Tabelle 2.

Boden	Rollwiderstandsbeiwert		Druck bei 2,5 cm Eindringtiefe		K % (35 % Schlupf)	c kp/cm²	tan ρ
	Vorderachse	Hinterachse	100 Ø kp/cm²	200 Ø kp/cm²			
Sandboden A							
Stoppel	0,081	0,064	6,7	6,3	40,7	0-0,4	0,75
gepflügt	0,098	0,097	2,7	2,3	34,3	—	≈ 0,6
Sandiger Lehm B							
Stoppel	0,048	0,044	4,5	3,5	57,5	0,1-0,16	0,75
gepflügt	0,130	0,118	0,6	0,43	52,7	—	≈ 0,75
Sandigtoniger Lehm C							
Stoppel	0,068	0,063	4,8	3,4	58,3	0,24-0,1	≈ 0,75
geschält 32 % F	0,228	0,138	—	—	42,5	—	
geschält 24 % F	—	—	1,8	1,95	—	—	≈ 0,50

Auf dem sandigen Lehm B im gepflügten Zustand waren die Rollwiderstandsbeiwerte unter der Vorder- und Hinterachse rund 2,7 mal so gross wie auf dem Stoppelfeld. Es besteht eine tendenzmässige Uebereinstimmung zwischen den unterschiedlichen Rollwiderstandsbeiwerten und den entsprechenden Tragfähigkeiten des Bodens.

Die Rollwiderstandsbeiwerte auf geschältem, sandig tonigen Lehm C sind unter der Vorderachse 3,4 mal und unter der Hinterachse 2,2 mal so gross wie auf dem Stoppelfeld. Ein Vergleich mit den Ergebnissen der Stempeldruckversuche ist wegen der unterschiedlichen Feuchtigkeit bei den Fahr- und Stempeldruckversuchen auf geschältem Boden nur sehr bedingt möglich.

Auf Moorboden wurden keine Fahrversuche parallel zu den Stempeldruck- und Scherversuchen gemacht. Jedoch zeigt das zum Vergleich herangezogene Bild 2.07, dass die erreichbaren Zugkräfte sehr stark von der mittleren Flächenpressung in der Berührungsfläche zwischen Reifen und Boden abhängen. Bei dem einfachen Reifen 7-36 war die Tragfähigkeit des Moorbodens in diesem Falle erschöpft. Die Spurtiefe war hoch, und ein grosser Teil der Schubkräfte in der Berührungsfläche musste dazu benutzt werden, den Eigenrollwiderstand zu überwinden. Die erheblich grössere Berührungsfläche der Zwillingsreifen konnte sich mehr auswirken als die des breiteren Reifens 10-28 und die Luftdruckabsenkung.

Aus dem Vergleich der Stempeldruckkurven und der Rollwiderstandsbeiwerte auf Mineralböden lässt sich eine tendenzmässige Uebereinstimmung feststellen. Der Verlauf der Stempeldruckkurven wird jedoch durch Störeinflüsse wie Strukturänderungen durch Bodenbearbeitung oder Strukturschwellen infolge Bearbeitungsgrenzen und ähnliches beeinflusst. Auf landwirtschaftlichen Böden ist aber mit solchen Störeinflüssen zu rechnen. Für diese Böden ist daher eine Anpassung der Formeln von Gorjatschkin und Bekker zu erwägen.

3.2) Verlauf der Triebkraftbeiwerte und Scherversuche.

Auf dem Sand A ergaben sich auf dem Stoppelfeld gegenüber dem gepflügten Boden im günstigsten Fall um etwa 20% höhere Triebkraftbeiwerte. Bei Scherversuchen ergaben sich um 25 % höhere Scherspannungen und um 20 % höhere Gleitspannungen. Weiterhin wurden auf dem kohäsionslosen gepflügten Sand von den Reifenstollen bei grösserem Schlupf tiefe Spuren in den Boden eingefräst, die vermutlich ein Anwachsen des Rollwiderstandes und damit ein Absinken der Triebkraftbeiwerte zur Folge hatten. Damit lassen sich die Unterschiede der Triebkraftbeiwerte deuten.

Auf dem sandigen Lehm B, Stoppelfeld, waren die Zugkräfte nur um etwa 8 % höher als auf gepflügtem Boden. Bei den Scherversuchen waren die Reibungsbeiwerte bei kleiner Normalspannung kaum unterschiedlich. Jedoch ist beim Stoppelfeld eine Kohäsion von 0,1-0,16 kp/cm² vorhanden. Die maximalen Schubspannungen werden im Gegensatz zum gepflügten Boden nach sehr kleinen Scher- und Gleitwegen erreicht. Es handelt sich um einen Reibungsboden, bei dem vor allem der Reibungsbeiwert für die Zugkräfte massgebend ist, der von dem Lockerheitsgrad nicht wesentlich beeinflusst wird. Mit dem Schergerät konnten höhere Normalspannungen als 0,4 kp/cm² nicht untersucht werden, da der Scherring zu tief in den lockeren Boden einsenk, so dass die Grundplatte mit der Drehmomenten-Messeinrichtung auflag.

Auf dem sandig tonigen Lehm C sind die beträchtlichen Unterschiede im Verlauf des Triebkraftbeiwertes eine Folge des Schälens und der unterschiedlichen Feuchtigkeit. Die Scherversuche zeigten auf Stoppelfeld eine Kohäsion von 0,24-0,1 kp/cm² und erheblich höhere Reibungsbeiwerte als auf dem geschälten Boden; insofern stimmen sie in der Tendenz mit den Zugkraftmes-

sungen überein. Dabei bleibt jedoch der unterschiedliche Feuchtigkeitsgehalt des geschälten Bodens bei Fahr- und Scherversuch unberücksichtigt.

Beim Vergleich der Zugkraft-Schlupfmessungen und der Scherversuche konnte bisher nur eine qualitative Uebereinstimmung festgestellt werden. Bei dem Zugkraft-Schlupfverhalten spielt auch der Eigenrollwiderstand eine beträchtliche Rolle, da durch ihn bereits Schubkräfte in der Berührungsfläche verbraucht werden und nicht mehr für den Vortrieb wirksam werden können.

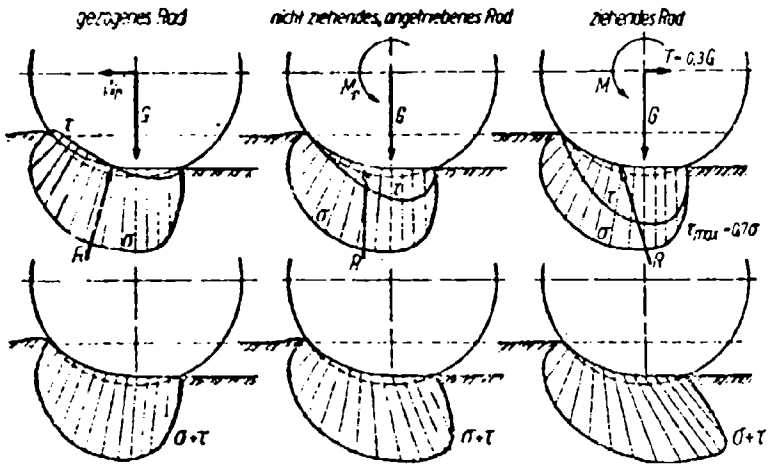


Bild 3.01. — Normal- und Tangentialspannungsverteilung an einem gezogenen, an einem nicht ziehenden angetriebenen und an einem ziehenden Rad.

Dies geht aus Bild 3.01 a-c hervor, in dem die Normal- und Tangentialspannungsverteilung am gezogenen, nicht ziehenden angetriebenen und am ziehenden Rad dargestellt sind. Obwohl der Schlupf bei Bild 3.01 c bereits so gross ist, dass am Ende der Berührungsfläche eine Tangentialspannung von $\tau_{max} = 0{,}7$ der Normalspannung erreicht wird, beträgt die resultierende Triebkraft nur 0,3 der Radlast.

4. - Zusammenfassung

Es werden Messmethoden und Messeinrichtungen beschrieben, mit denen Zugkräfte von Schleppern in Abhängigkeit vom Schlupf, Fahrwiderstände und bodenmechanische Kenngrössen gemessen werden können.

Für die Messung von Zugkraft und Fahrwiderstand wird ein Messwagen mit hydraulischer Kraft- und mechanischer Schlupf-Messeinrichtung benutzt. Zur Ermittlung der bodenmechanischen Kenngrössen wurden ein Ringscher- gerät und ein Druckstempelgerät als Anbaugeräte am Schlepper entwickelt, die mit der Schlepperhydraulik betrieben werden.

Mit diesen Einrichtungen wurden auf drei Mineralböden und auf Moorboden Vergleichsversuche durchgeführt. Da durch die Bodenbearbeitung landwirtschaftlich genutzter Flächen der Bodenzustand und damit die Zugfähigkeit von Schleppern im

starken Masse beeinflusst werden, wurden die Versuche jeweils auf Stoppelfeld und auf gepflügtem Boden gemacht.

Durch die Bearbeitung wurde, wie zu erwarten, in jedem Fall die Zugfähigkeit verschlechtert und der Rollwiderstand erhöht! Die Stempeldruckversuche zeigten, dass nur bei abgesetzten gleichmässig feuchten *Mineralböden* der Druckanstieg angenähert der Formel von Gorjatschkin $p = k \cdot z^n$ folgt. Erhebliche Abweichungen ergeben sich bei lockeren Mineralböden mit einer Bearbeitungsgrenze oder überhaupt bei Böden mit Struktur- und Feuchtigkeitsschwellen. Bis jetzt konnten die Formel von Bekker $p = \left(\frac{k_c}{b'} + k_\rho\right) \cdot z^n$ und die hieraus abgeleiteten Rollwiderstandsformeln für Reifen noch nicht auf landwirtschaftlich genutzten und bearbeiteten Böden mit ihren grossen Streuungen und den Strukturgrenzen angewandt werden.

Für *Moorböden* erwies sich die Formel von Gorjatschkin als nicht anwendbar. Im Gegensatz zu Mineralböden, bei denen mit zunehmender Eindringtiefe die Flächenpressungen immer anwachsen, nehmen sie bei Moorböden nach Ueberschreiten eines Maximums wieder ab oder bleiben gleich. Weiterhin wird der Verlauf der Flächenpressung von einer verwurzelten Grasnarbe oder einer festeren und trockeneren Oberschicht sehr beeinflusst.

Wie die Scherversuche zeigen, beeinflussen die von der Bodenbearbeitung und dem Pflanzenbewuchs herrührenden Struktur-Aenderungen von Mineralböden den Verlauf der Schubspannungen in Abhängigkeit von Scher- und Gleitweg, während selbst eine sehr intensive Bearbeitung den Höchstwert der Reibung bei gleicher Feuchtigkeit und Flächenpressung nicht wesentlich ändert. Die Kohäsion ändert sich in Abhängigkeit von der Textur sehr. Durch die landwirtschaftliche Bearbeitung kann sie aber für einige Zeit aufgehoben werden. Jedoch ist ihr Einfluss auf die Zugfähigkeit von Ackerschlepperreifen offenbar grösser, als nach der Coulomb'schen Formel zu erwarten ist.

Deshalb muss versucht werden, Methoden und Geräte so zu verbessern, dass eine bessere Korrelation zwischen den physikalischen Kenngrössen und den Koeffizienten für Fahrwiderstand und Zugkraft gefunden werden kann.

SCHRIFTTUM

1) Bernstein R. Abriss einer Motorpflugmechanik. In: Martiny, B: Die Motorpflüge als Betriebsmittel neuzeitlicher Landwirtschaft Bd., 2, S. 121. Berlin, M. Krayn, 1917.

2) Freise H. Schlupfmesser für Räder- und Kettenfahrzeuge. VDI-Ztg. Bd. 81, Nr. 33, S. 967, 1937.

3) Zschange F. Schlupfschreibgerät für Räder- und Kettenfahrzeuge. Zeitschrift Feingerätetechnik, VEB Leipziger Druckhaus, Nov. 1957.

4) Söhne W. Reibung und Kohäsion von Ackerböden. Grundlagen der Landtechnik H. 5, Düsseldorf VDI-Verlag, 1953.

5) Bock G. Zugkraftmessungen an leichten Ackerschleppern auf kultivierten Moorböden. Landtechnische Forschung, 1953.

DISCUSSIONS

F. J. SONNEN. — In der Drucksache Nr. 32 wurde ausgeführt, dass der Verlauf des Triebkraftbeiwertes K in Abhängigkeit vom Schlupf auf landwirtschaftlich genutzten Böden dargestellt werden kann durch die Funktion

$$K = K_{max} - A\,e^{-k\,s}$$

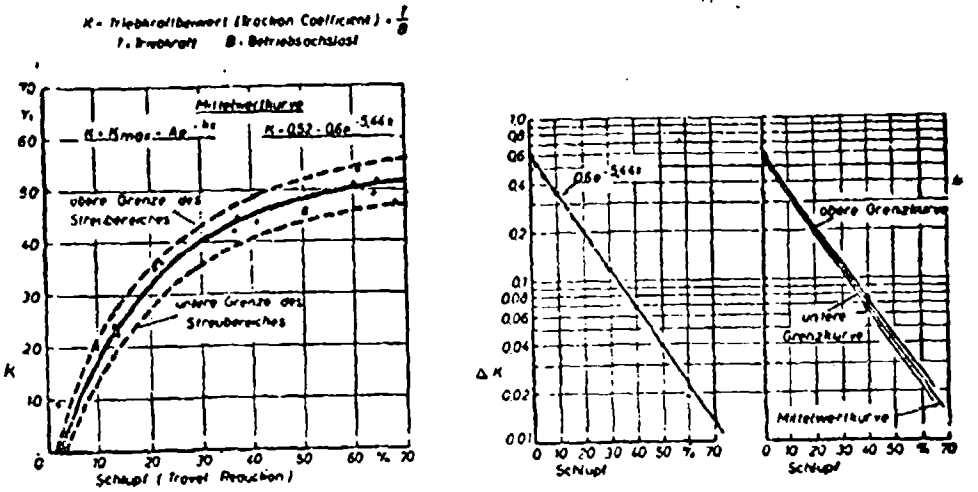


Bild 1. — Rechnerische Ermittlung des Verlaufes des Triebkraftbeiwertes K.

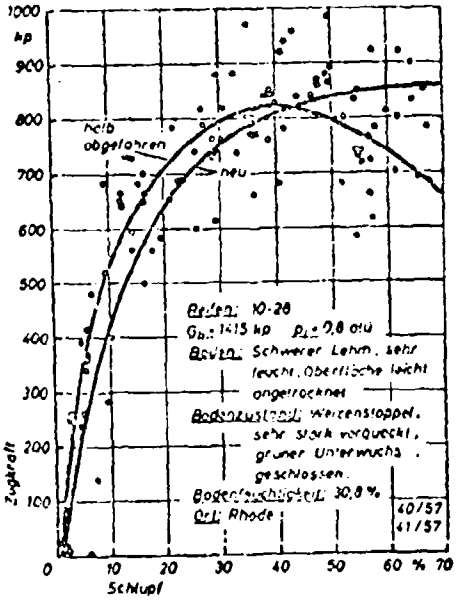


Bild 2. — Verlauf der Zugkraft bei neuen und halb abgefahrenen Reifen.

Die Brauchbarkeit dieser Formel ist seit etwa 3 Jahren an den Ergebnissen zahlreicher, im Institut für Schlepperforschung durchgeführter Feldversuche geprüft worden. Mit ihr konnten Kurvenverläufe des Triebkraftbeiwertes auf allen in diesem Zeitabschnitt untersuchten Bodenarten und -zuständen wiedergegeben werden, die Uebereinstimmung war gut.

Bei ungünstigen Bodenverhältnissen kann es bei Feldversuchen vorkommen, dass die Triebkraftbeiwertkurve nicht im Ursprung des Koordinatensystems beginnt, sondern bei Schlupfwerten von etwa 5-10 %. Zur Beschreibung solcher Kurvenverläufe ist im 2. Glied der Gleichung der Faktor A erforderlich, der nach der bisherigen Erkenntnis eine Funktion des Rollwiderstandes ist und bei Beginn der Kurve im Koordinatenursprung zu K_{max} wird. Im Bild 1 wird ein solcher Verlauf des Triebkraftbeiwertes gezeigt, der auf einem gepflügten, feuchten schweren Lehm gewonnen wurde. Im Diagramm ist die Streuung der Messwerte eingetragen, ebenfalls die obere und untere Grenze des Streubereichs.

In mittleren Teil des Bildes wurde auf halblogarithmischem Papier für die Mittelwertkurve als Ordinate die Differenz $K_{max} - K$ aufgetragen, als Abszisse der Schlupf. Man sieht, dass die Mehrzahl der Punkte auf einer Geraden liegt, die auf der Ordinate den Wert A abschneidet und deren Steigung durch den Wert k charakterisiert ist. Unter Zuhilfenahme von halblogarithmischem Papier lassen sich also die Konstanten verhältnismässig einfach finden und die Gleichung leicht auswerten.

Zur Auffindung der Mittelwertkurve kann der in der Darstellung ganz rechts gezeigte Weg beschritten werden. Dort wurden zunächst die Geraden für die obere und untere Grenze des Streubereiches gezogen. Unter der Voraussetzung, dass die Streuung der Messpunkte sich gleichmässig um die Mittelwertkurve verteilt, kann dann für bestimmte Punkte die Lage der die Mittelwertkurve bestimmenden Geraden durch Halbieren des Abstandes der beiden Grenzgeraden gefunden werden. Im Beispiel wurde dies für den Schlupf 40 % und für den Einlaufpunkt der Mittelwertkurve bei 2,5 % Schlupf durchgeführt. Der Einlaufpunkt kann bei der von uns verwendeten Messmethode berechnet werden. Das beschriebene Verfahren hat den Vorteil, dass auch bei verhältnismässig grosser Streuung der Messpunkte die Mittelwertkurve mit vergleichsweise geringem Aufwand und guter Sicherheit gefunden werden kann.

Die angegebene Gleichung kann nur stetig ansteigende Kurven voll wiedergeben, wie z. B. den in Bild 2 angegebenen Kurvenverlauf des neuen Reifens; Kurvenverläufe, die ein Maximum aufweisen, wie z. B. der des halbabgefahrenen Reifens, können durch die Gleichung nur bis zum Maximum beschrieben werden. Zu diesem Ergebnis kommen auch Z. Janosi und B. Hanamoto, die in der Drucksache Nr. 41 den Verlauf der Schubspannung in Abhängigkeit von der Dehnung ebenfalls durch eine e-Funktion darstellen. Dort wird der Verlauf der Kurve durch Konstanten bestimmt, die auf Bodenkenngrössen beruhen, und mit den an Modellfahrzeugen in Bodenrinnen ermittelten Werten vergleichen. Bei Betrachtung der guten Uebereinstimmung der im Feldversuch gemessenen Triebkraftbeiwerte mit den nach unserer Methode errechneten Kurvenverläufen scheint eine Verbesserung der Uebereinstimmung der in Bodenrinnen gewonnenen Ergebnisse durchaus möglich zu sein. Auf landwirtschaftlich genutzten Böden war es uns bisher nicht möglich, Triebkraftbeiwerte und deren Verlauf aus den Bodenkenngrössen abzuleiten.

E. LEMKE. — Zum Vortrag von Herrn Dr. Söhne möchte ich einige kleine Zusätze geben. Die Bilder, die Sie über die Bestimmung der Kenngrössen an Moorböden sahen, sind in Mooren gefunden worden, auf denen wir Fahrversuche durchgeführt haben; wir haben die Moore dabei — speziell dieses Moor — in einem extrem trockenen

Zustand befahren und fanden, dass sich dieser sehr trockene Zustand ganz besonders eignet zur Klassifizierung der Moore in Bezug auf Geländefahren. Die Moore verdienen also in dieser Hinsicht eine andere Behandlung als die Mineralböden, die ja bisher — und das mit recht — nach ihrem Verhalten im nassen Zustand, oder in einer nassen Jahreszeit, klassifiziert werden. Es zeigte sich dabei, dass wir in Mitteleuropa den entwässerten Mooren eine besondere Behandlung widmen müssen; wir haben fast nur künstlich entwässerte Moore in Mitteleuropa, und müssen also hier ganz anders als etwa in Nordamerika vorgehen. Die künstliche Entwässerung bringt zustande, dass die Moore in diesem trockensten Zustand von der Oberfläche her austrocknen, und dass sich damit eine Art tragender Teppich bildet, der sich aus der Vegetation — meist Gras oder Binsenbewuchs — und einigen Dezimetern sehr stark ausgetrockneten Torfes zusammensetzt. In dieser Zeit, im Oktober '59, war dieser Teppich oder diese Decke etwa 30-70 cm dick. Wir haben dann Herrn Dr. Söhne gebeten, diese Versuche auf Moor auszuführen; leider war es organisationsmässig nicht möglich sie im unmittelbaren Zusammenhang auszuführen — es verging ein 3/4 Jahr — und daher ist eine gewisse Trennung der Versuchsbedingungen zustande gekommen. Während wir im Oktober '59, an diesen gezeigten Stellen 30-70 sogar 50 und 70 cm ausgetrocknete Decke vorfanden, waren 3/4 Jahr später nur noch etwa 20 cm übrig geblieben. In diesem trockensten Zustand war das Moor bei 40 cm an einer Stelle, bei 70 an einer anderen Stelle, sogar bis auf die Sohle nicht mehr nass. Der Zustand war so verschieden, dass in der trockenen Decke das Moor Bröckel bildete, die man kaum mit dem Finger zerdrücken konnte; an einer Stelle dann das Nichtzersetzte, der sogenannte Weisstorf, der aus Moos besteht, so fest war wie eine Filzsohle, und darunter das nasse Moor, etwa wie ein nasser Badeschwamm, und der zersetzte Schwarztorf sich etwa wie eine Zahnpaste verhielt. Also die Unterschiede im mechanischen Verhalten zwischen Decke und dem nassen Moor waren sehr extrem.

Insofern sind also auch die Kurven, die von den Kennziffern gebildet wurden, nicht mit dem extremen Trockenzustand direkt gleich zu setzen. Dieser extrem trockene Zustand ergab eine Klassifizierung für Moore nach der Mächtigkeit — in Moore bis 40 cm, bis 1 m, 2 m und über 2 m Mächtigkeit —. Und das ist sehr einfach zu verstehen. Wenn etwa 30 bis 70 zentimeter von der Oberfläche her austrocknen und tragend sind, dann ist es natürlich sehr wesentlich verschieden, ob das Moor nur ½ m mächtig ist, und damit die gesamte Mächtigkeit durchgetrocknet ist, oder 1 m und damit nur etwa die Hälfte vom Moor ausgetrocknet ist, oder das Moor etwa 2 m ist, und über 2 m und damit nur ein kleiner Prozentsatz des Moores trocken ist. Es zeigte sich, dass die Fahrzeuge mit mehreren 10 Tonnen Gewicht durch diese Decken durchbrachen, wenn eben die Mächtigkeit des Moores etwa mehr als 2 m stark war; dann wirkte sich das Gesamtgewicht bei den schweren Fahrzeugen so stark aus, dass diese Decke nicht mehr trug; ganz anders bei den Decken am Rand des Moores, bei denen unbegrenztes Befahren, auch mit schweren Fahrzeugen, möglich war. Also in diesem Falle eine ganz deutliche Auswirkung des Gesamtgewichtes auf das Fahrergebnis.

Ich möchte Herrn Dr. Söhne fragen, ob bei den veränderten Versuchsbedingungen, bei denen also die tragende Decke geschwunden war, auf 20 cm, dieser Zusammenhang mit dem Gesamtgewicht noch zu erkennen war. Ein anderes Interesse ist, nach welcher Richtung hin das mögliche, das anwendbare Gerät für Torfe und für Moore sich voraussichtlich entwickeln wird. Wir stellten fest, dass der Kegel-*penetrometer* uns keine verlässlichen Werte lieferte bei Mooren mit solch starken tragenden Teppichen oder Decken, er lieferte zu günstige Werte, die eben schon in der Decke steckenblieben und das Ergebnis entsprach, mindestens bei den Fahrzeugen von mehreren 10 Tonnen Gewicht, nicht den Gegebenheiten. Insofern erscheint es notwendig, dass für den weiteren

Gebrauch des Kegelpenetrometers Begrenzungen der Anwendbarkeit klar herausgestellt werden.

W. SOEHNE. — Ich habe mich eigentlich mehr auf landwirtschaftliche Fahrzeuge in der Grössenordnung 2-4 Tonnen Gewicht beschränkt. Bei erheblich schwereren Fahrzeugen mit erheblich grösseren und breiteren Gleitketten wäre es erforderlich, unsere Messeinrichtungen etwas zu modifizieren, dass man grössere Lasten, die in grösserer Tiefe wirken, einbringen kann. Und das wären dann die Voraussetzungen um solche Moorböden in grösseren Tiefen zu klassifizieren.

N. W. RADFORTH. — My colleague, Dr. Lemke, has just communicated a most significant observation on Dr. Söhne's results. I congratulate him and in concurring am not unmindful of the valuable basic contribution that Dr. Söhne has unquestionably made.

Humification and water loss from the surface of organic terrain by artificial or seasonal influence may indeed induce the formation of a crust which has different bearing potential and other properties than the original values. Therefore there may be a secondary state to which Dr. Söhne's results may relate; they would in this event not be valid for the initial or primary condition. Also this crust varies as to properties characteristically from place to place. The reasons for this phenomenon are two. In the first place humification causes one order of differential. Secondly, peat in its natural constitution differs characteristically as to phisical properties (Radforth, Can. Jour. Eng., 1953, Et. Sez.). In our laboratory we recognize 16 categories of peat which differ as to mechanical properties (loc. cit.).

There should be no discouragement from an idea that because of this difference the mechanical analysies of peats is impractical and likely to be undependable. On the contrary organic terrain can be validly classified to account for both orders of variability indicated because of the kind of organization inherent this terrain. (See Radforth paper).

N. 34

The powered vehicular wheel plane-rolling in equilibrium: a consideration of slip and rolling resistance

Considerazioni sullo scaricamento e la resistenza al rotolamento di una ruota motrice piana in equilibrio

J. R. Phillips *)

ABSTRACT. — *When a flexible vehicular wheel rolls on deformable ground with a driving, or a braking couple applied at the hub, difficulties arise in specifying the phenomena «slip» and «rolling resistance». The paper attempts to clarify the basic issues involved.*

A definition, not entirely new, is offered for what is described as a «meaningful» coefficient of rolling resistance, and this definition is studied in the light of some well known definitions for slip. The question of «zero-slip» is studied in particular and shown to be of importance in the choice of meaningful definitions.

A criticism is made of current views on the matter of rolling resistance, it being argued that not sufficient attention is being paid to the questions of slip and zero-slip. It is argued, in fact, that currently used coefficients of rolling resistance are not meaningful, in that they do not relate to practical reality or to the fundamental mechanics.

Introduction. — The purpose of this paper is to discuss the equilibrium of the elastic plane-rolling wheel being steadily driven or braked while rolling over deformable ground. It aims to derive a useful expression for the forward (or rearward) thrust F on the chassis in terms of the couple M acting at the hub of the wheel and other variables. The phenomena «slip» and «rolling resistance» are studied in particular, and the algebraic argument purports to show that these are not clearly separable from one another: a carelessly conceived definition for rolling resistance may well be found to depend upon some arbitrarily chosen definition for slip.

The view is taken throughout that any coefficient ρ of rolling resistance ought to be defined in such a way that it remains analogous with the well known coefficient μ of sliding friction: if F be the horizontal component of the force which is acting from the chassis upon the wheel, then, when zero couple M is acting at the hub, the relation

$$F = -\rho G$$

*) University of Western Australia.

ought to hold, G being the vertical component of the force which is acting from the chassis upon the wheel.

Chudakov (1950) appears to have taken a similar view, and he derives on this basis two apparently different, though identical expressions for his coefficient ρ of rolling resistance. Both expressions for Chudakov's ρ involve the couple M at the hub, the forward « shift » a of the vertical reaction, and his two different rolling radii, k and k_m. These mentioned variables are all defined by the present author in substantially the same way as they are defined by Chudakov. Chudakov's paper, however, does not discuss the phenomenon « slip » as such, nor does it treat the case where the ground is considered deformable.

Definitions. — The wheel shown in the figs. 1 a and 1 b is both elastic and treaded: it may, for example, be a flexible pneumatic wheel or a hard wheel with hard strakes. The ground on which it rolls is level, longitudinally homogeneous, and deformable. In both diagrams the indicated forces and couples are acting, not on the chassis or on the ground, but on the wheel. In both diagrams, also, the wheel is travelling towards the right.

The couple M is the total couple acting at the hub. This couple is the algebraic sum of what we might call the driving couple, say M_p, and the friction couple at the bearing, say M_q. The separate couples M_p and M_q do not appear in the diagrams because in the overall view they are not important.

The force F is the horizontal component of the force which comes from the chassis and which acts upon the wheel at the hub-centre; G, the « load » on the wheel is the vertical component of this force. The horizontal force F on the chassis, equal and opposite to the force F on the wheel, is required of course to balance whatever other resistive or propulsive forces there may be acting on the chassis - those due to the presence, for instance, of other wheels, or to the action of external influences such as the towing by, or towing of, other chassis, or to the presence on the chassis of soil-working, road-making, or other tools.

The reaction R_r is the total reaction from the ground: it is the vector-sum of all the elementary forces distributed over the contact patch. If we assume that the wheel is travelling in the vertical plane of its own periphery (that is that the wheel is plane-rolling) and that the wheel itself is symmetrical about this plane, there is no couple associated with this reaction R_r: it is a pure force.

The force R_r, the line of action of whose vector is located in relation to the wheel, is divided in the diagrams into its horizontal and vertical components $(R_r)_x$ and $(R_r)_y$. Knowing that these components may be drawn anywhere provided they intersect on the located line of action of R_r, we see that $(R_r)_x$ has been drawn, quite arbitrarily, at the undisturbed ground level (UGL).

In view of the physical realities at the surface of any real ground, grass, roots, stones, etc., it will be clear that the UGL must be put at some arbitrarily

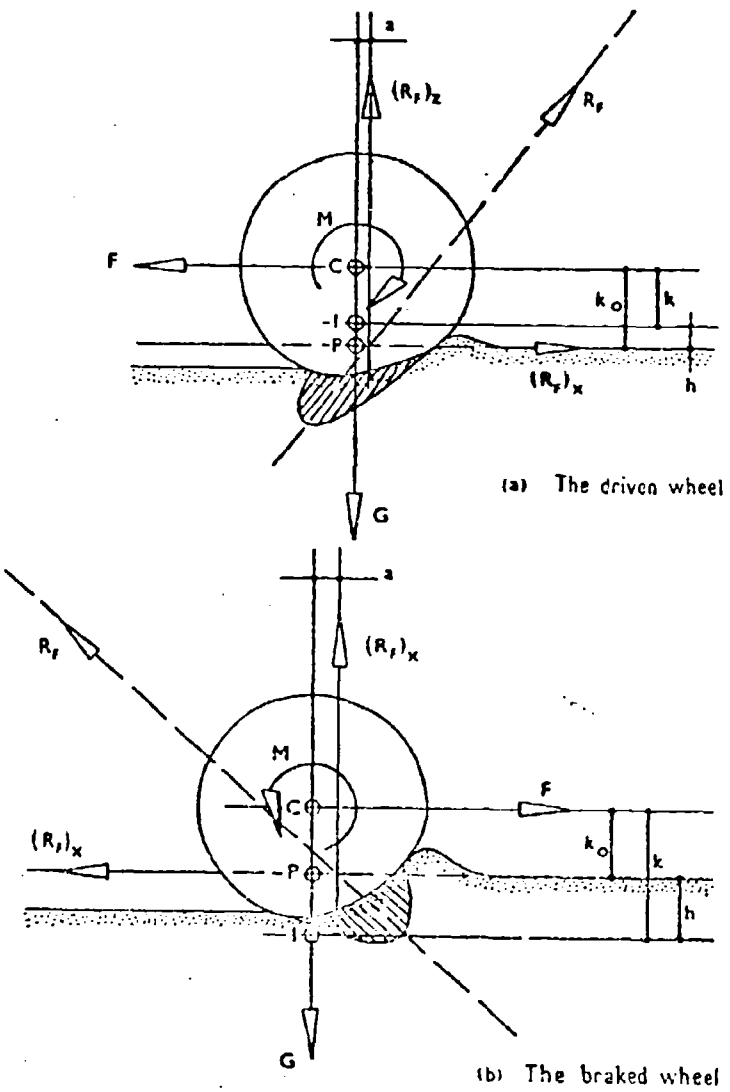

a
$(R_r)_z$
R_r
M
F
C
k_o
k
-I
-P
$(R_r)_x$
h
G
(a) The driven wheel
a
R_r
$(R_r)_x$
M
C
F
$(R_r)_x$
k_o
k
-P
h
-I
G
(b) The braked wheel

Fig. 1.

nominated level. The mathematical implications of this free choice are important; they are discussed in detail later.

The arbitrary choice for the location of $(R_F)_z$ has automatically located $(R_F)_z$. The length-dimension a, which nominates the position of $(R_F)_z$ in relation to the hub-centre, has been called by a number of Authors the forward (or rearward) «shift» of the vertical reaction.

The constant (clockwise) angular velocity of the wheel is ω, and the constant (towards the right) linear velocity of travel is v. If $v = k\omega$ then k is the distance down from the hub-centre (C) to the instantaneous centre of rotation (I) of the wheel relative to the ground.

Let us call k the «actual rolling-radius» of the wheel, for this is the radius one might imagine oneself using for calculating the actual distance travelled by the wheel in one revolution.

Clearly h, the height of the instantaneous centre (I) above the UGL, is such that $h = k_o - k$.

The distance from the hub-centre (C) down to the point (P) at the UGL is k_o, and this distance (which will remain approximately constant for a constant G and a constant ground) may, for obvious reasons, be called the «apparent rolling radius» of the wheel.

Let us call (P) the «ideal point of contact». Since, ultimately, the oblique-rolling circumstance ought to be provided for, we shall define the point (P) generally as being at the intersection of the following three planes: the plane of the UGL; the plane of the periphery of the wheel; the vertical plane through the wheel-axis. It will be noted that a knife-edged «hard» wheel rolling on «hard» ground will always make contact at this ideal point.

Sign conventions are chosen as follows. For horizontal forces and distances, and for linear velocities, the positive direction is towards the right. For couples and angular velocities, the positive direction is clockwise. The height h is positive when (I) is above (P), and the radius k is positive when (I) is below (C).

It might be mentioned here that the enclosed shaded areas in the fig. 1 are after Söhne (1951). They are meant merely to suggest that the reaction R_F originates somehow in the ground.

Derivation of expressions for p. — If the wheel in the fig. 1 is in equilibrium, that is if the vectors v and ω are constant, the following three equations may be written:

$$(R_F)_z = G$$

$$F = (R_F)_x$$

$$M = (R_F)_x a + (R_F)_z k_o$$

and from these it follows that

$$F = \frac{M}{k_o} - G\frac{a}{k_o} \qquad (1a)$$

This equation (1 a) is simply an equation of equilibrium: it may be obtained directly by taking moments about the point (P).

At this early stage of the argument it will be seen how the often-mentioned ratio a/k_o (sometimes called the Coulomb coefficient) has come to be quoted in textbooks as the « coefficient of rolling resistance » — it being argued, presumably, that, if it were not for the rolling resistance « obstacle » Ga/k_o, F would equal, simply, M/k_o.

There are faults in this textbook argument however: the expressions M/k_o and Ga/k_o will both take numerical values depending upon the arbitrary choices made for the various datum-levels. It has already been shown that the value taken by the length-dimension a will depend upon the level chosen for the horizontal component of reaction $(R_F)_x$. Also the value taken by k_o will depend entirely upon the arbitrary choice of level made for the UGL. Only in the very special case of a wheel rolling with zero moment M at the hub, and with its $(R_F)_x$ chosen at the UGL, will the ratio a/k_o remain independent of the location of $(R_F)_x$ and the UGL.

In general, that is whenever M is not zero and whenever the ground is not such that a « physical » UGL might be chosen with certainty, the ratio a/k_o may in fact be given whatever numerical value we wish to arrange for it. The expression Ga/k_o, accordingly, cannot be a useful measure of whatever we might *imagine* to be the « rolling resistance force ».

In his paper already quoted (1950) Chudakov deals with an elastic wheel rolling on hard ground; his implied UGL is at the hard ground level, and his $(R_F)_x$ is at the UGL. In his analysis he also rejects the expression Ga/k_o as being a useless measure for the « rolling resistance force ». He does this, however, not because of the argument pursued above, but because he finds by experiment (with a braked wheel) that, as the braking couple increases, that is as the couple M at the hub becomes more and more negative, the length-dimension a decreases and even becomes negative. He asks: how can Ga/k_o be a measure of a « rolling resistance force » when a is sometimes zero and often even negative?

Chudakov writes another equation. He writes, in essence, not only that

$$M = Ga + Fk_o \qquad (1\,b)$$

but also that

$$M\omega = (R_F)_x v + \rho (R_F)_x v \qquad (2\,a)$$

where $M\omega$ is the power-input at the hub, $(R_F)_x v$ is the power-output to the chassis, and $\rho (R_F)_x v$ is an expression (including the dimensionless coefficient ρ) for the power-loss to the ground at the contact patch.

Obviously, in the equation (2 a), the force $(R_F)_x$ is not considered as working on the wheel at the velocity ρv; the expression $\rho (R_F)_x v$ for the power-loss to the ground is a sound one nevertheless. The idea is, not that the force $(R_F)_x$ is working, but that the (admittedly somewhat mythical) horizontal force $\rho (R_F)_x$, or ρG, is working at the velocity v. The fact is that, by choosing to write the

expression $\rho\ (R_F)_z\ v$ for the power-loss to the ground, we are taking a short cut to a definition for ρ.

Had the algebra of equation (2 a) been written more nearly according to first principles, the rate of working of the force R_F would have been considered. The point of application of the force R_F is moving (in the direction of R_F) at the velocity $\omega a\ (R_F)_z/R_F + \omega h\ (R_F)_x/R_F$, so the power-loss to the ground, which is the product of R_F and this velocity, is $\omega a\ (R_F)_z + \omega h\ (R_F)_x$. But $\omega = v/k$, $(R_F)_z = G$, and $(R_F)_x = F$, so the power-loss to the ground may be written $(a/k + h/k \cdot F/G)\ (R_F)_z\ v$. Note that the expression within the brackets here is identical with the first of the expressions derived for ρ.

By simply repeating the equation (1 b), and by rewriting the equation (2 a) by putting $(R_F)_z = G$, $(R_F)_x = F$, and $\omega = v/k$, we get

$$M = G a + F k_0 \tag{1 b}$$

$$M = F k + \epsilon G k \tag{2 b}$$

and from these, first by eliminating M, and then by eliminating F, we arrive at the following alternative expressions for ρ:

$$\rho = \frac{a}{k} + \frac{F}{G} \cdot \frac{h}{k} \tag{3 a}$$

$$\rho = \frac{a}{k_0} + \frac{(M/k)}{G} \cdot \frac{h}{k_0} \tag{3 b}$$

Substantially, these are the expressions derived by Chudakov. They are applicable here, however, for deformable ground.

The independence of ρ. —If $(R_F)_z$ had been put elsewhere, say at some distance m above or below the UGL, the equations (1) and (2) and the expressions (3) for ρ would still have been obtainable. The distance m would simply have complicated the algebra somewhat in the early stages. This means that, whereas the simple a/k_0 was dependent upon the level chosen for $(R_F)_z$, the expressions (3) for ρ are not.

It will also be seen that the UGL itself may be shifted, either upwards or downwards, without affecting the expressions (3) for ρ. This means that, during some series of experiments in the field where perhaps ρ was being measured, we could afford to nominate the UGL as being anywhere, that is, we could measure k_0 in any way we chose, provided, for the sake of comparison with other work, we consistently chose to measure it in some particular way.

To demonstrate the truth of the statement that ρ is independent of our measure of k_0, suppose that the UGL were nominated as being at some distance, say Δ, below (or above) the level shown in the fig. 1. Putting $(R_F)_z$ at this new UGL, we see that the new a, say a', becomes $a \mp \Delta \tan \Phi$, where Φ is the

inclination of R_F to the vertical, and that the new h, say h', becomes $h \pm \Delta$; so the new ρ, say ρ', using the expression (3 a) becomes

$$\begin{aligned}\rho' &= \frac{a \mp \Delta \tan \Phi}{k} + \frac{F}{G} \cdot \frac{h \pm \Delta}{k} \\ &= \frac{a \mp \Delta (F/G)}{k} + \frac{F}{G} \cdot \frac{h \pm \Delta}{k} \\ &= \frac{a}{k} + \frac{F}{G} \cdot \frac{h}{k} \\ &= \rho\end{aligned}$$

which is what was required to show.

This fact that the expressions (3) for ρ are independent of arbitrarily chosen levels is an important (and convenient) one; but notice also that, when M is zero, $\rho = a/k_o$ and $F = -\rho G$; this latter infers that the coefficient ρ as defined above does satisfactorily conform to the requirement asked of it, namely that it remain analogous with μ.

Slip and zero-slip. — Before discussing some algebraic implications of the above expressions for ρ, the questions of « slip » and « zero-slip » ought to be examined.

Suppose that a « hard » wheel of radius k_o was rolling on « hard » ground and that it was travelling in each revolution a distance $l_o = 2\pi k_o$. It would be agreed by most observers, firstly that the UGL might be taken at the hard ground level, and secondly that this hard wheel was rolling with « zero-slip ». If on the other hand it was travelling in each revolution some other distance, say $l = 2\pi k$, it would be agreed by most observers that the wheel was slipping, and that the actual extent of the slip could be quantified by quoting one or both of the following ratios: $(l_o - l)/l_o$; $(l_o - l)/l$. These latter are the well known « travel-reduction » and « spin » slip ratios respectively.

Now if n_o was the number of revolutions required of this hard wheel to travel a certain distance when the slip was zero, and n the number of revolutions required of the same wheel to travel the same distance when the wheel was slipping, it will be seen that

$$\frac{h}{k_o} = \frac{l_o - l}{l_o} = \frac{n - n_o}{n} \qquad (4\,a)$$

and that

$$\frac{h}{k} = \frac{l_o - l}{l} = \frac{n - n_o}{n_o} \qquad (4\,b)$$

where h, k_o and k have the same meanings as they had before.

Fig. 2 demonstrates the ways in which h/k_o and h/k will vary with v/ω,

that is, with k. Notice that whereas h/k$_o$ varies linearly with k, h/k does not. The wheel-diagrams below the curves in fig. 2 are all of the same hard wheel rolling on hard ground; each has been drawn with its UGL opposite its relevant

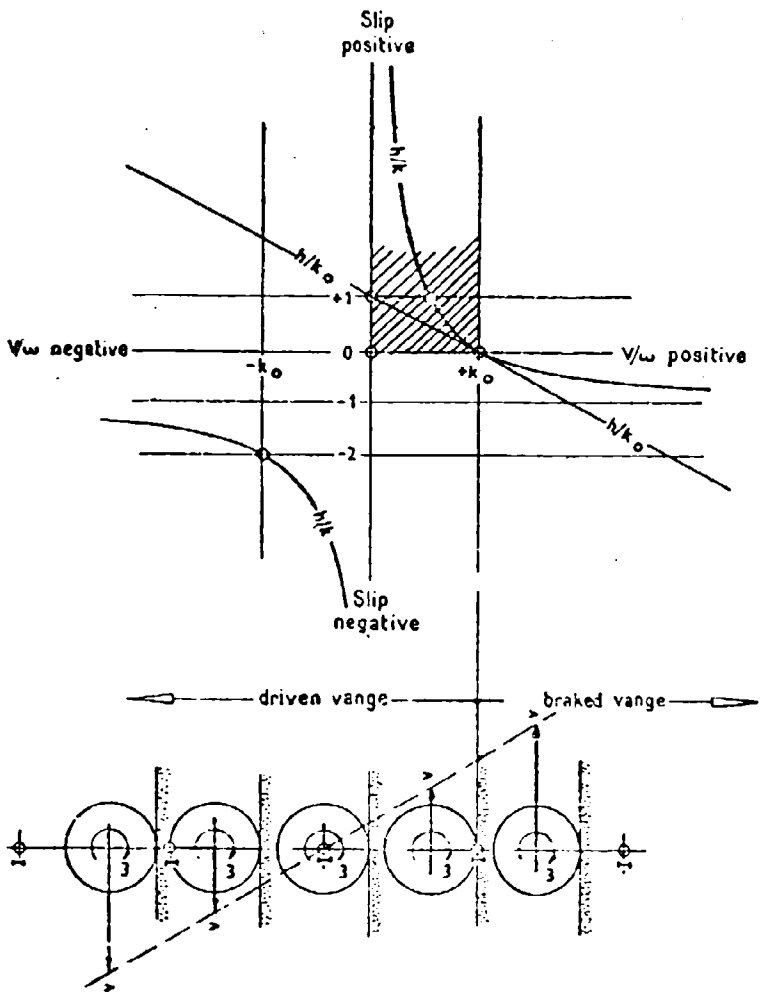


Fig. 2.

point on the v/ω-axis, and as a group they are intended to show how the radius k may vary all the way from positive-infinity through zero to negative-infinity. It has already been shown in (4 a) and (4 b) that, for a hard wheel on hard ground, h/k$_o$ is the travel-reduction slip while h k is the spin slip.

Now it must be observed here that the equalities (4) apply without ambiguity only in this hypothetical circumstance of the hard wheel being driven over hard ground. When we define this hypothetical « hard-wheel-hard-ground »

circumstance we require among other things that the height h and the equal and opposite forces F and $(R_F)_x$ diminish to zero when the couple M diminishes to zero and vice versa. These requirements do not obtain in practice however; for when we drive a real wheel over real ground neither h nor F necessarily diminishes to zero when M diminishes to zero, nor, conversely, does M diminish to zero when either h or F diminishes to zero. In the « real-wheel-real-ground » circumstance, moreover, we must ask: where is the UGL?

It will be obvious that there are a number of different criteria available for the notion « zero-slip », each one leading, of course, to a different length l_o; and the most sensible and convenient of these would seem to be, (a) when h is zero, or (b) when F is zero, or (c) when M is zero.

In fig. 3 a certain real wheel is imagined to have been driven from the same starting-line through N revolutions over three similar stretches of the same real ground. On the first run (a) the wheel has been driven in such a way that the instantaneous centre (I) has remained at the UGL, on the second (b) in such a way that the force F has remained at zero, and on the third (c) in such a way that the couple M has remained at zero. The various indicated arrangements of the vectors have been drawn so as to require no written explanation. Fig. 3 purports as a whole to show that the respective distances travelled in each of the three mentioned circumstances are all different; the three diagrams offer, in other words, a clarification of the statement that the three mentioned criteria for zero-slip are all different.

Of the three criteria one might imagine that the third, the zero-M criterion, would be the most sensible and most convenient; for, when M = 0, the reaction R_F passes through the hub-centre of the wheel, and the wheel might be said to be « free-rolling ». In ordinary field practice, however, this condition is difficult to achieve: the wheel must be driven by a driving couple M_p, carefully adjusted so as to balance exactly the friction couple M_q.

The second, the zero-F criterion, has the advantage that we could argue that when the slip is zero the soil experiences no longitudinal distortion at the contact patch; also, when F = 0, the whole energy-input at the hub is being lost at the contact patch, and the efficiency of the wheel as a machine is zero. The zero-F condition obtains, for example, at all four wheels of a four-wheel driven vehicle when it travels at constant speed across a level stretch of ground. This condition is, however, like the zero-M condition, very difficult to achieve in ordinary experimental practice in the field.

The first, the zero-h criterion, on the other hand, has the advantages: (i) that the distance l_o can easily be determined in the field; and (ii) that the ratio h/k_o appears as a dimensionless number in the expression (3 a) for ρ. In the field one would need only to measure a number of times (with some suitably- footed height gauge) the height k_o — the gauge, incidentally, would fix the UGL — and then to obtain the distance $l_o = 2\pi k_o$. Measured distances l would subsequently determine radii k, and thus numerical values for the ratio h/k_o.

After considering the various possibilities the present writer has chosen as

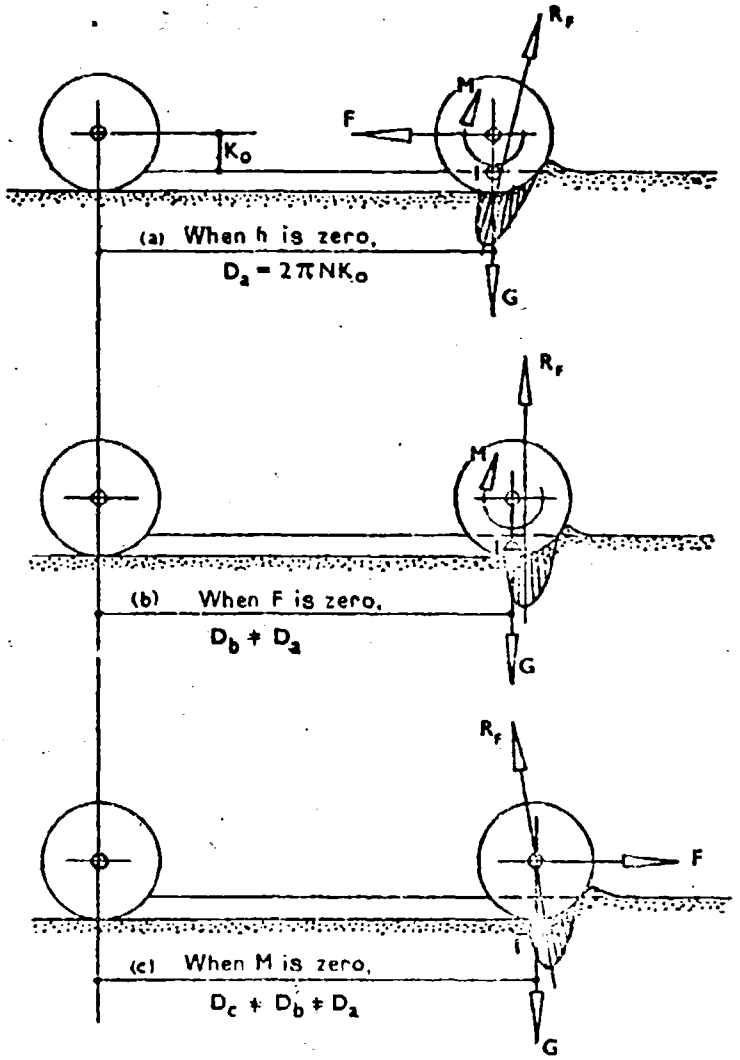


Fig. 3.

his measure for slip the ratio h/k_o and, as his criterion for zero-slip, the circumstance when h is zero.

It may be argued that this scheme has the following disadvantages: (i) that the value taken by the ratio h/k_o will depend upon the choice of level for the UGL, that the measure for slip, in other words, will depend upon the nature of some arbitrarily chosen instrument for measuring k_o; (ii) that a small percentage « error » in the measurement of k_o will cause a large percentage

alteration in h, and thus in h/k_o; (iii) that the ratio h/k_o will often be highly negative, even when M is positive and the force F on the chassis is positive.

These objections, however, may be remarked upon respectively as follows: (i) any definition for slip must depend upon some arbitrarily chosen zero, so the particular zero chosen by the instrument is as good a one as any other; the UGL, moreover, has got to be chosen somehow, so why not use some special instrument for choosing it?; (ii) this objection is linked with the first in that the value taken by h/k_o will depend upon the measuring instrument and the skill of the operator using it; on rough ground, however, it would be wise to measure k_o a number of times and then to quote an average value; (iii) the phenomenon slip is less important in the fundamental mechanics than is the phenomenon rolling resistance; it is much better to have some « unmeaningful » measure for slip than to have some unmeaningful ρ; it is better, in other words, simply to regard h/k_o as some useful ratio (like a/k_o is a useful ratio) which happens to figure in the determination of the meaningful ρ.

That ρ is a meaningful coefficient is discussed in the following section.

The meaning of ρ. — By rearranging equation (2 b) and by quoting again the expression (3 a) for ρ we get

$$F = \frac{M}{k} - \rho G \qquad (2\,c)$$

$$\rho = \frac{a}{k_o} \frac{M/k}{G} \frac{h}{k_o} \qquad (3\,a)$$

and then, by substituting (3 a) in (2 c), we get

$$F = \frac{M}{k} - \left[G\left(\frac{a}{k_o}\right) + \frac{M}{k}\left(\frac{h}{k_o}\right)\right] \qquad (5)$$

This expression (5) for F infers the obvious, namely that, if it were not for the rolling resistance force ρG (contained within the square brackets), F would equal, simply, M/k. We know from ordinary experience, however, that F is always less than M/k: we know, in other words, that ρ is always positive: F always falls short of the « ideal » M/k by the positive amount of force ρG.

There is of course a clear circularity in the above reasoning; the argument has concluded, in effect, that the force ρG is the force ρG; the equation (5) is simply another form of our chosen definition for ρ.

This particular form, however, is a useful one, because it collects together into a single statement all of the variables which are important from the practical point of view: G, M, k, and F. It shows clearly how the two dimensionless ratios, a/k_o and h/k_o, figure in the determination of F; and it shows that these ratios (which will vary) must be determined independently by experiment. It could in fact be argued that the form of equation (5) suggests the experiments

by means of which the variations of a/k_o and h/k_o might be studied, but such notions are beyond the scope of the present paper.

It will be more instructive, perhaps, to study the meaning of ρ by considering the algebraic consequences of some limiting conditions. Refer to equation (5) and consider the following:

When h is zero, that is when the point (I) is at the UGL, of vice versa, equation (5) reduces to

$$F = \frac{M}{k_o} - G\frac{a}{k_o}$$

because, when $h \to 0$, $k \to k_o$, and $\rho \to a/k_o$. It is worth observing here that, if the UGL were chosen at some other level, the point (I) remaining fixed, the ratio a/k_o would be altered; but so also would h be altered — it would no longer be zero. The value for ρ would be found to remain the same.

When F is zero, that is when the chassis accepts nor gives no thrust, equation (5) reduces to

$$M = Ga$$

which is not surprising because, when F is zero, R_F is vertical and equal to G. The length-dimension a is not determined by the choice for the UGL in this particular case. Also, when F is zero,

$$\rho G = M/k$$

which means that the force ρG of rolling resistance becomes equal to the whole of the « ideal » F, namely M/k.

When M is zero, that is when the wheel is « free-rolling », equation (5) reduces to

$$F = -G\frac{a}{k_o}$$

which shows that the expression for ρ becomes a/k_o not only when h is zero but also when M is zero. It also shows again that ρ accords with the requirement asked of it, that it remain analogous with μ.

When k tends to zero, that is when the wheel approaches the condition where it rotates yet makes no progress,

$$\rho G \to \infty$$

which is not surprising; ρ has been defined as that dimensionless number which, when multiplied to Gv, gives the power-loss to the ground at the contact patch. The power-loss ρ Gv must remain finite always, so, as $k \to 0$, that is as $v \to 0$, ρ must tend to infinity. But also, as k tends to zero,

$$F \to \infty - \infty$$

which shows that the force F remains, in the limit, finite though indeterminate.

A relevant remark here is that when the wheel does finally arrive at this limiting condition, the ground on which it is rolling is no longer being « continuously » deformed; the radius k_o is decreasing.

When k tends to infinity (either positive or negative) the wheel approaches the condition where it no longer rotates but continues to travel along. As $k \to \pm \infty$, $h \to \mp \infty$, and $h/k \to -1$. So, as $k \to \pm \infty$,

$$\rho G \quad \to \quad + G \frac{a}{k_o} - \frac{M}{k_o}$$

which has a finite value. But also, as $k \to \pm \infty$, $M/k \to 0$, so

$$F \quad \to \quad - G \frac{a}{k_o} + \frac{M}{k_o}$$

This means that the force ρG of rolling resistance tends, in the limit, to become equal and opposite to the (towing) force F. This is not surprising because, in the limit, all the power Fv being put into the wheel from the chassis is being lost, ρGv, at the contact patch; the couple M is doing zero work. When, in other words, ω finally becomes zero, ρ in fact becomes the well known coefficient of sliding friction μ.

When, on the other hand, the radius k_o approaches zero the hub-centre of the wheel approaches the nominated UGL and the equal and opposite forces F and $(R_p)_x$ (at the UGL) tend to become colinear and cancel. If, in the limit, we remove $(R_p)_x$ to some distance, say m, below the UGL we are still unable to write the equation (1) so that it features F or $(R_p)_x$; the two variables simply disappear. When $k_o = 0$, $h = -k$, and $h/k = -1$; so when we put $k_o = 0$ in the equation (5) we get

$$F = \frac{M}{k} - [\infty - \infty]$$

which is also disappointing: it seems we cannot find an expression for the presumably finite ρG either. It is of course easy to show from first principles that, when $k_o = 0$,

$$M = Ga$$

but this result also tells nothing about the force F or the force ρG.

There is a real difficulty in this last consideration which appears to be due to the absence of missing information. It is conceivable, for instance, that if we know some functional relationship between say a and h, we would be able to write an expression for ρG in the limit as k_o tends to zero.

Before finally concluding this section on the meaning of ρ a criticism must be offered here of the opposite, more widely-held view on the question of rolling resistance.

It is argued by a number of authors that the power-loss to the ground at the contact patch is legitimately divisible into two separate parts: (i) that which

is due to slip; and (ii) that which is due to deformations of the wheel and of the ground. A definition for slip (with its arbitrarily chosen zero) is chosen first. From this a « power-loss due to slip » is calculated. Then a coefficient ρ is finally nominated to deal with the remaining power-loss « due to the deformations ».

It is true that any ρ defined in this way will never approach infinity, but it would appear that such coefficients are unmeaningful; they depend so obviously upon arbitrarily chosen definitions for slip and zero-slip (or upon no definition at all for the latter), and they thus necessarily refer, not to the total power-loss at the contact patch, but to some other, often unspecified amount of power which can have little or no relevance to the fundamental mechanics. It may have been noticed in this connection that graphs of « slip » and of « rolling resistance » are often drawn in the literature so as to be vague in the neighbourhood of the origin.

The ρ that has been derived above by the Chudakov-method, however, is in the writer's present opinion a meaningful ρ. It does make sense in the context of reality and it is, unlike a number of other coefficients ρ, non-self-contradictory.

BIBLIOGRAPHY

Chudakov E. A. K voprosu o kachenii elastichnogo automobil'nogo kolesa. (An enquiry into the rolling of elastic motor car wheels). Reports of the Academy of Sciences, USSR, vol. 70, no. 5, pag. 773, 1950.

Söhne W. Das Mechanische Verhalten des Ackerbodens bei Belastungen, unter rollenden Rädern sowie bei der Bodenbearbeitung. (The mechanical behaviour of soil under load, under rolling wheels, and on soil working). Grundlagen der Landtechnik, Heft 1: 9 Konstrukteurheft, pag. 87, 1951.

DISCUSSIONS

V. E. GOUGH. — As a person whose experience is largely in the field of tyres on hard ground and this is a conference largely attended by people with experience in soil mechanics, may I be so bold as to express some doubts about the diagram seen in so many papers, namely:

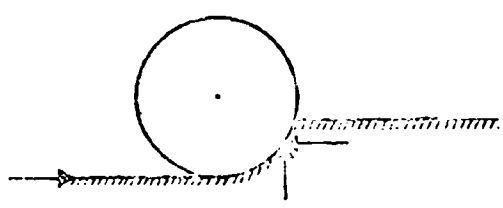


Fig. 1.

In this diagram the choice of points of application of the various forces appears to be arbitrary and empirical. In our work on hard ground, we have found some dangers in such approaches. In view of this I wish to welcome the analysis in the paper which is based on first principles. While I received this paper only yesterday when I came to this conference and have not found time in my room to study this paper I am sure that it is in agreement with a similar analysis which I included in Tyre-to-ground contact stresses (Wear. vol. 2, 1958-1959). (I have since confirmed this).

In this connection we are talking of resultant forces in those cases where all forces are co-planer and in such cases there is a single resultant force only. More knowledge than arbitrary assumption is needed to know what stresses lead to that resultant. For example it is an assumption to draw two separate horizontal forces in the diagram one representing soil shear in the entry region and one representing traction in the exit region. The level at which this latter force acts is an arbitrary assumption. Even in the hard ground case there are two equations one based on energy and one on moments and further data is required to relate the two and to relate the virtual centre in relation to the ground level.

In the three dimensional case the resultant can be expressed in terms of a force normal to a given plane and a force in the plane (ibid). We find this representation valuable in the case of our studies with our own six component rig of tyres on hard surfaces — we take as our reference plane the ground surface — in studies on soft ground I would suggest it would be the mean ground plane.

J. R. PHILLIPS. — I am sure that Mr. Gough is correct when he suspects this kind of picture. Perhaps also Mr. Gough and others are not bold, and they are correct when they suspect the kinds of pictures we find in our literature, where the curve drawn in the neighbourhood of the origin is on purpose left vague. It is this difficult question of what occurs near the origin. In the case of ordinary comparatively hard wheels on comparatively hard ground, the neighbourhood of the origin contracts almost to a point, and it is possible to argue over this difficulty. But in the generalized case where we have very flexible wheels or very deeply straked wheels rolling in very deformable ground, for example the milling cutter in a milling machine, the neighbourhood of the origin will not reduce to a conveniently small area which we may ignore and call a point.

A. R. REECE. — Mr. Chairman, Gentlemen, I think that Dr. Phillips has done a very good job in drawing our attention to the arbitrary nature of the usual definition of rolling resistance and rolling radius. For example, in a recent test that we made of a small tractor in very soft ground we found that the rolling radius (defined as in the international standard tractor test code) was twice the actual wheel radius. Having drawn attention to the arbitrary nature of the normal definition of rolling resistance Dr. Phillips goes on to propose that we adopt the Chudakov rolling resistance coefficient. This I am sure is totally unacceptable to all of us interested in soil vehicle mechanics. It is quite clear from equation (2a) that the coefficient μ covers all the losses involved in the wheel, lumping together both slip and rolling loss. While this may be adequate for the study of pneumatic tyres on hard roads it is quite useless for hard or resilient wheels on soft ground. In my study of the mechanics of a wheel on the soil the slip losses (due to horizontal deformation)

and the rolling losses (due to vertical deformations) will be computed separately. We therefore require that the losses are allocated to these two sources from the results of a wheel test. This can be quite simply done using equation (1b) by replacing k_u by the rolling radius of the wheel. The rolling radius would need to be rather arbitrarily assigned but for most practical wheels and tyres this can be done in a simple and meaningful way.

Dr. Phillips goes on to suggest that there is some particular merit in the distance from the centre of the wheel to the undeformed ground surface instead of the more usual rolling radius. It is clear to most people now that this distance is not a constant for a particular wheel in a particular soil, but is a function of slip. Dr. Phillips is therefore, suggesting that we replace the rolling radius by a dimension which varies in some complex way with slip. This seems to be little short of ridiculous. Having admitted that the rolling radius is an arbitrary dimension let us keep it, at least as a constant dimension for one wheel at a particular load on a given soil.

There is another important point concerning rolling resistance that needs to be made. From the point of view of soil vehicle mechanics it would be useful to define rolling resistance as the sum of the backward pointing horizontal components of the soil forces on all the elementary areas within the contact patch. Unfortunately it is impossible to obtain this force from a wheel test in which only the forces at the hub of the wheel are measured. In this type of test it is only really possible to assign a quantity of energy lost to rolling resistance. It is not possible to measure an actual force.

W. F. BUCHELE. — I want to congratulate Dr. Phillips for his basic paper concerning the behavior of the wheel. In the laboratory (in my Soil Dynamics Course) we have conducted experiments concerning the contact patch and the behavior of the resultant force R_{VD}, we have developed an analysis similar to that presented by Dr. Phillips for the driven wheel.

The polar pressure distribution curve has been drawn in fig. 1, using Dr. Phillips notation. A theoretical relation exists between the moment arm r_m of the resultant force R_{VD} and the radius of the solid wheel r_1.

$$r_m = r_1 \sin \Theta \qquad (1)$$

Where:

r_1 = Radius of a solid wheel

$\Theta = \tan^{-1} \mu$

$\mu = \dfrac{S_s A}{W_D}$

$S_s = C + p \tan \Phi$

A = Area of contact patch

W_D = Dynamic weight

R_{VD} = Resultant force of driven wheel

R_{VU} = Resultant force of undriven wheel

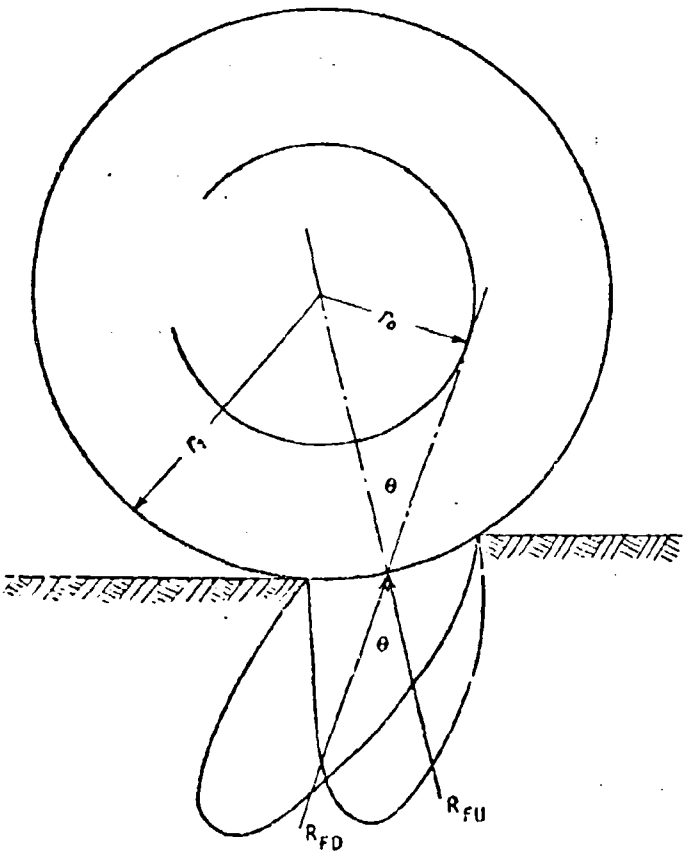


Fig. 1.

If the dynamic weight on the tire and the Coulomb parameters are known, the value of the R_{FD} can be calculated by equation 2.

$$R_{FD} = \frac{CA + W_D \tan \Phi}{\sin \Theta} \tag{2}$$

The direction of R_{FD} is dependent on the position of R_{FC}, as shown in figure 1. The position of R_{FC} is dependent upon the rolling resistance of the wheel.

N. 35

The ideal tractive efficiency of soils *)

Condizioni ideali del terreno ai fini della trazione

G. W. STEINBRUEGGE **)

ABSTRACT. — *The soil upon which a tractor operates is the intermediate link between the energy source at the traction members of a tractor and the energy output at the tractor drawbar. The transfer of energy from traction member to drawbar is subject to the efficiency with which the soil can effect the transfer. This efficiency reaches a maximum for any given pressure exerted upon the surface of the soil when increases in the amount of energy transferred are offset by proportional increases in the amount of energy lost by additional soil displacement and deformation. The maximum tractive efficiency attainable within a soil varies for different soil surface pressures. The maximum tractive efficiency of a soil attainable under given conditions of surface pressure is the ideal tractive efficiency of the soil for that pressure.*

Knowledge about the ideal tractive efficiency of soils is useful in evaluating the optimum performance of tractors and other soil engaging machines. Such knowledge is essential to the prediction of soil reactive thrust for tractive operations and to the prediction of forces involved in soil fracturing operations.

The overall tractive efficiency of a tractor operating upon the surface of a soil can be determined from the ratio of the output power of the tractor delivered at the drawbar to the input power delivered by the tractor to its driving members. The tractive efficiency thus attained is dictated largely by both the characteristics of the tractor and the characteristics of the soil [1,2]. If the tractor is operated upon a soil of different physical characteristics, a different overall tractive efficiency will be obtained. The change in tractive efficiency is due primarily to the change in soil characteristics. This concept implies that overall tractive efficiency must be due in part to the tractive efficiency of the tractor and in part to the tractive efficiency of the soil.

The tractive efficiency attributable to the soil may be defined as the ratio of the useful work accomplished by a tractor operating upon the soil to the sum of the work thus accomplished plus traction losses encountered within the soil. This relationship may be considered from the standpoint of an ideal tractor having no traction losses whatsoever operating upon a soil in which losses occur because of deformation and displacement of the soil. In this case

*) Published with the approval of the Director as Paper no. 1098, Journal Series, Nebraska Agricultural Experiment Station.

**) The Author is Professor of Agricultural Engineering at the University of Nebraska, a member of the Nebraska Board of Tractor Testing Engineers and a member of the American Society of Agricultural Engineers.

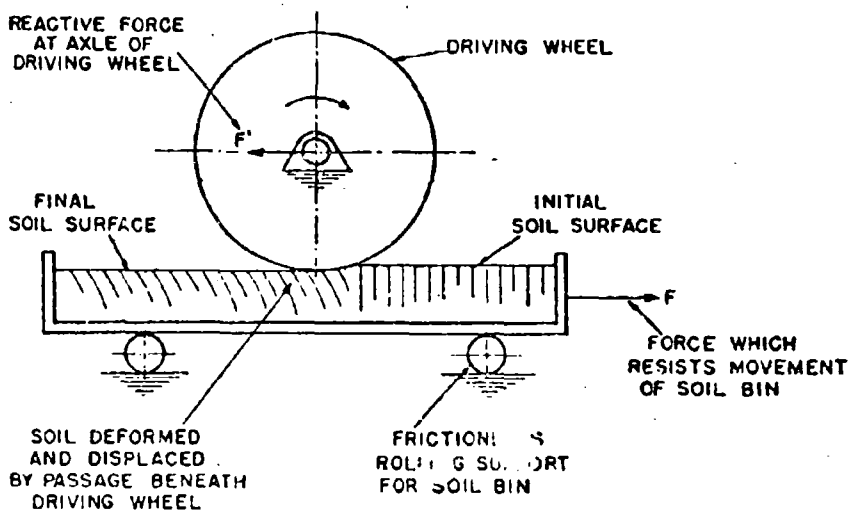


Fig. 1.

let the soil be contained within a trough or bin mounted so that it can move laterally under contact with a driving wheel of a stationary tractor[3]. Let the movement of the bin which results from rotation of the wheel be resisted by some means for absorbing the energy transmitted through the soil to the bin (fig. 1). Under these conditions the energy input to the soil is equal to the energy output from the soil plus the energy losses within the soil, and the efficieney of energy transmission through the soil can be stated algebraically as:

$$\text{Soil tractive efficiency} = \frac{\text{Energy output}}{\text{Energy output} + \text{Soil energy losses}}$$

If the soil bin is held stationary and translatory motion of the driving wheel permitted, the energy output is through the tractor frame to which the wheel is attached. In this case the energy transmitted to the soil is in turn delivered through the intermediary of the tractor to the tractor drawbar. The resultant tractive efficieney of the soil is again equal to the energy output divided by the energy output plus the energy losses within the soil. The energy output of the soil through the intermediary of the tractor is equal to the product of the drawbar pull of the tractor multiplied by the distance traveled by the tractor. Soil tractive efficieney may then be stated as follows:

$$\text{Soil tractive efficiency} = \frac{\text{drawbar pull of tractor}}{\text{pull} + \dfrac{\text{soil energy losses}}{\text{distance of tractor travel}}}$$

If the drawbar pull in the above equation is expressed in pounds per square inch of surface contact area, then the soil energy losses must be expressed in inch-pounds per square inch of surface contact area per inch of tractor travel. The energy losses within the soil are equal to the sum of the horizontal and vertical soil energy losses which result from the horizontal and vertical soil displacements.

Each soil has associated with it a maximum tractive efficiency attainable for each traction member supporting a given total weight per unit soil contact area. This maximum tractive efficiency of the soil is attained by the action of

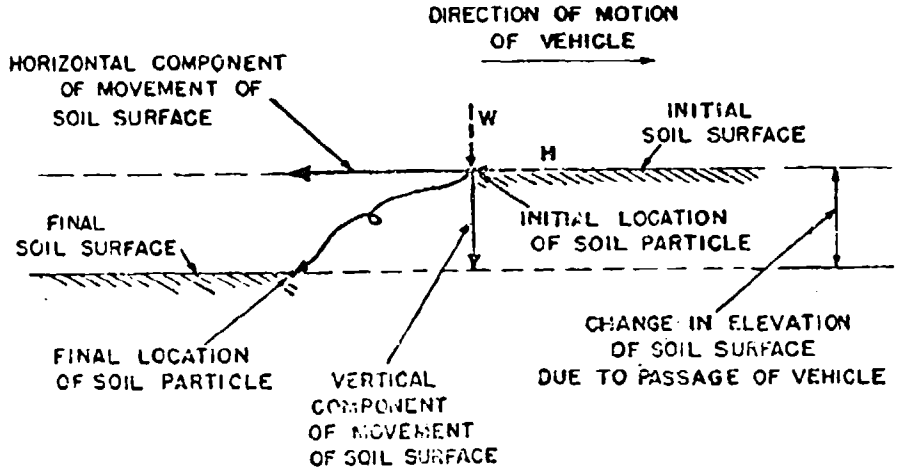


Fig. 2.

traction members which produce minimum disturbance of the soil necessary to the production of reactive soil thrust. Energy should not be wasted in unnecessary disturbance of the soil. The tractive efficiency thus achieved under the given surface pressure conditions is the ideal tractive efficiency of the soil for these conditions.

Determination of the ideal tractive efficiency of a soil may be made by an analysis of the displacement of the soil surface when subjected to the action of appropriate horizontal and vertical forces exerted upon the surface of the soil by an ideal tractor having no traction losses. The movement of a particle of soil at the surface may be resolved into horizontal and vertical components of movement (fig. 2). The horizontal component of soil movement determines the magnitude of horizontal thrust [1]. The horizontal thrust is equal to the horizontal shearing strength of the soil and may be determined by means of a suitable soil shear testing apparatus. A testing apparatus suitable for this determination should minimize the edge effects associated with the use of small plates on soil surfaces. The relationship between horizontal thrust and horizontal soil displacement varies for soils of different physical characteristics. The variation of soil thrust with changes of surface deformation for an average

agricultural soil [1] is shown as curve A in fig. 3. The area under curve A is representative of the energy expended upon the soil in displacing the surface horizontally. The relationship between total energy expended and horizontal displacement is shown as curve B in fig. 3.

The energy loss accompanying the horizontal movement of a soil surface is equal to the product of the average thrust and the horizontal displacement.

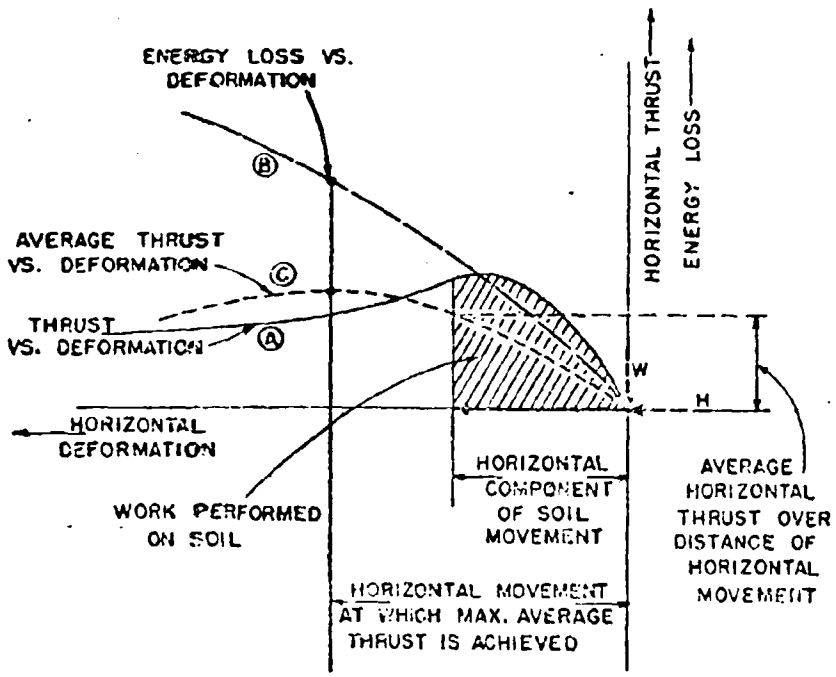


Fig. 3.

If the energy area under curve A is divided by the length of the area, the average thrust is determined. A plot of the average thrust needed to horizontally displace the soil surface is shown as curve C in fig. 3. This average thrust equals the total soil reaction which a traction member would encounter during displacement of the soil surface. The horizontal displacement of the soil surface at which maximum average thrust is achieved is indicated in fig. 3. The magnitude of the horizontal energy losses within the soil which accompany maximum thrust is also shown.

The soil displacement at the leading edge of the contact area of a traction member is equal to zero. If the displacement at the trailing edge is equal to x, the displacement at a point along the contact length of the traction member is a fraction of x. This fraction is equal to the ratio between the distance from the point x to the leading edge and the total contact length [1]. The soil reaction which a traction member encounters while moving over the surface of a soil

is dependent upon the average thrust reaction over the distance of total soil displacement and the area of soil contact. The energy expended upon the soil during this forward movement is equal to the product of the total average thrust and the distance of tractor movement. If the distance of soil movement is expressed in inches and the average thrust in pounds per square inch of soil contact area, energy expenditure is an inch-pounds per square inch. The unit of energy expenditure per inch of tractor movement is then inch-pounds per square inch per inch.

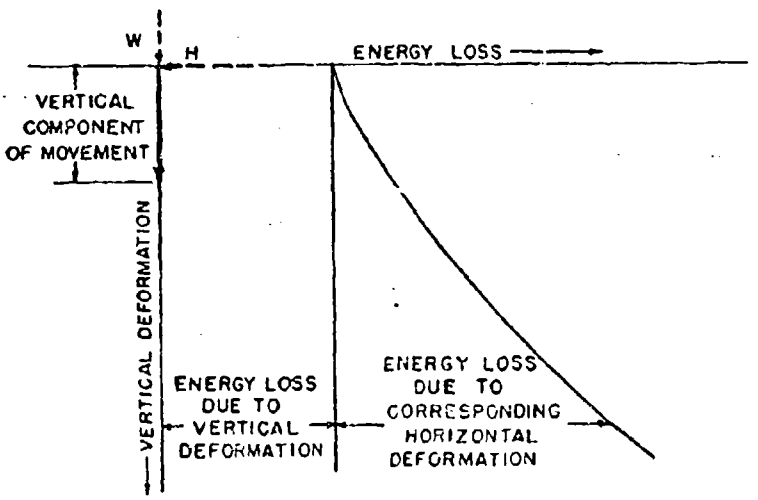


Fig. 4.

The vertical displacement which results from action of a vertical pressure upon a soil [6] together with the characteristics of the soil determines the vertical energy loss. If the pressure causing vertical displacement is p and the differential of vertical movement is dz, then the vertical energy loss is the integral of pdz. A soil of given physical characteristics will undergo a uniform displacement if acted upon by a uniform surface pressure. In the case illustrated in fig. 2-5, the vertical energy loss per unit area is a constant.

The total energy loss as shown in figure 4 is the sum of the vertical and horizontal energy losses. The vertical energy loss is a constant for a constant weight tractor. The horizontal energy loss is the same as that determined by curve B in figure 3.

In the total energy losses of figure 4 are plotted as abscissa and if the corresponding average thrusts depicted by curve C, figure 3 are plotted as ordinates, the corresponding tractive efficiencies may be determined as in figure 5. The maximum tractive efficiency for the given soil subjected to the given surface pressure may be found by determining the tangent to the curve of figure 5 which passes through the origin.

In this example it was assumed that the displacement of the soil surface was the result of action upon that surface by a tractor having no inherent traction losses. All losses encountered were soil losses. The maximum tractive efficiency indicated in figure 5 is the efficiency of the soil alone. This maximum efficiency is therefore the ideal tractive efficiency of the soil.

Studies were made of the performance of an agricultural crawler tractor operating in the adverse tractive conditions presented by the dry sands of

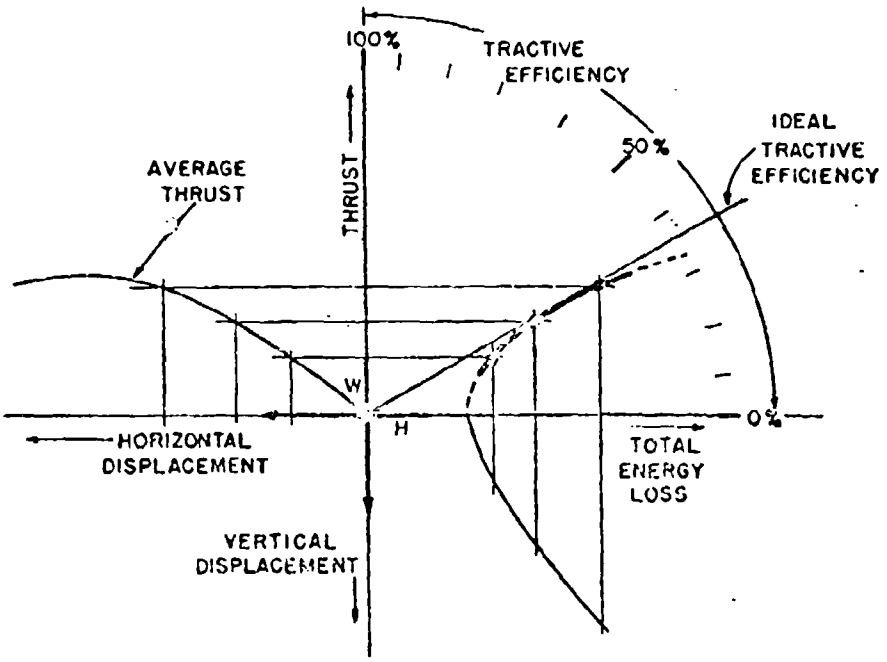


Fig. 5.

the Nebraska Sandhills area[3]. The soil was loose Valentine Fine Sand of 0.8 % moisture content. The horizontal thrust and vertical pressure responses of the soil to horizontal and vertical displacements were secured by means of soil shear and penetrometer tests. Analysis of the data indicate that the ideal tractive efficiency of the soil was 0.547 at a surface pressure corresponding to that presented by the tractor. The analysis of the data and computation of the ideal tractive efficiency of this dry sandy soil is given in the Appendix.

Individual soils have ideal tractive efficiencies associated with each unit pressure exerted upon the surface of the soil. Energy is expended in the establishment of reactive thrust within a soil. This energy is used to relocate masses of the soil relative to each other. Such relocation results in compaction of the soil, fracturing of the soil, or other changes in the relative positions of adjacent soil particles. The ideal tractive efficiency of soils is a measure of the ability of soils to provide reactive thrust with minimum energy absorption.

BIBLIOGRAPHY

1) Bekker M. G. Theory of land locomotion. The University of Michigan Press, Ann Arbor, Michigan, 1956.
2) Bekker M. G. Off-the-road locomotion. The University of Michigan Press, Ann Arbor, Michigan, 1960.
3) Greer Charles H. A laboratory study of some factors affecting the efficiency of tractor drive wheels (graduate thesis). Dept. of Agr. Engr., Univ. of Nebraska, May 1934.
4) Harrison W. L. et Al. A soil value system for land locomotion mechanics. Research report No. 5, Dec. 1958. Land Locomotion Research Branch, Research and Development Division, Ordnance Tank, Automotive Command, Dept. of the Army.
5) Berns David K. Effect of compaction and moisture content on the trafficability constants of Valentine Fine Sand and medium quartz sand (graduate thesis). Dept. of Agr. Engr., Univ. of Nebraska, June 1960.
6) Czako T. and Bekker M. G. Determination of vehicle sinkage parameters by means of rigid wheels (part 1). Report No. 33, May 1958. Land Locomotion Laboratory, Research Division, Ordnance Tank, Automotive Command, Dept. of the Army.
7) Nelson Leon F. The relationship of pull, slip and soil moisture content for a track type tractor operating in Valentine Fine Sand, unpublished report, Dept. of Agr. Engr., Univ. of Nebraska, Nov. 1959.

APPENDIX

The ideal tractive efficiency of a soil is determined by the force response and energy absorption of the soil during horizontal and vertical displacement. Computation of the ideal tractive efficiency of a loose dry sand follows:

The soil: USDA Soil Survey Classification: Valentine Fine Sand. Location: Loup County, Nebraska, Sec. 6, TWP 22 N, R 20 W. Soil Particles: irregular in shape, jagged edges, approx. 75 % of the particles fall into a size range between 0.1 and 0.3 mm.

Bouyoucos Hydrometer Test: 95.0 % sand; 1.4 % silt; 3.6 % clay.

Particle Density: 2.65 gram/cc.

Bulk Density: 1.43 gram/cc. uncompacted; 1.38 gram/cc. compacted.

Moisture Content: 0.8 % (dry basis).

Soil Test Equipment: Type: Bevameter, Instrument No. 3 (Loaned to the University of Nebraska by the Land Locomotion Research Branch, O.T.A.C. Detroit, Arsenal).

The Bevameter consists of two instruments used in evaluation of the soil:

1) A torsional shear displacement head measures the horizontal force necessary to shear the soil. The vertical pressure on the shear head may be varied. A recording mechanism plots a chart of shearing stress vs. horizontal deformation.

Calibrated Shearing Stress (plotted as the ordinate) 2.2518 PSI per inch of chart height for 7 inch O.D. shear head. Shearing area of 7 inch shear head, 14.726 sq. in.

Horizontal Deformation (plotted as the abscissa) 1.266 times displacement on chart = Deformation at shear head.

2) A penetrometer measures the sinkage of a flat plate with increases of surface pressure. Penetrometer plates of different sizes may be used. A recording mechanism plots a chart of vertical load vs. sinkage.

Calibrated Vertical Load (plotted as the ordinate) 59 lbs. per inch of chart height.

Vertical Deformation (plotted as abscissa) 1 inch of chart displacement = 1 inch of sinkage.

The Soil Characteristics: The physical soil characteristics as determined through the use of the Bevameter and expressed by the parameters of the Land Locomotion Soil Value System are:

From the shear head data:

$c = .06$;
$\Phi = 27°$;
K_1 = not determined;
$K_2 = \infty$;
d (opt) = .823 inches (at the soil surface).

From the penetrometer data:

$K_c = -9.6$ *);
$K_\phi = 14.9$;
$n = 0.88$.

The above values computed from data taken during controlled testing in the laboratory. Values indicated are an average of at least six determinations each.

The Test Tractor: International TD-6, 8450 lbs. total weight.

Tracks: number = 2; width = 18 inches each; contact length = 60 inches each; average ground pressure = 3.92 PSI; Max. pull, 3350 lbs. @ 3.82 % slip.

The Computation of the Ideal Tractive Efficiency. — ***The Horizontal Thrust and Energy Loss***: The maximum soil shearing stress per square inch of contact area is:

$S_{max} = c + p \tan \Phi$ where $c = .06$ PSI
$S_{max} = 2.06$ PSI $p = 3.92$ PSI
$\tan \Phi = \tan 27° = .51$

If successive areas of the curve:

$$\frac{S}{S_{max}} = \frac{e^{(-K_2 + \sqrt{K_2^2 - 1})\, K_1 d} - e^{(-K_2 - \sqrt{K_2^2 - 1})\, K_1 d}}{e^{(-K_2 + \sqrt{K_2^2 - 1})\, K_1 d_{max}} - e^{(-K_2 - \sqrt{K_2^2 - 1})\, K_1 d_{max}}}$$

are planimetered when

$S_{max} = 2.06$ PSI
$K_2 = \infty$
$d_{max} = .823$ inches
$d = .1\ d_{max}, .2\ d_{max}, 3.\ d_{max}$, etc.

the following values of average thrust will be found. The product of d and S_{av} is the horizontal energy loss.

*) A statistical analysis of the variance of K_c in loose sand tests indicated not only a lack of precision in the measurement of K_c but also that K_c has negligible effect on the sinkage properties of sand.

		d, inches	Sav. PSI	Horizontal energy loss inch lbs/in²/in
—		0.000	0.00	0.00
.1	d_{max}	0.082	0.24	0.02
.2	»	0.165	0.47	0.08
.3	»	0.247	0.77	0.19
.4	»	0.329	0.97	0.32
.5	»	0.412	1.17	0.48
.75	»	0.617	1.37	0.85
1.0	»	0.823	1.55	1.28
1.5	»	1.234	1.72	2.12
2.0	»	1.646	1.81	2.98
3.0	»	2.469	1.89	4.67
5.0	»	4.115	1.96	8.07
10.0	»	8.230	2.01	16.53
—		∞	2.06 (asymptote)	∞

The vertical energy loss:

$$Z = \left[\frac{p}{\frac{K_c}{b} + K}\right]^{\frac{1}{n}} = \left[\frac{3.92}{\frac{-9.6}{18} + 14.9}\right]^{-\frac{1}{.88}} = .23 \text{ inches sinkage.}$$

When Z = .23, the vertical energy loss $= \int_0^z pdz = .49$ inch lbs/in²/in.

The tractive efficiency:

$$\text{Tractive efficiency} = \frac{\text{thrust}}{\text{thrust} + \text{total energy loss per inch of travel}}$$

Thrust PSI	Total energy loss in lbs/in²/in	Tractive efficiency of the soil	
0.00	0.49	.000	Tractor does not slip.
0.24	0.51	.320	
0.47	0.57	.452	
0.77	0.68	.531	
0.97	0.81	.545	
1.17	0.97	.547	Ideal tractive efficiency. This occurs at a soil surface deformation of 0.41 inches.
1.37	1.34	.505	
1.55	1.77	.467	
1.72	2.61	.397	
1.81	3.47	.343	
1.89	5.16	.268	
1.96	8.56	.186	
2.01	17.02	.106	
2.06	∞	.000	Tractor slips 100 %.

The ideal tractive efficiency of Valentine Fine Sand of 0.8 % moisture content when subjected to a surface pressure of 3.92 PSI is 54.7 %.

N. 36

Soil trafficability classification scheme

Schema di classificazione del suolo in base alle possibilità di traffico su di esso

S. J. Knight *) - M. P. Meyer **)

ABSTRACT. — *A study was made of pertinent soil trafficability data collected during the wet season at more than 1360 sites located principally in humid-temperate regions of the United States. The soils were identified according to the Unifed Soil Classification System and U. S. Department of Agriculture textural classification system, topographic position, and two general levels of wetness. A scheme for classifying soils according to their trafficability was developed. The scheme lists the soil types in order of decreasing strength under each of four topography-general wetness level categories, and shows the probability of successful passage on each soil for vehicles with known soil strength requirements. This scheme permits the estimation of the probability of a successful operation under given soil type, topography, and gene.al wetness level conditions. Given the choice of several routes and vehicles, the determination can be made of the vehicles with the best chances of success over a given route or which route is best for given vehicles.*

Introduction. — Trafficability, the ability of a soil to permit the passage of a military vehicle, varies principally with soil type and moisture content. Moisture content is influenced by numerous environmental factors, the principal factor being weather, the vagaries of which are known to all. At first glance, the classification of soils according to their trafficability appears to be a very difficult task. However, the task is immediately halved if one recognizes that all soils are about equally trafficable when they are comparatively dry, and under dry conditions there is no real need to differentiate them from each other. Considering wet conditions, the task of classification would still be difficult were it not for the fact that naturally occurring soils attain high moisture contents early in the wet season (defined later in this paper) and maintain them with little deviation for several months of the year. Since one soil type will have distinctly better or poorer trafficability than another soil type under wet-season conditions, classification of soils from a trafficability standpoint becomes feasible.

This paper summarizes a study of pertinent trafficability data collected from soil during the wet season over a period of several years by personnel of the Army Mobility Research Center, U. S. Army Engineer Waterways

*) Engineer, Chief, Army Mobility Research Center, Soils Division, U.S. Army Engineer Waterways Experiment Station, Vicksburg, Miss.

**) Engineer, Trafficability Section, Army Mobility Research Center, Soils Division, U. S. Army Engineer Waterways Experiment Station, Vicksburg, Miss.

Experiment Station (WES), and their collaborators. Summary data are presented as a scheme for the classification of soils from a trafficability standpoint. A detailed report[1] on the data, their analysis, the soil trafficability classification scheme derived therefrom, and related studies will probably be published during late 1961.

Data were collected from a wide range of soil types at more than 1300 sites located principally in a humid-temperate climate in the United States. At each site, moisture content and density were determined, samples were obtained for mechanical analysis and determination of Atterberg limits, soil strength was measured in suitable trafficability units, and depth to water table, topographic position and other environmental features pertinent to soil trafficability were ascertained. Many of the sites were visited several times during the wet season.

A preliminary analysis of these data considered the effect on trafficability of soil type, parent material, topography, time since last rainfall, water-table level, grain-size distribution, plasticity, and vegetation. The present analysis is restricted to the most significant parameters, namely, soil type, topography, and a general wetness level based on time since last rainfall and the water-table level.

Each of the sites examined was therefore identified according to its soil type, topography, and general wetness level. Since many of the sites were visited several times during the wet season, it was feasible to identify the same site at the two general wetness levels to be described. Pertinent trafficability data from all sites in the same soil type-topography-general wetness level category were then subjected to determination of statistical means and ranges. A comparison of the statistical means and ranges of these data serves as a technique for comparing and rating the trafficability of soils during the wet season, i.e., a scheme for classifying soils from a trafficability standpoint.

Soil type. — The soils were subjected to standard laboratory tests for determination of grain sizes and Atterberg limits, and the results of these tests were used to classify the soils according to two well-known systems, the Unified Soil Classification System (USCS)[2], developed by the U.S. Army Corps of Engineers and the U.S. Bureau of Reclamation, and the U.S. Department of Agriculture (USDA) textural classification system. The scheme for classifying the trafficability of soil is therefore available in both USCS and USDA terms. In the interest of brevity, this paper is restricted to USCS terms of reference.

Topography. — A study of the data revealed the feasibility of classifying the topography of a site into one of two classes, called simply low topography and high topography. Low-topography sites were those at comparatively low elevation with respect to surrounding terrain, and high-topography sites were those at comparatively high elevation. Absolute elevations had no significance in identifying the topography class. The sites identified as low-topography sites were usually poorly drained. Sites known to have water tables occurring within 4 ft of the surface at some time during the year were automatically classified as low-topography sites; sites known to be always free of water

tables within 4 ft of the surface were automatically classified as high-topography. These sites were usually medium-well to well drained.

Fig. 1 is a graphic representation of the two topography classes considered in this study.

General wetness levels. — Two general levels of wetness, termed « wet-season condition » and « high-moisture condition », were employed in the analysis. Wet-season condition is the average moisture condition, i.e., the average of the varying moisture content, of the soil in the wet season. The wet season,

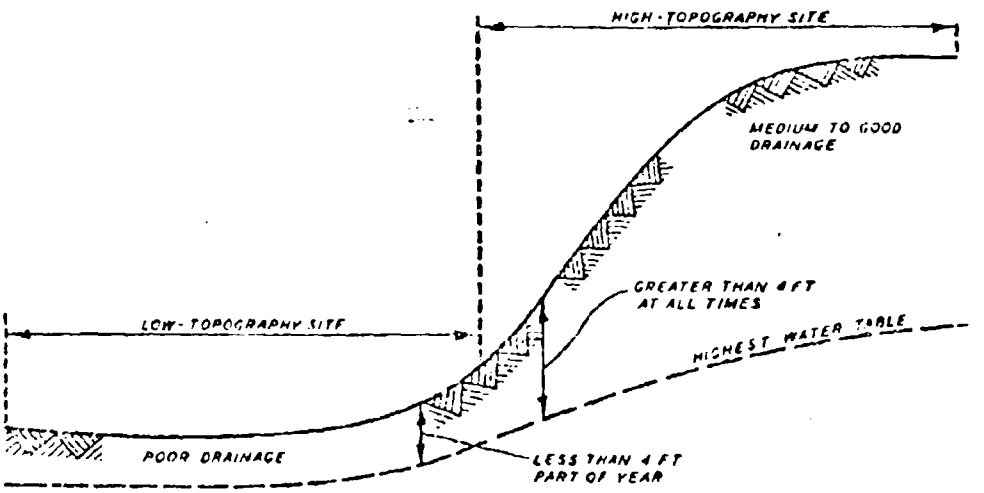


Fig. 1. — Topography classes.

defined as the period of the year of generally high soil moisture, is one of generally high precipitation and low evapotranspiration, and it occurs in the winter and early spring months in humid-temperate regions of the United States. The second moisture reference, high-moisture condition, refers to the highest moisture content that may occur, i.e., during rains or immediately after rains. Fig. 2 graphically illustrates the variation in moisture content during the dry and wet seasons for a low-topography site. The two general wetness levels employed in this analysis are shown in the wet season. A high-moisture condition also can occur during or following heavy rains in the dry season, but this condition usually occurs infrequently and does not last long. High-topography sites exposed to the same weather conditions would reveal a more-or-less parallel moisture trace, but lower in values of moisture content.

Absolute moisture content values under high-moisture condition for low-topography soils range up to 6 % higher than values under wet-season condition, depending on soil type. The corresponding difference in terms of rating cone index, a measure of soil strength discussed later in this paper, is about 69 units.

Topography-general wetness level categories. — For purposes of the classification scheme, the topography and general wetness level references were combined into four categories as follows:

a) low topography, high-moisture condition;
b) low topography, wet-season condition;
c) high topography, high-moisture condition;
d) high topography, wet-season condition.

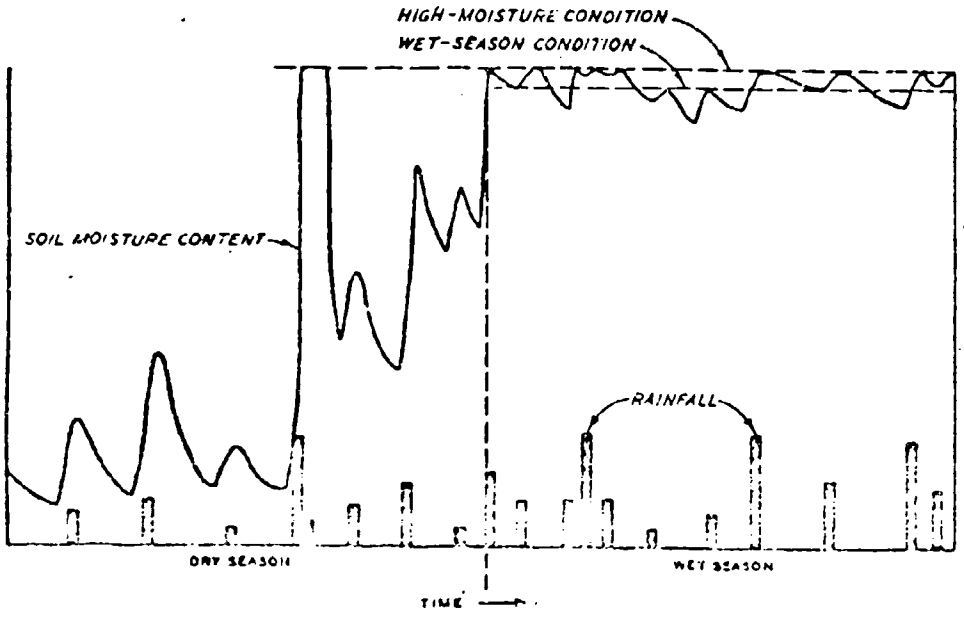


Fig. 2. — General wetness levels for a low-topography site.

Because of the requirements for brevity, this paper discusses the classification scheme for only one category-low topography, wet-season condition.

Soil strength and vehicle cone index terms. — The classification scheme is essentially a listing of soils in order of decreasing strength. Strength is measured in terms of an index, termed rating cone index, which is a physical evaluation of the bearing and traction capacity of a remolded soil, i.e., the trafficability of a soil. The rating cone index is obtained by multiplying a cone index by a remolding index. The cone index is a measure of the initial strength of a soil (before remolding) obtained by means of a cone penetrometer. This instrument is composed of a 5/8-in.-diameter, 3-ft-long staff with a 1/2-sq-in., 30-degree circular cone on one end and a proving ring, dial, and handle on the other end. The force necessary to push the cone slowly through the soil is registered on a dial that ranges from 0 to 300. The measured value is the cone index. The remolding index obtained by special test equipment is

a measure of the proportion of original strength that the soil will retain under traffic. If the cone index of a soil is 100 and the remolding index is 0.60, the rating cone index will be 60. The rating cone index is particularly significant in that it can be compared to a vehicle index, termed vehicle cone index, to determine whether a vehicle can or cannot traverse the soil. If the vehicle cone index is less than the rating cone index, the are may be considered as passable, and 50 vehicles of this type can pass in careful straight-line traffic or one vehicle can execute severe maneuvers without becoming immobilized. If the vehicle cone index is higher than the rating cone index, the area is considered impassable for the vehicle. For example, a rating cone index of 60 would represent a passable situation for vehicles with indexes of 55 and an impassable situation for vehicles with indexes of 65.

Correlations between vehicle performance and soil strength are most consistent when the strength in the critical soil layer is considered. For most U. S. Army vehicles this layer lies between 6 and 12 in. below the surface. The classification scheme is therefore in terms of data from this layer.

A complete description of instruments and techniques employed in measuring the trafficability of soils may be found in the paper « Measurement and Estimation of the Trafficability of Fine-Grained-Soils »[4].

Cumulative frequency of rating cone index. — If a given soil type under a given topography-general wetness level condition always had the same strength, a simple classification scheme in which the rating cone index of that soil was compared with the vehicle cone index could be developed to show whether a vehicle could or could not « go ». However, the rating cone index of a given soil varies widely under a given set of general topography-moisture conditions. Therefore, the range of rating cone indexes that can occur must be considered. This was done by drawing a cumulative frequency graph and using it for estimating probabilities of occurrence of rating cone index values greater than a given value and, thus, probabilities of « go » for vehicles with a known vehicle cone index.

Fig. 3 shows the cumulative frequency (in per cent) of decreasing rating cone index for a USCS ML (silt) under low-topography, wet-season condition. ML soils for 104 sites were used in the analysis. Fifty per cent of the sites had rating cone indexes greater than 77; this means that vehicles with a vehicle con index of 77 would be able to « go » 50 % of the time. Seventy-five per cent of the soils had rating cone indexes greater than 47; thus vehicles with indexes of 47 would have a 75 % probability of « go ». Ninety per cent of the soils had rating cone indexes greater than 32; thus vehicles with a vehicle cone index of 32 would have a 90 % probability of « go ». If probability of « go » is substituted for cumulative frequency in per cent and vehicle cone index is substituted for rating cone index, a probability of « go » can be read from the graph for any vehicle cone index. This graph, as previously mentioned, is for an ML soil under the low-topography, wet-season condition. Similar graphs have been developed from the data for other soil types and within each type for other topography-wetness level conditions. The graph for high-

topography, wet-season condition shows a higher range of strength and thus parallels and lies to the right of the graph in fig. 3. The graph for low-topography, high-moisture condition shows a lower range of strength and thus parallels and lies to the left of the graph for the low-topography, wet-season condition in fig. 3.

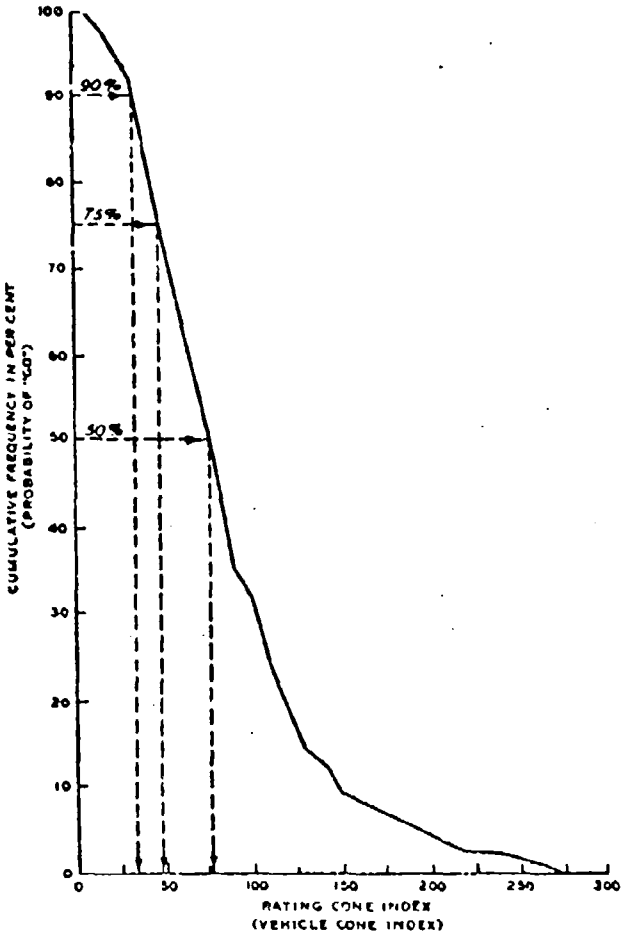


Fig. 3. -- Cumulative frequency of rating cone index for a USCS ML soil under low-topography, wet-season condition.

Soil trafficability classification scheme. — The product of the foregoing analysis, the soil classification scheme itself, is illustrated in fig. 4. The illustration includes only the more important USCS soil types and applies only to one of the four topography-wetness level categories, i.e., the low-topography, wet-season condition. (The complete scheme for USCS and USDA

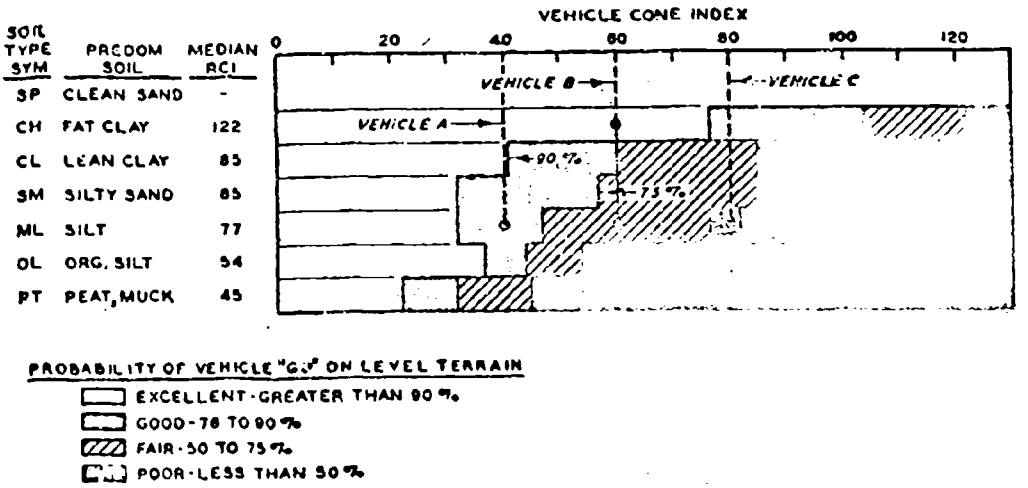


Fig. 4. — Soil trafficability classification in USCS terms for low-topography, wet-season condition.

soil types will be included in the WES technical memorandum previously mentioned [9]. The predominant soil corresponding to the USCS soil type is shown in the second column of fig. 4 and the soils are listed in the order of their decreasing median cone indexes. The median cone index is the value of the rating cone index at 50 % cumulative frequency and is represented in fig. 4 by the vehicle cone index value at 50 % probability of « go ». Studies have shown that the SP soils, the clean sands, are clearly the best soils from a trafficability standpoint. Unless complicated by slope or unusual conditions of high moisture, clean sands are trafficable to all tracked vehicles and wheeled vehicles with the proper tires and inflation pressures, regardless of the cone index of the sand. They therefore have been given a distinct place at the top of the list and have not been subjected to statistical analysis.

Probability of « go ». — Probability of « go » was arbitrarily classified into four ranges, and each range was provided with a descriptive term. Greater than 90 % probability of « go » was considered to be excellent; 75 to 90 %, good; 50 to 75 %, fair; and less than 50 %, poor. The information is presented in the scheme (fig. 4) by a series of bar graphs, one graph for each soil type. Data used in determining the divisions for each graph, i.e., the vehicle cone index corresponding to 50, 75, and 90 % probability of « go », were read from the cumulative frequency graph for the soil type. The vehicle cone indexes for the ML soil at 50, 75 and 90 % probability of « go », as previously mentioned, were 77, 47, and 32, respectively.

Application. — The classification scheme may be used in several different ways. As an example, assume three different vehicles — A, B, and C — are being considered for possible travel over a low-lying ML soil area during a

period several days after a rain in the wet season, i.e., under low-topography, wet-season condition. See fig. 4. Vehicle A with a vehicle cone index of 40 would have a good chance of success; vehicle B with an index of 60 would have a fair chance of success; and vehicle C with an index of 80 would have a poor chance of success. As another example, assume two different routes are being considered, one where the soil is ML and the other where the soils is CH. Vehicle B with an index of 60 would have an excellent chance of success on the CH soil and only a fair chance of success on the ML soil.

Limitations. — The soil classification scheme has certain limitations. It was based on information for soils in a temperate climate and therefore may not necessarily apply to soils in other climates. It is quite probable that tropical soils will require separate statistical analyses because ranges in pertinent trafficability parameters will be different for the same soil types. Limited information indicates the scheme will probably be adequate for subaretic and arctic soils, but this remains to be verified. The scheme appears limited in that it applies to level terrain, but this limitation can be resolved easily by incorporating a slope index which considers the detrimental effects of a specific slope on the vehicle probability of «go». (This has been done and will be included in the WES technical memorandum to be published [3]). The scheme obviously does not cover obstacles.

BIBLIOGRAPHY

1) U. S. Army Engineer Waterways Experiment Station Technical Memorandum No. 3-240. Trafficability of soils, 16th supplement; Soil classification. Vicksburg, Miss., 1961.
2) U. S. Army Engineer Waterways Experiment Station Technical Memorandum No. 3-357. The unified soil classification system. Vicksburg, Miss., March 1953.
3) Knight S. J. and Rula A. A. Measurement and estimation of the trafficability of fine-grained soils. Submitted to the First International Conference on the Mechanics of Soil-Vehicle Systems, Turin Institute of Technology, Turin, Italy, 1961.

N. 37

Influence of multiple compartment tires on off-the-road vehicle mobility

Influenza dei pneumatici a compartimenti multipli sulla mobilità fuori strada del veicolo

NORMAN W. Mc LEOD *)

ABSTRACT. — *The usual approach to tire design to obtain vehicle mobility over soft ground, has been the development of a large tire with very low inflation pressure. In effect, these tires are inflated large bags that are circular in cross-section. The very large size of these single compartment, low inflation pressure tires presents a number of disadvantages.*

Vehicles equipped with conventional high pressure tires become immobilized on natural ground (clay) after a rain, because of the deep ruts they form in the layer of very soft wet soil at the surface. By applying principles of soil mechanics to the vehicle mobility problem in this case, it is easily shown that this deep rutting (and vehicle immobility) occurs because the load on the tire exceeds the bearing capacity of the soft soil layer. On the basis of soil mechanics principles, it can also be demonstrated that when a tire rests on a layer of soft soil, the bearing capacity of the soil increases between the edge and the centre of the contact area of the tire on the soil. This observation points directly to a modification in tire design that would improve vehicle mobility over a layer of soft soil. Since the bearing capacity of the soil layer is lowest near the edge of the contact area under a tire, and is highest at the centre of the contact area, it is obvious that no advantage of this difference in bearing capacity can be taken when using a conventional single compartment tire that applies pressure more or less uniformly over the entire contact area. On the other hand, by going to a multiple compartment tire consisting of two or more annular compartments spaced within each other at different distances from the outer casing, and by inflating each compartment to a different pressure, the tire load that can be placed on a layer of soft soil without failing it, can be greatly increased without any increase in the overall dimensions of the tire. With this type of tire, each compartment will subject a concentric annular portion of the contact area between the tire and soil to a different unit pressure. For example, the centre compartment of the tire would be inflated to the highest pressure because the bearing capacity of a soft soil layer is highest at the centre of the contact area. The outer compartment of the tire would be inflated to the lowest pressure because the bearing capacity of a soft soil layer is least at the edges of the area loaded by a tire. By adjusting the inflation pressures of the different compartments, the bearing capacity of the soil would not be exceeded at any point under the tire.

Calculations based on soil mechanics indicate that depending on the nature of the soft soil, and upon the relative size of the tire and depth of the soft soil layer, the load that can be applied by a multiple compartment tire can be more than one hundred per cent greater than the maximum load that could be applied by a conventional single compartment tire of the same overall dimensions, without causing failure (deep rutting) of the soft soil layer.

The ability of a multiple compartment tire to apply much greater load to a layer of soft soil without failure, than a single compartment tire of the same size, can be easily demonstrated by simple working models.

---

*) Asphalt Consultant, Imperial Oil Limited, Toronto (Ontario, Canada).

Synopsis

This paper indicates that on the basis of well known principles of soil mechanics, a layer of soft soil can support a greater load applied by a multiple compartment tire than by a conventional single compartment tire of the same overall dimensions. Under conditions where space for tires is limited, this greater load carrying capacity of multiple compartment tires could be utilized advantageously for off-the-road mobility over a layer of soft soil.

Introduction

Vehicles equipped with conventional high pressure tires become immobilized on a layer of soft soil. The soft soil may consist of loose sand, or a layer of soft clay soil that forms after a rain. Immobility results when the load on a conventional tire exceeds the bearing capacity of the soft soil layer. Deep ruts develop because the overloaded soft soil is squeezed out laterally from under the tire.

One method for providing vehicle mobility over soft soil employs large tires of such low inflation pressure that the bearing capacity of the soil is not exceeded. These large low pressure tires tend to float the load over even very soft soil.

It is the purpose of this paper to describe another possible method for achieving vehicle mobility over a layer of soft soil. This method, which involves a tire constructed with multiple more or less concentric annular compartments, results from the application of well known principles of soil mechanics.

Conventional single compartment tires

1) High pressure tires. — In figure 1, the variation in pressure on the transverse axis of the contact area formed by a loaded conventional tire resting on a flat surface is indicated by the curve labelled « tire pressure distribution curve ». The pressure rises quickly from zero at the edge of the contact area to a peak pressure due to tire wall stiffness, falls off slightly at the centre of the contact area, rises to a second peak, and again falls off rapidly to zero as the other edge of the contact area is approached [1].

The differences in load carrying capacity of a layer of soft soil at points along the transverse axis of the contact area under a loaded conventional tire is shown in figure 1 by the curve labelled « soil strength curve ». The gradual increase in strength of the layer of soft soil between the edge and the centre of the contact area is due to the frictional resistances between the soft soil layer and the tire, and between the soft soil layer and the firmer soil on which it rests. Jurgenson [2] made use of these two frictional resistances in his squeeze test for measuring the shearing strength of clay. Incidentally,

Jurgenson's squeeze test shows that the load carrying capacity of a layer of soft soil increases between the edge and the centre of the loaded area, and provides verification for the general slope of the « soil strength curve » of figure 1.

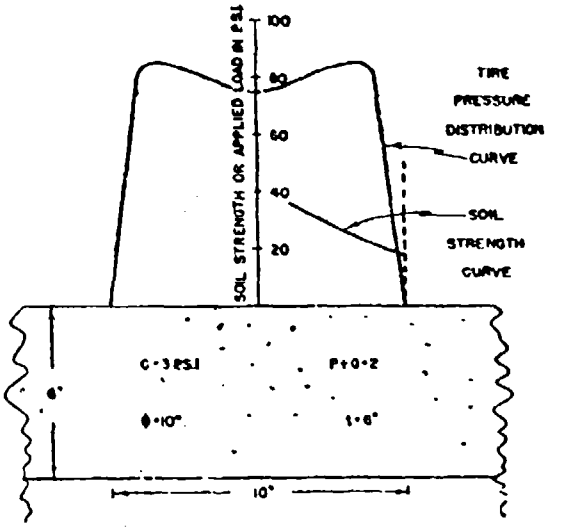


Fig. 1. — Illustrating overloading of a layer of soft soil by a conventional high pressure truck tire.

The general equation employed for calculating points on the « soil strength curve » of figure 1 is:

$$V = 2c\sqrt{\frac{1+\sin\Phi}{1-\sin\Phi}} + 2cK\sqrt{\frac{1+\sin\Phi}{1-\sin\Phi}}\left(\frac{1+\sin\Phi}{1-\sin\Phi}\right) + \frac{d}{t}(P+Q)(c+V'\tan\Phi)\left(\frac{1+\sin\Phi}{1-\sin\Phi}\right) \quad (1)$$

where

V = strength in p.s.i. developed by the soft soil layer at any point on the contact area;
c = unit cohesion in p.s.i. obtained from the Mohr diagram for the soft soil;
Φ = angle of internal friction obtained from the Mohr diagram for the soft soil;
K = a constant which may be taken equal to unity for conservative design;
P = ratio of frictional resistance fV' between the soft soil and the tire to the shearing resistance of the soft soil represented by the Coulomb equation $s = c + V' \tan \Phi$, and therefore has a maximum value of unity;
Q = ratio of frictional resistance gV' between the soft soil layer and the firmer soil below to the shearing resistance of the soft soil $s = c + V' \tan \Phi$, and has a maximum value of unity;
f = coefficient of friction between soft soil layer and tire;

g = coefficient of friction between soft soil layer and the firmer soil below;

d = distance in inches from the edge of the contact area to any point on the contact area where the value of the strength V of the soft soil layer is required;

t = thickness of the soft soil layer in inches;

V′ = the average vertical pressure exerted by the tire between the edge of the contact area and any point on the contact area where the strength V of the soft soil layer is required.

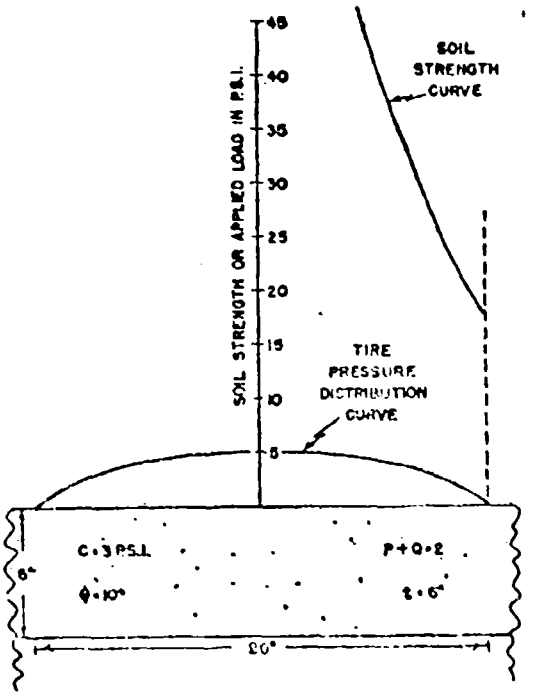


Fig. 2. — Illustrating inability of a low pressure conventional tire to utilize the potential load carrying capacity of a layer of soft soil.

The derivation of equation (1) has been given elsewhere [3-4].

For the layer of soft soil, c = 3 p.s.i., Φ = 10°, and 6 inches thick shown in figure 1, the strength curve for the layer of soft soil lies well below the curve representing the tire pressure distribution across the contact area. Figure 1 demonstrates very clearly that a loaded conventional high pressure truck tire will exceed the strength of this soft clay layer by a very wide margin. The soft soil layer will fail by being squeezed out from under the tire and a deep rut will form. It is for this reason that trucks and all other vehicles equipped with tires inflated to high or even to moderate pressures lose off-the-road mobility when they encounter a layer of soft soil.

2) **Low pressure tires.** — Figure 2 illustrates the case where vehicle mobility over a layer of soft soil is achieved by using a large tire with a

very low inflation pressure. In effect, some of these tires are basically inflated bags of circular cross-section.

As demonstrated by figure 2, the curve representing the distribution of tire pressure may lie well below the strength curve for the soft soil layer across all or most of the contact area.

Figures 1 and 2 make it clear that with conventional single compartment tires, only a portion of the potential load carrying capacity of a layer of soft soil can be utilized. A conventional single compartment tire applies pressure more or less uniformly to the contact area, whereas the strength of a soft soil layer increases from the edge to the centre of the contact area.

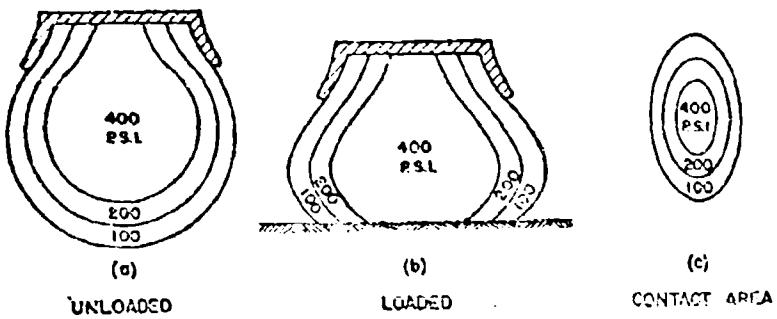


Fig. 3. — Diagram of multicompartment tire.

Multiple compartment tires

Figure 3 illustrates a multiple compartment tire. It consists of two or more annular compartments spaced at different distances from the outer casing. Each compartment can be inflated to a different pressure. Under an applied wheel load, the tire deflects or flattens and the contact area is subjected to different unit pressures as illustrated by figure 3 (c). These can be increased between the edge and the centre of the contact area as shown.

The ability of a layer of soft soil to support a greater load applied by a multiple compartment tire than by a single compartment tire of the same size, can be easily demonstrated by a simple experiment. Fill a shallow pan with relatively unstable sand. Place a regulation soccer football or basketball on the layer of sand and apply pressure. The sand is displaced under a moderately light load. Next insert a standard tennis ball into a toy balloon, and inflate the balloon to the size of the football or basketball. Place the inflated balloon containing the tennis ball on the layer of sand. The weight of a man can be exerted on the tennis ball without causing the layer of sand to displace.

Figure 4 illustrates the increase in total wheel load that could be applied to a layer of soft clay soil, 4 inches thick, for which $c = 3$ p.s.i. and $\Phi = 10°$, by means of a 2 compartment tire $36 \times 20 \times 16$ inches, as compared

with a single compartment tire of the same dimensions. The contact area is assumed to be square, and the spacing between the inner and outer compartments of the 2-compartment tire is 3 inches. The safe wheel load is 10,940 pounds for the 2-compartment tire versus 8,000 pounds for a conventional single compartment tire of the same size.

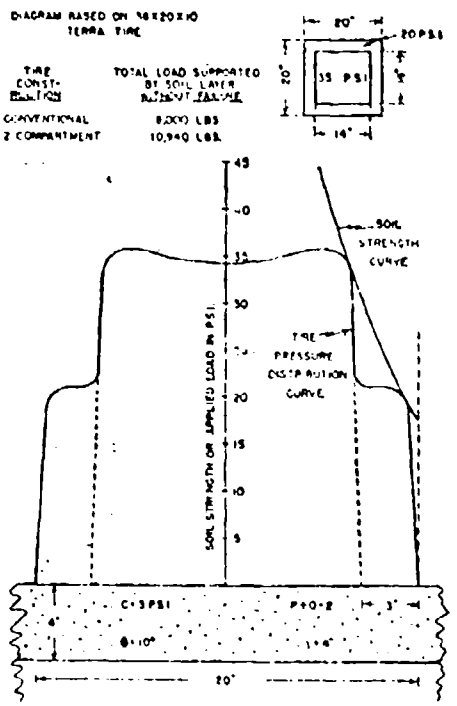


Fig. 4. — Illustrating increased load supporting capacity of 2 compartment versus conventional tire on 4 inches of soft clay.

The increase in wheel load on the 2-compartment tire is achieved by inflating the outer compartment to 20 p.s.i., and the inner compartment to 35 p.s.i. As illustrated by figure 4, these inflation pressures provide a tire pressure distribution curve that more nearly coincides with the strength curve of this particular soft soil layer. In general, the curve representing the tire pressure on the contact area lies below the soil strength curve, the two curves being tangent to each other at two points. Consequently, while the soft soil layer will be compressed somewhat under the 2-compartment tire loaded to 10,940 pounds, since the strength of this layer is not exceeded at any point on the contact area, there is no tendency for the layer of soft soil to be squeezed out from under the tire.

Figure 4 illustrates the two basic objectives of multiple compartment tires:

a) to more effectively utilize the potential strength of a soft soil layer, which increases from the edge to the centre of the contact area;

b) to float the loaded wheel over the soft soil layer without causing it to fail by lateral displacement.

Figure 5 provides a similar comparison between the two types of tire construction for a 6-inch layer of unstable sand for which c = 0 and Φ = 30°.

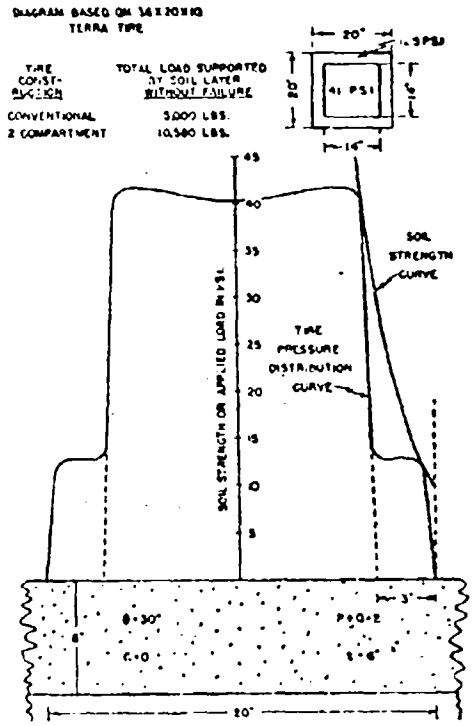


Fig. 5. — Illustrating increased load supporting capacity of 2 compartment versus conventional tire on 6 inches of weak sand.

In this case, the safe wheel load for a single compartment 36 × 20 × 10 inch tire is 5,000 pounds, but is 10,580 pounds for a 2-compartment tire of the same dimensions.

Table 1 lists comparative data calculated for a 2-compartment tire, 36 × 20 × 10 inches, versus a conventional single compartment tire of the same size. The data compare the safe maximum wheel loads that can be applied by the two types of tires to a 4-inch and to a 6-inch layer of soft clay soil for which c = 3 p.s.i. and Φ = 10°, and to a 4-inch and a 6-inch layer of unstable sand for which c = 0 and Φ = 30°. In all cases the spacing between the outer and inner compartments of the 2-compartment tire is 3 inches, and the contact areas of the tires on the soil are assumed to be square. The data

of Table 1 for the 4-inch soft clay layer, and for the 6-inch layer of unstable sand, are illustrated in figures 4 and 5, respectively.

The figures in the right hand column of Table 1 indicate the per cent increase in the safe wheel load that could be applied by employing the 2-compartment tire rather than a single compartment tire of the same size. The increase in wheel load ranges from 26 per cent for the 6-inch layer of soft clay soil, to 155 per cent for the 4-inch layer of unstable sand.

It is recognized that much remains to be learned about the reaction between a tire and the ground. However, unless certain assumptions are made, based upon principles of soil mechanics, and concerning the reaction between ground and tire, it is not possible to undertake the calculations required to guide even an initial testing program. Consequently, the calculated values listed in Table 1, and illustrated in figures 4 and 5, for loads and inflation pressures that may be applied by tires of different designs to a layer of soft soil without causing it to fail by lateral displacement, may not be quantitatively correct. Nevertheless, since all calculations were made on a similar basis, the comparisons shown between the maximum loads that can be applied by the single and 2-compartment tires should have some value as a qualitative guide, at least for the static condition.

Tests by the Defence Research Board of Canada

The Defence Research Board of Canada has published[5] the results of some large scale tests made with a 2-compartment $36 \times 20 \times 10$ inch tire, and with a single compartment tire of the same dimensions, similar to those for which the data of Table 1 were calculated.

Very briefly, their findings were:

1) On a rigid surface, the pressures exerted on the contact area by the 2-compartment tire corresponded very closely to those estimated from the different inflation pressures applied to the two compartments.

2) A controlled wheel load test over a layer of soft sand indicated no increase in load carrying capacity for the 2-compartment tire.

3) A large increase in drawbar pull was observed when the loaded 2-compartment tire was pulled over a layer of soft sand, as compared with the single compartment tire of the same dimensions.

4) Failure of the layer by lateral displacement, and slippage of the tire occurred, when the 2-compartment tire was pulled over a layer of quite unstable sand.

Discussion

It is useful to consider why the full scale trials by the Defence Research Board of Canada did not verify the better vehicle mobility over a layer of soft soil that might have been expected for the 2-compartment tire on the basis of principles of soil mechanics, and the calculated values listed in Table 1. It is believed that there are two quite simple explanations.

a) There was sufficient sinkage of the 2-compartment tire into the layer of unstable sand, that the outer casing was folded against the casing of the inner compartment. Consequently, the 2-compartment tire was acting in this case as though it consisted of only the inner compartment. This has been pointed out by White [5].

TABLE 1. — *Comparison of maximum loads supported by layers of soft soil when applied by 2-compartment and conventional single compartment tires of the same overall dimensions.*

Nature and thickness of soft soil layer	Maximum loads supported by soft soil layer					Increase in load supported by soil layer due to two-compartment tire
	Conventional 36 × 20 × 10 terra-tire		Two-compartment 36 × 20 × 10 terra-tire			
	Inflation (psi)	Load (lb)	Inflation O.C. [1] (psi)	Inflation I.C. [2] (psi)	Load (lb)	%
6 in. soft clay	19	7690	19	29	9560	26
4 in. soft clay	20	8080	20	35	10940	37
6 in. layer weak sand	12.5	5080	12.5	41	10580	112
4 in. layer weak sand	18	7280	18	75	18350	155

1) O.C. = outer compartment.
2) I.C. = inner compartment.

Assumptions on which data of table 1 are based:
1) Loaded radius: 15 inches.
2) Contact area: 20 inches square (load on tire divided by inflation pressure).
3) Spacing between boundaries of contact areas of inner and outer compartments of 2-compartment tire: 3 inches.

It is a major function of the outer compartment of a 2-compartment tire to place a maximum of restraint on the layer of soil without overloading it, thereby increasing its stability and enabling a higher pressure to be applied by the inner compartment. This higher unit pressure cannot be applied by the inner compartment when the outer compartment fails to function as intended. The data listed in Table 1 are based on the assumption that there is a spacing of 3 inches between the boundaries of the contact areas of the outer and inner compartments, that is, the inflation pressure of the outer compartment is intended to act as a restraint on the soil layer under the outer 3 inches of the contact area. Because of tire sinkage into the layer of sand, with resulting tendency for the casing of the outer compartment to fold against that of the inner compartment, the spacing between the boundaries of the contact areas of the outer and inner compartments seems to have largely disappeared in this case, and as reported by White [5], the 2-compartment tire acted as though it consisted of only the inner compartment.

In view of the tire sinkage, and the resulting curvature of the contact area, that is inevitable on soft soils even when no lateral displacement occurs, it should be emphasized that it is the spacing between the *horizontal projections*

of the boundaries of the contact areas of the outer and inner compartments that becomes important. For operation over a layer of soft soil, it is evident that the spacing between the casings of the outer and inner compartments of the experimental 2-compartment tire used in this ex ; was inadequate. To establish the optimum spacing between these casing would require further full scale tests.

b) The larger drawbar pull (3.28 times great for the layer of weaker sand) measured for the 2-compartment as compared with the conventional single compartment tire, can also be easily explained.

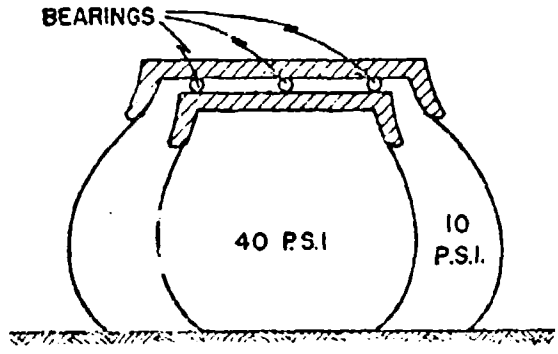


Fig. 6. — Diagram of a mechanical arrangement to enable both compartments of a 2-compartment tire to rotate independently of each other, thereby eliminating friction between outer and inner casings.

Both compartments of the experimental 2-compartment tire were mounted on the same rim, e.g. figure 3. Because of the spacing of about 3 inches between the casings of the outer and inner compartments, the circumference of the outer casing was about 9 inches or so longer than that of the inner casing. Consequently, as the wheel rotated when pulled over the layer of sand, it was necessary for the inner surface of the outer casing to slide over the outer surface of the inner casing. This had a similar overall effect to the application of a braking force to the wheel to which the 2-compartment tire was attached, and was chiefly responsible for the observed increase in drawbar pull. This braking force due to friction between the two casings where they came together over the contact area, was large enough during the trial over the weaker of the two sands tested, to cause the tire to partly skid as well as roll on the surface of the sand layer. As a result, progressively deeper rutting, and failure of the sand layer by lateral displacement, occurred as the 2-compartment tire was pulled over it. In this case, appreciable skidding or slippage of the tire on the surface of the sand would be expected as soon as the braking force on the wheel due to friction between the two casings, approached the frictional force provided by the coefficient of friction between the outer casing and the sand (shearing strength of the sand).

The failure of the sand by lateral displacement under the tire, that accompanied the slippage or skidding of the tire on the sand, provided deeper rutting that also contributed to greater drawbar pull for the 2-compartment tire.

The results of the tests made with this first full scale model of a 2-compartment tire as reported by White [5], make it apparent that the problems presented by the friction between the casings of the outer and inner compartments where they come together over the contact area, must be solved before the 2-compartment tire is able to function effectively. No anti-friction lubricant is likely to be sufficiently satisfactory. One method that might be employed for this purpose is illustrated in figure 6. It consists of mounting each casing for a 2-compartment tire on a separate rim, with one rim capable of free rotation on the other. This arrangement would eliminate the friction between the casings of the outer and inner compartments due to differences in their circumferential lengths.

Space limitations prevent any general discussion of other factors related to the use of multiple compartment tires. However, some of these have been referred to elsewhere [4].

Conclusions

1) Multiple compartment tires should be considered for improving off-the-road vehicle mobility under the following conditions:

a) When the soft soil exists as a surface layer. As shown by equation (1), the effectiveness of a multiple compartment tire depends upon the ratio of width of tire to depth of soft soil layer. Its effectiveness in terms of load supporting capacity, as compared with that of a conventional single compartment tire of the same size, is increased when this ratio is high.

b) When the space available for wheels and tires must be limited. This condition could exist when designing landing gear for aircraft intended to operate on natural ground. It could also be encountered in the design of land vehicles of various kinds such as trucks, construction equipment, agricultural machinery, etc., for operating off-the-road. Whenever the space available for wheels and tires on these vehicles is a critical factor, the greater load carrying capacity of the multiple compartment tire over a layer of soft soil, could provide an important advantage over conventional tires of the same size.

2) More full scale testing is required to establish optimum conditions for use of the multiple compartment tire, and to compare its effectiveness with that of alternative methods which might be employed to improve vehicle mobility over natural terrain.

ACKNOWLEDGMENTS. — Grateful acknowledgment is made to Mr. C. L. Perkins for his assistance with the calculations for the table and charts, and for his skilful drafting of the diagrams.

BIBLIOGRAPHY

1) Teller L. W. and Buchanan J. A. Determination of variation in unit pressure over the contact area of tires. Public Roads, vol. 18, No. 10, 1937.

2) Jurgenson Leo. The shearing resistance of soils. Contributions to Soil Mechanics 1925-1940, Boston Society of Civil Engineers, 1940.

3) McLeod Norman W. The design of bituminous mixtures with curved mohr envelopes. Proceedings of the Association of Asphalt Paving Technologists, vol. 22, 1953.

4) McLeod Norman W. Influence of tire design on pavement design and vehicle mobility. Proceedings, Highway Research Board, vol. 31, 1952.

5) White M. G. Multi-compartment aircraft tire-dynamic testing. Defence Research Board, Ottawa (Canada), February 1960.

N. 38

On the slip and the tractive effort

Sullo scorrimento e lo sforzo di trazione

A. D. Sela *)

ABSTRACT. — *The track or the wheel of a vehicle transfers to the soil horizontal forces in order to move the vehicle forward. The soil reaction to these forces induces shear stresses that are followed by shear displacement. There is a sound relation between these stresses and strain and it depends on the soil characteristic.*

The soil displacement along the contact of the track and the ground, and due to that the shear stresses, are to a great extent influenced by the track shape, dimensions and other characteristics.

The study of the interrelations of the track and its characteristics, the soil and its characteristics and other conditions that are developed in this track-soil system, enables arriving at a better vehicle design, with better traficability, and in this particular case, better traction, that will be specially fitted to any kind or to a particular soil.

The soil displacement along its contact with the track depends on the rate of slip and the distance from the first contact Point of the track and the ground.

$$d = i\,x \tag{1}$$

When:

i = Rate of slip %.
x = Distance from first contact (cm).
d = Soil shear displacement (cm).

The shear stress-displacement relation is given by Bekker's equation:

$$s = \frac{c + p \tan \Phi}{y_{max}} \left[e^{(-k_2 + \sqrt{k_2^2 - 1})\, k_1 d} - e^{(-k_2 - \sqrt{k_2^2 - 1})\, k_1 d} \right] \tag{2}$$

Where:

s = Shear stress (Kg/cm²).
c = Soil cohesion (Kg/cm²).
p = Mean ground pressure Kg/cm².
Φ = Internal friction angle.
$k_1\ k_2$ = Soil parameters.
y_{max} = The max. value of the expression in the brackets $[\ ] = y$.

In order to enable easier mathematical analysis of equation (2), it was altered as follows:

Assume:

$$-k_2 + \sqrt{k_2^2 - 1} = -a \tag{3}$$

But:

$$\left[-k_2 + \sqrt{k_2^2 - 1} \right] \left[-k_2 - \sqrt{k_2^2 - 1} \right] = 1$$

then:

$$-k_2 - \sqrt{k_2^2 - 1} = -\frac{1}{a} \tag{4}$$

*) Dipl. Eng. Bs. C. Ordnance Corps Israel Army - Israel.

By introducing the value of (3) and (4) to equation (2):

$$s = \frac{c + p \tan \varphi}{y_{max}} \left[e^{-a k_1 d} - e^{-\frac{k_1 d}{a}} \right]$$

A rather easy analysis of the equation may be performed and its characteristics may be investigated.

Thus it was enabled:

a) To prepare a nomogram in order to make an easy evaluation of soils parameters from experimental stress-strain curves.

b) Easy mathematical operations enabled obtaining the mean value of $y = e^{-a k_1 d} - e^{-\frac{k_1 d}{a}}$ *along any length d of displacement.*

c) A study of the equation of the means value of $y = \bar{y}$ *may be performed.*

Such a study as mentioned in para. c. above, shows that this mean value $\bar{y}$ *has a maximum, and this maximum is obtained when y and* $\bar{y}$ *curves intersect. From this it follows that* $\bar{y}$ *obtains its maximum value when a certain displacement which is typical to each soil, is obtained at the point of departure of the track from the ground. As the maximum value of* $\bar{y}$ ($\bar{y} = \bar{y}_{max}$) *yields the maximum tractive effort that may be obtained from a given track, then, this information assumes a great importance, since in order to obtain this value of displacement — (dc) — a certain slip should be performed according to eq. (1).*

$$dc = il \qquad (1)$$

where l equals the length of contact between ground and track, and thus any predetermined slip may be obtained by governing the length of ground contact.

The influence of ground pressure distribution along the ground contact on the tractive effort has been investigated too, and it is apparent that although cohesive soils are not effected by the pressure distribution, yet friction soils react in better traction when the ground pressure increases to the rear of ground contact area. This fact has a direct effect on load distribution when traction is mostly needed-namely when the vehicle is climbing, accelerated or performing a tough towing. Accordingly, the location of the vehicle center of gravity may be properly selected.

In closure, it may be said that this study enables a proper understanding of the inter-influence of the components of a vehicle-soil system with relation to the development of tractive-effort. It enables analysing qualitatively each of the factors, and permits quantitative computation when a new vehicle is designed or when estimating the performance of exist vehicles.

A track or a wheel of a vehicle transfers to the ground horizontal forces in order to move the vehicle forward. The soil reaction to these forces induces shear stresses that are followed by shear strain, or displacement, and there are direct relations between the soil strain and soil stress on one hand, and between the track slip and the tractive effort it develops on the other hand.

The subject of this paper is to study this relationship, and to see if and how the soil characteristics will influence the design of a vehicle tracks or wheels in order to obtain the maximum tractive effort that the soil may allow. It will also be possible, on the basis of this study, to make a fairly accurate estimate of the performance of an existing vehicle in this respect.

A) The slip of the track and the horizontal displacement of the soil. — When a vehicle is in motion, its tracks or wheels develop thrust in the soil, and in order to do so — a certain slippage is in existance between the ground and

the vehicle. This slip causes a horizontal displacement that varies along the contact surface of the track and the soil. It is of importance to know how this displacement varies in order to evaluate the stress function along the contact surface.

Because of this slip, the actual velocity (Va) of the vehicle will be lower than the theoretical (Vt).

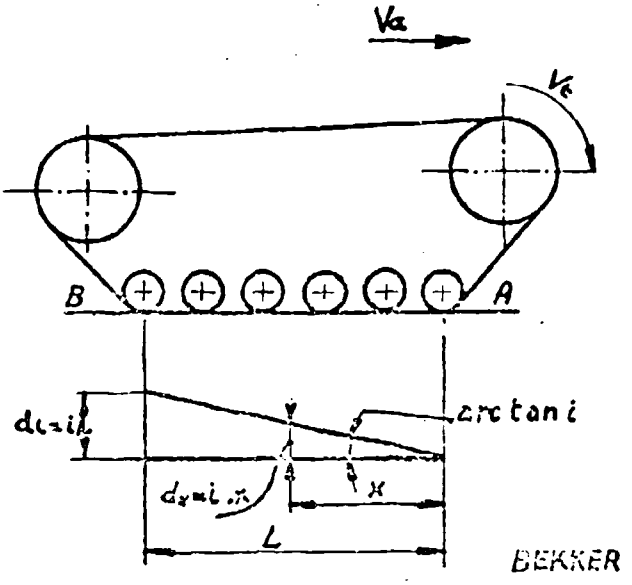


Fig. 1. — Shear strain, dx with respect to the slip-i.

Fig. 1 illustrates a track travelling on the ground with theoretical velocity (Vt) and actual velocity (Va). Any point of this track making its first contact with the ground (at point A, fig. 1) and after a certain time, t, this point will be at distance x from A. The value of x is given by the equation:

$$x = Vt \cdot t$$

At the same time the vehicle moved forward only a distance s, equal to:

$$s = Va \cdot t$$

The difference between x and s is the shear strain that occurred in the soil at any point, x cm. from A (fig. 1).
Thus:

$$d = x - s$$

or:

$$d = (Vt - Va)\,t = \left(1 - \frac{Va}{Vt}\right) Vt \cdot t$$

The expression $\left(1 - \frac{Va}{Vt}\right)$ is defined the rate of slip, and denoted « i ».

$$i = \left(1 - \frac{Va}{Vt}\right) \tag{1}$$

and $Vt \cdot t = x$, thus it follows that the soil shear strain at any point under the track at distance x from A (fig. 1) is directly proportional to the rate of slip i and to the distance x from A.

$$d_x = i\,x \tag{2}$$

And the displacement at the point of departure of the track from the ground equals to the rate of slip multiplied by the length of contact.

$$d_1 = i \cdot l$$

where l is the length of contact.

It is seen that the shear displacement varies along the contact of the soil and the track, being zero at the first point of contact A, and taking its maximum value at the point of departure « B » (fig. 1) and from here it follows that the shear stresses will also vary along the contact surface, and will depend on the displacement d, and on the nature of shear stress-strain relations of each particular soil.

B) **The shear-stress-strain relation in soils.** — Bekker investigated the shear stress-strain relation and found it to be expressed by equation (4):

$$s = (c + p \tan \Phi) - \frac{y}{y_{max}} \tag{4}$$

where:

s = Shear stress Kg/cm²
c = Soil cohesion Kg/cm²
p = Ground pressure Kg/cm²
Φ = Soil internal friction angle Deg.

y is a function that governs the form of the curve and is expressed by equation (5):

$$y = e^{(-k_1 + \sqrt{k_2^2 - 1})\,k_1 d} - e^{(-k_1 - \sqrt{k_2^2 - 1})\,k_1 d} \tag{5}$$

k_1 and k_2 being soil parameters and y_{max} is the maximum value of this expression. This expression is cumbersome for mathematical operations, and it will be altered, in order to facilitate its study, as follows:

It is obvious that:

$$\left[-k_2 + \sqrt{k_2^2 - 1}\right]\left[-k_2 - \sqrt{k_2^2 - 1}\right] = 1$$

then if:

$$-k_2 + \sqrt{k_2^2 - 1} = -n$$

it will be seen that:

$$-k_2 - \sqrt{k_2^2 - 1} = \frac{1}{n}$$

introducing these values to equation (5) will give:

$$y = e^{-n k_1 d} - e^{-\frac{k_1 d}{n}} \tag{6}$$

and thus the stress-strain relations may be expressed by equation (7):

$$s = (c + p \tan \Phi) \frac{e^{-n k_1 d} - e^{-\frac{k_1 d}{n}}}{e^{-n k_1 dopt} - e^{-\frac{k_1 dopt}{n}}} \tag{7}$$

where dopt is the value of strain that will give the maximum value of y, and

$$s_{max} = c + p \tan \Phi \tag{8}$$

and this is in agreement with Coulomb's equation. Fig. 2 describes the shear stress-strain relation of two different soils.

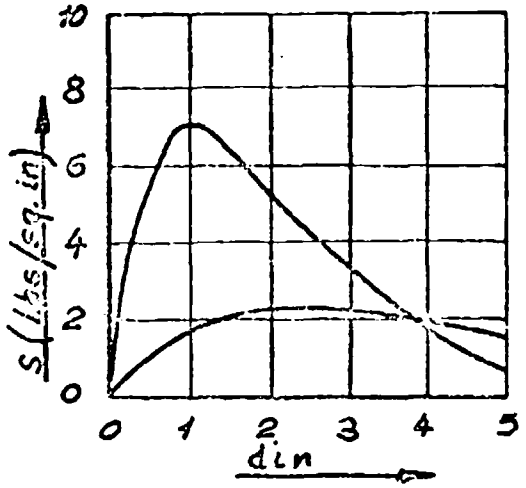


Fig. 2. — Shear stress with respect to shear strain. - A) Undisturbed silt; B) Undisturbed sandy Loam (Bekker).

The study of this curve may now be performed:

If:

$$-k_2 + \sqrt{k_2^2 - 1} = -n$$

then:

$$k_2 = \frac{1 - a^2}{2a}$$

and curve A in fig. 3 shows this relation for all values of a and k_2.

The maximum value of $y = y_{max}$ will be found by means of equating the first derivative of y to zero.

$$y = e^{-a k_1 d} - e^{-\frac{k_1 d}{a}} \tag{6}$$

$$\left(\frac{dy}{dd}\right)_{d = dopt} = -a k_1 e^{-a k_1 dopt} + \frac{k}{a} e^{-\frac{k_1 dopt}{a}} = 0$$

thus:

$$a^2 = e^{-\frac{k_1 dopt}{a}} (1 - a^2)$$

or:

$$k_1 dopt = \frac{2a \ln 1/a}{1 - a^2}$$

Curve b, fig. 3, shows the relation between k_1 dopt and a, for all value of a.

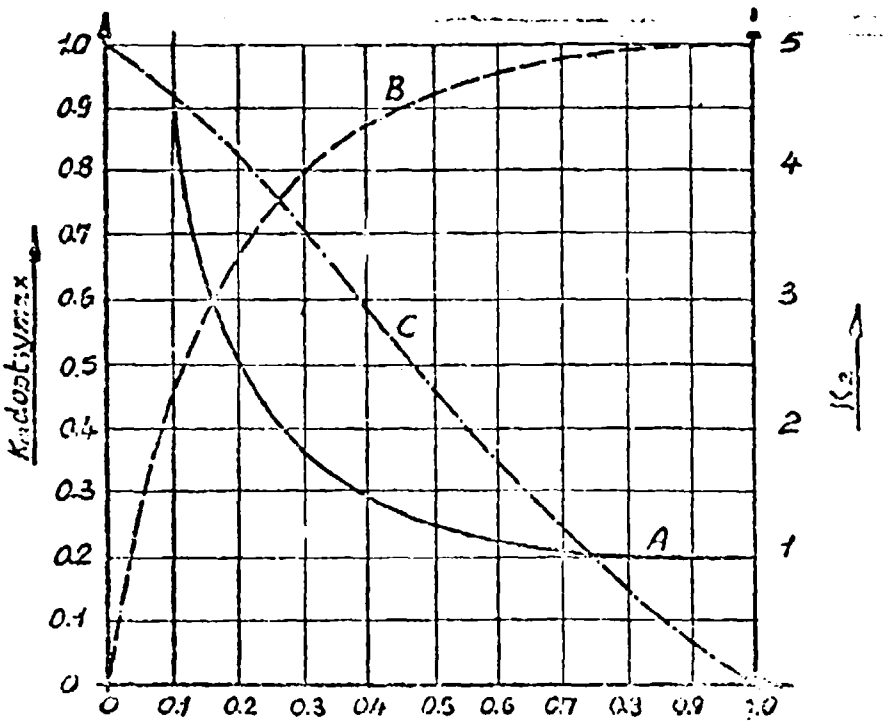


Fig. 3. — Values of k_1x dopt, y max, and k_2 with respect to a.
——— k_2; — — — k_1 dopt; — · — · — y max.

By introducing the values of k_1 dopt from equation (8) to equation (6), the value of y_{max} with respect to a may be obtained (equation 9):

$$y_{max} = e^{-\frac{2a^2 \ln 1/a}{1-a^2}} - e^{-\frac{2 \ln 1/a}{1-a^2}} \qquad (9)$$

Curve c, fig. 3, shows how y_{max} varies with respect to a for all values of a.

In the same way, by equating the second derivative to zero it may be found that the y curve achieves its point of infection where d assumes the value of 2 dopt:

$$k_1 \, d \, inf = 2 \, k_1 \, dopt = \frac{4a \ln 1/a}{1-a^2} \qquad (10)$$

C) **The soil parameters k_2 or a, and k_1 or k.** — It is explained by Bekker [1], that k_1 represents the soil compaction, its values go up with soil compaction and brittleness. Its dimension is l^{-1}. On the other hand, k_2 or a, are dimensionless.

This parameter governs the whole shape of the curve. The numerical value of a goes up with soil compactness and down for dry loose soils like sand.

Table 1 gives typical values of a and k_1 for three kinds of different soils.

TABLE 1. - *Values of soil parameters k_1, a.*

Soil	a	k_1 (1/cm.)
Silt, undisturbed	0.64	0.40
Sandy loam	0.27	0.12
Loose sand	0.14	0.68

In order to extract these soil parameters from experimental shear stress-strain curve, the procedure described hereon may be followed:

Fig. 4 contains 4 quarters, in quarter 1 the experimental curve should be drawn, with the relative stresses $\left(\frac{s}{s_{max}}\right)$, against soil displacement d.

Then, the ratios $\frac{d}{dopt}$ should be marked on the d axis for the values:

$$\frac{d}{dopt} = 0{,}25;\ 0{,}5;\ 0{,}75;\ 1.0;\ 1{,}5;\ 2{,}0;\ 3.0;\ 4.0,$$

and the respective points on the curve should be marked. (Points 1, 2, 3, 4, etc. marked on the curve in quarter 1).

Quarter 2 of fig. 4 contains a family of curves according to equation (12).

$$y_{max} = \frac{e^{-\frac{2a^2 \ln 1/a}{1-a^2} \cdot \frac{d}{dopt}} - e^{-\frac{2 \ln 1/a}{1-a^2} \cdot \frac{d}{dopt}}}{e^{-\frac{2a^2 \ln 1/a}{1-a^2}} - e^{-\frac{2 \ln 1/a}{1-a^2}}} \qquad (12)$$

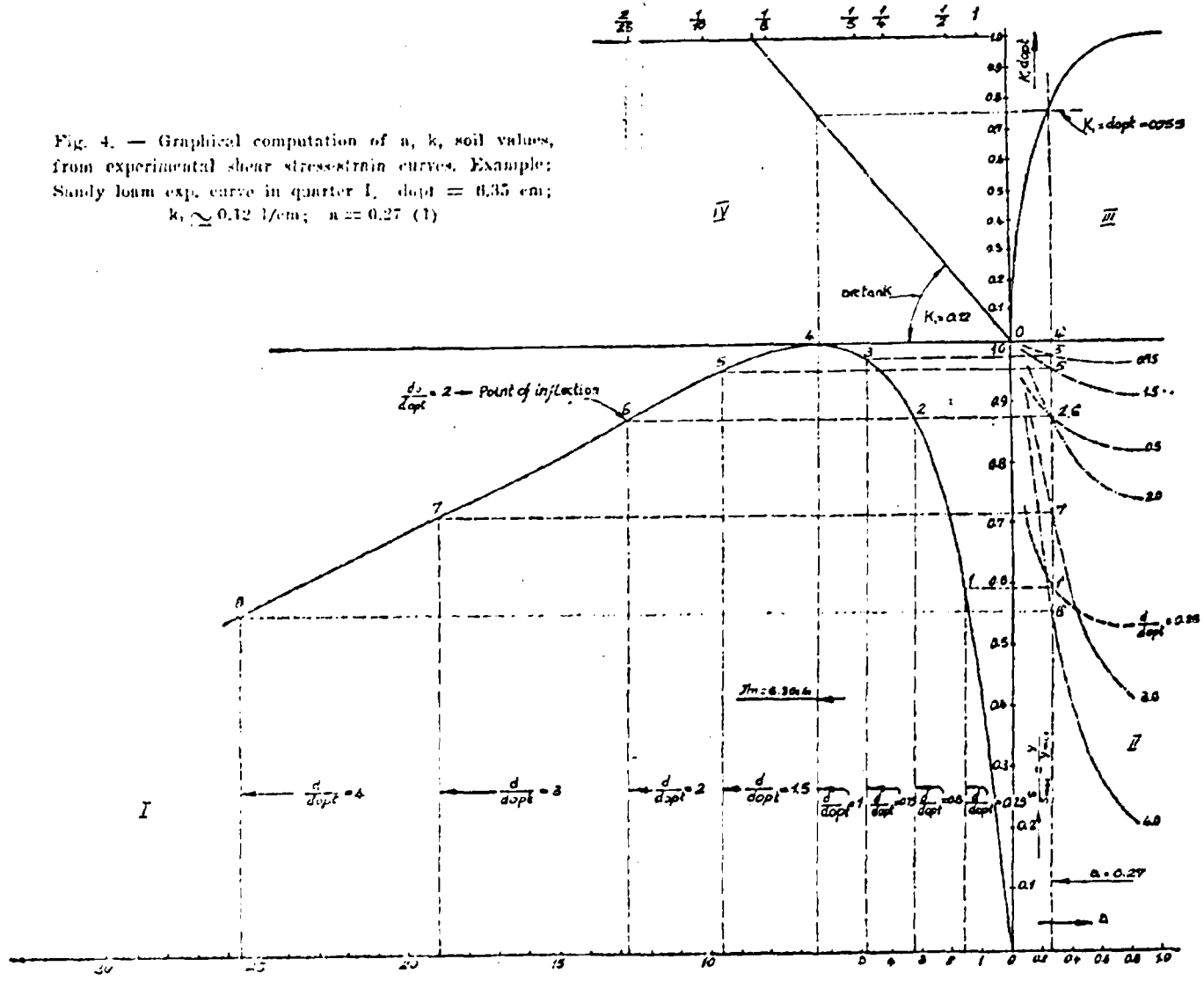


Fig. 4. — Graphical computation of a, k, soil values, from experimental shear stress-strain curves. Example: Sandy loam exp. curve in quarter I. dopt = 0.35 cm; $k_1 \simeq 0.12$ 1/cm; a = 0.27 (1)

The independent variable in this equation is a, and $\frac{d}{dopt}$ serves as a parameter. The horizontal axis of quarter 2 represents a, and the vertical axis represents $\frac{y}{y_{max}} = \frac{s}{s_{max}}$

here again the parameter $\frac{d}{dopt}$ takes the value = 0.25; 0.50; 0.75; 1.0; 1.5; 2; 3; and 4 thus a family of 8 curves is obtained. Each one curve of this family will have one common value with any experimental curve, drawn in quarter one, and these common values will be on a horizontal line, that is connecting the common point for the same $\frac{d}{dopt}$ values in the two quarters.

But as each $\frac{s}{s_{max}}$ curve has its one particular a value, it follows that the intersections of the horizontal lines with their respective curves in quarter 2 will occur on one vertical line which corresponds with the respective a value that belongs to the experimental curve.

Thus, after marking the points 1, 2, 3, ... 8, as described previously on the curve in quarter 1 — horizontal lines should be drawn from this point to the right, until these lines intersect their corresponding curves in quarter 2, and thus the value of parameter, a, will be obtained.

Quarter 3 describes the value of k_1 dopt related to a, (equation 8)

$$k_1 dopt = \frac{2a \ln 1/a}{1 - a^2} \qquad (8)$$

so if the previously described vertical line obtained in quarter 2 will be continued until it is intersecting the k_1 dopt curve in quarter 3, its value can be read on the corresponding point of the vertical axis of this quarter.

Quarter 4 serves to evaluate k_1 values. The values of dopt is known from the experimental curve, so if a vertical line were drawn through the point $\frac{s}{s_{max}} = 1$ (Point 4 on the expression curve) into quarter 4, until it is intersected by a horizontal line through the appropriate value of k_1 dopt obtained as described previously, then the tangent of the line that will be drawn from this point of intersection to the origin of quarter 4 will be equal to k_1.

Thus by the procedure described above one might easily be able to evaluate the values of a and k_1 soil parameters.

D) **The tractive effort.** — The previous chapters helped to understand and estimate the values of the displacement of the soil under the track and along the contact surface from one hand, and how the stress-strain curve will

behave on the other hand. Now, by tying them together it will be possible to compute the tractive effort that may be produced by the track.

If s is the minute shear stress under each point of the track, then:

$$dT = b \cdot s \cdot dl$$

where:

T = tractive effort, kg.
b = width of track, cm.
l = length of track, cm.

and the tractive effort (T)

$$T = b \int_0^l s \cdot dl \tag{13}$$

by introducing the value of $d = il$ to the stresses equation (7) and introducing equation (7) to equation (13) the total tractive effort may be computed.

$$T = b \int_0^l \frac{c + p \tan \Phi}{y_{max}} \cdot \left(e^{-akil} - e^{-\frac{kil}{a}} \right) dl$$

as $\frac{c + p \tan \Phi}{y_{max}}$ is constant, it may be placed to the left of the integral sign, and then the equation may be multiplied and divided by l:

$$T = \frac{b \cdot l \cdot (c + p \tan \Phi)}{y_{max}} \cdot \frac{\int_0^l \left(e^{-akil} - e^{-\frac{kil}{a}} \right) dl}{l} \tag{13 a}$$

In this equation, the integral divided by l, represents the average value of $-y$.

This average value of y will be denoted $\bar{y}$ and so the equation may be written thus:

$$T = b \cdot l \cdot (c + p \tan \Phi) \frac{\bar{y}}{y_{max}} \tag{14}$$

or

$$s = \frac{T}{bl} = (c + p \tan \Phi) \cdot \frac{\bar{y}}{y_{max}} \tag{14 a}$$

where s = the mean shear stress (kg./cm.²).

The study of this equation is very interesting:

bl is the magnitude of the contact surface between the soil and the track.

$(c + p \tan \Phi)$ is the maximum shear stress that any one point of the contact surface might produce, then the multiplication

$$bl \ (c + p \tan \Phi)$$

expresses the tractive effort that may be obtained if all the contact surface

will be under this value of shear stress ($c + p \tan \Phi$), but as this is not the case, it is obvious that:

$$\frac{y}{y_{max}} < 1$$

then, it follows that this theoretical thrust can never be obtained in practice, and it is also seen that if $\bar{y}$ will once obtain any maximum value, then, the practical thrust will become maximum.

Accordingly, the value of $\bar{y}$ will be now studied:

$$\bar{y} = \frac{1}{de} \int_0^{de} \left(e^{-ak_1 d} - e^{-\frac{k_1 d}{a}} \right) dd \qquad (15)$$

where de is the shear strain at the point of departure of the track from the ground.

By solving the integral within the limits $o \leq d \leq dl$ the value of $\bar{y}$ is obtained.

$$\bar{y} = \frac{1}{k_1 dr} \left[\frac{1}{a} \left(1 - e^{-ak_1 dr} \right) - a \left(1 - e^{-\frac{k_1 dr}{a}} \right) \right] \qquad (16)$$

and hence the thrust will be:

$$T = \frac{b\, e\, (c + p \tan \Phi)}{y_{max} \cdot k_1 dr} \left[\frac{1}{a} \left(1 - e^{-ak_1 dr} \right) - a \left(1 - e^{-\frac{k_1 dr}{a}} \right) \right] \qquad (17)$$

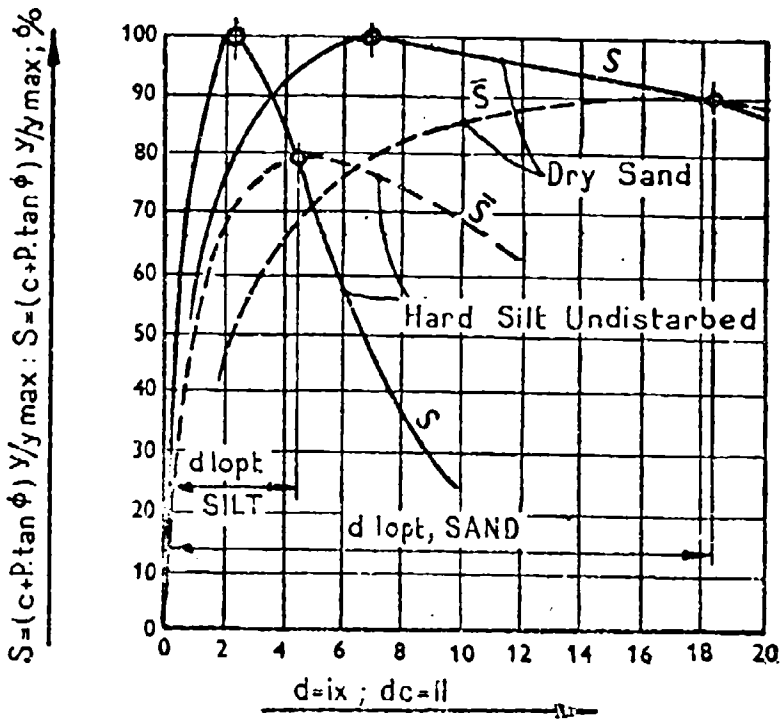
As it was said previously, the thrust will take its maximum value if $\bar{y}$ will take its maximum value. Again by deriving $\bar{y}$ with respect to de and equating to zero, it will be found if and when does $\bar{y}$ assumes its maximum value.

$$\frac{d\bar{y}}{dde} = \frac{k_1 dr}{k_1 dr^2} \left\{ \left(e^{-ak_1 dr} - e^{-\frac{k_1 dr}{a}} \right) - \frac{1}{k_1 dr} \right.$$

$$\left. \left[\frac{1}{a} \left(1 - e^{-ak_1 dr} \right) - a \left(1 - e^{-\frac{k_1 dr}{a}} \right) \right] \right\}$$

and by equating this derivative to zero:

$$e^{-ak_1 dr} - e^{-\frac{k_1 dr}{a}} = \frac{1}{k_1 dr} \left[\frac{1}{a} \left(1 - e^{-ak_1 dr} \right) - a \left(1 - e^{-\frac{k_1 dr}{a}} \right) \right] \qquad (18)$$



——— $\frac{s}{s_{max}}$ with respect to shear displacement d;

– – – $\frac{\bar{s}}{s_{max}}$ with respect to shear displacement at the point of departure-di.

Fig. 5.

The left hand side of equation (18) is the value of y (the value of y at the point of departure). The right hand side of equation (18) is the value of $\bar{y}_1$ (the average value of y along the contact surface).

From this it followed that if once the average value of y will take the minute value of y ($i \cdot e \cdot y_1 = \bar{y}$) at the point of departure of the track from the ground, then the point of departure of the track from the ground, then the thrust will be at its maximum. If the curves $y = f(d)$ and $\bar{y} = F(d_1)$ will be drawn in common coordinate system, they will intersect at a certain value of $d = d_1$, and at this point of intersection $\bar{y}$ will be at its maximum (see fig. 5).

It may also be seen that for each soil there is a certain typical value of dl that will valid this maximum value of $\bar{y}$ and hence, maximum value of thrust. This value of dl will be denoted d k, opt, and it will be understood, that as this shear displacement is achieved at the point of departure of the track from the ground then the maximum thrust has been obtained.

TABLE 2.

Soil	d opt cm.	dl opt cm.	$\frac{\bar{y}_{max}}{y_{max}}$
Silt, undisturbed	2.42	4.6	0.80
Sandy loam	6.35	13.2	0.85
Loose sand	7.02	18.5	0.9

It was shown in equation (14) or (17) that the value of the thrust will be:

$$T = b \cdot l \cdot (c + p \tan \Phi) \frac{\bar{y}}{y_{max}} \qquad (14)$$

hence

$$T_{max} = b \cdot l \cdot (c + p \tan \Phi) \frac{\bar{y}_{max}}{y_{max}}$$

Table 2 gives typical values for some typical soils of this ratio $(\frac{\bar{y}_{max}}{y_{max}})$, and it is seen that this ratio goes down to 0.8 or less in cohesive soils and comes up to about 0.9 in friction soils. However, its value is always lower than unity.

In order to achieve maximum thrust, it was explained that a certain shear displacement dlopt should be achieved.

It has also been shown that this displacement behaves according to equation (3), then:

$$dlopt = iopt \cdot l \qquad (3)$$

or:

$$iopt = \frac{dlopt}{c} \qquad (19)$$

and equation (19) shows that in order to achieve the maximum traction with a given track and a given soil, the slip should go up to a certain value. If the rate of slip i is too high, it follows by excessive wear and tear, of the tracks (or of the tyres), the power losses due to the slip are great, the actual velocity of the vehicle is reduced too much, and the soil is spoiled for the motion of following traffic.

For these reasons and others the rate of slip should be kept as low as possible, and once its magnitude has been decided upon, the length of contact may be computed.

$$l = \frac{dlopt}{iopt} \qquad (20)$$

An illustrative example will be given by the comparison of tracked vehicle with a length of contact with the ground (l) of 370 cm., to a wheeled vehicle that has a contact length of 18.5 cm., which are both travelling in dry loose sand.

The first one will develop its maximum thrust at 5 % slip, while the second one will do this at 100 % slip, or practically it will come to a standstill and dig itself in.

E) The effect of ground pressure distribution on the thrust. — Until now the ground pressure was assumed constant and equal to the mean ground pressure all over the contact surface. The effect of uneven pressure distribution will now be studied.

According to equation (4)

$$s = (c + p \tan \Phi) \frac{y}{y_{max}} \qquad (4)$$

Now, instead of p = constant, it will be introduced as a function of x or: p = p (x):

$$s = (c + p_x \tan \Phi) \frac{y}{y_{max}} \qquad (21)$$

from here it is seen that purely cohesive soil remains indifferent to the pressure distribution with respect to tractive effort. On the other hand, soil with friction will respond sensitively to such a variation. Hence the analysis will be done on a soil with friction only, and the equation will take the form:

$$s_f = p_x \tan \Phi \frac{y}{y_{max}} \qquad (22)$$

where

s_f = shear stress in friction soil.

For the sake of simplicity only two pressure distribution functions will be examined.

a) The pressure will be increased linearily from zero at the first point of contact to its maximum value at the point of departure.

b) The pressure will be decreased linearily from its maximum value at the first point of contact to zero at the point of departure.

Accordingly:

$$p_a = \frac{2 p x}{l} \qquad (23)$$

$$p_b = 2 p \frac{l - x}{l} \qquad (24)$$

Where p is the mean ground pressure Kg/cm².

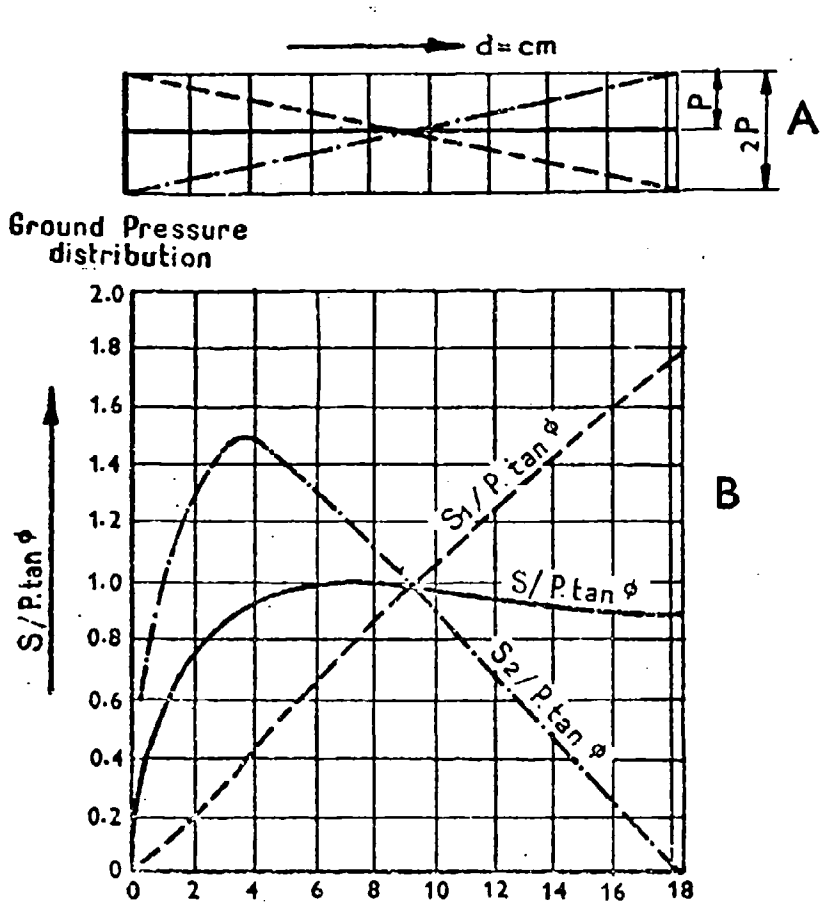


Fig. 6. — Shear stresses a long d with respect to various functions of the pressure distribution.

By introducing p_a from equation (23) to equation (22) it will be obtained:

$$s_{fa} = \frac{2\,p\,x}{y_{max}\,l} \cdot \tan\Phi \left(e^{-akix} - e^{-\frac{kix}{a}}\right) \qquad (25)$$

or:

$$s_{fa} = \frac{2\,p}{y_{max}} \cdot \frac{d}{d\,l} \cdot \tan\Phi \left(e^{-akid} - e^{-\frac{kid}{a}}\right) \qquad (26)$$

In the same way, by introducing the value of p_b to equation (22) the stress-strain equation will be:

$$s_{fb} = \frac{2\,p}{y_{max}} \frac{d\,l - d}{d\,l} \tan\Phi \left(e^{-akid} - e^{-\frac{kid}{a}}\right) \qquad (27)$$

It is interesting to note that the value of s_{fb} equals twice the value of s (even pressure distribution) minus s_{fa} [equation (26)].

$$s_{fb} = 2s - s_{fa} \tag{28}$$

Fig. 6 (A) describes three possibilities of pressure distribution:

$p = p_{mean}$; $p = p_a$; $p = p_b$.

Fig. 6 (B) describes the shear stress distribution for these three cases.

It must be noticed that the stress curves are prepared for the case where the rate of slip is such that $dl = il$ takes the value of dl_{opt}, namely the shear displacement at the point of departure of the track from the ground is of the value that will produce the maximum thrust, where the ground pressure is constant all over the contact surface.

The value of the mean shear stresses in each case will be computed by integrating the stresses in the limits $0 \leqslant d \leqslant dl$ and dividing by dl. Hence:

$$\frac{\bar{s}_{fa}}{p \tan \Phi} = \frac{}{y_{max}\, dl^2} \int_0^{dl} d \left(e^{-akd} - e^{-\frac{kd}{a}} \right) dd \tag{29}$$

The solution of this integral is

$$\frac{\bar{s}_{fa}}{p \tan \Phi} = \frac{2}{y_{max}} \left\{ \frac{1}{k^2 dl^2} \left[\frac{1}{a^2} \left(1 - e^{-akdl} \right) - a^2 \left(1 - e^{-\frac{kdl}{a}} \right) \right] \right.$$

$$\left. - \frac{1}{kdl} \left(\frac{e^{-akdl}}{-a} - a\, e^{-\frac{kdl}{a}} \right) \right\} \tag{30}$$

and if:

$$2 \left\{ \frac{1}{k^2 dl^2} \left[\frac{1}{a^2} \left(1 - e^{-akdl} \right) - a^2 \left(1 - e^{-\frac{kdl}{a}} \right) \right] \right.$$

$$\left. - \frac{1}{kdl} \left(\frac{e^{-akdl}}{a} - a\, e^{-\frac{kdl}{a}} \right) \right\} = \bar{y}_{fa}$$

then equation (30) will take the form:

$$\bar{s}_{fa} = p \tan \Phi \cdot \frac{\bar{y}_{fa}}{y_{max}} \tag{31}$$

And from here it also follows that:

$$\bar{s}_{fb} = p \tan \Phi \cdot \frac{2\bar{y} - \bar{y}_{fa}}{y_{max}} \tag{32}$$

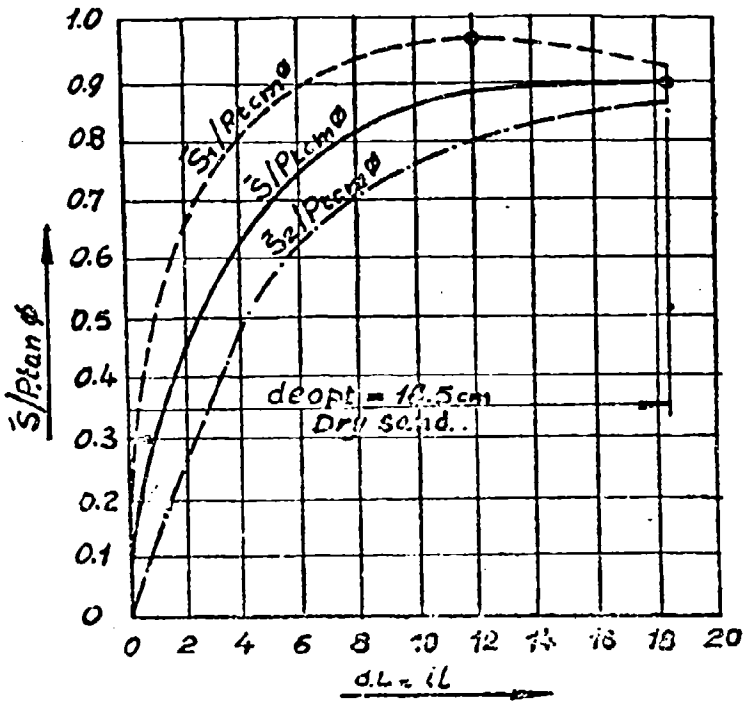


Fig. 7. — Mean shear stresses s, s_1, s_2 with respect to de = il.

Figure 7 shows three curves; the higher of the three shows $\frac{\bar{s}_{(a}}{p \tan \Phi}$ with respect to the displacement at the point of departure dl = il. The middle curve shows $\frac{\bar{s}}{p \tan \Phi}$ (even pressure distribution), and the lower curve is $\frac{\bar{s}_{(a}}{p \tan \Phi}$.

From the results of this study, it may be concluded that in such soil where the internal friction angle Φ is of appreciable value, the load distribution must be transferred to the rear when the thrust assumes its higher values. By that means, a higher maximum thrust will be achieved, and it will be achieved at lower slip rates.

The higher thrust values are mostly needed when the drawbar pull is high, when climbing hills and when accelerating the vehicle. Fortunately, in all these three cases there is weight transfer to the rear, and accordingly, if the center of gravity of the vehicle will be properly located, optimum values of thrust may be obtained when they will be most needed.

F) This paper deals solely in the study of tractive effort with relation to the rate of slip. The results of this study may be used either for design considerations of new vehicles or to estimate the performance of existing vehicles.

Anyway, it must not be overlooked that the rollig resistance has not been considered here, and it must be borne in mind that in some cases the maximum net drawbar pull will take place, because of the effect of the rolling resistance at values of slip rates different than those that will give the maximum thrust.

BIBLIOGRAPHY

1) Bekker M. G. Theory of land locomotion.
2) Nicklethwait E. W. E. Tracks for fighting vehicles.
3) Berger, Carleton, Mc Kibbon and Painer. Tractors and their power units.
4) Ordnance Proof Manual, Vol. II, Automotive Testing, Aberdeen Proving Ground, Maryland.
5) Little L. F. Some problems in the design of crawler tractors.

DISCUSSION

M. G. BEKKER. — I have been very gratified and pleased that an equation which I proposed some ten years ago has become the subject of a study by Mayor Sela; and I also would like to congratulate the Major for the excellent mathematical solution of that equation, which we have seen on the blackboard. I wish to add that the solution which we worked out during my association with the Land Locomotion Laboratory in Detroit also, was not too satisfactory to us. Actually it was very difficult to find exact K_2 values in the higher range, because they were increasing too rapidly in an asymptotic way, the solution which Major Sela has proposed is much more accurate and elegant.

Let me also add that during the 10 years which have elapsed since this equation has been proposed as a definition of the stress-strain relationship, for the horizontal direction of vehicle motion, our thinking has been somewhat changed, in a certain sense. We found that there are a great many soils which do not have peaks in stress-deformation characteristics; that applies — as Major Sela mentioned — to granular masses, frictional masses, such as sands in particular; we found that a much more simple equation can be used in solving the same problems which we have been trying to solve using the original equation. This matter will be discussed in detail by Mr. Janosi, Mr. Harrison, Mr. Hanamoto and Pavlics; I believe, I am not making any premature disclosure if I mention that Dr. Söhne in Braunschweig-Völkenrode has a similar solution, and I think that Prof. Reece also has modified our equation more or less in the same direction. All this seems to indicate to me that the method by means of which we define the discussed stress-strain relationship is basically correct, and that this relationship can be expressed, and perhaps, must be expressed, by an equation of the type which was the subject of an analysis by Major Sela.

Thank you very much.

N. 39

Il fenomeno dell'aderenza di un cingolo fuori strada

The phenomenon of the adhesion of a track off the road

ALESSANDRO ORLANDI *)

ABSTRACT. -- *An examination is made of the phenomenon of the adhesion of a tracked vehicle running in open country, on ground identified by the factor of cohesion C and by the coefficient of attrition tg φ.*

If we admit as acceptable a law of proportion between pressure and sequezing of soil, there operates the law of variations of the tangential tension under the track and its slip.

There arises, through the characteristics of the tractor (weight and size of the track) and the of the soil (C, tg φ), the position in which we no longer have the condition of adherence between track and ground.

The most suitable method for a study of terrain in the laboratory is given.

Introduzione

Un cingolo in movimento fuori strada si comporta come se marciasse ingranando in una specie di cremagliera. Si può supporre cioè che i ramponi, di cui sono muniti i pattini, penetrino nel terreno fino a che sia raggiunto l'equilibrio fra il carico gravante sui cingoli stessi e la reazione del suolo.

L'andamento delle reazioni specifiche del terreno non è costante, anche a cingolo fermo, ma varia, specialmente secondo una sezione trasversale.

Il diagramma delle pressioni dipende dalle caratteristiche del terreno e dalla base di appoggio. Si vedano per esempio le ricerche compiute dal Press **). In fig. 1 sono riportati alcuni diagrammi, ottenuti con corpi di carico rigidi, caricati con un peso P, nei tre terreni-tipo: sabbia, limo e argilla; si passa cioè da un terreno incoerente ad altro coerente.

Questi diagrammi dimostrano l'influenza del terreno e delle dimensioni della base di carico.

Si vede infatti che per una base larga 50 cm. vi sono nei diagrammi di carico delle escursioni maggiori che non nel caso di larghezza di cm. 60.

Questo comportamento sarebbe dovuto ai fenomeni di rifluimento che hanno tanta maggiore importanza quanto minori sono le superfici di appoggio.

---

*) Università di Bologna - Italia.

**) Press, da Cestelli Guidi: Meccanica del terreno. Ed. Hoepli, pag. 147, 1957.

DIAGRAMMI DI CARICO
(Press)

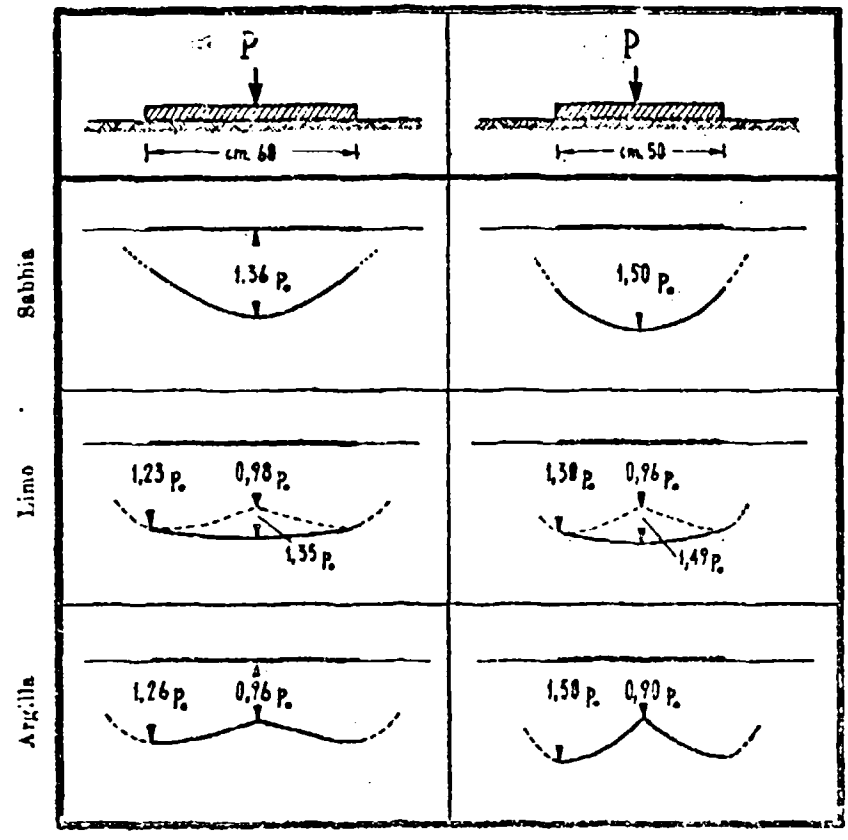


Fig. 1.

Il Lemeyer *) sperimentando con una base circolare rigida, su diversi terreni, trovò che l'andamento del diagramma dipende dal tipo di terreno (v. fig. 2). Si noti in particolare il caso dell'argilla molle che si comporta analogamente ad un terreno incoerente.

In complesso (Cestelli Guidi, opera citata) la spiegazione dei diversi comportamenti può essere la seguente: in un terreno coerente anche le zone periferiche del basamento partecipano utilmente alla deformazione essendo il terreno dotato di resistenza alla trazione (coesione) e in tal modo si crea una ulteriore resistenza sotto la zona perimetrale del basamento; in un terreno incoerente, non solo manca questa collaborazione ma la terra posta sotto il contorno del basamento rifluisce, dando luogo ad una notevole diminuzione della capacità portante.

Concludendo, per le piccole superfici di appoggio, quali appunto i cingoli,

*) Lemeyer, da Cestelli Guidi, opera citata, pag. 148.

DIAGRAMMI DI CARICO
(Lomeyer)

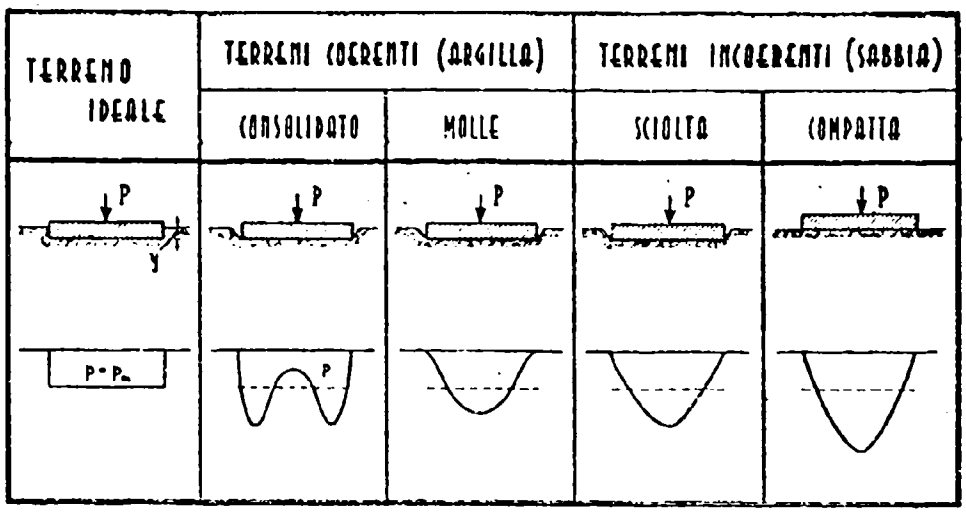


Fig. 2.

la terra ai lati, sotto l'azione dei carichi, rifluisce verso l'esterno in misura maggiore o minore a seconda che il terreno sia incoerente o coerente *).

Questo fenomeno, che è maggiormente sentito per le superfici minori (quindi per i cingoli, ed in particolare per quelli più stretti), fa sì che il terreno sottostante alla base agisca contro quello circostante come un vero e proprio cunco, con espulsione della terra verso la periferia.

Le pressioni sul terreno non sarebbero quindi tali da far accettare l'ipotesi di una ripartizione uniforme.

Tuttavia il Garbari **) ammette, nel caso di mezzi cingolati lenti (6-12 Km/h), che si possa ritenere

$$p = p_m$$

con

$$p_m = \frac{P}{b \cdot L} \qquad (1)$$

essendo:
- p = pressione effettiva locale;
- p_m = pressione media;
- P = carico gravante su un cingolo;
- b = larghezza del cingolo;
- L = lunghezza del cingolo a terra.

*) I diagrammi del Press e del Lomeyer ora riportati, furono ottenuti sotto carichi statici. Tuttavia sono ugualmente interessanti per illustrare il comportamento del suolo secondo le sue caratteristiche geofisiche.

**), Garbari, Rendiconti Congresso, ATA, pag. 69, febbraio 1949.

Sollecitazioni

Come si è detto il movimento del veicolo cingolato in terra smossa, e comunque « fuori strada », è caratterizzato da un « ingranamento » dei ramponi col terreno stesso (v. fig. 3).

Il comportamento del terreno non risulta in genere facilmente definibile in quanto esso dipende da moltissimi fattori, quali le caratteristiche geofisiche, il grado di umidità, la compattazione; oltre alle dimensioni e forma del pattino, del rampone, ecc.

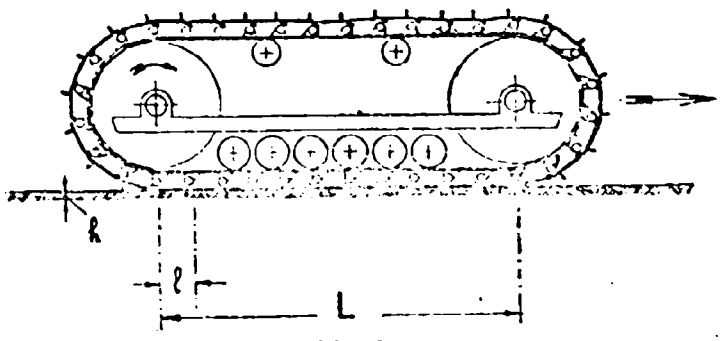


Fig. 3.

Tuttavia possiamo pensare che gli n ramponi del tratto di cingolo in quel momento a contatto col terreno (escludendo quindi l'ultimo che sta per rialzarsi) suddividano la porzione del suolo, costituente l'orma del cingolo, in n segmenti di dimensioni

$$b \cdot \frac{L}{n} = b \cdot l$$

e li sollecitino tangenzialmente con una forza che, complessivamente, è uguale allo sforzo al « cerchione » T che il cingolo stesso sviluppa durante il moto (v. oltre, fig. 4).

Detti segmenti, sono pure soggetti ad una pressione verticale p_i trasmessa dal pattino al terreno, tale che per il pattino i-esimo si abbia in generale:

$$p_i \cdot b \cdot l = \Delta P_i \qquad (2)$$

Il rampone trasmette al terreno uno sforzo orizzontale ΔT_i che comprende sia lo sforzo trasmesso propriamente dalla fronte del rampone, sia dal pattino in virtù dell'aderenza fra pattino e terreno *); definendo t_i lo sforzo tangenziale

*) La T è dovuta non soltanto alle forze trasmesse dai ramponi ai segmenti di terreno, ma anche dall'aderenza del piano orizzontale del pattino nel tratto AA' contro il terreno; il che permette una distribuzione dello sforzo T_i su tutto il segmento. Tuttavia agli effetti delle considerazioni che seguono supporremo tutta la forza ΔT_i concentrata nel rampone.

medio nel segmento i-esimo trasmesso al terreno in un piano situato a profondità h sotto il piano del cingolo (v. fig. 4), scriveremo:

$$\Delta T_i = b\,l\,t_i \qquad (2.1)$$

Compiessivamente risulta per tutto il cingolo:

$$P = \Sigma_1^n \Delta P_i \qquad T = \Sigma_1^n \Delta T_i \qquad (3)$$

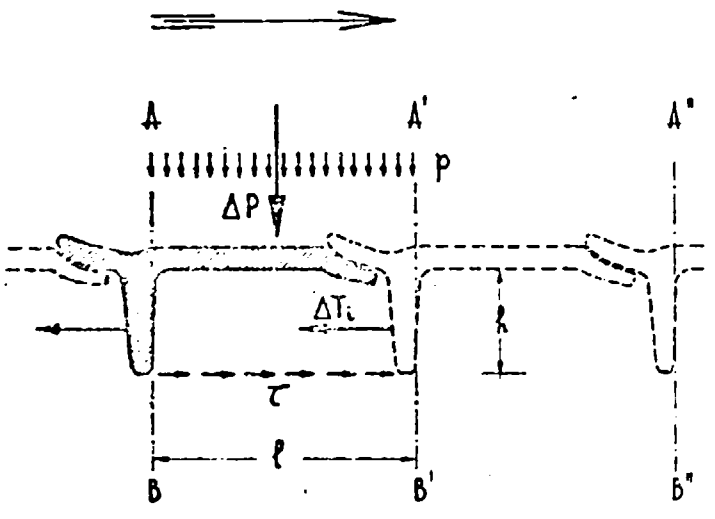


Fig. 4.

Tuttavia in quanto segue supporremo valida la (1): $p_m = \frac{P}{b \cdot L}$, per cui risulterà $\Delta P = \frac{P}{n}$.

Ricerchiamo ora le reazioni tangenziali τ del terreno che sopportano gli sforzi ΔT_i, reazioni che, impedendo gli strisciamenti del cingolo, permettono al veicolo di spostarsi per compiere il lavoro cui è adibito.

Abbiamo visto che il cingolo affonda i suoi ramponi nel terreno fino a quando la somma delle pressioni con le quali il suolo reagisce è pari al carico gravante sul cingolo stesso. Questo equilibrio avviene per lo più quando tutto il cingolo è a contatto col terreno, anzi il terreno generalmente si costiperà un poco, prima che venga raggiunto l'equilibrio.

Si ammetta valida la relazione di proporzionalità fra reazioni e affondamenti

$$p = Ky \qquad (4)$$

dove K (kg/cm³) è il «coefficiente di sottofondo» (Bettungziffer; Subgrade reaction).

Ma poichè per la (4) l'equilibrio è stato raggiunto solo dopo l'affondamento misurato da y, si può supporre che le pareti laterali dei segmenti di terra sotto il cingolo non offrano pressochè più la possibilità di resistenza allo sforzo tangenziale. Infatti l'affondamento y, senza il quale non si manifesta la reazione p del suolo, non può avvenire senza una certa lacerazione del materiale terroso sulle pareti laterali (E' indubbio che la sollecitazione è sentita maggiormente dagli strati più superficiali, cioè più vicini al pattino affondante, ma data la scarsa profondità di h i fenomeni di rottura della coesione del terreno si propagano per tutto lo spessore suddetto).

Non potendosi contare sull'apporto resistente delle pareti laterali di dimensioni l · h per le ragioni suddette, lo sforzo $T = \Sigma \Delta T_i$ dovrà essere quindi sopportato esclusivamente dalla somma delle tensioni tangenziali agenti sulle aree di base, di dimensioni b · l, dei segmenti delimitati dai singoli pattini *) **), sul piano a profondità h anzidetto (fig. 4).

La tensione ΔT esercitata da un rampone non resta costante durante tutto il tempo in cui questo artiglia il suolo, cioè dal momento in cui, rotolando attorno al rocchetto anteriore, entra in contatto col terreno, fino a quando è preso dal rocchetto motore e sollevato da terra.

Si ritenga infatti il terreno cedevole secondo la (4), e il cingolo assolutamente inestensibile e rigido. Supposto ora il veicolo in marcia, si consideri il pattino che, svoltosi dal rocchetto anteriore, è appena entrato a contatto col terreno. Sia I questa configurazione istantanea, mentre sia II la configurazione del cingolo relativa ad un intervallo di tempo successivo, per la quale il pattino in oggetto è preceduto da un altro, ossia si trova in seconda posizione.

Ora il rampone del 1° pattino quando si trova in posizione I, agisce sulla parete AB, fig. 4, del segmento di terra con una forza ΔT_1 che provoca, per la (4), un cedimento orizzontale δ.

Con l'avanzare del cingolo (pos. II) il rampone di un nuovo pattino viene a trovarsi in testa e si comporta come il precedente, determinando a sua volta uno stesso cedimento δ che si ripercuote necessariamente su tutta la lunghezza del cingolo in tensione, considerato inestensibile. In particolare il secondo cedimento si somma a quello che il pattino, ora secondo, aveva già subito, determinando quindi uno spostamento 2δ.

Ne consegue che ogni segmento di terreno, man mano che il cingolo avanza, subisce ulteriori schiacciamenti orizzontali il cui valore complessivo è definito da:

$$\Delta_i = i \cdot \delta \qquad (5)$$

proporzionale al numero d'ordine della posizione i-esima.

---

*) Ignorare il contributo alla resistenza delle pareti laterali costituisce un errore a tutto favore della sicurezza di marcia.

**) Si trascurano gli spessori degli speroni, che peraltro sono dell'ordine del 5 ÷ 6 % della lunghezza l del pattino.

Quindi anche le ΔT_i, che per la (4) sono proporzionali ai rispettivi cedimenti Δ_i, sono proporzionali al numero d'ordine della posizione, e cioè hanno una variazione lineare lungo il cingolo.

Cedimenti e tensioni

Posto che l'intero cingolo è formato da z pattini, essendo δ il cedimento elementare di ogni pattino, ad ogni giro completo il cedimento totale sarà $z \cdot \delta$ e quindi se il cingolo percorre in un giro la distanza $\pi D + 2L$ (con D diametro di rotolamento) è possibile esprimere lo scorrimento relativo s nella forma:

$$s = \frac{z\,\delta}{\pi D + 2L} \tag{6}$$

E' interessante studiare l'andamento delle tensioni tangenziali in funzione dei cedimenti Δ, poichè questo fenomeno, che dipende anche dal terreno, caratterizza la marcia del veicolo fuori strada.

Si esaminino pertanto le condizioni di equilibrio di ogni segmento del suolo genericamente individuato dalla sua coesione $c > 0$ e dal suo coefficiente di attrito interno $tg\,\varphi$; e si prenda in considerazione il segmento i-esimo di dimensioni $b \cdot l \cdot h$.

Per quanto detto sopra un generico segmento è sollecitato complessivamente attraverso il pattino dalle forze: orizzontale $\Delta t_i = b\,l\,t_i$ e verticale $\Delta P_i = b\,l\,p_i$ che per la (1) diventa $\frac{P}{n} = \Delta P = p\,b\,l$.

Tenendo conto della resistenza al taglio solo della base del segmento, cioè trascurando per quanto detto prima l'apporto dei fianchi, il pattino i-esimo risulterà in equilibrio finchè sarà valida la relazione:

$$t_i < \tau \tag{7}$$

essendo τ la tensione di taglio massima che può sopportare il terreno in esame nelle condizioni di sollecitazione in cui si trova.

La tensione τ è legata alla pressione p dalla nota relazione di Coulomb

$$\tau = c + p\,tg\,\varphi \tag{8}$$

che è sempre valida per terreni coerenti e no, per il principio di corrispondenza.

In fig. 5 si è rappresentato l'andamento delle tensioni t in funzione dei cedimenti Δ per un dato terreno soggetto ad una pressione p.

Si è diviso il diagramma in tre zone:

1° zona = dell'aderenza: $t < \tau$;

2° zona = rottura dell'equilibrio che si verifica quando $t = \tau$;

3° zona = degli slittamenti.

Per piccoli cedimenti è verificata la (7) che per la legge di Coulomb espressa dalla (8) mette in relazione le caratteristiche del terreno (c, φ) con le condizioni di lavoro del cingolo (t_i, p).

Aumentando lo sforzo di trazione, per certi segmenti di terra potrà non verificarsi più la (7): potrà risultare cioè $t_i > \tau$, quindi non essere più verificata la condizione di aderenza; pertanto si passerà nella zona III di figura 5, mentre per la validità della seconda delle (3): $T = \sum_1^n \Delta T_i$ parte dello sforzo (dato che in fase di scivolamento $\tau_s < \tau$) verrà a gravare sui

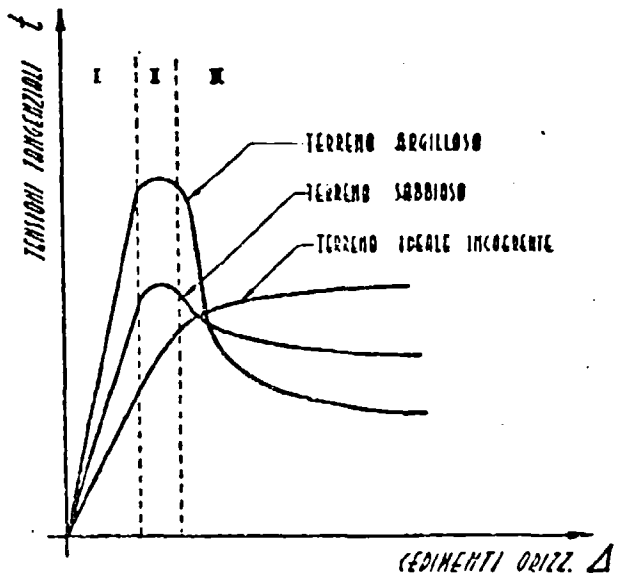


Fig. 5.

ramponi agenti su segmenti di terra che precedono, ossia meno sollecitati. Questi a loro volta potranno però raggiungere in seguito il limite di resistenza.

E' molto interessante esaminare l'andamento del fenomeno dell'aderenza dai diagrammi della figura 5 e tenendo presente la relazione di Coulomb.

Finchè si resta nel campo dei piccoli cedimenti, le τ crescono proporzionalmente a questi, a conferma della già indicata (4): $p = K y$ che, si ricorda esprime la proporzionalità, in un terreno, fra le pressioni e i corrispondenti schiacciamenti.

Le tensioni τ crescono molto più rapidamente per i terreni coerenti ossia, a parità di cedimento, le sollecitazioni tangenziali che un terreno è capace di sopportare senza che si rompa l'equilibrio, sono maggiori, in virtù della coesione c.

Raggiunto il valore τ_{max}, dato dalla formula di Coulomb, nel campo dei terreni coerenti si ha un crollo della resistenza, appunto per la mancata prestazione di c, fino a scendere ad un valore, per gradi Δ, inferiore a quanto si ha

per i terreni incoerenti i quali hanno degli angoli di attrito interno φ maggiori che non i terreni coerenti.

Si nota però una piccola caduta di τ anche nella curva dei terreni sabbiosi nel passare dalla II alla III zona, per effetto di un sia pur piccolo valore di c.

In base a quanto si è visto finora, l'andamento delle tensioni tangenziali sotto un cingolo in marcia fuori strada, può essere indicato come in figura 6.

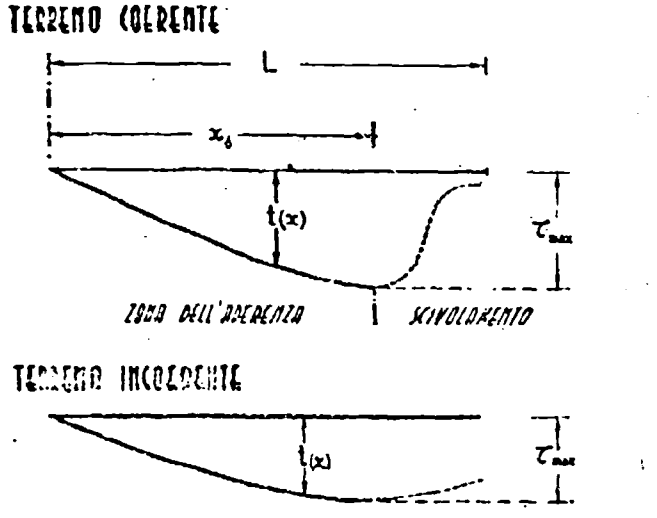


Fig. 6.

Nel primo caso, terreno coerente, le tensioni crescono circa linearmente da zero ad un valore massimo dato dalla formula di Coulomb, dopo di che esse calano rapidamente ad un valore τ, che rimane più o meno costante.

Invece in un terreno incoerente (sabbia) si ha un andamento dapprima crescente, poi raggiunto il valore limite di τ, dato dalla solita espressione di Coulomb, la tensione tangenziale si mantiene invariata.

In un terreno reale si potrà verificare un caso intermedio fra i due estremi sopra indicati, secondo il rapporto sabbia/argilla, il grado di umidità e la situazione di compattazione del terreno stesso.

Determinazione dell'ascissa critica dell'aderenza

Cerchiamo in quale punto, sotto il cingolo, si può verificare la condizione critica

$$t(x) = \tau_{max}$$

per la quale il segmento, sollecitato al massimo delle possibilità del terreno, viene tagliato dando luogo a vistosi fenomeni di scorrimento.

Non conoscendo la relazione analitica rappresentante l'andamento reale di dette tensioni tangenziali in funzione dell'ascissa, si pongono le seguenti ipotesi semplificative:

— che sia valida la (4), $p = K y$, e quindi la legge di variazione di $t(x)$, che pertanto sarà lineare, cioè la $t(x)$ sarà proporzionale alla distanza x del segmento stesso dall'inizio dell'orma del cingolo;

— che in fase di scorrimento la tensione si mantenga costante e uguale a τ_s dal punto in cui si verifica la condizione $t = \tau_{max}$, fino all'estremo posteriore dell'orma.

L'andamento delle tensioni sarà del tipo rappresentato in figura 7 a.

Lo sforzo di trazione T risulterà in una situazione generica:

$$T = b \sum_{o}^{x_s} t(x) \cdot \Delta x + b t_s \cdot (L - x_s) \tag{9}$$

dove per le ipotesi fatte, dovrà essere:

$$t(x_s) = \tau_{max} = c + p \operatorname{tg} \varphi$$
$$t_s = \tau_s = p \operatorname{tg} \varphi \tag{10}$$

Quindi la (9) diventa:

$$T = \frac{1}{2} b \tau_{max} \cdot x_s + b \tau_s (L - x_s) \tag{11}$$

Ritenendo valide le (10) e (11), e quindi i diagrammi di figura 7, si possono verificare i tre seguenti casi-tipo:

terreno corrente: $\tau_s < \tau_{max}$ (e in particolare $\tau_s < \frac{\tau_{max}}{2}$) il massimo sforzo di trazione

$$T = \frac{1}{2} b \tau_{max} \cdot L$$

si ottiene quando la tensione sotto l'ascissa $x = L$ è la massima. Superato in tal punto la τ_{max} [data come al solito dalla (8)] tutto il cingolo entra in slittamento e lo sforzo di trazione possibile diventa minore: $T = \tau_s b L$ (fig. 7 b);

terreno incorrente: $\tau_s = \tau_{max}$ (e in particolare $\tau_s > \frac{\tau_{max}}{2}$) il massimo sforzo di trazione si ottiene quando tutto il cingolo è in fase di slittamento. In questo caso lo sforzo di trazione $T = \tau_s b L$ è quindi il massimo (fig. 7 c);

terreno intermedio: $\tau_s = \frac{\tau_{max}}{2}$. In questo particolarissimo caso lo sforzo di trazione T resta costante in qualunque condizione di aderenza o di slittamento parziale o totale del cingolo.

Cioè si ha:

$$T = \frac{1}{2} b \tau_{max} \cdot L = b \tau_s L = \frac{1}{2} b \tau_{max} \cdot x + b \tau_s (L - x)$$

come si può verificare ponendo $\tau_s = \frac{\tau_{max}}{2}$ (fig. 7 d).

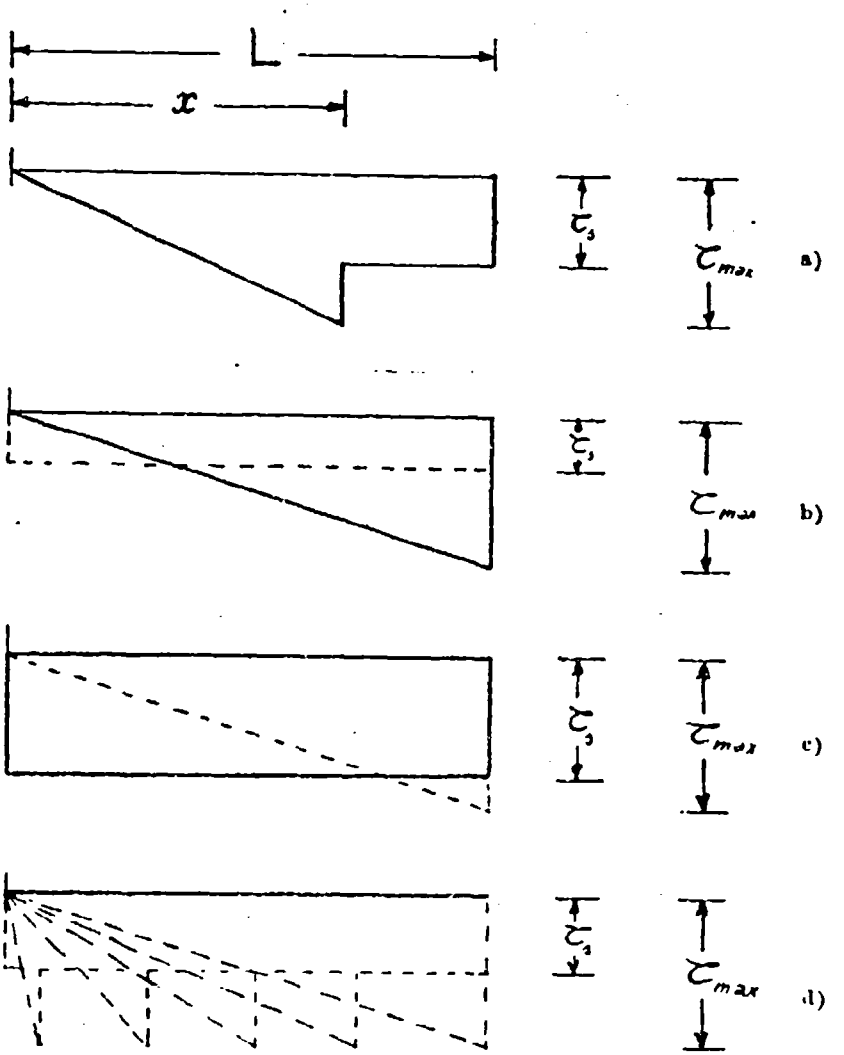


Fig. 7.

Questi risultati, dedotti da considerazioni riferite ad uno schema delle tensioni semplificato notevolmente per comodità di studio, hanno un valore puramente qualitativo.

Prove di laboratorio

Vista l'importanza di conoscere i termini che intervengono nella espressione di Coulomb, sarà opportuno determinarli con la massima cura, cercando, nella riproduzione del fenomeno in laboratorio, di mantenersi il più possibile aderenti all'andamento reale del fenomeno stesso.

Esistono diversi procedimenti per ricavare c e φ, fra cui molto noti sono quelli dell'apparecchio triassiale e della scatola di Casagrande.

Quest'ultimo, forse il primo in ordine di tempo, è indubbiamente il più adatto alla ricerca in oggetto perchè riproduce esattamente l'azione del pattino e del rampone sul terreno.

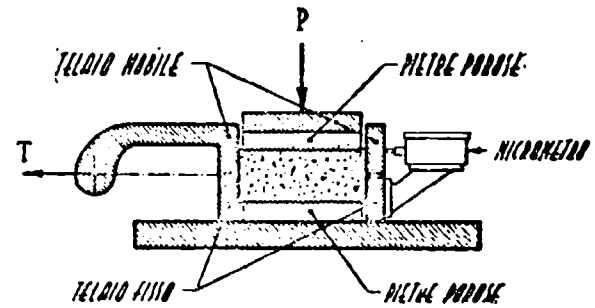


Fig. 8.

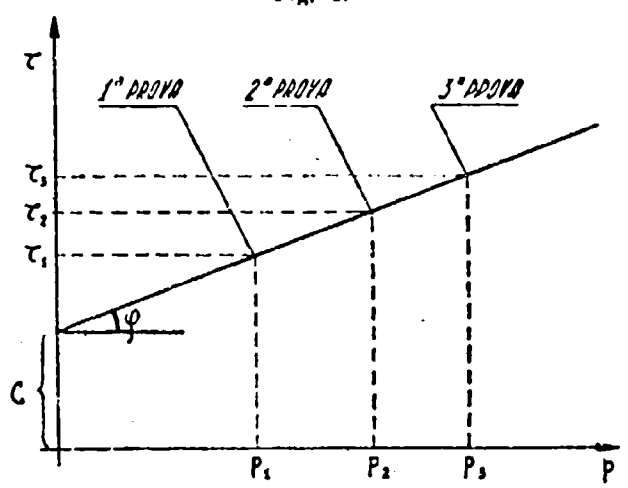


Fig. 9.

L'apparecchio consiste (fig. 8), in una coppia di telaietti quadrati di area S che, sovrapposti vengono chiusi sopra e sotto da opportune pietre porose fra le quali è stato precedentemente posto il provino di terra in esame.

Il telaietto inferiore è fisso al banco, mentre il superiore, sulla cui pietra porosa è posto un carico P verticale, viene sollecitato a spostarsi da una forza orizzontale T. Un micrometro misura gli spostamenti relativi dei due telaietti.

Si ha pertanto: $\tau = \frac{T}{S}$; $p = \frac{P}{S}$.

Fissato P, si aumenta T finchè non si produce un sensibile spostamento del telaietto mobile.

Si ripete la prova diverse volte variando P, e di conseguenza T, e si disegna il diagramma di figura 9 che individua i termini cercati c e φ, permettendo di scrivere la formula di Coulomb: $\tau = c + p \operatorname{tg} \varphi$.

Il metodo della scatola di Casagrande è utile e pratico anche per determinare il coefficiente φ del terreno a contatto con un corpo di altra natura, per esempio una lastra metallica.

E' il caso del cingolo con pattino piatto di cui sono generalmente fornite le gru e le escavatrici da cantiere.

Si sostituisce allora uno dei due telaietti della scatola di Casagrande (meglio il superiore) con una lastra metallica e si ripetono le prove sopra descritte.

Esistono due tipi di questo apparecchio secondo le misure del provino di terra: cm. $7 \times 7 \times 2$ e cm. $30 \times 30 \times 15$.

Indubbiamente per compiere le ricerche in materia di cingoli si presta meglio la scatola di dimensioni maggiori.

Proposizione conclusiva

E' possibile studiare le condizioni di aderenza di un mezzo cingolato fornito di pattini a ramponi in marcia fuori strada, conoscendo le caratteristiche del trattore (b, l, L, P, T) e quelle del terreno (formula di Coulomb).

Riguardo a questo si può ricordare che i mezzi cingolati che lavorano alla costruzione di grandi opere in terra (argini, dighe, rilevati stradali, ecc.) si ritrovano per lo più a percorrere un terreno di cui sono note e sufficientemente costanti le caratteristiche geofisiche, e quindi non è azzardato pensare che, nell'impostare il calcolo dei cicli di trasporto per la costruzione di quell'opera, il tecnico possa utilizzare vantaggiosamente le conoscenze « a priori » del suolo sul quale passeranno i mezzi cingolati.

N. 40

Factors affecting wheeled tractor traction on sandy loess soils

Fattori influenzanti la trazione del trattore a ruota su terreno sabbioso

MORDECHAI WEINBLUM - SAMUEL ORLOVSKI *)

ABSTRACT. — *This work was devoted to the investigation of the effects of several factors on traction of a wheel-type tractor in sandy-loess soil. An attempt was also made to determine the relation between traction and soil strength as measured by several field methods. The following factors were investigated: a) weight on the driving wheels; b) forward speed; c) dual tires; d) reversed direction tires; e) retractable grousers, front and rear half tracks and four wheel drive; and f) soil strength.*

Drawbar pull versus slip, tractive efficiency and drawbar horse-power were determined for each factor. These curves were calculated after linear transformation of the exponential function connecting slip and drawbar pull ($S = Ae^{BP}$). Observations fitted this function well in the measured range of slip (up to 50 %). The comparison between treatments was made with drawbar pull at 20 % slip as a criterion.

Soil strength was measured by a penetrometer and by a vane shear apparatus. Comparison of these methods was made under both field and laboratory conditions.

Results of these tests show that the condition of the soil has a deciding effect on the traction. At 20 % slip, additional weight on the driving wheels increased pull under all soil conditions. A definite tendency of increase in the coefficient of traction with increase in weight was also determined. Dual tires, retractable grousers, and front half tracks caused no improvement in traction. No effect of forward speed on drawbar pull at 20 % slip was found in the range 1.22 till 2.44 m/sec. (except one test). The combination of weight on the driving wheels and forward speed was chosen so that the efficiency of engine power would be maximum.

Rear half tracks and four wheel drive improved traction.

Observations from both the penetrometer and the vane shear apparatus showed a tendency to linear correlation with the pull coefficient. It seems that the penetrometer is more sensitive than the second device, especially in soil with a non-uniform profile.

The effect of weight on the driving wheels in loose sandy-loess soils has not been sufficiently clarified in these tests.

Introduction

The use of wheel-type tractors for agricultural purposes in areas of sandy or semi-sandy soils is very limited. Use is limited to those jobs that can be accomplished at high speeds and that do not demand high drawbar pull. Efficient use of wheel tractors for low-speed, high-power jobs is impossible in these areas because of low soil strength and poor traction. If we consider the various economic and functional advantages of wheel-type tractors, the necessity

*) Research Engineer, Farm Machinery Division, National and University Institute, Beth Dagon, Israel and Senior Lecturer, Head of Farm Machinery Section, Department of Agricultural Engineering, Israel Institute of Technology, Haifa, Israel.

of finding ways to widen the scope of wheel tractor use to these areas while increasing low-speed efficiency becomes apparent.

The purpose of this study was to determine the factors influencing tire grip in the sandy-loess soils of the Ze'ilim area, and ways of measuring them, as well as to find the soil characteristics that best correlate with tire grip so that results would be adaptable to conditions differing from those of the experiment.

Work procedures

1) During the research the following factors were tested: a) Weight on the driving wheels, b) Forward speed, c) Retractable grousers, front half-tracks, rear half-tracks, dual tires, four wheel drive and direction of tire tread, d) Condition of soil surface. An additional aim was to determine a field procedure for measuring soil strength which would permit an evaluation of the wheel tractor's traction on the tested soil.

2) Planning of field tests: the tests included: seven static weights on the drive wheels: a) 1900 kg., b) 1960 kg., c) 2100 kg., d) 2200 kg., e) 2330 kg., f) 2360 kg., g) 2650 kg.; three forward speeds: I) 4.5 kph.; - 4.7 kph., II) 6.0 - 6.3 kph., III) 8.5 - 8.8 kph; and four surface conditions: 1) Packed soil covered with a loose layer, 2) Uncultivated soil, 3) Plowed soil, and 4) Wet soil. Each factor was examined in groups according to the following arrangement.

	1	2	3	4
I	b, c, d, g			
II	b, c	a, e	a, e	a, f
III	b, c			

Subsequently, comparative tests were carried out at one speed (II) and on three soil conditions (2, 3, 4) between a tractor with regular tires and each of the following: A) Dual tires (fig. 16), B) Tires with reverse treads, C) Retractable grousers attached to the tires (fig. 17a, b), D) Front half-tracks (fig. 18), E) Rear half-tracks (fig. 19), F) Four wheel drive (fig. 20).

3) Work methods. The basis for calculation of the traction of the tractor was the P-S curve which shows the relation between drawbar pull and slip for each test. The forward speed and rolling resistance were also measured for the calculation of drawbar horse power, rolling resistance horse power, slip horse power and tractive efficiency.

4) Laboratory tests. Two methods for soil strength measurements were compared under controlled conditions: a) resistance to a penetrometer, b) the moment needed to turn a vane shear apparatus. The same methods were used also in the field tests.

The soil. — Soil samples were prepared at two moisture contents: a) hygroscopic moisture, b) 8-10 % moisture content.

Soil samples from each moisture group were compressed under five pressures: 1) noncompressed, 2) 0.5 kg/cm², 3) 1 kg/cm², 4) 1.5 kg/cm², 5) 2 kg/cm². Compression was achieved in a special device. Each treatment was repeated at least three times.

Observations. — Two readings of resistance to the penetrometer and one reading of the shearing moment of the vane shear apparatus were taken for each sample of a certain treatment. Soil density for the entire depth (17.5 cm) was measured every 2.5 cm for each treatment. Moisture distribution was also measured.

Direct shear. — For comparison, soil strength was also measured by direct shear in the laboratory. These measurements were made at both moisture contents and four stages of compression. The horizontal deformation curves in relation to shearing stress were determined, and the normal stress versus shear stress curve was also obtained through calculation. The comparison of the results of this test with those of the penetrometer and the vane shear apparatus test is strictly qualitative.

Results. — 1) Soil classification. The average mechanical composition of the soil on which the tests were conducted is: clay 4 %, silt 1 %, fine sand 51 %, coarse sand 44 %.

Classification will now be made of the four soil conditions. 1) After seven subsurface cuttings of couch grass every ten days, the area was disked before tests were made, creating a 10 cm layer of loose soil over a hard bottom. The soil was dry (hygroscopic moisture). 2) Uncultivated soil. This area had not been cultivated for several years. The land was slightly rolling, and was covered by sparse, dry vegetation. The moisture was only hygroscopic. 3) Uncultivated soil plowed to a depth of 30 cm. After plowing the surface remained level. The moisture was hygroscopic. 4) The soil was compacted after twelve subsurface cuttings. This field was irrigated for three hours, four days before testing began. During the test the average moisture at different depths was 0-10 cm 5 %, 10-25 cm 5.8 %.

Soil strength. The average observations of soil strength for each of the four soil conditions are listed in table 1.

Drawbar pull versus tire slip curve. — 2) Analysis of results. It is necessary to express this curve in a functional form by means of the measured data.

After several attempts to fit functions to the measured points by statistical regression methods, the following function was found to be most suitable: $S = Ae^{BP}$, S - slip (%), P - drawbar pull (kg), A, B - empirical constants. Fitting the function to measured points was accomplished after the linear transformation. $\ln S = \ln A + BP$, and after determination of the regression line of P in relation to lnS by the accepted method of least squares.

Criterion of comparison. — The drawbar pull at 20 % slip was chosen as the criterion for comparison.

The value of drawbar pull at 20 % slip (P_{20}) was determined from the calculated curve. For statistical comparison between the various treatments, the standard error of the points from the regression line was chosen as the best approximation of the variance around P_{20}.

Drawbar horsepower. — Drawbar horsepower curves were obtained from data measured during the tests. Expressing the drawbar horsepower as a function of slip, and inserting $S = Ae^{BP}$, deriving the expression for P and equating to zero, we obtain an equation in which the value of P for maximum drawbar horse power is: $e^{BP}\ (BP = \frac{100}{A})$. The value of pull, slip and maximum drawbar horse power were determined for each treatmeat by trial and error.

Tractive efficiency. — Engine power was not measured during the tests. Efficiency can be estimated by the following expression:

$$\eta = \frac{P}{P + R}\left(1 - \frac{S}{100}\right)$$

when η tractive efficiency and R-rolling resistance. By inserting equation (1), deriving and equating the expression to zero, the following equation was obtained from which it is possible to calculate efficiency at maximum pull and the corresponding drawbar pull and slip: $e^{BP}\ (BP^2 + BRP + R) = \frac{R}{A}\,100.$

3) Traction as affected by weight on driving wheels. The P versus lnS regression lines for different weights on the drive wheels under the various soil conditions previously described are shown in fig. 3. Analysis of the results is given in table 2.

4) Traction as affected by forward speed. Results for this part are not uniform (fig. 4, table 3).

5) The results concerning dual tires are given in fig. 5.

6) Reversed direction tires as compared to ordinary tires.

On the supposition that the accepted direction of tire treads causes soil movement from the center of the tire towards its sides, and that this is a negative phenomenon in the particular soil of these tests, an experiment was made to determine the effect of reversing tread direction on traction. Fig. 14 clearly shows the greater soil deformation created by ordinary tread action. Results of the experiment (fig. 6) are not uniform. For soil condition 3 no difference was found. For soil condition 4 reverse treads caused a 20 % increase in drawbar pull over ordinary treads. This difference proved to be statistically significant.

7) The results concerning retractable grousers and front half-tracks are given in fig. 7 and table 4.

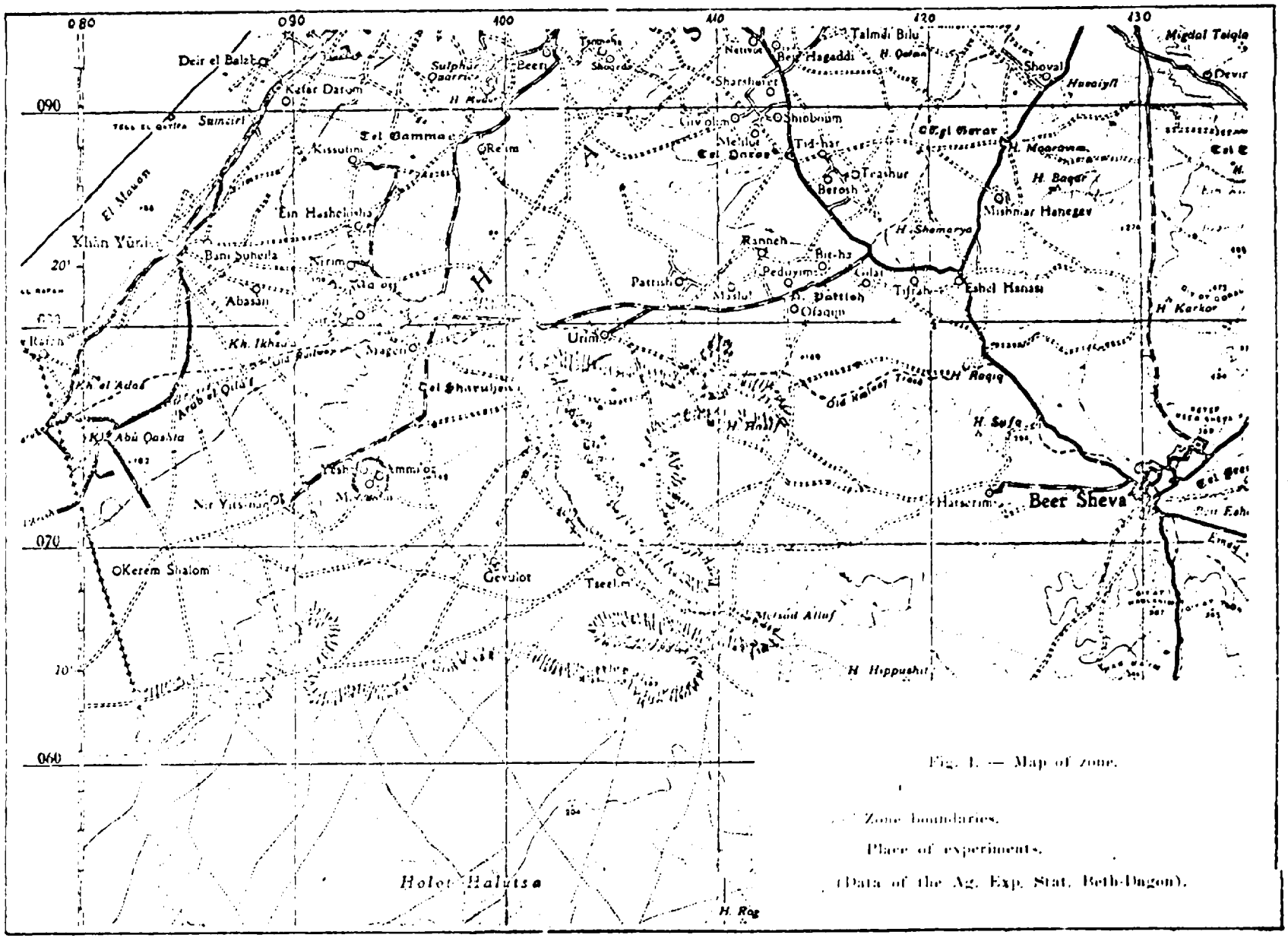


Fig. 1. — Map of zone.

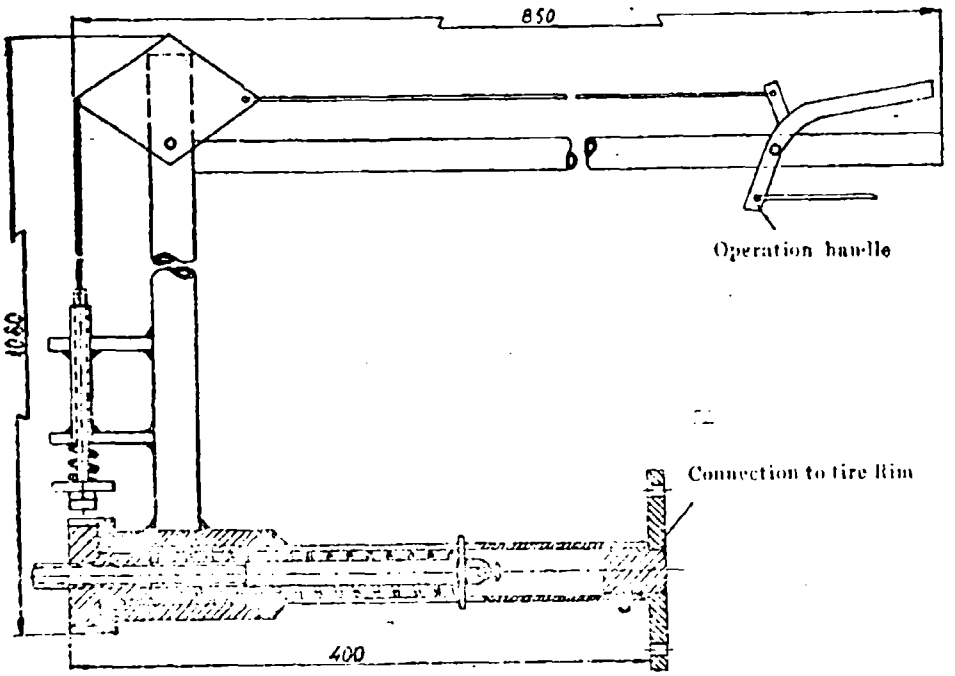


Fig. 2. — Apparatus for slip measurement (general view).

8) The results concerning rear half tracks and four wheel drive are given in fig. 8 and table 5.

9) Condition of the soil. Effect on drawbar pull and methods of measurement. Results (fig. 9, table 6) clearly show the pronounced effect that soil condition has on traction. Traction can be expressed as a single number by using the coefficient of traction at 20 % slip. This coefficient changed from 14.5 % for soil condition 3 to 34 % for condition 4. Only slight difference was found between conditions 1 and 4, and this indicates that the loose layer had a negligible effect on traction. The effect of soil condition on maximum drawbar horse power and maximum tractive efficiency was pronounced.

The relation between soil characteristics and traction. — The various soil conditions differed from each other in density of the surface, depth of the loose layer and moisture content. Except for condition 1, the soil was uniform to a depth of at least 30 cm. The curves relating coefficient of traction and soil strength are shown in fig. 10. The number of soil conditions is too small to permit definite conclusions as to this relationship. It seems from these curves that a correlation exists between the coefficient of traction and the average strength measurements as measured by the two instruments, although penetrometer readings give better agreement. The vane shear apparatus readings are not accurate for soils with a non-uniform cross section. Therefore, the results for

TABLE 1. — *Observations from penetrometer and vane shear apparatus.*

Soil Condition	Vane shear apparatus performance					Energy for penetrometer to 20 m.			Kgm
	No. of obser.	Aver. max. Mom. kgm	Standard deviation	Aver. friction Mom. kgm	Standard dev.	Condition	Number of observations	Average	Standard deviation
1	42	585	215	220	55	1	38	5.3	3.15
2	4	390	25	170	32	2	12	4.0	1.64
3	12	160	35	110	16	3	10	0	0
4	26	590	103	300	67	4	14	7.3	1.55

TABLE 2. — *Traction as affected by weight on the driving wheels.*

S × 10³	A	Weight transfer (Kg)	Max. tractive efficiency			Max. drawbar horse power			Probable error of estimation	Significance between the tractors	No. of observations	Standard error	Variance from regression line	Additional drawbar pull (Kg)	Addition of weight (Kg)	Drawbar pull at 20 % slip (Kg)	Static weight on driving wheels (Kg)	Treatment
			Slip (%)	Tractive effic. (%)	Towing coeff. (%)	Slip (%)	Drawbar pull (Kg)	Power (H.P.)										
3.03	2.73	230	16	590	57	30	780	12.1	0.322		4	4	66	—	—	660	1960	I b, 1
2.79	2.01	260	14	650	60	28	965	15.0	0.371	Significant	5	19	1813	170	140	830	2100	I b, 1
2.81	1.22	340	11	850	64	25	1150	19.2	0.381	Significant	5	30	3211	240	550	1070	2650	I g, 1
3.03	2.54	330	19	390	46	30	490	7.7	0.210		8	25	5100	—	—	410	1900	II a, 2
2.32	4.05	350	19	610	53	32	830	12.5	0.265	Significant	9	23	3224	230	430	640	2330	II e, 2
2.56	7.59	300	29	330	31	37	450	6.3	0.145		6	7	276	—	—	280	1900	II a, 3
4.15	4.75	360	24	460	32	32	480	7.0	0.139	Significant	9	8	518	50	430	330	2330	II c, 3
2.30	4.05	210	15	570	60	30	820	12.7	0.314		8	17	2418	—	—	690	1900	II a, 4
1.53	4.84	260	16	760	63	33	1170	17.5	0.364	Significant	11	29	4282	210	460	900	2360	II f, 4

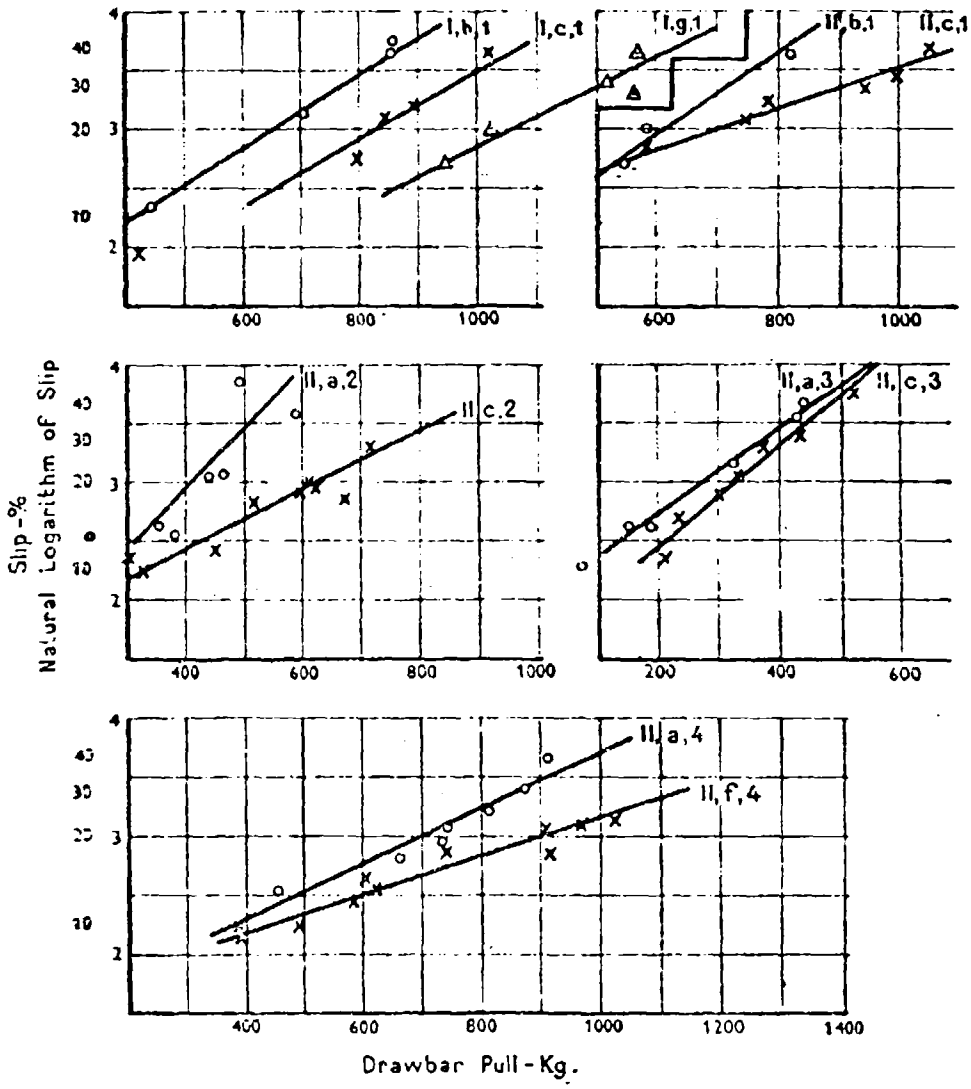


Fig. 3. — Traction as affected by weight on driving wheels.

this instrument were not used in determining the relationship for soil condition 1.

The extent of agreement between penetrometer and vane shear apparatus data as found from laboratory tests can be seen in fig. 11. Both instruments permit clear distinction between the strength of dry and wet soil. In contrast, strength increase caused by precompression was so small that it was impossible to find a distinct relationship between the data. In any case, it seems that the penetrometer was more sensitive to slight changes in soil strength.

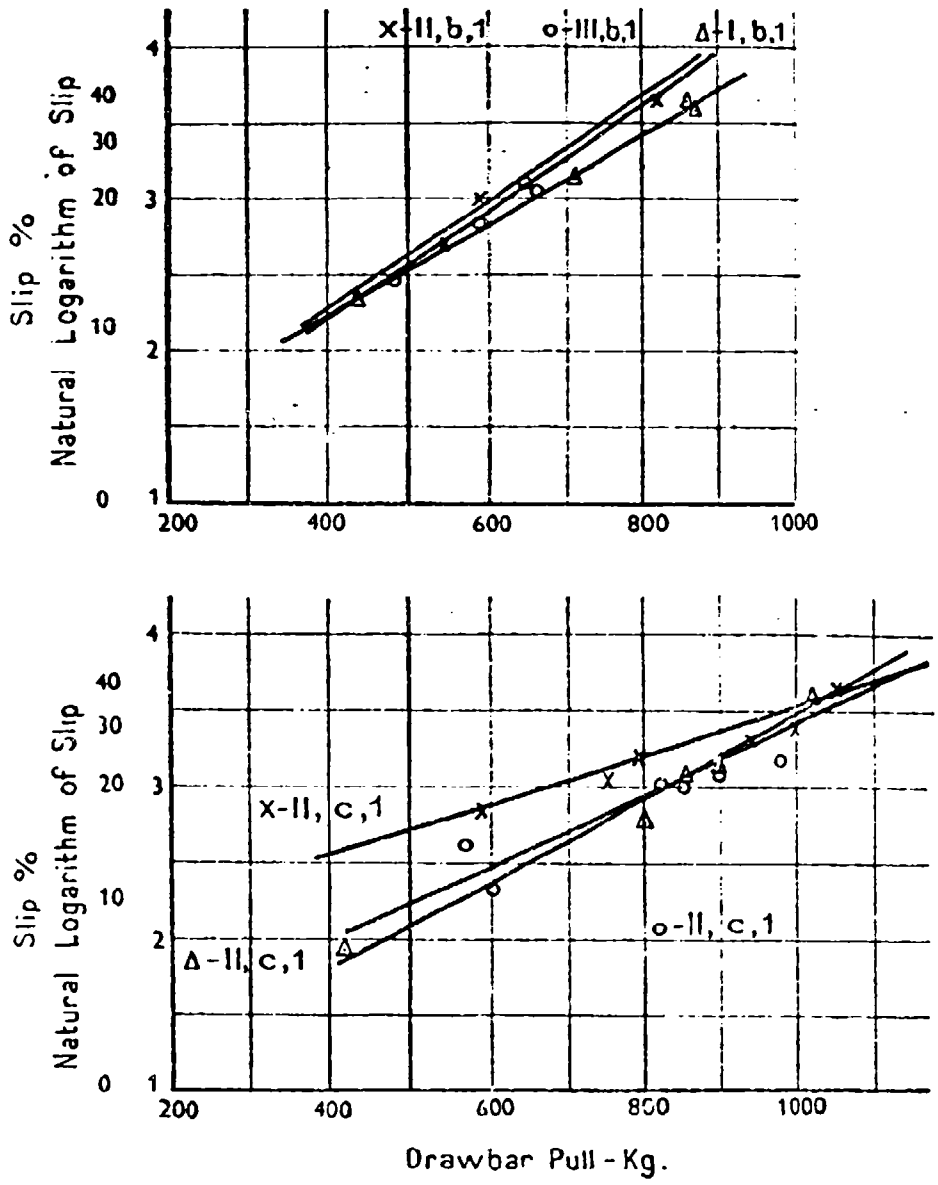


Fig. 4 — Traction as affected by forward speed.

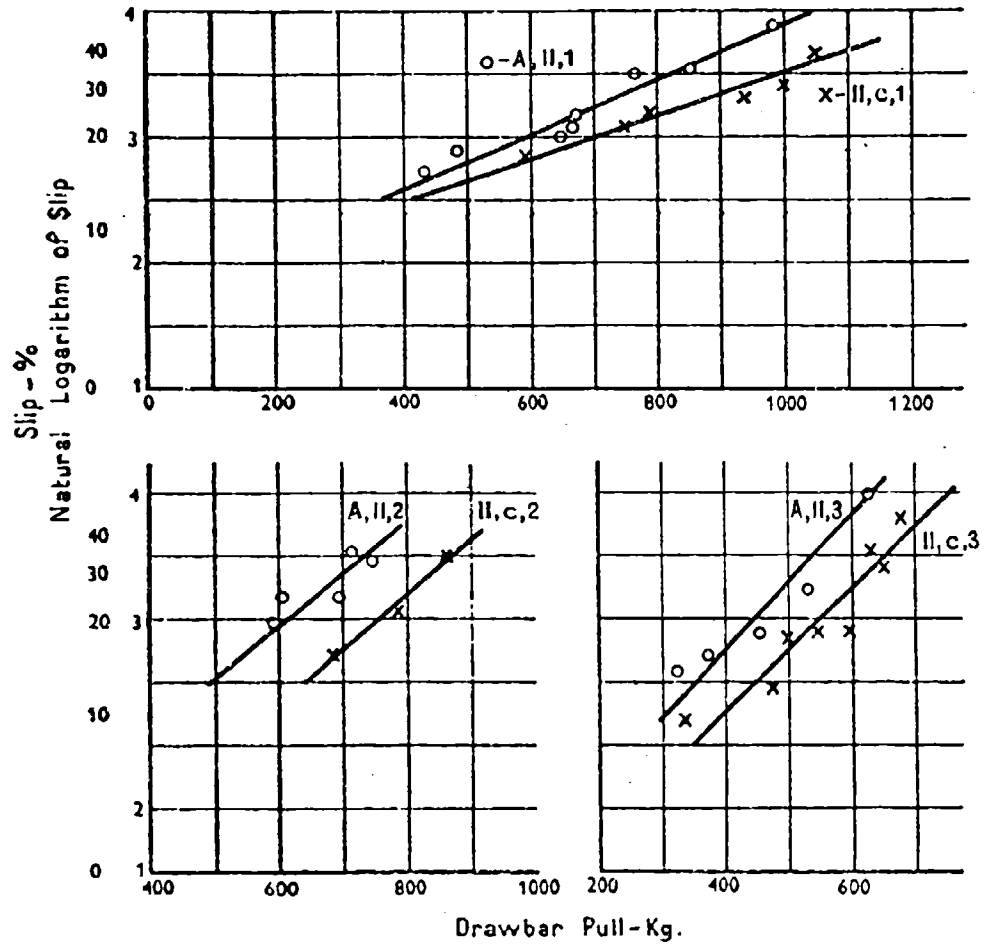


Fig. 5. — Dual tires vs ordinary tires.

The basic difference between dry and wet soils was evident from direct shear tests in the laboratory. In dry soils, the cohesion coefficient does not change with precompression and remains zero, while precompression in wet soils causes an increase in cohesion coefficient values, and a decrease in the friction angle.

It should be noted that in both direct shear and tractor action soil shear occurs under a normal load. The two instruments used for measuring soil strength, however, do not produce a normal load. The discrepancy between the techniques of measuring traction and soil strength demands that further research be done on instrumentation.

TABLE 3. — *Traction as affected by forward speed.*

B × 10⁻³	A	Rolling resistance (Kg)	Max. tractive efficiency: Slip (%)	Max. tractive efficiency: Drawbar pull (Kg)	Max. tractive efficiency: Tractive efficiency (%)	Max. drawbar horse power: Slip (%)	Max. drawbar horse power: Drawbar pull (Kg)	Max. drawbar horse power: Drawbar horse power (H.P.)	Dynamic coefficient of traction	Significance between treatments	No. of observations	Standard error	Variance from regression line	Additional drawbar pull (Kg)	Addition of weight (Kg)	Drawbar pull at 20 % slip (Kg)	Static weight on driving wheels (Kg)	Treatment
3.65	2.73	280	16	580	57	30	780	9.1	0.318	Non signif.	4	4	66	—	—	660	1960	I b, 1
3.39	2.49	250	15	530	58	28	710	11.0	0.305	Non signif.	3	118	58366	40	0	620	1960	II b, 1
3.56	2.13	280	14	530	57	28	690	15.6	0.305	Non signif.	4	50	8242	— 10	0	630	1960	III b, 1
2.79	2.01	290	14	680	60	27.5	935	11.3	0.370	Significant	5	19	1813	—	—	830	2100	I c, 1
1.64	6.41	290	24	790	56	28	900	14.0	0.314		6	28	2280	— 140	0	660	2100	II c, 1
2.36	2.80		15	700	60	30	1000	22.0	0.373	Significant	6	37	5161	+ 130	0	820	2100	III c, 1

TABLE 4. — *Retractable grousers and front alf tracks VS ordinary tires.*

B × 10⁻³	A	Rolling resistance (Kg)	Max. tractive efficiency: Slip (%)	Max. tractive efficiency: Drawbar pull (Kg)	Max. tractive efficiency: Tractive efficiency (%)	Max. drawbar horse power: Slip (%)	Max. drawbar horse power: Drawbar pull (Kg)	Max. drawbar horse power: Drawbar horse power (H.P.)	Dynamic coefficient of traction	Significance between treatments	No. of observations	Standard error	Variance from regression line	Additional drawbar pull (Kg) *	Addition of weight (Kg)	Drawbar pull at 20 % slip (Kg)	Static weight on driving wheels (Kg)	Treatment
2.65	9.00	735	30	460	27	40	540	7.2	0.127	Significant	11	40	5191	— 30	—	300	2330	C, II e, 3
4.57	9.75	600	33	270	21	41	320	4.2	0.070	Significant	9	12	806	— 175	—	155	2200	D, II d, 3
4.35	4.75	560	24	400	32	32	460	7.0	0.147		7	8	518	—	—	330	2330	II e, 3
1.80	8.90	485	25	580	41	37	740	10.5	0.188	Significant	11	42	9073	— 190	—	450	2330	C, II e, 2
5.06	2.83	350	27	480	42	38	620	8.5	0.174		9	18	2676	— 250	—	390	2200	D, II d, 2
2.52	4.05	330	19	610	53	32	830	12.5	0.265		9	25	3284	—	—	640	2330	II e, 2

*) As compared to a single tire.

TABLE 5. — *Rear half tracks and four wheel drive US ordinary tires.*

B × 10⁻³	A	Max. tractive efficiency		Max. drawbar horse power		Dynamic coefficient of traction	No. of observations	Standard error	Variance from regression line	Additional drawbar pull (Kg) **	Drawbar pull at 20 % slip (Kg)	Total weight (Kg)	Static weight on driving wheels (Kg)	Treatment
		Rolling resistance (Kg)	Slip (%)	Drawbar pull (Kg)	Slip (%)	Drawbar horse power (H.P.)								
2.28	3.68	230	15	610	62.5	30	929	14.2	0.314	7	20	2208	—	750	2050	2130	H c, 4
2.24	1.11	235	9	929	72	25	1380	23.0	0.415	11	22	5174	540	1290	3770	2950	E H, 4
2.12	0.45	360	×	1350	72.5	22	1870	32.4	0.430 *	9	41	13932	1050	1800	4500	2940	F H, 4

*) The coefficient of traction is calculated in relation to the total weight of the traction.

**) As compared to a single tire.

TABLE 6. — *Traction as affected by soil.*

B × 10⁻³	A	Max. tractive efficiency		Max. drawbar horse power		Max. shear moment (KGCM)	Energy to force penetrometer to 20 cm (KGCM)	Dynamic coefficient of traction	Coefficient of rolling resistance	Rolling resistance (Kg)	No. of observations	Standard error	Additional drawbar pull (Kg)	Drawbar pull at 20 % slip (Kg)	Weight on driving wheels (Kg)	Treatment
		Slip (%)	Drawbar pull (Kg)	Slip (%)	Drawbar horse power (H.P.)											
3.50	7.13	29	280	37	450	6.3	160	0	0.115	0.183	500	6	1	280	1000	H a, 3
3.05	4.2	19	390	30	490	7.7	160	4.0	0.210	0.110	300	×	25	130	1000	H a, 2
3.39	2.49	15	530	28	710	11.4	580	5.3	0.305	0.090	250	3	118	210	1000	H b, 1
3.30	4.05	15	570	30	820	12.7	590	7.2	0.347	0.088	240	6	17	70	1000	H a, 4
4.35	4.75	24	400	32	430	7.0			0.139	0.178	500	11	×	—	2330	H c, 8
3.52	4.05	19	610	32	830	12.0			0.266	0.105	350	×	25	310	2330	H c, 2
1.58	4.84	16	760	32	1170	16.5			0.388	0.085	260	11	29	260	2330	H c, 4

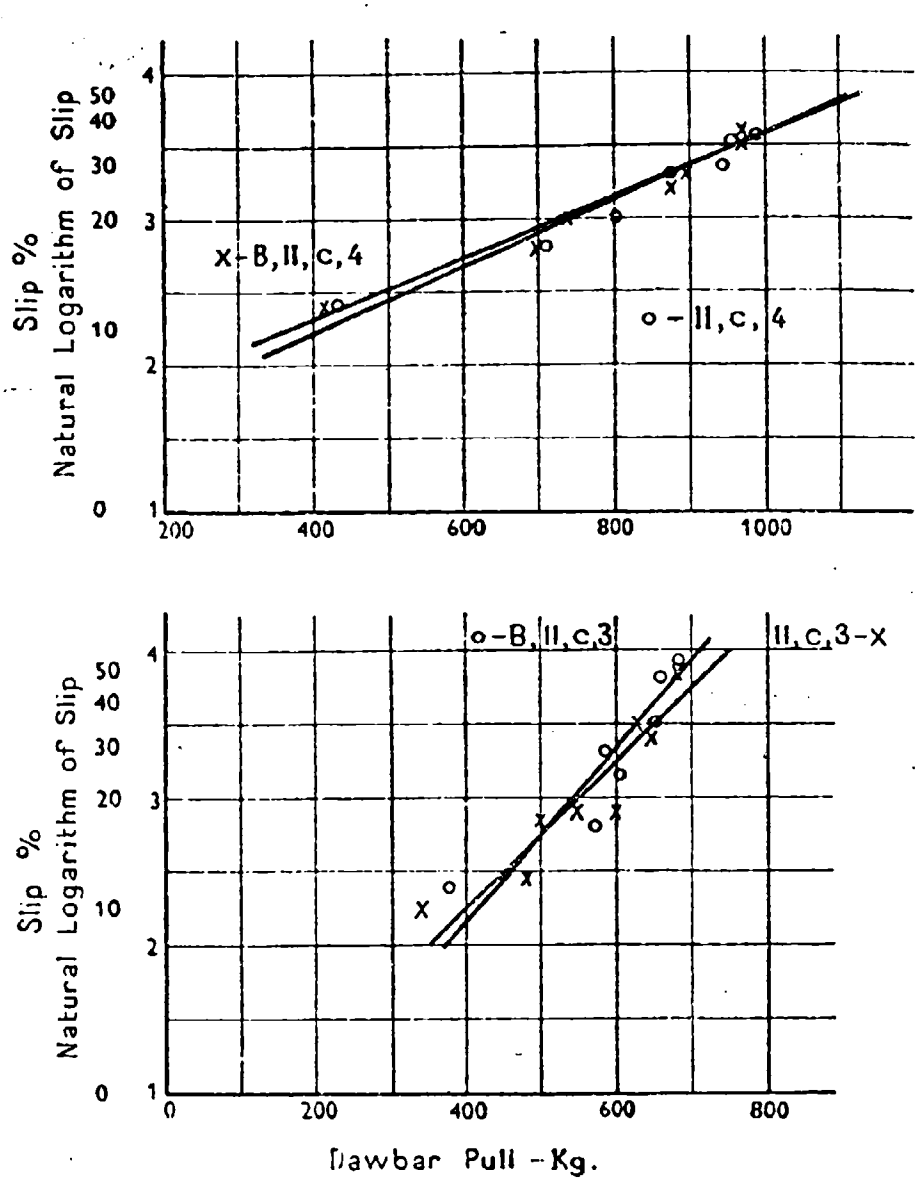


Fig. 6. — Reversed-direction tires vs ordinary tires.

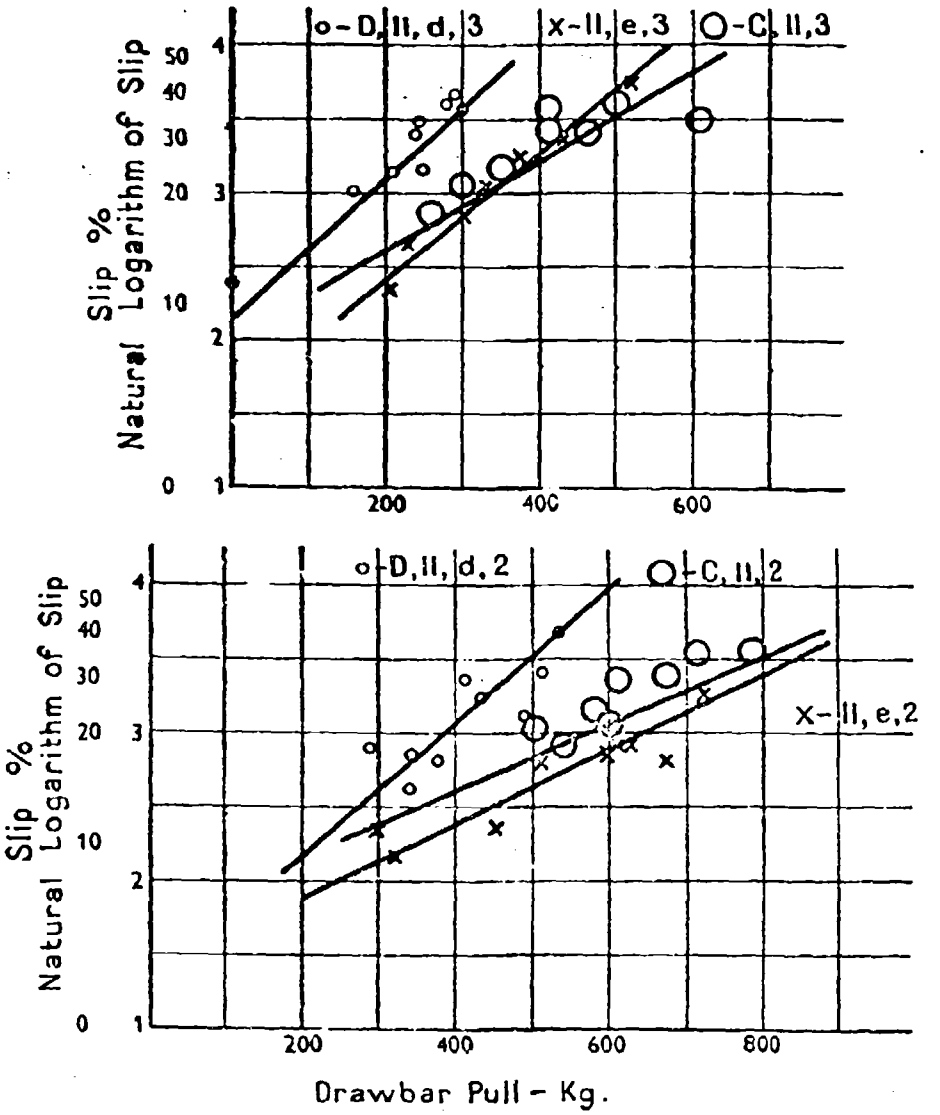


Fig. 7. — Retractable grousers and front half tracks vs ordinary tires.

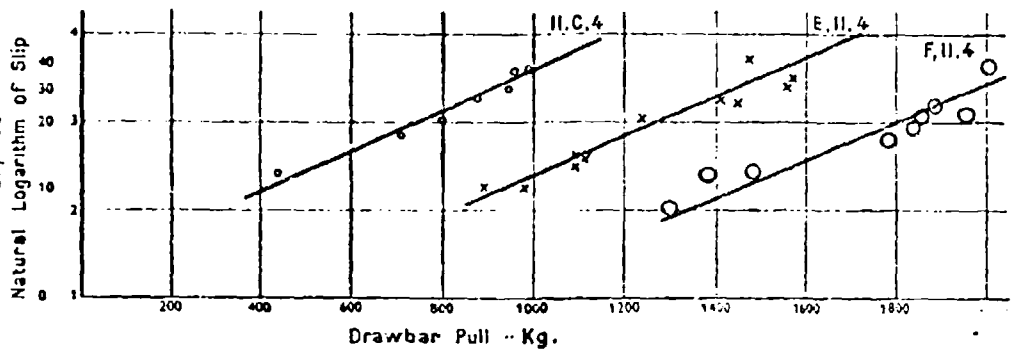


Fig. 8. — Rear half tracks and four-wheel drive vs ordinary tires.

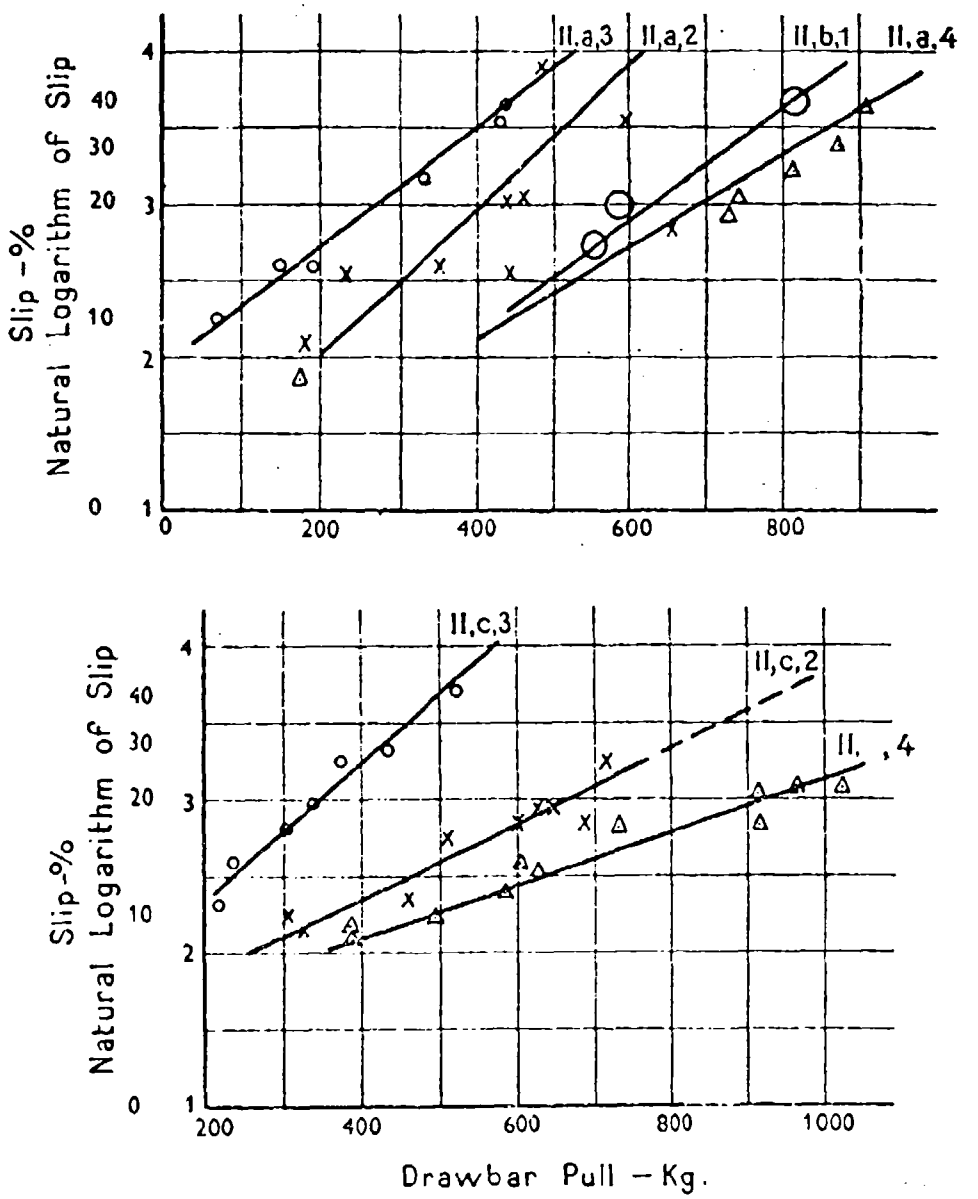
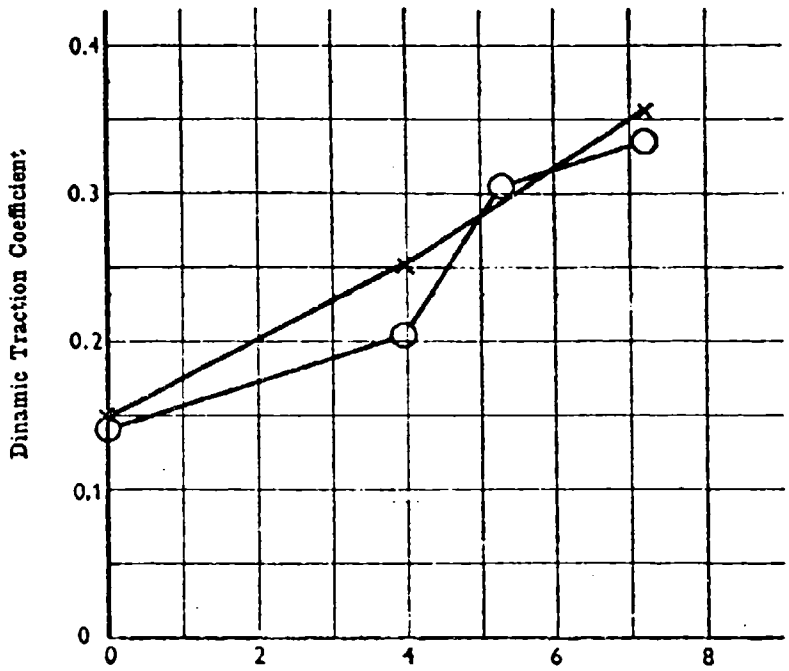


Fig. 9. — Traction as affected by soil.

a. Soil Strength measured by Penetrometer



b. Soil Strength measured by Vane Shear Apparatus

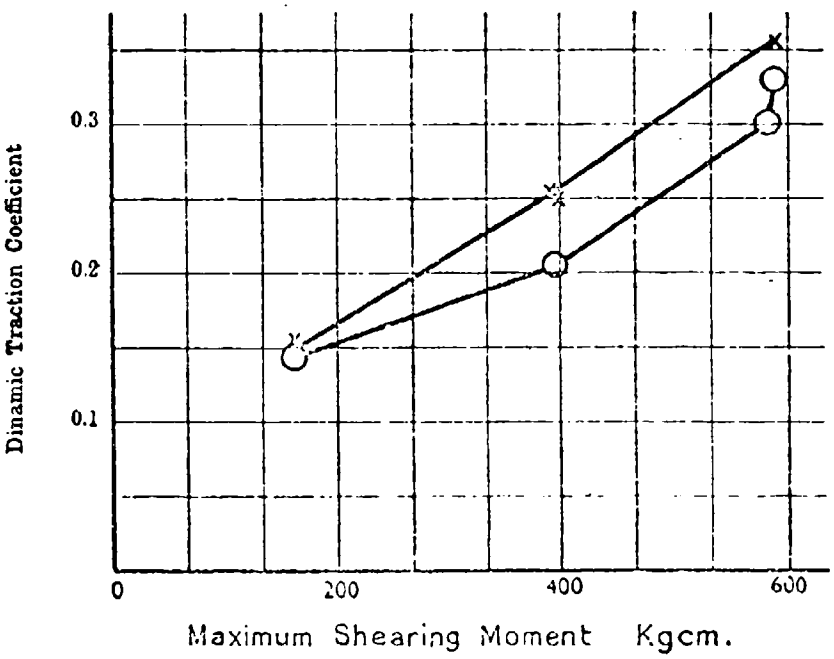


Fig. 19. — The dynamic traction coefficient vs soil strength.

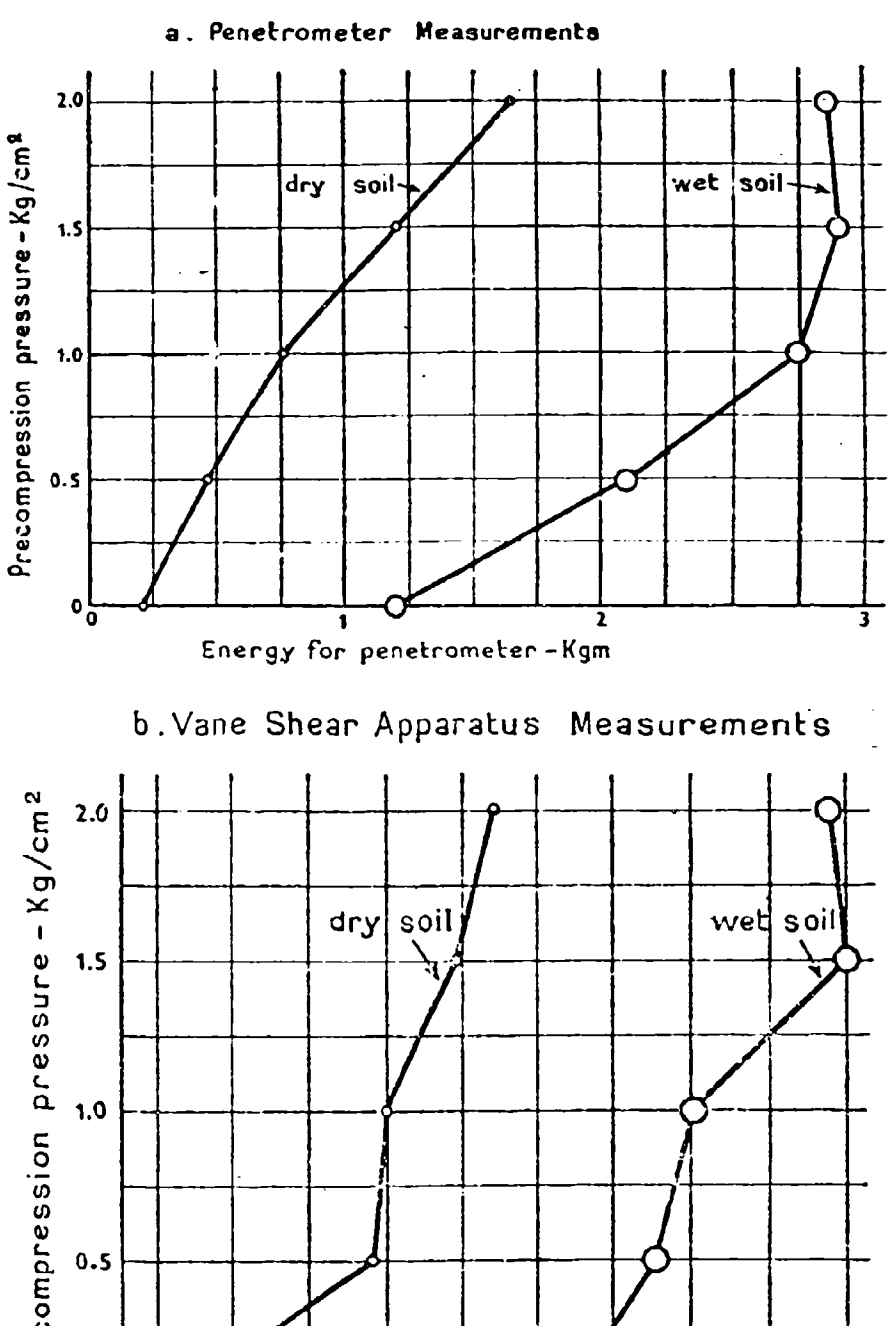
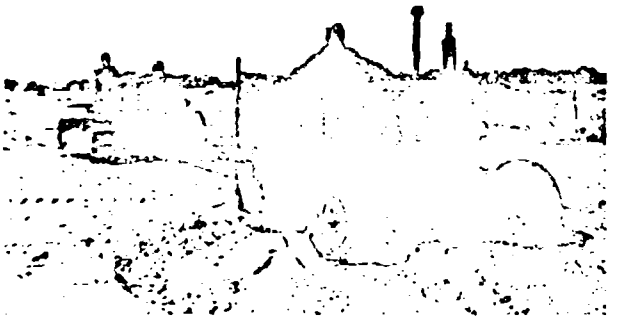


Fig. 11. -- Penetrometer and vane shear apparatus measurements in laboratory conditions.

Fig. 12. — Tracklayer as a regulating load for the tested tractor.



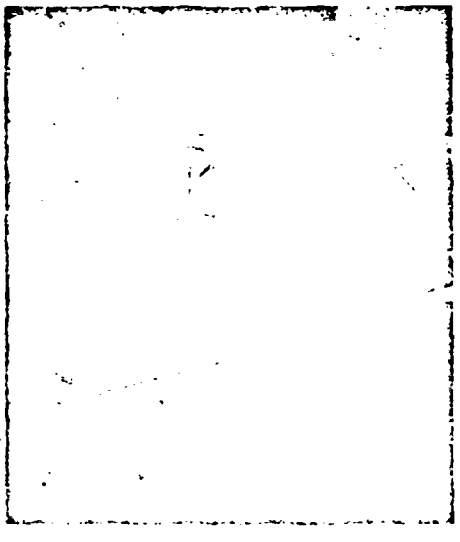


Fig. 13.
Recorder of amsler dynamometer.



Fig. 14. — Rolling resistance measurement.

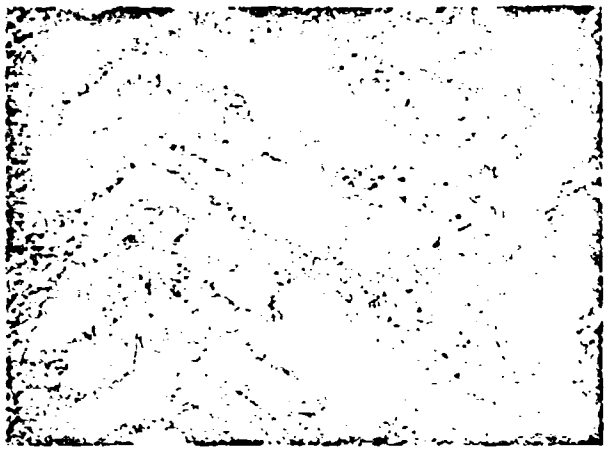


Fig. 15. — Tire patterns; left, reversed direction. Right, ordinary direction.

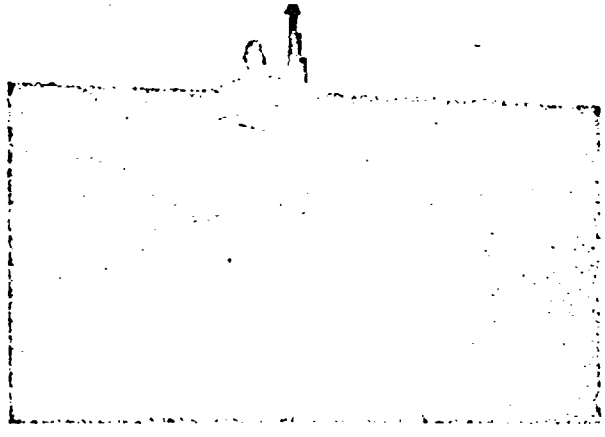


Fig. 16. — Dual tyres.

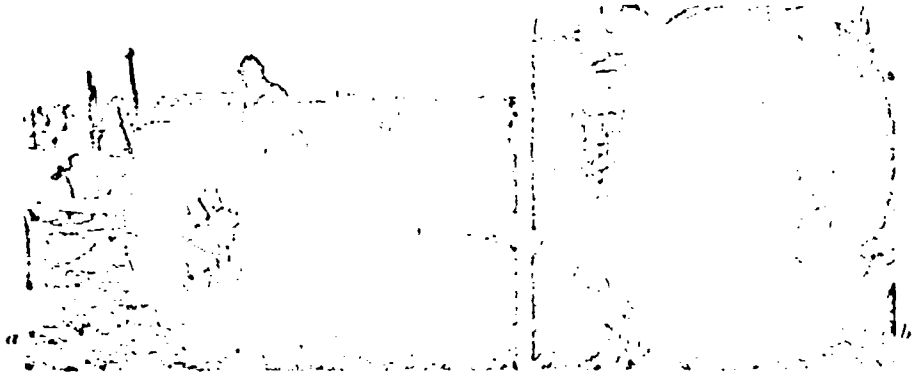
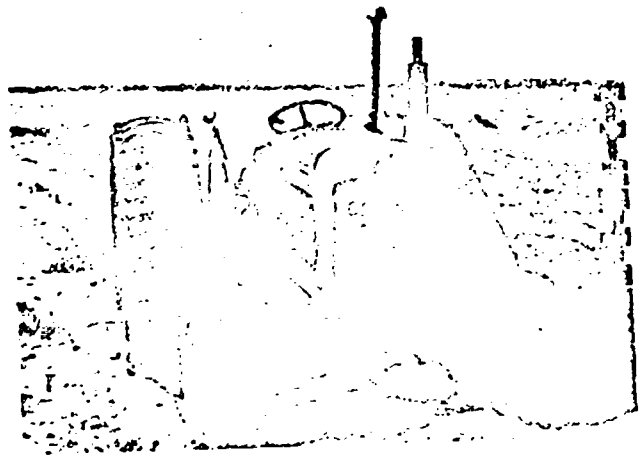


Fig. 17. — a) Retractable grousers in action. — b) Grousers out of action.

Fig. 18. — Front half track.



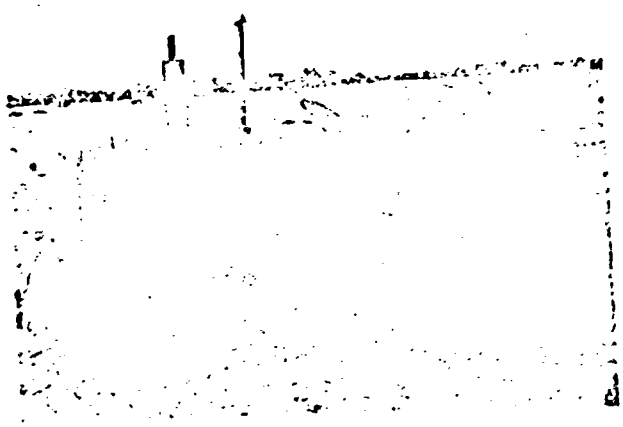


Fig. 19. — Rear half tracks.

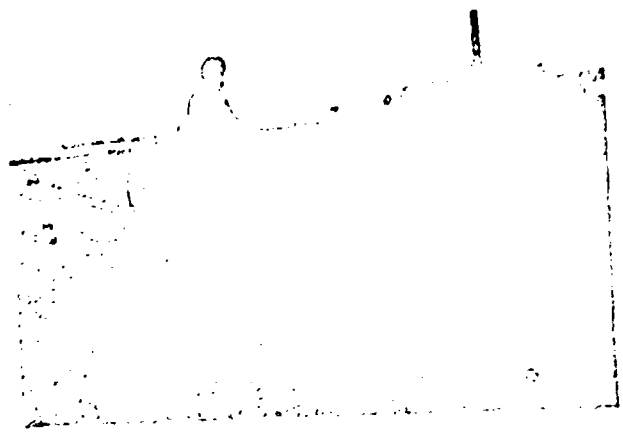


Fig. 20.
Four wheel drive tractor.

Conclusions

1). The exponential function $S = Ae^{BP}$, expressing the connection between drawbar pull and tire slip, fitted field observations well in the range of 0-50 % slip. This function permits analytical determination of maximum drawbar horse power and maximum tractive efficiency values.

2). Additional weight on the driving wheels caused an increase in drawbar pull at 20 % slip.

3). Additional weight on the driving wheels caused an increase in the dynamic coefficient of traction under all soil conditions except condition 3.

4). Additional weight on the driving wheels caused an increase in the maximum drawbar horse power. This output was achieved at high slip values (about 30 %) for most treatments. This exceeds the normal range of slip during work.

5). The maximum tractive efficiency increased only slightly with additional weight on the driving wheels.

6). No effect of forward speed on drawbar pull at 20 % slip or on maximum tractive efficiency was found for most treatments.

7). The data compiled in these tests enables determination of the optimal combination of weight on the driving wheels and forward speed that will insure more efficient use of engine power for pulling while limiting slip to 20 %.

8). Dual tires, retractable grousers and front half tracks proved inefficient as aids for increasing the traction of the wheeled tractors on sandy loess soils for all four tested conditions.

9). Rear half tracks increased slightly the dynamic coefficient of traction.

10). The four wheel drive tractor increased slightly the coefficient of traction for soil condition 4. Superior traction as compared to the ordinary tractor also arises form the total weight utilization realized in four wheel drive tractor.

11). Soil condition has a pronounced influence on the traction of a wheel-type tractor. A tendency toward correlation was found between penetrometer and vane shear apparatus data and the coefficient of traction.

Penetrometer measurements proved more sensitive to changes in soil strength than those of the vane shear apparatus for soils with non-uniform strength profiles.

12). Results permit a rough estimate to be made of the coefficient of traction through data obtained from one of the methods.

13). Future work wheel tractor action in sandy loess soils was investigated from the point of view of traction only. Other aspects of the problem, such as stability, steering, manoeuverability, etc. have yet to be investigated.

The economical aspect was also omitted from this work, although this will be a decisivie factor in determining the scope of wheel tractor use in these areas.

Field determination of soil strength and the correlation between soil strength data and traction in sandy loess soils have yet to be improved, and additional research is needed on this subject.

DISCUSSION

H. MEYER. — Meine Herren, ich glaube, dass aus den Vorträgen und Diskussionsbeiträgen dieses Vormittages gewisse Schlussfolgerungen gezogen werden können. Ich möchte den Ausführungen von Professor Bekker am Schluss der Tagung nicht vorgreifen, aber mir scheint es doch richtig zu sein, auf folgendes hinzuweisen.

Uns allen gemeinsam ist das Interesse an der Theorie, an der wissenschaftlichen Durchdringung der Vorgänge, um zu erfahren: warum sind die Dinge so? nachdem wir festgestellt haben: wie sind die Dinge? In der Anwendung der Theorie scheinen sich mir aber die Wege zu teilen, in einen landwirtschaftlichen und in einen mehr militärischen Weg, der sich weitgehend mit den Interessen des Erdbaues, der Exploration und ähnlicher Zwecke deckt.

Auf der landwirtschaftlichen Seite handelt es sich um die Ausübung einer Zugkraft durch einen im allgemeinen relativ leichten Traktor auf Arbeitsgeräte oder auf Fahrzeuge. Hierbei muss sehr auf den Boden Rücksicht genommen werden, damit er für die landwirtschaftliche Nutzung nicht geschädigt wird. Auf der militärischen und industriellen Seite handelt es sich aber in erster Linie um die eigene Fortbewegung der Fahrzeuge und der von ihnen getragenen Lasten, weniger um einen Zug angehängter Fahrzeuge.

Hier muss auf den Boden nur soweit Rücksicht genommen werden, wie es etwa nachfolgende Fahrzeuge verlangen. In der Diskussion ist die Frage nach dem Wirkungsgrad für den Fall aufgeworfen worden, dass keine Zugkraft ausgeübt wird. Diese Frage ist nicht weiter behandelt worden, sie ist aber für die militärische Seite wichtig.

Manche Bemerkungen deuten darauf hin, dass in Rücksicht auf die sehr unterschiedlichen Gewichte der militärischen und landwirtschaftlichen Fahrzeuge für die Untersuchung der Böden verschiedene Einrichtungen bei gleicher Methode verwendet werden müssen. Ich möchte glauben, dass wir allen Anlass haben, gemeinschaftlich unsere Anstrengungen für eine Verbesserung der Theorie zu verstärken, wenn wir auch in der Anwendung je nach Zielsetzung verschiedene Wege gehen müssen.

Ich darf mit diesen Bemerkungen die Vormittagssitzung schliessen und den Vortragenden und den Diskussionsrednern für ihre interessanten Ausführungen und für ihre teilweise erfreuliche Kürze danken.

SIMILITUDINE
FRA VEICOLI IN GRANDEZZA NATURALE
ED IN SCALA RIDOTTA

SIMILARITY BETWEEN FULL SIZE
AND SMALL SCALE VEHICLES

Problèmes de similitude: déclaration d'ouverture

Problemi di similitudine: discorso d'apertura

J. Truelle *)

Monsieur le Recteur, mon Général, Messieurs,

En ouvrant la session consacrée à la Similitude, je tiens tout d'abord à signaler que ma présence à cette table revêt une double signification:

1) Je représente ici le Secrétaire Général Adjoint de l'Alliance Atlantique, chargé des Affaires Scientifiques. Or la Division des Affaires Scientifiques de l'Alliance Atlantique, qui est dégagée des préoccupations militaires immédiates, s'intéresse essentiellement à la Recherche Scientifique fondamentale et à la Coopération Internationale dans ce domaine.

Ainsi, la participation de cette Division Scientifique à vos travaux marque tout l'intérêt que nous attachons à leur valeur, en tant que Recherche Scientifique faite en coopération.

2) Réciproquement, l'invitation que vous nous avez faite d'apporter notre contribution à votre Conférence démontre aussi tout l'intérêt que vous portez à l'activité scientifique de l'Alliance Atlantique, et au nom de la Division Scientifique de cette Alliance, je vous en remercie.

Abordant maintenant le sujet dont nous allons discuter, je crois utile d'attirer votre attention sur l'importance des études qui y ont été consacrées.

Les études de similitude, qui conduisent à expérimenter sur des modèles réduits, permettent de faire des économies très sensibles sur les frais d'essai, mais aussi de gagner beaucoup de temps; et c'est ce dernier facteur qui me paraît le plus important.

En prenant connaissance des communications déjà faites ici-même, j'ai été très impressionné par la variété infinie des sols sur lesquels doivent se déplacer des véhicules appropriés, et subséquemment par le nombre des solutions les plus diverses qui ont été imaginées pour résoudre ces problèmes multiples.

Une imagination fertile comme celle du Comte Bonnartini a largement pourvu ces techniques de la mobilité d'une grande richesse de solutions théoriques, et de réalisations concrètes.

Mais M. Bonnartini lui-même nous dirait qu'au stade de l'invention, il est souvent difficile de faire un choix entre des solutions diverses, qui ne peuvent être essayées toutes, ne serait-ce, par exemple, pour la seul raison qu'on ne peut pas attendre la pluie favorable pour obtenir exactement le type de terrain prévu. Les méthodes de la similitude ont été une solution élégante à ces genres de problème.

Remarquons toutefois que, dans le domaine des terrains, la théorie de la similitude est singulièrement plus difficile qu'en Aérodynamique, où elle s'est montrée si féconde: il ne s'agit pas seulement de faire des comparaisons entre des ensembles complexes

*) Président de la Session.

où les longueurs, les surfaces et les volumes ne varient pas dans la même proportion, mais où par surcroît le milieu par rapport auquel on se déplace ne peut plus être assimilé à un fluide homogène.

Ainsi, le sol peut être considéré tantôt (mais rarement) comme un fluide homogène, tantôt comme un solide discontinu, tantôt comme un corps intermédiaire, avec dans tous les cas des effets de caractère capillaire au contact du véhicule avec le sol.

Il va sans dire que, pour analyser tous ces phénomènes, comportant un grand nombre de paramètres variant dans de très larges limites, de nombreux calculs sont nécessaires, et que dans ce domaine comme en bien d'autres, pour définir l'appareil optimum correspondant à un ensemble de conditions données, la Recherche Opérationnelle est appelée à jouer un rôle considérable.

Pour terminer, je ferai une simple remarque d'ordre personnel en rappelant que les trois Auteurs qui vont présenter des communications font tous appel aux références scientifiques antérieurement établies par le Professeur Bekker: c'est un hommage implicite au Maître, qui a sans doute apporté le premier une contribution essentielle à la théorie de la locomotion.

A similitude study of the drag and sinkage of wheels using a system of soil values related to locomotion *)

Studio su modelli simili della resistenza all'avanzare e dell'affondamento delle ruote usando un sistema di caratteristiche del terreno relative al movimento

HENRY H. HICKS, jr. **)

ABSTRACT. — *Analytical and experimental studies of wheel performance in soils have been hampered by the lack of a valid system of soil values. The sinkage parameters constitute one proposed system of soil values which have been used with some success in the prediction of wheel performance by analytical means, but there is generally no way to distinguish between those discrepancies that are chargeable to the analysis and those that may be due to a possible inadequacy of the soil value system.*

In the work presented here, a successful similitude correlation of wheel performance in sand was obtained using the sinkage parameters. This confirms their validity for sand, and defines the method for extending the correlations to cohesive soils. The tests were made in the laboratory under simulated field conditions, and include an investigation of wheel sinkage and drag as related to wheel shape, diameter, load, and soil depth.

Introduction

Theoretical and experimental investigations of the drag and sinkage of wheels in soil were initiated long ago[1]. Early experimental investigations consisted of isolated tests conducted without reference to quantitatively measured soil properties, and the results obtained are therefore unrelated to each other, or to any particular system of soil-wheel mechanics.

Theoretical investigations have been hampered fundamentally by the lack of a generally valid system of soil parameters and practically by the complexity of the analytical methods. These efforts have nevertheless produced some working formulas for the prediction of wheel performance that are fairly accurate over limited ranges of conditions, but precise predictions of broad applicability have yet to be achieved.

About a decade ago, Nuttall[2] conducted an investigation of wheel performance by testing scale models in the laboratory. In this investigation, two of

*) This paper was originally prepared for Land Locomotion Laboratory, U.S. Army, Ordnance Tank Automotive Command, Detroit, Michigan.

**) University of Michigan Research Institute, Ann Arbor, Michigan.

the sinkage parameters proposed by Bernstein[3] were redefined in terms of the Coulomb soil properties. The third parameter was retained as well as the essential form of Bernstein's prediction equations. Good correlations were obtained over a limited range of test conditions, but even so there are several objections to be made to this work. For example, no rational argument is given for discarding part of the sinkage parameters. Furthermore it is nearly certain that the Coulomb properties are inadequate to describe the unconsolidated soils on which vehicles frequently operate. In addition, by redefining a part of the sinkage parameters in terms of basic soil properties, there remains an incomplete accounting for the inhomogeneities the soil may have. Finally, a scale effect exists between model and prototype that was not considered, but this has apparently not been considered by anyone else previously.

With these objections in mind, but believing that the scale-model-laboratory approach has great potential application and value, an investigation has been conducted at the University of Michigan to determine if scale-model wheel tests can be correlated on a similitude basis using the sinkage parameter system of soil values. This investigation is continuing, and the results to date are most encouraging.

Theory

Rational analyses[2] indicate there is an intimate connection between wheel sinkage and drag. Thus, it is reasonable to assume that they are both functions of the same independent variables. Among these variables are those termed the sinkage parameters. The sinkage parameters considered here are those advocated by Bekker[1] and are obtained from the stress-strain relationship obtained by forcing a rectangular flat plate into the soil with an instrument called a bevameter. The parameters obtained are as follows:

k_ϕ = Sinkage modulus (frictional) lb/in^{n+2};
k_c = Sinkage modulus (cohesive) lb/in^{n+1};
n = Sinkage index (Non. Dim.).

For low-speed tests on solid, rectangular cross-sectional, wheels the remaining independent variables are taken to be,

d = Wheel diameter (in.); Wheel aspect ratio (Non. Dim.);
D = Soil depth (in.); Coeff of friction (soil-wheel);
W = Wheel load (lb).

Dependent variables are,

R = Wheel rolling resistance (lb);
z = Wheel sinkage (in.).

In evaluating the sinkage parameters it is assumed that the stress-strain relationship is expressible by an equation of the form

$$p = (k_\phi + k_c/b)\, z^n \tag{1}$$

and the sinkage parameters are the constants of this equation.

A dimensional analysis of the above listed variables yields the following equations:

$$R/W = (d/D)^{a_1}\,(W/d^{n+2}k_\phi)^{a_2}\,(k_c/dk_\phi)^{a_3}\,(n)^{a_4}\,(\alpha)^{a_5}\,(\mu)^{a_6} \tag{2}$$

$$z/d = (d/D)^{b_1}\,(W/d^{n+2}k_\phi)^{b_2}\,(k_c/dk_\phi)^{b_3}\,(n)^{b_4}\,(\alpha)^{b_5}\,(\mu)^{b_6} \tag{3}$$

Since it was decided to study the effect of the independent variables W, D, d, and α on the dependent variables z and R, the model rules require the following conditions to be met:

$$k_c = c_1\, d\, k_\phi \tag{4}$$

$$W = c_2\, k_\phi\, d^{n+2} \tag{5}$$

$$D = c_3\, d \tag{6}$$

These equations require that, to obtain complete similitude with geometrically scaled models, the tests must be conducted in soils whose qualities change as the scale of the model changes. More specifically, laboratory test soils must be available in which k_c may be varied independently of K_ϕ, n, and μ.

We do not yet have the ability to compound laboratory test soils that will satisfy these particular requirements, but progress is being made on the problem and for the present valuable work may be done in sand for which k_c is essentially zero. For this soil the model rules require only that

$$W = c_2\, k_\phi\, d^{n+2} \tag{5}$$

$$D = c_3\, d \tag{6}$$

These conditions can be met in a single soil.

The particular forms of equations (2) and (3) permit a considerable simplification in testing, for by taking the soil parameters only in semi-infinite homogeneous beds with a single bevameter plate, the soil parameters are constant for all conditions of test. Changes in the boundary conditions due to finite test bed depth are accounted for by the depth coefficient (d/D). Those effects due to wheel shape are accounted for by the aspect ratio α. These are the conditions that have been applied in our laboratory tests which are believed to be of the utmost value in relating these tests to practical field conditions.

The d/D ratio represents a type of inhomogeneity which is easily produced in the laboratory and simulates what is probably the most frequently occurring inhomogeneity of natural soils; namely that of a more or less homogeneous soil bed overlying a hard pan at some depth.

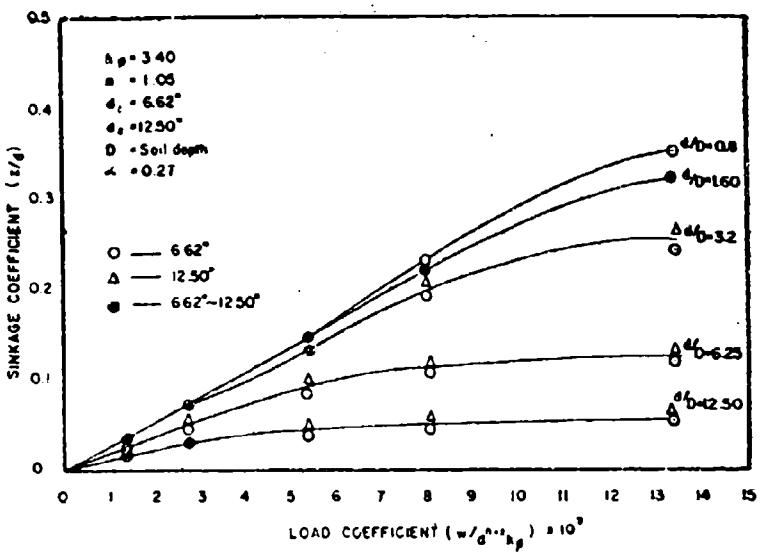


Fig. 1. — Plot of non-dimensional sinkage coefficient (z/d) vs. non-dimensional load coefficient ($w/d^{n+2}k_\phi$) for rectangular cross-sectional wheels.

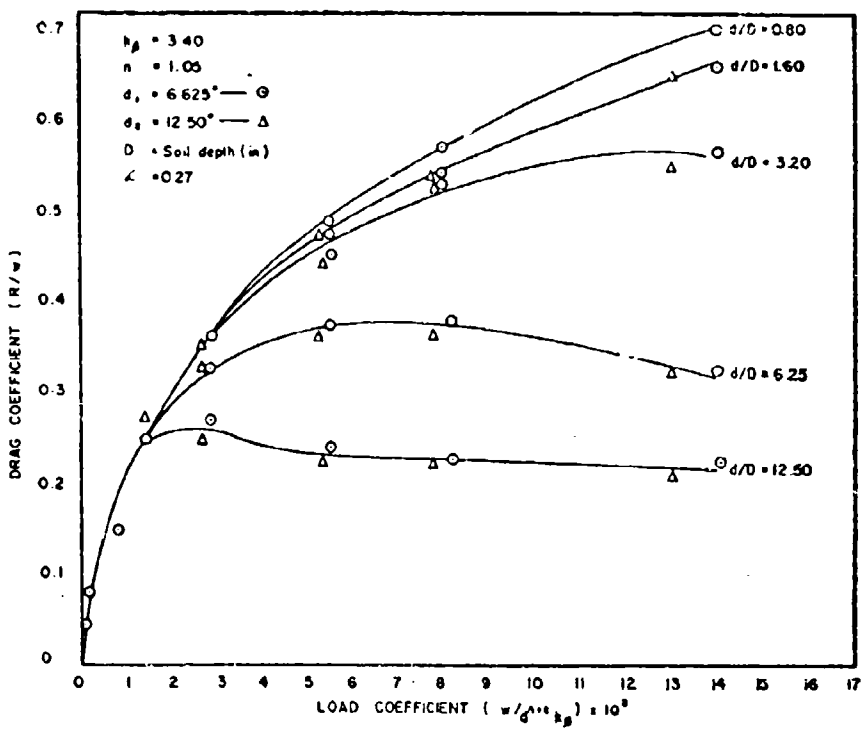


Fig. 2. — Plot of non-dimensional drag coefficient (R/w) vs. non-dimensional load coefficient ($w/d^{n+2}k_\phi$) for rectangular cross-sectional wheels.

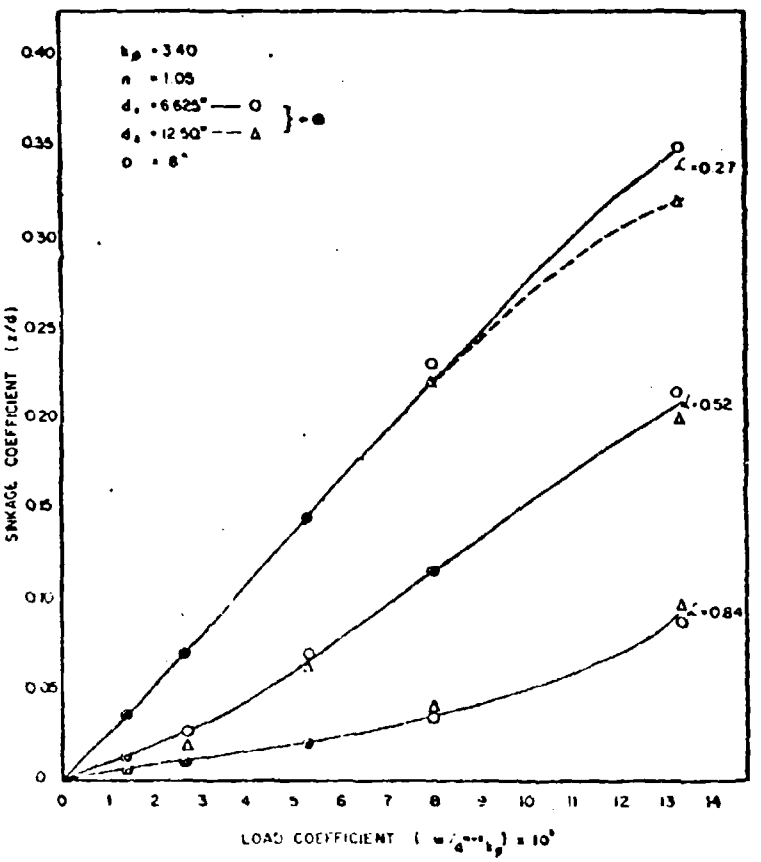


Fig. 3. — Plot of non-dimensional sinkage coefficient (z/d) vs. non-dimensional load coefficient ($w/d^{n+2}k_\phi$) at various aspect ratios for rectangular cross-sectional wheels.

Experimental work

In accordance with the preceding theory, low-speed drag and sinkage tests were conducted on two geometrically similar, solid, aluminum wheels of rectangular cross section, the diameters of the wheels being 6.625 in. and 12.50 in. The aspect ratios of the wheels tested were 0.27, 0.52 and 0.84. The soil used was a sand for which k_ϕ = 3.40 and n = 1.05 are most probable values. The tests with variable aspect ratio were conducted in deep beds of soil corresponding to practically semi-infinite conditions, while the tests conducted in various depths of soil were made at the single aspect ratio α = 0.27. All tests were conducted at the relatively low speed of 0.25 ft/sec. This was done because experimental difficulties are minimised at low speed,

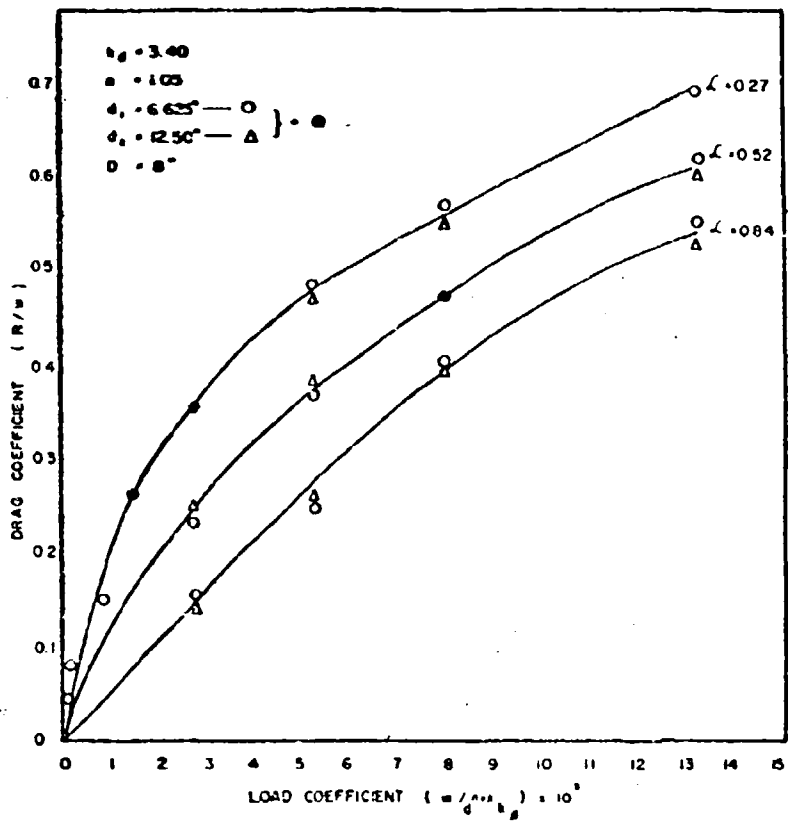


Fig. 4. — Plot of non-dimensional drag coefficient (R/w) vs. non-dimensional load coefficient ($w/\delta^{n+2} k_\phi$) at various aspect ratios for rectangular cross-sectional wheels.

and is justified by the results of other tests[5] which showed the effect of speed to be negligible below a speed of 5.0 ft/sec. with a 12.5 inch diameter wheel.

It should be noted that unexpected experimental difficulties are encountered in a work of this type. The principal difficulty is the preparation of the soil to a uniform and repeatable consistency. This problem was never completely solved and consequently the data presented here represent the mean of many test runs, in some cases numbering twelve. Another problem is associated with the large span of forces to be measured, covering a range of approximately a hundred to one. This demands considerable precision and ruggedness in the test apparatus, qualities that are somewhat mutually exclusive.

The test results are given in figures 1-4. In figures 1 and 2, the sinkage and drag coefficients are given vs the load coefficient with the depth ratio as a parameter. In figures 3 and 4, the sinkage and drag coefficients are given vs the load coefficient with the aspect ratio as a parameter.

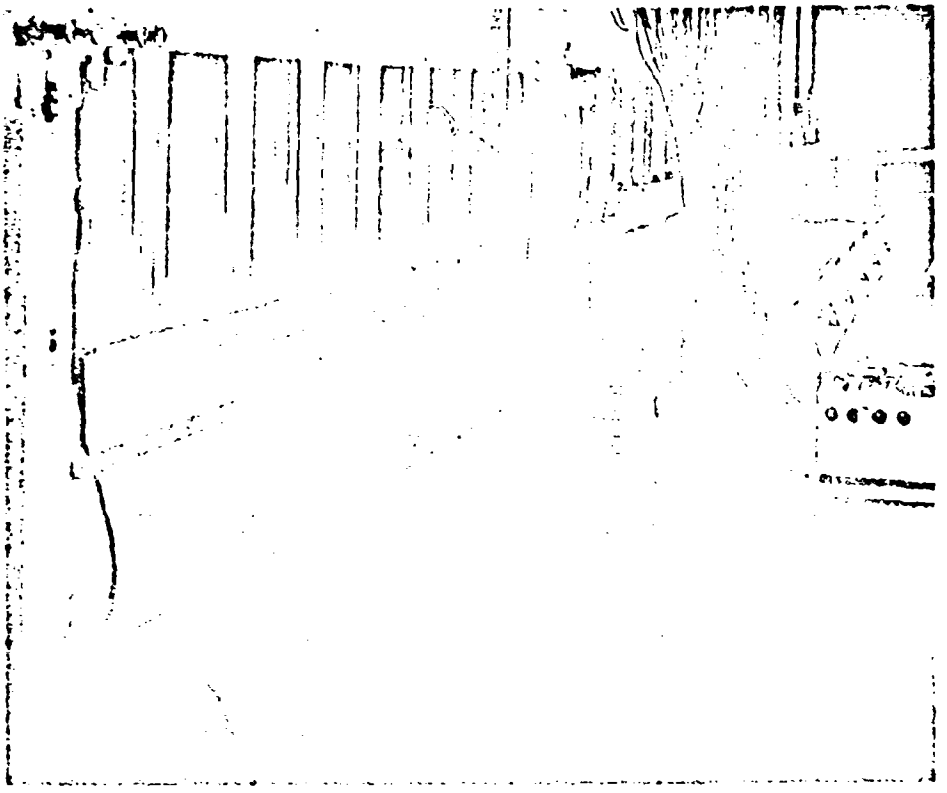


Fig. 5. — General view of test facility.

A general view of the test apparatus is shown in figure 5, and a detailed view of the wheel carriage is shown in figure 6.

Discussion

The plotted data make it apparent that a high degree of similitude has been attained in the tests, and that the independent variables selected are appropriate to the system. Accordingly, the results should be applicable to wheels of any scale as long as the assumed parameters are maintained. It is consequently important to consider carefully what this condition requires.

The sinkage parameters used are those obtained with a single (1 by 3 in.) bevameter plate, penetrating a semi-infinite bed of homogeneous soil. This means that the parameters obtained depend only on the inherent mechanical properties of the soil, and on the shape and size of the bevameter plate. If a different soil is placed under the bevameter plate, changes in the sinkage parameters will result which can be due only to changes in the mechanical properties of the soil.

Consistent with this framework of ideas, there exists a particular wheel having some diameter and aspect ratio, whose sinkage characteristics are similar to those of the bevameter plate used. In other words an analogy exists, and because of this any variations in the basic mechanical properties of the soil will not only produce changes in the sinkage parameters as measured by the bevameter, but will also cause a change in the sinkage of the wheel.

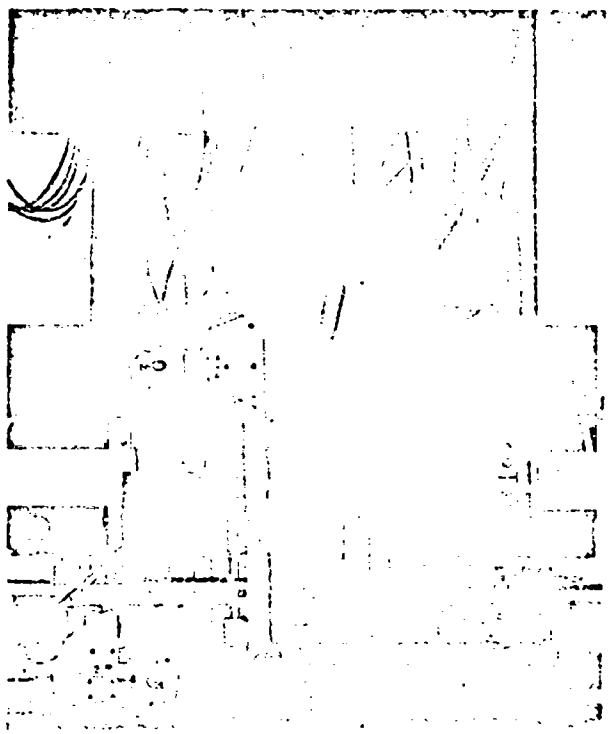


Fig. 6. — Detailed view of wheel carriage.

Consequently the sinkage of the analogous wheel is uniquely related to the measured sinkage parameters.

If a fixed quality soil and variable geometry wheel are considered instead of the converse above, then variations in the size and shape of the wheel produce sinkages that are related to the sinkage of the analogous wheel and hence to the sinkage parameters through these geometrical variations alone. The preceding reasoning is now repeated, but the soil is considered to be of finite depth and the first effect to be observed is that a new set of sinkage parameters is obtained that is related to the original set by some factor that describes the relative « infiniteness » of the boundaries. The ratio of the characteristic dimension « b » of the bevameter plane to the soil depth « D » or specifically the b/D ratio is a factor that satisfies this requirement. It is

further evident that the analogous wheel will describe a new sinkage that is uniquely related to the new sinkage parameters, but also to the original sinkage parameters through the b/D ratio. Similarly, new relations describing the effects on sinkage of changes in wheel geometry and soil quality will be obtained that are related to the original relations through the b/D ratio. Finally since there exists an analogous wheel of characteristic dimension « d », all effects of changes in soil depth may be related to the ratio d/D instead of the ratio b/D. It is thus possible to construct a self-consistent system based on analogy, which preserves the idea of sinkage parameters that are determined by soil properties only and which accounts for variations in wheel geometry and soil depth. In this system, it is obviously necessary to take account of the d/D ratio in the correlation of test results, as this is the source of the scale effect mentioned earlier. Failure to do this can lead to difficulties in obtaining correlations. This was observed by Ozako and Bekker[6] in an attempt to obtain sinkage parameters from the analysis of tests on wheels. Wheels of a range of diameters were tested in a bed of soil of fixed depth, and only one of these wheels having a particular diameter gave sinkage parameters comparable to those obtained with the bevameter. Apparently the analogy of wheel, soil, and bed depth to bevameter, soil, and bed depth was an optimum for this particular wheel. This observation is a manifestation of the scale effect and this difficulty has been entirely overcome in the present tests by observing the depth ratio (d/D).

An infinite variety of conditions exist with natural soils in the field, but it is believed that the most frequently occurring condition is that of an approximately homogeneous soil overlying a hard pan at some depth. To the degree that this is true, the results given here should be applicable to natural soils in the field.

It was noted earlier that prior theory and experiment had produced working formulas for wheel drag that were fairly accurate over limited ranges of conditions. One of these equations due to Bernstein[3] can be expressed in the form:

$$R/W = 0.86\ (W/\alpha\, k\, d)^{n-1.3}$$

and another due to Nuttal[2] and applicable to sand can be expressed as:

$$R/W = 0.50\ (W/\alpha^{n-2}\, g\, \rho\, d^4)^{n-1}$$

Both of these equations, especially Nuttall's, predict drag coefficients that are in reasonable agreement with selected areas of the data presented here, but neither of them follows the trend of aspect ratio very well. A better understanding of the source of this divergence can be obtained by writing these equations for a wheel of variable width which carries a constant load « c » per unit of width. For these conditions the formulas reduce to:

$$R/W = 0.86\ (c/k\, d^2)^{n-1.3}$$

and:

$$R/W = 0.50\ (c/g\, \rho\, d^2)^{n-1}\, \alpha^{n-2}$$

In the first case it is seen that the aspect ratio drops out entirely, implying that shape has no effect on the drag coefficient and that end effects are negligible. In the second case it is apparent that

$$\lim_{a \to \infty} R/W = \infty$$

and:

$$\lim_{a \to 0} R/W = 0$$

There is no physical basis for these conclusions nor do the data support them. It is apparent, moreover, that additional analytical work is needed in this area.

One of the more interesting features of the drag data is the way the drag coefficient decreases with large loads in shallow soils. This possibly may have practical application, but in any event this result demonstrates the value of conducting experiments that simulate natural soil conditions.

The effect due to variation of aspect ratio also has some interesting features. The increase of the drag and sinkage coefficients of the low-aspect-ratio wheels is apparent. Some considerations in logic indicate that the drag coefficient may become infinite for zero aspect ratio wheels, but approaches a limiting finite value for infinite-aspect-ratio wheels.

Conclusions

It is concluded from the work presented here that the sinkage parameters are appropriate variables for predicting the drag and sinkage of wheels in beds of homogeneous sand of varying depth. The application to cohesive soils of the approach made here depends on the development of suitable laboratory test soils, and it now appears that this problem can be practically solved.

Nomenclature

b = Wheel width or characteristic dimension - L, (in.).
c = Proportionality constant - n.d.
d = Wheel diameter - L, (in.).
D = Soil depth - L, (in.).
g = Acceleration due to gravity - L/T^2 (ft/sec^2).
k_c = Sinkage modulus (cohesive) - F/L^{n+1} (lb/in.$^{n+1}$).
k_ϕ = Sinkage modulus (frictional) - F/L^{n+2} (lb/in.$^{n+2}$).
n = Sinkage index - n.d.
R = Wheel rolling resistance - F, (lb).
W = Wheel load - F, (lb).
z = Wheel sinkage - L, (in.).
α = Wheel aspect ratio - n.d.
μ = Coef. on friction (wheel to soil) - n.d.
ρ = Soil density - M/L^3 (slugs/ft^3).

BIBLIOGRAPHY

1) **Bekker M. G.** Theory of land locomotion. Univ. of Mich. Press, Ann Arbor, 1956.

2) **Nuttall C. J.** The rolling resistance of wheels in soil. Stevens Inst. of Tech., Hoboken, New Jersey. Exp. Towing Tank Rpt. no. 418, July 1951.

3) **Bernstein R.** Problem einer experimentellen Motorfluguechanick. Der Motorwagen, 16, 1913.

4) **Bekker M. G.** Off the-road locomotion. Univ. of Mich. Press, Ann Arbor, 1960.

5) **Vincent E. T., Hicks H. H. Jr.** and **Kapur D. K.** Performance coefficients for free running wheels in sand, UMRI Rpt. 2544-31-F, Ann Arbor, July 1960.

6) **Czako T.** and **Bekker M. G.** Determination of vehicle sinkage parameters by means of rigid wheels, part I, dept. of the army, O.T.A.C., Land Locomotion Laboratory, Rpt. no. 33, Center Line, Mich., May 1958.

N. 42

Scale models of vehicles in soils and snows

Studio su modelli in scala del movimento di veicoli su terreno e su neve

C. J. Nuttall Jr. *) - R. P. McGowan **)

ABSTRACT. — *The history of research into the use of scale-models to study vehicle performance in soils is reviewed. The current research program in this field of the U.S. Army Transportation Research Command is outlined, and a method for characterizing soils and snows for scale-model test purposes, growing out of this work is presented. Some correlations between scale-model and full-size performance in natural snow and sand terrains are given. Finally, design data on the performance of 4 × 4 pneumatic-tired vehicles in sand and snow are offered together with appropriate information on probable minimum material strengths to be anticipated. The current dimensional analysis upon which the research is based is presented in detail in an appendix.*

The place of scale-models and dimensional reasoning in vehicle-soil research. — It is important, in beginning any discussion of vehicle-soil scale-models, to emphasize that the understanding of fundamental vehicle-soil relationships necessary to prepare a valid, useful dimensional analysis — a prerequisite to proper understanding of scale-model systems — is precisely the same as the minimum required to undertake any more formal analysis of equal validity. Research in the use of scale models deals primarily with identifying the basic factors influencing vehicle-soils systems behavior. Results of this research are thus of fundamental interest quite apart from whether or not scale-models are useful or practical in studying any particular design problem. The same minimum understanding may be reached by other paths, but, however reached, it must stand the same test of predicting effects of simply changing the scale of the system.

As a matter of fact, the research summarized below has not only clarified many basic vehicle-soil interactions, but has also resulted in the development of practical, economical techniques for the use of scale-model tests in direct support of vehicle design work. This is fortunate, because the complexity of natural terrains and of real vehicles is so great as reasonably to preclude — within the scope of support that this type of study normally receives — complete solutions to practical problems solely by mathematical means.

Background of scale-model vehicle work. — Although Kamm and Schmid, during the late 1930's, used scale-models to study the dynamic behavior of

*) Wilson, Nuttall, Raimond, Engineers, Inc. Chestertown, Maryland.

**) U.S. Army Transportation Research Command, Ft. Eustis, Virginia.

vehicles on highways (ref. 1), consideration of the use of models to study soft-ground crossing performance appears to have begun with Markwick, in a short wartime note for the British « Mud Committee » (ref. 2). Markwick prepared a simple dimensional analysis of the problem, based upon the assumption that the soil could be characterized in terms of its Coulomb coefficients (c, cohesion; and Φ, angle of internal friction), its density, and a viscosity coefficient. He pointed out the several dilemmas raised by his analysis from the view point of practical scaling procedures, but concluded that scale-model methods probably could be developed. The current dimensional analysis of the problem, which is but little changed in fundamentals from Markwick's original proposal, is given in appendix I.

The first serious experimental exploration of the use of scale-model vehicles in soils began in late 1945, under the auspices of the U. S. Army Ordnance Corps, at the Davidson Laboratory (then the Experimental Towing Tank). This work started by attempting to validate Markwick's analysis experimentally. Tests were conducted in the laboratory with families of small wheels rolling slowly in a light loam having low moisture content, and in an air-dry silty sand. At the time that this program was suspended in 1949, positive results had been achieved for the limited range of soils considered (ref. 3). Shortly thereafter an independent study was begun in England by M'Ewen and Willetts which embraced a larger range of test objects, and reached substantially the same conclusions (ref. 4, 5).

Since that time scale-model/dimensionally-oriented research, per se, has been continued by the U. S. Army Transportation Research Command (USATRECOM) from 1956 to date (ref. 6-11), and by the University of Michigan from 1958-1960 [12]. The latter work was based upon laboratory tests in sand, and was hampered for a time by an attempt to utilize dimensionally unsound parameters to describe the soil.

Outline of the complete USATRECOM program. — The USATRECOM program to develop vehicle mobility scale-model understanding for all types of soft terrain was initiated in 1956. The approach was to postulate the types of mechanical behavior involved, to conduct critical tests within the framework of the dimensional analysis based upon these postulates, and to modify and simplify the analysis in accordance with the test results until a satisfactory level of correlation was achieved. It has now been demonstrated that, by proper dimensional treatment, scale-model test results can be interpreted not only in terms of the performance of a wide range of similar vehicles of different size from the one tested, but also for a range of terrain conditions as well.

The USATRECOM program used geometric scale-models of existing vehicles, and the tests were planned so that direct comparisons of model and full-size performance could be made. The scale ratios were made large (about $\frac{1}{4}$) and the tests performed in the field in essentially natural terrains. This eliminated the problem of reproducing natural terrains in the laboratory, and permitted direct comparison of model and full-size test results in the same real terrains of interest. This was desirable because natural terrains are, in general,

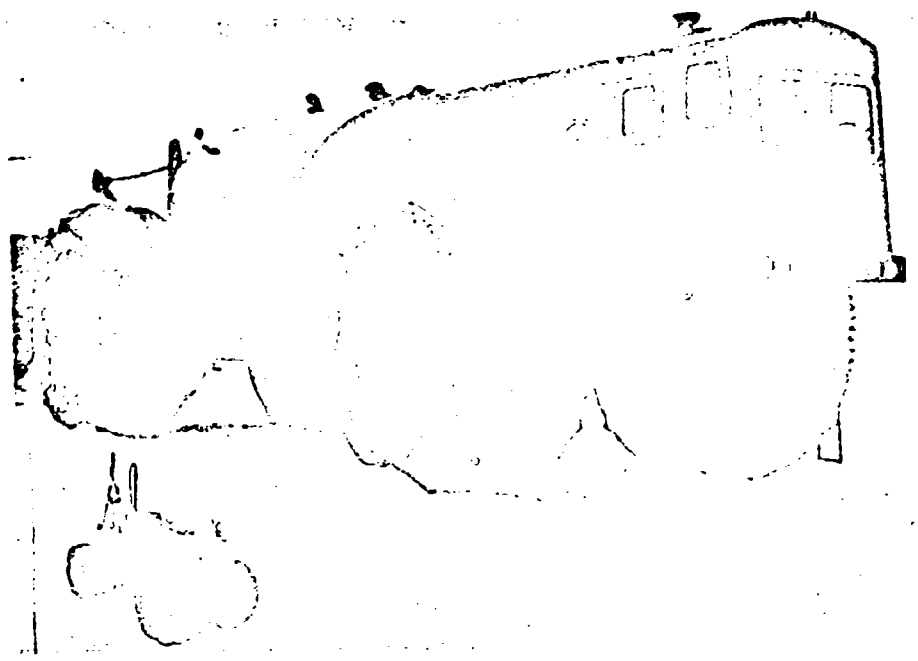


Fig. 1. — Logistical cargo carrier and ¼ scale model.

highly stratified in horizontal planes. This stratification is a characteristic that strongly affects actual vehicle performance. The relatively large (but entirely practical) scale-ratios made the size of the models commensurable with the expected dishomogeneities in natural conditions, and minimized errors associated with any necessary neglect of proper scaling of secondary factors.

The first tests were made in snow with the power car of the U. S. Army Logistical Cargo Carrier (LCC) and a ¼ scale model of it (fig. 1). The LCC power car is a 4 × 4, 30-ton vehicle utilizing tires 16 feet in diameter and 4 feet wide. In typical sub-arctic snows, this heavy vehicle operates only when limited snow depth permits « ground support ». Correlations were obtained between the model and full-size prototype primarily on the basis of snow depth, although the manner of reducing snow depth for the model tests resulted in an essentially constant snow condition for the model tests [6].

Further correlation tests in snow were conducted in Michigan, during 1957 and 1958, with a lightweight wheeled vehicle capable of operating in soft snows of any depth; i.e. a « flotation » vehicle (Marsh Buggy); and a model to approximately ¼ scale (fig. 2). In 1959, the dimensional/scale-model understanding was applied in tests that evaluated the « flotation » performance of a wide range of other tire shapes. (See appendix II and fig. 3). In 1960, this work was extended to include performance in the « ground support » region of loads, snow strengths, and snow depths [7].

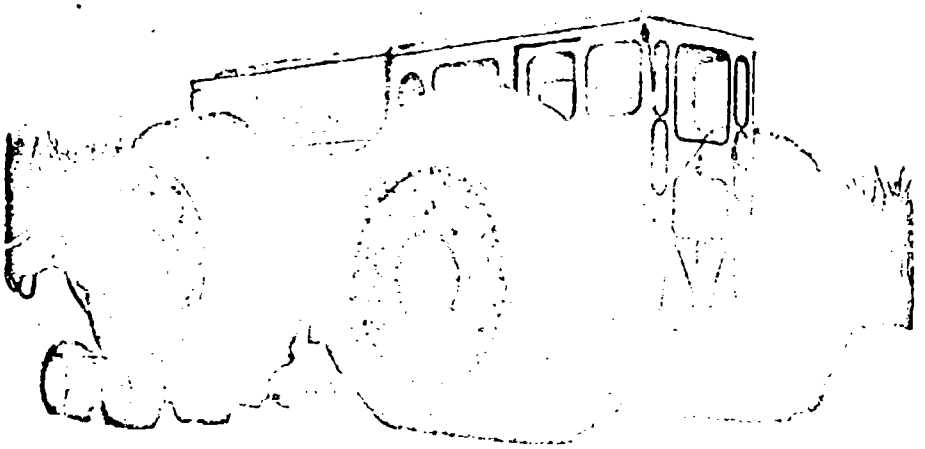


Fig. 2. — Marsh Buggy and ¼ scale model.

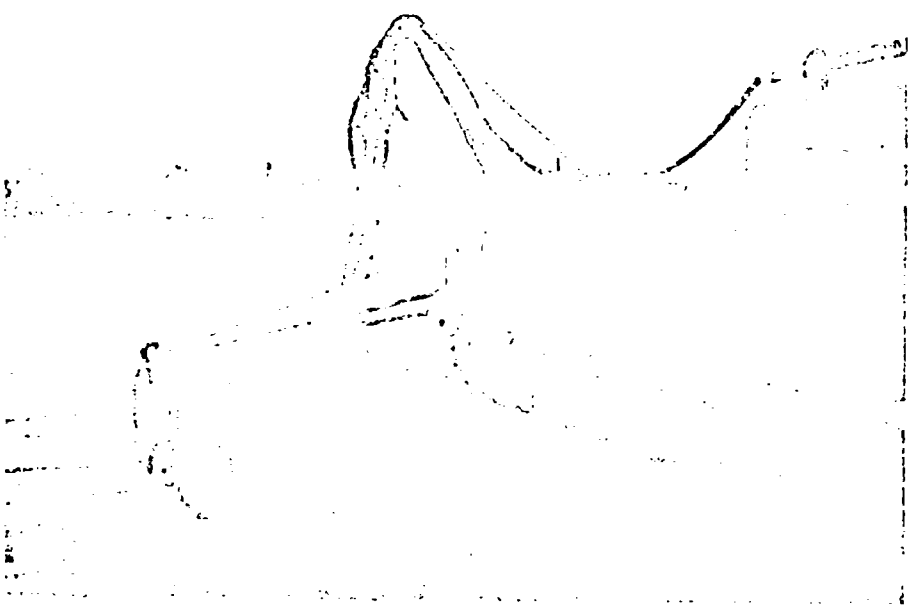


Fig. 3. — Snow flotation test in progress.

Correlation tests were conducted with the LCC and its ¼ scale model in beach sands during the summer of 1956. Further correlations in sand were developed with the Marsh Buggy and other full-size vehicles and models during 1958, 1959, and 1960 [8, 9]. The dimensional/scale-model capability was again exploited in the evaluation and analysis of the performance of a wide range of tire shapes [9].

A method for characterizing soils and snows for scale-model test purposes. — In appendix I will be found the current dimensional analysis on which the research is based. This presentation concludes with functional equations for operation in sands, dry snows, and other primarily frictional materials, as follows:

$$z = d\,\Theta \quad (W/c_s d^2,\ \Phi,\ S,\ h/d) \tag{1a}$$

$$D = W\,\Theta' \quad (W/c_s d^2,\ \Phi,\ S,\ h/d) \tag{1b}$$

$$\alpha = \Theta'' \quad (W/c_s d^2,\ \Phi,\ S,\ h/d) \tag{1c}$$

where the symbols are as defined in the appendix. If tests are run in a terrain for which the dynamic internal friction of the material (Φ) may be presumed to be relatively constant with depth, the problem of correlating scale-model and full-size tests, if the analysis is correct, reduces primarily to that of evaluating the load numeric, $W/c_s d^2$. This in turn becomes a problem of assigning a value to the average effective structural cohesion, c_s, for the strata utilized.

In theory, the desired value is a weighted average of actual mechanical measurements in each stratum — which no one yet knows quite how to make, much less how to average. To circumvent this complex measurement and interpretation problem, relative values may be induced from the results of pressure-penetration tests of a series of circular plates considered as scale-models and prototypes within themselves.

This is done by assuming, a priori, that the tests on two sizes of plate, which will be governed by a simplified version of equation (1 a),

$$z_p = d_p\,\Theta''''\,(q/c_s) \tag{2}$$

(where q = average penetration pressure, and the subscripts « p » refers to the plates) must correlate if appropriate values of c_s are known. Relative rather than actual values will evidently be sufficient. In accordance with this assumption, arbitrary values for c_s are assigned which force a « best-fit » correlation of the test results from two plates.

It is further assumed that the same relative but arbitrary values for c_s will serve in the load numeric describing results of tests in the same terrain on other scale-model and full-size objects in the same scale-ratio, one to the other, as the plates — provided the plate tests have each sampled the terrain to the same general depth as will their respective counterparts. It should be emphasized at this point that these gross assumptions are supported, in the

final analysis, only by the fact that their use results in a useful degree of correlation between model and full-size vehicle performance.

To illustrate the procedure, consider the data shown in figure 4, which shows typical plate-penetration test results for four diameters of plate, each with two replications. All data were recorded in a single, deep, dry, snow pack within a small area and a short period of time. The data are plotted in quasi-dimensionless form; i.e. q vs. z/d. It is evident on inspection that the shape of

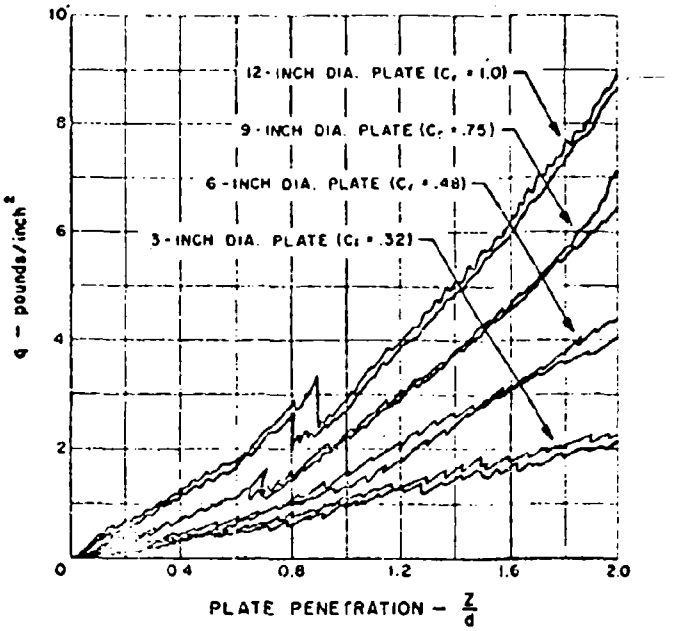


Fig. 4. — Four plate sizes tested in the same snow pack.

the average curve for each size is similar, and that if proper values of c_s could be assigned to complete the load numeric (q/c_s), the four groups of tests would display a good degree of correlation when plotted in fully dimensionless terms.

By arbitrarily assigning a unit value to the average strength experienced by the 12-inch diameter plate, and by assigning to the curves for other diameters the relative values shown (as c_r, where the subscript « r » denotes « relative » values), the four average curves can be made to correlate as illustrated in figure 5. Based upon this result, we could proceed to conduct tests on a prototype under the assumption that it was operating in a snow pack having an average strength of $c_r = 1$; while tests on a $\frac{1}{4}$ scale model would accordingly be conducted under the assumption that the pack, used by the model to only one-quarter the depth used by the prototype, had an average strength of $c_r = 0.32$, which was the value giving the best correlation of the 3-inch diameter plate with the full-size 12-inch diameter plate.

In order to generalize the method, however, all plate data are compared to a typical « standard » curve for a 12-inch diameter plate (fig. 6) — arbitrarily chosen after inspection of a great deal of data covering tests from 1954-1958 — rather than to each other. In recognition of the fact that many shapes of curve other than the one selected are possible, especially in other types of snow packs, the « standard » curve shown in figure 6 is designated as « type I, typical of light, dry, tree-belt snow packs ». As a matter of fact,

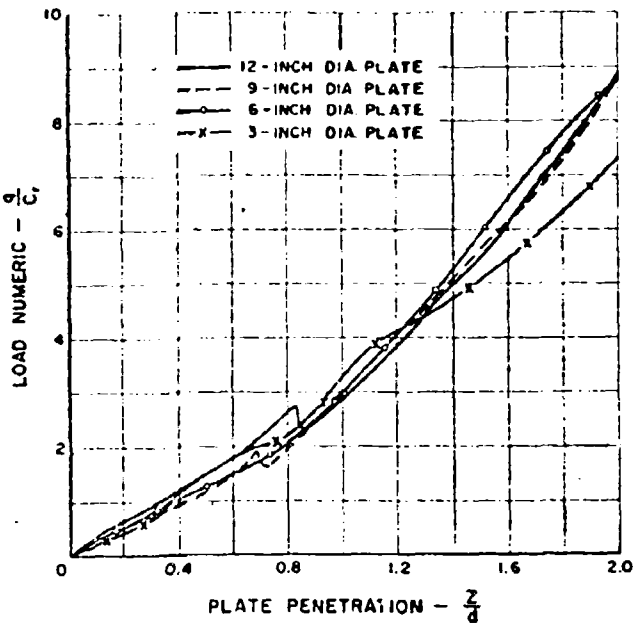


Fig. 5. — Four plate sizes correlated by c_r.

assignment of c_r values by making a « best-fit » to the type I curve even when the test curve is not closely related has worked well, although the basic philosophy behind the method would suggest that when the shapes were not similar, correlation should not be expected a priori.

Finally, to complete the generalization of the method, it was arbitrarily decided that plate diameter used to determine (or to predict) c_r in snow should be 1/10 of tire diameter.

The method has been successfully extended to sands, in which, however, a new « standard » curve was established (for a 4.6-inch diameter plate, fig. 7); and test-plate diameter, as a practical measure, was taken as 1/25 of tire diameter. As a result of these changes the approximate relationship between the relative-strength numbers assigned to a given sand or snow (-like) material by the two methods is:

$$(c_r)_{sand} = 0.06\ (c_r)_{snow} \qquad (3)$$

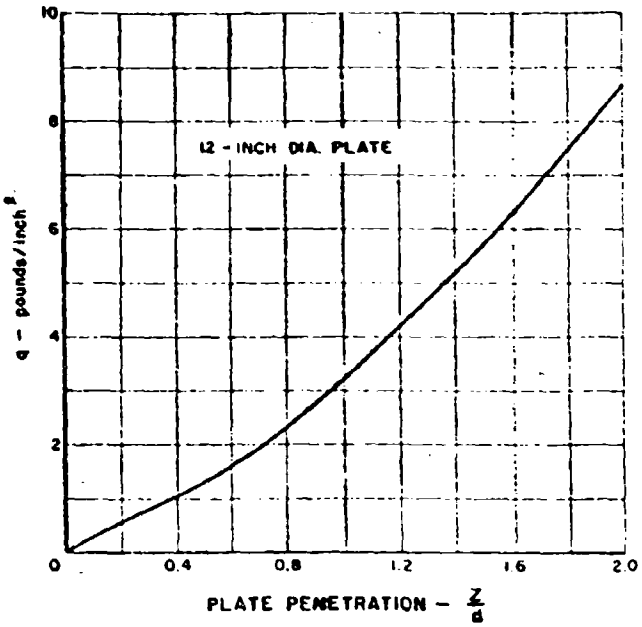


Fig. 6. — Type I snow, typical of dry tree belt snow packs.

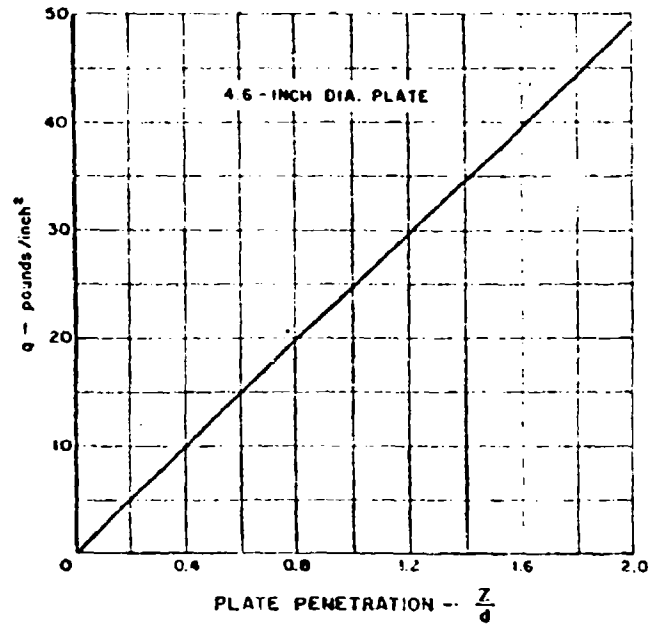
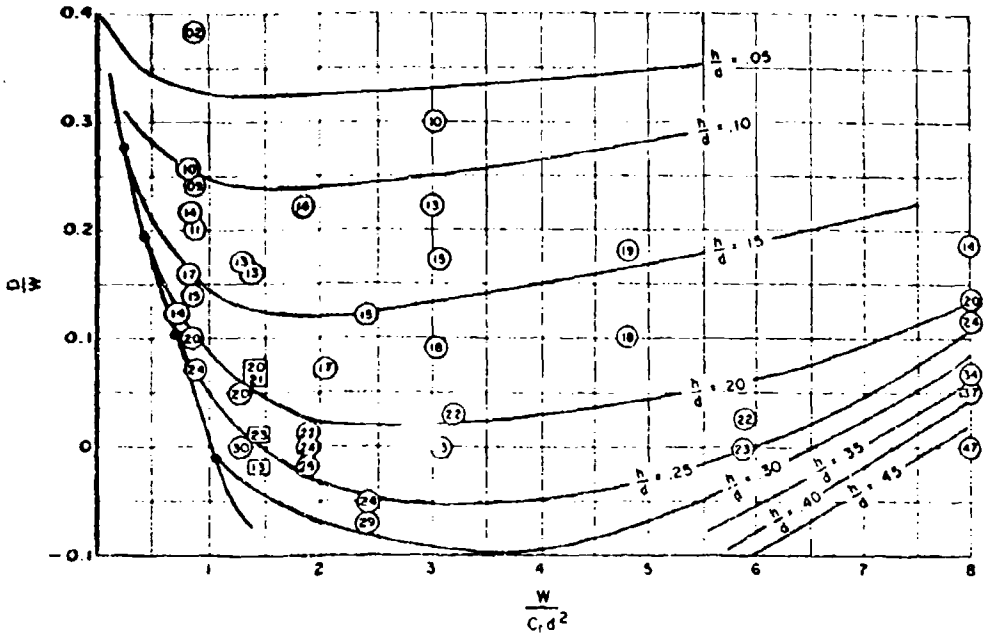


Fig. 7. — Standard curve established for soft sand, LCC 4 × 4 vehicle, equal weight distribution.

LCC 4 × 4 vehicle, equal weight distribution.



Note: Data shown for ground support only.

● Start of ground support.

○ LCC model, ground support tests; snow depth (h/d), in one hundredths, indicated within symbol.

□ LCC, full size; snow depth (h/d) indicated.

Fig. 8. — LCC type tires in snow, flotation and ground support.

i.e., a material intermediate between a typical snow and a typical sand would appear to be a strong snow ($c_{r\,snow}$ would be high), where, tested by the « standard » sand procedure the same material would appear to be a weak sand ($c_{r\,sand}$ would be *low*).

Correlation achieved by use of the method. — The method just described has been utilized, with growing refinement, in the analysis and correlation of tests in snow and sand covering a period of four years. Figure 8 shows the composite data, at a reasonable, fixed tire deflection, from tests of the LCC power-car prototype and ½-scale model in snow, from the « flotation » region through the « ground-support » region (where snow depth and, or tire loading is such that the snow pack is disturbed right down to the ground beneath). Dimensionless drawbar pull (D/W) at 25 percent slip (always near the maximum pull) is plotted as a function of the load numeric $W/c_r d^2$.

The points plotted were each read from the « faired » results of numerous carefully conducted drawbar pull vs. slip tests. A typical set of data curves from one such series in snow is shown in figure 9.

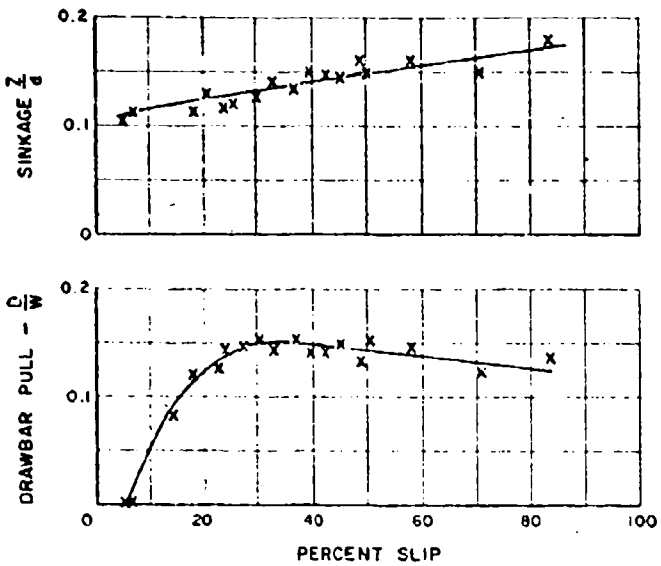


Fig. 9. — Typical data from drawbar pull vs. slip tests.

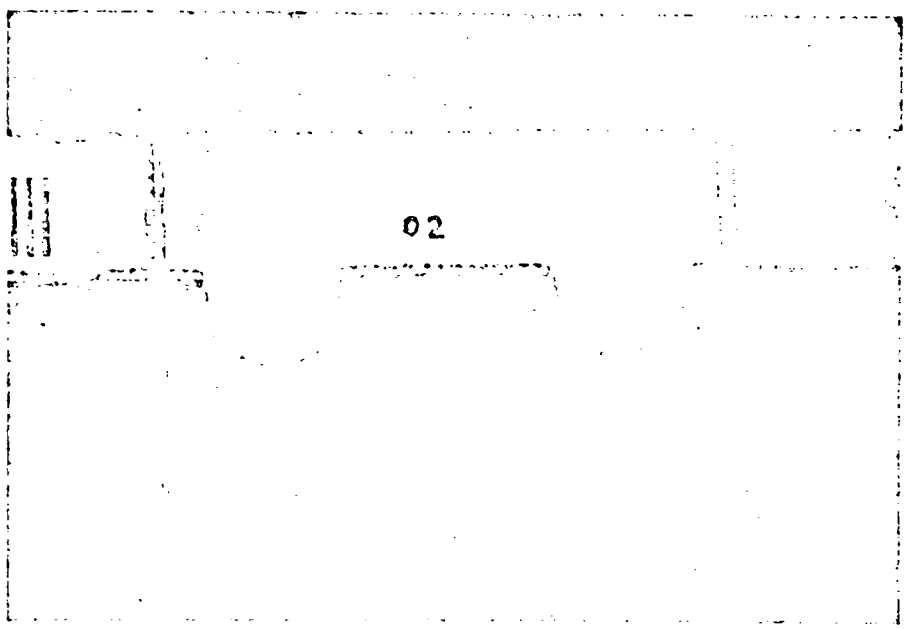


Fig. 10. — Nakaya rearing beam reveals stratifications and deformation of snow.

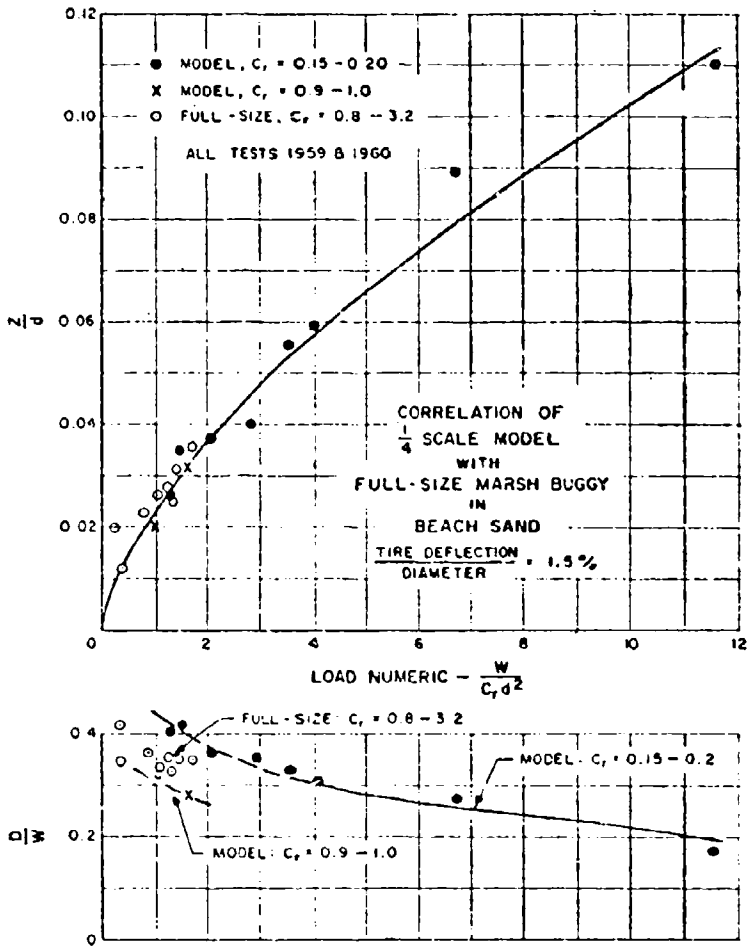


Fig. 11. — Correlation of Marsh Buggy and model in sand.

The beginning of « ground-support » was determined from study of photographs taken of cross sections of the snow pack cut across the vehicle ruts and treated by the « roaring bonfire » method first reported by Nakaya [3]. Figure 10 shows such a photograph, in which it will be seen that the extent to which the snow pack has failed under vehicle action is clearly visible.

Figure 11 presents similar composite data from tests in sand of the light Marsh Buggy (on low-pressure tires 10 feet in diameter, at a single deflection) and a scale-model of it to approximately $\frac{1}{4}$-scale. The important vehicle parameter, tire pressure, was controlled in all snow and sand tests by adjusting tire deflection, under test load and on a hard surface, to a fixed percentage of

Performance of 4 × 4 vehicles in dry, tree belt snow

$$\frac{\text{tire deflection}}{\text{diameter}} = 0{,}06$$

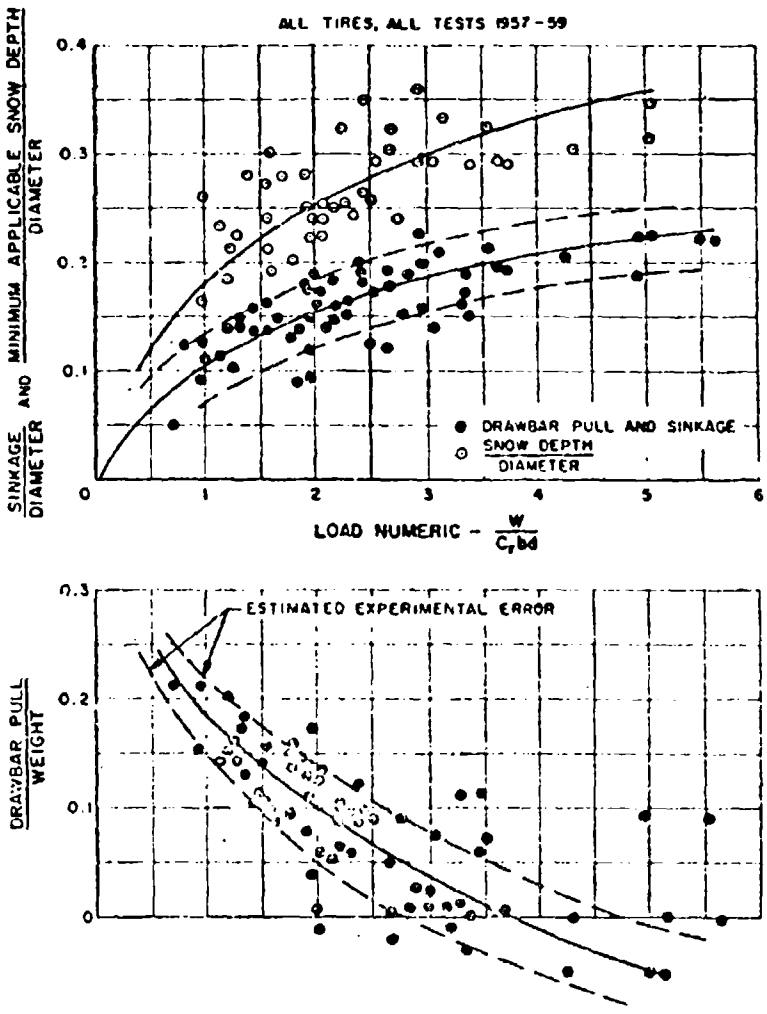


Fig. 12. — 4 × 4 vehicles in snow.

outside diameter for any given series of tests; i.e., the deflection ratio, δ/d, was held constant, in accordance with the requirement for geometric similarity.

We consider the degree of correlation shown in these figures to be entirely acceptable and useful. The fact that, in each type of material, it is achieved on the basis of only one soil parameter (after-collapse internal friction was, apparently, substantially constant) makes it particularly useful in design, for

it means that tests at several loads in one test area may be generalized to predict results in other areas having either more or less strength.

Some 4 × 4 design charts. — The usefulness of the present understanding is readily demonstrated, and the degree of correlation achievable by the methods discussed is further supported by the data in figures 12 and 13. Figure 12 presents the results of hundreds of tests in dry, tree-belt snow packs of a series of tires of widely differing configuration, sizes and loads, at a single deflection ratio (δ/d). The characteristics of the several tires are shown in appendix II.

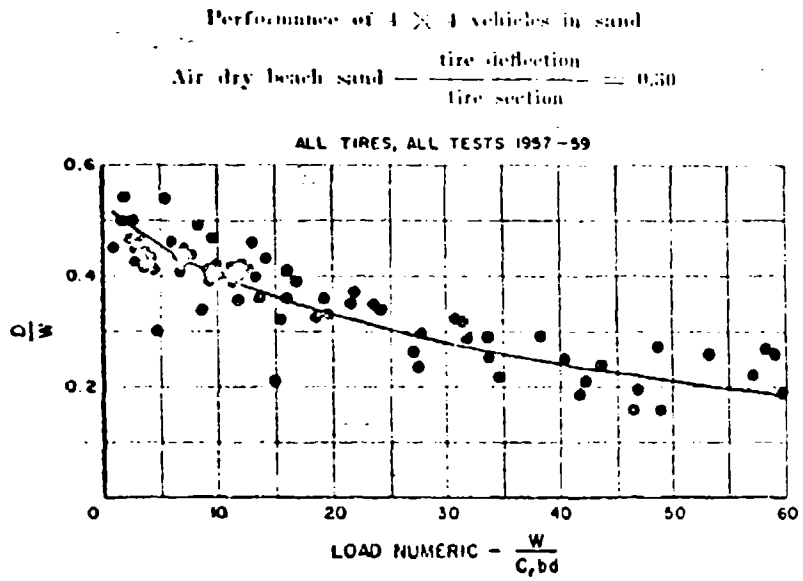


Fig. 13. — 4 × 4 vehicles in sand.

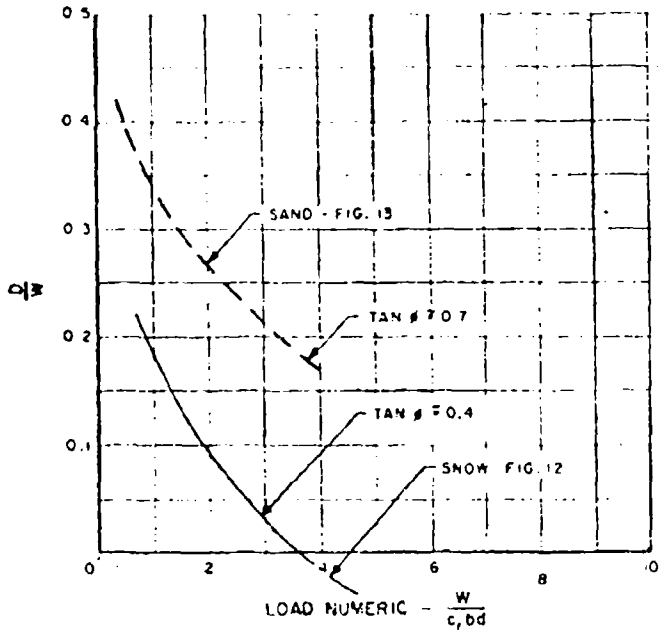
It will be seen that, simply by replacing the numeric $W/e_r d^2$ by its dimensional equivalent $W\ e_r bd$ (where b = overall tire width), the flotation performance in dry snow over a period of three years, of a wide range of tires, 24 to 120-inches in outside diameter, under loads from 50 lb/tire to 3000 lb/tire, in snow packs of varying strengths, all plot within a wide but entirely usable scatter band.

Figure 13 shows the sand performance of these same tires similarly treated. In this case, tire loads ranged from 50 lb/tire to 50,000 lb tire. The scatter is less, and the possibility for reducing it through the use of a more complex form of the load numeric is evident in a more detailed presentation. However, the error in using a single curve to predict either sand or snow performance from the data in figures 12 or 13 is well within the accuracy with which field conditions can be predicted for practical design purposes.

The two « single line » D/W vs. $W/e_r bd$ curves for sand and snow, reduced

to a common base in terms of the approximate relationship given by equation (3), are shown in figure 14. The remaining difference may, for the moment at least, be attributed to the large difference in usual, average internal friction in sand and dry snow ($\tan\Phi = 0.7$, and $\tan\Phi = 0.4$, respectively).

It remains, in order to make the data of figures 12 and 13 useful in design, to assign reasonable values to c, for various conditions. A preliminary survey of tree-belt snow areas was begun in 1960, which, together with the accumulated



(ALL REFERRED TO TYPE I SNOW CURVE)

Fig. 14.

test site data from previous years, has resulted in the approximate relationships between c, and plate diameter (and hence, via the standardized procedure, tire diameter) shown in figure 15[5]. It has been observed that, in general, immobilizations of 4×4 vehicles in level terrain will not occur regardless of snow strength (within observed limits) if snow depth is less than approximately 30 percent of tire diameter. Data considered at each plate diameter were accordingly limited to those obtained in snow packs greater than three times the plate diameter.

It will be remarked that the snow strength upon which a vehicle may depend increases almost linearly with tire diameter. Thus a large diameter tire benefits not only from its size, per se, but also from a lesser likelihood of meeting critical snow depths and from the probability that by using the deep packs to greater depths than do smaller tires it will encounter greater

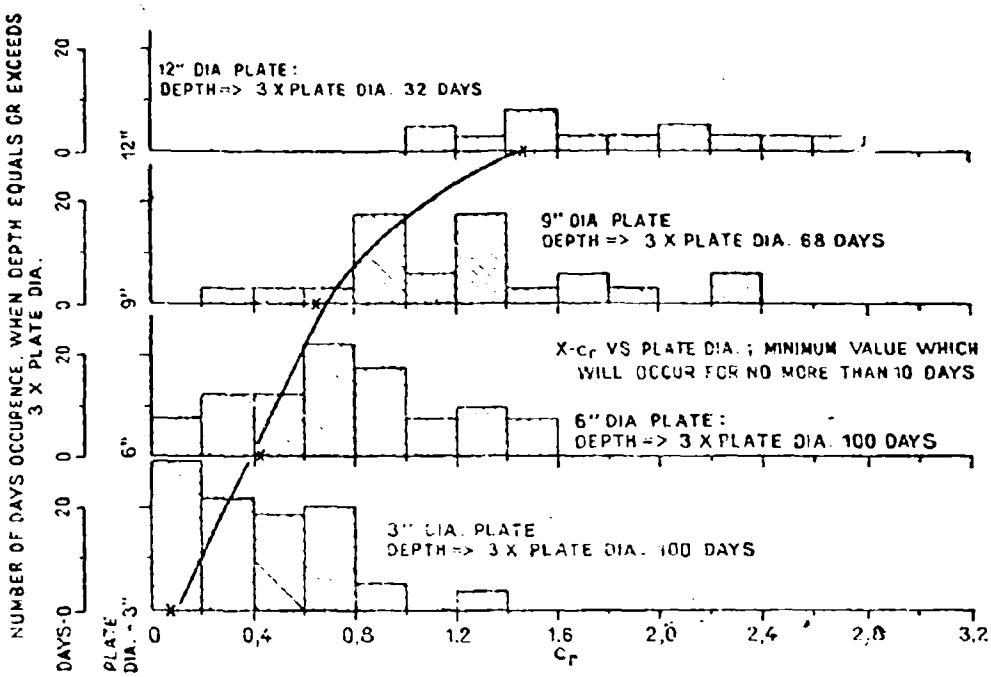


Fig. 15. — Distribution of snow strength for 100 day season of difficult snow from preliminary survey of tree-belt areas (1958-1960).

average strengths. The latter fact may be explained qualitatively in terms of increased snow strength in the lower, older layers of a typical, dry, tree-belt snow pack.

Although a similar survey has not been begun in natural sand areas, experience in the test areas, conservatively interpreted, indicates that minimum c_r values in sands will be of the order of

$$(c_r)_{min} = d_p/6 \qquad (4)$$

where d_p = plate diameter in inches. The approximate linear increase in c_r with depth may reflect some influence of body forces in sands, in place of, or in addition to, an increase in structural strength with depth due to stratification, increasing consolidation, etc.

Conclusions. - Although the work is still in progress and, if ship and aircraft experience is any guide, will never be entirely finished, we believe we can now fairly state that:

1) Scale-model tests to determine the performance of proposed designs in sands, dry snows, and similar frictional/collapse materials are now entirely practical and reliable.

2) These types of materials can be adequately characterized for design and test purposes in terms of a relative structural cohesion, an effective coefficient of internal friction, and, as necessary, the depth of the material to a substantially stronger stratum.

3) On the basis of data already developed, vehicle designers can now reliably estimate the performance of 4 × 4 vehicles on any type of tire in dry tree-belt snow areas, and in sand areas, with useful accuracy.

4) There are clear indications that similar, practical scale-model test methods in other types of materials can be developed, provided that dimensionally sound parameters are used to characterize the terrain soil behavior and provided that trivial parameters are excluded on the basis of valid experimental evidence.

APPENDIX I

The dimensional framework for treating scale-model vehicles in soft terrains

The principal requisite for a valid, useful dimensional analysis of a given type of mechanical system is a complete, minimum list of the truly important independent parameters influencing its behavior. An analysis will be incorrect if any major variable is overlooked, and will be misleading and less useful than it might be if the list is not pared of all factors whose influence is negligible.

Factors relating to the vehicle.

1) The *geometry* or configuration of the vehicle, which may be specified by the ratio of each important linear dimension of the machine, such as length (y), wheel base (m), lug depth (a), tire section width (b), and wheel spacing (s), tire deflection (δ), etc., to a single, characteristic linear dimension such as the wheel diameter (d). Thus,

$$y/d,\ m/d,\ a/d,\ b/d,\ s/d,\ \delta/d,\ \text{etc.}$$

The statement of geometric similarity between a model and a full-size prototype means that each such ratio for the model equals the corresponding ratio on the full-size vehicle. Their influence on the complete system is thus constant for a given configuration, and may be pooled with other constants relating to the system. They need not appear in the functional equation that is the final expression of a dimensional analysis performed in relation to the use of geometrically similar scale-models.

2) d = a characteristic linear dimension of the vehicle, such as its wheel diameter, which expresses its *size*. The ratio d_m/d_f, in which the subscripts m and f refer to scale-model and full-size prototype respectively, is the linear scale ratio, λ.

3) W = the gross *weight* of the vehicle. Where important, the ratios of component weights to the gross weight must also be specified. However, the requirement for complete dynamic similarity between two sizes of vehicles includes the condition that corresponding ratios on each be equal, so that, as in the case of the geometry, these ratios need not appear in the final equations.

Factors relating to the operation of the vehicle.

4) V = a characteristic *speed* related to the vehicle, such as peripheral wheel speed relative to the vehicle. At a given moment, all other velocities and components in the system may be expressed in terms of ratios to this speed.

One ratio of particular importance in dynamic systems is the slip ratio (S): $S = V_s/V$, where V_s = the slip speed, or average speed of the wheel contact area relative to the undisturbed soil or snow.

It is to be noted that while the slip ratio is usually conceived in terms of speeds, it also has a simple geometric interpretation:

$S = j/l_c$ where « j » is as defined below S, and l_c = distance from front to rear of running gear contact area, along the same path over which « j » is measured (usually parallel to the average surface of the material).

In terms of speeds, the slip ratio implies dynamic soil reactions arising from inertia and/or viscous effects. In terms of distances, the ratio implies essentially static material reactions, determined primarily by displacement and but little influenced by time-rate of displacement.

5) j = slip distance of a tractive element relative to the undisturbed material during one cycle in contact with the material.

Factors relating to the soil bed or snow pack.

6) h = total *depth* of material of interest. Boundaries of significant layers, and hence their thicknesses as well, may be specified by measurements from the surface, $_1h$, $_2h$, etc. The ratios $_1h/h$, $_2h/h$, etc. are presumed equal under the assumption of geometric similarity which extends to the geometry of the terrain as well as of the vehicle.

7) $_nc_s$ = before-collapse, or *structural cohesion* of the material at depth $_nh$. This will in general vary at a given spot and time from layer to layer, and hence with depth, i.e. $_nc_s = F\ (_nh)$.

8) $_n\tau_0$ = the full, unit after-collapse or *dynamic shearing resistance* of the material originally at depth $_nh$. For any depth, it may be approximated by Coulomb's assumption:

$$_n\tau_0 = {}_nc_i + \sigma \tan {}_n\Phi$$

where σ = unit normal loading on the shear plane. On this basis, τ_0 may be replaced by $_nc_i$ and $\tan_n \Phi$, where these are, respectively, the effective cohesion and the tangent of the effective angle of internal friction of the collapsed material originally at depth « $_nh$ ».

9) $_n\gamma$ = the before-collapse bulk specific weight of the material at depth $_nh$.

10) $_n\beta$ = plastic kinematic viscosity at depth $_nh$.

11) A = slope of the surface of the material.

12) $_nf_i$ = coefficient of friction of soils or snows at depth $_nh$ on the material of part i of the vehicle. The use simply of the factor f in the analysis will signify this entire set of frictional phenomena.

13) $_nB$ = shear stress/strain parameter characterizing dynamic shearing resistance in layer n. Dynamic shearing resistance develops only after some consolidation and reorientation of the grains of the collapsed material. The typical relationship in weak,

loose materials between unit shearing resistance and shear travel may be approximated by the equation:

$$\tau = \tau_m (1 - e^{-j/B})$$

Because Bj must be dimensionless, the dimension of the parameter B is L.

The list might be further lengthened by the inclusion of soil or snow elastic properties, but the phenomena of interest regularly involve large, permanent deformations of the material, so that elastic forces may probably be neglected from the outset, at least until experimental evidence of their importance dictates otherwise.

Factors relating to the system as a whole.

14) g = acceleration of gravity.

Dependent Variables.

15) z = sinkage of vehicle.

16) α = trim of vehicle.

17) D = drawbar pull, or measurable margin of tractive capacity over external motion resistance. Drawbar pull of a given machine in a given material is largely influenced by slip ratio (S) and/or grouser travel (j). Either drawbar pull or slippage may be taken as the independent variable, and the remaining one as dependent. In testing it is convenient to control slippage and to measure drawbar output. In practice, the drawbar load is fixed, at any given moment, by terrain and towed load, and slippage becomes the dependent variable.

Resulting Equations.

From this list the dimensional equations may be written *):

$$z = d\,\Theta \quad (W/c_c d^2,\ c_1/c_c,\ \Phi,\ W/\gamma d^3,\ A,\ V^2/g\,d,\ V\,d/\beta,\ f,\ S,\ j/B,\ h/d) \qquad (I-1\,a)$$

$$D = W\,\Theta' \quad (W/c_c d^2,\ c_1/c_c,\ \Phi,\ W/\gamma d^3,\ A,\ V^2/g\,d,\ V\,d/\beta,\ f,\ S,\ j/B,\ h/d) \qquad (I-1\,b)$$

$$\alpha = \Theta'' \quad (W/c_c d^2,\ c_1/c_c,\ \Phi,\ W/\gamma d^3,\ A,\ V^2/g\,d,\ V\,d/\beta,\ f,\ S,\ j/B,\ h/d) \qquad (I-1\,a)$$

Some possible simplifications.

It is evident from the equations that unless some factors are eliminated, preferably upon the basis of sound experimental data, the analysis does little to clarify vehicle-soil relationships, and makes the possibilities for the use of scale-models appear remote indeed. Some of the more interesting possibilities for simplification, from a practical viewpoint, are discussed below. Only equation (I - 1 a) is modified, it being understood that the form of equations for « α » and « D » follow accordingly.

There has been no indication in the data for the past several years of any marked effect of vehicle speed, per se, upon vehicle performance in soils or snows over the range of rather slow speeds at which quantitative tests have been run. On the basis

*) For a thorough discussion of the philosophy and techniques of dimensional analysis see Langhaar [2].

of this experience, it is possible to eliminate (for similar tests) all terms related to speed, except the slip ratio. The apparent influence of slip ratio upon vehicle performance at slow speed is undoubtedly due to its geometric meaning, which remains valid regardless of any lack of actual speed effects.

Further, in relation to the vehicle and test procedures utilized in the present program, the factors A (equals zero for tests in level terrains) and f may be considered constant. On these bases, eliminating all terms relating to V, A, and f, equation (I - 1) becomes:

$$z = d\,\Theta^{I} \quad (W/c_z d^2,\ c_1/c_z,\ \Phi,\ W/\gamma d^3,\ S,\ j/B,\ h/d) \qquad (I-2)$$

If, as past experience in nonplastic soils and dry snows indicates, body forces may be considered negligible, factors related to γ may also be neglected.

Accordingly, equation (I - 2) may be further simplified:

$$z = d\,\Theta^{II} \quad (W/c_z d^2,\ c_1/c_z,\ \Phi,\ S,\ j/B,\ h/d) \qquad (I-3)$$

Finally, if the unit dynamic shearing resistance of a material (such as disaggregated snows and sands) is considered to be entirely frictional and constant with depth, equation (I - 3) becomes:

$$z = d\,\Theta^{III} \quad (W/c_z d^2,\ \Phi,\ S,\ j/B,\ h/d) \qquad (I-4)$$

It has been found in practice that both of the above assumptions are reasonably close to the facts for sands and dry snows, at least in so far as these may be ascertained by means of present shear vane tests, although some small cohesion (usually less than 0.1 psi) is often registered.

There remains the question, at low slippages, of whether expansion of model data to full-size predictions should be made on the basis of the slip ratio (S) or of the numeric j/B. In order to satisfy both conditions simultaneously,

$$B_m = \lambda B_f \qquad (I-5)$$

i.e., barring an unlikely, relatively steady decrease in material «stiffness» with depth (measured from the surface), the two conditions cannot both be satisfied by tests of model and prototype in the same terrain.

At this moment, little is known of the structure or behavior of the parameter B. It is not known how, or even whether, it varies with normal and/or shear stress in a given soil or snow, to what extent it is a property independent of size of the test sample or test apparatus, etc. The importance of at least one such parameter, whatever its final form, must be recognized, however, for it offers the only acceptable explanation yet advanced for the characteristic shape of curves of drawbar pull vs. slippage for all types of vehicles. This basic explanation was first offered and discussed by Bekker (Ref. 14). On the basis of experience to date, however, it is (somewhat arbitrarily) considered that present use of scale models should utilize expansion with the *slip ratio* as the controlling numeric, rather than j/B. Accordingly, equation (I - 3), upon which practical vehicle mobility tests of vehicles using models in any type of terrain should be planned and interpreted, becomes;

$$z = d\,\Theta^{IV} \quad (W/c_z d^2,\ c_1/c_z,\ \Phi,\ S,\ h/d) \qquad (I-6)$$

Thus, in a given terrain (Φ relatively constant) dimensionless sinkage, **z/d** (and likewise drawbar pull, trim, etc.), of a given vehicle and its scale model is a function primarily of the loading, $W/c_n d^2$, the slip ratio, S, cohesion ratio, c_t/c_n, and where depths are such that « hard-pan » or « ground-support » comes into play, the dimensionless depth h/d. All may readily be adjusted and/or controlled if means are available to measure « c_n » and « c_t », or relative values thereof, in relation to some arbitrary « standard ». In materials which may be considered purely frictional the cohesion ratio, of course, also may be dropped; i.e. finally,

$$z = d\,\Theta \quad (W/c_n d^2,\ \Phi,\ S,\ h/d) \tag{1a}$$

$$D = W\,\Theta' \quad (W/c_n d^2,\ \Phi,\ S,\ h/d) \tag{1b}$$

$$\alpha = \Theta'' \quad (W/c_n d^2,\ \Phi,\ S,\ h/d) \tag{1c}$$

APPENDIX II

Characteristics of test tires

Tire size and type	Outside diameter	Section width	Section height **)	Width ÷ dia.	Tread depth	Plys
6.00 - 16	27.8	6.5	5.2	0.23	1/16	2
9.00 - 14, Marsh Buggy Model	25.9	9.0	5.1	0.35	Smooth	2
LCC Model	29.9	12.0	6.1	0.40	1/4	4
Torus	31.7	17.0	14.5	0.49	Smooth	2
6.00 - 16, Dual	27.8	14.6 *)	5.2	0.52	1/8	2
Rolling Bag, 22 × 36	36.0	22.5	11.9	0.62	Smooth	4
Rolling Bag, 24 × 36	24.3	24.3	8.5	1.00	Smooth	4
Marsh Buggy, full-size	114.7	38.6	23.0	0.34	Smooth	4
LCC, full-size	120.0	48.0	24.1	0.40	1	12
18.00-25, Lark	60.7	18.6	16.4	0.32	1/2	12
29.50-25, Goer	73.4	31.5	20.7	0.43	2	12

*) Includes two inch spacing.

**) Measured from rim flange to outside diameter of undeflected tire.

NOTE: All dimensions in inches.

BIBLIOGRAPHY

1) Kamm W. and Schmid C. Das Versuchs-und Messwesen auf dem Gebeit des Kraftfahrzeugs. Berlin, 1938.

2) Markwick A. H. O. Dimensional analysis of the bearing capacity of soils under tracked vehicles and its application to model tests. Road Research Laboratory, October 1941.

3) Nuttall C. J. Jr. Scale-model vehicle testing in non-plastic soil. Stevens Institute of Technology, ETT Report 394, December 1949.

4) Willetts B. F. The performance of footings on and cultivation implements in soils. Thesis submitted for degree of doctor of philosophy, University of Durham, June 1959.
5) M'Ewen E. and Willetts B. F. The sinkage of dynamically loaded footings. Fighting Vehicles Research and Development Establishment, Report BR 122, January 1955.
6) Nuttall C. J. Jr. and Raimond V. M. Sealed vehicle mobility factors. Final report, Wilson, Nuttall, Raimond Engrs. Inc. Report, 18-2 July 1956.
7) McGowan R. P. Sealed vehicle mobility factors (tires in snow). U. S. Army Transportation Research Command, Fourth Interim Report, September 1961.
8) McGowan R. P. Sealed vehicle mobility factors (tires in sand). U. S. Army Transportation Research Command, Third Interim Report, June 1961.
9) Wilson C. W. and Nuttall C. J. Jr. Sealed vehicle mobility factors (tires in sand). U. S. Army Transportation Research Command, Sixth Interim Report, July 1961.
10) McGowan R. P. Sealed vehicle mobility factors (Marsh tests). U. S. Army Transportation Research Command, Report No. 380-6, January 1959.
11) Vincent E. T. et al. Research in vehicle mobility: performance coefficients for free-running wheels in sand. University of Michigan Research Institute, Report no. 2544-31-F, July 1960.
12) Nakaya U. et al. The physics of skiing: the preliminary and general survey. Journal of the Faculty of Science, Hokkaido Imperial University, 1936.
13) Langhaar H. L. Dimensional analysis and theory of models. New York, 1951.
14) Bekker M. G. Traction and slippage of crawlers and wheels. Society of Automotive Engineers, January 1954.

DISCUSSION

Z. JANOSI. -- Mr. Chairman, I hope that you are familiar with the analysis which is presented in Mr. Nuttall's and Mr. McGowan's paper, otherwise the comments I am going to make will not be of much use to you. I am sure that most of you have noticed that the United States is represented here by three major groups. A number of speakers are associated with the Land Locomotion Laboratory which is supported by the Ordnance Corps of the U. S. Army, another group works for the Army Mobility Research Center, Corps of Engineers, U. S. Army and some participants are affiliated with the Transportation Research Command, U. S. Army.

It appears that there is not much in common between our approaches except that we agree in utilizing vertical soil penetration tests. Fortunately, however, these methods are not really divorced, as I intend to demonstrate in connection with the previous presentations.

Let us assume that the vertical soil stress-strain relationship can be expressed by Bekker's equation which is used by the Land Locomotion Laboratory. For circular plates we have

$$p = \left(\frac{k_c}{D} + k_\phi\right) z^n$$

Or using the notation of the authors of the paper on hand

$$q = \left(\frac{k_c}{D} + k_\phi\right) z^n$$

It was shown by Mr. Nuttall and Mr. McGowan that the dimensionless curve representing the relationship between q/c_r and z/D is independent of the size of the plate used in the test.

I would like to show that this important observation may be verified by Bekker's equation.

Introducing a new variable $f = z/D$ one can write that

$$q = D^n \left(\frac{k_c}{D} + k_\phi\right) f^n$$

Notice that f is the dimensionless sinkage.

For the reference plate whose diameter may be called D_1 we have

$$q_1 = D_1^n \left(\frac{k_c}{D_1} + k_\phi\right) f^n$$

and for any other plate

$$q_1 = D_1^n \left(\frac{k_c}{D_1} + k_\phi\right) f^n \quad .$$

Hence c_R the characteristic factor used by Mr. McGowan and Mr. Nuttall, called the relative structural cohesion, can be expressed by means of the Bekker formula as follows:

$$\frac{1}{c_R} = \frac{q_1}{q_1} = \frac{D_1^n}{D_1^n} \left(\frac{k_c}{D_1} + k_\phi\right) \frac{1}{\left(\frac{k_c}{D_1} + k_\phi\right)}$$

Now we can express

$$\frac{q_1}{c_R} = D_1^n \left(\frac{k_c}{D_1} + k_\phi\right) f^n$$

Notice that $\frac{q_1}{c_R}$ is a function of f only, for a given soil, if one agrees to use a reference plate of diameter D_1. This conclusion is well justified by the empirical curves obtained by the authors for dry snow and sand. The curves — figures 5 in the paper — are of parabolic shape as predicted by the last equation:

$$\frac{q_1}{c_{R1}} = \text{Constant} \times f^n$$

I hope that further efforts will be made to investigate the possibility of integrating the two methods, which would eliminate a great amount of work overlap.

Thank you very much.

N. 43

Analytical prediction of performance for full size and small scale model vehicles

Previsione analitica della prestazione dei veicoli a grandezza normale ed a scala ridotta

WILLIAM L. HARRISON, JR. *)

ABSTRACT. — *This paper presents the current techniques in use by the Land Locomotion Laboratory for determining vehicle performance predictions.*

Factors which must be considered in practical applications of the equations describing soil-vehicle relationships are presented.

The current techniques for determining analytical prediction of vehicle performance and the experimental evaluation of vehicle performance are illustrated in the evaluation of six vehicles of which three are full size and three are 1/4 scale models.

It is demonstrated that the equations defining soil-vehicle relationships are not influenced by scale factors and are equally valid for analytically determining the performance of full size or scale model vehicles.

Experimental tests were conducted and compared to the analytical predictions. The results show an accuracy of predictions within ± 10 per cent.

Key to symbols and definitions

k_c	=	Cohesive modulus of sinkage (lbs/in^{n+2}).
k_ϕ	=	Frictional modulus of sinkage (lbs/in^{n+2}).
b	=	Width of wheel or a rectangular footing; radius of circular footing used in soil penetration tests (in).
n	=	Exponent of sinkage.
D	=	Diameter of a wheel (in).
β_o	=	Central angle between the vertical radius and the radius associated with the soil level (°).
X	=	Horizontal coordinate axis; distance between vertical radius and wheel perimeter, horizontal travel of a point on the wheel perimeter (in).
Y	=	Vertical distance between the center of the wheel and an arbitrary point on the perimeter; ordinate of a point on the wheel perimeter measured above the root (in).
R_v	=	Motion resistance due to vertical reaction P (lbs).
R_H	=	Resistance due to horizontal pressure (P_H) (lbs).
c	=	Cohesion (lbs/in^2).
Φ	=	Angle of shear resistance; angle of internal friction (°).
J	=	$\frac{i_o l}{K}$
K	=	Deformation modulus of a soil shear stress-strain curve (in).
i_o	=	Slip.

*) Land Locomotion Laboratory - U.S. Army Ordnance Tank Automotive Command, Detroit, Michigan.

α	=	Turning angle of a wheel while the endpoint of the radius moves from the bottom of the wheel to a point characterized by X and Y (°).
α'	=	$-\alpha$ (°).
V_t	=	Theoretical speed of the wheel calculated from the radius and the RPM (in/sec).
R	=	D/2 (in).
β_v	=	Central angle at which the tangent of the path of a point of the wheel perimeter is vertical (°).
β	=	$\beta_v - \alpha'$ (°).
H (H_G)	=	Gross tractive effort, traction, thrust (lbs).
H_1	=	Thrust developed on that part of the perimeter which lies between $\beta_v - \beta_o$ and β_v (here $\beta_o < \beta_v$).
W	=	Gross vehicle weight (lbs).
$\bar{X}$	=	Abscissa of center of gravity of vehicle (in).
γ	=	Density of soil (lbs/in³).
K_o - K_b	=	Constants dependent on the angle of internal friction Φ and angle of repose Φ' with respect to the angle of inclination of the rupture plane for the determination of the bulldozing resistance R_b (6).
DP (H_D)	=	Drawbar pull (lbs).
R_M	=	Sum of the various resistances imposed upon the vehicle by the soil.
R_c	=	Resistance due to compaction (lbs).
R_b	=	Resistance due to bulldozing (lbs).
W_R	=	Vertical load on the rear axle of a vehicle (lbs).
W_F	=	Vertical load on the front axle of a vehicle (lbs).
A	=	Ground contact area (sq in).
Z	=	Sinkage (in).
Z_o	=	Maximum sinkage of a wheel or a track.
l	=	Ground contact length (in).

Introduction

The significance of accurate analytical descriptions of natural phenomena is often overlooked until one is faced with a problem for which no such discipline exists. This paper does not aim to justify or expound a theme of a need for an analytical base for a prediction technique. However, for the moment entertain the thought of the welter of confusion and conflicting opinion that has surrounded vehicle design for the past years. This state of confusion has been suffered because of a lack of a discipline to relate the behavior of the vehicle to its environment; the soil.

Since the advent of the Bekker soil value system and a series of relating equations in use by the Land Locomotion Laboratory *) [1] predictions of vehicle « reaction » to various soil conditions have been analytically produced with acceptable accuracy. For the past five years, methods and techniques of applying the equations of Land Locomotion Mechanics to the prediction of vehicle performance have been subjected to continuous refinement to achieve increased

*) Land Locomotion Laboratory, Research Division, Research and Engineering Directorate, Ordnance Tank-Automotive Command, Detroit, Michigan.

accuracy. The accuracy of any analytical solution will depend in general on a number of factors. However, even if the equations are perfect in their description of a phenomenon, the accuracy of the solutions they produce will only be comparable in accuracy to that of the input data. For the problem at hand, the input data can be in the form of physical and geometric soil characteristics and physical characteristics of vehicles. This paper is limited to the physical characteristics of soil and the vehicle dimensions pertinent to predicting the performance of vehicle, both wheeled and tracked, operating in soft deformable soils or snow. Vehicle performance over hard bumpy terrain requiring use of geometric characteristics of the soil structure and additional vehicle dimensions will not be included in this presentation.

Background

The term, « vehicle performance » as used throughout this paper will be limited to a general definition from which specific performance criteria can be extracted. This general definition will be in terms of net traction or more commonly expressed as « drawbar-pull ». This is a measure of the additional thrust that a vehicle can develop in excess of that which is required for self-propulsion. This additional thrust, or « drawbar-pull » is measured experimentally by determining the maximum towed load a vehicle can pull while maintaining a constant velocity-slip condition. Analytically, the « drawbar-pull » is determined by algebric summation of the thrust a vehicle can develop in a given soil and the resistance to motion. This relationship was expressed in equation form by M. G. Bekker [2-3] as follows:

$$DP = H - R_M \qquad (1)$$

where H is the gross traction developed and R_M is the summation of the various resistance imposed upon the vehicle by the soil. The equations for H and R_M proposed by Bekker have since been modified [4-5-6] and are currently utilized in the form shown on plates I and Ia.

The derivation and experimental verification of these equations utilized soil models. Application of these equations to practical solutions involving complete vehicles, rather than a single wheel or track operating under ideally prepared conditions, requires techniques directed toward consideration of all pertinent soil and vehicle characteristics which can affect the net thrust to be predicted by use of equation (2) to (6). The pertinent soil characteristics which must be considered are:

1) Variation of soil values within a specified area; 2) proper interpretation of stress-strain curves; 3) the existence of hardpans at shallow depths; 4) change in soil strength due to deformation.

The method of obtaining soil values has been described in a presentation to this group by Mr. F. Pavlics [7], General Motors Corp., Detroit, Michigan.

$$H = H_1 = b R \int_{\beta_v - \beta_o}^{\beta_v} \left\{ c + \left(\frac{k_c}{b} + k_\phi \right) R^n \left[\cos (\beta_v - \beta) - \cos \beta_o \right]^n \tan \Phi \right\}$$

$$\left\{ 1 - e^{-\frac{R}{K} \left\{ \sqrt{2 i_o - i_o^2} \left[\cos (\beta_v - \beta_o) - \cos \beta \right] + (1 - i_o) \left[\sin (\beta_o - \beta_v) + \sin \beta \right. \right.} \right.$$

$$\left. \left. + (\beta_v - \beta_o) - \beta \right] \right\} \left. \right\} \cos (\beta_v - \beta) \, d\beta$$

$$\beta_o < \beta_v \qquad (2a)$$

$$H = b R \int_{0}^{\beta_v} \left\{ c + \left(\frac{k_c}{b} + k_\phi \right) R^n \left[\cos (\beta_v - \beta) - \cos \beta_o \right]^n \tan \Phi \right\}$$

$$\left\{ 1 - e^{-\frac{R}{K} \left\{ \sqrt{2 i_o - i_o^2} \left[\cos (\beta_v - \beta_o) - \cos \beta \right] + (1 - i_o) \left[\sin (\beta_o - \beta_v) + \sin \beta \right. \right.} \right.$$

$$\left. \left. + (\beta_v - \beta_o) - \beta \right] \right\} \left. \right\} \cos (\beta_v - \beta) \, d\beta -$$

$$- b R \int_{\beta_v - \beta_o}^{0} \left\{ c + \left(\frac{k_c}{b} + k_\phi \right) R^n \left[\cos (\beta_v - \beta) - \cos \beta_o \right]^n \tan \Phi \right\}$$

$$\left\{ 1 - e^{-\frac{R}{K} \left\{ \sqrt{2 i_o - i_o^2} \left(\cos \beta - \cos \beta_o \right) (1 - i_o) \left[\sin \beta_o - \sin \beta + \beta - \beta_o \right] \right\}} \right\} \cos (\beta_v - \beta) \, d\beta$$

$$\beta_o > \beta_v \qquad (2b)$$

Plate 1.

$$R = R_v + R_H = (k_c + k_\phi) \left[\frac{Z_o^{n+1}}{n+1} \left(1 - \frac{Z_o}{D/2 \, (n+2)} \right) \right] +$$

$$\int_{D/2 - Z_o}^{D/2} Y^{n-1} \left(1 - \frac{D/2 - Z_o}{Y} \right)^n \left[(D/2)^2 - Y^2 \right]^{1/2} \qquad (3)$$

$$H = A c + W \tan \Phi \left[1 - \frac{1}{J} \left(1 - e^{-J} \right) \right] \qquad (4)$$

$$J = \frac{i_o l}{K} \qquad (4a)$$

$$R_c = \frac{2 b k Z^{n+1}}{n+1} \qquad (5)$$

$$R_b = 2 b \left(2 Z c K_b + \gamma K_o Z^2 \right)$$

Plate 1a.

Plate 1, 1a. — Equations used in the performance predictions of wheeled and tracked vehicles.

The majority of tests both in laboratory and field conditions require statistical techniques for determining the range of soil values that properly represents the distribution of soil strengths. Proper interpretation of stress-strain curves obtained from vertical load vs. deformation and shear stress vs. deformation tests is quite significant for accurate predictions of vehicle performance. The load limits used to establish the stress-strain curves must correspond to pressures imposed on the soil by the vehicle to be evaluated. This later may be particularly significant for some soil conditions since tests have shown that in many soils and snow there are two distinct sets of vertical load parameters (k_c, k_ϕ, n) within pressure limits of 1-10 psi.

The pressure limits are equally important in obtaining the horizontal shear-deformation parameters (c, ϕ, K). In many soils horizontal shear under very low normal pressures will not produce soil failure. This will result in apparent horizontal shear parameters of different magnitudes than those resulting from soil failure. However, usually by measuring the shear parameters within the corresponding limits of vehicle ground pressure, appropriate values will be obtained for application to performance predictions.

The existence of « hardpans » at shallow depths requires additional analysis. It can be determined from the vertical load-deformation curves whether the vehicle to be evaluated will achieve flotation in the layer covering the hardpan or reach a limited sinkage due to the hardpan. In the latter case the properties of the cover layer would be used to determine resistance while the gross tractive effort would be determined from properties of the hardpan [5].

The quantitative significance of the change in soil values after deformation by lead wheels of multi-axle wheel vehicles and the lead tracks of multi-unit tracked vehicles is unknown. Current investigations by the Land Locomotion Laboratory and by Goodman at Syracuse University will determine whether the effect will be significant enough to warrant inclusion in the determination of vehicle performance.

The pertinent vehicle characteristics which must be considered are:

1) Conventional characteristics such as wheel diameter and width, track contact area, load distribution, etc.

2) Number of powered wheels or track units.

3) Location of all wheels and tracks relative to each other.

4) Change in axle loads due to drawbar loads.

5) Vehicle trim attitude.

6) Tracked vehicles - number of road wheels and spacing between roadwheels.

The sum of the tractive forces developed by each powered wheel or track determines the gross tractive effort. The total resistance will depend on the number of wheels or tracks following in the ruts made by the lead wheels.

The change in load distribution between front and rear axles of wheeled vehicles caused by the application of drawbar loads warrants consideration when predicting performance. The change in load distribution is most significant for vehicles with relatively small wheel-base dimensions.

Change in load distribution is also quite apparent by the attitude of trim when vehicles are moving over mud or deep snow. Methods for predicting the angle of trim and the resulting load distribution, and vehicle performance is described in a first effort by S. J. Weiss et al.[9] and in later field and laboratory correlation studies[10-11].

In the analysis of tracked vehicle performance, the number and the spacing between road wheels must be considered for an accurate prediction[12]. These factors will have a bearing on the effective ground pressure of the vehicle. To calculate the performance of tracked vehicles under the assumption that the ground pressure is evenly distributed over the ground contact area will cause significant error for vehicles having few and widely spaced road wheels.

Caterpillar Tractor Model D-4.

	Full scale	¼ scale model
Gross vehicle weight (W) .	15600 lbs	200 lbs
Track length (l)	72"	18"
Track width (b)	16"	4"
Number of road wheels . .	5	5
Spacing of road wheels . .	9-1/2" O.C.	2-3/8" O.C.

Truck, ¾ Ton, 4 × 4 M-4.

Gross vehicle weight (W) . .	7150 lbs	340 lbs
Weight, front axle (W_F) . .	3300 lbs	156 lbs
Weight, rear axle (W_R) . .	3850 lbs	184 lbs
Wheel width (b)	9.6"	2.6"
Wheel diameter (D)	35.2"	8.5"
Center of gravity (s) . . .	58" ahead of rear axle	14.5" ahead of axle

Farm Tractor, FMC, Model Cot.

Gross vehicle weight (W) . .	3975 lbs	rear axle
Weight, front axle (W_F) . .	1318.5 lbs	248.4 lbs
Weight, rear axle (W_R) . .	2656.5 lbs	82.4 lbs
Front wheel width (b) . . .	5.9"	166 lbs
Front wheel diameter (D) . .	28.4"	1.5"
Rear wheel width (b) . . .	11"	7.0"
Rear wheel diameter (D) . .	50"	3.7"
Center of gravity (s) . . .	24.4" ahead of rear axle	12.5" 6" ahead of rear axle

Plate 2. -- Characteristics sheet of vehicles tested.

Application of the equations discussed earlier and the technique for the prediction of full scale and reduced scale model vehicle performance can best be portrayed by describing the analytical predictions of six vehicles and showing the correlation to actual performance obtained by experimental tests.

Three different types of vehicles are used to demonstrate the methods of prediction. They are:

1) Tracked vehicle - Caterpillar Tractor Co., Model D-4, full scale and 1/4 scale.

2) Wheeled vehicle (4 × 4) Truck, 3/4 ton, 4 × 4, M-43, full scale and 1/ scale.

3) Wheeled vehicle (4 × 2) - Farm Tractor, FMC, Model 601, full scale and 1/4 scale.

The equations and soil constants are identical in statement and application for both full scale and reduced scale model vehicle. There are no dimensional projections of the results of scale model performance to full scale vehicle performance; however, it is repeated that the same principle for prediction and testing apply to both. The characteristics of the vehicle are shown on plate number 2.

The soils in which the vehicles were evaluated (analytically and experimentally) were by general definition, sharp dry sand, and a typical Michigan farm soil which can be categorized as a sandy loam. The sandy loam was maintained at a moisture content of 20 % ± 1 %. Grain size distribution diagrams of the two soils are shown on plates 3 and 4.

The soils in which the tests were conducted are located in the Land Locomotion Laboratory full scale and scale model soil bins. The large soil bins, in which full size vehicles are tested, have dimensions of 12 feet by 120 feet by 4 feet deep. The small soil bins in which scale model vehicles are tested have dimensions of 4.5 feet by 30 feet by 1.5 feet deep.

Statistical sampling techniques were applied in obtaining the Bekker soil values. The maximum and minimum values taken from the frequency distribution of each soil parameter (k_c, k_ϕ, n, c, ϕ) were used in computing the performance predictions. These values listed on plates 3 and 4 represented a range covering approximately 90 % of the soil parameters occurring throughout the test bins. For field tests in which no control over the soil condition is attempted and the scatter of soil parameters is much larger, the range of soil values is selected from the frequency curve to include those values within the 80 % probability of occurrence points.

To describe the procedure for predicting performance in detail, a curve of drawbar pull vs % wheel slippage for the FMC Model 601 Farm Tractor in dry sand will be determined. All of the equations of land locomotion are programmed for high speed computations on electronic digital computers, allowing practical application of equations 2 to 6 described earlier in this paper.

The first step will be to determine the change in axle loads due to drawbar-pull forces. This is illustrated in plate number 5. The change in weight distribution was computed under static conditions although it has been shown by Bekker [3] and Janosi [5] that the vertical reaction occurs ahead of the centerline when dynamic conditions exist. The approximation obtained by assuming static loading conditions is of sufficient accuracy because the off-set distance is rela-

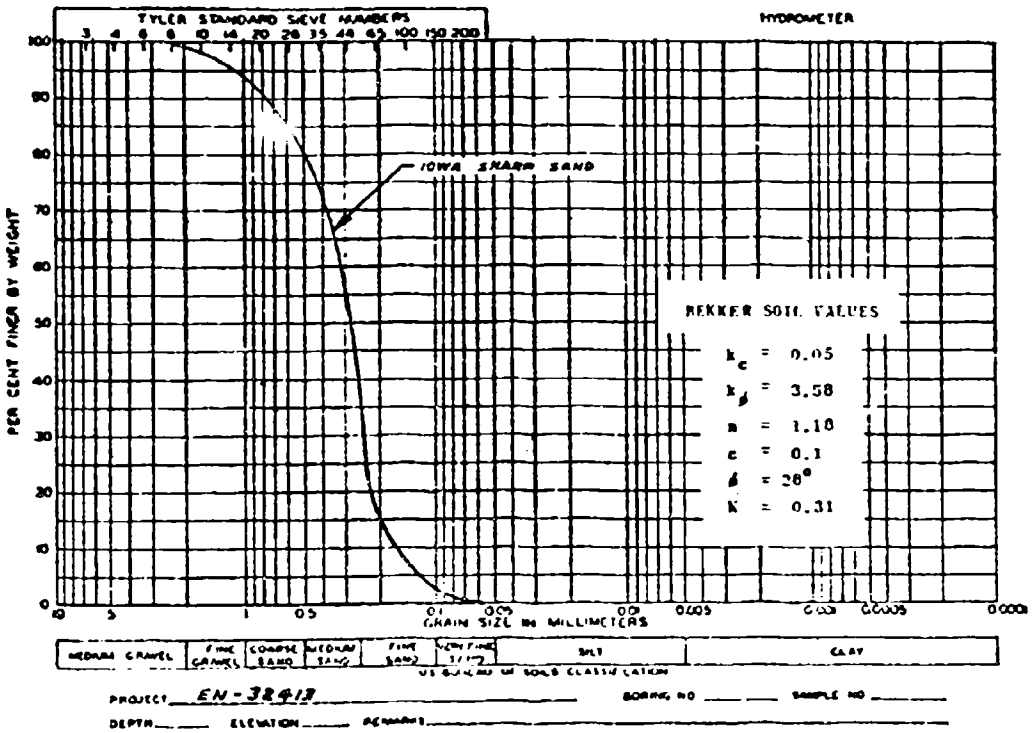


Plate 3. — Grain size distribution diagram of Iowa sharp sand and Bekker soil values.

tively small and the overall distance between front and rear wheel reactions are, for practical considerations identical to dynamic conditions.

Read axle loads ranging from 2660 lbs to 2800 lbs and front axle loads ranging from 1320 lbs to 1180 lbs were chosen as the weight input to equations 2 and 3. Other vehicle data entered in the equations is as follows:

b = 5.9 inches (front wheels); b = 11.0 inches (rear wheels); D = 28.1 inches (front wheels); D = 50 inches (rear wheels).

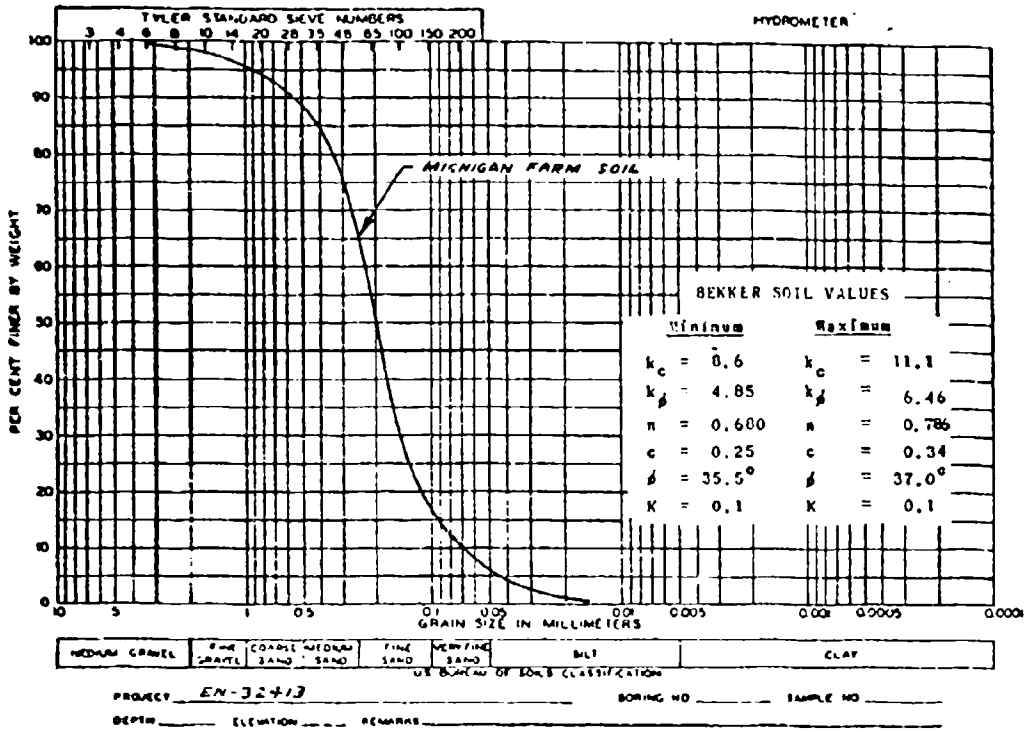
The Bekker soil values for the dry sand are as follows:

k_c = 0.05; k_ϕ = 3.58; n = 1.18; c = 0.10; Φ = 28°; K = 0.31.

Statistical sampling was not used in obtaining the soil values in dry sand for the magnitude of variation was negligible.

The numerical results from equations 2 and 3 are received from the digital computer in the form shown on plates 6 and 6 a. The following steps are used to plot the curve of drawbar-pull (DP) vs % wheel slip (i_s):

1) Since only the rear wheels of the tractor are powered the curve representing the change in axle load for the rear wheels W_R on plate number 5 is the only one considered to determine gross tractive effort (H). Since the



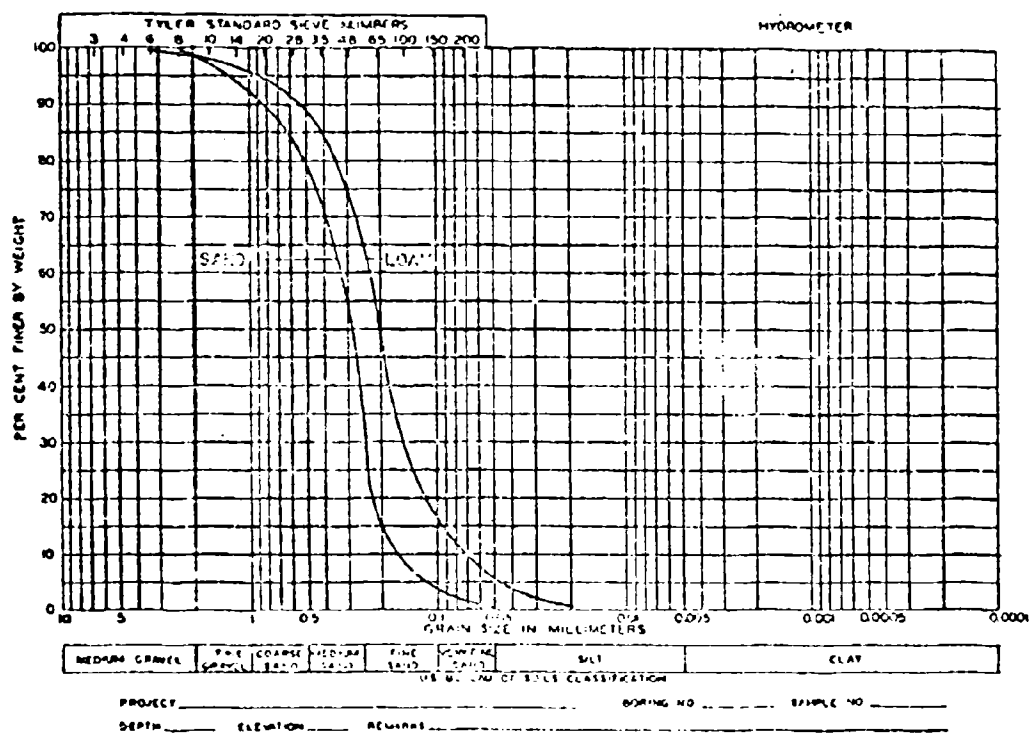


Plate 4. — Grain size distribution diagram of Michigan farm soil and Bekker soil values.

change in axle load is computed for static conditions, drawbar pull (H_N) and gross tractive effort (H_G) are equal, no motion resistance occurs. A value for W_R is selected from the ordinate of the graph on plate 4 and projected until intersection is made with the curve of W_R. The corresponding value of H can then be read from the abscissa. This load (W_R) divided by a factor of 2 represents the load on each rear wheel. From the column of values computed for

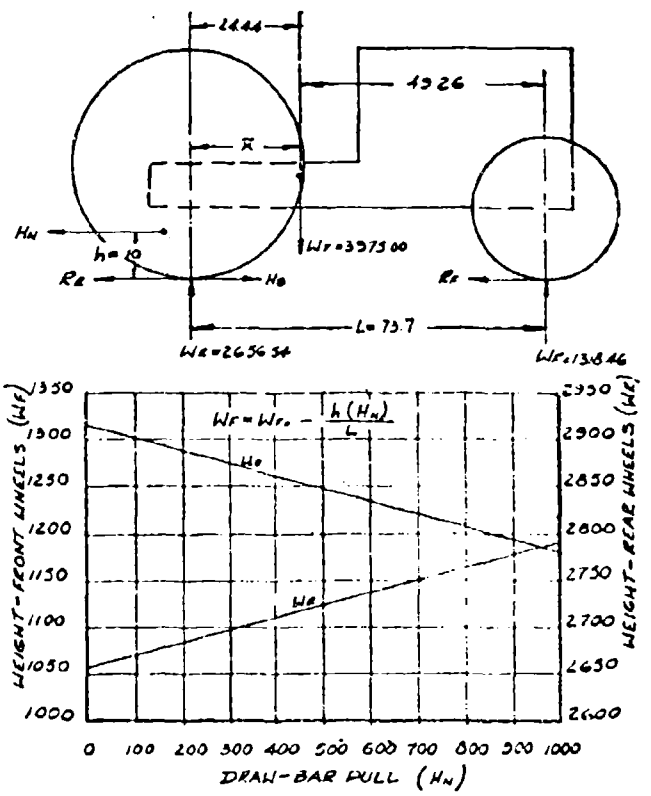


Plate 5. — Change in load distribution due to drawbar load for the farm tractor (FMC Model 601).

this selected load shown on plates 6 and 6 a, the corresponding value of H from the curve on plate number 5 is located. In the column adjacent to this value of H appears a corresponding value of % wheel slippage (i_o). This value of H and the corresponding wheel slippage represent one point on a curve of gross tractive effort vs % wheel slippage (H vs i_o).

For example, an axle load of 2740 lbs (W_R) on plate number 5 gives a value of H equal to 610 lbs and a wheel load of 1370 lbs. There values occur simultaneously on plates 6 and 6 a at a wheel slippage of 25 %. This procedure is repeated for increasing values of rear axle load (W_R) until a % wheel slippage range of 10 to 80 % has been covered.

Plate 6.

H		t_n		$W_H/2$	
+ 18378	+ 03	+ 100	— 00	+ 134	+ 04
+ 46960	+ 03	+ 200	— 00	+ 134	+ 04
+ 65264	+ 03	+ 300	— 00	+ 134	+ 04
+ 73293	+ 03	+ 400	— 00	+ 134	+ 04
+ 76010	+ 03	+ 500	— 00	+ 134	+ 04
+ 76753	+ 03	+ 600	— 00	+ 134	+ 04
+ 76920	+ 03	+ 700	— 00	+ 134	+ 04
+ 76951	+ 03	+ 800	— 00	+ 134	+ 04
+ 18476	+ 03	+ 100	— 00	+ 135	+ 04
+ 47256	+ 03	+ 200	— 00	+ 135	+ 04
+ 65705	+ 03	+ 300	— 00	+ 135	+ 04
+ 73810	+ 03	+ 400	— 00	+ 135	+ 04
+ 76557	+ 03	+ 500	— 00	+ 135	+ 04
+ 77310	+ 03	+ 600	— 00	+ 135	+ 04
+ 77479	+ 03	+ 700	— 00	+ 135	+ 04
+ 77511	+ 03	+ 800	— 00	+ 135	+ 04
+ 18580	+ 03	+ 100	— 00	+ 136	+ 04
+ 47552	+ 03	+ 200	— 00	+ 136	+ 04
+ 66146	+ 03	+ 300	— 00	+ 136	+ 04
+ 74327	+ 03	+ 400	— 00	+ 136	+ 04
+ 77105	+ 03	+ 500	— 00	+ 136	+ 04
+ 77867	+ 03	+ 600	— 00	+ 136	+ 04
+ 78039	+ 03	+ 700	— 00	+ 136	+ 04
+ 78071	+ 03	+ 800	— 00	+ 136	+ 04
+ 40696	+ 02	+ 500	— 01	+ 137	+ 04
+ 20102	+ 03	+ 100	— 00	+ 137	+ 04
+ 36074	+ 03	+ 150	— 00	+ 137	+ 04
+ 50179	+ 03	+ 200	— 00	+ 137	+ 04
+ 60927	+ 03	+ 250	— 00	+ 137	+ 04
+ 68292	+ 03	+ 300	— 00	+ 137	+ 04
+ 72934	+ 03	+ 350	— 00	+ 137	+ 04
+ 75659	+ 03	+ 400	— 00	+ 137	+ 04
+ 77160	+ 03	+ 450	— 00	+ 137	+ 04
+ 77940	+ 03	+ 500	— 00	+ 137	+ 04
+ 78324	+ 03	+ 550	— 00	+ 137	+ 04
+ 78503	+ 03	+ 600	— 00	+ 137	+ 04
+ 78582	+ 03	+ 650	— 00	+ 137	+ 04
+ 78616	+ 03	+ 700	— 00	+ 137	+ 04
+ 78629	+ 03	+ 750	— 00	+ 137	+ 04
+ 78634	+ 03	+ 800	— 00	+ 137	+ 04
+ 78636	+ 03	+ 900	— 00	+ 137	+ 04
+ 78636	+ 03	+ 950	— 00	+ 137	+ 04
+ 78636	+ 03	+ 100	+ 01	+ 137	+ 04
+ 18788	+ 03	+ 100	— 00	+ 138	+ 04
+ 48141	+ 03	+ 200	— 00	+ 138	+ 04
+ 67027	+ 03	+ 300	— 00	+ 138	+ 04
+ 75360	+ 03	+ 400	— 00	+ 138	+ 04
+ 78199	+ 03	+ 500	— 00	+ 138	+ 04
+ 78980	+ 03	+ 600	— 00	+ 138	+ 04

Explanation of computer printout code + 137 + 04 is interpreted as $+ 0.137 \times 10^{4}$.

(follows plate 6)

H		h_o		$W_R/2$	
+79157	+03	+700	—00	+138	+04
+79191	+03	+800	—00	+138	+04
+18891	+03	+900	—00	+139	+04
+48435	+03	+200	—00	+139	+04
+67406	+03	+300	—00	+139	+04
+75875	+03	+400	—00	+139	+04
+78745	+03	+500	—00	+139	+04
+79537	+03	+600	—00	+139	+04
+79717	+03	+700	—00	+139	+04
+79751	+03	+800	—00	+139	+04
+18985	+03	+100	—00	+140	+04
+48729	+03	+200	—00	+140	+04
+67965	+03	+300	—00	+140	+04
+76391	+03	+400	—00	+140	+04
+79292	+03	+500	—00	+140	+04
+80093	+03	+600	—00	+140	+04
+80276	+03	+700	—00	+140	+04
+80310	+03	+800	—00	+140	+04

Plate 6 a.

$W_R/2$		D		b		R_V		R_H		$R_V + R_H$	
+5900	+03	+2810	+02	+5900	+01	+1471	+03	+6469	+02	+2118	+03
+6000	+03	+2810	+02	+5900	+01	+1502	+03	+6652	+02	+2167	+03
+6100	+03	+2810	+02	+5900	+01	+1533	+03	+6836	+02	+2217	+03
+6200	+03	+2810	+02	+5900	+01	+1561	+03	+7022	+02	+2267	+03
+6300	+03	+2810	+02	+5900	+01	+1596	+03	+7211	+02	+2317	+03
+6400	+03	+2810	+02	+5900	+01	+1627	+03	+7400	+02	+2367	+03
+6500	+03	+2810	+02	+5900	+01	+1659	+03	+7591	+02	+2418	+03

$W_R/2$		D		b		R_V		R_H		$R_V + R_H$	
+1340	+04	+5000	+02	+1100	+02	+2539	+03	+7199	+02	+3288	+03
+1350	+04	+5000	+02	+1100	+02	+2563	+03	+7390	+02	+3322	+03
+1360	+04	+5000	+02	+1100	+02	+2587	+03	+7681	+02	+3355	+03
+1370	+04	+5000	+02	+1100	+02	+2611	+03	+7773	+02	+3388	+03
+1380	+04	+5000	+02	+1100	+02	+2635	+03	+7867	+02	+3422	+03
+1390	+04	+5000	+02	+1100	+02	+2659	+03	+7958	+02	+3455	+03
+1400	+04	+5000	+02	+1100	+02	+2684	+03	+8051	+02	+3489	+03

Plate 6, 6a. — Predicted results of H, R_V, R_H for the farm tractor (FMC Model 601) in Iowa sharp sand.

2) Resistances are computed for the same range of wheel loads used in the determination of gross tractive effort (1). The load on the front wheels (W_F) will decrease with increasing drawbar-pull. Horizontal and vertical components of the motion resistance are determined and listed separately on plates 6 and 6 a (R_v and R_H) for appropriate application. Both components of the resistance will be used for the front wheels but only the vertical component (R_v) is normally used for the rear wheel. This assumption is possible due to the fact that the rear wheel operates in the rut made by the front wheel so that the horizontal resistance component (R_H) becomes negligible. However, since the

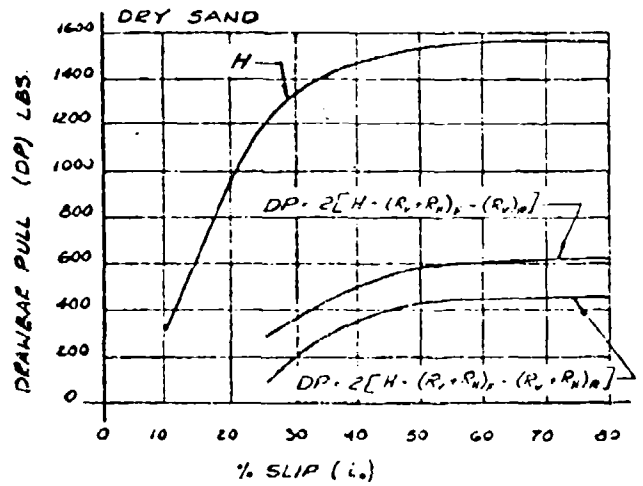


Plate 7. — Predicted results of farm tractor (FMC Model 601) in Iowa sharp sand.

width of the front wheel in this case is much smaller than the rear, the resistance for the rear wheel will be an unknown value between R_H and (R_v + R_H). We find then, the resistance for the front wheel at a load of 620 lbs is 227 lbs per wheel and 261-338 lbs per wheel at a load of 1370 lbs for the rear wheels.

3) The algebraic summation of the gross tractive effort and the resistance to motion as expressed in equation 1 for each % wheel slippage plotted in the range of 10 to 80 % will give the final curve of drawbar-pull vs % wheel slippage. Accordingly, the gross tractive effort for the example will be 2H = 1220 lbs, and the resistance will be 2R, to 2 (R_v + R_H) for the rear wheels plus 2 (R_v + R_H) for the front wheels giving a total resistance of 976 to 1128 lbs. The resulting drawbar-pull will be 92-244 lbs at 25 % slip. The total results of the predicted performance curve for the tractor on dry sand are shown as a band of points on plate number 7. The same general procedure is used to predict the performance of the truck, 3/4 ton 4 × 4, M43 with the exception that all wheels are powered as compared to two wheels on the FMC farm tractor.

Equations (4), (5) and (6) shown on plate number 1 a were used to predict

the performance of the Caterpillar tractor. It is first determined whether the vehicle will travel in a level attitude or assume an angle of trim of sufficient degree to affect the results of the predictions. If the vehicle sinkage is computed to be minor the assumption is made that the vehicle will maintain a level attitude while in motion. If the vehicle sinkage is relatively large, the evaluation must be made assuming that an angle of trim exists and the ground pressure is non-uniform along the track contact area. This requires the use of equation (4) in the following form:

$$H = A \left\{ c \left[-\frac{1}{J} \left(1 - e^{-J} \right) \right] + k Z_0^n \tan \Phi \left[\frac{1}{n+1} - \frac{1}{I^{n+1}} \int_0^I X^n e^{-\frac{I_0 X}{k}} dX \right] \right\} \tag{7}$$

where

$$Z_0 = \left[\frac{(n+1) W}{A k} \right]^{\frac{1}{n}} \tag{8}$$

and equation (5) for resistance (R_c) becomes

$$R_c = \frac{2 b k Z_0^{N+1}}{n+1} \tag{9}$$

In the performance prediction of the Caterpillar tractor for the dry sand and Michigan farm soil, the sinkage was considered to be minor and equations (4) and (5) were applied to the solutions.

The performance predictions for the 1/4 scale models were computed in the same manner as the full scale vehicles.

Discussion of tests

Experimental tests were conducted in the laboratory to verify the analytical predictions. Plate number 8 shows a view of the Caterpillar tractor model D-4 in the soil bin containing the Michigan farm soil. The tractor is attached to a dynamometer carriage which provides the drawbar load. The skid located behind the carriage provided additional drawbar load. Instruments for recording the drawbar load and track slippage are shown mounted on the platform of the dynamometer carriage. A view of the load cell used to measure the magnitude of the drawbar load is shown connected between the test vehicle and the dynamometer carriage in plate number 9. Plate number 10 is a view showing the full scale D-10 tractor in dry sand prior to a test run. Plate number 11 shows a view of the 3/4 ton truck, M43 in the soil bin.

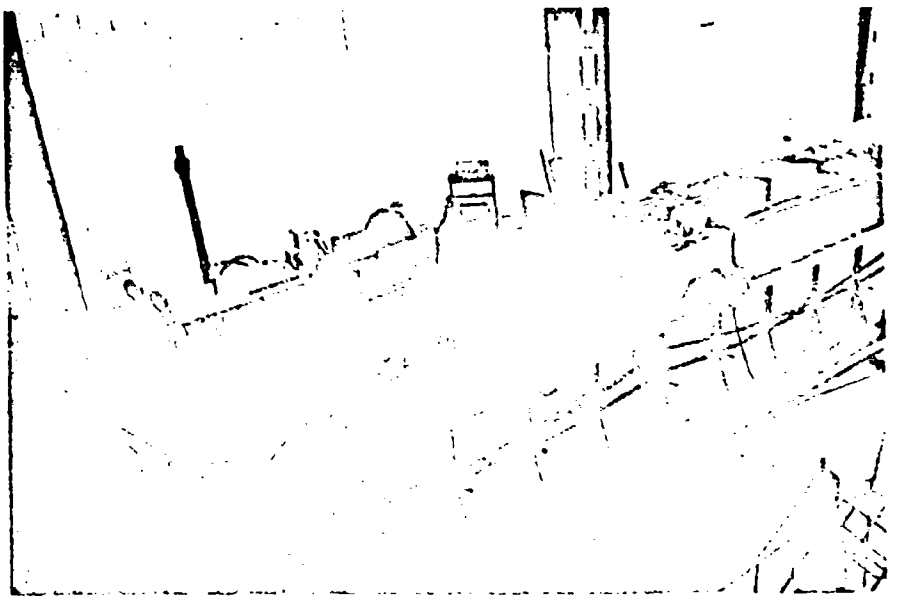


Plate 8. — Caterpillar tractor, model D-4, in soil bin containing Michigan farm soil.

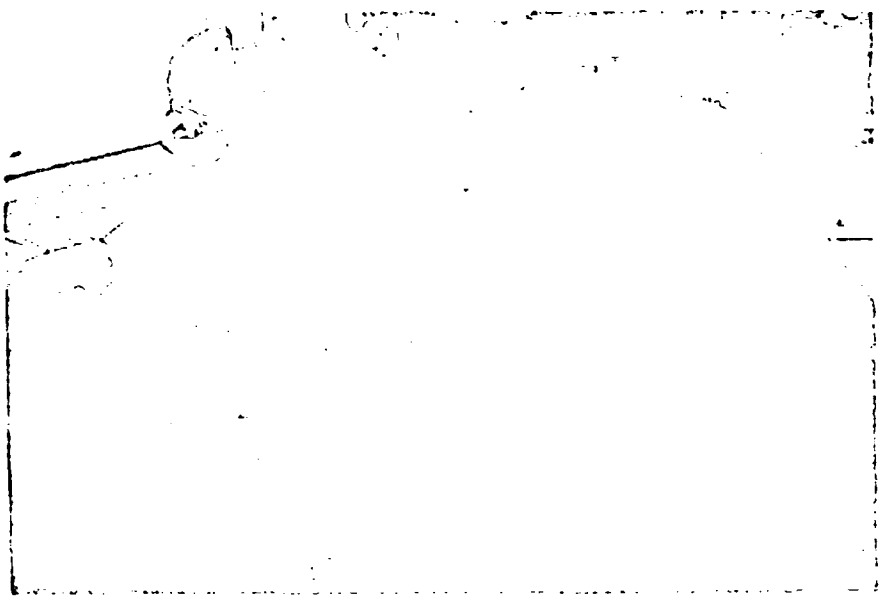


Plate 9. — Load cell for measuring the magnitude of drawbar loads.

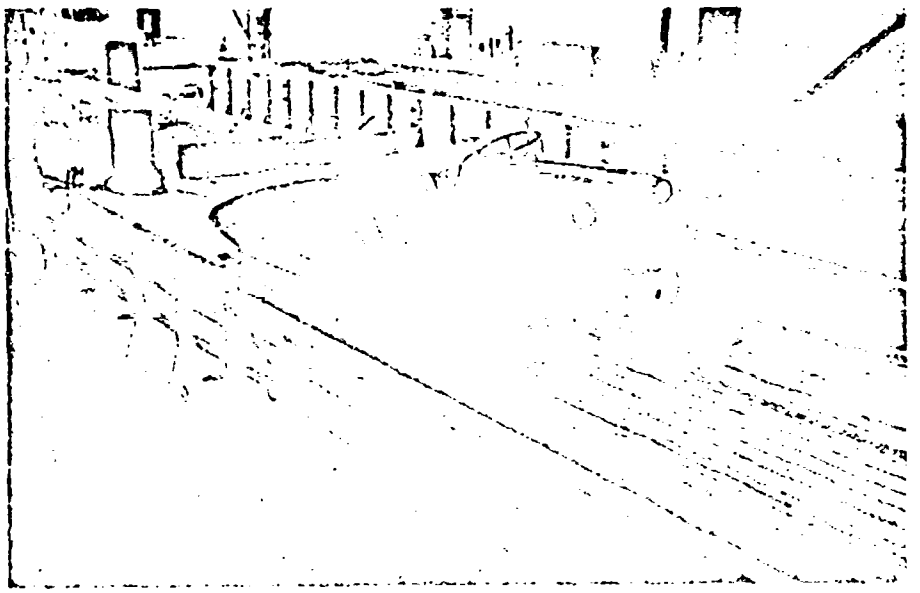


Plate 10. — Full scale FMC farm tractor in dry sand bin.

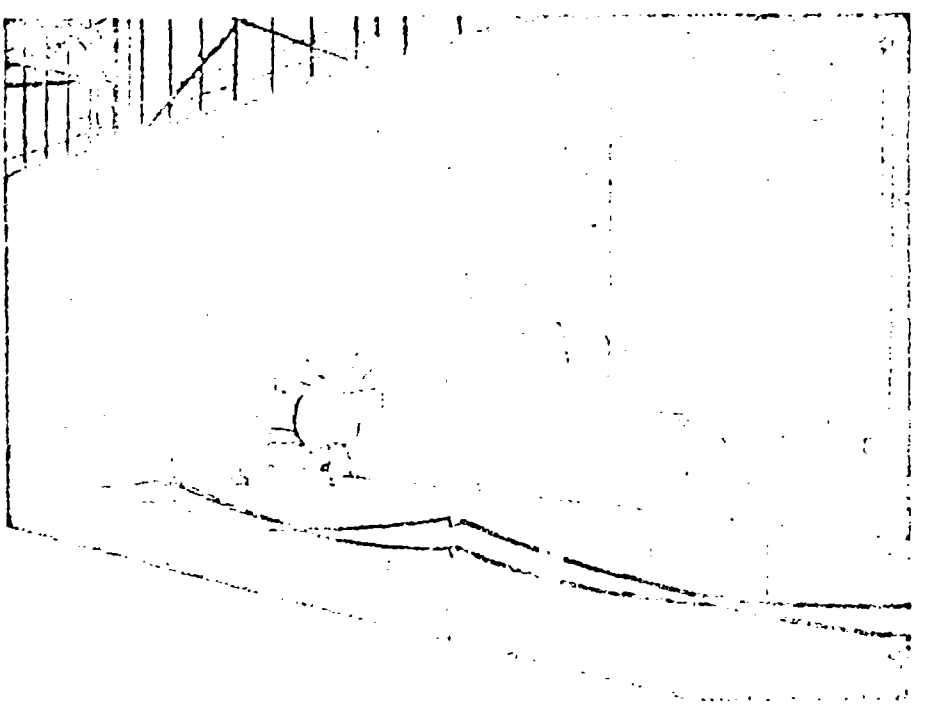
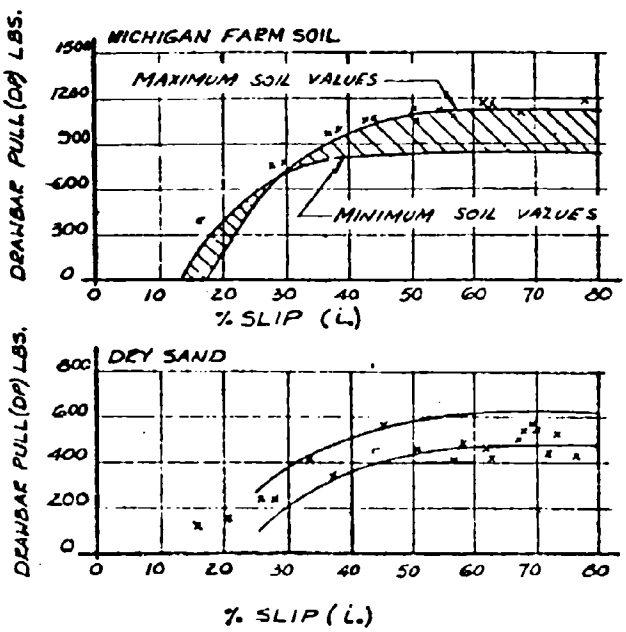


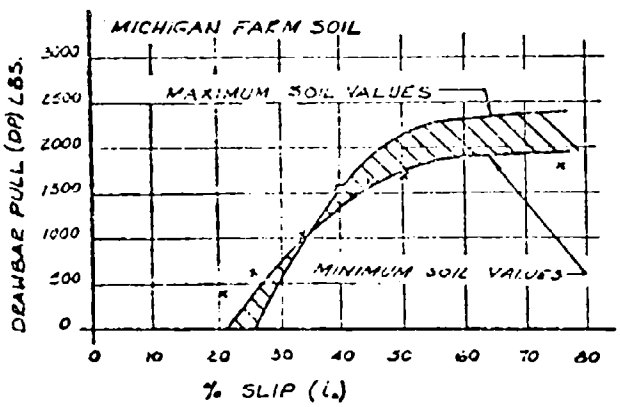
Plate 11. — 3/4 ton truck, M 43, connected to dynamometer carriage.



——— Computed values. XXX Measured values.

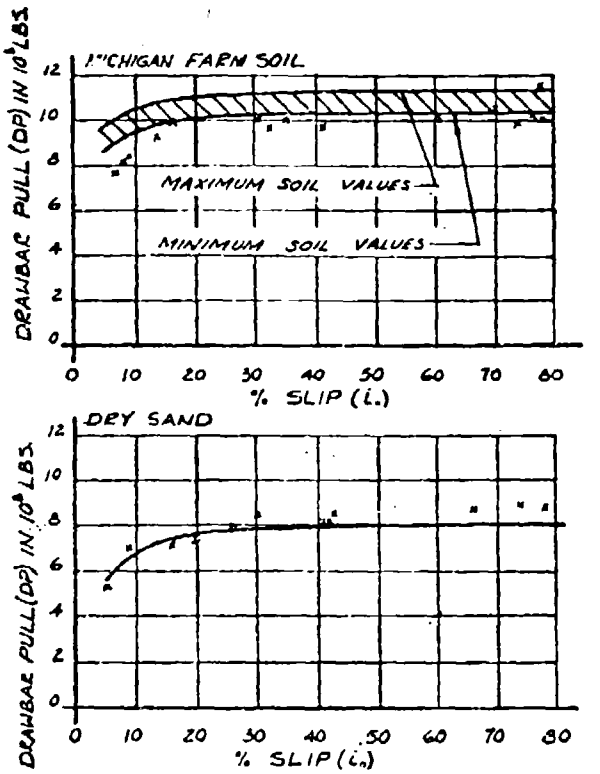
Plate 12. — Test results and predicted results of the FMC farm tractor in sand and Michigan farm soil.

Truck, 3/4 ton, 4 × 4, M43.



——— Computed curves. XXX Measured points.

Plate 13. — Test results and predicted results of the truck M 43 in Michigan farm soil.



——— Computed curves. XXX Measured points.

Plate 14. — Test results and predicted results of the Caterpillar tractor, D-4, in sand and Michigan farm soil.

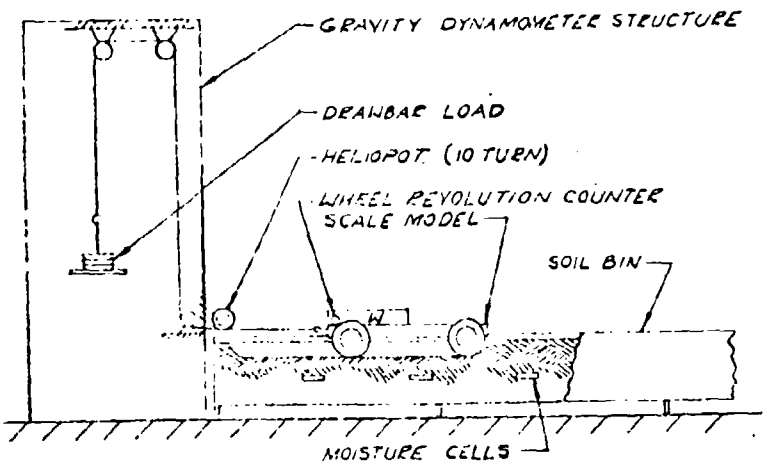


Plate 15. — Model testing facility.

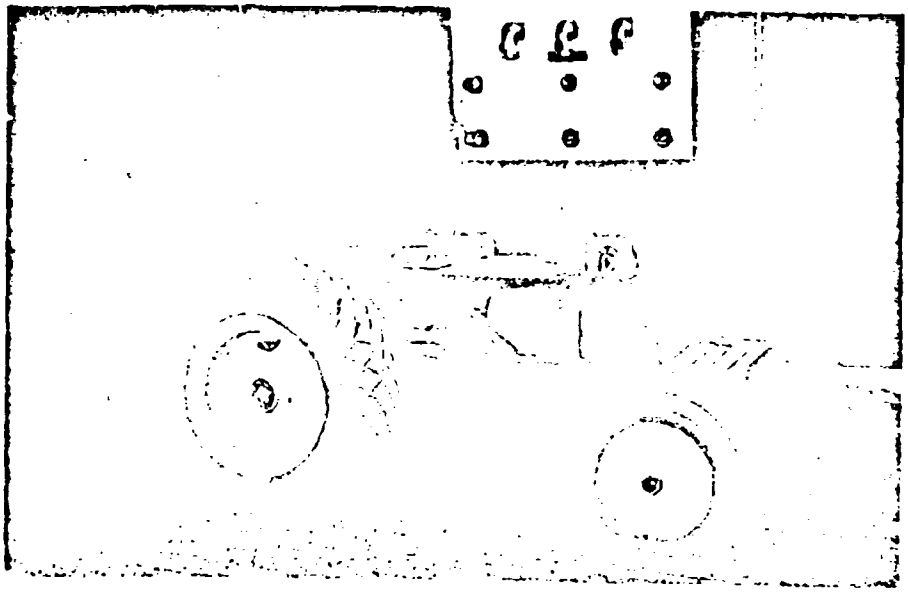


Plate 16. — 1/4 scale FMC farm tractor in model test bin.

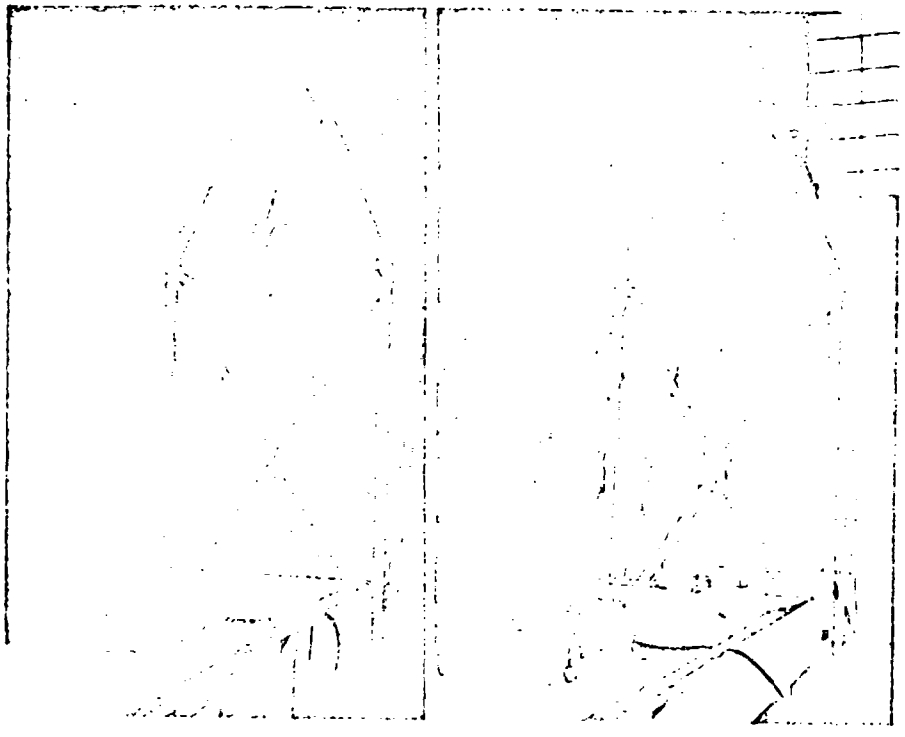


Plate 17.

Plate 18.

Plate 17. — 1/4 scale Caterpillar tractor, D-4, in model test bin.
Plate 18. — 1/4 scale truck, M 43 in model test bin.

The drawbar-pull vs slip curves of the full scale vehicles were obtained by applying a load to the vehicle through the dynamometer carriage and recording the resulting wheel or tack slippage. Each test run contributed one point to the curve. The load on the drawbar was increased until a wheel or track slippage of 80 % was attained. The measured curves of drawbar pull vs slip in

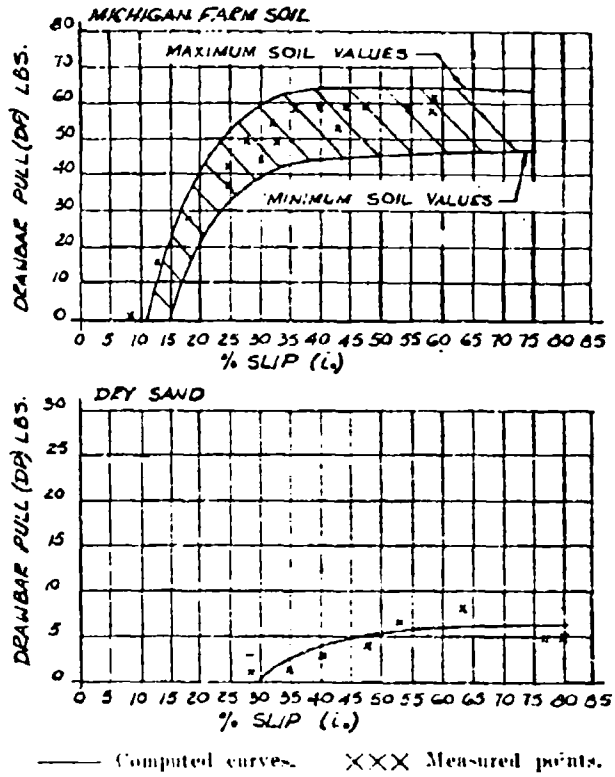
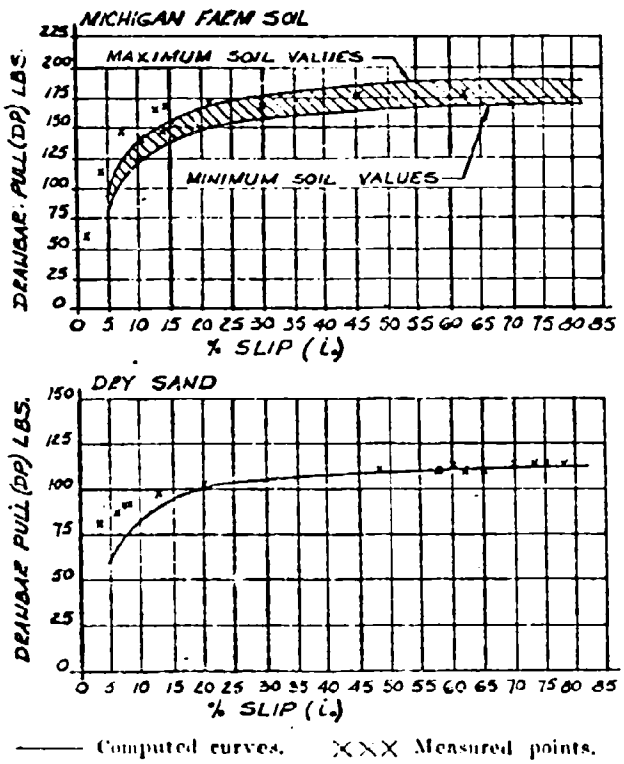


Plate 19. — Test results and predicted results of the 1/4 scale FMC farm tractor in sand and Michigan farm soil.

dry sand and loam for the full scale vehicles are compared to the predicted curves on plates 12, 13, and 14. The 3/4 ton truck, M43, was unable to negotiate the dry sand. The sand is not compacted but rather in a very loose condition. The relatively small tires on the M43 truck and the magnitude of the load per wheel were the prime reasons for the lack of sufficient flotation.

Plate number 15 is a sketch of the model test facility. Drawbar-pull tests of the 1/4 scale models were conducted by attaching a known load to the vehicle by means of the gravity type dynamometer and measuring the per cent of wheel or track slippage. Slippage was determined by recording the actual distance traveled by the vehicle by means of a 10 turn heliopot. Simultaneously, the

distance traveled by a point on the wheel or track circumference of the vehicle was measured and the slippage established. Plate number 16 shows the 1/4 scale FMC farm tractor undergoing a drawbar-pull vs slip test in Michigan farm soil. The 1/4 scale Caterpillar tractor and the 1/4 scale truck, M43 are shown in plates 17 and 18 respectively. The measured results of the 1/4 scale



——— Computed curves. XXX Measured points.

Plate 20. — Test results and predicted results of the 1/4 scale Caterpillar tractor, D4, in sand and Michigan farm soil.

model tests in dry sand and Michigan farm soil are shown in comparison with the predicted curves in plates 19, 20 and 21. The 1/4 scale model truck, 3/4 ton, M43 was unable to negotiate the dry sand was the case with the full scale truck, M43.

Conclusions

The performance of vehicles in deformable soils can be predicted through the application of Land Locomotion Mechanics utilizing the Bekker soil value system. The accuracy of predictions for vehicles operating in homogeneous soil conditions is accurate to within ± 10 %.

The current equations used by the Land Locomotion Laboratory to describe soil vehicle relationships do not produce any scale effect. That is, the equations are equally accurate for predictions of model performance or predictions of full scale vehicle performance.

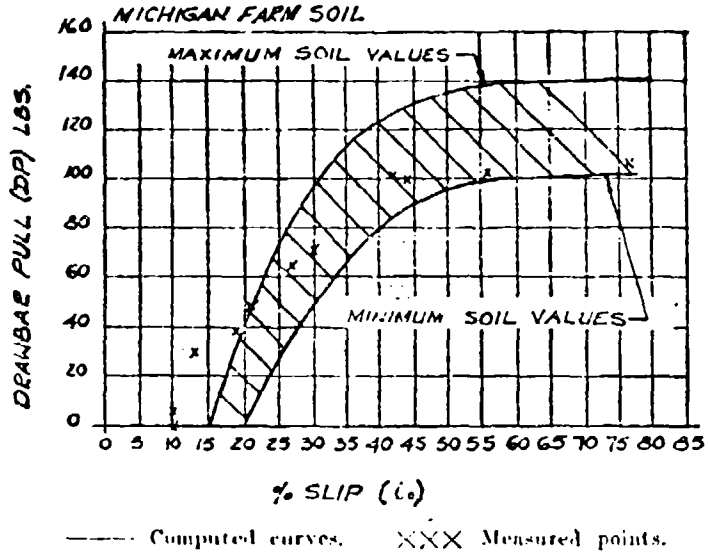


Plate 21. — Test results and predicted results of the 1/4 scale truck, M43, in Michigan farm soil.

The use of scale models to establish the order of merit of competitive vehicle concepts is a valid technique. This method of evaluation eliminates the high cost in time and money associated with evaluation tests utilizing full scale prototypes.

Programming of the soil vehicle relationships for computation by means of electronic computers provides the capability of analytically predicting the performance of a large number of vehicles at an even greater saving in time and money than possible using model technique. With complete acceptance by the design engineer of the analytical predictions, the use of scale model testing and full scale prototype testing will be required only as a final verification.

Studies currently in progress by the Land Locomotion Laboratory to determine the significance of such factors as; the change in Bekker soil values when the soil is deformed by the passing of a wheel or track; the effect of wheel or track slippage on vehicle sinkage and motion resistance; and the effect of multi-layer soils on vehicle performance will further improve the accuracy of vehicle performance predictions beyond the current 10 %

BIBLIOGRAPHY

1) **Bekker** M. G. A proposed system of physical and geometrical soil values for the determination of soil trafficability and vehicle performance. Interservice Vehicle Mobility Symposium, Stevens Institute of Technology, Hoboken, New Jersey, April 1955.

2) **Bekker** M. G. A practical outline of the mechanics of automotive land locomotion. Detroit Arsenal Land Locomotion Laboratory, January 1955.

3) **Bekker** M. G. Theory of land locomotion. University of Michigan Press, Ann Arbor, Michigan, 1956.

4) *Janosi* Z. An analysis of pneumatic tire performance in deformable soils. Paper to be presented at the First International Conference on the Mechanics of Soil-Vehicle Systems, Turin (Italy), 1961.

5) *Janosi* Z., Hanamoto B. The analytical determination of drawbar pull as a function of slip for tracked vehicles in deformable soils. Paper to be presented at the First International Conference on the Mechanics of Soil-Vehicle Systems, Turin (Italy), 1961.

6) *Hegedus* E. A simplified method for the determination of bulldozing resistance. Land Locomotion Report No. 61, OTAC, Detroit Arsenal, 1960.

7) *Pavlics* F. A new type of field apparatus for measuring locomotive stress-strain relationship in soils. Paper to be presented at the First International Conference on the Mechanics of Soil-Vehicle Systems, Turin (Italy), 1961.

8) *Hanamoto* B. Soil testing at fort Know, Ky. Land Locomotion Laboratory Report No. 39, OTAC, Detroit Arsenal, June 1958.

9) *Weiss* S. J., Harrison W. L., Abarca Li L. C. and Bekker M. G. Preliminary study of snow values related to vehicle performance. Technical Memorandum M-02, Detroit Arsenal, Land Locomotion Laboratory, September 1956.

10) *Harrison* W. L. Study of snow values related to vehicle performance. Land Locomotion Laboratory Report No. 23, OTAC, Detroit Arsenal, December 1957.

11) *Harrison* W. L. and Czako T. Over-snow vehicle performance studies. Land Locomotion Laboratory Report No. 68, OTAC, Detroit Arsenal, November 1960.

DISCUSSIONS

R. P. MCGOWAN. — I would like to make one comment, which I believe Mr. Harrison will agree with, that the performance of vehicles in the various types of soil conditions is actually somewhat more complicated then even are represented in his equations, and that therefore they would require verification over the range of soil types and values, and over the range of vehicle sizes and types also. So that, while his approach is an analytical approach versus the scale model approach, it still will require a verification over a wide range of conditions. The procedure, therefore, while analytical, still requires empirical verification. We like the scale model approach because it requires a minimum understanding of a complex situation and will produce usefull results. Also I might add, that it is the same road that has been followed in aerodynamics and hydrodynamic fields. I have a brief question, that Mr. Harrison might be able to answer, about his method. The bevameter, when it is used in limited depths of soil, does the bevameter reading include the ground effect or not?

W. L. HARRISON. — I agree with Mr. McGowan that scale model testing is an easy way out. However, I do not think we can afford to take the easy way out and not understand the relationship between the soil and the vehicle. In addition, we do not use the analytical approach in lieu of the scale model technique. As I stated in my paper, we can predict scale model vehicle performance as well as full scale vehicle performance. In answer to the question concerning the bevameter, it does observe what you refer to as the ground effect. The vertical load versus sinkage curve produces a strength profile of the soil, and when properly obtained that is within the range of pressures that will be applied to the ground by the vehicle which you are interested in evaluating, you may accurately determine what its performance will be.

R. P. MCGOWAN. — I would just like to comment briefly a bit further, that if the bevameter measurement includes in the measurement quantities others than what are in the soil, then it too is a scale model test of a sort. And also I recall — I think it was Mr. Pavlics' presentation —, that the new type of rolling wheel bevameter produced values that were substantially different than those produced by the original model of the bevameter, and this, of course, means that the bevameters are acting as scale models measuring relative soil properties rather than absolute soil properties.

W. L. HARRISON. — I did not intend to give the understanding that the bevameter recorded values which are not in the soil. And in reference to Mr. Pavlic's presentation, the one parameter that he said was different from that which you obtain with the bevameter is the tangent modulus, which merely determines the location of peak point along the horizontal axis of the stress strain curve, of the shear stress.

C. J. POWELL and J. L. SMITH. — Mr. Harrison presents test data which effectively confirm his prediction equations for the conditions of his tests. Some discussion regarding the range of applicability of the equation to varied vehicle and soil conditions seems pertinent, however. The equations the Author uses to predict wheeled-vehicle performance were developed by the Land Locomotion Laboratory for a rigid wheel operating in a homogeneous soil. While Mr. Harrison has not included information on the inflation pressures that were used in his tests, it is assumed that they were high enough so that the tires acted essentially as rigid wheels.

Prediction of drawbar pull by the formulas proposed by Mr. Harrison involves the use of a computed value for motion resistance due to sinkage of the wheel into the soil (Eqs. 1 and 3). Mr. Harrison apparently has been able to make this computation satisfactorily for the Michigan farm soil since he shows predicted drawbar pull curves for tests in this soil. A review of Mr. Janosi's paper (No. 45) reveals that he was unable to determine reliable soil values for the Michigan farm soil because the equation, $p = k Z^n$, did not describe the shape of the penetration curve. Therefore, he did not find it possible to predict motion resistance. Since Mr. Harrison worked with the same type of soil and the same soil value system, it would be of interest to know the equation he used to describe the load-penetration curve.

In the tests with the 3/4-ton truck and its corresponding 1/4-scale model, both the full-size vehicle and the model were immobilized in loose sand. It would be interesting to see the prediction curves for these tests even though no test data could be developed.

It is noted that the equations proposed in this paper have been tested experimentally in loose, nonplastic soils only (the farm soil does not contain sufficient fines

to have a measurable plasticity by the Atterberg Limit test). Before they are accepted for general use, additional tests should be made in nonplastic soils at different densities and plastic soils at different densities and moisture contents.

W. L. HARRISON. — In answer to the first question by Messrs. Powell and Smith, I used the same equation as Mr. Janosi ($p = kZ^n$). The difference can be simply explained as follows: Mr. Janosi tilled his soil to a depth of only 4 to 6 inches, while the soil in which I conducted my tests was tilled to a depth of 24 inches.

In answer to your next question, if you have some doubt as to the immobilization of the 3/4 ton truck and model in loose sand, all of the necessary input data and the equations for prediction are included in this paper and you may easily calculate the performance in question.

And finally, the equations used in this paper have already been accepted for general use by the Land Locomotion Laboratory and many others. Fortunately, the soil strength inputs to the equations are based on stress-strain relationships of soil under vertical and horizontal loads and are not affected by the definitions of plasticity as defined by the Atterberg limit test or any others. Soil strength is measured, as near as possible, akin to the mode of soil failure caused by a vehicle when traveling across the soil. Any effects of density, moisture content, plasticity or nonplasticity will naturally be contained in the soil stress-strain relationship.

Problèmes de similitude: commentaire final

Problemi di similitudine: conclusioni

J. Truelle

Je n'aurai que quelques mots à ajouter, à l'issue de cette session consacrée à la Similitude, pour souligner le travail très sérieux représenté par les communications que nous venons d'entendre. Je pense que cet apport constituera un excellent outil de recherche, à la disposition des théoriciens.

Je remarque, pour terminer, que la plupart des formules présentées ont un caractère encore empirique: cela ne doit pas nous décevoir, si ces formules sont précisément conformes à l'expérience. Mais nous devons en conclure que la théorie de la locomotion en tous terrains, et de la similitude en particulier, est très complexe, que des formes mathématiques satisfaisantes sont encore à trouver, et qu'il reste par conséquent beaucoup à faire dans ces études, dont on doit souhaiter qu'elles soient approfondies.

TEORIA E PREVISIONE DELLE PRESTAZIONI

THEORY AND PREDICTION

The analytical determination of drawbar pull as a function of slip for tracked vehicles in deformable soils

Determinazione analitica dello sforzo di trazione alla barra dei veicoli cingolati in funzione dello scorrimento su terreni cedevoli

Z. Janosi - B. Hanamoto *)

ABSTRACT. -- *Equations are deduced by means of the Bekker soil value system and a soil shear stress-strain relationship, first suggested in this paper, to predict the drawbar pull of track laying vehicles as a function of slippage. Test results indicating reasonable accuracy of the method are presented.*

Conclusions are drawn concerning possible means of achieving improved tracked vehicle design, and the direction of future research.

Key to symbols and definitions

H	=	Traction, tractive effort, thrust. The gross tractive effort developed by the vehicle (lbs).
i_o	=	Slip, slippage. A ratio between the difference of the theoretical and actual speed and the theoretical speed.
S	=	Shear stress in the soil (lbs/in^2).
S_{max}	=	Maximum shear stress in the soil (lbs/in^2).
c	=	Cohesion (lbs/in^2).
p	=	Pressure normal to the shear-plane (lbs/in^2).
p_{max}	=	Maximum normal pressure under a track which occurs at Z_o sinkage (lbs/in^2).
Φ	=	Angle of shear resistance, the angle of internal friction (Degrees).
A	=	Vehicle-ground interface, ground contact area (in^2).
W	=	Load (lbs).
K_1	=	Slippage coefficient (in^{-1}).
K_2	=	Slippage coefficient.
Y_{max}	=	Maximum value of terms included in the brackets in equation 3.
x	=	Horizontal distance between an arbitrarily chosen point on the track and the leading point of the interface (in).
l	=	Length of the track (in).
j	=	Soil deformation in the horizontal direction (in).
K	=	Deformation modulus of a soil shear stress-strain curve (in).

*) Land Locomotion Laboratory U.S. Army Ordnance Tank Automotive Command, Detroit, Michigan.

b = Width of one track (in).
h = Heighth of grousers (in).
D P = Drawbar pull, net tractive effort. The thrust lessened by the motion resistance (lbs).
R = Motion resistance (lbs).
Z = Sinkage at a point defined by x (in).
Z_o = Maximum sinkage of a track, sinkage at the end of the interface (in).
k_c = Cohesive modulus of sinkage (lbs/in^{n+1}).
k_ϕ = Frictional modulus of sinkage (lbs/in^{n+1}).
n = Exponent of sinkage.
m = Number of terms considered in the series in equation 20.
J = Traction exponent, abbreviation for $\frac{i_o l}{K}$.
T = Torque needed to turn the shearhead of the bevameter (in lbs).
r_i = Inside radius of the shearhead (annulus) (in).
r_o = Outside radius of the shearhead (annulus) (in).
r = Radius of shearhead associated with d F (in).
d F = Elemental area $r\,dr\,d\Theta$ (in^2).
$d\Phi$ = Angle at center of annulus associated with d A.
$\bar{S}_{max}$ = Arithmetical average of measured S_{max} values (psi).
g = Regression coefficient.
$\bar{p}$ = Arithmetical average of applied p values (psi).
i = Numbers of S_{max} and p values considered in the regression analysis.

1) **Background.** — Micklethwaite [1] was the first to attempt to relate soil shearing strength as used in soil mechanics to determine the available thrust for a given soil. Starting with Coulombs well known equation [2]

$$S_{max} = c + p \tan \Phi \tag{1}$$

he multiplied both sides by the ground contact area

$$H_{max} = S_{max} A = c A + p A \tan \Phi$$

For uniform normal pressure distribution the relationship between weight and pressure is: $W = p A$. Thus Micklethwait's equation took the following form:

$$H_{max} = c A + W \tan \Phi \tag{2}$$

Bekker [3] suggested a more general equation which has been successfully used by the Land Locomotion Laboratory to predict track laying vehicle performance in snow [4]. Bekker made use of the fact that the form of soil shear stress-strain curves are similar to the shape of the displacement-natural frequency diagram of an aperiodic damped vibration [5] (see fig. 1).

By replacing the damping constant and the spring constant by appropriate soil parameters he arrived at the following equation:

$$S = \frac{c + p \tan \Phi}{Y_{max}} \left[e^{(-K_2 + \sqrt{K_2^2 - 1})\, K_1 i_o x} - e^{(-K_2 - \sqrt{K_2^2 - 1})\, K_1 i_o x} \right] \tag{3}$$

The shear stress can be integrated along the track-soil interface. For constant normal pressure distribution, Bekker derived the following equation.

$$H = \frac{2\,l\,b\,(c + p\tan\Phi)}{K_1 i_0 Y_{max} l}\left[-\frac{1}{-K_2 + \sqrt{K_2^2 - 1}} + \frac{e^{(-K_2 + \sqrt{K_2^2-1})K_1 i_0 l}}{-K_2 + \sqrt{K_2^2 - 1}}\right.$$

$$\left. + \frac{1}{-K_2 - \sqrt{K_2^2 - 1}} - \frac{e^{(-K_2 + \sqrt{K_2^2-1})K_1 i_0}}{-K_2 - \sqrt{K_2^2 - 1}}\right] \qquad (4)$$

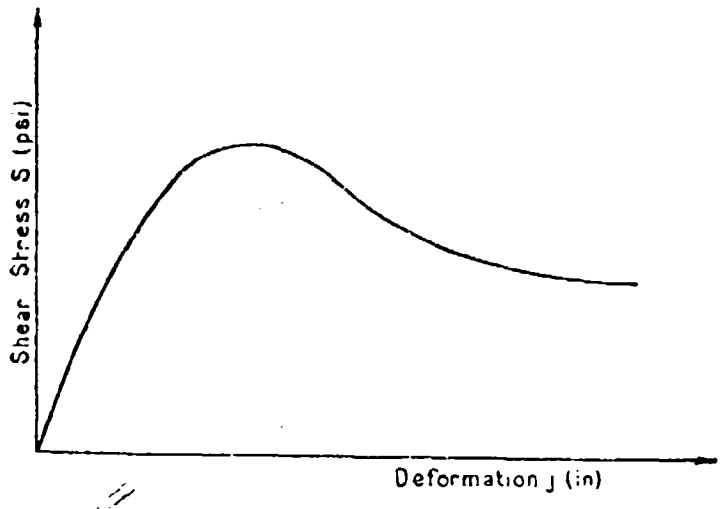


Fig. 1. — Soil shear stress-strain curve with a « hump ».

For more complicated pressure distribution, geometrical solutions have been applied [6]. It has been found at the Land Locomotion Laboratory that in the majority of the cases the soil does not exhibit a hump and a decay in the shear stress-strain curve (figure 2). Thus it is seldom necessary to use an involved equation such as equation 3. Also, it has been difficult to establish the numerical value of K_2 when the curve does not drop after reaching its maximum. These observations lead the authors to suggest the following simpler equation to describe soil shear stress strain curves of the type shown in figure 2:

$$S = (c + p\tan\Phi)\,(1 - e^{-j/K}) \qquad (5)$$

Note that for very large deformation equation 5 approaches Coulomb's formula:

$$(S \to c + p\tan\Phi) \text{ as } j \to \infty$$

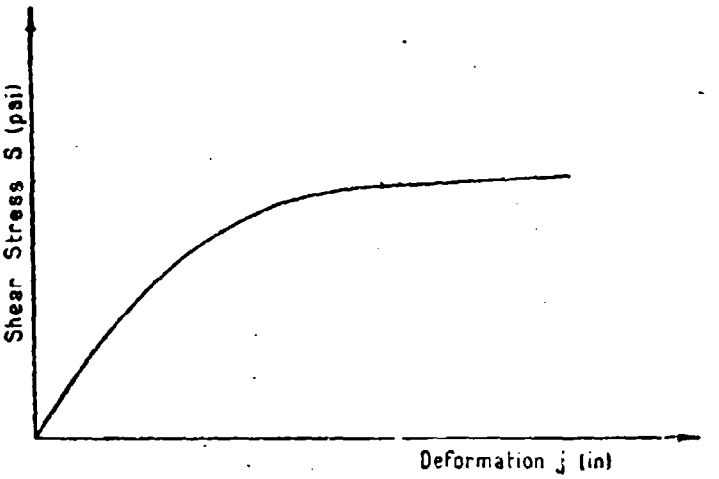


Fig. 2. — Typical soil shear stress-strain curve.

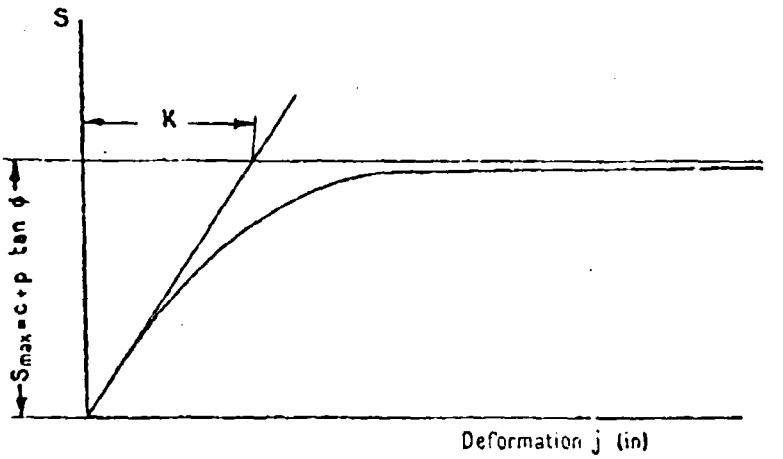


Fig. 3. — Evaluation of « K » from a typical soil shear stress-strain curve.

Differentiating both sides of equation 5 and setting j equal to zero the following is obtained:

$$\left(\frac{dS}{dj}\right)_{j=0} = \frac{c + p \tan \Phi}{K} \qquad (6)$$

Equation 6 represents the slope of the tangent drawn at the origin (figure 3), therefore K may be obtained from the experimental shear stress-strain curve as the distance between the intercept of the tangent drawn at the origin

and the line given by $s = c + p \tan \Phi$ and the s axis. K is called the deformation modulus of a soil shear stress-strain curve.

II) **Discussion of the theory.** — The total tractive effort exhibited by a track is obtained by integrating the shear stress along the ground contact area. Thus from equation 5 assuming constant width (b):

$$H = 2b \int_0^l (c + p \tan \Phi) (1 - e^{-j/K}) \, dx \qquad (7)$$

There are two variables other than x in the integrand: p and j. Hence equation 7 can only be evaluated if the function $p = p(x)$ and $j = j(x)$ are known.

A) Uniform normal stress distribution

1) **Traction.** — The case of uniform pressure distribution, p = constant, is considered first. The soil deformation under a track is proportional to the distance of the soil particle from the front end of the soil-vehicle interface (x). The factor of proportionality is defined as slip (i_o).

Thus:

$$j = i_o x$$

Hence equation 7 may be rewritten in the following form:

$$H = 2b (c + p \tan \Phi) \int_0^l (1 - e^{\frac{-i_o x}{K}}) \, dx \qquad (8)$$

The integration yields:

$$H = 2b \left[c + p \tan \Phi\right] \left[l + \frac{K}{i_o} (e^{\frac{-i_o l}{K}} - 1)\right] \qquad (9)$$

Using the following notations:

$$A = 2bl, \quad W = pA \quad \text{and} \quad J = \frac{i_o l}{K}$$

equation 9 becomes:

$$H = (Ac + W \tan \Phi) \left[1 - \frac{1}{J} (1 - e^{-J})\right] \qquad (10)$$

Thus Micklethwait's solution (equation 2) always yelds too high values except for infinite length. However the error committed will be insignificant if J is a large number.

2) **Effect of grousers.** — In case a track is equipped with grousers the maximum thrust is somewhat higher than that predicted by equation 10. The additional thrust may be calculated by means of an equation established by Bekker[3]. Accordingly equation 2 becomes:

$$H = A c \left(1 + \frac{2h}{b}\right) + W \tan \Phi \left\{1 + 0.64 \left[\frac{h}{b} \cot^{-1} \left(\frac{h}{b}\right)\right]\right\}$$

Thus a refined form of equation 10 may be established as shown below:

$$H = \left\{ A c \left(1 + \frac{2h}{b}\right) + W \tan \Phi \left\{1 + 0.64 \left[\frac{h}{b} \cot^{-1} \left(\frac{h}{b}\right)\right]\right\}\right\} \left[1 - \frac{1}{j} \left(1 - e^{-j}\right)\right] \tag{11}$$

It has been assumed that the shear stress may be expressed with the same relationship in both vertical and horizontal planes.

3) **Drawbar pull.** — In order to obtain the drawbar pull one has to substract the motion resistance from the traction:

$$DP = H - R \tag{12}$$

The total resistance consists of several components. Only the resistance due to soil compaction is considered here because its magnitude is dominating in most cases.

According to Bekker[3] the compaction resistance may be expressed as follows:

$$R_c = 2 \frac{k_c + b k_\phi}{n + 1} Z_0^{n+1} \tag{13}$$

where

$$Z_0 = \left[\frac{W}{A \left(\frac{k_c}{b} + k_\phi\right)}\right]^{\frac{1}{n}} \tag{14}$$

It should be emphasized that a relationship which would enable one to consider the sinkage as a function of slippage is lacking as yet. Equation 13 and 14 are accurate for small slippages only.

B) Linear sinkage

1) **Traction.** — If the sinkage is linearly proportional with x the solution is somewhat more involved. The vertical pressure under a footing as a function of the sinkage may be expressed by an equation first introduced by Bekker[1].

$$p = \left(\frac{k_c}{b} + k_\phi\right) Z^n \tag{15}$$

From figure 4

$$Z = Z_o \frac{x}{l} \tag{16}$$

Using equations 15 and 16, equation 5 now becomes

$$S = \left[e + \left(\frac{k_c}{b} + k_\phi\right) \left(\frac{Z_o}{l}\right)^n x^n \tan\Phi\right] \left(1 - e^{\frac{-i_o x}{K}}\right) \tag{17}$$

and

$$H = 2b \int_0^l \left[e + \left(\frac{k_c}{b} + k_\phi\right) \left(\frac{Z_o}{l}\right)^n x^n \tan\Phi\right] \left(1 - e^{\frac{-i_o x}{K}}\right) dx \tag{18}$$

Equation 18 reduces to the following form:

$$H = A \left\{ e \left[1 - \frac{1}{J}\left(1 - e^{-J}\right)\right] + p_{max} \tan\Phi \left[\frac{1}{n+1} - \frac{1}{l^{n+1}} \int_0^l x^n e^{\frac{-i_o x}{K}} dx\right] \right\} \tag{19}$$

Here $p_{max} = \left(\frac{k_c}{b} + k_\phi\right) Z_o^n$, and Z_o is given by equation 25.

The integral in the last term can only be solved in a closed form if n is an integer. Numerical solutions presented in this paper have been obtained by means of a Datatron 204 Electronic Computer.

When a digital computer is not available the solution may be obtained by means of power series. It can be shown that this method yields the following equation:

$$H = A \left\{ e \left[1 - \frac{1}{J}\left(1 - e^{-J}\right)\right] + p_{max} \tan\Phi \sum_{m=1}^{\infty} \frac{J^m (-1)^{m+1}}{m!\,(m+n+1)} \right\} \tag{20}$$

Since the number of terms required in the series may be quite large, a simpler approximative solution is now presented.

If $\frac{i_o}{K}$ is not a very small number and l is a large number the following approximation may be applied:

$$\int_0^l x^n e^{\frac{-i_o x}{K}} \approx \int_0^\infty x^n e^{\frac{-i_o x}{K}} dx$$

The right hand side can be rewritten as:

$$\frac{1}{(\frac{i_o}{K})^{n+1}} \int_o^\infty (\frac{i_o}{K} x)^n e^{\frac{-i_o x}{K}} d(\frac{i_o x}{K})$$

The integrand is the so called Gamma function[3] of $n + 1$.

Thus:

$$\frac{1}{(\frac{i_o}{K})^{n+1}} \int_o^\infty (\frac{i_o}{K} x)^n e^{\frac{-i_o x}{K}} d(\frac{i_o x}{K}) = \frac{\Gamma(n+1)}{(\frac{i_o}{K})^{n+1}} \qquad (21)$$

It is known that: $\Gamma(n + 1) = n!$

Thus when using equation 21 the total tractive effort becomes:

$$H = A \left\{ e \left[1 - \frac{1}{J} (1 - e^{-J}) \right] + p_{max} \tan \Phi \left[\frac{1}{n+1} - \frac{n!}{J^{n+1}} \right] \right\} \qquad (22)$$

2) **Grouser effect.** — The effect of grousers may be included again. The solution is then (see equation 19).

$$H = A \left\{ e \left(1 + \frac{2h}{b} \right) \left[1 - \frac{1}{J} (1 - e^{-J}) \right] + \right.$$

$$p_{max} \tan \Phi \left[1 + 0.64 \left(\frac{h}{b} \cot^{-1} \frac{h}{b} \right) \right] \left[\frac{1}{n+1} - \right.$$

$$\left. \left. - \frac{1}{J^{n+1}} \int_o^J x^n e^{\frac{-i_o x}{K}} dx \right] \right\} \qquad (23)$$

and the approximate solution is:

$$H = A \left\{ e \left(1 + \frac{2h}{b} \right) \left[1 - \frac{1}{J} (1 - e^{-J}) \right] + \right.$$

$$\left. p_{max} \tan \Phi \left[1 + 0.64 \left(\frac{h}{b} \cot^{-1} \frac{h}{b} \right) \right] \left[\frac{1}{n+1} - \frac{n!}{J^{n+1}} \right] \right\} \qquad (24)$$

3) Drawbar pull. — It has been shown * that the maximum sinkage may be calculated by means of the following equation:

$$Z_o = \left[\frac{(n+1)\,W}{A\left(\frac{k_c}{b} + k_\phi\right)} \right]^{\frac{1}{n+1}} \tag{25}$$

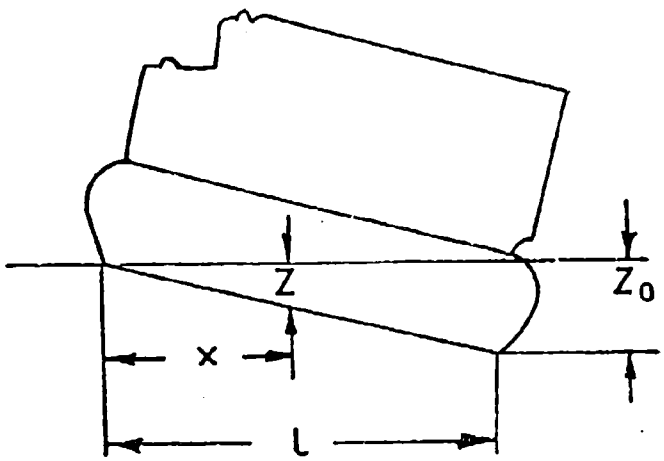


Fig. 4. — Tracked vehicle in « trimmed » position.

and the compaction resistance is again:

$$R_c = \frac{\left(\frac{k_c}{b} + k_\phi\right) Z_o^{n+1}}{n+1} \tag{26}$$

where Z_o is given by equation 25.
The drawbar pull of the vehicle may be found as:

$$DP = H - R_c$$

where H is given by equation 23 or 24 and R_c by equation 26.

III) Tests. — In order to check the accuracy of the theory presented above, numerous full scale vehicle and model tests have been carried out by the Land Locomotion Laboratory in 1960. These tests are reported in another paper, « Prediction of performance for full size and small scale model vehicles ». Here only the results of a series of scale model tests conducted by the Authors are presented.

a) *Test apparatus.* — Powered small scale models were run in different soils with varying loads on the tow hook and the slip was measured. The

loading system was a gravity dynamometer (figure 5). The drive shaft of the model was fitted with a hexagon nut to trip a micro-switch which actuated a counter resulting in a trace on the recording paper of a Brush recorder. This enabled one to compute the theoretical distance covered by the vehicle. A potentiometer connected to the load dynamometer pulley measured the actual distance traveled.

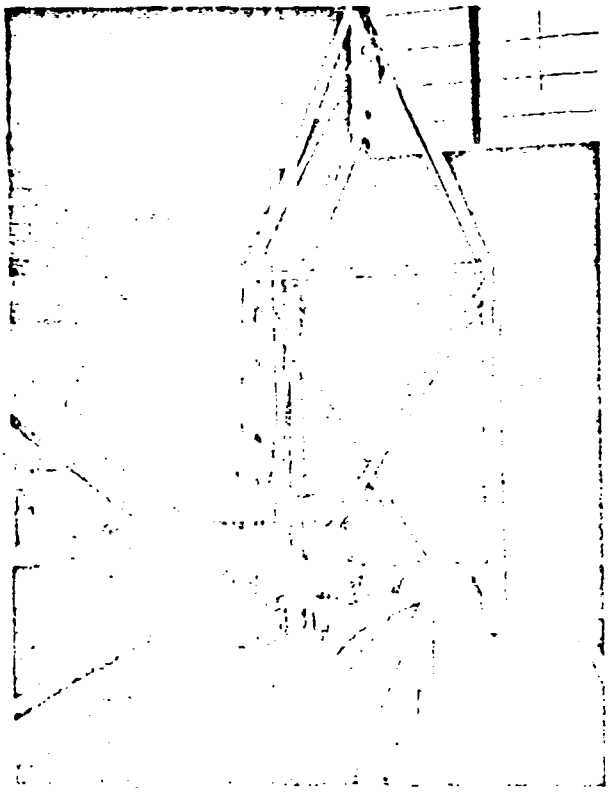
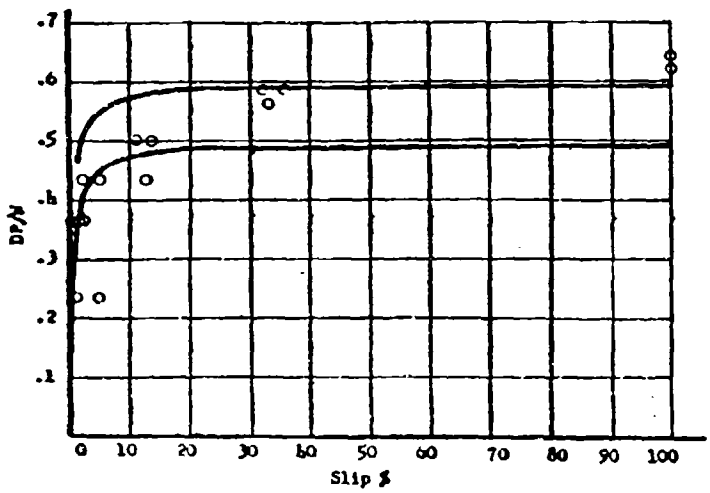


Fig. 5. — Model vehicle in test bin with gravity dynamometer.

Model « R » weighed 162 lbs and its tracks had the dimensions 17.1 × 2.375; Model « B » weighed 162 lbs and had tracks with the dimension 17.1 × 1.875 inches. The height of the grousers was 5/32" for both models.

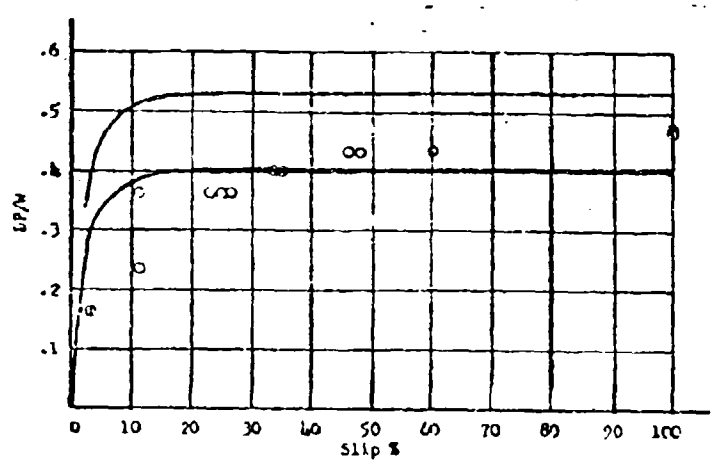
b) *Test procedure*. — 1) The soil was processed by a rotary tiller and either rolled with a lawn roller or tamped with an air temper depending upon the moisture of the soil.

2) Bevameter soil measurements[7] were taken at random locations throughout the length of the soil bin. Two sets of load-sinkage and shear stress-strain measurements were taken.



○ Measured; —— Computed 6 May 1960, Dry Mich. Farm Soil Model R, Wgt 162 lbs.

Fig. 6. — Predicted « band » and measured values of drawbar pull pro unit weight as a function of slip for model « R » in dry farm soil.



○ Measured; —— Computed 11 May 1960, Dry Mason Sand Model R, Wgt 162 lbs.

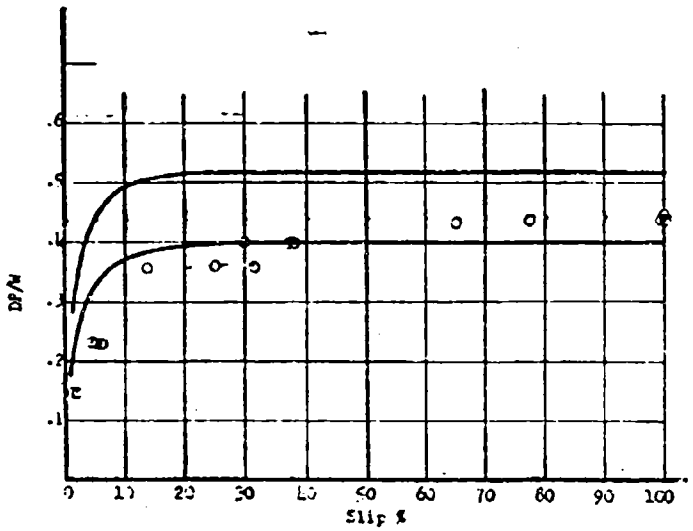
Fig. 7. — Predicted and measured DP/W values as a function of slip for model « R » in dry mason sand.

3) Moisture content samples were taken at each end and in the middle of the bin.

4) Step 1 repeated.

5) The model was placed in the bin and started. The load on the dynamometer pan was increased in ten pound increments until the vehicle stalled in order to determine the range of loads to be tested.

6) The model was moved six inches from the ruts of the previous run.



○ Measured; —— Computed 11 May 1960. Dry Mason Sand Model B, Wgt 162 lbs.

Fig. 8. — Predicted and measured DP/W values as a function of slip for model « B » in dry mason sand.

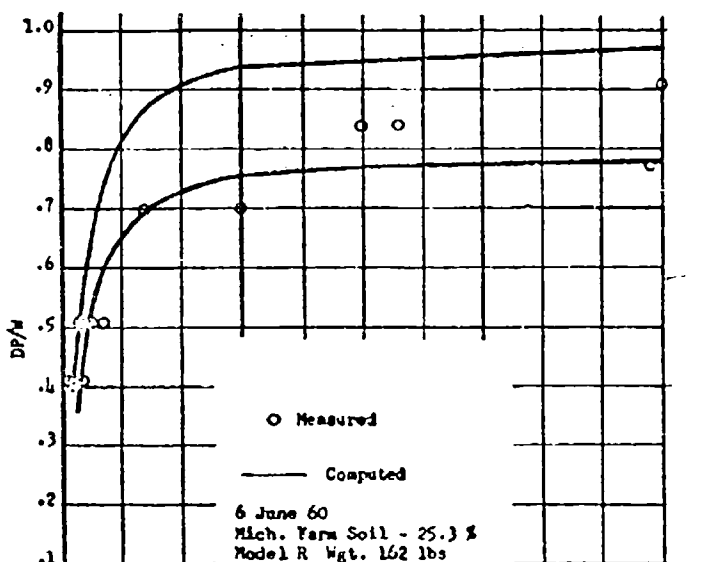


Fig. 9. — Predicted and measured DP/W values as a function of slip for model « R » in farm soil of MC = 25.3 %.

Each following run was completed with one of the loads within the established range. Thus the entire slip range was covered with at least 4 different loads, each repeated 3 times.

c) *Evaluation of test data.* — It was realized that the problem of keeping the soil consistent for each set of runs would have been difficult. The moisture content samples indicated that there were differences along the

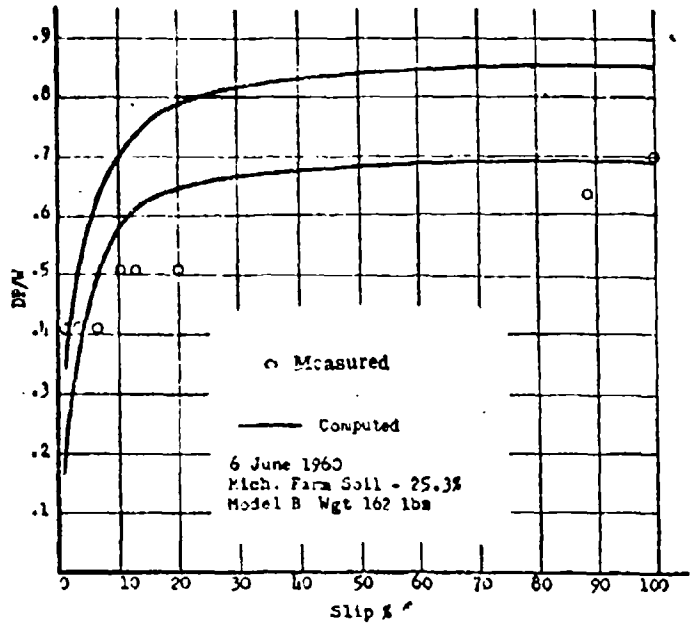


Fig. 10. — Predicted and measured DP/W values as a function of slip for model « B » in farm soil of MC = 25.3 %.

length of the bin for any one run. To encompass the performance of the models within the soil variations, each set of shear curves was analyzed separately. A linear regression analysis was performed with each set of data [11]. The straight line of Coulomb's shear stress equation for the four sets of data taken, were plotted and the maximum and minimum shear stress at the ground pressure of the model were determined. The corresponding c and Φ values were used to determine the maximum and minimum drawbar pull predictions. Thus instead of predicting a single drawbar pull vs. sinkage curve, a « band » was established. The predicted and measured values are presented in figures 6 - 16. A sample of the computations is presented in the appendix.

IV) Conclusion. — It is believed that correlation of tested data obtained by the theory presented demonstrates the usefulness of an analysis based on empirical soil stress-strain relationships.

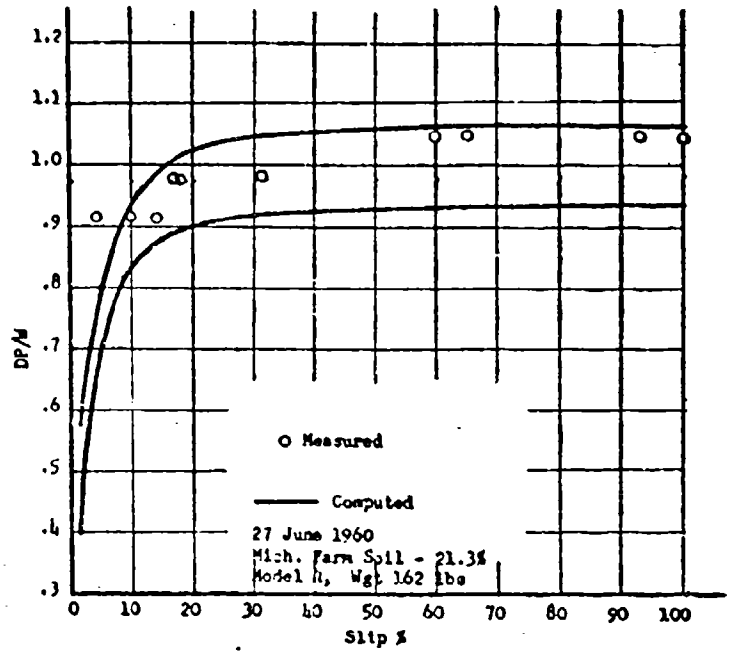


Fig. 11. — Predicted and measured DP/W values as a function of slip for model « R » in farm soil of WC = 21.3 %.

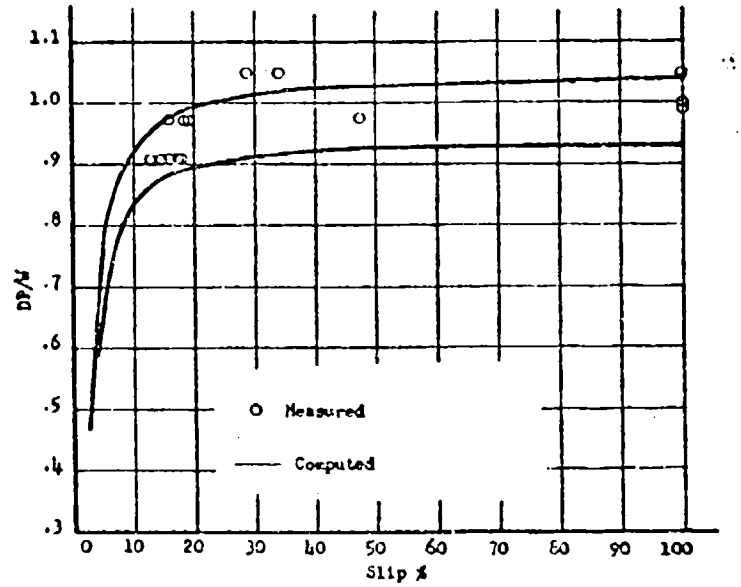


Fig. 12. — Predicted and measured DP/W values as a function of slip for model « B » in farm soil of WC = 21.3 %.

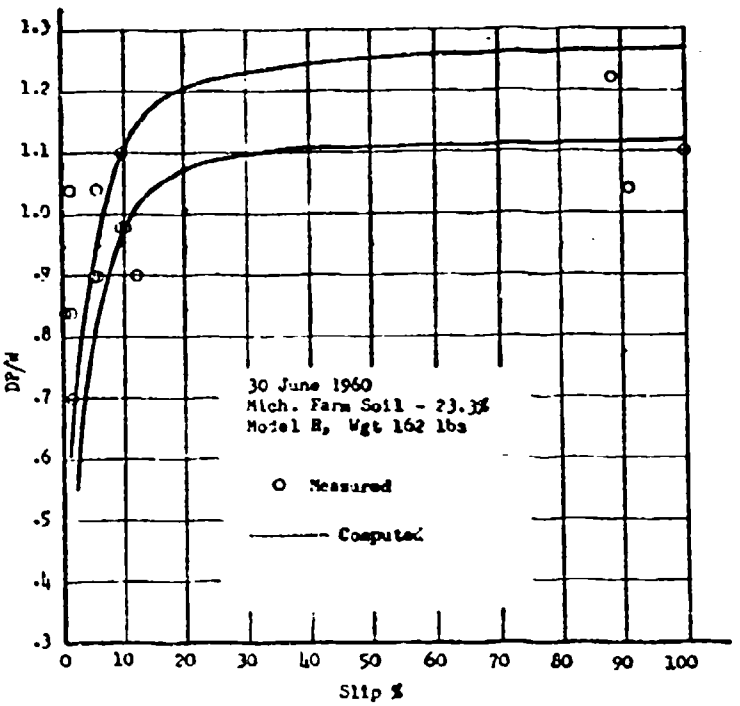


Fig. 13. — Predicted and measured DP/W values as a function of slip for model « B » in farm soil of WC = 23.3 %.

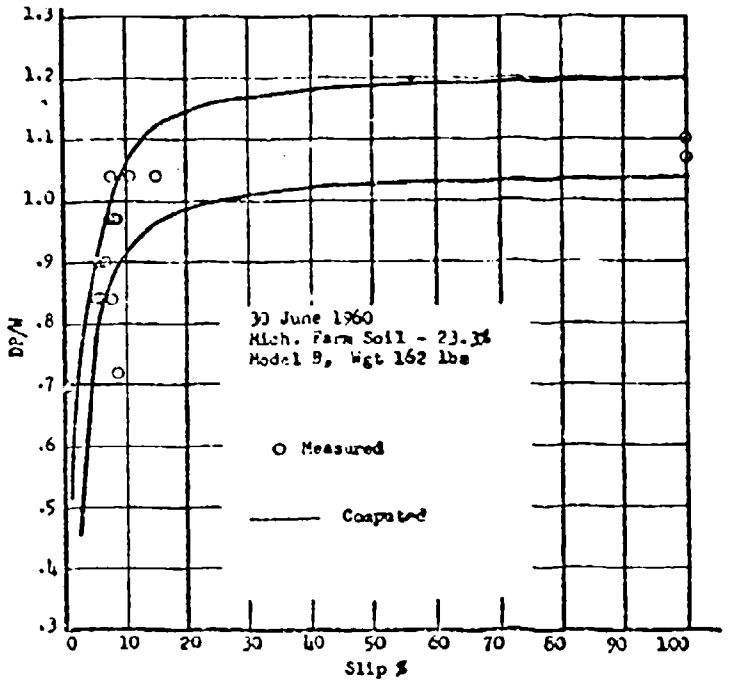


Fig. 14. — Predicted and measured DP/W values as a function of slip for model « B » in farm soil of WC = 23.3 %.

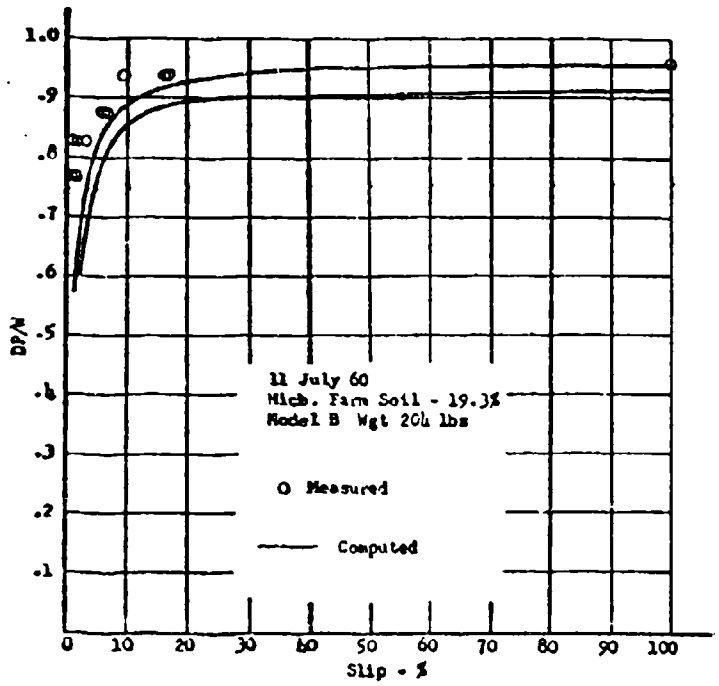


Fig. 15. — Predicted and mensured DP/W values as a function of slip for model « R » in farm soil of WC = 19.3 %.

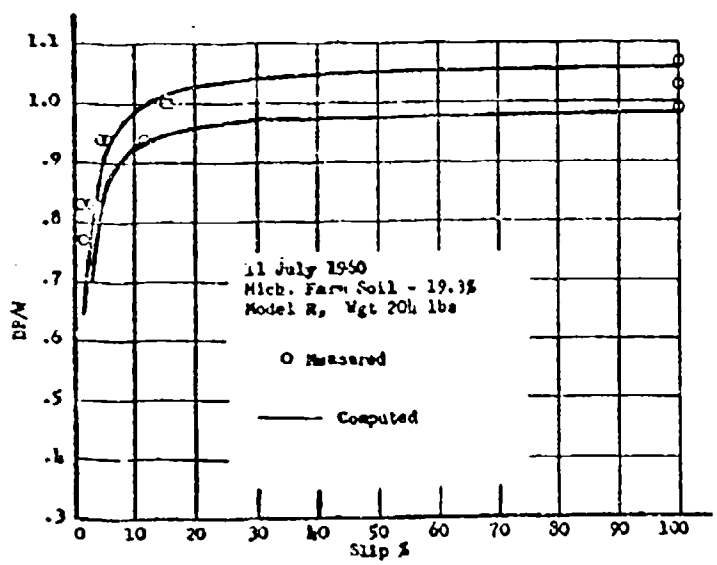


Fig. 16. — Predicted and measured DP/W values as a function of slip for model « R » in farm soil of WC = 19.3 %.

2) The equations presented are accurate if the road wheels are close to each other, thus forming a «solid footing». In case of excessive track slack and more involved pressure distribution, a geometric method to describe track behavior seems to be the most promising.

3) Further research is needed to establish the sinkage - slippage relationship.

4) An additional conclusion based on an analysis of the equations derived is that for a given ground contact area (or mean ground pressure) the longer and narrower track is advantageous. Since, however, a too long track encounters difficulties in steering, the concept of articulated vehicle arises as a possible avenue toward the improvement of present design trends, as first emphasized by Bekker [10].

BIBLIOGRAPHY

1) Micklethwait E. W. E. Soil mechanics in relation to fighting vehicles. Military College of Science, Chobham Lane, Chertsey, 1944.
2) Terzaghi K. and Peck R. B. Soil mechanics in engineering practice, pag. 97. John Wiley & Sons, New York, 1958.
3) Bekker M. G. Theory of land locomotion. The University of Michigan Press, Ann Arbor, 1956.
4) Harrison W. L. Study of snow values related to vehicle performance. Land Locomotion Research Branch Report No 23. Detroit Arsenal, Center Line, Michigan, December 1957.
5) Den Hartog J. P. Mechanical vibrations. Mc Graw-Hill, New York, pag. 38, 1956.
6) Gamalski T. C. Drawbar pull of tracked vehicles. Research report No. 5, Land Locomotion Research Branch, OTAC, Center Line, Michigan, 1958.
7) Bekker M. G. A proposed system of physical and geometrical terrain values for the determination of vehicle performance and soil trafficability. Research report No. 4, Land Locomotion Laboratory, OTAC, Center Line, Michigan, 1956.
8) Sokolnikoff I. S. and Sokolnikoff E. S. Higher mathematics for engineers and physicists. Mc Graw Hill, New York, 1941.
9) A soil value system for land locomotion mechanics. Research report No. 5. Land Locomotion Laboratory, Detroit Arsenal, Center Line, Michigan, 1958.
10) Bekker M. G. An introduction to research on vehicle mobility. - Part I. Stability problem (chapter XII). U.S. Ordnance Corps Land Locomotion Research Branch, OTAC, Detroit, 1958. (First printing: Canadian Department of National Defense, Ottawa, 1948).
11) Hald A. Statistical theory with engineering applications. John Wiley & Sons, New York, 1952.

APPENDIX

On 27 June 1960 the following soil moisture data were measured at three different locations in the test bin.

TABLE 1. — *Soil moisture data at 8:30 A.M.*

	North end	Middle	South end
Weight of sample (gr.)	107.2	131.5	119.8
Weight of dry soil sample (gr.)	88.7	107.9	98.2
Weight of water (gr.)	18.5	23.6	21.6
Water content %	20.85	21.87	20.99

Here the water content is the following:

$$\text{Water content } \% = \frac{\text{Weight of water}}{\text{Weight of dry soil sample}} 100$$

TABLE 2. — *Soil moisture data at* 3:30 *P.M.*

	North end	Middle	South end
Weight of sample (gr.)	102.0	127.4	131.0
Weight of dry soil sample (gr.)	84.7	104.8	107.1
Weight of water (gr.)	17.3	22.6	23.9
Water content %	20.42	21.56	22.32

The mathematical average of the six water content data is 21.3 %.

Shear test evaluation:

Date: 27 June 1960.
Soil: Michigan farm soil.
Water content: 21.3.

Shear tests were performed by means of a bevameter[9]. The following equations were used to evaluate the shear stress:

$$\int dT = S \int_{r_i}^{r_o} \int_{o}^{2\pi} r \, dF = S \int_{r_i}^{r_o} \int_{o}^{2\pi} r^2 \, dr \, d\theta$$

Hence:

$$S = \frac{3T}{2\pi (r_o^3 - r_i^3)}$$

since, for the annulus used the dimensions were: $r_o = 3.50$ in and $r_i = 2.75$ in (yielding an area of $F = 14.72$ in^2)

$$S = 0.02158\, T$$

The unloaded shearhead weighed $W_e = 13.5$ lbs.

Linear regression analysis.

In order to determine the best fitting straight line for $S_{max} = f(p)$ (see equation 1) to the measured shear stress data the following equation was used:

$$S_{max} = \overline{S}_{max} + g(p - \overline{p}) \qquad (27)$$

Here

$$g = \frac{\Sigma p S_{max} - \frac{\Sigma p \, \Sigma S_{max}}{i}}{\Sigma p^2 - \frac{(\Sigma p)^2}{i}} \qquad (28)$$

TABLE 3. — *Shear test data.*

Location and time	Load applied on shearhead W (lbs)	Pressure $p = W + W_c/F$ (psi)	Measured torque T (in.lbs.)	Max. shear stress S_{max} (psi)	Deformation modulus K (in)
South half of	21.5	1.46	63	1.36	0.36
bin at	29.5	2.00	87	1.88	0.29
8:30 A.M.	37.5	2.54	113	2.44	0.31
	45.5	3.09	126	2.72	0.36
	53.5	3.63	148	3.19	0.42
North half of	21.5	1.46	73	1.58	0.22
bin at	29.5	2.00	92	1.99	0.29
8:30 A.M.	37.5	2.54	113	2.44	0.42
	45.5	3.09	137	2.96	0.31
	53.5	3.63	155	3.34	0.22
South half of	21.5	1.46	63	1.36	0.33
bin at	29.5	2.00	83	1.79	0.29
3:00 P.M.	37.5	2.54	103	2.22	0.31
	45.5	3.09	122	2.63	0.33
	53.5	3.63	150	3.24	0.33
North half of	21.5	1.46	68	1.47	0.36
bin at	29.5	2.00	82	1.80	- -
3:00 P.M.	37.5	2.54	107	2.31	0.33
	45.5	3.09	129	2.78	0.36
	53.5	3.63	153	3.30	0.31

K was determined from the shear-stress strain curve S (see fig. 3).

Figures 17 and 18 were obtained using p and S_{max} values as listed in Table 3 and equation 27.

The average ground pressure for model « B » was 2.40 psi for which the smallest S_{max} value was 2.1 psi and the largest S_{max} was 2.33 (see figures 17 and 18).

The corresponding c and Φ values as determined from figure 17 and 18 were $c = 0.0925$ psi, $\Phi = \tan^{-1} 0.847$ (rad) and $c = 0.358$ (psi), $\Phi = \tan^{-1} 0.827$ (rad) respectively. (Note that the minimum S_{max} is not necessarily associated with the minimum c or Φ values).

These c and Φ values were used in equation 23 to obtain the upper and lower drawbar pull vs slip curves in figures 6-16.

For the evaluation K was assumed to be 0.30 (in) which corresponds to the average ground pressure of model « B » (see Table 3).

In order to compute

$$p_{max} = \left(\frac{k_c}{b} + k_\phi\right) Z_o^n$$

and R_c (equation 26), k_c, k_ϕ and n were needed. Since small sinkages of the order of 0.25 in. were observed during the test runs the effect of k_c, k_ϕ and n on the drawbar pull was assumed negligible and therefore a regression analysis similar to that described above was not performed on the measured data.

The arithmetical average for four penetration tests performance on 27 June 1960 $k_c = 3.5$; $k_\phi = 3.5$ and $n = 0.40$ were used in equation 26 to obtain figures 6-16.

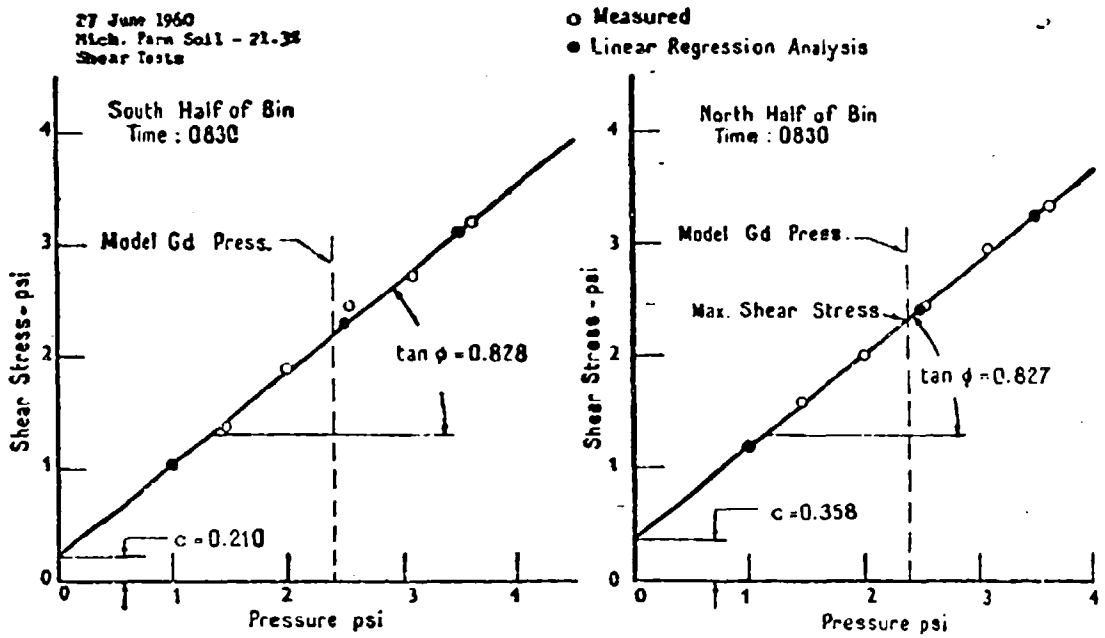


Fig. 17. — Evaluation of « c » and « ϕ » from a maximum shear stress vs. normal pressure curve obtained with a bevameter and corrected by means of linear regression analysis.

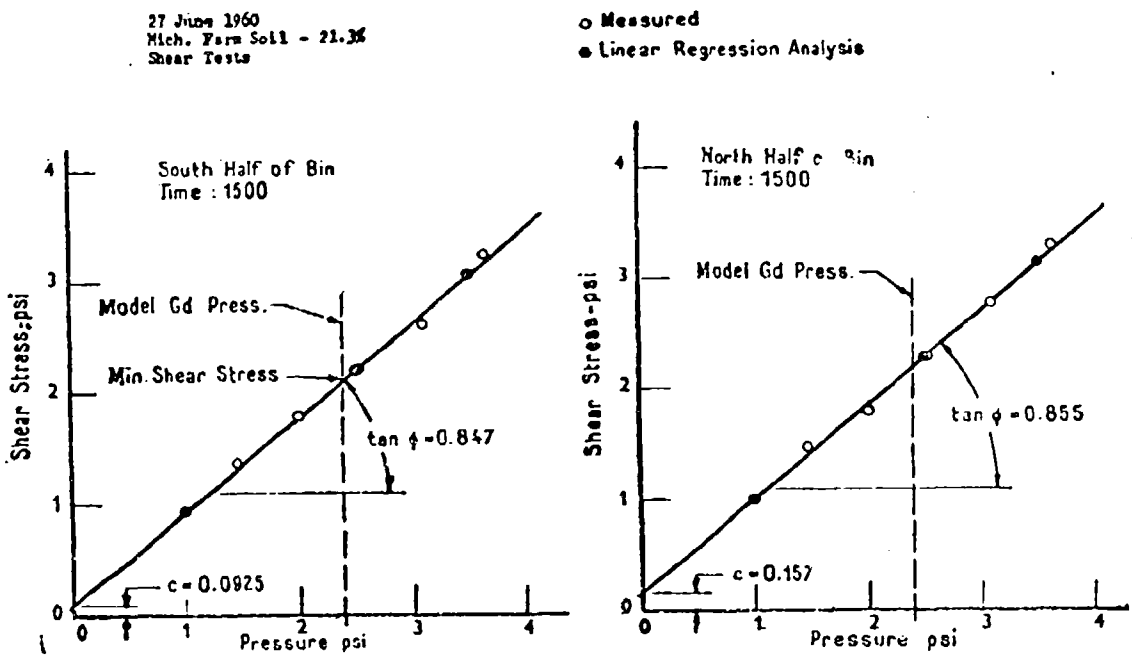


Fig. 18. — Evaluation of « c » and « ϕ » from a maximum shear stress vs. normal pressure curve obtained with a bevameter and corrected by means of linear regression analysis.

DISCUSSIONS

A. R. REECE. — I would like to congratulate Mr. Janosi and Hanamoto on their two papers numbers 41 and 42. It is remarkable that there is only one other paper in the whole Conference Proceedings which really attempts to relate vehicle performance with soil properties. I think that they will agree that their aim has not been to present a final analysis, but rather a hypothesis which can be used to guide future experiments and from which can be developed improved theories.

We have been using equation 5 at King's College for some time now. We had not looked upon it as anything new, but rather as a special case of Bekkers equation 3. In equation 3 as K_2 tends towards infinity we obtain

$$S = S_{max} (1 - e^{-\frac{j}{2K_1K_2}})$$

It then is rather more convenient to replace $2K_1K_2$ by a new constant $\frac{1}{K}$.

The Authors propose that K is obtained from the slope of the tangent at the origin. This is not a very good way of obtaining K because it only uses a small part of the stress strain curve and we have observed that in the vicinity of the origin the curve becomes rather erratic. For example, it is not uncommon for quite large shear stresses to be developed with no measureable deformations to begin with. It is better to rewrite equation 5 as

$$1 - \frac{S}{S_{max}} = e^{-\frac{j}{K}}$$

and hence

$$\text{Log}_e \left(1 - \frac{S}{S_{max}}\right) = -\frac{j}{K}$$

From this equation a straight line can be plotted on log/linear graph paper and the slope gives K. This method uses all of the stress strain curve.

We have long thought that this type of equation is rather inappropriate to describe the soil shear stress strain curve. This equation gives a family of curves as in figure 1 a in which increasing normal stresses give increasing shear stresses but constant deformations. This is a rather unlikely arrangement because it is well known that as the normal load is increased so is the volume of soil under stress and therefore one would expect the deformations to increase similarly.

Figure 1 b shows a much more likely set of curves in which it is seen that deformations grow in a progressive manner with increasing normal loads. This family of curves is obtained by making the Authors constant a linear function of normal pressure. We have found experimentally that this equation

$$S = (c + \sigma \tan \Phi)\left(1 - e^{-j\frac{\sigma}{K}}\right)$$

has in our very limited experience fitted the stress strain characteristics of a single track on light frictional soils quite well. Unfortunately we have found that tracks of different shapes and sizes require a different value for the K although the range of K is quite small.

It is noticeable that the Authors figures 6, 7, 8, 9 and 10 do not show good agreement between their K measured with a bevameter and the K appropriate to the vehicle they are testing. This can be seen because the K determines the shape of the slip pull curve. It can be seen from these figures that the experimental results are much more gently curved than the predictions indicating that too small values of K had been used.

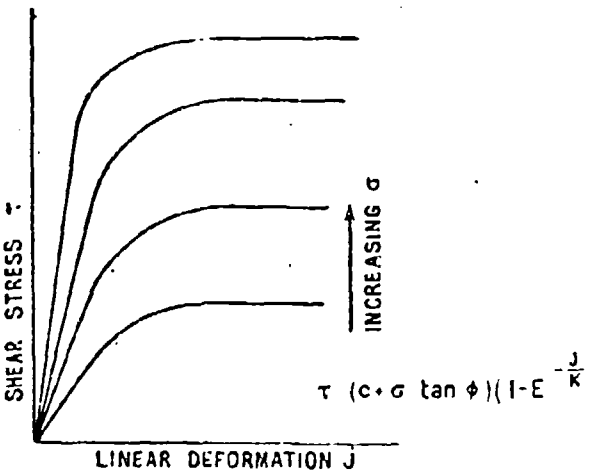


Fig. 1 a.

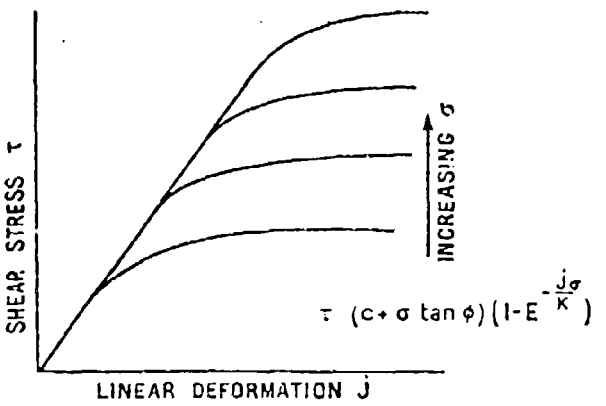


Fig. 1 b.

SHEAR STRESS-DEFORMATION MODULI

Mr. Pavlics in his description of the wheel type bevameter (paper 22) reported that it gave values of K about twice as high as the torsion annulus. This is probably due to the greater loads and the different shape of the loading area.

I was most interested to read the Authors sentence following equation 14 on page 9. Here they say that « It should be emphasized that a relationship which would enable one to consider the sinkage as a function of slippage is lacking as yet. Equations 13 and 14 are accurate for small slippages only ».

I think that this is one way of expressing the major limitation of the analysis in both papers number 41 and 42. In both papers there is the unstated assumption that the Principle of Superposition applies to soil vehicle mechanics. Of course it does not. It is assumed that the phenomena which occurs in the two Bekker tests separately occur in the same magnitudes when the horizontal and vertical loadings are applied together.

SINKAGE IN A SHEART TEST

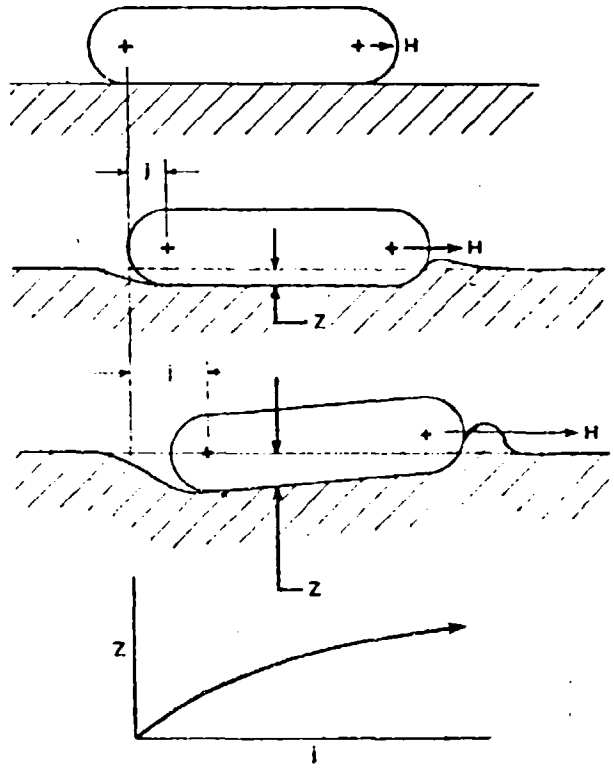
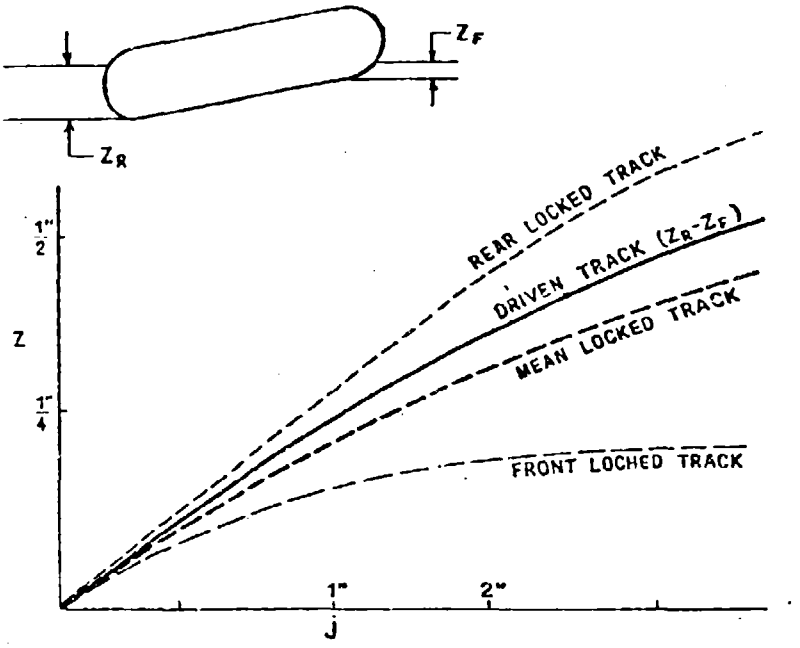


Fig. 2.

In this limited experience which we have managed to gain in our Department at King's College, we have noticed that the new factor which usually appears when vertical and horizontal loadings are applied together is extra sinkage. Figure 2 shows the way in which we have carried out shear deformation tests. We have not used a bevameter but proceeded to drag the actual track that we were going to test, locking it against rotation. The figure shows three stages in the test. As the applied force H grows so does the horizontal deformation j in exponential manner as previously described. However, along with the increase in j comes an increasing sinkage. At first the track sinks in a fairly level manner but later as soil piles up at the front of the track and a hole developes at the back then the track begins to tilt. If the mean sinkage at the centre of the track is plotted against j another exponential curve is obtained similar

to that shown in the figure. A similar sinkage occurs beneath a bevameter annulus but here of course the difficulty of the non-uniform sinkage is eliminated.

Our experiments have shown that the theory put forward by the Authors applies quite well to a crawler operating in easy conditions. As the load on the tracks is increased the sinkage becomes greater and the predicted results become progressively less in accord with the facts. It becomes more necessary to take into account the relationship between sinkage and slip. This can be done by relating Z with X by



COMPARISON OF SINKAGE IN SHEAR TEST AND TRACTION TEST

Fig. 3.

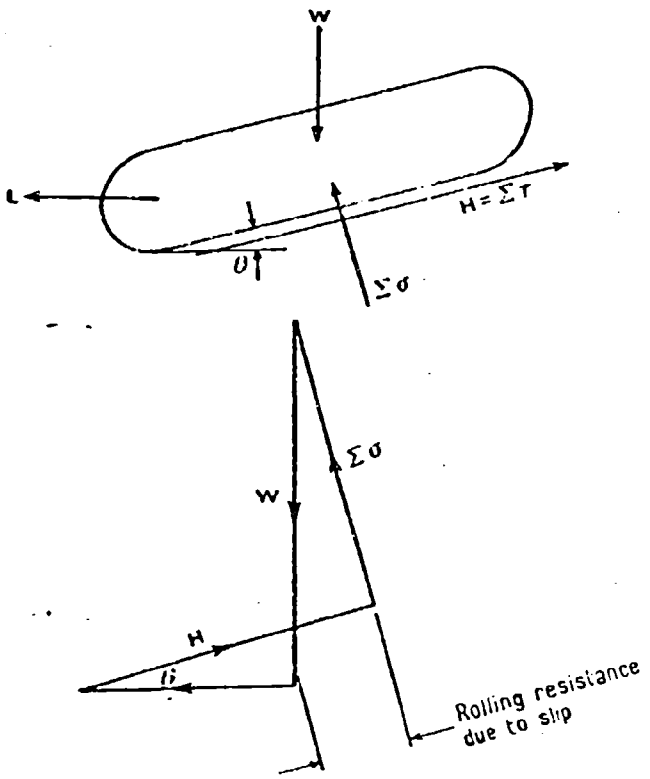
means of the Z — j relationship obtained from figure 2. We have observed that this in fact can be done. Figure 3 relates the measured difference in sinkage between the front and back of a driven track with the mean sinkage beneath the locked track at comparable linear displacements.

Because the deformations grow along the track to a maximum at the rear, so do the sinkages and this is the reason why vehicles in difficult going always adopt a tail down attitude. It results from this attitude that the normal pressure along the track does not act vertically, and has a backward component which constitutes additional rolling resistance, and also the shear stress is not horizontal. The balance of the external forces on the track is as shown in figure 4. It is quite easy to calculate the reduction in thrust due to the tail down attitude using the polygon of forces shown in figure 4.

The effect of adding this analysis to the Authors is shown in figure 5. Here we have experimental slip pull curves for three small crawlers of different track size but

constant weight together with predicted performance obtained by the Authors method. It will be seen that as the track becomes smaller the agreement becomes worse. Almost complete agreement is regained by taking account of the slip sinkage.

The data in figures 4 and 5 have been obtained by Mr. J. Adams a post-graduate student at Durham University.



ROLLIN RESISTANCE DUE TO SLIP

Fig. 4.

I find it difficult to understand section B of the authors analysis concerned with linear sinkage. They do not state why the vehicle has taken up this particular attitude. It may be that they think that it has occurred because the vehicle weight is concentrated towards the back of its track area due partly to load transfer and partly to the static weight distribution. In this case surely, it would be necessary to specify the position of the vehicles centre of gravity and also the height of its drawbar. Since these dimensions are not specified I can only conclude that the analysis does not take account of the three conditions of equilibrium, $\Sigma F_x = 0$, $\Sigma F_y = 0$ and $\Sigma M_o = 0$. It seems that the last condition is ignored.

In the field of vehicle mechanics everything that takes place in the soil is complex and uncertain and this is all the more reason for making sure that the theories fit all the three conditions of equilibrium which are about all that is known for sure.

I believe that the fundamental reason for the tail down attitude taken up by tracked vehicles in loose soils and snows is the reduction of supporting capacity caused by horizontal deformations, that I have already discussed. If this is so, then it follows that the analysis must be based on the slip sinkage relationship and

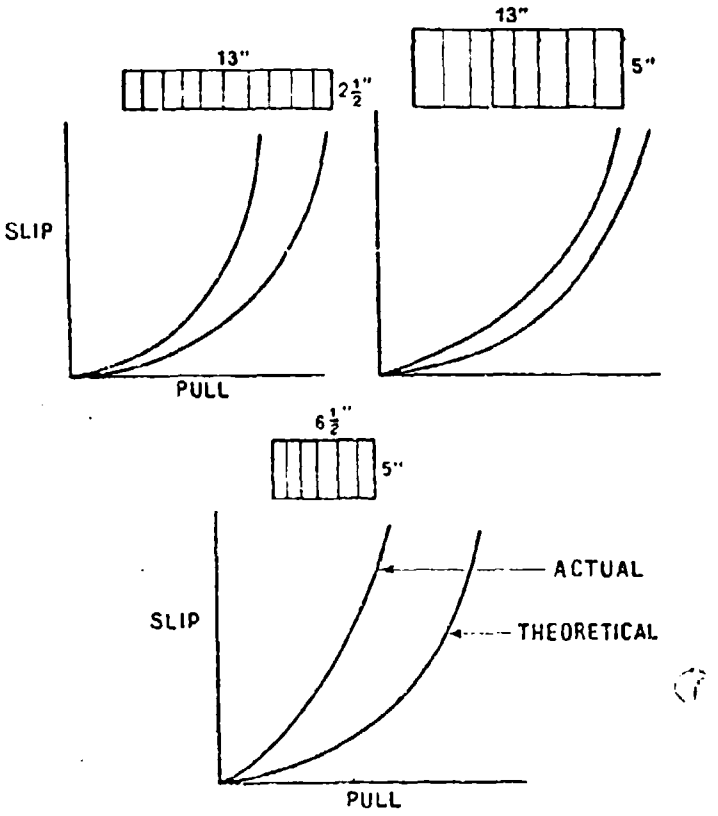


Fig. 5.

will have an entirely different bases to that attempted by Mr. Janosi. It should be noted that in the experiments, the results of which are shown in figure 5, the resultant of the pressure beneath the tracks was kept central by moving a balance weight to counteract the load transfer due to drawbar pull. Despite this the tractors took up an increasingly tail down attitude with increasing slip.

Discussion on paper number 42. — I think that Mr. Janosi's paper can perhaps be criticized because it does not make sufficiently clear the assumptions on which the analysis is based. It may be that this is the fault of the Conference Organization

in restricting the length to a certain number of pages, but there can be no doubt that is reduces the value of the work.

The major assumption made is that which I have drawn attention to with reference to the preceeding paper, concerning the superposition of the information from the two Bekker tests. I think that in most cases of a wheel operating in soft going it is necessary to take into account the phenomena of slip sinkage. This becomes increasingly important as the contact pressure becomes greater and the contact length smaller and I would expect it to make a very considerable difference to the performance of wheels. The very interesting film shown at this Conference by Mr. Turnbull and Freitag of the Waterway's Experimental Station showed very clearly a wheel in loose sand in which the sinkage was obviously primarily a function of the slip.

I think that slip sinkage is also a possible explanation for the difficulties experienced by Professor Vincent (paper no. 46) in trying to relate a theory similar to Mr. Janosi's to experimentally observed phenomena. One would expect that if the soil deformations grow towards the point immediately below the axle so the supporting capacity would be reduced and therefore the contact pressure would be reduced in this region. This will help to explain why the pressures do not grow to a maximum at this point.

A further example of an unstated assumption made by Mr. Janosi is to be found on page 711 after equation (7). He says here that:

The horizontal pressure components may be expressed according to figure 4 as follows:

$$P_H = p_r \tan \alpha$$

This follows from assuming that the shear stresses around the rim of the wheel are zero. This of course is not true as is shown for example by Mr. Uffelman's figure 14 in his paper number 7. It is to be expected that in general this pattern of equal amounts of positive and negative shear stress would be found, in the case of the self propelled wheel.

It is interesting to observe that Mr. Janosi finds that his theory under estimates the measures rolling resistance. I think that this is because he has completely ignored the energy absorbed in the horizontal soil deformations due to the previously mentioned shear stresses and also due to the horizontal components of the normal stresses. It may be that this is what he calls bulldozing resistance but this does not seem to be a very justifiable name since these losses would be called slip losses if the wheel was producing some tractive effort.

It is very easy to be critical. The fact that it is possible to criticize Mr. Janosi's papers does not detract at all form its very great value. I am convinced that his basic approach is the correct one and he has done a very great service in boldly attempting what is at the present time probably an impossible task.

Z. JANOSI. — I would like to say I am very sorry that we meet Prof. Reece so seldom and have to attend an international conference to have an opportunity to exchange ideas. Now, to discuss Prof. Reece's comments I would like to emphasize 8 points.

1) Equation (5) is not just a special form of equation (3) which one may obtain by replacing $2K_1K_2$ by $1/K$ when $K_2 \to \infty$, because $e^{-2K_1K_2} \to 0$ as $K_2 \to \infty$ and therefore one obtains $s = s_{max}$, which does not represent a curve of the desired shape.

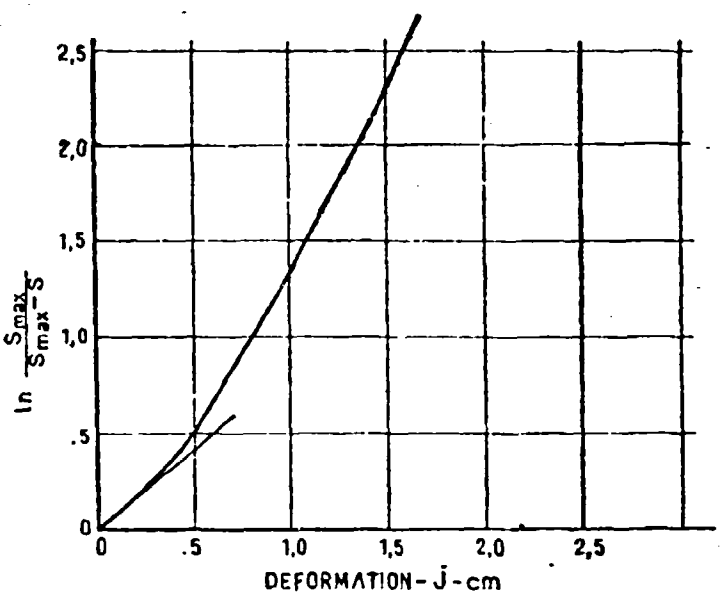

2,5
2,0
1,5
1,0
.5
0
0
.5
1,0
1,5
2,0
2,5
$\ln \frac{S_{max}}{S_{max}-S}$
DEFORMATION - J - cm

Fig. 1.

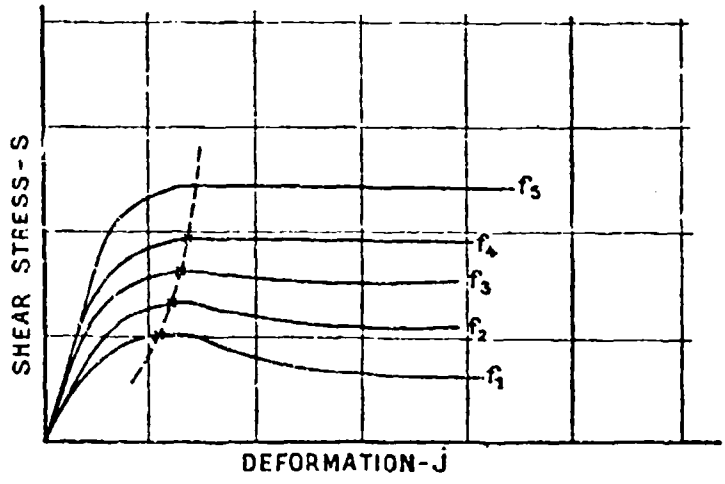

SHEAR STRESS - S
f_5
f_4
f_3
f_2
f_1
DEFORMATION - J

Fig. 2.

2) The « logarithmic technique » recommended by Prof. Reece seems to be more accurate than the « tangent solution » for the determination of the numerical value of K.

We should bear in mind, however, that when « in the vicinity of the origin, the curve becomes rather erratic » then the replotting procedure will be difficult to carry out accurately. It is advisable to use that portion of the experimental curve which falls between $s = 0$ and $s = s_{max}$ and not « all the stress strain curves » because a replotted shear stress strain curve is very seldom one straight line. It rather looks like the curve shown in figure 1. In this case the technique recommended by Prof. Reece is more complicated and more inaccurate than the « tangent method ».

3) It is true that shear stress-strain curves do not follow the trend shown in figure A in Prof. Reece's comments (which was assumed in our paper), but unfortunately figure 1B does not show the real situation either. An extensive amount of test data obtained at the Land Locomotion Laboratory in 1959 reveals that shear curves behave as shown in figure 2 when the normal pressure varies. It does not seem to be worth while to use the exponent $\frac{-jp}{K}$ instead of $\frac{-j}{K}$ because the inaccuracy will become even greater at higher p values and the analysis would be more complicated. This difficulty was largely reduced by using a K value which was obtained at that normal pressure (p) which was estimated to occur under the vehicle. Our intention is, however, to introduce a correction factor which would improve the accuracy of the equation at a later date. Since K remains constant above a fairly low p value we felt that the validity of the analysis would not be greatly reduced by using K = constant for various p values. The variation of K as a function of the shape of the footing is included in the analysis both in the paper on hand and that of Mr. Harrison. We found that the length of the footing l is the important influencing factor. Fortunately it was found that the relationship between K and l proved to be very close to a linear one.

4) We think that mathematical simplifications have contributed considerably to the difficulties Mr. Payles reported on.

5) We have to admit that the principle of superposition is theoretically not admissible when one works with soils. If one attempts to consider the very important problem of the slip-sinkage relationship by means of actual drag tests, one finds that in some cases the static sinkage decreases instead of increasing. Therefore, one may conclude that the phenomena involved can not be so easily explained as it was done by Prof. Reece. Since test results obtained by means of experiments conducted with actual size vehicles were in good agreement with theoretical predictions, we concluded that the application of the principle of superposition does not result in considerable errors and it may be used until much more is known about the behavior of soils under vehicles.

We are fully aware of the importance of a valid sinkage-slippage relationship and we plan to investigate this problem quite extensively.

There is another argument against the use of the « drag test ». If one has the opportunity to pull the tracked vehicle in a given soil one may also measure the drawbar pull as a function of slip very easily and there is no further need for analytical predictions.

6) The effect of the trim angle was not included in the analysis because it was considered negligible. If one investigates, however, extremely short tracks as was done by Prof. Reece in figure 5 of his comments, this effect may be quite substantial.

7) If one tries to analyze the performance of a track which operates with trim, it is not possible to satisfy all three equations of equilibrium unless the true pressure distribution is known. The pressure distribution is a function of the drawbar pull which is, in turn, a function of the slip. Thus a variable pressure distribution pattern is to be considered for an exact solution. Unfortunately we do not have enough information at the present time on these phenomenon. The question remains then whether one should satisfy the moment equilibrium equation and postpone the analysis until a pressure distribution law compatible with the equations of equilibrium is found or work with Bekker's equation ($p = kz^n$) and check the magnitude of the error involved. As test results show under normal conditions, the equation yields a good approximation.

8) We agree with Prof. Reece's statement that the slip-sinkage relationship should be included in the analysis of wheels. Furthermore it is true that friction between the wheel and the soil was neglected. The first question can not be answered as yet, while the second problem was not considered important enough to complicate the analysis which is much involved anyhow. We have not completely neglected, however, the resistance due to shear stresses and that due to p_0. These are partially included in the term denoted by H_2.

I believe that the underestimation of the rolling resistance is due to the incorrect assumption as to the pressure distribution under the wheel, which had to be employed at the present time. The pressure distribution is currently studied by Prof. Vincent and also by Mr. Hegedus in our Laboratory. I hope that this problem will be clarified in the near future.

Finally I would like to express my gratitude to Prof. Reece, who not only recognized the main unsolved problems but presented very valuable suggestions as to their solution. As he said, it is an impossible task to establish a rigorous solution of the problems investigated at the present time because the semi-empirical soil value system is not suitable to account for all the important phenomena involved in its present form.

I believe, however, that the improvement in our system which is constantly attempted in our Laboratory will allow us to improve the accuracy of our predictions and expand the generality of its possible applications. The papers presented are not regarded as final solutions but rather as a summary of the present state of the art. Meanwhile the basic laws of soil dynamics are studied by our contractors. These studies are hoped to lead to the point where we will be able to abandon empiricism and establish rigorous solutions at least for some important but relatively simple cases.

N. 45

An analysis of pneumatic tire performance on deformable soils

Analisi della prestazione dei pneumatici sui terreni cedevoli

Z. Janosi *)

ABSTRACT. — *This paper presents the current state of the art of the semi-empirical method established in the Land Locomotion Laboratory **) to predict the performance characteristics of a tire operating in deformable soils. The equations for sinkage, motion resistance and drawbar pull as a function of load, geometry, inflation pressure and soil characteristics are based on the soil value system first proposed by Bekker.*

The results show reasonable agreement between experimental data and precalculated values for homogeneous soils.

Key to symbols and definitions

P_v	=	Vertical component of ground pressure acting on the wheel-soil interface (psi)
k_c	=	Cohesive modulus of sinkage (lbs/in^{n+1})
k_ϕ	=	Frictional modulus of sinkage (lbs/in^{n+2})
b	=	Width of wheel or a rectangular footing; radius of circular footing used in soil penetration tests (in)
n	=	Exponent of sinkage
Z	=	Sinkage of an arbitrary point on the wheel perimeter (in)
W	=	Vertical load on the wheel (lbs)
D	=	Diameter of a wheel (in)
β_o	=	Central angle between the vertical radius and the radius associated with the soil level (°)
X	=	Horizontal coordinate axis; distance between vertical radius and wheel perimeter, horizontal travel of a point on the wheel perimeter (in)
Z_o	=	Maximum sinkage of a wheel (in)
Y	=	Vertical distance between the center of the wheel and an arbitrary point on the perimeter; ordinate of a point on the wheel perimeter measured above the root (in)
F	=	$(D/2 - Z_o)$ Distance between the center of the wheel and the undisturbed soil level (in)
P	=	Vertical reaction acting against the moving wheel (lbs)

*) Land Locomotion Laboratory U.S. Army Ordnance Tank Automotive Command, Detroit, Michigan.

**) Located at the U.S. Army Ordnance Tank Automotive Command.

M = Moment of P with respect to the center of the wheel (lbs in)
f = Distance between P and the center of the wheel; (in)
R_v = Motion resistance due to vertical reaction P (lbs)
p_H = Horizontal component of ground pressure acting on the wheel-soil interface (psi)
R_H = Resistance due to horizontal pressure (p_H) (lbs)
R_m = $R_v + R_H$ (lbs)
$P_{g\,max}$ = Maximum ground pressure acting under the tire (psi)
P_i = Inflation pressure of a tire (psi)
P_c = Carcass pressure; difference between $p_{g\,max}$ and p_i, a pressure due to stiffness of the carcass (psi)
R_c = Resistance due to soil compaction under the tire (lbs)
R_d = Resistance due to hysteresis losses; due to carcass stiffness (lbs)
f_i = Experimental coefficient indicating proportionality between R_d and W
P_{i_o} = Optimum inflation pressure, at which the resistance is minimum (psi)
l_1 = Length of the « flat » part of the soil-tire interface at low inflation pressures (in)
l_2 = Difference between the length of the horizontal projection of the tire-soil interface area and l_1 (in)
$P_{i\,crit}$ = Inflation pressures which separate the « rigid » and « soft » pressure domains for a tire (psi)
c = Cohesion (lbs/in²)
p = Normal pressure on the wheel-soil interface (psi)
Φ = Angle of shear resistance; angle of internal friction (°)
j = Horizontal soil deformation (in)
K = Deformation modulus of a soil shear stress-strain curve (in)
i_a = Slip
α = Turning angle of a wheel while the endpoint of the radius moves from the bottom of the wheel to a point characterized by X and Y (°)
α' = $-\alpha$ (°)
V_t = Theoretical speed of the wheel calculated from the radius and the RPM (in/sec)
V_a = Actual speed (in/sec)
r = Radius of a fictitious wheel which would cover the same distance as the wheel does after α angle had been covered, but without slip (in)
R = D/2 (in)
Y_c = Ordinate of the instantaneous center ($Y_c = R - r$) (in)
β_v = Central angle at which the tangent of the path of a point of the wheel perimeter is vertical (°)
β = $\beta_v - \alpha'$ (°)
X_β = Abscissa of the path of a point on the wheel perimeter associated with angles β, β_o and β_v respectively (in)
$X_{\beta v o}$
H = Gross tractive effort, traction, thrust (lbs)
H_1 = Thrust developed on that part of the perimeter which lies between $\beta = \beta_v - \beta_o$ and $\beta = \beta_v$ (Here $\beta_o < \beta_v$)
H_2 = Reaction due to shear stresses, negative thrust developed on that part of the perimeter which lies between $\beta_v - \beta_o = \beta$ and $\beta = \beta_v$ (Here $\beta_o > \beta_v$)
j' = Horizontal soil deformation in the direction of the motion (to be considered if $\beta_o > \beta_v$) (in)
j_{Z_o} = Maximum horizontal soil deformation in the direction of the motion (in)

I) Background

Some outstanding studies are listed in the following which represent important yardsticks in the development of the mechanics of tires under off-the-road conditions.

The problems related to rigid wheel behavior in soft soil have been investigated by several researchers and some important phenomenae have been observed for which numerous useful solutions have been proposed.

The sinkage and motion resistance of a towed wheel was first analyzed by Bernstein [1]. Russian investigators improved Bernstein's basic equation and obtained a more general solution [2].

Garbari published a very useful paper [3] in which he suggested some new notions such as the critical inflation pressure. A further improvement in the basic soil stress-strain relationship led Bekker to equations of more general value [4].

Vincent of the University of Michigan has observed some new relationships as to the pressure distribution under a towed rigid wheel in sand and the flow of soil past the wheel [5].

The kinematics of a rigid wheel has been analyzed by Russian scientists in great detail; the equation of the path of a soil particle under the wheel has been found. Their achievements, however, are of purely academic value because of the lack of a soil stress-strain relationship [6].

As for soft tires Omelianov's empirical equation for resistance prediction is frequently published in Russian textbooks [7]. Another Russian paper by Ageikin [8] reveals an equation for sinkage similar to that published by Bekker and the author of this paper [9-10-11]. Experiments by the National Tillage Laboratory [12], by the Waterways Experiment Station of the U. S. Army Corps of Engineers [13], by Soehne [14] and by a group consisting of researchers from the National Tillage Laboratory and Michigan State University [15] elucidated some important aspects of the pressure distribution under soft tires operating in soft soil. Kerr [16] and some French researchers [17] investigated tire performance in desert sand.

A new, radial ply, tire design introduced by the Pirelli Co. [18] proved to be superior to the conventional one according to tests conducted by the company itself, by the National Tillage Laboratory [19] and by the Ford Motor Co.

Bekker's condual tire concept [21] appeared to be promising in view of theoretical considerations and some limited test results.

Richey suggested the mounting of a radial ply tire on a narrow rim and conducted field test which proved that the concept had significant advantages over tires of conventional rim dimensions [20].

Soehne published a very thorough analysis of tire behavior [22] but seemed to be hindered by the lack of some kind of soil stress-strain rela-

tionship in attempting to establish an analytic method to describe basic tire mobility characteristics.

Various aspects of tire behavior on hard ground have been analyzed by a great number of researchers and institutions. An excellent digest of these studies has been presented by Hadekel [23].

II) Theoretical approach

The problem of investigating pneumatic tires operating in deformable soils can be divided into four parts as follows:

1) Towed tire: a) Rigid. b) Soft.
2) Driven tire: a) Rigid. b) Soft.

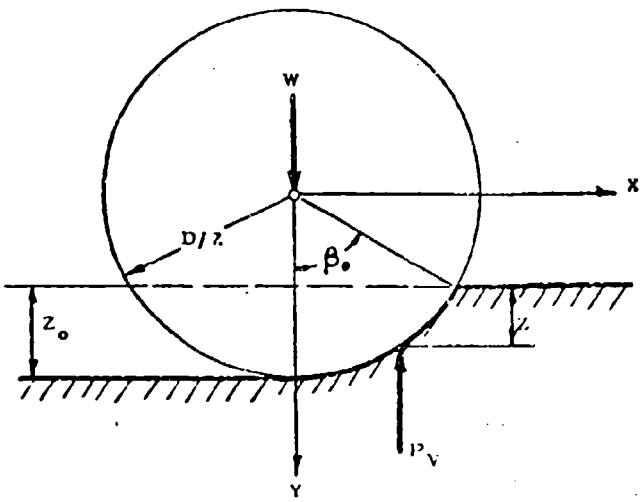


Fig. 1. — Vertical pressure acting under a rigid wheel operating in deformable soil.

1 *a)* **Tower rigid tires.** — The tire may be considered rigid if the inflation pressure is higher than the so called critical pressure (defined in section 1b).

Assuming that the vertical pressure under the wheel may be expressed by Bekker's basic relationship [4]:

$$p_v = \left(\frac{k_c}{b} + k_\phi\right) Z^n \qquad (1)$$

the equilibrium of vertical forces can be expressed as follows (figure 1)

$$W = b \int_0^{D/2 \cos \beta_o} p_v \, dx \qquad (2)$$

Bekker has shown that [4] the sinkage may be expressed from equation 2 by the following equation:

$$Z_o = \left[\frac{3W}{(3-n)\left(\frac{k_c}{b} + k_\phi\right) b \sqrt{D}} \right]^{\frac{2}{2n+1}} \tag{3}$$

The main component of the motion resistance is due to the ground pressure distributed along the wheel-soil interface.

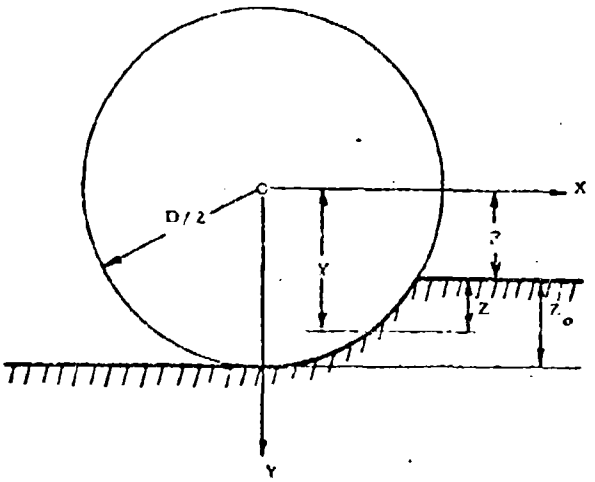


Fig. 2. — Relationship between y, Z, F and Z_o.

Experiments conducted in the Land Locomotion Laboratory [21] indicate that the vertical pressure component may be expressed by equation 1.

From figure 2

$$x^2 + y^2 = (D/2)^2$$

or

$$x^2 + (Z + F)^2 = (D/2)^2$$

and

$$x\,dx = -(Z + F)\,dZ \tag{4}$$

The elementary vertical reaction is:

$$dP = b\,p_y\,dx$$

The elementary reaction-moment taken to the center of the wheel:

$$dM = b\,p_y\,x\,dx$$

Using equation 4

$$dM = -b\,p_y\,(Z + F)\,dZ \tag{5}$$

The abscissa of the resultant vertical reaction is:

$$f = \frac{\int dM}{\int dP}$$

Since $W = \int dP$ and using equation 5 one obtains:

$$f = \frac{k_c + b k_\phi}{W} \int_{Z_o}^{\bullet} Z^n (Z + F)\, dZ$$

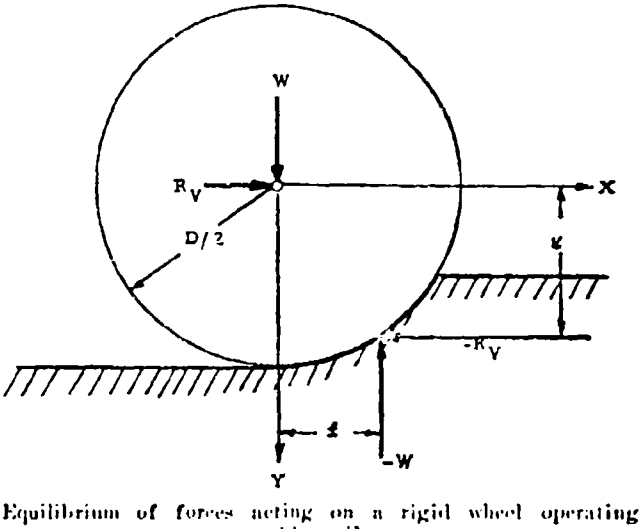


Fig. 3. — Equilibrium of forces acting on a rigid wheel operating in deformable soil.

Considering that $F = D/2 - Z_o$ the following is obtained:

$$f = \frac{k_c + b k_\phi}{(n+1) W} Z_o^{n+1} \left[\frac{D}{2} - \frac{Z_o}{n+2}\right] \qquad (6)$$

To overcome the moment caused by the vertical pressure components one has to apply a force (R_v) at the axis. Clearly if $D/2 \simeq g$ (see figure 3)

$$R_v = \frac{W f}{D/2}$$

Hence using equation 6

$$R_v = \frac{k_c + b k_\phi}{n+1} Z_o^{n+1} \left[1 - \frac{Z_o}{D/2} \frac{1}{n+2}\right] \qquad (7)$$

The horizontal pressure components may be expressed according to figure 4 as follows:

$$p_H = p_v \tan \alpha$$

or

$$p_H = \left(\frac{k_c}{b} + k_\phi\right) Z^n \tan \alpha$$

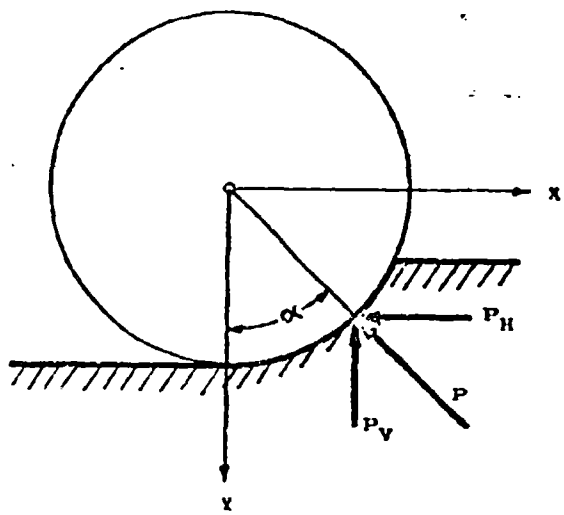


Fig. 4. — Horizontal and vertical pressure components acting under a rigid wheel.

It can be seen that

$$\tan \alpha = \frac{x}{\sqrt{(D/2)^2 - x^2}}$$

Thus

$$p_H = \left(\frac{k_c}{b} + k_\phi\right) Z^n \frac{x}{\sqrt{(D/2)^2 - x^2}}$$

The resistance due to horizontal pressures:

$$R_H = b \int_{D/2 - z_o}^{D/2} p_H \, dy$$

From here considering that $Z = y - F$ and $x = \sqrt{\left(\frac{D}{2}\right)^2 - y^2}$

$$R_H = (k_c + b k_\phi) \int_{D/2 - z_o}^{D/2} y^{n-1} \left[1 - \frac{D/2 - z_o}{y}\right]^n \left[(D/2)^2 - y^2\right]^{1/2} dy \qquad (8)$$

Equation 8 has been programmed for a Datatron computer by the Dynamics Simulations Laboratory located at the Ordnance Tank-Automotive Command. Thus the total resistance considered in this study is the sum of R_v and R_H.

$$R_m = R_v + R_H = (k_c + b k_\phi) \left[\frac{Z_o^{n+1}}{n+1} \left(1 - \frac{Z_o}{D/2\,(n+2)}\right)\right] + \int_{D/2 - Z_o}^{D/2} y^{n-1} \left(1 - \frac{D/2 - Z_o}{y}\right)^n \left[(D/2)^2 - y^2\right]^{1/2} \tag{9}$$

1 b) **Low inflated towed tires.** — The theory used in this paper has been explained in details in reference 10.

The sinkage of a tire with low inflation pressure will result in a maximum ground pressure equal to the inflation pressure plus a pressure due to the deflection of the stiff carcass (p_c)

$$p_{z\,max} = p_i + p_c$$

Using equation 2 one arrives at the following formula:

$$Z_o = \left[\frac{p_i + p_c}{\frac{k_c}{b} + k_\phi}\right]^{1/n} \tag{10}$$

Since it is assumed that the tire-ground interface is flat, resistance due to vertical pressures is considered. It has been shown by Bekker [1] that the resistance due to vertical reaction pressure in the soil may be approximated as follows:

$$R_c = \frac{k_c + b k_\phi}{n+1} Z_o^{n+1}$$

Using equation 10:

$$R_c = \frac{b \left(\frac{k_c}{b} + k_\phi\right)^{-1/n}}{n+1} (p_i + p_c)^{\frac{1+n}{n}} \tag{11}$$

Another important component of the total rolling resistance is due to carcass flexture (hysteresis losses). The « deflection resistance » has to be obtained by means of experiments on hard ground. The experimental resistance vs. inflation pressure curve can be described mathematically for

each tire. For example the deflection resistance varies in the following way in case of a 14-20 tire.

$$R_d = f_t W$$

where:

$$f_t = 0.0225 - 0.025 \log \frac{p_i}{40} \qquad (12)$$

Thus the total resistance considered in this paper is obtained by combining equations 11 and 12.

$$R = \frac{b}{n+1} \frac{1}{\left(\frac{k_c}{b} + k_\phi\right)^{1/n}} (p_i + p_c)^{\frac{n+1}{n}} + W \left[0.0225 - 0.025 \log \frac{p_i}{40}\right] \qquad (13)$$

Equation 13 shows that the compaction resistance is directly proportional, while the deflection resistance is inversely proportional with the inflation pressure. The total resistance, therefore, will have a minimum value at an optimum inflation pressure. The optimum inflation pressure may be found for a 14-20 tire if one solves the equation

$$\frac{dR}{dp_i} = 0 \text{ for } p_i$$

From equation 13 the following is obtained:

$$(p_{i_o} + p_c)\, p_i^n = \left[\frac{k_c}{b} + k_\phi\right] \left[\frac{0.0108\, n\, W}{b}\right]^n \qquad (14)$$

If the soil values, the carcass pressure, the load and the width of the tire are known the optimum inflation pressure can be found from equation 14.

In order to separate the rigid and soft operational conditions one has to investigate the equilibrium of a towed tire. It has been found [10] that the length of the flat part of the interface is (figure 5 a):

$$l_1 = \frac{W}{b(p_i + p_c)} - \frac{1}{n+1} l_2$$

As l_1 aproaches zero (hence p_c vanishes too) the inflation pressure approaches a critical value:

$$p_{i\,crit} = \frac{(n+1)\, W}{b \sqrt{D Z_o - Z_o^2}} \qquad (15)$$

where

$$l_2 = \sqrt{D Z_o - Z_o^2} \qquad \text{(see fig. 5 b)}$$

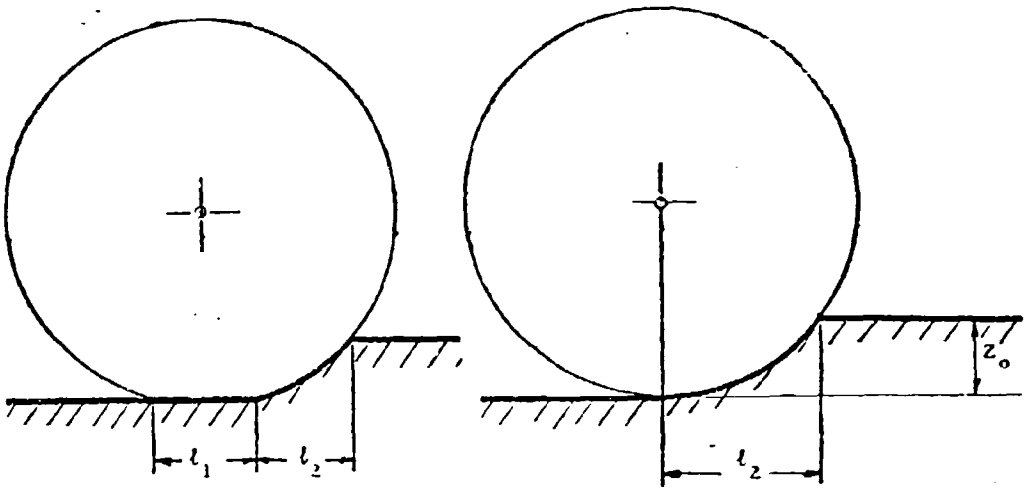


Fig. 5 a. Fig. 5 b.

Fig. 5 a. — Assumed shape of a low inflated tire operating in deformable soil.
Fig. 5 b. — Shape of a highly inflated tire operating in deformable soil.

2 a) **Driven wheels.** — Only rigid tires will be considered in this section. It is assumed that the sinkage and the resistance can be expressed as shown in the previous discussion although it is known that both are functions of the slippage. This problem awaits further research.

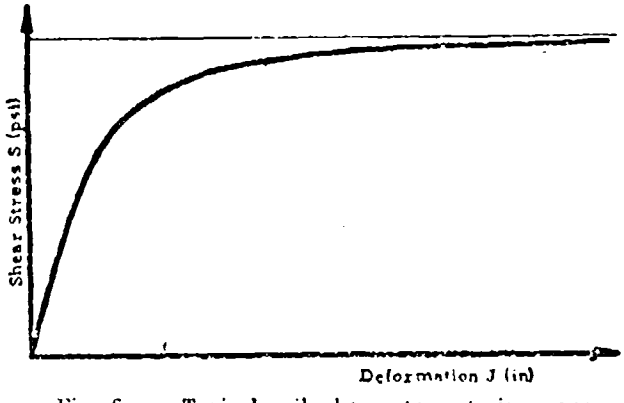


Fig. 6. — Typical soil shear stress-strain curve.

Furthermore, it is assumed that traction is due to horizontal shear stresses occurring under the wheel. Hence it is first necessary to examine a typical soil shear stress-strain curve (figure 6).

A simple empirical relationship suitable to describe a soil shear stress-strain curve has been suggested recently by the author [2a].

$$S = [c + p \tan \phi] [1 - e^{-j/K}] \qquad (16)$$

The traction may be obtained if one integrates equation 16 along the wheel soil interface.

To that end one has to express j in terms of the slippage and geometric dimensions. If the driven wheel moves with a certain slip (i_s) a point on the wheel perimeter describes a looped cycloid. The parametric equation of the path is the following:

$$x = r\alpha - R\sin\alpha$$

$$y = R\,(1 - \cos\alpha) \qquad (17)$$

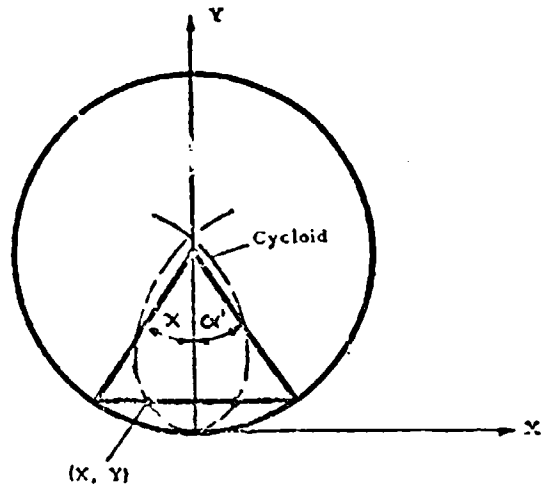


Fig. 7. — Relationship between α and α' for a driven wheel.

If one introduces $\alpha' = -\alpha$ then equation 17 becomes (figure 7)

$$x = R\sin\alpha' - r\alpha'$$

$$y = R\,(1 - \cos\alpha') \qquad (18)$$

The slippage is defined as:

$$i_s = \frac{V_t - V_a}{V_t} = 1 - \frac{V_a}{V_t}$$

But according to figure 8

$$\frac{V_a}{V_t} = \frac{r}{R}$$

hence

$$i_o = 1 - \frac{r}{R} \quad \text{and} \quad r = R\,(1 - i_o)$$

The ordinate of the instantaneous center of motion is y_c:

$$y_c = R - r = i_o R$$

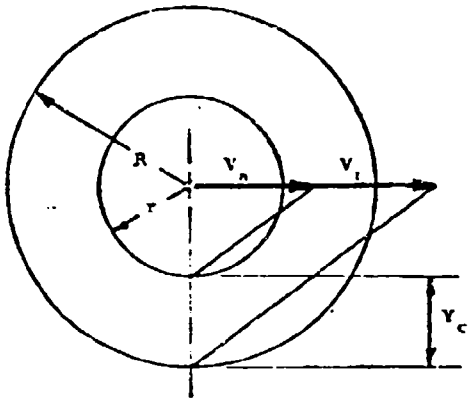


Fig. 8.

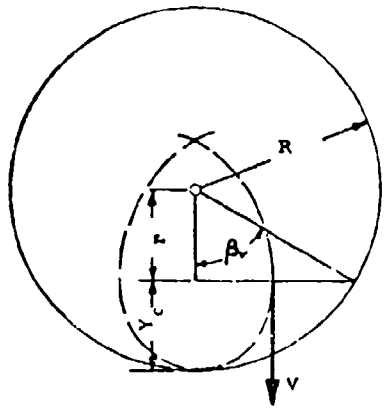


Fig. 9.

Fig. 8. — Relationship between the theoretical and actual velocities for a driven wheel.

Fig. 9. — Definition of β_v.

Hence equation 18 may be rewritten in the following form:

$$x = R\,[\sin\alpha' - (1 - i_o)\,\alpha']$$

$$y = R\,[1 - \cos\alpha'] \qquad (19)$$

Define β_v as the angle at which the tangent of the cycloid is vertical (figure 9).

Then

$$\beta_v = \cos^{-1}\frac{r}{R} = \cos^{-1}(1 - i_o) \qquad (20)$$

A new variable β which is defined as follows (figure 10) can be introduced:

$$\beta = \beta_v - \alpha'$$

Then equation 19 becomes:

$$x = R\,[\sin(\beta_v - \beta) - (1 - i_o)\,(\beta_v - \beta)]$$

$$y = R\,[1 - \cos(\beta_v - \beta)] \qquad (21)$$

But

$$\sin(\beta_v - \beta) = \sin\beta_v \cos\beta - \sin\beta \cos\beta_v$$

since

$$\cos\beta_v = (1 - i_w); \quad \sin\beta_v = \sqrt{1 - \cos^2\beta_v} = \sqrt{2i_w - i_w^2}$$

Thus

$$x = R\left[\sqrt{2i_w - i_w^2}\cos\beta - (1 - i_w)(\sin\beta + \beta_v - \beta)\right] \qquad (22)$$

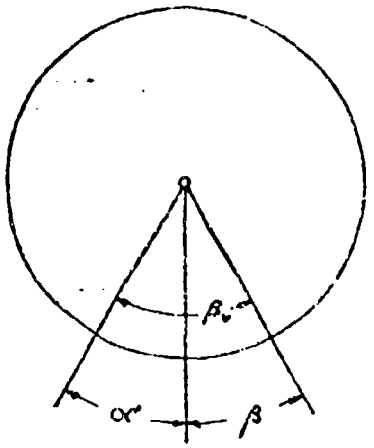


Fig. 10.

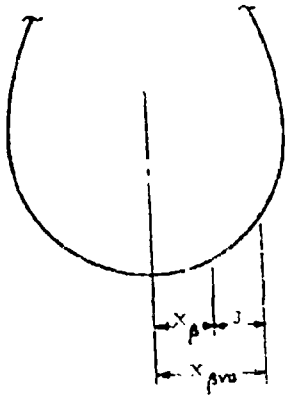


Fig. 11.

Fig. 10. — Relationship between β_v, α and β.
Fig. 11. — Relationship between x_β and j.

The deformation at angle β may be expressed as the difference of $x_{\beta vo}$ and x_β (figure 11). Note that $\beta = 0$ at $x = x_{\beta_v}$.

Thus:

$$j = R\left\{\sqrt{2i_w - i_w^2}\cos(\beta_v - \beta_w) + (1 - i_w)\left[\sin(\beta_v - \beta_w) + \beta_v - (\beta_v - \beta_w)\right]\right\} -$$

$$- R\left[\sqrt{2i_w - i_w^2}\cos\beta - (1 - i_w)(\sin\beta + \beta_v - \beta)\right]$$

So:

$$j = R\left\{\sqrt{2i_w - i_w^2}\left[\cos(\beta_v - \beta_w) - \cos\beta\right] + \right.$$

$$\left. + (1 - i_w)\left[\sin(\beta_w - \beta_v) + \sin\beta + \beta_v - \beta_w - \beta\right]\right\} \qquad (23)$$

According to figure 12 the sinkage is:

$$z = z_o - y = z_o - R\,[1 - \cos(\beta_v - \beta)] =$$
$$= R\left\{z_o/R - [1 - \cos(\beta_v - \beta)]\right\}$$

but

$$\cos\beta_o = 1 - \frac{z_o}{R}$$

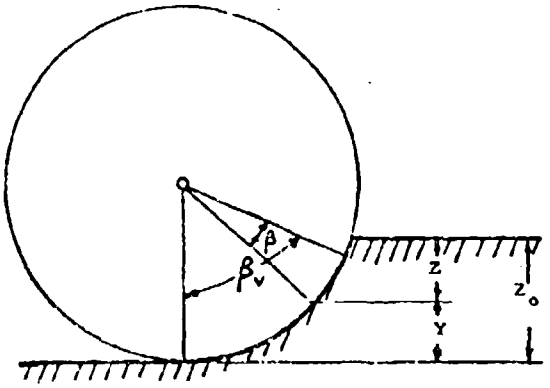


Fig. 12. — Relationship between the sinkage of an arbitrary point (Z) and β.

Therefore

$$z = R\,[\cos(\beta_v - \beta) - \cos\beta_o] \qquad (24)$$

Using equations 23 and 24 equation 16 may be integrated along the soil-wheel interface:

$$H = \int_S\int (c + p\tan\Phi)\,(1 - e^{-j/K})\,ds$$

$$= \int_S\int \left\{c + \left(\frac{k_c}{b} + k_\phi\right) R^n\,[\cos(\beta_v - \beta) - \cos\beta_o]^n \tan\Phi\right\}$$

$$\left\{1 - e^{-\frac{R}{K}\left\{(\beta_v - \beta_o) - (1 - i_o)\,[\cos(\beta_v - \beta_o) - \cos\beta] + \right.}\right.$$

$$\left.\left. + (1 - i_o)\,[\sin(\beta_o - \beta_1) + \sin\beta + \beta_v - \beta_o - \beta]\right\}\right\} ds$$

The surface element (dA) may be expressed as (figure 13):

$$dA = R\,b\,d\beta$$

Its horizontal projection is the effective area element with respect to horizontal shearing stresses

$$dS = dA\cos(\beta_v - \beta)$$

Therefore:

$$H_1 = b R \int_{\beta_v - \beta_o}^{\beta_v} \left\{ e + \left(\frac{k_c}{b} + k_\phi \right) R^n \left[\cos(\beta_v - \beta) - \cos\beta_v \right]^n \tan\Phi \right\} \left\{ 1 - e^{-\frac{R}{K} \left\{ \sqrt{2 i_o - i_o^2} \left[\cos(\beta_v - \beta_o) - \cos\beta \right] + \right.} \right.$$

$$\left. \left. + (1 - i_o) \left[\sin(\beta_o - \beta_v) + \sin\beta + \beta_v - \beta_o - \beta \right] \right\} \right\} \cos(\beta_v - \beta)\, d\beta \qquad (24\,a)$$

When $\beta_o > \beta_v$. However, another effect has to be included.

As can be seen on figure 14 the path of the points on the wheel perimeter as a positive x component between the points 1 and 2.

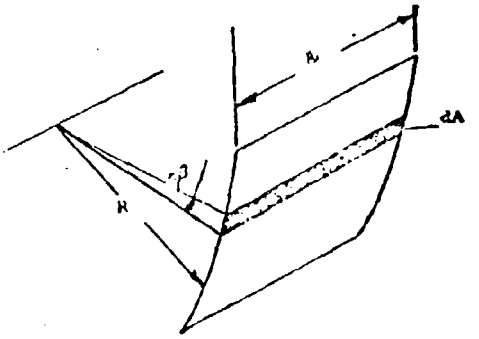


Fig. 13. — Area element on the rim.

Thus a resistance is created (H_2) due to shear-stresses on section 12, while traction is developed along section 23. In order to find H_2 one has to express j'as shown in figure 15.

$$j' = j_{\beta_o} - j = R \left[\sqrt{2 i_o - i_o^2} (1 - \cos\beta_o) + (1 - i_o) (\beta_o - \beta_o) \right]$$

$$- R \left[\sqrt{2 i_o - i_o^2} (1 - \cos\beta) - (1 - i_o) (\sin\beta - \beta) \right]$$

Thus

$$j' = R \left[\sqrt{2 i_o - i_o^2} (\cos\beta - \cos\beta_o) + (1 - i_o) (\sin\beta_o - \sin\beta + \beta - \beta_o) \right] \qquad (25)$$

The resistance is then:

$$H_2 = b R \int_{\beta_v - \beta_o}^{\alpha} \left\{ e + \left(\frac{k_c}{b} + k_\phi \right) R^n \left[\cos(\beta_v - \beta) - \cos\beta_o \right]^n \tan\Phi \right\}$$

$$\left\{ 1 - e^{-\frac{R}{K} \beta} \right\} \cos(\beta_v - \beta)\, d\beta \qquad (26)$$

If equation 26 has to be used ($\beta_o > \beta_1$) then the lower limit of integration in equation 24 a is zero, and the traction of the wheel is:

$$H = H_1 - H_2$$

If $\beta_o < \beta_1$ $H = H_1$ where H_1 is given by equation 24 a.

The integrals cannot be solved in a closed form therefore the equations have been programmed on a Datatron 204 electronic computer.

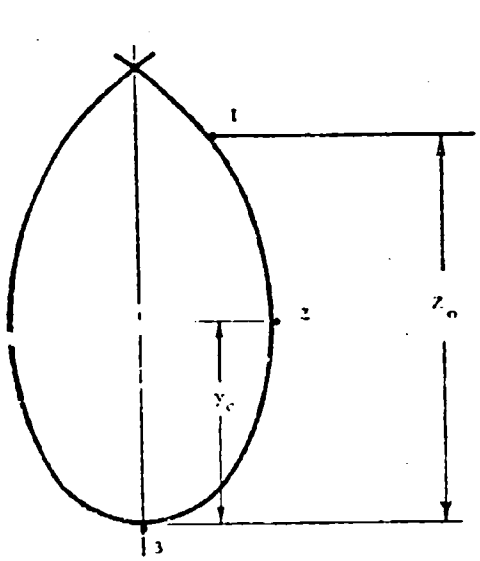


Fig. 14.

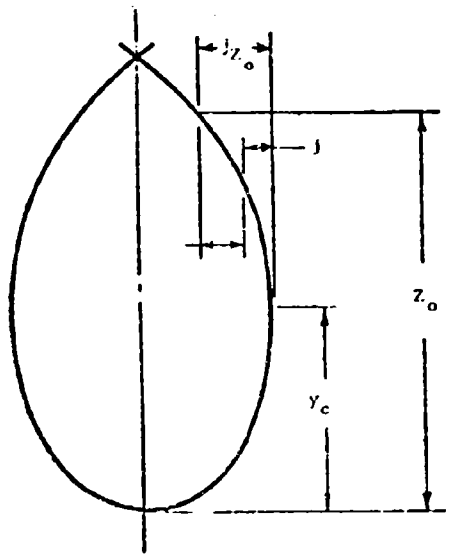


Fig. 15.

Fig. 14. — Resistive (12) and tractive (23) portions of the active segment of the path of a point located on the wheel perimeter.

Fig. 15. — Relationship between j and j' for the resistive domain of the path.

III) Tests

The test program designated to check the validity and accuracy of the theory presented consisted of two major phases:

a) Single wheel tests (towed and driven wheels).

b) Wheeled vehicle tests.

Towed single wheel tests are reported in this paper. The following tires were tested in sand: 7.00-16, 11.00-20; 14.00-20; 11.00-28 conventional tractor tire and 11.0-28 radial ply tractor tire. The 7.00-16 and the 14.00-20 tires were also tested in a particular loam soil. Driven single wheels had not been tested before the deadline date set for submittance of papers for this con-

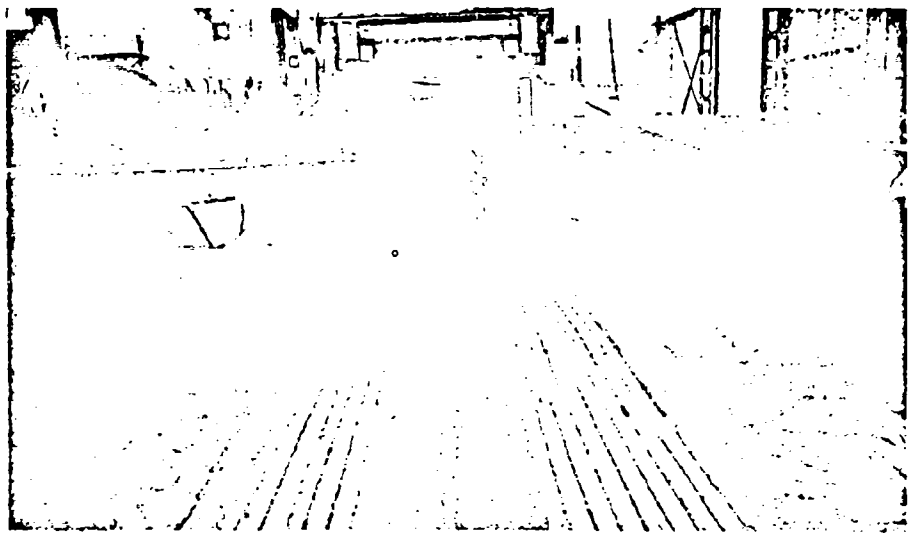


Fig. 16. — Test bin and tire test carriage.

ference because of time limitations. Equations 24 a and 26 (Drawbar pull as a function of slip driven wheels) were used, however, in another paper to be presented by Mr. Harrison from the Land Locomotion Laboratory at this conference (« Analytical Prediction of Performance for Full Size and Small Scale Model Vehicles »).

1) **Test apparatus.** — A simple carriage was built (fig. 16 and 17) to accomodate towed tires. The carriage was pulled by means of a parallelogram bar system (A), hence the load (W) was solely supported by the tire. Two load cells (B) mounted on each side of the wheel axle provided the motion resistance readings which were recorded on a Brush roll-paper type recorder (fig. 18). The sinkage of the carriage was determined by means of a potentiometer (fig. 19), the housing of which was firmly attached to a fixed bar while its shaft was free to follow the vertical movement of the carriage (c). The variation of the carriage sinkage was continuously plotted on the Brush recorder used to record motion resistance. The electric Bevameter (25) and an XY plotter were mounted on the test rig enabling one to take soil value readings quickly and efficiently.

2) **Test procedure.** — Tests were carried out in the following steps:

a) The soil was loosened by means of rakes to a depth of 18 inches and leveled with a heavy plate mounted vertically in front of the dynamometer carriage.

b) Penetration tests were performed with the Bevameter using cir-

cular footings 3 and 4 inch diameters. The load vs sinkage curves were recorded on the XY plotter.

c) The carriage was lifted with an overhead crane so that the tire barely touched the soil level. The instruments were then adjusted so that zero motion resistance and sinkage was established on the recorder.

d) The tire was then towed along the bin while the motion resistance was recorded by the two load cells and the carriage sinkage by the potentiometer.

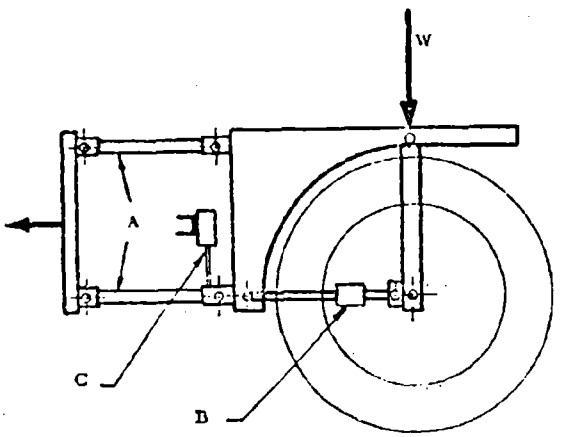


Fig. 17. — Sketch of the tire test carriage.

e) The actual wheel sinkage was measured at three places in the rut left by the tire. (This was not always possible in sand because of the cave-in of the rut walls).

f) The load and/or the inflation pressure was changed.

g) Step a was repeated, etc.

Tests were also run on a hard surface to obtain R_a, the deflection resistance. The resistance was measured for the same inflation pressures and loads used for tests in deformable soils.

The ground contact area was established by a special technique since the high lugs prevented the use of the « hard surface and paint » method which is usually used for the experimental evaluation of the magnitude of the ground contact area for conventional automobile tires. To overcome this difficulty tire imprints were taken in sand and plaster of Paris was poured in the print until its depth exceeded the heights of the lugs by 1/4 inch. The ground contact area was established for each load at pressures less than the critical pressure, by measuring the area enclosed by the contour of the dry plaster cast (fig. 20).

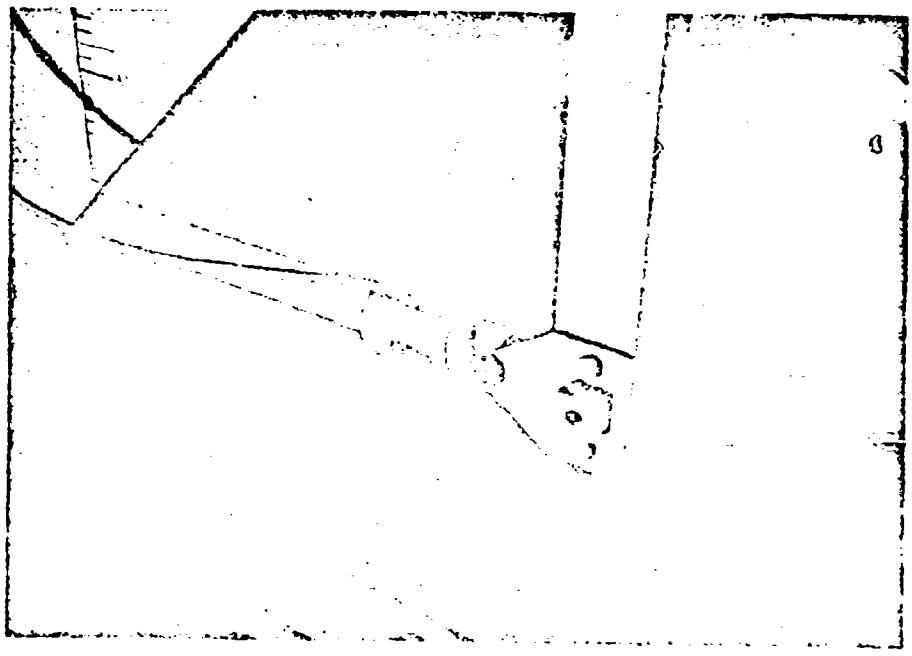


Fig. 18. — Load cell to measure motion resistance.

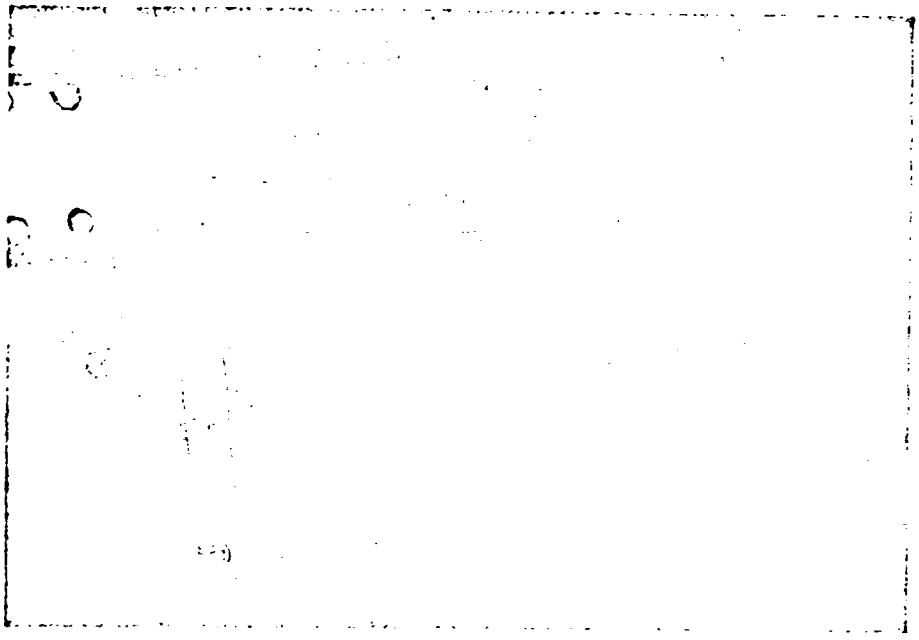


Fig. 19. — Potentiometer to measure sinkage.



Fig. 20. — Cast of low inflated tire imprint.

3) **Evaluation of tests.** — Soil values were evaluated by using the well known technique established by the Land Locomotion Laboratory [25]. Since the soil values obtained in sand exhibited a very high degree of consistency no attempt was made to apply statistical methods to evaluate a band instead of a curve for the predicted resistance vs inflation pressure relationships. However, certain difficulties arose with the evaluation of the soil values of the loam.

The average motion resistance was obtained by establishing the mean ordinate of the recorded curve. The area under the curve was found by means of a planimeter and divided by the base considered.

Since the recorded carriage sinkage is the sum of the tire sinkage and the deflection of the tire, the rut depth was measured separately. The difference between the recorded carriage sinkage and the depth of the rut is the deflection. The exact value of the sinkage is not really critical unless one is interested in bellying. In order to correlate the measured resistance curve at low pressure p_i had to be obtained. To this end the ground contact area (A) was evaluated as described above and the following equation was used:

$$\frac{W}{A} = p_i + p_c$$

For pressures lower thant the critical inflation pressure (equation 15) the resistance was predicted by means of equation 11 (see figs. 22-26). For high pressures the equation derived for rigid wheels was used (equation 9). In the case of a rigid wheel the theoretical resistance does not depend on the

inflation pressure, thus the curve is a horizontal line for $p_i > p_{cr}$. It seemed to be advisable to avoid any attempt to predict the resistance for inflation pressures slightly below the theoretical critical pressure because the assumption of flat ground contact area may not be justifiable for that case. Therefore, the predicted resistance values for low pressure were connected by a straight line with the « rigid wheel resistance » at the critical pressure.

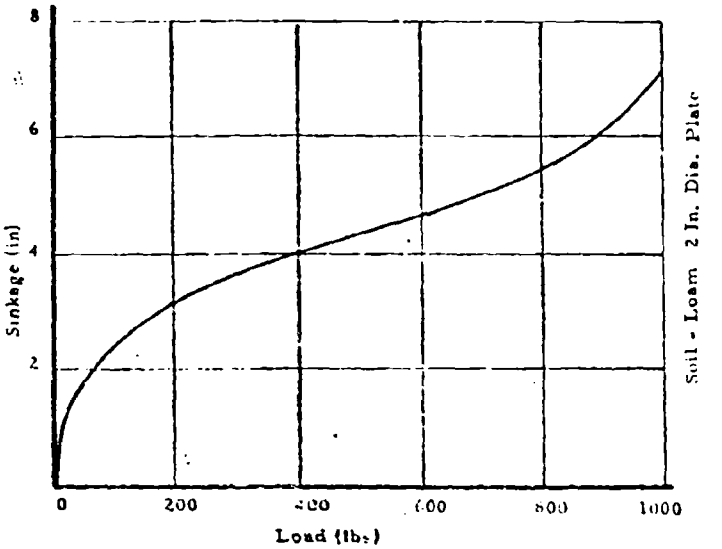


Fig. 21. — Typical load vs. sinkage curve obtained in the loam soil in which tire tests were performed.

It has been observed by the writer that when a wheel operates in a so called multi-layer soil the equations presented are not always applicable. A multi-layer soil may not be characterized by a single set of sinkage parameters if the layers are shallow. The loam soil in which the 7.00-16 and the 14.00-20 tire were run proved to be of this particular multi-layer character. A typical penetration curve as shown in fig. 21 will reveal that an expression of the form $p = kz^n$ is not suitable to represent the vertical stress-strain relationship for that soil condition. Work has been started in the Land Locomotion Laboratory to devise a geometric method to solve this problem.

4) **Discussion of test results.** — The motion resistance as a function of inflation pressure (figs. 22-26) varied according to the trend predicted by theory. At high inflation pressures the tire does not deform in deformable soils and the resistance only depends on the load. If the inflation pressure is lowered below the so called critical pressure the resistance begins to decrease and reaches a minimum value at p_{opt}, (see equation 14). At very

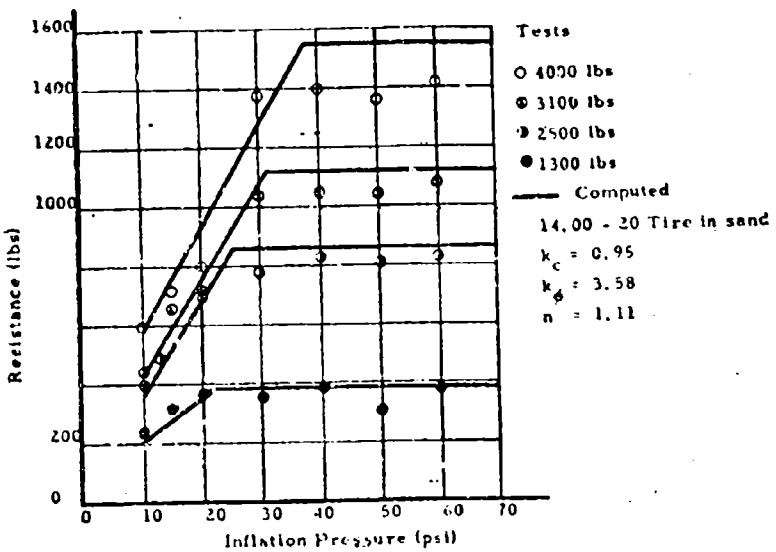


Fig. 22. — Resistance in function of inflation pressure for a 14.00-20 tire operating in sand.

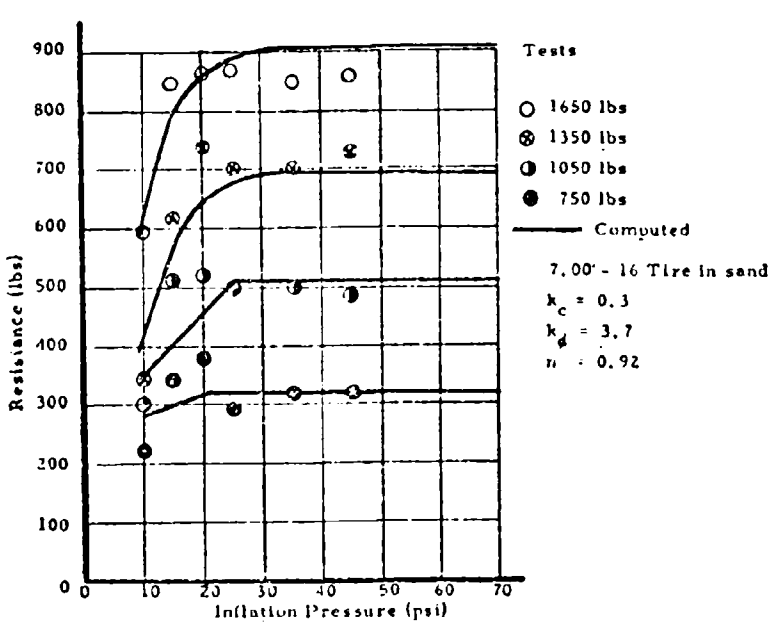


Fig. 23. — Resistance in function of inflation pressure for a 7.00-16 tire operating in sand.

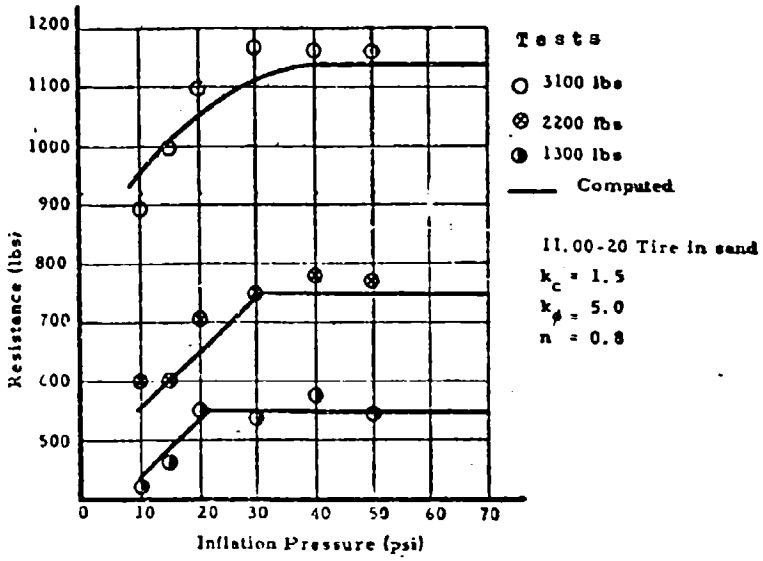


Fig. 24. — Resistance in function of inflation pressure for a 11.00-20 tire operating in sand.

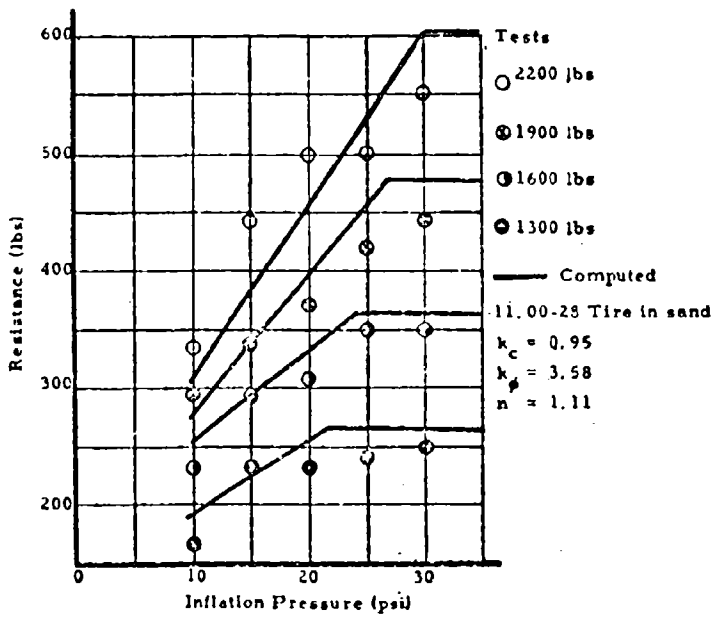


Fig. 25. — Resistance in function of inflation pressure for a 11.00-28 radial ply tractor tire operating in sand.

low pressure the resistance increases again due to high hysteresis losses. The latter trend was clearly shown in reference 16. During the test series presented in this paper the inflation pressure was not reduced below the optimum (p_i). It is interesting to note that the sinkage is practically independent of the load at low inflation pressures. An increase in load results in more deformation while the sinkage and hence the bulk of the resistance stays constant. The increase in resistance is due to an increase in the deflection.

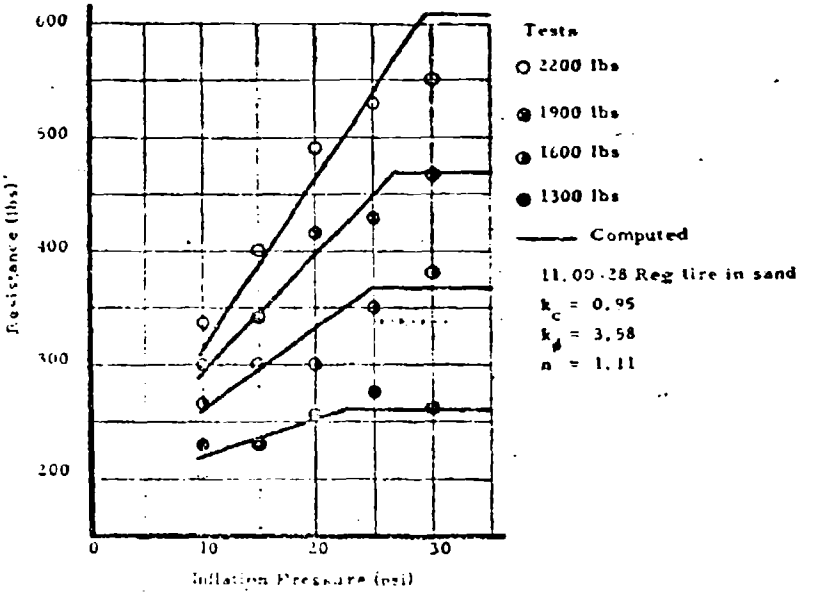


Fig. 26. — Resistance in function of inflation pressure for a 11.00-28 conventional tractor tire operating in sand.

This condition prevails (within the limits set by the tire geometry) until the inflation pressure reaches the neighborhood of the critical pressure.

It is believed that the critical pressure is a very important operational characteristic. A soft tire deforms rather than sinks, thus yielding less resistance and more ground contact area than a rigid tire. The advantage of a soft tire may only be exploited if inflation pressure is reduced below critical pressure. The theoretical value of the critical pressure may be found if the Bekker soil values, the load and the tire geometry is known (equation 15).

The correlation between the tested and predicted curves may be judged satisfactory, especially if one considers the great number of assumptions introduced in the theory in an attempt to keep the solution on a practical level.

IV) Conclusions

a) It is believed that the usefulness of empirical stress-strain curves in predicting vehicle performance has been confirmed by this work.

b) The notion of critical pressure is of paramount importance when one attempts to cross a particularly adverse terrain with wheeled vehicles.

c) Equations 9 and 13 show that a narrow and large diameter tire encounter less resistance than a wide and small one. In other words a longitudinal ground contact area is favorable.

d) As for driven rigid wheels one may conclude that there exists a slippage determined by the load, the geometry and the soil, above which the increase in drawbar pull is off-set by the decrease in tractive efficiency.

BIBLIOGRAPHY

1) Bernstein R. Probleme zur experimentellen motorpflug mechanik. Motorwagen, 1913.
2) Goryachkin V. D. (Collective work) Teoria i prosivoslstuvo sielskohoziayniti mashin. Moscow, 1936.
3) Garbari F. Resistenza al movimento dei veicoli a ruote su terreno cedevole. ATA, Rendiz Congr. 9-11 Roma, 1950.
4) Bekker M. G. Theory of land locomotion. (Chapter VI). University of Michigan Press, Ann Arbor, Michigan, 1956.
5) Vincent E. T. Pressure distribution on and flow of sand past a rigid wheel. First International Conference on the Mechanics of Soil-Vehicle System, Turin, 1961.
6) Weiss J. S. Preliminary study of snow values related to vehicle performance. Report No. 2. Ordnance Corps Land Locomotion Laboratory, Detroit Arsenal, 1956.
7) Onelanov A. E. O Primenii pneumaticheniik koles. Selhoz mashima No. 5, 1948.
8) Ageikin Y. S. Opredelchenie deformatsii parametrov kontakta shiny s myagkim gruntom. Avtom trakt prom, 1959 (5).
9) A soil value system for land locomotion mechanics. Research Report No. 5, Land Locomotion Laboratory, OTAC, Center Line, Michigan, 1958.
10) Bekker M. G. and Janosi Z. Analysis of towed pneumati tires moving on soft ground. Report No. 62, Land Locomotion Laborator OTAC, Center Line, Michigan.
11) Bekker M. G. Off-the-road locomotion. University of Michigan Press, Ann Arbor, Michigan, 1960.
12) Reed I. F. Pressure patterns for conventional and radial ply tires. Presented at the meeting of the ASAE Committee on Tractive and Transport Efficiency, at the National Tillage Laboratory Auburn, Alabama, 1960.
13) Thomson A. B. and Smith M. E. Stresses under moving vehicles. Technical Report No. 3-5415 Report 2, U. S. Army Engineer Waterways Experiment Station, Corps of Engineers, Vicksburg Mississippi, 1960.
14) Soehne W. Druckverteilung im boden und bodenverformung unter schlepperreifen. Grundlagen der Landtechnik, Vol. 5, 1953.
15) VanDenberg G. E., Cooper A. W., Erickson A. E. and Carleton A. E. Soil pressure distribution under tractor and implement traffic. Agricultural Engineering, Vol. 38, No. 12, Dec., 1957.
16) Kerr R. C. A design guide for the application of pneumatic tires to vehicles intended for off-road service. Arabian American Oil Company, 1955.
17) Chapoux E. Pneumatic pour vehicules sahariens. Engineur de L'Automolvill, Vol. XXXII, No. 11, 1959.
18) Mazza C. and Amici. Essais sur pneus pour tracteurs influence de la structure de la carcasse. R. G. C., Vol. 36, No. 10, 1959.

19) Reeds I. F. Tests of lugged radial ply and conventional tires. Presented at the meeting of the ASAE Committee on Tractive and Transport Efficiency, at the National Tillage Laboratory, Auburn, Alabama, 1960.
20) Richey C. B. Techniques of field test comparisons of tractor tire efficiency. Presented at the meeting of the ASAE Committee on Tractive and Transport Efficiency at the National Tillage Laboratory, Auburn, Alabama, 1960.
21) Hegedus E. Evaluation of conical tire model. Report No. 60, Land Locomotion Laboratory, OTAC, Detroit Arsenal, Center Line, Michigan, 1960.
22) Soehne W. The Transmission of force between tractor tires and farm soils. (in German) Grundlagen der Landtechnik, Vol. 3, 1952.
23) Hadekel R. The mechanical characteristics of pneumatic tires. Issued by T.P.A. 3 Technical Information Bureau for Chief Scientists, Ministry of Supply, 1944.
24) Hegedus E. Pressure distribution under a rigid wheel. To be published by the Land Locomotion Laboratory, OTAC, Center Line, Michigan.
25) Pavlics F. OTAC Instruments for the measurement of physical soil values, paper No. 4. Research Report No. 5, Land Locomotion Laboratory, OTAC, Center Line, Michigan, page No. 40, 1958.
26) Janosi Z. and Hanamoto B. The analytical determination of drawbar pull as a function of slip for tracked vehicles in deformable soils. Paper presented at the First International Conference on the Mechanics of Soil-Vehicle Systems, Turin (Italy), 1961.

DISCUSSIONS

R. D. WISMER and M. E. SMITH. -- The study of the performance of pneumatic tires on deformable soils is quite complex. In this interaction both the soil and the tire yield and, as is well known, the relative amount of deflection of each may have a profound effect on performance. Mr. Janosi has chosen to analyze one aspect of this problem, that of the towed pneumatic tire at various inflation pressures, and in doing so has made a very worthwhile contribution to the rather meager amount of information on this subject.

However, a fundamental assumption in Mr. Janosi's analysis of pneumatic tire performance is that the vertical pressure under the tire may be expressed by Bekker's pressure-sinkage relation [1].

$$p = \left(\frac{k_c}{b} + k_\phi\right) z^n$$

He obtains the soil values k_c, k_ϕ, and n used in this relation from plate penetration tests. Ideally, the pressure-sinkage relation for plates with different dimensions describes a family of parabolas which plot as parallel straight lines on logarithmic paper, one for each plate (see figure 1). The slope of these lines is the coefficient, n, while the pressure intercept at $z = 1$ is the constant term,

$$\frac{k_c}{b} + k_\phi$$

The plate size term, b, is the width of a rectangular plate or the radius of a circular plate. The two terms k_c and k_ϕ are obtained by solution of simultaneous equations or by graphical construction (see figure 1).

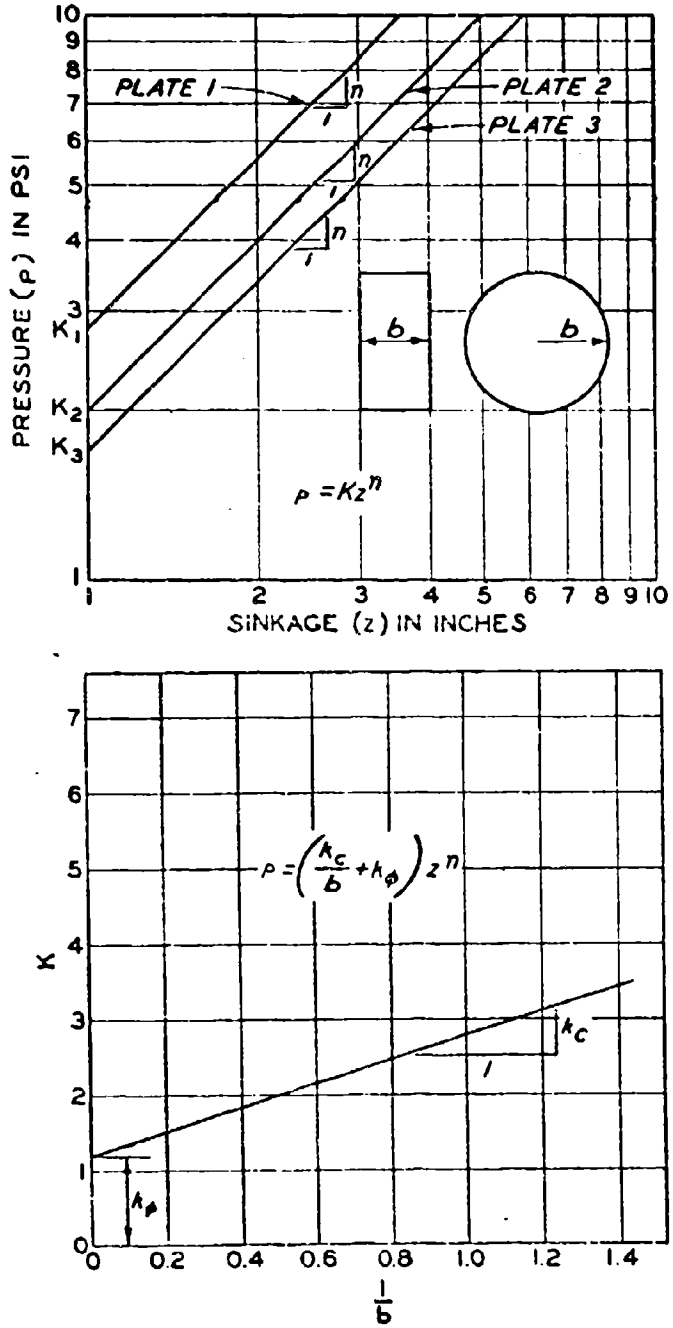


Fig. 1. — Pressure-sinkage relation.

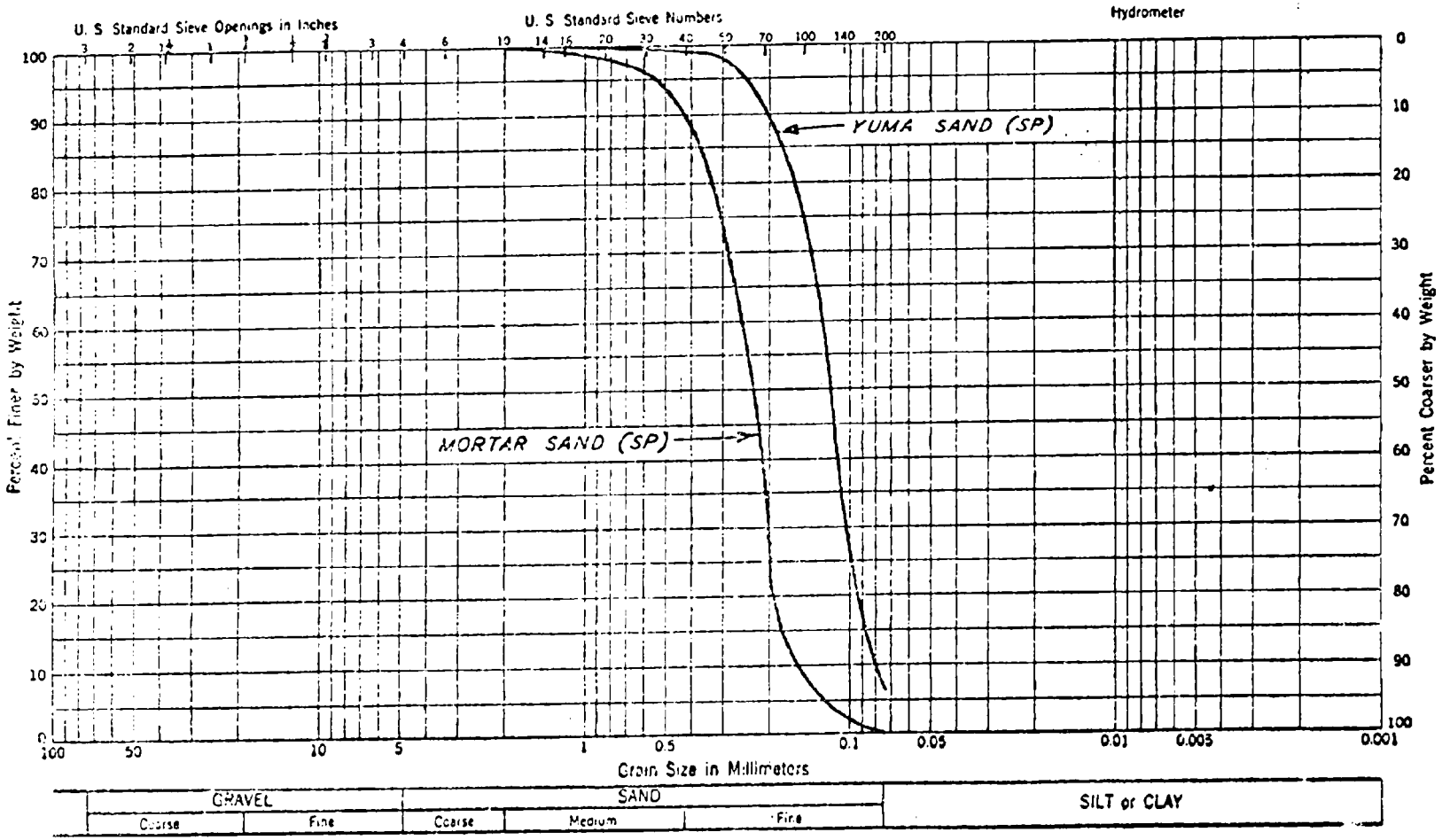
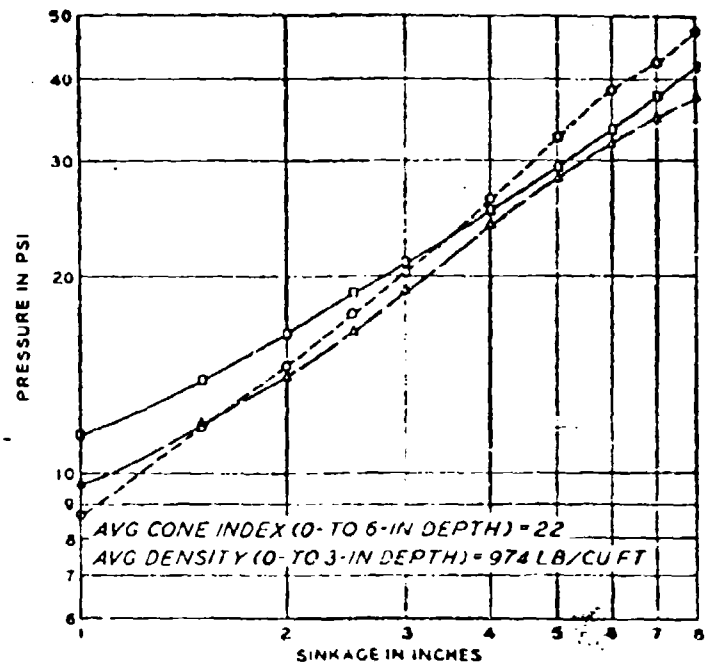


Fig. 2. — Soil classification data.



a

LEGEND

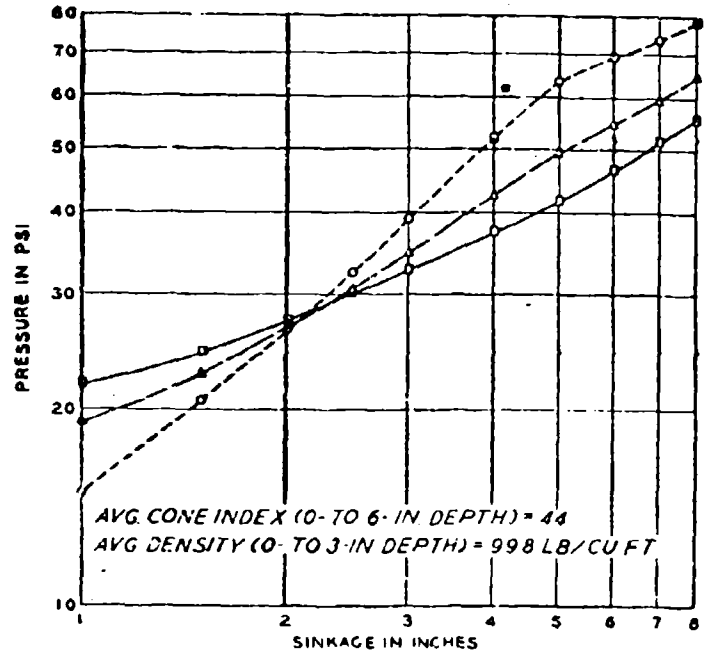
○ 1.1 in diam plate
□ 4.2 in diam plate
Δ 2.8 in diam plate

Note: Properties of the sand are:

C = 0
φ = 33°-36°
γ_{Min} = 88.0 LB/CU FT
γ_{Max} = 103.2 LB/CU FT

Fig. 3. — Plate penetration curves, yuma sand.

Some investigators have reported considerable difficulty in obtaining reliable values of k_c, k_ϕ, and n from plate penetration tests. Goodman and Lee (paper No. 4) encountered a tremendous spread in values of k_c and k_ϕ in their work with lacustrine clay; Sohne and Sonnen (paper No. 33) found that $p = Kz^n$ did not adequately describe the penetration curve in an agricultural soil; Steinbrugge (paper No. 35) obtained negative values of k_c in sand, although he used an average of at least six determinations; and Hicks (paper No. 41) assumed $k_c = 0$ for sand and used only one plate size, thereby eliminating some of the difficulties of the method which have plagued other investigators. Even Mr. Janosi reported difficulty in obtaining reliable soil values in the loam soil described in his paper. The Army Mobility Research Center (AMRC) of the U. S. Army Engineer Waterways Experiment Station has also found the pressure-sinkage relation to be inconsistent, as will be discussed.


PRESSURE IN PSI
SINKAGE IN INCHES
AVG CONE INDEX (0- TO 6-IN DEPTH) = 44
AVG DENSITY (0- TO 3-IN DEPTH) = 99.8 LB/CU FT

b

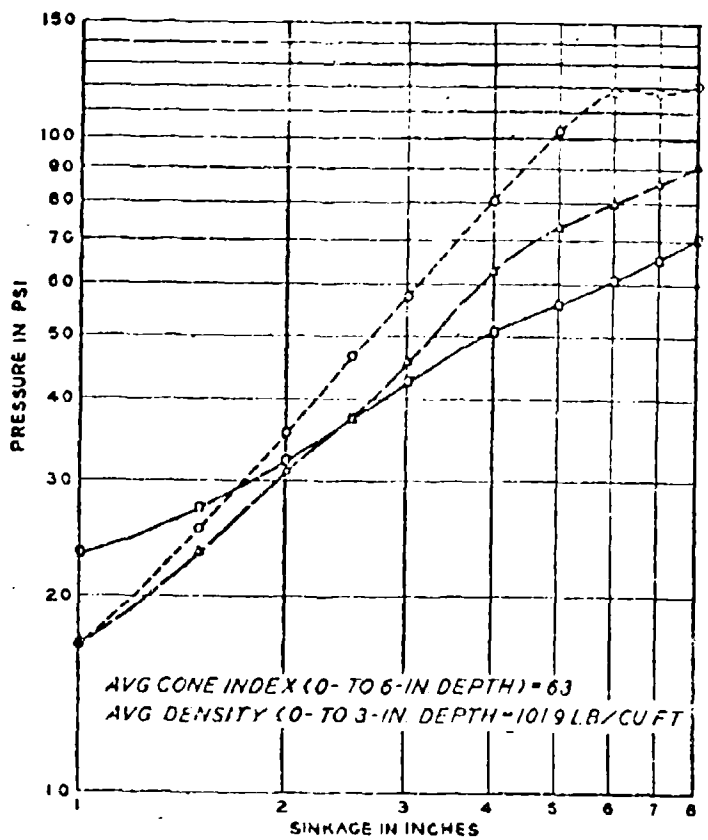
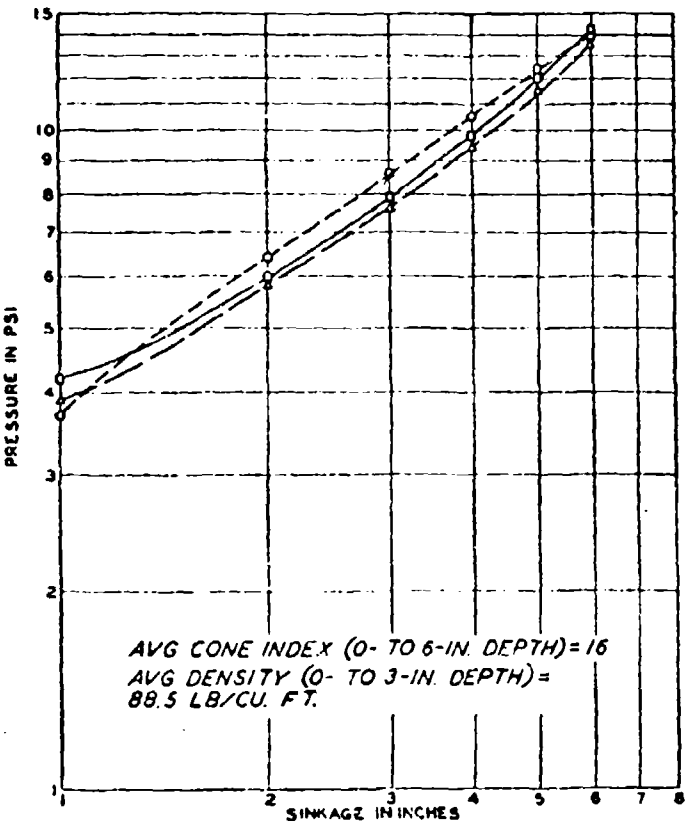

PRESSURE IN PSI
SINKAGE IN INCHES
AVG CONE INDEX (0- TO 6-IN DEPTH) = 63
AVG DENSITY (0- TO 3-IN DEPTH = 101.9 LB/CU FT

Fig. 3.

c



a

LEGGEND

○·····○ 1.4 in diam plate
□ ——— □ 4.2 in diam plate
Δ— - - - —Δ 2.8 in diam plate

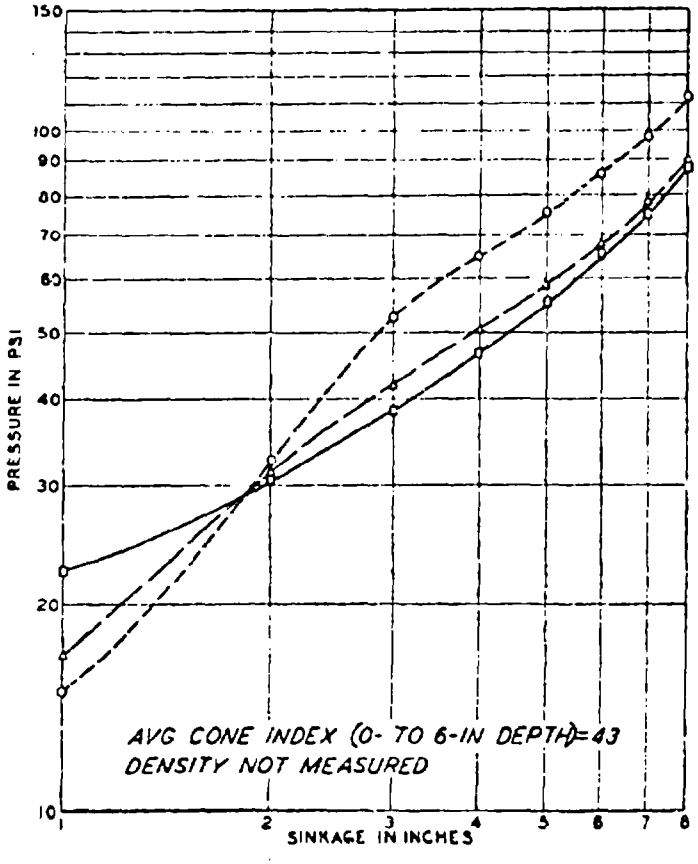
Note: Properties of the sand are:

C	=	0	γ_{Min}	=	87.4 LB/CU FT
Φ	=	32°-38°	γ_{Min}	=	106.1 LB/CU FT

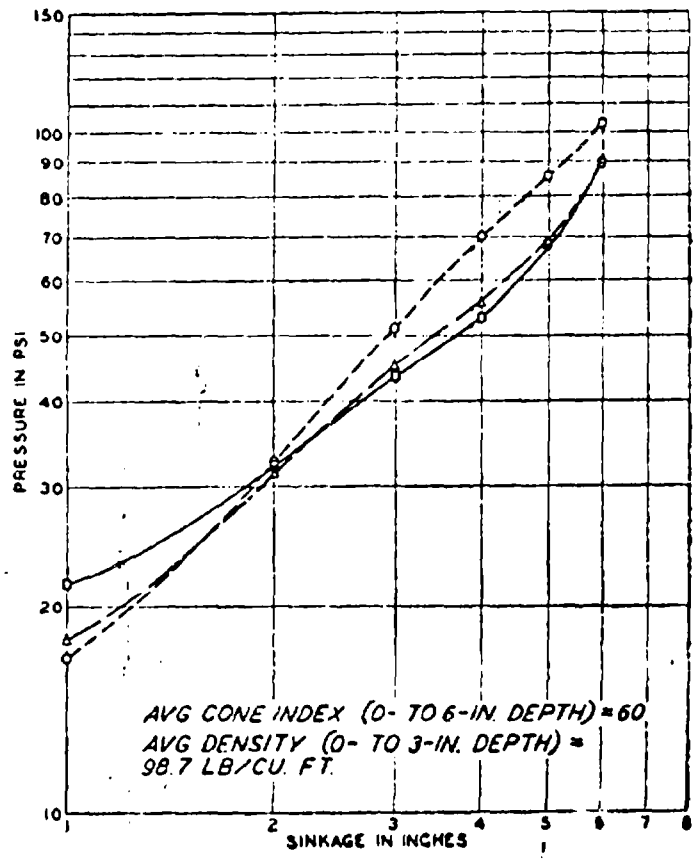
Fig. 4. — Plate penetration curves, mortar sand.

Pressure-sinkage curves have been developed by the AMRC for a dune sand from Yuma, Arizona, and a mortar sand. Both sands are classified SP on the basis of the Unified Soil Classification System[2]. The grain-size distribution curves for these sands are presented in figure 2.

Typical pressure-sinkage curves for plate penetration tests made in dry (moisture content less than 1 per cent) Yuma sand are presented in figure 3; similar data for tests made in dry mortar sand are presented in figure 4. These data represent


PRESSURE IN PSI
SINKAGE IN INCHES
AVG CONE INDEX (0- TO 6-IN DEPTH)=43
DENSITY NOT MEASURED

b


PRESSURE IN PSI
SINKAGE IN INCHES
AVG CONE INDEX (0- TO 6-IN. DEPTH) = 60
AVG DENSITY (0- TO 3-IN. DEPTH) =
98.7 LB/CU. FT.

c

Fig. 4.

a range of soil strength and three plate sizes. All the data were obtained with circular plates but tests using rectangular plates produced similar results.

It is apparent that the pressure-sinkage curves for different plate sizes cross each other and are not straight, particularly for sand at intermediate and high densities. Thus, k_c, k_ϕ, and n appear to vary with the size of the bearing area and even with the sinkage, z.

Bekker's assumed pressure-sinkage relation appears to be a valid approximation only for sand in a very low-density condition (figure 4a). Although the pressure-sinkage curves cross each other and are lightly curved for this condition, the data could be approximated by a single straight line. This would satisfy the assumed pressure-sinkage relation with $k_c = 0$.

The soil values quoted by Mr. Janosi (k_c = 0.3 to 1.5, k_ϕ = 3.58 to 5.0, n = 0.80 to 1.11) have been found in tests by the AMRC to correspond approximately to an 0- to 6-in. average cone index of 16 (see figure 4a). This finding is verified by tests reported by Mr. Janosi[3] in which a sand with an 0- to 6-in. average cone index of 17 exhibited soil values of $k_c = 0$, k_ϕ = 4.3, and n = 1.01. This represents about the loosest state at which sand can exist-even in the laboratory.

Of more than 1000 vehicle tests conducted by the AMRC in natural beach and desert sands, only four instances were recorded of an 0- to 6-in. average cone index being less than 20 when the sand was not inundated[4,5].

BIBLIOGRAPHY

1) Czako T. and Hegedus E. Physical soil and snow values for the determination of vehicle motion resistance. Research Report No. 5, Land Locomotion Research Branch, Centerline Michigan, p. 3, 1958.

2) U. S. Army Engineer Waterways Experiment Station, CE. The Unified-Soil Classification System. Technical Memorandum No. 3-357, Vicksburg, Mississippi, March, 1953.

3) Janosi Z. Prediction of «WES cone index» by means of a stress-strain function of soils, Report No. 46, Land Locomotion Laboratory, Centerline, Michigan, pp. 15-17, 1959.

4) Knigth S. J. U. S. Army Engineer Waterways Experiment Station, CE. A summary of trafficability studies through 1955. Technical Memorandum No. 3-240, 14th Supplement, Vicksburg, Mississippi, December, 1956.

5) Rush E. S. U. S. Army Engineer Waterways Experiment Station, CE. Test on coarse-grained soils with self-propelled and towed vehicles, 1956 and 1957. Technical Memorandum No. 3-240, 15th Supplement, Vicksburg, Mississippi, June, 1959.

Z. JANOSI. — 1) I would like to say that the phenomenon Dr. Söhne reported on, difficulties in certain loose soils, really exists. This is what we call the multi-layer soil which exhibits different properties as the penetrometer sinks. This can be registered by the bevameter and we have to assign two or more sets of soil values for that soil, but I have to admit that then the analysis of such a soil becomes more difficult.

2) k_c can take a minus value, and there is nothing wrong in this. We have to be concerned only if $(k_c/b + k_\phi)$ altogether takes a minus value, which I haven not seen to happen yet.

Now, as to the difficulty of predicting the sinkage of a wheel in sand I have to say the following. We were visited by some of the engineers from Vicksburg who carried out a great number of tire tests just before they visited us, and they told

me what follows. By considering the large amount of data obtained, they set up the following equation for sinkage, based on these experimental data:

$$Z = k \left[\frac{P_1 + P_2}{C}\right]^{1.27}$$

I do not remember whether the factor 1.27 is quite correct.

I was glad to see this equation in which P_1 is the inflation pressure, P_2 is the carcass pressure and C is the cone index. The cone index is also a measure of soil strength, as k_ϕ, k_c and n, so actually what they had was a certain constant times my equation. 1/n was in their case 1.27. So I was very happy that this equation was confirmed by other investigators, and is was also confirmed by a Russian scientist in another paper.

E. LEFLAIVE. — Je veux mentionner très brièvement deux points:

1) La formule qui est utilisée donnant la contrainte de cisaillement maximum est très intéressante par le fait qu'elle fait intervenir les déformations; il faut remarquer cependant qu'elle n'est valable que sur les directions pour lesquelles

$$\frac{\tau}{p + c \cot g \varphi}$$

est maximum, c'est-à-dire les lignes de glissement. L'Auteur de la communication a-t-il des éléments expérimentaux qui le renseignent sur les lignes le long desquelles l'intégration peut être faite?

Je m'excuse si la réponse à cette question est évoquée dans la communication écrite, dont je n'ai pas encore pu prendre connaissance.

2) J'ai été très intéressé par l'intervention du Professeur Reece; je signalerai seulement que les phénomènes qui ont été décrits, sur l'enforcement dans le sol d'un objet lorsqu'il est soumis à un effort horizontal, correspondent tout à fait aux résultats des calculs de force portante inclinée effectués dans l'hypothèse de la plasticité idéale classique.

W. L. HASLSON. — Mr. Turnbull has questioned my ability to obtain good results from stress strain curves whose logarithmic plots are not straight lines, but rather were seemingly scattered. This question has been covered in detail in my report. It is concerned with the proper interpretation of the soil stress strain curves. As I stated in my paper, as many as three different sets of soil values may exist within pressure limits of 1 to 10 psi. It is improper to fair one straight line through the points within the entire pressure range. The ground pressure of the vehicle which will operate across the soil determines which set of soil values to use. If this procedure is followed, good results can be obtained consistently in predicting vehicle performance.

F. L. UFFELMANN. — 1) As a static problem on the towed wheel there appears to be no justification for the calculation of an « R_H » component of rolling resistance (due to horizontal stress components over the area of contact of the rim) the total rolling resistance being estimated in the « R_v » component (due to the vertical stress distribution on the rim).

2) The R_v component is evaluated as a torque resistant $\frac{1}{2} R_v D$ opposing W.f where f, the horizontal action distance, has been calculated from the assumed vertical stress distribution on the rim given by the Bekker sinkage-stress relationship. The use of a true vertical action distance (g) instead of $\frac{1}{2}$ D would have increased the numerical value of this term.

3) For the estimate of R_H the horizontal elemental stress is stated to be the (vertical elemental stress) · tan α where α is the angle of sinkage of the element. There appears to be no justification for this assumption (and which indeed means an infinite horizontal stress at $\alpha = 90°$) particularly as the tangential rim stresses have been neglected and the resultant elemental stresses cannot all be normal to the rim. A more reasonable assumption for the calculation would have been to assume a radial pressure distribution as measured by Prof. Vincent in paper No. 46 when the separate resultant force components and their action distances (g and f) could be estimated without the erroneous tan α assumption.

4) Additional odd errors have occurred in the calculations, the most noticeable being the expression for tan α on page 743. This error however has been rectified in equation 8.

5) In view of the above indicated miscalculations it is difficult to believe the close agreement with experiment using this «refined» rolling resistance formula, reported by Mr. Harrison in paper No. 40.

F. FAUSTI. — Mr. Janosi prende in considerazione la resistenza al rotolamento di due pneumatici della misura 11.00 - 25, uno di tipo convenzionale, l'altro radiale: dai diagrammi pubblicati nella relazione risulta che essi avrebbero all'incirca le stesse caratteristiche di resistenza al rotolamento. Non vogliamo discutere il metodo di prova usato da Mr. Janosi; peraltro dobbiamo sottolineare che nelle ormai numerose prove condotte in tutto il mondo dai principali Centri di ricerca per l'Agricoltura, la resistenza al rotolamento delle coperture cinturate, od in genere delle radiali, è stata trovata costantemente inferiore a quella delle coperture convenzionali nella misura del 10 - 20 %. Voglio qui citare solamente le prove condotte dal National Institute of Agricultural Engineering di Silsoe, England.

Restiamo a disposizione degli interessati per ulteriori informazioni.

Z. JANOSI. — I cannot say too much about this. I can only say that we carried out those tests, and we measured those resistance values and we plotted them. I think that a radial ply tire should have higher motion resistance than a conventional one at low inflation pressures, because it deflects more and the hysteresis losses are greater. But, of course, we recognize that it has great advantages if it is used as a driven wheel, which outweighs the little disadvantage of having somewhat higher rolling resistance. The net drawbar pull is still much greater than that of conventional tires.

N. 46

Evaluation and selection of optimum vehicle types under random terrain conditions *)

Valutazione e scelta del tipo di veicolo « optimum » in base alle differenti condizioni del terreno

M. G. Bekker **)

ABSTRACT. — *Cross country vehicles operate in random terrain-climate environment. Therefore predictions of performances, evaluation of design concepts, and selection of optimum vehicle types can be performed only statistically, in terms of probabilities.*

To achieve this goal with customary empirical methods has been impossible. However, the latest developments in the mechanics of land locomotion based on physical soil measurements and on mathematical models of soil-vehicle relationship make a solution of this problem entirely feasible.

A method leading to that solution is expounded and illustrated by means of practical examples, such as a selection of an optimum agricultural tractor either of crawler or wheel type. –

Introduction. — Evaluation and selection of an optimum vehicle type which is expected to operate in an unchanging environment has been a relatively simple problem. A small number of experiments usually leads to the optimization of design and performance features; with sufficiently advanced experience most of the testing may be eliminated, enabling the evaluator to make an outright decision on the basis of previously accumulated data. Such has been the case of railroad and highway vehicles.

In off-the-road locomotion, however, where « roads » change in a random way, depending on geography, geology and climate, the problem becomes enormously complex. Its solution is unattainable within the present purely empirical techniques since no one can test all the possible vehicles choices, in all the possible terrain conditions under consideration.

Hence, the present proving ground testing and evaluation techniques can not produce results which would generally answer, for instance, the question of « track versus wheel ». They must also preclude answers to many other important questions such as an optimization of large arrays of vehicular configurations that are either theoretically possible on the drafting board or practically available on the market.

---

*) This paper was partially prepared during the Author's association with Land Locomotion Laboratory, U. S. Army Ordnance Tank Automotive Command, Detroit.

**) General Motors Corporation, Defense Systems Division, Land Mobility Laboratory.

The failure of present techniques to provide a basis for the quantitative prediction of the optimum of performance and design in a random terrain has been caused by the persistent seeking for deterministic fixed values where the answer can only be produced in statistical values. In addition, the selection of test sites has invariably ignored quantitative sampling techniques which would give the evaluator a truly representative probability density function of soil changes that affect locomotion under given geographical and climatic conditions.

The most pointed examples of such a state of affairs are the internationally adhered to Tractor Test Codes which call for testing vehicles only on two hard surface courses, one of which is made of concrete slabs[1].

Tractors developed on that basis have been produced and sold in all parts of the globe, although many realize that this completely ignores the existing differences in soil types, and the climate. Only in a qualitative manner has the fact been recognized that a vehicle which may achieve a certain level of performance with a satisfactory frequency in one terrain will perform in a different way on another.

This may have been tolerated as long as everybody was starting from the same premise encompassed by the purely empirical school of thought. However, with the development of land locomotion mechanics and new methods of a quantitative determination of soft ground performance[2-3-4-5-6-7-8-9] a need for a statistical adaptation of vehicles to the changing environment of operations is becoming more and more recognized. For that is expected to produce not only further progress through a more rational competitive effort which today is mainly wasted in marginal and accessory improvements, but also considerable savings in national economies.

The so-called underdeveloped countries would be particularly interested in this approach for obvious reasons. Their example may eventually accelerate progress even in those areas where less economic vehicles developed on the basis of present day empirics can still be afforded.

The whole concept is not new. Identical problems exist in other fields of engineering whenever a random process is involved. The widespread use of statistical methods in these fields has made it certain that similar methods must be and will be introduced sooner or later in the field of off-the-road locomotion. Work performed by the present writer has aimed in that direction since the end of World Was II[9].

However, the design and performance evaluation could not have been carried in terms of terrain probability density functions as long as mathematical models of soil-vehicle relationship were not established. An effort by the writer in the systematization of various attempts made with that respect[9] had resulted in the formulation of the methodology[9-10], which in turn has demonstrated that the only missing link in a comprehensive treatment of the problem was the lack of a generalized physical system of soil values. The subsequent development of such a system[9-11] by the Author, and its practicability shown in a solution of a variety of mobility questions[4-9-12] suggest that

the time may be ripe to discuss the problem with reference to soil-vehicle systems under random terrain conditions.

The implications of such an approach cannot be underestimated; for a manufacturer who can predict performance-design parameters with greater accuracy and thus can produce a better vehicle capable of operating in the

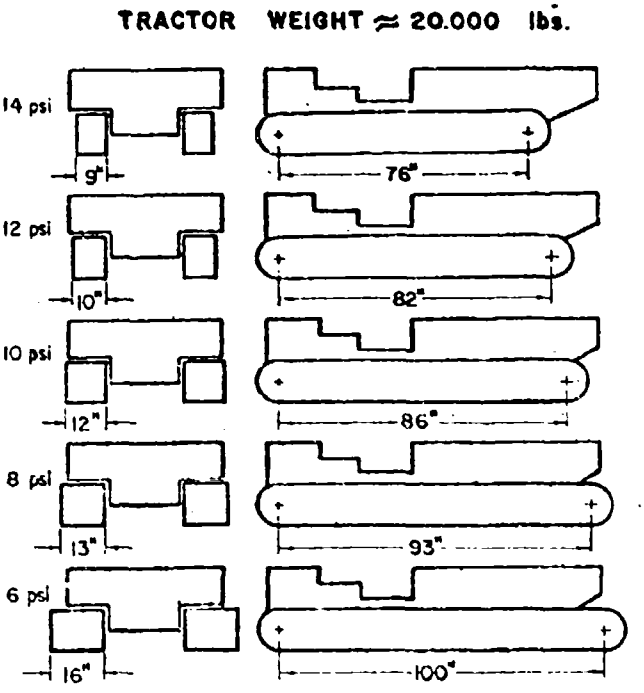


Fig. 1. — All values are given in round numbers.

given area at a guaranteed level of performance with, say, 75 % probability will force out of the market a less advanced competitor capable of operating even at the same level with, say, 50 % probability.

As the statistical method used in this paper has been exhaustively treated in a variety of text-books [2-5], it will not be described here. Instead its application to a hypothetical, but plausibly practical case, will be presented in a detail which may be considered useful to demonstrate the argument.

An example of a family of tracked vehicles to be evaluated. — Assume that there are on the market five tracked tractors as shown in figure 1. All weigh the same (20,000 lbs) and have, for practical purposes, the same engines and transmissions. However, they differ in the size of the running gear. As a result they exercise a ground pressure varying from 14 psi maximum to 6 psi minimum. The most compact tractor (14 psi) is the cheapest, the least

compact (6 psi) is the most expensive. The user wants to determine if he should buy a 14, 12, 10, 8, or 6 psi tractor. Tests performed in accordance with accepted Tractor Test Codes on hard surface have not shown significant differences or consistent merit trends.

Terrain moisture function and the probability distribution of terrain values. — To evaluate such a trend, soft ground performance must be determined. This, however, could hardly be done without a generalized terrain

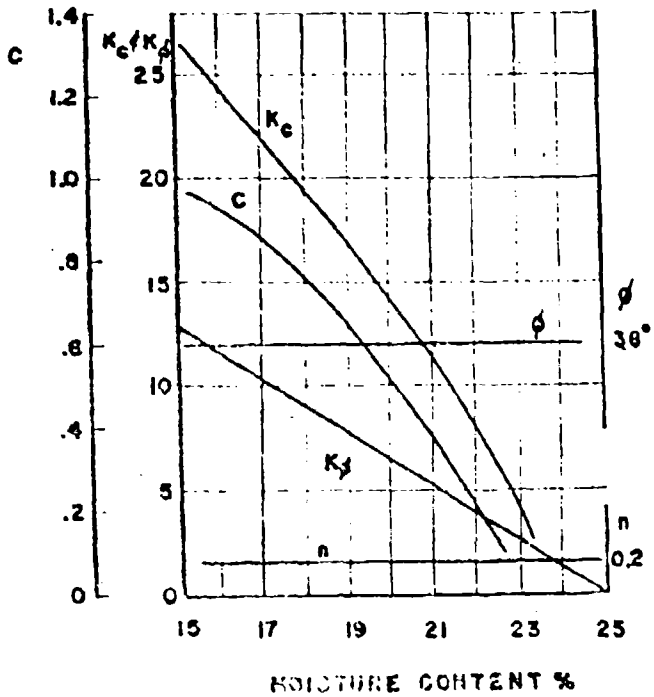


Fig. 2.

characteristic which would consider random variation of stress-strain relationships of soil in the considered area, due to weather cycles.

It has been shown in references [1,2,3] that, for practical purposes, maximum shearing stresses which the ground can withstand are definable in terms of ground pressure p, friction Φ and cohesion c. Stresses due to sinkage may be defined in terms of moduli of deformation k_c, k_ϕ and the exponent of deformation n [4,5,11].

Work performed for the Land Locomotion Laboratory, OTAC *), notably that by Hegelus [9] and Trask, Skjei and Kiehn [10,12] has indicated further

*) OTAC is the abbreviation of the Ordnance Tank Automotive Command, Detroit, Michigan.

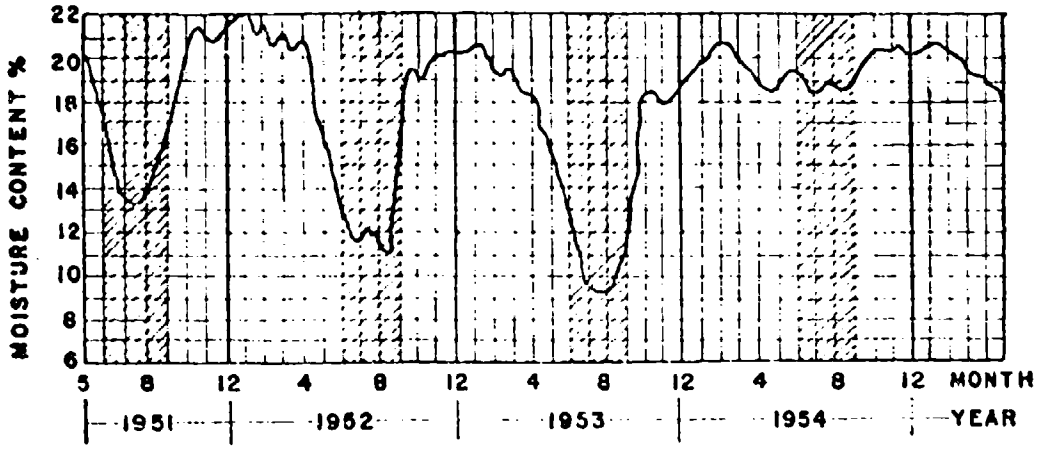


Fig. 3.

that each set of c, Φ, k_γ, k_ϕ n-values required to define the given stress-strain relationship can be empirically correlated with the corresponding moisture content M_c of the given soil. Thus, conversely when knowing the variation of M_c within the given area and the considered weather cycle, it is possible to define the variation of soil values from the predetermined $\Phi(M_c)$, $c(M_c)$, $k_\phi(M_c)$, $k_\gamma(M_c)$ and $n(M_c)$ functions. An example of these empirical functions found in typical homogeneous sandy loam is shown in figure 2.

The variation of M_c with time over the considered soil type and weather cycle will be called Terrain Moisture Function $M_c(t)$. That function implicitly defines temporal variation of Φ, c, k_γ, k_ϕ, n-values within the given area.

Assuming M_c as a random variable changing with t the probability of not exceeding the given moisture content M'_c and hence the given soil consistency defined by the corresponding c, Φ, k_γ, k_ϕ, n set of values may be defined according to standard practice[12,13]:

$$\text{Prob}\left\{0 < M_c(t) < M'_c\right\} = F_t(M'_c) = \int_0^{M'_c} f_t(M_c)\,dM_c$$

where $f_t(M_c)$ is the probability density function.

Terrain variation for average moisture contents measured between 1 to 2 feet of depth, only which is significant in locomotion problems[7], is shown in figure 3. The data have been reproduced from measurements performed for over 4 years in a Middlesex area by the Road Research Laboratories in Hammondsworth, England[18].

Frequencies of moisture content percentages assembled from graph, figure 3, are shown in table 1. The standard deviation of their distribution is $\delta = 1.63$, and the mean value $\bar{M}_c = 19.5$. A check of the data will show that the considered probability density may be assumed for the sake of the argu-

ment, at least in this presentation, as a function having the normal distribution of variable M_c, and is:

$$f_t(M_c) = [1/\delta(t) \sqrt{2\pi}] \exp [-(M_c - \overline{M}_c)^2 / 2\delta(t)]$$

Distribution curve based on this equation has been plotted on the moisture content histogram in figure 4. The probability density curve is shown in figure 5.

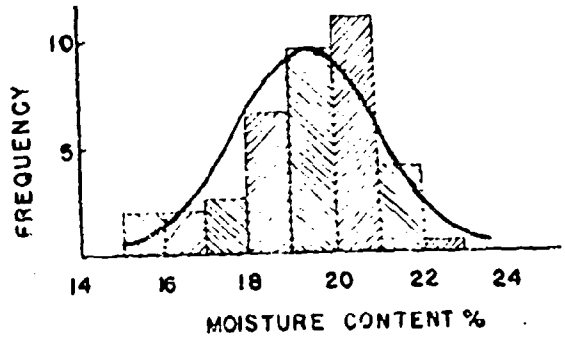


Fig. 4.

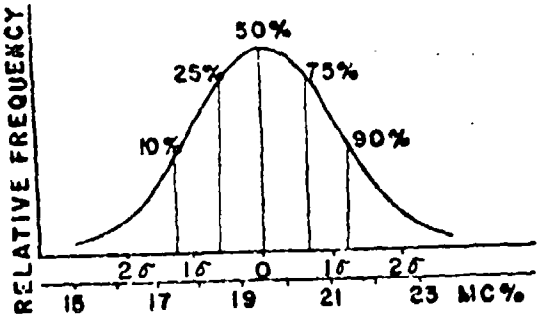


Fig. 5.

TABLE 1.

Interv.	Mid. Value	Frequency n.
15-16	15.50	2.0
16-17	16.50	2.0
17-18	17.50	2.5
18-19	18.50	6.5
19-20	19.50	9.5
20-21	20.50	11.0
21-22	21.50	4.0
22-23	22.50	0.5
		38.0

Table I was plotted under assumption that low moisture contents, below 15 %, produce hard surfaced soil and do not affect performance. Thus in the weather cycle of one year, measurements taken between 1 June and 1 September have been eliminated. When taking a complete one year cycle a skewed distribution would be obtained.

To perform specific computations for the considered tractors it will be assumed that Terrain Moisture Function, figure 3 refers to $c\,(M_c)$, $\Phi\,(M_c)$, $k_c\,(M_c)$, $k_\phi\,(M_c)$ and $n\,(M_c)$ functions as shown in figure 2. This enables one to calculate performance and design parameters provided that mathematical models of relationship between soils values c, Φ, k_c, k_ϕ, n and pertinent vehicles values are available. Values c, k_c, k_ϕ and n are monotone decreasing functions of M_c.

Mathematical models of soil-vehicle relationship. — Many such models have been made recently available, and enable one prediction with an acceptable degree of accuracy [2,3,4,5,6,7]. Since it would be impossible to discuss here a larger number of performance types as a function of a large set of design variants, even within one soil spectrum, only the thrust/weight ratio (τ/p) of the vehicle as function of its ground pressure (p) will be discussed. The reader will realize that in a similar manner all other performance types such as fuel consumption, cargo carrying capacity, slope climbing, accelleration, etc., may be determined [8,9,10].

It has been shown in reference [4] that

$$\tau/p = (c/p) + \tan\Phi - (p)^{1/n}/\left[1\,(n+1)\,(k_c/b + k_\phi)^{1/n}\right] \qquad (1)$$

where l is the lenght and b is the width of the track contact area, figure 1. In order to present equation 1 in a more convenient form one may note that the morphological relation between track dimensions and ground pressure as shown in figure 1 may be expressed by the equation: $l/b = 3p^{0.69}$. In addition, when further considering, for the sake of simplicity, a uniform load distribution one may write: $p = (W/2)/lb$, where W is vehicle weight. Substitution of the last two equations in equation 1 will yield:

$$\tau/p = (c/p) + \tan\Phi - p^{(1+0.309n)/n}/$$

$$\left\{1.7\,(n+1)\,\sqrt{W/2}\,\left[1.7\,k_c\,p^{0.69n}/\sqrt{W/2} + k_\phi\right]^{1/n}\right\} \qquad (2)$$

Equation 2 represents here the relationship between ratio τ/p expressed as a function of random soil values Φ, c, Φ, k_c, k_ϕ, n, and fixed in the given design vehicle values p and W. τ/p ratio also is a monotone increasing function of Φ, c, k_c, k_ϕ, and n.

Probability of operating on the desired level of thrust/weight ratio. — Assume that a farmer wants to select one of the tractors shown in figure 1, to operate in terrain described by graphs reproduced in figures 2 and 3. He also realizes that there are a few slopes on his farm which never exceed,

however, $\tau/p = 0.2$. In addition, he wants the tractor to pull implement with $\tau/p = 0.5$; hence the total level of performance with which the operation is intended amounts to $\tau_t p = 0.2 + 0.5 = 0.7$. To choose a tractor the farmer wants to know the probability with which each vehicle can achieve that level of performance. Knowing this and the cost involved he will be able to make his decision.

To this end curves of $\tau_t p$ versus p must be traced, for various probabilities of success. Take first the probability of 50 % that a certain moisture content M_c will not be exceeded in the considered area. By definition [12-13], such a moisture is $\overline{M}_c = 19.5$ % (figure 5). It produces soil values of the following approximate magnitude (figure 2):

$$c = 0.55; \quad \Phi = 38°; \quad k_c = 16; \quad k_\phi = 7; \quad n = 0.2$$

If these soil values and tractor values (by tractor values we understand dimensions and weights as shown in figure 1) are fed in equation 2, thrust τ/p will be expressed by the formula:

$$\tau/p = (0.55/p) + \tan 38° - p(1 + 0.55 \times 0.2)/0.2 \left\{ 1.7\,(1 + 0.2) \right\} \overline{20000/2} \times$$

$$\left\{ 1.7 \times 16\, p^{0.6/5} / \left\{ \overline{20000/2} + 7 \right\}^{1/0.2} \right\} \qquad (3)$$

Since by definition $\overline{M}_c = 19.5$ % is the moisture content that will not be exceeded with probability of 50 %, the considered set of soil values defines a «weakest» type of soil which may be not exceeded with the same probability. Hence, equation 3 defines the lowest value of thrust/weight ratio τ/p that may be encountered with 50 % probability in the considered area and the weather cycle. When changing p as a variable in equation 3, curve II shown in figure 6 will be obtained. This curve gives the relation between unit draw-bar pull and ground pressure that will occur with 50 % probability.

In a similar manner, a curve for the probability say, of 75 % will be obtained. To this effect the moisture content M_c which may not be exceeded with that probability has to be determined with the help of tables of normal distribution available in literature [12-13]. It will be found in such tables that for P = 75 %, the M_c-$\overline{M}_c$ / σ value equals approximately 0.68, and hence, according to previous denotations:

$$(M_c - 19.5)/1.63 = 0.68$$

or, $M_c = 20.6$ % (figure 5). If for this moisture content corresponding c, Φ, k_c, k_ϕ, n-values are selected from figure 2 and fed in equation 2, the 75 % probability curve III or $\tau_t p$ vs p will be obtained. Following a similar course of action curves of 90 % and 25 % may be constructed as plotted in figure 6, and denoted by I and IV.

Figure 6 provides the answer as to what tractor should be selected. From the location of the line corresponding to $\tau/p = 0.7$, results that the above level of performance required by the farmer may be achieved with the following ground pressures and related probabilities:

Probability %	**25**	**50**	**75**	**90**
Approx ground pressure of the tractor (psi) necessary to obtain $\tau/p = 0.7$	17	14	13	8.5

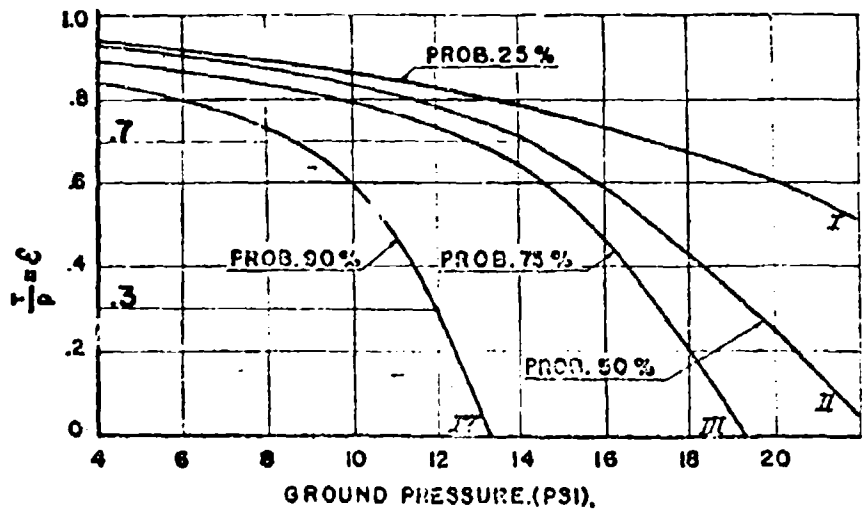


Fig. 6.

Thus if the farmer has enough money to buy an expensive tractor in order to work at the at the discussed level with 90 % probability he will buy the 8 psi vehicle (figure 1). He will definitely discard the need for the most expensive 6 psi tractor. He also may be tempted to buy a cheaper 12 psi equipment as he would loose relatively little of his 90 % chance to operate it at $\tau/p = 0.7$, since he would be operating above the 75 % probability of success producible by the 13 psi of ground pressure (figure 6).

Graph figure 6 replotted as shown in figure 7 will show that the reduction of ground pressure between 6 and 14 psi does not affect very much the probability of achieving given performance levels up to say, $\tau/p = 0.4$. Proper selection of ground pressure, however, is all important for higher thrust/load ratios.

Figure 7 also shows that there is a point of diminishing returns where little gain may be expected when selecting expensive low ground pressure vehicles instead of the cheaper standard equipment with higher ground

pressure. This applies to both tracks *and* wheels as it will be shown later. The random variation of soil types and moisture distributions makes thus the statistical study of design and performance imperative, if more rational and more economic vehicles are to be developed and used.

Track versus wheel problems. — To illustrate further the usefulness of the method presented in this paper the problem of a wheel will be discussed.

It was shown [1] that the drawbar weight ratio (DP/W) of a rigid wheel may be expressed by equation:

$$(DP/W) = (cA/W) + \tan\Phi - \left\{ [3W/(b\sqrt{D})]/(3-n) \right\}^{(2n+2)/(2n+1)} \times 1/W\,(n+1)\,(k_c + bk_\phi)^{1/(2n+1)} \qquad (4)$$

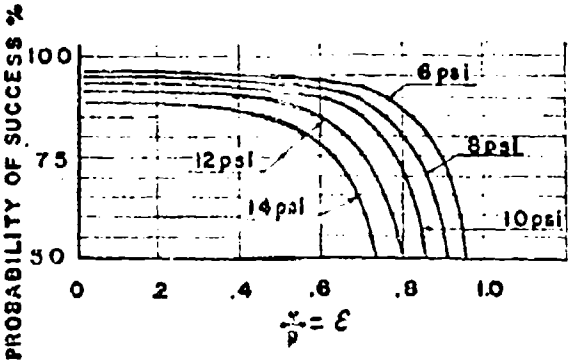


Fig. 7.

In equation 4, W is wheel load (lb), A is the ground contact area (sq in) and D wheel diameter (in). Value cA/W is very small in a case of practically every wheel and may be neglected. Thus equation 4 may be transformed as follows:

$$(DP/W) = \tan\Phi - [3/(3-n)]D]^{(2n+2)/(2n+1)}\ [W/(k_c + bk_\phi)]^{1/(2n+1)} \times 1/(n+1) \qquad (5)$$

Assume that D = 40 in, and b = 11 in. By feeding in equation 5 the above data and the soil data corresponding to 25, 50, 75 and 90 % of probability, and changing W, in the same manner in which that was done when changing p in equation 2, a family of curves of DP/W versus W, shown in figure 8 will be obtained.

Figure 8 gives the wheel load required to achieve the desired pull/weight ratio with the given probability of success. Again it will be seen that for low loads there is not much difference between the performances at various

probabilities. For higher axle loads, however, the DP/W drops rapidly and the probality of achieving the given performance rapidly decreases.

With the help of graph figure 8 one may compare the relative merits of tracks and wheels. Assume that there also is available a wheeled tractor, in addition to the tracked tractors sketched on figure 1. It has four wheels of D = 40 inches and b = 11 inches, each loaded with W = 5000 lb.; it thus weighs 20000, i.e. the same as the previously discussed vehicles.

The first conclusion which may be reached by means of graph figure 8 is that such a tractor could operate at DP/W = 0.7 with practically zero

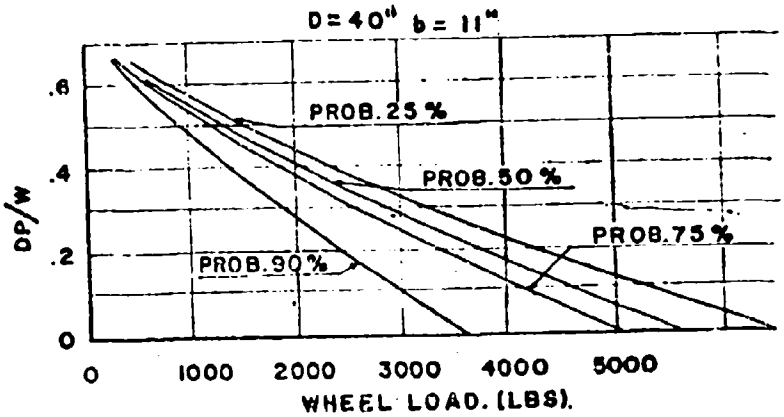


Fig. 8.

probability. Hence it would not satisfy the previously desired level of performance. To achieve that level it would have to have wheels loaded to less than 1000 lb i.e., would have to be equipped at least with 20 wheels of the assumed dimensions, which is absurd. Hence, under the assumed conditions the wheel cannot replace the track.

One may also wish, to compare the tracks and the discussed wheel on the basis of the probability of « go no go », i.e., for r/p = DP/W = 0. From graphs figures 6 and 8 the following table can be readily written.

Probability of « go » %	90	75	50	25
Required min. track ground pressure (psi)	13.2	19.2	23	Very large
Permissible max. wheel load	3600	5000	5500	(550)
Required No. of wheels for W = 20,000	5.5	4	3.6	3

The considered wheeled vehicle would be made more attractive if the wheel diameter is increased. To investigate the new relationship between DP/W and D, as well as the probabilities involved, graph shown in figure 9 may be computed using equation 5. In this procedure D is the variable and

W was assumed constant and equal to 5000 lb per wheel. The computation was performed in the same manner as that previously described.

Select D = 65 in, b = 11 in. This will produce DP/W = 0.3 at 90 % probability as shown in figure 9. If the performance requirement of the tracked tractors is reduced to $\tau/p = 0.3$, it will be seen (figure 6) that the

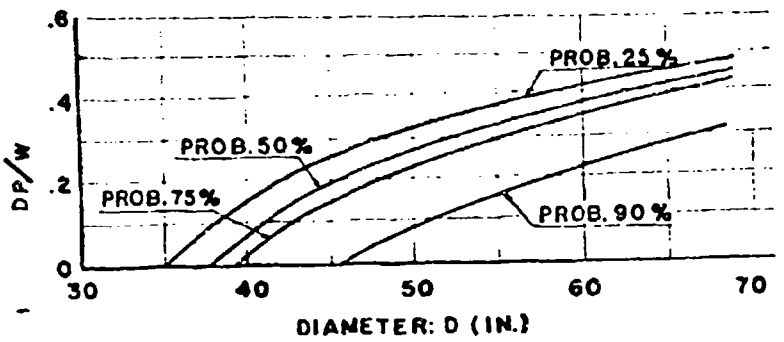


Fig. 9.

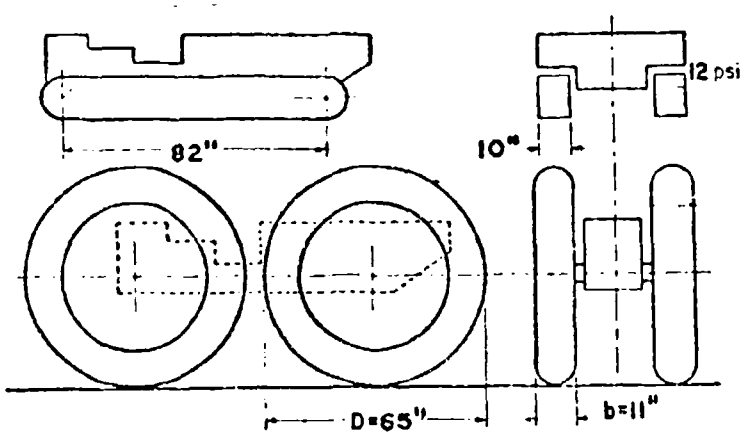


Fig. 10.

12 psi tractor will produce that very performance with the same probability. On that basis one may say that the 12 psi tractor (figure 1) and the 4 wheel tractor having D = 65 in, b = 11 in (figure 10) are equivalent in the soil described on figures 1 and 2, assuming performance level $\tau/p = 0.3$. To present a general picture of the relative forms and sizes of both tractors their outlines have been sketched in figure 10. This sketch casts again doubts, as to the practicability of replacing the tracker tractor with a wheeled one even if only $\tau/p = 0.3$ is expected to be achieved in the considered area with 90 % probability.

These examples illustrate the solution of track versus wheel problems from a soil-vehicle viewpoint. As may be seen, then, predictions of performance and design parameters can be made in quite a rigorous way. However, they can never be expressed in terms other than probabilities. There are no fixed values in off-the-road locomotion. There is only chance.

Conclusions and remarks. — To increase the accuracy and reliability of discussed predictions, and the safety of choices made, mathematical models of soil-vehicle relationship such as shown in equations 1, 2, and 4 ought to be further refined. As the writer attempted to show [1-2-3-4-5-6], and as it results from works by others [21-22-23-24-25], the above is entirely feasible within the concepts of applied mechanics; it is only a matter of a sufficiently large research effort before such a task will be accomplished.

Methods of prediction of soil moisture have been worked out with a surprising accuracy [26]. What remains then to be done is to determine, in the field and/or in the laboratory, statistical relations of $c \cdot (M_c)$, $\phi(M_\phi)$, $k_c(M_c)$, $k_\phi(M_\phi)$ and $n(M_n)$ types as shown on figure 2. This in turn appears to be a rather straightforward work which has already been started when measuring soil values [4-5-19].

One may thus conclude that it is only a matter of time to fully develop the discussed methods and to enable one to evaluate and select optimum vehicle types under random terrain conditions.

This would constitute a conscious effort of man to develop and adapt the vehicle to the terrain in the same manner in which natural selection of evolutionary forces has adapted animal locomotion to their environment [27].

ACKNOWLEDGMENT. — This work has been completed during the author's association with the Land Locomotion Laboratory of the U.S. Army Ordnance Tank Automotive Command and has been published by permission of the Command.

BIBLIOGRAPHY

1) Hurlbut L. W., Larson L. E., Steinbrueggе G. W. and Sulek J. J. The nebraska tractor tests. Agricultural Engineering, vol. 41, No. 4, April 1960.

2) Bekker M. G. Latest developments in off-the-road locomotion. Journal of the Franklin Institute, vol. 263, No. 5, May 1957.

3) Bekker M. G. Mechanics of vehicle mobility in off-the-road locomotion. Applied Mechanics Reviews, vol. 11, No. 8, August 1958.

4) Bekker M. G. Off-the road locomotion - Research and development in terramechanics, 272 pp. The University of Michigan Press, Ann Arbor, Michigan, 1960.

5) Bekker M. G. Theory of land locomotion - Mechanics of vehicle mobility, 497 pp. University of Michigan Press, Ann Arbor, Michigan, 1956.

6) Collective Work. Research Report No. 5. Land Locomotion Laboratory, OTAC, Detroit, Michigan, December 1958.

7) Bekker M. G. Mobility of cross country vehicles. - Thrust for propulsion - Flotation and motion resistance - Track and wheel evaluation - Optimum performance and future trend. Series of articles in Machine Design, Penton Publishing Co. Cleveland, Ohio, December 24, 1959; January 7, 1960; January 21, 1960 and February 4, 1960.

8) Janosi Z. Soil values in land locomotion. Journal of Agricultural Engineering Research. The British Society for Research in Agricultural Engineering, vol. 5, No. 1, 1960.

9) Bekker M. G. An introduction to research on vehicle mobility. Canadian Dept. of Natl. Defense 1946, Ottawa, Ontario. Second Printing, Aberdeen P. G., 1953, Aberdeen Md. Third Printing Land Locomotion Research Branch, OTAC, Detroit, Michigan, 1958.

10) Bekker M. G. Methods of evaluation of off-the-road locomotion. Report No. 274, Operations Research Office, Johns Hopkins University, Chevy Chase, Maryland, August 17, 1953.

11) Bekker M. G. A system of physical and geometrical soil values for the determination of vehicle performance and soil trafficability. Proc. Interservice Symposium, Stevens Institute of Technology - Duke University. Office of Ordnance Research and Land Locomotion Research Branch, OTAC, Detroit, Michigan, 1955.

12) Mode E. B. Elements of statistics. Prentice Hall, New York, 1953.

13) Bowker A. H. and Lieberman G. J. Engineering statistics. Prentice Hall, Englewood Cliffs, New Jersey, 1959.

14) Hegedus E. Effect of water content on bevameter values of soil. Land Locomotion Laboratory, OTAC, Report No. 27 (working paper), February 1958.

15) Trask P. D. and Skjei R. E. Pressure - Sinkage tests on mixtures of montmorillonite and elastic silt. Waves Research Laboratory, University of California, Ser. 116, Issue 3, Berkeley, California, July 1958.

16) Trask P. D. and Klehn H. jr. Pressure sinkage tests on mixtures of kaolin and illbite with elastic silt. Waves Research Laboratory University of California, Ser. 116, Issue 4, Berkeley 4, California, September 1958.

17) Trask P. D. and Klehn H. jr. Pressure - Sinkage tests on mixtures of clay with sand of varying grain size. Waves Research Laboratory, University of California, Ser. 116, Issue 5, Berkeley, California, January, 1959.

18) Field studies of the movement of soil moisture. Road Research Lab. Dept. of Scientific and Industrial Research. Tech. Paper No. 44, London, 1958.

19) Bekker M. G. Operational definitions of mechanical mobility of motor vehicles. Land Locomotion Research Branch, OTAC, Report No. 40, Detroit, Michigan, 1958.

20) Carlson C. A. and Horton J. S. Information of predicting moisture in the surface foot of various soils. Tech. Memo No. 3-331, Reports 1 and 5, Corps of Engineers, Vicksburg, Mississippi, 1957 and 1959.

21) Soehne W. Das mechanische verhalten des ackerbodens bei belastungen unter rollenden radern sowie bei der bodenbearbeitung. Grdl. d. Landtechn. Heft 1, 1951.

22) Swieznwski T. Toczenie Kola. Czasopismo Techniczne, Nos. 2-6, Lwow, 1932.

23) Ageikin Ya S. Opredelenie deformatsii i parametrov kontakta shiny s myagkim gruntom. Avtom. tract. Prom No. 5, 1959.

24) Chajoux E. Pneumatiques pour vehicules Sahariens. Ingenieurs de l'Automobile, vol. XXXII, No. 11, 1959.

25) Garbari F. Resistenza al movimento dei veicoli a ruote su terreno cedevole. ATA Rendic. Congr. 9-11, Roma, 1950.

26) Bekker M. G. Relationship between soil and a vehicle. SAE Transactions, 1950.

27) Bekker M. G. Mechanica de vehiculos en locomotion fuera del camino. Ciencia y Technica, vol. 126, No. 632, Buenos Aires, 1958.

28) Bekker M. G. Performance improvement in track type tractors. Agricultural Engineering, vol. 39, No. 10, 1958.

29) Bekker M. G. Evolution of animal and man-made locomotion. ASME Annual Meeting, New York, New York, December 1960.

30) Bekker M. G. Ueber die Wechselbeziehung Zwischen Fahrzeug und Boden bei Gelandefahrt. Automobiltechnische Zeitschrift., vol. 62, No. 7, July 1960.

DISCUSSIONS

F. L. UFFELMANN. — The probability functions used in this paper have been evaluated on a time basis and give the probability of success of a particular vehicle to cross uniform ground described by parameters which vary only with time. Surely the user, in addition, requires to know the probability on a distance basis, the probability of crossing one yard of ground having random variation of parameters with distance being higher than that required to cross one mile of the same ground.

The total probability of crossing a particular distance at a particular time would be the product of the two relevant probabilities.

M. G. BEKKER. — The probability functions used in this paper have been evaluated with reference to time over the surface of the assumed sample area. They thus encompass an area-time continuum. I used only one line to denote moisture change in order not to complicate the issue. One should use a band which would denote the minimum acceptable and the maximum desirable probability of ground surface distribution of the moisture in the sampled area. This is the problem of sampling, statistical inferences, and two-dimensional probability.

If you are interested in a « directional » probability function along a certain path, one yard or one mile long, then the samples should be taken along representative narrow strips instead of over a wide area.

Land Locomotion Laboratory, in cooperation with Professor Jehe of the University of Michigan, has started working on these problems almost two years ago when I was still associated with that group. I understand they have made some progress, and suggest that you contact them.

S. J. KNIGHT and M. P. MEYER. *(Received by letter after the closure of the Conference).* — Mr. Bekker has shown the feasibility of selecting an optimum-type vehicle for operation under random terrain conditions. By making use of the hypothetical probability of occurrence of the soil values Φ, c, k_c, k_ϕ, and n in a given area and the relations of the vehicle parameters W, p, l, b, and D to the soil values named, he demonstrates a method for estimating drawbar pull ability, the most important characteristic of an off-road vehicle, to illustrate his point. The examples used are clear-cut and straightforward. The selection of a family of tractors with dimensions that yield a specific relation of l, b, and p serves to simplify the illustration. The Author concludes that « it is only a matter of time to fully develop the discussed method and to enable one to evaluate and select optimum vehicle types under random terrain conditions ».

Though one may accept, for the sake of argument, the validity and accuracy of the vehicle-soil model suggested, one cannot but question the practicability of defining soils on a world-wide basis in terms of Φ, c, k_c, k_ϕ, and n. Anyone familiar with the vagaries of natural soils and the time and patience required to establish these soil values for even one soil condition is bound to be overwhelmed by the prospect of setting out to classify the soils of the world in these terms. Goodman and Lee, in their paper « Effects of Remolding on Soil Values Related to Vehicle Mobility » (paper No. 4), produce data which show extremely wide variation of

k_c, k_ϕ, and n in a natural clay. They further declare that, « Experimental data to date show a marked reduction in the spread of cohesive and frictional moduli of soil deformation from remolding », and suggest that « in predicting vehicle performance in a given location, the soil values must be determined for the soil in the most critical condition expected from traffic type and amount ». The Author makes no mention that the soil values in his model should represent this condition.

Mr. Bekker states that prediction of vehicle performance, selection of optimum vehicle types, etc., are impossible by customary empirical methods. However, the U. S. Army Engineer Waterways Experiment Station has had for many years an admittedly empirical method for accomplishing the same objectives. The method as it applies to fine-grained soils is implicit in papers 24 and 35, « Measurement and Estimation of the Trafficability of Fine-Grained Soils » and « Soil Trafficability Classification Scheme », respectively. An example of the Waterways Experiment Station method follows.

Example

Assumptions. — *Vehicles.* - Assume the same family of tractors as in Mr. Bekker's paper plus one tractor at W = 20,000 lb, p = 5 psi, and b = 18 in., and one tractor at W = 20,000 lb, p = 16 psi, and b = 8 in. Assume all tractors to have track grousers less than 1-½ in. high, 14 bogie wheels on the portion of the tracks in contact with the ground, track shoes 8 in. long, clearances of 14 in., engines with horsepower greater than 10 hp per ton of gross weight, and hydraulic transmissions.

Soil. - Assume the soil to be the USCS *) ML type in a low-topography area in a temperate climate and under average wet-season condition.

Problem. — Determine capabilities of the given tractors on the given soil conditions (in any area in a temperate climate) in probability terms.

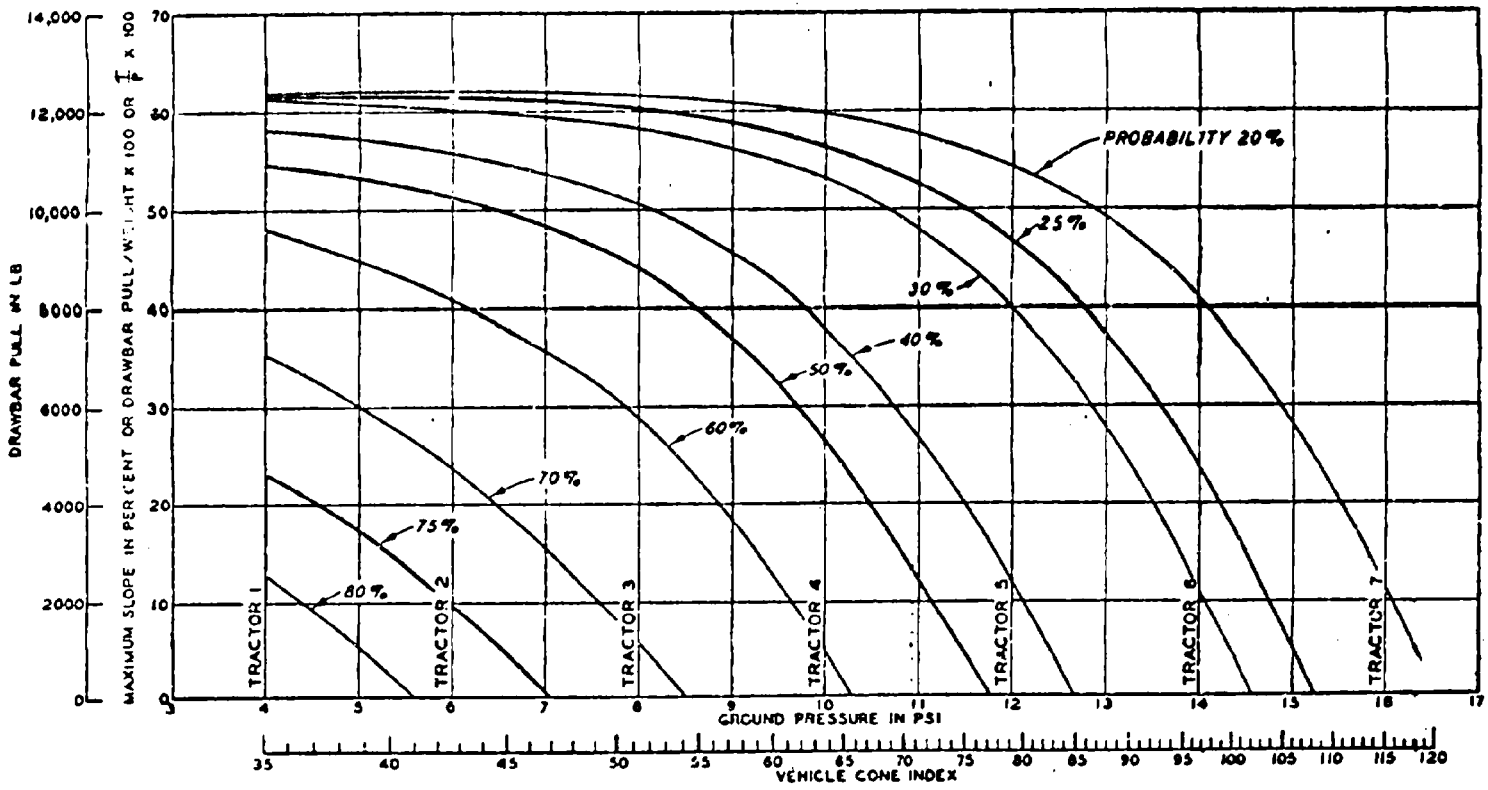
Solution. — Determine vehicle cone index (VCI) for each tractor by using formula on page B1 and figure B1 of paper No. 24.

Establish relationship between ground pressure and VCI and indicate relationship as a double scale on abscissas of figure attached, as shown.

Refer to figure 3 of paper No. 36. Determine rating cone index (RCI) corresponding to 25 % probability (RCI = 108). This means that 108 RCI or greater will occur in about 25 % of all areas of the ML soil (in a temperate climate in a low-topography area and under wet-season conditions), or that a vehicle with a VCI of 108 with no tow load can operate (40 to 50 trips in the same path or severe maneuvers) successfully in 25 % of the level areas. Plot 108 at 0 drawbar pull, and indicate 25 % probability.

For next point on the 25 % probability line, determine the VCI a tractor must have to negotiate a 10 % slope (or develop a drawbar pull equal to 10 % of its own weight on level ground) with 25 % probability. Refer to center curve of figure 3 in paper No. 24. At 10 %, the corresponding RCI equals 4.5. Subtracting 4.5 from 108 = 103.5. Plot 103.5 at 10 % slope.

*) US Army Engineer Waterways Experiment Station Technical Memorandum No. 3-357, The Unified Soil Classification System, March 1953, Vicksburg, Mississippi.



Performance of 20,000 lb tractors on a low-topography USRC ML soil under wet-season conditions.

Continue, as described, to develop curves for any desired probability. VCI for 50 % probability is 77, for 75 % probability is 47, etc.

Use of solution. — The solution of this problem (see attached figure) can be used to answer the following-type questions: (Assume, as in Mr. Bekker's example, that the cost of tractors varies inversely with their ground pressures).

a) Which tractor must be selected to insure that at least 50 % of the level areas can be traversed? (Answer: Tractor No. 4. Probability for No. 5 is approximately 47 %).

b) Which tractor can negotiate 10 % slopes with no drawbar load and with 75 % probability? (Answer: Tractor No. 2).

c) Which tractor should be selected to negotiate at least 75 % of the level areas and also be able to operate on 30 % slopes with at least 50 % probability of success? (Answer: Tractor No. 2. Tractor No. 2 is the least expensive tractor which will satisfy the former requirement and it will also satisfy the latter).

d) What performance can be expected from tractor No. 3? (Answer: Tractor No. 3 will be able to trasverse approximately 71 % of the level areas, 68 % of the 10 % slopes, 64 % of the 20 % slopes, etc. It will be able to exert a drawbar pull of 12,000 lb in 25 % of the level areas, etc.).

e) What maximum drawbar pull can tractor No. 3 exert while climbing a 20 % slope, with 25 % probability? (Answer: Tractor No. 3 requires 51 RCI to propel itself on level ground. RCI greater than 108 will occur in 25 % of the areas. Therefore, RCI units = 108 — 51 = 57 are available as soil strength over and above that required for mere self-propulsion. This strenght can be utilized to develop drawbar pull or to climb slopes. To climb a 20 % slope will require 10 of the 57 RCI units. (This figure, 10, is the difference in VCI (on the abscissa) for any probability curve between 0 slope and 20 % slope or may be found at slope = 20 on the center curve in figure 3 of paper 24). With the remaining 47 RCI units (57 — 10) the tractor can develop a tow load equal to 57 % of its weight. This figure, 57 %, is obtained by reading the center curve of figure 3, paper No. 24, at + 47 RCI. The answer, therefore, is tractor No. 3 can tow 11,400 lb while climbing a 20 % slope, in 25 % of the areas.

Discussion of example. — While the example refers to a given set of tractors and a particular soil type, data and techniques are available to predict the performance of any existing vehicle or any vehicle still on the drawing board (provided it is not radically different from existing vehicles) on any fine-grained soil in a temperate climate under wet-season conditions and also high-moistare conditions (see paper No. 35 for definitions). Slightly different techniques (which are available) will permit a similar analysis for coarse-grained soils in any climate.

Also, while the example provided for random variation in the strength (RCI) of a given soil type, it would have been just as practicable to solve the problem for a given area with a known moisture regime, as Mr. Bekker did in his example.

Tropical soils and arctic soils are expected to respond to similar analysis; however, basic data relating soil strength and climate have not yet been accumulated.

It is pointed out that the Waterways Experiment Station analysis considers the remolded s[illegible] not merely the in-situ undisturbed soil. It is also emphasized that multiple passes (40 to 50 in the same path) are an inherent condition of the present analysis. It has been found empirically that the soild strength which will

permit 40 to 50 passes of a vehicle will also permit severe maneuvers of a vehicle, i.e., sharp turns, backing out and crossing its own tracks, etc. The analysis therefore is in terms of practical operation of tractors. A similar analysis also could have been made on the basis of one straight-line pass of the tractors.

Summary. — The figure attached is qualitatively similar to figure No. 6 in Mr. Bekker's paper. Quantitative comparisons cannot be made since different soil conditions were assumed.

Because the two solutions are qualitatively similar, it would seem reasonable to assume that there is merit in both of the methods used to obtain the solutions. If two empirical methods are available to accomplish the same purpose, how can one be judge superior to the other? In a final sense, the only means of doing this is to test both methods simultaneously under the same vehicle and soild conditions a sufficient number of times to establish which method is the more accurate.

Empirical or quasi-theoretical methods are frequently employed for expediency or because truly theoretical solutions are complex or not available. Such is the case today in the field of off-road locomotion of vehicles. However, an acute awareness of the importance of the problem is drawing more and more researchers into this field. It is hoped that the problem will be approached along fundamental lines, for it is clear that unless the interrelations between moving vehicles and the media upon which they move are more thoroughly understood, significant improvements, in vehicle mobility off the road probably will not be attained.

DISCUSSIONE SUGLI ASPETTI DEL MOVIMENTO SULLA SUPERFICIE DELLA LUNA

PANEL DISCUSSIONS ON LUNAR SOILS

N. 47

Some predictions as to the possible nature and behavior of the lunar soils

Qualche previsione sulla probabile natura e sul comportamento del suolo sulla luna

JOHN A. RYAN *)

ABSTRACT. — *The effects of the lunar environment in determining the nature and behavior of the lunar soil are considered. The environmental parameters discussed are vacuum, gravity, temperature, corpuscular and electromagnetic radiation, and meteorite impact. These parameters are discussed individually and some predictions are made as to their combined effect. Areas in which experimental data are needed are outlined with emphasis given to those data which can be obtained in terrestrial laboratories.*

It is found that the lunar soil should not cause serious locomotion problems and in fact the soil behavior may be such that the locomotion problems are, in general, comparable to or less severe than those posed by terrestrial soils.

Introduction. — A considerable amount of work has been done in an effort to improve our understanding of terrestrial soil behavior. With the advent of the space age and the distinct possibility of lunar and planetary occupation in the foreseeable future, it has become necessary for us to extend our interests to non-terrestrial soils. Of course, not until landings are made will it be possible to determine the nature and behavior of such soil with any high degree of certainty. However, only by obtaining as much information as possible prior to such landings may we be able to anticipate some of the problems that could arise.

The first manned landings will most likely be made on the moon and for this reason the present discussion will be confined to the moon. This discussion will consist of three parts: a brief description of the lunar surface environment, an outline of present ideas as to the characteristics of the lunar soil, and finally, consideration of the effects of the lunar environment on the soil behavior.

The lunar environment. — There are six lunar environmental factors that are of importance to this study.

1) The moon essentially has no atmosphere.

2) The lunar surface gravitational force is roughly one-sixth that at the terrestrial surface.

*) Missiles and Space Systems Engineering, Santa Monica Division, Douglas Aircraft Company, Inc.

3) The temperature changes at the lunar surface are more extreme than here on earth, the day to night temperature variation being roughly 270° C at the subsolar point.

4) The lunar surface is exposed to a greater solar electromagnetic flux in the ultraviolet and in certain sections of the infrared than is the earth's surface and at no frequency is the flux less than at the earth's surface.

5) The lunar surface is directly exposed to corpuscular radiation, both cosmic and solar.

6) The lunar surface is unprotected against the impact of meteorites.

Current ideas as to the nature of the lunar soil. — The two principal theories as to the origin of the lunar surface features are meteoritic impact [1], and defluidization and volcanic action [2]. The actual mechanism is probably some combination of the two. The composition of the lunar soil will depend upon which mechanism dominates. From meteoritic impact it would be expected that meteoritic debris along with disrupted surface material would be scattered over the lunar surface. Most meteorites are thought to be of cometary origin and their composition is unknown [3-6]. For the remainder, those of possible asteroidal origin, nickel-iron would be expected [7], but most of the material would consist of silicates such as olivine and pyroxene, and such non-silicates as troilite (FeS), cohenite (Fe_3C) and graphite [8-9]. The disrupted surface material could be composed of igneous rock fragments. From volcanic action it would be expected that, in addition to igneous rock, unconsolidated materials such as volcanic ash and dust would be present [2-10]. Early experimental work [11] was concerned with comparing the low degree of polarization of the light from the moon with the polarization produced by various terrestrial materials. It was concluded that the lunar surface materials are most likely in powder form, possibly powdered pumice. Recent work [12] has extended this earlier work with the conclusion reached that the lunar surface behavior was most closely reproduced by powdered tuffaceous rock and volcanic ash.

There is wide variance in the ideas as to the thickness of this soil layer. Some believe the layer to be quite thick, on the order of one kilometer or more [13]. Most values given, however, are less than this. From considerations of meteorite influx, estimates of one to two meters have been made [14-15]. From considerations of the volcanic hypothesis [2-10], it has been estimated that the thickness in the maria could be as great as 1 meter, and elsewhere up to possibly 1000 meters. From infrared and microwave measurements [16-17-18-19-20-21], it has been shown that the data can be explained by a thin layer of dust over a hard substratum. However the data do not preclude the presence of a thick layer of dust [16-17-22-23]. In any case it is to be expected that the thickness of the soil layer will vary over the lunar surface.

The lunar soil material would, from both the volcanic and meteoritic hypotheses, be expected to consist of much fine grained material. From infrared measurements [20-24-25] the grain sizes have been estimated to be about 0.3 mm or less. Polarization measurements [11-12] indicate the presence of much dustlike

material (< .25 mm). Laboratory measurements of the electromagnetic parameters as a function of grain size for various soil materials [26] and comparison of the results with calculated values for the electromagnetic parameters of the lunar surface [27] also indicate that the surface material is dust.

Environmental effects on the nature and behavior of the lunar soil. — Since the environment determines the soil we should be able to obtain some general ideas as to the nature and behavior of the lunar soil by considering the effects of the lunar environment on the lunar surface. The environmental factors we will consider here are vacuum, gravitational force, radiation, temperature and meteoritic impact. To do this we will first consider each environmental factor separately and then will combine the effects of each to determine the possible nature and behavior of the lunar soil.

A) Environmental factors

1. *Vacuum.* — One possible effect of a vacuum on soil could be on its internal friction. It is well known [28] that the mechanical friction between contacting surfaces is appreciably greater in vacuo than in air. In many, but apparently not in all cases, outgassed surfaces in vacuo will adhere and sliding along the interface will no longer be possible. Unfortunately, this fact has been little appreciated insofar as its effect on the internal friction of lunar soils is concerned and as a result no internal friction data in vacuo are available. There are, however, data on the static friction of a few possible lunar soil materials. The coefficient of static friction for freshly cleaved mica surfaces is about $\mu = 1$ which, with exposure of the surfaces to air, falls to about $\mu = 0.4$. The coefficient of static friction for graphite, $\mu = 0.15$ in air, rises to about $\mu = 0.56$ in vacuo [28]. Nickel and iron, which are possible lunar soil materials, have been found to weld in vacuo. Though these data were obtained for purposes unrelated to the study of soil behavior, they serve to indicate that a considerable increase in the mechanical friction component of the internal friction could occur.

Whether or not the internal friction of a soil in vacuo is greater than that of cohesionless terrestrial soils depends on the effect of vacuum conditions on the soil porosity. Vacuum conditions will tend to increase both the soil porosity and the internal friction by increased grain angularity due to the lack of terrestrial-type erosional processes, and by the increase in mechanical friction. However, since internal friction decreases as porosity increases, it may well be, assuming all other factors to remain the same, that the porosity will be greater than and the internal friction will be comparable to that of cohesionless terrestrial soils (such as dry sand).

2. *Gravity.* — The porosity, among other factors, depends upon the soil weight and the external load. The porosity of a soil formed under the lunar gravity would be greater at any given depth than an equivalent soil formed

under terrestrial gravity. In addition, the porosity will depend on the manner in which gravity affects the soil accretion mechanism. For a given accretion mechanism such as grain transport parallel to the soil surface or grain impact (from a given height) upon the surface at velocities below that at which comminution may occur, the resultant porosity would be greater for smaller values of gravity. For grain impact at cosmic velocities, though information is lacking, one would expect that this porosity-gravity relationship should be the same. Thus, the porosity should be greatest for the soil formed under the smallest gravitational force.

It is quite apparent then, that for a given load placed on the soil surface the amount of compaction will be greatest for the soil under the smallest gravity. However, it is not immediately evident whether this will also be true for a given mass placed on the soil surface. Which soil will compact more depends on the slopes of the respective porosity-load curves, in the load range of interest. It would be expected that with a given applied mass the compaction of the lunar soil will exceed that for cohesionless terrestrial soils only if the initial lunar soil porosity is quite high.

As the porosity increases, the amount of interlocking and hence the angle of internal friction will decrease. Thus the internal friction will be smallest for the soil formed under the smallest gravitational force, all other factors remaining the same.

3. *Radiation.* — Solar and cosmic radiation incident upon the lunar surface may have an appreciable effect on the nature of the surface materials and on the soil behavior. It has been variously postulated that this incident radiation may act, through radiation damage, to break up the surface material into a very fine powder [13], that corpuscular radiation impact may produce a large amount of sputtered material with some of this sputtered material being redeposited at the surface to form a cement between the grains [14], and that molecular fragments and free radicals may be formed and accumulate in areas of low temperature [4-30].

Considering the possibility of radiation damage, the available experimental data can be divided into two classes, studies of artificial irradiation, and studies of rocks and minerals that have been exposed to natural irradiations [31-32-33-34-35-36-37-38-39-40-41-42]. The results of these investigations, insofar as those parameters which may affect soil behavior are concerned, may be summarized by saying that the irradiation generally produced a decrease in density, a decrease in strength, and in some cases partial disruption of the material into powder form. Unfortunately, as with the experimental work on high-vacuum friction, this work was done for purposes unrelated to the study of soil behavior so that the materials investigated are, in general, not typical of materials one would expect at the lunar surface and the data are in a form not readily applicable to soil behavior studies.

One cannot conclude, then, what degree of radiation damage may exist at the lunar surface since the amount of damage depends on the type of material, the type of crystalline structure, the radiation level, the duration of exposure,

and the rate of recovery from the radiation damage. The rate of recovery is of particular importance since for some minerals exposed to radioactive material, the recovery rate at room temperature is great enough so that the amount of radiation damage remains small[38]. On the other hand, the radiation may produce components which the moon cannot retain so that recovery cannot occur.

There are certain soil parameters which this damage, if present, may affect. The evidence indicates that the hypothesis of the incident radiation reducing surface material to a fine powder may be correct. Radiation could thus act as a soil accretion mechanism, forming fine grained material from larger particles and from exposed rock faces. In addition to a reduction of grain size, one would expect a decrease in the angularity of at least the larger grains though the finer grains produced would themselves be angular.

Considering the effects of sputtering, it has recently been shown[43] that sputtered material does indeed act as a cementing agent. As for the effect of sputtering on the soil parameters, it is apparent that should the lunar surface consist of granular material, sputtering will tend to reduce the soil porosity unless such sputtering has an appreciable effect on the grain spacing. On the other hand, if the surface should consist only of sputtered material, it would be expected that the porosity of this material should be quite high. Not much can be said about the effects of sputtering on the internal friction since the resultant internal friction will depend upon the porosity, upon the strengths of the bonds formed, and upon the percentage of grains which are cemented.

Though there is no experimental evidence available, it is possible to make some predictions as to what the bond strength may be. From some rather qualitative arguments it can be reasoned that if a considerable percentage of the lunar surface consists of cemented material, then the bonds must be quite weak. These arguments come from consideration of the experimentally determined lunar infrared temperature. From these data, and assuming that $c = 0.2$ cal/gm °C, where c = specific heat, it is found that for the lunar surface material, $\rho k \sim 5 \times 10^{-3}$, where ρ = bulk density (gm/cm^3) and k = effective thermal conductivity (cal/cm sec °C). For any reasonable value of the bulk density (with the assumption that the material density is 3 gm/cm^3 reasonable values for ρ are taken as those corresponding to a porosity of 97 % or less) it is found that the effective thermal conductivity must also be quite small ($< 5 \times 10^{-5}$). Such low values for the thermal conductivity can be reached by granular materials in vacuo. The primary mechanism of heat transfer in such a case is by conduction through the grains and across the grain contacts. The conduction across the grain contacts is of particular importance, since at these points the thermal resistance is quite high. If the grains are cemented, then in order to maintain this high contact resistance and hence retain a thermal conductivity corresponding to a reasonable value of the bulk density, it is necessary that the porosity of the cement be quite high. Such a high porosity implies a low bond strength. This conclusion is valid, of course, only if the cemented material constitutes a major portion of the lunar surface.

4. *Temperature.* — The great temperature changes at the lunar surface may cause spallation of exposed rock material, but such spallation should be but a minor contributor to the accretion of the lunar soil. The mechanical friction component of the internal friction of soils may change with temperature. There are no data available for soil materials, but from the results obtained for other materials it appears that significant changes in mechanical friction could occur, particularly at temperatures below 0 °C [4].

5. *Meteorite impact.* — Meteorite impact is a major soil accretion mechanism, both from the addition of matter from space and the breakup of surface material. To determine how such impact affects the lunar surface it is necessary to consider the mechanics of impact. Most but not all of the impacts will be of the hypervelocity type [14-15], that is at velocities high enough so that melting and vaporization of meteorite and target material can occur. Though the mechanics of impact are not completely understood and there is no experimental information available for impact upon granular material, the processes likely to occur during such impact can be outlined. Melting should occur in the immediate vicinity of the impact point. Some of this molten material may be hurled outward in the form of a rather fine spray. This spray could act as a cementing agent, provided that at the time of deposition the droplets are still molten. That material which remains in the crater should be highly charged with gas, so that as it cools a slag or froth-like material may be formed. Some material may be vaporized. Much of this may escape from the moon, but that which remains can act as a cementing agent. In addition, a shock wave will be propagated outward from the impact point. This shock wave, besides being the cause of the melting and vaporization, may act to disrupt solid material, to break cemented bonds formed by previous impacts and to hurl such disrupted material away from the impact area.

Considering the effect of meteorite impact upon the porosity, it appears that an « equilibrium » porosity may be achieved which could be reasonably high. As for grain size, the effect of the impact would be to produce finer grains, within limits. As for the grain shape, most would be quite angular with those produced from breakup of the froths perhaps tending to be « platy ». In addition, a small percentage of spheroidal grains could be formed if some part of the molten spray solidifies prior to deposition.

B) Combined effect of the environmental factors

1. *Soil accretion and transport.* — It has been found that there are two possible soil producing mechanisms acting at the lunar surface, meteorite impact and corpuscular radiations. In addition to these, there are two mechanisms which have not been discussed, but which may also act. These are volcanic action and seismic activity. All four of these can act also as transport mechanisms under the influence of gravity.

2. *Grain size and shape for the unconsolidated portion of the surface.* — Experimental evidence indicates that the lunar soil consists of grains predominantly of dust size (< .25 mm). The effects of incident radiation and meteorite impact are to produce such fine grained material. As for the grain shape, radiation should tend to reduce grain angularity by erosion of the grain surfaces, but at the same time it would be expected that any dustlike material produced by this radiation would itself be angular. In addition, meteorite impact should generally act to increase grain angularity and terrestrial-type erosional processes are absent. Thus it is quite likely that the lunar soil grains should be statistically more angular than the grains of typical cohesionless terrestrial soils.

3. *Porosity.* — An increase of mechanical friction, a reduced gravity and a greater grain angularity indicate that the porosity of the lunar soil should be considerably greater than that of typical cohesionless terrestrial soils. Meteorite impact and cementation may however place a limit upon how high the porosity can be. One would expect that a soil formed by impact would have a porosity less than that of a soil formed by a mechanism of accretion involving predominantly movement parallel to the soil surface. Unfortunately, there is not sufficient information available at present on impact phenomena, particularly for hypervelocity impact, to conclude what the net effect of such impact may be. However, the available experimental evidence indicates that the soil porosity may be quite high, perhaps as great as 90 % [22-23-26-27]. Because of this and because all the soil parameters, with the possible exception of the impact phenomena, indicate a porosity greater than that of cohesionless terrestrial soils, it seems likely that any compactive tendencies meteorites may have are not sufficient to counteract those effects which act to produce a high porosity.

We cannot conclude at present whether or not the lunar soil porosity may be as great as 90 %. There are, however, two factors, a high coefficient of mechanical friction with appreciable adhesion, and considerable grain angularity, that could produce such a high porosity. No data are available for the mechanical friction. As for grain angularity, it has been demonstrated a number of years ago that the porosity of a loosely formed sand-mica mixture is greater than that of the sand alone [15]. In fact, for a mixture containing 40 % by weight mica, the porosity was found to be 84 %.

4. *Angle of internal friction.* — The factors tending to cause the angle of internal friction to be greater than that for terrestrial soils are the increased mechanical friction, the increased grain angularity and *perhaps* cementation and slag formation. The factors tending to cause the angle of internal friction to be less than that for terrestrial soils are the high porosity and *perhaps* cementation and slag formation.

It cannot be concluded at present what the angle of internal friction may be. However, due to the highly frictional nature of the soil, for a given porosity the angle of internal friction should be considerably greater than that of a cohesionless terrestrial soil at the same porosity.

5. *Compaction.* — If the lunar soil porosity is comparable to or not much greater than that of cohesionless terrestrial soils, the amount of compaction under load should not be excessive. However, since problems may arise if the porosity is as great as 90 %, it is of interest to consider this possibility.

In the work discussed previously concerning the porosity of sand-mica mixtures, the porosity was also measured after application of a load of 1 Kg/cm² in air. The sample initially at a porosity of 84 % was reduced to a porosity of 74 % by this load. In this experiment, the soil was confined within a graduate (presumably 1000 ml) so that for soil in situ the change in porosity should be greater. However, the loads of interest for lunar locomotion considerations are much less than the 1 Kg/cm² used in this experiment, the coefficient of mechanical friction will be higher, and cementation may be present. In addition, the porosity should decrease and the internal friction increase with depth. These considerations imply, though they certainly don't prove, that even should the initial lunar soil porosity be as great as 90 %, locomotion problems should not be too serious. In fact, when one considers the lack of water and the highly frictional nature of the lunar soil, it is hard to imagine that the problems could be as serious as those posed by terrestrial soils.

6. *Lateral variations in the nature and behavior of the soil.* — We have made a number of predictions as to the nature and behavior of the lunar soil. We have not, however, considered the possibility of marked lateral variations in the soil behavior. Before concluding this discussion it is of interest to consider briefly what lateral variations may occur. First, it is quite possible that in the vicinity of impact and volcanic craters appreciable amounts of large rock fragments and boulders may exist in the soil. Second, the amount of cementation will vary over the surface, being least in the vicinity of the lunar poles and in sheltered areas. There may also be pockets in the soil where cementation is lacking. Such pockets would occur in areas in which a large amount of soil material has been deposited in a short time. Third, as mentioned earlier, the soil layer thickness can be expected to vary over the surface. Fourth, the mechanical friction will vary. In areas containing a large percentage of materials which can weld in vacuo, the mechanical friction will be quite high. Such areas could cause locomotion difficulties if the vehicle bearing surface is composed of material which will adhere to the soil. In other areas where gas is seeping through the soil, the mechanical friction may be comparable to that of terrestrial soils and the bearing capacity may be quite low. Finally, it is to be expected that the soil porosity will vary. Since the lateral changes in lunar soil behavior can conceivably be quite large, it is important that we be able to recognize areas that may present special problems and determine from experimental work the magnitudes of the changes that may occur.

Conclusions. — The following comparisons between lunar and cohesionless terrestrial soils can be made:

1) The lunar soil grains are generally of dust size, comparable to fine sand.

2) The lunar soil grains are statistically more angular.

3) The lunar soil porosity should be higher and may be as great as 90 %.

4) The internal friction of the lunar soil may be greater or smaller depending upon the value of the porosity and on whether or not cementation is present.

5) If the porosity is as great as 90 % there may be some locomotion problems. However, if the porosity is not much greater than that of cohesionless terrestrial soils there should be, in general, no locomotion problems.

6) Finally, as with terrestrial soils, marked lateral changes in soil behavior can be expected.

We have seen that there is a large amount of experimental data that can and should be obtained in terrestrial laboratories. It is important that these experiments be performed since the results obtained will aid in making better predictions as to the lunar soil behavior and the magnitude of the locomotion problems that may arise.

REFERENCES

1) Baldwin R. B. The Face of the Moon. Univ. of Chicago Press, 1949.
2) Green J. Astronautical Sciences Review, pag. 9, Jan.-Mar., 1960.
3) Whipple F. L. J. Geophys. Res, v. 64, No. 11, pag. 1653, 1959.
4) Platt J. R. Science, v. 125, pag. 1502, 1958.
5) Robey D. H. J. Brit. Interplan. Soc., v. 17, pag. 21, 1959.
6) Whipple F. L. Astrophys. J., v. 111, pag. 315, 1950.
7) Urey H. C. Proc. Lunar and Plan. Explor. Coll., v. 1, No. 3, pag. 1, Oct. 1958.
8) Mason B. Principles of Geochemistry. John Wiley & Sons Inc., New York City, 1952.
9) Mason B. J. Geophys. Res., v. 65, No. 9, pag. 2965, 1960.
10) Green J. Proc. Lunar and Plan. Explor. Coll., v. 1, No. 4, pag. 1, Jan. 1959.
11) Wright F. E. Proc. Nat. Acad. Sci., v. 13, pag. 335, 1927.
12) Barabashov N. P. and Chekirda A. T. Soviet Astron. (trans.), v. 3, No. 5, pag. 827, March-April 1960.
13) Gold T. Vistas in Astronautics, v. 2, pag. 261, Pergamon Press, 1958.
14) Opik E. J. Tech. Rep. 157, Physics Dept., Univ. of Maryland, College Park, Oct. 1959.
15) Whipple F. L. Vistas in Astronautics, v. 2, pag. 267, Pergamon Press, 1958.
16) Piddington J. H. and Minnett H. C. Aust. J. Sci. Res., Ser. A, v. 2, pag. 63, 1949.
17) Jaeger J. C. Aust. J. Phys., v. 6, pag. 10, 1953.
18) Jaeger J. C. and Harper A. F. A. Nature, v. 166, pag. 1026, 1950.
19) Jaeger J. C. Proc. Camb. Phil. Soc., v. 49, pag. 755, 1953.
20) Wesselink A. J. Bull. Astron. Inst. Neth., v. 10, No. 390, pag. 351, 1948.
21) Gibson J. E. Proc. I.R.E., v. 46, pag. 280, 1958.
22) Giraud A. Tech. Rept. 03544-1-T, Radiation Lab., Coll. of Eng., Univ. of Michigan, Ann Arbor, Sept. 1960.
23) Brown W. E. J. Geophys. Res., v. 65, No. 10, pag. 3087, 1960.
24) Pettit E. and Nicholson S. B. Astrophys. J., v. 71, pag. 102, 1930.
25) Pettit E. Astrophys. J., v. 91, pag. 408, 1940.
26) Tech. Rept. 03544-1-F, Radiation Lab., Coll. of Eng., Univ. of Michigan, Ann Arbor, Nov. 1960.
27) Senior T. B. A. and Siegel K. M. J. of Res., Nat. Bur. of Stand., v. 74 D, No. 3, pag. 217, May-June 1960.
28) Bowden F. P. and Tabor D. The Friction and Lubrication of Solids. Clarendon Press, Oxford, 1950.

29) Bowden F. P. et al. Proc. Roy. Soc. (Lond.), v. 212, pag. 485, 1952.
30) Windsor M. W. Nature, v. 184, pag. 1556, 1959.
31) Handon J. et al. Bull. Geol. Soc. Am., v. 68, pag. 1203, 1957.
32) Leivo W. J. Phys. Rev., v. 91, pag. 245, 1953.
33) Wittels M. and Sherrill F. A. Phys. Rev., v. 93, pag. 1117, 1954.
34) Frondel C. Amer. Mineralogist, v. 30, pag. 432, 1945.
35) Lind S. C. and Bardwell D. C. J. Franklin Inst., v. 196, pag. 521, 1923.
36) Przibram K. Irradiation Colours and Luminescence. Transl. and revised by J. E. Coffyn, Pergamon Press, 1956.
37) Pabst A. Amer. Mineralogist, v. 37, pag. 137, 1952.
38) Hurley P. M. and Fairbairn H. W. J. App. Phys., v. 23, pag. 1408, 1952.
39) Hurley P. M. and Fairbairn H. W. Bull. Geol. Soc. Am., v. 64, pag. 659, 1953.
40) Berman R. Amer. Mineralogist, v. 42, pag. 191, 1957.
41) Mügge O. Zbl. Miner. Geol. Paläont., v. 721, pag. 753, 1922.
42) Faessler A. Zeit. Kristal., v. 104, pag. 81, 1942.
43) Wehner G. K. Amer. Rocket Society Jour., v. 31, pag. 438, 1961.
44) King R. F. and Tabor D. Proc. Phys. Soc. (Lond.), v. 66, pt. 2, pag. 728, 1953.
45) Terzaghi K. Public Roads, v. 8, pag. 41, 1927.

• • •

Discussions on this paper are included with those of the following one.

Gli interventi su questa relazione sono conglobati con quelli della relazione seguente.

Probable soil conditions on the moon and terrestrial planets

Probabili condizioni del suolo sulla luna ed altri pianeti

N. A. Weil *)

ABSTRACT. — *A review is presented of the current state of knowlege of surface conditions existing on the moon and terrestrial planets (Mercury, Venus, Mars), as derived from the results of scientific investigations reported in the open literature.*

From evidence available to date, conclusions are drawn in regard to the environmental and soil conditions most likely to exist on these celestial bodies. Based upon available data, reasonably firm conclusions can be presented regarding surface conditions likely to exist on the moon; information in this regard is much more hypothetical concerning the terrestrial planets.

Finally, conclusions are drawn as to the logical areas to be sought out for lunar landings. It is suggested that such landings be aimed at the convex maria preferentially, and the concave maria as a second choice. Crater rims, lunar highlands or the floors of ring-walled planes are not recommended as landing targets, since each of these appear to pose difficult problems in regard to a vehicle alighting on these surfaces.

Introduction

As part of the United States space exploration program, research is currently in progress for developing spacecraft and impact payloads for lunar landings. Current plans formulated by the National Aeronautics and Space Agency call for three series of unmanned lunar exploratory studies: the Ranger series (operational in 1962), the Surveyor (operational by 1965) and the Prospector series (operational in 1968). The Ranger shots will carry instrumented packages sending back information from some distance above the lunar surface. The instrument package, however, will crash at a considerable velocity into the moon's surface, and is not expected to survive landing impact. The Surveyor series will be a « soft landing » package, impacting the surface at a speed low enough to cause no damage to the instruments container in it. Upon landing, the Surveyor is expected to gather data regarding the intensity of cosmic radiation, atmospheric composition, temperature conditions, surface hardness and composition, subsurface radioactivity, thermal gradients and seismic activity at the lunar surface. The Prospector series will gather roughly

*) Director of Mechanics Research, Armour Research Foundation of the Illinois Institute of Technology, Chicago, Illinois, U.S.A.

similar information, except that this package will be able to penetrate the surface to a much greater extent than the Surveyor, and the package will also be equipped with means for locomotion, giving it considerable mobility to explore the lunar surface. Remote controls and telemetering will be used in all three series to transmit commands and obtain information and data gathered by the instruments. This initial phase will be followed by manned landings on the moon as part of man's probing toward the planets and, subsequently, the stars.

In any attempt to land on the moon and later on the planets, there is a need to prepare for the worst surface conditions that might be encountered. Unfortunately, very little is firmly known about the surface even of our nearest celestial neighbor, the moon. According to one hypothesis the moon's surface may be covered with a dust layer perhaps kilometers in depth; according to alternate views held, the maria are the result of lava flows or consist of agglomerated particles of shallow depth. At least in regard to the moon, enough fragmentary information exists to allow for the formulation of (sometimes head-on opposite) theories. Knowledge regarding the surfaces of the terrestrial planets (Mercury, Venus, Mars) is so scarce that no coherent theories have been formulated regarding soil conditions likely to be encountered there.

This paper, accordingly, is concerned with an attempt to define the surface conditions likely to be encountered on the moon and the terrestrial planets. First a review will be made of the current state of knowledge on this subject, followed by a definition of the most probable surface conditions likely to exist on the moon and nearby planets. It should be emphasized that these are merely hypotheses, and represent no more than the Author's views on the subject under consideration.

State of knowledge of the lunar surface

The dominant features of the lunar landscape are its rather conspicuous craters and smooth appearing large dark areas, referred to as a « maria » (seas). Let us examine these two features sequentially.

a) **Maria.** — These areas comprise about 40 per cent of the visible surface of the moon, and are generally assumed to be the result of lava flows. As Tombaugh [1] point out, this view is supported by the following considerations:

1) The remains of partially destroyed craters can be observed near the « shores » of the maria.

2) The floors of large craters (mountain-ringed planes) are frequently thousands of feet below the mean surface elevation of the moon. Some of the large craters near the borders of maria show evidence of lava invasion. An example is the mountain-walled plane of Gassendi (55 miles in diameter) near Mare Humorum, whose floor is darker than the surrounding mountains and slopes toward the southern rim which has been partially melted. Even greater destruction was suffered by the 40-mile Dopplemeyer crater.

3) Large clefts border the maria, paralleling shore lines. It is assumed that these clefts represent fissuring resulting from contraction after cooling. Three concentric cracks, over 100 miles long, have been noted at the western edge of Mare Humorum; a crack in Mare Nubium passes through a mountain range.

4) Fracture occurance seems to indicate the massive laval nature of the maria. A prominent escarpment called the Straight Wall, 60 miles in length, has its maria side 800 feet lower than is the other side.

5) Bright ray systems radiating from large craters (Tycho, Kepler, Aristarchus) traverse both mountainous areas and maria. Their contrast is largest on the maria, where they show up as very bright lines against a dark background. By analogy, pulverized rock is far brighter than massive rock. Thus the rays are assumed to consist of finely pulverized material thrown out by violent impact over the solid igneous rock of the maria.

There is less agreement regarding the nature of origin forming the lavas that constitute the maria. Thus, Kuiper [2] subscribes to the view that all the maria are volcanic in origin, and resulted from lava flow that welled up through fissures in the surface during periods of high internal activity. This view of the plutonic origin of the maria is firmly supported by leading authorities [3,4] at least for the case of Mare Tranquillitatis which, because of its very black color and irregular outline, is assumed to be the result of laval flow over rough terrain.

Less agreement exists in regard to the other maria. For instance, early researchers thought that the maria were the result of meteoric impact on a vast scale. Thus, Gilbert [5] suggested that the Mare Imbrium was created by an object 100 miles in diameter which struck the moon at an oblique angle, creating first the « inlet » known as Rainbow Bay and then coming to rest in the center of the sea. Its flying fragments were reasoned to have cut the deep valleys that radiate from Mare Imbrium.

While the purely meteoric origin of the maria is largely discounted today, the possibility is still upheld that the maria were formed by the melting and subsequent solidification of lunar rocks due to impact of huge meteors crashing onto the lunar surface. Thus, Urey [6,7] showed that the meteor required to create the Mare Imbrium had to have a mass of about 1.5×10^{23} g, travelling at a velocity of 2.38 km/sec. The energy liberated during collision would then have been on the order of 4.15×10^{32} ergs. Although the better part of the planetesimal would have vaporized upon impact, sufficient energy would have remained to account readily for the heating of lunar rocks over a large area.

b) **Craters.** — Unlike the maria, which are assumed to be the result of lava flow of whatever origin, the craters are generally regarded as having been created by meteoric impact.

This view is, by no means, unanimous. Thus, frequent suggestions have been made in the past that the craters, too, were the result of volcanic activity. The most recent of these views were put forth by Moon [8] who favored the

platonic origin theory on account of the ordered nature (doublets, pairs and chains) rather than random distribution of lunar craters.

Nevertheless, this theory is unlikely to be correct. It was pointed out very early [5] that lunar craters bear virtually none of the features characteristic of terrestrial volcanoes. Terrestrial volcanoes are characterized by slopes which vary with the age of the mountain, but are not dependent upon its size; the older the volcano, the milder its slopes. The crater of terrestrial volcanoes is also independent of their size, and generally small as compared to the overall bulk of the mountain. Furthermore, the crater floor is never below the level of the surrounding plane, and secondary volcanoes exist in it in only the rarest instances.

Lunar volcanoes display just about head-on opposite features. Their bulk is very small as compared to the size of the crater; the cross section of the larger craters shows a thin and sharp rim surrounding a very broad crater (hence the name, «wall-ringed plane»). Most often the crater floor is substantially below the mean elevation of the surrounding area, and central craters within craters are frequent. Moreover, the larger the crater, the milder the slope of its inner wall; this is shown in Table I, taken from Kiess and Lassavasky [9].

TABLE I. — *Crater slopes on the moon.*

Crater diameter, km	Average Diameter, km	No. of observations	Max. inner slope, deg.	Mean inner slope, deg.
0-30	12	113	33.5	11.5
30-50	38	14	22.7	9.0
50-100	76	22	14.8	7.2
100+	144	8	11.6	6.0

Another uncommon feature of some of the larger lunar craters are the bright rays radiating from them. Tycho, one of the largest craters, has a particularly well developed set of radiating rays. The rays emanate at times from the center of the crater; at times they are tangential to it. They are seen best under oblique illumination, when they appear as bright streaks against a darker background. Under the normal illumination of the lunar noon, they all but vanish. The rays extend uninterrupted over all features of the moon, other craters as well as mountains and planes. They seem to be associated with the «younger» and more rugged craters on the moon, and appear to be the result of pulverized matter thrown out violently upon impact of the lunar surface by impinging meteorites.

If then, as most students of the subject agree [10], the craters of the moon are the result of meteoric collisions and not volcanic action, some puzzling questions still remain to be resolved. Amongst these are: a) why does this meteoric impact formation of craters apparently not continue to date and, b) what is the reason for the lack of existence of small craters?

As to the lack of crater formation in recent geological times, agreement is rather general that all of the prominent features of the moon were formed

soon after its birth, and that large scale surface shaping activity has essentially ceased since.

The lack of existence of small lunar craters is more apparent than real. Statistical probability calculations, extrapolating form the known distribution function of observable craters, indicate that small craters must exist in large numbers. The reason appears to lie more in the limitations of telescopic equipment used to photograph the lunar surface. A feature on the moon can be observed visually only if it is in excess of 1000 feet; photographic plates, incapable of mentally correcting for image instability due to atmospheric turbulance (as done by the human eye), cannot register surface details less than 2500 feet in extent on the moon.

While crater creating forces have apparently abated, those eroding the crater walls apparently have not. More will be said about this later. The important item to be observed here, as already noted in part in table I, that the angle of repose of lunar dust on the well eroded slopes[a] of large craters appears to be only 6°.

c) Lunar soil conditions. — Telescopic observations, as already noted above, yield only limited information on the finer details of the lunar surface. An important advance in this regard, however, took place in 1957 by way of radio observations conducted at Jodrell Bank in England[11]. These took advantage of the fact that any electromagnetic radiation strinking the surface of a smooth sphere will be reflected back as though coming from a single point in the interior of the sphere. With a rough surface the reflected radiation will be diffused, and the entire surface will appear to be illuminated.

The visible light reflected from the lunar surface is very diffused; hence the surface is rough on the scale of the length of light waves, i.e., at a range of 400-800$\mu\mu$. On the other hand, radio observations appear to come back only from the center of the moon's disk; therefore, at the 10-cm length of radio waves, the moon is perfectly smooth. This holds for the mountainous regions of the moon's visible center as well as for the maria (represented in this case by Sinus Vaporum), despite the rather jagged appearance of the moon's features.

The lack of pits and irregularities on the order of magnitude of inches may be understood if one assumes that all lunar features are covered with a dust layer at least several inches deep, including crater walls. Two explanations exist as to why this dust layer is smooth, despite meteoric impact which must continue to take place. One is due to Gold[12] who proposed that solar protons bombarding the moon would impart to dust particles a positive electrostatic charge. Under the influence of forces of electrostatic repulsion, the particles hop about on the surface and fill in all cavities or pits present in a flat terrain. Gold was able to reproduce this behavior in the laboratory, by bombarding dust particles with electrons[13]. This may mean that the moon's highlands are scoured clean, while its depressions are filled with dust to a considerable depth.

Another mechanism that may account for particle mobility on the moon is the phonon pressure of sunlight. While this pressure is extremely low, of

order of 10^{-8} psi at total reflection, it could exert sufficient force to mobilize extremely fine particles.

If, indeed, there is dust on the lunar surface to account for its apparent smoothness at the wavelength of radio waves, then one must be able to answer the question as to where this dust came from and how much of it may exist on the surface, by each of the dust generating mechanisms assumed.

Dust may have accumulated on the lunar surface under the action of three mechanisms: the alternate heating and cooling of the surface corresponding to the lunar day and night, the condensations of meteors vaporized upon impact and the settling of cosmic dust floating in the universe. It is interesting to examine the degree in which these mechanisms could have contributed to the formation of dust layers on the lunar surface.

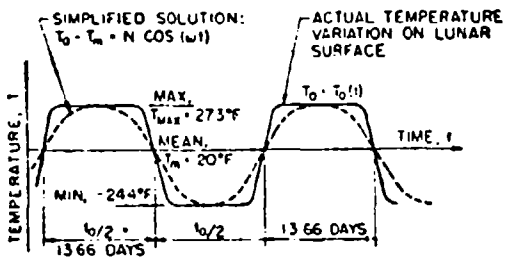


Fig. 1. — Temperature cycle at lunar surface (for values quoted, see references 8-12).

1) *Dust formation by thermal defoliation.* — The amount of dust formed by the mechanical break-up of surface rocks (thermal defoliation) on the moon is very difficult to estimate correctly. One can, however, develop an upper limit for the depth to which this mechanism may have been operative.

The equatorial temperature variation corresponding to the diurnal cycle of the moon, according to the best information available at present, is shown in fig. 1. Making now the vast simplification that the density (ρ), specific heat (c) and thermal conductivity (k) are independent of depth from the lunar surface, the one-dimensional heat conduction equation takes the form

$$\frac{\partial \theta}{\partial t} = a \frac{\partial^2 \theta}{\partial x^2} \tag{1}$$

where $a = k/\rho c$ is the thermal diffusivity and x is the depth counted from the surface. Let us further simplify conditions by approximating the actual surface temperature variation with the function, shown in fig. 1

$$\theta_0 = \theta_{max} \cos(\omega t) \tag{2}$$

where

$\theta = T - T_m$ = relative temperature
$\omega = 2\pi f$ = circular frequency
$t_0 = 1/f$ = period of temperature cycle

and t designates running time while T is the temperature. The solution of the system of Eqs. 1 and 2 is given by [14]

$$\theta = \theta_{max} e^{-mx} \cos(\omega t - mx) \tag{3}$$

$$m = (\omega/2\alpha)^{1/2}$$

As shown in fig. 2, the amplitude of thermal fluctuations decreases with depth according to

$$\theta_{max,x} = \theta_{max} e^{-mx} \tag{4}$$

and the depth, x_n, at which $\theta_{max,x}$ is reduced to 1/n of the value of θ_{max} is given by

$$x_n = 1.30 \log_{10} n(\alpha t_o)^{1/2} \tag{5}$$

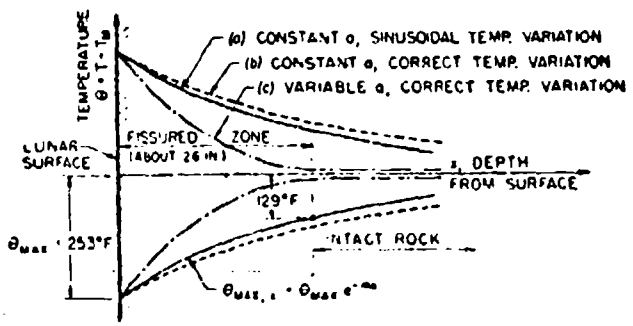


Fig. 2. — Profiles of maximum temperature amplitudes (envelopes) for various conditions.

We next have to relate thermal variations to fracture phenomena in rocks. There is very little direct experimental evidence in this regard; only three references can be quoted [15-17] that relate to the problem at hand. Thus, Charles [15] showed that rocks were clearly subject to cyclic thermal fatigue, in the presence or absence of environments inductive of corrosive attack. Lindman and Bobrowski [16] showed that the resistance of brittle materials to thermal shock, other things being equal, varies in direct proportion to their tensile strength, while Howie [17] obtained correlations of crack depth with severity of thermal shock in silica brick. A convenient correlation of thermal shock severity with the strength of the brittle substance, covering the present case of an infinite film coefficient, was stated by Kingery [18] in the form

$$\sigma_t = E\alpha\theta/(1 - \nu) \tag{6}$$

where E is the modulus of elasticity of the material, α is coefficient of thermal expansion and ν is Poisson's ratio. Eq. 6, naturally, corresponds to the case of complete arrest of thermal expansion and, as such, will yield conservative (upper bound) values.

Numerical data required to develop specific answers can be obtained as follows: a good average value for the modulus of elasticity of igneous rock is 7.5×10^6 psi; Poisson's ratio for almost all rocks is 0.25. The coefficient of thermal expansion, compressive strength and specific gr ity of differe.. rock formations are listed in table II.

TABLE II. — *Physical properties of igneous rocks.*

Type of Rock	Coefficient of thermal expansion α, 10^{-6}/°F	Compressive strength, 10^3 psi	Specific gravity
Granite Porphiry .	34	17.7	2.67
Biotite Granite . .	39	23.5	2.66
Muscovite Granite .	45	24.7	.62
Hornblende Granite .	37	25.8	2.63
Quartz Syenite . . .	37	21.6	2.67
Gabbro Diorite . .	39	25.0	3 02
Olivine Basalt . . .	22	24.0	2.75
Basalt Porphiry . .	26	18.8	2.81
Diabase	31	23.3	2.85
Orthoclase Gabbro .	30	26.4	2.87

Supported by other values obtainable from the literature, these compilations allow for a rough characterization of lunar rocks in the form of the data presented in table III.

TABLE III. — *Anticipated physical and mechanical data representative of lunar rock.*

Property	Symbol	Value
Modulus of Elasticity . . .	E	7.5×10^6 psi
Coeff. of thermal expansion	α	3.5×10^{-6}/° F
Poisson's ratio	ν	0.25
Compressive strength . . .	σ_c	22×10^3 psi
Tensile strength (est.) . . .	σ_t	4.5×10^3 psi
Specific gravity	γ	2.80
Specific weight	ρ	175 lb/ft^3
Specific heat	c	0.19 B/lb — °F
Thermal conductivity . . .	k	1.6 B/hr — ft — °F
Thermal diffusivity	a	0.048 ft^2/hr
Surface energy	γ_s	0.0057 in-lb/in^2

The following additional data can be obtained from fig. 1:

$$t_0 = 27.32 \text{ days}$$
$$\omega = 2\pi/t_0 = 0.00957 \text{ hr}^{-1}$$
$$m = (\omega/2a)^{\frac{1}{2}} = 0.3163 \text{ ft}^{-1}$$
$$\theta_{max} = 253° \text{ F}$$

Then, by Eq. 6, the temperature amplitude still capable of inducing thermal fissuring in lunar rocks is $\theta = 128.6°$ F. Further, by Eq. 4 the maximum depth to which this temperature swing can penetrate below the surface is x = 25.7 inches. Therefore, this simplified approach predicts that thermal degradation of lunar rocks may have affected the top 26 inches of the lunar surface.

Because of the simplifying assumptions made in this analysis, the result of 26 inches is an absolute upper bound and is undoubtedly excessive. As opposed to assumptions made here, the actual surface conditions of undisturbed

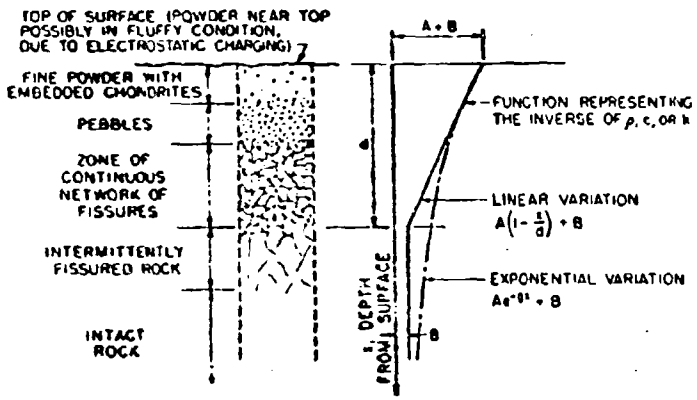


Fig. 3. — Assumed stratification of undisturbed top surface of moon (in maria) and accompanying variation of heat transfer parameters.

areas on the moon (the maria) probably consist of a dust layer at the top (containing possibly a few large embedded chondrites), followed by successively coarser constituents below, as depicted in fig. 3.

If this hypothesis is correct, its principal result would be that ρ, c and k will become functions of x, each increasing with depth. This requires that the « lumped constant » heat transfer Eq. 1 be replaced by its original form of

$$\rho c \frac{\partial \theta}{\partial t} = \frac{\partial}{\partial x}\left(k \frac{\partial \theta}{\partial x}\right) \tag{7}$$

This equation would have to be solved then subject to the correct boundary conditions shown in fig. 1, rather than the idealized sinusoidal temperature boundary value of Eq. 2. The result will be a far sharper depthwise attenuation of temperature fluctuations, as presented tentatively in fig. 2. Under these conditions thermal defoliation will be operative to a far shallower depth than the upper bounding value gleaned form the simplified solution.

For lack of research, specific values of the degree of reduction cannot be given; there are no data available on the thermal conductivity, specific heat and even density of highly comminuted soils under a hard vacuum. With what

meager indications exist to date, one may assume that the degree of reduction is at least one, and possibly two, orders of magnitude, Therefore, the mechanism of thermal defoliation may have broken up the lunar rocks to a depth of about 1-3 cm. Further thermal comminution would cease if the dust cover so formed remains undisturbed. If, however, the dust is removed by some mechanism, such as the instability of slopes of steeper crater walls exceeding the angle of repose of electrostatically charged dust in a vacuum, the freshly re-exposed rock would again be subject to thermal defoliation.

2) *Dust formation by condensation of impacted meteorites.* — The hypothesis has been put forward [6-7] that the process of condensation of meteors vaporized upon impact could have deposited considerable quantities of dust on the lunar surface. For instance, Urey's calculations [6-7] regarding the size of the meteor required to create the Mare Imbrium show that the mass of this body, if completely vaporized and spread uniformly over the surface of the moon upon condensation, would have resulted in a dust cover 110 meters deep. Considering that this is only one of the many planetesimals that may have impacted the lunar surface, the dust cover formed by this mechanism could be several km deep.

If this mechanism were really operative in the early stages of the moon's life, the dust so created could have spread quite uniformly over the lunar surface. Thrown out at explosive velocities, and in the absence of a lunar atmosphere to apply drag, the condensing dust particle could have readily travelled several times around the moon's perimeter, attracted only by the relative weak gravitational field (roughly 1/6th that of the earth at the surface) of this celestial body.

Nonetheless, what little direct evidence exists indicates that this dust forming mechanism must be largely discounted: if it were really operative, considerable amounts of meteoric dust should have condensed out from the impacts that created the lunar craters. This dust formation can be rather readily traced in the form of the ray-systems radiating from some of the craters. While stretching over enormous distances (some of the rays of Tycho can be traced for a distance of 5000 miles) the rays are known to be very shallow. They have no observable shadow even under the most oblique illumination, meaning that their depth cannot exceed a few centimeters. Therefore, the formation of deep lunar dust beds resulting from the vaporization and condensation of impacting meteorites must be largely discounted at our current state of knowledge.

3) *Micrometeorite accumulation.* — The third source of fine particles on the lunar surface is due to the settlement of cosmic dust attracted by the gravitational field of the moon. Some results in this regard can be inferred form the recent work of La Gow and Alexander [20] who calculated the micrometeorite flux from measurements made on the satellites 1958 Alpha and 1959 Eta. A flux of 8.5×10^{-3}/m^2 sec was reported by 1958 Alpha. Assuming a mean impacting velocity of 30 km. sec, the threshold mass of the least particle observed turns out to be 8.33×10^{-10} g. Data from 1959 Eta show an impact

rate of $1.74 \times 10^{-3}/m^2$ sec. for a threshold mass of 3.33×10^{-9} g. These points are plotted on a logarithmic scale in fig. 4, and the mass distribution curve is drawn by assuming a straight line relationship, described by an equation of the form

$$\dot{n} = cm^k \tag{8}$$

where $\dot{n}$ is the impact rate of a given particle size, m the particle mass, while c and k are constants. Then the total mass influx rate, $\dot{M}$ (g/m² sec), will be given by

$$\dot{M} = \int_{m_a}^{m_b} \dot{n}\, dm \tag{9}$$

where m_a and m_b are the least and largest masses occurring in the micrometeorite population. Substituting Eq. 8 into Eq. 9 and integrating, there results

$$\dot{M} = \frac{c}{k+1}\left[m_b^{k+1} - m_a^{k+1}\right] \tag{10}$$

Then the total micrometeorite accumulation, counted since the formation of the solar system, will be

$$M = \dot{M}\tau = \frac{c\tau}{k+1}\left[m_b^{k+1} - m_a^{k+1}\right] \tag{11}$$

The age of the solar system can be assumed to be near 7×10^9 years [21]. Furthermore, the minimum micrometeorite particle size in the solar system is limited by the Poynting-Robertson effect to about 10^{-12} g. Thus, the numerical data required by Eq. 11 are:

$$\tau = 221 \times 10^{15} \text{ sec}$$
$$c = 3.02 \times 10^{-13} \text{ (m}^2 \text{ sec)}^{-1}$$
$$k = -1.14$$
$$m_a = 10^{-12} \text{ g}$$

The values of c and k shown above were obtained from fig. 4. The exact value of m_b turns out to be irrelevant since, at $k < -1$ $m_b^{k+1} \to 0$ as $m_b \to \infty$. Substitution of these values into Eq. 11 yields

$$M = 228 \times 10^3 \text{ g/m}^2$$

At a particle density of 3.3 g/cm³ and assuming absolutely no porosity, this influx would be equivalent to solid layer 7.6 meters high.

This result implies the condition that micrometeorite flux is uniform throughout the solar system, and equal to the rate measured in near-earth

orbits. Such cannot be the case since the earth's gravitational field exerts a strong attractive force. A rational assumption is that flux density is proportional to field strength. Ignoring then minor perturbations such as the moon's own gravitational field (field strength 1/80'th that of earth) and periodic shadowing effects of the earth, this would mean that the micrometeorite flux becomes inversely proportional to the square of the distance from earth.

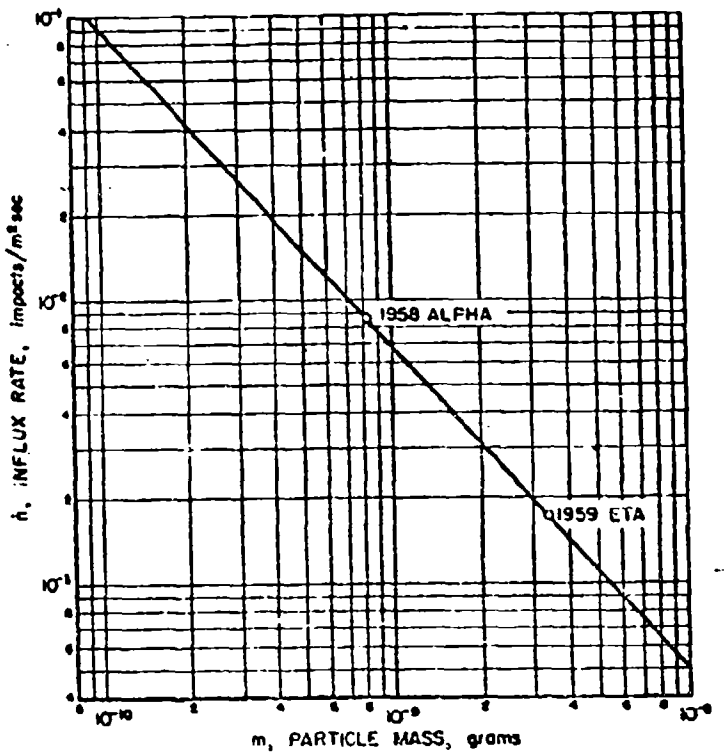


Fig. 4. — Assumed mass distribution curve for micrometeorite flux.

Accepting this tenet, the solid density accumulation of micrometeorite flux on the lunar surface would amount to 2.3 mm. At a void ratio of 75 %, which is probably a conservative assumption, the depth of dust layer traceable to this source would, therefore, amount to nearly 1 cm.

4) *Total dust accumulation and general surface conditions.* — As the calculations carried out above show, the most plausible assumption regarding the effect of dust forming mechanisms on the lunar surface is that thermal defoliation may be responsible for having degenerated a layer of rock of 1-3 cm into dust, galactic dust settlement may account for a layer 1 cm deep, additive to which is an unknown contribution due to the condensation of vaporized meteorites which, however, is assumed to be negligibly small.

All this seems to indicate that on open surfaces of the moon, such as the maria, there is a dust layer whose depth cannot amount to much more than a few centimeters. The situation is different only in craters and ring-walled plains. Here, the slopes exceeding the natural angle of repose of fine matter under lunar environmental conditions would have been re-exposed to thermal decomposition by repeated slides of the dust bed. In these places, therefore, it is conceivable that comparatively deep dust beds could have formed by this mechanism on the inside of lunar craters.

It is interesting to compare these deductions with hypotheses put forward by other researchers. The fact that the moon's surface is covered by a thin layer of fine dust was established many years ago by Pettit and Nicholson. However, their thermal observations during lunar eclipses also showed that this dust must be underlain by a layer of insulating material, having a thermal conductivity similar to pumice. This observation was later frequently misquoted in the context that the surface of the moon contains pumice-like material, ostensibly originating from volcanic eruptions (Pettit and Nicholson said nothing of the sort). In fact, even the « pumice-like » insulating layer analogy is open to question, since it rests on thermal conductivity data obtained by Smoluchowski on porous materials down to pressures of 5×10^{-2} mm. Hg, which is at least ten orders of magnitude larger than those existing on the moon. Because of this, Urey postulated recently [1] that the surface of the moon is nearly like fine sand rather than dust, while Gold [2] holds out for an extremely fine dust, created largely by light erosion. The most recent literature, in turn, contains speculation that the surface of the moon is covered with chondritic material such as that found in stone meteorites. This would mean that the moon's surface consists of gravelly material mixed with fine iron-nickel metal particles of the body-centered and face-centered cubic iron-nickel phases. Alternatively, a substantial school [22] maintains views similar to those advanced here, postulating that convex maria have a very shallow dust cover, not exceeding 2-3 centimeters, although allowing that flat or concave maria may contain a greater thickness of dust.

5) *Meritic composition.* — The last question that must be reviewed is the particle size spectrum of the lunar dust. This question gains importance since the response of lunar soils to imposed loads is likely to vary substantially, depending on whether one deals with a very fine powder or a stratum consisting of coarse aggregates.

Taking the dust forming mechanisms one by one, thermal defoliation cannot produce particles of extreme fineness. Once the intact rock has been fissured, further break-up of individual chunks becomes a matter of transient thermal stresses in the pieces, rather than restrained thermal expansion of a semi-infinite medium. The action, therefore, depends on heating or cooling rates that occur near the lunar terminator. These are quite steep. On the other hand, for a given heat flux, thermal stresses will become smaller as the size of the body diminishes. Therefore, as a crude guess, one may say that thermale defoliation will result in particles of a rather uniform size, ranging up to 100 μ at the

surface, with progressively increasing sizes below where thermal action is less severe.

To the extent that the condensation of meteors vaporized upon impact has contributed to dust formation, the particles originating from this source must be extremely fine. Cooling of the vapors is quite rapid and, despite the weaker gravitational field, their flight paths would tend to be short for lack of drag forces in the lunar atmosphere.

Much the same can be said for the particles accumulated from the galactic dust raining down on the moon's surface. In accordance with data given above, the least particle size represented is 0.83 μ, while the mean of the population is at about 6 μ with a strong skewing to the smaller particle sizes in the spectrum.

Thus, the mechanisms contributive to dust formation would tend to generate a powder with particle sizes ranging from 1-100 μ at the surface. Intermingled with this very fine powder are larger particles, represented by chondritic and achondritic meteorites, which escaped vaporization either because of their grazing angle of incidence upon the moon's surface, or because they impacted into existing powder beds rather than hard rock.

Proceeding downward from the surface, the particle size grows and aggregates increase in size, in keeping with schematic view presented in fig. 3, until one arrives at solid bedrock.

The surface of the terrestrial planets

Because of the more imminent interests, and their relative proximity to Earth, this discussion will be confined to an examination of information available on the surface conditions of the terrestrial planet: Mercury, Venus and Mars. These bodies are called terrestrial planets because their density, composition and probable interior structure are reasonably similar to those of Earth. Facts regarding their probable surface condition are extremely meager; a few data characterizing these bodies are presented in Table IV.

TABLE IV. — *Data for the terrestrial planets.*

Planet	Mean distance from sun, astr. units	Mean diam. miles	Vol. rel. to earth	Mass rel. to earth	Avg. spec. gravity	Surface gravity, g	Albedo	Mean temp. visible surf., °C	No. of satellites
Mercury	0.387	3150	0.06	0.042	3.80	0.27	0.07	+370	0
Venus	0.723	7700	0.92	0.81	4.86	0.87	0.59	−35	0
Earth	1.000	7920	1.000	1.000	5.52	1.00	0.29	+15	1
Mars	1.524	4215	0.150	0.108	3.96	0.38	0.15	−25	2

a) **Mercury.** — Mercury appears to be very comparable in most of its aspects to our moon. It has a period of rotation equal to its period of revolution around the sun (88 sidereal days), and an albedo and density very comparable to lunar values. The low value of the albedo, and negative nature of spectroscopic observations indicate that Mercury has virtually no atmosphere. The best

current estimates[23-24] obtained with polarimetric techniques indicate the existence of a thin atmosphere of unknown composition. The atmospheric pressure at the surface is assumed to be 3×10^{-4} atm., or 0.23-mm Hg. The surface temperature on the side permanently facing the sun averages 370° C; on the unlighted side, it is near absolute zero. For lack of atmosphere, there

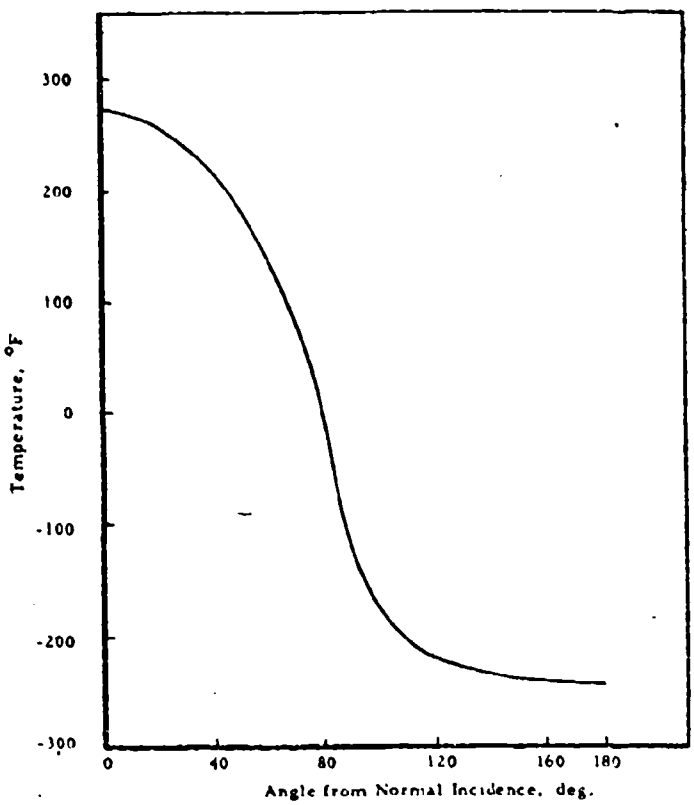


Fig. 5. — Lunar temperature variation at subsolar point during one-half lunar day.

is very little convective heat transfer from one side to the other, and the unlighted side of Mercury is probably the coldest solid surface in the entire solar system.

The polarization of reflected light and albedo being the same for Mercury and the Moon, the surface conditions of these two bodies are also assumed to be similar. There are some dusky surface markings on Mercury, whose existence was repeatedly confirmed by observers[24-25]. Thermal defoliation of surface rocks is unlikely to occur, since surface temperatures on the planet are steady. Because of the low albedo, one may assume the presence of igneous basalt and dark lava[25], forming a very irregular rough surface. Owing to the surface temperatures on the lighted side, there are likely to be molten pools of zinc

and tin, if these elements exist on the planet. Its location being near the sun, the density of particulate cosmic shower descending upon Mercury is likely to be much greater than at the earth orbit. Therefore, the planet's surface is probably covered with a layer of dust several times as deep as the estimated minimum of 2-3 cm covering the moon. Mercury's surface, like the moon's will also be found to show extensive crater formations caused by meteoric impact.

b) **Venus.** — This planet has physical characteristics most closely approaching those of the earth. However, we know virtually nothing about its surface, since all we see is its atmosphere.

The temperature at the top of this atmosphere is — 38° C mean, as determined by either thermoelectric or radiometric measurements [29]. The solid surface temperatures at the bottom of this atmosphere are assumed to be in the range of 200-350° C [25-28]. The only detectable element in this atmosphere is CO_2 [29-30]; spectroscopic investigations show no trace of water or oxygen. The great albedo of Venus' atmosphere induced investigators to believe that it is laden with globules of liquid or solid material somewhat over 2 μ in size [31], although polarimetric measurements do not confirm [32] the existence of solid dust in the atmosphere. It is not known how high the atmosphere is, but the barometric pressure has been estimated as high as 10 atm. [33] at the surface. This value, however, appears to be excessive when considering that the escape velocity for Venus is about the same as that of the Earth. Estimates [34] of a surface pressure not quite 2 atm. appear to be more reasonable.

Because of their similarity, we can assume that volcanic activity on Venus was similar to that of the earth and may still be in progress. This could account for the presence of CO_2 and lack of water on this planet [35]. While some argue [32] that the surface is completely covered by oceans, the lack of any detectable water vapor in the atmosphere makes such an assumption unlikely [36]. Photodissociation is certain to have created CO in the Venusian atmosphere (see discussion for Mars), which would have been retained by the planet in view of its comparatively high escape velocity (near that for Earth). The atmosphere is also certain to contain CH_4, which would again remain on the planet.

The inferred surface temperatures make it improbable that there is any liquid material on the surface of Venus. Because of shifting streaks, nebulous bands and changeable bright areas observable in the atmosphere when photographed in ultraviolet light [31], it is generally assumed that the atmosphere is in a state of violent motion, swirling great clouds of dust to large heights. The accompanying erosive action has probably covered the surface with a deep layer of finely eroded sand.

c) **Mars.** — Mars is the only celestial body, excepting the Moon, whose surface features can be photographed and measured under telescopic observation. Information accumulated to date shows the existence of white polar caps, large areas whose color changes from grey to dark green with seasonal variations and which are reminiscent of lunar maria; vast permanent orange expanses; and a network of thin lines sometimes identified as « canals ».

The axis of Mars is inclined at 24° to the plane of its orbit, which makes for very pronounced seasonal variations. Because of its rotational period (687 earth days), the seasons are about twice as long as those on earth, and the surface temperature is believed to range from — 120° C to + 30° C; at perihelion the northern hemisphere is in the « winter season ». The dark-green areas change to brownish-grey at the approach of winter, which forms the basis of speculation about the existence of some simple form of life (lichens, mosses) on Mars. The reddish-orange areas show little change in color with the seasons.

The retreat of polar caps during summer is not uniform [8]; there are small patches, always in the same location, that hold out for weeks after the whiteness disappeared from the surrounding area with the advance of summer. This suggests the presence of substantial differences in elevation on the Martian surface, the plateaus being colder than the surrounding planes. These plateaus are expected to have very mild slopes and heights not exceeding 10,000 ft., since no irregularities have been noted in photographs near the terminator, where they should otherwise be seen with ease.

The polar caps are almost certainly formed of water (snow or ice), in view of the prevailing Martian temperatures (too high for dry ice to form), the reflectivity of the caps (far lower than that corresponding to CO_2) and because of recent polarimetric measurements [23].

The true color of Martian soil (exclusive of the maria) is moderately reddish [9], the reflected ligh having wavelengths varying between 0.46 and 0.64 microns. These areas cover about 75 % of the Martian surface and are assumed to be barren deserts consisting of a granular or powdery form of iron oxide (ilmenite or limenine), the latter a hydrated ferric oxide of reddishbrown color. The graininess of the surface and the opacity of grains is confirmed by the low albedo of Mars [10]. These regions are also supposed to be the source of thin yellow clouds frequently observed in the Martian atmosphere. In fact, these clouds are more numerous when the planet is near perihelion (which agrees with the fact that most of the « deserts » providing the dust for these clouds lie in the southern hemisphere), and their polarization of reflected sunlight is identical with that of powdery soil [24].

Contrary to Moon and Mercury, Mars is « limb-dark » and is surrounded by a « blue haze » (whose color is actually red, by all standards). Therefore it definitely has an atmosphere. The Martian atmosphere is known to be some 40 Km. high, with rather good agreement that its surface pressure is about 65 - 85 mm. Hg [25-39-40]. This is about 10 percent of the terrestrial sea-level value, and corresponds to atmospheric pressures existing at an elevation of 55,000 feet on Earth. Spectroscopic evidence [41-42-43] has shown the presence of only CO_2 in the Martian atmosphere (which appears to be twice as abundant as on Earth), with no indications of water vapor, oxygen methane, nitrogen or noble gases. This is understandable if one considers that the escape velocity for Mars is about 5 Km./sec., as compared to 11.2 Km./sec. for Earth. Hence, molecules 5 times heavier should escape with equal ease from Mars than

those from Earth (ignoring the small effect of different temperatures at the exospheric base). Atomic oxygen, methane and water vapor should have escaped from the Martian atmosphere with even greater ease than is the case for helium on Earth.

The Martian atmosphere is very likely to contain carbon monoxide, formed by the decomposition of CO_2 under solar radiation [4]; the atomic oxygen so formed, in turn, escapes. CO on account of its high dissociation energy (11.0 eV), will be little affected by photodissociation, and will stay in the atmosphere. So will nitrogen, which has an even higher dissociation energy (15.6 eV). Furthermore, water vapor is known to exist on Mars, as evidenced by the polar caps, and by brilliant white shiftings spots in the atmosphere [5] which appear to behave like terrestrial cirrus clouds. Moreover, spectrographic evidence would not be expected to show the presence of nitrogen and noble gases. From known data of temperature and pressure, however, it appears [7] that 93.8 % of the atmosphere is made up of N_2, the balance being CO_2 (assumed concentration: 2.2 %), CO, H_2O and argon, the latter formed as the natural decay product from K_{40} in the surface.

Probable planetary surface conditions

The background information presented before permits certain conclusions and hypotheses to be drawn regarding the probable surface conditions of the moon and the terrestrial planets. This is presented below.

a) **Moon.** — Only the lunar highlands and the rims of lunar craters are free of dust. In these regions, bare rock is likely to be encountered, which is very slowly being decomposed into dust under thermal defoliation due to the alternation of lunar night and day, light erosion, and the impact of meteorites on the hard surface of exposed rock.

The slopes of lunar craters are likely to be covered by a layer of dust, whose thickness may increase to several hundred feet as one descends to lower elevations. This dust is relatively loose, because of the lessened gravitational field of the moon, and on account of the repulsive force of electrostatic charges. The surface of the dust layer is disposed on an inclination seldom exceeding 6°, equaling the angle of repose of this material under its environmental conditions. This dust is slowly migrating downhill, under pressure of reflected sunlight, solar proton bombardment and lunar gravitation. It may also be assumed that the dust covering lunar slopes is in a state of rather precarious equilibrium; any substantial disturbance (as created by lunar seismic activity, the impact of large meteors or the landing of instrument packages) might set off a lunar « dust avalanche ».

The bottoms of lunar craters are probably filled with dust strata that may range up to several kilometers in thickness. Under the weight of the overburden, the dust must be more compacted in lower stratifications. The electrostatic charging that the lowermost layers may once have acquired has

long since leaked away. It is also possible that deep layers of lunar dust contain some moisture, originating mostly from impacted meteors. The bottom layers, therefore, are compacted by the overburden, lack electrostatic charges, and may be cemented by moisture frozen into ice at the low temperatures prevailing here. Their apparent cohesion must be very high, since friction between the grains is likely to be substantial for absence of gaseous or liquid lubrication. Hence the bottom layers are likely to be quite hard. Even greater hardness would be encountered in areas where that heat of impact of colliding planetesimals acting on the lunar surface created localized lava flows.

Proceeding upward from the bottom of crater dust beds, density and apparent cohesion drop, until one arrives at the surface where the same fluffy conditions (under action of electrostatic forces) are expected to hold in the layers constituting the uppermost few feet as those already described for lunar slopes.

The dust cover of the maria is far thinner, by comparison. In convex maria the dust cover is of the order of centimeters in thickness; flat or concave maria are overlain by dust up to several decimeters thick. Beneath this thin mantle of dust lies rock of plutonic origin, basaltic in nature if it is the result of igneous processes or the melting of impacting asteroids, and of an iron-nickel composition if it represents the outpouring of a once-molten core.

The particle spectrum distribution of the lunar dust is likely to vary over quite a broad range, encompassing about five orders of magnitude (1 μ - 10 cm.), with a distribution highly skewed toward the finer particles. The finer constituents originate from the galactic dust shower and the condensation of meteoric material vaporized upon impact. The medium size particles are the result of the thermal defoliation mechanism, while the largest particles are made up of chondrites, achondrites and metallic meteorites which remained relatively intact upon impacting into the loose dust surface.

Excepting for the very bottom layers formed during the first few eons of the Moon's existence (when crater-shaping meteoric activity was high), the remainder of the dust, its source being mostly lunar rock and captured « galactic dust », is likely to be very close in composition to the chemical constituents forming the moon. This, in turn, is expected to be quite well represented by chondritic material, at least 40 % of which is composed of SiO_2. This may be interspersed with iron-nickel particles coming from iron meteorites, giving the dust a « raisin-bread »[3] appearance. The prevalence of iron-nickel components may be higher at the bottom, due to intensified meteoric impacts during the early stages in the life of our celestial companion.

This hypothesis for the lunar surface would help to explain the telescopic and radio observations regarding surface roughness. On the visible scale, the lunar surface would be rough, since most of the constituent particles of the lunar dust are larger than the wave length of visible light. On the other hand, lunar gravitation acting on the electrostatically excited surface dust would keep the upper layer smooth on the order of wave length of radio-observations (10 cm.); any impacting meteor or meteorite would be instan-

tancously enveloped into the surface dust and sink to lower elevations (since electrostatic forces in regard to larger particles are likely to be insignificant as compared to their effect on small particles, in direct proportion to the mass/surface ratio).

b) **Terrestrial planets.** — In brief, the terrestrial planets (excepting Earth) may be expected to possess the following surface conditions:

Mercury has a rugged surface, with extensive crater formations and a dust layer which is thin, but probably exceeds 10 cm. as a minimum. The origin of most of this dust is traceable to galactic dust; the mechanism of thermal defoliation is relatively inactive. Mercury always turns the same face toward the sun; its sun-baked side may hold molten pools of zinc, tin or mercury, while the shadowy side is frozen at a few degrees above absolute. Its atmosphere is very thin, at a surface pressure of about 0.2 mm. Hg; there are no violent storms nor any erosive forces acting on its surface. The planet is « dead », much like our moon.

Venus' surface is in a murky twilight, hot (300° C) and dry, overlain by an atmosphere that exerts a surface pressure of about 1500 mm. Hg and is composed principally of CO_2, CO, N_2, CH_4 and possibly O_2 and H_2O. The atmosphere is rent by violent storms, generating huge dust clouds, and exerting an enormous erosive action. Because of this, there are likely to be extensive and deep dust beds on Venus, but few surface features breaking the monotony of the terrain. The dust is ground to a particle size on the order of 2 μ or finer.

Erosive action is also forceful on *Mars* which, however, has retained some differences in elevation, as evidenced by plateaus and relatively narrow and shallow depressions (the canals). Most of the surface is dry desert land consisting of granulated or powdery iron oxide. A thin layer of vegetation covers about 1/4 of the surface, and a very thin ice-cap forms at the poles, the size of both of these regions changing with the seasons. The atmosphere is thin, its pressure being only about 1/10 that of the earth. This atmosphere, consisting of N_2, CO_2, CO, H_2O and noble gases is in violent motion and generates great dust storms. Oxygen, hydrogen, and helium are not expected to form part of the atmosphere. Because of the filtering action of the atmosphere, objects on the surface would acquire a deep reddish tint.

Considerations for landing on the moon

So little is firmly known about the surface conditions of the terrestrial planets that any hypothesis regarding their soil conditions must be considered, at best, as an educated guess. Therefore, we cannot indulge in the luxury of predicting conditions to be encountered upon landing on Venus, Mars, or Mercury, until scientific studies and further space explorations turn up more factual information on this subject. Fortunately, the need for this knowledge

is still some distance away, since Venusian or Martian landings are planned to take place only about a decade from now.

Landings on the *moon*, on the other hand, will be attempted very shortly. These landings (apart from the instrument package of Rover which is not expected to survive lunar impact) will consist of stationary instrument packages (the Surveyor series) and mobile land-roving instrumented vehicles (the Prospector series) partially controlled by remote command which will telemeter information back to earth. This will be followed, no doubt, by manned landings after sufficient data have been collected to make this adventure realistically safe. In this light is becomes a problem of immediate interest to consider the probable conditions pertaining to lunar landings.

By token of what was said before, the possible choices for a lunar landing would either be the barren rock of lunar crater rims, the shallow dust layers of the maria, of the deep dust beds of lunar low lands. As stated before, landings on lunar slopes may be disastrous.

Landings on the exposed rock of lunar highlands entail few unknown conditions. However, such landings would pose serious problems on account of the fact that these areas constitute only an extremely small part of the lunar surface. The guidance problems required to be solved to assure a correct impact location would appear to rule out this alternative. Also, cushioning or retro-rockets required to dissipate the energy of landing on the hard surface would incur added weight penalties for the package to be shot into a lunar trajectory.

Most logically, the landing target should be one of the lunar maria. These areas are reasonably smooth and wide open; therefore, comparatively easily impacted even without a control system of the most demanding accuracy. Landings in the maria, if their surface is as envisioned here, would be somewhat softened by dissipating some portion of the landing energy to permit the vehicle to scatter and partially settle into the thin dust layer covering the maria. Exploration of the craters and high topographic features would then be conducted from base camps established in the maria, utilizing tracked land locomotion vehicles.

The floors of craters (or mountain-ringed planes) would appear to offer a poor landing target. If our hypothesis is correct, and crater floors are filled with a thick layer of loose dust, the landing vehicle may settle into this dust until it is completely swallowed up. The use of retro-rockets would tend to help little, since this may only succeed in blowing a hole in the dust whose collapsing walls would finally engulf the vehicle.

Even for landings in the maria, one will have to learn what conditions of impact, deceleration, stability, resistance, consolidation, settlement and locomotion are likely to exist in dust layers in the centimeter-meter thickness range exposed to lunar environments. Some of this work is in progress now. However, much more research will be required before any firm conclusions can be drawn regarding the problems reviewed in this paper.

BIBLIOGRAPHY

1) Tomlinsugh C. W. Aerospace medicine conf. School of Aviation Medicine, San Antonio Texas, January 1960.
2) Kuiper G. P. Vistas in astronautics, II, 273-311, 1959.
3) Jastrow R. The exploration of the moon. Sci. Am., 202, 61-69, 1960.
4) Urey H. C. The moon. Science in Space, Chapter IV, N.A.S.N.R.C. Jt. Publ., 1960.
5) Gilbert G. K. Bull. Phil. Soc., Wash., 12, 241, 1893.
6) Urey H. C. Origin of the moon's surface features. - I) Sky and telescope, I, 108, January 1956.
7) Urey H. C. Origin of the moon's surface features. - II) Sky and telescope, p. 161, February 1956.
8) Moore P. Some lunar crater problems. Sky and Telescope, p. 201, March 1956.
9) Kiess C. C. and Lassovsky K. The known physical characteristics of the moon and the planets. ARDC-TR-58 41, ASTIA Doc. No. AD 115-617, July 1958.
10) Baldwin R. B. The face of the Moon. University of Chicago Press, 1949.
11) Fiehler G. J. Brit. Astr. Assn., 67, 8, 1957.
12) Gold T. Monthly notices of the R.A.S., 115, 585, 1955.
13) N.A.S.A. Lunar Research Conference, Astronautics, 45, 71-75, May 1960.
14) Jakob M. Heat transfer, vol. 1, p. 292-297. J. Wiley and Sons, N. Y., 1959.
15) Charles R. J. Fracture, p. 225-250. J. Wiley and Sons, N. Y., 1959.
16) Lindman W. G. and Bobrowsky A. R. NACA Techn. Note No. 1918, 1949.
17) Howie T. W. Trans., Brit. Cer. Soc., 45, 45, 1946.
18) Kingery W. D. Property measurements at high temperatures, p. 185-204. J. Wiley and Sons, N. Y., 1959.
19) Whipple F. L. Vistas in astronautics, 2, 267, 1958.
20) La Gow H. E. and Alexander W. M. Proc. First Internat. Space Symp., Nice, France, p. 1033-41, 1960.
21) Hoyle F. Am. Sci., 40, 188, 1961.
22) Green J. The physical characteristics of lunar surface. Proc. Lunar and Planetary Explor. Coll., 1, 1, 11-15, 1958.
23) Dollfus A. Comptes Rendus, Paris, 231, 1430, 1950.
24) Antoniadi J. Roy. Astr. Soc. of Canada, 27, 402, 1931.
25) Camichel. The Astrophys. Journal, 101, 258, 1945.
26) Sinton W. M. and Strong. Phys. Rev., 44, 99, 1933.
27) Mayer, McCullough and Sloanaker. The Astrophys. Journal, 127, 1, 1958.
28) Kraus. Nature, 178, 33, 1956.
29) Adams W. S. and Dunham T. Phys. Rev., 44, 99, 1933.
30) Schoenberg. Preuss. Akad. Wiss., 21, 353, 1930.
31) Hulst. Progr. in Phys., 13, 247, 1950.
32) Menzel and Whipple. Astr. Soc. of the Pacific, 67, 161, 1955.
33) Dole S. H. The atmosphere of Venus. The Rand C., Santa Monica, Cal., 27, 1956.
34) Herpberg J. Astr. Soc. of Canada, 45, 100, 1951.
35) Urey H. C. The planets. Yale Univ. Press, New Haven, 1952.
36) Kuiper G. P. The threshold of space. Pergamon Press, New York, 1957.
37) Richardson. Astr. Soc. of the Pacific, 67, 304, 1955.
38) Opik E. J. Journal Geophys. Res., 65, 3057, 1960.
39) Dollfus A. Astr. Soc. of the Pacific, 70, 56, 1958.
40) De Vaucouleurs G. Comptes Rendus, Paris, 220, 388, 1945.
41) Kiess C. C. et al. Astrophys. Journal, 126, 579, 1957.
42) Kuiper G. P. Atmospheres of Earth and Planets. Univ. of Chicago Press, 1949.
43) Richardson R. S. Astr. Soc. of the Pacific, 69, 23, 1957.
44) Opik E. J. Irish Astr. J., 5, 137, 1959.
45) Wright W. H. Astr. Soc. of the Pacific, 51, 202, 1939.

DISCUSSIONS

J. A. RYAN. — There are a number of comments which need to be made concerning this paper.

The first comment concerns the efficacy of electrostatic forces as a soil transport mechanism and as the cause of the high lunar soil porosity. Electrostatic forces can act as a transport mechanism and can cause high soil porosity provided « loose » material of sufficiently small size to be affected by such electrostatic charges is present and provided electrostatic charging occurs at the lunar surface. Let us consider these points in order.

As for « loose » material existing at the lunar surface we see that there are two mechanisms, sputtering and meteorite impact, which tend to produce cemented material [1,2,3]. However, since it is not to be expected that all the surface material is cemented [3], « loose » material can exist. The next question is whether material fine grained enough to be affected by electrostatic charges exists. To answer this question we can draw on the work done in the Soviet Union over the past thirty years on the photometry of the moon. This impressive volume of data has been analyzed, theoretically and experimentally, by two Russian investigators [4,5]. The results of this work are quite interesting, in fact they are almost too interesting since these investigators working independently but with the same data reach different conclusions about the nature of the lunar surface. However, they do agree that the optical behavior of the lunar surface cannot be reproduced in the laboratory by granular material less than about 70-100 μ in size. It would appear then that « loose » particles of a size small enough to be affected by electrostatic forces could at best constitute only a small percentage of the lunar soil material.

The final question is then whether the moon is electrostatically charged. The answer here seems to be that it is. A considerable amount of work has been done concerning the magnitude of this charge [6]. The best results to date indicate that the lunar surface may have a positive potential of 20-25 volts [6]. If one uses these values and considers what the charge density over the lunar surface must be to produce such a potential, it is found that even should the lunar soil consist only of grains small enough to be affected by electrostatic forces, the percentage of such grains which could maintain a charge at any one time must be quite small. It can be concluded, then, that as far as can be judged at present it is unlikely that electrostatic charges contribute significantly to soil transport or that such charges are the cause of the apparently high lunar soil porosity.

The second comment concerns the possibility of lunar surface temperature variations acting as a mechanism for the production of the lunar soil. The Author, in his mathematical treatment of thermal stresses, uses as a boundary condition the observed lunar infrared temperature changes. This is of course incorrect. The boundary condition which should be specified is the flux since if the lunar surface consisted of solid rock the temperature changes observed should be much less rapid and quite likely much small in magnitude than presently observed. The problem of a semi-infinite medium with the flux specified at the boundary has been solved by Jaeger [7]. Should the Author apply this treatment to his thermal stress calculations, he is likely to find that the maximum upper bound for the depth to which thermal fracturing could occur is considerably less than that given.

Another problem involved here is whether the theoretically calculated thermal

stresses are actually realized in the rock. A considerable amount of work has been done on the problem as to whether thermal fracturing is a factor in the mechanical disruption of rocks at the terrestrial surface[9-10-11-12]. It has been shown that thermal fracturing at the terrestrial surface is unlikely. Included in this work are experimental studies on various rock samples. These rock samples were heated rapidly to various temperatures and then plunged into ice water. It was found that the non-crystalline rocks could withstand such treatment without any microscopically visible change even when heated to temperatures somewhat in excess of 250° C. The polycrystalline rocks could withstand significantly higher heating temperatures. It can be shown theoretically that in many cases the rock samples should have broken yet they did not. These rocks have been formed by cooling from an initially molten state (≈ 1200° C). For the polycrystalline rocks, the various crystals have contracted by different amounts leaving gaps in the rock. Upon subsequent heating, sufficient expansion to close these gaps must occur before the thermal stresses can be realized. As for the non-crystalline rocks, the answer is not so obvious but it may be that innumerable small fractures, formed during cooling from the melt, may exist in the rock. During *any* subsequent heating these also must be closed before the thermal stresses can be realized.

One final problem is the possibility of fatigue from stress cycling. The best experimental results on fatigue available are those by Griggs[12]. He cycled a slab of granite over a temperature range of 110° C roughly ninety thousand times. At the end of this time microscopic examination showed no change in the specimen.

In addition to this, Tarr[9] heated various granite specimens to temperatures as high as 1000° C. These were then cooled, by water or air, and the compressive strength measured. It was found that up to a temperature somewhat greater than 250° C, no decrease in strength over that at 0° C occurred. In fact the strength increased slightly. At higher heating temperatures, a gradual loss in strength was noted. The maximum temperature changes at the lunar surface for exposed granitic rock are likely to be significantly less than 250° C. In addition, no moisture should be present. The effects of moisture on causing fatigue have been considered by Griggs[12] and Charles[13]. It cannot be concluded that fatigue does not occur at the lunar surface. However, the references quoted[9-12] indicate that if it does it must be an extremely slow process.

It can be concluded, finally, that it is quite unlikely thermal fracturing could play much of a role in the production of the lunar soil and that in fact there is no evidence which demonstrates that thermal fracturing will occur under the insolation variations extant at the lunar surface.

The third comment concerns radar reflection from the lunar surface. The Author states that reflections appear to come back only from the center of the visible disk and that the moon is perfectly smooth at radar wavelengths. As for the first statement, recent work has shown that signal is returned even from the limbs of the moon. An interesting paper in this regard is that by Leadabrand[14]. Concerning the second statement, there is a considerable amount of disagreement as to what the radar reflections do tell us about the lunar surface. Senior and Siegel[15] conclude that over large areas the moon is perfectly smooth at radar wavelengths. Daniels[16] concludes that the surface is pockmarked with innumerable craterpits covering a wide range of diameters. Pettingill[17] concludes that a reasonable fraction of the surface must have irregularities comparable to the wavelength of radar at 10 cm. Leadabrand[14] concludes that the moon in the vicinity of the center of the visible disk acts as a quasi-smooth reflector, but elsewhere behaves more like a rough scatterer. It is easy to see that there is no unanimity of opinion here so that the only thing that can be concluded at this

time is that on *the* scale of interest to lunar locomotion, paraphrasing Thomas Gold, the terrain is *closer* to that of the Sahara desert than to that of the Italian Alps.

The fourth *comment* concerns the angle of repose of the lunar soil. The Author states that the *angle* of repose of the lunar soil is about 6°. However, it has quite definitely been *shown*, experimentally and visually, that the lunar soil remains on even the very steep *slopes*. Thus the value of 6° is actually the average angle at which the soil reposes *rather* than the angle of repose.

The fifth *comment* concerns the question of how much exposed rock exists at the lunar surface. The Author states that the lunar highlands may be « scoured clean » of any dust cover. This view is refuted by all available evidence. This evidence includes the infrared, microwave, photometric and radar reflection results.

The final *comment* concerns the question of cosmic dust « infall ». The Author pictures this as *slowly* settling onto the lunar surface. However, it would appear unlikely that the *velocity* of these particles in space relative to the moon is small. In most cases it would be expected that this relative velocity (caused by terrestrial, lunar and cosmic *dust* motion in space and by the gravitational fields of the earth and moon) would *be* quite high, possibly well into the hypervelocity realm (> 6-7 km/sec for impact upon *rock*). The only reason small particles may « drift » down to the terrestrial surface *is* that a retarding atmosphere is present. Now, it is certainly true that such small *particles* as must comprise the cosmic dust will be affected by any electrostatic fields *existing* around the moon, but it is hard to believe, particularly if the initial relative *velocity* is high, that such particles would be slowed to the extent that they « drift » *down* to the lunar surface.

BIBLIOGRAPHY

1) Whipple F. L. Vistas in Astronautics, v. 2, pag. 267, Pergamon Press, 1958.
2) Wehner G. K. Amer. Rocket Society Jour., v. 31, pag. 438, 1961.
3) Ryan J. A. Some predictions as to the possible nature and behavior of the lunar soil. 1st International Conf. on the Mech. of Soil-Vehicle Systems, Turin (Italy), 1961.
4) Barabashov N. P. and Chekirda A. T. Soviet Astron. (trans.), v. 3, No. 5, pag. 827, March-April 1960.
5) Sytinskaya N. N. Soviet Astron. (trans.), v. 3, No. 2, pag. 315, March-April 1959.
6) Opik E. J. and Singer S. F. J. Geophys. Res., v. 65, No. 10, pag. 3065, 1960.
7) Jaeger J. C. Aust. J. Physics, v. 6, pag. 10, 1953.
8) Jaeger J. C. Proc. Camb. Phil. Soc., v. 46, pag. 634, 1950.
9) Tarr W. A. Econ. Geol., v. 10, pag. 348, 1915.
10) Blackwelder E. J. Geology, v. 35, pag. 134, 1927.
11) Blackwelder E. Amer. Jour. Sci., v. 26, pag. 97, 1933.
12) Griggs D. T. J. Geology, v. 44, pag. 783, 1936.
13) Charles R. J. Fracture, pag. 241, J. Wiley and Sons, N.Y., 1959.
14) Leadabrand R. L. et al. J. Geophys. Res., v. 65, No. 10, pag. 3071, 1960.
15) Senior T. B. A. and Siegel K. M. J. Res. Nat. Bur. Stand., v. 74 D, No. 3, pag. 217, May-June 1960.
16) Daniels F. B. USASRDL Tech. Rept. No. 2163, Nov. 1960.
17) Pettingill G. H. Lunar studies - Summer seminar. Mass. Inst. Tech., Aug. 1960.

N. A. WEIL. — The Author wishes to express, first of all, his appreciation for the interesting and enlightening comments made by Dr. Ryan to the paper on the probable surface conditions on planetary bodies. Since Dr. Ryan's comments are pertinent to lunar considerations only, the closing statements of the Author will be restricted to this body.

The discussion concerning the effect of electrostatic forces on particle migration

contributes some interesting information on this subject without, however, settling the arguments concerning this point. Until more is learned about this item, either by carefully controlled additional experiments or by data telemetered back by lunar landing satellites, one must assume that electrostatic charging of small particles may contribute to their mobility on the lunar surface.

The discussor suggests that the Author's approach to the treatment of thermal stresses in the lunar crust, by means of using known surface temperatures as the boundary values, is incorrect; instead, Dr. Ryan advocates the use of the solar flux as the correct boundary condition to be used in thermal calculations. This suggestion is spurious and poorly defined. While flux could be used as an indirect indication of boundary conditions, such could be done only if one knew (a) the total flux of solar energy radiated, (b) the portion of this flux that is turned into heat energy upon impingement on the lunar surface, (c) the reflectivity and emissivity of the lunar surface, (d) the reradiation from the surface into space. In addition, such an approach would have to take into account the incident angle of radiant energy.

Of the questions posed above, only (a) and (d) is known with any degree of certainty. Thus, the total solar energy radiated is about 1400 watts/m^2 and, for reradiation purposes, space can be assumed to be a black body at a temperature of 3.2° K. The other questions are not known with any degree of certainty. Moreover, while the discussor does not define the type of flux he has in mind, a correct application of his boundary conditions must lead to the same answers for subsurface temperatures as those obtained from surface temperatures as boundary values.

The lunar-surface temperatures, on the other hand, are known with a great deal of certainty from observed infrared measurements; Fig. 5 shows the temperature variation experienced over one-half a lunar day at the subsolar point. This surface temperature, if represented as an analytical function, is the direct and correct boundary condition that should be applied to the calculation of subsurface temperature. As stated in the paper, the real uncertainties in regard to this question are posed by the depthwise variation of thermal diffusivity in the lunar soil.

As concerns the case of fatigue of lunar rocks due to thermal stress cycling, evidence available to date is insufficient to establish firmly the influence that this effect might have had in degrading surface rocks. However, the evidence cited by the discussor is not directly applicable to this problem; thus, Tarr's work (discussor's reference 9) entailed a single thermal cycle, while Greggs' paper (discussor's reference 12) reports on tests of up to 9×10^4 cycles over a temperature range of 110° C. In contrast, lunar rocks experience a temperature range of about 290° C at the subsolar point, having been exposed to this cycling over some 8×10^{16} temperature reversals.

Some light can be shed on this question by the work of Coffin [1], Manson [2], Swindeman and Douglas [3], and Major [4], who have satisfactorily established that thermal cycling can be reasonably represented by mechanical fatigue conducted at the mean value of the temperature range and employing a stress range identical to the thermal stresses. At completely restrained thermal expansion, and for values of E and ν as shown in Table III of the text, this would call for mechanical cycling of representative lunar rocks with a stress range of 13,500 psi at a temperature of 0° F over a minimum of 10^7 cycles representative of the endurance limit of materials. Although to date no fatigue work has been carried out on allegedly brittle materials, such work will shortly be in progress, at least on single and poly-crystals of MgO and Al_2O_3, on a broad program dealing with the fundamentals of brittle fracture in ceramic materials [5].

The discussor's comments in regard to recent progress on radar reflection observations from the lunar surface are valuable. The principal recent contribution in this

regard is that of Leadabrand, who shows that considerable reflection takes place from the limbs of the moon, although in the vicinity of the center of the visible disk the moon acts as a smooth reflector. In this regard it should be considered that the lunar surface contains many irregularities, the most obvious of these being the craters, some of which are visible with the naked eye. If the surface is smooth at the 10 cm wavelength of radio waves, but contains roughness at larger distances, such a condition would still appear as a smooth surface at radio wave lengths under normal incidence. At oblique incidence, however, surface irregularities would become foreshortened proportionally to the sine of the incident angle. When this angle becomes small enough, the larger scale surface roughness will begin to show up even at the wave-length of radio waves. This phenomenon will become most pronounced at grazing incidence, that is, near the limbs of the moon.

Leadabrand's observations thus only add support to the picture of the lunar surface presented in the text. Even though the most pronounced crater chain happens to cut diagonally across the visible face of the moon, radar reflections from the center of the disk still indicate a smooth surface. Thus, the surface must be assumed to be smooth at the 10 cm scale, with limb reflections of radio waves traceable to the grosser surface irregularities of the lunar terrain.

The last comment of the discussor, discoursing on the supposed statement of the Author concerning the «slow settlement» of galactic dust on the lunar surface, is somewhat puzzling: a careful rereading did not turn up any such statement made in the text. If «slow» was inferred at any place, such referred to a time-wise slow accumulation of galactic dust; as the text shows, this may have amounted to a solid layer of only 2 mm in depth over a span of 7×10^7 years. Moreover, it is well known that the average speed of micrometeorites may range about 30,000 ft/sec; furthermore, the absence of a lunar atmosphere, and its corresponding drag forces was pointed up in Section II (c) of the text, under the discussion of Meritic Composition. Therefore, the discusser's comments on «drift» in the terrestrial atmosphere, and «slow settling» on lunar surface, while diverting, appear to have little relation to the subjects discussed in the paper.

BIBLIOGRAPHY

1) Collin L. F. Trans. ASME, 76, 931-950, 1954.
2) Manson S. S. Heat Transfer Symposium. U. of Mich., pag. 9-75, 1953.
3) Swindeman R. W. and Douglas D. A. Trans. ASME, 81 D, 203-212, 1959.
4) Major H. Jr. ASME Preprint No. 105, 1958.
5) Armour Research Foundation, «Studies on the Fundamental Factors Affecting the Brittle Behavior of Ceramics», in progress under direction of N. A. Weil on Contract No. AF33(616)-7465.

J. A. RYAN. — The Author has made a number of interesting comments [1] on this writer's paper [2] which deserve discussion. The discussions will follow the order in which the comments were presented by the Author.

The first comment concerns the effect of a vacuum on the internal friction. As stated by the writer [2], the presence of a vacuum will not necessarily increase the internal friction. Rather, it will increase the mechanical friction. Whether or not this will cause the internal friction to increase will depend upon the effect of increased mechanical friction on the soil porosity.

The second comment concerns the lunar soil porosity. It was not stated in the paper [2] that the lunar soil porosity is 90 %. Rather, it was suggested that, since radar

reflection results indicate a 90 % porosity and since there are processes acting at the lunar surface which may cause a high porosity, this possibility should be considered. In the extreme case where the soil consists of material that can cold-weld in vacuo, or where the soil is cemented, almost any porosity would theoretically be possible. Even if, as is likely, the soil is only partially cemented and the mechanical friction generally insufficient to cause welding, the additional presence of a reduced gravitational force makes it hard to believe that a lunar soil porosity of 90 % is not possible. As for the Author's statement that «the maximum porosity the lunar soil may have is that corresponding to the undisturbed settlement of particles», comments concerning the likelihood of undisturbed settlement have been made previously [2].

The third comment concerns the effects of radiation and meteorite impact upon soil grain shape. As for the effect of radiation, the Author has given an incomplete, hence misleading, quotation from the writer's paper. The complete statement reads, «radiation should tend to reduce grain angularity by erosion of the grain surfaces, but at the same time it would be expected that any dustlike material produced by this radiation would itself be angular». Further, radiation is not a «fracture mechanism» as such. The evidence showing that radiation could act as a soil producing mechanism comes primarily from studies of the metamict minerals. These are minerals which have been exposed to natural radioactivity over long periods of time and as a result have lost all vestiges of crystal structure. In addition, they have lost most of their internal strength, in some cases to the degree that they disintegrate into a powder. If radiation is to act as a dust forming mechanism at the lunar surface it will be through metamictization such as described here and not through fracture of crystalline grains. The products of such metamictization would tend to be angular. However, if the amount of radiation damage decreases with depth below the grain or rock surface, then this radiation damage could cause slow surface erosion, resulting in a reduction of angularity for the parent grain. Sputtering can also act to reduce grain angularity through grain surface erosion.

Only a brief comment needs to be made concerning the effect of meteorite impact on grain shape. There is no question that material mechanically disrupted by impact will tend to be quite angular. As for vaporized or liquefied material, this could only form spherical grains if it solidified prior to deposition and if the velocity at which these grains impact the surface is below that at which comminution can occur. It cannot be concluded at this time what percentage of spherical grains may exist at the lunar surface. However, it would seem to this writer that the percentage would be small.

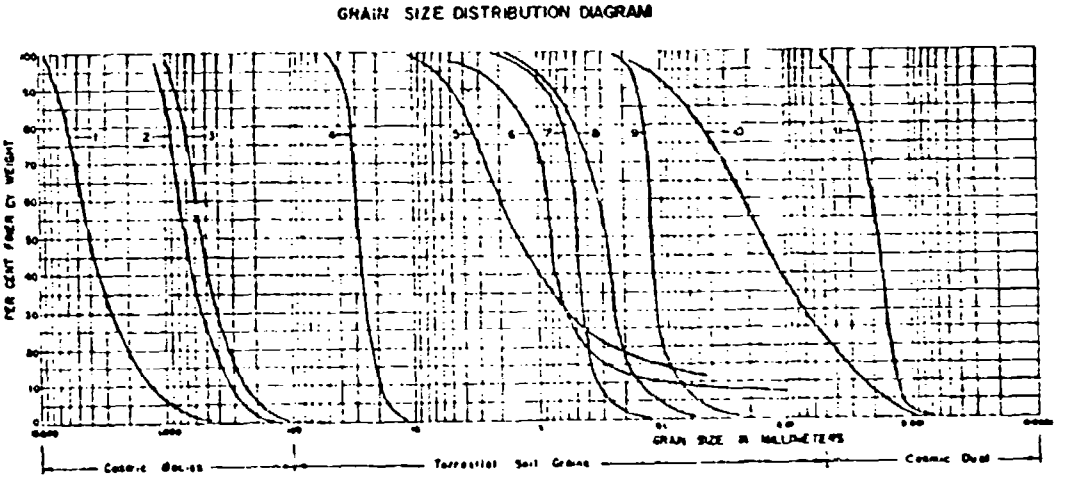
The fourth and last comment concerns the lunar soil grain size. The classification used by the Author (sand = 2.0-0.06 mm) is, of course, the M.I.T. classification. The classification used by the writer is the Bureau of Soils Classification. Fine sand, in this classification, is defined as consisting primarily of grains in the size range 0.25-0.1 mm. This classification has been used since the writer believes it to correspond roughly to the size range, for the unconsolidated portion of the surface, into which the greater percentage of lunar soil grains fall. The Author, however, believes the grains will be much smaller than this. Comments concerning this point are contained in the present writer's discussion [3] of the Author's paper [4].

BIBLIOGRAPHY

1) Weil N. A. Discussion to paper, Some predictions as to the possible nature and behavior of the lunar soils by J. A. Ryan. 1st Internat. Conf. on the Mech. of Soil-Vehicle Systems, Turin (Italy), 1961.

2) Ryan J. A. Some predictions as to the nature and behavior of the lunar soils. 1st Internat. Conf. on the Mech. of Soil-Vehicle Systems, Turin (Italy), 1961.
3) Ryan J. A. Discussion on paper, Probable soil conditions on the moon and terrestrial planets by N. A. Weil. 1st Internat. Conf. on the Mech. of Soil-Vehicle Systems, Turin (Italy), 1961.
4) Weil N. A. Probable soil conditions on the moon and terrestrial planets. 1st Internat. Conf. on the Mech. of Soil-Vehicle Systems, Turin (Italy), 1961.

M. G. BEKKER. — The short time alotted to this discussion prevents me from commenting on Dr. Ryan's and Weil's remarks concerning lunar soils. I would like, however to contribute to the discussion by reporting to this conference some details regarding the possible particle size distribution of lunar soils.



Note: 1: Asteroids (H. Brown); 2: Iron methеorites (H. Brown); 3: Stone meteorites (H. Brown); 4: Cheril bank gravel (England); 5: Hong Kong decomposed granite; 6: San Paolo Sand (Brazil); 7: Cape Cod Sand (U.S.A.); 8: Mason Sand (Otae, Detroit, U.S.A.); 9: Pumice, grade 0 (G.M., U.S.A.); 10: Upper Silesia Sand (Poland); 11: Cosmic Dust (Oort).

Professor Brown of California Institute of Technology has recently published a paper in which he compared the size distributions of meteors and asteroids. He found that respective frequency distribution curves are similar, and suggested that there may be a universal cosmic law which shapes these curves.

Professor Brown's curves have been replotted by the Land Mobility Laboratory of General Motors Corporation; on the same graph we have plotted particle size distribution of graded terrestrial soils, as shown on the slide. In this manner, we produced comparable curves pertaining to the distribution of the celestial bodies having a few kilometers, and the soil grains having a few microns in diameter.

The similarity of these curves is striking and further suggests the existence of a «universal» law as proposed by Professor Brown.

The ungraded soils 5 and 10 as shown on our graph have different distributions. This indicates that the forces that tend to eliminate the extreme sizes on both ends of the curve during the grading process are independent of the environment of their operation.

What now remains to be done is to locate a few points of lunar soil distribution, if there is such a thing on the moon. The one could probably safely assume the shape of the curve similar to that for meteors, asteroids and graded soils.

May I note, as a curiosity that particle size distribution of pumice which we use in the Land Mobility Laboratory (curve 9) has by a strange coincidence almost the same shape of distribution curve at that of the meteors.

J. J. MURRAY. — If a significant dust layer covered the lunar surface, then meteorite impact should have given rise to dust rings in orbit about the moon. Since no such rings are observable would it not appear that the surface must be essentially solid?

J. A. RYAN. — I am not sufficiently familiar with the dynamics of ring formation to be able to say what percentage of the material disrupted by impact could enter a closed lunar orbit nor how stable such orbits might be. I would, however, tend to believe that the amount in orbit at any one time would be small.

As for the surface being essentially solid, and I presume you mean the exposure of bare rock at the surface, all the experimental evidence indicates that little or no such rock is exposed.

E. SAIBEL. — I would like to say a few words about the fracture of brittle materials. There have been two points of view presented here on the nature of fracture as it might or might not have arisen from thermal action. Now, testing a rock or testing a glassy substance on a small scale has relatively little, in fact almost nothing, to do with its behaviour in a large mass. The fracture of glassy materials on rocks, or for that matter most brittle substances, is a matter of the imperfections or the stress raisers that exist in these materials. And certainly there must be, in the rocky structure of the moon, billions and billions of these imperfections. No matter how small the motion may be, whether it be due to thermal stresses, whether it be due to tidal action of the sun, or vibrations of one sort or another these elements of rocks are going to be stressed in fatigue, and sooner or later, I would say that it is almost certain, fractures will occur.

J. A. RYAN. — The difference between Dr. Weil's opinion and my own concerns the degree to which thermal fracturing (from variations in insolation) can occur and can act as a soil producing mechanism at the lunar surface. I certainly cannot prove that thermal fracturing does not occur, but I do not believe it could occur to the degree postulated by Dr. Weil.

As for fractures existing on the lunar surface, this is certainly the case. Observation of the moon has shown the existence of many such fractures. Since the moon at one time was closer to the Earth than it is at present it may be that these were formed by the increased tidal pull. It has been postulated that on a small scale (below that which can be seen through the telescope) innumerable fractures may exist. I would not be surprised if this is so. However, even if some of these were of thermal origin, which I doubt, there is a big step involved between saying that such fractures are present and saying that this is a soil producing mechanism. A considerable size difference is involved.

W. J. TURNBULL. — The papers by Messrs. Ryan and Weil are very interesting, and particularly interesting was the lively discussion between the two Authors following the presentation of their papers. This discussion left little room and need for discussion

by the panel members; however, it is desired to make a few comments, especially with respect to possible behavior of lunar soils.

A most comprehensive treatment of the effects of pressure, temperature, radiation, and gravity on the bearing and shearing strengths of lunar dusts is found in the papers Messrs. Ryan and Weil prepared for this meeting. Ryan states that the net effect of vacuum conditions on lunar dust may cause little change in internal friction and that the effects of lunar gravity would decrease the internal friction. It would appear then that the internal friction of the lunar soils would be less than that of cohesionless terrestrial soils. He states that this would certainly be the case if the lunar soil porosity is as great as 90 per cent. However, if due to the effect of meteoritic impact the porosity is not much greater than that of cohesionless terrestrial soils, or if cementation is present, the internal friction of lunar soils may well be greater than that of such terrestrial soils. Ryan concludes that the determination of which case is more likely must await experimental data on soils in vacuo and data concerning lunar soil porosity. Ryan does not consider possible peculiarities of soil structure resulting from in-vacuo deposition, or peculiarities in grain shape or structure. If eventually we find that lunar soils have porosities approaching 90 per cent, due to particle shape, electrostatic charges, or other factors, we can well be in plenty of trouble trafficability wise if the lunar dust layers have appreciable thickness.

Some experiments concerning soils in vacuo have been conducted by the Radiation Laboratory of the University of Michigan. These investigations indicated that, within the limits of the particle sizes studied, falling steel balls penetrate deeper under vacuum conditions than under atmospheric pressure. Three grades of fairly angular silica sand with grain size ranges of 11 to 90, 90 to 177, and 177 to 420 microns were studied. A suggested explanation is that when air is removed, the particles of sand form a wider spaced lattice due to their rough edges touching. In other words, the rough edges may support the particles in a more unstable array; and when the ball hits, it breaks down this loose lattice. Another possible explanation is that compression of air within the layer of sand or dust retards penetration.

From a soil mechanics standpoint one may postulate that lunar soils, exclusive of any cementation effects, are likely to be angular and granular and hence exhibit no cohesion. Thus, their behavior would be expected to be analogous to that of dry sands. We have practically no knowledge at present to indicate the effects of gravity, vacuum, radiation, etc., on the soil properties; thus, we cannot say with certainty whether lunar soils would be stronger or weaker than terrestrial sands. If the particle size of lunar soils is very small, then they may exhibit properties akin to rock flour.

If the foregoing turns out to be a fair picture of the case, then soils engineers will not be confronted with the problems of cohesive soils. In this respect the problems of cohesionless granular materials will be simpler to deal with unless it so happens that the particle sizes are those of rock flour, in which case severe mobility problems could exist, particularly for tires.

The things the soils engineer would want to know about lunar soils are: particle size gradation, particle composition, angularity, degree of packing (void ratio), cementation of particles or lack thereof, and effects of vacuum, radiation, reduced gravity, etc., on the soil properties. Once these are known or can be postulated, a reasonable estimate of lunar soil behavior can be made.

Of the many avenues of study which might be pursued, two are:

a) The study of stone meteorites (whose origin is presumably known) as to composition and structure, and then, by analogy, a determination of the most nearly similar terrestrial rocks. Once these are found, a study could be made of their residual

soils, in place. The rocks could also be subjected in the laboratory to lunar conditions of stress and temperature. This could contribute to an improved hypothesis of the origin of lunar soils.

b) More detailed and comprehensive studies of rock flour and fine and medium sands in vacuo as to their physical characteristics and behavior.

J. A. RYAN. — Thank you, Mr. Turnbull. I have a few brief comments that may be of interest here. The first comment concerns the possible 90 % porosity for the lunar soil. Whether or not a 90 % soil porosity is a «dangerous» condition depends upon what causes this high porosity. The second comment concerns the work done at the Radiation Laboratory of the University of Michigan. I am familiar with this work and might mention that Dr. D. Bowen, North American Aviation, Inc. (Proceedings of the Lunar and Planetary Exploration Colloquium, Vol. 1, No. 1, p. 12, 1958) performed similar experiments and concluded that the sphere did not penetrate as deep in vacuo as it did in air. Prof. G. Kennedy, Institute of Geophysics, University of California at Los Angeles (unpublished paper entitled «Surface characteristics of the Moon») also performed such experiments, but concluded there was no difference in penetration depth.

R. L. SCHIFFMAN. — There seems to be a very serious question as to whether or not there is any appreciable «dust» layer on the moon. It appears that in the absence of any direct information one can build reasonably good arguments on either side of the argument.

Certainly from the Soil Mechanics point of view, any considerations of vehicle mobility must assume that there is a surface layer of fine particles of sand and silt sizes. These remarks are predicted on this speculation.

From a mobility standpoint, the complete absence of other coherent forces, result in shearing strengths of the dust far lower than we are accustomed to dealing with on earth. As a result the areas of very fine dust particles are likely to be in a state that will prevent traverse without stabilizing treatment. The most obvious treatment is a chemical being sprayed in advance of the traversing vehicle. To my knowledge the present chemicals used for stabilizing granular soils require oxygen to complete the reaction. Thus is will become necessary to develop chemicals which will solidify in the attenuated atmosphere of the moon.

It appears to me that there is so much speculation concerning the nature and properties of lunar material that the first step that is needed is a rather substantial investigation of the surface of the moon. I believe that the present programs for a lunar investigation will go a long way towards determining if there is a dust layer in the first place and if so the nature of this material. It is my hope that the instrumentation of the presently planned lunar exploration probes will be of such a nature as to send back information on the nature and quality of lunar surface materials that would be applicable to mobility design.

J. A. RYAN. — I might make a comment on this. The source of the information that there was a large dust could formed at the impact point was a Hungarian observatory. At a meeting in Los Angeles, held shortly after this lunar impact, Prof. Z. Kopal from the University of Manchester stated that these particular observers were «notoriously unreliable» (Proceedings of the Lunar and Planetary Exploration Colloquium, Vol. 2, No. 1, p. 32, 1959).

SUOLO E VEICOLI

SOIL AND VEHICLES

N. 49

A suggested empirical combination between the Bekker and the Vicksburg methods in trafficability analyses of deep loose sands

Proposta di una combinazione empirica tra i metodi di Bekker e di Vicksburg per l'analisi delle possibilità di traffico su sabbia sciolta

TRAFFICABILITY RESEARCH TEAM *)

ABSTRACT. — *There are two methods used in trafficability analyses of soils. They are the Vicksburg and the Bekker methods. The Bekker method is a theoretical one. Its computation procedure follows a series of nomograms, once a number of physical factors have been established either experimentally or from recorded past knowledge. The Vicksburg method is an empirical one particularly applicable to fine grained soils. Soil strength, which is a measure of trafficability, is measured in terms of cone index and is known to vary with moisture content for a given soil.*

Graphical relationships have been established by the Vicksburg method for the vehicle classes of tanks, half track, and wheeled vehicles, correlating cone index differences with per cent climbing slopes in fine grained soils.

In sands no generalization may be made. Cone index versus per cent climbing slopes must be established for each individual vehicle. The need for reducing such costly and time consuming evaluations demands development of a more efficient method.

Observations from trials performed by the Israeli Army have led to a suggested empirical short cut method of establishing the desired cone index versus slope graphs for deep loose sands.

The Bekker factors of $K_c = 0$, $K_\phi = 3.5$, $n = 1/2$ for deep loose sands were shown experimentally to correspond to a 70 cone index by the Vicksburg method.

For $K_c = 0$, $K_\phi = 3.5$, $n = 1/2$ one may compute with the aid of the Bekker's nomograms the maximum climbing slope of a desired vehicle. Having this value and the corresponding 70 cone index, one point is already available for constructing the graph. With the aid of a second theoretical point of $\sim 60\,\%$ climbing slope corresponding to an optimum obtainable cone index of 300, one may now proceed and draw the desired graph which has a tendency to follow a straight line.

Future work is suggested to be aimed at comparing a wide range of the Bekker's factors with cone index values.

Introduction. — There are two methods in use in trafficability analyses of soils: the Vicksburg method and the Bekker method. A basic difference exists between the Vicksburg method developed by the Corps of Engineers U.S. Army and the Bekker method developed by the Ordnance Corps, U.S. Army.

*) Corps of Engineers, Israel Army.

The first one is an empirical and a statistical method designed to fulfill the requirements of the Corps of Engineers. The second method is a theoretical one being used in the development of new vehicles.

This paper introduces a suggested empirical application of the Bekker method to the Vicksburg method in the trafficability analyses of deep loose sands.

Observations thus far have only been made on sands of one type, those corresponding to the Bekker factors of $K_c = 0$, $K_\phi = 3{,}5$ lb/in^{n+2}, $n = 1/2$.

Characteristics of the two methods. — *The Bekker method.* - In his book [1] « Theory of Land Locomotion », Bekker lists 11 factors needed in defining the exact performance ability of a vehicle in a cross-country locomotion.

Seven of the factors are considered to vary with changes in moisture content. They are:

- c = cohesion;
- Φ = angle of friction;
- k = moduli of sinkage, depending on cohesion and friction angle (k_c, k_ϕ);
- n = exponents of sinkage;
- K_1 = exponents of slippage;
- K_2 = exponents of slippage;
- γ = bulk density.

Their evaluation require special laboratory conditions and various instruments.

Other factors are related to the surface and not assumed to vary with changes in moisture contents i.e. climatic changes. They are:

- L_w = Length of surface wave;
- hw = Height of surface wave;
- ho = Height of obstacle;
- Lo = Width of trench.

In report 41 [2] « A definition of soil trafficability » (June 1958), Bekker points out that for his method to be applicable to a wide range of soils there must be a gathering of extensive data and an elaborate cataloguing of the above mentioned seven factors from a great number of soils. Such a cataloguing work is not available as yet for it requires a long period of time, thereby limiting a direct employment of the Bekker procedure.

The Vicksburg method. - In place of the seven variable factors used by Bekker, the Vicksburg method employs one single value, called the Cone Index value. The Cone Index is an instrumentally measurable factor. It measures the mechanical strength of the soil. Although an empirical and a statistical value. The Cone Index is a practical parameter because it is easy to obtain and to interpret by the military man who is not an engineer.

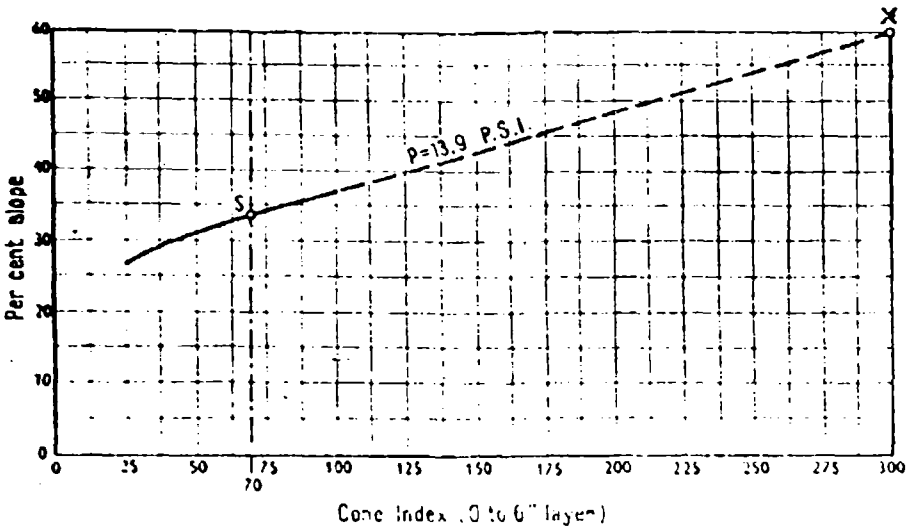


Fig. 1. — Performance of M-4 medium tank in deep loose sands (7).

Land is heterogenous within short distances with regard to soil strength and a large number of Cone Index values are hence required. The Cone Index approach has the advantage that it does not necessitate a large and highly trained crew to determine soil strength satisfactorily. Cone Index may also be related to changes of soil moisture contents in different soils.

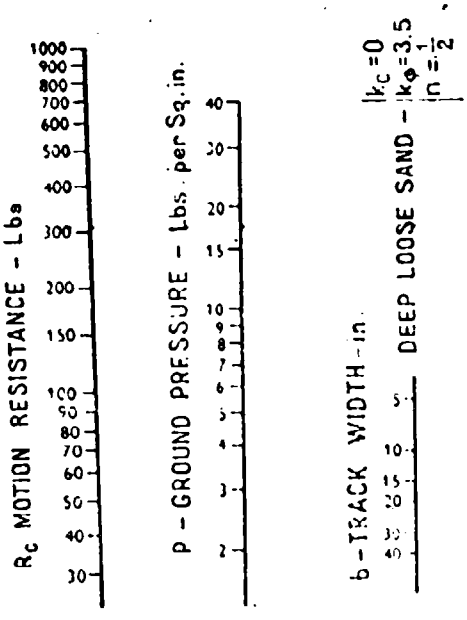
Drawbacks in the Vicksburg method in analysis of deep loose sand. — By the Vicksburg method, any vehicle has a specific and computable Vehicle Cone Index. It remains constant for that vehicle depending upon the vehicle's mechanical characteristics.

A difference in values between Soil Cone Index and Vehicle Cone Index is a measure of that soil's trafficability on slopes [8].

For cohesive, fine grained soils where the Soil Cone Index is a factor dependent on moisture conditions, the Vicksburg method has been able to correlate the differences between Soil Cone Index and Vehicle Cone Index with climbing slopes for whole classes of vehicles, such as tanks, Half tracks, wheeled and towed vehicles.

Such correlations for the four great vehicle classes could not be obtained in coarse grained soils (non cohesive deep loose sands) [7-9]. In this case the function of Cone Index versus climbing slope has to be established separately for each and every individual vehicle, by laborious field trials.

Thus, saving in costly and time consuming trials would result in greater efficiency. The incentive was thus furnished for seeking possible combinations between the theoretical Bekker method, computable in an office, and the Vicksburg method, to see if the number of field trials could be reduced.



This chart is based on the equation:

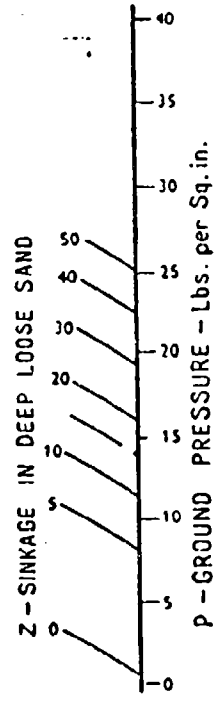
$$R_c = \frac{1}{(n+1)\ (b\,k_\phi)^{1/n}} \left(\frac{W}{l}\right)^{\frac{1+n}{n}}$$

Where:

R_c = Resistance to motion
W = Total track load (lbs)
P = Ground pressure (lbs./sq. in.)
b = Track width (in.)
l = Length of contact area (in.)
k_ϕ,n = Empirically determined soil parameters

Combine the corresponding values on b and P. Extend the line to R and read where it is being intersected.

Fig. 2. — Resistance to off-the-road motion of track produced by soil compaction.



This chart represents the equation:

$$P = (k_\phi)\ Z^n$$

Where:

P = Ground pressure (lbs./sq. in.)
Z = Sinkage experienced under static loading (in.)
b = Track width (in.)
k_ϕ, n = Empirically determined soil parameters

Sinkage is being directly obtained from ground pressure.

Fig. 3. — Sinkage of track.

This chart is based on the equation:

$$R_b = \frac{b \sin(\alpha + \phi)}{2 \sin\alpha \cos\phi} (\gamma Z^2 k_\gamma) + \frac{\pi \gamma t^3 (90 - \phi)}{540}$$

$$k = \left[\frac{2N}{\tan\phi} + 1\right] \cos^2\phi$$

Where:

R_b = Resistance to motion produced by bulldozing of soil (lbs.)
b = Track width (in.)
α = Angle of approach 45°
Z = Sinkage of track (in.)
t = $Z \tan^2(45 - \phi/2)$
γ = Specific weight of the soil 0.05 lb. per cu. in.
ϕ = Angle of internal friction of the soil.

Combine corresponding values on Z and b. Extend the line to R_b and read where it intersects.

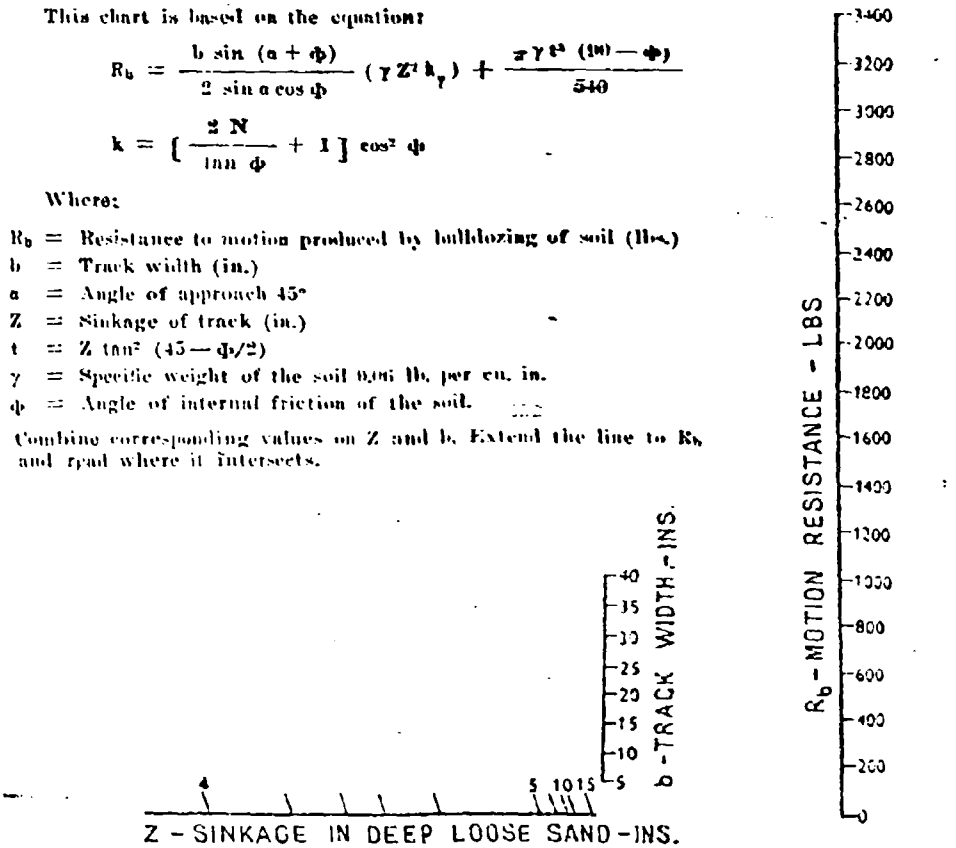


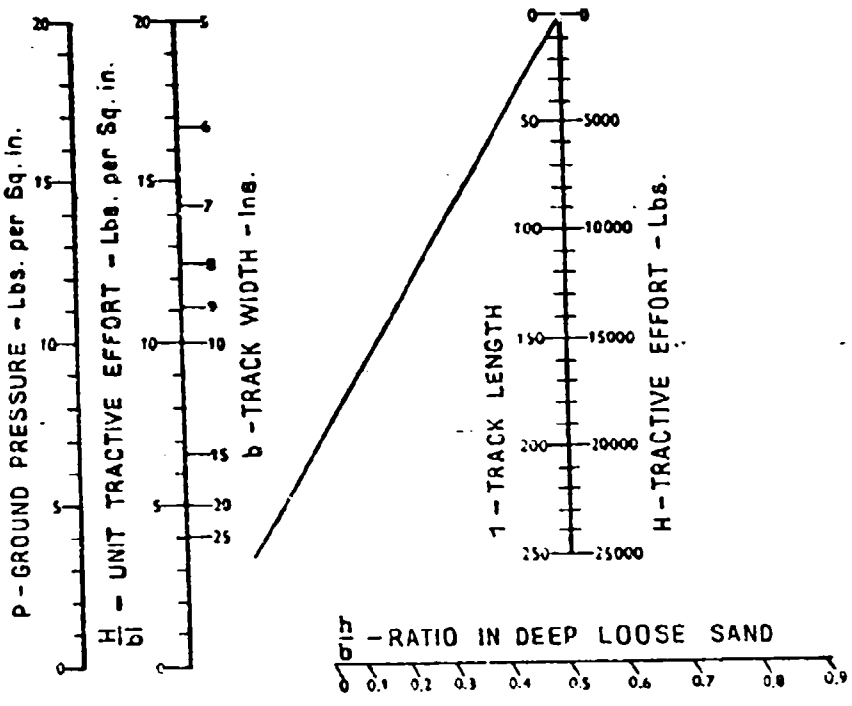
Fig. 4. — Resistance to off-the-road motion of track produced by bulldozing of soil.

Investigations in the field, and subsequent analyses were made for this purpose.

Figure 1 [5] depicts the performance capability of a M4 Sherman tank in deep loose sands as established by the Corps of Engineers. The abscissa represents the sand Cone Index of the 0-6" layer and the ordinate represents the per cent climbing slope.

A suggested empirical method of combining the two methods. — It should be stressed again that the Bekker method is a theoretical one used in the design and development of vehicles.

Computations by this method follow a series of nomograms adapted for deep loose sand from Bekker's work [3], and shown in figures 2-3-4-5. From these nomograms a theoretical performance capability may be found. The performance capability expressed in the maximum climbing slope of a tank,



This chart is based on the equation:

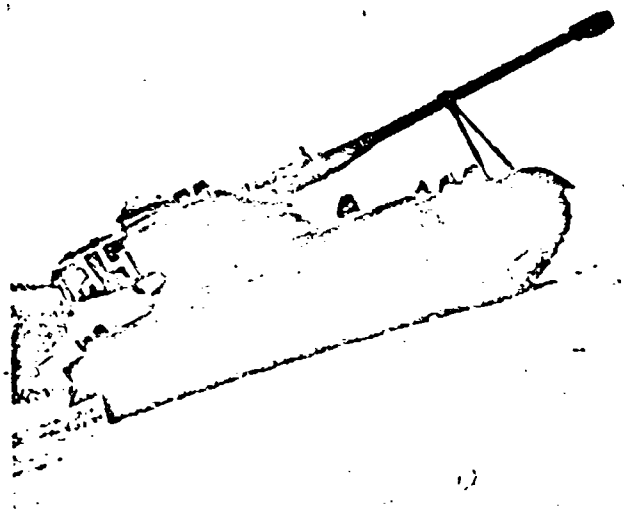
$$H = W \tan \phi \left\{ 1 + 0.64 \left[h/b \cot^{-1} \left(\frac{h}{b} \right) \right] \right\}$$

Where:

H = Gross tractive effort lb,
W = Load on track Lb.
P = Ground pressure Lbs./Sq. in.
b = Track width ins.
l = Contact length of track ins.
h. = Grouser height ins.
ϕ = Angle of internal friction

Combine the corresponding values of l and b. Mark the point of intersection with the tilted line as d. Combine P with $\frac{h}{b}$. Mark the point of intersection with $\frac{H}{bl}$ as f. Combine f and d and extend the line to read off H.

Fig. 5. — Tractive effort of track.



W = 31800 Lbs.
b = 13.5 ins.
L = 110 ins.
h = 1 in.
P = 10.7 Lbs./Sq. in.

Fig. 6. — A M X (French) Tank - Tecnical data.



R = R_C + R_h = 7400 Lbs. (Reading)
R_C = 1800 Lbs. (Computed)
R_h = 5600 Lbs. (Computed)

Fig. 7. — Resistance to off-the-road motion (total) for the A M X Tank.

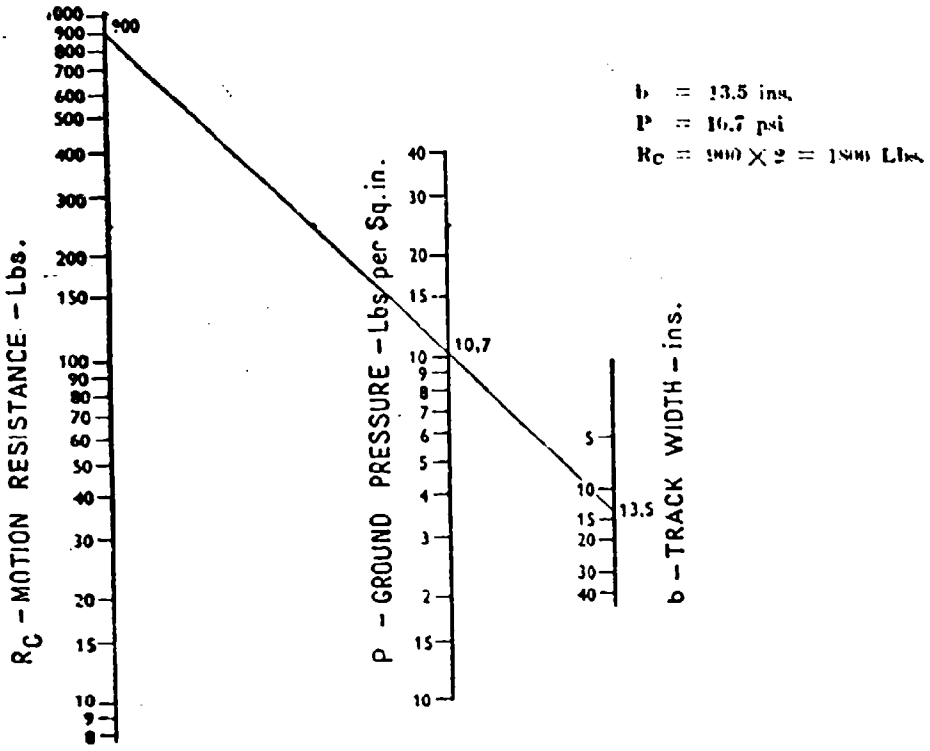


Fig. 8. — AMX (French) Tank.

or in the power difference that exists, with which a tank could pull other vehicles.

A prerequisite to the solution by this method is the establishing of the Bekker's soils factors. For deep loose sands, Bekker had worked with the factors: $k_c = 0$, $k_\phi = 3{,}5$ lb/in^{n+2}, $n = 1/2^{+4}$.

Trials in Israel were performed in deep loose sand regions apparently possessing the same values for the three factors. These factors were evaluated by an indirect measurement. Dynamometer tests were made at the sites and revealed that the Rolling resistance of several tanks on a level ground equalled the values computed by the Bekker procedure, assuming the three factors to have values as above. The corresponding Cone Index readings were determined to be 70 by field tests at the same time.

Thus, 70 Cone Index found corresponding the Bekker factors of $k_c = 0$, $k_\phi = 3.5$, $n = 1/2$, on that particular flat and level sand site.

Trials at other sites in the region revealed that the sand there had similar physical properties, when actual climbing slopes equalled those computed by the nomograms, assuming k_c, k_ϕ and n as above. For those sites as well, the same Cone Index of 70 was also found.

The relationship depicted by Fig. 1 is a slightly curved line, tending to follow a straight line for Cone Index values beyond point S (higher than 70). A definite relationship as shown by a solid line in fig. 1, is shown only up to Cone Index values of about 100, since higher Cone Index values are rare

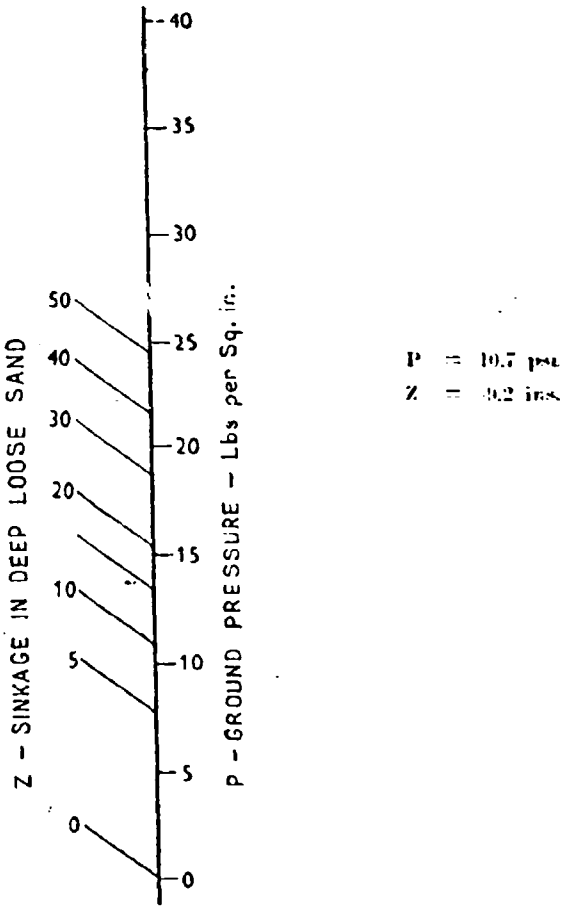


Fig. 9. — A M X (French) Tank.

in deep loose sands. The broken line section of the graph, however, has been drawn to represent a hypothetical relationship for higher Cone Index values. It is possible to predict the location for higher values for a very firm material, as represented by a Cone Index of 300. The corresponding maximum climbing slope of the M-4 tank is 60 ½ °. Hence, this point may be established theoretically, as represented by X on fig. 1.

Being able to establish those two points, X and S, one may proceed and

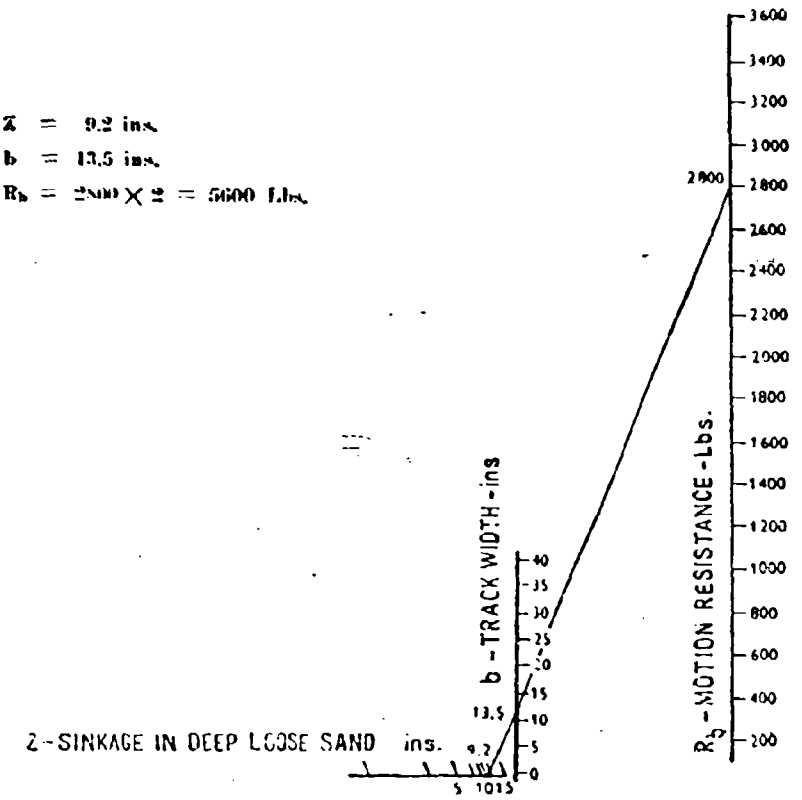


Fig. 10. — A M X (French) tank.

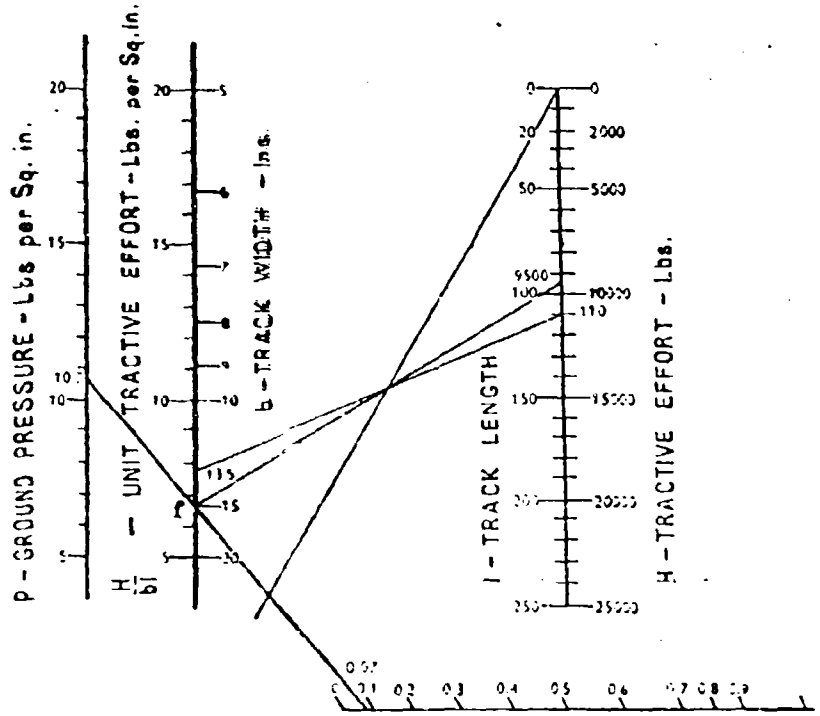
draw a Cone Index versus per cent slope relationship for a desired tank, as a straight line between X and S, curved downward gradually for values lower than S.

Sample computation for the French A M X tank. — Figs. 2 to 5 inclusive in the appendix represent Bekker's nomograms used in the computations.

Fig. 6 shows the French A M X tank technical data as required for the computations by the nomogram procedure.

Fig. 7 depicts the total rolling resistance R of the A M X tank as obtained by a dynamometer reading.

Figs. 8 to 12 inclusive depict the computation procedure for the A M X tank, following the system of the nomograms; figs. 2 to 5. The rolling resistance $R_b + R_c = R$ was determined to be identical to the dynamometer reading demonstrating that the factors as proposed by Bekker for deep loose sands were applicable to this area. The maximum climbing slope thus obtained was 37 %, as shown in fig. 12.



b = 13,5 ins.; l = 110 ins.; h = 4 in.; P = 10,7 psi.
H = 9500 × 2 = 19000 Lbs.

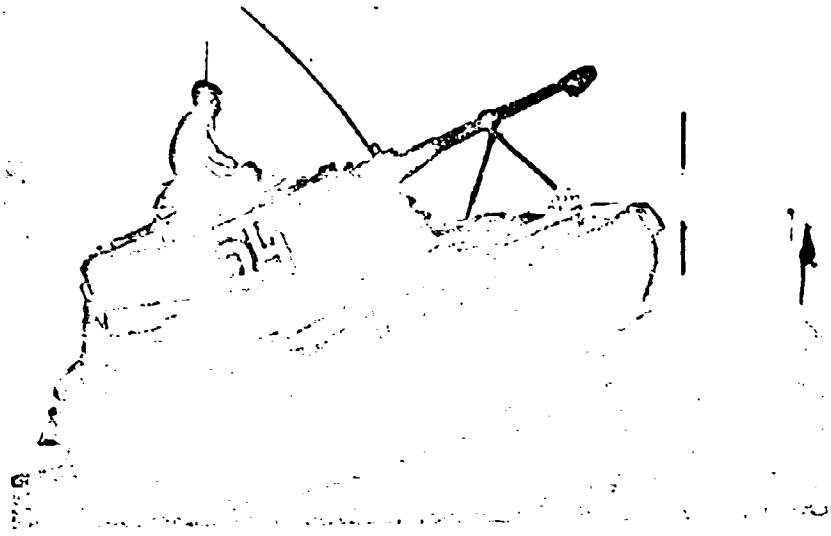
Fig. 11. — A M X (French) Tank.

Fig. 13 was drawn with the aid of point X, 300 Cone Index versus 60 % slope and the aid of point S, 70 Cone Index versus 37 % slope. These two points were joined by a straight line and the extension of the line to values lower than 70 was curved gradually. The other points marked on the graph represent field trials readings, as listed in table 1, taken to check the theoretical computations.

TABLE 1. — *A M X Tank field trials.*

Average	Cone Index *)			If stopped	Slope	Region	No.
	6"	3"	0"				
31.6	53	42	0	No	29,3	IV	1
50	94	55	0	Yes	35,1	IV	2
68	134	72	0	Yes	38,1	IV	3
34	58	45	0	No	29,3	IV	4
32	46	51	0	Yes	46,4	IV	5
36,6	63	47	0	No	27,1	IV	6
36,3	65	42	0	No	21,8	IV	7

*) Each tabulated Cone Index value is an average of 10 field readings.



D.P. = H − R
H = 19000 Lbs.
R = 7400 Lbs.

$$i_{max} = \frac{D.P.}{W}$$

D.P. = 19000 − 7400 = 11600 Lbs.
W = 31800 Lbs.

$$i_{max} = \frac{11600}{31800} \cong 37\,\%$$

Fig. 12. — AMX (French) Tank - Maximum climbing slope.

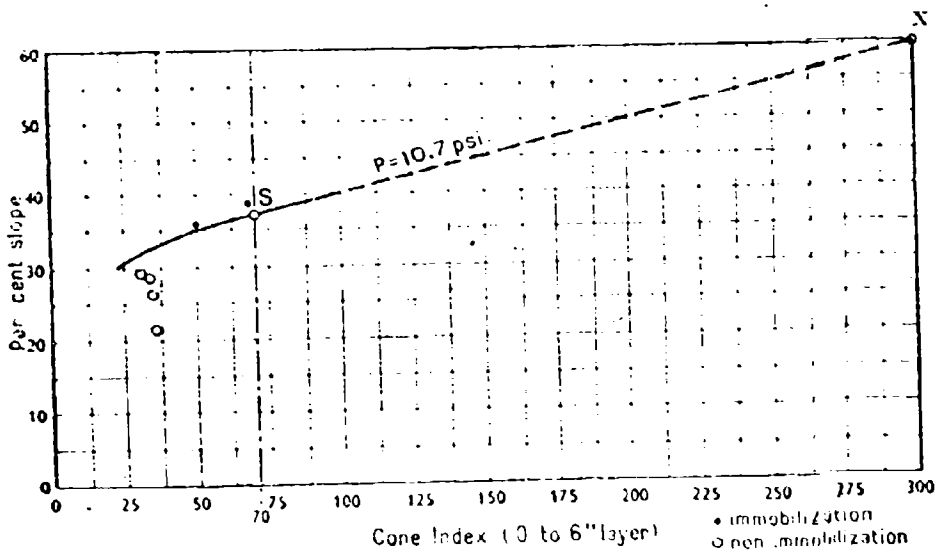


Fig. 13. — Performance of AMX (French) Tank in deep loose sands.

Conclusions. — The empirical method suggested above leads to the conclusion that there is scope for trafficability prediction for deep loose sand.

Should this study be continued more extensively there can be much time and effort saved in computing trafficability for such soils, where both the Bekker and the Vicksburg methods contribute to the solution.

This study had thus far been limited to Bekker's factor of $K_c = 0$ $K_\phi = 3.5$ $n = 1/2$ and 70 Cone Index. Future work is proposed to concentrate on correlating a range of Bekker's factors with Cone Indices in conjunction with vehicle performances.

ACKNOWLEDGMENT. — The Trafficability Research Team wishes to acknowledge its gratitude to Professor Joseph G. Zeitlen, Chairman, Department of Soil Engineering, Israel Institute of Technology, Haifa, for his guidance and assistance in the preparation of this paper.

BIBLIOGRAPHY

1) Bekker M. G. Theory of Land Locomotion.
2) Bekker M. G. A definition of Soil Trafficability. Report No. 11, Land Locomotion Research Branch, Ordnance Corps, June 1958.
3) U. S. Ordnance Corps. Research Report No. 4, Land Locomotion Research Laboratory, 1956.
4) Weiss S. J. Techniques for the evaluation of track and road wheel design. Report No. 4, March, 1956.
5) U. S. Ordnance Corps. Interservice vehicle mobility symposium. Land Locomotion Research Laboratory, 1955.
6) U. S. Corps of Engineers. Trafficability studies. Research and Development Reports. Supplements 1 to 12 (inclusive), 1948-1954.
7) U. S. Corps of Engineers. Pilot study, tests on Coarse. Grained Soils, Supplement 13, Research and Development Report, November, 1955.
8) U. S. Corps of Engineers. A summary of trafficability studies through 1955, Supplement 14, Research and Development Reports, December, 1956.
9) U. S. Corps of Engineers. Test on Coarse Grained Soils with self-propelled and towed vehicles 1956-1957. Supplement 15, Research and Development Report, June, 1959.

DISCUSSIONS

Z. JANOSI. — Mr. Chairman; we have heard about an effort to correlate Bekker's soil value system and the method based on the cone index. It is logical to assume that such a relationship must exist, because both system derive their parameters from load sinkage data obtained by penetrating different footings into the ground. The Land Locomotion Laboratory investigated this problem in 1958, and our findings were published in report N. 46 in 1959. We found that it was not possible to predict the Bekker soil values from a given cone index as used by the Army Mobility Research Center, since there is an infinite number of sets of soil values which would yield the same cone index. It was, however, simple to express the cone index by means of the three Bekker values if one equated the load required to penetrate the cone into the ground with the sime of the stresses resisting the

cone. The resulting equation was checked by data obtained from simultaneous cone penetrometer and bevameter tests in various soils. The agreement between the predicted and tested cone index values was acceptable. As far as I know, the Army Mobility Research Center also ran numerous tests to check the validity of this equation and found that the above relationship was valid. I hope that this paper, which was also published by the Land Locomotion Laboratory in Research Report N. 5, will be of help to the Corps of Engineers of the Israelian Army in their effort to establish a relationship between the two systems.

D. R. FREITAG and E. S. RUSH. — The Israeli Trafficability Research Team has described a proposed analytical method of establishing trafficability performance curves for vehicles operating in sand. They suggest that the maximum slope negotiable by a vehicle be computed by Mr. Bekker's techniques for one sand condition measured in terms of k_c, k_ϕ, and n; that these values be converted to an equivalent cone index by actual measurement; and that a curve of maximum slope versus cone index be constructed for the vehicle, using the single point thus derived, a somewhat arbitrary maximum point, and the general shape of empirical curves of slope versus cone index developed by the Army Mobility Research Center (AMRC) of the U. S. Army Engineer Waterways Experiment Station. The example given is for a loose, dry desert sand for which cone index is 70, k_c is 0, k_ϕ is 3.5, and n is 0.5.

The cone index of 70 agrees well with the values found by the AMRC in its field tests on dry desert sands. The AMRC did not measure the Bekker soil values at the time of these field tests and cannot therefore verify the relation of cone index to soil values. However, many comparative sets of data have been collected subsequently in the same desert sand at the same moisture content and density, but in the soil bins of the AMRC testing facility [1,2]. These comparisons reveal that soils values $k_c = 0$, $k_\phi = 3.5$, and $n = 0.5$ can be associated with cone index in the order of about 15, not 70 [2]. Also sinkages of tracked vehicles measured by the AMRC in desert sand with a cone index of 70 were considerably less than the 9.2 in. reported for the AMX tank. It would be of considerable interest to determine the reason for the marked difference between these relations and those found by the Israeli team. However, regardless of the accuracy of the relation of cone index to k_c, k_ϕ, and n, the Israeli proposal is of interest if it can be shown to be of general validity.

TABLE 1. — *Pertinent data for tracked vehicles.*

Vehicle	Test Weight lb	One Track		Shoe Length in.	Both Tracks Avg		Bogies Per Side	Ground Clearance in.
		Contact Length in.	Contact Width in.		Total Contact Area sq in.	Contact Pressure psi		
1/4-ton M29C weasel	5,560	78	20	4.25	3120	1.8	8	11.0
Standard D4 engineer tractor	14,870	61	13	6.50	1586	9.4	6	11.0
Standard D6 engineer tractor	22,667	86	16	6.75	2752	8.2	6	12.5
Standard D7 engineer tractor	27,000	95	20	8.00	3800	7.1	7	15.0
13-ton M5A4 hi-speed tractor	25,230	117	17	5.50	3878	6.5	5	20.0
18 ton M4 hi-speed tractor	28,700	131	17	6.00	4454	6.4	5	20.0
M4 medium tank	67,700	150	23	6.00	6900	9.8	6	17.0

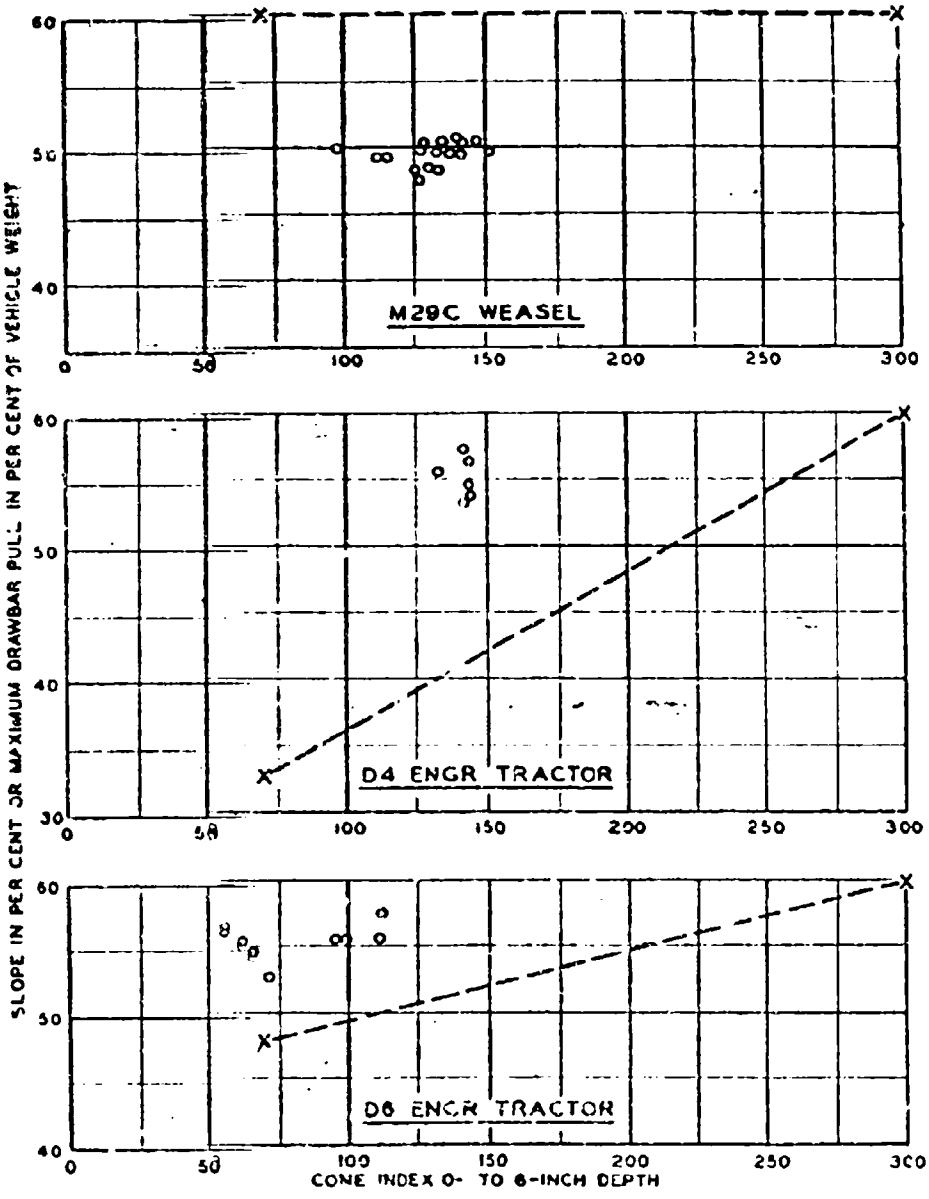


Fig. 1. — Comparison of actual and predicted performance: M29C weasel, D4 engineer tractor, D6 engineer tractor.

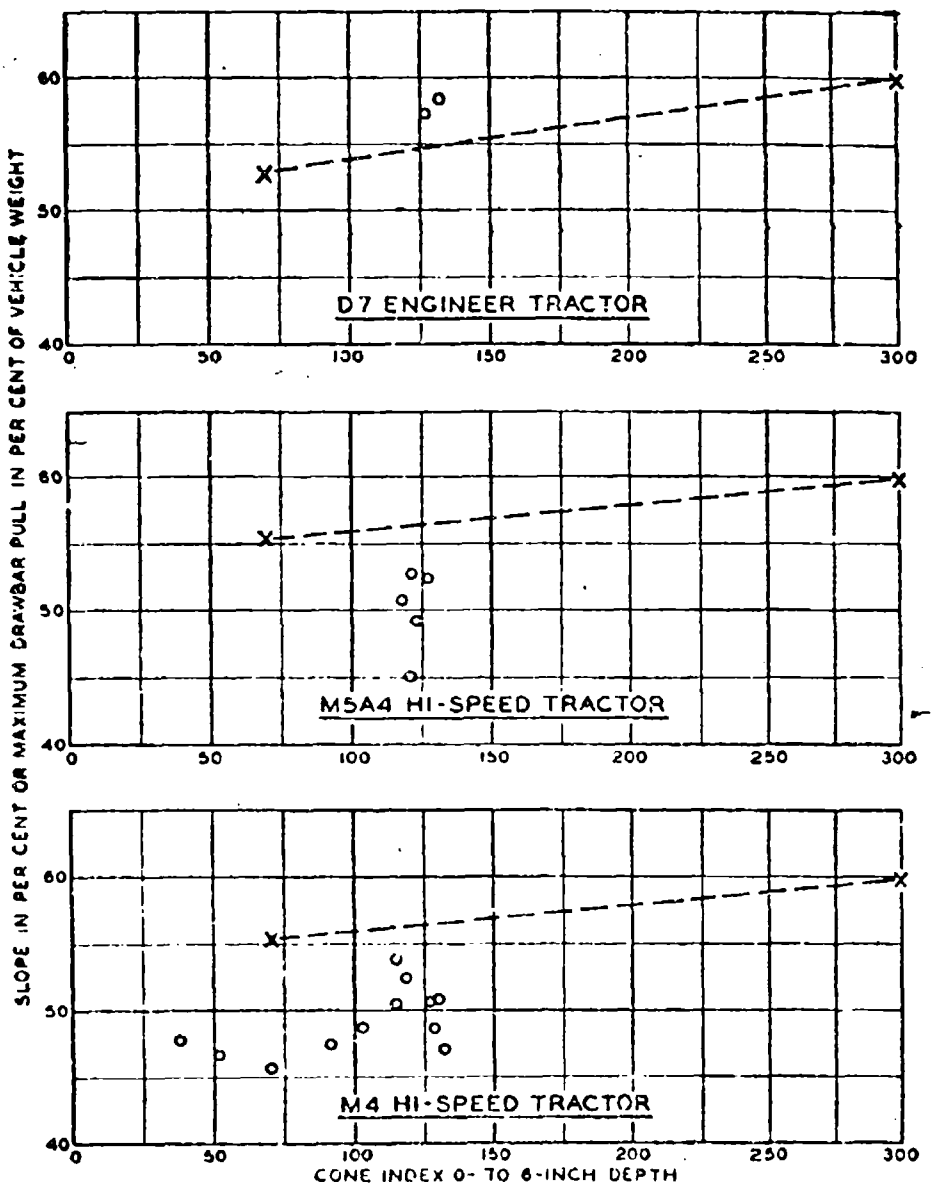
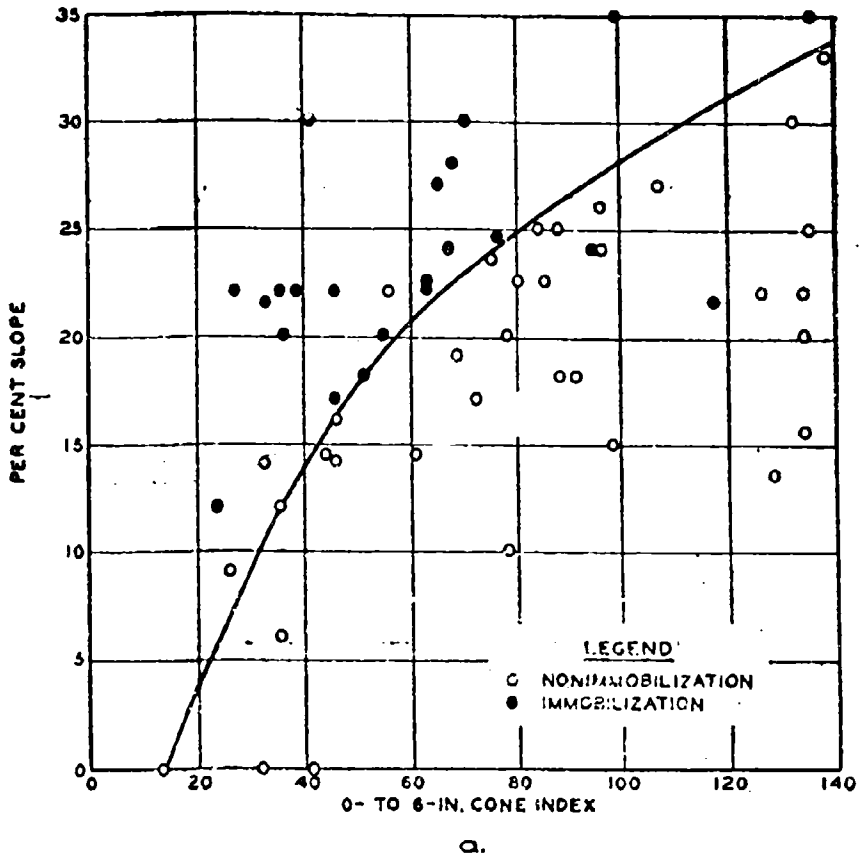


Fig. 2. — Comparison of actual and predicted performance: D7 engineer tractor, M5A4 hi-speed tractor, M4 hi-speed tractor.

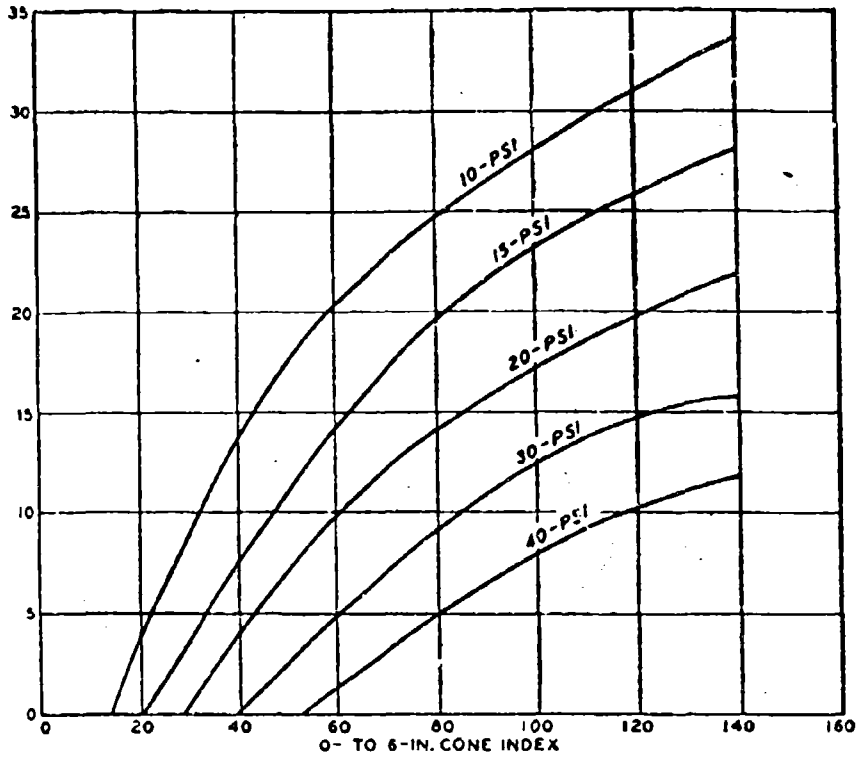


a.

Figure 3. — Vehicle performance, 2-1/2-ton 6 × 6 trucks, 11.00-20, 12-pr tires (single), dry-to-moist sand. - a) 10-psi tire pressure; b) family of tire pressure curves.

In its study of the trafficability of sands the AMRC used six different tracked vehicles in addition to the M4 tank referred to by the Authors. (It should be noted at this point that the M4 tank used was the wide-tracked version having a nominal ground pressure of about 9.8 psi, not 13.8 psi as assumed by the Authors. Unfortunately complete dimensions of this vehicle were not given in WES Technical Memorandum No. 3-240, thirteenth Supplement, « Trafficability of Soils, Pilot Study, Tests on Course-Grained Soils », listed as reference 7 in the Israeli paper). Pertinent characteristics of all the tracked vehicles tested are given in table 1.

Performance curves have been derived for each of the tracked vehicles using the methods proposed by the Israeli Trafficability Team, assuming that $k_c = 0$, $k_\phi = 3.5$, and $n = 0.5$ correspond to cone index = 70. These curves, together with results of field tests, are shown in figures 1 and 2. The derived points plotted at cone index = 70 were computed by the proper equations rather than read from the nomograph to insure accuracy. The data points plotted were obtained from drawbar-



b.

Figure 3.

pull tests on level sand by assuming that the ratio of maximum drawbar pull to weight is equivalent to the tangent of the angle of maximum climb. It can be seen that calculated performance is reasonably close to the actual performance for the D7 engineer tractor; but for the others, it is either much higher or much lower. It will be noted that the actual performance of the three engineer tractors (D4, D6, and D7) was somewhat better than predicted, while for the other three vehicles, performance was poorer than predicted. The data suggest that the strength of sand has little influence on performance at least within the strength range tested. All the engineer tractors can be considered to be able to climb about the same maximum slope (about 55 %). The three military tractors also have about the same performance that can be characterized by a slope-climbing coefficient of about 50 %. The difference in the performance of the two groups of vehicles appears to be related to the type of track. The military vehicles have relatively flexible tracks designed to provide good « ride » at fairly high speeds. The engineer tractors have a more rigid track system. It would appear that any formulas intended to predict performance of tracked vehicles in sand must be able to evaluate the influence of the track stiffness factor.

TABLE 2. — *Pertinent data for wheeled vehicles.*

Vehicle	Test Weight lb	Tire Description			
		Nominal Width in.	Rim Diam in.	Ply Rating	No. of Tires
1/4-ton M38A1 4 × 4 truck	2,975	7.00	16	6	4
3/4-ton M37 4 × 4 truck	5,645 7,085 7,085	9.00	16	8	4
2-1/2-ton M211 6 × 6 truck	12,792 17,960 20,034	9.00	20	8	10
2-1/2-ton M135 6 × 6 truck	12,450 17,330 22,705	11.00	20	12	6
5-ton M41 6 × 6 truck	18,115 28,175 32,380	14.00	20	12	6
5-ton M52 6 × 6 truck	22,310	11.00	20	12	10
5-ton M54 6 × 6 truck	30,635	11.00	20	12	10
Bucket loader 4 × 4 tractor	13,595	14.00	24	8	4
Tournadozer 4 × 4 tractor	31,070	21.00	25	16	4
3-ton Jumbo 4 × 4 truck	21,100	18.00	26	10	4

Most of the trafficability studies conducted on sand by the AMRC have been concerned with wheeled vehicles. This emphasis was deliberate because wheeled vehicles do not perform as well as tracked vehicles in sand, and because seemingly small changes in tire size, inflation pressure, etc., can cause great variations in performance. These studies have resulted in the production of families of curves to show vehicle performance[4]. Curves, such as the one given in figure 3, have been determined for the first five vehicles listed in table 2. The test data for the other vehicles listed are not as numerous at this time and curves have not yet been established.

As pointed out by the Israeli Trafficability Research Team, it is highly desiderable to establish performance curves for new vehicles without the necessity of extensive testing. The AMRC is now endeavoring to develop mobility index equations that will make this feasible for wheeled vehicles. One of the several systems currently being evaluated is summarized in figure 4. It is a purely empirical arrangement of factors considered to influence the performance of wheeled vehicles. Other systems under study are based in dimensional reasoning and are similar in many respects to the system currently being utilized by the U. S. Army Transportation Research Command[5]. It is anticipated that a report describing a proposed mobility index system will be prepared soon by the AMRC.

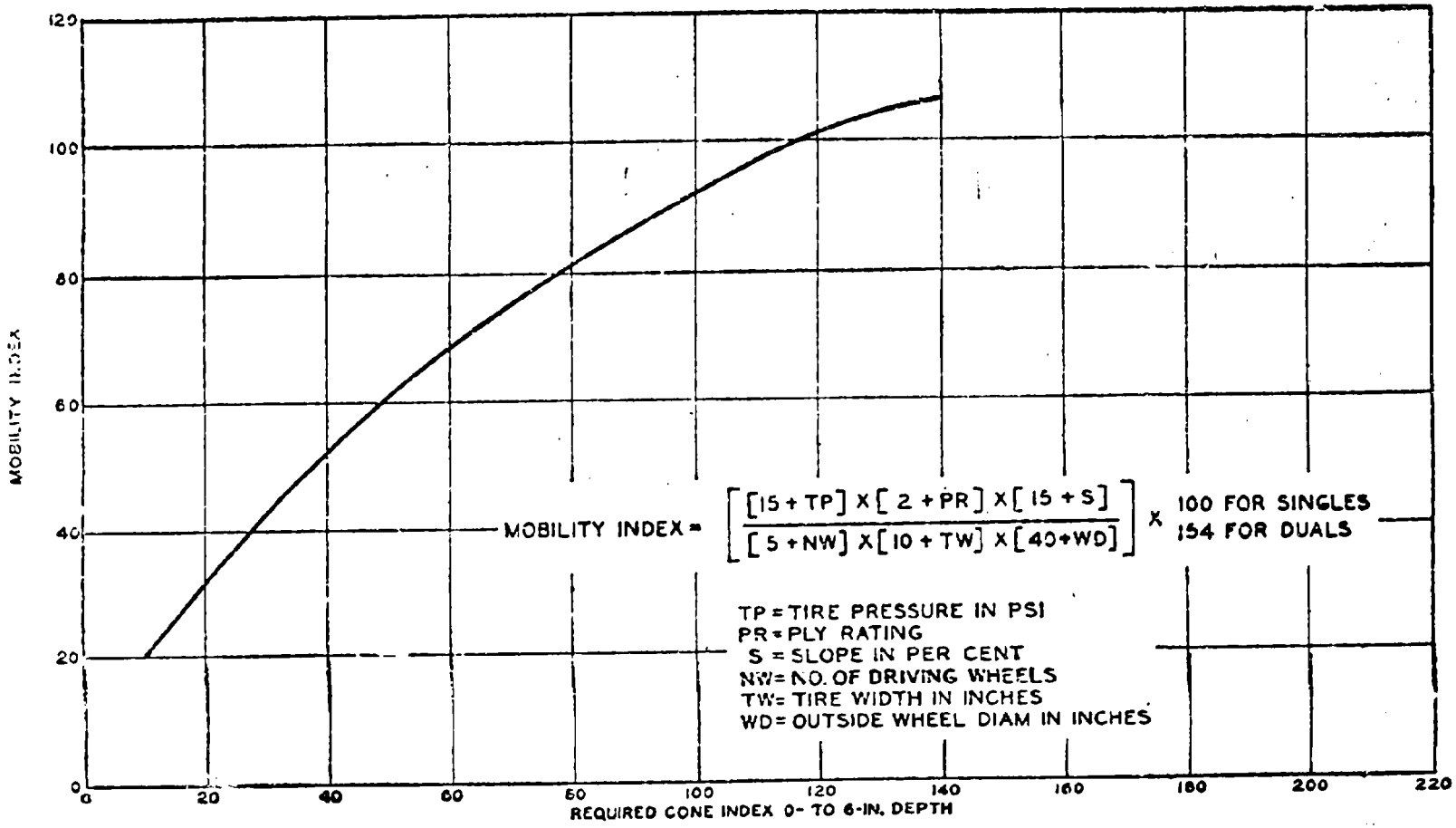


Figure 4. — Mobility index for wheeled vehicles, clean sands, preliminary.

BIBLIOGRAPHY

1) **Knight S. J.** The army mobility research center, The Military Engineer (Society of American Military Engineers, Mills Bldg., Pennsylvania Ave., at 17th St., N. W., Washington 6, D. C.), vol. 52, No. 347, pp. 208-212, May-June, 1960.

2) **Turnbull W. J. and Freitag D. R.** The behavior of sand under pneumatic tires. First International Conference on the Mechanics of Soil-Vehicle Systems, Turin Institute of Technology, Turin (Italy), 1961 (Paper No. 31).

3) **Wismer R. D. and Smith M. E.** Discussion of Paper No. 45, An analysis of pneumatic tire performance on deformable soils by Z. Janosi. First International Conference on the Mechanics of Soil-Vehicle Systems, Turin Institute of Technology, Turin (Italy), 1961.

4) **Rush E. S.** Test on coarse-grained soils with self-propelled and towed vehicles, 1956 and 1957. Technical Memorandum No. 3-240, 15th Supplement, U. S. Army Engineer Waterways Experiment Station, Vicksburg, Mississippi, June, 1959.

5) **Nuttall C. J. jr. and McGowan R. R.** Scale models of vehicles in soils and snows. First International Conference on the Mechanics of Soil-Vehicle Systems, Turin Institute of Technology, Turin (Italy), 1961 (Paper No. 42).

N. 50

Pressure distribution on and flow of sand past a rigid wheel *)

Ripartizione della pressione e spostamento della sabbia al passaggio di una ruota rigida

E. T. Vincent **)

ABSTRACT. — *This work is an attempt to contribute to the understanding of the process occurring during the passage of a rigid wheel on a dry sandy soil. Results of experimental work done at the University of Michigan are presented.*

Various loads were charged on a given wheel runned at a given speed. The shapes of the mounds of sand ahead and along the sides of the wheel produced by the movement of the wheel were measured.

With a small pressure transducer on the surface of the wheel was possible to measure the distribution of the loading on the wheel.

The experiments done pointed out that the passage of a wheel does not only compact but moves the sand. The assumption of both effects has little influence upon the theoretical relationships for sinkage, drag, etc. provided the correct avarage values for the soil constants are employed.

Introduction

The analytical approach to the relationship between load, drag, and sinkage of a rigid wheel based on the soil relationships developed by M. G. Bekker are outlined in Refs. 1-2. The results obtained with these methods have considerable accuracy, particularly as regards sinkage in sand *; the predicted values, however, do appear to diverge both at high and low loads, and particularly so when plastic soils are employed. The accuracy obtained, however, is sufficient for most engineering evaluations at the present time since there still remain many other unknowns in the soil relationship.

This paper is an attempt to contribute to the understanding of the fundamental nature of the process and the relationship between the variables, together with the manner in which the soil moves during the passage of a rigid wheel. These comments pertain to the use of a fine dry sand as the soil.

---

*) This paper was originally prepared for Land Locomotion Laboratory, U. S. Army Ordnance Tank Automotive Command, Detroit, Michigan.

**) The University of Michigan, Ann Arbor, Michigan.

The present theory of wheel action assumes that the soil is compacted vertically by the passage of the wheel and that the pressure against the wheel surface at any depth below the free soil surface is given by a relation of the form $P = (\frac{k_c}{b} + k_\phi) Z^n$, where k_c and K_ϕ are cohesive and fractional moduli, and b is the narrowest dimension of the bearameter. Such an approach leads to a pressure distribution of the form shown in figure 1,

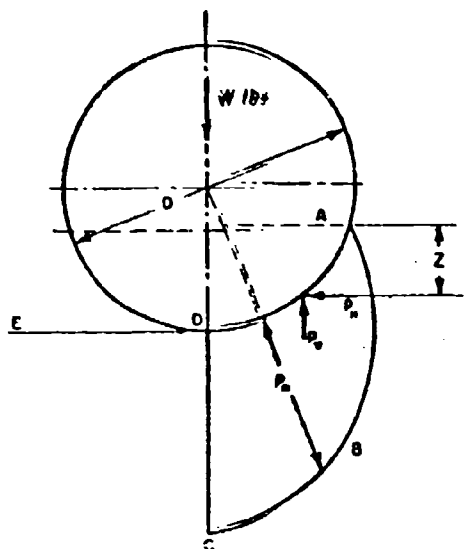


Fig. 1. — Pressure against wheel face by Bernstein's equation.

were A B C D represents the normal pressure p_n exerted on the wheel face to produce the vertical component whose value is given by

$$p_v = (\frac{k_c}{b} + k_\phi) Z^n$$

It is seen that this method of attack, generally attributed to Bernstein and Letoshney [3-4] results in a discontinuity at the point of ground contact D where, theoretically, the wheel leaves the surface. But surface E D is also a free surface, and an instantaneous change of stress, at the surface, of the type shown does not appear reasonable since sinkage relative to E D is zero at D. Although the soil in this region is considered to have been compacted by the passage of the load and thus will have different values of k_c and k_ϕ compared with the original soil, any such change in soil properties does not enter into the relationships developed. Secondly, when the loads are high, the sinkage is great, which means that soil compaction would be of considerable

magnitude. However, a well-settled sand is not readily compressible, at least not to the degree required by the relationships given, and, observing a wheel in motion through a typical dry sand, it is quite apparent that effects other than compaction do exist. It is believed that some compaction and/or elasticity exist at light loads, and in such cases the analytical treatment should take this into account. Under such small sinkages there is no particular problem in transporting loads of such magnitude over soils; the troubles all begin when sinkage begins to assume considerable magnitude. The effects on the the sinkage of the wheel does not produce a corresponding compaction of the soil. over a considerable area round the wheel contact. This of course means that the sinkage of the wheel does not produce a corresponding compaction of the soil. When motion occurs, this heaving is transmitted ahead of the wheel at all times, approximately along the lines of the Rankine theory, but with motion there is also considerable bulldozing occurring ahead of the wheel with the result that a « bow wave » is formed. This « bow wave » in the case of sand builds up to a definite form and the slopes of the surface exceed the angle of repose of the soil, with the result that sand on top of the wave moves both forward and laterally relative to the wheel so that the displaced sand is eventually disposed of by flowing past the sides of the wheel and falling into the rut behind the wheel made by the sinkage. There is thus a flow process in addition to the one of compaction.

Some of these facts are discussed in detail below, and the requirements for a theory are established which will indicate a method of approach with conditions closer to those actually existing than is now the case.

Cycloidal action

In a theoretical analysis it is possible to assume some idealized conditions. Let it be assumed that it is possible for a towed wheel loaded with a weight of W lb, sinking to a depth of Z in., to roll without slipping on the soil (experiment has indicated slippage occurs even at quite light loads).

Under such assumptions, it follows that a particle of soil located in the free surface of the sand, at point « a » of figure 2, will travel along the path a a' a'', a portion of a cycloid. Thus the soil is compacted the vertical distance ab and bulldozed a horizontal distance ba''.

The equation for the path aa'' is given by

$$x = D/2\,(\theta - \sin\theta)$$
$$y = D/2\,(1 - \cos\theta) \qquad (1)$$

Let the wheel be rotated one revolution from position A to B. Then the soil at a' will have work done on it in moving from a' to a''; a corresponding particle with the wheel at position B has already had work done on it from a,

to a''_1 or a total distance of aa''; consideration of all other particles will also show that the work done in one complete revolution of the wheel is that of overcoming the resistance along the complete path such as $e\ e'\ e''$. It follows that the work done on the soil ehg in one revolution is the same as that done on a rectangular block $edfg$. In effect the block $edfg$ is moved forward the distance ba'' and depressed through the vertical distance ab.

The above method of approach does not take into account any flow past the wheel, but does show how a «bow wave» can be formed despite the assumption of compaction only. This analysis perhaps represents the process for small sinkages with some degree of accuracy, though even the smallest sinkages tend to show some small degree of flow.

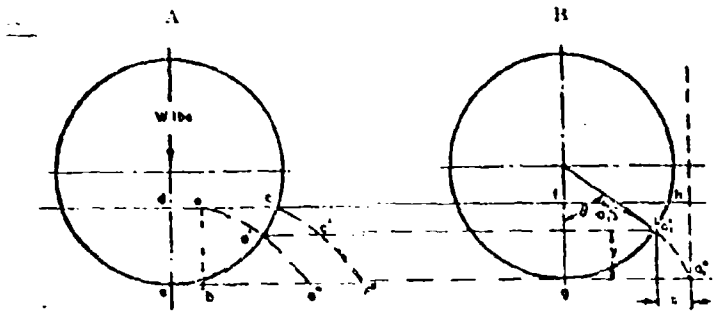


Fig. 2. — Cycloidal motion.

Consider the above approach in a little greater detail:

On the present general assumption, viz. that the sand ahead of the wheel is undisturbed as far as wheel action in concerned, the horizontal component of the cycloidal motion of the soil must all be accounted for by compaction. Unless compaction exists to the degree assumed, the horizontal displacement produced by the cycloidal motion must result in a heaving of the soil ahead of the wheel and the effective value of Z will change. If compaction were zero, a volume of sand equal to that given in Eq. (2) must be displaced ahead of the wheel.

$$\text{Horizontal displacement} = bZ\pi D \text{ cu in/rev} \tag{2}$$

With zero compaction, flow of the sand must occur past the wheel uniformly along the length of the path; it follows that the area of the mounds produced, above the original soil surface, at the center of the wheel must have a total cross-sectional area given by:

$$\text{Cross-sectional area} = \frac{bZ\pi D}{\pi D}$$

$$= bZ \text{ sq in.} \tag{3}$$

This is illustrated in figure 3. For this to occur, the bulldozing effect must build up a bow wave of sufficient magnitude so that flow of the sand in the lateral direction of the wheel must occur at the same rate as it is displaced, and the bow wave ahead of the wheel must have inclined sides at an angle greater than Φ (the angle of repose); then flow of the sand will occur both in the direction of motion and at right angles to it.

On the assumption that compaction does exist to some extent, but of insufficient magnitude to account for the total displacement by the wheel, we can write:

$$\text{Total displacement} = \text{Compaction} + \text{flow} = bZ\pi D \text{ cu in./rev} \quad (4)$$

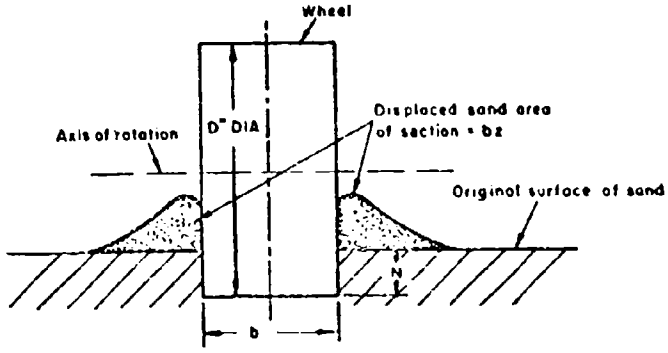


Fig. 3. — Sinkage accompanied by displacement.

To express the compaction factor in terms of W, bZ, D, etc., much more would have to be known regarding soils than is the case at the present time such as:

1) depth of soil affected by the load;

2) degree of compaction possible for the soil in question;

3) the maximum load pressure applied to the soil by load W;

4) effects of load on surrounding soil as well as that immediately below tread.

Present evidence indicates that compaction is of rather small magnitude, e.g., a lightly loaded wheel resting on the surface of sand does sink a small amount, but at the same time the soil round the wheel also heaves to a small extent despite the low load.

Little is known about the maximum local soil stress, item 4, at the present time. Bernstein's relationships give a distribution of the type shown in figure 1, with a maximum equal to D.C. occurring under the centerline of the wheel; however, as already noted, such a distribution of stress does not seem

to be a possible solution in actual practice. To approach this problem as a whole, it becomes necessary to obtain information regarding the relative effects of flow and compaction together with the stress pattern over the load-bearing surface of the wheel. Some preliminary jest work was carried out at The University of Michigan under the auspices of the Office of Ordnance Research to provide some answers to this problem, with the following results.

Flow of sand past a rigid wheel

A number of tests were run at various loads with a given wheel towed at given speeds, and the shape of the mounds of sand left as a result of the motion were measured. The shapes measured ahead of and along the sides of the wheel were those left when the wheel had been brought to rest; thus they differ slightly from those existing when in actual motion.

The wheel employed in these tests was a model 12-1/2-in. diameter with a face of 3-1/2 in. or an aspect ratio of $a = 0.28$. It was loaded with 25, 50, and 100 lb, respectively.

If the rut left behind the wheel during its normal motion is considered (in this case the results do represent the actual results produced by the wheel and its load when moving at velocity), traces such as those shown in figure 4 (a, b, and c for loads of 25, 50, and 100 lb, respectively) are obtained.

To estimate the approximate displacements of the sand, the shape of the mounds were considered to consist of flat surfaces extended so that the intersection of the sloping surfaces was at a point in place of the actual rounded condition of the mound itself. The error introduced by this approximation is considered to be small. By calculation it can be shown that:

Wheel load = 25 lb
Area of sand above original soil surface = 2.0 sq. in.
Area of trough in sand below original soil surface = 2.35 sq. in.
Compaction = 0.35 sq. in.
Angle Φ_1 = 32° approx
Angle Φ_2 = 14° approx

Wheel load = 50 lb.
Area of sand above original soil surface = 2.81 sq. in.
Area of trough in sand below original soil surface = 3.02 sq. in.
Compaction = 0.21 sq. in.
Angle Φ_1 = 32° approx
Angle Φ_2 = 24° approx

Wheel load = 100 lb.
Area of sand above original soil surface = 2.76 sq. in
Area of trough in sand below original soil surface = 4.68 sq. in.
Compaction = 1.92 sq. in.
Angle Φ_1 = 30° approx
Angle Φ_2 = 33° approx

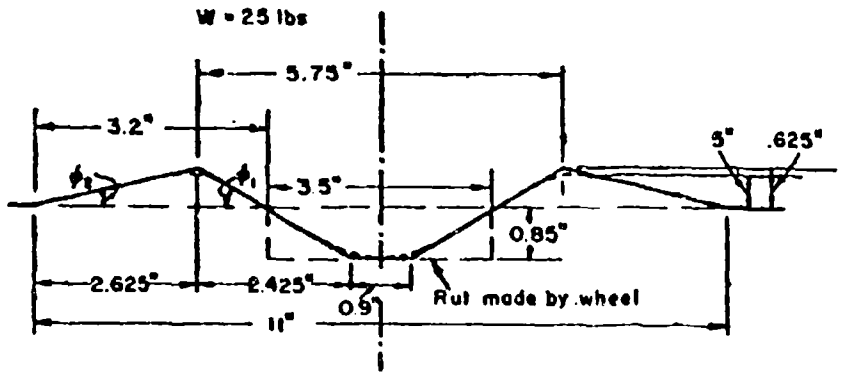


Fig. 4 a.

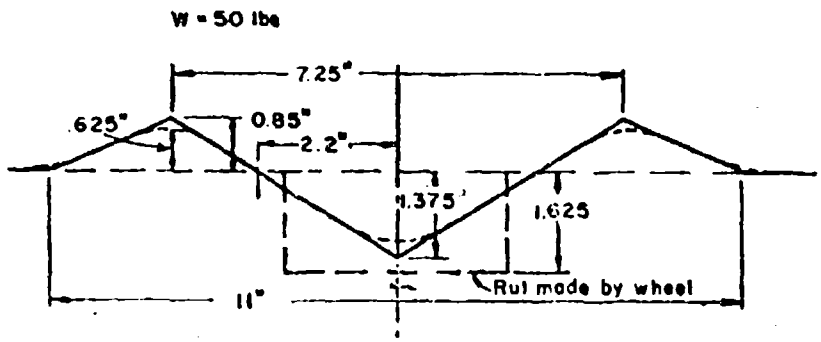


Fig. 4 b.

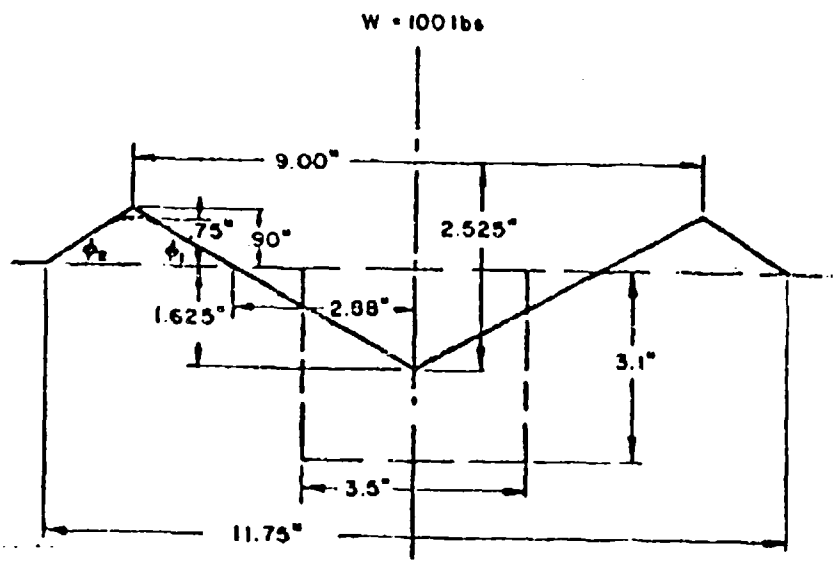


Fig. 4 c.

Fig. 4. — Typical ruts left by wheel at various loads.

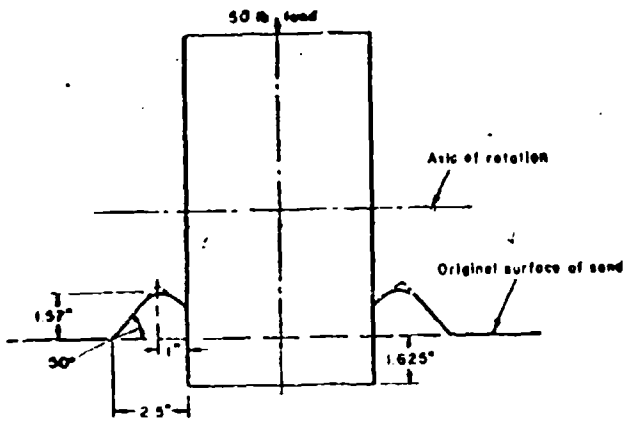


Fig. 5 a.

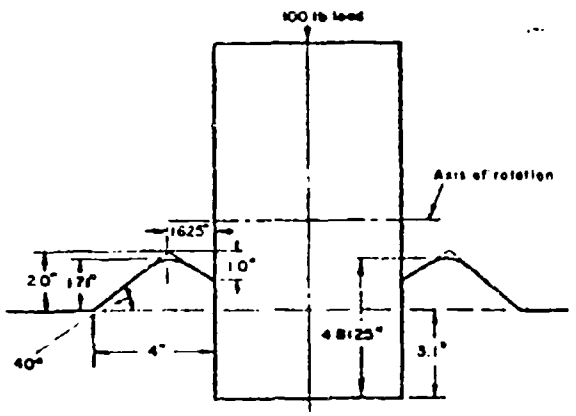


Fig. 5 b.

Fig. 5. — Typical side displacements.

If the section of the mound at the vertical centerline of the wheel is considered, the soil surface appears as shown in figures 5 a and b for the 50 and 100 lb, respectively. Calculating the area of the sand piled above the original surface of the soil in this case and comparing it with the area displaced by the wheel sinkage, the following is obtained:

Load, lb	Area of Mound, sq. in.	Area of Displacement, sq. in.	Difference, sq. in.
50	5.0	5.7	0.7
100	9.6	10.7	0.9

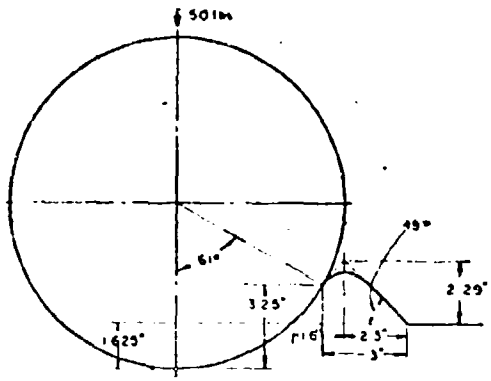


Fig. 6 a.

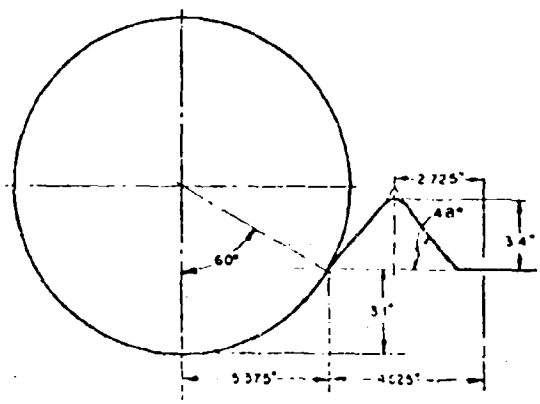


Fig. 6 b.

Fig. 6. — Typical « bow waves ».

Taking the dimensions of the bow wave shown in figures 6 a and b for the two loads in question, we obtain:

Load, lb	Vol of Sand in Wave, cu in.	Displacement of Wheel per 1 in. Travel, in.
50	27.5	10.85
100	15.7	5.7

It is seen that the bow wave appears to be approximately three times the rate of displacement of the wheel per 1 in. of forward motion to provide sufficient slope to initiate the lateral motion necessary for flow round the wheel.

Comparing the hights of the mounds ahead along the sides of the wheel, it is seen that the wave has heights of 2.3 in. and 3.4 in. respectively, while

the sides are 1.6 in. and 2.0 in. while the mound behind the wheel amount to 0.85 and 0.9; there is a head to produce the necessary flow.

In addition, the flow past the wheel is seen to be roughly a constant amount less than the wheel displacement. This could be a measure of the compaction of the sand and indicates that compaction is only slightly affected by the change of maximum pressure to which the sand is subjected, from about 3 to 4-1/2 psi. in this case, a rather small change. The main increase in load-carrying capacity appears to come from the increasing area of contact of the wheel with the sand as a result of additional sinkage.

Looking at the pattern behind the wheel, the soil displaced above the original surface is in general somewhat smaller than the rut left by the wheel, again indicating that some compaction is occurring; at the high load, a considerable difference exists behind the wheel, despite reasonable agreement of the volumes when compared at the vertical center line of the wheel. It should be emphasized again that accurate reading of the dimensions is difficult and the high-load results could be in error.

It follows that the theory assuming compaction of the soil alone under the action of the wheel does not represent the case with accuracy. Flow round the wheel in the case of a dry sand appears to be of greater importance. It is appreciated that vastly different conditions may exist in the case of a plastic soil. The effects of this change in nature of the process on the present system of calculations for load, drag, sinkage, etc., will be discussed later.

Stress pattern on wheel surface

To measure the actual loading per unit area on the face of the wheel, a small pressure transducer was installed in the surface of the wheel, consisting of a plunger (1/4-in. diameter) attached to a differential transformer incorporated into an appropriate circuit whose output was led to a recorder so that a trace proportional to the variation of the load on the plunger could be obtained. A true point reading is not secured but at least the load recorded is fairly typical of the actual variations of the stress.

Figures 7, 8 and 9 show the results obtained, the first with the pressures plotted round the surface of the wheel showing the loaded area, the second with the same data plotted on an expanded angular base. The wheel employed in these tests was 12-1/2-in. diameter with a face width of 6-1/2 in. or an aspect ratio of $\alpha = 0.52$. Figure 7 shows the pressures with the pick-up at the center of the wheel face where the motion can be considered two-dimensional, while figure 9 shows the effects of placing it near the edge of the wheel where three-dimensional flow is undoubtedly occurring. Comparison of the diagram shows a definite change in the distribution of pressure for the two positions, but it does not appear to be of a serious nature for the locations recorded. In what follows, the central location only will be employed and the motion of the sand is considered to be of a two-dimensional nature.

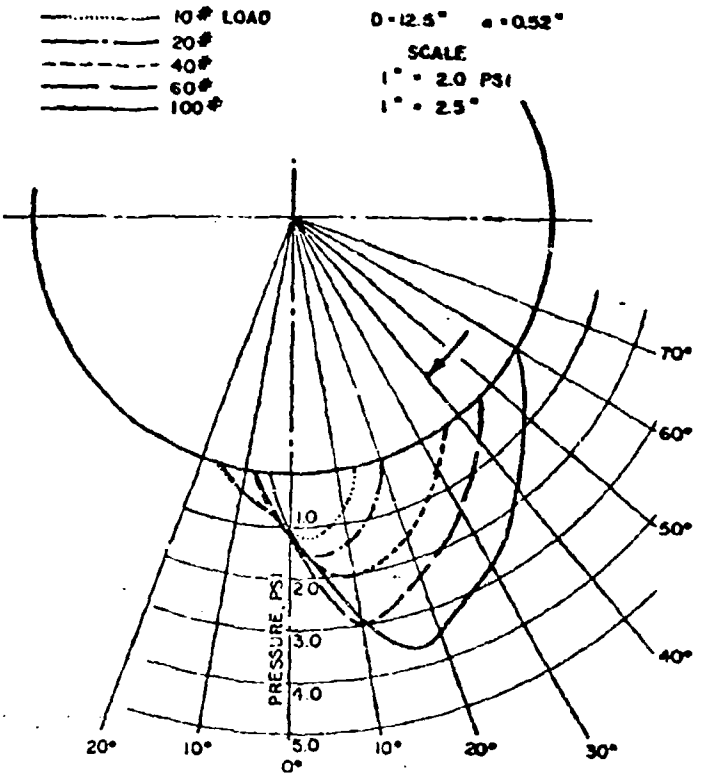


Fig. 7. — Variation of loaded area and pressure under center of wheel.

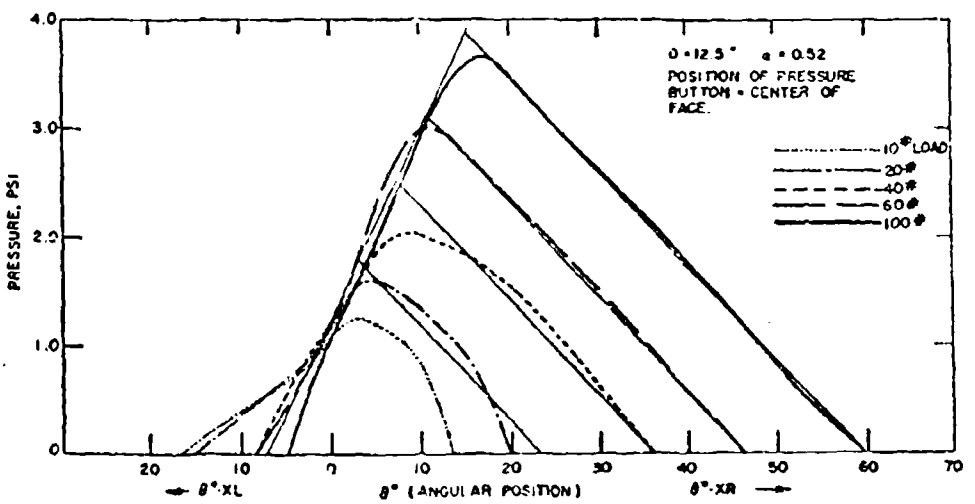


Fig. 8. — Variation of angle of contact and pressure on wheel with load.

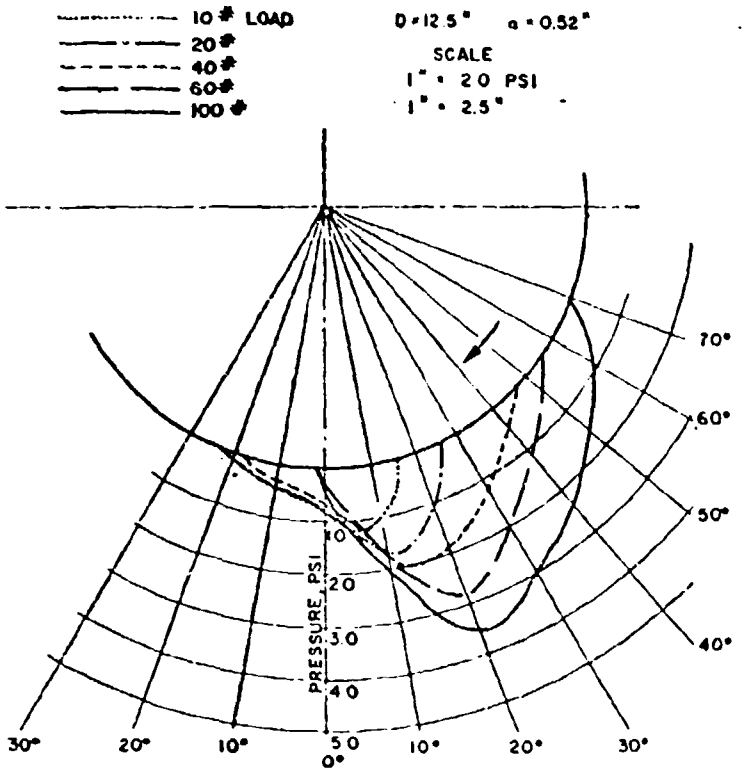


Fig. 9. — Variation of loaded area and pressure near edge of wheel.

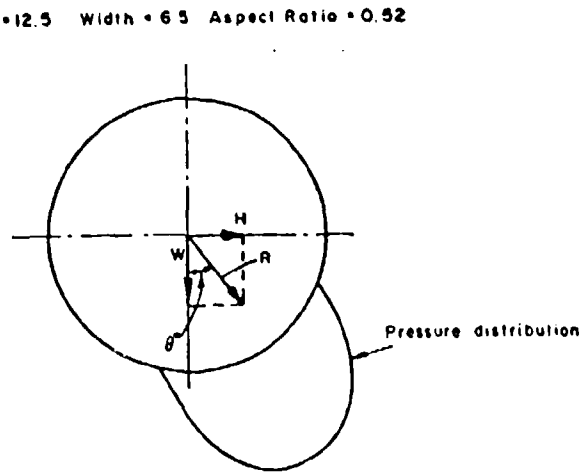
One thing is immediately apparent from figure 7 that there is a definite change in the stress pattern between the light loads with small sinkage, and the heavier loads where sinkage and compaction are great.

Examine the stress diagram for the 10- and 20-lb loads. Stress begins at 13-1/2° before vertical and ends at 16-1/2° after for the 10-lb load, and at 20° and 15° for the 20-lb load. These values indicates a roughly elastic medium with little if any permanent compaction of the soil although a very shallow rut is left behind. At such light loads extremely small differences in soil level and small errors in the instrumentation could account for the differences in angular contact before and after the centerline. These loads are accompanied by a mixiumun soil stress of 1.22 and 1.6 psi, respectively.

The remaining diagrams, for the 40-, 60-, and 100-lb loads, show a stress pattern as follows.

Load	Angle at Which Stress Begins in Degrees Before B.D.C.	Angle Past B.D.C. at Which Stress Ends	Maximum Stress, psi.
40	36	8	2.02
60	46	8	3.00
100	39.5	5	3.62

The soil no longer appears elastic to any great extent; in fact, the point of wheel contact ends, for all practical purposes, at one constant angle, 7°, if the stress curves are averaged out by using a straight line for the trailing side of the pressure curves, which fig. 8 indicates as a possibility. Before any general conclusions are drawn, a more detailed investigation of the loadings is necessary.



Load (lb)	Drag (lb)	Resultant (lb)	θ°	Sinkage (in.)
10	1.25	10.07	7°	0.17
20	4.10	20.4	11.5°	0.25
40	13.65	42.2	19°	0.57
60	24.40	64.8	22°	0.97
100	52.00	112.6	27.5°	2.31

Fig. 10. — Resultant forces on rigid wheel.

Let us examine the loads applied to the wheel when in motion. These consist of the applied vertical load, W lb, plus the horizontal drag of the wheel, H lb, necessary to overcome the rolling resistance. It follows that there is a resultant force, R lb, acting at some angle θ° to the vertical as shown in fig. 10. With respect to this resultant load, acting during motion of the wheel, the angular positions of beginning and end of the pressure diagrams become:

Load	Stress Begins Degrees Before Resultant R	Stress Ends Degrees After Resultant R
10	6.5	23.5
20	8.5	26.5
40	17.0	27.0
60	24.0	30.0
100	32.0	32.5

It will be observed that the majority of the contact area lies behind the direction of the resultant force when the loads are light, while at heavy loads the contact is roughly equally divided on either side of the resultant.

If the 10- and 20-lb loads are neglected, the remaining diagrams can be represented with considerable accuracy by a series of similar triangles, as

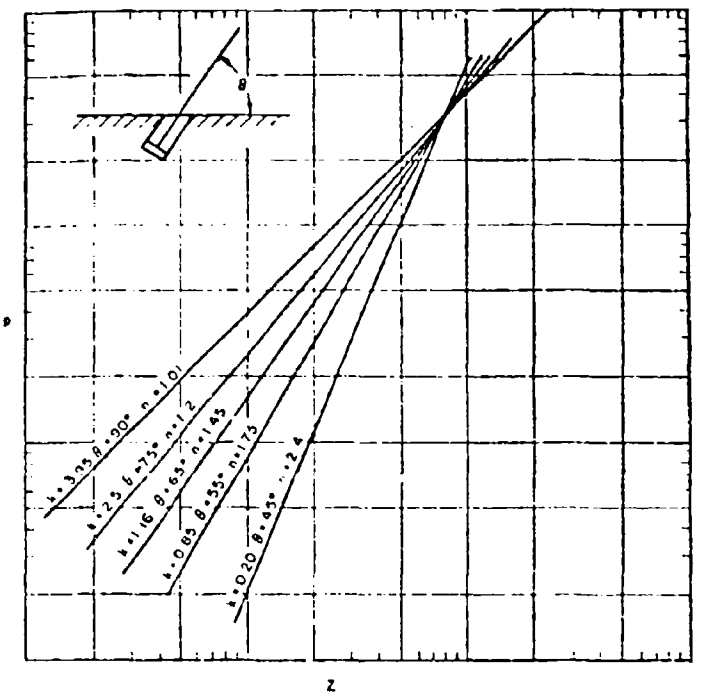


Fig. 11. — Stress-sinkage relations for various angular penetrations.

shown superimposed in fig. 8, with the maximum stress occurring at an average of 72 % of the angular contact area measured from the leading edge of contact with the sand.

The similarity of the diagrams suggested some common constant relationship between depth of sinkage below the surface, the angle of contact, and the stress; various methods of calculation for such a relation were examined. Soil penetrations were carried out with the bevameter normal to the surface of the sand and inclined to it in the manner in which a wheel surface contacts the soil at high sinkage under a cycloidal motion. Typical results are shown in fig. 11; it is observed that the slope of the log-log plots increases as the angle θ to the soil surface reduces, and that all these lines meet in a common point, which appears to indicate that, given an infinitely large bed of homogenous sand, the direction of application of the load does not matter after a conside-

rable depth is reached. It would be assumed that past the common point of intersection one common line would represent all angles. The value of « n » varied from 1.0 to 1.3 for various sizes of the plate on the bevameter and the 90° position, to 2.4 for the 45° one. There is a problem as to where the penetration Z should be taken as zero when in an angular position, when the side

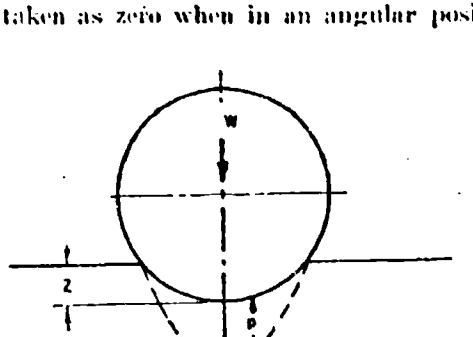


Fig. 12 a.

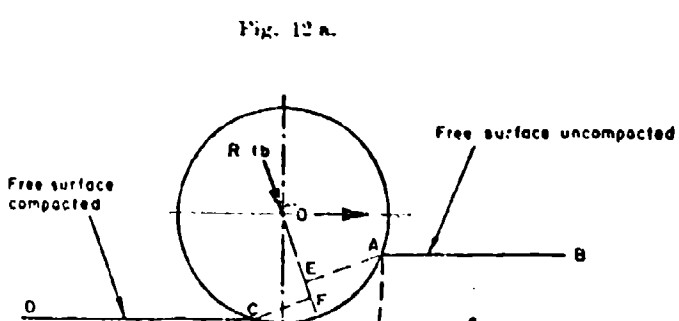


Fig. 12 b.

Fig. 12. — a) wheel loaded statically; b) load on wheel in motion.

of the foot first touches the soil or when the whole width of the plates contacts the soil. Plotting these data in the different ways, considerable differences in the value of n result. For example, if the 45° line is plotted on the basis of when the first contact is made with the sand, and also when corrected for the sinkage being considered zero when the centerline of the plate and bevameter is at the soil surface, then « n » changes from 2.4 to 1.74. When $\Theta = 75°$, the change in value of « n » for similar plots is quite small, as would be expected. In any case, for all methods of plotting the value of « n » increases as the angle is reduced, compared with the normal 90° position.

Consideration of the conditions under which the soil is operating under a rolling wheel indicates that some variation in the value of the soil constants is to be expected before and after loading. As the wheel rolls forward, the uncompacted soil near the surface is loaded and compaction results, increasing presumably up to the point where the stress reaches a maximum. Further rotation of the wheel continues the displacement of the soil downward, if compaction is the only method in force, not with increasing stress as is generally

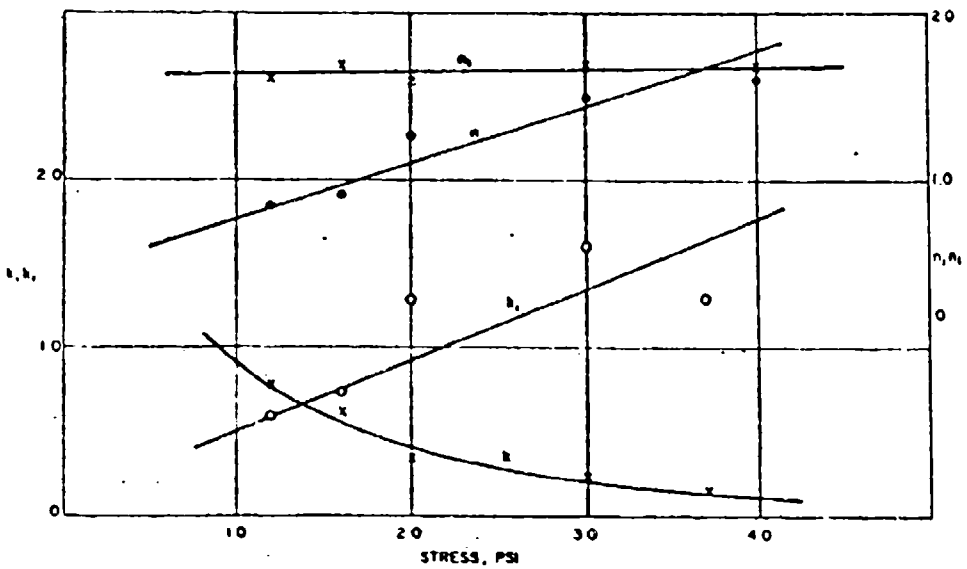


Fig. 13. — Variation of soil constants with stress.

assumed, but with a reducing one (which is not possible according to the Bernstein theory). In a bevameter test the load p in $p = kZ^n$ continues to increase at all times as Z increases; thus there is a distinct difference in the action of the soil in the two cases. This suggested the following solution.

A static wheel subjected to a load W sinks some distance Z in the soil as shown in fig. 12 a. It is reasonable to suspect that the point value of the pressure against the wheel surface varies from zero at the surface to some maximum directly under the load, i.e., a symmetrical stress-strain curve, would exist and the value of « n » in the pressure-sinkage relationship for each side of the diagram would be identical, i.e., the soil is the same on each side of the center. In the case of a towed wheel, the conditions are such that from the original surface of the sand to the point of peak load the soil is being compacted, and a certain value of « n » exists for this type of action on the soil. Beyond the peak pressure, where maximum compaction has occurred, it is conceivable that new values of k and « n », say k_1 and « n_1 », exist due to the compaction.

Working on the assumption that the sand, up to the point of maximum

pressure, has one set of soil properties, and a different set of values after the peak is reached (that is, the soil compaction has reached its limits for the load in question at the peak stress and despite further sinkage, relative to the original soil surface, there is a reduction of stress), calculations were made for the values of k and n for the curves of pressure before and after the peak pressure with the results shown in the table below and in fig. 13:

Load	k	k_1	n	n_1
10	7.8	6.0	0.85	1.62
20	6.1	7.3	0.91	1.7
40	3.5	13.0	1.27	1.5
60	2.4	16.0	1.5	1.6
100	1.6	13.0	1.6	1.6

The method of plotting was that the point of contact of the original soil surface with the wheel at A of fig. 12 b formed the reference for the values of p and Z from which k and n were determined while the point C of the compacted surface CD was employed for a sinkage reference for k_1 and n_1, Z being measured along the line of OG normal to AE and CF, the zero for Z being E in the uncompacted case and F for the compacted portion of the curve. In effect, the soil contact with the wheel was that provided by a static wheel loaded with the resultant force R along OG but with two different soil properties, one on each side of the line of application of the load.

The log-log plots of the 40-, 60, and 100-lb loadings could be averaged into the relationship given by $p_1 = 13.0\ Z_1^{1.6}$ with reasonable accuracy but in the case of the k and n values only « n » could be averaged with a moderate degree of accuracy at the value of n = 1.42; the k's appeared to have a definite variable value with the load. The 10- and 20-lb loads could be represented by the relationships: $p = 7.0\ Z^{0.9}$; $p_1 = 7.0\ Z_1^{0.9}$ within a reasonable error.

The original uncompacted soil tested by the bevameter gave an average of $p = 3.9\ Z^{1.1}$. Thus the figures in the above confirm some changes in the values of k and n as stress is applied. In fact, the log-log plots under the various loads did indicate a gradual departure from the straight-line relationship as the stress approached the maximum value, indicating a continued increase in « n » with the stress.

To establish and check this idea, a bevameter test was carried out on the original soil and again after the passage of a loaded wheel, the values of k and n obtained are shown below.

	k	n
Original soil	3.0	1.0
Compacted soil		
60-lb load	3.4	1.0
100-lb load	4.3	1.0

Soil reaction

The application of an external load and drag to a wheel result in a resultant load of R lb at some angle $\theta°$ to the vertical and must of course induce an equivalent reaction in the soil, as represented by the load diagrams of figs. 7, 8, and 9.

To check how closely this measured reaction agreed with the load applied, the average load per square inch of contact area and its point of application was obtained from three of the diagrams with the following results.

Vertical Load	Resultant R	$\theta°$	Radial Component of Soil Reaction	
			lb	$\theta°$
100	112.7	27.5	83	27.3
60	64.9	22.2	53.2	17.0
40	42.3	18.8	34.8	13.0

In view of all the various factors involved, the agreement between the applied load and the measured reaction can be considered reasonable.

Effect of friction on soil reaction

In the actual case with motion, there is an additional force involved: friction which results from the slippage occurring between the wheel and sand. This force is of course normal to the wheel surface at all points and would result in some modification of the supporting forces and the resultant point of application.

Tests were run to determine the magnitude of the tangential force necessary to cause slip of a rigid wheel under various loads[4]. These tests indicate that an average value for the coefficient of friction to be expected is of the order of 0.48; however, the relationship $F = \mu W$ does not represent the results too well, particularly at high loads where the sinkage is large. However, using this relationship for simplicity, when friction is added to the radial pressures the combined resultant soil forces become, for the 100-lb load:

Resultant Load	Soil Reaction, lb
112.7	90.2

Much more would have to be known regarding the variation of the frictional forces with pressure before an accurate estimate of the resultant reaction of the soil and its direction of application on the wheel surface is known.

Discussion

The experimental work reported here establishes that the passage of a wheel over a dry sand does not result in compaction of the soil alone; there is considerable flow around the wheel. The theories in general use at present assume the former only, and thus the question arises how accurately the relationships developed by the use of compaction alone agree with the actual case.

The results reported here indicate a change in the effective values of k and n with load from a value of about 8.0 and 0.85 for the 10-lb load, to 1.6 and 1.6, respectively, at the higher loads.

The results is that the calculated theoretical sinkage at low loads will be higher, and at the high loads lower, than the values determined by the present theory with n = constant = 1.0 to 1.3. Comparison of these results with Ref. 2 indicates that the corrections are in the right direction, with the result that experiment and theory will agree to a higher degree of accuracy than is now the case, at least for sand.

One other aspect of this change from compaction to flow with compaction are the effects that will be introduced into determining the drag forces, etc. The drag at present is obtained theoretically by equating the work done on the wheel by the towing device, to the work of soil compression. In actual practice, soil flow (in the case of sand) appears to be the major factor, in place of compaction. With flow it has been shown that the pressure against the wheel surface is still of the form $P = kZ^n$ as with the compaction theory; thus, using values of « k » and « n » which do represent the actual conditions on the wheel surface, the forces to move the wheel must be the same, and the work done is unchanged, whether compaction or flow results. The correct solution to the analytical problem appears to depend more on the values of « k » and « n » existing in practice than on the exact nature of the process itself. The variation of the parameters from the Bekker soil-value system is sufficiently limited to permit the use of suitable correction factors, but more must be learned about a wider range of soils and wheels to obtain such factors. In fact, it is suggested that the values of k and n depend on the state of stress of the soil, as well as on its general physical properties. Tests for soils properties under a variable applied stress are planned, with the applied stress being of a flexible nature so that similar heaving of the soil, etc., can occur as with present test procedures.

The variable value of « n » with load does not simplify the problem. Actually, it is rather the opposite: it indicates soil properties that are a function of the applied stress, and the complications in handling the analytical portion of the problem will be multiplied. Perhaps this is not too important in these days of computers, but it would be a problem for calculations by any other means.

Many more tests will be necessary before the changes indicated here can

be accepted for general application, tests *not* only of the soil itself but also of the loading created by the wheel and their effects on soil properties.

It may be assumed that soil properties will have to be secured under various stress levels as indicated above to proceed with any accurate theory or calculations; however, it has already been shown that the soil properties as measured by the Bekker system do give results within the required limits for many general engineering problems.

Conclusions

As a result of this work, it can be concluded that, for a towed wheel in a dry sand:

1) Compaction effects are small.

2) Flow of sand occurs as a result of bulldozing forming a « bow wave ».

3) The normal pressure of the sand against the surface of a rigid wheel is of the form $p = k/^n$.

4) The pressure of the sand on the surface of a rigid wheel can best be represented by two sets of soil values, one during the compaction phase, and the other as the stress is relieved.

5) The assumption of either compaction or flow has little effect upon the theoretical relationships for sinkage, drag, etc., provided the correct average values for the soil constants are employed.

6) No assumptions are made in the bevameter test concerning compaction or flow; thus the use of the soil constant for either process appears legitimate.

7) Acknowledging flow the main process for the conditions considered offers a more realistic approach to the problem without throwing out all existing analyses.

KNOWLEDGMENTS. — The Author wishes to thank the Office of Ordnance Research for support provided which permitted this work to be carried out, and to the following personnel who contributed their time in the conduct of the various tests: H. H. Hicks, A. J. Johnson, and C. Leonard.

This work was performed for Land Locomotion Laboratory, U.S. Army Ordnance Tank Automotive Command.

BIBLIOGRAPHY

1) Bekker M. G. Theory of Land Locomotion, Univ. of Mich. Press, 1956.

2) Ehrlich I. R. Wheel Sinkage in Soil, doctoral dissertation, Univ. of Mich., 1960.

3) Hart W. H., Peloquin E. A. and Young W. H. Friction Tests of a Rigid Wheel, M.S. thesis, Univ. of Mich., 1959.

4) Liston A. Determination of Friction Forces Between a Rigid Wheel and a Frictional Soil, M.S. thesis, Univ. of Mich., 1958.

DISCUSSION

Z. JANOSI. — The presentation given by Professor Vincent is of great significance because it uncovers a fallacy that has hindered the application of analytical methods established in the past.

The pressure distribution under a wheel has been assumed to follow a relationship of the form $p = kz^n$.

According to test results obtained by the speaker, for towed wheels the resultant of the vertical reaction pressures acts ahead of that obtained by the theory. Hence, the magnitude of the motion resistance will be greater than that obtained by means of equations derived for the so-called compaction resistance. This is fully supported by experimental observations.

If one had an accurate picture of the true pressure distribution one would be relieved from the burdensome problem of matching the experimental resistance values by introducing additional terms into the theoretical evaluation which accounts for the bulldozing effect. Initial pressure distribution test results obtained at the Land Locomotion Laboratory fully support the validity of the trends shown by Professor Vincent. It is our aim to investigate the effect of slip on the pressure pattern.

The idea of analyzing the effects caused by the cycloidal motion of the wheel seems to be promising too. The path of a soil particle under the wheel has been investigated by Russian researchers in great detail. The influence of slip and the friction angle has been also included in their analysis. This problem cannot be circumvented when one attempts to predict the traction of a wheel and should also be considered in calculating the resistance acting against it.

While the present analytical methods yield results of acceptable accuracy in most cases, it has long been known that they are not general enough. Professor Vincent's paper points out some important new aspects that hold promise for further refinements and generalizations in the theory of land locomotion.

N. 51

Etude de l'adhérence, en partant des moyens actuellement pratiqués pour tenter de l'améliorer

Study of adhesion with the practical available means, to achieve improvement

Studio per migliorare l'aderenza usando i mezzi pratici attuali

J. Remus *)

ABSTRACT. — *On 10 years' experiments and researches, first of all the Author deals with the principle of displacement of an off-the-road vehicle.*

Then he sums up the story of the agricultural tractor pneumatic tire according to researches for better adhesion.

Afterwards he mentions the available means fitted to increase the adhesion of tractor and of agricultural machinery.

He draws up the principles that, consciously or nor, guided the researches: weight, bearing surface *(nature, shape and elasticity)*, variability *of weight and bearing surface*, coupling elasticity *between engine and motion organs, and lastly a* diminished resistance to motion *for a convenient investigation about plowing devices.*

Préambule

Depuis que les hommes ont découvert que des grains jetés sur le sol ne donnaient qu'une infime proportion de plantes adultes, le travail initial de toute culture est le travail du sol. Ce sol oppose une résistance mécanique à tous les outils. La plupart d'entre eux (charrue, herse, semoir, canadien, etc.) travaillent en éclatant le sol devant eux dans une direction constante.

Toutes les machines de travail du sol doivent *vaincre une résistance* qui tend à s'opposer directement à leur avancement.

D'une façon plus générale, toutes les machines tractrices ou automotrices (y compris les machines agricoles) doivent pouvoir avancer sur les terres et perdent toute utilité si elles ne se déplacent pas en même temps qu'elles ne travaillent. A l'inverse de ce qui se passe à l'usine, *en Agriculture c'est l'outil qui se déplace sur la matière première.*

*) Ingénieur Agricole, Conseiller Technique de la S. A. Dunlop, Paris - France.

Or, le *sol agricole* connaît une infinité de *variations* selon :

1) son relief ;

2) sa structure à l'état vierge, avant toute culture, pour autant qu'on puisse s'en faire une idée. (En particulier, la nature chimique et la granulométrie des composants sont des facteurs de variation) ;

3) la nature de la végétation qui le recouvre ;

4) les conditions momentanées de climat, température, humidité et l'amplitude diurne de leurs variations ;

5) le « passé » de ce sol, c'est-à-dire tous les apports d'amendements d'engrais, de fumier et les travaux mécaniques anciens, ainsi que les effets des saisons passées.

Par ailleurs, tous les travaux que reçoit le sol ont pour but de briser et d'émietter la terre pour y faciliter la circulation de l'air et de l'eau, mais, par voie de conséquences, tendent *à rompre la cohésion* de cette terre et à rendre difficiles les déplacements des véhicules et des machines.

La recherche d'une possibilité acceptable de déplacement se présente pour un Agriculteur sous deux aspects :

1) **Le rendement correct de la source de l'énergie.** — Il faut que, sur l'ensemble du travail d'une heure, d'un jour ou d'un an, la quantité de travail fait soit une part raisonnable du travail fourni par les moteurs. C'est un problème de bilan énergétique.

2) **La nécessité de reculer au maximum le passage à la limite.** — Nous verrons que lorsque la résistance à l'avancement s'accroît, on arrive très vite à une limite pour laquelle toute l'énergie motrice se dépense sans aucun avancement. En outre, la machine s'enlise le plus souvent au même moment.

On peut donc trouver des conditions de travail où, momentanément on acceptera un très mauvais rendement, mais où il faudra passer « à tout prix » à travers la zone difficile pour éviter le catastrophique enlisement.

Par ailleurs, l'avancement économique ne peut être détaché d'autres préoccupations : il faut que la machine porte sur le sol *sans enfoncer*, d'abord parce que c'est une condition nécessaire à l'avancement mais aussi parce qu'il ne faut ni perturber le sol en profondeur, ni creuser des ornières, ni nuire aux racines des plantes qui sont en cours de développement.

Il faut également *éviter de tasser le sol* pour ne pas asphyxier ces mêmes racines ou empêcher la germation des grains.

Il faut que l'avancement se produise *sans usure* excessive des organes de contacts avec le sol non seulement sur le champ, mais surtout sur le sol dur des routes où toutes les machines ont également à se déplacer.

Donc, problèmes complexes, offrant une infinité d'exigences souvent contradictoires, échappant à toute loi générale et qui se résume à cette question :

Comment faire avancer une machine agricole dans un champ ?

S'il n'y a pas d'adhérence, il n'y a plus d'Agriculture possible.

Cette question préoccupe les cultivateurs du monde entier, qu'ils soient

en zones périodiquement humides comme c'est le cas de l'Europe Occidentale ou en zones constamment sèches, car dans ces dernières zones les sols sont le plus souvent pulvérulents et dépourvus de cohésion.

L'année qui vient de s'écouler a connu bien des inquiétudes et des déceptions dans ce domaine.

Or, on doit constater qu'il existe *une très grande variété de méthodes, de dispositifs mécaniques* et de *conceptions diverses, de machines* destinés à améliorer l'adhérence et il ne se passe pas de semaine sans que soit déposé un nouveau brevet sur cette question.

Bien plus, chaque paysan a une idée personnelle et arrêtée sur ce que « devraient » faire les Industriels pour que ces machines adhèrent mieux.

Essayons de dresser *l'inventaire des moyens d'avancement* sur le sol, de rechercher *l'idée qui a déterminé leur adoption, d'en voir l'efficacité*, de déterminer les parentés qui existent entre ces moyens et peut-être de voir à travers les succès et les échecs si l'on peut définir *les conditions de l'adhérence*.

Quels sont les modes de déplacements terrestres connus a ce jour?

1) *Le glissement* de l'objet traîné ou poussé *sur le sol* ; son avancement dépend de sa forme générale, du coefficient constamment variable de glissement de ce corps sur la terre, des obstacles plus ou moins déformables qu'il rencontre sur son trajet.

2) *Le glissement sur une surface choisie et construite* ; c'est la pierre que les bâtisseurs de pyramides poussaient sur des madriers, retirant ceux-ci, derrière, au fur et à mesure de l'avancement, pour les reposer en avant.

On peut considérer que depuis les pyramides, le progrès que constitue la chenille se résume essentiellement à ceci : on a supprimé l'homme qui déplaçait les madriers et celui qui poussait la pierre.

3) *Le levier* : c'est en particulier le principe utilisé dans la *roue* : si l'on considère un instant très bref du déplacement d'une roue motrice d'un tracteur, on constate que l'effort moteur (le point de contact de la roue au sol étant supposé fixe dans cet instant) tend à éloigner le centre de gravité du tracteur vers l'avant, grâce à un effet de couple. Ou, ce qui revient au même, l'effort tend à éloigner le point de contact avec le sol vers l'arrière.

Si l'adhérence est bonne, c'est le centre de gravité qui avance et le roulement de la roue qui s'amorce.

Mais le déplacement par effet de levier est, en fait, celui de la plupart des animaux et celui de l'homme : On peut très bien concevoir un mode de déplacement mécanique constitué par une succession d'implantation sur le sol, sans glissement, et par un mouvement du type « levier ». C'est le pas prudent du héron posant une patte après l'autre sur la vase. C'est aussi à un certain point de vue, l'avancement du tracteur à chenille se déplaçant mécaniquement (par roulement) par rapport aux patins supposés immobiles pendant leur appui sur le sol.

4) On doit aussi citer un mode particulier de déplacement qui est le *hâlage*. Il consiste à tirer un corps mobile à distance depuis un point fixe.

Ce procédé est d'un emploi limité mais il est à peu près indifférent à la nature du contact avec le sol, et à la pente. Il est utilisé encore pour les cultures en montagne dans le labour au treuil, ou dans l'emploi de motoculteurs auto-hâleurs.

Ainsi donc, quel que soit le mode de locomotion, ils procèdent toujours des mêmes modes de progression (qui peuvent d'ailleurs très bien être associés) : *glissement* et *effet de levier*, ce dernier étant produit par rapport aux points de contacts du véhicule avec le sol ou par rapport à un point fixe extérieur (hâlage).

On ne peut faire déplacer un corps par glissement qu'en le laissant obéir à la gravité sur une pente, en le poussant, ou en le tirant. Ces deux derniers cas supposent soit le hâlage, soit l'emploi d'une machine mobile pour tirer ou pousser, ce qui pose à nouveau la question du déplacement de cette machine.

Par contre, l'effet de levier provoque par lui-même la déplacement vers l'avant de la machine, dans la mesure ou il y a une réaction du sol qui s'oppose au glissement vers l'arrière.

Ce sont les péripéties de cette recherche d'effort de levier sans glissement qui constituent l'histoire de l'adhérence, et nous allons tout d'abord les envisager à propos de l'évolution du pneumatique de tracteur agricole.

Ce faisant, nous aurons toujours constamment à l'esprit ces deux causes de non adhérence que sont : la présence d'outils accrochés dans le sol et qui retiennent le tracteur comme un câble retient un bateau au rivage, et l'inaptitude des sols agricoles à faciliter l'adhérence.

Comment le pneumatique agricole s'est adapté aux besoins de l'adhérence?

Nous avons déjà eu l'occasion d'étudier l'évolution du *pneumatique agricole;* résumons-en les étapes [1] :

En 1930, on a monté sur un tracteur agricole, par hasard, des pneus d'avion inutilisés. Il s'agissait de pneus très *volumineux* et lisses. On a constaté qu'ils portaient bien le tracteur et ne se détruisaient pas en quelques heures de service, comme on l'avait craint tout d'abord. Aucun document n'est parvenu jusqu'à nous pour nous dire si des efforts de traction avaient été mesurés.

Très vite, on a constaté qu'ils glissaient sur eux-mêmes. L'effet de levier ne jouait donc pas en faveur de l'avancement.

On a réalisé sur la surface du pneu des *barrettes* ou *crampons* analogues à ceux des roues en fer. L'idée (informulée) était la suivante : prendre appui sur une plus grande épaisseur de terre et tirer profit de la résistance du sol au cisaillement. On ne s'apercevait pas qu'en fait c'était à son poids énorme que le tracteur à roues fer devait le plus clair de son adhérence.

Très vite, d'ailleurs, on est arrivé à cette constatation : la résistance au cisaillement joue peu, la terre se bourre entre les sculptures, et on a remplacé le glissement caoutchouc-terre par un glissement terre sur terre.

Apparaissent alors les pneumatiques à « *centre ouvert* ». Les barrettes sont indépendantes les unes des autres pour que la terre se dégage plus facilement.

A la même époque, le tracteur devenu machine motrice pour tous les travaux s'allège considérablement. Un besoin plus aigu d'adhérence se fait sentir.

On découvre alors que le glissement diminue si le pneu est *souple*, déformable, parce qu'il présente alors une surface d'appui réel plus grande et que les barrettes rendues ainsi mobiles dans le roulement se débarrassent plus aisément de la terre. C'est *l'auto-nettoyage*.

Pour obtenir un pneu souple, il faut une carcasse déformable et une faible pression de gonflement.

La pression de gonflement joue un rôle complexe : elle doit être assez forte pour tenir le pneu serré sur sa jante et limiter sur route l'usure et les fatigues dûes à un travail excessif de la carcasse, mais il faut aussi qu'elle soit assez faible pour donner une bonne adhérence. Le cultivateur doit donc adapter la pression de gonflement à la nature de son travail.

Donc, on a cherché d'abord à *accrocher* le pneumatique dans le sol, puis à *l'étaler* sur le sol sans bourrage de terre.

Mais les tenants de l'accrochage n'avaient pas dit leur dernier mot : ils préconisèrent de hautes et étroites barrettes destinées à aller prendre appui en profondeur sur les « couches fermes », sans que quiconque se préoccupe d'ailleurs de savoir si de telles couches existaient. Le résultat le plus clair fut de fraiser le sol et d'obtenir, en outre, sur route, une usure rapide et une fatigue du matériel. On revint donc à des barrettes de hauteur raisonnable, et on améliore les angles de dépouille pour augmenter le dégagement de la terre.

Mais on s'aperçut très vite qu'aucun perfectionnement de pneumatique n'est efficace si l'on tombe au-dessous d'un certain *rapport poids-puissance*.

Nous avons dit que les tracteurs s'étaient allégés en 15 ans en passant de 120 Kg/cheval à 50 Kg par cheval.

Or, si l'on veut que le point d'appui inférieur du levier ne glisse pas vers l'arrière, il faut bien que cet appui soit suffisant. Si la terre obéit trop docilement au cisaillement (cas des terres sablonneuses et légères) il faut redonner un court instant à ce sol une cohésion suffisante pour qu'il donne la réaction que l'on attend de lui. Autrement dit, il faut lui faire subir une compression momentanée. Nous reviendrons tout à l'heure sur cette question, mais une troisième arme apparaît donc dans l'arsenal après l'accrochage et la souplesse : *le poids*.

On constate à la même époque que le moteur diesel, beaucoup moins souple que le moteur à essence, transmet brutalement l'effort moteur sans baisser de régime lorsque l'effort résistant s'accroît, et qu'il favorise ainsi les amorces de patinage. On commence peut être à soupçonner à partir de ce moment, *qu'une plus ou moins grande souplesse dans la liaison entre le moteur et le point d'appui joue un rôle dans l'adhérence*.

Le tracteur s'allégeant toujours, on revient à l'idée d'une *surface d'impact plus grande* : sur un même tracteur, on met des pneus plus grands, sans très

bien réaliser qu'augmentant la surface et diminuant le poids par centimètre carré, on a peu de chance d'aboutir à un résultat appréciable.

On cherche également à donner au pneu un impact plus grand en le montant sur une jante aussi large que possible (c'est actuellement la tendance américaine dite : *extra wide base*) ou en donnant une forme telle au pneu, qu'à volume égal il ait une bande de roulement plus large et des flancs moins élevés (*low section height tires*). Les gains d'adhérence restent modestes.

Il nous semble que, si les premières améliorations apportées au pneu d'avion promu accidentellement pneu agricole engendrèrent un progrès considérable, chaque perfectionnement nouveau apporte un progrès de moins en moins important, et surtout de moins en moins général. Cette série décroissante veut-elle dire que nous allons vers une limite au delà de laquelle seule une formule vraiment révolutionnaire permettra de faire un pas réel en avant? Il est trop tôt pour le dire.

Quelles sont maintenant les plus récentes étapes de cette tentative de perfectionnement du pneu?

Il semble que ce soit la *carcasse* qui soit à l'ordre du jour. La première étape fut de l'alléger pour la rendre plus souple. Les textiles actuels à haute ténacité permettent de le faire en conservant une marge de sécurité importante. Il faut toutefois limiter l'amincissement pour que les épines cheminant entre les fils n'atteignent pas la chambre à air.

On cherche ensuite à lui donner une forme plus *aplatie* pour augmenter la part du pneu qui est au contact du sol.

C'est le cas (mais ce n'est pas la seule solution) du pneu avec carcasse radiale et ceinture : la nappe textile tendue autour de la zone de roulement oblige le pneu à s'aplatir au gonflage, ce qui lui donne une très bonne « assiette », en particulier sur les sols légers et secs. Cette formule donne aussi une bonne résistance à l'usure mais parfois au détriment de la souplesse souhaitable au niveau de la bande de roulement.

On s'intéresse aussi aux *rapports* qui existent *entre la bande de roulement et les flancs*, et entre les *diverses parties de la bande de roulement* elle-même.

La souplesse des flancs est une qualité (sauf en terrain très accidenté) parce qu'elle aide à la souplesse de l'ensemble. C'est un heureux effet de la carcasse radiale qui corrige ainsi dans une certaine mesure la rigidité de la bande de roulement.

Mais cette souplesse a aussi un autre rôle à jouer : absorber les augmentations momentanées d'effort à la jante (cas du moteur diesel) sans amorce de patinage. La rotation de la bande de roulement doit avoir une certaine indépendance par rapport à celle de la jante, et les flancs jouent alors un rôle d'amortisseurs.

Enfin des recherches sont faites en vue de *rendre indépendantes les unes des autres les sections successives de la bande de roulement*, pour que, étant au

sol, elles ne subissent pas la compression venant de la partie de la bande de roulement qui est en avant, et pas davantage la traction de celle qui est en arrière.

C'est la recherche des *points d'appuis successifs indépendants* que nous évoquions au début de cet exposé.

Les idées formant les lignes de force de l'évolution la plus récente du pneumatique pour roue motrice de tracteur intéressent donc :

— *l'amélioration de la structure de la partie du pneu qui est au contact du sol;*

— *l'amélioration des rapports entre cette zone de contact et l'effort d'entraînement.*

Ensemble des moyens d'adhérence du tracteur agricole

Envisageons maintenant l'ensemble des moyens préconisés pour améliorer l'adhérence, dans le cas précis du tracteur agricole. Nous y retrouverons d'ailleurs les étapes de l'évolution du pneumatique.

A) Moyens d'adhérence ne comportant ni accessoires particuliers ni transformation du tracteur.

Le réglage de l'outil : il s'agit de donner essentiellement à la charrue une position telle que la résultante des forces (résistance de l'outil, poids sur les deux essieux, résistance à l'avancement, etc.) passe au voisinage des points de contact des roues motrices du tracteur avec le sol, et ait une composante verticale aussi importante que possible (dans les limites de sécurité et de possibilité de travail).

On cherche donc à augmenter au maximum la *force verticale* qui appuie les roues motrices sur le sol.

Les techniques dites de *transfert de charges instantanées* permettent de modifier à tout instant l'importance de cette force, et donc de *l'adapter aux conditions constamment changeantes du terrain.*

L'emploi de la remorque semi-portée répond aussi à l'idée d'une augmentation de poids sur l'essieu moteur du tracteur, lorsque la charge à tirer s'accroît.

Les augmentations directes de poids : le tracteur s'étant allégé par son mode de construction, et certain travaux ne nécessitant pas une forte traction (binage, transport sur sol dur) on a recours *momentanément* à des surcharges par apport de masses en métal ou d'eau dans les pneus.

Il serait sans doute plus rationnel d'ajouter ces masses sur l'essieu même du tracteur, l'augmentation de poids étant plus efficace sur la partie transportée de la machine que sur le levier lui-même, c'est-à-dire la roue. Mais, pour des raisons de commodité, on place en général ces masses sur le roues.

Le lestage à l'eau constitue une méthode complémentaire et économique

d'augmentation de poids, mais il est de réalisation assez malaisée (nécessité d'un antigel) et, à poids égal, il donne des résultats inférieurs à ceux des masses de métal [2].

Tous les moyens que nous venons d'indiquer sont directement ou indirectement des recours à un accroissement du poids sur l'essieu moteur. On agit exactement comme si l'on voulait retrouver le poids perdu depuis que les tracteurs se sont perfectionnés.

Mais le grand progrès est que l'on peut n'ajouter ce poids qu'aux seuls moments où on en a effectivement besoin.

Abaissement de la pression de gonflement des pneumatiques. — Nous en avons parlé précédemment.

Il a pour but d'augmenter la surface d'impact sur le sol et de mieux répartir les zones de pression. Il rend le pneu plus souple et plus « moulé » sur le sol. Il facilite l'auto-nettoyage en augmentant la mobilité des barrettes (tout au moins dans les pneumatiques à carcasse conventionnelle). Il a peu d'influence sur le cisaillement et sur la pression moyenne exercée sur le sol par unité de surface.

Au total, il donne une amélioration très sensible à l'adhérence mais est limité par le risque de tourage sur jante à environ 800 grs de pression par centimètre carré.

Le retournement des pneus sur leurs jantes. — Ce procédé est utilisé en sols sablonneux secs, là où le plus grand risque est souvent constitué par l'enfoncement de la roue dû à l'écoulement du sable sur les côtés du pneu.

Le profil qui est destiné, dans le sens de rotation normale, à écarter et dégager la terre collée aux pneus, tend, une fois retourné, à rassembler le sable sous le pneu et l'empêcher de s'enfuir.

Choix d'un rapport de vitesse et d'un régime moteur appropriés. — Nous revenons à la transmission des efforts du moteur à la bande de roulement.

Lorsque le tracteur avance sur un terrain de médiocre adhérence et qu'il fournit un effort élevé (75 % de sa puissance motrice par exemple) avec un patinage qui devient important, il suffit d'une très légère et brusque augmentation de l'effort moteur pour passer au patinage total.

Ce léger effort peut être une réponse à un accroissement de la résistance de l'outil dans le sol. Si la transmission est très démultipliée et le régime élevé, ce régime (dans le cas du diesel) ne baisse pas sous l'effet de cette résistance : le moteur « répond » à la résistance plus forte par un effort plus grand, et c'est le patinage total.

Sur un terrain de mauvaise adhérence, il faut donc choisir une démultiplication plus petite (par exemple le 3ème au lieu de la 2ème) et un régime plus bas pour augmenter les chances de fléchissement momentané du moteur sous l'effet des accroissements de résistance.

Embrayage sans progressivité. — Ceci n'est nullement en contradiction avec ce qui précède.

Nous nous plaçions dans le cas où le tracteur avançait à son régime et au voisinage de l'effort maximum.

Ici, nous envisageons le démarrage. Celui-ci demande un effort élevé puisqu'il faut vaincre l'inertie du tracteur et souvent celle de la charrue déjà à demi engagée dans le sol.

L'expérience montre que l'embrayage sans progressivité permet le démarrage si le rapport de vitesse a été choisi correctement; ceci dans des terres agricoles de médiocre cohésion ou trop glissantes.

Nous parlons, bien entendu, d'un tracteur muni de pneumatiques agricoles à sculptures.

Un embrayage progressif et, en particulier, un embrayage hydraulique donnent, par contre, des résultats médiocres à l'opposé de ceux qu'ils peuvent fournir sur un sol ferme.

On peut rapprocher ces phénomènes des constatations que nous avons pu faire en mesurant les compressions de sol agricole sous le passage des roues de tracteur. On remarque, en effet que la terre, se comportant comme un solide semiélastique, se comprime momentanément sous la roue [3]. La déformation est d'autant plus grande que le poids par centimètre carré est plus élevé, mais d'autant plus faible que la passage de la roue a été plus rapide.

Dans le cas du démarrage, la terre qui est immédiatement en arrière de la barrette est comprimée vers l'arrière; elle obéit d'autant moins à cette sollicitation que le temps d'effort est plus court. Elle a donc, dans ce cas, une réaction élastique meilleure et l'effet de levier joue en faveur du déplacement du tracteur vers l'avant.

On voit au passage le rôle important que jouent les barrettes au moment du démarrage.

B) Dispositifs complémentaires d'adhérence.

Jumelage des pneumatiques. — Il double la surface d'impact mais diminue de moitié la pression moyenne par centimètre carré.

Son principal mérite est de permettre un abaissement plus important de la pression de gonflement (450 grs) ce qui transforme les pneus, si leur carcasse est assez souple, en véritables ventouses posées sur le sol.

Si le jumelage est utilisé pour augmenter l'effort de traction, il soumet le pont et les transmissions à des contraintes considérables.

Les chaînes d'adhérence : elles sont destinées à obtenir un plus fort cisaillement. Ce qui suppose donc que le sol a déjà une résistance honorable au dit cisaillement.

Les chaînes d'adhérence ont souvent le défaut de se charger très vite de terre et d'être, pour cette raison, difficiles à retirer en bout de champ. Il leur est interdit de rouler sur la route. Ce sont, en général, les plus simples qui sont les meilleures.

Les griffes d'adhérence et les roues-squelettes. — Ces griffes fixées à l'extérieur des roues, ou ces roues très plates en métal dont les rayons mé-

talliques se prolongent en bêche au-delà de la jante reprennent une même idée : aller chercher la couche dure sous les zones superficielles sans cohésion.

Si cette couche existe réellement, elles peuvent être efficaces. Mais les cas en sont assez rares.

Citons, cependant, celui des rizières récentes dont le sol est mal stabilisé parce qu'il a été apporté au-dessus du niveau primitif pour des motifs de nivellement, et parce qu'on a eu l'imprudence de la labourer l'hiver.

Citons aussi les terres d'argile labourées depuis un siècle à la même profondeur et où le talon de la charrue a lissé, à 30 cm de profondeur, une couche dure qui retient l'eau et rend le sol boueux à la moindre pluie.

Mais c'est un équipement barbare pour la mécanique du tracteur.

Les cages extérieures et les roues cages. — Elles appellent les mêmes réserves mécaniques que ce qui précède, mais peuvent être efficaces dans les cas désespérés.

La roue cage est un cylindre fait de tube ou de fer en T, qui remplace la roue normale.

Elle peut avoir plus d'un mètre de large (rizières). Son rôle n'est pas comme on le croit souvent d'augmenter la surface d'impact (puisqu'elle est à claire-voie) mais de multiplier les points de cisaillement.

La cage est dite extérieure lorsque, au lieu d'être substituée à la roue normale munie d'un pneumatique, elle y est au contraire fixée. Elle constitue un perfectionnement par rapport au système précédent en ce sens que, grâce à son diamètre légèrement inférieur à celui du pneumatique, elle n'entre en action qu'au moment où ce dernier commence à s'enfoncer.

Les semi-chenilles. — Elles sont nées de l'idée d'augmenter en sol glissant la surface d'impact.

Le réglage de la roue de tension, en avant de la roue motrice du tracteur, permet en théorie de répartir la charge sur l'essieu arrière au long de la zone d'impact de cette semi-chenille.

Mais on a diminué la pression unitaire au sol. De plus ce dispositif rend malaisé le braquage. Il est, néanmoins, apprécié dans certaines terres à betteraves.

Surdimension des pneumatiques. — Nous en avons parlé à propos de ceux-ci. On cherche, en général, à surdimensionner par l'emploi de pneumatiques de plus grand diamètre.

On se trouve limité dans l'élargissement des pneumatiques par la largeur de la raie de labour ou par la nécessité de passer dans une culture en végétation.

En surdimensionnant par accroissement de diamètre, on choisit sans le savoir la solution mécanique qui est le plus souvent la meilleure.

Nous verrons, en effet, tout à l'heure que la longueur de l'impact du pneu sur le sol a plus d'importance pour l'adhérence que la dimension perpendiculaire, c'est-à-dire la largeur.

Mais la surdimension en diamètre augmente les efforts à l'essieu et modifie les rapports de vitesse d'avancement et de rotation de la prise de force.

L'amélioration du couple à la jante qui résulte de la surdimension en diamètre, peut toutefois dans les terres dépourvues de cohésion présenter un inconvénient.

Ainsi, lors d'essais dans les sables des Landes, nous avons constatés que les pneus de grande diamètre, accrochant énergiquement dans le sol et conservant sans défaillance leur vitesse angulaire dans le passages difficiles, avaient une tendance plus grande que les autres à passer en patinage total, et à d'enliser.

Pour être plus précis, on doit donc dire que la surdimension en diamètre permet la meilleure transmission des efforts mais que dans des sols vraiment dépourvus de cohésion cette qualité va à l'encontre du but à atteindre et qu'il vaut mieux préférer une surdimension en largeur. Celle-ci limite l'enfoncement et par conséquent l'effort demandé au moteur.

Par contre, sur un terrain portant bien et de bonne cohésion, le pneu de grand diamètre donnera un effort au crochet supplémentaire.

Les montages sur jante *Extra wide base* et les pneus dits « *Low section height tires* » que nous avons évoqués au chapitre précédent, constituent eux aussi des tentatives de surdimension, mais cette fois-ci sans variation de diamètre [4].

Tous les auteurs sont d'accord et nos propres essais nous ont toujours confirmé que le gain d'adhérence dû à la surdimension est extrêmement faible si celle-ci ne s'accompagne pas de l'augmentation de poids sur l'essieu correspondant.

Autrement dit, si un pneu de plus grand diamètre ou de plus grande section a une capacité de charge plus grande que le pneu d'origine, il faut ajouter sur l'essieu un poids correspondant à l'écart de charge portante des pneus considérés pour enregistrer un gain effectif de traction.

Changement de dimension des roues avant. — Ce changement est motivé par le souci de diminuer dans des terrains portant mal la cause de résistance à l'avancement que constituent les roues de faible diamètre et de faible section qui s'enfoncent facilement, creusent une ornière et poussent devant elle un bourrelet de terre qui résiste à l'avancement. En les remplaçant par des roues plus grandes et plus larges, on rend la direction un peu plus dure mais on élimine en grande partie cette résistance.

C) Choix d'un tracteur ou d'une machine en se plaçant au seul point de vue de l'adhérence.

Le tracteur à quatre roues dont deux motrices est, en général, le plus répandu. La répartition classique de poids est pour le tracteur nu : ⅓ à l'avant, ⅔ à l'arrière.

Une souplesse suffisante du moteur (et en particulier une possibilité importante de variation de régime) et un nombre élevé de vitesses sont bénéfiques pour l'obtention d'une bonne adhérence.

Il est vraisemblable qu'un entraînement hydro-statique des roues appor-

ternit une amélioration dans ce domaine, sauf peut-être, comme nous l'avons vu, pour le démarrage ou même les déplacements à vitesse très lente.

Le premier perfectionnement dont l'avantage est évidente est le *blocage de différentiel.*

Il a pour but, lorsqu'une roue est ralentie momentanément dans sa rotation par la nature du sol ou par un changement dans la ligne de traction de l'outil, ou par un alourdissement dû à l'inclinaison du tracteur, d'éviter que l'autre roue n'accélère son mouvement et ne perde toute adhérence.

Le rôle normal du différentiel qui est de limiter l'usure dans les courbes sur sol dur, est en effet sans objet dans ce cas.

Le tracteur à quatre roues motrices est un autre progrès sensible; il permet de doubler la surface des impacts « actifs » sur le sol, et d'utiliser le poids sur l'essieu avant, sans qu'il soit nécessaire d'effectuer un report de charge.

La meilleure répartition de poid est de la moitié à l'avant et la moitié à l'arrière; les quatre pneus doivent être de même diamètre. Le principal obstacle à l'emploi de ces tracteurs est leur prix.

Un type particulier de tracteur est celui dont les autres roues (motrices) *ne sont pas braquables*, mais montées sur essieux fixes. Les essieux sont eux-mêmes reliés entre eux par des chaînes enfermées dans des caissons à huile. L'ensemble mécanique est puissant et brutal. On a comparé de tels engins à des tracteurs munis de chenilles isolées du sol. En fait, ce sont des tracteurs dont les quatre roues motrices sont solidaires et liées par une absence générale de différentiel.

Il existe, toutefois, un prototype de tracteur à quatre roues non braquables, dont les roues peuvent être désolidarisées par un ensemble complexe de différentiels.

On diminue également la demande d'adhérence faite au tracteur *en facilitant le travail de l'instrument tracté.*

Abandonnant de plus en plus le moteur auxiliaire, on demande au moteur du tracteur, par l'intermédiaire de sa prise de force, de fournir à l'outil la part d'énergie qui est (toujours) inemployée dans ce tracteur: entraînement des pièces travaillant sur les machines de pseudo-labour ou de récolte, des roues porteuses de la remorque, de la charrue-rotative.

Ce dernier instrument encore assez peu employé en Europe, sauf dans les cultures maraîchères, provoque une dislocation des couches superficielles plus intense qu'une charrue ordinaire, en demandant une traction plus faible.

La prise de force du tracteur est donc un instrument qui contribue à la résolution des problèmes d'adhérence.

Reste enfin *le tracteur à chenilles*, si toutes les solutions précédentes ont échoué.

La chenille permet d'éviter l'enfoncement sur les sols sans cohésion, et de accroître la surface de contact sur les sols glissants. Elle a peu évolué depuis les tout-des prototypes de la fin du siècle dernier et les premiers chars de combat de 1914-1918.

Aussi, on lui reproche son prix élevé d'entretien et les dégâts qu'elle

commet par ripage sur les routes, ainsi que son faible horaire annuel d'utilisation dans une ferme.

L'emploi de petites bobines de caoutchouc ou de petits pneus fixés sous le patin et pouvant rouler sur sol dur dans une direction perpendiculaire à l'axe du tracteur, facilite l'évolution, augmente la vitesse de déplacement et limite l'usure.

Deux domaines d'amélioration s'offrent aux chercheurs: rendre aussi peu solidaires que possible les patins pour limiter la transmission des efforts longitudinaux (c'est le même problème que pour le pneu) et améliorer le roulement du tracteur sur la face interne des patins.

Pouvons-nous après ces inventaires, essayer de classer les modes d'adhérence?

Le poids: c'est l'élément le plus anciennement utilisé. Son rôle est de constituer sous la roue un volume de terre plus dense résistant mieux au cisaillement. C'est dans les sols légers, sablonneux, que le poids est le plus nécessaire au tracteur.

Or, on doit constater que la plus grande anarchie règne dans les charges sur l'essieu moteur du tracteur, puisque, à puissance de moteur égale, elles varient dès le rapport de 1 à 2,5.

Si le poids est trop faible, on atteint le patinage total bien avant que le moteur n'ait donné sa puissance maximum. S'il est trop fort, le moteur s'étouffe avant patinage total. On peut déterminer pour un modèle de tracteur et sur un sol donné le rapport poids-puissance le plus favorable.

On est limité dans l'augmentation de poids par le fait qu'elle entraîne celle de la résistance à l'avancement.

En outre, le poids peut provoquer l'enlisement dans un sol sans cohésion si le pneu ou la chenille n'ont pas un profil approprié.

Enfin, on risque de tasser le sol et d'asphyxier les racines. Seuls les sols correctement travaillés et modérément humides reprennent complétement leur structure primitive après le passage d'une charge qui les a comprimés.

Le poids est donc lié à une surface portante appropriée.

La surface portante: Sur un sol argileux, compact et glissant, l'augmentation de poids est de faible utilité à partir du moment où les barrettes pénètrent dans le sol: le pneu s'enrobe de terre et l'on reconstitue une roue lisse.

Il faut accroître le nombre des unités de résistance au glissement et ceci d'autant plus qu'elles ont une faible valeur. On cherche donc à accroître la surface de contact.

Il faut presque toujours avoir une surface importante pour éviter l'enfoncement, car le patinage élevé est à la rigueur tolérable momentanément si le tracteur ne s'enlise pas.

La forme et les proportions de cette surface ne sont pas indifférentes.

Nous savons que si un pneu large résiste à l'enfoncement (mais aussi à

l'avancement) un pneu de grand diamètre adhère mieux mais peut accroître le patinage dans des sols sans cohésion.

Il existe (toutes choses étant égales par ailleurs) des rapports entre la section d'un pneumatique et son diamètre, qui sont plus favorables que d'autres à une bonne adhérence, parfois dans des limites très étroites et sans qu'on sache toujours pourquoi.

Pour un pneu déterminé, il existe une largeur de jante optimum qui n'est pas obligatoirement la plus importante.

Le rapport entre la hauteur et l'épaisseur des barrettes, ainsi que le rapport entre *leur épaisseur et les espaces qui les séparent* jouent également un rôle qui varie d'ailleurs selon les terrains.

On a essayé de combiner surface et accrochage pour la chenille en munissant les patins de crampons. A moins de donner à ceux-ci un développement considérable, les résultats sont assez peu démonstratifs.

La forme des patins de chenilles, leur rapport entre leur largeur et l'espace qui les sépare a fait également l'objet d'études particulières [7].

Pour revenir au pneu, il est vraisemblable que les liaisons entre un sol d'une granulométrie déterminée et la surface d'un pneu ne sont pas les mêmes selon qu'il s'agit d'un *grand* pneu ou d'un *petit*.

L'abaissement de pression et la souplesse de l'enveloppe qui en découlent (et qui augmentent quand l'épaisseur de la carcasse diminue) jouent le rôle que nous avons signalé: surface plus grande et mieux répartie, meilleur auto-nettoyage.

Mais cet aplatissement de la bande de roulement n'est effectif que si le pneu est suffisamment chargé. Il doit l'être pratiquement au *voisinage de sa charge nominale*.

Un pneu qui a, de par sa construction une large bande de roulement, ou qui a un aplatissement important pour un faible abaissement de pression (ou une faible surcharge) a donc bonne aptitude à l'adhérence.

Signalons au passage la contradiction qui existe entre le besoin de se débarrasser aisément de la terre entre barrettes et la nécessité de maintenir, d'enfermer sous le pneu, un sol dont on veut augmenter la cohésion sous l'effet du poids.

Différents essais ont d'ailleurs été faits pour réaliser, à l'intention de la culture dans les sables, des pneus dont la bande de roulement infléchie dans sa partie médiane, tente *d'empêcher l'écoulement* latéral de ce sable.

Mais, lorsqu'on aborde un sol suffisamment consistant et sec, l'étalement du pneu devient inutile et même nuisible en raison de l'usure.

Il faut donc pouvoir faire varier cette pression.

Variabilité des moyens d'adhérence. — En raison du caractère changeant des sols et de la variété des travaux, il faut que les moyens d'accroître l'adhérence puissent être modifiés facilement, rapidement et avec une grande progressivité: réglage des outils, masses amovibles, transfert des charges répondent à ces exigences. Il serait souhaitable que le conducteur d'un tracteur puisse à tout moment changer la pression de ses pneus sans descendre de son siège.

Ce genre de dispositif n'existe à notre connaissance que sur des tracteurs forestiers russes.

Signalons aussi les élargissements amovibles des patins de chenilles et la possibilité, sur certains modèles de tracteurs, de faire varier la longueur de chenille en contact avec le sol.

Une grande souplesse dans les liaisons entre roulement et moteur est également souhaitable. Soit que cette souplesse provienne du moteur lui-même, soit qu'elle provienne des transmissions, soit enfin qu'elle soit donnée par les flancs du pneumatique (qui doivent néanmoins être très robustes).

Certains chercheurs ont expérimenté des roues ayant une liaison souple entre la jante et l'essieu, mais ces dispositifs sont restés des curiosités mécaniques.

La souplesse est, en particulier, nécessaire pour pouvoir travailler avec un effort important et des patinages momentanés élevés. Il est sans importance dans ce cas de travailler près du patinage total pourvu qu'on ne l'atteigne pas.

Il est utile de *diminuer l'effort résistant* des machines tractées ou portées en les modifiant ou en les recréant pour qu'elles puissent utiliser l'énergie disponible à la *prise de force* du tracteur.

Enfin, le recours à des dispositifs qui prétendent aller *prendre appui en profondeur* dans le sol est, sauf cas particuliers, dépourvu d'intérêt.

Conclusion

Dans la recherche d'un résultat favorable de l'effort de notre levier, c'est-à-dire du mouvement en avant, nous avons examiné les moyens employés et tenté d'en dégager quelques principes.

Ce n'est pas, dans la pratique, à un point de contact sur un sol déterminé que nous avons affaire, mais à une surface d'appui plus ou moins définie, plus ou moins grande, plus ou moins souple, plus ou moins sculptée qui repose sur une infinie variété de sol.

Le roulement agricole est enfermé dans des contraintes beaucoup plus sévères que les autres roulements « out of the road » pour les raisons suivantes :

Le cultivateur doit parcourir la surface entière de chaque pièce de terre.

Il doit créer une structure déterminée du sol, et ensuite ne pas perturber la surface qu'il a créée.

Il doit concilier des nécessités apparamment inconciliables : comprimer le sol sans le tasser, adhérer sans user, etc.

Il doit tenir compte dans ses dates de roulement et de travail du temps nécessaire au développement des végétaux qu'il plante ou sème.

Il ne doit recourir pour assurer son adhérence qu'à des techniques rentables.

C'est pourquoi, nous pouvons dire que l'étude des problèmes de roulement en agriculture constitue la meilleure école pour la résolution des problèmes de roulement tous terrains.

BIBLIOGRAPHIE

Remus J. Problèmes posés aux manufacturiers de pneumatiques par l'évolution de la motoculture. Revue Générale du Caoutchouc, Juillet 1957.

Reed I. F., Reaves C. A. and Shields J. W. Comparative performance of farm tractor tires weighted with liquid and wheel weights. Agricultural Engineering, June 1953.

Remus J. Technique nouvelle dans l'étude des sols. La sonde extensométrique. Agriculture, 1952.

Reed I. F. Some effects on oversizing rear tractor tires. Agricultural Engineering, 1955.

Walters F. C. and Worthington W. H. Low section height tires. Society of Automotive Engineers at Milwaukee, Wis, September 1955.

Reed I. F. and Shields J. W. The effect of lug height and of rim width on the performance of farm tractor tires. SAE National Tractor Meeting Milwaukee, September 1950.

Sonnen F. J. Dimensions et charges portantes des pneus de roues motrices de tracteurs. Landtechnik, Mars 1959.

Luhrs H. Charge de service optimale des essieux moteurs des tracteurs et les dimensions de pneus les plus appropriées qui en résultent. Landtechnische Forschung, n. 9, 1959.

Bekker M. G. Relations entre le sol et le véhicule. Rapport S.A.E., 9 Janvier 1950.

Bekker M. G. Theory of land locomotion. The University of Michigan Press, 1956.

Bekker M. G. Performance improvement in track-type tractors. Agricultural Engineering, Octobre 1958.

N. 52

Triebkraftsteigerung bei Geländefahrzeugen durch das Schub-Schritt-Verfahren

Increased draft for wheeled vehicles operating outside the roadway by the « thrust-stride-system »

Su un mezzo per aumentare lo sforzo di trazione dei veicoli destinati al movimento fuori strada

HANS VON SYBEL - FRANZ GROSSE-SCHARMANN *)

ABSTRACT. -- *A basic study of soil-wheel mechanics has revealed that you can transfer a considerable stronger draft to soil outside the normal roadway by a resting wheel than you can do this by a normally driven rolling wheel. Therefore a periodically agitated two-cycle driving system is proposed for vehicles with pneumatic tyres, such system being supposed to become effective under occasional difficult conditions only.*

This variation of applying a draft is characterized by an alternating movement of performing a stride, whilst the wheel is rotating with little or without pull, to be followed by a locking cycle of the same wheel non-revolving, during which cycle the tractor is pushed forward against the resting wheel by suitable mechanical or hydraulic means. On striding forward wheels may be discarged of weight in order to make decrease the rolling resistance. The kinematics of stopping and striding are synchronized such that an almost perfect continuation of vehicle velocity and pushing force is achieved.

Tests of this device in soil, which were executed by the Munich Institute of Agricultural Engineering, have shown the expected pull increased in comparison with a normally driven wheel. This is due to a first soil-deformation stage achieved by a better use of soil cohesion within the gripping length and to an additional deformation incurred by the anchorage reaction of the pressed soil masses acting on the wheel sunk meanwhile less or more. A muddy soil provides the locked and sinking wheel with more time for getting in touch with the underground resisting more effectively, after the wheel has pushed away the slush. A yet more favourable anchorage effect is achieved, if — depending on step-length and wheel-distance — the tread pressed before can be used by the following wheels striding and stopping in the same manner.

Wie wir zum Thema gelangten

Vor geraumer Zeit wirkte und webte im Bayernland als schöpferisch begabter Ingenieur mit universalem Blick ein bescheidener Landedelmann, der sein Sinnen zeit seines Lebens der Technik in der Landwirtschaft zuwandte:

*) Technische Hochschule, München (Germany).

Clemens Freiherr von Bechtolsheim, Bild *1*. Während sein Dünnschicht-Strömungsprinzip in der Schleuder, damals *nur* Milchschleuder, verbunden **mit um ein** Vielfaches erhöhter Trennschärfe *und* gesteigertem Mengendurchsatz **heute in** aller Welt noch unverändert *genutzt* wird, ist das stille **Ringen um den Schreitwagen**, das seinen Lebensabend *aus*füllte, aus dem Schatten einer **kinematischen Studie**[1] und einer Versuchsaus*führung* kaum herausgetreten,

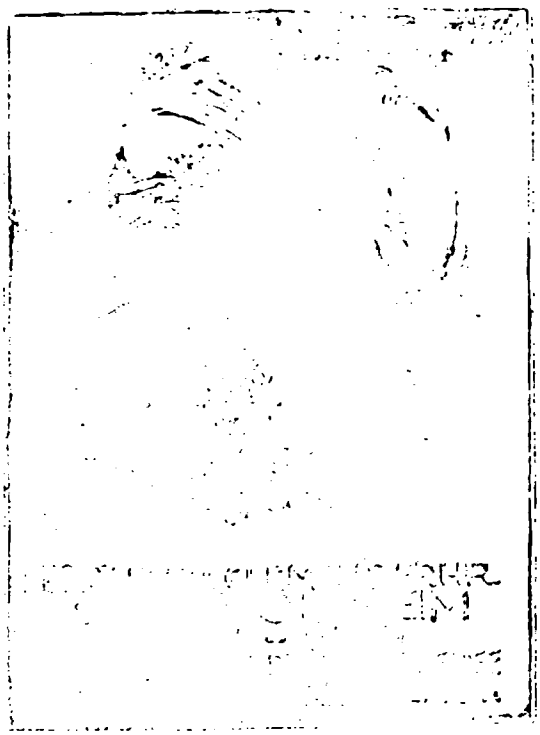


Bild 1. — Die Schreitkinematik erfüllte seinen Lebensabend.

Bild 2. Ob dabei wohl ein Unterbewusstsein *mit*spielte, dass bei der Abkehr vom stapfenden Zugtier zum rollendem Trieb*rad* irgendetwas verkehrt sein müsse, wer vermag es noch zu sagen. Uns blie*b* als anregendes Vermächtnis, der Wahrheit auf den Grund gehend zu erforschen, warum eigentlich der stapfende Huf mehr Zugkraft auf den Boden *ab*stützen solle, als das stetig vorrollende Triebrad.

Um dabei jedoch die Nutzanwendung in *rea*listischem Geleise zu halten, galt es doch wohl vorbehaltlos anzuerkennen, dass der abrollende Plattfuss des Niederdruck-Ackerluftreifens mit seinem bei tragbarem Schlupf annehmbaren Wirkungsgrad der Energ übertragung und in *be*sondere mit seiner Eignung für höhere Geschwindigkeiten auf der Strasse *eine* für die meisten Gelände-

bedingungen äusserst befriedigende Lösung darstellt, die durch eine Schreitmechanik zu ersetzen, ganz und gar ausscheidet. Aber für schwierige Fälle, in denen der Luftreifen zu versagen droht, wäre immerhin die Frage, ob dann nicht ein Schreiten des Luftreifens selber die erahnte und bisher nicht hinreichend begründete Triebkraftsteigerung erbrächte. In solchem bescheidenerem Rahmen der Ergänzung gesehen, galt es also nicht über die noch so reizvolle

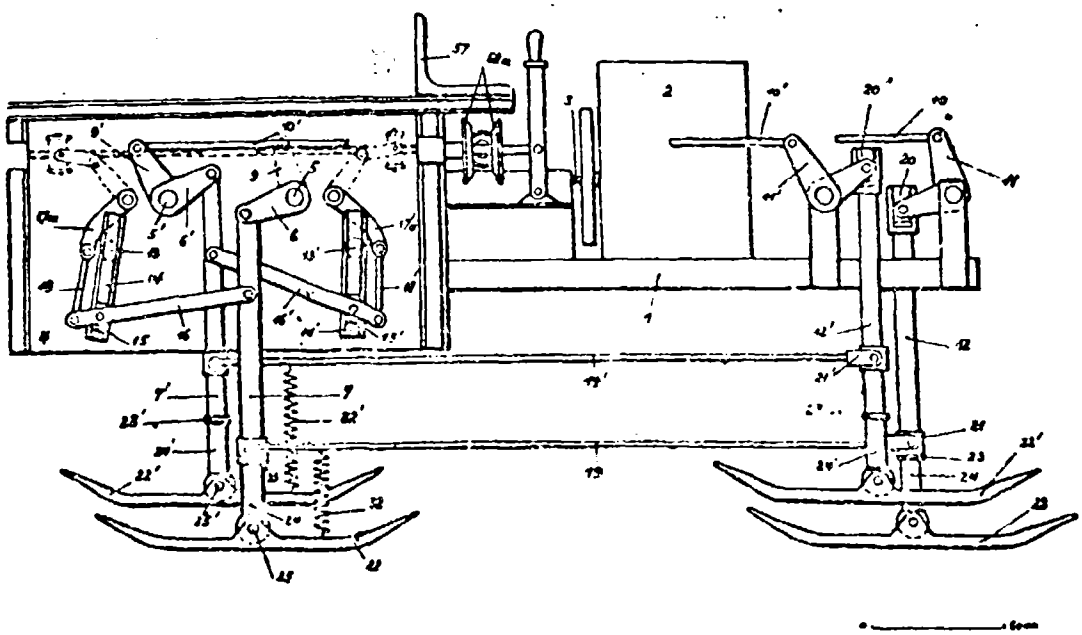


Bild. 2. — Der Schreitwagen des Freiherrn v. Bechtolsheim. DRP 554354 aus dem Jahre 1913.

Kinematik des Getriebes der krabbelnden Vielfüssler, sondern allein über den wahlweise rollend oder schreitend treibenden Luftreifen nach einer intermittierenden Antriebsvariante zu suchen, die eigentlich nur im Notfall in Funktion träte, während es in der Regel beim kontinuierlichen Vorrollen des Triebrades verbliebe.

Bei der experimentellen Verfolgung des Abstützeffektes im Schreiten konnten wir an Vorstellungen von Kurt *Schröter* anknüpfen, einem Fahrzeugpionier aus Thüringen, der schon vor zwanzig Jahren Anhänger mit unter der Ladefläche in Zugrichtung verschiebbarer Hinterachse ausgerüstet hatte; dabei bewirkte ein durch Zapfwelle betätigter Zahnstangentrieb abwechselnd das Vorrollen des Achssatzes unter der dabei stillstehenden Ladepritsche und dann bei blockierten Rädern das Vorschieben derselben. Während des Vorziehens des Achssatzes liess man in diesen erfolgversprechenden Versuchen den Schlepper bis zu 100 % schlüpfen.

Die Idee des Schub-Schritt-Verfahrens *)

Unter Schub-Schritt-Verfahren ist hiernach die besondere Art und Weise der Fortbewegung eines Geländefahrzeuges zu verstehen, bei der die Räder abwechselnd stillstehen und dabei Schubkräfte auf den Fahrzeugrumpf übertragen, und dann wieder um eine bestimmtes Stück (Schritt) gegenüber dem Fahrzeugrumpf vorrollen. Die Bewegungen der jeweils stillstehenden, triebkraftabstützenden Räder und der jeweils rollenden Räder sind so aufeinander abgestimmt, dass eine möglichst kontinuierliche Schubkraft und gleichmässige Fahrgeschwindigkeit des Fahrzeuges entsteht. Werden die jeweils vorrollenden Räder teilweise oder ganz von senkrechter Last befreit, so kann man dadurch den Rollwiderstand beträchtlich senken und bei vollkommener Entlastung sogar zum Verschwinden bringen. Die Entlastung der vorrollenden Räder hat weiterhin eine zusätzliche Belastung der währenddessen stillstehenden, Triebkraft abstützenden Räder zur Folge, wodurch diese wiederum grössere Triebkräfte abstützen können. Aus Stabilitätsgründen ist eine vollkommene Entlastung jedoch erst bei einem sechsrädrigen Fahrzeug praktisch zu verwirklichen. Wird keine oder nur eine teilweise Entlastung der vorrollenden Räder vorgenommen, so können diese beim Vorrollen zur Triebkraftabstützung mit herangezogen werden, wenn man sie rotierend antreibt.

Hauptmerkmale der die geschilderte Fahrweise verwirklichenden Konstruktion sind die mit einer Sperrvorrichtung versehenen Räder, die in vertikaler Ebene um horizontale Achsen durch Steuerzylinder hydraulisch geschwenkt und ausserdem in Richtung der Radstütze hydraulisch be- oder entlastet werden, wie dies in Bild 3 für ein allradgetriebenes zweiachsiges Geländefahrzeug skizziert ist.

Der rotierende Antrieb der Räder kann mechanisch zum Beispiel über Gelenkwellen vom Differentialgetriebe aus oder hydraulisch durch in die Räder eingebaute Oelmotore erfolgen. Im Falle des Differentialgetriebes kommt, wenn das eine Rad gesperrt wird und das andere dann mit doppelter Geschwindigkeit voreilt, im Mittel dieselbe Vortriebsgeschwindigkeit zustande, als ob beide Räder wie normal gleichzeitig rotierend angetrieben werden. Beim hydrostatischen Antrieb ist die gleiche Differentialwirkung durch Parallelschalten der Radmotore zu erreichen. Das Einstellen der Schub-Schritt-Einrichtung hat daher auf die Fortbewegungsgeschwindigkeit des Fahrzeuges keinen Einfluss.

Die Sperrung des Rades während der Abstützperiode kann mechanisch oder hydraulisch erfolgen: Mechanisch zum Beispiel durch den Einbau bekannter Sperrvorrichtungen wie Freilauf oder Klinkengesperre in die Räder, die die Drehung des jeweils zurückbleibenden Rades entgegen der Fahrtrichtung verhindern. Bei Verwendung von Rad-Oelmotoren wird die Blockierung durch Abschalten des Oelflusses erreicht.

---

*) Anmerkung: Dieser Beitrag enthält gleichzeitig auszugsweise die Dissertation des zweitgenannten Verfassers aus dem Institut für Landmaschinen der Technischen Hochschule München, eingereicht 1960.

Beim allradangetriebenen Zweiachsfahrzeug mit Schub-Schritt-Einrichtung erfolgt das periodische Abbremsen und Vorlaufen der Räder so, dass sowohl auf jeder Fahrzeugseite als auch an jeder Achse das eine Rad abgebremst ist, während das andere voreilt, wodurch ein periodisches Auseinanderlaufen und wieder Zusammenlaufen der Räder auf jeder Fahrzeugseite, ähnlich dem Passgang des Kamels, zustande kommt. Beim allradangetriebenen Dreiachsfahrzeug mit Schub-Schritt-Einrichtung (Bild 4) erfolgt das periodische Voreilen

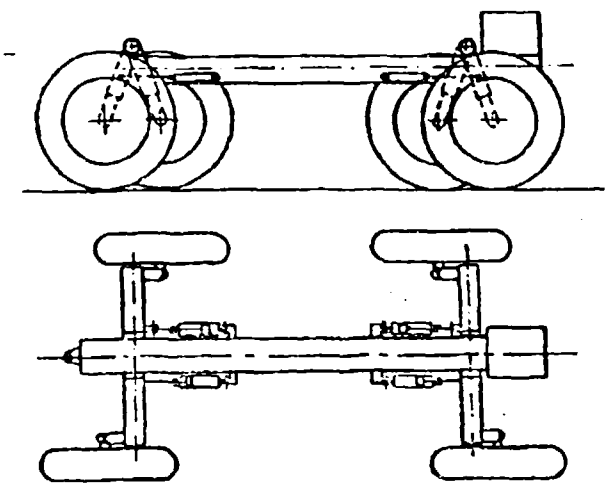


Bild 3. — Zweiachsfahrzeug mit Allradantrieb und Schub-Schritt-Einrichtung; Räder auf der einen Seite zusammenlaufend, auf der anderen auseinanderstrebend, wie beim Passgang.

und Abbremsen der Räder so, dass auf jeder Fahrzeugseite jeweils ein Rad voreilt, wobei es teilweise oder ganz von senkrechter Last befreit ist, während die anderen zwei Räder gesperrt sind und in der beschriebenen Weise Vortriebskräfte auf den Fahrzeugrumpf übertragen.

Die durch den rechten Zylinder hin- und hergeschwenkte Radstütze ist in Bild 5 als hydraulisches Federbein adgebildet, wobei durch Steuerung des Oeldruckes im linken Zylinder die beschriebene Entlastung der Räder beim Vorrollen vorgenommen werden kann. Das schematisch angedeutete Federelement kann als Schraubenfeder oder Gummifeder oder auch als Luftfeder ausgebildet sein. Die Luftfederung beispielsweise ausgeführt als eine mit Druckluft gefüllte Blase, welche durch den Oeldruck zusammengepresst wird, kann auch ausserhalb der Radstützen angeordnet werden; hierdurch wäre gewährleistet, dass die Federung unabhängig von der mit dem Oeldruck veränderlichen Länge der Radstützen voll erhalten bleibt. Der Fahrzeug lenkung dient ein Drehzapfen, um und den das ganze Hydraulik-Radgestell mit seiner Achse schwenkbar ist.

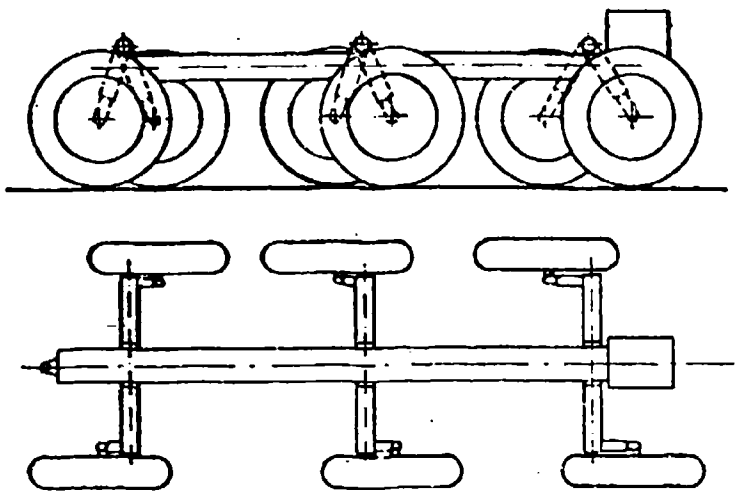


Bild 4. — Dreiachsfahrzeug mit Allradantrieb und Schub-Schritt-Einrichtung; auf jeder Seite ein Rad (gegebenenfalls entlastet) vorrollend, zwei Räder abstützend.

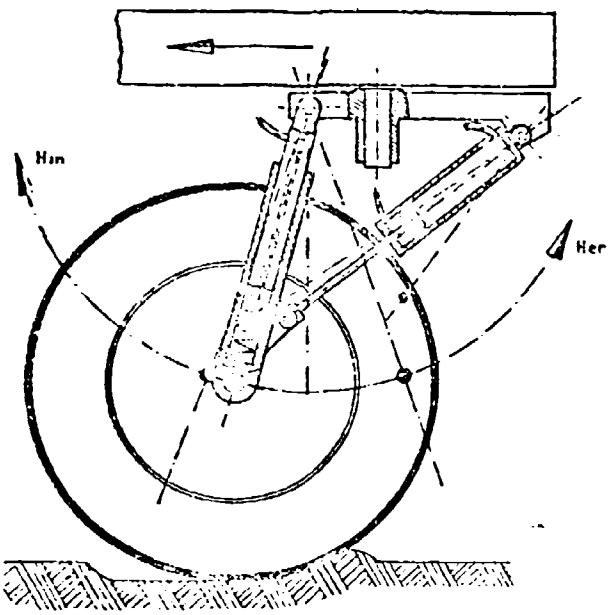


Bild 5. — Die Hydraulik der Radabstützung. Radschwenkung durch rechten Kolben. Hin = Schritt. Her = Schub. Möglichkeit der Radentlastung beim Vorrollen mit dem linken Kolben. Ausserdem: Abfederung und Lenkung des schreitenden Rades.

Die Theorie des Schub-Schritt-Verfahrens

Mit welchen Vorstellungen kann man nun theoretisch Klarheit in den Vorgang der Triebkraftabstützung erstens bei einem blockierten Rad und zweitens bei einem rotierenden Triebrad hineinbringen?

Bekanntlich baut sich die Triebkraft auf den Schubspannungen in der Auflagefläche auf. Diese Schubspannungen τ verlaufen in einem bindigen Boden mit zunehmender Verformung x wie in Bild 6 dargestellt. Ab einem bestimmten Verformungsweg ist die Kohäsion c des Bodens überwunden und die Schubspannung fällt von ihrem Höchstwert τ_s (Scherfestigkeit) auf einen blossen Reibungsanteil $\sigma \cdot \tan \varphi$. Hierin bedeuten σ die Normalspannung und φ den Winkel der inneren Reibung.

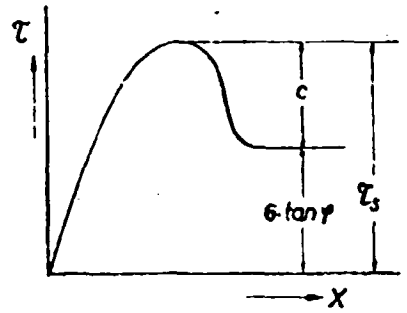


Bild 6. — Schubspannung und Verformung eines kohäsiven Bodens (Schematisches Diagramm).

Triebkraftabstützung beim blockierten Rad. — Setzt man nun ein durch ein Gesperre blockiertes Rad auf dem Boden auf und belastet es mit einer senkrechten Last G, so ergibt sich in der Auflagefläche eine Druckspannungsverteilung σ, die je nach Raddurchmesser und Breite, Reifenluftdruck und Reifensteifigkeit, Bodenzustand u.s.w. verschiedenartig ausfällt, die aber zunächst als gleichförmig angenommen werden möge.

Zieht man mit einer horizontalen Zugkraft T an dem blockierten Rade, so verschiebt sich dieses in Richtung der Zugkraft nach rückwärts. Zum besseren Verständnis soll der Abstützvorgang unterteilt werden:

In einem ersten Abschnitt möge die Verformung noch an keiner Stelle bis zum Abscheren gediehen sein. Auch soll der durch die geringe Verschiebung hinter dem Rade entstandene Erdhügel noch ausser Betracht bleiben. Dann tritt unter dem Rad ein Verformungs- und Spannungsverlauf auf, wie in Bild 8 c bis e für die vereinfachende Annahme konstanter Druckbelastung σ in der Auflagefläche A dargestellt ist. Unter dem Reifen verformt sich der Boden horizontal in einer nach Bild 8 a und b dargestellten Weise. Wie die eingebrachten Kreidestränge bestätigen, ist der Verformungsweg an jeder Stelle e über die Eingriffslänge E der gleiche. Daraus ergibt sich, dass auch die

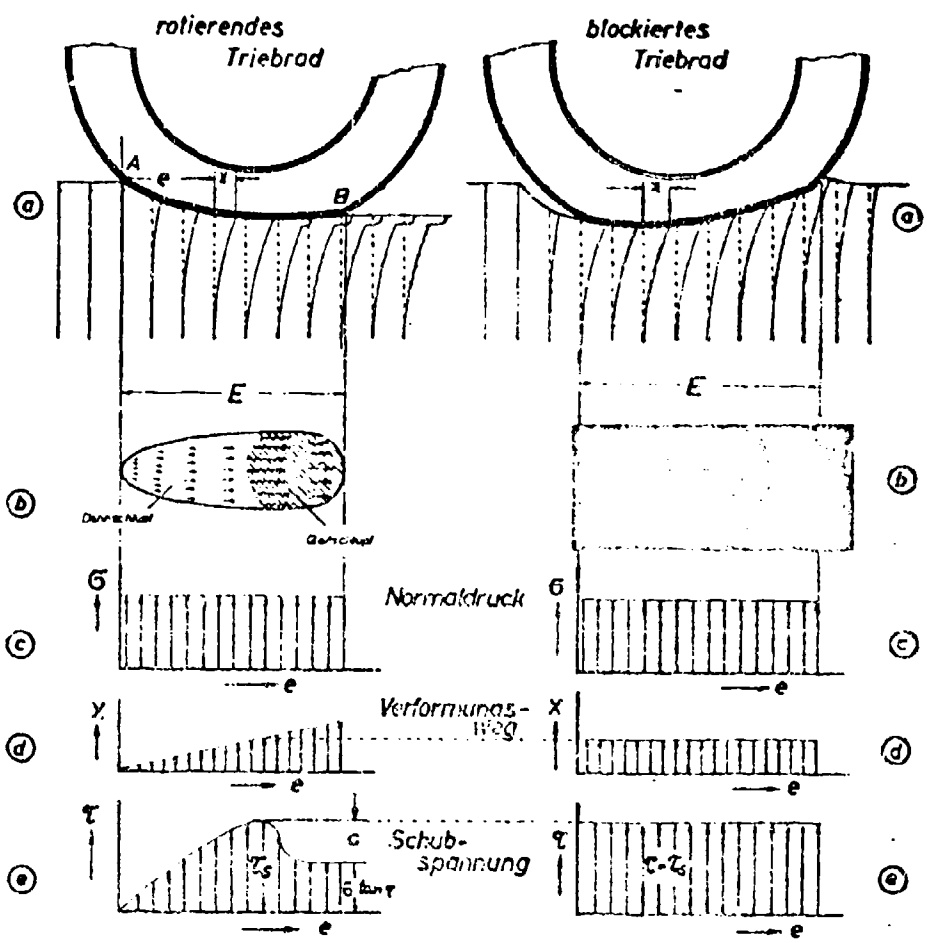


Bild 7.

Bild 8.

Bild 7. — Aufbau der Triebkraft am rotierend angetriebenen Rad. a) Längsschnitt durch senkrechte Radebene; b) Plattfuss: Schubspannungen zunehmend von vorne nach hinten; c) Annahme konstanter Druckbelastung; d) Verformung linear zunehmend; e) Schubspannung nach Höchstwert abfallend; je grösser der Schlupf, desto früher beginnt das Abfallen. (nach W. Sölne) [27].

Bild 8. — Aufbau der Triebkraft am gesperrten Schwenkrad im ersten Abschnitt der Verschiebung. a) Längsschnitt durch die senkrechte Radebene; b-d) Konstante Verformung entlang der Eingriffslänge; e) Annahme konstanter Druckbelastung; c) Konstante Schubspannung im Bereich des Plattfusses.

Schubspannungen über die Eingriffslänge E konstant sind. Hat sich das Rad soweit verschoben, dass gerade die Scherfestigkeit τ_s erreicht ist, so nimmt die Triebkraft ihren höchsten Wert an, nämlich

$$T = \int_{(A)} \tau_s \cdot dA = \tau_s \cdot A$$

Triebkraftabstützung beim rotierend angetriebenen Rad. — Der entsprechende Vorgang der Triebkraftabstützung beim rotierend angetriebenen Rad wurde erstmals von W. Söhne[2], und zwar ebenfalls mit der vereinfachenden Annahme konstanter Normalspannung σ in der Auflagefläche, gemäss Bild 7 c beschrieben: Hiernach nimmt die Bodenverformung x bei einem über die Eingriffslänge als konstant vorausgesetztem Schlupf vom ersten Berührpunkt A bis zum Abhebepunkt B linear zu, wie in Bild 7 d für einen bestimmten Schlupf angedeutet ist. Zur Bodenverformung an jeder Stelle e gehört aber nach Bild 6 eine entsprechende Schubspannung τ. Deren Verteilung für den zugrundegelegten Schlupf ist in Bild 7 e wiedergegeben. Die Schubspannungen steigen vom Berührpunkt A (Bereich elastischer und plastischer Verformung), bis an einer bestimmten Stelle der Auflagefläche A die Scherfestigkeit τ_s erreicht und die Kohäsion überwunden ist. Dann fallen die Schubspannungen auf den konstanten Wert der niedrigeren Gleitspannung $\sigma \cdot \tan \varphi$ ab.

Das Integral der Schubspannungen in der Auflagefläche ergibt wiederum die Triebkraft:

$$T = \int_{(A)} \tau \cdot dA$$

Der Wert dieses Integrals ändert sich natürlich mit dem Schlupf; niemals aber kann hier die Triebkraft den Betrag $T = \tau_s A$ erreichen, der sich als maximaler Wert beim blockierten Rade ergeben hatte. Hiernach ist klar, warum am blockierten Rad theoretisch eine grössere Triebkraft zu erwarten ist, als an einem kontinuierlich rotierenden Triebrad.

Zweiter Abschnitt der Verschiebung beim blockierten Rad. — Im zweiten Abschnitt der Verschiebung eines blockierten Rades (Verschiebung so gross, dass an allen Stellen der Auflagefläche der Boden bereits abgeschert ist) sinkt das Rad weiter in den Boden ein und schiebt Erdmassen vor sich her, verdichtet diese dabei und bildet vor sich einen Erdhügel. Dieser entsteht durch Heben des Bodens von unten her. Zur Klärung des hierbei erfolgenden Abstützvorganges sei auf das theoretische Gleitlinienfeld unter einer Streifenlast* zurückgegriffen, Bild 9 a. Wenn auch beim Rad in der Form der Abstützfläche die Bedingungen für eine Streifenlast (Länge sehr viel grösser als Breite) nicht erfüllt sind, so kann dieser Vergleich doch zu einer Vorstellung über den Vorgang der Triebkraftabstützung nützlich sein.

Beim Rad bildet sich unter der Abstützfläche eine aktive Rankinesche Zone (Bild 9 b), die praktisch als Keil verdichteten Bodens bei der Verschiebung nach rückwärts mit dem Rad fest verbunden bleibt. Neben dem aktiven Bereich entstehen passive Rankinesche Zonen, in denen ebenfalls mit Verdichtung und

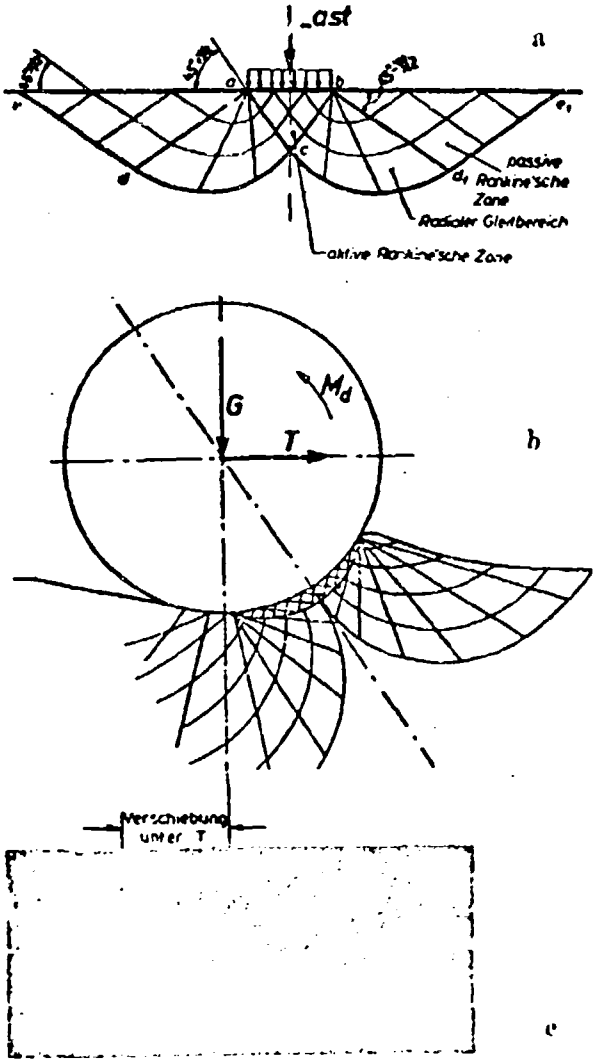


Bild 9. — a) Das theoretische Gleitlinienfeld unter einer Streifenlast; b) Vermutetes Gleitlinienfeld unter blockiertem, eingesunkenem Triebrad, einschliesslich des zweiten Abschnitts der Verformung; c) Bestätigung des zu vermutenden Fliessverhaltens durch ein Netz eingebrachter Gipsstränge: Aktive Rankine-Zone am blockierten Triebrad haftend und nach abwärtsrückwärts mit dem Rade verschoben.

Zunahme der scheinbaren Kohäsion zu rechnen ist. Die daraus resultierende Abstützkraft ist demzufolge umso grösser, je grösser das dem Rad vorgelagerte beanspruchte und verformte Bodenvolumen ist, d.h. auch je tiefer das Rad eingesunken ist.

Wegen der beim blockierten Triebkraft abstützenden Rad erfolgenden Verschiebung nach rückwärts hat man es beim Schub-Schritt-Verfahren auch mit einer Art Schlupf zu tun. Die theoretische Schrittlänge l (Bild 10) wird

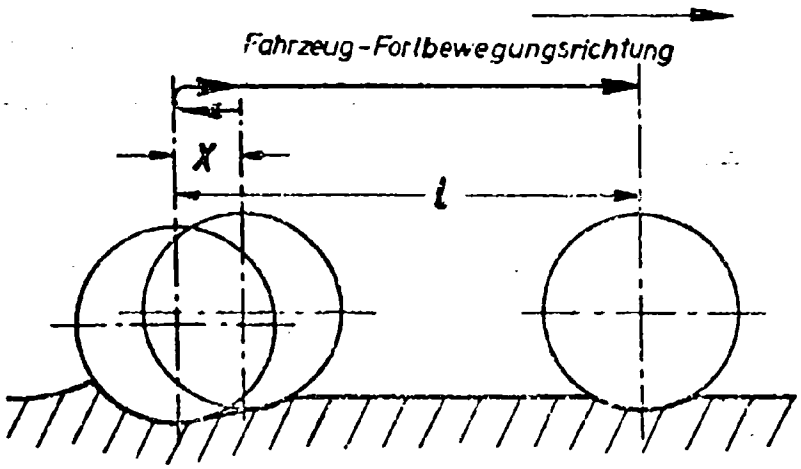


Bild 10. — Kinematischer Schlupf beim Schub-Schritt-Verfahren:
$s' = x/l$; x = Deformation; l = Schritt Stride.

bei jedem Schritt um die Verschiebungsstrecke x des Rades bei der Triebkraftabstützung verkürzt. Aehnlich dem Schlupf beim rotierend angetriebenen Rad kann man hier einen kinematischen Schlupf definieren durch die Beziehung

$$s' = \frac{x}{l}$$

Das Wesen dieser Beziehung ist vergleichbar mit dem Zurückrutschen des Fusses beim Schreiten. Es unterscheidet sich vom Schlupfvorgang beim rollenden Rad, da es sich um einen diskontinuierlichen Vorgang handelt. Der Schlupf s' nimmt mit wachsender Schrittlänge l ab, wenn man für die Verschiebung x zunächst einen konstanten Wert annimmt. Da ein grosser kinematischer Schlupf s' mit einem grossen Leistungsaufwand verbunden ist, soll ein möglichst langer Schritt l angestrebt werden. Die Grenze der praktisch durchführbaren Schrittlänge ist konstruktiv bedingt. Wird die Verschiebung x gleich der Schrittlänge l, so ergibt sich 100 % Schlupf, was bedeutet, dass das Fahrzeug sich nicht mehr vorwärtsbewegt.

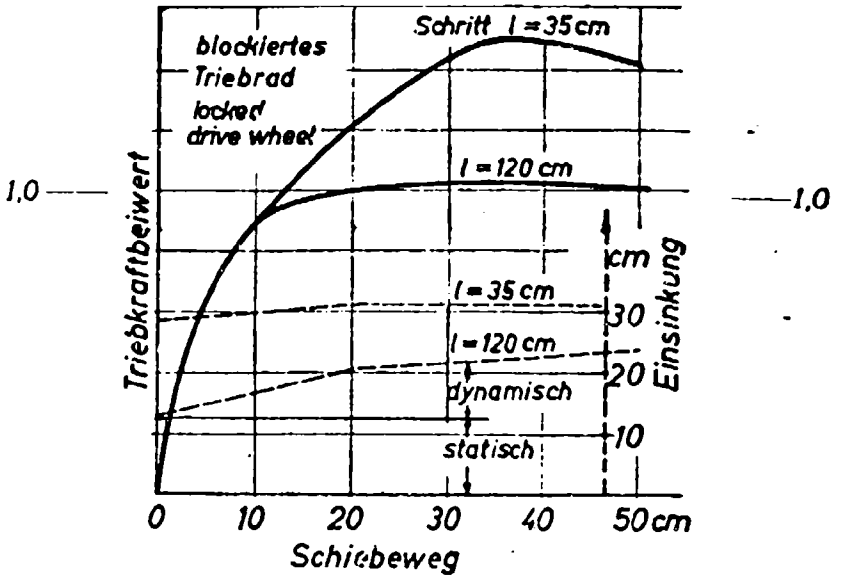


Bild 11.

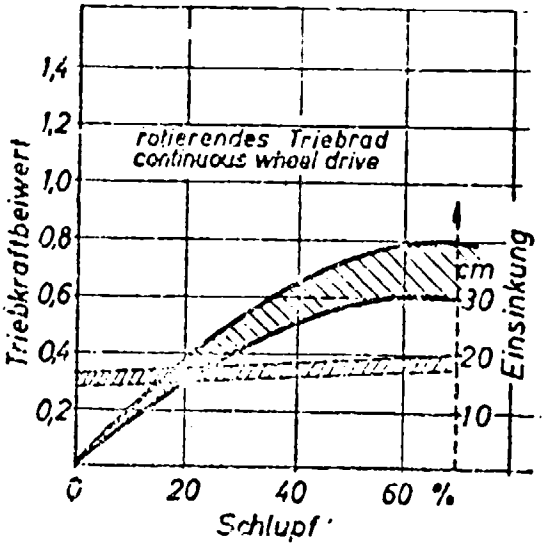


Bild 12.

Bild 11. — Triebkraftbeiwert und Einsinkung beim Schub-Schritt-Verfahren. Im ersten Abschnitt bis etwa 10 cm Verformung sind nur die Schubspannungen wirksam daher Kurven zusammenfallend. Erst nach Abscheren im zweiten Abschnitt Ausnutzung der Verdichtung hinter eingesunkenem Rade zur Abstützung.

Bild 12. — Triebkraftbeiwert und Einsinkung beim kontinuierlich rotierenden Triebrad. Bei tragbarem Schlupf niedrige Triebkraftbeiwerte im Vergleich zum Schub-Schritt-Verfahren.

Experimentelle Untersuchungen

Zur Nachprüfung der theoretischen Betrachtungen und zur quantitativen Ermittlung der Triebkraftsteigerung beim Schub-Schritt-Verfahren gegenüber dem rotierenden Triebrad wurden in unserer Bodenrinne Vergleichszugkraftversuche mit einem rotierend angetriebenen Rad und mit einem blockierten Rad, beide in natürlichem Massstab durchgeführt. Der Boden in der Prüfrinne ist nach Lührs[3] als mittelschwerer Lehmboden anzusprechen. Für die Versuche wurde die von Lührs[3] gebaute Apparatur benutzt, bei der unter Verwendung eines Einzelrades Radlastkonstanz unabhängig von der Grösse der auftretenden Triebkraft gesichert ist. Es wurden Reifenabmessungen, Reifenluftdruck und Reifenprofil, Radlast, Schrittlänge, Verschiebungsgeschwindigkeit, Radentlastung beim Vorwärtsrollen, Bodenfeuchtigkeit und der Porenanteil des Bodens variiert. Die über Dehnungsmessstreifen gemessene Zugkraft, Rollwiderstand und Radeinsinkung wurden als Funktion des Weges mit einem Oszillographen registriert. Ausserdem konnte durch Konstanthalten der Raddrehzahl beim rotierend angetriebenen Rad durch Aufbringen einer Zeitmarke auf die Oszillogramme der Schlupf erfasst werden.

Darstellung der Versuchsergebnisse. — Wie allgemein üblich, machen wir die Triebkraft T durch Bezugnahme auf die Radlast G dimensionsfrei. Dieses Verhältnis $T/G = \varkappa$ wird als Triebkraftbeiwert oder Kraftschlussbeiwert bezeichnet. In demselben ist offengelassen, inwieweit der Coulombsche Reibungsgesetz zutrifft, d.h. reine Reibung zum Kraftschluss beiträgt, oder beim Aufbau der Triebkraft noch eine Kohäsion mitwirkt.

Der mit der Bodenverformung fortschreitende Aufbau der Abstützung einer Triebkraft oder Zugkraft (Verankerung) mit dem zugehörigen Verlaufe der Einsinkung sei nur für einen bestimmten Beispielsfall unter Gegenüberstellung der Messergebnisse am blockierten, nach rückwärts gezogenen Rad in Bild 11 und am rotierend angetriebenen Rad in Bild 12 verdeutlicht.

Das Verhalten des Rades bei Blockierung. — Für das Schub-Schritt-Verfahren kam das gesperrte Rad nach jedesmal verschiedener Schrittlänge im unbefahrenen, lockeren Boden zum Einsatz. In Bild 11 sind nur die Kurven für die grösste und kleinste Schrittlänge angegeben. Im ersten Abschnitt der Verschiebung (bis etwa 10 cm) steigt der Triebkraftbeiwert für beide Kurven gleich steil an. Das erklärt sich daraus, dass die Triebkraft in der Hauptsache auf den in der Auflagefläche auftretenden Schubspannungen beruht, während die Abstützung an den vorgelagerten Erdmassen noch kaum gewirkt haben kann. Nach etwa 10 cm Verschiebungsweg setzt der Abschervorgang ein, was besonders deutlich an der Kurve der grossen Schrittlänge zu erkennen ist. Dass $\varkappa$ bei weiter zunehmender Verformung nicht abfällt, wie nach dem Abscherdiagramm zu erwarten wäre, liegt daran, dass die Abstützwirkung an den vorgelagerten Erdmassen die verlorengegangene Kohäsion ausgleicht. Die viel stärkere Steigerung von $\varkappa$ bei kleiner Schrittlänge beruht darauf, dass

das Rad sich noch an den vom vorhergehenden Abstützvorgang verdichteten Untergrund abstützt. Die dermassen abstützbare Triebkraft ist umso grösser, je öfter kurze Schritte nacheinander ausgeführt werden, da sich dadurch das Volumen der vorgelagerten, verdichteten Erdmassen erhöht.

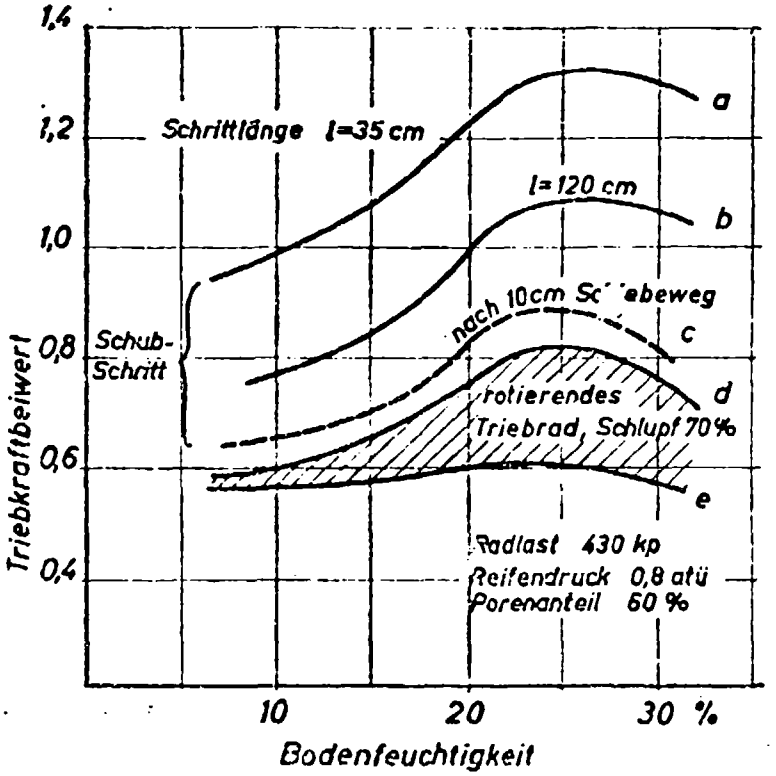


Bild 13. — Bei nur 10 cm Schieben, alsdann noch unbeeinflusst von der Schrittlänge, ergibt das Schub-Schritt-Verfahren (e) bereits höhere Triebkraftbeiwerte als das rotierende Triebrad bei 70 % Schlupf mit verschiedenen Reifen (Bereich zwischen den Kurven d und e). Höchstwerte (Kurven a und b) nach grösserem Schieben sind von der Schrittlänge abhängig.

Neben der Bodenpackungsdichte hat vor allem die Bodenfeuchtigkeit den grössten Einfluss auf die Höhe der erreichbaren Triebkraft, weil sich mit ihr die Kohäsion weitgehend ändert. Im Bild 13 sind die aus vielen Versuchsreihen ermittelten Triebkraftbeiwerte über dem Wassergehalt des Bodens aufgetragen. Die Triebkraftbeiwerte steigen mit zunehmendem Wassergehalt an und fallen schliesslich bei höheren Wassergehalten wieder leicht ab. Die Messwerte der verschiedenen Reifen liegen innerhalb der auftretenden Streuung, sodass man von einer deutlichen Überlegenheit einer bestimmten Reifenabmessung nicht sprechen kann. Es ist jedoch zu erwähnen, dass der Reifen

kleineren Volumens, der infolge seiner kleineren Auflagefläche tiefer einsinkt, im zweiten Abschnitt, wo es auf die Einsinktiefe ankommt, grössere Triebkräfte abstützen kann.

Ein Einfluss des Reifenluftdruckes konnte selbst bei grosser Variation von 0,2 bis 2,0 atü auf dem sehr weichen, lockeren Boden nicht festgestellt werden. Diese Tatsache lässt sich auch leicht erklären: Der Reifen sinkt auf nachgiebigem Boden sehr weit ein und plattet sich überhaupt nicht oder nur auf einer verhältnismässig kleinen Fläche ab. Dort herrscht der maximale Flächendruck, der sich aus Reifenluftdruck und Reifensteifigkeit zusammensetzt, während in dem weitaus grösseren Teil der Auflagefläche ein niedrigerer Flächendruck auftritt, auf den infolge der relativ grossen Reifensteifigkeit der Reifenluftdruck praktisch keinen Einfluss mehr hat. Somit trägt die Anwendung grossvolumiger Reifen viel mehr zur Vergrösserung der Auflagefläche bei, als die Senkung des Reifenluftdruckes. Erst wenn auch die Reifensteifigkeit im Vergleich zum Reifenluftdruck weitgehend gesenkt werden könnte, würde der Einfluss des Reifenluftdruckes auf die Grösse der Auflagefläche auch bei nachgiebigem Boden an Bedeutung gewinnen.

Das Profil des Reifens hat die Aufgabe, eine Verzahnung mit dem Boden herzustellen. Ist nun der Boden in allen Schichten homogen, so ist es gleichgültig, in welcher Schicht der Boden abgeschert wird. In diesem Falle vergrössert das Profil lediglich den Durchmesser des Reifens. Da es sich in der Bodenrinne um einen in allen Schichten homogenen Boden handelte, reichte selbst die geringe Rauhigkeit eines profillosen Reifens aus, um eine Verzahnung mit dem Boden herzustellen. In der Praxis jedoch ist die Homogenität des Bodens meist nicht vorauszusetzen. Die Oberschicht des Bodens kann feuchter oder lockerer sein, es kann zum Beispiel durch einen Regenschauer eine dünne Schmierschicht entstanden sein, oder der Boden kann mit Pflanzen bewachsen sein, die beim Befahren zerdrückt werden und dann ebenfalls eine schmierende Oberfläche ergeben.

Will man die Schrittlänge verkleinern, um eine möglichst hohe Triebkraft aufgrund der Erkenntnisse aus Bild 11 zu erreichen, so muss man mit Anwachsen des kinematischen Schlupfes rechnen, also auch mit einem Mehraufwand an Leistung. Ein gesteigerter Effekt kann auch dadurch erreicht werden, dass man die Abstände und die Schrittlängen der zwei oder drei auf jeder Fahrzeugseite angeordneten Räder so aufeinander abstimmt, dass die nachfolgenden Räder jeweils die von den vorderen Rädern verfestigte Schritt-Spur wieder benutzen, wodurch ebenfalls der beschriebene Verfestigungseffekt ausgenutzt ist. Damit erreicht man also auch bei grossem Schritt, d.h. bei kleinem kinematischen Schlupf und mässigen Massenkräften höchste Triebkraft.

Der Gewinn an Triebkraft aus der Verdichtung infolge Radbelastung fällt nur bei lockerem Boden ins Gewicht. Fester Boden hat bereits in seinem natürlichen Zustand hohe Kohäsion, die sich im Schub-Schritt-Verfahren nicht ohne weiteres noch zusätzlich steigert.

Das Verhalten des rotierend angetriebenen Rades. — Die Vergleichsversuche mit dem rotierend angetriebenen Rad wurden jeweils unter den gleichen

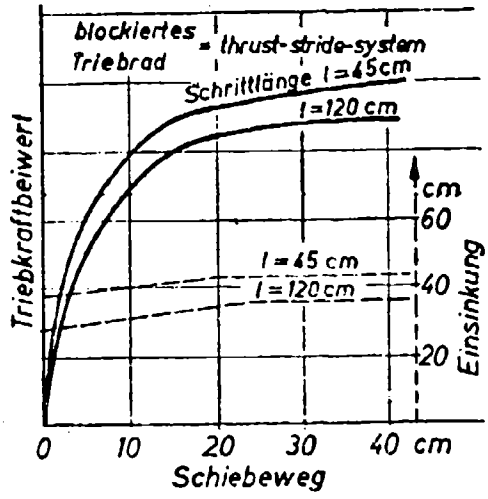


Bild 14.

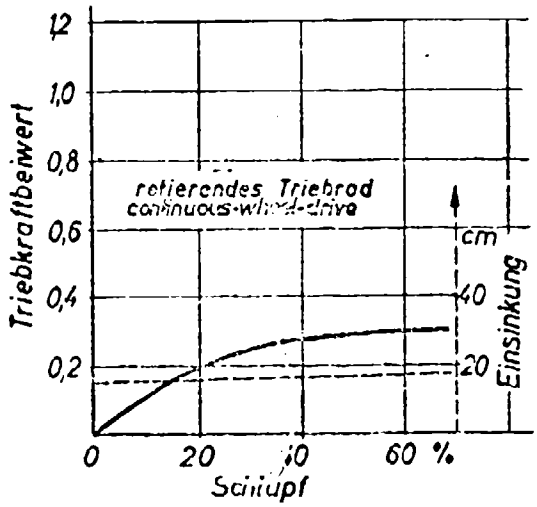


Bild 15.

Bild 14 und 15. — Vergleich zwischen normal kontinuierlichem Radantrieb und Schub-Schritt-Verfahren in 10 cm-Schlammschicht auf festem Untergrund. Radlast 430 kp, Reifendruck 0,8 atü, 8·24 AS.

Bedingungen wie beim blockierten Rad durchgeführt (Bild 12). Im allgemeinen haben sich hier die schon bei anderen Autoren[2-6] gewonnenen Erkenntnisse bestätigt. Es fällt in allen Diagrammen, in denen die Triebkraft und die Radeinsinkung gleichzeitig aufgeschrieben wurden, auf, dass erst bei etwa 30 bis 40 % Schlupf die Radeinsinkung beträchtlich zunimmt und der Anstieg des Triebkraftbeiwertes bedeutend geringer wird. Das lässt darauf schliessen, dass bei diesem Schlupf im grössten Teil der Reifenaufagefläche der Boden abgeschert wird und damit das Gleiten einsetzt. Mit zunehmendem Schlupf fräst sich der Reifen immer tiefer in den Boden ein.

Das Ausmass der Triebkraftsteigerung beim Schub-Schritt-Verfahren

Wie aus Bild 13 sowie aus der Gegenüberstellung der Bilder 11 und 12 hervorgeht, sind selbst nach einem kurzen Verschiebungsweg von 10 cm die erreichten Triebkräfte bereits höher als beim rotierend angetriebenem Rad bei 70 % Schlupf. Wird der erläuterte Abstützeffekt an den vom vorhergehenden Abstützvorgang stark verfestigten Erdmassen noch ausgenützt, so lässt sich die Triebkraft bis auf das Doppelte steigern.

Während bei den bisherigen Versuchen der Boden in allen Schichten homogen war mit gleicher Feuchtigkeit und gleichem Porenanteil, ist in der Praxis solche Homogenität nicht vorauszusetzen. Dieser Fall wurde in die Untersuchung mit einbezogen und hierzu der Boden in der Prüfrinne mittels Vibrator verdichtet. Auf diesen festen, praktisch wasserundurchlässigen Untergrund wurde dann eine Schlammschicht von 10 cm Dicke aufgetragen. Es wurden Versuche sowohl mit blockiertem als auch rotierend angetriebenem Rad darauf durchgeführt. Dabei konnte beobachtet werden, dass beim Einsetzen des Rades der Schlamm zur Seite gedrängt wird, bis das Rad den festeren Untergrund erreicht hat. Dieser Verdrängungsvorgang ist von der Zeit abhängig, d.h. das Rad wird um so sicherer den festen Untergrund erreichen, je mehr Zeit ihm dafür zur Verfügung steht. Da nun beim Schub-Schritt-Verfahren das Rad bedeutend länger an einer Stelle verharrt als das rotierend angetriebene, ist auch hier das Schub-Schritt-Verfahren überlegen. Während ferner das angetriebene Rad infolge des Schlupfes dauernd neuen Schlamm unter seine Auflagefläche fördert, der dann Schmiermittel zwischen Reifen und festem Boden ist, dringt das blockierte Rad nach Erreichen der festeren Unterschicht beim Verschieben noch ein wenig in diese ein, wo es dann festen Halt vorfindet und beim Verschieben den Schlamm vor sich herschiebt, ohne den festen Griff am Untergrund zu verlieren. Im Bild 14 sind die Versuche mit dem Reifen 8-24 AS für das blokierte und in Bild 15 für das rotierend angetriebene Rad dargestellt, die die grosse Ueberlegenheit des Schub-Schritt-Verfahrens auf Boden auch mit schlammiger Oberschicht bestätigen.

LITERATURANGABEN

1) Stiebling A. Die schreitende Zugmaschine des Freihern von Bechtolsheim. Dissertation, TH München, 1933.

2) Söhne W. Druckverteilung im Boden und Bodenverformung unter Schlepperreifen. In: 11. Konstrukteurheft, 2. Teil, VDI-Verlag Düsseldorf. Grundlagen der Landtechnik, Heft 5, S. 49-63, 1953.

3) Lührs H. Wirkungsgraduntersuchungen an Ackerschleppertreibradreifen, ihre Bedeutung für den Schlepperkonstrukteur. Dissertation TH München, München, 1959.

4) Bekker M. G. Theorie of Land Locomotion. Ann Arbor, The University of Michigan Press, 1956.

5) Söhne W. Die Kraftübertragung zwischen Schlepperreifen und Ackerboden. In: 10. Konstrukteurheft, VDI-Verlag Düsseldorf. Grundlagen der Landtechnik, Heft 3, S. 75-87, 1952.

6) Buck G. Beobachtungen bei Feldversuchen über die Zugfähigkeit von Schleppern. In: 11. Konstrukteurheft, 2. Teil, VDI-Verlag Düsseldorf, Grundlagen der Landtechnik, Heft 5, S. 42-48, 1953.

7) Söhne W. Einige Grundlagen für eine Landtechnische Bodenmechanik. In: 13. Konstrukteurheft, VDI-Verlag Düsseldorf, Grundlagen der Landtechnik, Heft 7, S. 11-27, 1956.

8) Terzaghi K. und Jelinek R. Theoretische Bodenmechanik, Berlin, 1954.

9) Söhne W. Reibung und Kohäsion bei Ackerböden. In: 11. Konstrukteurheft, 2. Teil, VDI-Verlag Düsseldorf, Grundlagen der Landtechnik, Heft 5, S. 64-80, 1953.

N. 53

Traffic over frozen or crusted surfaces

Movimento su terreno gelato o superfici ghiacciate

A. Assur *)

ABSTRACT. — *Traffic over crusts is one of the problems encountered in off-the-road locomotion, in particular in polar regions and especially over ice sheets. Three failure stages of the crust and their relation to elastic theory for regular and plastic theory for emergency operations are outlined. Solutions of the differential equations for circular, elliptic and arbitrary loads are given. Failure under punching requires the computation of combined stresses. The location of the circumferential crack is analyzed and equations for the collapse load under plastic yielding are given. Large-scale loading tests show how the failure is related to the duration of loading and how much time elapses before final breakthrough occurs after circumferential cracking. A nomogram for the computation of the critical resonance speed is given. Then it is shown how to determine the stiffness modulus of crusts and how a variation in the profile of Young's modulus affects the flexural strength.*

Vehicles travelling off the road may easily encounter conditions where the surface of the terrain is sufficiently hard but the layers underneath may be too soft to support the load. If the hard surface layer is sufficiently thick it will distribute the load over an area wide enough to be supported by the unreliable foundation underneath without exceeding the strength of the crust. If the stresses originated in the surface layer or on the foundation are too large the vehicle will break through and may be a complete loss.

Such conditions exist in swamps with an organic cover, especially when frozen, in muskeg or, in general, in terrain with a relatively thin frozen surface layer. Natural snow with a hard crust is another example, as well as the ice cap with a compacted surface layer or frozen slush. In other regions we may encounter dry surface layers over muddy foundations or salt lakes covered with a dangerous hard crust, as in North Africa. The ideal case for theoretical discussions, of course, is an ice sheet over a water body. We will be primarily concerned with this case. In principle, or at least approximately, the mechanics of other crusted surfaces is the same, only the parameters to be used differ.

Numerous heavy loading tests performed by Sipre on fresh and salt ice sheets have clarified the failure mechanism of such crusted surfaces.

*) Chief, Applied Research Branch, USA Cold Regions Research and Engineering Laboratory (formerly Sipre).

Three failure stages have to be distinguished. At first a tension failure in the radical direction occurs at the bottom of the ice sheet, accompanied by a loud explosive noise on fresh ice or a dull rumble on sea ice. This failure can be computed by means of elastic analysis. Although without immediate dangerous consequences such failure is not desirable for ice sheets under frequent use. Corresponding aircraft landing criteria, for regular operations, were computed by Assur [1].

In the next phase numerous radical cracks develop until a circumferential crack occurs at some distance from the load. Then the load suddenly sags, but is still held by the wedging of the ice fragments. This condition can be predicted by means of plastic analysis. Only for emergency operations a crusted surface can be used close to collapse. Criteria for these cases can be found in reference 1.

Final breakthrough occurs by failure in a shearing zone which follows closely the outline of the loading surface.

Another type of failure is the punching of the crusted sheet due to a highly concentrated load. A number of loading tests of this type were made by Sipre, including tests last winter at Point Barrow, Alaska.

For the elastic case (regular operations) the differential equation

$$\frac{d^4 w}{d r^4} + \frac{2}{r}\frac{d^3 w}{d r^3} - \frac{1}{r^2}\frac{d^2 w}{d r^2} + \frac{1}{r^3}\frac{d w}{d r} = -\frac{w}{l^4} \qquad (1)$$

leads to a general solution in terms of Kelvin functions (2)

$$w = C_1 \operatorname{ber}\rho + C_2 \operatorname{bei}\rho + C_3 \operatorname{ker}\rho + C_4 \operatorname{kei}\rho \qquad (2)$$

with

$$\rho = \frac{r}{l}$$

W = deflection at the distance r from center of coordinates.

$$l = \sqrt[4]{D/K} \qquad (3)$$

a characteristic length, designated by us as the « action radius ». K = the reaction of the foundation, equal to the density of the liquid.

$$D = \frac{E h^3}{12 (1 - \mu^2)}$$

the flexural rigidity.

E = Young's modulus, h = thickness of the crusted layers, μ = Poisson's ratio. Detailed tables of the Kelvin function involved in equation (2) were recently published by Sipre [3].

The common objection that Hooke's law does not hold is not valid for ice, for which stress is proportional to strain virtually until failure as long as the rate of loading is greater than 0.5 kg/cm^2 sec^{-1}. This is true for any moving load,

for parked loads the validity of equation (1) is impaired; under rapidly moving loads resonance oscillations may be created which complicate the situation.

Satisfying the necessary boundary conditions and making the total hydrostatic reaction from the liquid layer on the crusted layer equal to the concentrated load P, the solution is

$$w = -\frac{P \operatorname{kei} \rho}{2 \pi k l^2} \tag{4}$$

which gives

$$w_m = \frac{P}{8 k l^2} \tag{5}$$

for the maximum deflection.

In our work we use the nondimensional function

$$\psi = \frac{w}{w_m} = -\frac{4}{\pi} \operatorname{kei} \rho \tag{6}$$

The integration over a uniformly loaded circular area of the radius yields the bending moment

$$M = \frac{1+\mu}{8} P \frac{1}{\alpha} \frac{d\psi}{d\alpha} \tag{7}$$

with $\alpha = a/l$ and the maximum developed flexural stress

$$\sigma = 6 M/h^2 \tag{8}$$

For small loading areas an equivalent radius rather than the actual α has be used to account for the thick plate effect.

For elliptical loads, such as tires,

$$m = M/P = \frac{1+\mu}{8} \frac{1}{\alpha} \frac{d\psi}{d\alpha} + \frac{1}{8\pi} \frac{1-\epsilon}{1+\epsilon} (1-\mu) \tag{9}$$

ϵ = ratio of short to long diameter.

Tests have shown that highly concentrated loads fail by punching under roughly 45°. The vertical tensile stress on the 45° cone is then

$$\sigma_1 = \frac{P}{(2a + h) \pi h} \tag{10}$$

Meyerhof [4] limits his computation to this stress. We prefer to add vectorially the tensile stress created under bending at the radius a + h.

Wyman [5] gives for the deflection field around a circular load

$$w = \frac{q \alpha}{k} (\operatorname{ber}' \alpha \ker \rho - \operatorname{bei}' \alpha \operatorname{kei} \rho) \tag{11}$$

q = intensity of uniform loading.

Further developing the theory we find the following relation

$$-S\,\alpha\,m_z = \beta_r'(\alpha)\left[\psi(\alpha_1) + \frac{\psi_r'(\alpha_1)}{\rho}(1-\mu)\right] +$$

$$+ \beta'(\alpha)\left[\psi_r(\alpha_1) + \frac{\psi'(\alpha_1)}{\rho}(1-\mu)\right] \qquad (12)$$

$$2\,\mathrm{ber} = \beta_r\,; \quad 2\,\mathrm{bei} = \beta\,; \quad \mathrm{kei} = -\frac{\pi}{4}\psi\,; \quad \mathrm{ker} = -\frac{\pi}{4}\psi_r$$

$$\alpha_1 = \frac{a}{l} + \frac{h}{l}$$

The corresponding stress is

$$\sigma_z = \frac{6\,P\,m_z}{h^2}$$

and the resultant stress for failure in punching under bending

$$\sigma_3 = \sqrt{\sigma_1^2 + \sigma_z^2}$$

For larger loads the stress σ under the center of the load will exceed the combined stress near the edge of the load.

Also of interest is the location of the maximum radial stress, where one would expect the formation of a plastic hinge under prolonged loading.

A rather lengthy derivation leads to

$$1-\mu = \frac{\rho\left(\psi' + \psi_r'\dfrac{\beta'(\alpha)}{\beta_r'(\alpha)}\right)}{\psi + \dfrac{2\psi_r'}{\rho} + \left(\psi_r - \dfrac{2\psi'}{\rho}\right)\dfrac{\beta'(\alpha)}{\beta_r'(\alpha)}} \qquad (13)$$

The argument ρ for ψ and ψ_r is omitted.

Upon numerical evaluation for $\mu = \frac{1}{3}$ it was found that the results can be approximated by

$$\frac{L_c}{l} = 2.06 + \frac{\alpha}{3} \qquad (14)$$

with L_c = the location of the circumferential crack.

The « action radius » l which can be derived from (14) and experiments leads to a very small « stiffness modulus » E. Also one should consider that the location of maximum radial stresses travels towards the center of coordinates with increasing load and longer application of the load.

Not much can be done if one limits himself to an analysis of circular loads. Most actual loads have an arbitrary configuration of the loading surface on the crust. A method had to be found to compute the stresses for any loading configuration.

This can be done by dividing the loading surface into a number of small circular loads with varying loading intensity at various locations.

By using the fundamental relations for the radial and tangential moments

$$M_r = -D\left(\frac{d^2 w}{d r^2} + \frac{\mu}{r}\frac{d w}{d r}\right) \tag{12 a}$$

$$M_t = -D\left(\mu\frac{d^2 w}{d r^2} + \frac{1}{r}\frac{d w}{d r}\right) \tag{12 b}$$

and considering that for orthogonal moments

$$M_\varphi = M_r \sin^2\Theta + M_t \cos^2\Theta \tag{13 a}$$

or

$$2 M_\varphi = M_r (1 - \cos 2\Theta) + M_t (1 - \cos 2\Theta) \tag{13 b}$$

with Θ the angle between the direction of the moment and the reference axis; and the relations

$$w = w_m \omega \tag{14 a}$$

$$\frac{d w}{d r} = \frac{w_m}{l}\frac{d \omega}{d \rho} \tag{14 b}$$

$$\frac{d^2 w}{d r^2} = \frac{w_m}{l^2}\frac{d \omega}{d \rho} \tag{14 c}$$

with $w_m = P/Skl^2$ the maximum deflection under a point load and $\omega = w/w_m$ which is easy to prove, we find, considering equation (11), after rearranging the terms

$$-16\,m = (A + B\cos 2\Theta) + \mu\,(A - B\cos 2\Theta) \tag{15}$$

with

$$A(\rho, \alpha) = \frac{\beta_r'(\alpha)}{\alpha}\psi + \frac{\beta'(\alpha)}{\alpha}\psi_r \tag{16 a}$$

$$B(\rho, \alpha) = \frac{\beta_r'(\alpha)}{\alpha}\left(\psi + 2\frac{\psi_r'}{\rho}\right) + \frac{\beta'(\alpha)}{\alpha}\left(\psi_r - 2\frac{\psi'}{\rho}\right) \tag{16 b}$$

The argument ρ for ψ and ψ_r is omitted.

The evaluation causes no difficulty by using a digital computer which originates the Kelvin functions involved. For manual computations it is more advantageous to approximate the loading configuration by a system of point loads.

This gives

$$A(\rho) = \psi_r(\rho) \tag{17 a}$$

$$B(\rho) = \psi_r(\rho) - 2\frac{\psi'(\rho)}{\rho} \tag{17 b}$$

Equation (15) combined with (16 a, b) of (17 a, b) can be used for any loading configuration except for loads in the immediate vicinity of the center of coordinates where the stresses are computed. These special precautions must be taken.

The emergency criteria computed by Assur [1] were based upon the principle of collapse loads with reasonable safety.

There is still no entirely satisfactory theory available for the final collapse of ice sheets. This is primarily because part of the ice sheet, no doubt, remains in the elastic state, while the plastic state is reached near the load under prolonged loading.

The most satisfactory approach can be derived from studying the equilibrium of a wedge with its apex at the center of a circular load. Radial yield lines progress outwards until the radial yield moment perpendicular to a circular line equals the tagential yield moment perpendicular to the radial yield lines.

An analysis of this concept leads to the expression

$$\sigma_o = \frac{P_o}{\pi h^2}\left[1 - \frac{1}{3}\left(\frac{\pi}{2}\right)^{\frac{1}{3}} \alpha^{\frac{2}{3}}\right] \tag{18}$$

for the maximum radial stress. This can be expressed also as

$$P_o = \frac{4\pi}{1 - \frac{1}{3}\left(\frac{\pi}{2}\right)^{\frac{1}{3}} \alpha^{\frac{2}{3}}} M_o \tag{19}$$

The first approach along the line was made by Johansson [3]. Meyerhof [4] recently derived the approximate expression

$$P_o = 3{,}3\pi\left(1 + \frac{3}{E}\alpha\right) M_o \tag{20}$$

for

$$0{,}05 \leq \alpha \leq 1$$

He uses a more advanced concept in deriving the deflection profile. The main disadvantage in the derivation of equation (20) is the assumption that the whole hydrostatic reaction is confined within the hinge circle and also the assumption that the radius of the hinge circle is equal to the radius of the deflection dish in the elastic case. Both of these assumptions are contradicted by our large scale loading tests.

It must be pointed out also that while « Young's modulus » E can be derived from the « action radius » l by means of

$$E = 12\,(1-\mu^2)\,\left(\frac{l}{h}\right)^4 k\,, \tag{21}$$

in the elastic case this is not so in case of a plastic moment, when Hooke's law with its triangular stress profile does not hold any more. In that case

$$E_p = 6\,\left(\frac{l}{h}\right)^4 k\,l \tag{22}$$

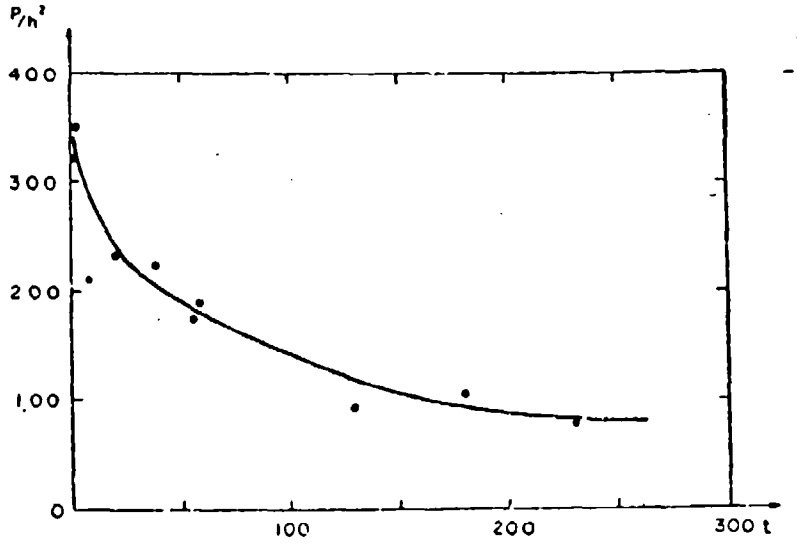


Fig. 1.

should be used for the « stiffness modulus » E_p computed from the action radius l in case of plastic failure.

The theory leading to equation (20) does not furnish the location l_c of the circumferential crack, the theory leading to equation (19), however, yields

$$\lambda \quad \frac{l_c}{l_p} = \sqrt[3]{\frac{32}{\pi}}\,\alpha \tag{23}$$

This agrees with equation (14) fairly well in a given range. For small loading areas the circumferential crack should approach the center rapidly as is also actually observed.

The « stiffness modulus » E to be used in the computation of l_p in equation (23) is very small according to equation (22). A value of 2300 t_m/m^2 for example, was found for sea ice, 25 cm thick.

Some results of complete failure experiments on fresh ice sheets, performed in 1954 by the author and subsequently by Frankenstein (Sipre), supplemented by the experience of tractor train operators in Alaska are shown in fig. 1. Most of these data correspond to a 12 ft circular load P [metric tons]. As a first approximation the « loading factor » P/h^2 can be used to characterize the intensity of loading (ordinate) h ice thickness in m. Although $P/h^2 = 100$ is widely recommended for traffic over ice, which is quite sound for loads of short duration, complete breakthrough does occur with such a loading factor after

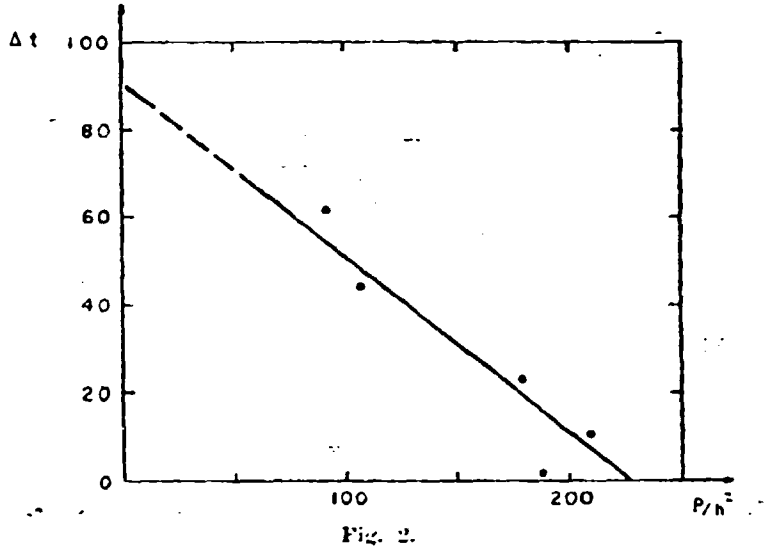


Fig. 2.

prolonged parking. The graph is also particularly interesting in the respect that part of the advantage of using the plastic yielding concept rather than the elastic theory is lost because of the phenomenon illustrated. Elastic theory applies for quick loading, plastic theory for loads of long duration.

The curve in fig. 1 can be represented by an equation of the type

$$\frac{P}{h^2} = A^{-1/6} + C \tag{24}$$

As mentioned above complete collapse occurs only some time after a circumferential crack has formed. As long as the loads are not excessive this may take as long as 90 minutes (fig. 2), giving plenty of warning for parked loads. With high loads the « grace period » is much shorter. With a loading factor of 227 t_c/m^2, complete breakthrough occurs instantaneously after the formation of a circumferential crack.

$$\Delta t = 90 - 0.395 \frac{P}{h^2} \tag{25}$$

High loading factors may be used under emergency conditions if one is prepared for a rapid breakthrough without much warning.

Finally another phenomenon must be mentioned, which has been the cause of many accidents in the past. Although the ice sheet was safe according to accumulated experience, vehicles have gone through if a resonance frequency was amplified within the ice sheet. The « critical speed » (v) depends primarily upon the depth of water in the case of shallow water bodies and primarily upon the thickness h and modulus of elastic E in the case of deep water bodies.

The corresponding solution, based primarily upon the differential equations discussed by Greenhill [6], is:

$$v^2 = \frac{bl}{\cosh \frac{H}{\epsilon l} + \epsilon \left(\frac{l}{l_1}\right)^{3/4}} \qquad (26)$$

with

$$b = g\epsilon \left[1 + \left(\frac{1}{\epsilon}\right)^4\right]$$

and

$$\epsilon = \rho/\epsilon$$

H = water depth

$$l_1 = \frac{E}{12\, g\, \rho_w\, (1-\mu^2)}$$

g = acceleration of gravity

$\rho = \rho_i/\rho_w$

ρ_i = density of ice

ρ_w = density of water

$\epsilon = S/2\pi$

$S = L_c/l$

L_c = dominant wavelength

The factor s was derived from a Fourier analysis of the Kelvin functions produced theoretically by a load moving over ice.

Figure 3 gives a nomogram for practical purposes. The graph is entered with Young's modulus of the ice sheet on the line M N E, in this case, is much higher due to dynamic loading: 30×10^4 t$_s$/m^2 may be used for sea ice, 45×10^4 for snow ice, 60×10^4 for clear fresh ice. The intersection with the ice thickness lines h (in inches) gives a l_1 value (m). In case of « deep water » the critical speed can be read directly on the right scale. For shallow water (anything to the left of the line A-A, depending upon l_1), the intersection of the l_1 line with the corresponding depth will give the critical speed in MPH. For example, clear ice 20" thick gives $l_1 = 24$ and a critical velocity of 42 MPH in a water body 100 ft. deep.

The true resonance speed is slightly below the theoretical critical speed due

to damping. The stresses originated under resonance may be 250 % of the static stresses. They are negligible for loads moving at very high speeds.

In conclusion a few words may be devoted to the determination of the stiffness modulus E. This can be done from a deflection record under a slowly moving load, from a least square fitting of the theoretical deflection curves to data obtained by levelling, or from the location of the circumferential crack according to equations (13), (14) or (23).

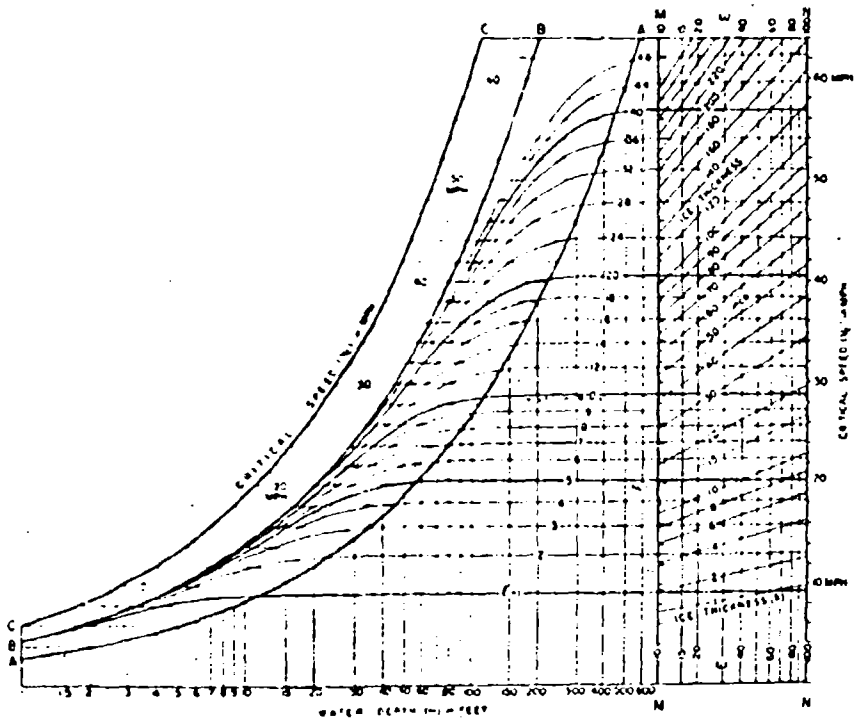


Fig. 3.

Another method is to observe the deflection both in the center w_0 and at the edge w_a of a large circular load, such as in the tank tests mentioned above. It can be shown that

$$1 - \omega = \frac{\alpha \ker' \alpha \,(1 - \operatorname{ber} \alpha) + \alpha \ker' \alpha \operatorname{bei} \alpha}{1 + \alpha \ker' \alpha} \tag{27}$$

Plotting the theoretical relation $\frac{1-\omega}{\omega}$ versus $\alpha\, l = a/\alpha$ can be determined once $\omega = w_a/w_r$ is observed.

The theory requires $w_a \sigma w_r$ for any load. The proportionality limit extends in some cases up to the formation of a circumferential crack but usually

σ declines with the higher loads indicating progressive plastic yielding. Values from 43,000 to 54,000 t_o/m^3 were found by this method for ice sheets composed largely of snow ice.

Another difficulty is that in most crusts, in particular in sea ice Young's modulus changes with depth within the crust. This problem can be met by making an adjustment in the flexural rigidity D.

Also the flexural strength will be affected by a vertical variation of E within the crust. A « transformed cross section » has to be used in such a case.

Assuming a linear variation of E within the profile the ratio R_b between the flexural strength of an assumed isotropic crust and the true maximum stress in the bottom layer is

$$R_b = 1 + \frac{(r+1)(r-1)}{2(2r+1)} \qquad (28)$$

with r the ratio of Young's modulus E at the top of the crust to E at the bottom.

Substituting 1/r for r in (28) to compute the ratio R_t concerning the stress in the top layer we derive

$$\frac{R_t}{R_b} = \frac{2r+1}{r(r+2)} \qquad (29)$$

for the ratio between the flexural strength with tension at the top and the flexural strength with tension at the bottom. This is important for an evaluation of circumferential cracking (tension on top) and first radial cracking (tension at the bottom).

The flexural strength of ice sheets is measured conveniently in situ by means of simply supported beams cut within the ice sheet.

BIBLIOGRAPHY

1) Assur A. Airfields on floating ice sheets, Sipre Report, 36.
2) Wyman M. Deflections of an infinite plate, Canad. J. Res, A, 28, 293-302, 1950.
3) Nevel D. E. Tables of Kelvin functions and their derivatives. Sipre Technical Report 67, 1959.
4) Meyerhof G. G. Bearing capacity of floating ice sheets. Proc AMSCE, # 2627, EM 5, 1960.
5) Johansson A. Försök med armerade betong-platter på elastiskt underlag (Swedish), (Experiments on reinforced concrete plates on an elastic foundation), Betong, H 3, 1947.
6) Greenhill A. G. Wave motion in hydrodynamics. Am. T. Math., vol. IX, 1887.

ASPETTI DIDATTICI DEGLI STUDI DEL MOVIMENTO FUORI STRADA

EDUCATIONAL ASPECTS OF LAND LOCOMOTION STUDIES

N. 54

Land locomotion in United States universities

Il movimento fuori strada nelle università americane

E. T. Vincent *)

ABSTRACT. — *The establishment of various courses on off the road locomotion have been stimulated by the publication of M. G. Bekker papers of 1956. There only have been before some lectures at Stevens Institute of Technology of Hoboken in 1953.*

A table shows the American Universities where at present are held lectures on land locomotion and points out the number of students enroled and graduated.

These lectures have a good frequency considering that young people are mostly attracted by other problems as space or nuclear, but are only the first step of a program that must have a larg development.

The university seams to be the best place for studies requiring a deep knowledge of the ground as well as locomotion. For the moment mainly Agricultural Engineers are interested in the subject but the importance of the problem (excluding military requirements that have to be considered temporary) spread over not only agriculture but all kind of locomotion. We could think to have in the future roads for fast travel, and for slow locomotion (20-25 m.p.h.) use a good off-the-road vehicle and cross the country.

Locomotion on the moon is a hard problem difficult to solve.

The instructional programs at various Universities in the United States were, in general, started under the stimulus of Mr. M. G. Bekker, together with his active assistance in many cases. One very necessary ingredient for growth was, of course, the existence of a text book for use in such instruction; it follows that the publication of «Theory of Land Locomotion» by M. G. Bekker, University of Michigan Press, 1956, marked the beginning of most of the present day courses. There is one exception, that being the Courses and Research in the Mechanics of Motor Vehicles offered in the Graduate School of Stevens Institute of Technology, Hoboken, New Jersey from 1951 to 1953, these appear to be a pioneer effort in the field of Land Locomotion, and were offered by Mr. Bekker.

The next major step in course offering followed the publication of the above mentioned text in 1956; and consisted of graduate courses (a) Theory of Land Locomotion, (b) Land Locomotion Laboratory at the University of Michigan in the fall of 1956 by the writer.

The growth in the United States since that time can be represented best by the data in Table I, the order of presentation is not necessarily chronological.

*) University of Michigan, Ann Arbor, Michigan.

TABLE I.

Institution	Course No. and description	Level and % devoted to land locom.	Credits	Average No. of students per semester	Make-up of students attending courses to date PhD	MS	BS
Stevens Institute of Technology	ME 334 mechanics of motor vehicles I	Graduate 100 %	2 hrs	8		32*	
	ME 335 mechanics of motor vehicles II		2 hrs	8			
University of Michigan	ME 240 theory of land locomotion	Graduate 100 %	3 hrs	8	2*	20*	2*
	ME 242 land comotion lab.		3 hrs	4		12*	
University of Illinois	AE 346 farm tractors	Senior 15 %	3 hrs	7			
	AE 446 farm tractors	Graduate 50 %	3 hrs	5		5	
Michigan State University	AE 840 advanced power machinery	Graduate 15 %	3 hrs	25	7*	6*	50*
	AE 991 soil dynamics	Graduate 50 %	3 hrs	6			
University of Nebraska	AE 125 agricultural tractors I	Senior 15 %	3 hrs	13			13
	AE 225 agricultural tractors II	Senior 20 %	3 hrs	11			11
	AE 325 land locomotion	Graduate 80 %	3 hrs	5		5	
Purdue University	AE 335 farm tractors and their power units	Senior 20 %	3 hrs	Undergraduate course to be introduced spring 1961	2*		

*) Total to date. All others per semester.

In this table the per cent course work specifically directed to the field of Land Locomotion as judged by course content, is indicated in column 5. This applies particularly to the Agricultural Engineering Course where this type of work is usually included with the farm machinery courses. In addition the approximate number of students graduated at the various levels in these programs is also indicated, together with an approximate distribution among the various types of degrees involved.

If the general trend in Engineering Education in the United States is considered in conjunction with the data presented in Table I, the growth in the Land Locomotion Mechanics Program can be considered to be of reasonable proportions for the short period covered by its development; since this growth has occurred during a period when broad general science training has been the vogue with little or no detail or applied courses being required in any one field, and in many cases, a complete lack of instruction in how many important

basic principles can be applied in practice. That is, the education has been scientific and not engineering.

In the conventional engineering fields the lack of detailed knowledge of any one applied subject is perhaps not too serious since, due to long use, a good understanding of the subject has been acquired over the years and much has worked its way into many general books; thus it is easy for a well trained man to read and understand what is necessary in any one field, then given some experience, competency results. This cannot be done in the Land Locomotion field, there is little to read and still less written or known as to the application of such laws as appear to apply at the present time.

The well trained man in basic science can do research in the field if given a year or so in which to become familiar with the requirements; however, anything associated with such mundane subjects as surface locomotion, receives little attention today from young modern trained persons; space and nuclear problems occupy almost all their attention. The fact that in the near future more and more of the earth's surface must be traversed by machinery, not only for war, but for the raising of crops to feed the present and continuing population explosion, does not appeal.

It does seem to the writer that the present place of land locomotion courses lies with the Agricultural Engineers; it is here that its presence might have the most immediate and lasting effect. It is hoped, at least, that in a relatively few years the various nations of the earth will realize that nobody, even the victor, gains as a result of a major war; thus the efforts in the field under discussion directed toward military objectives, though they are extremely important at the present time, should be treated as a temporary requirement.

Turning again to the civilian applications, other than farming, there are many small villages and towns in the U.S.A. that are getting cut off from large scale economical supplies due to the shutting down of uneconomical railroad transportation. The highways must now carry the necessary supplies; but again good roads on which the vehicle sponsored by the modern trend of the automotive industry must travel, at least in the United States, are also extremely expensive to build and how long the present trend in road construction with its ever increasing taxation can continue is problematical. A good off-the-road vehicle capable of cross country journeys even at 20-25 miles per hour would be a great boon for many; using the main highways for fast travel over the long distance to the nearest point followed by off-road distribution to the final destination of both goods and materials.

To make such a scheme possible a greater knowledge of the properties of the earth's surface is a first necessity followed by increased knowledge of how these properties can be combined with those of a suitable mechanism to produce the desired off-road speed and comfort necessary for such operations. At the present time the Universities appear to be the only source of supply of men for such operations and an educational and research program of sufficient magnitude staffed by first class personnel appear the only way of arousing

student interest in such projects and thus produce the men capable of carrying on the necessary developments and designs.

If one lets his imagination run wild, there are other phases of land locomotion which could attract the scientist interested in space, but phases which without adequate support, probably governmental, could not be tackled. The moon is, at present, foremost in many minds. Do the early arrivals on that planet explore it on their own two feet when they get there or wait and build roads for automotive equipment with the possibility that, to begin with, all of the important ingredients for roads must be shipped from the earth. There are some suggestions that the moon's surface is a deep layer of dust; if so, present off-the-road equipment would be useless. It follows that education and study of as much of the problem as is possible from our home base is first necessary and from such knowledge an engineering approach to a possible suitable vehicle could be made. Such equipment would probably have a better chance of success than shipping any of the present vehicles, automotive, agricultural, road-making, etc. to the moon.

It is considered that the land locomotion courses such as those given in Table I represent the first step in a much broader program than is contemplated by many and which will take much longer to solve successfully than that of reaching the moon itself. It follows that efforts to lay some groundwork for an engineering approach to some simple cases of designing a vehicle to suit the material on which it is to operate (other than a hard surface road) does merit considerable study and research. If this simple one can be solved, it may point the way to solutions of the far more complicated problems likely to be met in the future. Without continued study and research at Universities, the main object of which is the training of men for various duties in science and industry, there seems little chance of experienced men in any number being available for much future development work in the field under discussion.

The writer wishes to thank all his colleagues at the various schools for their contributions which made this analysis possible.

DISCUSSIONS

L. AMICI. — Volevo solo dire al conferenziere che noi in Italia teniamo un Corso al Politecnico di Torino, già da sei anni, sul pneumatico, sulle sospensioni pneumatiche per autoveicoli e su tutte le applicazioni in gomma ai veicoli.

Questo corso è tenuto presso l'Istituto del Prof. Pellone al Politecnico di Torino, a cui l'Oratore potrà rivolgersi per avere informazioni sulle materie trattate durante questo corso. Grazie.

A. R. REECE. — Mr. Chairman, Gentlemen, our Department at Durham University is the only Department of Agricultural Engineering in England. We have been going for about 15 years and we are very concerned to establish Agricultural Engineering as a worthwhile University subject.

We considered it important to develop those subjects which can be considered unique to agricultural engineering and here of course the field of soil dynamics in

its two branches of soil implement and soil vehicle mechanics is of the utmost importance. A lot of agricultural engineering is really only ordinary mechanical engineering applied to a machine used in farming. We consider it most important to develop subjects which are unique to agricultural engineering in preference to these.

We are therefore, devoting a large proportion of our research effort to developing the soil mechanics studies and to integrating them into our teaching. We are running a brief course in vehicle mechanics at the moment and one of the very good features of such a course is its realism. It makes a pleasant change from the normal fossilised basic engineering material to be able to teach ideas which will almost certainly be obsolete within a matter of a few years. It is stimulating to the students for them to carry out experiments, the results of which do not really fit the theory they have been taught.

J. R. PHILLIPS. — We appear to be discussing, gentlemen, the question of agricultural engineering courses in the Universities and technical colleges. Perhaps it may be interesting for you to hear something of the arguments and developments which have been taking place in Australia on this matter. Briefly, in Melbourne, in the eastern part of Australia after the very hard work from some twenty years of a certain Mr. Vasey, there is now organized in the University of Melbourne, and in a way connected with the standard tractor testing authority set up under the auspices of the University of Melbourne, a full degree course in agricultural engineering. The students there take the first three years of this course more or less in common with other engineers. In the final year, however, they specialize and graduate with the degree « Bachelor of Agricultural Engineering ». One of the big difficulties in Australia, and I expect elsewhere, revolves around the argument that Mr. Reece has mentioned: what is it that constitutes the specialness in agricultural engineering as a discipline worthy for a separate title? It is very easy to say that agricultural engineering is simply one of the fields in which any responsable and well trained engineer may ultimately operate. Once this argument and discussion has been resolved, however, in one direction or the other, it is then important, if you wish to discuss the content of courses, to ask the question: « What shall we teach? ». Immediately the though arises that if agricultural engineering is to be a discipline in its own rights, it will need to deal not only with the question of mechanism and machines in agriculture, but it must deal with hydraulogy the study of water, the geography of strata, geology, crops growing, weather and many other of these related topics. However, the argument continually comes back to the question of soil mechanics and soil; here attempts in Melbourne have been made to produce a soil science subject, or discipline, which may have relavance to the question of engineering and agriculture. The question that I continue to ask of the people who design these courses is this. I say the study of soil mechanics, as so far developed in the text books, is the soil mechanics of the civil engineer. The soil mechanics of the civil engineer, it seems to me, deals almost exclusively with soil in its compacted state. They are concerned with the questions of foundation, of carrying capacity, and so on. The agricultural engineer, however, would need to study, I imagine, the soil mechanics not of soil in its compacted state, but soil soil in its dispersed state. And here, in this field, as far as I can see, there are hardly any established scientific principles at all. The result is in the University discussion in Australia, to do with the designing of such course, the result is that a three term year is devided between three separate lecturers. We have one lecturer from a civil engineering department who teaches, willy-nilly, everything that he knows about soil mechanics. We have a

soil physicist from the department of agriculture who tells what he knows about soil physics and the classification of soils, according to a welle established principle along these lines. We also have lectures from the soil microbiologist and the soil chemist. Now, it is my experience, in discussing with the lecturers concerned in this work in Melbourne, I have said to them: « How do you integrate these three different disciplines and join them into a new separate discipline which has application for the matter of agricultural engineering ? And from each one of those three months comes the answer: « I am unable to discuss my discipline with my collegue, he doesn't understand me; moreover, I don't understand him ». I say: « Where then does the integration come from? ». And the answer always is again: « We hope that this year, or next year, or perhaps in ten years, a brilliant student will listen to all three of us and somehow join these three disciplne together ».

W. F. BUCHELE. — For the past two years I have taught the graduate course, soil dynamics, at Michigan State University. This course is for masters degree and doctoral degree candidates and deals with tillage energy, the behavior of soil under the action of wind, water, and tillage forces, and the movement of vehicles on the soil. I like to describe the course this way; we deal with movement in or over the soil.

During my graduate work, I took a split major between agricultural engineering and soil physics. I took a number of courses dealing with soil physics, plant physiology and machine design which Dr. Phillips spoke about.

Information from the above courses is integrated with Coulombs equation, the Bekker equations, and new research information and taught as a basic course in an emerging science.

I also teach a certain amount of soil value information in my undergraduate course, advanced power and machinery. In this manner, some 20 to 25 students are acquainted with the knowledge being developed in this field.

E. SAIBEL. — We are in the midst right now of revising our engineering curriculum, and our endeavour is to revise it toward greater generality. We wish to see fewer special courses and more general, basic work. In fact, we are getting to the point now where practically all of our undergraduate engineers will take a common three years. After that, we are not sure how we'll proceed; whether after a fourth year in a speciality a man will get a Bachelor's Degree, or perhaps after a fourth and fifth years he will get a Master's Degree. But, in any event, the general idea is to give a solid three or four years of mathematics, substantial physics, substantial chemistry; and to do this not because it's pointed towards the automotive industry, or because it's pointed towards the steel industry, or because it's pointed toward any other industry but because at the undergraduate level, all the work should be basic.

My point is simply this: I hope that this meeting will not lead any school toward greater specialization. I would hope that it would lead in toward less specialization and more general aspects of basic science.

OSSERVAZIONI CONCLUSIVE GENERALI

SUMMATION AND CLOSING REMARKS

Where do we go from here?

Conclusioni e previsioni per il futuro

M. G. Bekker*)

Your Excellencies, Ladies and Gentlemen:

It is a great honor and privilege to be asked by the Organizational Committee do deliver a closing address to this Congress. I have accepted it with a great hesitation for fear that I may fail to perform this task in a manner satisfactory to this audience. I hope that your indulgence and patience may help me to make this presentation interesting and useful to all concerned.

It is safe to assume that you may expect from me more than a mere summation of what has been said at this Conference. If this is correct, I should like to take the liberty of giving you not an abstract, but some kind of a synthesis of our discussions and a conclusion regarding the present « state-of-the-art » and an answer to the question as to « Where do we go from here? ».

For the first time in the history of engineering, off-the-road locomotion became the sole subject of an international gatherin. This alone makes our Conference the most outstanding event in its field. To look upon it in a proper perspective, I should like to go as far back as 1913, and render homage to the man who, in my opinion, is a precursor of a first general approach to the problem of soil-vehicle relationship. I am speaking of R. Bernstein whose paper entitled: « Probleme zur experimentellen Motorpflugmechanik », published in Volume 16 of « Der Motorwagen » is, in my opinion, a classic that has survived practically unchanged in its importance all the perturbations of our age.

To give you an example of Bernstein's influence, let me say that as recently as 1960, Y. S. Ageikin published in the No. 12 issue of the « Avtomobilnya i tractornya promyshlennost », an article on soil-wheel relationship based on Bernstein's methodology. This is not surprising as Russian engineers took much interest in Bernstein's research since Goryatchkin published in 1936 his collective work entitled « Teoria i proisvodstvo selskohosyainih mashin ».

---

*) General Motors Corporation.

The second man whose name I wish to record at this Conference is E. W. E. Micklethwait. As a wartime advisor to the British Ministry of Supply, Micklethwait published in 1944, through the British Military College of Science, a short treatise entitled: «Soil Mechanics in Relation to Fighting Vehicles». That work laid down the foundation for a solution of what had remained untouched by Bernstein, although a similar, independent work was carried on by myself in Canada at the same time. Micklethwait, to my best knowledge, was first to write on the application of classical principles of soil mechanics to locomotion problems, and to call the attention of automotive engineers to works by Professor Karl Terzaghi, generally recognized as the father of soil mechanics.

Terzaghi, in his book entitled «Theoretical Soil Mechanics», sees two fundamental problems concerning the whole issue: The first, related to the state of stresses that precede soil failure due to the plastic flow, which he calls the Stability Problem; and the second, related to the stress-strain relationship that exists after the flow takes place, which he calls the Plasticity Problem. If I may use a metaphor, I should say that Micklethwait approached the stability problem while Bernstein attacked the plasticity problem. Thus, these two men together put the cornerstone under the foundation of the mechanics of land locomotion in its present form, and implicitly outlined a methodology for a solution of the totality of problems of soil-vehicle relationship.

This has been first recognized in early work on land locomotion mechanics conducted during and after the Second World War, under the auspices of the Canadian Army, Canadian National Research Council and more recently, the United States Army Ordnance Corps. The Land Locomotion Laboratory of the Ordnance Tank Automotive Command was particularly instrumental in establishing basic philosophy and methodology of the new approach to this old problem.

The above approach, however, was not unique. During the same war years, a young Doctor of Engineering and Officer of the Italian Army, named Ferruccio Garbari also worked on problem of off-the-road locomotion. In a paper entitled: «Resistenza al movimento dei veicoli a ruote su terreno cedevole» published in the 1949 Volume of ATA Rendiconti della II Riunione Annuale, he treated the problem within the same methodological framework as that which guided the above-mentioned Canadian and United States research work.

We were not aware, in America, of the work by General Garbari. When is was brought to our attention by Mr. James J. Murray, whom you have met as a Chairman of last Thursday's Session, we felt this more than a mere coincidence. The fact that people across decades have followed, in different countries, the same path to the same goal suggested that the time may be

ripe for getting together. General Garbari felt the same way. This is how the idea of this Conference was born. Thanks to the support of His Magnificency Rector Professor Capetti, the Co-Chairman of this Conference, and the interested faculty members of the Institutes of Technology of Torino and Milano, of the Universities of Bologna and Roma, of the Servizio Tecnico della Motorizzazione dell'Esercito Italiano, the United States Army Research Office, and particularly the Land Locomotion Laboratory of the U.S. Army Ordnance Tank Automotive Command, the idea became a reality.

The distinguished members of the Organizational Committee, the National Secretaries of all the countries represented here, all the speakers and all those who have taken part in this Conference have done the rest. I feel that a new era has started in this most ancient field of man's locomotion.

That the Conference has been a success seems to be no doubt. Fifty-two papers from nine countries and 329 participants in the discussion speak for themselves. It would be impossible to mention in this short address all the contributions made, and to attempt to evaluate their significance.

In a conviction that the Conference will bear upon future developments in off-the-road locomotion, I would like with your permission, Ladies and Gentlemen, to dwell only on those aspects of the present state-of-the-art which, in my mind, offer a methodological clue to the future, and a hope of a generalization of solutions of our problems, within the mechanics of soil-vehicle systems. I shall bypass the areas which have been either worked out for the past 20 years to the utmost of their capabilities, which have been previously discussed in technical journals and magazines, or which contain information difficult to assess because of lack of quantitative data.

I mentioned at the beginning of my address that the land locomotion mechanics, as we see it today presented at this Conference, started with Bernstein, Micklethwait and Terzaghi. That goes back more than half of the century. It even goes further into the past if we recall that some fundamental principles of a solution of soil mechanics problems were actually published in 1773 by Coulomb in his « Essai sur une application des regles de maximis et minimis a quelques problèmes de statique relatifs à l'architecture », or by Boussinesq, in 1885, in his « Application des potentials à l'étude de l'equilibre... etc. ». Is thus our general approach to the problem divorced from modern thought? Is land locomotion mechanics in such a primitive state of development that it makes no use of the existing theories of plasticity, or of various models of visco-elastic behavior of soils?

The answer is not simply « yes » or « no ». The land locomotion mechanics based on Coulomb-Mohr criterion of failure, and on semi-empirical definitions of stress-strain relationship that exist in sinkage, as reported by a large group of papers discussed here may be considered primitive and far from being rigorous. But there have been no other general solutions presented at this

Conference, or available elsewhere. That latter point has been clearly made in an indirect fashion in the paper by Professor Drucker who stressed that:

« Although the art of soil mechanics is old and in many respects well established, the science of soil mechanics is relatively recent... In soil Mechanics (the science), the essential set of equations clearly should be relations between stress and strain. Except for elastic and simple visco-elastic behavior, no such equations are now in actual use ».

Professor Haythornthwaite stressed the same point:

« In the case of soils, much fundamental works needs to be done to establish appropriate stress-strain relations, and to explore the consequences ».

Thus, there seems to be little choice: While exploring the fundamentals, one must proceed with simple solutions of urgent practical problems by using less rigorous methods. It seems to me that the Conference has stressed the importance of both approaches, and that it has also stressed a need for the search for a general method rather than for a solution of a specific problem. That is, I believe, a great achievement. For, if I mai paraphrase the words of one of the foremost philosophers of our century, Alfred North Whitehead, I would say that the greatest invention is the invention of the method of invention.

A word of caution against extremes, however, may be in order. One should not expect too much practical gain from the refinements of a rigorous scientific treatment of land locomotion because of the statistical character of soil changes. This appears to be particularly true when much effort is spent on complex computations which produce a result, let us say, with $\pm$ 5 % accuracy, when no predictable variation of soil that may occur within one hundred square meters or one hour may reach enormous proportions, and produce a 100 % error. On the other hand, empiricism which goes as far as to operate with physically undefined quantities and coefficients that hide all the unknown of the problem has been shown to lead only to a stalemate, at least on a long range basis.

The discussion has thus shown that the statement of the problem, from locomotion viewpoint, and not necessarily from soil mechanics viewpoint, is most important. I have always felt strongly in that respect, particularly when planning the strategy of the research effort and its budget. For instance, it has always appeared to me that while a study of soils based on visco-elastic models must continue for the sake of the scientific explanation and for the delight of the researcher, its practical value may be somewhat academic at this time, for the following reason: soils which display much elasticity are strong soils, and pose no problem in off-the-road locomotion. Soils which are predominantly viscous are a problem, but viscous forces depend on velocity of deformation. Since, however, we cannot move fast in a thick viscous mud or clay, for economic and engineering reasons, the problem loses much of its practical significance. The confirmation of this truism I have seen in many experiments.

The necessity for a continuous balancing of basic and applied research, if I may use these words in the context of my remarks, appears to be particularly important for two reasons: first, because the development of land locomotion mechanics is a new development, and has not yet established a generally recognized and accepted school of thought, such as that established in aerodynamics and fluid mechanics; second, because most of present or potential contributors to this study are part-time workers whose main interest and professional background can be traced in fields other than the mechanics of soil-vehicle systems, and who naturally may gravitate to their main line of endeavor rather than to this relatively new activity. Some papers presented here seem to indicate that trend.

This emphasizes a need for a fully professional treatment of the complex problems outlined by the Conference. The enormity of problems discussed here cannot be coped with on a part-time basis at least below a certain level, if they are going to be solved. It needs professionals. An educational activity discussed by Professor Vincent could be most helpful in that respect. It has produced encouraging results in the United States. When teaching land locomotion mechanics at Stevens Institute of Technology, and the University of Michigan, I saw a great potential in the young graduates, some of whome have become prominent professional workers in the discussed fields.

To emphasize this conclusion, let me note that the existing university programs of automotive engineering appear to be somewhat behind the spirit of our time. They could possibly be re-vitalized by the introduction of broad studies of transportation systems, which would include the mechanics of soil-vehicle systems. A study of that type would make use of all the disciplines with which this Conference has been concerned. To look upon a vehicle from the viewpoint of plasticity, elasticity, dynamic response to random input, statistics, stochastic processes, plus all the engineering sciences that help to make a vehicle, would be undoubtedly attractive even to a student who wants to travel in Space. In that particular case, I would even visualize a fascinating study of lunar soil mechanics concerned, for example, with the bearing capacity of a granular mass placed in a vacuum and reduced gravitational field, and exposed to the bombardment of protons. The paper by Dr. Ryan on lunar soils certainly suggests the vastness of such a problem, and the challenge which anyone can meet without the need for the astronomical amount of money which other phases of space exploration demand.

A truly professional approach to the mechanics of soil-vehicle systems necessitates a close cooperation within the same methodology of all those interested. This implies a need for common language such as basic definitions, symbols, etc. The Conference has shown, in my opinion, that in this area much is to be accomplished.

To illustrate further that point, I would not only suggest that we attempt an international standardization of terminology, but also the establishment of a common intellectual heritage by the most careful and objective referencing

of all the papers, publications and presentations. A need for this is seen in Conference papers, which use different symbols and nomenclature. As an example, one of the papers captions a paragraph with a sub-title which proposes a novel « plasticity theory ». At the end of the paragraph, however, one finds an equation which when properly « translated » is nothing else but a specific case of Bernstein's equation published in 1913. The lack of proper references makes it impossible to assemble a body of knowledge for professional use, and tends to forestall any professional cooperation, without which there can be little progress.

A number of ideas pertaining to new vehicle designs have been proposed at this Conference. I think there were good ideas. What struck me, however, was the fact that some of them were rather old. Being good, why have they not been accepted for so many years?

It would appear that the question may be answered in a general way, and not only with reference to the inventions discussed at this Conference. In land locomotion, as in many other fields, there are no panacea: Every vehicle is good in one soil, and bad or mediocre in another. In order to find de balance between the bad and the good, we must specify the environment and the frequency with which particular situations occur. In other words, we must go into operational studie in addition to the engineering studies. That is where most engineers fail. A good idea worked out and presented without an appropriate analysis of the whole soil-vehicle system cannot be possibly judged. It will live orphaned for years without being either disqualified, or adopted.

A good example of that point may be seen in the development of the so-called articulated vehicles; i.e., vehicles composed of a number of units hooked together in accordance with what I call the « Train Concept ». The first patent in this field was taken in England in 1917, by Diplock. Here in Italy, Pavesi produced a remarkable vehicle of the same type in the nineteen twenties. But the real interest in these vehicles at least in the United States and Canada, was not provoked until 1950-1956, when very comprehensive studies of the whole problem were made and published: These studies have originated, so to speak, the development of vehicles described in Mr. Thomson's and in one of Mr. Nuttall's papers.

This convinced me again that many good ideas presented at this Conference could be easily sold if backed by both engineering and operational analyses. That alone warrants further development of such analyses. Here, however, comes a word of caution. The analyses must belong to a recognized methodological school of thought. They ought to be generally accepted within the framework of applied mechanics and operations research for, if one starts to prove that his vehicle is better than someone elses because his « index » is higher than that of the competitor, then the argument will switch to what the « index » means, and not to what the vehicle does.

It would appear, then, that it is in the interest of everyone concerned

to work on a commonly recognized ground, i.e., within the context of a definite physico-geometrical system of values, measures and definitions. All the attempts to correlate purely empirical, dimensionally nonspecified indices with performance and design of vehicles have not helped anyone, as far as I know.

International gatherings are not necessarily a forum for display of unanimity and consent. This Conference, however, is an exception at least from one viewpoint. It seems to me that we all have been concerned with the same thing, namely with the predictions of an optimum of vehicle performance and design. This can be seen in theoretical papers, since the ultimate of the theory is its applicability to prediction; in papers describing experimental work, since experiment is the only means to verify or refute a theory; in dissertations on measuring techniques and instrumentation, as measurements are an essential part of the experiment.

Even those who presented new vehicle designs, undoubtedly, went through some process of prediction to reassure themselves in the validity of their concepts.

Predictions which I have in mind are engineering prediction. They are based on plausible assumptions, physically defined numbers, mathematical equations and calculations. This process of prediction methodologically is simple: First, we take values which matter. Those are meters, feet, volts, ampers, centigrades, calories, torques, moments, and what not; second, we construe formulae which express functional relationship between these quantities; and third, we feed the above available values in our equations, and by solving them find the desired answer, i.e., the prediction of what will happen under the assumed conditions.

That method has reached a fantastic accuracy since one today can hit the moon with a rocket at the distance of some 350.000 kilometers.

Actually, we need not go that far. Here on the earth, in aeronautical engineering, for instance, we have all the measurements and equations pertaining to the air and the plane. In naval architecture, there is all that is needed to known about water and the ocean in order to build and navigate a ship. There are formulae composed of viscosities densities, temperatures, gradients; velocity distributions of streams, currents and gusts; there are loads, powers, aspect ratios, stresses and strains. There are available values pertaining not only to air and sea vehicles, but also to the environment in which they operate.

Now, can I ask how many physically defined values do we measure on the ground? Is it not true that the consistency of the ground and its load bearing capacity are more capricious and unpredictable because of climate and geography than those of the air and water; would it be not logical then to expect that because of that complexity, we must measure more things on the ground than we measure in the atmosphere and on the seas?

The paradox is that for more than a decade we have debated what to

measure, and as a result, *we do not measure anything at all*. When trying to design efficient soil-vehicle systems, we can predict the behavior of every nut and bolt in the vehicle, but we cannot predict the behavior of the whole vehicle in the soil. Of course, without measuring soil, one cannot calculate; without calculation, one cannot predict. This, Ladies and Gentlemen, is in my opinion, the stumbling block which must be removed before our making any general progress whatsoever.

This Conference, I believe, has demonstrated that rational methods of engineering prediction based on soil measurements can be developed. It is now up to the rank and file of engineers and research workers either to adopt something which was presented at this Conference or modify it, or create something new. But this we must do, and do it with the highest priority. For there is no use to develop equations if one is not going to have the soil data which have to be fed into the formulae to make them practically meaningful. Should we fail to do so, it may take twenty years or more to test all new vehicle concepts, in all possible soil-climate conditions in order to arrive at an optimum solution which we are lacking today.

The fact that the presently used process of « trial and error » did not produce optimum solutions even after 30 years of testing agricultural tractors, for instance, is seen in the editorial published in the 17 February 1961 issue of the « Engineer ». At the Tenth British National Power Farming Conference, the farmer:

« Contended as plegmatically as he can with the whims and fancies of Nature... Nature has successfully kept nearly all machinery out of fields. Indeed, it was suggested during one of the discussions at the Conference that perhaps Hovercraft could be adopted to get implement to work where tractors bogged down. Our impression was that although the suggestion was meant to be humorous, there was in the mind of the speaker a wistful hope that the day will come when his machinery would not bog down ».

In my humble opinion, that day will not come until we start measuring statistically soil properties and their changes due to climate, and to design vehicles to perform the job under the assumed conditions with the desired degree of probability of success, or with that probability for which we are ready to pay. The present deterministic approach to locomotion values, stressed in many Conference papers cannot, in my opinion, produce practical results, because the soil may change its values on the same field by 100 % within a small area and a short time. Thus, one cannot look for fitting a straight line between scattered points, but has to « average » soil parameters in the same manner in which the vehicle itself will « average » its performance. Only in strictly controlled laboratory conditions is a satisfactory point-to-point correlation possible between soil and vehicle data. That, I believe, has been demonstrated by a number of papers.

To measure probabilities of success and their cost, in a competitive way, every tractor and off-the-road equipment manufacturer will, undoubtedly use

soil measurements and soil mechanics laboratories equipped with soil bins in the same manner in which airplane manufacturers use aerodynamic laboratories with wind tunnels and with all atmospheric measurements.

It seems to me that this Conference has not only shown a necessity for this type of approach, but also it has proven that this approach is entirely feasible and uniquely successful. It is my belief that the Conference has demonstrated the following:

1) Pure empirics has ended its usefulness.

2) Theoretical, although not quite rigorous solutions, are possible when starting with recognized definition of applied mechanics.

3) All the solutions are statistical in nature, and must be optimized in an operational analysis.

4) Hence, new vehicle designs cannot be fully evaluated and vehicle performance cannot be predicted without prior definition of the terrain, expressed in terms of physico-geometrical properties of soil and its surface.

I propose these conclusions for your consideration, Ladies and Gentlemen, as far as human frailty will permit, to speak without prejudice. I think I am in a position to do so, and when I say this, I say it not only for myself, but for a sizeable group of research workers in the United States and abroad with whom I have been very closely associated.

If I may elaborate and attempt to answer the question as to where do we go specifically from here, I would like to show you a picture which illustrates some sort of a synthesis of my thoughts.

We all agree that in order to meet the challenge in off-the-road locomotion, we must predict. Predictions have to be made within engineering mechanics, and have to be verified experimentally in the laboratory and in the field. To this end, we must calculate. One cannot calculate without measuring. Since we are interested in a soil-vehicle system, we must measure both soils and vehicle values. However, only vehicle values may be deterministic; soil values are statistical, therefore, all our predictions will be concerned with chance and operations research. Soil measurements and their statistical changes, as well as analyses of vehicle concepts, will express only a probability of achieving success in the given environment, but that is very significant. It also is, in my opinion, the minimum which one must try to attain. The outcome of our attempts may become the Shakespearean «to be or not to be», in this competitive world. This is where we go from here as I see it, in the light of the deliberations by this Conference.

Within such an approach, there is an ample need and opportunity for an international cooperation. It is my hope that we will meet again. At the next meeting, we should be able, I am sure, to discuss many more results arrived at within a definite school of thought. To establish such a school should be our goal, if you agree. Until the Second International Conference, then!

Before closing, let me say a few words of appreciation addressed to our hosts. I do not have any mandate to speak for anyone; I am sure, however, that I express the thoughts of all of us gathered here and particularly of the American group, when conveying sincere thanks to our Italian friends for the magnificent organization of the First International Conference on the Mechanics of Soil-Vehicle Systems.

Grazie ai nostri amici italiani per la magnifica organizzazione di questo Primo Convegno Internazionale del Movimento Fuori Strada.

Let me also express my personal feelings which, I believe are the sentiments of all of us, the feelings which reflect our deep regrets that General Garbari who dedicated himself to this Conference was unable to attend. Our prayers and best wishes for his speedy recovery are extended to him along with sincere thanks for all that he has done to assure the success of this Conference. Thank you.

R. A. Weiss *)

First of all, Mr. Chairman, I want to express on behalf of my fellow representatives of the United States Army and myself our appreciation to General Garbari and Rector, Prof. Capetti and their committee's work in making possible this opportunity to meet together to discuss problems of mutual interest, and to see this beautiful section of Italy. The list of groups and individuals to whom our thanks are due is indeed a long one, for a meeting of this magnitude requires a great deal of cooperative effort. Our appreciation goes to the General Inspectorate for Motorization, and the Technical Service of Motorization of the Italian Army; to the Politecnico di Torino, the National Unity Centennial Committee, FIAT, the Regional Administration, and to the many other groups helping with this conference. I think you all join me, too, in a special word of thanks to the untiring efforts of Colonel Tajani and to the capable translators, projectionists, secretarial assistants, and the many others behind the scenes who made our meetings more useful and our stay more pleasant.

As I review in my mind the results of this first conference on the mechanics of the soil-vehicle systems, I feel that there have been some and major substantial accomplishements here. Even more, however, I feel that the conference has underscored needs and future goals. One senses an atmosphere

*) Navy and Scientific Director Office, of the Chief of Research & Development, Army Research Office, Head Quarter Department of Army, Washington 25, D.C.

of preparation, of beginning. While a great deal of very meaningful work has been done, as reported upon in these sessions, vastly more still remains to be accomplished.

Let me mention briefly what I feel are the principle broad needs or problem areas in land locomotion research. These requirements, as you will notice, are closely correlated. First of all, there is a need for recognition that the study of soil-vehicle systems is an integrated field of theoretical and practical research, as so well pointed out by Dr. Bekker. As the unity and significance of this field gain in acceptance, we can hope for the corresponding growth of interest on the part of the scientific community. Only by mobilizing such interest can there develop a sufficiently large and stable corps of scientists and engineers devoted to the solution of land locomotion problems.

A second need or requirement is for better recognition on all sides of the full magnitude of the problem which we are considering. As the papers presented here so clearly illustrate, the basic question of how best to move by vehicle in off-road situations has many varied aspects. These must be tied together in a broad conceptual framework which can serve to unify the specialized work of, for example, the soil engineer, the tire designer, the dimensional analyst, and the agricultural expert. Perhaps it is not necessary that this conceptual framework or grand design be specifically stated. It must, however, be at least tacitly agreed upon as the outline into which the pieces of the puzzle fit.

A third need, I feel, is for maintaining a variety of approaches toward the solution of ground mobility problems. Your lively discussions here are strong evidence that there may be many different ways to handle these questions, and certainly the real, practical problems of locomotion, while like in genus, differ greatly in specifics. For the time being, at least, many avenues of research need to be explored. This variety of approach is not inconsistent with the unity of the field which I have already stressed.

Finally, as a corollary to the third requirement, there is a need for greatly improved interchange of ideas among those of you, both theoreticians and experimentalists, working in the cross country movement field. Only when ideas are freely and frankly exchanged can the best ideas be carried out further, and the sterile approaches abandoned. It is, of course, concerned awareness of the need to mix ideas which motivated the originators of this first international conference on the mechanics of soil-vehicle systems. You will, I am confident, merit this opportunity they have given you by nurturing carefully the new contacts made in these four busy days. Without seeking to deprive General Garbari and Rector Capetti and their Committees of the full credit which they alone deserve, Mr. Chairman, I assure you that the United States Army is pleased to have been associated with the sponsorship of this most worthwhile conference.

CONCLUSIONE

Al termine dei lavori, alcuni convenuti hanno rilevato l'opportunità che i contatti che si sono stabiliti in occasione del presente Convegno fra gli scienziati ed i tecnici che si occupano dell'argomento nei vari Paesi, vengano mantenuti e sviluppati, anche in vista dell'organizzazione di un futuro Secondo Convegno Internazionale del Movimento fuori strada.

Dopo varie proposte, ci si è trovati d'accordo di dar mandato ai segretari nazionali del Primo Convegno, di mantenersi in rapporto fra di loro ai fini predetti.

CONCLUSION

At the end of the meetings some of the Members remarked that it would be advisable for the contacts realized by technicians from different Contries, interested in off-the-road locomotion to be kept up and developped, also in view of the organization of a future Second International Conference on the Mechanics of Soil-Vehicle Systems.

After various proposals it was agreed that the National Secretaries of the First Conference should contact one another on the above mentioned objects.